Environmental Science and Technology

(2012)

Volume 1

Edited by

George A. Sorial
Jihua Hong

ISBN 9780976885351

Library of Congress Cataloging-in-Publication Data

Environmental Science and Technology 2012 (1)

Proceedings from the Sixth International Conference on Environmental Science and Technology, held on June 25-29, 2012 in Houston, Texas, USA

Includes bibliographical references
ISBN: 9780976885351

I. Sorial, George A.
  II. Hong, Jihua
III. International Conference on Environmental Science and Technology
(6th : 2012 : Houston : Texas)

Printed in the United States of America

Email: press@AASci.org
Website: www.AASci.org/conference/env

ISBN 9780976885351

Environmental Science and Technology

(2012)

Volume 1

Edited by

George A. Sorial
Jihua Hong

American Science Press, Houston, USA

TABLE OF CONTENTS

INTRODUCTION

PLENARY SESSION

WATER POLLUTION AND WATER QUALITY

Rivers, Lakes and Estuary Systems

Watershed Management

Water Resources and Assessment

Groundwater

Non-point Sources

Wastewater Discharge Management

In-Situ Measurement and Monitoring

Drinking Water

Water Quality Assessment/Management

Nitrogen-Phosphorus Wastewater Treatment / Sludge Treatment

Sludge Treatment

Municipal Wastewater Biotreatment

Industrial Wastewater Biotreatment

Adsortion/Desorption for Wastewater Treatment

Physico-chemical Wastewater Treatment

Reactions and Degradation of Wastewater Contaminants

Nanotechnology Applications

AIR POLLUTION AND AIR QUALITY CONTROL

Aerosol/ Air Quality Assessment

Transport of Pollutants / Waste Gas Control Techniques

Air Pollutant Monitooring

Hazardous Gas Biofiltration

Fuel Gas DeSOx, DeNOx, and Metal Removal

Air Pollution Prevention and Management

ECOSYSTEM ASSESSMENT AND RESTORATION

Ecosystem Assessment

Urban Ecosystems

INTRODUCTION

The Sixth International Conference on Environmental Science and Technology 2012 was held in Houston, Texas, USA, June 25-29, 2012. The Program included 16 sections, containing 60 sessions with approximately 850 platform and poster presentations. This conference series strives to provide a platform for an extremely diverse group of environmental topics for engineers and scientists from around the world.

Authors of the presentations accepted for the program were invited to submit their papers to the Conference Organizing Committee. More than 160 papers were received and then reviewed by the editors, session chairs, and the members of the Scientific/Technical Committee of the conference. Those papers and abstracts accepted for publication were assembled into two volumes.

Sections are arranged basically according to their order listed in the original program except the sessions entitled Land (Soil, Waste Solid) Pollution and Remediation. This exception was made to balance the length of the two volumes. The conference also consisted of having a plenary session with four speakers from different universities at the United States and other countries.

Environmental Science and Technology 2012 (I) contains the following sections:

- Plennary Presentation
- Water Pollution and Water Quality Control
- Air Pollution and Air Quality Control
- Ecosystem Assessment and Restoration

Sections included in Environmental Science and Technology 2010 (II) are as follows:

- Land (Soil, Waste Solid) Pollution and Remediation
- Bio-Assessment and Toxicology
- Wetlands and Sediments
- Global Warming
- Metals (Distribution, Removal, Remediation, Speciation, and Phytoremediation)
- Chlorinated and Other Persistent Organic Compounds
- GIS for Environmental Assessment, Database, and Remote Sensing Applications
- Environmental Analysis and Measurements
- Society and the Environment
- Environmental Planning and Management

- Renewable Energy Development

We would like to especially thank the session chairs who were instrumental in the success of the conference. The Conference was sponsored and organized by the American Academy of Sciences, with financial contributions from the co-sponsors and supporting organizations.

The papers in these proceedings represent the authors' results and opinions. No sponsors, cosponsors, participating organizations or editors should be construed as endorsing any specific contents or conclusions in the proceedings.

George A. Sorial, Ph.D.
University of Cincinnati

Jihua Hong, Ph. D.
American Academy of Sciences

PLENARY PRESENTATION

DATA DRIVEN ESTIMATES OF AIR QUALITY IN HOUSTON WITH CONTINUOUS SPATIAL AND TEMPORAL RESOLUTION*

Katherine B. Ensor (Statistics Department, Rice University, Houston, Texas, USA)

Using the dense network of air quality monitors in Houston, Texas and advanced statistical methodologies we develop a near real-time spatial-temporal estimator of pollution levels in the greater Houston metropolitan area. The focus is on the main criteria pollutants and small particulates. The statistical methodology couples hierarchical Bayesian methods with kriging and multivariate time series, providing estimates of pollutants continuously in time and space with clear measures of uncertainty. Uncertainty measures increase in sparsely sampled areas. In addition to extensive cross-validations studies based on the existing network, we augment the out-of-sample empirical testing of our estimation methodology through strategic use of the City of Houston's Mobile Ambient Air Monitoring Lab. We also present preliminary empirical results related to expected changes in air quality dynamics when examining the proximity to roadways and vehicle kilometers traveled.

* Loren H. Raun (Statistics Department, Rice University, Houston, Texas, USA), Arturo Blanco and Don Richner (Department of Health and Human Services, Houston, Texas, USA) participated in this study.

ISBN 9780976885351

CHALLENGES, STRATEGIES, AND PRACTICES OF WATERSHED POLLUTION CONTROL IN CHINA*

Zheng Zheng (Fudan University, Shanghai, China; Email: zzhenghj@fudan.edu.cn)

China has achieved enormous economic growth during the past three decades, with its national gross domestic product increasing by over 80 times between 1980 and 2010. Nevertheless, the economy growth was realized at tremendous environmental costs. China is now faced with pervasive water pollution issues. Water quality of many water bodies could not even meet the lowest Category V standard in China, indicating that they are not suitable for the purposes of irrigation or scenic views.

Realizing the urgency to mitigate its serious water pollution situations, China has made great investment in water pollution control such as its recent launch of the national key research program in water pollution prevention and control. So far, the huge investment has only resulted in partial success. Point pollution sources such as industrial and municipal wastewater in the country have been largely put under control. Nevertheless, the trend of deteriorating water quality has yet to be reversed.

At least two factors contribute to the dichotomy between huge investment and limited results in China's endeavors of water pollution control. First, in the past China has put the majority of its emphasis on point-source pollution treatment. It is increasingly realized that the previously largely ignored nonpoint pollution sources are the major cause of water pollution in many parts of the country. Second, China has been overly relying upon engineering approaches to water pollution control, ignoring the important roles of non-engineering approaches and stakeholder participation.

In addition, compared to developed countries, non-point source pollution in China has the unique characteristics of strong intensity and composition complexity due to its special socioeconomic conditions. First, China is faced with the daunting task of rural sewage treatment. More than 50% of its 1.3 billion people are rural. Sewage from the majority of the rural households is discharged either without or only with minimal treatment using simple methods such as septic tanks. Second, China is plagued with serious agricultural pollution due to prevalent improper application of fertilizers and pesticides. Finally, increasing living standards have stimulated appetites for meat consumption and led to mushrooming concentrated animal feeding operations, most without adequate waste disposal facilities. Overall, pollutant loads have far exceeded environmental assimilation capacity in many parts of China, and there is no readily available approach to tackle this serious situation.

Integrated watershed approach has been shown a potentially effective approach for non-point source pollution control worldwide. On the basis of global successful experiences as well as our own years of work in non-point source pollution control, a complete watershed pollution control framework has been put forward with three guiding principles: (1) prioritize pollution control based on the watershed's environmental capacity; (2) control pollution from source to discharge; (3) emphasize high-value nutrient recycling and watershed ecosystem recovery.

Through years of extensive research, interim progress has been made to implement the above framework to mitigate pollution from various nonpoint sources such as rural sewage, rural waste, and agriculture. In rural sewage treatment, we have developed a series of technologies with the advantages of low construction and operation costs, easy maintenance, and high pollutant removal rates. In rural waste disposal, we have developed a systematic approach aiming at the full closure of nutrient cycles and production of high-value added products. This approach consists of anaerobic co-digestion of rural wastes, biogas refinement, high-quality fertilizer production with biogas residues, nutrient conditioning, fertilizer packaging, plant configuration, and habitat rehabilitation. In agricultural pollution abatement, we have developed a so-called "clean river network" approach, which makes full use of local landscape and river networks, and fortify them with appropriate physical, chemical, and biological pollution treatment structures so as to achieve pollution reduction during transport.

* Xiaoying Yang and Xingzhang Luo (Fudan University, Shanghai, China) participated in this study .

ISBN 9780976885351

ANALYSIS OF *ESCHERICHIA COLI* O157:H7 SURVIVAL IN MAJOR LEAFY GREEN PRODUCING SOILS BASED ON TOPOLOGICAL DATA ANALYSIS*

A. Mark Ibekwe (USDA-ARS U. S. Salinity Laboratory, Riverside, CA 92507, USA)

Shiga toxin-producing *E. coli* O157:H7 has been implicated in many foodborne illnesses caused by the consumption of contaminated fresh produce. However, data on its persistence in major fresh produce-growing soils are limited due to the complexity in datasets generated from different environmental variables and bacterial taxa. There is a continuing need to be able to distinguish the various environmental variables and different bacterial groups to understand the relationships among these factors and the pathogen survival. Using Ayasdi's Topological Data Analysis (TDA) methods, we reconstructed the relationship structure of *E. coli* O157:H7 survival in 32 soils (16 organic, 16 conventional) from California (CA) and Arizona (AZ) with a multi-resolution output. Our goal was to correlate the survival time of *E. coli* O157:H7 in soils with soil properties and 16S rRNA 454-pyroseqnence based bacterial community composition. Results showed that the longest survival time, *ttd* (detection limit of 100 CFU g^{-1} dry soil) of *E. coli* O157:H7 was observed in the soils from northern CA and in organic soils from AZ. *E. coli* O157:H7 survival in soils was negatively correlated with electrical conductivity (EC), while water soluble organic carbon (WSOC) and total nitrogen (T-N) were positively correlated. A laboratory experiment with soils spiked with increasing salt concentrations confirmed that the concentration of Na^+ in soil water extracts negatively affected ($P < 0.001$) *ttd*. Bacterial diversity as determined by the Shannon diversity index had no significant ($P = 0.635$) effect on *ttd*, but individual bacterial phyla had different effects. The survival of *E. coli* O157 was significantly enhanced by *Actinobacteria* ($P < 0.001$) and *Acidobacteria* ($P < 0.05$), and significantly suppressed by *Proteobacteria* and *Bacteroidetes* ($P < 0.05$). Our data showed a complex interaction between *E. coli* O157:H7, soil microbiota, and soil properties in the survival of this pathogen in the soils studied. Therefore, good agricultural practices must be followed during pre-harvest operation to prevent the introduction of *E. coli* O157:H7 into produce-growing soils, and reduce the potential public health impact and economic losses associated with foodborne outbreaks.

* Jincai Ma[1,2], David E. Crowley[2] and Ching-Hong Yang[3] participated in this study ([1]USDA-ARS U. S. Salinity Laboratory, Riverside, CA 92507, USA; [2]Department of Environmental Sciences, University of California, Riverside, CA 92521, USA; [3]Department of Biological Sciences, University of Wisconsin, Milwaukee, WI 53211, USA).

ISBN 9780976885351

THE CARBON CONUNDRUM: ONE OR MULTIPLE SOLUTIONS?*

Farid Benyahia** (Chemical Engineering, Qatar University, Qatar)

The green house gas emission reduction debate seems to go on for an extended period with no major breakthrough on large scale deployment of sequestration technologies despite the launch of several high profile CCS projects around the world. This situation stems from unresolved issues that are related to the limited availability of suitable CO_2 storage sites on a global scale, the risks associated with potential leaks and the concern on the state of the art of modeling of CO_2 transport fate in reservoirs, despite advances made in the field. Given the massive scale of global carbon emissions coupled with insufficient capacity of suitable geological formations or depleted reservoirs that can store safely captured CO_2, it is imperative to consider alternatives to underground storage in order to address the carbon conundrum. The reality is that a single solution to mitigating global carbon emissions is neither feasible nor safe. Indeed, it is much safer to consider a range of carbon management options with a view to manage the risk involved in each option and prevent further delays in addressing the global green house gas emission reduction. The main focus of this work is to accurately characterize the carbon conundrum and provide a balanced analysis of various carbon management options from the feasibility, effectiveness and risk point of view. Such alternative methods to underground storage include mineralization, biofixation, carbon conversions and energy efficiency. The approach has clearly demonstrated that a mix of options in carbon management will probably be the most practical solution given the diversity of geology, energy consumption and industrial growth across the globe. An Arabian Gulf case study based research work addressing two environmental problems in one solution is presented. The work that promised to address simultaneously desalination brine reject and carbon emission through a mineralization chemical reaction based solution at relatively low temperature showed a great potential for this dual solution approach. Important experimental conditions were identified to enable a pilot plant study prior to deployment for full scale.

*Karam Al-Ahmed (Chemical Engineering, Qatar University, Qatar) participated in this study.
**Email: farid.benyahia@qu.edu.qa

ISBN 9780976885351

WATER POLLUTION
AND
WATER QUALITY CONTROL

WATER QUALITY IN UTAH LAKE TRIBUTARIES OVER 40 YEARS

Gordon Killarney Liljenquist, ***Brett Borup****, Woodruff Miller, and Gustavious P. Williams

(Brigham Young University, Provo, UT, USA)

ABSTRACT: Utah Lake is a large, approximately 380 km^2, freshwater lake at an elevation of 1,400 m and an average depth of 2.7 m. Due to its size and depth, evaporation accounts for approximately 40% of the outflow and total dissolved solids (TDS) are a main concern. A predictive statistical model for TDS in the lake has been developed over the past 40 years, with data from the tributaries and the outlet that correlates TDS and ion concentrations with flow. This model was updated with extensive data collection from March 2009 through May 2011. The data included total dissolved solids, bicarbonate, sulfate, calcium, chloride, magnesium, potassium, sodium, water temperature, pH, conductivity, turbidity, dissolved oxygen, and flow rates. These data were used to develop new predictive statistical correlation equations. We compared the new correlation equations with the previous equations to determine how or if water quality had changed in the tributaries. Generally water quality has not changed significantly in the past 40 years. However, in tributaries that experienced heavy development, such as Hobble Creek, changes were identified but showed complex trends.

INTRODUCTION

Site Description. Utah Lake has a surface area of approximately 380 km^2, an average depth of 2.7 m, and is fed by approximately 50 tributaries (Rice, 1999; Miller, 1980). It is the largest freshwater lake in Utah and the second largest west of the Great Lakes. The Jordan River is the only natural, surface outflow which carries water to the Great Salt Lake (Miller, 1980).

The water in Utah Lake serves many purposes with a substantial portion used for irrigation. Economic losses would result if this water quality deteriorated (Brimhall, 1981). Utah Lake supports a host of recreational uses and wildlife including an endangered, endemic species of fish, the June Sucker, *Chasmistes liorus*. These uses depend on maintenance of the water quality (Marelli, 2010).

Purpose. Due to the size and depth, evaporation accounts for approximately 40% of the outflow and total dissolved solids (TDS) are a main concern. A predictive statistical model of Utah Lake for TDS was developed over the past 40 years, using data from the tributaries and the outlet. Land use in the watershed has changed greatly in 40 years. We updated this data collection and developed new correlation equations to predict lake conditions based on measured data. This study compares the new correlation equations to those developed over the past 40 years to assess changes and impacts from development.

Eight parameters were analyzed; total dissolved solids (TDS), bicarbonate (HCO3), sulfate (SO4), calcium (Ca), chloride (Cl), magnesium (Mg), potassium (K), and sodium (Na). These variables were grouped based on seasons (months of the year) and tributary flow rates.

ISBN 9780976885351

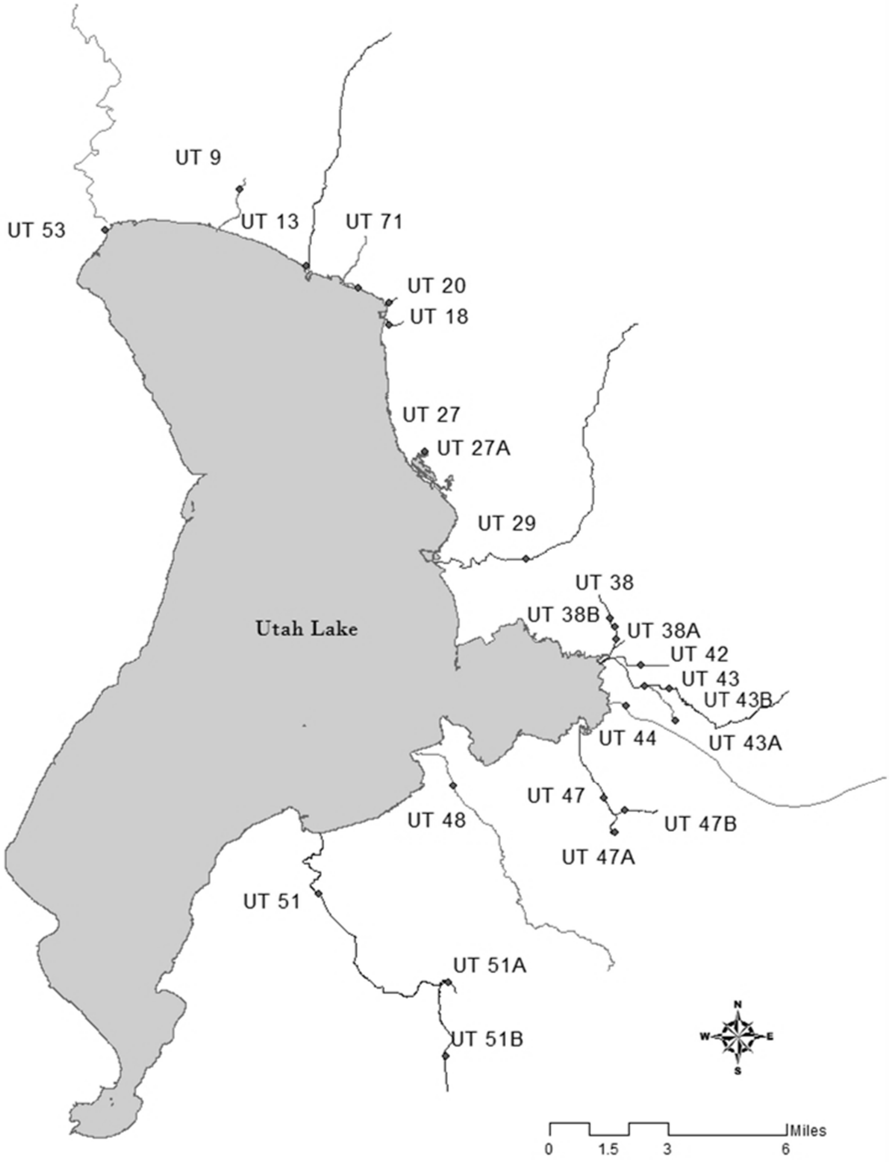

FIGURE 1. The location of the sampling sites for the tributaries and the outlet.

METHODOLOGY

Data Acquisition. From March 2009 to May 2011, monthly samples were collected at 18 different sites from the Utah Lake major tributaries and the Jordan River (UT 53). During high flow periods, from April to June of each year, samples were taken twice a month.

Of the 14 original sites, 4 were located downstream from waste water treatment plants (WWTPs). Beginning in October 2009 to May 2011, additional data were collected upstream of these WWTPs. Field measurements of water temperature, pH, conductivity, turbidity, and dissolved oxygen were taken with a Hach HydroLab DS 5 water probe. Weather conditions were also noted. The water samples were sent to the Utah Unified State Laboratory for TDS and ion concentrations measurements.

Flow rates were measured simultaneously with the samples. The flow rates for the Provo River (UT 29) and Hobble Creek (UT 44) were taken from the United States Geological Survey gaging records. Jordan River flow rates were provided by the Jordan River/Utah Lake Commissioner (Dye, 2012).

Flow was calculated by measuring the depth and velocity at three or four subsections within the cross section. The velocity was measured using a Flo-Mate Model 2000 Portable Flow Meter, (Marsh-McBinney, Inc). The velocity was measured at 0.4 (from the bottom) of the surface depth to obtain the average of the velocity profile for each subsection. Flow was computed by multiplying the sub-section area by the average velocity. The total tributary flow rate is the sum of the subsection flows (Dye, 2012).

From November 2009 to May 2011, data for the various wastewater treatment plants (WWTP) and the Geneva Steel Site (UT 20) were acquired directly from the State of Utah. Prior to November 2009, the values for the flow rates and ion concentrations at the Geneva Steel Site were measured by the study team.

Data Analysis. Data were organized by site locations and matched with flow measurements. We then computed averages, standard deviations, and maximum, and minimum values for each sample set. We then removed the outliers in the data sets.

The data sets were separated by seasons. Past projects characterized the seasons in different ways (O'Neill, 1992). We divided the year into three seasons: March through June (spring), July through September (summer), and October through February (winter) which produced the most logical and consistent results.

Each TDS and ion concentration was plotted against flow. The data were then fitted with trend lines; linear, exponential, power, logarithmic, or polynomial. The trendline type chosen was based mainly on which type produced the best coefficient of determination (r^2). However, the number of available data points was limited. Therefore, if a trendline produced a high r^2 value, but did not realistically project values that went beyond those of the available data points, that trendline was not selected. Any r^2 value less than 0.4 was deemed unacceptable to maintain consistency with past studies (Marelli, 2010).

If an equation could not accurately predict TDS and ion concentrations, then mean values were used. In past reports, both overall mean values and seasonal mean values were used to predict TDS and ion concentrations. We calculated seasonal and overall mean values and used them to predict TDS and ion concentrations, if no reliable trendline equation could be determinedTrendlines and concentration values were plotted so a visual verification of accuracy could be done.

The original predictive model assumed flows from WWTPs discharged into Utah Lake separate from their tributaries. Realistically effluent from the WWTPs is carried by tributaries. We treated tributaries which carried WWTP effluent differently from those without WWTP effluent.

Only four tributaries carry WWTP effluent: Millrace (UT 38B), Spring Creek (UT 43), Dry Creek (UT 47), and Benjamin Slough (UT 51). The effluent flow rates from these WWTPs were obtained from plant operators, with the flow rate for the Salem WWTP (UT 51C) assumed to be constant at 1.2 cfs. This was justified since the effluent from this WWTP is discharged from ponds with small fluctuations. The Timpanogos WWTP Ponds (UT 71) and Orem WWTP (UT 27A) both discharge directly into Utah Lake.

For Millrace, Spring Creek, and Dry Creek the water quality data upstream from the WWTP were used in the original predictive model with the flow rate values downstream set equal to the flows minus the WWTP discharge flow rates. If the WWTP discharge was not available, the seasonal mean discharge was used. This assumption was made since the difference in flow rates between the upstream measurements and the downstream measurements were within 3 cubic feet per second (cfs). Benjamin Slough (UT 51) sustained a greater difference and the influence of the Payson WWTP (UT 51A) and Salem WWTP (UT 51C) on UT 51 was removed using a mass balance equation.

Limitations. In past, similar studies trendline equations with high r^2 values, often greater than 0.9 were produced. In this study the average r^2 values were about 0.6. Since the collected data for this study only span a 26 month period, the lower r^2 values were deemed to be reasonable.

We noted that the equations and averages might be considerably different if data had also been collected during average and low runoff years, instead of the three high runoff years of 2009 - 2011. For example, the average 47 year Provo River flow at the Woodland station is 211 cfs, where the average flow rate for the past three years is 257 cfs, and the average 83 year Spanish Fork River flow at the Castilla station is 237 cfs, where the average flow rate for the past three years is 287 cfs. The average precipitation for the past 30 years at the Provo/BYU station is 20.13 inches, where the average precipitation for the past three years is 23.14 inches.The average Spanish Fork precipitation for the past 30 years is 21.55 inches, where the average for the past three years is 25.74 inches.

The trendline equations likely work best at predicting lake TDS and ion concentrations when the flow rates are within the maximum and minimum flow rates measured in the 26 month period. Beyond these flow rates, the predicted concentration values may be significantly inaccurate.

RESULTS AND DISCUSSION

Results. The data collected from each site were plotted similar to those shown in Figure 2. If the overall r^2 value was less than 0.4, then mean values were plotted (as shown for the SO_4 plots in Figure 3).

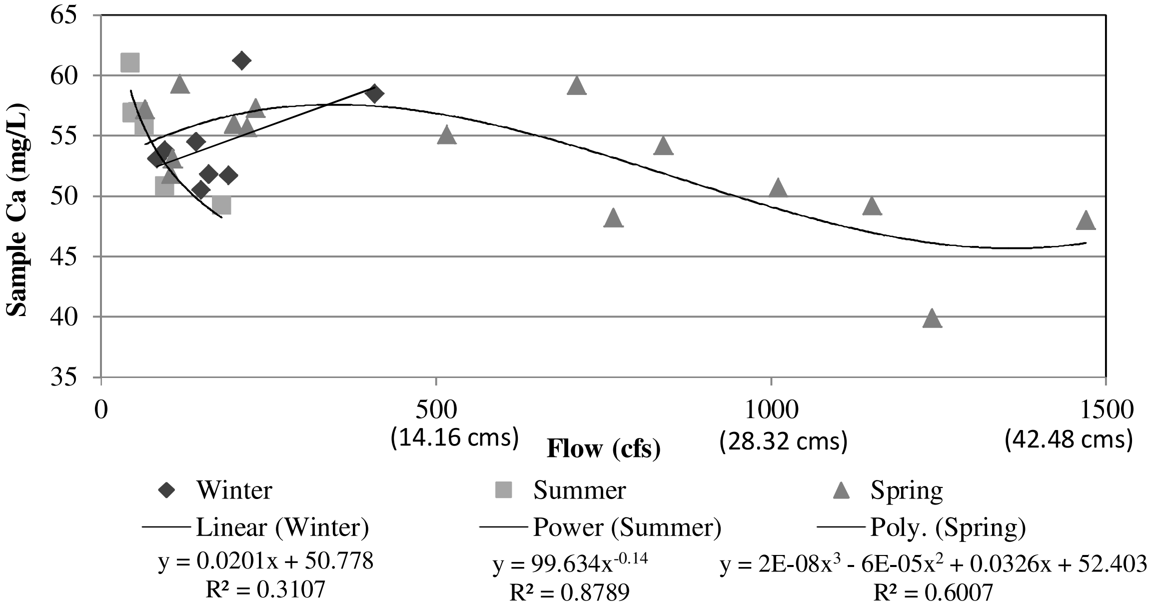

FIGURE 2. The trendlines that were found to have the reasonably best fit were used to predict concentrations of Ca in UT 29, lower Provo River.

Discussion. No equation was developed to predict the varying SO_4 concentrations, so a seasonal mean was used (Figure 3). However, in many cases the seasonal means could not accurately simulate the SO_4 trends. The annual mean concentrations of Mg and Na decreased over the past 40 years with the difference in Na being greater than that of Mg (Figure 4). Complex trends exist among these seasonal concentrations. Both of these tributaries, Provo River and Hobble Creek, have experienced heavy development over the past 40 years which may have contributed to the changes observed between the new and old data sets.

For every station, the new data proved more accurate than the previous model. Among the 21 sites analyzed in this study, new equations were found for 67 percent of the TDS and ion concentrations. However, the data from the seven WWTPs generated fewer equations, overall, than the 13 Utah Lake tributaries and the Jordan River. Only 55 percent of the TDS and ion concentration values for the WWTPs could be simulated with an acceptable equation. Conversely, 75 percent of the TDS and ion concentrations for the Utah Lake tributaries and the Jordan River could be simulated with an acceptable equation.

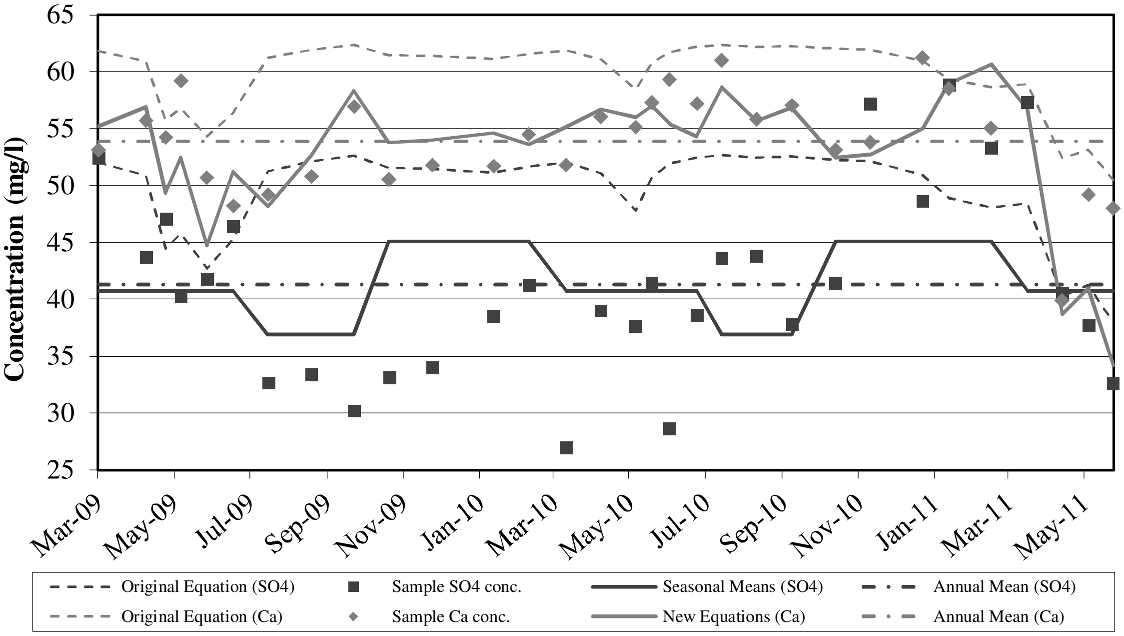

FIGURE 3. A predictive equation for Ca concentrations was found, but seasonal mean values were used to predict SO_4 concentrations in UT 29, lower Provo River.

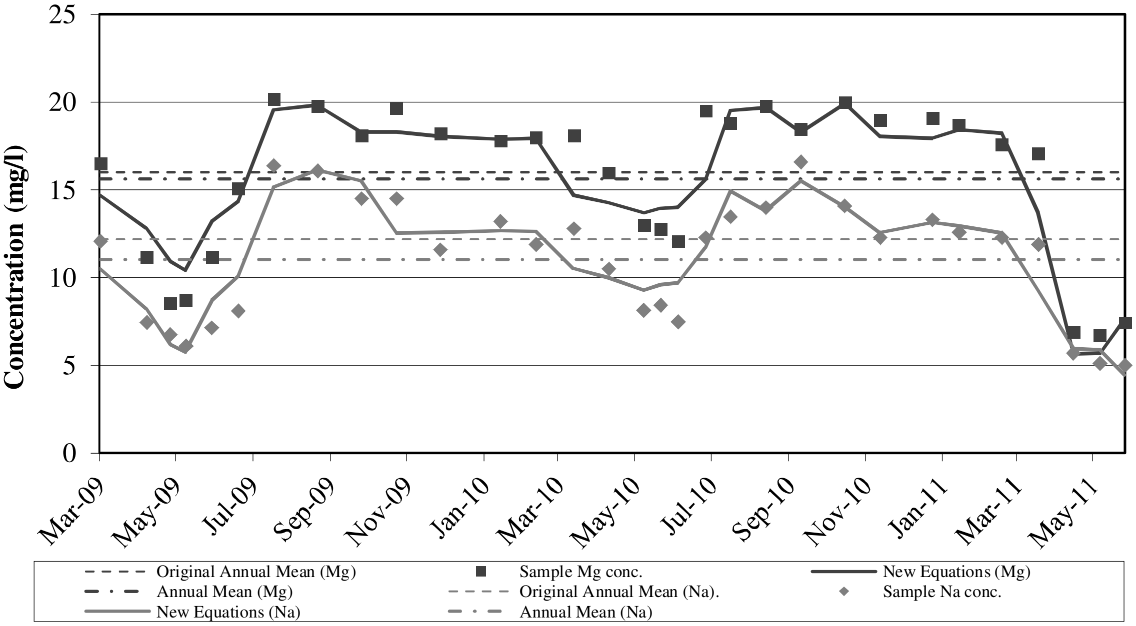

FIGURE 4. The original predictive model used annual means from 40 years ago, but recent data have produced predictive equations for both Mg and Na in UT 44, Hobble Creek.

The poor percentage of acceptable equations for the various WWTPs may have occurred because there was a comparatively low variation among the flow rates. For example, the Salem WWTP (UT 51C) had a relatively constant flow of 1.2 cfs. Thus, no acceptable trendline equations were produced to correlate flow with the TDS and ion concentrations.In this case, the seasonal mean values were used and seem to be sufficient to predict TDS and ion concentrations.

About 64 percent of the trendlines were polynomial equations. Although the data points that had polynomial trends were best described by this type of equation, polynomial equations are poor at data extrapolation and results outside the sample range are suspect.

CONCLUSION

The water quality of Utah Lake is of great importance to agriculture, recreation, and wildlife. We compared new correlation equations developed from recently gathered data over a 26 month period to those that were developed over the past 40 years . We found that few significant changes in water quality have occurred in the past 40 years. However, the new equations developed by this study, more accurately predict water quality of Utah Lake using tributary flow rates of the tributaries and the time of the year

REFERENCES

Brimhall, W. H. and Merritt, L. B. 1981. *Geology of Utah Lake: Implications for Resource Management. Great Basin Naturalist Memoirs*, No. 5, 24-42.

Dye, J. M. 2012. *Utah Lake Tributary Flow Analysis for the Central Utah Water Conservancy District*. M.S. Project, Brigham Young University, Provo, UT.

Marelli, J. 2010. *Update and Calibration of the Utah Lake Water Salinity Model (LKSIM)*. Brigham Young University, Provo, UT.

Miller, S. L. 1980. *Utah Lake Phase 1 Report #26*. Eyring Research Institute, Inc.

O'Neill, R. E. 1992. *Statistical Analysis of Major Ions of Selected Tributaries of Utah Lake*. M.S. Project, Brigham Young University, Provo, UT.

Rice, D. W. 1999. *Update and Calibration of the Utah Lake Water Quality Salinity Model (LKSIM)*. Brigham Young University, Provo, UT.

A PARAMETRIC STUDY FOR INVESTIGATING THE EFFECT OF INPUT PARAMETERS ON BACTERIAL CONCENTRATION IN SURFACE WATER FROM BRIDGE NESTING BIRDS

Manjura Maula Md. Nayamatullah*[*] and Sazzad Bin-Shafique
(University of Texas at San Antonio, San Antonio, TX, USA)

To understand the effect of direct droppings from the bridge nesting birds on bacterial contamination of surface water, a water quality model using QULA2Kw is developed for the bacterial impaired section of Guadalupe River near Kerrville, Texas. Concentration of three indicator bacteria, such as fecal coliforms, *E. coli*, and Enterococci are monitored at upstream, below the bridge, and downstream of the River for one and a half year. The model was calibrated with the measured bacterial concentration at different locations along the bridge. A decay constant estimated from the model was found to be 6.5/day for *E. coli*, and 5.5/day for fecal coliforms and 3.5/day for Enterococci. A parametric study is conducted to investigate the effect of the input parameters, such as decay rate, flow at the River, water temperature, and settling velocity. From the parametric study, it can be suggested that the decay rate and headwater flow has the highest impact on fate and transport of pathogens. The water temperature moderately affect the fate and transport of pathogens, whereas, the settling velocity of bacteria did not show any significant effect.

∗Email: jzb292@my.utsa.edu

ISBN 9780976885351

SPATIAL GROUPING AND TEMPORAL TRENDS IN OTOLITH CHEMISTRY OF AN ESTUARINE FISH

***Ana Judith Giraldo*, Travis Elsdon and Bronwyn Gillanders**
(University of Adelaide, Adelaide, SA, Australia)

Elemental concentration in otoliths provides a unique opportunity to discriminate among fish that live in different habitats, and to estimate population structure. Therefore, we examined spatial and temporal patterns in otoliths of juvenile 0^+ black bream (*Acanthopagrus butcheri*), to discriminate stocks of fish living in different estuaries. Fish were sampled in up to 13 estuaries of Kangaroo Island and the Fleurieu Peninsula each year over five year period (2008 – 2011). Otoliths were examined to determine if individual estuaries or groups of estuaries differed in chemical concentrations (tags), and to examine inter- annual variation in chemical tags. Tags differed among individual estuaries and in some cases adjacent estuaries shared similar chemical tags. Differences in chemical tags were detected among all estuaries in two of the year's comparisons. Similarities in otolith tags were detected for five of the seven estuaries in 2010 and 2011. Grouping together estuaries with similar chemical tags enhances the classification accuracy of individual estuaries and those groups, and therefore the ability to discriminate stock structure based on otolith chemistry. Temporal differences in chemical tags were detected among years for several estuaries; however, there were no clear trends in the differences between years. The result highlight that the population of black bream from different estuaries or group of estuaries have unique chemical tags that can be used to trace cohorts of fish. Chemical tags in juvenile black bream can therefore be used to estimate connectivity, population movements, and the function of estuaries as nursery areas for this species in subsequent years.

ISBN 9780976885351

PHYSICO-CHEMICAL PARAMETERS AND PLANKTON DIVERSITY OF GHANPUR LAKE, WARANGAL, AP. INDIA

T. Ravinder Reddy, D. Balakrishna, K. Vasumathi Reddy and D.Samatha.
(Department of Zoology, Kakatiya University, Warangal, Andhra Pradesh, India)

The planktonic population and the physico chemical parameters of the Ghanpur Lake have been studied for a period of twelve months. Ghanpur Lake was situated Warangal district, Andhra Pradesh, India. The physico chemical parameters and planktonic diversity was studied from February 2009 to January 2011. The physico chemical parameters includes Temperature, pH, Transparency, Turbidity, Conductivity, Total Dissolved Solids (TDS), Dissolved Oxygen (DO), Free CO2, Alkalinity, Total Hardness, Chlorides, Sulphates, Phosphates, Biological Oxygen Demand (BOD) and Chemical Oxygen Demand (COD). During summer Temperature, pH, Conductivity, TDS, DO, Alkalinity, Total Hardness, Chlorides and BOD was found to be increased and gradually decreased in rainy season. Sulphates and phosphates were found to be high in winter season and low in summer season. Therefore this lake has rich number of species and biodiversity of aquatic animals. A high rate of primary production was observed (326.060 mg/m2/hr). A total of 13 Zooplanktons were identified among these rotifers 7 species, Copepods 3 species, Cladocera 2 species, Ostracoda 1species, of which rotifers and copepods are dominating. Rotifera, Cladocera and Copepod populations were high during summer season and low in rainy season. While the Ostracode species were recorded high in rainy season and low in winter season.

ISBN 9780976885351

SEA-AIR TRANSFER OF MERCURY IN POST-DESULFURIZATION SEAWATER DISCHARGED FROM COAL-FIRED POWER PLANT

Lumin Sun, Shanshan Lin, Lifeng Feng and ***Dongxing Yuan*** *
(Xiamen University, Xiamen, Fujian, China)

To reduce air pollution of sulfur dioxide, more and more coal-fired power plants built in coastal areas have been equipped with seawater flue gas desulfurization systems. After neutralization of sulfur dioxide in fuel gas, the waste post-desulfurization seawater is discharged from such plants and carries pollutants such as mercury from the fuel gas into the adjacent seas. However, very limited impact studies have been carried out. The present study targeted at the distribution and sea-air transfer and flux of volatile mercury in seawater, taking a typical plant in Xiamen as an example, to trace the fate of the discharged mercury other than sediments.

Samples in 28 sampling sites were collected in the sea area around two discharge outlets of the plant, daily and seasonally. Total mercury, dissolved gas mercury, dissolved total mercury and reactive mercury in seawater, as well as total gas mercury above the sea surface, were investigated. Some ancillary parameters, including seawater pH, temperatures of air and water, salinity, dissolved oxygen, wind speed, solar radiation, suspended substance and dissolved organic carbon, were also determined.

The concentrations of all mercury species showed a gradient from the discharge point to outer sea area, indicating the discharged waste seawater was the source of mercury pollution. The distribution showed that the significant influenced region was about one square kilometer. The values of mercury species in summer and day time were usually higher than those in winter and night time, revealing that water temperature and solar radiation were the key factors for mercury concentration and transformation. The relationship between dissolved gas mercury and solar radiation further confirmed their significant correlation.

Mean values of dissolved gas mercury and total gas mercury in the area were 183 and 4.48 ng per cube meter in summer and 116 and 3.92 ng per cube meter in winter, which were hundreds times higher than those in a reference site. Based on the flux calculation, the transfer of the volatile mercury was from sea surface into atmosphere, and more than 4.8 kg mercury, occupying about 1.3% of the total discharge amount of the coal-fired power plant, in one square kilometer area was emitted to the air annually.

The study result strongly suggests that the impact of volatile mercury in waste post-desulfurization seawater on the air should not be neglected, and the research data would be useful for the relative air pollution control.

ISBN 9780976885351

A COMPREHENSIVE COMPARISON BETWEEN OSE II, MECHANICAL METHODS AND CHEMICAL DISPERSANTS IN LAYMEN'S TERMS

Steven Pedigo (OSEI Corporation, P.O. Box 515 429, Dallas, TX 75251, USA)

Oil Spill Eater II is the name of a non-toxic product which provides the means for moving oil spill response out of its current 19th Century methodology into the realm of advanced technological 21st Century breakthroughs for swiftly addressing and remediating *100% of any spill in any environment*. In comparison, current response methods employed by three major oil companies - BP, Exxon and Shell - are obsolete and obtain dismal results.

Most recently, BP, Exxon, and Shell have utilized *mechanical clean up* on the Gulf of Mexico Deepwater Horizon (DWH) oil blowout, the Yellowstone River oil spill in Montana, and the recent oil spill in the North Sea, respectively. Mechanical clean up in calm seas only has the capability of remediating somewhere between 2 and 8% of a spill; a woefully inadequate response.

Also utilized in the Gulf of Mexico blowout was Exxon's outmoded invention *Corexit,* a chemical dispersant licensed to Nalco Holding Company for manufacturing and distribution. The label on this horrifically toxic dispersant clearly states it can cause kidney failure and death and the MSDS (Material Safety Data Sheet) specifically warns, "Do not contaminate surface water" with it. Additionally, toxicity testing in regards to marine species shows little tolerance by all forms of sea life; thus, applying it on spills as a preferred response method increases the toxicity of the spilled oil on which it is used. Despite this, millions of gallons of Corexit have been sprayed on and injected into the Gulf's wateres.

ISBN 9780976885351

MANAGEMENT MULTI-OBJECTIVES OF WATER FUNCTIONAL ZONE IN CHINA

Lingling Bin, Chengzhong Pan, Xinyi Xu, Aizhong Ding
(College of Water Sciences, Beijing Normal University, Beijing 100875, PR China)

ABSTRACT: The problems of water resources shortage, water pollution, water ecological degradation has become the focus of attention of the society, and exert a direct influence on social and economic development in China. Water functional zone, which is the basis for water resources development and protection, is defined to manage water resources in a scientific way. Water function compartment is beneficial for water administration to finely control water quantity and quality, define important protection zone and improve the distribution of water resources in different water functional zones. In this study, management objectives and its setting methods of water functional zone for water quality, water quantity and water ecological conservation was proposed analyzing the existent problems and demands of the management. Then, results of water quality indicators, water quantity indicators aquatic ecosystem indicators were calculated in Huai River Basin as an instance, which provide a foundation for river basin water resources management and protection.

Key words Management objectives • Water functional zone • Indicators • Huai River Basin

INTRODUCTION

Various resources and environmental problems such as water pollution, unreasonable development and utilization of water resources, water ecological degradation result in damage of aquatic systems and degradation of its service function, affecting public health and social security directly and restricting social and economic sustainable development in China. Water functional zone (WFZ), which is the basis for water resources development and protection, is defined to manage water resources in a scientific way. Four types of first-grade zone and seven types of second-grade zone are included (FIGURE 1), while the second-grade zones are extended out from the utilization zone. At present, 3216 first-grade zones were divided; of which 248 were lakes type, more for rivers type. Water function compartment is beneficial for water administration to finely control water quantity and quality, define important protection zone and improve the distribution of water resources in different WFZs. However, only the objective for the water quality was focused at the present management, while little attention was paid to indicators of water quantity and aquatic ecosystem. What's more, areal variation of the evaluation

---

ISBN 9780976885351

method and frequency results in deficiencies in the process of implementing the water functional zone management (WFZM). Therefore, study on water quantity, water quality, and aquatic ecosystem management objectives is very necessary for ensuring the safe water supply, protection of the ecological environment and facilitating harmonious development of economic society and water resources. The result of this paper can provide basis for administration.

MATERIALS AND METHODS

Study area. As the case study area, Huai river basin (30°55'~36°36'N, and 111°55'~121°25'E) was located in eastern China (FIGURE 2), about mid-way between the Yellow River and Yangtze River, the two largest rivers in China, and like them runs from west to east. It flows through five provinces of China, namely Hubei, Henan, Anhui, Shandong and Jiangsu. It is the seventh largest river basins in China, having a length of 1,078 kilometers and a drainage area of 187,000 square kilometers. The population living in the basin is 165 million. Its average population density is approximately five times the nation's average. Although the annual mean precipitation and water resource of the basin are 920 mm and 85.4 billion m3respectively, water resources per capita and per unit area is less than one-fifth of the national average. Moreover, more than 50% of the water resources are overexploited, and is much higher than the recommended rate for international inland rivers (30%) (Zhang and Xia et al., 2010). In recent years, the water pollution accidents occur frequently and ecological environment get worse. Therefore, to make effective water management objectives of the water functional zone for the protection of water resources and ecological environment is especially important.

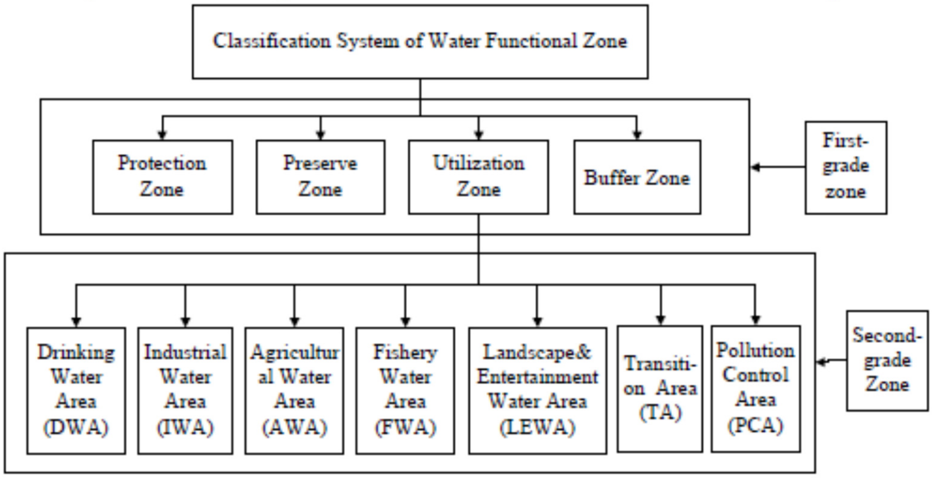

FIGURE 1 Classification System of Water Functional Zone

Data collection. Historical data were collected from different sources. For the management indicators propose and calculation, materials about water functional zoning were collected. Meantime, month average discharge and water level (WL) data (1956-2009) and water quality monitoring data (2010-2011) were collected. Water resource data was shown in TABLE 1. For this paper is to provide a basis for managers, relevant national standards were referred (TABLE 2).

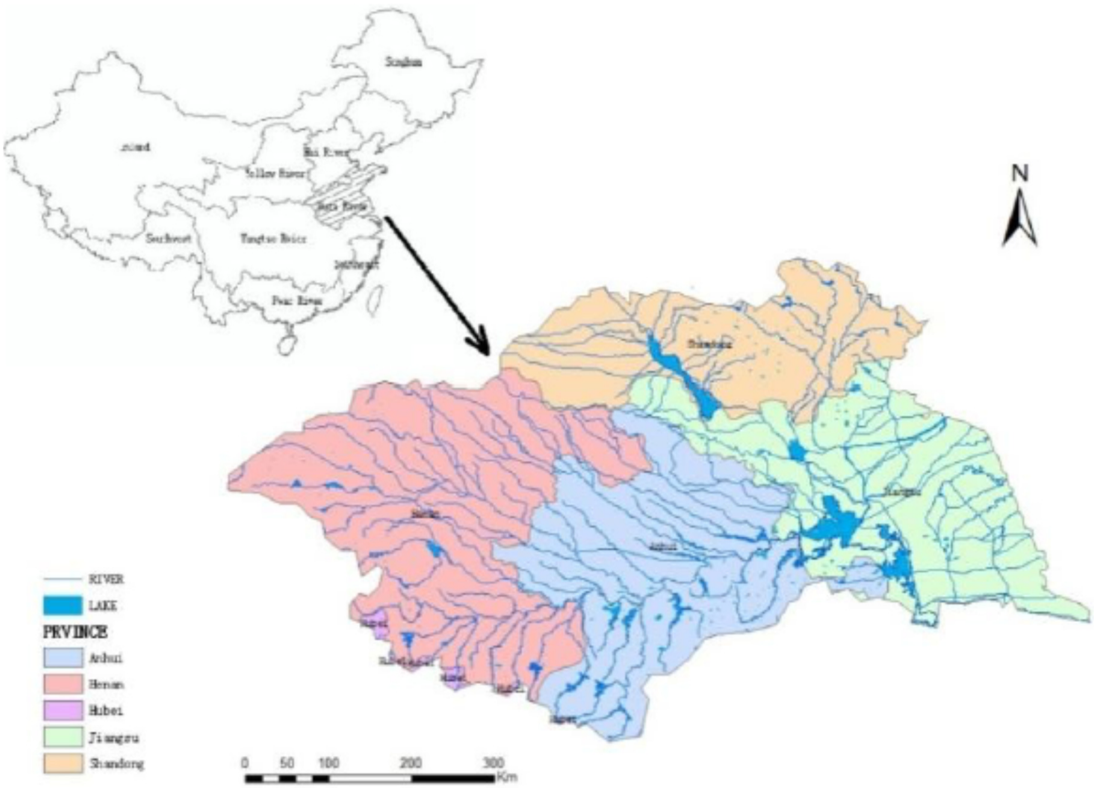

FIGURE 2 Location of Huai River Basin in China

Management Objectives Setting. In order to set the management objectives of water functional zone, it is necessary to know the demand of the management. By analysis of economic and social situation in the water functional zone, as well as the ecological environment, indicators of water quantity, water quality and water ecological conservation were selected. Then, results were calculated in Huai River basin as an instance.

Water quantity objective. To meet the requirements of the different functional areas for water resource, and to facilitate management and assessment, stream flow and water level (lakes and reservoirs) were chosen as the indicators for the WFZ. Stream flow was divided into function flow (FF) and environmental flow (EnF); the former was the flow that can meet its function demand and environmental flow was the minimum flow to improve the water quality. A global review of the present status of environmental flow methodologies revealed the existence of some 207 individual methodologies, recorded for 44 countries within six world regions (Tharme, 2003). In China, we take the average discharge in 90% assurance rate under the condition of the most withered month. In the WFZM, because of protection zone and drinking water area allowing no sewage, only function flow was given, for other WFZs, we take the smaller value of the two kinds of flow for evaluation.

TABLE 1 Surface Water Resource of the main river in Huai River Basin

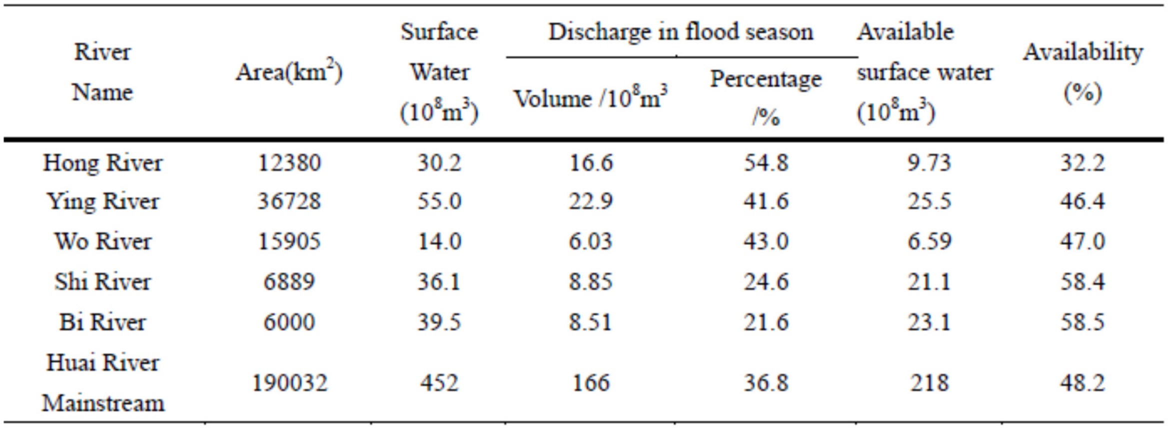

River Name	Area(km^2)	Surface Water (10^8m^3)	Discharge in flood season		Available surface water (10^8m^3)	Availability (%)
			Volume /10^8m^3	Percentage /%		
Hong River	12380	30.2	16.6	54.8	9.73	32.2
Ying River	36728	55.0	22.9	41.6	25.5	46.4
Wo River	15905	14.0	6.03	43.0	6.59	47.0
Shi River	6889	36.1	8.85	24.6	21.1	58.4
Bi River	6000	39.5	8.51	21.6	23.1	58.5
Huai River Mainstream	190032	452	166	36.8	218	48.2

TABLE 2 Standards referred in the paper

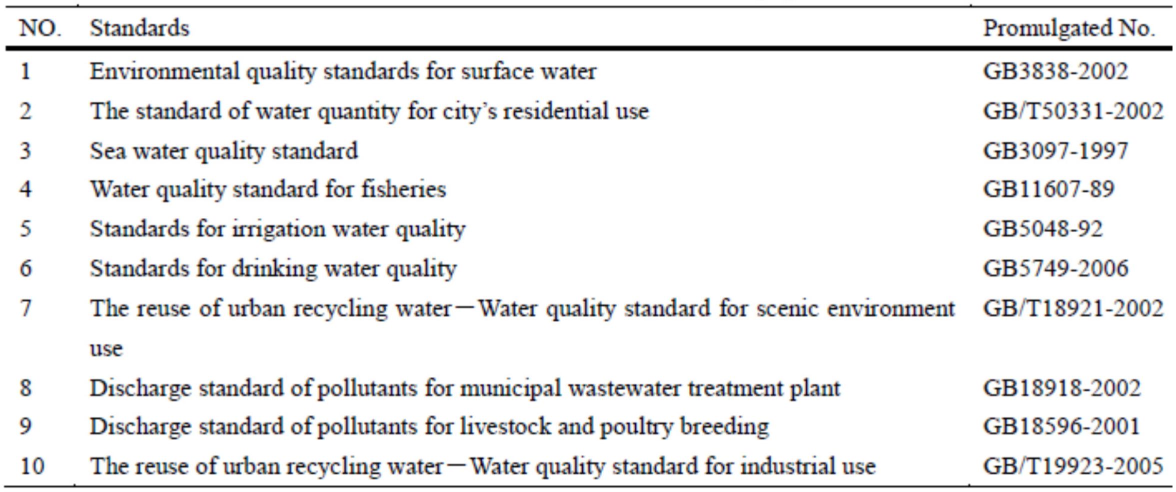

NO.	Standards	Promulgated No.
1	Environmental quality standards for surface water	GB3838-2002
2	The standard of water quantity for city's residential use	GB/T50331-2002
3	Sea water quality standard	GB3097-1997
4	Water quality standard for fisheries	GB11607-89
5	Standards for irrigation water quality	GB5048-92
6	Standards for drinking water quality	GB5749-2006
7	The reuse of urban recycling water—Water quality standard for scenic environment use	GB/T18921-2002
8	Discharge standard of pollutants for municipal wastewater treatment plant	GB18918-2002
9	Discharge standard of pollutants for livestock and poultry breeding	GB18596-2001
10	The reuse of urban recycling water—Water quality standard for industrial use	GB/T19923-2005

Water quality objective. For the prevention and control of water pollution, the State Environmental Protection Administration, allied with the General Administration of Quality Supervision, Inspection and Quarantine promulgated environmental quality standards for surface water, which is applied for the rivers, lakes, canals, channels, reservoirs and other surface water areas, it is also proper for WFZ. However, WFZ was divided in accordance with its function; many other standards all in table 2 were referenced in the process of setting objectives. The various functional areas must meet the corresponding water level requirements according to the surface water quality standard. All the indexes in surface water quality standards and the respective reference standards must be assessed. For example, there are 24 water quality indexes in environmental quality standards for surface water, 5 supplementary items and 80 specific items in drinking water sources areas, so there are 109 items should be assessed in the zones which have the function of drinking water resource. In addition to water quality indicators in the standard, environmental capacity (EC) is also included for the management objectives of the WFZ. Using environmental flow as the design flow, one-dimensional river water quality model was selected to calculate the environmental capacity. Now that no sewage discharges was allowed in protection zone and drinking water area, and buffer zone is set to coordination of conflicts between provinces, EC in these zones is need not to calculate.

Water ecology objective. The health of aquatic ecosystems is a comprehensive reflection of the quality of the aquatic environment and physical habitat. At present, China's aquatic ecosystems deteriorated seriously due to various pollutants discharged. As early as the middle of the last century, health of aquatic ecosystems was studied abroad, and a lot of mature evaluation and management methods were proposed (Frissell and Bayles, 1996; Allan and Johnson, 1997; Pollard and Huxham, 1998). Based on the study at home and abroad, taking into account the current status of watershed management in China, ecological flow (EcF) for rivers and ecological water level for lakes were set as ecological indicators.

Table 3 Management Objectives of WFZ in Huai River Basin

Category	River	Name	Water Quantity		Water Ecology	Water Quality		
			FF/WL	EnF (m^3/s)	EcF (m^3/s)	Level	EC（t/yr）	
							COD	NH_3-N
Protection Zone	Canal	PZ in Xuzhou	31.3-32.8m	2.00	2.84	III	0	0
Preserve Zone	Huai River	PZ in Xinyang and Suizhou	3.62m^3/s	8.00	10.76	III	836	26
Buffer Zone	Huai River	BZ in Anhui and Jiangsu		102	28.5	III	0	0
Drinking Water Area	New Shu River	DWA in Lianyungang	3.58 m^3/s	1.27	0.28	II	0	0
Industrial Water Area	Yi River	IWA in Yinan	0.12 m^3/s	3.35	0.05	III	374	18.8
Agricultural Water Area	Old Shu River	AWA in Tancheng	1.92 m^3/s	0.69	1.14	III	449	21
Landscape & Entertainment Water Area	Huai River	LEWA in Benbu	19.79 m^3/s	77.8	49.6	III	21385	1314.7
Pollution Control Area	Huai River	PCA in Xi county	23.75 m^3/s	16.4	5.1		5196	644.7
Transition Area	Chi River	TA in Mingguang	4.46 m^3/s	1.03	0.8	III	34	56.2

RESULTS

Through methods stated above, 10 WFZs in Huai River Basin has selected as an example, indicators of water quantity, water quality and water ecology were calculated (Table 3). Watershed management organizations can calculate all the indicators and announce to their subordinate departments, then assess regularly. Once assessment results fail to meet the established requirements, organizations should require the subordinate departments to improve the management.

CONCLUSION AND DISCUSSION

Research on the objectives of WFZ by methods on hydrology, ecology, and environment is not only a new task in the basin management in China, but also one of the active international research areas and challenges. This paper analyzed the current management problem in WFZM and put forward the assess framework and the indices at a basin scale; all the results can be used as a scientific basis for WFZM. However, because of ecological monitoring program and information deficiency, more water ecological indicators should be proposed in future research.

ACKNOWLEDGEMENTS

This study was supported by Key Project of Protection of Water Resources Integrated Management System organized by the Ministry of Water Resources.

REFERENCES

Allan, J. and L. Johnson 1997. "Catchment - scale analysis of aquatic ecosystems."*Freshwater Biology* 37 (1): 107-111. Frissell, C. A. and D. Bayles 1996. "ECOSYSTEM MANAGEMENT AND THE CONSERVATION OF AQUATIC BIODWERSITY AND ECOLOGICAL INTEGRITY." *JAWRA Journal of the American Water Resources Association* 32 (2): 229-240.

Pollard, P. and M. Huxham 1998. "The European Water Framework Directive: a new era in the management of aquatic ecosystem health?" *Aquatic Conservation: Marine and Freshwater Ecosystems* 8 (6): 773-792.

Tharme, R. E. 2003. "A global perspective on environmental flow assessment: emerging trends in the development and application of environmental flow methodologies for rivers." *River Research and Applications* 19 (5-6): 397-441.

Zhang, Y. and J. Xia, et al. 2010. "Impact of water projects on river flow regimes and water quality in Huai River Basin." *Water resources management* 24(5): 889-908.

UNDERSTANDING FARMERS' PERCEPTIONS TOWARDS WATER POLLUTION CONTROL IN THE YANGTZ DELTA, CHINA

Xiaoying Yang*, Xingzhang Luo, and Zheng Zheng (Fudan University, Shanghai, China)

It is increasingly realized that non-point pollution sources contribute significantly to water environment deterioration in China. Chinese government has been trying to shift its emphasis in water pollution control towards an integrated watershed approach for non-point source pollution control. Nevertheless, most efforts have been limited to engineering projects for end-of-pipe treatment with scarce promising outcomes. Farmers, who are both the major non-point source pollution dischargers and water environment deterioration victims, have been largely left out of water pollution control programs. Little research has been conducted to understand farmers' perceptions of water pollution and their attitudes towards water pollution control. To fill in the gap, in-house surveys of more than 200 randomly selected farmers have been conducted in Yixing, Huzhou, and Shanghai of the Yangtz River Delta to gain insights of the current situations of fertilizer use, rural water use, rural sewage treatment, and farmers' viewpoints towards water quality and water pollution control in economically developed regions of China. Study results have revealed widespread dissatisfaction with environmental quality, deficiency in environmental awareness, and lack of willingness to participate among the interviewed farmers. Without significant improvement with farmers' involvement capacity, it will be extremely difficult to implement effective watershed pollution control in China.

ISBN 9780976885351

Environmental Sceince and Technology 2012 (I)

PERFORMANCE ASSESSMENT OF GOVERNMENT MANAGED AT IMPROVED MAIN IRRIGATION NETWORK IN THE NILE DELTA

Ahmed Mohsen and Arif Alam (Tottori University, Tottori, JP)
Yoshinobu Kitamura, Katsuyuki Shimizu (Tottori University, Tottori, JP)
Taleet El-Gamel (National Water Research Centre, Cairo, EG)

ABSTRACT: The improvement of irrigation systems in the Nile Delta is one of the most important attempts in Egypt to implement more effective irrigation technology by improving the existing irrigation networks. One of the major forms of development is to apply the demand delivery system by using of mechanical gates to automatically divert water through irrigation networks. This paper discusses evaluating main irrigation networks system under the government managed before and after improvement in the Nile Delta. The overall results indicate that policy of using the demand delivery concept through irrigation networks is successful by improving water delivery performance among them than the rotation delivery concept that used before. It is provided fair share of water delivery among irrigation districts and available water in the end of irrigation network, although this system located in an end of irrigation networks in the Nile Delta.

Keywords water delivery performance, irrigation district, automation system, rotation system, Nile Delta.

INTRODUCTION

The Global water crisis is reaching a peak and increasing intensity due to the pressure of environmental degradation and high demand for food by increasing population in all over the world. This crisis affect negatively on the available water resources, which represent the mantle heavily on the countries of the world in the management of water resources' development. Egypt is one of the African countries that could be vulnerable to water stress under climate changes in the future. An array of serious threats resulting from climate change in Egypt, the most important is the rise in sea level that could affect the Nile Delta area. Therefore, the Egypt's policy has permitted cultivation of paddy fields in Delta's area to annexation and compressor having the largest fresh water as possible to stop the overlap of sea water, which these particular areas characterise with a low-level contour. The most important rice-producing countries in Mediterranean region are Egypt (6,600 km^2), (Ferrero, A. 2006). Even so, these areas consume around 25% of Egypt's quota from Nile flow, (WAGS. 2008). So, the water management in the Nile Delta, the scarcity of water irrigation, and high-profit paddy field cultivation considered the major challenge the form crops map of the Egypt. This management is the main task of the Egyptian government. The improvement of irrigation systems in the Nile Delta is one of the most important attempts in Egypt to implement more effective irrigation technology by improving the existing irrigation networks. One of the objectives of irrigation system improvement is to increase the reliability of irrigation water supply to meet the water demand more efficiency and effectively. One of the major forms of development is to apply the demand delivery concept in the main irrigation system by installing automation gates in secondary canals' level (branch canal). Depending on the rotation system was used before, the gate hoisting mechanism on the canal control structures are operated manually by head keeper. This causes difficulties to adjust gate opening in response to rapidly changing demand. As a result, there was often too much or as well as little flow in the canal. Fluctuation of water levels in the canal would promote bank instability and unreliable supply to the secondary canals.

Such development and change will have impacts on the decisions of water management and use. Therefore, performance of water delivery systems needs to be defined and assessed under these conditions before and after improvement. This paper highlights the water management in the Nile Delta zone in Egypt and presents the operation criteria and mechanisms in operation of the irrigation system by using performance evaluation tools. This paper discusses to evaluate main irrigation network system through season (2004) before improved and season (2007) after improved system in command area in the Nile Delta of Egypt by using the performance indicators proposed by Molden and Gates (1990).

ISBN 9780976885351

MATERIALS AND METHODS

Study Area. The Wasat command area, within the Kafr El-Shakh governorate, is located on the northern edge of the middle Nile Delta and extends from the outskirts of Kafr El-Shakh city to the shores of Lake Burullus (Eid, H. M., et al 2001). The command area is fed from the tail reaches of the main canal, Mit Yazeed, which in turn is supplied from the principal canal, Bahr Shebin, **FIGURE 1**. Owing to its location at the tail of the feeder canal system, the Wasat command area suffers from inadequate water supplies. This problem is exacerbated by the tendency of farmers to plant more paddy rice area than they are licensed to. Nevertheless, this area is famous for its rice production, which contributes 40% of Egypt's one (MSEA 2008).

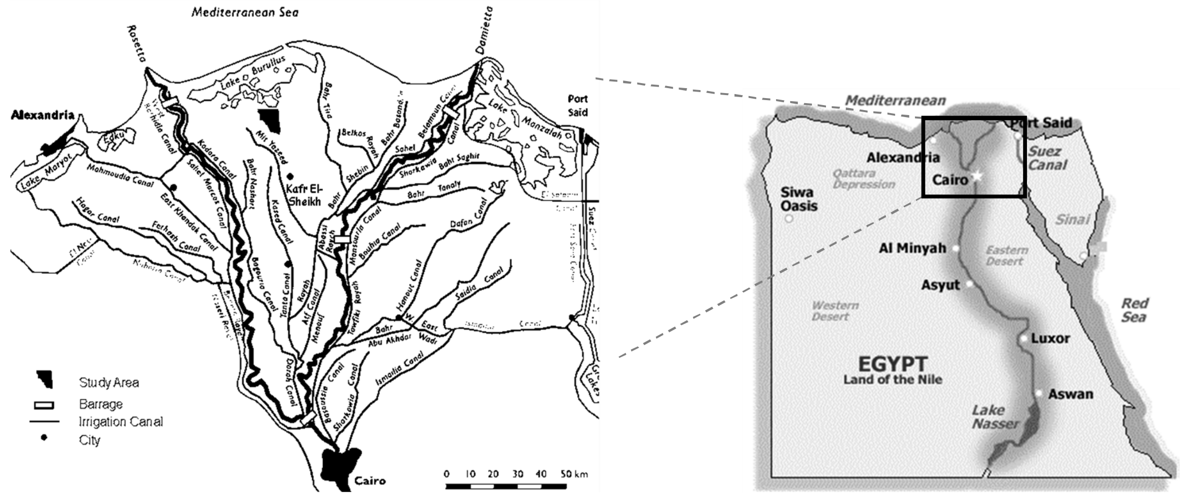

FIGURE 1 Layout of irrigation networks in Wasat command area

Characteristics of Irrigation Districts. In this study, was measured performance of irrigation networks through three selected irrigation districts that share in main canal (Mit Yazeed) at downstream El-Wasat regulator (km 34.7 on main canal), as presented in **FIGURE 2**. Each irrigation district was selected irrigation system (branch canal) to represent behavior of operation, as Dakalt canal in Kafr El-Shakh district, Baseis canal in El-Reyad district, and Shalma canal in Sidi Salam district.

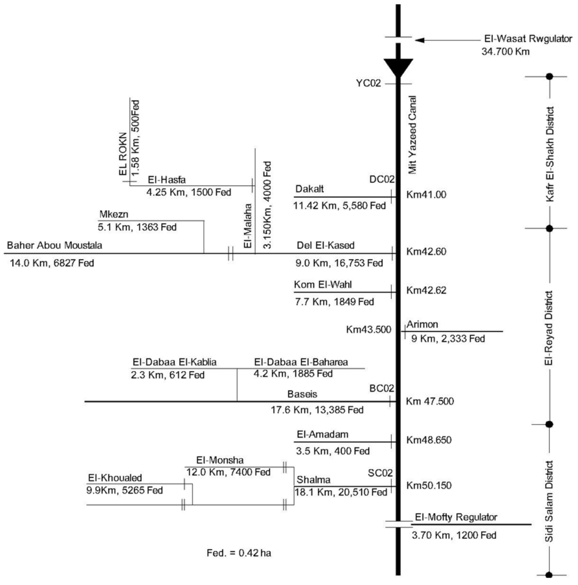

FIGURE 2 Schematic outlines of the water delivery canals

Before improving the system in the study area, the branch and distributaries canals system were operated according to agricultural rotation principal. There are two systems of rotation; two-turn rotation and three-turn rotation. Under the two-turn rotation, the canal system is divided into two groups. Each canal group is opened for 7 days and closed for another 7 days resulting in a length of irrigation interval of 14 days. The rotation system for rice is usually two-turn rotation with 4 days on and 4 days off. Under the three-turn rotation, the canal system is divided into three groups. Each group is opened for 5 days and closed for another 10 days giving an irrigation interval of 15 days. The demand delivery system is applied after improved the system. The basis is downstream control of irrigation network, although downstream control does not necessarily mean demand scheduling. The discharge is controlled by the end user from downstream end of the system. (Laycock, A. 2007). This offers the chances of increased crop yield, a reduction in water wastage. It means a free choice of crops as long as water is available, but also an increased capacity of the downstream end of the system.

Water Delivery Performance of the System. Water delivery performance through irrigation networks level of irrigation district was determined according to the indicators of adequacy, efficiency, equity, and dependability (Molden, D. J. et al 1990).

Adequacy: Distribution of required amount $P_A = 1/T\sum_{T=1}^{T}\left(1/R\sum_{R=1}^{R} p_A\right)$ (1)

Efficiency: Conservation of water resources $P_F = 1/T\sum_{T=1}^{T}\left(1/R\sum_{R=1}^{R} p_F\right)$ (2)

Equity: Distribution of fair amount $P_E = 1/T\sum_{T=1}^{T}\mathrm{CV}_R\left(Q_D/Q_R\right)$ (3)

Dependability: Uniform distribution overtime $P_D = 1/R\sum_{R=1}^{R}\mathrm{CV}_T\left(Q_D/Q_R\right)$ (4)

The indicators compare the volume of water delivery (Q_D) with water required (Q_R) of a certain region (R) during a certain time (T). Spatial averages are weighted against the surface of the irrigation network through branch canals in order to take into account their relative importance. For this study, the region (R) consists of the total area covered by the selected samples and the period (T) covers seven months of winter season and also covers five months of summer season. Therefore, water delivery and requirement were calculated overall interval of two weeks for branch canals. From the computed values, performance was classified as "good", "fair", or "poor" according to Molden and Gates (1990).

TABLE 1 Evaluation criteria for each indicator (Molden 1990)

Measure	Performance Classes		
	Good	Fair	Poor
P_A	0.90 - 1.00	0.80 - 0.89	< 0.80
P_F	0.85 - 1.00	0.70 - 0.84	< 0.70
P_E	0.00 - 0.10	0.11 - 0.25	> 0.25
P_D	0.00 - 0.10	0.11 - 0.20	> 0.20

Determination of Crop Water Requirements and Water Delivery. We estimated crop water requirements with the CROPWAT model of the UN's Food and Agriculture Organization (FAO), which uses Penman–Monteith methods to calculate reference crop evapotranspiration. Water application efficiency (by surface irrigation) was assumed to be 70%, while conveyance efficiency was assumed equal to 80% for main canal (EHWR 2003). The calculations were based on 15-day time steps that related to the cropping pattern and calendar.

But, the performance indicators used in this study requires the calculation of the water volumes that were delivered to certain reaches of the sample branch canals. Such calculations were not possible unless continuous discharge records were available. Since the water levels were continuously monitored using automatic water level recorders at upstream and downstream of head regulator for selected branch canals, and then, it was important to establish a relationship between the water levels and the discharges such that the continuous records of water levels can be converted to continuous records of

TABLE 2 Head discharge relations for head regulators

No.	Canal	Status	Relation	R^2
1	Dakalt	Submerged	$Q/H^{0.5} = 5.65 * GO - 0.05$	0.84
2	Basies	Submerged	$Q/H^{0.5} = 9.09 * GO - 0.84$	0.87
3	Shalma	Submerged	$Q/H^{0.5} = 12.63 * GO - 0.22$	0.92
		Free	$Q = 0.07 * WL^{6.67}$	0.77

R^2 = Correlation Coefficient; Q = Discharge (m^3/sec); WL = Water Level (m); H = Head Level (m); and GO = Gate Opening (m) discharges as precisely as possible. These flow heights were converted into discharge using individual rating curves of each point. The rating curves of these canals, constructed to standard geometric shapes. These curves were checked at each measurement point by using the flow velocities measured by current meter, and the area of flow cross section as present in **TABLE 2**.

RESULTS AND DISCUSSION

Cropping Pattern and Values of Q_D and Q_R. TABLE 3 depicts as percentage of the cropping patterns for Wasat command area. The maximum legal rice quota is 50% of a branch canal's command area (WAGS 2008), while the rice areas in head location accounted for over 55% of the area during before improvement, and increased to 63% in 2007. In other side, the crop rate in middle and tail locations was fixed through irrigation season. For cotton crop, the increasing of crop was luck for Dakalt canal, which its area of cotton was increased to 30% after improved against maize crop. Alfalfa is the most favourable winter crop to many farmers since it can either be used as fodder or sold for cash, especially in middle and tail locations. While in head location, this crop was decreased after improved systems. Wheat occupied between from 28% to 44% of cropping before improved and after that it was decreased through all locations. Sugar beet is the third main winter crop due to its cash value as it is sold to the sugar factories there.

TABLE 3 Irrigated crop patterns of branch canals in 2004 and 2007

Crops	Branch Canals					
	Head		Middle		Tail	
	(Daqalt)		(Basis)		(Shalma)	
(%)	2004	2007	2004	2007	2004	2007
Rice	57	63	44	41	52	52
Cotton	19	30	14	18	32	38
Maize	13	3	17	4	8	3
Citrus	0	0	2	2	0	0
Other (Sum)	11	4	23	35	8	7
Total	100	100	100	100	100	100
Alfalfa	37	27	22	29	26	36
Wheat	40	28	28	20	44	36
Sugar Beet	16	15	18	18	24	15
Citrus	0	0	2	2	0	0
Other (Win)	7	30	30	31	6	13
Total	100	100	100	100	100	100

TABLE 4 Q_D and Q_R values by branch canal position in 2004 and 2007

Season	**Month**	Branch Canals					
		Head		Middle		Tail	
		m^3 / ha (ha= 0.01 km^2)					
		Q_D	Q_R	Q_D	Q_R	Q_D	Q_R
Sum 04	May	1,235	1,680	1,016	1,571	1,017	1,768
	Jun	1,947	1,968	1,080	1,777	1,481	2,074
	Jul	2,066	2,243	939	2,133	1,231	2,269
	Aug	1,783	2,092	948	2,070	1,366	2,030
	Sep	621	1,118	792	1,069	734	1,048
Win 04/05	Oct	941	267	393	394	446	241
	Nov	700	461	544	490	439	445
	Dec	841	338	622	360	284	331
	Jan	313	407	274	413	261	418
	Feb	942	521	597	434	328	567
	Mar	856	834	488	763	525	978
	Apr	693	804	700	817	517	949
Sum 07	May	1,088	1,859	1,047	1,760	993	1,852
	Jun	1,725	2,183	1,315	1,866	1,307	2,160
	Jul	1,707	2,322	1,493	2,127	1,137	2,293
	Aug	1,474	2,053	1,653	2,037	1,332	2,003
	Sep	691	1,108	736	1,037	599	1,026
Win 07/08	Oct	904	393	725	432	655	304
	Nov	879	495	414	494	640	472
	Dec	615	362	325	369	449	345
	Jan	339	412	754	412	510	407
	Feb	368	390	628	421	389	477
	Mar	1,012	658	1,131	763	724	808
	Apr	759	681	1,123	937	1,835	873

Q_D and Q_R for the selected branch canals are given in **TABLE 4**. The water delivery in summer season was higher than winter season due to control for operation in regulators according to less water demand for winter crops. While in summer season, the gates were opened continuous owing to the greater demand by large proportion of paddy field. The water supply was increased after improved system at downstream main canal and that impact positively on middle and tail locations of branch canals. It is noticeable that the water delivery for the branch canals after the development was equal of values among themselves, which indicated that the automation system is distributed evenly among the districts of irrigation in the same time. While the system before development, the rotation system shifts are given in the head of irrigation district provided its full without taking into account; there are other districts of irrigation.

Water Delivery Performance of the System

Spatial Values of Performance Indicators. The adequacy values for spatial function are given in **FIGURE 3 (a, b)**. The highest *P*A values before improvement were found in June month at summer season around 0.8, and between October to December months at winter season around 0.9 to 1.0. For after improved system, the values of *P*A were almost fixed to range from 0.6 to 0.7 through summer months and 0.9 to 1.0 through winter months. The performance of water delivery among irrigation districts to water demand are fixed after improved its system in both irrigation seasons. Although, the values of *P*A are poor degree at summer season that is a normal case because this area locates in end of irrigation waterway in Nile Delta and faces water shortage during all the time due to cultivate paddy rice. However, the automation systems succeed to keep the ratio of available water delivery to water demand among irrigation months.

Spatial values of *P*F closed to 1.0 through all months in all summer seasons that indicated not good efficient water but water shortage in **FIGURE 3 (c)**. For the system before improved in winter season, the values were fluctuated through months for season in **FIGURE 3 (d)**. This rate is between good and fair degrees due to operate according to agricultural rotation principle among delivery canals, and there are not control points to distribute water among them. While after improved, the rate is fair through all months due to equal efficiency of automation gates of irrigation system at all time.

For the system after improved, the spatial values of CV_R were good degree through summer season as presented **FIGURE 3 (e, f)**, while the values were poor degree through winter months. This result indicates the ratio of water delivery to water demand among irrigation districts that are the same through months of irrigation seasons due to high efficiency of new gates to operate in same the time. This performance confirms the more equitable water delivery among irrigation district after its improved. As for system before unimproved, the values of CV_R were fair in summer seasons and between fair to poor in winter seasons because there are some abuse among the irrigation system during applying rotation principle.

Temporal Values of Performance Indicators. For the system before improved, the temporal values of *P*A in summer or winter seasons for head location were higher than other locations, as shown in **FIGURE 3 (a, b)**. This is a natural fact for available water in the head irrigation district at the main canal by using a rotation system among other irrigation systems. For the system after improved, the values of *P*A at different locations through irrigation seasons were fixed, except tail location in summer season. It indicates success of the operating automation gates under capacity of water required in downstream through irrigation systems and the chance of irrigation among districts become the same, especially the tail location.

From **FIGURE 3 (c)**, the temporal values of *P*F in summer season for the system before and after improved were good degree not because of more efficient water use by operation irrigation systems, but because of water shortages during this season. For winter season as shown in FIGURE 3 (d), the values of *P*F for the system before improved for head location were 0.7 that indicate to deliver more the water to irrigation system than required, in contrast, to other locations were facing water shortage. There is no cooperation or participation clear among irrigation districts in the operation.

CV_T values were closed to 0.2 for the system before improved **FIGURE 4 (g, h)**, the dependability performance of all three irrigation systems is poor because head location gets its full share of water through the application of rotations, while other sites get their share incomplete as a result of water-deficit region. While for system after improved, the values of CV_T were closed to 0.1 in summer season and 0.3 in winter season, and in addition, there were same values among them through irrigation season. The reason for these is the successes of applying continuous flow through a main canal than a rotation system that applied before.

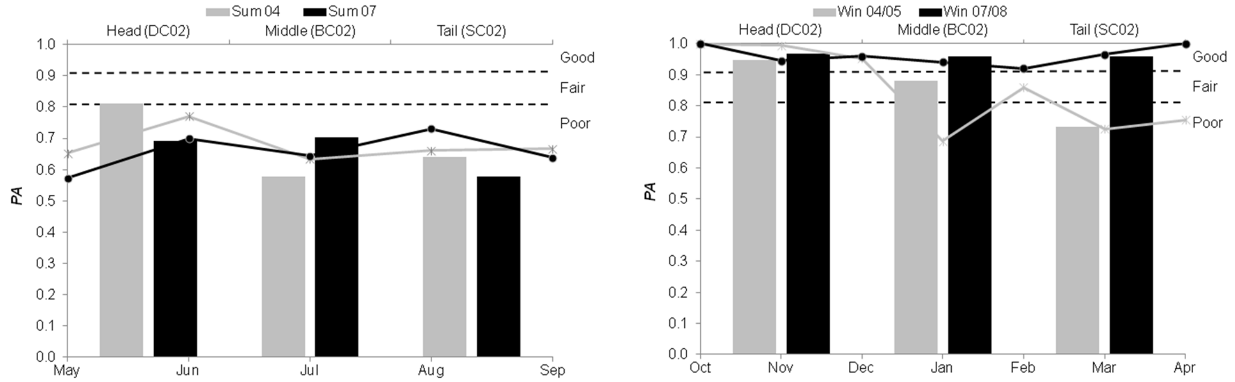

(a) PA values in summer season **(b) PA values in winter season**

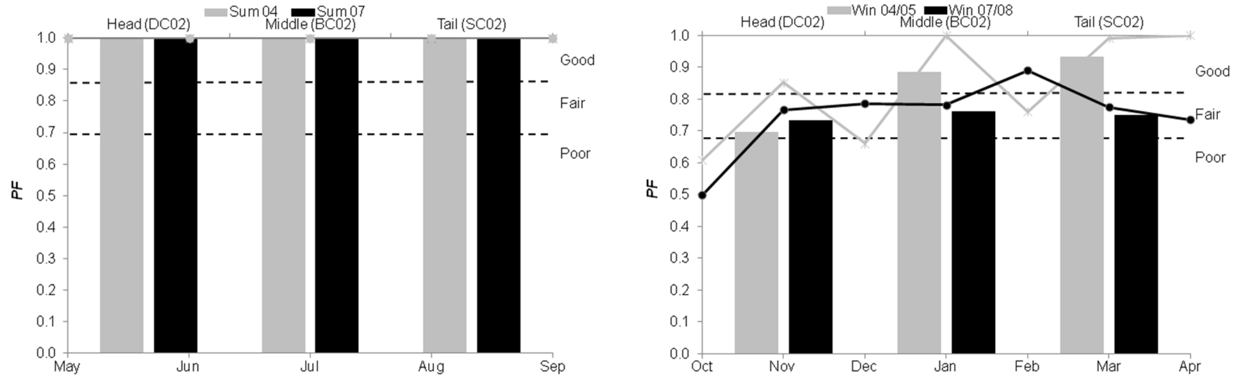

(c) PF values in summer season **(d) PF values in winter season**

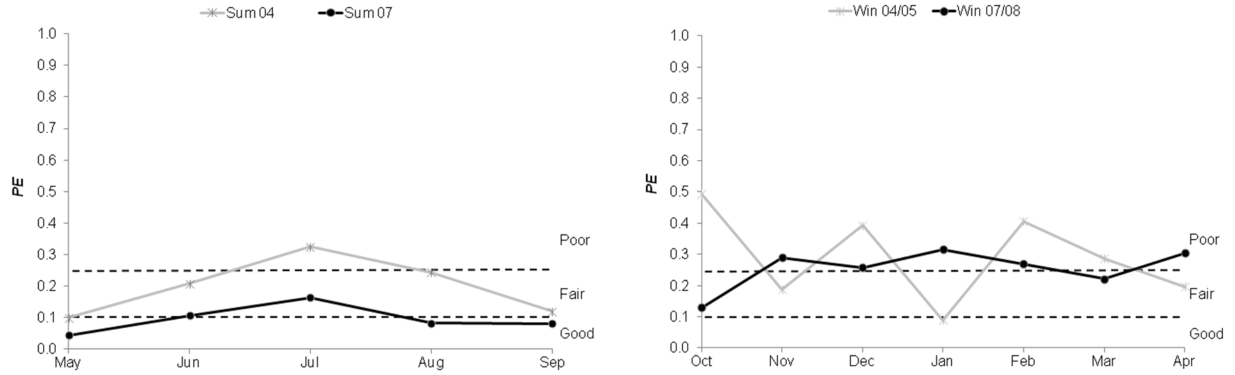

(e) CV_R values in summer season **(f) CV_R values in winter season**

FIGURE 3(a-f). Spatial and temporal values of PA, PF, CV_R, and CV_T for irrigation seasons 2004 and 2007

CONCLUSION

Based on the evaluation of indicators in this study, it can be concluded that the increase in the number of irrigation districts in one main irrigation network system is difficult to continuous monitoring of the water management and distribution among them by using rotation delivery system because there are not control points to distribute water among them and the most important elements of current control between irrigation district and next for equitable distribution under the dependence of water level. But applying demand delivery flow through irrigation networks by using automation systems, it is improved water delivery performance to equal share water among them during irrigation periods. As a result of cancellation of the human element in controlling the distribution of water among them according to water needs in downstream, despite the occurrence of the region at the ends of the irrigation networks.

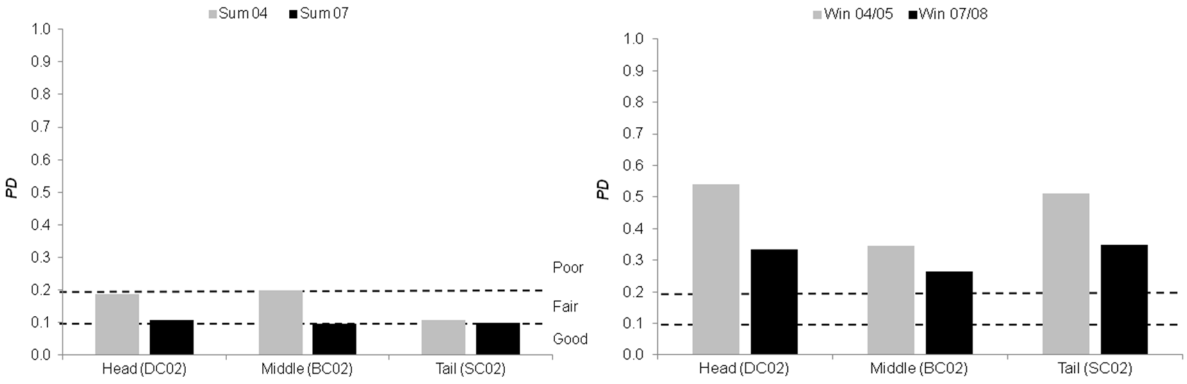

(g) CV_T values in summer season **(h) CV_T values in winter season**

FIGURE 4(g-h). Spatial and temporal values of PA, PF, CV_R, and CV_T for irrigation seasons 2004 and 2007

ACKNOWLEDGEMENTS

The author wishes to thank Global Centre of Excellence for Dry-land Science (GCOE) in Arid Land Research Centre of Tottori University for the funding on this research. This work was supported by Water Management Research Institute (WMRI) of National Water Research Centre (NWRC).

REFERENCES

EHWR: Egyptian Handbook for Water Resources. 2003. *Module 1: Management of Irrigation and Drainage Networks*. National Water Research Centre, Cairo, (in Arabic).

Eid, H. M., El-Marsafawy, S. M., and Ouda, S. A. 2001. *Assessing the impact of climate on crop water need in Egypt*: *the CROPWAT analysis of three districts in Egypt*. Agriculture Research Centre, Cairo.

Ferrero, A. 2006. "Challenges and opportunities for a sustainable rice production in Europe and Mediterranean area". J. of Paddy Water Environ. 4: 11-12. doi:10.1007/s10333-005-0025-3

Laycock, A. 2007. *Irrigation systems (design, planning and construction)*. British library, London, UK.

ISBN-13: 978 1 84593 263 3.

Molden, D. J., and T.K. Gates. 1990. "Performance Measures for Evaluation of Irrigation Water Delivery Systems." J. Irrig. Drain. Eng. 116/6: 804–823. ASCE, ISSN 0733-9437/90/0006-0804

MSEA: Ministry of State for Environment Affairs. 2008. *Environmental characterization of Kafr El-Sheikh city*. Environment Affairs Sector, Kafr El-Sheikh, Egypt. (in Arabic).

WAGS: Water Awareness and Guidance Sector. 2008. *Rice Problem in Egypt*. Ministry of Water Resources and Irrigation. Cairo. Egypt. (in Arabic).

CLEANER PRODUCTION POTENTIALITY ANALYSIS OF ELECTROLYSIS MANGANESE PRODUCTION IN CHINA

Fan Wang, Xiaojuan Gao
(Chinese Research Academy of Environmental Sciences
/ China National Cleaner Production Center)

ABSTRACT: In this paper, over 40% electrolysis manganese plants in China were investigated, including the raw materials, main process, power consumption, and waste treatment. Through material balance analysis, some process steps which contain high consumption and pollution were given out. It was also researched that why these process steps cause resources waste and high pollution, and some cleaner production technologies were introduced to solve these problems.

Key Words: Electrolysis Manganese, Cleaner Production

INTRODUCTION

Manganese is an important metal resource in modern economy. It is widely used in steel smelting, chemical, electricity, air and space craft, and military industries. After 2000, electrolysis manganese industry was promoted rapidly in China, which brought large benefits and gave important contribution for local economy development. Now, China is the largest producer, consumer, and exporter of electrolysis manganese, which covers about 98% output in the world [1]. On the other hand, electrolysis manganese production also generated lots of wastes and caused serious environmental problem in some area of China. Before 2005, in the boundary area of Hunan, Guizhou and Chongqing province (which is called "manganese triangle"), the wastewater and residue were discharged from electrolysis manganese factories directly to the river. It caused extreme pollution that in the river around "manganese triangle" the concentration of manganese and ammonia were over 100 times higher than the National Standard. After several years' effort, the pollution was controlled. But because of the undeveloped manganese producing technology, so large quantities of wastes from electrolysis manganese process can't be extinguished by the traditional treatment [2].

There are two parts of serious problems [3]. First, in the wastewater treatment system, all valuable substances are transformed to slag, and some secondary pollution can also happen if the slag can't be disposed safely. In addition, high concentration NH_3-N is not treated in the wastewater system and discharged directly into river, which can cause water system eutrophication [4]. Second, there are several kinds of pollutant, such as manganese, in residue [5]. It could cause surface waster and ground water pollution that the untreated residue was piled in the valleys. In China, the manganese factories generate over 10 million tons residue every year. Because most of the slag yards were not constructed normatively, so much piled residue can cause dangerous accidents, such as dam collapse and electrolyte leakage. In this condition, there are many safety problems and hidden water pollution dangers around manganese factories in China.

There three "non-cleaner" in electrolysis manganese process are considered as the main reasons of high pollution [6]. The first is non-cleaner resources. In China, low grade manganese ore has widely been used to produce electrolysis manganese, which needs high sulfuric acid consumption and gives out large quantities of residue. The second is non-cleaner process. In the electrolysis manganese production, selenium dioxide and potassium dichromate are used, which are toxic materials and can cause serious pollution problems. The third is non-cleaner control system. There are few automatic system in electrolysis manganese factories. Most of the processes are operated manually, kinds of measurement are not accurate, and most equipment are not sealed. In order to solve the problems, cleaner production was

---

ISBN 9780976885351

strongly recommended to reduce the resource consumption, recycle the valuable elements and diminish the wastes generation.

Figure 1. Residue piled in the valley

Figure 2. Wastewater treatment system

INVESTIGATION

There are 60 electrolysis manganese factories were investigated, which covered about 40% electrolysis manganese plants in China. The investigation contents include electrolyte preparation, electrolysis, residue, slag, and wastewater. Because a similar technology is used to produce manganese in most of Chinese factories, the resource consumption, energy, and wastes generation are in same grade in these factories. The paper only lists some data from 3 typical factories.

Resource consumption. Resource consumption can indicate the cleaner production level. Lower consumption means higher efficiency and lower pollutant generation. Compare with Manganese Metal Company (MMC) in South Africa, resource and assistant material consumption in Chinese manganese factories is higher. The investigation results of resource consumption were given in table 1.

Table 1 Resource consumption in Chinese factories and MMC

Item	Unit	Factory A	Factory B	Factory C	MMC
Ore grade	%	14	<16	<16	44
Ore consumption	t/t	8.689	8.25	8.44	2.67
H_2SO_4	t/t	1.837	1.91	1.82	0.25
SeO_2	kg/t	1.389	1.01	1.71	0
$K_2Cr_2O_7$	kg/t	0.477	0.35	0.74	0
Fresh water	t/t	3.3	3.4	3.7	0.48
Power consumption	kw.h	6335.8	6925.63	6350	9800

In table 1 we can see that the grade of ore used in Chinese electrolysis factories is lower than 16%, but that in MMC is about 44%. The sulfuric acid consumption in Chinese factories is higher than 1.8 tons/ton product, and that in MMC is about 0.25 tons/ton product. It is easily found that because of lower ore grade, the ore and sulfuric acid consumption in Chinese factories is higher than that in MMC. Selenium dioxide and potassium dichromate are both used in Chinese factories. Even their amount is not large, but because the high toxicity, these two materials will be forbidden to be used in manganese production after 2013 in China.

MATERIAL BALANCE ANALYSIS

The place where main element loses can be found by material balance analysis, and a special cleaner production technology can be devised to solve the problem. So, material balance is an important tool in cleaner production potentiality analysis. In this project, two main elements manganese and chromium are selected to do material balance analysis.

Manganese balance analysis. All the manganese in ore and assistant materials was quantified and calculated, and all manganese in product, wastewater, residue, anode slag is also quantified and calculated. Fig 3 shows the manganese balance.

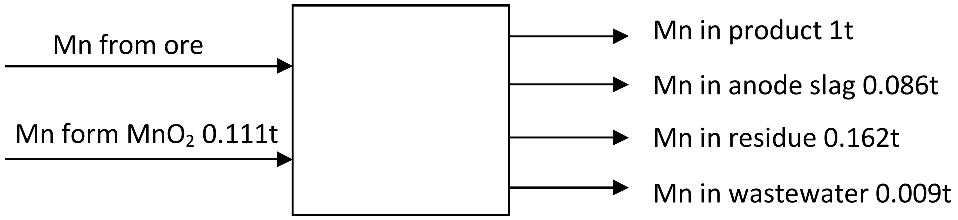

Figure 3. Manganese balance

The manganese balance figure shows that it needs 1.257 tons manganese in ore and assistant materials to produce 1 ton electrolysis manganese, the convert ratio is only about 80%. Manganese in anode slag, residue, and wastewater is about 0.086t, 0.162t, and 0.009t respectively, and the total amount in wastes is about 20% of that in raw materials. These kinds of manganese are discharged into environment and caused serious pollution problems. On the other hand, the manganese in wastes is difficult to be used again and causes resources loss.

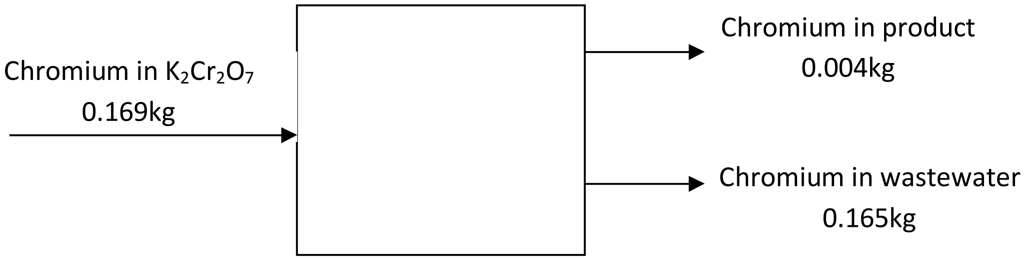

Figure 4. Chromium balance

Through manganese balance analysis, it is found that the production generates large amount of residue while producing 1 ton electrolysis manganese. There is about 0.162t manganese, about 12.9% of that in raw material, in discharged residue when producing 1 ton electrolysis product. In China, while producing 1 ton product manganese factories discharge 8~10 ton residue, in which the manganese concentration is about 3~4%. According to the yield of manganese in China, about 10,000,000 tons residue are given out annually in recent years, and about 300,000~ 400,000 tons manganese are discharged as pollution into the environment. If the manganese in residue was recovered, it would not only reduce the serious pollution but also bring large benefits to manganese factories. This is where the most important cleaner production chance of manganese production.

Chromium balance analysis. Potassium dichromate is used for manganese flasks passivation after electrolysis. Through washing the product, dichromate is cleaned from the manganese flakes and stayed into wastewater. Fig 4 shows the chromium balance.

0.456kg potassium dichromate which contains 0.169kg chromium is used for passivation to produce 1 ton electrolysis manganese. 0.004kg chromium is retained in product, and 0.165kg in wastewater. In Chinese manganese factories, while produces 1 ton product it generates about 3~4 ton wastewater, in which the concentration of chromium (VI) is 200~350mg/L, 400~700 times higher than the National Wastewater Discharge Standard (GB8978-1996). Because of its high toxicity, chromium (VI) is constrained to be treated till the concentration is lower than the National Standard. In traditional wastewater treatment system, chromium (VI) is transformed to chromium hydroxide and deposited from the water. But the chromium hydroxide is also hazardous solid waste and can cause secondary pollution if it is not treated safely. On the other hand, because dichromate is a valuable material, it could reduce potassium dichromate consumption and bring benefit to factories if the chromium (VI) was recovered and reused. So, it is another cleaner production chance here.

BRIEF INTRODUCTION OF CLEANER PRODUCTION TECHNOLOGIES

Double leaching [7, 8]. To solve the problem that there is large amount of manganese in residue which cause serious pollution, double leaching technology has been used in some factory for cleaner production engineering demonstration. Its mechanism contains 4 parts; first the residue is double-leached by using the acid in anolyte; then the residue is washed to reduce manganese remains in residue; and at the third step the residue is neutralized by ammonia; at last combine all the technologies above to a membrane filter, to finish the double-leaching technology.

Figure 5. the scene of double leaching technology demonstration plant

Wastewater whole process control. The result from the demonstration engineering shows that, by using the double leaching technology, over 50% soluble manganese is recovered. It means to use this technology; the manganese convert ratio can be increased up to about 90%. For example, the double leaching technology used in the demonstration factory (yield 30,000 ton Mn/a) can recover about 3,000 ton manganese annually and bring about 30 million CNY to the factory per year. Meanwhile, the technology can also reduce the manganese concentration 50% in residue, and decrease the environment risk of the residue which piled in the valley.

Double leaching technology is now being used in Hu'nan DongFang Manganese Company. Figure 5 shows the scene of demonstration plant.

To solve the problem that the wastewater which contains chromates causes serious pollution and secondary pollution risk, the wastewater whole process control technology was developed and demonstrated in an electrolysis manganese factory. The waste water whole process control technology contains two parts: the first is Automation System of Post-Electrolysis Process, including auto-lifting/

scraping/ counter-washing/ drying/ stripping/ finishing/ pickling/ polishing/ immersing/ and cathode inserting [9]; and the second is Anion Exchange System [10-11], which recover the chromate in the waste water. By wastewater controlling, wastewater is reduced three times and reused twice automatically in this technology. The Three Times Reductions includes: reduce adhered electrolyte by scraping while cathode lifting, reduce adhered chromate by scraping after passivation, and reduce wastewater amount by multi-grade counter-washing and needle jet. The Twice Reuses includes: reuse chromate to passivation by anion exchange, and reuse wastewater which contains Mn^{2+} and NH_3 to ore leaching.

Figure 6. the scene of traditional post-electrolysis operation

4. Co

Fig 7 the scene of the wastewater whole control technology demonstration plant

The result of wastewater whole process control technology demonstrated in a electrolysis manganese factory (yield 30,000 ton Mn/a) shows that 300 ton manganese and 86 ton chromates can be reduced and reused annually, which valued about 3.52 million CNY. Meanwhile it can also reduce 240 ton deposit annually, which is generated by traditional wastewater treatment system and can cause secondary pollution. Because all the operation steps are devised to be run automatically in this technology, about 300 workers is reduced and save labor cost about 6 million CNY.

In addition, by using automation in waste water whole process control technology, Cathode Lifting/ Pulling/ Inserting are operated enclosed in a special field, so as to avoid electrolyte and passivation liquid drops on workers' bodies directly. So the technology can also reduce the hurt of workers caused by electrolyte and passivation liquid, which contains many pollutants such as chromates, manganese, selenium and lead.

The wastewater whole process control technology is now being used in Hu’nan Jinxu Manganese Company. Figure 6 shows the scene of traditional post-electrolysis operations, and Figure 7 shows the scene of this technology and automation system demonstration plant.

Most of the production technologies used in Chinese electrolysis manganese factories was developed in 1935. Although some modification have taken place in some factories, but the technologies have not been improved essentially. Electrolysis manganese is still an undeveloped industry in China. As the technologies related in the paper, many cleaner production change can be found in electrolysis manganese factories. By using cleaner production technologies, it can not only help the factories to increase their benefits, but also solve the environment problem radically.

REFERENCES

[1] Tan Zhu-zhong, The Development of “11`5 Plan” and the Forecast of “12`5” Plan in Chinese EMM Industry’s, China’s manganese industry, 2011, 29(1): 1-4

[2] Zhou Chang-bo, Yu Xiu-ling, Zhou Shuang, The Urgency of Performing Clean Production in the Electrolysis Manganese Industry and the Relevant Recommendations, China’s manganese industry, 2006, 24(3): 15-18

[3] Ning Duan, Wang Fan, Zhou Chang-bo, Analysis of pollution materials generated from electrolytic manganese industries in China, Resources Conservation and Recycling, 2010, 54: 506 -511

[4] Wang Qi-nian, Wang Fan, Gao Xiaojuan, Research Progress in the Treatment of EMM Wastewater in China, China’s manganese industry, 2011, 29(2): 10-13

[5] Duan Ning, Zhou Chang-bo, Yu Xiu-ling, Analysis of sustainable development of the electrolysis manganese industry, Resources and Environment in the Yangtze Basin, 2007, 16(6): 764-768

[6] Duan Ning, Dan Zhi-gang, Song Dan-na, Current Status and Directions for Development of Cleaner Production Technology of Electrolysis Manganese Metal Industry in China, Journal of Environmental Engineering Technology, 2011,1(1):75-81

[7] Liu Gui-hua, Pan Cen-xuan, Zhu Ke-song, Ru Zheng-guang, Wei Jian, Manganese Extraction from Slag with Membrane Filter Press, China’s manganese industry, 2010, 28(2): 36-38

[8] Du Bing, Zhou Chang-bo, Recovery of soluble manganese in electrolysis manganese residue, Environmental protection of chemical industry, 2010, 30(6): 526-529

[9] Wang Qi-nian, Wang Fan, Xu Dong-yao, Preliminary Discussion on Control Measures for Cleaner Production with Wastewater Reduction in Electrolytic Manganese Metal Industry, China’s manganese industry, 2011, 29(3): 6-9

[10] Wei Jian, Wang Fan, Zhu Chun-lei, Ma Cong, A Study on the Treatment of Wastewater Containing Mn^{2+} with Ion Exchange Method, China’s manganese industry, 2009, 27(4): 25-29

[11] Gao Xiao-juan, Wang Fan, Liu Bin, Wang Qi-nian, Removal of high-concentration ammonia nitrogen in electrolytic manganese wastewater by copper-loaded resin, Industry water & wastewater, 2011, 42(4): 55-59

NUTRIENT LIMITATION OF PHYTOPLANKTON IN THE TAIHU LAKE OF CHINA

Jiajia Liu, Peifang Wang *, Chao Wang and Jin Qian
(Hohai University, Nanjing, Jiangsu, China)

ABSTRACT: The relationship between phytoplankton and nutrient was important to understand the ecological process of lake. As Blue-green algae were always blooming in Taihu Lake, nutrients, like nitrogen and phosphorous, were monitored in the whole water area of the Lake in Apirl and July, 2009 to analyze the nutrient limitation on the growth of phytoplankton and the principles of nutrient transformation. It showed that the content of inorganic nitrogen and phosphate was high in offshore regions, especially in the Zhushan Bay. The content of chlorophyll *a* manifested the growth of phytoplankton, and that it was higher in summer than in spring. The content of chlorophyll *a* with variety of inorganic nitrogen and phosphate differed obviously with season and region. There was a positive correlation between chlorophyll *a* and inorganic nitrogen , negative correlation with phosphate. When the ratio of inorganic nitrogen and phosphate (DIN:OP) was 16:1, it was the most appropriate condition on the growth of phytoplankton. This shows that the phytoplankton growth is likely to be limited by nitrogen in spring and by phosphorus in summer in the Taihu lake area.

INTRODUCTION

Phytoplankton is an important primary producer in the ecological process of lake, plays an important role in material circulation and energy conversion process. Chlorophyll *a* is a good index about plantation of phytoplankton, is also the main photosynthetic pigment of phytoplankton(Xia Bin et al., 2000). Phytoplankton growth in aquatic systems are regulated by a number of factors, such as temperature (Pomeroy and Wiebe, 2001), predation, substrate supply (inorganic and organic nutrients) (Elser et al., 2007;) and virus infection (Wilhelm and Matteson, 2008).Nutrient is an important material base for the phytoplankton growth, and dissolved inorganic nitrogen (DIN), activated phosphate (OP) are the most important nutrient and the most common limited elements (Wang Hanlui et al., 2002). When the ratio of inorganic nitrogen and phosphate (DIN:OP) was 16:1(Redfield, 1958), it was the most appropriate condition on the growth of phytoplankton.(Healey F P et al., 1980). In lake systems, phytoplankton growth is generally limited by the availability of P, while in marine systems N (nitrogen) is often considered the primary limiting nutrient(Rejas et al., 2005).

Taihu Lake situated in the coordinates of 31°10′N and120°09′E. With an area of 2,250 km² and an average depth of 1.9 metres, it is the third largest freshwater lake in China. Taihu Lake is an important water resource of drinking water, irrigation and industrial water and also for its fishery resources. The lake has become increasingly eutrophic since the 1980's due to abundant and diverse incoming pollutants. The subsequent release of organic matter and nutrients to the water column from the decomposition of algae leads to a positive feedback cycle providing increasingly more nutrients for the growth of new algae. There were many research about Nitrogen and phosphorus of Taihu Lake, but very few for the relationship of chlorophyll *a* and nutrient. 34 stations were sampled in the whole Taihu Lake (Fig.1). Through the investigation, this article reported the effects of nutrients on the growth of phytoplankton and the relationship of chlorophyll *a* and nutrient from Taihu Lake. The data from this study provides an increased insight into the mechanisms of nutrient limitation and providing the reference and evaluation to the comprehensive research of Taihu Lake ecosystem.

ISBN 9780976885351

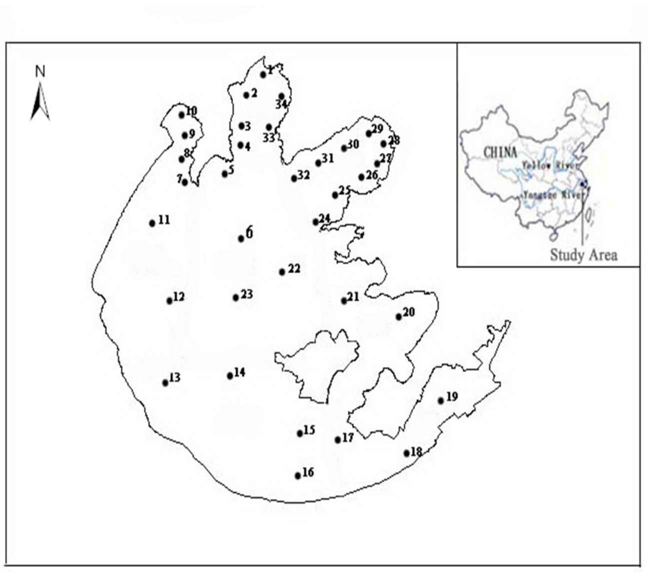

FIGURE1. Sample locations in the Taihu Lake of China

METHODS AND MATERIALS

With the GPS positioning in April and July 2009, we use plexiglass water sampler to collect surface waters for each station and placed them into three polycarbonate bottles. The water was immediately transported to the lab, at 4 ℃ for save. Water collected for nitrate (NO_3-N), nitrite nitrogen(NO_2-N), ammonium (NH_4-N) and phosphate analyses was filtered through filter membrane (0.45 μm pore size). Nitrate and orthphosphate analyses were measured according to Gross and Boyd. Nitrite nitrogen was measured by ultraviolet spectrophotometry and ammonium was measured by the Nessler's reagent method. To determine Chl *a* concentration, water samples were filtered through lter membrane (0.45 μm pore size), the residue extracted by 90% acetone, and then the absorbency were measured in 750, 663, 645, 630 nm to calculate the chlorophyll *a* concentration by colorimetry.All statistical analyses were carried out using the program SPSS 16.0 for Windows. Data are given as mean and standard deviation of three replicates.

RESLUTS AND DISSCUSION

Distribution Characters of Inorganic Nitrogen: The forms existing in the Taihu lake are dissolved nitrogen, ammonium, nitrate, nitrate nitrogen and organic nitrogen.Figure 2 and 3 describe the spatial distribution of DIN in Taihu Lake in spring and summer. Overall, the average concentration of DIN in spring (0.968 mg/L) is lower than that in summer (1.233 mg/L), and the range of it is 0.221~4.454 mg/L in spring and 0.349～3.269 mg/ L in summer. When spring, phytoplankton and large aquatic plants begin to multiply and grow at high flow period , the content of inorganic nitrogen falls. In summer, high temperature cause death algae soon broken down in the water body and nutrient will come out into the water（Yang et al.,2003）.Generally speaking, the concentrations of DIN decrease from north to south. However, there is a area with high concentration of DIN (0.671~0.997 mg/L) established between Gonghu Bay and Meiliang Bay in spring, and another one with low concentration (0.221~0.442 mg/L) in the middle of the lake. And in summer, there is an area with high concentration of DIN established around Zhushan Bay, but the area is reduced.

Distribution Characters of Phosphate: Which phosphate is the main form dissolved by the plant. Phosphorus in the lake has an important influence on primary productivity and lake system of nutrition state. Figure 4 and 5 describe the spatial distribution of OP in Taihu Lake in spring and summer. Because of the allogenic nutrients from different sources and with diferent content, the concentration of OP is regionally distributed compared to DIN. Generally speaking, the average concentration of OP in spring (0.087 mg/L) is higher than that in summer (0.032 mg/L), which is opposite to DIN. There is some areas with high concentrations of DIN (0.117~0.224 mg/L) established in Gonghu Bay, east and west coasts in spring, but a low concentration area is established in the middle of the lake. In summer, the low concentration areas (lower than 0.041 mg/L) are located in Meiliang Bay and Gonghu Bay, however, the high one (higher than 0.075 mg/L) is located in Zhushan Bay.

Distribution Characters of Chlorophyll *a*: As shown in Figure 6 and 7, the average concentration of Chl *α* is 0.396 µg/L in spring. The low concentration areas are among Zhushan Bay, Meiliang Bay and Gonghu Bay, and the high areas (higher than 0.1 µg/L) are located in the middle of the lake and north coast due to fisheries developed and booming of plankton. On the other hand, the average concentration of Chl *α* is 2.640 µg/L in summer, and the spatial distrbution of Chl *α* is same as that in spring.Overall, the trend for space distribution of Chl *a* is mainly in north and the coast of west. The concentration of Chl *α* in North bay is obviously higher than other bays, and the east bay and the west bay have no obvious difference. The whole lake of Chl *a* present uniformity distribution.The content of Chl *a* in water is not only related with aquatic plant species and the development status, but also closely related with the nutrient content of nitrogen and phosphorus. Because of high nutrient in North bay, the algae can fully absorb nutrients and multiply, which results in frequent blue-green outbreaks.

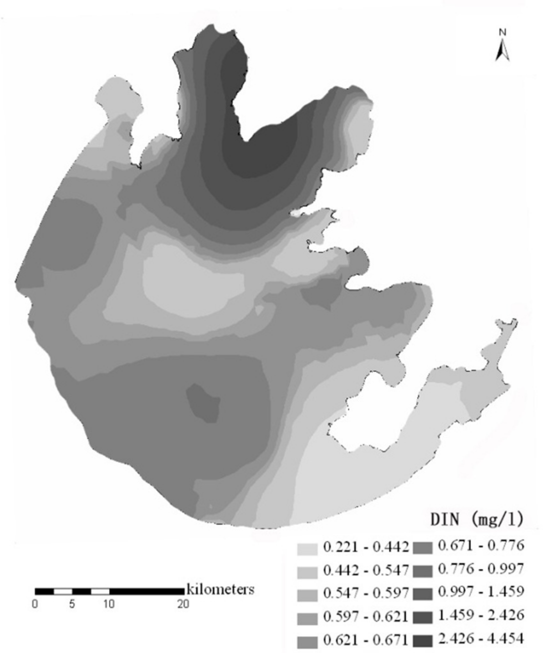

FIGURE2. The horizontal distribution of inorganic nitrogen(mg/L) in spring

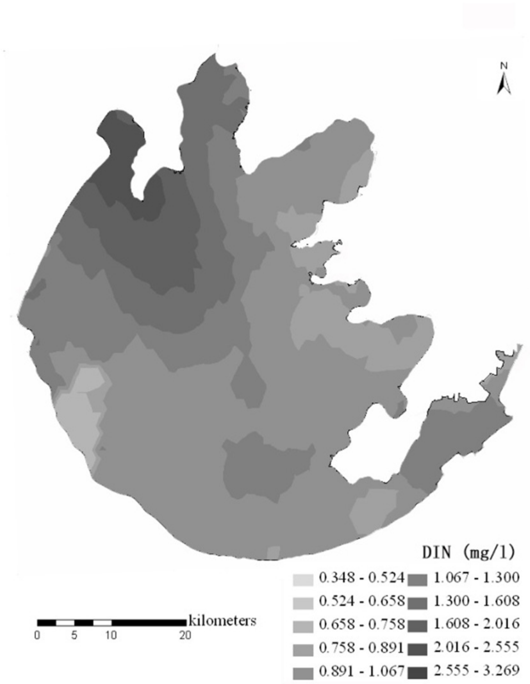

FIGURE3. The horizontal distribution of inorganic nitrogen(mg/L) in summer

Correlation Analysis of Nutrient and Chlorophyll *a*: In view of Chl *a* is the comprehensive index of phytoplankton biomass in water body, we choose it as an instructions factor. Through the analysis, mutual relationship between Chl *a* and nutrients expounds eutrophication characteristics of the Taihu lake.

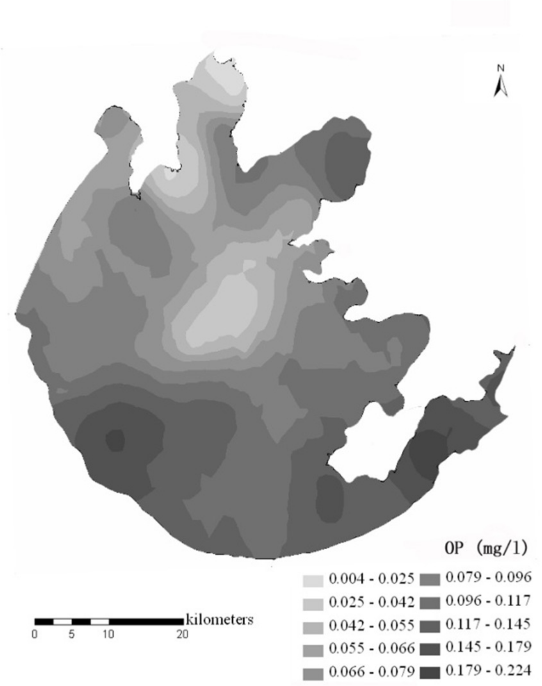

FIGURE4. The horizontal distribution of phosphate (mg/L) in spring

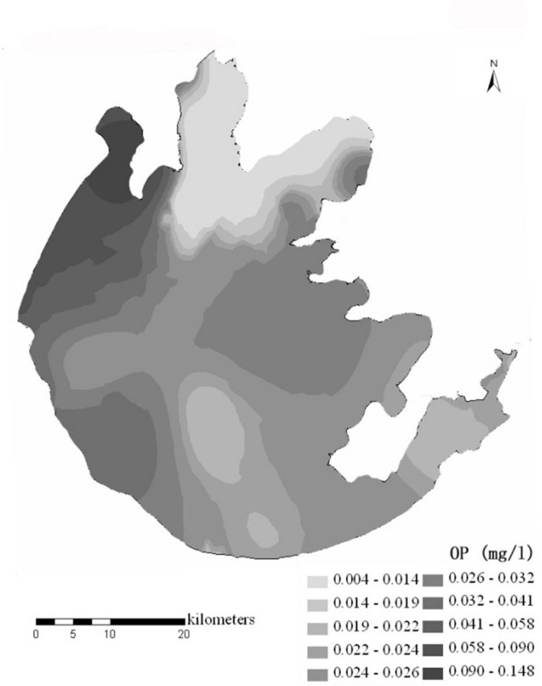

FIGURE5. The horizontal distribution of phosphate (mg/L) in summer

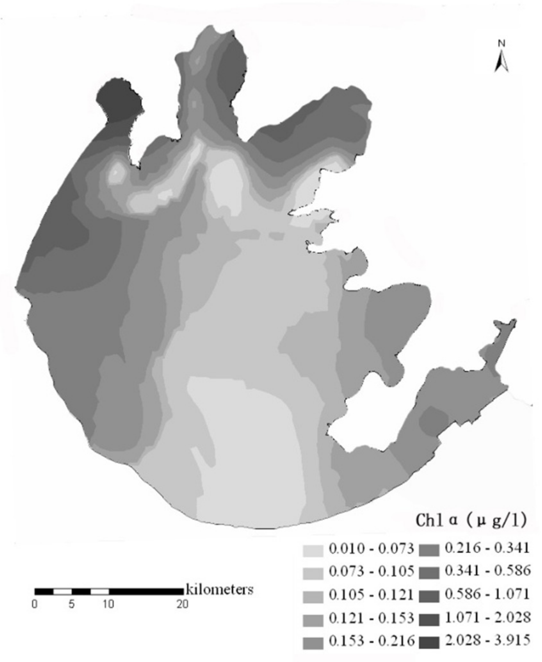

FIGURE6. The horizontal distribution of chlorophyll *a* (μ g/L) in spring

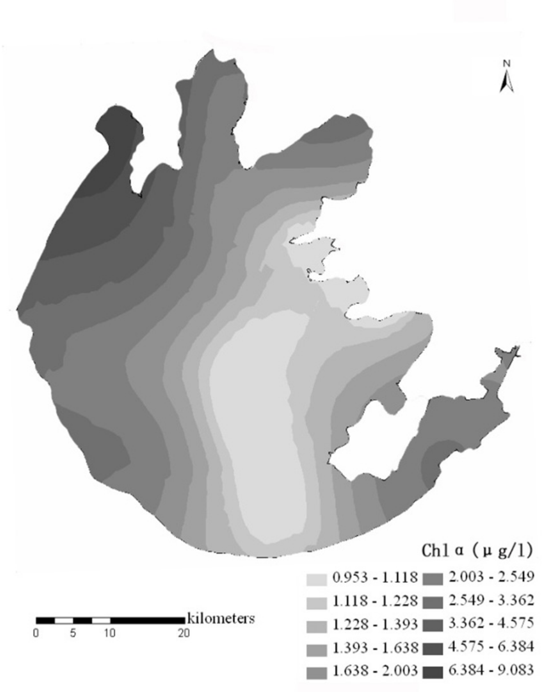

FIGURE7. The horizontal distribution of chlorophyll *a* (μ g/L) in summer

Ammonia nitrogen exists in water wtih free ammonia or ion ammonia form, and nitrate nitrogen is not stable, easy to resolve. Nitrate, nitrite nitrogen and ammonium concentrations showed signicant relevance with DIN concentrations (Table 1). DIN, nitrate, nitrite nitrogen and Chl *a* concentrations showed signicant positive correlation. There are very significant consistency between nitrogen, nitrate nitrogen and Chl *a*. OP concentrations showed signicant negative correlation with nitrate data. The high value area of chlorophyll *a* content corresponding trace area of activated phosphate, which explained that because of the phytoplankton growth, the consumption of nutrient was more than transsshipment, the distribution of activated phosphate was negatively correlated to chl *a*.This suggests that the content of N, P is in a quite high level in the Taihu lake, the rate of algae growth is restricted by nitrogen nutrition.

TABLE1. Correlation coefficients (r) for Chl *a* against nutrition at each sampling site for all data in Apirl and July (n= 68)

	NH_4-N	NO_3-N	NO_2-N	DIN	OP	chl *a*
NH_4-N	1	-0.012	0.067	0.886^{**}	0.094	0.056
NO_3-N	-0.012	1	0.275^{*}	0.445^{**}	-0.270^{*}	0.472^{**}
NO_2-N	0.067	0.275^{*}	1	0.265^{*}	0.080	0.669^{**}
DIN	0.886^{**}	0.445^{**}	0.265^{*}	1	-0.026	0.311^{**}
OP	0.094	-0.270^{*}	0.080	-0.026	1	-0.118
Chl *a*	0.056	0.472^{**}	0.669^{**}	0.311^{**}	-0.118	1

** $p<0.01$; *$p<0.05$

Nutrient Ratios in Spring and Summer: The ratio of DIN: OP was 16:1 in the cells of the general aquatic plants. When DIN: OP was 16:1, it was the most appropriate condition on the growth of phytoplankton, if DIN: OP fell below 16:1 indicating nutrient limitation to phytoplankton, above 16:1 indicating phosphate limitation to phytoplankton. (Jia Houlei et al., 2003). The change of DIN: OP in part reflects the nutrient renewable and migration mechanism.That survey shows that it's phosphate limitation. Phosphate is the limiting factor for the phytoplankton growth. For the most stations in spring, the ratios of N/P are less than 16, accounting for 74%, there are 9 stations always exceeded 16:1, located in Meiliang bay and Gonghu bay. Most area are nitrogen restrictions in Taihu lake, but Meiliang bay and Gonghu bay are still under phosphorus restrictions. For the most stations in summer, the ratios of N/P are greater than 16, there are 3 stations of 13.32, 9.71, 15.78, close to 16.

This shows that compared with the general lake, the phytoplankton growth is likely to be limited by nitrogen in spring and by phosphorus in summer in the Taihu lake area. The degree and scope of phosphorus limitation are mainly influenced by the exogenous input and seasonal change, and this is consistent to the research conclusion of Xia (2001) about yellow sea and east China sea of nutrient distribution and phytoplankton limited.

TABLE2. Statistical results of the N/P ratios in the upper layer of Taihu Lake

Season	average	min	StationsN/P>16	StationsN/P<16
Spring	33.01	1.33	9	25
Summer	79.18	9.71	31	3

CONCLUSIONS

Nutrients, like nitrogen and phosphorous were observed in the Taihu lake of China during Apirl and July in 2009, based on Chl *a* concentrations. Nutrients data showed the same spatial pattern as Chl *a* data, with decreasing concentrations of DIN off the shore. Generally speaking, the average concentration of DIN in spring is lower than that in summer, the average concentration of OP in spring is higher than that in summer . The content of chl *a* manifested the growth of phytoplankton, and that it was higher in summer than in spring.Chl *a* and OP showed signicant negative correlation while postive correlation between Chl *a* and DIN, nitrate, nitrite nitrogen. DIN:OP ratios suggested nitrogen limitation in spring, whilst posphorus limitation in summer.

With the control of input pollution, sediment will become the main pollution source. Sediment pollution especially with the winds and waves function is susceptible to suspension, thus speeding up the release of the nitrogen pollution, a direct impact on water quality. Therefore, with the advancement of Taihu lake management work, external pollution has been gradually control, sediment pollution control will be the focus of Taihu lake management.

ACKNOWLEDGMENTS

Support for the National Key Basic Research Development Program ("973" project) of China (No.2010CB429006), the National Natural Science Foundation of China (NO.50830304).

REFERENCES

Elser, J.J., Bracken, M.E.S. 2007. "Global analysis of nitrogen and phosphorus limitation of primary producers in freshwater, marine and terrestrial ecosystems ".*Ecol. Lett*,10, 1135–1142.

Healey, F P, Hendzel, L L. 1980. "Physiological indicators of nutrient deficiency in lake phytoplankton ". *Can J Fish Aquatic Sci*, 37: 442-453.

Jia Hou lei, Wen Yan mao, Shu Ting fei.2003. "Content and character of nutrient in water environment of cage culture, Yaling Bay ".*Marine Environmental Science*, 22 (3): 12-15. (in Chinese)

Pomeroy, R.L., Wiebe, W.J. 2001. "Temperature and substrates as interactive limiting factors for marine heterotrophic bacteria".*Aquat. Microb. Ecol,*23:187–204.

Redfield, A.C. 1958. " The biological control of chemical factors in the environment".*Am.Sci.* 46, 205–221.

Rejas, D., Muylaert, K., De Meester, L. 2005. "Phytoplankton–bacterioplankton interactions in a neotropical floodplain lake (Laguna Bufeos, Bolivia) ".*Hydrobiologia* ,543,91–99.

Wang Hankui, Dong Junde, Zhang Si, Huang Liang-min.2002. "Distribution of N/P ratio and its limitation to growth of phytoplankton in Sanya Bay ". *Tropic Oceanology*, 21(1): 33- 39. (in Chinese)

Wilhelm, S.W., Matteson, A.R.2008. " Freshwater and marine viroplankton: a brief overview of commonalities and differences".*Freshw. Biol*,53, 1076–1089.

Xia Bin, Lü Ruihua, Sun Peixi.2001. "Spatial-temporal Distributions and Size Compositions of Chlorophyll-a in the Typical Areas of the Yellow Sea and East China Sea in the Autumn of 2000". *Journal of Oceanograpgy of Huanghai &bohai Seas,*19 (4): 37- 42. (in Chinese)

Yang Dingtian, Chen Weimin, Jiang Jing, Ji Jiang, CaoWenxi.2003. "Effects of algal bloom on N,P and K contents in Meiliang Bay of Taihu Lake".*Chinese Journal of Applied Ecology*,14(6): 969- 971.(in Chinese)

ANALYSIS OF CHINA'S CONSTRUCTION WATER SHORTAGE BASED ON FUZZY MATTER-ELEMENT MODEL

LIANG Yuan, Xinyi Xu, Bo Pang and Jun GAO
(Beijing Normal University, Beijing, China)

ABSTRACT: Water shortage of construction is the main form in the southwest of China, which has not a uniform standard to define the shortage degree. The paper attempts to introduce fuzzy-element model and Euclid approach degree to the analysis of construction of water shortage degree, regarding the every city and the water shortage phases as the object of matter-element, through constructing evaluation index system, the writer determines the weight by entropy method based on the analytical hierarchy process method, calculates with the Euclid approach degree between the standard fuzzy matter-element and put forward a new construction water shortage evaluation method on the basis of the entropy method. The method applied to construction water shortage of all 16 cities of Yunnan Province in China, it provides a new reference for analysis of construction water shortage in China.

INTRODUCTION

The shortage of Engineering type, due to the lag of development and construction of waterworks, water resources, spatial and temporal deployment of the imbalance, resulting in insufficient water supply and water shortage(Xu, X. Y. et al, 2009) . Some cities and regions in water-rich region due to insufficient water supply project, there will be the Engineering shortage. Such as Southwest drought, Yunnan Province, rich in water resources in areas emergence of water scarcity, exposing the water infrastructure is still weak in Yunnan situation. After years of efforts, Yunnan water supply situation has greatly improved, but the Engineering shortage is still the main form of water shortage in Yunnan(Wang, J. C. et al, 2010)

At present, about the degree of engineering shortage less of its extent there is no uniform definition. Water shortage in urban water shortage report in Sichuan Province(Water Planning and Design Institute of Sichuan Province., 2007) in the proposed evaluation criteria of the shortage of urban engineering: water shortage is more than 20%, that the city is a serious water shortage in the city. Through the establishment of index system to calculate the water demand and engineering available water, draw water shortage rate, and ultimately determine the extent of the Sichuan Province, the city's Engineering shortage. On the basis of the matter element analysis, combined with the Euclid approach degree, and applications based on the analytic hierarchy process and entropy weight method to determine the weight to avoid the AHP method to determine the weight of subjectivity. Build the fuzzy matter-element model based on entropy weight, and Yunnan Province, the shortage of urban engineering of a comparative analysis.

MATERIALS AND METHODS

Fuzzy matter-element and compound fuzzy matter-element. To set things in the name of N ,

---

ISBN 9780976885351

On the characteristics c of value v, the ordered triple group, $R=(n,c,v)$, is viewed as a description of the basic things, referred the matter element. The value v is fuzzy, then known as the fuzzy matter-element. If things N has n features, $c_1, c_2 \cdots c_n$ and the corresponding fuzzy values $v_1, v_2 \cdots v_n$, Said R is n-dimensional fuzzy matter-element, denoted by $R=(n,c,v)$. So that constitutes the n-dimensional compound element R_{mn} of m things If the value of R_{mn} rewrite the fuzzy matter-element value, called the m things n-dimensional compound fuzzy matter element(Cai, W., 2000).

$$R_{mn} = \begin{bmatrix} & M_1 & M_2 & \cdots & M_m \\ c_1 & u_{11} & u_{21} & \cdots & u_{m1} \\ c_2 & u_{21} & u_{22} & \cdots & u_{m2} \\ \vdots & \vdots & \vdots & \cdots & \vdots \\ c_n & u_{1n} & u_{2n} & \cdots & u_{mn} \end{bmatrix} \tag{1}$$

Determination of favorably membership degree. A fuzzy value $u(x)$ is on behalf of degree of membership who's the corresponding value of x of things characteristic C.

1) More bigger more excellent, the transformation formula for:

$$u_{ij} = x_{ij} / \max x_{ij} \ (j=1,2,\cdots m; i=1,2,\cdots n) \tag{2}$$

2) More smaller more excellent, the the transformation formula for:

$$u_{ij} = \min x_{ij} / x_{ij} \ (j=1,2,\cdots m; i=1,2,\cdots n) \tag{3}$$

3) More close to a constant the more excellent, the transformation formula for:

$$u_{ij} = \min(x_{ij}, u_0) / \max(x_{ij}, u_0) (j=1,2,\cdots m; i=1,2,\cdots n) \tag{4}$$

Standard fuzzy matter element and squared difference compound fuzzy matter-element. By equation can constitute a standard program of the n-dimensional fuzzy matter element R_{0n}, all of which determined by the maximum or minimum value of favorably membership degree of R_{mn} (Zhang B. et al 1997),

$$R_{0n} = \begin{bmatrix} & M_0 \\ c_1 & u_{01} \\ c_2 & u_{02} \\ \vdots & \vdots \\ c_n & u_{0n} \end{bmatrix} \tag{5}$$

If $\Delta_{ij} (j=1,2,\cdots m; i=1,2,\cdots n)$ is on behalf of the difference square the between standard fuzzy matter element R_{0n} and the compound fuzzy matter-element R_{mn} that composed of the squared difference compound fuzzy matter.

$$R\Delta = \begin{bmatrix} & M_1 & M_2 & \cdots & M_m \\ c_1 & \Delta_{11} & \Delta_{21} & \cdots & \Delta_{m1} \\ c_2 & \Delta_{21} & \Delta_{22} & \cdots & \Delta_{m2} \\ \vdots & \vdots & \vdots & \cdots & \vdots \\ c_n & \Delta_{1n} & \Delta_{2n} & \cdots & \Delta_{mn} \end{bmatrix} \tag{6}$$

Weight determination based on the entropy. Entropy is the measure of the degree of disorder, can be used to measure the known data included in the amount of information and to determine the weight. When the difference value between the evaluation object indexes is larger, the entropy value is smaller, indicate that the index provides an effective amount of information larger, its weight also should be large; On the contrary, is no different(Qiu. W. H., 2001). That can eliminate the AHP and other methods to determine the weight of subjective factors.

Construction of the judgment of the evaluation matrix R of m things n evaluation indexes.

$$R=\left(r_{ij}\right)_{m\times n}\quad i=1,2,\cdots,n;j=1,2,\cdots m \tag{7}$$

Determine the matrix R normalized, get Normalized matrix, and B elements:

$$b_{ij}=\frac{r_{ij}-r_{\min}}{r_{\max}-r_{\min}} \tag{8}$$

Where: $r_{\max}$, $r_{\max}$ respectively, for different objects under the same evaluation most satisfied or most dissatisfied. According to the definition of entropy, entropy value determines the weight of entropy for m evaluation object of n evaluation index (Ruan, B. Q. et al, 2005).

$$H_i=-\frac{1}{\ln m}\sum_{j=1}^{m}f_{ij}\ln f_{ij} \tag{9}$$

$$f_{ij}=b_{ij}\Big/\sum_{j=1}^{m}b_{ij} \tag{10}$$

Where: $i=1,2,\cdots,n;j=1,2,\cdots m;0\leq H_i\leq 1$Clearly, when $f_{ij}=0$, $\ln f_{ij}$ is meaningless, so the need for f_{ij} to be amended, will be defined as

$$f_{ij}=\frac{1+b_{ij}}{\sum_{j=1}^{m}\left(1+b_{ij}\right)} \tag{11}$$

Using the entropy value evaluation of Entropy:

$$W^*=\left(\omega_i^*\right)_{1\times n} \tag{12}$$

$$\omega_i^*=\frac{1-H_i}{n-\sum_{i=1}^{n}H_i} \tag{13}$$

Where: $i=1,2,\cdots,n,$ and satisfies $\sum_{i=1}^{n}\omega_i^*=1$

Calculation Comprehensive weight of evaluation indexes.

$$W=\left(\omega_i\right)_{1\times n} \tag{14}$$

$$\omega_i=\frac{\omega_i^*\omega_i^{'}}{\sum_{i=1}^{n}\omega_i^*\omega_i^{'}} \tag{15}$$

Where: $\omega_i^{'}$ is subjective weight of evaluation index i.

Euclid approach degree. Approach degree refers to the approaching level each of evaluation sample and standard sample, the greater its value the closer the two, On the contrary, is no different(Sun, X. L. et al 2008).The calculation formula is a variety which can be used for two things. Taking into account the significance of this article with a comprehensive evaluation, the Euclid approach degree is calculated as follow(Pan, F., et al 2005):

$$\rho H_j = 1 - \sqrt{\sum_{i=1}^{n} \omega_{ij} \Delta_{ij}} \quad (j = 1, 2 \cdots, m) \tag{16}$$

Where: ρH_j is Euclid approach degree between j-evaluation sample and standard samples. This is used for constructing Euclid approach degree compound fuzzy matter element.

Sample selection All the 16 city, state selected Yunnan Province, as evaluation samples, including Kunming, Qujing,Yuxi, Bashan City, Zhaotong City,Lijiang City, Pu'er City, Lincang,Chuxiong Yi Autonomous Prefecture,Honghe Hani and Yi Autonomous Prefecture,Wenshan Zhuang and Miao Autonomous Prefecture,Xishuangbanna Dai Autonomous Prefecture, Dali Bai Autonomous Prefecture,Dehong Dai and Jingpo AutonomousPrefecture,Nujiang Lisu Autonomous Prefecture,Diqing Tibetan Autonomous Prefecture. Select 2010 as present situation level year,it all comes from Yunnan Statistical Yearbook 2011,Yunnan Province Water Resources Bulletin 2010 and 2010 in Yunnan Province Water Statistics Yearbook that all of 16 city, state water shortages evaluation index calculation required for the original data.

The establishment of evaluation indexes system Many factors affecting the Engineering water shortage, according to the water resources characteristics of Yunnan Province, , set the following indicators:

TABLE 1 **The Engineering Shortage of Water Resources Evaluation Index System**

Order	Index	Calculation	Unit
1	soil erosion area rate	the area of soil erosion/land area	%
2	rural drinking water safety population rate	the safety of drinking water in rural areas/rural population	%
3	Available water per capita	water conservancy total supply quantity/the total population	m^3 / person
4	The effective irrigation area rate	the effective irrigation area / arable land	%
5	The total capacity coefficient	water conservancy total capacity / multi-year average annual runoff	—
6	The compliance dike length rate	compliance the dikes length/total embankment length	%
7	The utilization rate of water resources development	the river outside the water supply quantity / the mean annual water resources quantity	%
8	The water conservancy investment rate	water conservancy investment/total investment	%

Engineering shortage level is divided into five levels, the indicator data collected 2000 to 2010 a total of 11 years in Yunnan Province around the city, state, cluster analysis, the degree of Engineering shortage is divided into five grades, get 5 grading standards of the respective evaluation values.

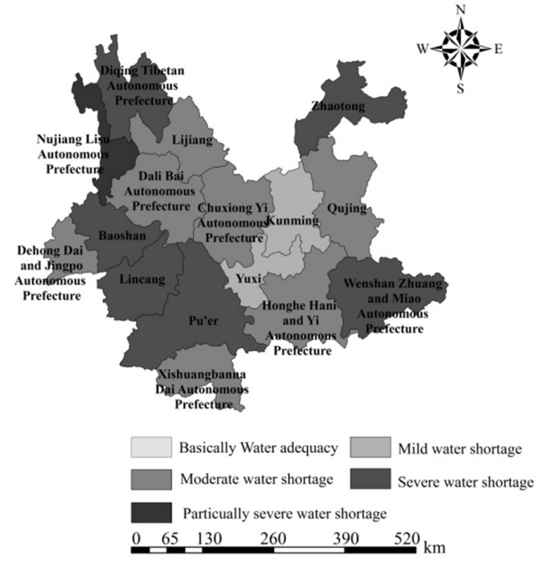

FIGURE 1. The degree of engineering Water shortage of the Yunnan

The model establishment. Build a compound fuzzy matter element. According to the data collected. Establish 20 programs of the compound fuzzy matter-element for each index value of 16 cities in Yunnan Province and the five grading standards program.

According to formula (2) - (4), calculate favorably membership degree, the soil erosion area rate can be calculated as "more smaller more superior" index, 6 indicators ,such as rural drinking water safety population rate, available water supply Per capita can be calculated as "more bigger more superior" index, utilization rate of water resources development in accordance with the constant type index calculation, get u_0=30 which takes the international commonly used 30% of water resources development and utilization (Wang, X. Q., 2008).

1) Constructed in the square of the difference of compound fuzzy matter-element in accordance with formula(5) and (6), determine the subjective index weight by Entropy method. First build judgment matrix according to measured value of the program, Subjective weights set, obtained using the analytic hierarchy process, has passed consistency test,$CR=0.035$,to meet the consistency.

2) Calculate the entropy of each evaluation index weight in line with formula (7) - (13), Calculated comprehensive weights for each index by amendment in light of formula (14) and (15).

3) Calculation of Euclid approach degree, according to formula (16). According to the square compound fuzzy matter element and each index weight calculated, compute that Euclid approach degree of every program. Calculation results of the degree of engineering water shortage in Figure 1

RESULTS AND DISCUSSION

It can be seen from Figure 1:there are varying degrees of Engineering shortage in every city of the Yunnan Province which according to Figure 1, due to rapid urban economic and social development, with a high concentration, the capacity factor and utilization of water resources development, Kunming and Yuxi City, to a lesser extent, mild Engineering shortage city. Because of the complex topography, difficult water resources development and utilization. There are more serious Engineering water shortages in the rest of Yunnan Province. Nujiang Prefecture, is the city of water shortage of particularly serious Engineering, Engineering water shortage is most severe. Nujiang Prefecture is located in Yunnan Province in western Yunnan the topography of by the majestic towering mountains and deep and fast flowing rivers, cutting a deep gorge of Nujiang, Lancang, Dulong River, three mountains, water resources development is extremely difficult, water resource development rate is very low. The results showed that, based on entropy weight fuzzy element method analysis it is authentic that , a reasonable assessment of the Engineering shortage extent of the study area, which provide the basis for decision making for regional water resources development.

CONCLUSIONS

Fuzzy matter-element method based on entropy weight directly selected indicators related to water scarcity, the use of entropy obtained by the weight, to avoid the subjectivity of the AHP method, by calculating the Euclidean approach degree to assess engineering degree of water shortage. The results showed that application of the model in Yunnan Province, authentic method of analysis is more consistent with the fact that, compared to more targeted than the previous method, but also have promotional value. The future research work, the method were applied in the same areas which is more serious problem of engineering water shortage such as Sichuan, Chongqing, Guizhou and Guangxi and other areas to provide a reference to solve the engineering water shortage problem in southwest China. The method of analysis for the degree of engineering water shortage, a new way of thinking, and provide a basis for decision making to address the engineering water shortage.

ACKNOWLEDGMENTS

The paper was completed under the guidance of my tutor Professor Xu Xinyi, The teacher's comments inspired my ideas and the article on the general framework. Then express my gratitude for Pangbo instructor and GaoJun classmate who give advice and help in the article details. I will continue to strive for more results.

REFERENCES

[1] Cai, W. 2000. Matter-Element Model and Application. 2nd. ed., *matter transformation,* pp.62-105. Science and Technology Literature Press, Beijing.

[2] Pan, F. et al 2005, “Fuzzy matter-element model for evaluating sustainable utilization of regional water resources” Advances In Water Science. 14(5): 271-275.

[3] Qiu. W. H., 2001. Management decision-making and the application of entropy 2nd. ed., *Entropy Application Foundation*,pp.102-157. Machinery Industry Press, Beijing.

[4] Ruan, B. Q. et al 2005, “Fuzzy comprehensive assessment of water shortage risk” Journal of Hydraulic Engineering. 36(8):906-912

[5] Sun, X. L. et al 2008, “Matter element extension evaluation model based on synthesis weights and approach degree and its application,” 2nd International Conference on Bioinformatics and Biomedical Engineering (ICBBE 08) IEEE Press, Nanjing, CA.

[6] Wang, J. C. et al 2010. “Yunnan Province, the water crisis and countermeasures.” China Rural Water and Hydropower. (12):52~56.

[7] Wang, X. Q., and Zhang, Y. 2008. “The Allowable Exploitation Rate of Rivers Water Resources of the Seven Major Rivers in China” journal of natural resources. 23(5):500-506

[8] Water Planning and Design Institute of Sichuan Province. 2007. Urban water shortage analysis of Sichuan Province,. Sichuan Provincial Department of Water Resources. MA.

[9] Xu, X. Y. et al 2009. “Classification and Counter Measure Research on Water Scarcity in China.” Journal of Beijing Normal University(Natural Science). 45(2):86~90.

[10] Zhang B. et al 1997. Fuzzy Matter-Element analysis. 1st. ed., *Fuzzy Matter Element Analysis Theory*, pp.8-38. Oil industry Press, Beijing.

CHARACTERIZATION OF RESISTANCE PATTERN F *BACILLUS* TO VARIOUS HEAVY METALS AND ANTIBIOTIC

Yamini Sisodia, Vivek Bajpai, Pallavi Sharma[1] and Pankaj Kumar Jain
Department of Science, MITS University, Lakshmangarh (Sikar) Rajasthan 332311, India
[1]Department of Microbiology, Bundelkhand University, Jhansi (U.P) 280129, India

Present study is carried out to systematically examine the pathogenic microorganisms in sewage samples isolated from Shekhawati region of Rajasthan. For this purpose survey was carried out at the Sewage Treatment plant of MITS residential campus, Laxmangarh, Sikar. In this survey we have isolated 26 bacterial strains and identified them using biochemical and molecular methods. Molecular identification of isolates was done by DNA isolation, PCR amplification using 16s rDNA primer and partial sequencing of purified product after sequencing, out of 26, 10 sequences were submitted in NCBI which designated accession no. Out of these 10 isolates *Bacillus pumilis, Bacillus subtilis and Bacillus licheniformis* were taken for further studies. Growth pattern of these isolates was observed on different pH, Temperature and at different concentration of various metals. There is growing awareness of the need for development of new antimicrobial agents for the treatment of human, animal and plant diseases. Keeping this fact in view, we have also did the antibiotic susceptibility of these isolates against various antibiotics (Ampicillin, Erythromycin, Chloramphenicol etc.) by measuring zone of inhibition in Mueller Hinton agar plate by Kirby Bauer method. Results of present studies indicates that the strains isolated from sewage water are resistant to most of the antibiotics and susceptible to Chromium , Cadmium, Mercury and some other heavy meals whereas Zinc and Iron are supporting the growth of bacillus at various parameters.

ISBN 9780976885351

IDENTIFICATION OF TECHNIQUES TO MEET PH STANDARD DURING IN-STREAM CONSTRUCTION

Dong Hee Kang and Mark M. Bundy (Estuarine Research Center, St. Leonard, MD, USA)
James G. Hunter (Morgan State University, Baltimore, MD, USA)
Z. Andrew Farkas (National Transportation Center, Baltimore, MD, USA)

Culverts constructed from a variety of materials and available in many different shapes and configurations are hydraulically short conduits necessary to convey stream flow through a roadway embankment or past some other type of flow obstruction. The service life of a culvert is subject to field conditions and the durability of the culvert material. Environmental conditions over time will deteriorate all culvert materials due to abrasion, corrosion, and removal of bedding materials (Norman et al., 2005). Therefore, proper attention must be given to this deterioration and periodic maintenance is required to increase the service life of a culvert. As water travels through the deteriorating culvert, water may also begin to travel outside of the culvert, eroding the soil bed and weakening the entire structure. The loss of soil and bedding beneath the road will eventually create voids, making the roadway unstable and the road pavement above may also fail.

Cementitious grout is often used in the repair and maintenance of culverts. However, consideration must be taken to ensure that grout paving materials used to reline the culvert do not adversely impact local water quality, particularly by spiking the pH due to hydrolysis of calcium oxide (CaO) which can increase pH to as high as 12.4 (Gupta et al., 2009). Consequently, the inundation of water over this reactive surface could produce caustic alkalinity and increases in pH that can raise the toxicity of other pollutants, impacting aquatic organisms. For example, the toxicity of ammonia is 10 times more severe to fish at a pH of 8.5 than it is at pH 7.5 (Turston et al., 1981).

Few studies have been conducted to ascertain the impact grout materials used during field application (Reiner, 2008). One previous study of note, a 2003 Virginia Department of Transportation (VDOT) study by G. Michael Fitch, illustrates that the use of grout materials can result in spikes to pH depending on the combination of stream flow rate and grout application rates. For newly paved culverts, proper precautions and actions (such as diversion and treatment) may be needed for high pH waters that exceed Maryland pH upper limit of 8.5. Due to this concern, it is undesirable for the Maryland State Highway Administration's (SHA) routine maintenance activities using grout paving to exceed the pH limit.

Each year, hundreds of SHA remedial structural activities require waterway permits issued by the Maryland Department of the Environment (MDE) and the U.S Army Corps of Engineers (USACE). The regulatory agencies are becoming increasingly concerned with water quality standards, particularly with Maryland's High Quality (Tier II) waters and have indicated the possibility of, as a first step in holding SHA accountable to State water quality standards, conditioning SHA permits to require pH monitoring. This is significant because if impacts to a waterway are unavoidable and cannot be justified, the Maryland Department of the Environment (MDE) and the U.S Army Corps of Engineers (USACE) will deny issuing applicable permits or approvals. With the safety of SHA's structures at stake, this research sets out to identify those maintenance construction techniques that allow SHA to comply with current state and federal water quality standards and remedial action(s) that are low-cost and dependable, so that there is compliance with Maryland water quality standards. Proposed for this study were field and laboratory tests of typical grout paving applications under various conditions to provide recommendations and a decision-making flowchart to meet Maryland's pH limit of 8.5. In addition, this study also identified potential remedial techniques for high pH waters contained within the work area and first flushes of the grouted work surface so that they meet Maryland's acceptable pH range of 6.5 and 8.5.

ISBN 9780976885351

THE U.S. FLOOD CONTROL PROGRAM AT 75

Peter E. Black (Distinguished Teaching Professor of Water and Related Land Resources, Emeritus, SUNY ESF, Syracuse, NY 13210)

Recent, recurring, and increased magnitude floods and their impacts on water supplies and developed areas with attendant economic loss demand reconsideration of flood control as an appropriate land and water management program. Measures afforded by the existing program encourage and enable investment in flood plains while violating several natural principles that make the situation worse**.** This paper critically and comprehensively reviews essentials of the seventy-five year old U. S. riverine Flood Control Program, including news reports, scientific articles, books, and landmark treatises. United States floods have continued (and will continue) to occur, causing increasing property damage and loss of life with growing fiscal loss. Causes include fundamental principles of physics, hydrology, and ecology, as well as environmental policy, economics, and common sense issues. This review examines pertinent basics of watershed ecology and hydrology as well as the importance of understanding the natural variation and distribution and ecological importance of floods. The well-documented evidence is overwhelming. A proposed alternative approach would enable and celebrate natural floods, managing their ecological and hydrological values and not attempting to control them. **Keywords:** Dams, flood, floodplain, flushing, hydrology, riverine ecology, stormwater runoff, watershed hydrology and management, benefit-cost analysis, earmarks, flood management.

ISBN 9780976885351

IMPORTANCE OF DIVERSION OF WATER FROM MAJOR RIVER TO IRRIGATION RESERVOIRS FOR BIRD DENSITY AND DIVERSITY IN SEMI-ARID ZONE OF CENTRAL GUJARAT, INDIA

Geeta Padate (Division of Avian Biology, Department of Zoology, Faculty of Science,
The M. S. University of Baroda, Vadodara-390002, India)

In the semi arid zone of central Gujarat, India, to satisfy the needs of water for irrigation and domestic use, several reservoirs have been constructed over the last century. This region in India mainly depends on monsoon water which is collected in depressions by constructing earthen dams. The monsoon lasts in the region from June to August or early September. As the water is utilized for various purposes the reservoirs start drying up. Over the turn of last century water from famous Narmada dam is being diverted to many of these irrigation reservoirs increasing hydro-period of the reservoirs in the area. The reservoirs which use to dry up in summer -April-May, has started retaining some water during this period.

One important reservoir in the area is Wadhwana Irrigation Reservoir which has been declared as a Wetland of Nationally Importantance in year 2005. The shallow areas of this reservoir have been inhabited by large number of migratory birds in winter. The changes in the bird density and diversity during midwinter waterfowl census have been evaluated as pre-Narmada and post-Narmada inundation. The density of dabbling ducks that prefer shallow areas have increased while that of diving ducks like pochards have decreased in the area. Similarly the diversity of small waders like stint and other plovers have decreased as water level has increased while those of larger waders like Egrets, Ibises, Spoonbill, etc. have increased. As the hydroperiod has increased large number of resident species of birds occupy the shallow water during summer occasionally crossing 1% criteria of Ramsar site. The importance of such diversions on density and diversity of birds in semi arid zone of central Gujarat, India is discussed.

ISBN 9780976885351

ULAANBAARTAR, MONGOLIA – SUSTAINABILITY FOR THE FAST DEVELOPMENT WITH LIMITED WATER RESOURCES?

Naranchimeg, B. and Nam C. Woo (Yonsei University, Seoul, Rep. of Korea)

Ulaanbaartar (UB), the Capitol of Mongolia, is one of the fastest growing cities in the world, with its fast population increase during the last decade. The main source of water supply is the Tuul River, of which water is abstracted through the well field developed along the fluvial deposits, and supplied to the central urbanized area. In Ger districts of the city surrounding the central area, groundwater is the sole source of water, developed mostly in the forms of dug wells. Issues related to the water resources of UB include, (i) rise of water demand due to population increase, and (ii) accumulated potentials of water-resource contamination by various residential and industrial activities without proper sanitations and preventive measures.

From a total of 28 locations covering the river, wells, and springs, water samples were collected in different seasons and analyzed for chemistry and stable-isotopic signatures. At three monitoring wells in the central water-supply well field, water level, temperature and EC have been monitored since August, 2010. Result of the cluster analysis clearly differentiates the water in central well field from the local groundwater in Ger districts. Local groundwater shows wide range of EC values and nitrate concentrations exceeding the drinking water guideline of 50 mg/L-NO3. Stable isotope ratios of hydrogen and oxygen with *d*-excess values indicate the seasonal changes in sources of water from the well field water-supply, and different recharge processes in shallow and deep wells. Continuous groundwater monitoring from the central well field also shows daily fluctuation of water levels due to pumping, seasonal changes, and water-quality changes. Since Ulaanbaatar has been the biggest and the fastest growing city in Mongolia, various types of potential sources of groundwater contamination have also been located inside the city boundary including tanning industries, coal-based thermal power plants, gas stations, etc. Thus, for the sustainable development of water supply sources of the City with protection it is warranted to develop better management measures with long-term and systematic monitoring schemes.

ISBN 9780976885351

HYDROGEN DISSOLUTION RATE IN HYDROGENOTROPHIC DENITRIFICATION PROCESS EQUIPPED WITH SOLID-POLYMER-ELECTROLYTE MEMBRANE ELECTRODE

Ryosuke Mine and Yutaka Sakakibara (Waseda University, Tokyo, Japan)
Masashito Komori (Yamato Co., Ltd, Gunma, Japan)

ABSTRACT: Hydrogen dissolution rates in Solid-Polymer-Electrolyte (SPE) membrane electrode were measured under different electric currents and packed material conditions. The packed material used in this study is a porous cube made of polyvinyl alcohol. Electric currents and volume of the packed material were set in the range of 1.0 to 4.0 A and 0.5, 1.0 L, respectively. In batch experiment, observed results showed that volumetric hydrogen transfer coefficients in liquid film (K_La) were represented by a linear function of hydrogen gas bubble production rates (GH2). By using our former mathematical model and the observed relation for K_La, hydrogen dissolution rates were calculated and compared with continuous experimental results, demonstrating that calculated results were in fairly good agreement with observed results.

INTRODUCTION

Nitrate pollution of groundwater has been a serious environmental issue in the world (Power and Schepers, 1989; Strebel et al., 1989). In human body, nitrate inhibits transportation of oxygen and changes to a carcinogen (Leach et al., 1987). According to The World Health Organization, the maximum allowable nitrate concentration is set at 11.3 mg-N/L (WHO, 2004). To treat nitrate contaminated groundwater, several treatment processes have been proposed. In heterotrophic denitrification process, organic matter is used as an electron donor. The process produces excess sludge and residual organic matter may exist in treated water. On the other hand, hydrogenotrophic denitrification process uses hydrogen as an electron donor. Hydrogen is a clean gas and doesn't harm to human body and environment. However, denitrification rates were not high in former studies (Gross et al., 1988; Ergas and Reuss, 2001) because of low hydrogen dissolution rates.

To achieve high denitrification rate, we proposed a biological denitrification process using hydrogen gas produced by SPE membrane electrode. This process can achieve high hydrogen dissolution rate and denitrification rate by applying electric currents. For further enhancement of denitrification performance, hydrogen dissolution rate or its control is still a key factor. The objective of this study was to evaluate the hydrogen dissolution rates under different electric currents and packed material conditions.

MATERIALS AND METHOD

Figure 1 shows a schematic diagram of the experimental apparatus used in this study, which consisted of a direct current (DC) supply (GPS-1850D, GW INSTEK), a SPE membrane electrolytic cell, a packed-bed reactor, a circulation pump, and an anodic water tank. The packed material was a porous cube made of polyvinyl alcohol whose size is 10 x 10 x 10mm. The anodic water tank was connected to anodic chamber and filled up with purified water (distilled and deionized water) whereas the packed-bed reactor was connected to cathodic chamber and filled up with tap water. Total volume of the reactor is 20 L. In cathodic chamber, water is flowing upward and controlled at a velocity of 1.5 m^3/h (corresponding to about 2.0 m/s in cathodic chamber) by a circulation pump.

SPE membrane electrode was purchased from Tanaka Kikinzoku Kogyo K.K., Japan. Design of the SPE membrane electrolytic cell is shown in Figure 2. An electrode made of platinum was attached to the both fluorinated ion exchange membrane (Nafion®117, Du Pont) using chemical plating method. The

ISBN 9780976885351

thicknesses of the electrode and membrane were 0.5 µm and 0.1mm, respectively. Geometric area of the electrodes was 20 cm^2 in anodic and cathodic sides. In the electrolytic cell, SPE membrane electrode was sandwiched by two titanium mesh plates electroplated with platinum and further by two titanium current feeders. The cell was supported by vinyl chloride plates and screwed on them so that anodic and cathodic chambers were isolated completely.

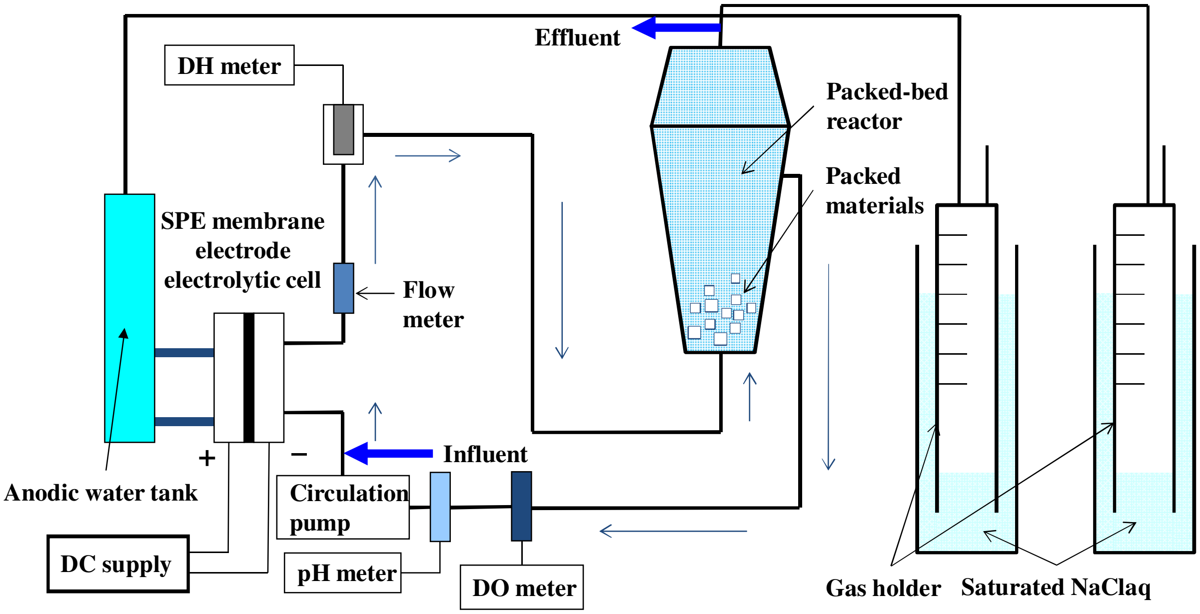

Figure1. Schematic diagram of the experimental apparatus

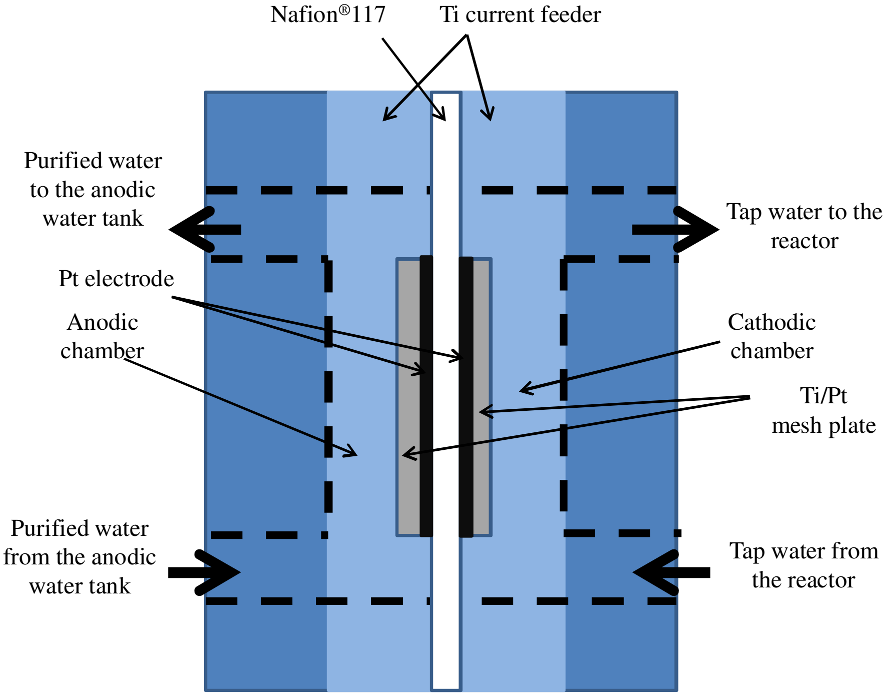

FIGURE2. Schematic cross section of SPE membrane electrode electrolytic cell

In this study, batch and continuous experiments were conducted to evaluate the hydrogen dissolution rates under different electric currents and packed material conditions. Electric currents and volume of packed material were set in the range of 1.0 to 4.0 A and 0.5, 1.0 L, respectively.

Packed materials were used as two bed types, fixed-bed and fluidized-bed. In batch experiments, time course change of dissolved hydrogen (DH) and hydrogen bubble production rate (GH2) were measured by a DH meter (DHM-100, DKK-TOA Corporation) and gas holder filled with saturated NaClaq, respectively. In continuous experiments, hydraulic retention time (HRT) was set at 1.0 h. As shown in Figure 3, oxygen gas is produced at anode (Reaction (1)), and hydrogen is produced at cathode after consuming dissolved oxygen at the electrode surface (Reaction (2)).

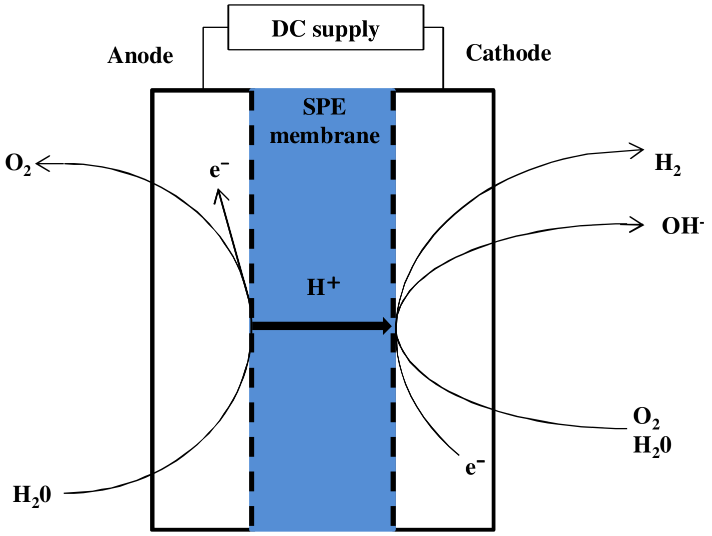

FIGURE3. Water electrolysis by SPE membrane electrode

Anode $2H_2O \rightarrow O_2 + 4H^+ + 4e^-$ (1)

Cathode
$$O_2 + 2H_2O + 4e^- \rightarrow 4OH^-$$
$$2H^+ + 2e^- \rightarrow H_2 \qquad (2)$$

RESULTS AND DISCUSSION

Hydrogen Dissolution Rate: In batch experiments, K_La was analyzed from time course changes of DH concentration (Figure 4). The results are shown in Figure 5. As shown in Figure 5, numbers of packing materials had no significant effect on the hydrogen dissolution rates and it was found that K_La was a linear function of GH2 (Equation (3)). In addition, in continuous experiments, the difference of hydrogen dissolution rates between packing materials and no materials was not observed. In batch experiment, values of DH had sometimes converged on a certain steady value before a DH meter reached a saturation value. In such cases, values of DH were modified linearly.

$$K_La = 26.02\left(\frac{R_{H2,G}}{V}\right) \qquad (3)$$

$$\frac{dC_{H2}}{dt} = -\frac{C_{H2}}{\theta} + K_La(C_{H2,S} - C_{H2}) + \frac{R_{H2,D}}{V} \qquad (4)$$

Where, $R_{H2,G}$ is the rate of hydrogen gas bubble production, V is total volume of reactor, C_{H2} is DH concentration, $C_{H2,S}$ is saturated concentration of dissolved hydrogen, $R_{H2,D}$ is the direct dissolution rate of hydrogen from the cathode without producing gas bubble, θ is HRT.

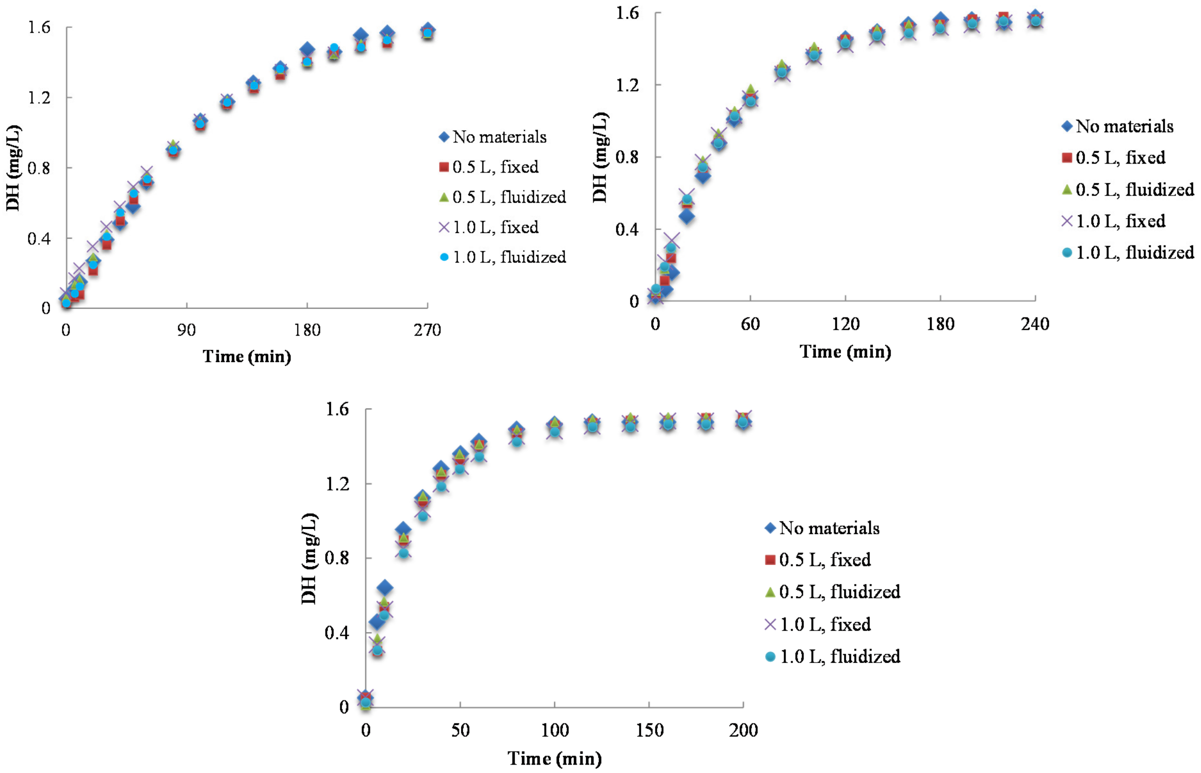

FIGURE4. Batch experiment results in different electric currents (1.0 A (top-left), 2.0 A (top-right), 4.0 A (down))

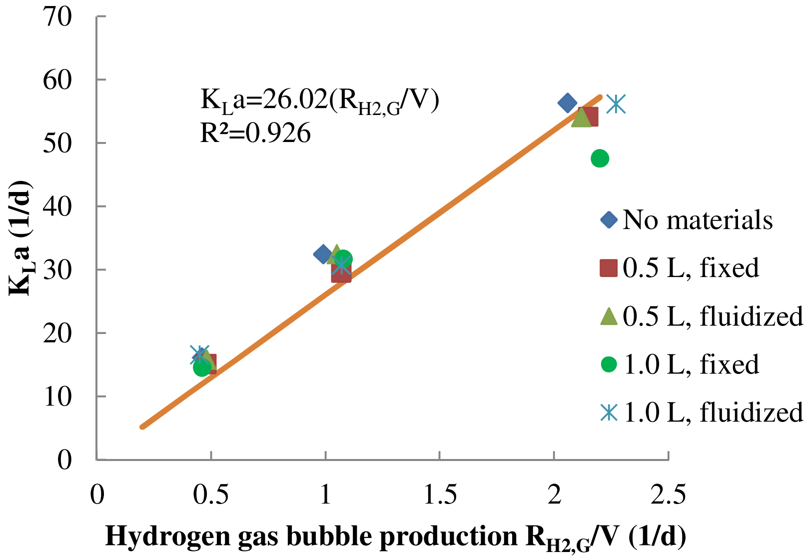

FIGURE5. Relation of K_La and GH2

In continuous experiments, observed results were compared with calculated results by our former mathematical model (Komori et al., 2008) (Eq. (4)) and Equation (3). As shown in Figure 6, experimental results were in fairly good agreement with observed results.

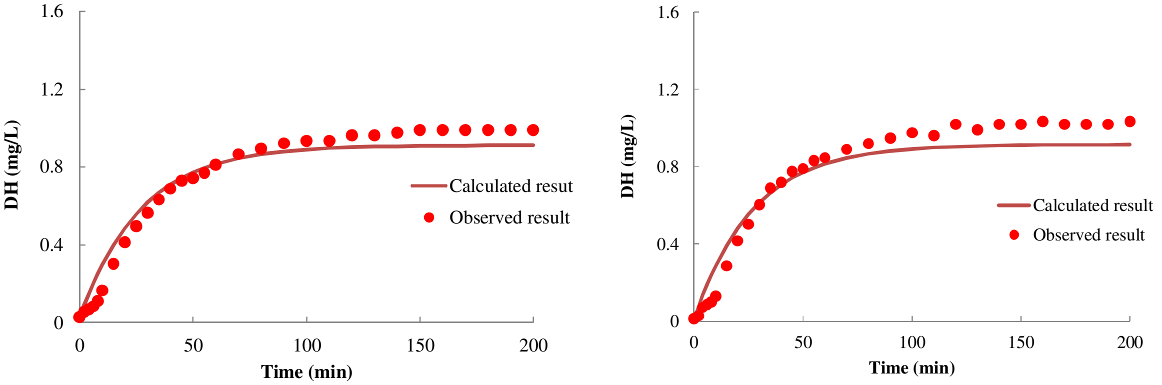

Continuous results (0.5 L, fixed-bed (left) and fluidized-bed (right))

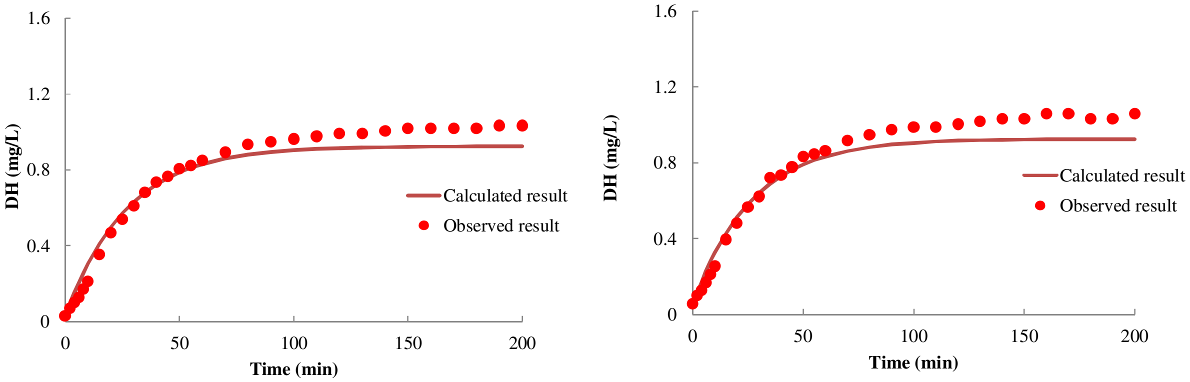

Continuous results (1.0 L, fixed-bed (left) and fluidized-bed (right))

FIGURE6. Comparison of calculated results and experimental results in different conditions.

Simulation of Continuous Denitrification. In our former mathematical model (Komori and Sakakibara (2008)), governing equations for nitrate concentration C_{NO3} and nitrite concentration C_{NO2} could be expressed by Equations (5) and (6), respectively.

$$V\frac{dC_{NO3}}{dt}=Q(C_{NO3,in}-C_{NO3})-V_R r_{NO3} \quad (5)$$

$$V\frac{dC_{NO2}}{dt}=-QC_{NO2}-V_R(r_{NO2}-\alpha\cdot r_{NO3}) \quad (6)$$

Where, $C_{NO3,in}$ is influent concentration of nitrate, Q is flow rate, V and V_R are total volume of reactor and the packed materials, respectively, γ_{NO3} and γ_{NO2} are denitrification rates for nitrate and nitrite, respectively, and α is the coefficient of assimilatory metabolism for nitrate.

Concentrations of dissolved hydrogen and oxygen, C_{H2} and C_{O2}, are expressed by Equations (7) and (8), respectively.

$$V\frac{dC_{H2}}{dt}=-QC_{H2}+V\cdot K_L a(C_{H2,S}-C_{H2})+R_{H2,D}-V_R r_{H2} \quad (7)$$

$$V\frac{dC_{O2}}{dt}=Q(C_{O2,in}-C_{O2})-V\frac{D_{O2}}{D_{H2}}K_L aC_{O2}-R_{O2,E}-V_R r_{O2} \quad (8)$$

Where, $C_{O2,in}$ is influent of concentration of dissolved oxygen, $R_{O2,E}$ is the consuming rate of oxygen on the cathode, γ_{H2} and γ_{O2} are the rates by which biomass utilizes hydrogen and oxygen, respectively. D_{H2} and D_{O2} are diffusive coefficients of hydrogen and oxygen, respectively. Table 1 shows the value of each parameter.

TABLE1. Parameters used in simulation

V	13.4(L)	D_{O2}	4.9×10^{-4}(m^3/d)
V_R	2.2(L)	D_{H2}	2.2×10^{-4}(m^3/d)
$C_{H2,S}$	1.5(mg/L)	$C_{O2,in}$	8.0(mg/L)
Q	52.8(L/d)	$C_{NO3,in}$	100.0(mg/L)
α	0.962	thickness of biofilm	100μm

By using Equations (3) to (7), denitrification performances were simulated for various material sizes. As shown in Figure 7, calculated concentrations for nitrate in the effluent were lower for smaller material size. This means that smaller materials could enhance larger working surface for biological reactions.

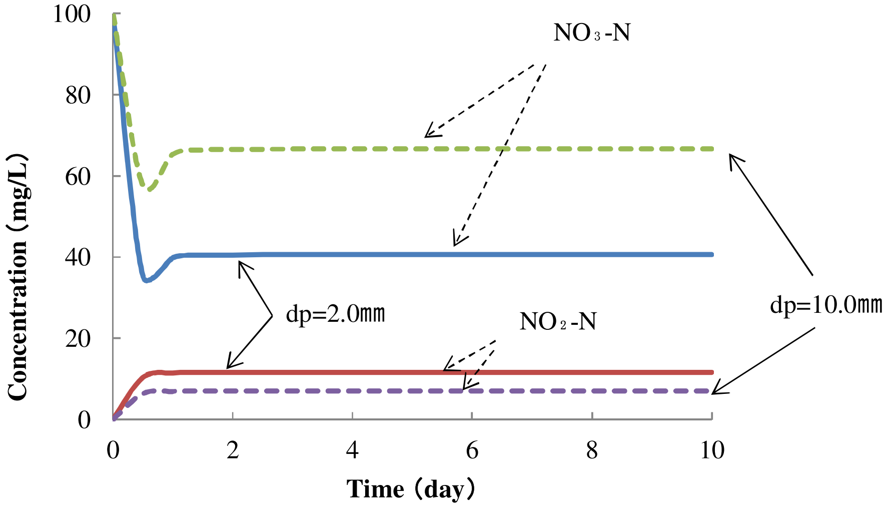

FIGURE7. Simulation results of denitrification performance

CONCLUSIONS

In this study, batch experiments were conducted to evaluate the hydrogen dissolution rates under different electric currents and packed material conditions. From experiments, it was found that packing carriers had no significant effect on the hydrogen dissolution rates and volumetric hydrogen transfer coefficients in liquid film (K_La) were represented by a linear function of hydrogen gas bubble production rates. Calculated hydrogen dissolution rates and dissolved hydrogen (DH) in the reactor were in fairly good agreement with observed results. Moreover, by using our former mathematical model and the observed relation for K_La, continuous denitrification performances were calculated and compared, demonstrating that smaller packed material had higher denitrification rate, because of increased surface area of packed materials and biomass concentration.

REFERENCES

Gross, H., Schnoor, G. and Rutten, P. 1988. "Bisological denitrification process with hydrogen-oxidizing bacteria for drinking water treatment." *Water Supply*, 6(3): 193-198.

Komori, M. and Sakakibara, Y. 2008. "High-rate hydrogenotrophic denitrification in a fluidized-bed biofilm reactor using solid-polymer-electrolyte membrane electrode (SPEME)." *Water Science and Technology*, 58(7): 1441-1446.

Komori, M., Matsutani, H., Akita, Y. and Sakakibara, Y. 2008. "Hydrogen dissolution and oxygen consumption in electrolysis of water with Solid-Polymer-Electrolyte (SPE) membrane electrode" *Proceedings of Environmental and Engineering Research*, 46: 137-143.

Komori, M. and Sakakibara, Y. 2008. "High-rate hydrogenotrophic denitrification of synthetic groundwater by a fixed-bed bioreactor equipped with SPE electrolytic cell." *Journal of Japan Society of Civil Engineers G*, 65(3): 153-163.

Leach, S.A., Thompson, M. and Hill, M. 1987. "Bacterially catalyzed N-nitrosation reactions and their relative importance in the human stomach." *Carcinogenesis*, 8: 1907-1912.

Power, J.F. and Schepers, J.S. 1989. "Nitrate contamination of groundwater in north America." *Agriculture, Ecosystems and Environment*, 26: 165-187.

Strebel, O., Duynisveld, W.H.M. and Bottcher, J. 1989. "Nitrate pollution of groundwater in Western Europe." *Agriculture, Ecosystems and Environment*, 26: 189-214.

World Health Organization. 2004. "Rolling revision of the WHO guidelines for drinking-water quality. Draft for review and comments. Nitrates and nitrites in drinking-water."

DEVELOPMENT OF A WATERSHED BASED GROUNDWATER VULNERABILITY ASSESSMENT TOOL

Mansoor A. Baloch* (Centers for Disease Control and Prevention, Atlanta, GA, USA)
Liora Sahar (Northrop Grumman Corporation, Atlanta, GA, USA)

The objective of this study is to assess and to characterize environmental risks and vulnerabilities of unregulated groundwater systems, incorporating an approach based on elements of the Safe Drinking Water Act's Wellhead Protection program. An evaluation strategy based on watershed characteristics is used to identify environmental contributing factors to groundwater contamination and to evaluate the effectiveness of protection measures stipulated by well-water protection ordinance of the state of Georgia. The steps involved in data gathering and preprocessing, and the methodology employed for the development of a geospatial environmental vulnerability assessment tool are also presented. Environmental data sources required for the analysis are identified and include septic systems, elevation, land-use and land cover data, soil, vegetation coverage, demographics and livestock. A geospatial overlay/Index modeling approach is developed to identify areas of higher vulnerability for groundwater pollution by taking into consideration watershed land-use, hydrology, and topography (LHT). The results are compared with those provided by U.S. EPA's DRASTIC model, a widely used intrinsic vulnerability assessment tool. It is concluded that geospatial vulnerability assessments provide meaningful tools to identify areas that are more likely than others to become contaminated in the absence of sophisticated data to conduct site specific monitoring and process based evaluation of groundwater systems. Public health practitioners can use vulnerability assessment maps to identify areas for prioritized intervention

---

ISBN 9780976885351

BIOREMEDIATION OF ENDOSULFAN CONTAMINATED GROUNDWATER USING NATURAL ZEOLITE SUPPORTED BIOBARRIER

Ayla Bilgin and ***Selim L. Sanin**** (Hacettepe University, Ankara, Turkey)

Endosulfan, a known toxic, bioaccumulant and endocrine disruptor pesticide, is recently enlisted in priority organic pollutants (POPs) list; will be banned from use globally starting 2012. It is widely applied on several agricultural plants, mostly in China and India, to eradicate insects but out of purpose use is also very common. Its hydrophobic nature increases its retention time in soil and endosulfan becomes a long term pollution source, with potential sporadic releases, for groundwater compared to other environmental reservoirs. Limited number of microorganisms is identified as endosulfan degrader.

Biobarriers are effective on removal of adsorbed trace contaminants from soils, in groundwater, if microorganisms on the support media are effective. Bacterial surfaces properties can be used to control microbial accumulation on soil, during biobarrier development. Bioremediation of endosulfan, using biobarriers, is not reported. This study aimed to isolate bacteria from different soils, determine their removal efficiencies under different physical conditions; then to attach a bacterial consortium on porous media developed by using natural zeolite, to develop economically feasible and sustainable biobarrier, for *in-situ* remediation applications.

In this study three new endosulfane degrading bacteria, *Sphingamonas sp. Methylobacterium rhodesianum and Afipia sp.*, are identified from different soils. No toxic degradation by-products such endosulfan-sulfate is observed. In 25 days endosulfan degrading sub-population was isolated from the microcosms. Selected cultures had five days of lag phase and exponential growth is completed within 20 days. Presence of secondary carbon source had effect on the growth rates, so is pH levels. Initial endosulfan removal efficiency of the columns were 50% and by 120th days both biobarriers reduced endosulfan to non-detectable levels. Hydraulic retention time in the column reactors did not change, but the receding tail is extended as an indicator of biofilm formation in the porous structure. In 140 days 22 grams of microbial mass is accumulated in the biobarriers with relatively homogenous distributions. In the outlet section there was slightly higher microbial mass which is an indicator of easily biodegradable chemicals. This observation is also consistent with the unclogged biobarriers during the operation. Sporadic endosulfan loadings didn’t affect the removal performance.

Our study clearly showed the contaminated groundwater can be remediated, if constructed bacterial consortium, on natural zeolite, is applied as biobarrier. The consortium, because of its members, is more tolerant to environmental changes. Unclogged porous structure extends the performance of biobarrier.

*sanin@hacettepe.edu.tr

ISBN 9780976885351

BIOREMEDIATION OF PENTACHLOROPHENOL CONTAMINATED GROUNDWATER USING BACTERIAL COMMUNITIES

Vaibhav V. Joshi*, M. Lynn Prewitt, H. Borazjani, Ken Willeford, Din Pow Ma (Mississippi State University, Mississippi State, MS, USA)

Pentachlorophenol (PCP) is a wide spectrum biocide commonly used as a wood preservative and has been classified as a priority pollutant by the U.S. Environmental Protection Agency. Extensive use and improper disposal of this toxic and recalcitrant compound in the environment for more than sixty years has resulted in groundwater contamination, which is a very serious health and environmental issue. Previous studies have reported individual bacterial and fungal species that actively degrade the PCP. However few studies have focused on indigenous microbial communities involved in PCP degradation at contaminated sites. Therefore the objective of this work is to compare PCP degradation by indigenous bacterial community and selected, pure cultured PCP degrading bacteria: *Sphingobium chlorophenolicum* and *Burkholderia cepacia*. In this study, PCP contaminated groundwater was collected from a former wood treatment site undergoing biosparging remediation. Experimental setup includes five treatments of native and known PCP degrading bacteria in water containing different concentrations of PCP. The following analyses will be determined on days 0, 21 and 42: 1) PCP concentration by gas chromatography; 2) gene expression of the PCP degrading genes: pcpB, pcpD, pcpC, pcpA and pcpE by Real-time PCR and 3) enzyme activity by spectrophotometrically monitoring substrate utilization over time. Statistical analysis of the data will be used to study the significant differences in PCP degradation by these bacterial communities. The results of this study should be beneficial for bioremediation of PCP in contaminated groundwater.

ISBN 9780976885351

APPLICABILITY OF SPANISH STANDARDS ROM5 FOR PORT BOURGAS SEA WATER ENVIRONMENTAL ASSESSMENT

Magdalena Korsachka, Elitsa Angelova, Roumen Marinov and ***Jordan Marinski**** (Bulgarian Academy of Sciences, Sofia, Bulgaria)
Stefan Tsakovski, (University of Sofia "St. Kl. Okhridski", Sofia, Bulgaria)

ECOPORT 8 project involves PAN-EU corridor VIII ports from Italy, Greece, Romania, Bulgaria, Montenegro and Albania, integrating existing international dialogue on developments in maritime traffic, docking in ports, with a common environmental policy aimed at defining shared standards. To check the applicability of the Spanish Standards ROM 5 [Puertos del Estados (Ed.), ***Quality of coastal waters in port areas***, December 2007, ISBN 978-84-88975-63-8] and their verification for South East European (SEE) ports is one of the research task of project work package 5 (WP5): Testing Monitoring Surveys. The testing phase is carried out in the port waters of Port of Bourgas, which is one of the Corridor 8 ports.

The aim of environmental monitoring of port Bourgas is to deliver reliable data for pollution risk assessment of port water body, characterization of port water body, and development of program for assessment and management of environmental risk. The environmental risk assessment and management programs usually include several monitoring plans and activities carried out after the characterization of investigated environmental media. Current investigations analyze the applicability of ROM 5 standards and propose conceptual scheme for characterization of water bodies. The abovementioned scheme includes three monitoring plans: systematic, continuous and visual inspection plan. The adoption of environmental monitoring program is accomplished by identification of contaminant emissions and environmental risk in the frame of preliminary monitoring plan by means of multivariate statistical analysis and calculation of integrated indices for ecological potential estimation. The priority pollutants and quality indicators included in the preliminary monitoring plan are: *Heavy metals* - Cd, Pb, Hg, Ni; *Organics* - tributyltin (TBT), benzine; *Indicators* - ΣPAH, ΣPCB, Σ phenols, oxygen sat.(%), turbidity, total hydrocarbons, detergents, chlorophyll "a".

Final assessment of the port water body is done by calculation of complex empirical quality indexes. The integrated indices and statistical results obtained from the preliminary monitoring data set are used for determination of sampling points which are included in systematic monitoring plan according to ROM standards manual (Part 7.1). The quality assessment of the water column is appropriate to be done by proposed indices I_{AG}. It could be concluded that environmental monitoring of water quality described in ROM standards is adequate for characterization of port Bourgas water body. Final schemes (pollutants, indicators and sampling points coverage) of systematic and continuous monitoring plans are optimized by multivariate statistical analysis of the obtained preliminary monitoring data set.

This research is conducted within the framework of the Environmental Management of Transborder Corridor Ports, ECOPORT 8 project Code SEE/A/218/2.2/X, funded by South East Europe Transnational Cooperation Programme under the Priority Axis 2: Protection and Improvement of the environment, Area of Intervention 2.2: Improve prevention of environmental risks.

ISBN 9780976885351

SYNTHESIS OF OILY NANOSCALE ZERO VALENT IRONS AND THEIR DECHLORINATION REACTIVITY IN THE NONAQUEOUS PHASE

Hsin-Lan Hsu (Industrial Technology Research Institute, Hsinchu, Taiwan, R.O.C.)
Chien-Yi Liao (National Taiwan University, Taipei, Taiwan, R.O.C.)

Remediation of groundwater contaminated by dense non-aqueous phase liquid (DNAPL) has been very challenging for decades. Although recently several novel nanoscale zero valent irons (NZVI) capable of targeting DNAPL had been proposed, their reactivity was only limited to the DNAPL/water interface while the reactivity inside DNAPL was desired. In this study, we synthesized a new oily remediation agent containing palladium-catalyzed NZVI modified with hydrophobic oligomers or polymers. The resulting oily NZVI was miscible with trichloroethylene (TCE) and could undergo dechlorination in the nonaqueous mixture with a half-life of about a week. The soil column test showed that the oily NZVI prepared using polymers moved farther than those using oligomers. This may be due to the higher dispersion stability provided by the polymers as suggested by the smaller colloidal sizes, which were measured by laser light scattering. Results here showed that direct dechlorination of DNAPL is possible and polymeric dispersants might be preferred.

ISBN 9780976885351

PHOSPHORUS CONTENT, SORPTION AND SATURATION OF TOPSOIL IN CHAOHU LAKE WATERSHED, CHINA

Huiping Zhou* (Nanjing Institute of Environmental Science, MEP, Nanjing, China)
Chao Gao (Nanjing University, Nanjing, China)
Hecang Zhao (Institute of Geological Survey of Anhui Province, Hefei, China)

ABSTRACT: The impact of non-point phosphorus pollution on surface and subsurface water quality is an important environmental concern in China, especially in the watersheds dominated by agriculture. A long term accumulation of phosphorus in agricultural topsoil will lead to phosphorus saturation and increase phosphorus loss risk. Studying spatial variance of phosphorus content, phosphorus fixation capacity and saturation of topsoil, is helpful to evaluate phosphorus loss risk and develop best management practices. A GIS-based geostatistical method was applied to analyze the spatial variance of topsoil total phosphorus in Chaohu Lake watershed. The phosphorus fixation capacity and saturation degree were also analyzed for different soil types and the soil under different landuse. The kriging results showed that total phosphorus had good spatial structure at NE-SW direction on a large scale. Tests for phosphorus sorption index showed general lower phosphorus fixation capacity of topsoil in Chaohu Lake watershed than Taihu and other areas in the world. Over 30% of the samples were phosphorus saturated with the saturation degree overpass 25%. Further studies are essential on a small scale to better explain the distribution of topsoil phosphorus and critical areas should be focused with management practices to control phosphorus loss.

INTRODUCTION

Phosphorus (P) loss from agricultural topsoil plays a key role in the eutrophication of surface water. A long term accumulation of P in agricultural topsoil will lead to P saturation, which would result in high P concentration in runoff and increase P leaching risk through the soil profile (Heckrath et al., 1995). High soil test P (STP) or total soil P (TP) levels are usually associated with increased P loss to water (Pote et al., 1996, 1999). It has been proved that the soil P content at different scales is spatial variable, which usually caused by natural process and management practices (Castrignanò et al., 2000). Studying the spatial variance of P content is helpful in soil nutrition management and non-point source pollution control. Many studies have demonstrated that the geostatistics is a useful tool in studying the spatial variance of soil properties (Liu et al., 2004; Askin and Kizilkaya, 2006; Chen et al., 2006). In addition to soil P content, soil P fixation capacity is also important in evaluating P loss potential. P sorption index (PSI) and degree of P saturation (DPS) have also been suggested as indicators of P loss risk from agricultural soil (Mozaffari and Sims, 1994; Indiati and Sharpley, 1995; Hooda et al., 2000a, 2000b; Nair et al., 2004). However, existing studies mainly focused on agronomic but not environmental purpose (Chen et al., 2006; Juang et al., 2002) and rarely on large scales (e.g. Zhang et al., 2004).

The main objectives of this study were: (1) to study the spatial variance of TP content of topsoil in Chaohu Lake watershed; (2) to compare the P fixation capacity between soil types and study the P saturation states in Chaohu Lake watershed.

MATERIALS AND METHODS

ISBN 9780976885351

Study Area: The Chaohu Lake watershed is located in central Anhui province, China (Fig. 1). It is situated between longitude 116°24′30″~118°00′00″ E and latitude 30°58′40″~32°6′00″ N, covering about 13 349 km^2. Annual precipitation in the subtropical monsoon climate is approximately 1100 mm. Geological structure presents as NE-SW aspect. Soil type in upland regions are typified by ferri-udic argosols while stagnic anthrosols is dominant throughout the plain. High agricultural production but poor environmental protection consciousness has resulted in substantial nonpoint source pollution (Yan and Wang, 1998). Nutrient loadings from nonpoint sources are believed to be the primary source of pollution of Chaohu Lake (Wang, 2003; Yin and Zhang, 2003).

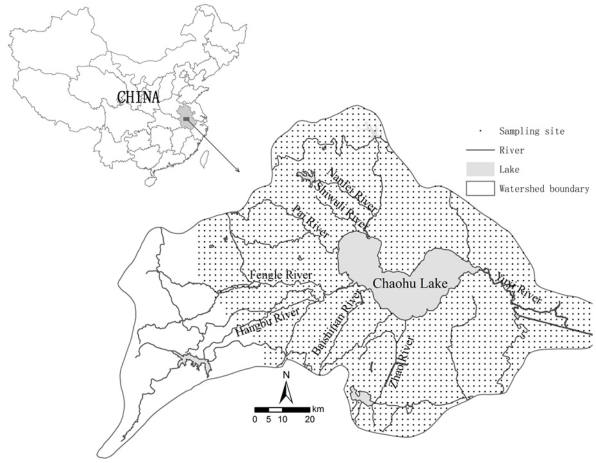

FIGURE 1 Study area and the distribution of soil data

Data Sampling and Analysis: Topsoil (0~20 cm) samples were collected in the watershed during a multi-purpose sampling campaign conducted by Anhui Institute of Geological Survey in 2003. The watershed was divided into 1×1 km grids. Four composite topsoil samples, with one sample in each grid, were collected from each set of four adjacent grids (2×2 km; total area of 4km^2). Equal amounts of these four samples were mixed to form a bulk sample which was submitted for laboratory analysis. Altogether, 2195 bulk samples were collected in the watershed (Fig. 1). TP was measured using XRF. Five grams of each air dried soil sample was first sieved to < 2 mm and then ground to <200 mesh in an agate mortar before compacted into a disc. Then the concentration of phosphors was determined with an ARL9800 XP + XRF. Soil PSI for each soil type was calculated using the quotient as below:

$$PSI = X/\log C \qquad (1)$$

where X is the amount of P sorbed, from one addition of 1.5 g P/kg of soil was determined after shaking for 24 hours at a water to soil ratio of 10:1 and C is the solution P concentration expressed as μmoles/L. Altogether 450 samples of 10 soil types from different regions were selected for PSI test. Soil DPS was determined by the approach of Pautler and Sims (2000), calculated based on P_{ox}, Fe_{ox}, and Al_{ox}:

$$DPS_{ox}\ (\%) = (P_{ox} / PSC_t)\times 100 \qquad (2)$$

$$PSC_t = \alpha(Al_{ox} + Fe_{ox}) \qquad (3)$$

where Al_{ox} ,Fe_{ox} , and P_{ox} are aluminum, iron, and phosphorus extracted by acid ammonium oxalate (mmol/kg), $\alpha$is an empirical parameter that is fixed to 0.5 as per Breeuwsma and Silva (1992).

Geostatistical Analysis. Geostatistics were used to estimate and map soil TP in unsampled areas. After sampling data were transformed to normally distributed, semivariograms were developed to establish the degree of spatial continuity of soil TP among data points and to establish the range of spatial dependence. Based on the spatial variance information, kriging's estimates are calculated as weighted sums of the adjacent sampled TP content. Geostatistical Analyst Module in ArcGIS was used as geostatistical analysis tool.

RESULTS AND DISCUSSION

Spatial Variance of Soil TP: The descriptive statistics showed that the coefficient of variation of sampling TP was high in this area (Table 1). The semivariogram analysis with isotropy revealed topsoil TP were moderate spatial autocorrelation, and the semivariogram model of topsoil TP was fitted by exponential model. Anisotropic analysis in direction NE20°and NE60° were also compared. The anisotropy was 0.9948 in direction NE20° and 1.5951 in direction NE60°. The major range in direction NE60° was 1.6 times the minor range. The lower ratio of nugget to sill (0.35 of NE60° and 0.40 of NE20°) explained the better spatial variance structure in direction NE60°. That is, the spatial variability of soil TP was mainly caused by structure factors while not random factors in this direction.

TABLE 1 Descriptive statistics of TP in topsoil

Sample Numbers	Maximum (g/kg)	Minimum (g/kg)	Mean (g/kg)	Median (g/kg)	Standard Deviation	Coefficient of Variation (%)
2195	3.74	0.23	0.54	0.49	0.21	39.2

The ordinary kriging interpolated map based on the fitted model showed that the TP distribution was band characteristics and good spatial structure at NE-SW direction, which is consistent to geological structure aspect on a larger scale (Fig. 2). The P-rich soils were mainly distributed in some riverine areas along the Nanfei, Hangbu, Zhao and Yuxi Rivers. Relative high levels of soil P are also associated with peri-urban land uses. Topsoil in the hill areas and riversides appeared to be higher TP mainly contributed by the landform, and the higher TP areas around the cities mainly contributed by the excessive input of fertilizers.

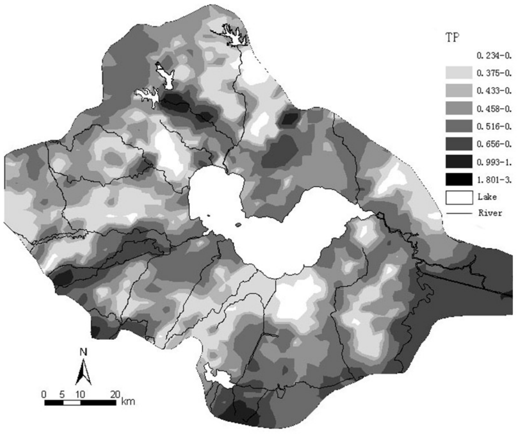

FIGURE 2 Kriging interpolated map of soil TP

P Fixation Capacity and P Saturation: Soil PSI test results showed that the average soil PSI (from 14.5 to 25.3 for different soil types) in the Chaohu Lake watershed was relatively lower than in other global regions (Table 2). It indicated that the soil P fixation capacity were relative weaker than other areas and therefore in high potential for P loss to water.

TABLE 2 P fixation capacity compared between soils from Chaohu watershed & other regions

Study Area	Sample Number	PSI Value			Literature Reference
		Mean	Standard Deviation	Range	
Chaohu watershed, China	450	18.8	7.4	4.3-56.5	This study
Taihu watershed, China	28	38.5	11.2	20.8-75.4	Gao et. al., 2001b
Northeast Scotland	25			5-64	Bache and Williams, 1971
Florida, USA	18			37-210	Porter and Sanchez, 1992
South Italy	32	28.2	15.9	4.3-54.2	Indiati and Sharpley, 1995

Existing studies proved that a certain range of soil organic matter content could increase soil P sorption, while the result would be reverse when organic matter content exceeds the upper limit

(Pierzynski et al., 1994). The lower P fixation capacity of soil in Chaohu Lake watershed probably has some relationship with the organic matter content, which is 19.8g/kg in average, lower than in Taihu Lake watershed with 27.2 g/kg (Gao et al., 2001a). P fixation capacity is an intrinsic property of soil, which are different among different soil types. Table 3 showed that the average PSI of Carbonati-Udic Argosols is relative higher than others, while Purpli-Udic Cambosols is relative lower. It is known that several factors such as the content of Fe, Ca and Al will influence soil P sorption properties. Generally, the higher soil P content and lower PSI resulted in the higher soil DPS. The DPS value of Purpli-Udic Cambosols samples showed that P is more saturated than other soils. The results also showed the DPS were notably different among all the tested soils. The study by Gao and zhang (Gao and Zhang, 2001) had demonstrated the DPS is a key factor determined the magnitude of P loss to water. Some researches suggested that a DPS value of 25% is a threshold for P loss from agricultural soil (Breeuwsma and Silva, 1992).

TABLE 3 PSI and DPS for different soil types

Soil Type	**Sample Number**	**PSI**			**DPS,%**		
		Range	**Mean**	**Standard Deviation**	**Range**	**Mean**	**Standard Deviation**
Argi-Udic Ferrosols	15	7.9-39.9	17.4	8.2	2.1-13.4	6.9	4.4
Ferri-Udic Argosols	45	6.1-47.5	17.8	7.2	5.4-33.9	20.6	11.4
Humic Ali-Perudic Cambosols	49	6.5-49.7	20.3	9.5	11.9-37.3	23.7	9.8
Albic Fe-accmuli-Stagnic Anthrosols	32	10.3-24.9	15.9	3.7	21.6-41.7	28.3	7.4
Gleyi-Stagnic Anthrosols	28	5.4-34.8	17.9	7.4	4.5-25.1	13.8	6.9
Hapli-Stagnic Anthrosols	32	10.1-27.1	17.4	4.3	4.9-32.2	19.6	8.8
Fe-accumuli-Stagnic Anthrosols	181	4.3-31.2	17.9	5.4	6.6-42.0	19.3	10.1
Purpli-Udic Cambosols	19	5.9-29.9	14.5	6.2	11.2-64.9	33.3	20.9
Carbonati-Udic Argosols	49	14.1-41.2	25.3	7.6	2-27.9	8.5	8.7

CONCLUSIONS

The spatial variance of TP content of topsoil and the soil P fixation capacity and saturation in Chaohu Lake watershed were discussed in this paper. We found that the soil TP distribution was band characteristics and good spatial structure at NE-SW direction. The spatial variations on a larger scale are largely due to geological influence, while spatial variations in local areas mainly reflect the land use and peri-urban agricultural activities. Soil PSI index was also tested and the results showed the fact that P fixation capacity of soils in this watershed are generally lower than those in other area. We found that PSI values of more than 94.3% of the samples are lower than 30 and obviously different among soil types. The P fixation capacity of Carbonati-Udic Argosols is relatively higher while the Purpli-Udic Cambosols is on the contrary. Soil DPS tests also showed over 30% of the samples are saturated with DPS values overpass 25%. It indicated high P loss risk will occur from these areas when soil P increased. More attentions should be paid on this watershed to find out the potential critical areas of P loss and control the non-point P pollution with best management practices.

ACKNOWLEDGEMENTS

We are grateful to Anhui Institute of Geological Survey for providing the latest soil survey data.

We would like to acknowledge the help of Qinyun Fan, Dengfeng Wang, and Juan Zhou in the laboratory experiment.

REFERENCES

Askin, T., and R. Kizilkaya. 2006. “Assessing Spatial Variability of Soil Enzyme Activities in Pasture Topsoils Using Geostatistics.” *European Journal of Sioil Biology.* 42(4):230-237

Bache B. W., and E. G. Williams. 1971. “A Phosphate Sorption Index for Soils.” *Journal of Soil Science* 22:288-301

Breeuwsma, A., and S. Silva. 1992. *Phosphorus Fertilization and Environmental Effects in the Netherlands and the PoRegion (Italy).* Report No. 57. Agricultural Research Department, Wageningen, The Netherlands.

Castrignanò, A., L. Giugliarini, R. Risaliti, and N. Martinelli. 2000. “Study of Spatial Relationships Among Some Soil Physico-chemical Properties of a Field in Central Italy Using Multivariate Geostatistics.” *Geoderma.* 97:39-60

Chen, F. S., D. H. Zheng, and X. Y. He. 2006. “Small-Scale Spatial Variability of Soil Nutrients and Vegetation Properties in Semi-Arid Northern China.” *Pedosphere*. 16(6):778-787

Gao, C., and T. L. Zhang. 2001. “Phosphorus Sorption and Desorption of Upland Soils in the Hilly Areas of Taihu Lake Watershed” (in Chinese). *Journal of Lake Sciences.* 13(3):255-260

Gao, C., T. L. Zhang, and W. D. Wu. 2001a. “Agricultural Soil Nutrient Status in Taihu Lake Area and Its Implication to Nutrient Management Strategies” (in Chinese). *Scientia Geographica Sinica.* 21(3):428-432

Gao, C., T. L. Zhang, and W. D. Wu. 2001b. “Risk Evaluation of Agricultural Soil Phosphorus Release to the Water Bodies” (in Chinese). *Acta Scientiae Circumstantiae.* 21(3):344-348

Heckrath, G., P. C. Brookes, P. R. Poulton, and K. W. T. Goulding. 1995. “Phosphorus Leaching from Soils Containing Different Phosphorus Concentrations in the Broadbalk Experiment.” *J. Environ. Qual.* 24(5): 904- 910

Hooda, P. S., A. R. Rendell, A. C. Edwards, P. J. A. Withers, M. N. Aitken, and T. W. Truesdale. 2000a. “Importance of Soil Phosphorus, Sorption and Desorption Indices in Assessing Phosphorus Loss in Agricultural Runoff.” *Journal of Environmental Quality*. 29:1166-1171

Hooda, P. S., A. R. Rendell, A. C. Edwards, P. J. A. Withers, M. N. Aitken, and V. W. Truesdale. 2000b. “Relating Soil Phosphorus Indices to potential Phosphorus Release to Water.” *Journal of Environmental Quality*. 29:1166-1171

Indiati, R., and A. N. Sharpley. 1995. “Soil Phosphate Sorption and Simulated Runoff Parameters as Affected by Fertilizer Addition and Soil Properties.” *Communications in Soil Science and Plant Analysis.* 26:2319-2331

Juang, K. W., D. C. Liou, and D. Y. Lee. 2002. “Site-specific Phosphorus Application Based on the Kriging Fertilizer-phosphorus Availablity Index of Soils.” *Journal of Environmental Quality*. 31(4):1248-1255

Liu, X. M., J. M. Xu, M. K. Zhang, J. H. Huang, J. C. Shi, and X. F. Yu. 2004. “Application of Geostatistics and GIS Technique to Characterize Spatial Variabilities of Bioavailable Micronutrients in Paddy Soils.” *Environ. Geol.* 46:189-194

Mozaffari, M., and J. T. Sims. 1994. “Phosphorus Availability and Sorption in an Atlantic Coastal Plain Watershed Dominated by Animal- based Agriculture.” *Soil Science.* 157: 97-107

Nair, V. D., K. M. Portier, D. A. Graetz, and M. L. Walker. 2004. “An Environmental Threshold for Degree of Phosphorus Saturation in Sandy Soils.” *Journal of Environmental Quality*. 33:107-113

Pautler, M. C., and J. T. Sims. 2000. “Relationships between Soil Test Phosphorus, Soluble Phosphorus, and Phosphorus Saturation in Delaware Soils.” *Soil Science Society of America Journal.* 64:765-773

Pierzynski, G. K., J. T. Sims, and G. F. Vance. 1994. *Soil and Environmental Quality*. Lewis Publishers, Boca Raton, Florida, USA.

Porter P. S., and C. A. Sanchez. 1992. “Effect of Soil Properties on Phosphorus Sorption by Everglades Histosols.” *Soil Science*. 154(5): 387- 398

Pote, D. H., T. C. Daniel, A. N. Sharpley, P. A. Jr. Moore, D. R. Edwards, and D. J. Nichols. 1996. “Relating Extractable Soil Phosphorus to Phosphorus Losses in Runoff.” *Soil Science Society of America Journal.* 60:855-859

Pote, D. H., T. C. Daniel, D. J. Nichols, A. N. Sharpley, P. A. Jr. Moore, D. M. Miller, and D. R. Edwards. 1999. “Relationship between Phosphorus Levels in Three Ultisols and Phosphorus Concentrations in Runoff.” *J. Environ. Qual.* 28:170-175

Wang, X. Y. 2003. *Nonpoint Source Pollution and Management*. (in Chinese). Oceanpress, Beijing.

Yan, W., and X. Wang. 1998. “Preliminary Study on Non-point Sources Pollution in the Chaohu Lake Drainage Basin” (in Chinese). *Scientia Geographica Sinica.* 18(6):264-267

Yin, F. C., and Z. Y. Zhang. 2003. “Survey of Chaohu Lake Eutrophication Research” (in Chinese). *Journal of Lake Science.* 15(4):377-384

Zhang, S. R., B. Sun, Q. G. Zhao, P. F. Xiao, and J. Y. Shu. 2004. “Temporal-spatial Variability of Soil Organic Carbon Stocks in a Rehabilitating Ecosystem.” *Pedosphere.* 14(4): 501-508

STREET DUST AND ITS POTENTIAL HEAVY METAL CONTAMINATION TO RUNOFF

Xuyong Li, Hongtao Zhao, Xiaoyan He (Research Center for Eco-environmental Sciences, Chinese Academy of Sciences, Beijing, China)

Street dust (SD) is an important carrier of heavy metal contaminants, and can remarkably contribute to urban runoff pollution. Significant administration difference among urban and rural areas causes SD variation along urban-rural gradient in China. More than ninety SD samples were collected along the urban-suburban-rural gradient from areas of five administrative units in the Beijing metropolitan region of China, including central urban (UCA), urban village (UVA), central suburban county (CSA), rural town (RTA), and rural village (RVA) areas. We investigated the quantity of SD per unit area, SD grain size, SD particulate mobility, and heavy metal concentrations in SD along urban-suburban-rural gradient. We also evaluated potential metal pollution in SD surface runoff through the washoff experiment using a rainfall simulator. Our results show that the SD mass per unit area increased among urban-suburban-rural gradient in the order UCA (21 ± 24 g/m^2) ≈ CSA (20 ± 16 g/m^2) < RTA (59 ± 63 g/m^2) < RVA (RVA, 147 ± 112 g/m^2) ≈ UVA (147 ± 198 g/m^2). Compared to SD from the other administrative units, SD from the UCA and CSA had higher metal concentrations and higher proportions of smaller particles, whereas that from the RVA and UVA had larger quantities of metals per unit area. UCA and CSA had lower potential runoff pollution contributions per unit area. The washoff percentage of the SD varied along the urban-rural gradient: UCA 15.8 ± 2.7 %, CSA 14.2 ± 1.6 %, RTA 12.7 ± 2.2 %, RVA 13.5 ± 2.5 % and UVA 11.6 ± 1.7 %. The average washoff loss proportion of the five metals (Cr, Cu, Ni, Pb, Zn) from SD was 24.3%, 56.8%, 34.3%, 22.8%, and 27.3% , respectively. The metal loss proportion of SD from washoff increased with the decrease of the particle size of SD, which was strongly affected by the urban-suburban-rural gradient. SD washoff loss among different SD particle sizes varied from 4.6% to 62.1%. Proportion of acid-extractable metal was higher in SD than that in washoff particles. Our findings help to make appropriate strategies for controlling metal pollution from SD washoff along the urban-suburban-rural gradient.

ISBN 9780976885351

EVALUATION OF BEST SAMPLING TIME FOR MEASUREMENT OF OIL AND GREASE

Zulkifli Yusop and Chow Ming Fai
(Universiti Teknologi Malaysia, Johor Bahru, Johor, Malaysia)

Accurate knowledge of the fate and transport of oil & grease carried by storm water runoff is important to assess the non point source pollution problem. This paper presents the results of best sampling time for measurement of oil & grease quality from stormwater runoff in a residential area in Skudai, Malaysia. Ten storm events were grab sampled and analyzed for the concentration of oil & grease. Event Mean Concentration (EMC) of oil & grease was computed for each storm event. The pollutograph of oil & grease for each storm event was examined to determine when a single oil & grease grab sample can closely approximates the event mean concentration value. Results showed that for a small catchment, the best time to collect a single grab sample ranged from 10 to 25 min after the beginning of storm runoff.

ISBN 9780976885351

INDUSTRIAL WASTEWATER MANAGEMENT IN VIETNAM, CURRENT STATUS AND SOLUTIONS

Le Tuyet Minh, Tan Soon Keat (Nanyang Technological University, Singapore, SG)
Nguyen Phuong Quy (SFC Vietnam Investment Development for Environment Corporation, Hanoi, VN)

ABSTRACT: In recent 20 years, Vietnam economy has been growing fast. Many industrial parks (IP) have been established with various industries developed. However, wastewater management was not properly concerned which resulted in numerous serious pollution cases. Consequently, “death rivers” were found easily in Vietnam these days. Currently, there are about 290 IPs with the total effluent of more than 600,000 m^3/day. Only 27% of discharged wastewater was treated properly. The rest was released to receiving bodies without any treatment method or with simple techniques only. To cope with those problems, regulations with tighter conditions and guidelines were issued; training to raise people’s awareness was also conducted. Above all of that, construction of wastewater treatment plants is necessary, with the consideration of investment and operation costs. Reasonable technologies that provide the lower cost but fulfil the treatment requirement are what the investors are looking for. Other than that, applying cleaner productions in both existing and new IPs also helps to lower the cost for water treatment. This study analysed the current status of industrial wastewater management in Vietnam; as well as appropriate technology solutions for wastewater treatment which applicable for climate conditions and, quality and investment requirements.

INTRODUCTION

Since 1990s, industrialisation in Vietnam has been developed rapidly and open with various types such as Food processing & Beverage, Wood and forest product, Textile, Tobacco, Leather and Chemical products, etc. Many of existing industrial clusters, industrial points and craft villages (which were observed more in the Northern part than in the Southern part of the country due to the manufacturing tradition) with outdated technologies and no wastewater treatment system has been locating inside the city or near residential area. Industrialisation blooming also leads to the rapid urbanisation. Therefore, the cities are required to be enlarged to meet with the population demands, and centralised by manufactures and small existing industrial park (IP). Mixture of industrial and domestic effluent also caused serious pollution to the urban surface water, ground water and air pollution due to the lack of investment in discharge facilities and proper treatment system. Rapid urbanisation with inadequate of facilities and infrastructures resulted in the overload for discharge system and severely pollution. IPs that stayed far from the urban areas were in the same situation, since environmental protection was not taken care in the first days of industry development. Industries that course severe pollutions are thermal power, cement and construction material production and mining industry (MOIT report, 2003).

If there were only 500 cities and towns in Vietnam in 1990, after 20 years the number of urban areas reaches to 754, which attract about 33% population of the country (MONRE report, 2010). Urbanisation and industrialisation lead to the increasing number of IPs to be built. Until this moment, there is no adequate investigation on total number of industrial clusters throughout the country. According to the Ministry of Natural Resources and Environment (MONRE), up to the end of 2011, there were about 283 IPs in Vietnam, among which 180 are in operation, which also means that 64% of industrial park was filled.

ISBN 9780976885351

CURRENT STATUS

Insufficient of Common effluent treatment plant (CETP). Vietnam Environment Administration (VEA) provided a summary on total capacity and typical pollutants' loading rates by key economic zone (KEZ) as shown below:

TABLE 1. Estimate flow capacity and pollutant loading rate in key economic zone (KEZ) (MONRE report, 2009)

KEZ	Q (m^3/d)	TSS (kg/d)	BOD (kg/d)	COD (kg/d)	TN (kg/d)	TP (kg/d)
Northern part	155,055	34,112	21,243	49,463	8,993	12,404
Centre part	58,808	12,937	8,057	18,760	3,411	4,705
Southern part	413,400	90,948	56,636	131,875	23,977	33,072
Cuu Long Delta	13,700	3,014	1,877	4,370	795	1,096
TOTAL	640,963	141,011	87,813	204,468	37,176	51,277

The data was estimated based on total land space used for industrial development. It can be seen that industries in the Southern part of Vietnam discharged more than 65% of total effluent volume. In average, each industrial park discharge ranging from 3,000 to 4,000 m^3/day.

Despite the fact that a regulation from Government cited that a CETP must be built prior the operation of the IP, up to end of 2011, only 65% of the 180 under operation IPs were equipped with wastewater treatment plant (WWTP). However, not all of them were operated properly with adequate and updated technologies. Many IPs provide WWTP just to deal with the regulation. The investigation from a VEA (MONRE report, 2009) showed that although a number of WWTP or CETP were built, the treatment efficiency of those plants were still low and did not meet the requirement for effluent standard. A large amount of effluent was in fact dumped directly to the public sewage system without any treatment. (LBCD Consultants inc., 2010)

World Bank (WB) conveyed studies to assess the impact of the releasing effluent from IPs to the river in two main river basins, which are Nhue-Day in the North and Dong Nai in the South of Vietnam. The study showed that lesser IPs export processing zone (EPZ) in the North was recorded. This is true because Southern part of Vietnam is considered the business centre of the country. Although it can be realised that lower percentage of Northern part IPs have CETP is than the South, it is in fact more IPs in Northern KEZ are applying for building CETP, or the CETP are under construction.

TABLE 2. Examples of industrial parks, industrial cluster, industrial points and craft villages (CV) that are not equipped with CETP (LBCD Consultants inc., 2010)

Region	IP & EPZ		Industrial Cluster		Industrial Points		Polluting CVs
	Total	**w/o CETP**	**Total**	**w/o CETP**	**Total**	**w/o CETP**	**No WWTP**
Northern KEZ							
Ha Noi	13	12	37	35	43	43	257
Nam Dinh	11	10	16	16			75
Ha Nam	11	10	6	6	5	5	14
Southern KEZ							
HCMC	15	2	30	28			
Dong Nai	29	20	43	42			
Binh Duong	28	9	9	8			
Binh Phuoc	19	18	17	17			
Ba Ria- Vung Tau	14	14	30	30			

Death rivers. Canal and sewage systems in Vietnam which were designed during the French colonisation (about 70 years ago), have been deteriorated and cannot afford for the rapid increasing of the population currently. The system becomes overload that easily damages the pipe system. It is impossible to rebuilt or replace the whole collection system in a short time due to the lacking of capital or the poor infrastructure.

In the big cities like Hanoi and Hochiminh, many canals and rivers are extremely shallow, and there is almost no flow velocity. In rural areas or even some small cities, there is even no drainage system and effluent from IPs has been discharged directly to irrigation canals and rivers. Water quality is steadily deteriorating, and the canal will soon be biologically dead. There are many examples of the river that was "killed" by this direct effluent discharge. In 2008, residents near Thi Vai river (Dong Nai province) informed that Vedan company discharged effluent directly to the river. The product from this company includes of Glutamic Acid, Monosodium Glutamate, Starch and other chemical productions. With nearly 5,000 m^3/d of effluent dumped directly and daily to Thi Vai river in many years, at some point of the river, DO was recorded as ranging from 0.5 to even 0.04 mg/l. Another example is Sonadezi Long Thanh IP, which receive wastes from rubber, leather, plastic and chemical industry, etc., recently was found to discharge wastewater to Ba Cheo canal (Binh Duong province), causing the damage of 95% aquatic life, and severely to poultry production, and water resources pollution (www.monre.gov.vn).

SOLUTIONS

Discharge permit: Vietnam Law on Environment has issued different standards and provided guidelines for wastewater quality to be discharged to receiving bodies. By times, more conditions have been provided to determine the limit concentration of pollutants in the effluent.

- In 1995: TCVN 5945-1995 standard, which is later replaced by TCVN 5945-2005. This standard helps the user to identify the limit value of pollutants and the maximum allowable concentration of pollutants in the industrial wastewater that can be discharged to the receiving bodies used for domestic water supply (Grade A); for irrigation, aquaculture (Grade B); and to the wastewater ponds, wastewater inlet sluice for dilution purpose (Grade C).
- In 2000: TCVN 6773-2000: standard for industrial effluent discharged into the irrigation system;
- In 2001: TCVN 6984-2001: standard for industrial effluent discharged into water bodies using for protect aquatic life.
- In 2009: QCVN 24: 2009/BTNMT: guidelines to determine the maximum concentration that is allowable to be discharged to the receiving body, based on the maximum concentrations that are regulated in TCVN 5945-2005, the flow rate and volumetric capacity of wastewater receiving facilities. This guideline has been using commonly these days.

Legislation: Similarly, legal documents related to this issue also show more effort of the government on preventing industrial wastewater pollution. The requirements have been tighter to the IP management.

- In 2007: The government issued Decree No. 88/2007/ND-CP urban and IPs drainage system, specially indicated that discharge of wastewater from IPs must follow the guidance and standards.
- In 2008: Decree 29/2008/ND-CP mentioned that CETP is necessary only if IP is preparing for expansion.
- In 2009: Circular 08/2009/TT-BTNMT indicated that CETP is required prior to the operation of the IP. For those IPs that have operated without a CETP, then the plant should be constructed and commissioned by the end of 2010. CETP must equip the online monitoring system for typical parameters such as pH, COD, TSS, DO and specific parameter if any.

Monitoring programme and training: Facing with the severe problems on water resources pollution, monitoring programme is required. Trainings on monitoring have been conducted since 2009, which was organised in 8 selected provinces. The programme helped to train government officers on using automated sampling and other online monitoring equipment. The owners of IPs are requested to conduct monitoring the effluent every 3 to 6 months, and report to local agencies every 6 months (LBCD Consultants inc., 2010).

Conferences have been organised to raise awareness of industries owners, as well as to introduce updated and efficient wastewater treatment technologies.

Polluter-pay-principle. The government applied this method to charge the IPs which are found discharging pollutants to receiving sources. Up to 2010, 12million USD of this fee has been collected, in which 20% kept by DONREs of the provinces to cover the cost for monitoring and fee collection; the rest of 80% will be sent to local Environmental Protection Fund and other local agencies to upgrade and maintain the drainage system. HCM City Industrial Park-Export Processing Zone Authority (HEPZA) is the only IP till now keeps 10% of the collected environmental fee to cover its environmental management expenses.

Cleaner production. Producing technology pays an important role in controlling wastewater capacity and the required components of WWTP. It can help to reduce effluent capacity (e.g. in Beer production or Food production) or to reduce dissolve dyes in textile dyeing industry, which are not easy to be treated.

Tran Van Nhan et al. (2005) conducted a study on implementation of cleaner production options in textile dyeing industry. The study showed that only by applying 30% of the proposed options that costs 120,000 USD, the annually benefit from it can be 6 times higher than the investment cost. However, to invest and apply an intervention to the existing production chain does not mean can reduce pollution effectively. The effect relies much on the expertise of operators. Cleaner production in Vietnam is still quite new field and lack of man-power and expertise in this area. Even though, it is a good opportunity to look at, especially to the new manufactures. This technology could be applicable in Pulp and paper, Food processing and Textile dyeing industries.

Relocation. Outdated technologies industrial points have been closed or relocated out of the centre of cities, leaving space for residential areas. High polluting industries have been given priority to move including of those that discharge toxic pollutants, such as paper, leather, rubber, pesticides and fertiliser productions. Small and old industries in the city are urged to close and move to planned areas for industry development. (Le Van Khoa et al., 2006; Quach To Dung, 2003)

Prevention of pollution. Construct a retention tank is a good option to overcome the situation when the CETP must close emergency for repairing or maintenance. Nhon Trach IP has used this solution, so that it avoids discharging wastewater directly to receiving source without any treatment.

Pre-treatment or stream separation is required, especially when there are mixtures in types of wastewater in an IP. Separate the sources that have higher load or special pollutant for pre-treatment is encouraged at the industry level. This step can help to lower pollutant load for the CETP, hence can help to reduce investment and O&M cost. IP management is expected to support or share the cost with the manufacturers (LBCD Consultants inc., 2010).

Technology selection: Those tools mentioned above will help to protect or reduce the environmental impact from the manufactures to human livings. However, an efficient wastewater technology is still necessary as required. The technology that brings more benefit to the owner is expected to meet those requirements:

- High treatment efficiency;
- Low or reasonable investment cost;
- Low operation and maintenance (O&M) cost;
- Convenience for expansion and
- Easily adapts with overload situation.

Several technologies have been applied for industrial wastewater treatment in Vietnam such as conventional aerated system (CAS), oxidation ditch, SBR, aerated lagoon, etc. SBR and CAS are used more popular due to the requirement of land savings, higher treatment efficiency and widely applicability to variety of wastewater types (LBCD Consultants inc., 2010). SBR is actually more preferable and seems to be the promising technology in future for industrial wastewater treatment in Vietnam. As compared to

CAS, SBR doesn't require a separate settling tank since both aeration and sedimentation happen in the same take. Construction cost since then is lesser, and operation is more convenience in batch.

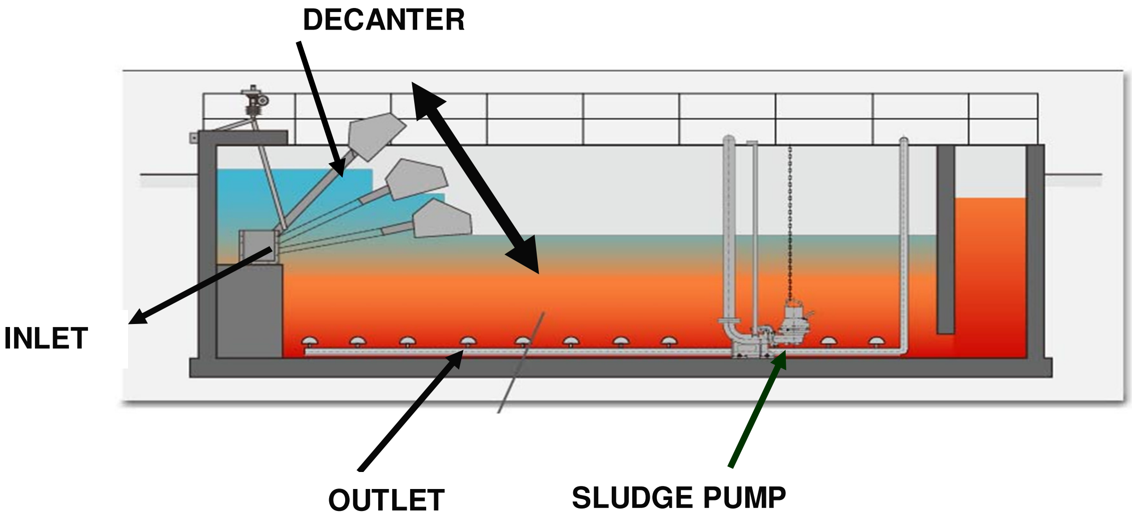

FIGURE 1. System Schematics of C-Tech

SFC Vietnam Investment Development for Environment Corporation (SFC) is a member of SFC Group who experienced in SBR technology. SFC has introduced its technology – the renovated SBR which is called C-Tech – for wastewater treatment in Vietnam. Besides, by maintaining both aerobic and anoxic condition during the whole process, C-Tech allows both organic contents and nutrients (nitrogen, phosphorous) removal in secondary treatment. (http://www.sfcvietnam.com.vn, http://www.sfc-group.net).

TABLE 3. Evaluation on the compliance of C-Tech and other conventional technologies with common requirements

S/N	Requirement	Technology					
		Biofilter	**CAS**	**Oxidation Ditch**	**A2O+MBR**	**SBR**	**C-Tech**
1	WWTP Effluent quality	Very good (Grade A)	Good (Grade B)	Good (Grade B)	Good (Grade B)	Good (Grade B)	Very good (Grade A)
2	O&M cost	High	High	Average	High	Average	Average
3	Overload tolerance	Low	Low	Average	Average	Normal	High
4	Requirement in O&M	High	High	High	High	Average	Average
5	Investment cost	Very high	High	High	High	Average	Average
6	Expansion ability	Low	Low	Average	Average	Average	High
7	Space requirement	Average	Very high	Higher Average	Higher Average	High	Low
	EVALUATION	5	5	4	3	2	1 (Best)

A2O technology is developed from a variety of practical and mature water treatment with highly optimised integration. A2O combines with MBR will give higher treatment efficiency and eliminate of secondary clarifier. However, back wash system is required. Table 3 shows that C-Tech has more advantage than other conventional technology and is considered the best option for investment, especially in Vietnam. Besides, experiments also showed that with controlled system operated efficiency, C-Tech can helps saving about 50% energy during operation, i.e only 0.3 kWh/kgCSB is required for C-Tech while SBR and CAS consume 0.77 and 0.84 kWh/kgCSB respectively.

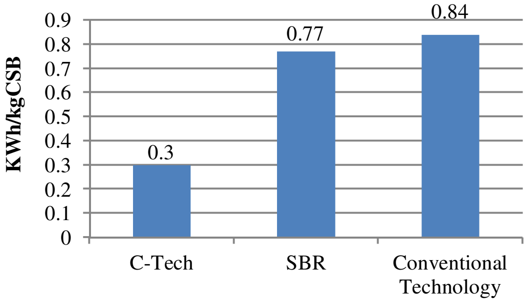

FIGURE 2. Comparison on energy usage among C-Tech, SBR and CAS

Since 2008, SFC has applied successfully C-Tech in some projects like CETP in Phu My II IP (4,000 m^3/day), Vietnam Singapore IP Bac Ninh (4,000 m^3/day), Bien Hoa 2 IP (4,000 m^3/day), Quang Tri rubber company (1,500 m^3/day), Bau Xeo IP (4,000 m^3/day), Song Cong IP (4,000 m^3/day), etc.

CONCLUSIONS

Industrial development blooming leads to water resources pollution seriously in cities and urban areas. Despite the fact that the government is tightening industrial development with environmental protection, the number of CETP is not sufficient. Wastewater treatment is a promising market in Vietnam. High and updated technologies are necessary. However, reasonable investment cost is preferable. Investment rate for a cubic metre of wastewater currently in Vietnam is about 500 – 1000 USD. The government is now pushing both existing IP and under construction IP to build and have the CETP in commissioning as soon as they can. To the IPs management board, it is obviously that they will prefer a solution that saves space, investment and is easy in operation.

Separation at source is one of the important key to help solve this problem. It can be reached by applying cleaner production and pre-treatment at the industry level if it is required. Total pollutant load is reduced and toxic pollutant can be eliminated at source that can help to CETP becomes simpler. Total investment for the CETP and support fee for the manufactures is possibly lower than investing for a CETP of a mixture stream. Unpredicted or a sudden monitoring and examine can help to prevent the owners from cheating.

C-Tech, with its experience worldwide, and has been applied successfully in Vietnam. Holding advantages such as high efficiency in treatment, easy operation, space and cost savings as compared to other conventional technologies, C-Tech shows its potentiality to satisfy the investors and environmental agencies.

ACKNOWLEDGEMENTS

The work is supported by Maritime Research Centre (Nanyang Technological University) and SFC Vietnam Investment Development for Environment Corporation.

REFERENCES

MOIT - Ministry of Industry and Trade. 2003. *Business Forum number 50*, pp.13. Vietnam.

MONRE - Ministry of Natural Resources and Environment. 2009. *National report on environment – Environmental problems of Industrial parks in Vietnam*. Hanoi, Vietnam

MONRE - Ministry of Natural Resources and Environment. 2010. *National report on environment*. Hanoi, Vietnam

MONRE - National technical regulation on industrial wastewater and National standards on effluent quality.

LBCD Consultants inc. & Experco International Ltd. 2010. *Industrial wastewater management in river basins Nhue-Day and Dong Nai project – Final report*. World Bank report no. 57863. Vietnam.

Le Van Khoa and Peter Ho. 2006. "Greening Through Industrial Relocation in Vietnam". *Greening Industries in Newly Industrializing Economies: Asian-style leapfrogging*, pp.107-135. Kegan Paul, London.

Quach To Dung. 2003. *Environmental Pollution Situation and Industrial Relocation Program in Ho Chi Minh city*. Proceedings of Kitakyushu Initiative Seminar on Industrial Relocation. Ho Chi Minh city, Vietnam

Tran Van Nhan. 2005. *Cleaner Production - a Cost-Effective Tool for Textile Industrial WastewaterManagement in Vietnam*. Science Council of Asia.

WEPA. 2009. *Outlook of Water environment management strategies in Asia*. Japan.

THE EFFECTS OF WATER TMS AND FUTURE DIRECTIONS IN KOREA

ByungKook Lee, Eulsaeng Cho* (Korea Environment Institute, Seoul Korea)
S.H. Kim (KECO, Incheon, Korea)
TaeJoo Park (Pusan National University, Busan, Korea)

ABSTRACT: The real-time water quality monitoring system based on Water Quality Tele-Monitoring System (Water TMS) to inspect the actual pollutants discharge load from the effluents of major point sources(MWTFs, ICWTPs, etc.) have been introduced in Korea since 2006. The parameters being monitored are pH, organic matters (BOD or COD), suspended solids (SS), total nitrogen (TN), total phosphorus (TP) and flow. Compared to the data before the installation of water-TMS in 2008, effluent water quality in 2011 has been improved with 41% and 33% reduction of effluent discharge concentration and load, respectively. The implementation of Water TMS can ensure the safety of the water environment with a valuable contribution towards preventing water pollution accident and promoting reliability, transparency and continuity in implementation of environmental policies. The success of water-TMS will be the footstone to integrate Water TMS, river water quality monitoring systems including manual, real-time automatic and IP-USN monitoring system, which can be useful for forecasting water quality in advance.

INTRODUCTION

Water Quality Tele-Monitoring System (water-TMS) is a real time monitoring system of effluent discharged from wastewater facilities by automatic measuring instrument. The water quality monitoring system based on Water-TMS in Korea was introduced to perform Pollutant Discharge Levy Program more scientifically based on actual discharge by real-time monitoring. In Korea, wastewater facilities are charged for pollutants discharged in excess of the emission limit. Conventional method of assessing excess effluent charge is based on “one-time measurement at a snap field inspection” and estimated on the assumption that the first measurement value continues until the improvement completion date, not on the real discharge amount and period. Supreme Court also ruled that the charging method was illegal in 1995. In 2006, the Ministry council of regulation reform decided to improve the imposition method more scientifically based on automatically measured data. In 2007, as a result, legislation and water-TMS control center were established. Water-TMS instrument was installed in wastewater facilities and has operated since 2008. Ultimately, the aims of water-TMS application and performance is to supervise discharge facilities in real time with remote monitoring instead of on-site inspection; and to efficiently and systematically manage the water quality of effluent from discharge facilities through improved methods of assessment.

POLICY OF WATER-TMS IMPLEMENTATION

Legislation: The general framework for water-TMS is under the legislation consisting of “Water Quality and Ecosystem Conservation law, enforcement decree and enforcement regulation. By Water Quality and Ecosystem Conservation law, it is mandatory for direct discharge facility over a certain size to

---

ISBN 9780976885351

install and operate water-TMS system; Article 38-2 [Obligation of water-TMS equipment installation], Article 38-3 [Forbidden Acts of wastewater facility running TMS Analyzer, and Standards for operation and management]. In the Enforcement Decree, subject, method and period of measuring instrument are specified; Article 35 [subject of water-TMS equipment installation, Method and Period of measuring equipment installation], Article 37 [Establishment and operation of Tele-Monitoring System Control Center]. The Enforcement regulation states the criteria of operation and management of automatic measuring instrument; Article 50 [Criteria of operating and managing analyzers]. Also, the enforcement notice can be issued according to this regulation, if necessary; Article 51 [Enforcement notice].

Subject of water-TMS installation & Monitoring Parameters: According to Water Quality and Ecosystem Conservation law, the on-line automatic measuring instrument should be installed at the following facilities treating more than 700 m^3 per day ; Municipal wastewater treatment facility (MWTF), industrial complex wastewater treatment facilities (ICWTF), individual business wastewater discharge facility (IBWDF). However, indirect wastewater discharge facility is exempted from the water-TMS policy. The parameters being monitored by on-line automatic measuring instrument for water-TMS are pH, organic matter (BOD or COD), suspended solids, total nitrogen, total phosphorus and flow. All data measured by automatic measuring instrument are recorded in data logger system and transmitted to water-TMS control center through internet (Figure 1).

FIGURE 1. Water-TMS facility and automatic measuring instruments in WWTP

Agencies involved for water-TMS implementation: The Water TMS is being implemented by four agencies: Ministry of Environment (MOE), Korea Environment Corporation (KECO), Local government and discharge facility (Figure 2). The MOE plays a role as a general manager, and the KECO operates water-TMS Control Center. Data received from each discharge facility are compiled at the server and managed via the systems in the Control Center. The Control Center plays a variety of roles in analyzing each effluent wastewater quality, including determination of compliance with effluent standards, and provision of data regarding assessment of effluent charges to administrative agencies. In addition, the Control Center is responsible for Quality Assurance (QA) and Quality Control (QC) inspection to verify the reliability of the monitored data, and provide technical support to discharge facilities for enhancing stable operation of Water TMS. Local government supervises discharge facilities in the completion of the installation or improvement of on-line automatic measuring instruments. Discharge facilities are operating and maintaining automatic measuring instruments, and transmitting the monitoring data to the water TMS Control Center.

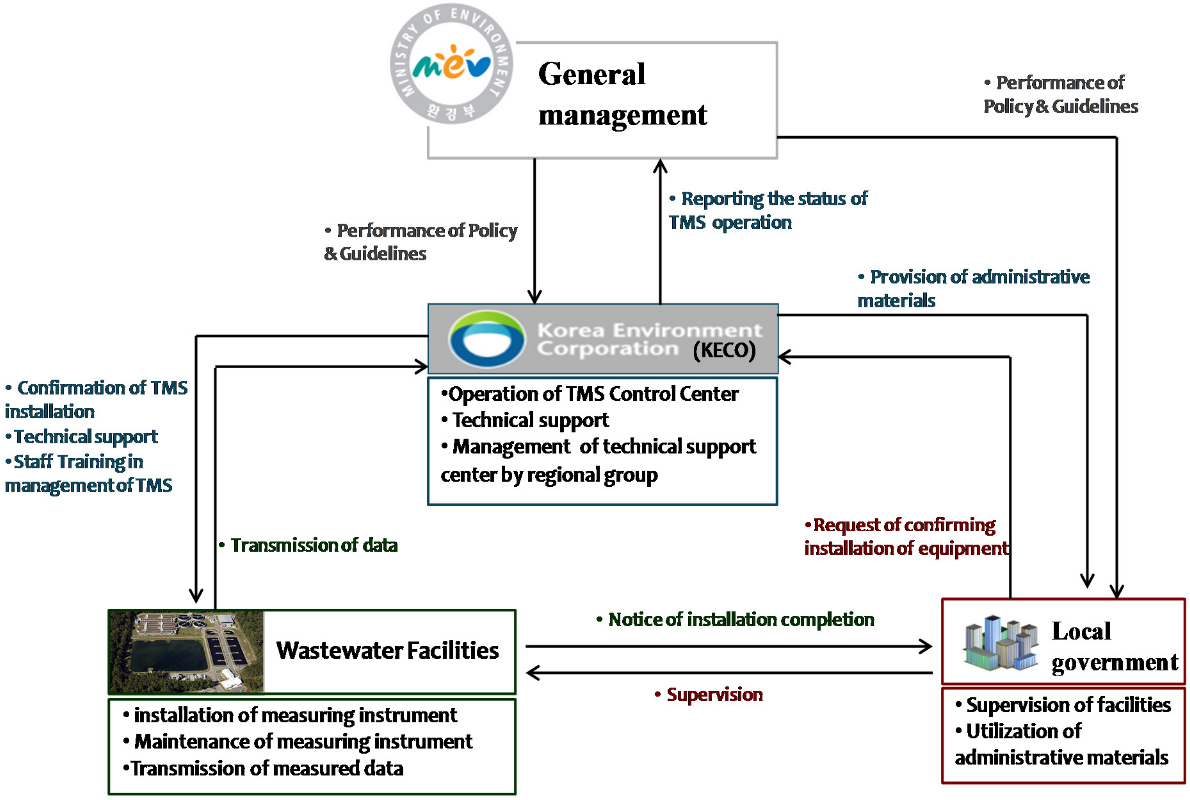

FIGURE 2. Implementation scheme of water-TMS

STATUS AND EFFECTS OF WATER-TMS APPLICATION

Status of water-TMS operation: As of December, 2011, water-TMS has operated in 653 wastewater facilities, including municipal wastewater plant (53%), industrial complex wastewater plant(13%), Individual business wastewater discharge facility (34%).

TABLE 1. Status of water-TMS installation and operation in wastewater facilities (KECO, 2012)

Type	Capacity (1,000 m^3)	Water-TMS installation & operation
MWTP	≥100	51
	10 ~ 100	140
	2 ~ 10	158
	subtotal	349
ICWTP	⩾10	28
	0.7~10	57
	subtotal	85
IBWDF	⩾0.7	219
Total		**653**

In terms of discharge volume, 97% of wastewater effluent discharged from MWTP is monitored by water-TMS. Industrial effluent wastewater quality is also observed in real-time at 98% from ICWTP and 73% from IBWDF, although it covers only small portion of the number of whole dischargers. Totally, point source pollution of 95% is managed systematically through on-line monitoring system (Table2).

TABLE 2. Status of wastewater Monitoring by Water-TMS (KECO, 2012)

Type	WWTP		TMS installed WWTP		Ratio of monitoring by TMS	
	No. of plant	Discharge Volume (m^3/d)	No. of plant	Discharge Volume (m^3/d)	No. of plant	Discharge Volume (m^3/d)
MWTP	465	19,190,600	349	18,581,677	**75%**	**97%**
ICWTP	145	521,967	85	803,613	**59%**	**98%**
IBWDF	14,380	1,574,385	219	1,152,756	**1.5%**	**73%**
Total	**14,990**	**21,586,952**	**653**	**20,538,046**	**4.3%**	**95%**

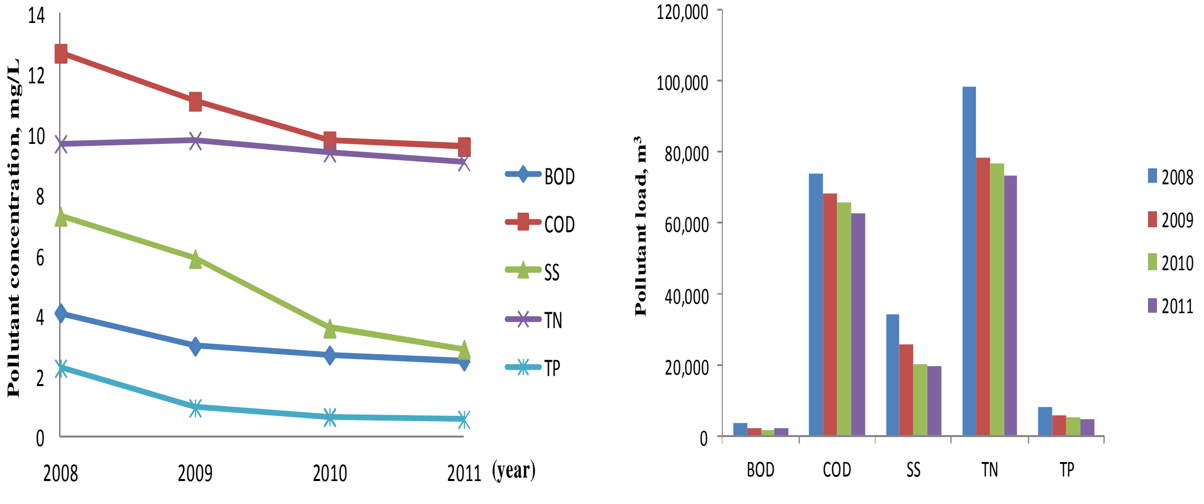

(a) (b)

FIGURE 3. Trends of effluent concentration(a) and load(b) from point source discharge facility.
(KECO, 2012 , MOE, 2008a; 2008b; 2008c; 2009a; 2009b; 2009c, NIER, 2011a; 2011b)

Achievements in water-TMS performance: After the operation of water-TMS, considerable effluent pollutant has been decreased compared to the data before the installation of water-TMS in 2008. Continuous reduction in the concentration and load of all pollutants being monitored by water-TMS parameters observed as shown in Figures 3. In the comparison of achievement between 2008 and 2011, the highest reduction appears in TP at 75% and 43% in terms of concentration and load, respectively, followed by SS, BOD, COD and TN. On an average, effluent discharge concentration and load has been reduced by 41% and by 33%, respectively for 3 years operation of water-TMS

CONCLUSION

The implementation of Water TMS can ensure the safety of the water environment with a valuable contribution towards preventing water pollution accident and violation of regulation by warning discharge status to related agencies and facilities. Also, real-time discharge monitoring data can be useful for promoting reliability, transparency and continuity in implementation of environmental policies. From the point of view of discharge facility, water-TMS encourage point source dischargers to voluntarily improve their treatment process efficiency by understating effluent water quality through season-based, time-based analysis of real-time monitoring data.

The benefit from the cut of conventional monitoring expenses and the reduction of effluent loads exceeded the cost of the expenses establishing water TMS consisted of the control center and TMS of each point sources. According to the cost-benefit analysis of water-TMS, it was evaluated that the benefits of cost saving on manual analysis and effects of water quality improvement(reduction in pollutant load) outweighted cost for construction and operation of water-TMS control cent and on-line automatic measuring instrument in wastewater facilities by 23 million USD per year(Cho et.al., 2011). This full-fledged introduction of Water TMS applied to the large-scale treatment plants make the basis of real-time control of point dischargers by covering most of point sources based on the total flow although it covers only small portion of the number of whole dischargers.

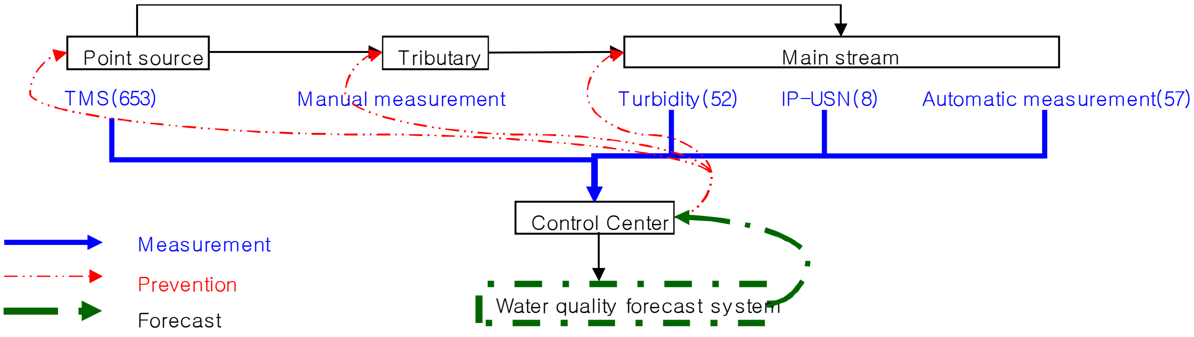

FIGURE 4. Water quality forecast scheme through integration of water quality monitoring data observed from point and non-point source.

In Korea, real-time monitoring system such as water-TMS for point source pollutant is expanding to non-point source discharge to protect the healthy water environment which provides drinking water and the aquatic ecosystem. Automatic river water quality monitoring system has operated at 56 stations at the main stream of four major rivers. The monitoring system based on Internet Protocol-Ubiquitous Sensor Network (IP-USN) has been tested at eight stations in the Four Major Rivers Restoration Project since 2010 to complement the existing real-time water quality monitoring system by giving more freedom of mobility and more chief cost by using mobile communication system

In the future, we expect to change current hybrid type water and water quality management system to fully real-time system. The success of Water TMS will be the footstone to integrate Water TMS, river water quality monitoring systems including manual, real-time automatic and IP-USN monitoring system. These real-time water management systems can be useful in enhancing more clean and healthy water environment, and can contribute to build a base infrastructure for a future advanced intelligent society. Now, Korea government is working to establish integrated water quality monitoring system for forecasting water quality a week in advance, contributing to prevention of water pollution accident (Figure 4).

ACKNOWLEDGEMENTS

This research was supported by Korea Environment Corporation (KECO) and accomplished by KEI.

REFERENCES

Cho E. S., Ahn. J. H., Choi. J. Y., Han D. H., Kim T.Y. 2010. Feasibility analysis for water-TMS expansion in monitoring parameter and subject.

Korea Environment Corporation (KECO). 2012. Water-Telemonitoring system (TMS) establishment and operation report. 2012.2

Ministry of Environment (MOE). 2008a. 2008 Operation state analysis of publicly owned treatment works. Sewerage Division.

Ministry of Environment (MOE). 2009a. 2009 Operation state analysis of publicly owned treatment works. Sewerage Division.

Ministry of Environment (MOE). 2010a. 2010 Operation state analysis of publicly owned treatment works. Sewerage Division.

Ministry of Environment (MOE). 2008b. 2008 Operation state analysis of Industrial complex wastewater treatment plant. Aquatic Ecosystem Conservation Division.

Ministry of Environment (MOE). 2009b. 2009 Operation state analysis of Industrial complex wastewater treatment plant. Aquatic Ecosystem Conservation Division.

Ministry of Environment (MOE). 2010b. 2010 Operation state analysis of Industrial complex wastewater treatment plant. Aquatic Ecosystem Conservation Division.

National Institute of Environment Research (NIER). 2011a. 2009 National water pollutant survey, Report/11-1480523-000429-10.

National Institute of Environment Research (NIER). 2011b. 2010 National water pollutant survey, Report/11-1480523-000429-01.

FLUORESCENCE FINGERPRINT PROPERTIES OF THE WASTEWATER OF AN INDUSTRIAL PARK*

C.B. XIE, ***J.WU***, Z.P.CAO, D.D. YIN (State Key Joint Laboratory of Environment Simulation and Pollution Control, School of Environment, Tsinghua University, Beijing 100084, P.R.China)

The conventional parameters to indicate organic pollution such as COD and BOD only represent the total amount of certain group of organic substances rather than the components. Fluorescence spectrum could exhibit organic components and unique for each sample like fingerprint, thus it is referred to as fluorescence fingerprint. This study investigated the properties of the fluorescence fingerprint of the wastewater of an industrial park in south China. The results showed that three main peaks A ($\lambda ex/\lambda em$=230/340 nm), B ($\lambda ex/\lambda em$=280/340 nm) and C ($\lambda ex/\lambda em$=235/440nm) located in all EEMs (see Fig.1). Peak A and B came from the domestic sewage and industrial wastewater from the park. Peak C was very likely mainly related to the textile wastewater. A peak locating at $\lambda ex/\lambda em$=285/440 nm in some samples may derive from the paper making wastewater. It is industrial wastewater, which accounted about 60-70% for the total wastewater, led to the big fluctuations in concentration and compositions of the industrial park wastewater. It seems that the fluorescence fingerprint could be a powerful tool to monitoring the variabilities of the wastewater components.

*Partially funded by 863 key project (SQ2009AA06XK1482350) and National major science and technology project about water pollution (2008ZX07313-007) and Tsinghua University Initiative Scientific Research Program (20101081863).

ISBN 9780976885351

#1083

ONSITE WASTEWATER TREATMENT SYSTEM FAILURE IN THE DICKINSON BAYOU WATERSHED

Aaron Forbis-Stokes, Clyde Munster, Bryan Boulanger, Binayak Mohanty (Texas A&M University, College Station, TX, USA)

Onsite wastewater treatment systems (OWTSs) are commonly used means of wastewater treatment in the Dickinson Bayou watershed, located between Houston and Galveston. The Dickinson Bayou is classified as “impaired” by the Texas Commission on Environmental Quality due to high levels of bacteria, specifically *E. coli*. Failing OWTSs within the bayou’s watershed are possible sources for the impairment of the bayou. Conventional OWTSs, comprised of a septic tank and a soil absorption field, rely heavily on soil treatment of effluent. The type of soils is a significant factor in treatment capabilities. In the Dickinson Bayou Watershed, soils are primarily composed of clays, which are known to be problematic for conventional systems as they restrict water flow and create perched water tables. These perched water tables may be flushed into surface waters during rainfall events. This project uses the HYDRUS modeling software to display OWTS water flow and contaminant transport through the soil profile to show system failure during rainfall events.

ISBN 9780976885351

REAL TIME MONITORING OF A SEQUENCING BATCH REACTOR WITH *IN-SITU* NIR SPECTROSCOPY

Nídia Dana Lourenço (Institute for Biotechnology and Bioengineering - Lisbon, Portugal)
Cláudio Fernandes de Almeida (Institute for Biotechnology and Bioengineering - Lisbon, Portugal)
João Almeida Lopes (REQUIMTE - Porto, Portugal)
Helena Maria Pinheiro (Institute for Biotechnology and Bioengineering - Lisbon, Portugal)

ABSTRACT: Sequencing batch reactors (SBR) present a high operational flexibility which is not fully exploited with the traditional monitoring approach of quantifying the incoming and the treated water quality parameters using retrospective and time-consuming analytical methods. For efficient operation, all wastewater treatment systems need real-time monitoring and supervision methods and this is an area where near-infrared (NIR) spectroscopy has a high application potential. However, the use of *in-situ* NIR spectroscopic data in this context has scarcely been reported. This study investigated the use of NIR spectra in multivariate statistical process control (MSPC) models for real-time monitoring and supervision of a laboratory-scale SBR treating a simulated textile wastewater with glucose as the main carbon source. Eight nominal cycles were used for MSPC modeling and 7 batches with imposed failures were monitored. All the imposed failures, including aeration failure and changes in the quality and quantity of the main carbon source, were detected in two statistical process control charts (Hotelling's T2 and SPE) derived only from *in-situ* NIR spectral information.

INTRODUCTION

Textile wastewaters are rated as the most polluting in all industrial sectors, including high organic loads and recalcitrant dyes. These dyes are resistant to degradation in conventional aerobic biotreatment, and thus alternative, staged anaerobic/aerobic regimes have been tested in sequencing batch reactor (SBR) systems, with clear success in the decolorization of the widely used azo dyes (Lourenço et al., 2001). One of the major advantages of SBR systems is their high operational flexibility but this advantage is not fully exploited with the traditional wastewater treatment monitoring approach that consists of quantifying the incoming and the treated water quality parameters using retrospective and time-consuming analytical methods in order to assess the compliance of the legal discharge requirements.

For efficient operation all wastewater treatment systems have urgent needs for efficient process supervision (i.e. monitoring quality and process variables, building and using process historical databases) and diagnosis methods. Online wastewater treatment monitoring became mandatory, particularly in industrial sites, and NIR spectroscopy has a high application potential in this area (Bonastre et al., 2005). In fact, NIR sensors are becoming particularly suitable for *in-situ* applications due to the availability of high-quality optical fibers and of robust spectrometers.

Multivariate Statistical Process Control (MSPC) methods are powerful tools for process supervision that have been successfully employed in several industries (Kourti, 2004), including wastewater treatment in SBR (Aguado et al., 2007, Villez et al., 2008). These methods comprise the establishment of multivariate control charts that allow the detection of deviations (faults) from normal operation and the diagnosis of possible causes. In spite of the recent availability of robust NIR immersion probes, the use of NIR spectra in MSPC models for wastewater treatment monitoring and supervision has scarcely been reported (Páscoa et al, 2008). This study investigated its use for real-time monitoring and supervision of a laboratory-scale SBR treating a simulated textile wastewater with glucose as the main carbon source.

ISBN 9780976885351

MATERIALS AND METHODS

Sequencing Batch Reactor Operation. A 1 liter SBR was inoculated with activated sludge from a full-scale wastewater treatment plant (WWTP) and was operated in 24-hour cycles with 5 discrete phases: static fill (45 min), reaction (21 h), settle (1 h), draw (1h) and idle (15 min). A glucose-based feed solution was prepared in aerated tap water with a theoretical chemical oxygen demand (COD) of 1000 mg O_2/L. This solution included 30 mg/L of an azo dye (Acid Red 14), 143 mg/L NH_4Cl, 760 mg/L KH_2PO_4 and 915 mg/L Na_2HPO_4. The reaction was divided in two sub-phases: an initial 12-hour mixed phase (starting after the end of the fill phase) and a subsequent 9-hour aerated phase. Air was supplied by an air pump through membrane diffusers and additional mixing was provided by magnetic stirring. Peristaltic pumps were used to fill and drain the SBR and the volumetric exchange ratio was fixed at 50%. The pumping, aeration and agitation functions were controlled by a computer using specifically developed software. Mixed liquor samples were collected along the SBR cycles and clarified by centrifugation for COD determination according to standard procedures (APHA, 1995). Daily purges of mixed liquor were taken manually towards the end of the mixed reaction phase in order to impose a sludge retention time (SRT) of 15 days.

NIR Spectra Acquisition. *In-situ* NIR spectra were acquired every 30 minutes along 22 batches with a portable NIR spectrophotometric system composed of a NIR512 temperature-regulated InGaAs array detector (Ocean Optics Inc.) effective in the 900-1700 nm spectral region, a tungsten light source model SL1 (StellarNet Inc.) and a T-300-RT-Vis-NIR transflectance dip probe (Ocean Optics Inc.) with a total optical path length of 1 cm. Optimized spectral acquisition conditions corresponded to setting detector temperature, integration time and number of scans to average to -4ºC, 650 ms and 80 scans, respectively. Blanks were performed with air (empty probe) and the OOIBase32 software (Ocean Optics Inc.) was used for spectrometer control and data acquisition.

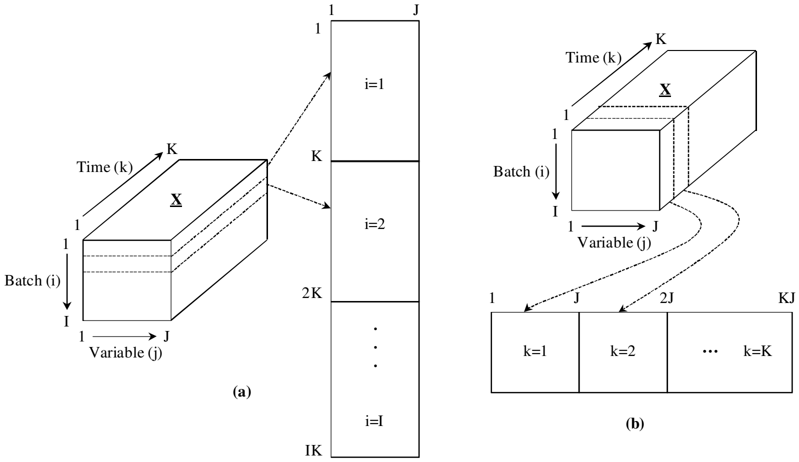

Figure 1 – Three-way matrix unfolding strategies used in the current work: (a) variable-wise unfolding and (b) batch-wise unfolding.

Chemometrics. Principal component analysis (PCA) of the acquired NIR spectra was performed for nominal batch selection. The main objectives of PCA are the transformation of the original data's co-ordinate system into a more relevant one and the reduction of the original system dimension through the use of a limited number of the Principal Components (PC's) which reflect the inherent structure of the data. A Principal Component model is an approximation to a given data matrix **X**, i.e., a model of **X** that is used instead of the complete original matrix, and can be represented according to $\mathbf{X}(n\times j) = \mathbf{T}(n\times d)\, \mathbf{L}^T(d\times j) + \mathbf{E}(n\times j)$, where *n* corresponds to the number of objects (samples), *j* to the number of variables (in the present case, wavelengths) and *d* to the number of PC's. **T** represents the scores matrix, **L** the loadings matrix, $\mathbf{L}^{\mathbf{T}}$ the transposed loadings matrix and **E** the residuals matrix.

For the particular case of spectroscopic data, PCA identifies the major sources of variance in the collection of spectra by defining a series of ranked components or factors and assigning each spectrum a score based on the relative contribution of each factor (Næs et al., 2002). The sources of variance, once identified, can aid in the visualization of the major data trends and the data collection can be reduced from a complicated multidimensional representation to a more easily visualized two or three-dimensional space (score plots) describing the main data information (Booksh, 2000).

A PCA-based approach was used for Multivariate Statistical Process Control (MSPC) model development. The three-way matrix $\underline{\mathbf{X}}$ consisting of *J* variables measured at *K* time points along each of the *I* batches was unfolded into a two-way matrix prior to PCA. This procedure is generally referred as Unfold PCA (U-PCA) and includes several possible unfolding strategies (Aguado et al., 2007). In the current work, only the variable-wise (Figure 1 (a)) and the batch-wise (Figure 1 (b)) unfolding strategies were tested. The acquired NIR spectra were exported to Matlab 7 (The Mathworks Inc.). PCA was performed with PLS_Toolbox 4.2 (Eigenvector Research Inc.) and MSPC models were developed in Matlab 7 using specifically in-house programmed chemometric functions. The standard normal variate (SNV) pre-processing method was used to correct spectral noise and background effects from the acquired spectra. The wastewater treatment process was monitored through the observation of two charts: the Hottelling T^2 chart, calculated from the selected principal components, and the squared prediction error (SPE) chart of the residuals, also referred as Q-statistic.

Spectra from 8 batches run under normal operating conditions (NOC) were used for MSPC model development. Seven batches with imposed abnormal operating conditions (AOC) were monitored and 7 additional batches (TEST, 1 nominal and 6 abnormal) were used to test the developed models. The main characteristics of these batches (SBR cycles) are described in Table 1.

Table 1 – Batches (SBR cycles) used for MSPC model development and validation.

Batch Number	Batch type	Characteristics
1-8	NOC	Nominal batches representative of adequate process behavior, used for MSPC model development
9, 11-15	TEST	Abnormal batches with several unintended mixing and aeration failures, used for test
10	TEST	Nominal batch used for test
16-17	AOC	Abnormal batches with acetate-based feed (1000 mg O_2/L as COD)
18	AOC	Abnormal batch with aeration failure
19	AOC	Abnormal batch with low glucose concentration (200 mgO_2/L as COD)
20-22	AOC	Abnormal batches with high glucose concentration (4000 mgO_2/L as COD)

RESULTS AND DISCUSSION

COD removal. Samples collected along the SBR cycles were clarified by centrifugation for COD determination and examples of typical COD removal profiles are presented in Figure 2.

It was observed that the nominal batches 8 and 10 had similar COD removal profiles, with the COD consumption occurring mainly during the first 8 hours of anaerobic reaction. In batch 16 the main carbon source was changed from glucose to acetate and the COD removal was negligible along this cycle. The wastewater fed in batch 19 had half the normal COD load and lower COD removal was observed in this cycle. In batches 20 and 21, the COD load of the feed solution had a 4-fold increase and despite the high removal levels attained during the anaerobic reaction, the residual COD was high at the end of batch 20 and accumulation was confirmed at the onset of the subsequent batch 21. Batch 12 had several mixing and agitation failures and the anaerobic COD consumption was compromised due to lack of biomass contact with the wastewater.

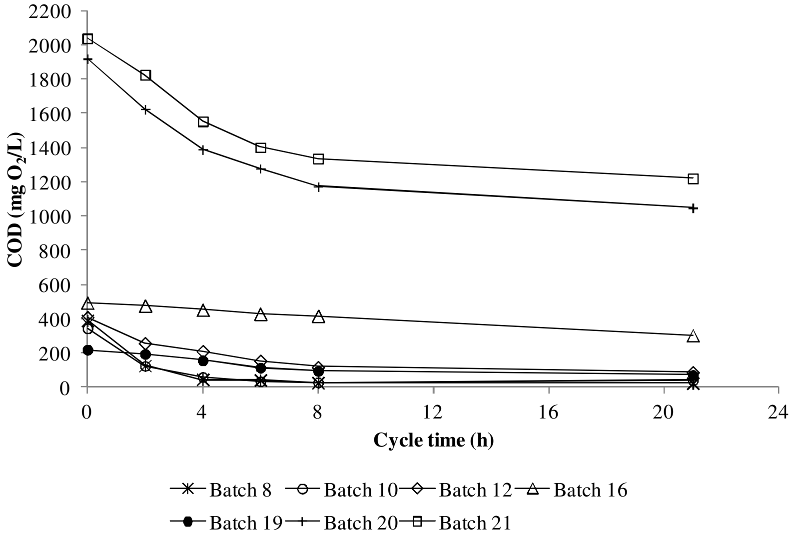

Figure 2 – Example of COD removal profiles observed during nominal and abnormal SBR cycles (batches).

Dataset selection. A preliminary analysis of the *in-situ* acquired NIR spectra was performed in order to detect abnormal (out-of-control) operation and ensure that only the in-control data, representative of the adequate process behavior, was used for MSPC model development. Four spectral regions (A, B, C and D, Figure 3) were excluded from the dataset. Regions A (880-965 nm) and D (1646-1720 nm) corresponded to saturation due to inherent equipment limitations. In region B (1215-1267 nm) the saturation was due to the presence of suspended biomass and in Region C (1319-1465 nm) it was attributed to the strong water absorption. Additionally, since during static fill, settling and discharge the NIR spectra were acquired with a low suspended biomass amount in non-homogenous mixed liquor, only the spectra acquired during the reaction phase were considered for MSPC model development.

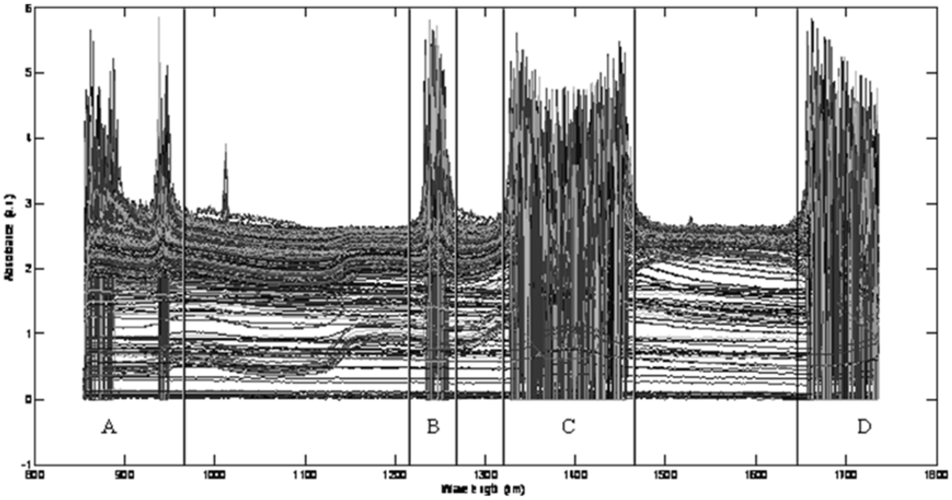

Figure 3 – *In-situ* NIR spectra acquired along 22 batches of SBR operation. Regions A (880-965 nm), B (1215-1267 nm), C (1319-1465 nm) and D (1646-1720 nm) were excluded in the developed models.

SBR monitoring with variable-wise unfolding MSPC models. One variable-wise unfolding MSPC model was developed with 8 NOC batches to monitor the SBR anaerobic/aerobic reaction phase and the corresponding statistical process control charts with projected TEST and AOC batches are presented in Figure 4.

It can be observed in Figure 4 that one sample of batch 8 is clearly above the confidence limits of the Hotelling's T^2 and SPE statistics, corresponding to an unusual variation both inside and outside the PCA model. This sample matched a mixing failure during the anaerobic reaction phase and the process returned to its normal state after mixing re-start. It can also be observed that the nominal TEST batch (batch 10) projected on the PCA model was identified as nominal in both statistics. All the other test batches exhibited significant deviations from normal behavior in both statistics of Figure 4. These deviations can be attributed to spectra acquisition with settled biomass due to unintentional repeated mixing and aeration failures throughout the batches. On the other hand, all the samples from the AOC batches are above the confidence limits in the SPE statistics, which is the statistic where most of the process faults are identified (Wise et al., 1999). In batches 16 and 17, the main carbon source was switched from glucose to sodium acetate. Batch 18 had an imposed aeration failure that was not accompanied by a mixing failure. Thus, the biomass was suspended due to mixing and the deviation observed was not as clear as those detected during the test batches with both aeration and mixing failures. Variable-wise unfolding models including only the anaerobic reaction or the aerobic reaction were developed and the results obtained were very similar to the ones obtained by modeling the two sub-phases simultaneously.

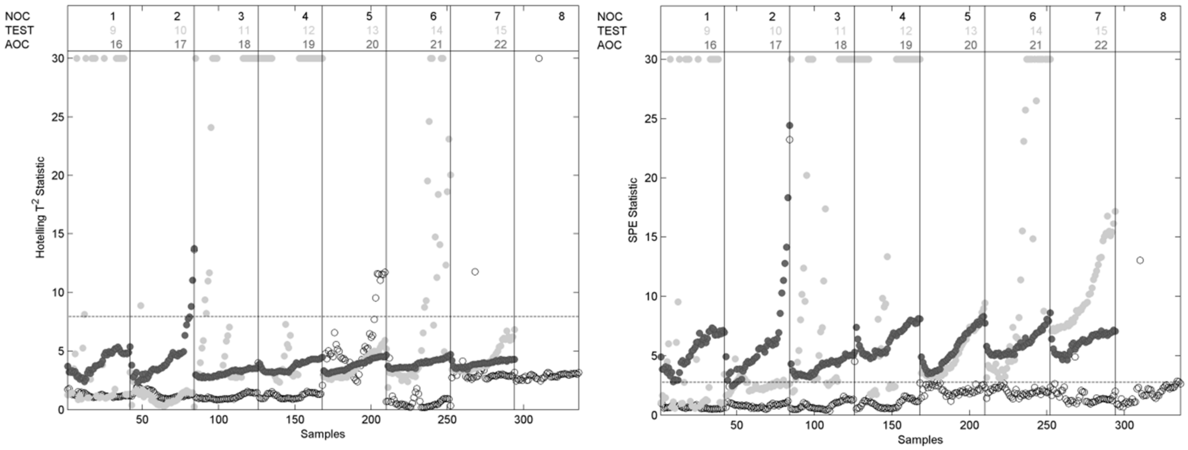

Figure 4 – Hotelling's T^2 and SPE statistics obtained for the variable-wise unfolding MSPC model developed to describe the SBR anaerobic/aerobic reaction phase. Dashed horizontal lines represent the 95% confidence limits, vertical lines divide different batches and top numbers identify SBR batches (Legend: ○ NOC, ● TEST, ● AOC).

In-situ NIR spectra obtained for the simulated textile wastewater with and without the azo dye were very similar (results not shown), which can be attributed to the low dye concentrations used in the current study. High color removal levels (> 90%) where attained in all monitored SBR cycles but failures related to color removal capacity of the system would not be identified by the developed MSPC models.

SBR monitoring with batch-wise unfolding MSPC models: Batch-wise unfolding MSPC models were developed with 8 NOC batches to monitor the SBR anaerobic/aerobic reaction phase and the corresponding statistical process control charts with projected TEST and AOC batches are presented in Figure 5.

It can be seen that the nominal TEST batch (batch 10) projected on the PCA model was identified as nominal in both statistics. All the other TEST batches were deviated from normal operation in the SPE statistic, similarly to the results presented in Figure 4 for the variable-wise unfolding model. The SPE statistic of the AOC batches with imposed failures was also above the confidence limit and all AOC batches were identified as abnormal. Batch-wise unfolding models including only the anaerobic reaction or the aerobic reaction were developed and the results obtained were very similar to the ones obtained by modeling the two sub-phases simultaneously.

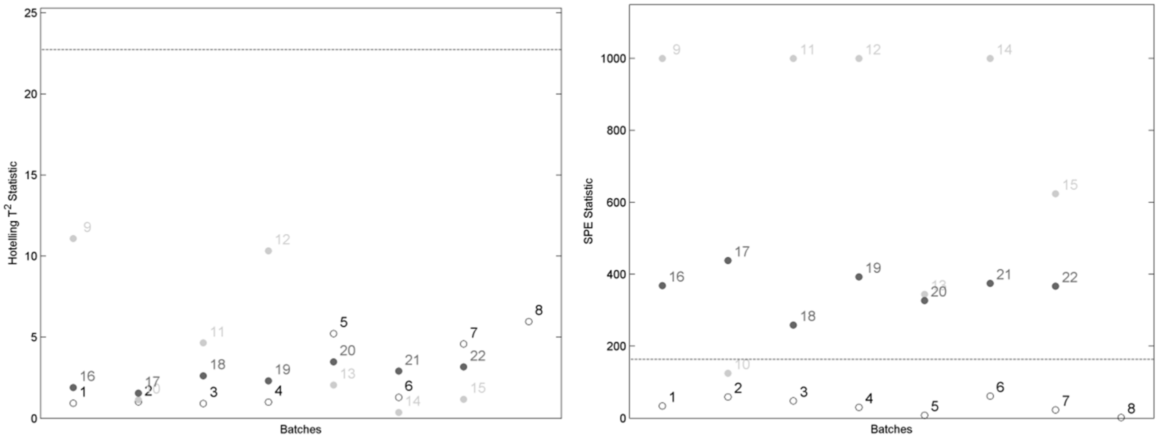

Figure 5 – Hotelling's T^2 and SPE statistics obtained for the batch-wise unfolding MSPC model developed to describe the SBR anaerobic/aerobic reaction phase. Numbers identify SBR batches (Legend: ○ NOC, ● TEST, ● AOC) and dashed horizontal lines represent the 95% confidence limits.

CONCLUSIONS

The use of *in-situ* NIR spectra revealed a high potential for real-time monitoring of the studied SBR system. All the developed models based on in-situ NIR spectra allowed the identification of deviations from normal process operation without the use of further analytical information. Mixing and aeration failures were easily identified, but batches with changes in the quality and quantity of the main carbon source were also detected. The models developed to monitor the anaerobic/aerobic reaction phase and the models developed to monitor the anaerobic reaction separately from the aerobic reaction, with variable-wise or batch-wise unfolding, presented good fault detection performance. Quantitative models should be developed with *in-situ* NIR spectra to predict COD along the SBR cycles. Further variables measured online (dissolved oxygen, redox potential, pH) could be incorporated in the models to enhance their diagnosis capabilities. In a laboratorial system several abnormal situations, which can hardly be imposed in a full-scale process, can be simulated in order to better evaluate MSPC model performance. However, the tools developed can be extended to continuous or batch full-scale systems.

AKNOWLEDGEMENTS

This work was financed by Fundação para a Ciência e a Tecnologia (FCT), Portugal, through the BIOTEXTILE project (PTDC/EBB-EBI/120624/2010). Nídia D. Lourenço acknowledges a post-doctoral fellowship from FCT (SFRH/BPD/31497/2006). This work has also been supported by Fundação para a Ciência e a Tecnologia through grant no.PEst-C/EQB/LA0006/2011.

REFERENCES

Lourenço, N. D., J. M. Novais, and H. M. Pinheiro. 2001. "Effect of Some Operational Parameters on Textile Dye Biodegradation in a Sequential Batch Reactor" *J. Biotechnol.* 89: 163-174.

Kourti, T. 2004. “Process analytical technology and multivariate statistical process control” *PAT – J. Proc. Anal. Technol.* 1(1): 13-19.

Bonastre, A., R.Ors, J. V. Capella, M. J. Fabra, and M. Peris. 2005. “In-line chemical analysis of wastewater: present and future trends” *Trends Anal. Chem.* 24: 128-137.

Aguado, D., A. Ferrer, J. Ferrer, and A. Seco. 2007. “Multivariate SPC of a sequencing batch reactor for wastewater treatment” *Chemom. Intell. Lab. Syst.* 85: 82-93.

Villez, K., M. Ruiz, G. Sin, J. Colomer, C. Rosén and P. A. Vanrolleghem. 2008. “Combining multiway principal component analysis (MPCA) and clustering for efficient data mining of historical data sets of SBR processes” *Wat. Sci. Technol.* 57(10): 1659-1666.

Páscoa, R.N.M., J. A. Lopes, and J. L. F. C. Lima. 2008. “In situ near infrared monitoring of activated dairy sludge wastewater treatment processes” *J. Near Infrared Spectrosc.* 16: 409-419.

APHA - American Public Health Association. A. D. Eaton, L. S. Clesceri, and A. E. Greenberg (Eds.) 1995. *Standard methods for the examination of water and wastewater.* 19th ed., Washington DC.

Næs, T., T. Isaksson, T. Fearn, and T. Davies. 2002. “Loadings and scores in principal component analysis (PCA)”. In *Multivariate Calibration and Classification*, pp. 39-42. NIR publications, Chichester, UK.

Booksh, K. S. 2000. “Chemometric methods in process analysis”. In R. A. Meyers (Ed.), *Encyclopedia of Analytical Chemistry*, pp. 8145-8169. Jonh Wiley & Sons Ltd, Chichester, UK.

Wise, B. M., N. B. Gallagher, S. W. Butler, D. D. White Jr, and G.G. Barna. 1999 “A comparison of principal component analysis, multiway principal component analysis, trilinear decomposition and parallel factor analysis for fault detection in a semiconductor etch process. *J. Chemometrics* 13: 379-396.

DISSEMINATION OF DECENTRALIZED WASTEWATER TREATMENT SYSTEM IN RURAL CHINA: OPPORTUNITIES AND CHALLENGES

Shikun Cheng, ***Zifu Li***, Heinz-Peter Mang, Sayed Mohammad Nazim Uddin, Xiaoqin Zhou and Elisabeth-Maria Huba*
(University of Science and Technology Beijing, Beijing, China)
(Technologies for Economic Development - TED, Maseru, Lesotho)

ABSTRACT: Domestic sewage and fecal sludge in rural areas of China is a peril to people's health that restricts the well-being life for rural inhabitants. Centralized wastewater treatment systems are costly to build and maintain, especially in rural China with low population densities and dispersed households. Alternatively, the decentralized approach for wastewater treatment which employs a combination of onsite and unpowered/low-powered cluster systems is attracting more attention. Currently, only a low percentage of wastewater is managed and treated in rural areas of China, against a large wastewater treatment gap. Opportunities for disseminating Decentralized Wastewater Treatment System (DEWATS) involve United Nations (UN) Millennium Development Goals (MDGs) and include the water pollution situation and deficiency of wastewater treatment facilities, intrinsic merits of DEWATS, national sanitation policy implication and reuse demand. Meanwhile, challenges faced are emphasized, which come down to: conventional centralized water-borne concept restrict the development of DEWATS and should be transformed, fund shortage results in the unaffordable of DEWATS, more reuse and resource recovery elements should be taken into consideration, final effluent quality from overcharged DEWATS is still uncertain, maintenance know-how of DEWATS should be informed, follow-up services is lagging and should be improved.

INTRODUCTION

In October of 2005, China government put forward the programme which is called New Socialist Countryside Construction. Against this backdrop, environmental protection in rural areas of China became more and more important. Therein, domestic sewage and fecal sludge in rural areas of China is a peril to people's health that restricts the well-being life for rural inhabitants.

Domestic wastewater in rural China is characterized by followings: firstly, population is scattered and sewage pipe network is unsound; secondly, water consumption is small but composition of mixed wastewater is complex; thirdly, the pollution of domestic wastewater is at a uncontrolled level and it contains a certain amount of synthetic detergent, virus, bacteria and parasite ova instead of heavy metal and other toxic substances; fourthly, nutrient elements such as nitrogen and phosphorus are high especial from toilet blackwater; fifthly, water quality as well as water quantity fluctuates a lot with a high daily variation coefficient (3.0-5.0 normally) (Cao and Liao, 2010; Yang, 2011).

As for wastewater treatment model, two ways could be chosen: centralized or decentralized. Centralized wastewater treatment systems are costly to build and maintain, and rely on additional huge water amounts for flush transport, especially in areas with low population densities and dispersed households. Alternatively, the decentralized approach for wastewater treatment which employs a

---

ISBN 9780976885351

combination of onsite unpowered/low-powered and water saving cluster systems is attracting more attention (May et al., 2009). DEWATS, short for Decentralized Wastewater Treatment System, was originated in China in 1988 as biogas septic tank. Starting in 1994, DEWATS have been further developed by contributing organizations from China, India and France under coordination of Bremen Overseas Research and Development Association (BORDA e.V.).

There are fewer discussions about DEWATS in China than other developing countries. This paper mainly presents the opportunities for dissemination of DEWATS in rural China; while there are many impediments and challenges towards DEWATS as well. Therefore, challenges faced are discussed afterwards.

OPPORTUNITIES FOR DEWATS IN RURAL CHINA

Millennium Development Goals. At the opening of new millennium, the United Nations (UN) Millennium Development Goals (MDGs) unveiled a special horizon - one that the entire developing world has been tasked to arrive at by 2015. To arrive at this moment of achievement, though, the world must first cross the water barrier (ADB/UNDP/UNESCAP/WHO, 2006). Providing reliable and affordable wastewater treatment in rural areas is a challenge in many parts of the world, particularly in developing countries. China is endowed with the largest population in the world, in which, rural population is 674 million (NBS, 2010). As roughly estimated, there is approximately 9 billion tons of domestic wastewater discharged every year in rural areas of China (Zhou et al., 2008).

The world is striving to meet MDGs while China is no exception. As most people without accessing to safe drinking water and sanitation dwell in rural areas, the efficiency of wastewater in rural areas plays a significant role in fulfilling MDGs. In China alone, the population in rural China that suffers from contaminated water sources reaches 90.84 million (NDRC/MWR/MOA, 2005). Popularization of DEWATS seems to increase the possibility of achieving some of the MDGs, i.e. mainly to halve, by 2015, the proportion of the population without sustainable access to safe drinking water and basic sanitation, ensuring environmental sustainability and reversing the loss of environmental resources. Increasing the accessibility to water and sanitation does not imply overexploitation of the existing resources, but improving their management by reducing, recycling and reusing as well as identifying new water sources such as storm water and reclaimed wastewater (Giovanni et al., 2012). DEWATS is a promising approach with the features of low investment cost, simple maintenance, wastewater reclamation, biogas production, nutrient reuse and sludge recycling, which fits the circumstance of rural areas well.

Intrinsic Merit of DEWATS. DEWATS are based on a set of treatment principles, which ensure treatment reliability, longevity, and tolerance towards inflow fluctuations. DEWATS work without or with very low energy input, so that the systems cannot be shut down accidentally and most of the materials/inputs are locally available; it therefore presents an affordable solution guaranteeing long-term, reliable operation (BORDA, 2009). Practice has shown that DEWATS have many advantages compared to centralized sewage plant. The lack of elaborate sewer systems dramatically reduces the investment and operation and maintenance costs. DEWATS can remove organic pollutants, pathogens and parasite eggs (Sasse, 1998), if possible with recovery of biogas as fuel. DEWATS could be constructed underground without occupying land. Moreover, DEWATS have less impact on environment and are suitable to the ecological sensitive region (Lu et al., 2009). DEWATS are not the best solution in every case. However, where skilled and responsible operation and maintenance cannot be guaranteed, DEWATS technologies are undoubtedly the best choice available.

Water Pollution and Infrastructure Deficiency. There is a trend that environmental pollution transfers from urban areas to rural areas. In this case, infrastructure construction aiming at wastewater treatment in rural areas is significant to improve rural environmental quality. Rural areas usually do not have sewage systems, about 96% of villages are absent of drainage and wastewater treatment system (Bai et al., 2008). Almost all of the domestic wastewater and runoff are discharged directly to the surface water. This situation has led to serious non-point pollution in many areas.

According to the 2nd Nationwide Agricultural Census, coverage of wastewater treatment at township level only reaches 19.4% via centralized way until the end of 2006 while the data at village level is not available yet. The absence of statistic at village level indicates the more scarcity of wastewater treatment facilities (NBS, 2008). What is more, the wastewater treatment facilities are very simple and primary. Mostly, only septic tank or biogas digester is built. These primary treatments cannot guarantee the harmless disposal of wastewater and effluent quality (Wang et al., 2011).

The absence and defect of infrastructure creates demand for DEWATS because the problems and limitations of the centralized approaches for wastewater treatment are progressively surfacing. Rural areas lack both the funding to construct centralized facilities and the technical expertise to manage and operate them. Alternatively, DEWATS allows for flexibility in management, and simple as well as complex technologies are available. DEWATS are ideal for treating the domestic wastewater of small cities, townships and villages as well as communities/ peri-urban areas, which have no sewage pipeline networks.

Government Support and Policy Drive. As early as 2000, former Ministry of Construction, former State Environmental Protection Administration (SEPA), Ministry of Science and Technology co-released Technical Policy on Municipal Wastewater Treatment and Pollution Prevention, which explicitly stipulated that the dispersive settlements without accessing to municipal sewage collection system should adopt onsite wastewater treatment approach and make the treated effluent meet the standard. In 2007, SEPA released Opinions on Strengthening Rural Environmental Protection Work, which explicitly specified to strengthen pollution control of wastewater in rural areas.

Ministry of Agriculture set a target of reducing emission level of agricultural pollutants by 50% during 11th Five-Year Plan (MOA, 2006). Until end of 2012, it is expected that treatment ratio of rural domestic wastewater will increase by 10% compared with 2010. During 12th Five-Year Plan, Ministry of Housing and Urban-Rural Development (MOHURD) will conduct to draw up technical guideline on rural domestic wastewater treatment. Demonstration project for wastewater treatment and reclamation in rural areas of China will be constructed. At the end of 2010, MOHURD firstly released the Guideline on Rural Domestic Wastewater Treatment (draft version).

Under the instruction of central government, lots of local regulations and policies were established, which are normally stricter than central government. For instance, Sichuan Province took the leading role in the implementation of DEWATS by the promulgation of a provincial policy.

Reuse Demand. China is a water-shortage country. According to statistics, 80 million rural people face the deficit of drinking water. As for agriculture, annual water-shortage gap reaches up to more than 30 billion m^3, 60% of cultivated land is lack of irrigation water. As a result, output of food is reduced by 35-40 billion tons per year (Li, 2012). On account of unreasonable use of chemical fertilizers, some farmlands were seriously polluted and excessive discharge of nitrogen and phosphorus causes eutrophication, which is disastrous for water bodies (Zhang and Zhang, 2008). Meantime, there is a great demand for organic fertilizers in China; especially producers of fruit aimed at export are in the need to fulfill ecological-label requirements. It is desired that waste can be recovered, not only reduce pollution but also improve environmental sustainability.

The idea of DEWATS is a closed-loop approach, which makes better use of the resources in wastewater and increase recycling rates. After DEWATS, wastewater from several flow streams is disposed to reach discharge standards and permit hygienic reuse in agriculture. Instead of treating a waste, a valuable resource is being exploited. Effluent from DEWATS is suitable for surface irrigation. Processed wastewater can be used for fish farming when diluted with fresh river water or after extensive treatment in pond systems. Sludge from DEWATS could be used to produce organic fertilizer. Theoretically, removal of each kg COD may produce 0.35 m^3 methane (Mang and Li, 2010). Organic wastewater could generate considerable biogas as a substitution of cooking fuel.

CHALLENGES FOR DEWATS IN RURAL CHINA

Conceptual Transformation. Public acceptance of DEWATS is an important issue for dissemination. Public awareness towards the problem of wastewater pollution has grown tremendously in recent years. However, rural people are still lack of knowledge and even have misperceptions about DEWATS. In some places, when residents or farmers were interviewed about the DEWATS in front of them, they had no idea about these structures. Local farmers prefer chemical fertilizer instead of organic fertilizer. They did not consider sludge from DEWATS as useful resources. On the contrary, they hope to be paid if they use the “waste sludge” from DEWATS (Cheng et al., 2010).

If DEWATS are to become accepted as a wastewater treatment solution, people need to be educated about the benefits of this choice. Educational materials directed to farmers or operators should explain proper wastewater disposal and maintenance practices, as well as provide information about the consequences of system failures (Aditi et al., 2011). Increased awareness about decentralized systems ought to help to reduce the number of failing systems and the eventual negative effects on groundwater and surface water.

Fund Shortage. The urban and rural dual structure in China renders the unbalanced investment between urban areas and rural areas. As economic level in rural areas is low, investment to wastewater treatment is limited. Since the DEWATS treat domestic wastewater in a decentralized way, the principle of building the system is: “Those who need wastewater treatment will be obliged to build the system (DEWATS); those who build the DEWATS will invest and benefit.” Money is often not the biggest problem, at least for pilot or demonstration projects. However, there is a general helplessness when it comes to individual implementation, and more so when it comes to active and well organized dissemination of DEWATS.

As it stands, the investment is normally borne by the user or beneficiary without government subsidy. For rural areas, it is not easy to take in social funds for rural areas and financing channel is single. The fund shortage in rural areas restricts the development of DEWATS. Even if DEWATS is endowed with the advantage of low maintenance cost, sometimes it still needs maintenance fee such as electricity and chemical agent.

Reuse Issues. Domestic installations have an impact on quality and quantity of domestic wastewater. Domestic wastewater mainly includes toilet blackwater, kitchen wastewater, shower and laundry greywater. Most of nutrient elements such as nitrogen and phosphorus in the domestic wastewater come from human and in farm households also from animal excrement (Li, 2011).

The currently existing DEWATS designs in China usually neglects reuse elements. The nitrogen and phosphorus resources are always not recovered and utilized (Yang et al., 2011). Source separation and collection of urine and feces should be taken into consideration when implementation of DEWATS; if the effluent fulfils irrigation standards, it can be applied on the fields for irrigation purposes; if the treated effluent fulfils the necessary standards, it can be used for landscape water body or groundwater recharge; if hygienically safe, sludge from anaerobic digestion can be used as fertilizer; biogas production should be encouraged.

Uncertain effluent quality. The inflow of rural domestic wastewater is of big fluctuation. Under the unsupervised circumstance, there is a possibility that DEWATS may be out of function, leading to the substandard effluent quality. Limited by conventional technology and design concept, many designers and equipment suppliers only put emphasis on removal of COD and BOD_5 but neglect denitrification and dephosphorization of DEWATS effluents, in case effluent is not agriculturally reused.

Additional, approved regulations and standards are absent in view of construction and acceptance of DEWATS. Moreover, there is still no special discharge standard aiming at rural domestic wastewater effluent. For the targeted wastewater in rural areas, designers often follow the different standards. It is suggested to draw up special effluent discharge standards for rural wastewater.

Follow-up Service and Management. At present, when one project is finished, there is no specification for completion acceptance to follow, thus quality of DEWATS cannot be controlled effectively. In some areas, the fact is that once DEWATS is built, no one will take care of it any more. DEWATS special literate staffs are in short supply in rural China and once out of function, it is left to be unrepaired for a long time. The users or operators may not be professional technician but at least be trained the know-how of DEWATS.

Wastewater treatment in rural areas is a kind of complicated system engineering, which is involved in mult-departments including construction, environmental protection, agriculture and forestry, hygiene, etc. When put into effect, DEWATS face the mult-management from different departments. That is to say, implementation of DEWATS must experience a series of examinations and approvals, which counterchecks the dissemination of DEWATS.

CONCLUSIONS

There are several opportunities for DEWATS development in rural China, including fulfilling MDGs, water pollution situation and deficiency of wastewater treatment facilities, advantages of DEWATS compared to centralized sewage plant, government support and policy drive for rural wastewater treatment, reuse demand for resources. Meantime, challenges are encountered and should be overcome, which include conventional concept restriction, fund shortage, reuse issues, uncertain effluent quality, follow-up service and management.

Training should be conducted to raise the level of DEWATS know-how during dissemination; more funds should be invested to rural wastewater treatment; more reuse element should be taken into consideration for DEWATS implementation; standards of DEWATS construction monitoring and effluent quality is suggested to make; measures should be taken to improve the follow-up service and management of DEWATS.

ACKNOWLEDGEMENTS

This research work was supported by the Fundamental Research Fund for the Central Universities of China and the authors would like to thank the sponsor.

REFERENCES

ADB, UNDP, UNESCAP, and WHO. 2006. *Asia Water Watch: Are Countries in Asia on Track to Meet Target 10 of the Millennium Development Goals? 2015.*

Aditi, M., and T. Sorada. 2011. "Review of socio-economic drivers of community acceptance and adoption of decentralised water systems." *J. Environ. Manage.* 92: 380-391.

Bai, X., W. Gu, F. Wo, C. Yang, and Q. Qiao. 2008. "Introduction and Outlook of Rural Domestic Wastewater Treatment" (In Chinese). *Agro-Environment & Development.* 6: 59-62.

BORDA. 2009. *DEWATS and Sanitation in Developing Countries: A Practical Guide.*

Cao, H., and Q. Liao. 2010. "Application of Decentralized Sewage Treatment Technology to the Domestic Sewage Treatment in Rural Areas" (In Chinese). *J. Anhui Agric Sci.* 38(29): 16431-16432, 16563.

Cheng, S., F. Wu, T. Wang, and X. Du. 2010. *A Field Study on DEWATS in Sichuan Province, China.*

Giovanni, L., A. V. Ghirardini, and F. Avezzù. 2012. "To Centralise or to Decentralise: An Overview of the Most Recent Trends in Wastewater Treatment Management." *J. Environ. Manage.* 94: 61-68.

Li, C. 2012. "Current Situation of Rural Water Resources and Countermeasures" (In Chinese). *Technology Innovation and Application.* 1: 165.

Li, Z. 2011. "Structure and Outlook of Water System in Eco-City" (In Chinese). *Construction Science and Technology.* 19: 32-35.

Lu, H., H. Yuan, Z. Jian, and L. Wang. 2009. "Expectation for Decentralized Sanitation and Reuse" (In Chinese). *Environmental Science and Technology.* 22, (S1): 76-78.

Sasse, L. 1998. *Decentralised Wastewater Treatment in Developing Countries.* BORDA, Bremen.

Mang, H., and Z. Li. 2010. *Technology review of biogas sanitation.* GIZ, Eschborn.

May, A. M., A.Tarhini, and J. A. Nasr. 2009. "Decentralized approaches to wastewater treatment and management: Applicability in developing countries." *J. Environ. Manage.* 90: 652-659.

Ministry of Agriculture (MOA). 2006. *National Agriculture and Rural Economic Development 11th Five-Year Plan* (In Chinese).

National Bureau of Statistics (NBS). 2008. *2nd National Agricultural Census* (In Chinese).

National Bureau of Statistics (NBS). 2011. *6th Nationwide Population Census* (In Chinese).

National Development and Reform Commission (NDRC), Ministry of Water Resources (MWR), and Ministry of Agriculture (MOA). 2005. *National Rural Drinking Water Safety Engineering Plan (2006-2010)* (In Chinese).

Wang, J., and L. Zhang. 2011. "Current situation and influence factor of rural decentralized wastewater treatment facility" (In Chinese). *Agro-Environment & Development.* 6: 65-70, 89.

Yang, L., Y. Huang, Y. Zhou. H. Wang, and J. Liang. 2011. “Technical Applicability for Decentralized Sewage Treatment in Rural Areas” (In Chinese). *J. Anhui Agric. Sci.* 39(15): 9199-9201.

Yang, X. 2011. “Patterns of Rural Sewage Treatment” (In Chinese). *Beijing Agriculture.* 5: 192-194

Zhang, Z., and W. Zhang. 2008. “The situation and trend of fertilizer application in China” (In Chinese). *Phosphate & Compound Fertilizer.* 23(6): 9-12.

Zhou, L., B. Lee, and J. Li. 2008. “Wastewater Facility Construction in Rural Korean and Apocalypse for Water Pollution Control in New Rural China” (In Chinese). *J. Agric. Sci. Tech.* 10(4): 42-47.

A MICROFLUIDIC PLATFORM FOR MULTI-PARAMETRIC WATER QUALITY ANALYSIS

John Cleary*, Damien Maher, Deirdre Cogan, Dermot Diamond (Dublin City University, Ireland)

A microfluidic analyser platform for a number of key water quality parameters has been developed. The platform utilises colorimetric reagent chemistry for detection and quantification of phosphate, nitrate, pH and chemical oxygen demand (COD). The system integrates microfluidic analytical systems, optical detection systems, and wireless communications into a low-cost, portable device capable of autonomous operation under environmental conditions for extended periods. The platform has been successfully tested and validated under various conditions including deployments in freshwater, estuarine water and municipal wastewater.

The system uses the vanadomolybophosphoric acid method for phosphate detection, the chromotropic acid method for nitrate detection, a combination of pH indicators for pH measurement, and a variation of the standard method using dichromate for COD analysis. In each case a colour change is developed after mixing the water sample with a reagent (or combination of reagents) in a microfluidic manifold where mixing and reaction take place. The colour change is detected using a light emitting diode (LED) and photodiode based optical detector, allowing quantification of the target analyte in the original sample. Data is stored on a Flash memory chip and also transmitted to the user via wireless communications. Wireless communication modes such as GSM or ZigBee radio are chosen according to the specific application in question. In this paper we describe the design and operation of the analyser platform and present data from laboratory and field trials of the system.

ISBN 9780976885351

#1113

PORTABLE LAB-ON-A-DISC WIRELESS SYSTEM FOR *IN-SITU* MULTIPARAMETER WATER QUALITY ANALYSIS

Monika Czugala, Damien Maher, Kevin J. Fraser, Dermot Diamond and Fernando Benito-Lopez*
(CLARITY: Centre for Sensor Web Technology, National Centre for Sensor Research, Dublin City University, Ireland), Jens Ducree and Robert Gorkin (National Centre for Sensor Research, School of Physical Sciences, Dublin City University, Ireland)

Miniaturization of analytical devices through the advent of microfluidics is an important step forward in the environmental monitoring, since sample accessing, reagents addition, measurements and calibration can be replicated on a micro-scaled equivalent to bench instruments. Micro total analysis systems provide a route to the generation of micro-dimensioned analytical instruments that can be operated in remote locations, enabling *in-situ* water analysis. In this work we report a novel system for the *in-situ* multiparameter water quality monitoring.

The micro-fluidic centrifugal platform, based on a pH dye/ionogel sensing area, offers many advantages over standard lab-on-a-chip systems such as the elimination of large power supplies and external pumps. The CD is combined with a low-cost, wireless optical sensor, paired emitter detector device (PEDD), and allows for monitoring the pH and the degree of turbidity of water samples in real time. The platform contains large chambers with several sub-compartments for various functions.

A low-cost, autonomous, custom designed CD analyser allows for the *in-situ* rotation of the disc as well as accurate measurements. The disc angular velocity and positioning are controlled using employed stepper motor. Apart from the low-power detection and the communication system, the integration of a wireless communication device allows the acquisition of parameters to be controlled remotely and to be adjusted according to individual needs, in addition to enabling data transfer.

The calibration of the sensor using standard buffer solutions at different pH resulted in a sigmoidal curve that is characteristic of the Bromocresol Purple dye, showing a pKa value of 6.6 for the solid-state pH sensor. Next, real samples from the River Tolka, Dublin (Ireland) were tested, and good correlation between pH results obtained using the PEDD system and a standard pH-meter was achieved. In the case of turbidity, although the samples contained low solid contents, it was possible to separate them from the sensing area, avoiding inaccurate pH measurements. We believe that this device will be of special interest in samples with a relatively high level of solid contaminants that could interfere with optical analytical measurements.

ISBN 9780976885351

AZO DYE BINDING INTERACTIONS WITH FRESHWATER AND TREATED WASTEWATER DISSOLVED ORGANIC MATTER

Tanveer Ahmed*, Keiichi Ohta and Masahiro Maruo
(University of Shiga Prefecture, Hikone, Shiga, Japan)

Binding interactions of Congo red (azo dye: CR) with extracted fulvic acid from Lake Biwa (LBFA), naturally organic carbon rich Shirakoma Pond water (SKPW) and treated sewage wastewater (TWW) dissolved organic matter (DOM) were investigated in low *in situ* dissolved organic carbon level (~ 3.5 mg/l). Binding coefficients (K_{oc}) were measured using fluorescence quenching techniques with a low inner filter effect (<1.05). K_{oc} values were compared for the similar DOM:CR organic carbon ratios and ionic strength (0.01 M, $Na\text{-}PO_4$ buffer soln.) along with the effects of different solution pH and temperature. K_{oc} at five different temperatures (20-35 °C) and three pH levels (4.0-9.0) were calculated using modified Stern-Volmer equation. Stern-Volmer plots and data obtained by high performance size exclusion chromatography (HPSEC) suggested about two folds higher binding magnitudes for higher molecular weight freshwater DOM samples than that of TWW DOM at solution temperature of 20 °C and pH 7.0. Effective distance between the CR complex (donor) and the DOM components (acceptor) of the freshwater and TWW samples were calculated to be in the range of 2-4 nm based on Förster's non-radioactive energy transfer theory. Negative ΔG and positive ΔS Values suggested that the binding interactions were spontaneous at higher temperature for all DOM-CR complexes with the predominance of hydrophobic interactions. However, unlike freshwater DOM-CR complexes, binding magnitudes for TWW DOM increased under alkaline condition (pH 9.0), which may be due to colloids/micellar formation, enhanced ionic or functional group activities. Under ambient temperature and pH ranges of 7.0-9.0, organic carbon rich water exhibited higher ability to uptake the CR complex compared to that in the elevated temperature and acidic water condition.

ISBN 9780976885351

MODELING THE TRANSPORT OF FECAL MICROORGANISMS IN NORWEGIAN DRINKING WATER SOURCES (LAKES)

Ingun Tryland, ***Torulv Tjomsland***, Dag Berge, Magdalena Kempa (Norwegian Institute for Water Research, Norway) and Venkat S. Kolluru (ERM, USA)

ABSTRACT: Lakes are often used as drinking water sources in Norway. The occurrence of fecal microorganisms at the deep water intake of lakes depends on the discharge of feces from warm-blooded animals, including humans, to the lake, and on the dilution, transport and survival of the fecal microorganisms in the lake. The hydrodynamic model GEMSS was used to model the transport of *E. coli* and microbial pathogens in Lake Maridalsvannet, the main drinking water source of Oslo, Norway's capital city. The modeled concentrations of *E. coli* at the deep water intake generally corresponded well with the observed concentrations. The model was used for exploring differences between different microbes, e.g. the transport of oocysts of *Cryptosporidium* with slow decay compared with *E. coli* which has a more rapid decay. The modeling effectively visualized the importance of different discharges to the lake and the impacts of potential future pathogen discharges if the current protective measures in the catchment area are loosened up. Combined with an approach based on quantitative microbial risk assessment (QMRA) to estimate the potential health risk associated with pathogen discharges and potential failure in the water treatment, such simulations provided good arguments for maintaining the protective measures in the catchment, even though the drinking water treatment plant has been upgraded.

INTRODUCTION

As Norway has very little ground water, lakes with deep water intake, are often used as drinking water sources. Protection of the drinking water sources has been an important principle in Norwegian drinking water management, and restrictions in the catchment area have often been implemented. Such protective measures include restrictions on house and cottage building, discharge of wastewater, livestock husbandry, as well as on recreational activities. Due to a generally good raw water quality, the water treatment at many Norwegian drinking water treatment plants has been simple, often only micro-sieving and chlorination. After a large waterborne disease outbreak caused by the chlorine-resistant parasitic protozoa *Giardia lamblia* in Bergen, Norway's second largest city, in 2004, several drinking water treatment plants were upgraded all over the country, with two hygienic barriers against most microbial pathogens. Upgrading the water treatment has raised a debate concerning the need for maintaining the restrictions in catchment areas of drinking water sources. Water supply managers are challenged both by politicians and the public, who want less stringent restrictions. For example, the main drinking water treatment plant of the city of Oslo was upgraded in 2008 and now includes coagulation, filtration, UV-treatment, (chlorination) and corrosion control. The raw water is taken from Lake Maridalsvannet. The catchment area of Lake Maridalsvannet is a very popular hiking area, and the public want to swim and fish in the lake. About 800 people live in the catchment area, and more people want to upgrade their cottages to permanent housing. At present, wastewater from toilets is collected in closed tanks and the grey water is treated in biofilters on site. There are also approximately 20 farms in the catchment area. Although commercial animal husbandry is not allowed, horse riding stables are growing more and more popular, and there are now approximately 100 horses in the valley, many which are owned by city residents. The new and costly water treatment plant is used as an argument for fewer restrictions that forbid swimming, fishing, camping, new house building and most farm animals in the catchment area. On the other hand, people responsible for the water supply are worried about the hygienic pollution such activities may represent. They are also aware of the fact that even the most modern water treatment plant can

---

ISBN 9780976885351

occasionally fail, and in some situations the old treatment plant with only micro-sieving and chlorination may still be used. A better understanding of the consequences different activities in the catchment area will have on the hygienic water quality at the deep water intake of the lake was therefore requested. Newly recognized threats, like UV-resistant viruses (Shin *et al*., 2009), in addition to chlorine-resistant parasitic protozoa, also call for a better understanding of processes like occurrence, retention and transport of different pathogens within the drinking water source itself. It is well recognized that oocysts of *Cryptosporidium*, cysts of *Giardia*, as well as some enteric viruses, may survive much longer in drinking water sources than the fecal indicator bacteria *E. coli* and intestinal enterococci (Espinosa *et al.*, 2008; Robertson and Gjerde, 2006), and that such indicators do not always correlate well with the occurrence of pathogens.

The occurrence of fecal microorganisms at the deep water intake of a lake depends on the load of human, animal (mammal) and bird feces to the lake, and on the dilution, transport, settling and survival of the fecal microorganisms in the lake. Hydrodynamic modeling, combined with modules which describe decay kinetics, is a useful tool for simulating the transport of pathogens in lakes, and to explore differences between pathogens with different properties (Hipsey *et al*., 2008). In the present work a pathogen transport model was set up for Lake Maridalsvannet. The model was used for visualizing the impacts of different “theoretical pathogen discharges” to the lake, on the raw water quality. This was combined with an approach based on quantitative microbial risk assessment (QMRA, WHO, 2008), for estimating the potential health risk associated with pathogen discharges and potential failure in the water treatment. The aim was to provide a tool for decision making in the discussion whether or not to lessen restrictions and protective measures in the catchment area, in light of the new and improved water treatment at the water work.

PATHOGEN TRANSPORT MODEL

A 3-D model package named GEMSS (Generalized Environmental Modeling System for Surface waters) was used. The model package has been developed by ERM's Surface water Modeling Group in Exton, USA (www.erm-smg.com). The core of the package is a hydrodynamic model, with modules for sediment transport, water quality, etc., which can be added when needed.

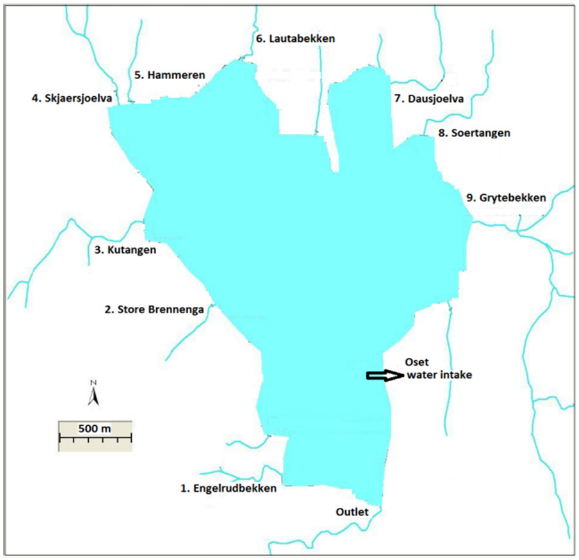

FIGURE 1. Lake Maridalsvannet with inlet streams, outlet river and raw water intake. The lakes area is 3.7 km^2, maximum depth 45 m and theoretical retention time 140 days. The catchment area is 252 km^2.

The model was used for simulating the transport of *E. coli* and “model pathogens” with different decay rates in Lake Maridalsvannet. Data about weather (air temperature, dew point temperature, solar radiation and wind) and water flows in the tributaries, outlet river and raw water intake are inputs to the model. The model was set up and run with data from 2006, which is considered a representative year. The data was provided by the Norwegian Meteorological Institute, Norwegian Water Resources and Energy Directorate and the City of Oslo, Water and Sewerage Works. The fecal indicator bacteria *E. coli* (or fecal coliforms) are monitored in the main inlet rivers and streams of Lake Maridalsvannet (monthly), as well as in the raw water intake at the water treatment plant (weekly). *E. coli* was therefore used for verifying the pathogen transport model. The main discharges of *E. coli* to the lake come from the inlets, as well as from bird droppings directly onto the lake surface. For simplification some of the inlets were combined reducing the number to 9 different "fecal discharge points" that were used in the model (Figure 1). The average discharges of *E. coli*, which are inputs to the model, were estimated based on historical data and varied from 100-1000 *E. coli* per 100 ml in the different inlet streams. The lake was divided in calculation cells, horizontal arrays of 150 m x 180 m and vertically 1 m in depth. The model calculated the concentration of *E. coli*/pathogens in each cell every hour over the year.

After calibration, the modeled concentrations of *E. coli* at the deep water intake (about 35 m depth) generally corresponded well with the observed concentrations (Figure 2). In Lake Maridalsvannet concentrations of *E. coli* in the raw water typically increase in November-December during the autumn lake turn over (circulation). In the period end of January to March, the lake is most often covered by ice, and with a stable water column in inverse temperature stratification below 4 ºC, the observed *E. coli* concentrations in the deep water are low. The spring turnover (in April) is often of short duration, and increased levels of *E. coli* are seldom observed in the weekly monitoring. Bird droppings and sedimentation with particles, were not included in the model, hence, occasional empirical observations of low levels of *E. coli* (1 per 100 mL) during the summer period when there is temperature stratification in the lake, were not revealed by the model (Figure 2). It was observed that the fecal loads from the different inlet streams varied widely, e.g. depending on the weather conditions (Berge *et al*., 2011). The modeling indicated that the raw water intake was only affected by *E. coli* from the inlets in the circulation period, and only two of the inlet streams (no. 4 and no. 7) affected the raw water intake with detectable levels of *E. coli*, i.e. ≥ 1 per 100 mL, given "average" discharges (Figure 2). After "worst case" discharges, which generally was associated with heavy rain, seven of the tributaries affected the raw water intake with at least 1 *E. coli* per 100 ml (results not shown). More detailed results about how the different inlet streams affected the raw water intake, have been published in Berge *et al.* (2011).

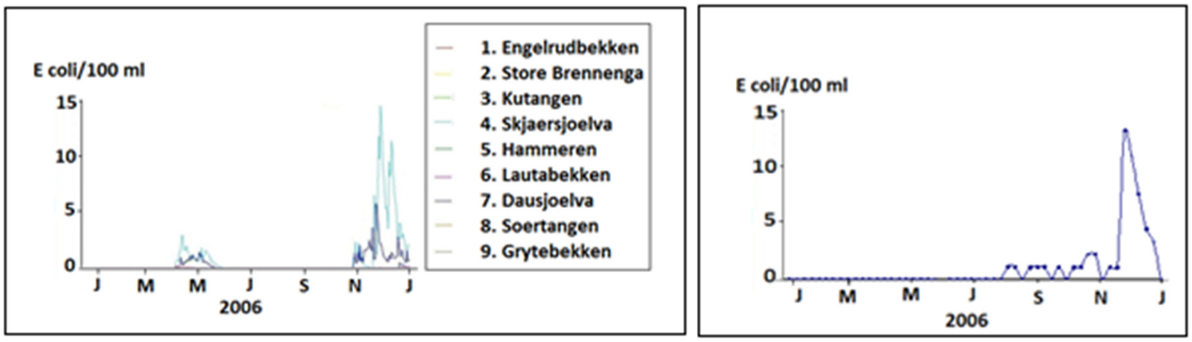

FIGURE 2. Modeled (left) and observed (right) *E. coli* concentrations at the raw water intake of Lake Maridalsvannet during 2006 (x-axis: J=January, M=March, M=May etc.) The modeled values differentiate between the different discharge points

In the model *E. coli* was given a decay rate of 0.7 day^{-1} at 20°C, which corresponds to a half-life ($T_{1/2}$) of 1 day at 20 °C and $T_{1/2}$ of 4.5 days at 4°C. For visualizing the effect of different decay rates, a continuous discharge of 10^{10} pathogens per day from the River Dausjoelva (discharge point 7) was modeled, using "model-pathogens" with different decay rates, i.e. $T_{1/2}$ of 1 day, 1 week and 1 month (Figure 3). The decay rates were set constant, i.e. did not vary with temperature. A $T_{1/2}$ of 1 month may be representative as worst case for *Cryptosporidium* oocysts in the cold Norwegian water (Robertson and Gjerde, 2006).

As shown in Figure 3 the simulated concentrations of pathogens at the deep water intake strongly varied with the decay rate, as it did by season, i.e. with or without circulation/stratification in the lake water column.

The discharges of pathogens to drinking water sources are not constant and continuous as simulated in Figure 3, but will vary depending on whether there are infected people or animals in the catchment area and whether their feces are transported to the lake. In scenario analysis one may assume that a single discharge occur on one specific day (e.g. fecal drop by infected animals or by swimmers that have acute diarrhea, or by surface runoff or wastewater leakage during heavy rain). As shown in Figure 4 the simulated concentrations of "model pathogens" at the raw water intake of Lake Maridalsvannet, after a single discharge of 10^{10} pathogens, strongly depended on when the discharge occurred and on the decay rate of the pathogens. A discharge of 10^{10} "model pathogens" on August 31st caused significant concentrations of model pathogens with $T_{1/2}$ =1 month at the deep water intake 2 months later when the water column circulated in the autumn turn over. Pathogens with $T_{1/2}$ =1 week only occurred at < 0.001 pathogens/L (Figure 4A). If the same discharge happened October 15th, only 1-2 weeks before the full-circulation, both pathogens with $T_{1/2}$ =1 month and $T_{1/2}$ =1 week strongly affected the deep water intake, while pathogens with $T_{1/2}$ =1 day occurred at < 0.001 pathogens/L (Figure 4B).

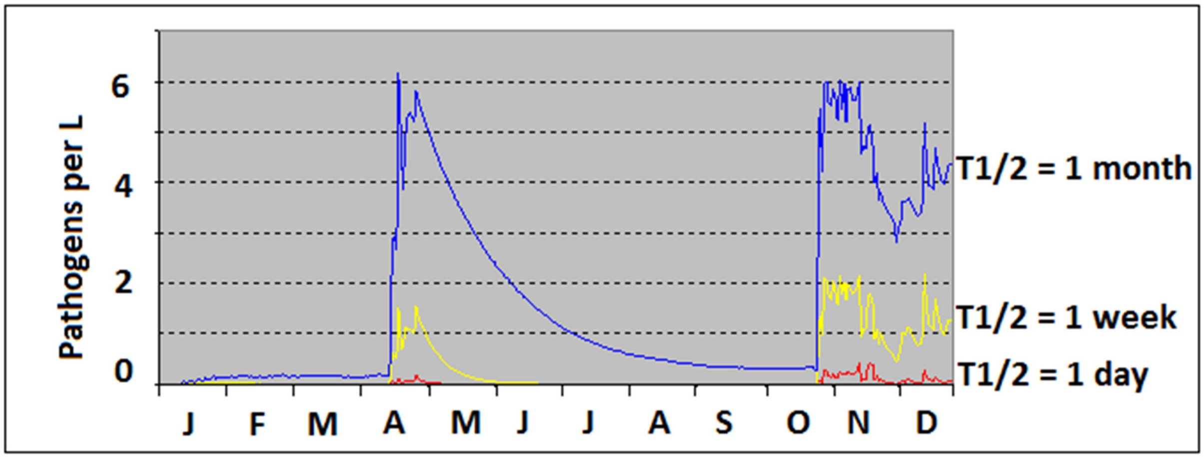

FIGURE 3. Simulated concentration of "model pathogens", with different decay rates, at the deep water intake of Lake Maridalsvannet during a year, after continuous discharges of 10^{10} pathogens per day from River Dausjoelva (discharge point 7)

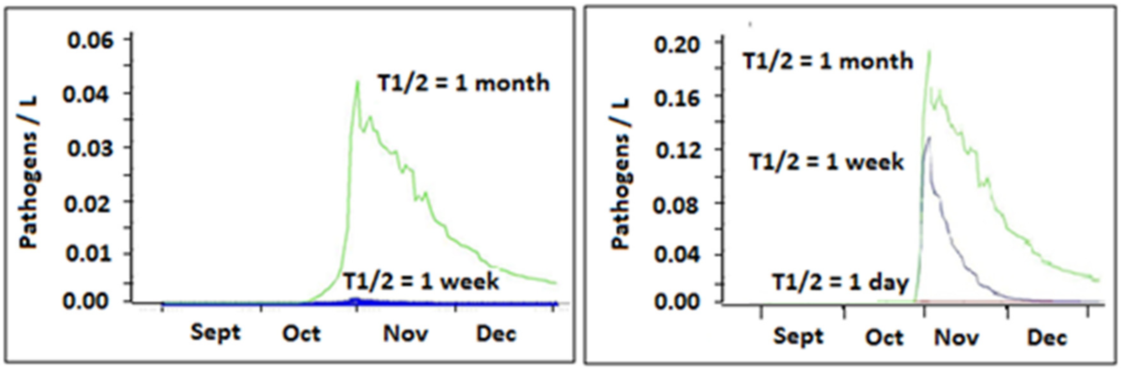

FIGURE 4. Simulated concentration of "model pathogens" with different decay rates at the deep water intake of Lake Maridalsvannet, after a single discharge episode of 10^{10} "model pathogens" from River Skjaersjoelva (discharge point 4), on August 31st (Figure 4A/left) and October 15th (Figure 4B/right)

A fraction of the pathogens may be associated with particles, and thus be removed from the water phase by sedimentation. Sedimentation rates will depend on the size and density of the actual particles present in the lake. Also the consumption and/or inactivation of enteric pathogens by autochthonous microbiota may be important for their fate and transport (Hipsey, 2008), e.g. predation (by bacteria), grazing (by larger eukaryotic organisms) or infections (by viruses). Such processes are difficult to quantify without comprehensive studies in the local lake, and therefore we used "typical", and not specific, decay rates in the pathogen transport model. In spite of the uncertainties, the output of the pathogen transport model was very useful as a part of risk assessment. The pathogen discharge, set to 10^{10} pathogens above, may be scaled up (e.g. to 10^{12}) or down (e.g. to 10^{7}) based on best qualified loading estimates, and the modeled concentrations at the water intake may be scaled thereafter.

RISK ASSESSMENT: MICROBIAL PATHOGENS IN LAKE MARIDALSVANNET

Most pathogens that may cause waterborne diseases originate from human or animal feces (WHO 2008). Fresh feces from humans, mammals and birds contain *E. coli*, but the concentration may vary from 10^{4}-10^{10} per gram (Havelaar *et al.*, 1986; Fergusson *et al.*, 2009). *E. coli* is generally not pathogenic, but the presence of *E. coli* indicates that the water is contaminated with fecal material and there is therefore a risk that pathogens may also be present. Human pathogens, including pathogenic bacteria, viruses and protozoa, are only excreted from infected individuals. While human pathogenic viruses are generally only transmitted from infected persons, some species and genotypes of the parasites *Cryptosporidium* and *Giardia,* and also some pathogenic bacteria (like *Campylobacter* spp., *Salmonella* spp. and *E. coli* EHEC), can also be transmitted from infected animals (Goss and Richards, 2008). In general, there is a higher risk associated with fecal material from humans than from animals, in particular in Lake Maridalsvannet where household animals often considered as "most risky" (cattle, pigs and poultry) are not allowed in the catchment area. Calves infected with *Cryptosporidium parvum* may excrete up to 10^{7} parasites per g feces (Fayer *et al.*, 1998). If such calves were present in the catchment area, with no protective grazing zones or restrictions, this could for example cause an average discharge of 100 g infected feces per day (10^{9} parasites per day) to Lake Maridalsvannet. Figure 3 indicates that the concentration at the raw water intake may be up to 0.6 parasites per L in the circulation period, given a discharge of 10^{9} parasites per day. According to QMRA model used by WHO (2008), the concentration of *Cryptosporidium* in the treated drinking water should be less than 0.00063 per L for obtaining an acceptable risk (1 ill person per 1600 per year). This will require at least 3 Log_{10} reductions of parasites in the water treatment plant after such discharges. Such reduction is obtained by the new water treatment plant (coagulation, filtration and UV-treatment). If the old treatment plant (micro-sieve and chlorination) is used, which happens in periods of repair and maintenance of the new one, no reduction of parasites will be obtained in the treatment process. By using a probability of infection per organism of 0.004, a risk of illness given infection of 0.7 and consumption of unheated drinking water of 1 L per day (WHO, 2008), 0.6 parasites per L may cause about 1 ill person out of 600 per day, which is an unacceptable risk. Similar discharges may also occur from a house with a person infected with *Cryptosporidium* (10^{7} parasites per g feces) where the wastewater is released directly to an inlet stream.

A scenario with an infected child that releases 100 g feces (10^{9} *Cryptosporidium* oocysts) to the water during bathing August 31st, may cause up to 0.005 oocyst per L in the raw water 2 months later when the water column circulates in the lake (Figure 4A). If the same discharge was generated by an infected fisher/jogger October 15th, up to 0.02 oocysts per L may be present at the raw water intake two weeks later (Figure 4B). Both these discharge scenarios gave higher concentrations of *Cryptosporidium* oocysts in the raw water than recommended by WHO for treated drinking water. This illustrates the importance of minimizing the discharges of human feces to drinking water sources, in particular <u>if the water treatment is poor</u>. The contamination potential of human feces may be even higher with regards to enteric viruses, since infected persons may excrete up to 10^{11} virus particles per g feces (Ashbolt *et al.*, 2010). Chlorination is an effective barrier (≥ 3 Log_{10} reductions) against viruses. The risk of norovirus should however be of concern due to its low infective dose, and enteric adenovirus due to its resistance to UV-treatment, if increased amounts of wastewater are discharged to Lake Maridalsvannet.

The risk of human pathogens in fecal material from dogs, horses, wild mammals and birds are lower than in fecal material from humans. Such animal feces may, however, contain e.g. human pathogenic *Cryptosporidium* oocysts, and the excretion may be about 10^{4} per gram feces (Himsworth *et al.*, 2010; Hamnes *et al.*, 2007; Graczyk *et al.*, 2007). If 0.00063 per L is considered as an acceptable concentration in raw water (assuming that the water treatment only consist of micro-sieve and chlorination), the modeling above indicated the following "acceptable loads" of such infected feces: 10^{6}

oocysts (= 100 g feces) per day if the discharge occur continuously over the year (Figure 3) or $3x10^7$ oocysts (=3 kg feces) if only a single release occur October 15th (Figure 4B) Such calculations are very uncertain, in particular since the excretion of pathogens from infected animals vary widely, from 10^0-10^2 per g for most of the infected animals, 10^3-10^4 per g (average of infected animals) to 10^7-10^8 per g from the most heavily infected individuals (Ogden *et al*., 2009; Fergusson *et al*., 2009).

CONCLUSION

Some human pathogenic parasitic protozoa and viruses may survive much longer than *E. coli* in water, and *E. coli* is not always a good indicator of the risk of pathogens in raw drinking water extracted from the deep layers of lakes. Several pathogens may represent an unacceptable risk in treated drinking water even at lower levels (< 0.001 per L) than is possible to measure by analytical methods. Modeling provides useful information about how different pathogen discharges may affect the pathogen concentrations at the raw water intake of drinking water sources. This information is important for determining the need for restrictions in the catchment area, and/or the need for hygienic barriers in the water treatment, or for optimum location of drinking water intake points in lakes and rivers. For obtaining a more reliable modeling, more information is required about the fate of different pathogens (in particular viruses) in water sources (decay, maintenance of infectivity, sedimentation with particles, etc.).

ACKNOWLEDGEMENTS

This study was financed by the City of Oslo, Water and Sewerage Works and by the Norwegian Institute for Water Research (NIVA).

REFERENCES

Ashbolt, N.J., M.E. Schoen, J.A. Soller, and D.J. Roser. 2010. “Predicting pathogen risks to aid beach management: The real value of quantitative microbial risk assessment (QMRA).” *Water Res.* 44:4692-4703.

Berge, D., I. Tryland, T. Tjomsland, L. Hem, and J. Røstum, J. 2011. “ ROS Lake Maridalsvannet – Oset”. NIVA-report: OR-6221. ISBN: 978-82-577-5956-8 (Norwegian).

Espinosa, A.C., M. Mazari-Hiriart, R. Espinosa, L. Maruri-Avidal, E. Mendez, and C.F. Arias. 2008. “Infectivity and genome persistence of rotavirus and astrovirus in groundwater and surface water.” *Water Res*. 42:2618-2828.

Fayer, R., L. Gasbarre, P. Pasquali, A. Canals, S. Almeria, and D. Zarlenga. 1998. “*Cryptosporidium parvum* infection in bovine neonates: dynamic clinical, parasitic and immunologic patterns”, *Int. J. Parasitol.* 28:49-56.

Ferguson, C.M, K. Charles, and D.A. Deere. 2009. “Quantification of microbial sources in drinking-water catchments. “ *Crit. Rev. Env. Sci. Tech*. 39: 1-40.

Goss, M., and C. Richards. 2008. “Development of a risk-based index for source water protection planning, which supports the reduction of pathogens from agricultural activity entering water resources.” *J. Environ. Manage.* 87:623-632.

Graczyk, T.K., A.C. Majewska, and K.J. Schwab, K.J. 2007. “The role of birds in dissemination of human waterborne enteropathogens.” *Trends Parasitol.* 24:55-59.

Hamnes, I.S., B.K. Gjerde, and L.J. Robertson. 2007. “A longitudinal study on the occurrence of *Cryptosporidium* and *Giardia* in dogs during their first year of life”. *Acta Vet Scand.* 11:49:22.

Havelaar, A.H., K. Furuse, and W.M. Hogeboom. 1986. “Bacteriophages and indicator bacteria in human and animal faeces.” *J. Appl. Bacteriol.* 60:255-262.

Himsworth, C.G., S. Skinner, B. Chaban, E. Jenkins, B.A. Wagner, N.J. Harms, F.A. Leighton, R.C. Thompson, and J.E. Hill. 2010. “Multiple zoonotic pathogens identified in canine feces collected from a remote Canadian indigenous community.” *Am J Trop Med Hyg*. 83:338-41.

Hipsey MR, Antenucci JP, Brookes JD. (2008). “A generic, process-based model of microbial pollution in aquatic systems.” Water Resources Research. 44, 1-26.

Ogden, I.D., J.F. Dallas, M. MacRae, O. Rotariu, K.W. Reay, M. Leitch, A.P. Thomson, S.K. Sheppard, M. Maiden, K.J. Forbes, and J.C. Strachan. 2009. “*Campylobacter* excreted into the environment by animal sources: prevalence, concentration shed, and host association.” *Foodborne Pathog. Dis.* 6:1161-1170.

Robertson, LJ., and B. Gjerde B. 2006. “Fate of *Cryptosporidium* oocysts and *Giardia* cysts in the Norwegian aquatic environment over winter”. *Microbial Ecol.* 52**:**597-602.

Shin G.A., J.K. Lee, and K.G. Linden. 2009. “Enhanced effectiveness of medium-pressure ultraviolet lamps on human adenovirus 2 and its possible mechanism.” *Water Sci. Technol.* 60:851-857.

WHO. 2008. Guidelines for Drinking-water quality. 3rd ed. Vol.1. Recommendations. Chapter 7. Microbial aspects. World Health Organisation. Geneva.

CHEMICAL AND BACTERIOLOGICAL QUALITY OF SOME CAMEROON BOTTLED DRINKING WATERS.

George Elambo Nkeng (National Advanced School of Public Works (ENSTP) Yaoundé-Cameroon)
Andrew Ako Ako (Hydrological Research Centre, IRGM Yaoundé-Cameroon)
Stephanie Abonoje Oyebog and Emmanuel Cheo Suh (University of Buea-Cameroon)

ABSTRACT: Eight domestic bottled water brands sold in Cameroon were analyzed for their health -related chemical (major and trace elements) and bacteriological quality. For the purpose of comparison, a sample of tap water was also analyzed. Inductively Coupled Plasma Mass Spectrometry (ICP/MS) was used for the analysis of major and traces elements. Ion chromatography (IC) was used for the analysis of anions. Total coliform bacteria and faecal coliform bacteria load were determined using the Multiple Tube Dilution technique.The results of the analysis were compared with the drinking water standards for drinking water to ascertain the suitability of these brands for human consumption. Generally, the bottled water samples were within the acceptable levels of the WHO guidelines and were lower than Maximum Contaminant Levels (MCL) established by the EPA. Notwithstanding, toxic and hazardous substances like lead, mercury and aluminium were detected in all the brands and the tap water sample. Total coliform bacteria are present in 3 brands (A, C and D) though no faecal coliform bacteria were detected in any of the brands. Chemical purity, including the absence of bacterial contamination of bottled water in contrast to tap water is not guaranteed, thus consumers should check the mineral content of their bottled water and choose the brand that is most appropriate for their individual dietary needs.

INTRODUCTION

In Cameroon, surface water resources such as rivers and streams together with groundwater (boreholes and springs) are the main sources of water supply in urban areas. Water from these sources is usually collected, treated and distributed to the populations by the Cameroon Water Utilities (CAMWATER). However, many people still rely on bottled water for drinking water for safety purposes, for infants (for formula preparation, drinking water and reconstitution of food) and other health reasons. Though the production of bottled started in 1999, it was only until 2007 that consumption got to its peak due to public conception about municipal water supplies. Between 1999 and 2009, 15 bottled water companies in Cameroon produced about 52,380,000 bottles of water and about 1,080,000l of water in sachets mostly from groundwater sources (MINEE, 2010). Bottled water is also imported from several European countries. Most brands are sold in 0.5 and 1.5 L disposable plastic bottles.

Despite the large market for bottled drinking water in Cameroon and the proliferation of bottled water producers, no research on the chemical and bacteriological quality of bottled water sold in Cameroon has been carried out.

This paper, a first of its kind in Cameroon, presents the results of a study aimed at evaluating the major, trace elements and bacterial composition of locally produced bottled water in Cameroon. The study is equally important because it will assure the consumers about the quality of their drinking water and also

---

ISBN 9780976885351

beneficial in detecting deterioration in quality and facilitate appropriate timely corrective actions with minimal negative impact on the health of the populace.

MATERIALS AND METHODS

This study is limited to eight popular bottling plants located across the South West and Littoral Regions of Cameroon. The 8 different bottled water brands (marked Brands A-H) were selected since these were the ones available to consumers. The bottled water brands were purchased from grocery shops, supermarkets, street vendors and distribution centres. To keep the brand names anonymous, the water samples were given alphabetical codes from A to H and this convention is used throughout the text. Physico-chemical parameters (pH, EC and temperature) of the samples were measured immediately after sample collection.

Analysis for anions was done at the Institute for Research in Agricultural Development (IRAD) Ekona laboratory. Bicarbonate (HCO_3^-) concentrations were determined by titration. The other anions (Cl^-, SO_4^{2-}, NO_3^- and PO_4^{3-}) and Ammonium ion (NH_4^+) were analysed by colorimetric/tubidimetric methods using a Perkin-Elmer Spectrophotometer 295E. The analysis of major and trace elements was carried by Acme Analytical Laboratory (Canada), an internationally accredited laboratory. Major and trace metals were determined by enhanced ICP-ES/ICP-MS. For comparison, a tap water sample from the study area was also analysed for its major and trace element contents.

Bacteriological analysis for total coliform bacteria and faecal coliform bacteria load was done in the Department of Life Science Microbiology Laboratory of the University of Buea. Total coliform bacteria and faecal coliform bacteria load were determined using the Multiple Tube Dilution technique. The Most Probable Number (MPN) of coliform bacteria per 100 ml of the water sample was then determined from statistical tables.

RESULTS AND DISCUSSION

Water chemistry and natural variation of elements. Results of measured physico-chemical and chemical parameters of the bottled water brands are presented in Table 1 .The ranges of values for the physico-chemical parameters are: 90–410µS/cm for electrical conductivity (EC) with a median of 294.7µS/cm; 6.34–7.91 for pH with a median of 7.28; 26.7-27.0 °C for temperature with a median of 26.8 °C; and 85-355 mg/l for total dissolved solid (TDS) with a median of 255 mg/l. There is a great variation between the EC values of the bottled water brands, which is related to the total dissolved solids (TDS) content, the origin of the water, and the treatment or purification method applied during bottling process. Electrical conductivity in water is usually used as a measure of ionic concentration. The low EC of brand D is due to its low ionic concentration.

Minimum pH is observed in brand E and maximum pH in brand B. The acidic nature of brand E could be resulting from organic acids in the soil as well from atmospheric sources. Since the brands were labelled as Natural Mineral Water, this might mean no carbon dioxide was present in the water. A pH value of 6.5 is the minimum recommended by WHO and EPA, brand E therefore falls short of this recommendation. Electrical conductivity and TDS values are below Maximum Allowable Values (MAV) (WHO, 2008; EPA, 2009). No standard is provided for temperature of water.

In this study, chemical analysis for 74 parameters was done for the 8 bottled water brands. The results show that the bottled water brands are quite different in chemical characteristics. Observed variations in the chemical constituents might be resulting from the origins of the water, residence time of the water in the rocks, atmospheric conditions and purification/treatment process employed by the manufacturers. Table 1 gives the analytical results of major constituents found in these brands.

Higher concentration of Ca^{2+} is observed in brand F from sedimentary terrain because of abundance of limestone. Calcium readily dissolved from rocks rich in calcium minerals, clay minerals, sulphates and other carbonate rocks especially limestone and gypsum. The exception was seen with brand D also from a sedimentary zone but with an extremely low Ca^{2+} content (0.67mg/l). Brand D actually has the lowest concentration of all major constituents with exception of Na^+.

Table 1 Physico-chemical parameters and major constituents for the 8 bottled water brands and tap water

	Brand code								
Parameters	**A**	**B**	**C**	**D**	**E**	**F**	**G**	**H**	**Tap water**
Temp (°C)	26.9	26.8	26.9	27	26.8	26.8	26.8	26.7	
EC (µS/cm)	334	275.1	216.1	90	314.3	292.9	410	171.9	
ph	7.34	7.91	7.5	7.81	6.34	6.73	7.26	7.34	
TDS (mg/l)	273	249	193	85	268	261	355	151	
Ca^{2+} (mg/l)	22.88	19.66	15.76	0.67	24.08	57.9	16.55	18.64	13.49
K^+ (mg/l)	6.15	3.59	2.14	0.19	9.04	3.86	9.18	1.56	8.88
Mg^{2+} (mg/l)	14.75	14.19	9.52	0.32	15.44	1.22	18.54	7.84	7.26
Na^+ (mg/l)	17.09	10.87	10.41	9.92	1.45	11.26	43.94	5.95	18.74
Cl^- (mg/l)	2	4	3	2	2	9	12	6	3
HCO_3^- (mg/l)	189.71	162.87	129.93	67.71	205.57	168.97	229.97	83.57	180
NO_3^- (mg/l)	0	0.2	0.08	0	0	1.58	0	0.5	0
SO_4^{2-} (mg/l)	5	4	2	2	3	5	11	3	4
SiO_2 (mg/l)	15.41	29.15	19.75	2.01	7.18	2.12	14.08	24.3	20.83

The exceptionally low concentration of Ca^{2+} but high Na^+ concentration in brand D may be an indication that the water is sourced from waters which have undergone natural softening by cation exchange. Higher Mg^{2+} concentration is generally observed among water from volcanic terrain (brands A, B, C, E, G and H). This is due to presence of magnesium-rich minerals such as olivine and pyroxene. The concentration of Ca^{2+} was greater than Mg^{2+} in all brands except brand G. This exception might be due to exchangeable sodium. This brand has Na concentration between ~ 27-42 units higher than the others. Primary source of sodium in natural water is from release of soluble products during the weathering of plagioclase feldspars. No health-based guideline value is proposed for Ca^{2+}, K^+, $Mg^{2+}$and Na^+ in drinking water by WHO due to contrasting views on health impacts of these elements..

High nitrate (NO_3^-) concentration (1.58 mg/l) in brand F relative to the others may be resulting from erosion of natural deposits or most likely from industrial and agricultural wastes. But this value is below standards/guideline set for nitrate in drinking water. The higher sodium, chloride and sulfate content in brand G relative to the others might be resulting from release of soluble products during weathering of plagioclase feldspars, salt water intrusion or chloride-rich rainwater. Brand E from volcanic area tends to have lowest concentration of Na^+ with respect to the others. No standards /or guideline value is proposed for HCO_3^- and SiO_2 in drinking water. The standards/guideline values provided for Cl^- and SO_4^{2-} are based on consumer's acceptability of taste and concentrations were below these values.

In terms of chemical quality, the tap water sample is richer in mineral salts than one bottled water brand (Brand D) putting in question the general notion that bottled waters are generally richer in mineral salts than tap water.

Table 2 Concentration of trace elements found in the 8 bottled water brands and tap water

Trace elements (µg/l)	Brand code								
	A	B	C	D	E	F	G	H	Tap water
Ag	1.05	0.94	0.8	0.11	0.16	0.12	0.13	0.13	0.25
Al	50	47	34	52	121	96	30	36	66
B	15	13	16	6	5	37	23	8	6
Ba	24.12	17.4	13.53	6.73	90.99	67.94	15.88	18.83	6
Br	10	16	17	18	9	90	52	29	14
Cd	0.07	0.15	0.07	0.1	0.09	0.14	0.17	0.11	0.11
Ce	0.98	0.4	0.35	0.29	0.38	0.4	0.28	0.3	0.38
Co	0.04	0.06	0.04	0.1	0.21	0.14	0.03	0.83	0.04
Cr	9	5.1	4.8	3.6	4.3	4.4	4.5	3.1	4.6
Cu	1.3	1.4	1	12.5	0.9	2.1	1	2	5.1
Fe	<10	28	<10	14	15	<10	12	52	29
Hg	0.1	0.1	<0.1	<0.1	<0.1	0.1	<0.1	<0.1	<0.1
La	6.51	0.56	0.22	0.12	0.14	0.23	0.11	0.16	0.15
Li	0.2	0.6	0.1	0.4	5.4	1.4	<0.1	0.2	0.1
Mo	1.5	1.2	1.1	0.1	0.1	0.2	4.4	0.5	1.5
Nd	2.93	0.19	0.08	0.06	0.05	0.11	0.05	0.06	0.06
Ni	0.5	0.8	1.5	1	2.3	0.8	0.4	0.9	0.5
P	118	258	193	81	146	0.8	197	107	205
Pb	6.4	2.5	1.2	5.9	1.5	2.1	2.2	1.9	2.9
Rb	9.88	7.79	5.91	0.49	16.66	4.93	23.59	5.09	20.81
Rh	0.02	0.03	0.01	<0.01	0.01	<0.01	<0.01	<0.01	0.01
Sb	0.31	0.18	0.44	0.06	0.44	0.76	0.78	0.74	0.13
Sn	0.55	0.52	0.35	0.17	0.21	0.21	0.15	0.18	0.21
Sr	78.96	198.8	128.05	4.67	48.26	27.69	125.04	222.38	129.1
U	0.04	0.03	0.05	<0.02	<0.02	0.03	2.25	<0.02	0.18
V	0.7	9	19.3	0.2	0.2	0.5	22.8	11.6	19.8
W	0.32	0.03	0.24	<0.02	<0.02	0.02	0.3	1.09	0.09

Concentration of trace elements. The analytical results of trace constituents are presented in Table 3. Higher concentration of Ag is observed in brands A, B and C with respect to others. Silver salts are used to maintain the bacterial quality of drinking water and this might be a reason for the observed concentrations in these brands. Maximum Ag concentration is below EPA standard value. Thorium and Bi in brands A and B may be originating from natural deposit or radioactive decay of uranium and its daughter products. Brand E tend to have very high Al, Ba and Li concentrations relative to others from same area. This might be due to relative mobility of these elements at lower pH. Aluminium tends to be the third most abundant element on the Earth's crust. Another possible source of Al might be from piping systems. The primary Ba mineral is barite but it often occurs in the lattices of some common silicates like feldspars. Ba is not very mobile (in the secondary environment) but it can be mobilized by acidic waters. Lithium is preferentially leached during the weathering of silicate rocks. K-feldspars, amphiboles and clay minerals have the most important contents of Li. Aluminium concentrations in brands D, E and F (from sedimentary terrain) are above the EPA lower secondary standard limit of 50µg/l.

The highest concentration of boron (B), bromide (Br), manganese (Mn) and zinc (Zn) was found in sample F from sedimentary areas. Boron is found naturally in groundwater. Boron compounds are also used in the manufacture of glass, soaps and detergents and as flame retardants. Boron from these sources may be a contributing source of the high boron content in brand F. However, maximum concentration of B (37 µg/l) is quite below the guideline value (500 µg/l) set by WHO (2008). Copper (Cu) concentration in brand D is higher with respects to the others. This might be originating from corrosion of plumbing systems or erosion from natural deposits. Germanium (Ge) in brand A may be from leaching of Ge catalyst used in production of PET. Maximum manganese concentration (in brand F) is above guideline value provided by EPA. With the exception of brand D (also in PET bottle), higher antimony (Sb) concentrations are observed in water from PET bottles than from HDPE bottle (brand B). The presence of Sb in these bottled water brands may include additional Sb leaching from the bottle material. However, concentration in these brands was below standard values. Iron is one of the most abundant metals in the Earth's crust. Sources of iron include weathering of pyroxenes minerals in volcanic areas and oxides, carbonates, and sulfides or iron clay minerals in sandstone areas. Maximum Fe concentration is below the value for standards used in Cameroon and EPA (2009). These values are set based on acceptability factors (taste and color). No health-based guideline value is proposed for iron in drinking water. Concentrations of Pb in brands A and D are about 4.5 and 4 times higher than concentration found in the other brands from same geologic terrain respectively. This higher concentration might be originating from lead pipes used to tap water from source to the bottling plants. Maximum Hg and Pb concentrations are below standards. Molybdenum (Mo) and vanadium (V) occur naturally in soils and may be entrained into water due to its mobility during weathering. U is release in water in these areas through erosion of natural deposits. Difference in the concentration of U may be due to U greater mobility under oxidizing conditions and it present in very varying concentrations in rocks.

Bacteriological Characteristics of Bottled Water Brands. In general, the presence of coliform organisms indicates the possible presence of microbial pathogenic agents. The results of the bacteriological analysis and estimate of the MPN of total coliform and faecal coliform bacteria counts per 100ml of water for the 8 bottled water brands are shown in Table 3.Total coliform bacteria were detected in 3 out of 8 (37.5 %) of the bottled water brands but none of the bottled water tested positive for faecal coliforms. Total coliforms count is highest in brand C (treated using UV light).

In comparison with the standards used in this study; all the three brands that tested positive for total coliforms are above the recommended values set by EPA and WHO. Brand C bridged all the standards EPA inclusive. Total coliform group include both faecal and environmental species. The negative test for faecal coliforms therefore means that the coliforms present in three samples that tested positive for total coliforms are mainly environmental species. The difference in the MPN of total coliforms between the brands is due to different water sources, and varying degrees of efficiency employed by the different manufacturers.

Table 3. Presumptive total coliform and faecal coliform counts per 100 ml of water sample

Brand code	Water volume (L)	MPN of total coliforms per 100ml	MPN of faecal coliforms per 100ml
A	1.5	4	0
B	1	0	0
C	1	9	0
D	0.5	4	0
E	1.5	0	0
F	0.5	0	0
G	1.5	0	0
H	0.5	0	0

It is not uncommon to find bottled water products stored under direct sunlight in unhygienic conditions. In view of this, the possibility of growth of microorganisms is greatly increased considering that temperatures in the study area may be as high as 30^{0}C. Nsaze and Babarinde (1999) demonstrated that the organisms multiply more easily between 25 and 37^{0}C. The normal room temperature (from 28 to 32^{0}C) in most of the bottled water storage facilities and grocery shops in the study area may also favour the growth of microbial pathogens.

CONCLUSIONS

General public opinion hails the benefits of drinking bottled water. Our study has shown that the bottled water brands' mineral contents are supposedly "within the required mineral contents". However, the variability of minerals and trace element contents is great from one brand to another. In our study, we found that all of our samples have detectable aluminium and lead in the ranges 30-121µg/l and 1.2-6.4 µg/l respectively. Aluminium concentration in brands D, E and F are above the lower guideline value set by the EPA. Maximum Pb concentration in Brand A (6.4µg/l) is regarded as high considering that it is close to the most stringent standard limit of 10µg/l. Total coliform bacteria are present in 3 brands (A, C and D) though no faecal coliform bacteria were detected in any of the brands. Differences in the bottled water brands and the tap water mineral and trace element contents have been established by our study.

ACKNOWLEDGEMENTS

This research was supported by a grant from the National Advanced School of Public Works (ENSTP) Yaoundé, Cameroon.

REFERENCES

Environmental Protection Agency (EPA). 2009. National primary/secondary drinking regulations. EPA 816-F-09-004, Washington, DC.

MINEE. 2010. Statistics on production of bottled water in Cameroon. Ministry of Water and Energy, Yaoundé.

Nsaze, H., and Z. Babarinde. 1999. Microbiological quality of bottled drinking water in the UAE and the effect of storage at different temperatures. Environ. Int., 25(1), 53–57.

WHO. 2008. Guidelines for drinking-water quality, 3rd edn. Incorporating the First and Second Addenda Vol 1 Recommendations. WHO, Geneva.

ROLE OF DO, pH AND ACTIVATED CARBON IN THE OXIDATION OF As(III)

T. Angele Ngantcha – Kwimi, Anjuman I. Islam, Brian E. Reed
Chemical, Biochemical and Environmental Engineering (University of Maryland, Baltimore County, MD, USA)

ABSTRACT: Preoxidation of As(III) to less toxic As(V) is usually needed in the treatment of arsenic in drinking water. The role of dissolved oxygen (DO) on As(III) oxidation by GAC 1240 at pH = 8.5 was investigated. The oxidative abilities of nine activated carbons as a function of 3 initial pHs (7.0, 8.5 and 9.2) were also examined in the presence of DO. The results indicated ~ 90% oxidation of As(III) to As(V) by GAC 1240 in the presence of 7.0 mg/L of dissolved oxygen. At an initial pH of 7, less than 90% As(III) was oxidized to As(V) due to the activated carbons. However, at an initial pH of 8.5, greater than 99% oxidation of As(III) to As(V) was noticed in the presence of five out of nine activated carbons. The remainder four of the nine activated carbons only achieved ~ 99% As(III) oxidation at an initial pH of 9.2. The oxidation of As(III) to As(V) by an iron-impregnated activated carbon, followed by the removal of As(V) via adsorption, offers a simple treatment which can be adopted for small communities and point-of-use systems for the removal of arsenic from drinking water.

INTRODUCTION

Arsenic has been linked to many health risks including cancers of the skin, lungs, liver and kidney and black foot diseases (Smith et al., 1992). To protect consumers from chronic exposure from drinking water, the maximum contaminant level of total arsenic was reduced from 50 to 10 µg/L in January 2006 (USEPA, 2001). Ninety seven percent of areas affected by the new MCL are small systems serving less than 10,000 people (http://water.epa.gov/drink/). As(V) is predominant under oxidizing conditions and is generally better adsorbed than As (III). As(III) occurs predominantly under reducing conditions, is more mobile in ground waters and is 60 times more toxic than As(V) (Jain and Ali, 2000). While the MCL is based on total arsenic, the difference in toxicity and chemical behavior requires that attention be paid to the fate of individual arsenic species in treatment systems. Enhanced coagulation/filtration is often used to remove arsenic from drinking water in large communities with centralized water treatment facilities; however, this technology is not suitable for small communities who often do not have a centralized treatment facility. In order for smaller communities to meet the lower arsenic standard relatively simple and effective arsenic removal technologies need to be developed. Adsorption is a relatively simple technology commonly used in drinking water treatment systems. Iron oxide impregnated activated carbons have an advantage over iron oxides and other adsorbents in that, they are durable and can potentially allow the concurrent removal of organic and inorganic contaminants. In iron-oxide adsorption systems As(III) that is present in the raw water is first oxidized to As(V) using chlorine or potassium permanganate (Ghurye et al.,2004; Johnston and Heijnen, 2001). Ngantcha et al., (2011) observed that As(III) was oxidized to As(V) in the presence of an iron oxide impregnated activated carbon. If the activated carbon can reliably oxidize As(III) to As(V) and the impregnated iron-oxide adsorb As(V) then a one step process can be used to remove both forms of Arsenic. The oxidation of As(III) to As(V) was also shown to occur when As(III) was adsorbed in the presence of an activated carbon by Daus et al., (2004). Schmidt et al., (2007) showed evidence of As(III) oxidation to As(V) from an X-ray absorption spectroscopy (XAS) analysis of an arsenite sample in the presence of zirconyl nitrate impregnated activated carbon (Zr-AC); As(III) was oxidized to As(V) in the presence of Zr-AC due to reducible carbon species on the adsorbent surface. Reducible surface species such as oxygenated surface groups have been shown to account for the catalytic oxidation of various compounds. Puri et al., (1958a) and Larson and Walton, (1940) found a

---

ISBN 9780976885351

correlation between the oxidation of inorganic salts like sodium nitrite and sodium sulfite and the acidic surface functional groups (carboxylic, phenolic, quinone type, and lactone groups), on the carbon surface. Meanwhile, Li et al., (2008) showed that basic functional groups on activated carbon fibers were responsible for the oxidation of hydrogen sulfide. Puri et al., (1958b) also showed that basic functional groups on the surface of charcoal accounted for the catalytic decomposition of hydrogen peroxide; the authors stated that the nature (functional groups) of the carbon surface and not the amount of the surface (surface area) was important in this reaction process. Ischizaki and Cookson, (1974) suggested that oxygen surface groups on Filtrasorb 200 accounted for the catalytic oxidation of n-butyl mercaptan to butyl disulfide in the presence of air. The authors attributed the oxidation to quinone type oxygen groups on the carbon surface. The authors reported insignificant oxidation in the presence of air but in absence of the activated carbon. In contrast, measurable oxidation was noticed in the presence of air and activated carbon, demonstrating the importance of oxygen in the oxidation process. Therefore, the objectives of this study are to investigate the role of dissolved oxygen, pH and activated carbon types in the As(III) oxidation process. This will serve as a preliminary study in investigating the role activated carbon surface functional groups play in the oxidation of As(III) and how these functional groups can be modified in drinking water treatment systems to improve the oxidation and removal of As(III).

MATERIALS AND METHOD

Role of DO in As(III) Oxidation: The role of DO on As(III) oxidation by GAC1240 was investigated in a series of experiments during which the DO concentration was set at either 7-7.4 mg/L or 0.7 to 0.9 mg/L. GAC 1240 was crushed so that 100% passed through a 200 and was retained by 400-mesh sieves. Two one-liter solutions of 1 mg/L As(III) at $I = 10^{-2}$ (as $NaNO_3$) were prepared and 0.225 g of GAC 1240 was added to each. One of the solutions was aerated so that the dissolved oxygen remained at a concentration range of 7 – 7.4 mg/L throughout a period of 4 hours; the other solution was deprived of oxygen by continuous nitrogen purging so that the dissolved oxygen remained at a range of 0.7 – 0.9 mg/L. Additionally, a sample with 1mg/L As(III) and no GAC 1240 was aerated throughout a period of 5 hours. The initial pH was set to 8.5 using 1N NaOH. Samples were collected at regular intervals of approximately 0.5 hrs., and filtered through a 0.45-µm membrane filter and filtrate was saved for arsenic analysis.

Effect of Activated Carbon Type on As(III) Oxidation: The oxidative abilities of nine activated (GAC 1240, Darco S-51, Norit RO 0.8, Norit PAC 200, Hydrodarco W, Norit GAC 400, Darco 20 x 40, Filtrasorb 200 and DSR-A 8 x 40) as a function of 3 initial pHs (7.0, 8.5 and 9.2) were examined in the presence of DO. Nine one-liter solutions of 1 mg/L As(III) at $I = 10^{-2}$ (as $NaNO_3$) were prepared and 0.225 g of each adsorbent was added resulting in a concentration of 0.225 g/L each. Three sets of nine 53-mLvials containing 3 glass bids for mixing (with no head space) were each filled with the above solution. 1N NaOH was added to the aliquots to adjust the initial pHs of each set to 7, 8.5 and 9.2. Vials were capped and shaken for 48 hours. After shaking, the equilibrium pH and dissolved oxygen were measured and the samples were filtered through a 0.45-µm membrane filter and the filtrate was analyzed for arsenic. Carbons showing 100% conversion to As(V) after 48 hours of shaking at pH 8.5 were not analyzed for the effects of pH at 9.2.

pH of Carbon: The pH of the carbons was determined for four (Norit R.O 0.8, Hydrodarco W, Darco S-51 and Darco 20 x 4**0)** out of the nine activated carbons. 1g of each carbon was added to 50 mL of deionized water and equilibrated for 24Hrs, after which the pH was measured. Samples with pH greater than the pH of the deionized water were considered to be basic and those with pH lower than that of deionized water were classified as acidic.

Analytical Methods: The filtrates were analyzed for total As using ICP and As(III) and As(V) were measured by IC-ICP. An Oakton epoxy glass pH electrode with Ag/AgCl reference cells was used for all pH measurements.

RESULTS AND DISCUSSION

Role of Dissolved Oxygen (DO) in As(III) Oxidation: Figure 1 shows approximately 10% oxidation of As(III) to As(V) by GAC 1240 in the presence of 0.7 - 0.9 mg/L dissolved oxygen. In contrast there was ~ 90% As(III) oxidation to As(V) by GAC 1240 in the presence of ~ 7.0 mg/L of dissolved oxygen, indicating that oxygen plays an important role in As(III) oxidation by GAC 1240. However, no As(V) was detected in the control sample (no GAC 1240) after 5 hours of aeration. Atmospheric oxygen has been reported to oxidize As(III) only in the order of weeks (Pierce and Moore, 1982). GAC 1240 requires oxygen to effectively catalyze the oxidation of As(III); the interaction of oxygen with As(III) could result in the formation of an oxygen radical (O2-) which oxidizes As(III) to As(V) (Hug and Lepin, 2003). The role of dissolved oxygen in the oxidation of As(III) has also been reported by various authors. Ischizaki and Cookson, (1974) noticed there was measurable oxidation of mercaptan to butyl disulfide by Filtrasorb 200 in the presence of air. Ona-Guema et al., (2010) reported the oxidation of As(III) by Fe(II) in the presence of oxygen only. Paritam et al., (2005) also reported the significant decrease in As(III) oxidation rate by TiO_2 in the absence of oxygen. In the absence of oxygen, however, ~ 10% of As(V) was still produced ; the formation of OH- radicals has been suggested as participating in the oxidation of As(III) in the absence of dissolved oxygen (Paritam et al., 2005). Other factors that could influence As(III) oxidation are pH and activated carbon type; the next series of experiments were conducted to assess these effects.

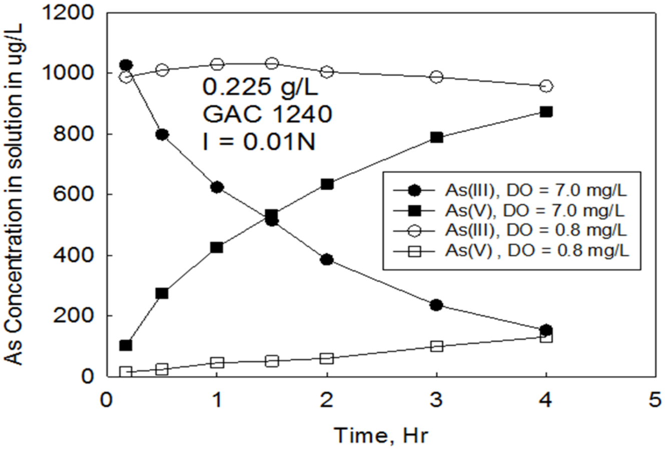

FIGURE 1 As(III) oxidation to As(V) as a function of dissolved oxygen ($As(III)_{init}$ = 1mg/L)

Effect of Activated Carbon Type and pH on As(III) Oxidation: Experiments were conducted to determine the effects of activated carbons on As(III) oxidation at different pHs. The selection of pHs levels were influenced by practical considerations of drinking water treatment systems. As(III) concentrations were 13uM(1 mg/L) and activated carbon loadings were 0.225 g/L. Table 1 shows the properties of the 9 activated carbons studied and the equilibrium pHs and DO of each of the activated carbons ; the activated carbons had various raw material precursors and were either granular or powdered with some being acid washed. The equilibrium DO ranged from 4.2 – 5.9, 4.2 – 5.9 and 8.0 - 8.3 mg/L at initial pHs of 7, 8.5 and 9.2 respectively. The DO did not change significantly across activated carbon type at initial pHs 7 and 8.5. However at pH 9.2, the DO increased noticeably.

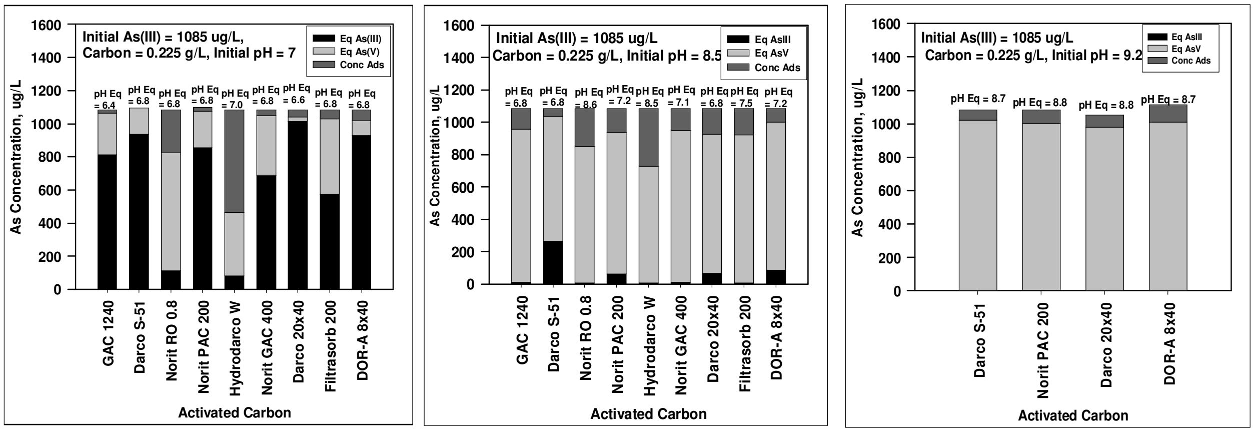

FIGURE 2 As(III) oxidation to As(V) at initial pHs of 7, 8.5 and 9.2 by different activated carbons

Table 1. Properties and Equilibrium Conditions for As(III) Oxidation by 9 Activated Carbons.

Carbon Type	Raw Material	Iodine # (mg/g)	Nature	Acid Washed	Initial pH = 7		Initial pH = 8.5		Initial pH = 9.2	
					Equilibrium pH	Equilibrium DO	Equilibrium pH	Equilibrium DO	Equilibrium pH	Equilibrium DO
Darco 20 x 40	Lignite	600	Granular	Yes	6.6	5	6.8	4.5	8.8	8.2
Darco S-51	Lignite	900	Powdered	Yes	6.8	6	6.8	5.6	8.7	8
DOR- A 8 x 40	Bituminous	750	Granular	No	6.8	4	7.2	4.2	8.7	8.3
Filtrasorb 200	Bituminous	850	Granular	No	6.8	4	7.5	4.3	-	-
GAC 1240	Bituminous	1020	Granular	No	6.4	6	6.8	6	-	-
Hydrodarco W	Lignite	500	Powdered	No	7	5	8.5	4.8	-	-
Norit GAC 400	Bituminous	1000	Granular	No	6.8	5	7.1	4.6	-	-
Norit PAC 200	Bituminous	900	Powdered	No	6.8	5	7.2	5	8.8	8.1
Norit RO-0.8	Extruded	1100	Powdered	No	6.8	6	8.6	5.2	-	-

Figure 2, shows that at an initial pH of 7, there was less than 90% oxidation of As(III) to As(V) by any of the activated carbons as indicated by the presence of As(III) in solution. The equilibrium pHs dropped slightly from 7, except for Hydrodarco W, which is later shown to be a basic activated carbon. Figure 1 shows that at an initial pH = 8.5, close to 100 % oxidation of As(III) to As(V) was noticed in the presence of five out of nine activated carbons (GAC 1240, Norit RO 0.8, Hydrodarco W, Norit GAC 400 and Filtrasorb 200). Again, there was a pH drop from the initial pH of 8.5 for all the carbons except for Norit RO 0.8 and Hydrodarco W. At the initial pH of 8.5, the highest percentage of As adsorbed was 33% compared to 57% at 7.5 and in both cases by Hydrodarco W. Similarly there was a slight decrease in adsorption by Norit RO 0.8 as the initial pH increased from 7 to 8.5. These two carbons also showed the highest oxidative abilities. However for the remainder of the activated carbons, adsorption increased with increase in pH from initial pH of 7 to 8.5. At pH 7 and 8.5, As(III) exist predominantly as a neutrally charged As(III) species. These differences are due to differences in adsorption behaviors, influenced by differences in the surface of the activated carbons. Figure 1 also shows that the least conversions to As(V) were by four (Darco- S 51, Darco 20 x 40, Norit PAC 200 and DOR A 8 x 40) of the nine activated carbons achieved ~ 100 complete oxidation until pH 9.2. For these carbons, the initial pH dropped from 9.2 to 8.7 and 8.8 suggesting acidic carbons.

Table 2, shows the amount of As(III) and As(V) left in solution after As(III) oxidation. From Table 2, we can infer that at the initial pH of 7.0, the activated carbons with the highest adsorptive arsenic abilities were Norit R.O 0.8, Hydrodarco W and Filtrasorb 200 meanwhile Darco S-51, DOR- A 8 x 40 and Darco 20 x 40 had the least adsorptive abilities. For the carbons that adsorbed As, it is difficult to ascertain exactly how much As(III) is being oxidized to As(V) from the initial As(III) concentration of 1085 µg/L in this experiment. However, we can infer from Table 2 that the highest amount of As(V) in solution resulted from Norit R.O 0.8, Hydrodarco W and Filtrasorb 200 and the least originated from Darco S-51, DOR- A 8 x 40 and Darco 20 x 40. Oxidation of As(III) by these nine activated carbons were favored at alkaline pHs, suggesting the presence of basic functional groups on the activated carbon like pyrones and chromenes which oxidize As(III) in the presence of dissolved oxygen. Li et al., (2008) and Puri et al., 1958b showed that basic functional groups carbons were responsible for the oxidation of hydrogen sulfide and hydrogen peroxide respectively; Puri et al., (1958b) stated that the nature and not the amount of the carbon surface was important in this reaction process.

Table 2. As(III) oxidation by 9 activated carbons, Equilibrium As(III) and As(V) concentrations. ($As(III)_{init}$ = 1085 µg/L)

Initial pH = 7					**Initial pH = 8.5**				**Initial pH = 9.2**			
Activated Carbon	**As(III) (µg/L)**	**As(V) (µg/L)**	**% As(V) Formed**	**% As Adsorbed**	**As(III) (µg/L)**	**As(V) (µg/L)**	**% As(V) Formed**	**% As Adsorbed**	**As(III) (µg/L)**	**As(V) (µg/L)**	**% As(V) Formed**	**% As Adsorbed**
Darco 20x40	1013.5	26.5	2.5	4.1	67.9	860	92.7	14.5	3.3	1006.2	99.7	7
Darco S-51	934.9	158.3	14.5	0	263.5	772.3	74.6	4.5	3.4	1018.1	99.7	5.9
DOR-A 8x40	927.9	88.1	8.7	6.4	87.3	913.6	91.3	7.8	3.4	975.3	99.7	9.8
Filtrasorb 200	573.2	456.1	44.3	5.1	7.5	913.2	99.2	15.1	3.4	1001	99.7	7.4
GAC 1240	810.9	255.1	23.9	1.8	10	947.3	99	11.8	N/A	N/A	N/A	N/A
Hydrodarco W	83.2	382.7	82.1	57.1	6.6	720.3	99.1	33	N/A	N/A	N/A	N/A
Norit GAC 400	688.6	359.1	34.3	3.4	9.2	942.4	99	12.3	N/A	N/A	N/A	N/A
Norit PAC 200	856.8	220.4	20.5	0.7	63.4	873.8	93.2	13.6	N/A	N/A	N/A	N/A
Norit RO 0.8	114.5	709.1	86.1	24.1	7.8	841.3	99.1	21.7	N/A	N/A	N/A	N/A

pH of Carbons: Based on initial results, the pH of four out of the nine activated carbons were determined. Two carbons with the highest oxidative abilities and two with the least oxidative abilities were selected for further investigation. The pH of Hydrodarco W and Norit Ro 0.8 were alkaline and were respectively 10.64 and 9.22. Whereas, those of Darco 2040 and Darco S-51 were acidic and were respectively 4.56 and 5.11. The pH of the carbons gives an indication of the functional groups present on the carbon surface which in turn influence oxidation.

CONCLUSIONS

Generally, we can conclude that the oxidation of As(III) by these nine activated carbons were favored at alkaline pHs and consequently basic activated carbons had higher oxidative abilities. Dissolve oxygen was also required for the oxidation process. It is therefore possible in a one step process to achieve the oxidation and removal of As by an iron oxide impregnated activated carbon; where by the activated carbon carries out the oxidation process and iron oxide the adsorption process. This study serves a pilot study on investigating factors that influence As(III) oxidation by activated carbons. Future work will characterize these functional groups responsible for oxidation after which activated carbons will be modified to enhance oxidation.

REFERENCES

1. Daus,B., Wennrich, R., and Weiss,H. 2004. " Sorption materials for arsenic removal from water : a comparative study." *Water Research.* 38:2948–2954
2. Ghurye, G., Clifford, D., and Tripp, A. 2004. "Iron coagulation and direct microfiltration to remove arsenic from groundwater." *J.-Am.Water Works Assoc*. 96:84-89.
3. http://water.epa.gov/drink/- Accessed in May 2011.
4. Ischizaki, C., and Cookson, Jr. J.T. 1974. "Influence of Surface Oxides on Adsorption and Catalysis with Activated Carbon." In (A.J Rubin, Ed.), *Chemistry of Water Supply, Treatment and Distribution*, pp 201 -231.Ann Arbor Sci Pub., Ann Arbor, MI.
5. Jain, C.K., and Ali, I. 2000. "Arsenic: occurrence, toxicity and speciation techniques." *Water Research* 34 : 4304-4312
6. Johnston, R., and Heijnen, H. 2001. "Safe Water Technology for Arsenic Removal." In (Ahmed, M. F., Ali, M. A., and Adeel, Z, Eds),*Technologies for Arsenic Removal from Drinking Wate*r, pp 1-22. The Bangladesh University of Engineering and Technology and the United Nations University.
7. Larson, E.C., and Walton. F.H.; 1940. Activated Carbon as a Catalyst in Certain Oxidation-Reduction Reactions. *J Phys. Chem.,* 44:70
8. Li,H., Monnell,D., Alvin M., and Vidic,R.D. 2008. "Factors affecting activated carbon-based catalysts for selective hydrogen sulfide oxidation." *Main Group Chemistry*. 7(3):239-250
9. Ngantcha,T.A., Vaughan, R., and Reed, B.E. 2011. "Modeling As(III) and As(V) Removal by an Iron Oxide Impregnated Activated Carbon in a Binary Adsorbate System." *Separation Science and Technology*, 46:1419–1429
10. Ona-Guema G., Morin, G., Wang, Y., Foster. A., Juillot, F., Calsa, G., and Brown, Jr.G. 2010. "XANES Evidence for Rapid Arsenic(III) Oxidation at Magnetite and Ferrihydrite Surfaces by Dissolved O2 via Fe2+-Mediated Reactions" *Environ. Sci. Technol.* 44:5416–5422
11. Paritam, K., Dutta, S., O. Pehkonen, Virendeh, K., Sharma, and Ajay, K. Ray. 2005 "Photocatalytic Oxidation of Arsenic(III): Evidence of Hydroxyl Radicals." *Environ. Sci. Technol.* 39:1827-1834
12. Pierce, M.L., and Moore, C.B. 1982. "Adsorption of arsenite and arsenate on amorphous iron hydroxides." *Water Research* 16: 1247–1253.
13. Puri, B.R., Sharma, L.R., Singh, D.D. 1958a. Studies in Catalytic Reactions of Charcoal, Part I. Catalytic Oxidation and Decomposition of Salt Solutions. *J. Ind. Chem. SOC.* 35: 765-769-774
14. Puri, B.R., Sharma, L.R., Singh, D.D. 1958b. "Studies in Catalytic Reactions of Charcoal, Part II. Catalytic Oxidation and Decomposition of Hydrogen Peroxide." *J. Ind. Chem. SOC.* 35: 770
15. Schmidt,G.T., Vlasova, N., Zuzaan, D., Kersten, M., Daus, B. 2008. "Adsorption mechanism of arsenate by zirconyl-functionalized activated Carbon." Journal of Colloid and Interface Science 317:228-234
16. Smith, A.H.; Hopenhayn-Rich, C.; Bates, M.N.; Goeden, H.M.; Hertz-Picciotto, I.; Duggan, R.; Wood, H.M.; Kosnett, M.J.; Smith, M.T. 1992. "Cancer risks from arsenic in drinking water. Environmental Health Perspectives." 97: 259–267.
17. U.S. EPA. Fed. Regist. 2001. 66: 20579–20584.

PERFORMANCE ATTRIBUTES OF MODIFIED BIOSAND FILTER WITH BRASS

Banu Sizirici Yildiz (Case Western Reserve University, Cleveland, OH, USA)

Access to safe drinking water is an essential requirement for human life. Unfortunately, more than one sixth of world population still lacks access to this precious resource. Point-of-use (POU) drinking water treatment technology enables these people to treat their water at home and to improve the water quality. All around the world, many companies propose POU water treatment technologies without adequate testing and this may lead to insufficient disinfection based on the World Health Organizations (WHO) drinking water guidelines. The recently promoted bio-sand filter (BSF) with granulated brass shaving "Chemical/Biochemical Water Purification Reactor US2008/079701" designed by Aqua Clara Water Purification Technology uses brass shaves as an extra disinfectant layer. Currently, this technology is being promoted without adequate testing. The aim of this study is to evaluate the pathogen reduction potential of modified biosand filter (MBSF) and to determine if brass corrosion yields metals (copper and zinc) at concentrations high enough to be of health concern. Two filters were designed; the conventional BSF filter was filled with gravel, pea gravel, coarse sand, and fine san and; the modified BSF (MBSF) was constructed in the same manner, with granulated brass disinfectant layer between fine sands. The filters were run intermittently twice a day with 8 liters of water collected from the Doan Brook Stream in Cleveland, OH. Physical and biological tests were conducted to compare the performance of the MBSF with the BSF over a three month period. Samples were collected from exit pipes and tested immediately for fecal coliform, total coliform, e-coli tests, flow rate, turbidity, pH, and dissolved oxygen. Test results showed 90.47% reduction in total coliform, 96.59% reduction in fecal coliform, 96.9% reduction in e-coli and 88.5 % reduction in turbidity for the BSF and 89.32% reduction in total coliform, 68.85% reduction in fecal coliform, 97.7% reduction in e-coli and 88.3% reduction in turbidity for the MBSF. The metal levels at the effluent were 0.024 ppm for copper and 0.24 ppm for zinc that is below WHO drinking water guidelines. Based on the test results, it was observed that the MBSF with brass has made no significant contributions to the improvement of the quality of water. The poor performance of brass, however, may be a result of integrating the disinfection layer into the lower depths of the BSF. There are more possible parameters that could be optimized; therefore, more study is necessary to develop a better understanding on MBSF with brass before promoting it for wide range use.

ISBN 9780976885351

USING SMART GRID TECHNOLOGIES AS A PUBLIC HEALTH PROTECTION TOOL

Trevor Hill and ***Graham Symmonds*** (Global Water Resources, Phoenix, USA)

In the early 1970's, the Safe Drinking Water Act (SDWA) was enacted, providing a cohesive federal set of standards for water quality delivered to consumers. As a result, utilities were required to meet maximum contaminant levels of certain constituents prior to water entering the distribution point. Today, the SDWA regulates 91 contaminants and the EPA is required to publish and maintain a Contaminant Candidate List and is required to make regulatory determinations on at least five potential contaminants every five years. Notably, however, the majority of these contaminants are regulated at the Entry Point to the Distribution System (EPDS) and not in the distribution system. In fact, only three of the SDWA rules require monitoring in the distribution system: the Lead and Copper Rule, the Total Coliform Rule, and the Disinfectant and Disinfection By-Products Rule. The result is that there are few regulatory requirements to monitor for water degradation in the distribution system. Distribution systems remain a vast array of potential problems for utilities. In fact, since the introduction of the SDWA, there has been marked reduction in the number of water-borne disease outbreaks attributed to water treatment systems. Over the same period, however, the percentage of disease outbreaks attributable to defects in the distribution system has increased exponentially. Interestingly, as a result of the continuous aging infrastructure employed by our water utilities, the number of water-borne disease cases has increased in the last decade. The smart grid for water can be used to significantly improve both the utility's understanding of water quality in the distribution system, but can dramatically increase the response time and provide the means to ensure public health protection. The answer lies in improving the temporal and spatial quality of the data. For example, by combining customer input via call centers, highly granular consumption data from the Customer Information System, SCADA and hydraulic modeling data and asset management with geo-referenced spatial data, a rapid, visual identification of water distribution system health can be built allowing operations staff to take action. Further, leak detection flags and reverse flow flags from AMI metering systems can be employed to both identify potential ingress of contaminants, and where hydraulic conditions exist that promote reverse flows. This paper will present the use of the Analytical Water Quality Assurance Program developed to provide instantaneous water quality notifications throughout the utility organization.

ISBN 9780976885351

HEALTH RISK OF DISINFECTION BYPRODUCTS IN RECYCLED WATER IN ABU DHABI

Aina Daniel, Maren Mieseler, Juan-Rodrigo Bastidas-Oyanedel, Farrukh Ahmad
(BioEnergy and Environmental Laboratory (BEEL), Water and Environmental Engineering Program,
Masdar Institute of Science and Technology, PO Box 54224, Abu Dhabi, United Arab Emirates)

Reuse practices of recycled water have become attractive options for extension of available water resources. Safe operation of water reuse systems depends on the reliability of disinfection step, which is the most important treatment process for public health protection. Generally, chlorination is used to inactivate pathogens in water. An undesirable side effect of the interactions between chlorine and residual organic matter in water is the formation of halogenated disinfection byproducts (DBPs) like trihalomethanes (THMs) and haloacetic acids (HAAs).The United Arab Emirates ranks eight in the world in water reuse. The enormous reuse practices of recycled water require a regulatory mechanism in ensuring public health safety. This study is aimed at developing both qualitative and quantitative approach at assessing human health risk posed by halogenated DBPs from reuse of recycled water in the emirate of Abu Dhabi. It will provide analysis of the principal functions of hazard identification, exposure assessment, and risk characterisation of THMs as they relate to specific usage patterns. Results of the exposure modeling exercise will help in determining the acceptable risk to human health so that policy guidelines related to recycled water use can be further refined.

ISBN 9780976885351

A NEW TREATMENT SYSTEM FOR GENERATING POTABLE WATER FROM MUNICIPAL AND INDUSTRIAL WASTEWATER

Yanguo Ma (PCDworks, Inc., Palestine, TX, USA)
Mike Musial (Active Water Sciences, LLC, TX, USA)
Kenneth Wilson (PCDworks, Inc., Palestine, TX, USA)
Mike Rainone (PCDworks, Inc., Palestine, TX, USA)

A new treatment system is being investigated for generating potable water from municipal and industrial wastewater. The system includes a biological reactor, filter and UV system. The significance of this system is that specific bacteria consortium is seeded in the bioreactor, which can enhance to mitigate not only common contaminates, such as biochemical oxygen demand (BOD), total suspended solids (TSS), but also some other emerging chemicals, which are being considered for regulation by USEPA. Local municipal wastewater and frac water are being used for this study. This study includes lab treatability study for the frac water and a pilot system testing for the municipal wastewater. The following parameters will be analyzed: BOD, TSS, total organic compounds (TOC), heavy metals, nitrogen and phosphorus. Preliminary results will be presented and discussed.

ISBN 9780976885351

ADSORPTION MECHANISMS OF COPPER ON FUNCTIONALIZED MULTIWALL CARBON NANOTUBES: CHEMICAL STRUCTURES

Shirley Rosenzweig* and George A. Sorial PhD (Environmental Engineering Program, College of Engineering & Applied Science, University of Cincinnati, OH); E. Sahle-Demessie PhD and Todd Luxton PhD (U.S. Environmental Protection Agency, Cincinnati, OH)

Multiwall carbon nanotube (CNT) surface functional groups and structure have important effects on the mechanisms of metal ions adsorption in aqueous solution, which is of upmost interest for future applications in drinking water treatment. Copper ions are of environmental interest due to corrosion reactions on household pipes. In many cases, the pH of water in the distribution systems drops below the pH at which the water left the treatment plant. Fluctuation of pH can cause disruption of copper passivation films and pitting of copper pipes, causing copper complexes precipitation or dissolution, introducing other contaminants in the water stream. This study investigates the influence of network forces formed by van der Waals bonds within the CNT bundles on the hydrophilicity, aggregate state and available sites for copper adsorption. Copper complexes are attracted to different oxygen radicals on the surface and within the bundles of CNTs. The adsorption isotherm curves show a strong effect of initial concentration, which is investigated as an impact of the different network forces and the presence of impurities leached from as-received CNTs. Isotherm and kinetic experiments compare alcohol (OH-CNT), acid (COOH-CNT) and pristine (P-CNT) CNTs adsorption capacity. A deprotonation process of COOH-CNTs reduced the van der Waals bonds, increasing available polarized sites for copper adsorption, improving adsorption capacity and removing the effect of initial concentration. The effect of purification of P-CNTs by oxidization (Ox-CNTs) is also investigated. Several methods are used to characterize all CNTs. FTIR spectra compare vibration peaks of hybrids and as-received CNTs. XPS spectra compare oxygen amount on the CNTs surface. TEM images confirm morphology and size. Zeta potential techniques study the effect of pH on copper adsorption. AAS techniques measure copper ion concentration, while ICP-AES analysis is used to measure the amount of several metals leaching from hybrids and as-received CNTs after different rinse cycles. The BET method confirms surface area. SEM/EDX experiments investigate the presence of solid copper and other species on as-received and hybrids CNTs (after copper adsorption). The isotherm and kinetic results suggest that network forces are stronger on COOH-CNTs, reducing its adsorption capacity. Consequently, adsorption of copper on OH-CNTs is better, followed by the deprotonated COOH-CNTs, as-received COOH-CNT, Ox-CNTs and finally P-CNTs. FTIR results show different peaks for hydroxyl groups and carboxyl groups associated to functionalization. Leached metal impurities show less than 1 mg/g of an eighteen-metal method applied, which is insignificant compared to the levels of copper in solution. Zeta potential experiments show that the electronegativity decreased (less negative surface charge) with increasing pH. Some conclusions driven from these results are that copper adsorption on to CNTs is attributed to the formation of an inner-sphere complex between copper and CNT surface functional groups. At pH values exceeding the PZC (point of zero charge), oxygen functional groups give rise to a net negative surface charge promoting metal cation adsorption. The solution pH dropped after equilibrium by release of H^+ from CNT surface. Kinetic studies demonstrate the copper adsorption rate on OH-CNTs, exceeded that of COOH-CNT surfaces. Network forces within acid and alcohol functionalized CNTs bundles suggest formation of different mesopore structures, leading to the conclusion of different diffusivity driving forces.

ISBN 9780976885351

APPLICATION OF COPPER OXIDE NANOPARTICLES TO REMOVE ARSENIC FROM NATURAL GROUNDWATER

Ajaya K. Sankara Warrier and K. J. Reddy* (University of Wyoming, Laramie, Wyoming, USA)

Arsenic (As) in water exists in two major oxidation states, arsenite (III) and arsenate (V), and it is difficult to remove both oxidation states simultaneously under a wide range of pHs and different concentrations of competing anions (e. g., phosphate, silicate, and sulfate). The objectives of this study were to evaluate the effectiveness of CuO (cupric oxide) nanoparticles in removal of As from groundwater under natural conditions, i. e., without adjusting the pH, oxidation state or spiking with competing anions (e. g., phosphate, silicate, and sulfate), and to determine the effects of CuO treatment on the chemistry of groundwater samples. Forty six groundwater well samples from rural domestic areas were tested in this study. Results suggested that more than 50 % of wells were found to contain arsenic level above the limit (>10 µg/L) set by US EPA (United States Environmental Protection Agency). Treatment of groundwater samples with CuO nanoparticles found to be efficient in removing arsenic to <10 µg/L. Results also suggested that CuO treatment did not alter the water chemistry and most of the water quality components remained within the US EPA MCLs (Maximum Contaminant Limit). Overall, results of this study show that CuO is an effective sorbent to remove arsenic from groundwater samples with a wide range of pHs and varying concentrations of competing ions.

ISBN 9780976885351

EFFECT OF CALCIUM ON MONOMER DISTRIBUTION AND TURBIDITY REMOVAL CAPACITY OF ALGINATE

Çiğdem Kıvılcımdan Moral (Akdeniz University, Antalya, Turkey)
Özdemir Doğan (Middle East Technical University, Ankara, Turkey)
F. Dilek Sanin* (Middle East Technical University, Ankara, Turkey)

Alginate which is a natural biopolymer composed of β-D-mannuronic and α-L-guluronic acids. It is currently extracted from marine brown algae. However, alginate can also be synthesized by some bacteria such as *Azotobacter vinelandii* and some species of Pseudomonas. *Azotobacter vinelandii* produces alginates first as mannuronic acid and then epimerizes it to guluronic acid by the action of seven different extracellular epimerases designated as AlgE1-7. These enzymes highly depend on calcium ion for their activity.

In this study, alginate was produced by *Azotobacter vinelandii* ATCC® 9046 in a laboratory fermenter with the ultimate goal of using the polymer produced for turbidity removal. During experiments, dissolved oxygen tension, mixing rate, pH and temperature were maintained constant at 5 % of air saturation, 400 rpm, 7.2 and 30 °C, respectively. The effect of variation of Ca^{2+} concentration (in the range of 25 to 100 mg/L) on alginate quality and quantity was investigated. It appeared that 50 mg/L of Ca^{2+} concentration was optimum for alginate production with the highest alginate concentration of 4.51 g/L. Similarly, a higher degree of polymerization seemed to be achieved at moderate level of Ca^{2+} dose. Monomer distribution of alginate was also affected by changing Ca^{2+} concentration. Almost equal amount of mannuronic and guluronic acids was obtained at moderate level of Ca^{2+} dose. On the other hand, alginates rich in mannuronic acid, 73 %, were produced at low Ca^{2+} concentration.

The alginate samples produced with the aforementioned experiments were then used in turbidity removal tests. The results from 10 NTU initial turbidity samples indicated that the effectiveness depended on the monomer distribution of the polymer. Bacterial alginate was generally able to reduce the turbidity values down to 1 NTU.

*e-mail: dsanin@metu.edu.tr

ISBN 9780976885351

COMMUNITY CHARACTERISTICS OF BIOFILMS FORMED ON WATER DISTRIBUTION PIPE MATERIALS

Sung-Chan Choi* (Hallym University, Chuncheon, Gangwon, S. Korea)
Hun-Joo Cha, Jung-Chul Suh (Samchully Co., Seoul, S. Korea)
Dooil Kim (Dankook University, Yongin, Gyeonggi, S. Korea)
Yeong-Kwan Kim (Kangwon National University, Chuncheon, Gangwon, S. Korea)

The surface-adherent bacterial entities known as biofilms that form on pipe surfaces in water distribution systems can lead to bacterial regrowth, increased chlorine demand, and problems with the taste and odor of the water. Changes in the diversity and structure of biofilm microbial communities may offer a key to understanding the generation and growth of biofilm in drinking water distribution systems. Annular Biofilm Reactor (ABR) equipped with coupons of three different pipe materials (STS 304, PVC, PE) was used to generate biofilm samples. During the sample generation period, average tap water quality was as follows: temp. 9.4°C, pH 6.9, turbidity 0.34 NTU, free residual chlorine 0.22 mg/L, NH_3-N 0.024 mg/L, PO_4^{3-}-P 0.027 mg/L, assimilable organic carbon (AOC) 37.3 μg/L, and heterotrophic plate counts 8 CFU/mL. AOC level clearly plays an important role that limits the formation of biofilm in this system. Nevertheless, terminal-restriction fragment length polymorphism (T-RFLP) analyses determined T-RF profile as early as 3 h of exposure on PVC coupons. Atomic force microscopic analyses showed an average surface roughness (R_a) of 125.7 nm for PVC, and this value was higher than STS (71.6 nm) and PE (74.0 nm). Surface roughness, however, did not seem to be the only factor that controls the initiation of biofilm development since the formation was faster on STS (6 h) than on PE (12 h). Upon detection of the T-RF peaks, richness (S) and diversity indices such as Shannon (H) and Simpson ($1/D$) demonstrated a rather slow increase until 48 h followed by rapid increase regardless of the pipe materials. Differences of microbial community structures among the biofilm samples were determined based on the cluster analysis using Jaccard coefficients (S_j). Pipe material and exposure time were found to be important in biofilm cluster formation. Biofilm communities on PVC or STS clustered together and the biofilm samples could be divided into two different groups according to the exposure time. First group of cluster contained a young (< 48 h) biofilm samples (10 out of 11) but second group contained a mature (≥ 48 h) samples (11 out of 14). Results suggested that the targeting of the first group of cluster is crucial for optimizing the management of drinking water distribution systems and controlling microbial growth due to the complexity of biofilm.

ISBN 9780976885351

DEVELOPMENT OF A WETTING TECHNIQUE OF CARBON ELECTRODES IN CAPACITIVE DEIONIZATION AND AN EVALUATION METHOD

Hsin-Lan Hsu and Yu-Tzu Chen (Industrial Technology Research Institute, Hsinchu, Taiwan, R.O.C.)

A higher degree of water filling in the pores of the carbon electrode in capacitive deionization application can enhance the desalination capacity. While several methods of surface modification had been suggested to alter the surface more water-wet, the surface modifier often increased the electrical resistance or blocked the pores, which reduced the available pores for electrosorption and thus lead to only several ten percent enhancement of desalination capacity. In this research, activated carbon electrodes conditioned with two proposed vacuum wetting techniques along with the commonly used soaking method were evaluated by pore water weight, cyclic voltammetry, and desalination capacity. The two vacuum wetting techniques, one with and the other without gaseous carbon dioxide assisted, both increased the pore water weight in the electrodes by 2-3 times. The one without carbon dioxide assisted also showed 2 times more desalination capacity and its high reproducible cyclic voltammetry curve suggested the water imbibition in the pores reach the steady state. These results showed that the water-filled pores in the hydrophobic carbon electrode can be increased by several times without trade-off.

ISBN 9780976885351

STRATEGIES FOR SUSTAINABLE DEVELOPMENT OF HYDROGRAPHIC ECOSYSTEMS IN WESTERN AND CENTRAL ROMANIA

Aurel Ardelean, Dorina Ardelean, Violeta Turcus, Iulian Octavian Stana and Mihai Sorin Pascu
("Vasile Goldis" Western University of Arad, Romania)

ABSTRACT: Mures River has a length of 766 km and collects water from a 29,767 km^2 area across the territory of two countries (Romania and Hungary). Over time along the river settlements were developed, some of which later became important industrial centers. Mures River Basin in Romania occupies 12% of the country and it gathers water from a network of 10,800 km watercourse. The ecological conditions of the river have an economic importance and its value is significant if we take into consideration all potential natural resources. By connecting two neighboring countries, the environmental problems of this river are not only national but they become international. The negative influence of people on the environment has turned against them, is known very well that human settlements suffer from the non-organic consumption of the environment.

The main objective is to develop a strategy for sustainable development and to ensure biodiversity, to combat cross-border pollution, to reduce the risk of pollution of one of the main tributaries of Danube River, through Tisza River Basin. Thus there were initiated a series of studies and international projects in "Vasile Goldis" Western University of Arad, in order to create opportunities for sustainable economic development, to enhance quality of life through the development and preservation of natural heritage and creation of a management and control system on environmental factors. For this study was chosen a sector from the lower course of Mures River, between two settlements, Zam and Pecica. To include the contribution of tributaries' pollutants and the impact of a city with a large population, sampling points were selected upstream and downstream of Arad. All samples were taken from boats during three subsequent days, in the order site 6 to site 1 opposite to the direction of the water flow.

The purpose of this paper was to investigate the pollution degree of Mures and its tributaries as well as to investigate the pollution at the level of aquatic communities. The most important sources of pollution for Mures River and its basin are the mining industry (affecting Aries River), metallurgical industry (tributaries Tarnava, Ampoi, Cerna, Strei), chemical industry (Tarnava), adding numerous water treatment stations, especially located on the river Mures.

From these studies we could demonstrate that it is necessary to implement a multidimensional approach into monitoring watercourse networks to improve the sensitivity and accuracy assessment of the ecological effects of pollution on the aquatic environment. In this context, the study of the Mures River and its tributaries is a priority. Based on this study we concluded that in order to increase the eco-toxicological quality of Mures River is required the retention of heavy metals (particularly cadmium and copper) at the sources of pollution, but also an effective treatment of fecal waste, the protection of landscapes and fragile ecosystems, the management of water system in relation to spatial planning, conservation of rivers and lakes, restriction of intensive use of land through the expansion of urban areas and intensive agriculture and flood prevention.

INTRODUCTION

The Mures river hydrographic basin is the largest river basin from Romania, with a surface of 29767km^2. The Mures river has a length of 766km, crossing the central and western part of the country, flowing into Tisa river, on the Hungarian territory, in Szeged. The Mures river hydrographic basin represents about 12% of Romania`s territory and gathers a network of tributaries with a total length of 10800km.

ISBN 9780976885351

Across the times, along the Mures river course, as along it`s tributaries, many settlements developed, out of which some are actually large human agglomerations, being important industrial centers.

Our study started from the hypothesis that the ecological qualities of the river courses and river basins have an important economic significance, not only through the quality and quantity of the resources provided, but also through the ecosystem services provided to the local communities and the general population.

The study was realized in the 2009-2012 period, the researches being realized along the whole length of the Mures river course. Along information gathered in the field, bibliographical data were discussed, to perform an integrated analysis of the human impact on the Mures river catchment ecosystems, and to propose necessary measures within a sustainable development strategy of the region.

MATERIALS AND METHODS

Mures river was investigated from it`s source to it`s Tisa river inflow, with the purpose to define it`s hydrographic, hydro-morphologic, water quality and ecosystems characteristics. In this respect water samples were collected, hydro-morphological and biodiversity assessments were performed, mostly upstream and downstream the confluence with it`s major tributaries, respectively: Niraj river: L = 82 km; S = 651 km^2, Aries river: L = 166 km; S = 3005 km^2, Tarnave river: L = 246 km; S = 6253 km^2, resulting from the junction of Tarnava Mica river (L = 196 km; S = 2071 km^2) and Tarnava Mare river (L = 223 km; S = 3666 km^2), Ampoi river: L = 57 Km; S = 576 km^2, Sebes river: L = 96 km; S = 1304 km^2, Strei river: L = 93 km; S = 1983 km^2.

Data regarding the multiannual water discharge of the Mures river was evaluated, in few different sections, in order to analyze the influence of the increased water discharge on the natural recovery of water quality, through the dilution of pollutants overflowing in the water bodies.

The multiannual water discharge of the Mures river increases from 1,05 m^3/s (33,1 mil. m^3/year) in Suseni section, to 105 m^3/s (3311,2 mil. m^3/year) in the Alba Iulia section, reaching to 186 m^3/s (5865,6 mil. m^3/year) in Nadlac section, where the river flows into Hungary.

The water discharge of the main Mures river tributaries in their confluence section, represented in the multiannual medium discharge, is the following: for Aries river the water discharge is 25,6 m^3/s (807,3 mil. m^3/year), representing 13% of the Mures river discharge in the Nadlac section. For Tarnave river the water discharge is 26,8 m^3/s (845,1 mil. m^3/year), representing 14,4% of the Mures river discharge in the Nadlac section. For Strei river the water discharge is 27,8 m^3/s (876,7 mil. m^3/year), representing 14,9% of the Mures river discharge in the Nadlac section.Measurements regarding water quality have been made for the following parameters: pH, dissolved oxygen, water conductibility, turbidity, temperature, nitrates, water hardness, CBO5, CCO-Cr, total nitrates, total phosphorus and others. The physical water parameters were measured with portable, real time, measuring devices. The chemical parameters were measured with portable, quick measurements, devices, in the field, and respectively measurements made in laboratory using standardized techniques and methodologies.

Assessments of hydro-morphological characteristics of the Mures river course were made with the RHS (British River Habitat Survey) methodology, modified to facilitate quicker assessment possibilities. Aspects as: river course sinuosity, debris (dead trees trunks), ridges, rocks and other bodies immersed which could produce turbulences, river shore stabilization, quality of the floodplain, type of riparian vegetation etc. were determined. Observations were realized considering river sectors with similar characteristics, the difference among two consecutive sectors being made when significant changes appeared at some point (example: tributary inflow > increase in the water discharge for the downstream sector, floodplain covered with forests next to a floodplain area covered with agricultural fields etc.). The evaluated characteristics were scored, and depending on the summarized value of the scoring the ecological quality of each river sector was established.

Data regarding the abiotic component of the aquatic ecosystems were correlated with data regarding the biodiversity of the studied area, plant and animal species being equally evaluated, as habitats characteristic for the humid areas, or habitats representing the living environment of the identified key species.

We realized maps which emphasize the human impact on the Mures river catchment ecosystems, as we realized maps which present in a descriptive manner the conclusions of our study and the measures necessary to promote the sustainable development of the communities living within the territory of the Mures hydrographic basin.

RESULTS AND DISCUSSIONS

After analyzing water quality and Mures river hydro-morphology the following punctual, significant, pollution sources were emphasized:

Human agglomerations. Above 2000 citizens equivalent which hold sewage systems, with or without water plants, with overflow in water bodies; under 2000 citizens equivalent, if they hold centralized sewage systems; human agglomerations with centralized sewage systems, which don`t have the capacity to collect and clean the mélange of sewage waters and rain water in periods with intense rainfalls.

TABLE 1: Situation of human agglomerations, water plants, and total organic charge, collected and cleaned in the Mures hydrographic basin.

Dimension of human agglomerations (citizens equiv.)	**Number of human agglomerations**	**Number of water plants**	**Total organic charge (citizens equivalent)**	**Collected organic charge**		**Cleaned organic charge**	
				Citizens equivalent	**%**	**Citizens equivalent**	**%**
> 150000	2	2	387000	243000	63	242000	63
15000 – 150000	19	19	712000	553000	78	199000	28
10000 – 15000	7	8	90000	46000	51	44500	49
2000-10000	215	16	881000	93000	11	31000	4
Total	243	45	2070000	935000	45	516500	25

TABLE 2: Organic substances and nutrients discharge of the human agglomerations from the Mures hydrographic basin.

Agglomeration categories/evacuated pollutants (citizens equivalent)	**Organic substances (CCO-Cr)**	**Organic substances (CBO5)**	**Total nitrates**	**Total phosphorus**
	t/year	**t/year**	**t/year**	**t/year**
> 100000	3782	1493	251	78
10000 - 100000	9678	3947	1822	191
2000 - 10000	515	223	37	8
< 2000	0	0	0	0
Total	13975	5663	2110	277

TABLE 3: Heavy metals discharge from punctual industrial and agricultural sources from the Mures hydrographic basin.

Industry type/evacuated pollutants	**Cu**	**Zn**	**Cd**	**Ni**	**Pb**	**Hg**	**Cr**
	t/year	**t/year**	**t/year**	**t/year**	**t/year**	**t/year**	**t/year**
IPPC industry	49652	13712	145	0	197	0	11
Non IPPC industry	1824	7053	7	9	21	0	5
Total industry	47015	22341	167	8	221	0	12
Other punctual sources	0	0	0	0	0	0	0

Industry. (1) Are represented by installations which enter under the incidence of the Commission Directive regarding the prevention and integrated pollution control – including the units inventoried within the Emitted Pollutants Registry (EPER) and which may impact water quality; (2) Industrial units which evacuate dangerous substances and/or priority risk substances over the legal limits; (3) Other industrial units which evacuate sewage waters within the water bodies and which do not comply with the actual regulations regarding the impact on water quality.

Agriculture. (1) Animal farms – including the units inventoried within the Emitted Pollutants Registry (EPER) and which may impact water quality; (2) Farms which evacuate dangerous substances and risk substances over the legal limits; (3) Other agricultural units with punctual evacuation and which do not comply with the actual regulations regarding the impact on water quality.

In the Mures hydrographic basin there was inventoried a number of 197 punctual pollution sources, which are overflowing used waters in surface water bodies. Among these, after field analysis regarding the quality of discharged waters, it was emphasized a number of 90 punctual significant pollution sources (42 urban, 32 industrial and 16 agricultural).

Along the punctual pollution sources, there were identified diffuse pollution sources. Principal categories of diffuse pollution were identified as being:

Human agglomerations. Human agglomerations which don`t have sewage systems or adequate collecting and elimination systems for the mud resulting from water plants, as the settlements which hold inadequate deposits for domestic wastes.

Agriculture. Animal farms which don`t have adequate systems to stock and use animal dejections, settlements identified as being vulnerable or potential vulnerable areas for nitrates pollution from agricultural sources, units which use pesticides and don`t conform with actual regulations, other units and agricultural activities which may lead to significant diffuse emissions.

Industry. RAW materials, finite products, auxiliary products deposits, stocking of wastes, units which produce accidental diffuse pollutions, respectively abandoned industrial sites.

TABLE 4: Industrial sources with high risk potential for accidental pollution from the Mures Hydrographic basin.

Crt. no.	**Name**	**Locality**	**Receiving water course**	**WRI ≥ 5,0**
1	Bicapa SA (sludge bed)	Tarnaveni/Mures	Tarnava Mica	7,3
2	Energo Mineral P.L. Abrud (sludge bed)	Abrud/Alba	Aries	9,1
3	EM Rosia Montana (sludge bed)	Rosia Montana/Alba	Aries	8.1
4	Minvest Deva, Filiala Ariesmin – Baia de Aries	Baia de Aries/Alba	Aries	7.5
5	CNCAPF Minvest Deva SA, Filiala Coranda (sludge bed)	Certej/Hunedoara	Mures	8.7

Table 5: Polluted areas with high risk potential from the Mures Hydrographic basin.

Crt. no.	**Area**	**Region**	**Receiving water course**	**Potential risk (m2 ≥ 250)**
1	Copsa Mica	Sibiu	Tarnava Mare	117 relevant
2	Mintia	Hunedoara	Mures	185 relevant

Other identified activities with potential negative impact. Another category of activities with impact on the Mures river course are the gravel pits – mostly in the minor river bed of the river. Their effect is materialized generally by the modification of the longitudinal profile, variability of the river bed deposits and the degrading processes – mostly lateral and depth erosion.

Gravel pits which exploit the high terraces deposits hold a potential risk by the penetration of the watertight clay strata which seal the depth aquifer from the surface aquifer, resulting in the contamination of the potable water resources for the local and regional human communities.

Based on the data gathered from the field and the bibliographical data, in conformity with the national and community regulations, protected areas for surface waters were identified and mapped.

Protected areas represent areas represent territories of the hydrographical basin, designated on the basis of special protection requirements drawn within the national and community regulations. Thus, in conformity with the Water Framework Directive, on the Mures river catchment territory the following categories of protected areas were analyzed and proposed:

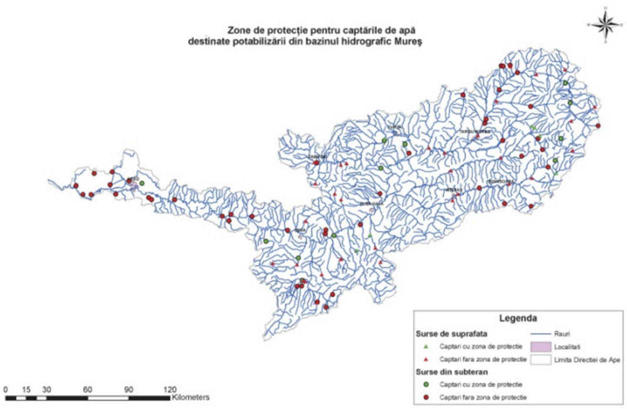

FIGURE 1: Protected areas for human use water intakes

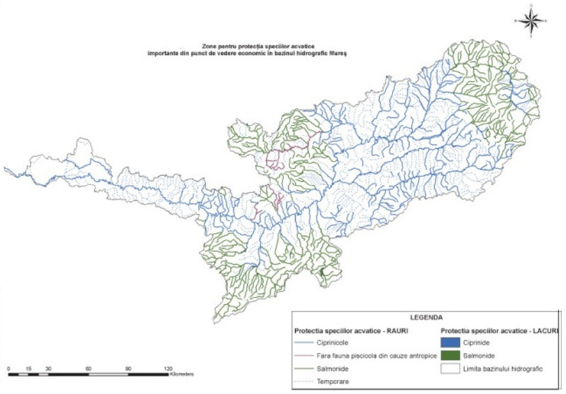

FIGURE 2: Trout and carp breeding areas

Areas for the protection of the human use water sources. There were inventoried 40 water intakes from surface waters, out of which 7 were insured with protection areas (17,5%). The medium tapped discharge was of 2158,97 l/s, and the population using these intakes is of 858557 citizens. For the underground water sources there were inventoried 58 intakes, out of which 13 were insured with protection areas (22.41%). The medium tapped discharge was of 652.49 l/s, and the population using these intakes is of 337585 citizens. In figure no. 1 the water intakes for human use from surface and underground waters from the Mures river basin are represented.

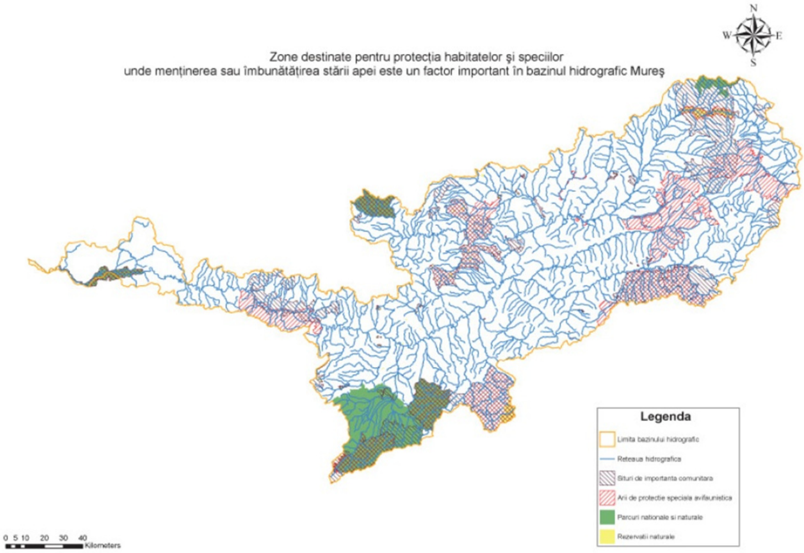

FIGURE 3: Areas for species and habitats protection

Areas for the protection of the aquatic species of economic importance. They comprise the water courses and lakes, important for fish farming. In figure no. 2 the actual situation at the level of Mures river basin is presented, regarding the trout and carp breeding areas, water courses without fish fauna due to human impact, and temporary water courses. The trout breeding areas have a total length of 3724km, which represent 34% of the total length of the entire hydrographic network, and a surface of 720ha of lakes. Out of the total length of 3724km, about 81% is located within natural protected areas.

Areas for the protection of the specific habitats and species. They comprise natural protected areas designated officially through national and community regulations and directives, which have a connection with the water bodies. Function of the management category, as one may observe in figure no. 3, in the Mures hydrographic basin, the areas for the protection of the specific habitats and species, where the preservation or the amelioration of the water status represents an important factor are within the extension of the following types of nature protection areas: national parks: 45623ha; natural parks: 178043ha; nature reserves: 30754ha; Special Protection Areas (SPA): 478435ha; Sites of Community Importance (SCI): 520710ha.

Thus, in the year of 2011, for the Mures river basin the areas designated for the protection of species and habitats summarize a number of 240 and a total surface of 696268ha, out of which one with cross-border character.

Some of the protected areas designated at national and European Community level, are recognized as Biosphere Reserves – Man and Biosphere Programme, and as Humid Areas of International Importance, designated by the Ramsar Convention Secretariat.

In order to emphasize the determinant character of the Mures river in shaping the landscape and generating the typical habitats which developed along it, we studied the biodiversity of a community importance site (SCI), localized within the inferior valley of the Mures river, having as central mark the Mures river course, respectively the ROSCI0064 Defileul Muresului Inferior (Inferior Mures Defile) Natura 2000 site. The site territory is developed on both sides of the river, on a surface of 34149ha, more extended on the right bank of the river, between the Gurasada, Hunedoara and Barzava, Arad localities. The site comprises the Mures river floodplain and the southern slopes of the Zarand Mountains. All the morphological elements have a microclimate strongly influenced by the Mures river.

The habitat of community importance with the largest distribution within the site is 91M0 – *Pannonian- Balkanic forests of Turkey Oak and Sessile Oak*. Within the Natura 2000 site, the habitat covers about 20% of it`s territory. This type of habitat is characteristic for the entire southern raw of Zarand Mountains, it`s presence being determined by the slopes exposition and the local climate.

The specific range was analyzed mostly with respect to bird species, especially bird species which use the Mures floodplain habitats as living environment, or at least feeding ground. Rare identified species, with high conservative importance, are: the Black stork – *Ciconia nigra*, the Lesser Spotted Eagle – *Aquila pomarina*, the Long-legged Buzzard – *Buteo rufinus*, the Corncrake – *Crex crex* etc. among the species characteristic to aquatic habitats we mention the Little Ringed Plover – *Charadrius dubius* and the Wood sandpiper – *Tringa glareola*, identified on the sandy banks which emerge along the Mures river islands. To these species a conservative management have to be performed, in order to insure their population perpetuation and even increase, as to participate to the sustainable development of the local human communities, through favorising the sustainable use of natural resources.

Among non wanted species, which realize strong invasions due to the favourable conditions offered by the Mures river, we mention the Amorpha – *Amorpha fruticosa*, the Ashleaf Maple – *Acer negundo*, the Prickly Cucumber - *Echinocystis lobata.* Their spreading has to be limited and they even have to be removed from some already occupied surfaces.

Areas sensible to nutrients and vulnerable to nitrates. On the territory of the Mures river basin there were identified 4 zones sensible to nutrients and nitrates: Podisul Transilvaniei (the Transylvanian Plateau), Mureşul Superior (the Superior Mures valley), Strei – Aries, Muresul Inferior (the Inferior Mures valley). Within these 4 areas 148 localities are to be found, distributed as follows: the Transilvanian Plateau – 67 localities, the Superior Mures valley – 9 localities, Strei-Aries – 50 localities, the Inferior Mures valley – 22 localities. The total surface of vulnerable areas within the Mures river basin is of 10672 km^2, divided as follows: the Transilvanian Plateau 3651 km^2, the Superior Mures valley 659 km^2, Strei – Aries 4544 km^2 and the Inferior Mures valley 1818 km^2.

CONCLUSIONS

The Mures river basin is an areal of surprising natural and cultural diversity. Even though there are significant pollution problems in some areas, the overall ecologic quality of the Mures river course and the Mures river basin remains high.

The Mures river ecosystems are not strongly fragmented by the building of dams and dykes. The Mures river banks are not strongly modified by river stabilization measures. The Mures river valley, and the Mures river catchment holds an important biodiversity, species and habitats of community importance. The most important activity which influences actually the river morphology is the gravel extraction, with effects on river dynamic. The actual ecological status of the Mures river may be used as support for the sustainable development of the local communities, through the sustainable use of natural resources.

As a final an comprehensive conclusion, we can state that the Mures river valley may be considered as one of the last major river courses of the Danube catchment which holds it`s natural characteristics, thus conservative measure should be imposed for it`s long term preservation.

REFERENCES

Balian, E.V. et all – 2008. *Freshwater Animal Diversity Assessment*. Springer Publishing, Dordrecht.

Chapman, D. [Ed.] – 1996. *Water Quality Assessments. A Guide to the Use of Biota, Sediments and Water in Environmental Monitoring*. 2nd edition, Chapman & Hall, London.

Furse, M. T. et all – 2006. *The Ecological Status of European Rivers*: Evaluation and Intercalibration of Assessment Methods. Springer Publishing, Dordrecht.

Gilbert, R.O. – 1987. *Statistical Methods for Environmental Pollution Monitoring*. Van Nostrand, Reinhold Co., New York.

Hildrew, A., Raffaelli, D. and Edmonds-Brown, R. – 2007. *Body Size* – the Structure and Function of Aquatic Ecosystems. Cambridge University Press, Cambridge.

Humpesch, U.H. – 1992. *Ecosystem study Altenwörth*: Impacts of a hydroelectric power-station on the River Danube in Austria. *Freshwater Forum*, **2**(1), 33-58.

Kresic, N. – 2009. *Groundwater resources* – Sustainability, Management and Restoration. McGraw Hill Publishing, New York

Namiesnik, J. and Szefer P. – 2010. *Analytical measurements in Aquatic environments*. 2nd edition, CRC Press, London.

Williams, G.P. – 1989. *Sediment concentrations versus water discharge during single hydrological events in rivers*. Journal of Hydrology, III, 89-106.

EVALUATION OF THE TMDL OF THE EAST CANYON RESERVOIR USING REMOTE SENSING

M. Brett Borup and David Fayol
(Brigham Young University, Provo, UT, USA)

ABSTACT: The objective of this paper is to determine if the implementation of the Total Maximum Daily Load (TMDL) in 2000 was successful in reducing excessive biological production in the East Canyon Reservoir using remote sensing. In this study, it was shown that data from the Landsat 5 Thematic Mapper (TM) could be used to compute the Chlorophyll-a concentration in the reservoir**.** A ratio of the blue (band 1) and green (Band 2) bands from the Landsat data were used to predict Chlorophyll-a concentrations. With this model 64 contour maps were produced showing the spatial distribution of the Chlorophyll-a over the East Canyon Reservoir for spring, summer and fall seasons from 1984 to 2010. A power equation model using these bands was fit to the data and found to have a correlation coefficient of 0.85 when compared to in-situ Chlorophyll-a measurements. An evaluation of these data showed at Chlorophyll-a concentrations in the reservoir were increasing in both the summer and fall prior to the implementation for the TMDL, but after TMDL implementation Chlorophyll-a concentrations in the reservoir are decreasing with time. In the spring it appears that Chlorophyll-a concentrations are continuing to increase with time even after TMDL implementations. These results may indicate that the TMDL does not control some source of phosphorous loading that occurs in the spring such as loads produced from agriculture and spring run-off. The evaluation of Chlorophyll-a concentrations using satellite imagery appears to be a useful tool in the evaluation of the effects of pollution control strategies.

INTRODUCTION

The East Canyon Reservoir is located) in the mountains northeast of Salt Lake City, UT, USA (Longitude / Latitude; 111 35 20 / 40 54 20. It was included in the "high priority" group for Utah's impaired waters in the 1998 list and thus needed a Total Maximum Daily Load (TMDL) plan to restore beneficial uses and water quality standards by targeting the reduction of the specific pollutant "total phosphorus." The TMDL was completed in 1999 (Judd, 1999) and strategies were implemented to reduce phosphorous levels in the reservoir in 2000. The results of the study indicated that the annual average load of phosphorus into the reservoir is 4182 Kg (9,220 lbs.) The target annual average load into the reservoir was determined to be 2561 Kg (5,647 lbs), so a load reduction of 1621 Kg (3,573 lbs) annually was required to meet the standard. The TMDL proposed activities to reduce the phosphorus load to East Canyon Reservoir to acceptable levels and thus to reduce the amount of nuisance causing algal growth that occurred in the reservoir.

Since 2000 phosphorus levels in East Canyon Reservoir have been monitored to determine the effectiveness of the TMDL activities, but little has been done to determine if the reduction in phosphorus load has had any effect on the algal populations in the reservoir which result from the high levels of phosphorus that existed in the reservoir prior to the implementation of the TMDL plan. The purpose of this study was to determine the effectiveness of those activities by assessing algal levels in East canyon

---

ISBN 9780976885351

Reservoir based on measuring chlorophyll-a concentration levels in the reservoir using remote sensing data.

MATERIALS AND METHODS

Using data from satellite images to predict chlorophyll-a concentration has been well studied (Fuller and Minnerick, 2007; Montana State Department of Environmental Quality, 2004; Han and Rundquist, 1997; Han and Jordan, 2005; and Brivio, et al, 2001 for example) and documented. In this study the following steps were completed to estimate chlorophyll-a concentrations in east Canyon Reservoir:

- The field chlorophyll-a data for the desired area was obtained and digitized.
- Cloud-free satellite imagery from approximately the same date as the field data collection was obtained.
- The imagery was corrected to compensate for geometric, radiometric, and atmospheric distortion in the imagery.
- A regression model was developed for each scene to relate the field data to the spectral data collected in each area of interest.
- The regression equation was applied to all image pixels in the satellite scene to predict chlorophyll-a concentration.

The Chlorophyll-a in-situ measurements were obtained from the Utah Division of Water Quality (UDWQ) and were taken between January 1995 and August 2008. Global positioning system coordinates were used to locate each of the samples. Results of these tests were used to calibrate the regression model.

All the images of the East Canyon reservoir for the time of study were downloaded from the United States Geological Survey (USGS). The choice of satellite was the Landsat 5 TM (Thematic Mapper) because it covers the entire time frame of our study. All of the Landsat 5 images that were used to calibrate the model and predict the Chlorophyll-a concentration were a Level 1T (Standard Terrain Correction). The Level 1T provides systematic radiometric and geometric accuracy by incorporating ground control points while employing a Digital Elevation Model (DEM) for topographic accuracy.

Additional criteria, such as cloud cover less than 10%, was chosen resulting in the highest quality of imageries to process the reading that were then processed using Exelis Visual Information Solutions (ENVI). Atmospheric correction in ENVI was performed using the dark subtraction method.

RESULTS AND DISCUSSION

Regression models from several previous studies were evaluated to determine the equation that best described the correlation between the in-situ data and the satellite imagery data. The model that was determined to be most successful based on a comparison of correlation coefficients used a ratio of data from Bands 1 and 2. A power fit equation (model) using these data was derived and a correlation of R^2= 0.8564 was determined:

$$\text{Chlorophyll-a, } \mu\text{g/L} = 1200.9 \exp [-4.077^*(\text{Band 1 value/Band 2 value})] \qquad \text{Equation (1)}$$

A graph of this equation and the observed data is presented in Figure 1. Using satellite image information and ArcMap it was determined 162 pixels covered East Canyon reservoir. The chlorophyll-a concentration for each individual was calculated using the satellite data and the correlation equation. This produces a spatial representation of the estimated chlorophyll-a concentration in East Canyon Reservoir at a given time. An example of the results of this method is shown in Figure 2.

Sixty-four maps were produced using these methods for each of three seasons: Spring (March, April, and May), Summer (June, July, and August), and Fall (September, October, and November). Maps were produced from days with Level T1 data and less than ten percent cloud cover between the years 1986 and 2010. This allowed further analysis of the reservoir during pre and post TMDL action time periods.

Data was not analyzed for the winter months since there was ice cover on the reservoir during much of this time period.

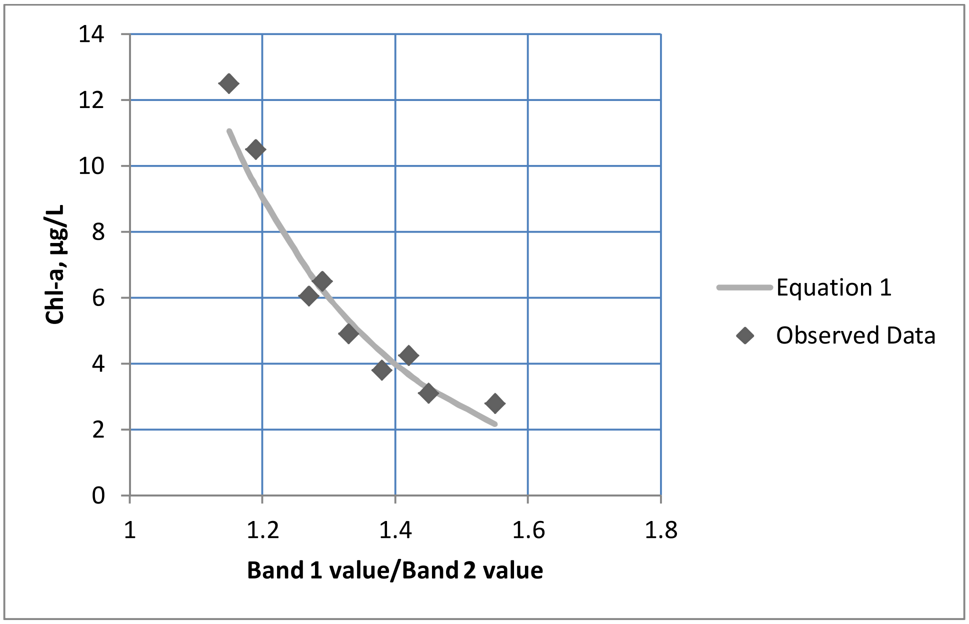

Figure 1. Power fit equation fit to observed data

.

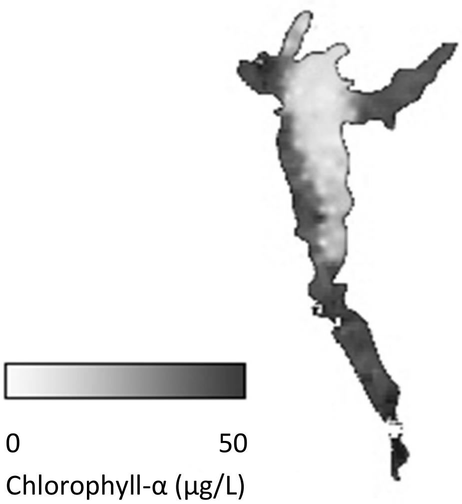

Figure 1. Estimated Chlorophyll-a Concentration for East Canyon Reservoir

Using the data obtained from the methods described above, the average chlorophyll-a concentration over the surface of the reservoir could be determined by taking a simple average of the values for each pixel on the reservoir. The seasonal average for each year can then be determined by averaging the results from each year during each of the seasons. These results are presented in Figures 3 through 5.

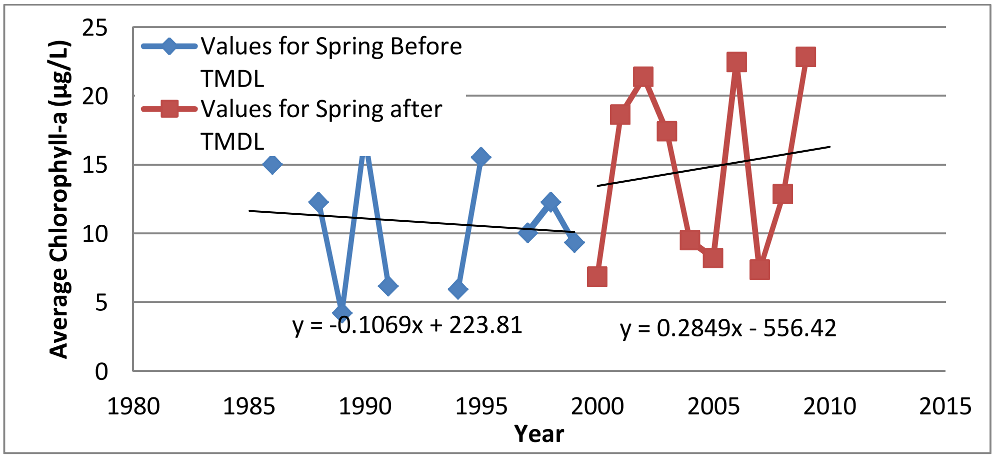

Figure 3. Average chlorophyll-a concentration for spring (East Canyon Reservoir)

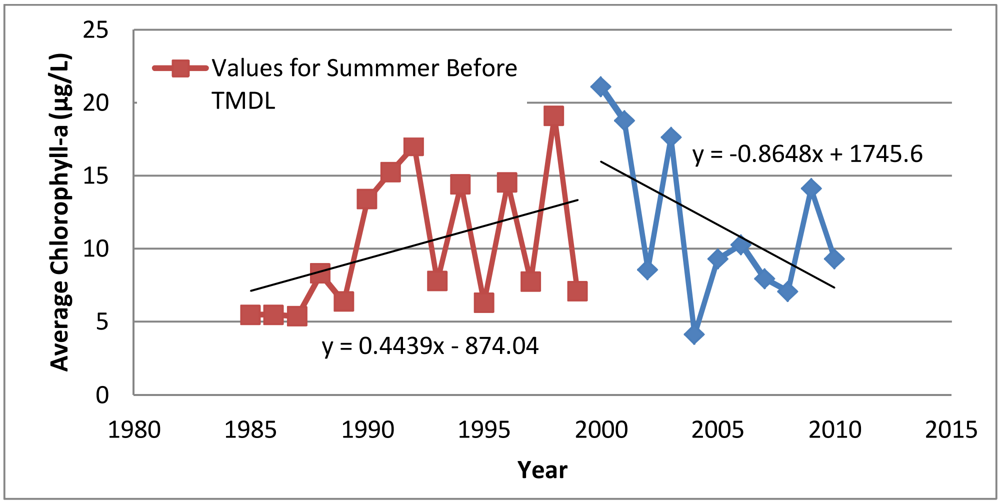

Figure 4. Average chlorophyll-a concentration for summer (East Canyon Reservoir)

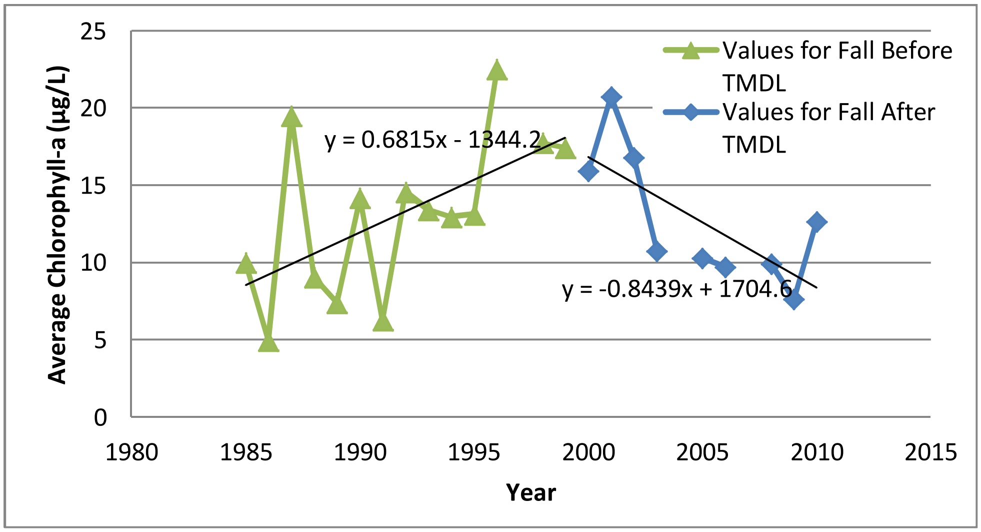

Figure 5. Average chlorophyll-a concentration for fall (East Canyon Reservoir)

Figures 4 and 5 show that the average annual chlorophyll-a concentrations in East Canyon Reservoir were lower after the TMDL actions were implemented in 2000 than they were before the TMDL. These figures also show that average annual chlorophyll-a concentrations in the reservoir were increasing over time before the TMDL, but were found to be decreasing with time after the TMDL was implemented in both summer and fall. This indicates that the TMDL measures were effective in helping to control biological productivity during these seasons.

While evaluating the data found in Figures 4 and 5 indicate that the TMDL measures appear to be effective during the summer and fall seasons, this same conclusion cannot be made for spring by evaluating Figure 3. Figure 3 shows that chlorophyll-a concentrations continue to increase over time even after the TMDL actions were implemented. The TMDL actions do not appear to be effective at reducing biological productivity during the spring season.

It is uncertain exactly why this is the case, but a couple of observations may be helpful. During the spring a large percentage of the nutrient load to East Canyon Reservoir comes from surface runoff (agricultural and natural sources). These sources are controlled by best management practices that are often not as effective as point source control. The main source of nutrient load during summer and fall is the point source load from a wastewater treatment plant. This source is effectively and very well controlled.

CONCLUSIONS

Remote sensing was found to be successful for the measurement of water quality such as Chlorophyll-a for the East Canyon Reservoir. A ratio of Band 1 and 2 was effective to predict the Chlorophyll-a concentration with a correlation of $R^2 = 0.8564$. Using remote sensing data average annual chlorophyll-a concentrations for the reservoir could be calculated.

These data were used to evaluate the effectiveness of a TMDL study performed at the reservoir. The implementation of the TMDL actions was found to be effective at reducing the amount of chlorophyll-a during the summer and fall seasons. On the other hand, for the spring season the concentration of chlorophyll-a was found to be greater after the TMDL.

REFERENCES

Brivio, P.A., C. Giardino, and E. Zilioli. 2001. "Determination of Chlorophyll Concentration Changes in Lake Garda Using an Image-based Radiative Transfer Code for Landsat TM Images." *Int. J. Remote Sensing. 22(2&3):487-502.*

Fuller, L.M. and R.J. Minnerick. 2007. *Predicting Water Quality by Relating Secchi-Disk Transparency and Chlorophyll a Measurements to Landsat Satellite Imagery for Michigan Inland Lakes, 2001–2006*— U.S. Geological Survey Fact Sheet 2007-3022, Date Posted: September 12, 2007:

Han L. and, Jordan KJ. 2005.Estimating and mapping chlorophyll-*a* concentration in Pensacola Bay, Florida using Landsat ETM+ data. *International Journal of Remote Sensing*. 26(23):5245-5254.

Han, L., and D. C. Rundquist. 1997. "Comparison of NIR/RED ratio and first derivative of reflectance in estimating algal-chlorophyll concentration: a case study in a turbid reservoir." *Remote Sensing of Environment* **62**(3): 253-261.

Montana State Department of Environmental Quality. 2004. "Mapping Chlorophyll Distribution Over Lakes of Northwest Montana." In *Water Quality Protection Plan and TMDl for the Swan Lake Watershed*, Montana State Department of Environmental Quality, Helena, Montana.

Utah Department of Environmental Quality. 2000. *Total Maximum Daily Load for East Canyon Reservoir.* Utah Department of Environmental Quality, Salt Lake City, Utah.

MAPPING AND MODELING CHLOROPHYLL- *a* CONCENTRATIONS IN UTAH LAKE USING LANDSAT 7 ETM+ IMAGERY

M. Brett Borup and Victor N. A. Narteh
(Brigham Young University, Provo, UT, USA)

ABSTRACT: Chlorophyll-*a* concentrations in the turbid surface waters of Utah Lake were determined using Landsat 7 ETM+ satellite imagery and field measured concentrations of chlorophyll-*a*. A log transformation of red/near-infrared reflectance (i.e. ln[Band3/Band4]) was used to estimate chlorophyll-*a and* had a high correlation with the field measured chlorophyll-a concentrations ($R^2 = 0.9337$). With this relationship, a model and 19 contour maps showing the spatial distribution of chlorophyll-a concentrations over Utah Lake was developed for the spring, summer, and fall seasons of 2003 to 2010. High concentrations of Chlorophyll-a (355µg/L and over) were observed mostly at the Provo Bay and Goshen Bay areas of the Lake. Occasionally, elevated levels of chlorophyll-*a* were observed at the northeastern, middle, and western sections of the lake. Utah Lake's average chlorophyll-*a* concentration is declining over time. Field measured concentrations of phosphorus and model estimates for chlorophyll-*a* concentrations were highly correlated ($R^2 = 0.9046$). This suggests that the elevated levels of chlorophyll--*a* might be a result of the point and non-point discharge of phosphorus-laden wastewater from treatment plants, municipal storm drains, and agricultural activities.

INTRODUCTION

Utah Lake is located in north-central Utah near the cities of Orem and Provo. It is the largest freshwater lake in the state, as well as the largest naturally occurring freshwater lake in the western United States. The beneficial uses of Utah Lake as designated by the State of Utah (Utah Administrative Code R317-2-13-12, June 01, 2006) include: secondary contact recreation (activities like boating, wading, etc.); warm water game fish and associated food chain; waterfowl, shore birds and other water-oriented wildlife and associated food chains; and agricultural water supply . The lake is 24 miles long and 13 miles wide, at its greatest, with a surface area of approximately 96,600 acres and a volume of 902,400 ac-ft. The relatively small volume of the lake is due to its shallow depth. The lake has a maximum depth of about 18 feet and the average depth is about 10 feet .

Utah Lake is a highly productive lake that experiences extensive algal blooms in the late summer and fall. The lake is listed on Utah's 2004 § 303(d) list for exceedance of state criteria for total phosphorus. Utah Lake is often considered to be a hyper-eutrophic ecosystem, with the highest algal diversity in spring and early summer, decreasing with the progression of the seasons.

Utah Lake is a large, shallow, semi-terminal water body that is fed by a very large, mostly Mesozoic-aged nutrient-rich sediment basin . Phosphorus, the nutrient that limits the growth of algae in surface waters, has a tendency to sorb onto these suspended sediments and settle at the bottom of the lake. Because of the lake's shallow depth, wind action constantly stirs up and mixes bottom sediments. This condition causes turbidity levels and suspended solids concentrations to be very high in the lake and causes phosphorus to be released from sediments in the benthic zone. The released phosphorus mixes with the oxygenated water at the epilimnion resulting in algae blooms. Other concerns associated with elevated total phosphorus concentrations include periphyton growth, low dissolved oxygen, increased pH, and cyanotin production by blue-green algae (cyanobacteria).

The purpose of this research is to develop a method to easily monitor the biological productivity of Utah Lake so that appropriate corrective actions may be taken to protect the beneficial uses of the lake.

ISBN 9780976885351

Landsat 7 ETM+ satellite imagery will be used to develop a method to estimate chlorophyll-*a* concentrations that will be used as a measure of productivity.

MATERIALS AND METHODS

Field data were obtained from seven sites on Utah Lake (Figure 1) between June 2008 and December 2010 and analyzed by the Utah Department of Environmental Quality, Division of Water Quality. These data were used to calibrate and validate the model developed from satellite imagery.

Figure 1. Utah Lake sampling locations

Satellite imagery was obtained from Landsat 7 using Landsat Enhanced Thematic Mapper plus (Landsat ETM+). Atmospheric correction was performed using Dark Subtraction—a method that subtracts the dark noise from the image. Prior to the correction, the Landsat Calibration option in ENVI version 4.7 was used to convert Landsat ETM+ digital numbers to exoatmospheric reflectance (reflectance above the atmosphere) using published post-launch gains and offsets found in the Landsat imagery metadata file. The pixel locator tool in ENVI 4.7 was used to correlate satellite reflectance data to the individual sample locations.

There have been relatively successful attempts in the United States to use Landsat Thematic Mapper imagery to determine chlorophyll-a concentrations in large open surface water bodies The presence of high suspended sediment concentrations, however, can dominate the spectrum and make chlorophyll-*a* concentration determination difficult. Several studies have shown that accurate measurements can be made under these conditions however (Han and Rundquist 2002; Yu, *et al,* 2007; Mittenzwey, 1992; and Dekker, *et al,* 1995). Several mathematical relationships between band reflectance values were compared to the field data to determine which of the models will yield the best correlation.

RESULTS AND DISCUSSION

Twelve different mathematical models that incorporated different combinations of band values were fit to the observed field data (Narteh, 2011). The model that was found to best fit the data was the following polynomial:

$$\text{Chlorophyll-}a = -205.91x^3 + 628.66x^2 - 619.72x + 207.58$$

Where: x = ln (Band 3/Band 4) reflectance ratio, and the estimated chlorophyll-*a* concentration is in g/L. A plot of the observed field data verses the model predicted values is found in Figure 2.

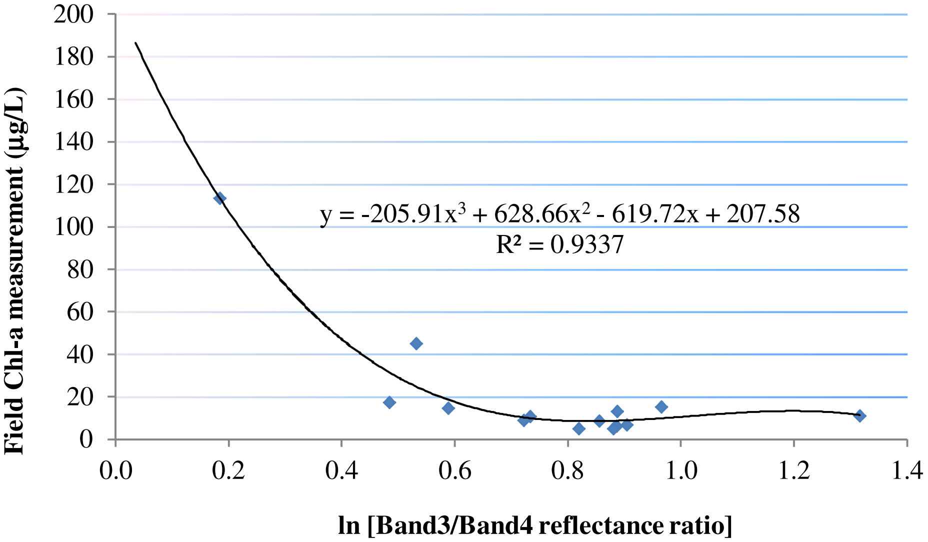

Figure 2. Field measured chlorophyll-*a* vs. model prediction

The spatial distribution of chlorophyll-*a* over the surface of Utah Lake was determined by applying the model to each individual pixel covering the lake. These data were then used to make illustrations of the chlorophyll-*a* spatial distribution using AcrMap. Examples of the plots are found in Figures 3 through 5.

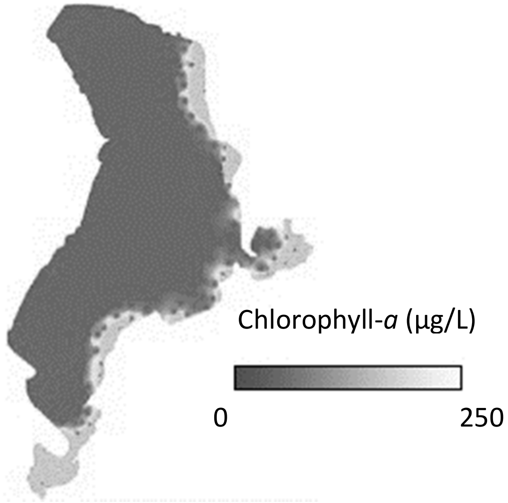

Figure 3. Chlorophyll-*a* concentrations in Utah Lake, spring

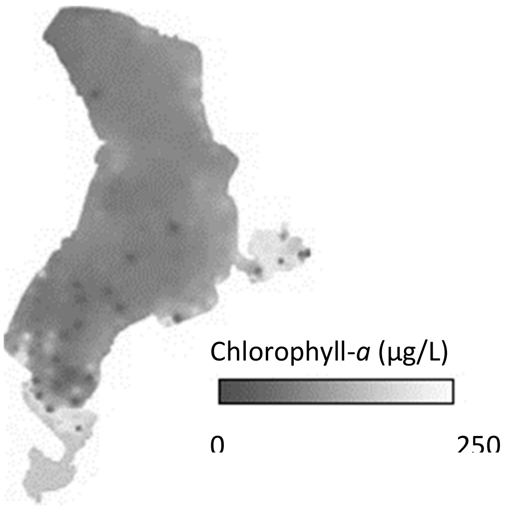

Figure 4. Chlorophyll-*a* concentrations in Utah Lake, summer

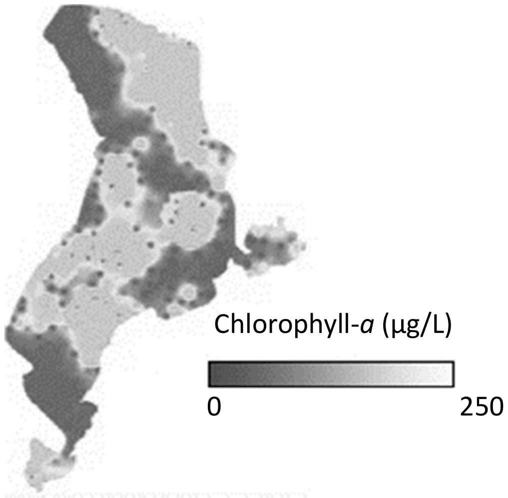

Figure 5. Chlorophyll-*a* concentrations in Utah Lake, fall

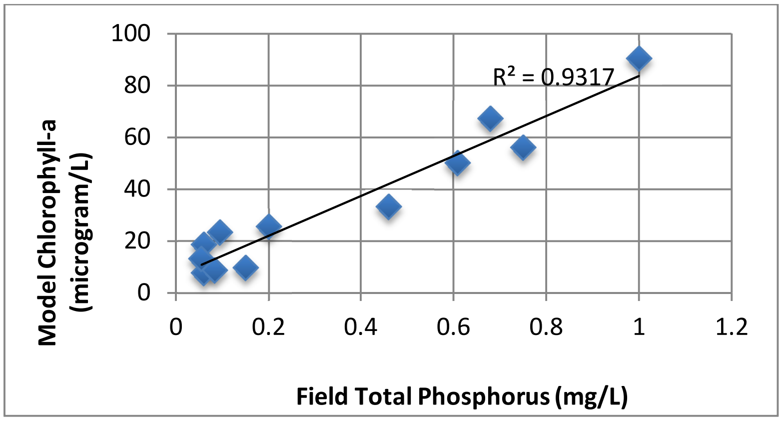

Figure 6. Correlation between field total phosphorus and model chlorophyll-*a* concentrations

It was also found that field phosphorus concentrations were strongly correlated with model predicted chlorophyll-a concentrations. Figure 6 shows the correlation between the total phosphorus concentrations (field measurement), and the chlorophyll-*a* concentrations (model estimates). From the plot it was established that phosphorus has a high correlation with chlorophyll-*a* ($R^2 = 0.9317$).

The contour maps reveal that the maximum values for chlorophyll-*a* concentration occurred mostly at the southern (Goshen Bay) and eastern (Provo Bay) sections of Utah Lake. Chlorophyll-*a* concentrations appear to be correlated with point source inputs from wastewater treatment plants that discharge to the lake and major tributaries. This would seem probable since these are the major sources of phosphorus input to the lake. Locations of treatment plants that discharge to the lake and major tributaries are illustrated in Figure 7.

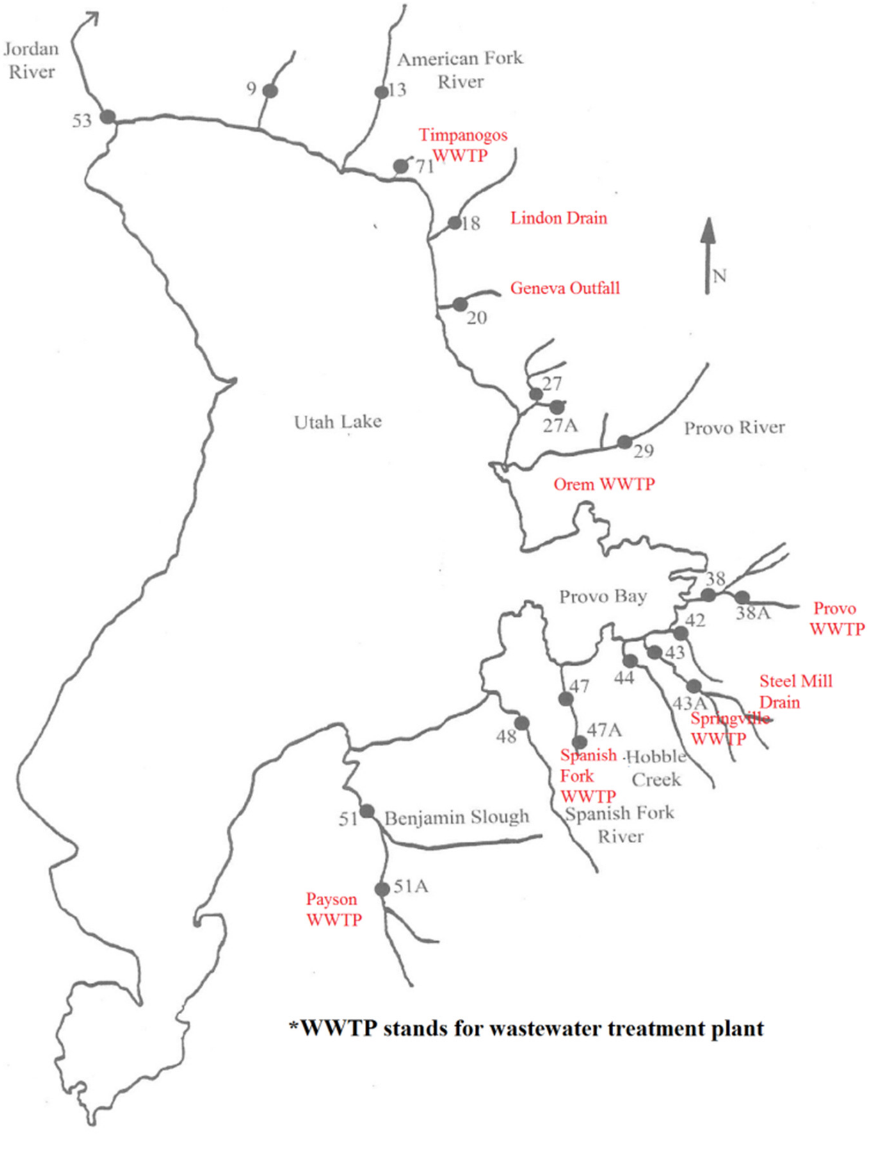

***WWTP stands for wastewater treatment plant**

Figure 7. Treatment plant and major tributary locations

CONCLUSIONS

This study shows that ln(Band 3/Band 4) or the log transformation of the red/near-infrared reflectance ratio is a good predictor of chlorophyll-*a* concentration in a turbid lake such as Utah Lake.

There was a strong correlation between concentrations of phosphorus and chlorophyll-*a*. This suggests that the spatial and temporal distribution of chlorophyll-*a* over Utah Lake is helpful in locating areas with high or low phosphorus concentrations.

High concentrations of Chlorophyll-a (355µg/L and over) were observed mostly at the Provo Bay and Goshen Bay areas of the Lake. Occasionally, elevated levels of chlorophyll-*a* were observed at the northeastern, middle, and western sections of the lake. This suggests maximum concentrations of phosphorus at the same area. This implies that the elevated levels of chlorophyll-*a* might be a result of the point and non-point discharge of phosphorus-laden wastewater from treatment plants, municipal storm drains, and agricultural activities

REFERENCES

Dekker, AG, TJ Malthus, and HJ Hoogenboom. 1995. "The Remote Sensing of Inland Water Quality." *Advances in Environmental Remote Sensing* (1995): 123–142.

Han, L., and D.C. Rundquist. 1997. "Comparison of Nir/Red Ratio and First Derivative of Reflectance in Estimating Algal-Chlorophyll Concentration: A Case Study in a Turbid Reservoir." *Remote Sensing of Environment* 62, no. 3: 253-261.

Mittenzwey, K.H., S. Ullrich, AA Gitelson, and KY Kondratiev. 1992. "Determination of Chlorophyll a of Inland Waters on the Basis of Spectral Reflectance." *Limnology and Oceanography* (1992): 147-149.

Narteh, V. N. A. 2011. *Mapping and Modleing Chlorophyll-*a *Concentrations in Utah Lake Using Landsat 7 ETM+ Imagery.* M. S. Thesis. Brigham Young University, Provo, Utah

Yu, K.P., J. Yoon, and B.K. Muhammad. "Developing a Monitoring Support Model for Chlorophyll a Concentration in the James River Estuary Using Modis Images." ASCE, 2007.

MEASURE DETERMINATION AND ZONING OF OIL POLLUTION (TPH) ON COSTAL SEDIMENTS OF BANDAR ABBAS (HORMOZ STRAIT) AND PROVING CONTROL STRATEGIES

Maryam Ehsanpour *(Islamic Azad University, Bandar Abbas Branch, Bandar Abbas, Iran. P.O.Box:79159-1311)
Majid Afkhami (Yung Researches Club, Islamic Azad University, Bandar Abbas Branch, Bandar Abbas, Iran. P.O.Box:79159-1311)

ABSTRACT: This study investigated the presence of hydrocarbon pollution in industrial waste water sediments found in west coast of Bandar Abass (Northern part of Hormoz strait).Therefore six transects from west of the city were selected. Each transects consists of three stations intervals 100, 600 and 1100 meter from the low tide were sampled in both the summer and winter season(July and January 2009). Physical and chemical parameters of water, concentration of total petroleum hydrocarbons (TPH) and soil tissue deposition were evaluated according to standard procedures of MOOPAM. Average results of dissolved oxygen were 6.42 mg/l, temperature 26.31°c, pH 8.55, EC 54.47ms/cm and salinity 35.98 g/l respectively. Result indicate that minimum, maximum and average concentration of total petroleum hydrocarbons(TPH) in sediments were, 60.18, 751.83, and 229.21 µg/kg respectively which are fewer than comparable studies in other parts of Persian Gulf.

INTRODUCTION

The Persian Gulf represents a highly stressful environment due to a combination of both prevailing natural conditions and development pressures along its coastline. The Gulf region has approximately two-thirds of the world's proven oil reserves and the eight riparian states (Iran, Iraq, Kuwait, Bahrain, Qatar, Saudi Arabia, UAE and Oman) currently account for approximately one-fourth of the world's oil production (Khan, 2002). Problems associated with oil pollution and non-living resources appear to be of greater significance in the Gulf compared with other regions (Munawar et al., 2002). This region has undergone considerable development, and consequently urbanization, industrialization, port areas and refineries have become major sources of pollution to the marine environment. Also, a combination of tanker traffic and either accidental or intentional spills have prevailed. The spill that took place during the 1991 Gulf War is only one of three major events (Fayad et al., 1996).

In 1994, two tankers collided spilling 16,000 tones of Iranian crude oil into the Gulf of Oman. Despite damage caused to the marine environment, studies demonstrated a significant decrease in contamination levels, almost returning to normal conditions within eight months of the accident (Shriadah, 1998; Shriadah, 2000). The recovery was likely accelerated as a result of the physical characteristics of the region and selfpurification processes. Enhanced degradation of the petroleum products was inferred due to the existence of microorganisms acclimated to oil pollution, and to The high ambient temperatures in the Gulf caused an increase in evaporation and photo-oxidation rates.

Anthropogenic hydrocarbon contamination of the marine environment is a significant concern throughout many countries. The sources of hydrocarbon pollution in marine waters include accidental oil spills from ships and oil extracting field platforms, discharge of oil-contained formation water during oil and gas exploration and production, industrial no refinery and refinery runoff, and urban sewage(Volkman et al., 1994).Hydrocarbon water pollution except oil spillage cannot be visually detected without analytical quantification of hydrocarbons. Various methods for determination of total petroleum hydrocarbons (TPH) In water are available for environmental monitoring. The most often used include gravimetric analysis, infrared spectroscopy, and high performance liquid or gas chromatography. However, the use of data on

---

ISBN 9780976885351

TPH concentration in hazard evaluation for marine biota is hindered by the lack of justified water quality criteria for TPH.The fast growing demand for petroleum products by developing industry increases the risk of hydrocarbon pollution of the marine environment and necessitates the revision of water quality criteria for TPH.

The present work evaluates marine contamination of petroleum hydrocarbons in the coastal zones of Bandar Abbas (in north coast of the Hormoz strait) based on the quality of sediment and some local seafood Species. Sediments are one of the many environmental compartments in which oil pollution accumulates. Therefore, sediments can hold and release pollutants causing detrimental effects to biota long after the initial input of pollution has ceased. These contaminants might be released slowly and be bioaccumulated in organisms that dwell in and around the sediment.

More recent data on concentrations levels of petroleum hydrocarbons in biota is needed to assess their contamination risk for human consumption. Overall, the results presented here for sediments and Biota contributes to the regional database for the Persian Gulf.

MATERIAL AND METHODS

Marine samples were collected from the Bandar Abbas coast line, which covers the north coast of the Hormoz strait. In general, all sampling procedures were carried out according to internationally recognized guidelines (UNEP, 1991). The sediments were stored frozen at 18 ºC in aluminum cartons prior to analyses. Following freeze-drying, samples were sieved through vibrating stacked stainless steel sieves with mesh sizes from 250 lm to 1000 lm. Sediments were then homogenized prior to extraction. Samples were Soxhlet extracted for 8 h into 250 ml of hexane: methylene chloride (1:1, v/v). A sulphur removal procedure was performed using activated elemental copper in order to avoid sulphur interferences UV fluorescence was used to quantify the total petroleum hydrocarbon (TPH) content in sediments and biota. Emission scans and synchronous excitation/emission scans were recorded to evaluate the relative fluorescence and to characterize the aromatic hydrocarbons. Standard response curves of fluorescence intensity versus concentration were generated for Kuwait crude (ROPME) oil and for the standard aromatic hydrocarbon, chrysene. Samples were diluted in order to give a reading within the linear calibration range of the fluorimeter. Conditions of the fluorimeter were adjusted as follows. For the first procedure, a fixed excitation wavelength of 310 nm was used; the emission wavelength was either 360 nm for single measurements or scanned from 320 nm to 550 nm.

RESULT AND DISCUSION

Measure determination of total petroleum hydrocarbons (TPH) in each station and season are summarized in Table 1. Results showed indications of some Oil contamination changes with 67-749 µg kg^{-1} in summer and 60.18-751.18 µg kg^{-1} total petroleum hydrocarbons as ROPME oil equivalents for winter in the region. Mean Oil contamination with 223.15 µg kg^{-1} in summer and 235.27 µg kg^{-1} for winter were determined.

Total petroleum hydrocarbons (TPH) in winter were more than summer season. Station 8 and 9 have higher amount 0f TPH in both seasons because of Splurge oil from boats repairs in this regions. The mean Total petroleum hydrocarbons (TPH) in Bandar Abass coastline was 229.21 µg kg^{-1} as ROPME oil equivalents that this levels was less than those measured in Persian Gulf (64300-143600 µg kg^{-1}) in 2005(Vossughi et al. 2005) and 6500-7000 in UAE (Shriadah 1999); less than range reported for near-shore marine sediments of the UAE in 1994, namely 400-212000 µg kg^{-1} (Abu-Hilal and Khordagui, 1994).

They are significantly lower that those reported from coastal areas of the ROPME Sea Area that were affected by the Gulf War Spill (Fowler et al., 1993; Readman et al., 1996) and similar to those measured in identical sites from Jebel Ali in 1991 (Fowler et al., 1993). According to some guidelines for pollution levels in bottom sediments of the Gulf (Massoud et al., 1996), concentration levels <15000 µg kg^{-1} as Chrysene equivalents are considered to be the natural background level in this region. This threshold value was surpassed in the sediment from this region (229.21 µg kg^{-1}). Absence of industries in this region leads to very low concentrations of TPH .The comparison of Total mean petroleum hydrocarbons (TPH) in sediment in other studies were summarized in Table 2.

Table 1. Mean Concentration of Total Petroleum Hydrocarbons (TPH) in Bndar Abbas Coastline Sediments (µg kg^{-1}).

Station	Summer	Winter	Mean
1	67.65	60.18	63.915
2	103.84	98.77	101.35
3	93.28	95.16	94.22
4	89.08	84.71	86.895
5	104.23	109.7	106.965
6	99.82	101.38	100.6
7	-	100	100
8	749.24	751.83	750.535
9	642.46	636.2	639.375
10	418.56	422.71	420.635
11	258.21	254.47	256.34
12	227.39	230.34	230.835
13	222.93	226.45	224.69
14	129.59	131.27	130.43
15	137.46	140.24	138.85
16	226.72	320.97	237.845
Mean ± SD	223.15	235.27	229.21±20.57

Table 2. Comparison of Total Mean Petroleum Hydrocarbons (TPH) in Sediment

Study Area	Unit	TPH Range	Reference
Kuwait	**µg kg^{-1}**	7430-458610	Metwally et al.1997
Persian Gulf	**µg kg^{-1}**	5400-92000	Abdali et al.1997
UAE	**µg kg^{-1}**	6500-7000	Shriadah 1999
Persian Gulf	**µg kg^{-1}**	6300-143600	Vossoughi et al. 2005
UAE	**µg kg**	100-16400	Tolosa et al. 2005
Qatar	**µg kg**	2200-8400	Tolosa et al. 2005
Bahrain	**µg kg**	16600-779000	Tolosa et al. 2005
Oman	**µg kg**	10-7600	Tolosa et al. 2005
India	**µg kg**	6.4-7.2	Ingole et al. 1995
Bandar Abbas	**µg kg**	50-750.535	Current study

Because there are so many different chemicals in crude oil and in other petroleum products, it is not practical to measure each one separately. However, it is useful to measure the total amount of TPH at a site. Chemicals that occur in TPH include hexane, benzene, toluene, xylenes, naphthalene, and fluorene, other constituents of gasoline, of jet fuels, of mineral oils, and of other petroleum products(ASTDR 1999).

CONCLUSION

Although the Persian Gulf is generally regarded as a heavily polluted water body with respect to oil, these screening results from north coast of the Hormoz strait indicate that the levels of petroleum contaminants were relatively low in sediments. Regular monitoring of the area and more specific analyses are recommended in order to determine if any dumping activities have taken place in this particular area. In respect to research from this study, it seems necessary to perform following actions to control environment quality in this region:

- Prevention maintenance of vessels and coast scrub
- Providing facilities equipped to deal with contamination
- Reception facilities centers at ports and docks
- Use of the private sector in dealing with pollution from ships and waste

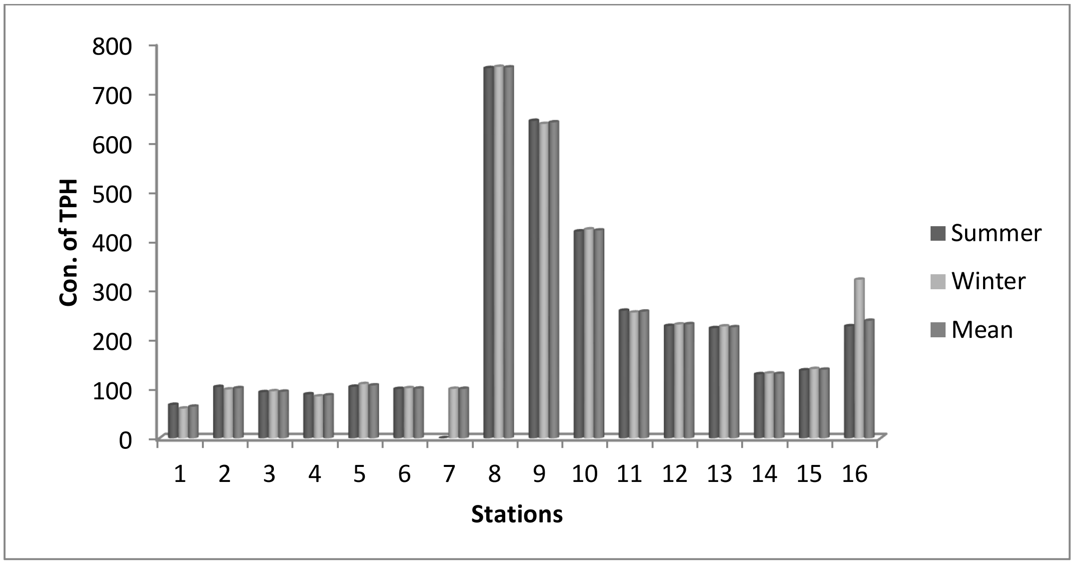

Figue 1. Concentrations of TPH in sediments at different stations

REFRENCES

Abdali. F.AL M.S. Massoud and A. N. AL-aghadban (1997). The status' of Oil Pollution in the Persian Gulf. *Environmental Pollution* . 24, 1, 11-22.

Abu-Hilal A.H. Khordagui H.K. (1994). Petroleum hydrocarbons in the near shore marine sediments of the United Arab Emirates. *Environ. Pollut.* 85, 315–319.

Agency for Toxic Substances and Disease Registry (ATSDR). (1999). Toxicological Profile for total petroleum hydrocarbons (TPH). Atlanta, GA: U.S. Department of Health and Human Services, Public Health Service.

Badawy M.I. Al-Mujainy I.S. Hernandez M.D. (1993). Petroleum derived hydrocarbons in water, sediment and biota from the Mina al Fahal coastal waters. Mar. Pollut. Bull. 26, 457–460.

Fayad N.M. El-Mubarak A.H. Edora R.L. (1996). Fate of oil hydrocarbons in fish and shrimp after major oil spills in the Arabian Gulf. Bull. Environ. *Contam. Toxicol.* 56, 475–482.

Fowler S.W. Readman J.W. Oregioni B. Villeneuve J.-P. McKay K. (1993). Petroleum hydrocarbons and trace metals in near shore Gulf sediments and biota before and after the 1991 war: An assessment of temporal and spatial trends. *Mar. Pollut. Bull.* 27, 171–182.

Ingole S.A Kadama A.N Mayadaco M.S Dhadke P.M Junt (1995).Petroleum Hydrocarbons in Intertidal Ecosystem along Bombay Coast, Indian Journal of Marine Sciences. Vol .24. 116-118.

Khan N.Y. (2002). Physical and human geography. In: Khan, N.Y., Munawar, M., Price, A.R.G. (Eds.), the Gulf Ecosystem: Health and Sustainability. *Bakhuys Publishers, Leiden*, pp. 3–21.

Massoud M.S. Al-Abdali F. Al-Ghadban A.N. Al-Sarawi M. (1996). Bottom sediments of the Arabian Gulf–II. TPH and TOC contents as indicators of oil pollution and implications for the effect and fate of the Kuwait oil slick. *Environ. Pollut*. 93, 271–284.

Methwally M. Al-Muzaini S. Jacob p. Bahlul M. Urushigawa Y. Sato S. Matsumura A. (1997). Petroleum Hydrocarbons and related Heavy Metals in the near shore Marine Sediment of Kuwait. *Environmental International.* 23, 115-121.

Munawar M.P. Price A.R.G. Munawar I.F. Carou S. Niblock H. Lorimer J. (2002). Aquatic ecosystem health of the Arabian Gulf: Status and research needs. In: Khan, N.Y., Munawar, M. Price, A.R.G. (Eds.), The Gulf Ecosystem: Health and Sustainability. *Bakhuys Publishers Leiden* pp. 303–325.

Readman J.W. Bartocci J. Tolosa I. Fowler S.W. Oregioni B. Abdulraheem M.Y. (1996). Recovery of the coastal marine environment in the Gulf following the 1991 war-related oil spills. *Mar. Pollut. Bull.* 32, 493–498.

Shriadah M.M.A. (1998). Impacts of an oil spill on the marine environment of the United Arab Emirates along the Gulf of Oman. *Mar. Pollut. Bull.* 36, 876–879.

Shriadah M.M.A. (2000). Levels and distribution of petroleum hydrocarbons in the coastal waters and sediments of the United Arab Emirates in the Arabian Gulf and Gulf of Oman. *Water Air Soil Pollut.* 119, 247–256.

Tolosa Imma. Stephen J. de Mora. Scot W. Fowler Jean Pierre Villeneuve. Jean Bartossi. Chantal Cattini (2005). Aliphatic and Aromatic Hydrocarbons in Marine Biota and Coastal Sediment from the Gulf and the Gulf of Oman. *Marine Pollution Bulletin.* 50. 166-1633.

UNEP (1991). Sampling of Selected Marine Organisms and Sample Preparation for the Analysis of Chlorinated Hydrocarbons. *Reference Methods for Marine Pollution Studies* No. 12, Rev. 2, UNEP, Nairobi, p. 17.

Volkman J. K. G. J. Miller A. T. Revill and D. W. Connell (1994). Oil spills. *In*: J. M. Swan, J. M. Neff, and P. C. Young, _Eds., Environmental Implications of Offshore Oil and Gas Development in Australia}The Findings of an Independent Scientific Review, pp. 509]695. *Australian Petroleum Exploration Association, Sydney.*

SOURCING DIOXIN FROM THE SAN JACINTO WASTE PITS INTO GALVESTON BAY

Taft Tucker and Hanadi Rifai
(University of Houston, Houston, TX, USA)

ABSTRACT: In 1965 and 1966, dioxin laden paper mill wastes were disposed of in the San Jacinto River Waste Pits (SJWP), bermed impoundments on the banks of the San Jacinto River (SJR). Regional land subsidence has caused submergence of portions of the waste pits, directly exposing the wastes to the San Jacinto River. Elevated levels of dioxin in sediment samples collected within and downstream of the waste pits indicate the waste pits have contributed dioxins to the SJR and Galveston Bay System (GBS). The site has been added to the EPA's National Priorities List (NPL). A qualitative investigation of dioxin distributions measured in sediments from the GBS identified 3 primary source profiles most likely representing dioxins from a) SJWP (paper mill) b) the Houston Ship Channel (HSC) upstream of its confluence with the SJR and c) Houston's urban air deposited via runoff or directly. Results of the PMF analysis returned source profiles similar to those identified qualitatively and indicated that industrial point sources have significant impact on nearby sediment quality with the HSC and SJR, but atmospheric sources are the dominant contributors to dioxins observed in the more open waters of Galveston and Trinity Bays.

INTRODUCTION

Site Background: In the 1965 and 1966, paper mill solid and liquid wastes were disposed of in the San Jacinto River Waste Pits. Since then, land subsidence in the area has exacerbated erosion of the waste pit berms and partial inundation of the pits allowing direct, constant contact between the San Jacinto River and the dioxin laden wastes in the pits. Elevated levels of dioxins in water, fish tissue, and sediment observed to date throughout the (HSC) system and in sediment samples collected near the waste pits indicate that the waste pits are a probable current source of dioxin into the San Jacinto River (Suarez, Rifai et al. 2006). As shown in Figure , the site and surrounding area has undergone considerable degradation between the 1960s and today.

Dioxins in Paper Mill Wastes: Polychlorinated dibenzo-*p*-dioxins (PCDDs) and polychlorinated dibenzofurans (PCDFs), more commonly referred to as "dioxins", can be present as one of 210 congeners, depending on the number and location of attached chlorine atoms. Of these congeners, only 17 are considered to exhibit "dioxin-like" toxicity; however, 2,3,7,8-tetrachlorodibenzo-*p*-dioxin is often given the dubious distinction of being the "most toxic man-made chemical" (Hites 2011), though toxicity varies significantly among the different congeners (Schwetz, Norris et al. 1973). Due to their high toxicity, persistence in the environment, and prevalence within industrialized settings (Wenning, Paustenbach et al. 1993), dioxins have received a significant amount of regulatory interest in recent years.

The use of molecular chlorine (Cl_2) as a bleaching during the paper pulp bleaching process is known to cause elevated levels of dioxins (Amendola, Barna et al. 1989; Clement, Tashiro et al. 1989). Evaluation of dioxin profiles in paper mill wastes and effluents has shown that particular congener patterns tend to emerge during the paper mill pulp bleaching process, particularly elevated levels of 2378-TCDF and 2378-TCDD (Ehrlich, Wenning et al. 1994), which are among the more toxic dioxin congeners. Samples and soil borings collected within the boundaries of the original waste pit berms exhibit a typical paper mill dioxin signature, see Figure . The formation and subsequent release of dioxins due to paper mill activities has steadily declined in recent years (USEPA 2006); however, impacted sediments have been

---

ISBN 9780976885351

shown that they can behave as long term sources of dioxins into an ecosystem (Yunker, Cretney et al. 2002).

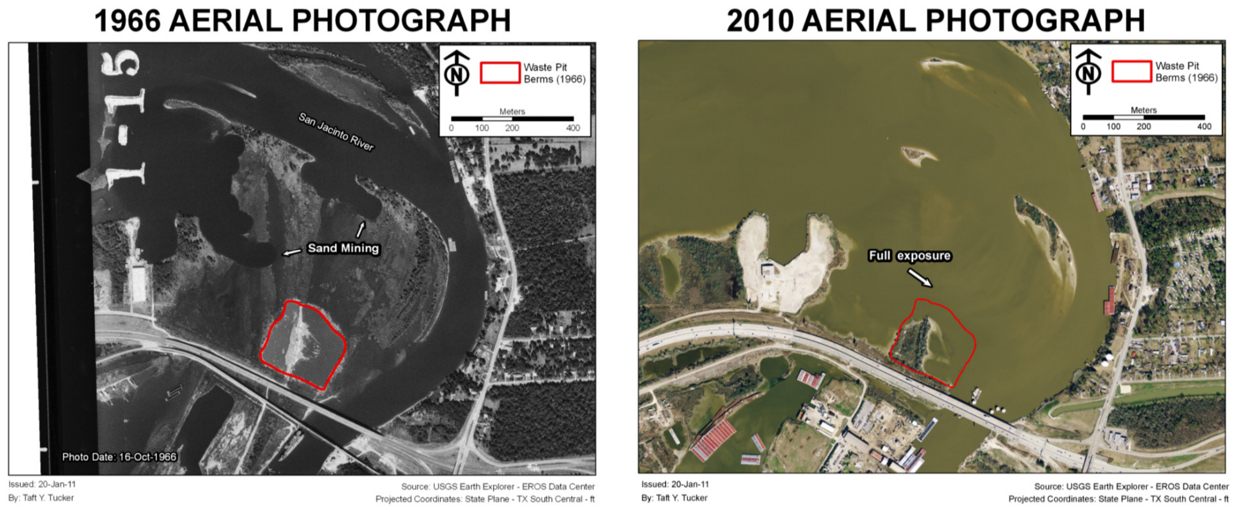

Issued: 20-Jan-11
By: Taft Y. Tucker

Source: USGS Earth Explorer - EROS Data Center
Projected Coordinates: State Plane - TX South Central - ft

Figure 1: Aerial photos taken of the study area during 1966 and 2010.

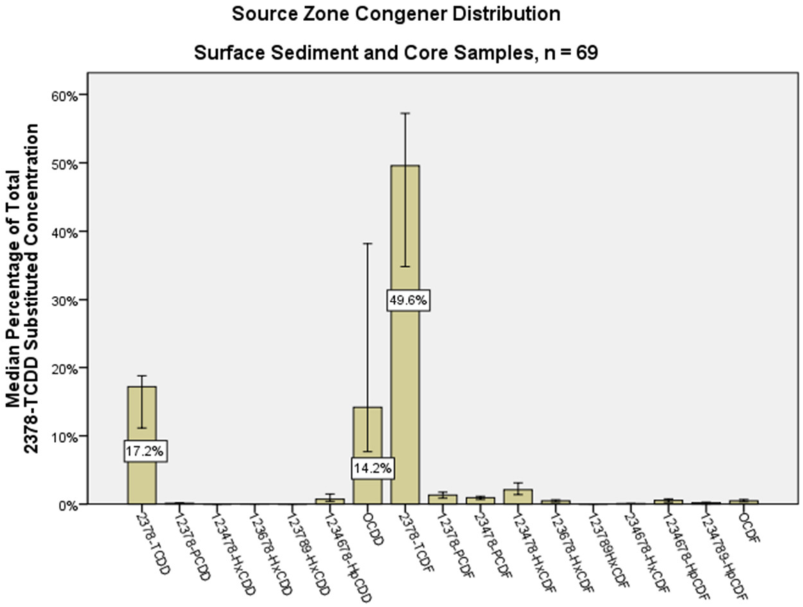

Figure 2: SJWP dioxin fingerprint

MATERIALS AND METHODS

Site Database: Numerous sampling events have been conducted since 1990, and a substantial dataset of dioxin concentrations in sediment, as well as other environmental media, collected throughout the GBS, has been generated. These data have been compiled in a site database accessible through the EPA Region 6 SJWP website. This study utilizes the approximately 400 surface sediment samples collected in the qualitative fingerprint analysis and in the application of a PMF source apportionment model.

Positive Matrix Factorization: PMF is a quantitative, multivariate source apportionment model that has become the most common model applied to environmental contaminants in sediment (Sundqvist, Tysklind et al. 2010). In PMF, the contribution of p independent sources to the original data matrix, X_{ij}, is modeled by,

$$X_{ij} = \sum_{k=1}^{p} F_{ik} G_{kj} + E_{ij} \tag{1}$$

where F_{ik} is the concentration of the ith analyte, e.g. congener or homologue group, in the kth factor, G_{kj} is the contribution of the kth factor to the jth sample, and E_{ij} is the model residual for the ith congener in the jth sample. The "object function", Q, is minimized to obtain an optimal solution and is represented explicitly as a weighted least squares problem by,

$$Q(E) = \sum_{i=1}^{m} \sum_{j=1}^{n} \left[\frac{E_{ij}}{s_{ij}}\right]^2 \tag{2}$$

where s_{ij} is the uncertainty of the concentration of the ith congener in the jth sample of the original dataset containing m congeners analyzed n samples (Paatero and Tapper 1994; Paatero 1997). For the PMF analyses run for this research uncertainty values, based off of recommendations of Polissar, Hopke et al. (1998) with minor changes as applied by (Sundqvist, Tysklind et al. 2010), were assigned.

RESULTS AND DISCUSSION

Fingerprint Analysis: Analysis of the homologue profiles generated during historical sampling revealed three identifiable source profiles which dominate contribution of dioxin mass into the HSC/GBS which are described below. Figure 3 shows homologue profile for samples collected near the HSC/SJR confluence during 2002 and is provided as an example.

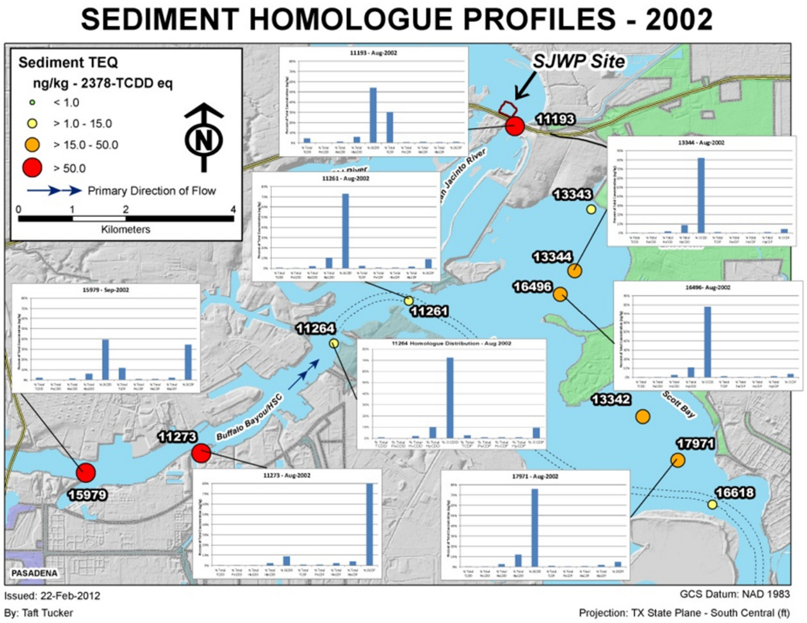

Figure 3: Homologue profiles for select sediment samples collected near the HSC/SJR confluence during 2002.

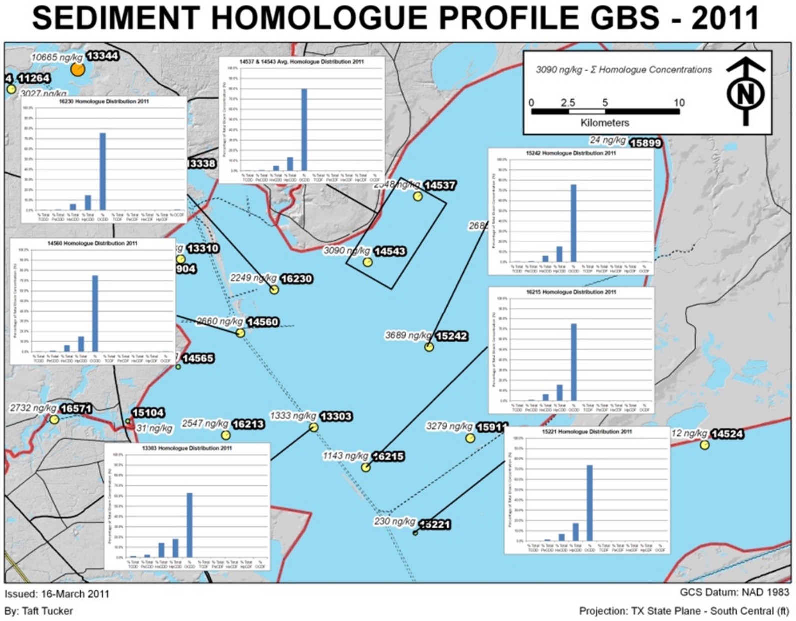

Figure 4: Sediment Homologue Profiles in Galveston Bay Sediments – 2011

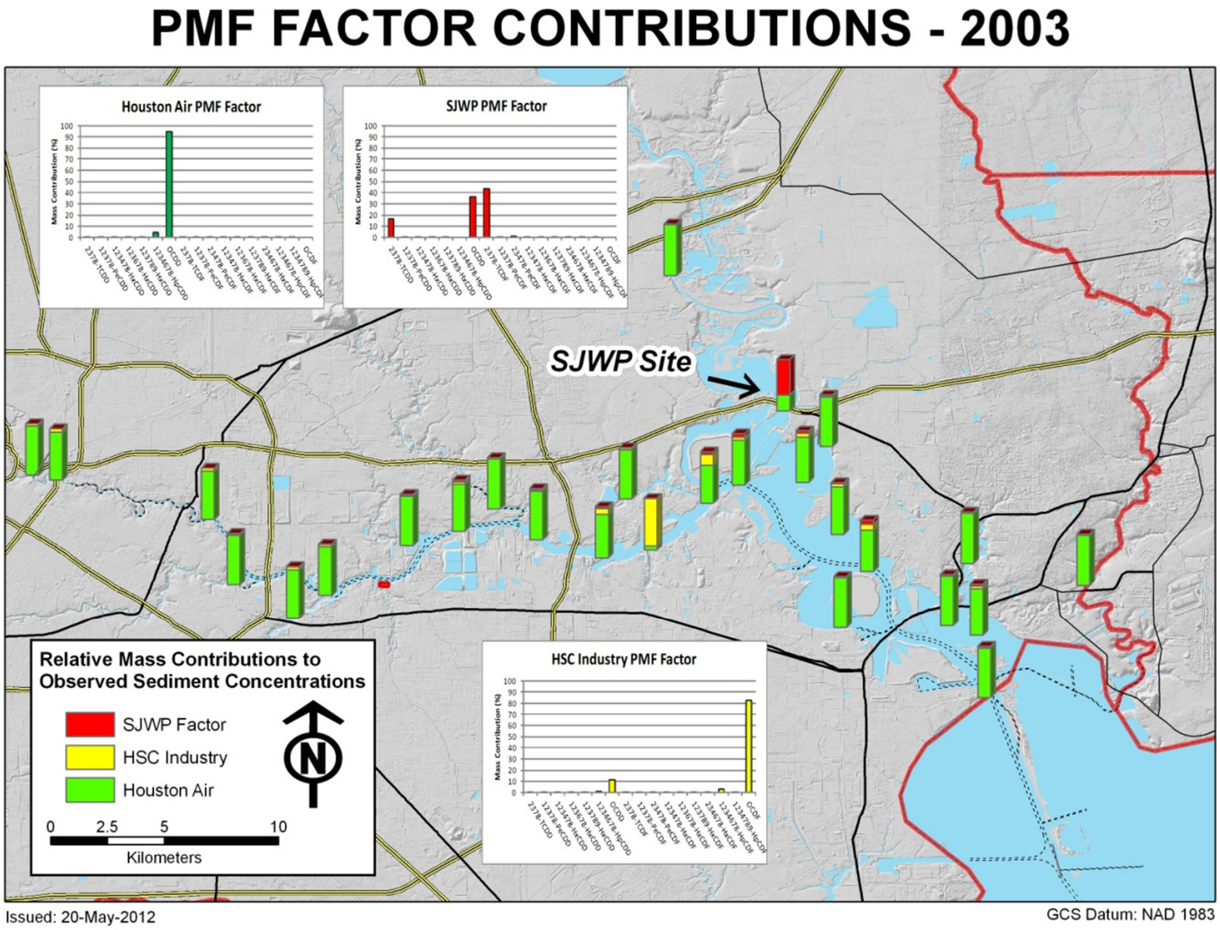

Figure 5: Relative PMF Factor Mass Contributions – 2003

The San Jacinto River Waste Pits – This profile is characterized by high levels of tetra-furan and tetra-dioxin, particularly 2378-TCDF and 2378-TCDD, which are typically present in a roughly 2.5-3 to 1 ratio. *Stations exhibiting this factor during 2002 sampling (Figure 3): 11193.*

HSC Industry – OCDF is the dominant congener in this signature. Patrick Bayou appears to be a major contributor of this dioxin profile. *Stations exhibiting this factor during 2002 sampling: 15979 & 11273.*

Houston Regional Air – This profile is predominantly OCDD along with other dioxins that decrease in concentration with decreasing chlorination level. Runoff likely delivers this profile to a certain degree (Correa, Raun et al. 2006), but the uniform distribution of this profile suggests that air deposition also plays an important role in delivering this profile to the system. *Stations exhibiting this factor during 2002 Sampling: 16496 & 17971.*

The influence of localized dioxin sources is apparent in sediments near the industrialized portion of the HSC, near the SJWP, and near the confluence of the HSC/SJR. This is contrasted with sediment samples collected from the open waters of Galveston Bay during the summer of 2011, see Figure 4, which closely resemble the fingerprint observed in Houston's air and runoff.

PMF Analysis: PMF was applied to surface sediment samples collected between 2002 and 2011 returning similar results to those observed during the qualitative fingerprint analysis. Outliers and samples with detections in fewer than 50% of 2378-TCDD substituted congeners were removed from the dataset prior to PMF analysis. PMF returned 3 primary source profiles, very similar to those discussed above, and their contributions to sediments decreased with increasing downstream distance from the HSC/SJR confluence. Figure 5 shows the results for samples collected during 2003.

CONCLUSIONS

This study indicated that industrial point sources have significant impact on nearby sediment quality with the HSC and SJR, but atmospheric sources are the dominant contributors to dioxins observed in the more open waters of Galveston and Trinity Bays.

REFERENCES

Amendola, G., D. Barna, et al. (1989). "The occurrence and fate of PCDDs and PCDFs in five bleached kraft pulp and paper mills." Chemosphere **18**(1â€"6): 1181-1188.

Clement, R. E., C. Tashiro, et al. (1989). "CHLORINATED DIBENZO-PARA-DIOXINS (CDDS) AND DIBENZOFURANS (CDFS) IN EFFLUENTS AND SLUDGES FROM PULP AND PAPER-MILLS." Chemosphere **18**(1-6): 1189-1197.

Correa, O., L. Raun, et al. (2006). "Depositional flux of polychlorinated dibenzo-p-dioxins and polychlorinated dibenzofurans in an urban setting." Chemosphere **64**(9): 1550-1561.

Ehrlich, R., R. J. Wenning, et al. (1994). "A MIXING MODEL FOR POLYCHLORINATED DIBENZO-P-DIOXINS AND DIBENZOFURANS IN SURFACE SEDIMENTS FROM NEWARK BAY, NEW-JERSEY USING POLYTOPIC VECTOR ANALYSIS." Archives of Environmental Contamination and Toxicology **27**(4): 486-500.

Hites, R. A. (2011). "Dioxins: An Overview and History." Environmental Science & Technology **45**(1): 16-20.

Paatero, P. (1997). "Least squares formulation of robust non-negative factor analysis." Chemometrics and Intelligent Laboratory Systems **37**(1): 23-35.

Paatero, P. and U. Tapper (1994). "POSITIVE MATRIX FACTORIZATION - A NONNEGATIVE FACTOR MODEL WITH OPTIMAL UTILIZATION OF ERROR-ESTIMATES OF DATA VALUES." Environmetrics **5**(2): 111-126.

Polissar, A. V., P. K. Hopke, et al. (1998). "Atmospheric aerosol over Alaska - 2. Elemental composition and sources." Journal of Geophysical Research-Atmospheres **103**(D15): 19045-19057.

Schwetz, B. A., J. M. Norris, et al. (1973). "Toxicology of Chlorinated Dibenzo-*p*-dioxins." Environmental Health Perspectives **5**: 87-99.

Suarez, M. P., H. S. Rifai, et al. (2006). "Distribution of polychlorinated dibenzo-p-dioxins and dibenzofurans in suspended sediments, dissolved phase and bottom sediment in the Houston Ship Channel." Chemosphere **62**(3): 417-429.

Sundqvist, K. L., M. Tysklind, et al. (2010). "PCDD/F Source Apportionment in the Baltic Sea Using Positive Matrix Factorization." Environmental Science & Technology **44**(5): 1690-1697.

USEPA (2006). An Inventory of Sources and Environmental Releases of Dioxin-Like Compounds in the United States for the Years 1987, 1995, and 2000. Washington, D.C., United States Environmental Protection Agency.

Wenning, R., D. Paustenbach, et al. (1993). "CHEMOMETRIC ANALYSIS OF POTENTIAL SOURCES OF POLYCHLORINATED DIBENZO-P-DIOXINS AND DIBENZOFURANS IN SURFICIAL SEDIMENTS FROM NEWARK BAY, NEW-JERSEY." Chemosphere **27**(1-3): 55-64.

Yunker, M. B., W. J. Cretney, et al. (2002). "Assessment of chlorinated dibenzo-p-dioxin and dibenzofuran trends in sediment and crab hepatopancreas from pulp mill and harbor sites using multivariate- and index-based approaches." Environmental Science & Technology **36**(9): 1869-1878.

COMPARISON OF SEAWATER PARAMETERS IN THE ARABIAN GULF AND THE GULF OF OMAN

Fadi Al Jallad and Muthanna Al Omar
National Energy and Water Research Center (NEWRC), Abu Dhabi Emirate, UAE

ABSTRACT: United Arab Emirate (UAE) has a coastline of about 734 Km along the Arabian Gulf, and 90 km along the Gulf of Oman. Arabian Gulf is a shallow semi-enclosed sea whose water properties are adversely affected by several natural and anthropogenic factors. On the contrary, the Gulf of Oman is a deep open sea, whose water is characterized by relatively low salt content as compared to the water of Arabian Gulf. Strait of Hormuz connects the Arabian Gulf with the Gulf of Oman and allows slow water exchange between water bodies of the two gulfs.

This work was established to measure and assess the physicochemical characteristics of seawater in the Arabian Gulf and the Gulf of Oman. The results were used to evaluate the suitability of seawater as a resource for desalination and to investigate the feasibility of expansion the existing cogeneration plants along Abu Dhabi coastline (Arabian Gulf) versus the construction of new plants along Fujairah coastline (Gulf of Oman).

During the period from November 2009 to September 2010, 43 composite seawater samples were collected from two locations in Arabian Gulf (Abu Dhabi Emirate) and Gulf of Oman (Fujairah Emirate). Samples were analyzed to determine various physicochemical parameters which include: anions (chloride, bicarbonate and sulphate), cations (sodium, potassium, magnesium, calcium and strontium) in addition to alkalinity, total hardness (TH), total dissolved solid (TDS), temperature and pH.

The results were statistically analyzed and the seasonal variation patterns for all parameters were determined. In the Arabian Gulf, the maximum values of Cl, SO_4, Na, K, Sr and TDS were observed in the hot season (May - September), while higher values of HCO_3, Mg, Ca, alkalinity, TH and pH were reported in colder season (November - February). On the other hand, the maximum values of Cl, K, Mg, Ca, Sr, alkalinity, TH and TDS in the Gulf of Oman were observed in the hot season, while higher values of HCO_3, SO_4, Na and pH were reported in colder season.

Generally, elevated levels of ion concentrations were found in the Arabian Gulf, where most of the physiochemical parameters were higher than their counterparts in the Gulf of Oman and other comparable regions. Consequently, the quality of seawater in the Gulf of Oman is relatively better and construction of new power cogeneration plants or expansion of the existing plants along Fujairah coastline (Gulf of Oman) is more feasible than the alternative along Abu Dhabi coastline (Arabian Gulf).

INTRODUCTION

United Arab Emirate (UAE) has a coastline of about 734 Km along the Arabian Gulf, and 90 km along the Gulf of Oman. The Arabian Gulf, referred to as the Persian Gulf in some countries, is a shallow semi-enclosed sea with mean depth of only 35 m (Smith et al., 2007). It represents the major water resource for most of the Arabian Gulf countries (Al-Barwani, 2008). Several natural and anthropogenic activities affect the quality of seawater in this gulf among them are; the limited inflow of freshwater, high evaporation rate, large quantities of brine discharge from the cogeneration plants and industrial campuses, in addition to the effects of different other human activities (Kampf and Sadrinasab, 2006). Lattemann and Höpner, (2008) reported that a large number of desalination plants are located along the coastline of Arabian Gulf, with a total capacity of approximately 11million m^3/day. The discharges of this industry as

---

ISBN 9780976885351

well as many other activities have adverse impact on the marine ecosystem and may lead to the deterioration of seawater quality (Altayaran and Madany, 2003).

The narrow Strait of Hormuz connects the Arabian Gulf to the Gulf of Oman, allowing a slow water exchange between the two water bodies, where the flushing time in the Arabian Gulf was estimated at approximately 3 - 5.5 years (Sheppard, 1993).

The Gulf of Oman is a deep open sea, whose water is characterized by relatively less salt content as compared to the Arabian Gulf. These characterizations can be attributed to better circulation of water body, deeper water and lower quantities of industrial discharges. The Gulf of Oman is directly connected to the Arabian Sea, where the depth of water may reach 5000 meter (ROPME 2000). The industrial effluents are relatively low since only five desalination plants are located along the Gulf of Oman with a total capacity of 1.1million m^3/day (Purnama, and Al-Barwani, 2006). However, few other minor industrial and domestic sources are established along the coast of the gulf which experiences high marine traffic density.

Seawater quality is usually described by its physical, chemical and biological characteristics. The chemical characteristics of seawater in three different locations (Eastern Mediterranean, Red Sea and Arabian Gulf) were determined and compared with typical seawater by Al-Mutaz (2000). Whereas the composition of seawater in Sur in the Gulf of Oman was determined by Mahmoudian (2006). The results of these research works are presented in Table 1, concluding that the characteristics of seawater vary widely depending on location.

TABLE 1. Major ion compositions of seawater in different regions compared to typical seawater (mg/L), Al-Mutaz (2000) and Mahmoudian (2006).

Constituent	Typical Seawater	Eastern Mediterranean	Red Sea (Jeddah)	Arabian Gulf (Kuwait)	Gulf of Oman (Sur)
Chloride (Cl^-)	18980	21200	22219	23000	22481
Sodium (Na^+)	10556	11800	14255	15850	11600
Sulphate (SO_4^{2-})	2649	2950	3078	3200	1657
Magnesium (Mg^{2+})	1262	1403	742	1765	1262
Calcium (Ca^{2+})	400	423	225	500	840
Potassium (K^+)	380	463	210	460	435
Bicarbonate (HCO_3^-)	140	-	146	142	109
Strontium (Sr^{2+})	13	-	-	-	-
Bromide (Br^-)	65	155	72	80	-
Borate (BO_3^{3-})	26	72	-	-	-
Fluoride (F^-)	1	-	-	-	0.7
Silicate (SiO_3^{2-})	1	-	-	1.5	-
Iodide (I^-)	<1	2	-	-	-
Others	1	-	-	-	-
Total dissolved solids (TDS)	**34483**	**38600**	**41000**	**45000**	**43775**

The main aim of this work is to measure the physicochemical characteristics of seawater in the Arabian Gulf and the Gulf of Oman and to identify their seasonal variations. Furthermore, the results of this study were used to evaluate the suitability of seawater as a resource for desalination and to investigate the feasibility of expansion the existing cogeneration plants along Abu Dhabi coastline (Arabian Gulf) versus construction new plants along Fujairah coastline (Gulf of Oman).

METHODOLOGY

The study was conducted in the coastlines of United Arab Emirate (UAE). Two study areas were selected for this work, the first of which is located along the Arabian Gulf in Abu Dhabi Emirate and has about 10 meter depth. The second study area is located along the Gulf of Oman in Fujairah Emirate and characterized by deep water (Figure 1).

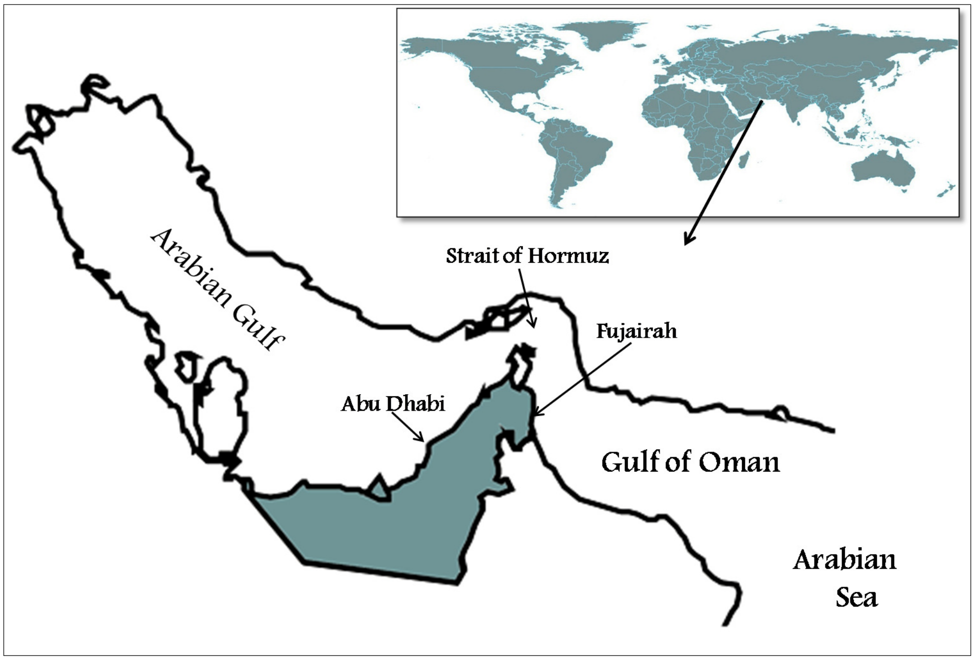

FIGURE 1. A map showing the study areas in UAE on both Arabian Gulf and Gulf of Oman.

During the period November 2009 to September 2010, a total number of 43 composite samples of seawater were collected manually on a biweekly basis from the Arabian Gulf (22 samples) and the Gulf of Oman (21 sample). The samples were collected in such a way that each composite sample comprised four subsamples; two of which were taken from near-shore (surface and bottom) whereas the other two were taken at about one kilometer away from shore (surface and bottom), the locations of the sampling points are illustrated in Figure 2.

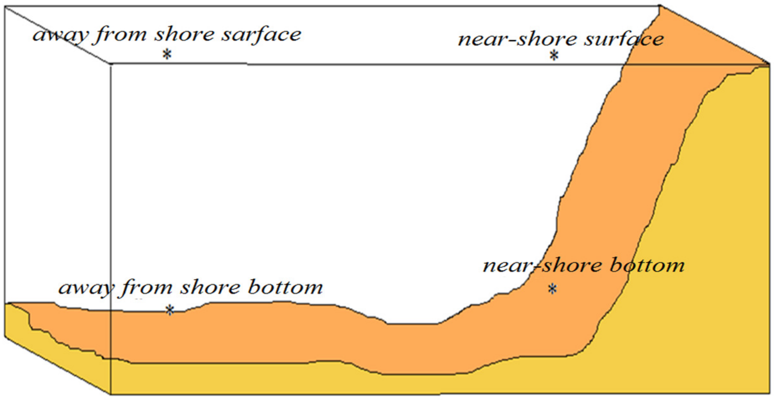

FIGURE 2. An illustrative diagram showing the locations of the subsample points of a composite sample.

Temperature and pH were measured in-situ using a portable meter (Hanna Instruments, USA, HI 9829). The seawater samples were collected, chemically preserved and handled according to the guidelines specified in the Handbook for Sampling and Sample Preservation of Water and Wastewater (US-EPA, 1982). The collected samples were analyzed in an accredited laboratory in Abu Dhabi to determine physicochemical parameters, which include; anions (chloride, bicarbonate and sulphate), cations (sodium, potassium, magnesium, calcium and strontium) in addition to alkalinity, total hardness (TH) and total dissolved solids (TDS). The chemical analyses were conducted according to Standard Methods for the Examination of Water and Wastewater (APHA, 1992). Monthly mean values of each parameter were calculated from the analysis results of biweekly samples.

RESULTS AND DISCUSSION

The results of statistical analyses for seawater parameters at the Arabian Gulf and Gulf of Oman during the study period are presented in Table 2. Minimum, maximum and average values of seawater temperature of the Arabian Gulf were 20.7 ^{o}C, 35.9 ^{o}C and 28.2 ^{o}C, respectively, whereas the counterpart values of the Gulf of Oman were 23.2 ^{o}C, 33.6 ^{o}C and 29.4 ^{o}C, respectively. The analysis results for pH showed almost similar values for the two locations, where the values varied from 7.9 to 8.3 and from 8.0 to 8.4 in the Arabian Gulf and the Gulf of Oman, respectively.

The alkalinity fluctuated from 110 to 130 mgCaCO$_3$/L and from 108 to 127 mgCaCO$_3$/L in the Arabian Gulf and the Gulf of Oman, respectively. Similar average value of 119 mgCaCO$_3$/L was observed in both locations. The maximum level was observed in January 2010 in the Arabian Gulf and in September 2010 in Gulf of Oman.

TH levels ranged from 7513 to 8354 mgCaCO$_3$/L and from 6159 to 7753 mgCaCO$_3$/L in the Arabian Gulf and the Gulf of Oman, respectively. The average value in the Arabian Gulf was 7902 mgCaCO$_3$/L which is 9% higher than the average value observed in Gulf of Oman. The maximum level was observed in February 2010 at the Arabian Gulf and in August 2010 at the Gulf of Oman.

TDS levels ranged from 44703 to 48477 mg/L and 40317 to 41352 mg/L in the Arabian Gulf and the Gulf of Oman, respectively. The average value in the Arabian Gulf was 46594 mg/L representing about 12% higher than the average value in the Gulf of Oman. Maximum concentrations for both locations were observed in July 2010.

The concentrations of chloride ranged from 22803 to 25152 mg/L and from 21716 to 25064 mg/L in the Arabian Gulf and the Gulf of Oman, respectively. The average concentration in the Arabian Gulf was 24346 mg/L representing about 8% higher than the average value observed in Gulf of Oman. The highest concentrations were recorded in August 2010 for both locations.

The analysis results showed that the contents of bicarbonate ranged from 90 to 118 and from 91 to 113 mg/L in the Arabian Gulf and the Gulf of Oman, respectively. Similar average values were observed in both locations with a value of 104 mg/L, while the maximum concentration was observed in November 2009 at the Arabian Gulf, where maximum value of 113 mg/L was recorded twice in November 2009 and January 2010 at the Gulf of Oman.

Sulphate concentrations fluctuated from 2928 to 3323 mg/L and from 2736 to 3106 mg/L, respectively. The average value (3188 mg/L) in the Arabian Gulf was higher than its counterpart in the Gulf of Oman by 10%. The maximum concentration was observed in September 2010 at the Arabian Gulf and in November 2009 at Gulf of Oman.

Sodium concentrations ranges were 11992 - 14309 mg/L and 12147 - 12498 mg/L in the Arabian Gulf and the Gulf of Oman, respectively. The average value of Sodium (13714 mg/L) in the Arabian Gulf was about 13% higher than average value in the Gulf of Oman. Maximum concentration was observed in July 2010 at the Arabian Gulf and in November 2009 at the Gulf of Oman.

Potassium concentrations ranged from 414 to 863 mg/L in the Arabian Gulf and from 387 to 508 mg/L in the Gulf of Oman. The average value (678 mg/L) in the Arabian Gulf was higher than its counterpart in the Gulf of Oman by about 33%. February and August 2010 experienced the highest concentrations for the Arabian Gulf and the Gulf of Oman, respectively.

Magnesium ranged from 1526 to 1722 mg/L and 1261 to 1596 mg/L in the Arabian Gulf and the Gulf of Oman, respectively. The average value in the Arabian Gulf was 1624 mg/L which represent about 10% higher than the average value in the Gulf of Oman. Maximum concentration was observed in January 2010 at the Arabian Gulf and in August 2010 at the Gulf of Oman.

Calcium concentrations ranged from 479 to 509 mg/L in the Arabian Gulf and 402 to 482 mg/L in the Gulf of Oman. The average value (490 mg/L) in the Arabian Gulf was higher than its counterpart in the Gulf of Oman by about 8%. Maximum concentration was observed in February 2010 at the Arabian Gulf and in August 2010 at the Gulf of Oman.

Finally, Strontium concentrations ranges were 9 - 11 mg/L and 8 - 12 mg/L in the Arabian Gulf and the Gulf of Oman, respectively. The average value of strontium in the Arabian Gulf (10 mg/L) was 11% higher than the average value in the Gulf of Oman. Maximum concentrations for both locations were observed in May 2010.

TABLE 2. Statistical analysis for seawater parameters at the Arabian Gulf and Gulf of Oman during the period from November 2009 to September 2010.

Parameter	Units	Arabian Gulf			Gulf of Oman			Percentage of increase
		Minimum	Maximum	Average	Minimum	Maximum	Average	
Temperature	^oC	20.7	35.9	28.2	23.2	33.6	29.4	4
pH	---	7.9	8.3	8.1	8	8.4	8.1	0
Alkalinity	mg/L*	110	130	119	108	127	119	1
TH	mg/L*	7513	8354	7902	6195	7753	7124	9
TDS	mg/L	44703	48477	46594	40317	41352	40845	12
Cl^-	mg/L	22803	25152	24346	20716	25064	22339	8
HCO_3^-	mg/L	90	118	104	91	113	104	0
SO_4^{2-}	mg/L	2928	3323	3188	2736	3106	2874	10
Na^+	mg/L	11993	14309	13714	11247	12498	11904	13
K^+	mg/L	414	863	678	387	508	452	33
Mg^{2+}	mg/L	1526	1722	1624	1261	1596	1456	10
Ca^{2+}	mg/L	479	509	490	402	482	453	8
Sr^{2+}	mg/L	9	11	10	8	12	9	11

**Expressed as $CaCO_3$*

CONCLUSION

The results of analyses indicate that the quality of seawater varies in the investigated locations. Generally, elevated levels of ion concentrations were found in the Arabian Gulf comparing with other regions (Eastern Mediterranean, Red Sea and the Gulf of Oman). Moreover, along the same coast line of Arabian Gulf, the levels of Chloride and Potassium in Abu Dhabi were higher than their counterpart in Kuwait.

The seasonal variations did not follow the same pattern for all studied parameters. In the Arabian Gulf, the maximum values of Cl, SO_4, Na, K, Sr and TDS were observed in the hot season (May - September), while higher values of HCO_3, Mg, Ca, alkalinity, TH and pH were reported in colder season (November - February). On the other hand, the maximum values of Cl, K, Mg, Ca, Sr, alkalinity, TH and TDS in the Gulf of Oman were observed in the hot season, while higher values of HCO_3, SO_4, Na and pH were reported in colder season.

Based on the results of present work, most of the physiochemical parameters in the Arabian Gulf were higher than their counterparts in the Gulf of Oman. Consequently, the quality of seawater in the Gulf of Oman is relatively better and construction of new power cogeneration plants or expansion of the existing plants along Fujairah coastline (Gulf of Oman) is more feasible than the alternative along Abu Dhabi coastline (Arabian Gulf). However, along the same coast line of the Gulf of Oman, the levels of Sodium, Sulphate, Magnesium and Potassium in Fujairah were higher than their counterpart in Sur in Oman.

ACKNOWLEDGMENT

The authors would like to thank Nashat Sabah, Elfadil Osman, Taher Ali and Jayeshkumar Shah for their contribution to this work by collecting the seawater samples from the study areas. The authors would like also to extend their sincere appreciation to Dr. Hamda Al-Thani, the Director of the National Energy & Water Research Center for her continuous support and encouragement.

REFERENCES

Al Mutaz M., 2000. Water desalination in the Arabian Gulf region. In: Goosen MFA, Shayya WH, eds. *Water management, purification and conservation in arid climates. Vol. 2. Water purification.* Basel, Technomic Publishing, pp. 245–265.

Al-Barwani H.H., 2008. Evaluating the Effect of Producing Desalinated Seawater on Hypersaline Arabian Gulf. *European Journal of Scientific Research*, 22: 279-285.

Altayaran, A.M. and I.M. Madany, 2003. Impact of a desalination plant on the physical and chemical properties of seawater, Bahrain. *Water Research,* 26(4): 435–441.

APHA, 1992. *Standard Methods for the Examination of Water and Wastewater*, 18th edition. American Public Health Association, Washington, D.C.

Kampf J. and M. Sadrinasab, 2006. The circulation of the Persian Gulf: a numerical study. *Ocean Science,* 2: 27–41.

Lattemann, S. and T. Höpner, 2008. Environmental impact and impact assessment of seawater desalination. *Desalination,* 220: 1–15.

Mahmoudian S. A., 2006. Practices and experiences of water and wastewater technology, Proceedings of the Seminar organized by the Regional Centre on Urban Water Management (RCUWM) -Tehran, October 2004. Muscat, Sultanate of Oman. Technical Documents in Hydrology, UNESCO-IHP-VI, No. 79, Paris, 75-91.

Purnama, A., and H.H. Al-Barwani, 2006. Spreading of brine waste discharges into the Gulf of Oman. *Desalination*, 195(1-3): 26-31.

ROPME, 2000. ROMPE Region from Space. Regional Organization for the Protection of Marine Environment (ROPME) and United Nations Environment Program (UNEP). Kuwait, March, 2000.

Sheppard, C.R.C., 1993. Physical-environment of the Gulf relevant to marine: an overview. *Marine Pollution Bulletin* 27: 3-8.

Smith, R., A. Purnama and H.H. Al-Barwani, 2007. Sensitivity of hypersaline Arabian Gulf to seawater desalination plants. *Applied Mathematical Modelling*, 31(10): 2347-2354.

US-EPA 1982. *Handbook for Sampling and Sample Preservation of Water and Wastewater.* United State Environmental Protection Agency. EPA-600/4-82-029.

NONYLPHENOLS AND THEIR ETHOXYLATES IN RIVERS AND HARBOR AREA OF KAOHSIUNG, TAIWAN

Bing-Jung Ku and ***Wei-Hsien Wang**** (National Sun Yat-Sen University, Kaohsiung, Taiwan)
Shu-Hui Lee (National Kaohsiung Marine University, Kaohsiung, Taiwan)

Alkylphenol ethoxylates (APEOs) are widely used nonionic surfactants. These substances have aroused much concern because of their ecotoxicological properties in aquatic environment. This work presents the results of an investigation on occurrence of nonylphenols (NPs) and their respective ethoxylates (NPnEOs) in rivers and harbor area in Kaohsiung, Taiwan. The total NPEOs (NP and NPnEOs) were 1.13-4.03 μg/L in river water and 0.038-0.19 μg/L in harbor seawater, 1285-5737 μg/Kg in river sediment and 72-556 μg/Kg in harbor sediment, respectively. The content of NP has a significant correlation with the total organic carbon in sediment samples. In rivers and harbor area of Kaohsiung, the concentrations of nonylphenolic substances in water and sediment are at a moderately to severely polluted level in comparison with other places in the world.

ISBN 9780976885351

STUDIES ON EVALUATION WATER QUALITY INDEX OF DARA DAM-MAHARASHTRA, INDIA

Anjali Mahajan, ***Tank S. K.***
(Department of Biosciences, Veer Narmad South Gujarat University, Surat – 395007, India)

Dara Dam is located at 21.46’ North Latitude and 74.26 east longitudes. Area of the Dam is 63.71 sq. km and it irrigates 4404 hectare land for agricultural production. Major interest of study was to find Water Quality Index of Dam as it is lifeline of the Tribal locality. Majority of the nearby inhabitants are economically very poor tribal people and depends on Dam for irrigation water. The need of the water is increasing day by day and now it is multiactivity like bathing, washing clothes, animals, vehicle cleaning, drinking and it is also consumed by the domestic and wild animals too.

To check the water quality, this study was under taken as water of the Dam is consumed by the local inhabitants. Present work includes hydrological parameters of dam at five different sites for twelve month and samples were collected once a month in the year 2009-2010. Total 28 parameters were analyzed , these were Temperature, pH, Turbidity ,DO,BOD, COD, TDS, TSS, Hardness, Alkalinity, Chlorides, Sulphate, Nitrate, Nitrite, Nitrogen(TKN),Sodium, Potassium, Magnesium, Total Coli form, Fecal Coli form and heavy metals like Hg, Pb, Cd, Cr, and Ar were analyzed. Arsenic was detected at one site only. Other heavy metals were not detected. Water color and odor were normal. For analysis of water samples, Methods followed was of APHA USA. Water Quality Index (WQI) was found out for each sampling site by using formula developed by Canadian Council of Ministry of Environment (CCME) prescribed by CCMEWQI. In our study of sampling station, WQI was 56.4 at site I, 71.06 at site II, it was 60.39 at site III, 41.14 at site IV and 36.41 at site V. From WQI of different sites and sampling stations, it can be concluded that water is not suitable for human consumption, 3 sampling sites are in fair condition and water from not a single site of sampling is in good or excellent condition. To find out significant parameters for the variation of WQI, correlation and regression analysis were done.

From our study it is clear that water quality is not good or excellent at any site according to standards laid by WHO. It is not consumable and it should not be consumed. Even then thousands of tribal people, being unaware of the water quality, consume this water.

ISBN 9780976885351

ARTIFICIAL NEURAL NETWORKS FOR LOCALIZATION OF CONTAMINATION SOURCES IN DRINKING WATER DISTRIBUTION SYSTEMS

Diogo Costa, Luís Melo and Fernando Martins (University of Porto, Porto, Portugal)

This paper addresses the problem of the localization of contamination sources after deliberate contaminations in drinking water distribution systems (DWDS) through the application of artificial neural networks (ANN). The aims of this methodology are: a) to determine the probability distribution of contamination source location for the entire DWDS; b) to estimate the corresponding time of contamination for nodes with probabilities different from zero.

The methodology requires the creation of two databases, generated using the hydraulic model of the entire DWDS, with the detection patterns (binary status for each sensor) and the times of detection in each sensor, coupled with their respective contamination scenarios. These databases are used to train an ANN to determine the probability distribution of contamination source location for the entire DWDS and to train an ANN per node to evaluate the corresponding time of contamination.

The tests performed for a simple DWDS allow concluding that the proposed methodology is able to identify the correct contamination source and to predict the time of contamination. In spite of the computational effort necessary to create the databases and to train the ANN, this step of the procedure only has to be taken once. Since the ANNs are trained, the application of this methodology requires a very small computational time.

ISBN 9780976885351

A NEW HYBRID AERATOR COMBINING A BUBBLE GENERATOR AND A SURFACE MECHANICAL AERATOR

Ajey Kumar Patel and Achanta Ramakrishna Rao
(Department of Civil Engineering, Indian Institute of Science, Bangalore-560012, India)

Aeration is an important process in a wastewater treatment plant. About 70 to 80 percent of energy used in wastewater treatment is in the aeration process. That shows the importance of the proper design of such systems. A novel design of a hybrid aerator is developed which maximizes oxygen transfer rate in wastewater. The hybrid aerator consists of: two independently rotating parts viz. a rotor with six flat blades as agitator and L-shaped hollow tube as bubble generator with one end in the atmosphere and other in the liquid. When L-tube is rotated air will be sucked into the tube and discharged into the water in the form of bubbles (application of Bernoulli's principle).The rotor rotates at a relatively lower speed than L-tube. The rotor creates turbulence in the wastewater body which helps in absorption of air from the atmosphere (according to two film theory) and mixing of air and water on forming the bubbles. So the dissolution of oxygen takes place from two mechanisms ie one from the agitated air-water interface and other from the interface of the bubbles introduced by the L-tube. The objective of the present work is to develop an optimal design of such a hybrid aerator for maximum oxygen transfer as dissolved oxygen into the wastewater body for reduction of BOD. The other objective is to develop a scale up criteria for oxygen transfer process for field applications. Dissolved oxygen is measured and recorded over time by Thermo Orion_ 5 Star Meter. Rotational speeds of rotor and L-tube have been measured with a digital tachometer. Reaeration experiments were conducted in circular shaped baffled aerator tanks of sizes A=1, 0.518, 0.168 m^2 and tap water is used for all experimental runs.

For hydraulic modeling of aeration systems the geometric configuration is very important. The various geometric parameters that influence oxygen transfer in hybrid aerators are: depth of submergence of L-tube, H_t; its radial position from the centre of the rotor shaft, R_l and the radius of the L-tube, l_a. The other dimensions are: the water depth in the tank, H; the diameter of rotor, D, with blade dimensions l and b; height of the top edge of the rotor blade from the horizontal bottom of the tank, h. The influence of these parameters has been studied and the optimal geometric dimensions obtained for L-tube are: $\boldsymbol{H_t/H = 0.173, R_l/D=0.65}$ **and** $\boldsymbol{l_a/D=0.36}$. The optimal ratio of speeds of rotor and L-tube is, $\boldsymbol{N_r/N_t = 0.0589}$. The other dimensions were maintained according to the following ratios: $\sqrt{A}/D = 2.88$; $H/D = 1.0$; $l/D = 0.32$; $h/D = 1.0$; N_b=4; B/D=0.5. The geometric ratio at which oxygen transfer rate is maximum is defined as optimal geometric dimension. Using optimal geometric parameters studies on the effect of dynamic parameters (Reynolds number, $R_e = N_rD^2/\square$ and Froude number, $F_r = N_r^2D/g$, where □□is the kinematic viscosity and g is gravitational constant) on re-aeration performance was conducted. The scaling effect was observed when using R_e and F_r for dynamic similitude. That means it is not possible to simulate oxygen transfer rate neither with R_e nor F_r. However when the same oxygen transfer data is plotted against theoretical power per unit volume parameter, $X_r = N_r^3D^2/(g^{4/3}\square^{1/3})$, then all the data from all sizes of aeration tanks fall on a unique curve, thus suggesting a dynamic similarity criteria for oxygen transfer in hybrid aeration system. The hybrid aerator performs about **4 times** better ie it absorbs **4 times** more oxygen for the same power consumed as compared to other aeration systems.

The optimal geometric parameters for hybrid aeration system have been obtained. The theoretical power per unit volume parameter is found to the suitable dynamic similitude criteria for oxygen transfer in geometrically similar hybrid aeration systems. The present design performs **4 times** better than previous designs, thus improving the efficiency of oxygen transfer process and incurring a substantial saving on power. The energy saved leads to a lower impact of such processes on the environment. The hybrid aerator developed is under patent.

ISBN 9780976885351

INVESTIGATION OF ANTIBIOTICS IN LONG-TERM WASTEWATER IRRIGATION SOIL IN TIANJIN, CHINA

Yali Shi Lihong Gao Wenhui Li Yaqi Cai*
(Research Center for Eco-Environmental Sciences, Chinese Academy of Sciences, Beijing, China)

Antibiotics, a particularly important pharmaceutical group, are wildly used as human medicine to prevent or treat infective diseases, and as veterinary drugs and growth promoters in livestock and aquaculture operations. They are regarded as “pseudo-persistent” contaminants because they are introduced into the environment continually. They are often excreted by the animals and end up in soils via grazing livestock or manure used as agricultural fertilizer. So soil is deemed to be the primary sink of antibiotics, which can persist in soil for a long time. Wastewater irrigation was considered as an important exposure route for the introduction of pharmaceutical compounds to the agricultural fields. However, water reclamation and reuse has become increasingly important and sustainable approaches in agricultural irrigation due to water resource scarcity and world growing demands for water, especially in China. Tianjin city, which is one of the most serious water resources shortage cities, has the largest wastewater irrigation area in China. It has been proved that the concentrations of heavy metals in the agricultural soil of Tianjin increased due to wastewater irrigation. However, there is limited information on the occurrence of antibiotics in the wastewater irrigation soil in Tianjin, China.

In our study, 22 antibiotics, including eight fluoroquinolones (FQs), nine sulfonamides (SAs) and five macrolides (MCs), were analyzed in total 87 soil samples collected from suburban areas (Xiqing, Dongli, Jinnan, Beichen), with the long-term wastewater irrigation, in Tianjin, China. The result showed that FQs were the predominant class of antibiotics, with the total concentrations of eight FQs (∑FQs) ranging from below the detection limits to 274.81 µg/kg. The mean ∑FQs (33.56µg/kg) was 30-fold higher than one of ∑MCs, which were the second dominant class of antibiotics. SAs showed the lowest level, with the total concentrations of SAs (∑SAs) ranging from below the detection limits to 5.05µg/kg. Among the group of FQs, norfloxacin was the predominant compound, with the mean concentration of 10.22 µg/kg. The spatial distribution of FQs showed the highest concentrations were found in Dongli district, which has longer reuse water irrigation than any other district. And in the Beichen district, where there is only shorter-term intermittent wastewater irrigation, the antibiotics showed the lowest level. So the wastewater irrigation was a potential source of antibiotics in the soil of Tianjin. The individual antibiotics levels in the present study were all below the trigger value (100µg/kg) set by the Steering Committee of Veterinary International Committee, indicating the low risk for organisms in the agricultural soils of Tianjin. However, it needs to further investigate the environmental fate of antibiotics in soils.

ISBN 9780976885351

THE OCCURRENCE AND TISSUE DISTRIBUTION OF PERFLUORINATED COMPOUNDS IN FARMED FRESHWATER FISH

Yali Shi Jiming Wang Yuanyuan Pan Yaqi Cai*
(Research Center for Eco-Environmental Sciences, Chinese Academy of Sciences, Beijing, China)

Perfluorinated compounds (PFCs) are a family of man-made fluorinated organic compounds which have been produced for several decades. Due to their oleophobic and hydrophobic properties, they are used extensively in food packaging, textile coatings, lubricants, surfactants, fire-fighting foams, and nonstick coatings for cookware. In recent years, human exposure to PFCs by intake of food, drinking water, air, and indoor dust has drawn growing concerns from environmental scientists due to their wide occurrence in the environment and human blood. In a previous study, it was indicated that humans are mainly exposed to PFCs through food consumption. In particular, the levels of PFCs in fish were relatively high among the foodstuffs analyzed, which implied that the intake of contaminated fish may be a significant source of PFCs in humans. However, there is still a dearth of information regarding PFC levels in farmed freshwater fish, especially its tissue distribution, in China.

In our study, the levels of fourteen PFCs were analyzed in the blood, liver, muscle, brain, and egg of popular farmed freshwater fish, including grass carp, snakehead, crucian carp, common carp, tilapia, and bighead from Beijing. Perfluorooctane sulfonate (PFOS) was the predominant compound in all the analyzed tissues, with the highest concentration at 70.7 ng/g wet weight (ww) found in the blood of bighead. The highest mean (or median) levels (in ng/g ww) of PFOS in blood and all tissues were observed in bighead (1.48-22.53 (0.70-12.19)) and the lowest in tilapia (0.26-1.63 (0.11-1.42)). In addition, perfluoroundecanoic acid was the second dominant PFC in blood, liver, muscle, and egg with the highest concentration at 19.17 ng/g ww found in blood. However, perfluorodecanoic acid levels (<limit of detection -0.963 ng/g ww) were similar to or slightly higher than perfluoroundecanoic acid levels (<limit of detection -0.918 ng/g ww) in the brain. Generally, the highest mean concentrations of PFOS and total PFCs (in ng/g ww) were found in fish blood (1.15-22.53, 6.16-31.4), followed by liver (1.63-14.14, 2.54-16.89), brain (0.51-5.51, 0.99-6.34) and muscle (0.26-1.48, 0.69-2.04), further support the premise that PFOS can more easily bind to serum proteins than fatty tissues. The egg to liver ratios as maternal transfer ratios were calculated for PFOS, which were in the range of 0.93 to 2.00. Furthermore, based on consumption information for fish in Beijing, the dietary intake of PFCs through fish consumption were estimated at 0.24 ng kg^{-1} d^{-1} for PFOS and 0.44 ng kg^{-1} d^{-1} for total PFC. These results indicate low health risk posed by PFCs to the residents of Beijing through consumption of fish.

ISBN 9780976885351

E. COLI BURDEN TO LAND AND DELIVERY TO WATER AT HEADWATER CATCHMENT SCALES

David M. Oliver (University of Stirling, Stirling, Scotland, UK)
Louise Heathwaite, Trevor Page, Ting Zhang, Keith Beven, Gareth McShane,
Heather Carter, Patrick O' Keenan & Philip M. Haygarth
(Lancaster University, Lancaster, England, UK)

This study reports on the accumulation of the faecal indicator bacteria (FIB) *Escherichia coli* on grazed pasture and its subsequent delivery to water following storm-driven transfers in the UK. The project developed and tested a field-based protocol for determining the dynamic burden (source loading) of *E. coli* in a small headwater catchment ($0.4 km^2$). We evaluated observations against an empirical model used to predict the temporal fluctuation in magnitude of *E. coli* burden on pasture. Water quality exported from the catchment was also monitored during ten storm events per year over a two year period in an attempt to determine the proportion of *E. coli* burden that was mobilised and delivered to the stream following rainfall. The results of our study indicated that an empirical model utilising key parameters linked to livestock excretion and FIB die-off was able to satisfactorily predict *E. coli* burden on pasture most of the time, with over 50% of sampling dates falling within the 5th and 95th percentile of predicted values. It was also evident that storm driven transfers were responsible for exporting high concentrations and loads of FIB from the catchment area. Minor storm events (e.g. relatively small changes in stream discharge) captured over the summer grazing season exported microbial concentrations from the catchment in excess of 1.2×10^5 *E. coli* per 100mL. However, one month after the removal of cattle from pasture, the concentration of cells exported during storm surges only reached levels approaching 8×10^3 *E. coli* per 100mL (2 orders of magnitude reduction in FIB concentration) despite stream discharge being approximately 7 times higher. While a first approximation of *E. coli* burden to land, this field-based protocol represents one of the first comprehensive approaches for providing a real estimate of a dynamic FIB source reservoir at the headwater catchment scale. The study also highlighted the utility of a simple dynamic empirical model for prediction of catchment-scale *E. coli* burden. Furthermore, preliminary findings are now beginning to couple temporally variable *E. coli* storm event dynamics, concentrations and loads to the antecedent *E. coli* burden on pasture to derive event-based delivery coefficients at the headwater catchment scale. Parallel work is being undertaken in two contrasting headwater catchments in the UK with differing livestock management and landscape characteristics to provide complementary datasets.

ISBN 9780976885351

CHINA'S REWARD MECHANISM FOR RECLAMATION OF SEWAGE AND REUSING OF RECLAIMED WATER

Xinxin Huang, Xinyi Xu, and Hongrui Wang (Beijing Normal University, Beijing, China)

Reclamation and utilization of sewage is an effective way to reduce the shortage of water resources and environmental stress. China is still in its infancy in this area, therefore it has great potential to develop the utilization of reclaimed water in China. This article lists out the current reward mechanisms for reclamation of sewage in nine major cities of China, which are almost administrative means. By analyzing the reward mechanisms, we know that the problems are focused on the scarcity of market means and technical support. More inducements therefore should be provided to incent the reclamation of sewage in China.

ISBN 9780976885351

QUALITY ASSESSMENT OF THE UPPER LITANI RIVER BASIN IN LEBANON

Mey Jurdi (American University of Beirut, Beirut Lebanon), Samira Korfali (Lebanese American University, Beirut, Lebanon), Mona El Rez, Nora Karahagopian and Khalil Kriedieh (American University of Beirut)

The Litani River is the largest and most important water resource in Lebanon. The river is 170 km in length with 60 km of tributaries, draining over 20% of the countries area, and totally contained within its boundaries. The implementation of watershed management and water supply schemes (irrigation and domestic) continue to be challenged by prolonged social and economical instability in the country. And, despite all invested efforts the water quality and quantity continue to be impacted by excessive exposure to pollution. As such, the study aimed at (a) updating the inventory of potential sources of pollution, (b) evaluating trends in water quality deterioration (d) reflecting on risks associated with multipurpose water usage (domestic, irrigation and recreational), and accordingly (e) proposing mitigation measures to upgrade quality and sustain the ecologic wellbeing. This is critical towards development of integrated river basin management (IRBM) to ensure the coordination, conservation, management and development of the Upper Litani River Basin.

ISBN 9780976885351

RESEARCH OF A NEW COMBINED TECHNOLOGICAL PROCESS USED FOR MICRO-POLLUTED WATER TREATMENT

Xin Da and Xu Xinyi* (Beijing Normal University, Beijing, China)
Liu Xin (Nanjing Forestry University, Nanjing, China)
Zhang Xin (Research Center for Eco-Environmental Sciences,
Chinese Academy of Sciences, Beijing, China)

A new combined technological process, which was used for micro-polluted water treatment, was developed. The bio-contact oxidation and ozone oxidation were used as the main technology. In the experiment a lake of Nanjing city was chosen as micro-polluted water source, after treatment, it was shown that CODMn、T-N、T-P、NH3-N、Color and NTU in effluent were lower than 1mg/L，0.3 mg/L、0.02 mg/L、0.01mg/L、15 and 1, respectively. all the index were reaching standards for drinking water quality（GB5749—2006）and the first class standard of surface water environment (GB38382～2002) of china. Also, the new process has advantages of auto running, easily operate and can be used in the place where there is no clear water.

ISBN 9780976885351

ASSESSING THE IMPACT OF WASTEWATER EXPENDITURES ON BACTERIAL WATER QUALITY

Roger M. Miranda* (University of Texas at Austin, Austin, TX, USA)

Evaluating the impact of tax-payer expenditures used to improve health and environmental conditions in low-income geographic areas is an important part of assessing the efficiency of these types of government programs. This article investigates the impact of US state and federal government expenditures on wastewater infrastructure in a populous border region of South Texas known as the Rio Grande Valley. The study uses a watershed approach, limiting the analysis to the geographic area encompassed by the watershed of the Arroyo Colorado, a water body that flows through the heart of the Rio Grande Valley and which is also the main receptacle of municipal wastewater in the area. The study shows that since 1999, capital expenditures in wastewater infrastructure in the Rio Grande Valley have significantly improved bacterial water quality in the Arroyo Colorado. However, water quality monitoring conducted after 2009 offers evidence of resurging bacteria levels, indicating the need to address issues associated with sustainability of sanitation efforts in this region of the US-Mexico border.

ISBN 9780976885351

ANALYSIS OF EFFECTS ON WATER QUALITY FACTORS USING DEVELOPED ALGAE BLOOMS FORECASTING MODEL

Mi Eun Kim, Young Su Jang, Ji Ye Im, Tae Seok Shon and Hyun Suk Shin*
(Pusan National University, Busan, Korea)

According to climate change all over the world, the issue on water quality management by increased water temperature and frequency of localized heavy rain in river and reservoir has been arisen in South Korea. For these reasons, automatic water quality monitoring system set up for preventing early algae blooms in five representative watersheds in South Korea. Also, Government concentrated on predicting variation of water quality factors on account of weather change and source of pollutants in the future using numerical models to manage water quality accidents. Many countries have conducted various studies about forecasting water quality by artificial neural network which has a number of advantages, as opposed to the traditional models based on methods like data driven self-adaptive methods, generalization through learning the data presented, universal functional approximators, and nonlinear for forecasting. Daecheong reservoir located in Geum river has a suitable environment for algae blooms because it has lots of contaminants that are flowed by rainfall in Daejeon and Chungcheong area. So this study selected Daecheong reservoir and used the data of the automatic water quality observation system. This model has been built to forecast the algae blooms over short periods (1 day, 3 and 7 days) using back propagation algorithm of feed forward neural networks. Also input parameters considered the hydrologic and water quality factors as following: inflow, outflow, average areal precipitation, air temperature, water temperature, dissolved oxygen (DO), total organic carbon (TOC), pH, chlorophyll-a (chl-a), total nitrogen (TN), and total phosphorous (TP) in Daecheong reservoir. And correlation analysis has been implemented to analyze lag time and components that sensitively responded to chlorophyll-a by referring the interpolated data and water quality and hydrologic factors in all. On the basis of results, after selecting input parameters for algae bloom prediction model, each case has been verified along with making various models. As a result of this study, the short term algae bloom prediction models showed minor errors in the prediction of the a day and 3 days. Components of water quality such as water temperature, pH and TOC showed the closest correlation with chlorophyll-a and the models have been built with them. Therefore, the models will be very effective to manage the water quality of Daecheong reservoir by predicting a day to seven days.

ISBN 9780976885351

THE MICROBE COMMUNITY AND DIVERSITY ON ANAMMOX BIOREACTOR

Yujie Qin and Shaoqin Zhou (College of Environmental Science and Engineering, South China University of Technology, Guangzhou, 510006 China)

ABSTRACT: Anaerobic ammonium oxidation (anammox) is a promising microbial pathway to remove ammonium from wastewater. In this paper, the anammox bacteria were successfully enriched in the UASB bioreactor, and the biosystem and its population were studied by conventional method, microtechnic and molecular biotechnology. The populations of mildew, actinomycete, yeast and bacteria were studied in the activated sludge and found that the concentration of bacteria was the highest, and the yeast and mildew were only a tiny minority. Based on 16S rRNA and phylogenetic analysis, we found four strains in the amplified DNA fragments. Three new species of anammox bacteria were found in this ecosystem.

INTRODUCTION

Anaerobic ammonium oxidation is a recently discovered nitrogen removal pathway in natural systems mediated by deep-branching members of the phylum Plancomycetes, the anammox bacteria. It was not until 1995 that the anammox process was confirmed in a fluidized bed reactor treating wastewater effluent(Mulder et al., 1995). The anammox reaction is a chemolithotrophic process in which 1 mole of ammonium is oxidized by 1 mole of nitrite to produce N_2 gas in the absence of oxygen (Strous et al., 1999).

The bacteria responsible for the anammox process reside within deep phylogenetic branches have not yet been isolated in pure culture. Molecular methods have been extensively utilized to identify the presence of anammox bacteria in environmental and wastewater samples. The first anammox bacteria, called Candidatus Brocadia anammoxidans, were enriched from bioreactor sludge of a wastewater treatment plant in The Netherlands (van de Graaf et al., 1995; Strous et al., 1998). Additional anammox bacteria have since been discovered in wastewater treatment systems: Candidatus Kuenenia stuttgartiensis (Schmid et al., 2000), Candidatus Scalindua brodae, Candidatus Scalindua wagneri (Schmid et al., 2003), Candidatus Anammoxoglobus propionicus (Kartal et al. 2007), Candidatus Brocadia fulgida (Kartal et al., 2008), and Candidatus Jettenia asiatica (Quan et al., 2008).

Microbial diversity and ecology of anammox bacteria have not yet been fully revealed due to limitations of 16S rRNA analysis. Information about the distribution, activity, and controlling factors of these anammox bacteria is still limited (Matthew et al., 2011). Herein, we cultivated the anammox bacteria from a UASB reactor because this reactor could provide high biomass concentration and a stable configuration that prevented substrate concentration shock (Buzzini et al., 2006; Jin et al., 2008). The reactor was started up for more than two years, and the removal efficiencies of ammonium and nitrite were more than 90%. We examine the population, the phylogenetic diversity of anammox and activity of anammox bacteria in the activated sludge from this UASB reactor.

MATERIALS AND METHODS

System configuration and experimental conditions: The activated sludge was collected form a UASB bioreactor. This UASB reactor contained a total volume of 3.2 dm^3, providing a reaction zone of 2.28 dm^3 and a settling zone of 0.92 dm^3 in the upside. The reaction temperature ranged from 32 to 34℃ and black cloth enclosure was used to shield the light in order to inhibit the growth of photosynthetic bacteria. The activated sludge from a landfill leachate wastewater treatment plant was inoculated the UASB reactor for start up. The volume of the inoculum was 0.75 times that of reactor. The influent was a synthetic solution

---

ISBN 9780976885351

of the following mineral composition (g/L): KH_2PO_4, 0.027; $MgSO_4{\cdot}H_2O$, 0.3; $CaCl_2$, 0.136; NaHCO3, 0.5; NH_4Cl, 0.153–0.497; and $NaNO_2$, 0.197–0.641; the microelements (g/L): EDTA, 5; $FeSO_4$, 5; $ZnSO_4{\cdot}7H_2O$, 0.43; $CuSO_4{\cdot}5H_2O$, 0.25; $MnCl_2{\cdot}4H_2O$, 0.99; $NiCl_2{\cdot}6H_2O$, 0.19; $CoCl_2{\cdot}6H_2O$, 0.24; and H_3BO_4, 0.014. $NaHCO_3$ was added to adjust the influent pH to the range of 7.5 to 7.8.

Isolation and identification of microbe: The activated sludge was taken from the reactor to study the microbe. The microbe was isolated by using the standard dilution. We used different medium to culture different kind microbe. Beef extract peptone, Potato Dextrose agar, Gause's medium，LB agar and some, and some other selective medium were used to isolation and culture the microbe of this sample from the UASB reactor. We identified the main microbe of the pure cells by the conventional methods and 16Sr RNA method.

Observing of the cluster in the sludge: The colony and cell morphology in the sludge were determined by using Ordinary optical microscope（phenix PH50-DB310U）, scanning electron microscopy (SEM, FEI-XL30，Netherlands).

DNA ectraction, PCR and 16 S rRNA sequence: 10 milliliter sludge samples for DNA extraction were collected from this UASB reactor after starting up for two years. The nucleic acids were extracted according to Logemann (1998). Amplifications of 16S rRNA from chromosomal DNA were carried out in a DNA thermal cycler model 2720 (Singapore) using two pairs of anammox primers. One primer pair is Pla46F (*Planctomyctales* primer, 3′-GGA TTA GGC ATG CAA GTC-5′) and AMX368R (the primer of all anammox organisms, 5′- CCT TTC GGG CAT TGC GAA-3′). The other pair of primers are Pla46F and AMX820R (*Candidatus* "Kuenenia stuttgartiensis" and *Candidatus* "Brocadia anammoxidans" primer, 5′- AAA ACC CCT CTA CTT AGT GCC C-3′). The two pairs of primers were designed to amplify the part of 16S rRNA genes of the anammox cluster containing 323 base pairs and 775 base pairs, respectively. The 16S rRNA Sequences obtained in this study were available from the GenBank sequence database under accession numbers.

RESULTS AND DISCUSSION

Optical and electronical microscopy analyses of sludge: The color of the sludge is different at the different stage. It is from the dark brown into the red. The sludge is dark brown at the first month starting up (Figure 1, A). After two years the color of the sludge is red (figure 1, B). The red color of anammox biomass is presumably attributed to the red Heme c-containing enxymes involved in anammox pathways, and the visual observation of the sludge color is used to roughly evaluate the performance of the anammox reactor(Li et al., 2012).

The surface of the sample from the UASB reactor is dotted many bacteria (figure 2). The microbe distribution on a granule depends on the pathway of the biodegradation they carry out. Consequently, ammonium and nitrite played an important role in establishing the predomination microorganisms. From figure 2, most of the cells were elliptical. The morphologically conspicuous bacteria had the same shape as that reported by Chamchoim (2007). The size of the cells was (0.6–0.8) μm × (0.9–1.2) μm.

The population of the microbe in the sample: The anammox bacteria were co-existence with other microbe in this ecosystem. Seven bacteria strains were purified by conventional methods, which are *Pseudomonas* sp., *Clostridium beijerinckii*, *Bacillus cereu*, two kinds of *Bacillus* sp., *Sphingosinicella microcystinivorans* and unidentified species; therefore *Pseudomonas* sp.(accession No. EU 301690) was the dominant bacteria of the seven stains. There were some mould, such as *Penicillium* sp., *Aspergillus* sp., *Cladosporium* sp. and so on.There were also some Actinomyces, which were *Micromonospora* sp. *Nocardia* sp., and some others. The concentration of most microbe was very low. From the three kinds microbe, the concentration of bacteria was the highest, and the yeast and mildew were only a tiny minority.

The species of purified bacteria in the anammox sludge: Seven strains were purified by conventional methods. Their numbers are fromE1 to E7. The seven species could grow under limited-oxygen and anaerobic condition. Based on the morphological, physiological, biochemical and 16Sr RNA analysis, these bacteria belonged to. The concentration of these bacteria was very low, except that E1 had a high concentration which was more than 10^7cell/ml; therefore E1 was one of dominant bacteria in the ecosystem. They might play an important role in the anammox reaction. The accession No. of E1 is EU 301690.

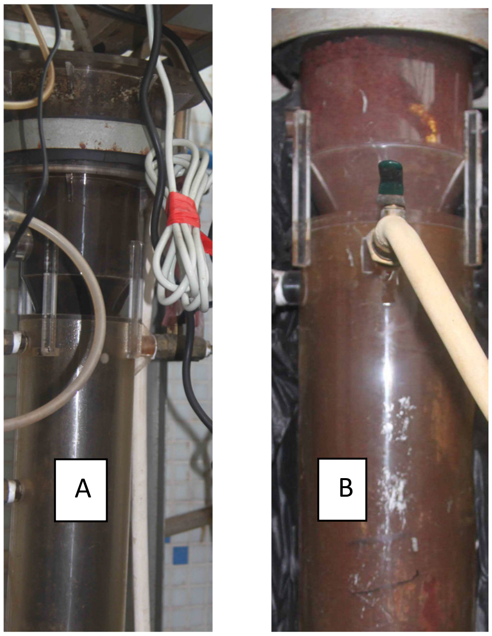

FIGURE 1. The color of the sludge in the UASB bioreactor. A. Starting up for one moth. B. Starting up for two years.

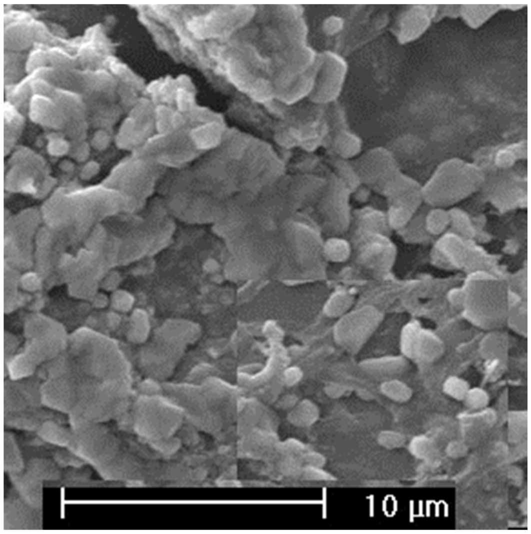

FIGURE2. Micrographs of biomass aggregate from anammox enrichment cultures.

Identification and phyligenetic analysis: The use of Pla46F and AMX368R primers resulted in a PCR product of the expected size and this was used to construct a clone library. Obtained sequences were aligned with anammox bacteria as present in GenBank and a phyligenetic tree was calculated. Based on the phylogenetic tree and the sequences of the clones (figure 3), we found that the anammox bacteria in the UASB reactor were to some extent related to the known anammox bacteria. Only one kind of anammox bacteria (CloneA238) was found before, and the other three (CloneA240, CloneA125 and CloneA224) were new species which had not been reported before. One ecosystem has one genus of dominant anammox bacterium. The biodiversity of anammox bacteria was not high.

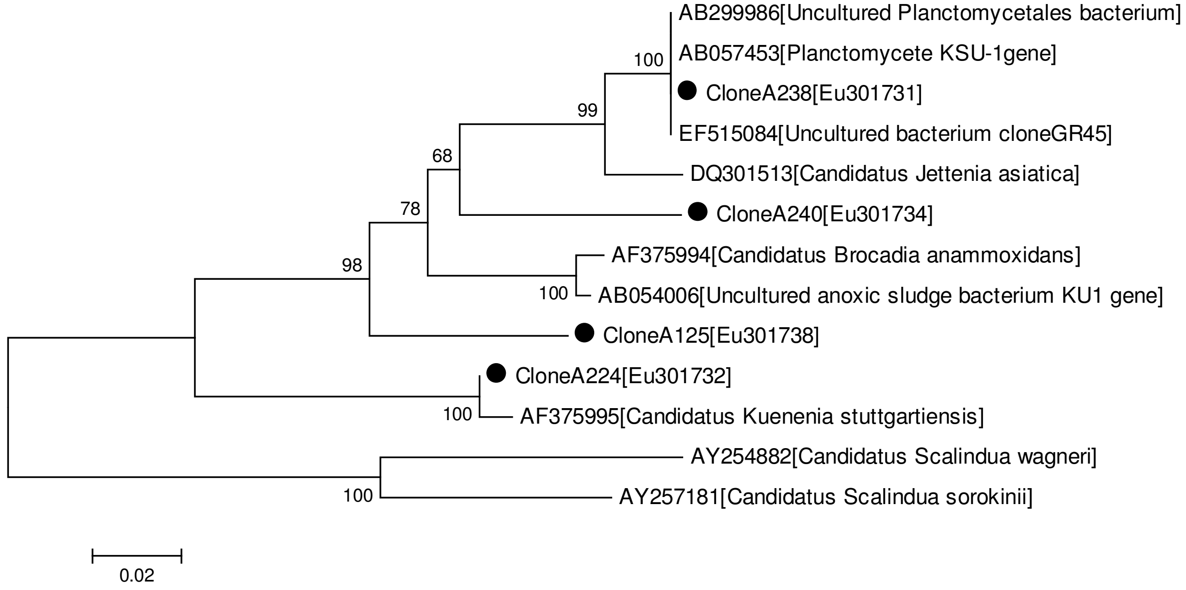

FIGURE3. Phylogenetic tree of the 16S rRNA sequences from clone libraries.
The bar below indicates the genetic distance between sequences

CONCLUSIONS

Anammox bacteria were successfully enriched in a UASB reactor. The removal efficiencies of NH_4^+–N and NO_2^-–N were both more than 90%. Different ecosystem has different population. From the anammox sludge, seven species of bacteria were isolated and purified by conventional methods. There are also some mould and Actinomyces in this sample.

The morphologically conspicuous bacteria were observed on micrographs. We cannot be certain that their key function is the anammox process, because there are no pure cells. This species adapts itself to dark, anaerobic and inorganic conditions, and we can conclude it represents chemoautotrophic bacteria. The shape of morphologically conspicuous cells allows us to compare this species with bacteria used in conventional treatment methods. We used two pairs of primes to clone anammox bacteria, and three new kinds of anammox species were found.

ACKNOWLEDGEMENTS

Support for this research by the Natural Science Foundation of Guangdong Province, K. C. Wong Education Foundation, the Fundamental Research Funds for the Central Universities and the State Key Laboratory of Subtropical Building Science is gratefully acknowledged.

REFERENCES

Buzzini A.P., I.K.Sakamoto, M.B.Varesche, and E.C.Pires. 2006. "Evaluation of the microbial diversity in an UASB reactor treating wastewater from an unbleached pulp plant". *Process Biochemistry*, 41(1):168-176.

Chamchoin N., and S. Nitisoravut. 2007. "Anammox enrichment from different conventional sludges". *Chemosphere*, 66(1):2225-2232

Hirsch M. D., Z. T. Long and B. Song. 2011. "Anammox Bacterial Diversity in Various Aquatic Ecosystems Based on the Detection of Hydrazine Oxidase Genes (hzoA/hzoB)". *Microbial Ecology*, 61(2):264-276.

Jin, R.C., B.L. Hu, P. Zheng, M. Qaisar, A.H. Hu and E. Islam. 2008. "Quantitative comparison of stability of ANAMMOX process in different reactor configurations". *Bioresource Technolog*, 99(6): 1603-1609.

Kartal B, L., van Niftrik, J. Rattray, J. L. C. M. van de Vossenberg, M. C. Schmid, J. S. Damsté, M. S. M. Jetten and M. Strous. 2008. "Candidatus 'Brocadia fulgida': an autofluorescent anaerobic ammonium oxidizing bacterium". *FEMS Microbiology Ecology*, 63(1):46-55.

Kartal, B., J. Rattray, L. A. van Niftrik, J. van de Vossenberg, M. C. Schmid, R. I. Webb, S. Shouten, J. A. Fuerst, J. Sinninghe Damsté, M. S. M. Jetten and M. Strous. 2007. "Candidatus "Anammoxoglobus propionicus"a new propionate oxidizing species of anaerobic ammonium oxidizing bacteria". *Systematic and Applied Microbiology*, 30(1):39-49.

Li H., S. Zhou, W. Ma, G. Huang, and B. Xu. 2012. "Fast start-up of ANAMMOX reactor: Operation strategy and some characteristics as indicators of reactor performance". *Desalination*, 286: 436-441.

Mulder A., A. A.van de Draaf, L. A.Robertson, and J.G. Kuenen. 1995. "Anaerobic ammonium oxidation discovered in a denitrifying fluidized bed reactor". *FEMS Microbiology Ecology* , 16(3): 177-183.

Quan Z. X., S. K. Rhee, J. E. Zuo, Y. Yang, J. W. Bae, J. R. Park, S. T. Lee, Y. H. Park. 2008. "Diversity of ammonium-oxidizing bacteria in a granular sludge anaerobic ammonium-oxidizing (anammox) reactor". *Environmental Microbiology*, 10(11):3130-3139.

Schmid M. C., K. Walsh, R. Webb, W. I. Rijpstra, K. van de Pas-Schoonen, M. J. Verbruggen, T. Hill, B. Moffett, J. Fuerst, S. Schouten, J. S. Damsté, J. Harris, P. Shaw, M. S. M. Jetten, and M. Strous. 2003. "Candidatus "Scalindua brodae", sp. nov., Candidatus "Scalindua wagneri", sp. nov., two new species of anaerobic ammonium oxidizing bacteria". *Systematic and Applied Microbiology*, 26(4):529-538.

Schmid M. C., U. Twachtmann, M. Klein, M. Strous, S. Juretschko, M. S. M. Jetten, J. W. Metzger, K. H. Schleifer, and M. Wagner. 2000. "Molecular evidence for genus level diversity of bacteria capable of catalyzing anaerobic ammonium oxidation". *Systematic and Applied Microbiology*, 23(1):93-106

Strous M., J. J. Heijen, J. G. Kuenen, and M. S. M. Jetten. 1998. "The sequencing batch reactor as a powerful tool for the study of slowly growing anaerobic ammonium-oxidizing microorganisms". *Applied Microbiology and Biotechnology*, 50(5):589–596.

Strous, M., J. A. Fuerst, E. H. Kramer, S. Logemann, G. Muyzer, K. T. van de. 152. Pas-Schoonen, R. Webb, J. G. Kuenen, and M. S. Jetten. 1999. "Missing lithotroph identified as new Planctomycete". *Nature*, 400(6743): 446-449.

Van de Graaf, A. A., A. Mulder, P. De Bruijn, M. S. M. Jetten, L. A. Robertson, and J. G. Kuenen. 1995. "Anaerobic oxidation of ammonium is a biologically mediated process". *Applied and Environmental Microbiology*, 61(4):1246-1251.

Logemann S., J. Schantl, S. Bijvank, M. van Loosdrecht, J. G. Kuenen, and M. Jetten. 1998. "Molecular microbial diversity in a nitrifying reactor system without sludge retention". *FEMS Microbiological Ecology*, 27(3): 239-249.

THE EFFECTS OF SILVER IONS ON ENHANCED BIOLOGICAL PHOSPHOROUS REMOVAL

Hong Chen and Yinguang Chen
(Tongji University, Shanghai, China)

ABSTRACT: With wide applications of silver ions (Ag^+), the toxicity on model organism and human health has been reported. However, their potential impacts on wastewater enhanced biological phosphorus removal (EBPR) have seldom been studied although the release to wastewater treatment plants has been detected. In this paper the effects of Ag^+ (0-5 mg/L) on EBPR were investigated. The phosphorus removal efficiency decreased to 48.8% at Ag^+ of 1 mg/L, and no net phosphorus was removed at Ag^+ greater than 2 mg/L. The mechanism study showed that the uptake of wastewater carbon source and the anaerobic and aerobic transformations of phosphorus, polyhydoxyalkanoates and glycogen were inhibited by Ag^+. Further investigation showed that Ag^+ caused the inhibitions on the activities of adenylate kinase(ADK) and expolyphosphatasep(PPX), which responded to the decreasing of phosphorus release, while the decreased phosphorus uptake was due to the generation of energy for phosphorus uptake being suppressed. Cell membrane integrity assay showed that the presence of 0-5mg/L Ag^+ did not lead to cell leakage and membrane damage.

INTRODUCTION

It is well known that silver ion (Ag^+) has always been used as an effective antimicrobial agent since ancient time. Ag^+ in the form of silver nitrate solution is the prototypical antimicrobial silver species. The biocidal effect of Ag^+ with its broad spectrum of activity including bacterial, fungal and viral agents, can be achieved at low concentration, and Ag^+ is currently used to control bacterial growth in a variety of applications, such as dental work, catheters and burn wound. (Crabtree et al., 2003) Their toxicity has been concerned by researchers for its wide applications. Ag^+ showed adverse effect on zooplankton, invertebrates and fish, and could change the cell membrane of bacteria and interact with ribosome and inhibited the expression of enzymes and proteins responsible for ATP production, which led to the death of cell. (Koo et al., 2008; Yamanaka et al., 2005)

The release of Ag^+ from the sources to the environment and finally entering wastewater treatment plants (WWTPs) have been reported in literatures. (Shafer et al., 1998) The report of the United States Environmental Protection Agency (EPA) indicated that Ag appeared in all of the sewage sludge samples, with the concentration ranging from 1.94 to 856 mg/kg (on a dry weight basis). In WWTPs, phosphorus can usually be removed from municipal wastewater by enhanced biological phosphorus removal (EBPR) method, which is characterized by circulation of activated sludge between anaerobic and aerobic conditions.(Oehmen et al., 2007) In general, microorganisms responsible for EBPR, *i.e.* polyphosphorus accumulating organisms (PAOs), are capable of storing organic compounds, such as short chain fatty acids (SCFA) as internal storage compounds (polyhydoxyalkanoates [PHA]) by utilizing energy and reduction equivalents mainly generated from the degradation of polyphosphate and glycogen, respectively, under anaerobic conditions. The phosphorus is therefore anaerobically released. Under subsequent aerobic conditions, PAOs use the stored PHA to produce energy for cell growth and maintenance as well

---

ISBN 9780976885351

as soluble orthophosphorus (SOP) uptake from bulk liquid to build up polyphosphorus. The net phosphorus removal can be achieved by wasting excess sludge with high phosphorus content because the aerobic phosphorus uptake is greater than the anaerobic phosphorus release. However, the effect of Ag^+ on enhanced biological phosphorus removal from wastewater has never been investigated in the literature.

The objective of this paper was to investigate the influences of Ag^+ on EBPR and to explore the mechanisms. The concentration of Ag^+ investigated in this study was in the range of 0-5 mg/L because it seemed impossible to have a higher concentration of silver in wastewater treatment plants.

MATERIAL AND METHODS

Determination of Activities of Adenylate Kinase (ADK), Exopolyphosphatase (PPX) and Polyphosphate Kinase (PPK) Aliquots of activated sludge were washed for 3 times with 1.5 M NaCl buffer (containing 0.01 M EDTA and 1mM NaF, pH 7.4).(McGrath and Quinn, 2000). Then, the resuspended pellets were sonicated at 20 kHz and 4 ^{o}C for 5 min to break down the cell structure of bacteria in activated sludge. The debris was centrifuged at 12000 g and 4 ^{o}C for 10 min and the crude extracts in supernatant were obtained for the enzyme activity measurement. All enzymes activities were based on protein content, which was determined by the method of Lowry et al. with bovine serum albumin as the standard. The methods of determination of ADK, PPX and PPK were according to the literatures. (van Groenestijn et al., 1989; Lee et al., 2006)

Cell Membrane Integrity Assay The cell membrane integrity of activated sludge was assayed by measuring the lactate dehydrogenase (LDH) release.(Wolterbeek and van deer Meer, 2005) The LDH release was determined by a cytotoxicity detection kit (Roche Applied Science) according to the manufacturer's instruction. At the end of the experiments, the aliquots were centrifuged at 12000 g for 5 min and then the supernatant was seeded on a 96-well plate, followed by the addition of 50 uL of substrate mixture (Roche Applied Science). After incubation at room temperature for 30 min in dark, 50 uL of stop solution (Roche Applied Science) was added to each well and the absorbance was recorded at 490 nm using a microplate reader (BioTek, USA).

Bacterial Viability Assay The numbers of bacteria with intact and damaged membranes in the presence of different concentrations of Ag^+ were determined by using a LIVE/DEAD Baclight bacterial viability kit (Molecular Probes, Invitrogen) and the microplate reader (BioTek, USA) according to the literature with modification. (Hu et al., 2003)

Other Analytical Methods The analyses of SOP, mixed liquid suspended solids (MLSS) and mixed liquid volatile suspended solids (MLVSS) were conducted according to Standard Methods. Protein, glycogen, acetic acid, PHA (including polyhydroxybutyrate (PHB), ployhydroxyvalerate (PHV) and polyhydroxy-2-methylvalerate (PH2MV)) were assayed according to our publication.

Statistical Analysis All tests were performed in triplicate and the results were expressed as mean ± standard deviation. An analysis of variance (ANOVA) was used to test the significance of results and $p<0.05$ was considered to be statistically significant.

RESULTS AND DICUSSION

The Effect of Ag^+ on the Net Removal of Soluble Ortho-phosphorus Compared to the control, the removal efficiency was decreased slightly from 99.7% to 97.3% at Ag^+ concentration of 0.5 mg/L, which was further decreased to 48.8% as Ag^+ was increased to 1 mg/L. There was no net phosphorus removal observed when the concentrations of Ag^+ were 2 and 5 mg/L. At the condition of Ag^+ concentration less than 0.5 mg/L, the phosphorus removal, anaerobic release and aerobic uptake were almost the same as those in the control. From the variations of SOP concentration during one cycle (Figure 1), the anaerobic and aerobic SOP transformations can be calculated. When a 0.5 mg/L of Ag^+ was in the reactor the anaerobic and aerobic SOP transformations, compared to the control, were decreased respectively from 85.3 and 100.3 mg/L to 82.7 and 97.3 mg/L, which were further decreased with the increase of Ag^+. It was noted that at Ag^+ concentrations of 2 and 5 mg/L, the amount of SOP uptake was lower than the corresponding SOP release, which resulted in no net SOP removals under these two conditions. Apparently, the presence of Ag^+ inhibited the SOP release and uptake, and the activated sludge process lost the EBPR performance at Ag^+ concentration greater than 2 mg/L. The reasons for Ag^+ showing different influence on SOP release and uptake were explored next.

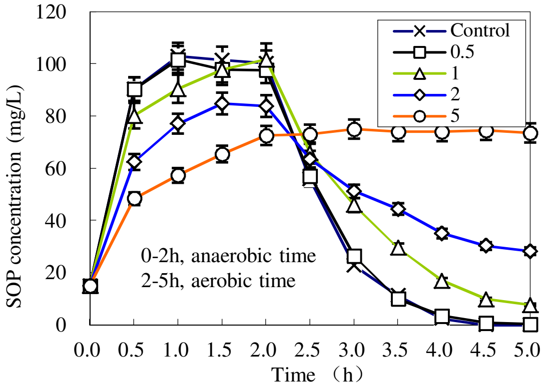

FIGURE 1. Effects of Ag^+ on the variations of SOP concentration during one anaerobic and aerobic cycle. Error bars represent standard deviations of triplicate tests.

As shown in Figure 2, with the increase of anaerobic time the concentrations of acetic acid in all reactors were decreased, which suggested that acetic acid was taken up under anaerobic conditions. The data also showed that although the uptake of acetic acid was not influenced by the presence of 0.5 mg/L of Ag^+, it was inhibited when the concentration of Ag^+ was 1 mg/L, and the inhibition was increased with the increase of Ag^+. All acetic acid was taken up within 1 h at Ag^+ concentrations less than 1mg/L, but there were still 19.5 and 51.0 mg/L of acetic acid left by the end of anaerobic time when Ag^+ concentrations were 2 and 5 mg/L, respectively. Obviously, with the increase of Ag^+, the acetic acid uptake was decreased. One possible reason was that acetic acid uptake required energy, which came mainly from polyphosphorus degradation (with the observation of phosphorus release), and the data in Figure 1 had indicated that the phosphorus release was decreased with Ag^+.

The influences of Ag^+ on the variations and transformations of PHA and glycogen in the anaerobic and aerobic time in reactors are shown in Table 1. The transformations of PHA and glycogen at Ag^+ concentration of 0.5 mg/L were almost the same as the control, but they were decreased linearly with the increase of Ag^+ from 0.5 to 5 mg/L. Acetic acid was the substrate of PHA synthesis, and the above study had indicated that the utilization of acetic acid was inhibited by Ag^+. PHA synthesis requires reducing equivalents, which is provided mainly by glycogen degradation. Thus the transformation of glycogen was decreased as PHA transformation was inhibited by Ag^+.

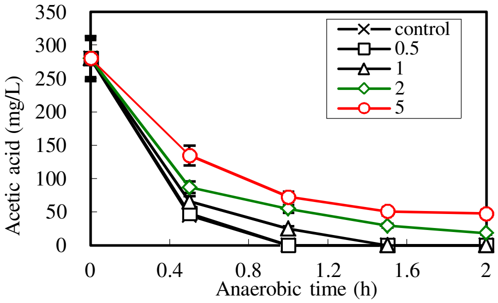

FIGURE 2. The effects of Ag^+ on the changes of acetic acid concentration in the anaerobic stage. Error bars represent standard deviations of triplicate tests.

Effect of Ag^+ on the Activity of Key Enzymes Involved in EBPR ADK, PPX, PPK are the key enzymes related to enhanced biological phosphorus removal. ADK and PPX are responsible for anaerobic phosphorus release, and the aerobic phosphorus uptake is relevant to the activity of PPK. As shown in Table 3 with the increase of Ag^+ concentration from 0.5 to 5 mg/L, both ADK and PPX were decreased. All these observations were in correspondence with the above observed anaerobic SOP transformation reported in Figure 1. It can also be seen from Table 2 that the activity of PPK remained relatively stable when the concentration of Ag^+ varied between 0-5 mg/L ($P>0.05$). It indicated that the aerobic SOP uptake should not be affected by Ag^+, which was in contradiction with the observation made in Figure 1. One possible explanation was that the SOP aerobic uptake required energy, which was generated mainly from PHA degradation, and the degradation of PHA had been proven in the above discussion to be negatively influenced by Ag^+ (Table 1). It seems that in the aerobic stage of EBPR the influence of Ag^+ on phosphorus uptake was mostly attributed to its inhibitory effect on the generation of energy other than phosphorus uptake enzyme (PPK).

TABLE 1. Effect of Ag^+ on the Anaerobic and Aerobic Transformations of PHA and Glycogen [a, b]

	Ag^+ Concentration (mg/L)			
	0.5	1	2	5
An (Ae) PHA[c]	2.51±0.21 (2.46±0.23)	2.52±0.23 (2.31±0.23)	2.36±0.24 (1.66±0.16)	1.86±0.18 (0.85±0.10)
An (Ae) glycogen	2.25±0.19 (2.36±0.09)	2.23±0.10 (2.26±0.11)	2.06±0.15 (1.71±0.22)	1.79±0.16 (1.06±0.15)

[a] The data (unit mmolC/g VSS) are the averages and their standard deviations of three different measurements.

[b] In the control the transformations of anaerobic (aerobic) PHA and anaerobic (aerobic) glycogen were 2.55 ± 0.25 (2.53 ± 0.23), and 2.27 ± 0.14 (2.41 ± 0.11) mmol C/gVSS, respectively.

[c] An: anaerobic; Ae: Aerobic.

TABLE 2. Effects of Ag^+ on the Activities of Key Enzymes Involved in EBPR [a]

	Ag⁺ concentration (mg/L)				
	0	0.5	1	2	5
ADK[b]	7.57±0.40	7.41±0.34	6.89±0.20	6.57±0.35	6.32±0.42
PPX[c]	0.09±0.01	0.09±0.01	0.05±0.01	0.04±0.01	0.02±0.01
PPK[b]	0.29±0.02	0.27±0.02	0.29±0.02	0.30±0.02	0.30±0.03

[a] The data reported are the averages and their standard deviations in triplicate tests.

[b] The unit is umol NADPH/(min·mg protein).

[c] The unit is umol *p*-nitrophenol/(min·mg protein).

In the literature cell leakage can be described by the measurement of LDH release. In this study the effects of Ag^+ on LDH release were shown in Figure 3. The statistical analysis indicated that the presence of 0-5 mg/L of Ag^+ did not significantly change the LDH release ($P>0.05$). Apparently, cell leakage did not occur in this study. Moreover, the data of live/dead assay (Figure 3), which was reported to predict cell membrane integrity, demonstrated that there was no membrane damage happened since the presence of 0-5 mg/L of Ag^+ did not significantly change the ratio of live/dead ($P>0.05$).

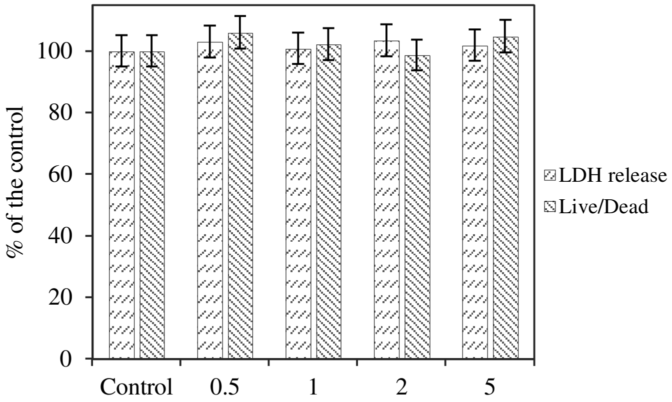

FIGURE 3. Effects of Ag^+ on LDH release and Live/Dead. Error bars represent standard deviations of triplicate tests.

CONCLUSIONS

The above studies indicated significant inhibitions occurred with the increasing concentration of Ag^+, and no net phosphorus was removed at Ag^+ greater than 2 mg/L. Further mechanism investigation showed the uptake of wastewater carbon source and the anaerobic and aerobic transformations of phosphorus, polyhydoxyalkanoates and glycogen were inhibited by Ag^+. However, the decreasing aerobic phosphorus uptake was mainly related to the restrained generation of energy provided by PHA degradation. However, the presence of 0-5 mg/L Ag^+, did not lead to cell leakage and membrane damage.

ACKNOWLEDGEMENTS

This work was financially supported by the Foundation of State Key Laboratory of Pollution Control and Resource Reuse (PCRRK).

REFERENCES

Crabtree, J. H.; Burchette, R. J.; Siddiqi, R. A.; Huen, L. L.; Hadnott, L. L.; Fishman, A. 2003. "Efficacy of silver-ion implanted catheters in reducing peritoneal dialysis-related infections." *Perit. Dial. Int.*, 23 (4): 368-374.

Hu, Z.; Chandran, K.; Grasso, D.; Smets, B. F. 2003. "Impact of metal sorption and internalization on nitrification inhibition." *Environ. Sci. Technol.*, 37 (4): 728-734.

Koo, H. C.; Jung, W. K.; Kim, K. W.; Shin, S.; Kim, S. H.; Park, Y. H. 2008. "Antibacterial activity and mechanism of action of the silver ion in Staphylococcus aureus and Escherichia coli." *Appl. Environ. Microbiol.*, 74 (7):2171-2178.

Jiang, Y. M; Chen, Y. G.; Zheng, X. 2009. "Efficient polyhydroxyalkanoates production from a waste-activated sludge alkaline fermentation liquid by activated sludge submitted to the aerobic feeding and discharge process." *Environ. Sci. Technol.*, 43 (20): 7734-7741.

Lee, S. J.; Lee, Y. S.; Lee, Y. C.; Choi, Y. L. 2006 "Molecular characterization of polyphosphate (polyP) operon from Serratia marcescens." *J. Basic. Microbiol.* 46 (2), 108-115.

McGrath, J. W.; Quinn, J. P. 2000. "Intracellular accumulation of polyphosphate by the yeast Candida humicola G-1 in response to acid pH." *Appl. Environ. Microbiol.*, 66 (9): 4068-4073.

Oehmen, A.; Lemos, P. C.; Carvalho, G.; Yuan, Z. G.; Keller, J.; Blackall, L. L.; Reis, M. A. M. 2007. "Advances in enhanced biological phosphorus removal: From micro to macro scale." *Water Res.*, 41 (11): 2271-2300.

Shafer, M. M.; Overdier, J. T.; Armstong, D. E. 1998. "Removal, partitioning, and fate of silver and other metals in wastewater treatment plants and effluent-receiving streams." *Environ. Toxicol. Chem.*, 17 (4): 630-641.

van Groenestijn, J. W. B., M. M.; Deinema, Zehnder,A. J. 1989. "Polyphosphate-degrading enzymes in acinetobacter spp. and activated sludge." *Appl. Environ. Microbiol.*, 55 (1): 219-223.

Wolterbeek, H. T., and van deer Meer, J.G.M. 2005. "Optimization, application, and interpretation of lactate dehydrogenase meaurements in microwell determination of cell number and toxicity." *Assay Drug Dev. Technol.*, 3 (6): 675-682.

Yamanaka, M.; Hara, K.; Kudo, J. 2005. "Bactericidal actions of a silver ion solution on Escherichia coli, studied by energy-filtering transmission electron microscopy and proteomic analysis." *Appl. Environ. Microbiol.*, 71 (11): 7589-7593.

PHOSPHORUS REMOVAL AND RECOVERY FROM WASTEWATER BY AN ELECTROCHEMICAL PROCESS

Hiroaki Yoshino and Yutaka Sakakibara
(Waseda University, Tokyo, Japan)

ABSTRACT: The possibility of removing and recovering phosphate from wastewater by an electrochemical process in a multi-electrode system was investigated experimentally and theoretically. In the process, electrodes were immersed in an electrolytic reactor treating synthetic wastewater and direct current (DC) was applied to crystallize phosphate on the surface of cathodes. Batch experimental results demonstrated that phosphate was removed by an application of electric currents, and at the same time, a crystalline substance, hydroxyapatite was produced on the surface of the cathodes and then settled down to the bottom of reactor. This phosphate removal with crystalline production increased with increasing electric currents, and was verified in continuous experiments. In addition, a simplified kinetic analysis was conducted to estimate pH profiles near working cathodes, demonstrating that the constituents were supersaturated for the formation of hydroxyapatite. From these results, we concluded that the proposed electrochemical process would be a feasible alternative to conventional advanced treatment processes distributed small-scale wastewater treatment and resource-recycling systems.

INTRODUCTION

Phosphorus compound is a causative substance of eutrophication, which links to the generation of blue-green algae and discolored water. Especially in closed water body, this problem has been observed worldwide. On the other hand, phosphorus compound is one of the most valuable resources as fertilizer. Though phosphate rock can be produced in some countries, such as U.S.A, China and Morocco, its depletion problem is of great concern (Kato et al., 2007). Furthermore, the amount of phosphorus compounds in municipal wastewater and animal waste was estimated to be roughly about 30 million ton-P/year, which is nearly equal to the annual production of phosphorous ores (Nakajima et al., 1998). Therefore, the development of a new treatment process which can achieve removal recovery of phosphorus compound will be important.

There are two treatment processes to recover phosphorus compounds as highly-pure crystal, i.e. hydroxyapatite (HAP) crystallization and struvite (MAP) crystallization methods. In addition, an electrolytic crystallization process was studied by Tanaka et al. (2009). It was reported that the formation of HAP in the cathode and that the material appropriate for the electrolysis was platinum coated on titanium.

In this study, an electrochemical process for removing and recovering phosphate from wastewater was proposed and the treatment performance was studied experimentally and theoretically. To increase the treatment efficiency, a multi-electrode system (Sakakiabra and Nakajima, 2001) was used in batch and continuous experiments.

MATERIALS AND METHODS

Figure 1 illustrates an experimental apparatus used in this study. This apparatus whose housing was made from acrylic plates was composed by one anode and porous platinum cathodes. The surface area of the electrode was about 114 cm^2 per piece, and the distance between the anode and the cathodes was set at 3.5 cm. In the anode compartment, glass beads were filled up. The volume of the anode and cathode

---

ISBN 9780976885351

compartments were 82 ml and 518 ml, respectively. A synthetic wastewater was prepared with KH_2PO_4 and $CaCl_2$, and the ratio of Ca/P was 1.67. In the continuous experiment, HRT was fixed at 3.0 hours.

During the experiments, constant electric currents (or current densities) were applied and the measurements were made for phosphate concentrations, dissolved oxygen, and pH at bulk liquid versus elapsed time. The applied-electric currents were in the range of 5 to 20 mA.

All liquid samples were filtrated with a membrane filter (Advantec CS045AN, pore diameter=0.45 μm). Phosphate concentration was measured using the spectrophotometer (Shimadzu UV-160A). Analysis of crystalline deposits was conducted using X-ray diffraction (XRD) analyzer (Rigaku RINT-UltimaШ).

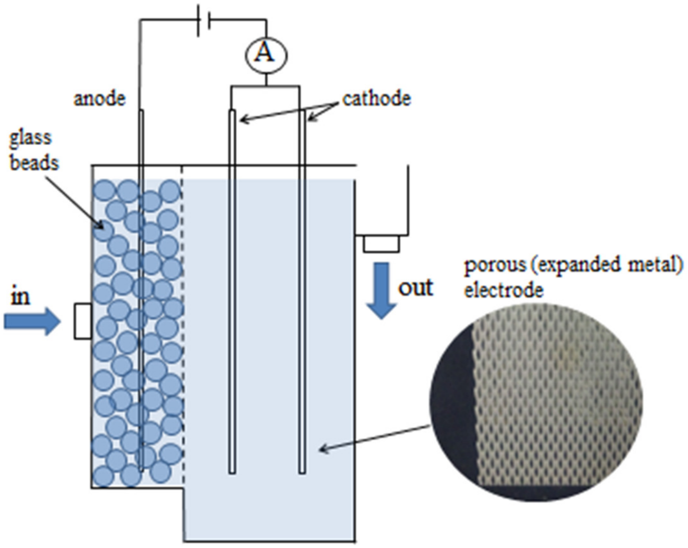

FIGURE 1 Schematic diagram of experimental apparatus

Reaction (1) shows HAP (hydroxyapatite) formation. In general, it is formed by adding $CaCl_2$ and $Ca(OH)_2$ as pH adjuster to the reactor where pH is controlled in the alkaline condition. In HAP formation, seed crystal which can be the core of crystallization and facilitated the crystalline growth is essential in the reactor. As a seed crystal, calcium silicate, phosphate rock, or bone black has been studied. In this study, no seed crystal was used in experiments.

Equation (2) shows the solubility product (K_{sp}) of HAP. From this equation, calculation was made to estimate pH above electrodes surface.

$$5Ca^{2+} + 3PO_4^{3-} + OH^- \rightarrow Ca_5(PO_4)_3(OH) \quad (1)$$

$$[Ca^{2+}][PO_4^{3-}][OH^-] = 10^{-55.9} \quad (2)$$

RESULTS AND DISCUSSION

Phosphorus Removal and Recovery: Figure 2 shows concentration changes of phosphate and dissolved oxygen (DO) versus elapsed time at different electric current conditions. Phosphate and DO concentrations decreased with time at higher rate when applying higher current. Equations (3) and (4) show the reaction of water electrolysis. In cathode compartment, by the electrolysis of water and consumption of DO, hydroxide ion was produced and observed pH increased from 4.5 to 6.0 or 6.5. During the experiment, although deposits were observed on the surface of cathodes, the amount of the deposits was too small to analyze using X-ray diffraction (XRD).

$$2H_2O \rightarrow O_2 + 4H^+ + 4e^- \qquad (3)$$

$$2H_2O + 2e^- \rightarrow H_2 + 2OH^- \qquad (4)$$

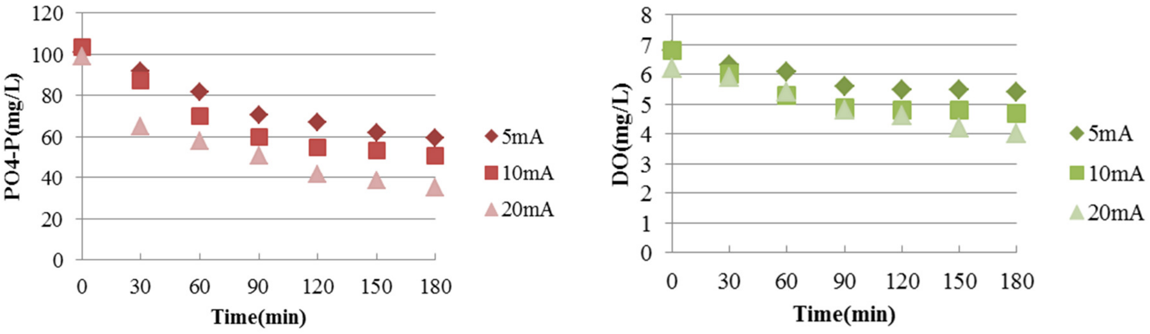

FIGURE 2 Time course changes in phosphate concentration and DO

PHOTOGRAGH 1 The condition on the surface of the cathode

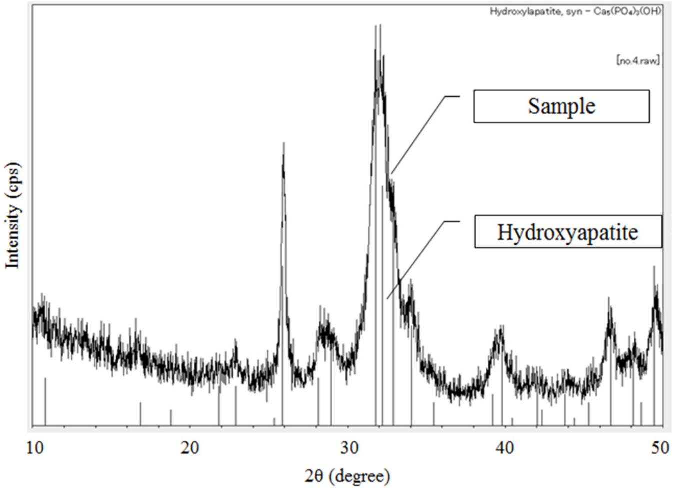

FIGURE 3 The result of X-ray diffraction analysis

Photogragh 1 is a picture inside the cathode compartment in the continuous experiment. Crystalline substance was produced on the surface of cathodes and then settled down to the bottom of reactor.

Deposits at the bottom of the reactor were recovered, and were analyzed after drying. Figure 3 shows the result of XRD analysis, demonstrating that peaks of the deposits corresponded to those of hydroxyapatite. From this result, it was found that the crystalline substance was composed mainly of hydroxyapatite.

pH Profiles on the Surface of Electrodes: Figure 4 illustrates a profile of hydroxyl ion (OH^-). Flux of OH^- is governed by Fick's law of diffusion and is expressed by,

$$J = -D\left.\frac{\partial C}{\partial x}\right|_{x=0} \tag{5}$$

where J is the flux of hydroxyl ions (mol/cm^2/sec), D is the diffusion coefficient (cm^2/sec), C is the concentration (mol/l), x is the distance from the electrode surface (cm), respectively. Assuming most electrons are transferred by OH^-, J is also expressed by J=i/F, where i is the current density (C/cm^2/s), and F is the Faraday constant (=96500 C/mol). That is,

$$J_{OH^-} = \frac{i}{F} = D_{OH^-}\frac{([OH^-]^* - [OH^-])}{\delta} \tag{6}$$

where D_{OH^-} is the diffusion coefficient of hydroxide ion (=5.3x10^{-5} cm^2/sec), $[OH^-]^*$ is the hydroxide ion concentration at the surface of cathode, $[OH^-]$ is the concentration at bulk liquid, and δ is the thickness of liquid layer, respectively. So, pH on the surface of cathodes (pH*) can be expressed by

$$pH^* = -\log_{10}\left(\frac{K_w}{\frac{i}{F}\times\frac{\delta}{D_{OH^-}} + [OH^-]}\right) \tag{7}$$

where K_w is the ion product of water.

Figure 5 shows calculated results for pH profiles on the surface of the cathode, where pH of bulk liquid was assumed at 3.5 or 6.5. Liquid film thicknesses were set in the range of 10 to 1,000 µm. From these calculations, even if pH at bulk liquid was acidic, alkaline conditions (pH = 8.6 to 11.2) were created on the surface of cathode when electric current density was larger than 0.02 mA/cm^2. That is, appropriate zones for crystallization of hydroxyapatite could be produced by an application of electric current.

Consideration on Crystallization: By Eq. (2) and referring former study (Murata., 1992), solubility curve (solid line) and super solubility curve (dotted line) were shown in Fig. 6 under different PO_4-P and pH conditions. Based on calculated pHs and phosphate concentrations in experiments, conditions on electrode surface in this study were estimated and plotted in Fig. 6. Calcium ion concentration was set at 216 mg/l.

It is generally known that there were three zones, stable zone (ionic condition), metastable zone, and unstable zone. In metastable zone, crystals could be produced only with some sort of catalysts (seed crystals), and in unstable zone, microscopic crystals could be produced rapidly. Comparing these zone and present study, it was found operation conditions in this study were in the unstable zone. Therefore, it was thought that after microscopic crystals of HAP were formed on the surface of the electrode, they could grow-up with time and settle down to the bottom.

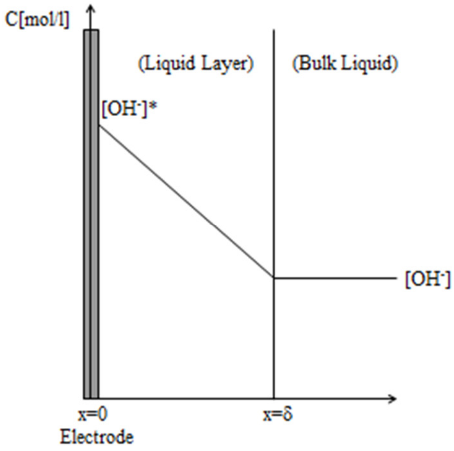

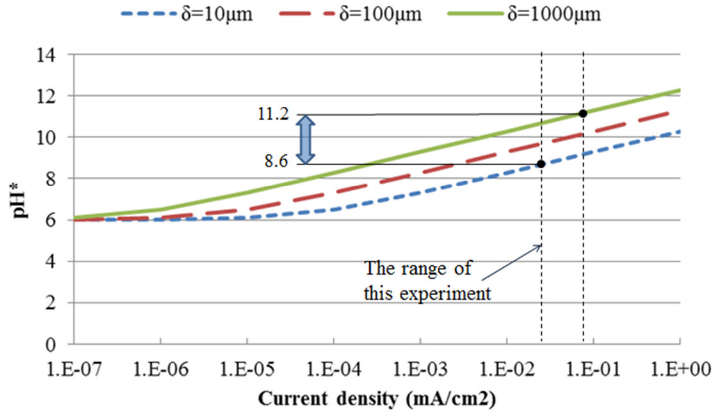

FIGURE 4 Illustration of the mass transfer boundary layer

FIGURE 5 pH profiles of the electrode surface

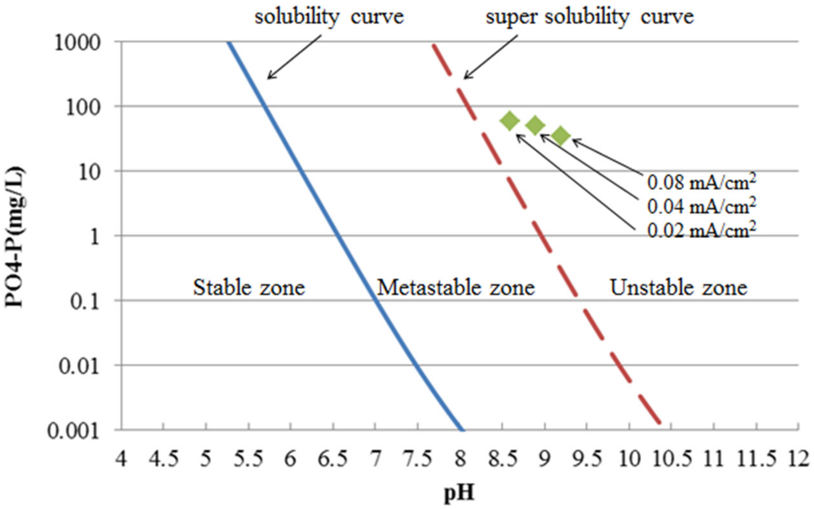

FIGURE 6 Estimation of the condition on the cathode surface (Ca^{2+}=216 mg/l)

CONCLUSIONS

The possibility of removing and recovering phosphate from wastewater by electrochemical process was demonstrated. By applying electric currents ranging from 0.02 to 0.08 mA/cm^2, phosphate was crystallized on the surface of the cathode. The removal amount was increased with increasing electric current. It was also found from X-ray diffraction (XRD) analysis that the crystalline substance was composed mainly of hydroxyapatite. In addition, by calculating pH profiles on the surface of the cathodes, it was thought that unstable zone was created on the surface of electrode so that microscopic crystals of HAP were formed, grow-up with time, and then settle down to the bottom of reactor.

REFERENCES

Hosni, K., S. B. Moussa., and M. B. Amor. 2007. "Conditions Influencing the Removal of Phosphate from Synthetic Wastewater: Influence of the Ionic Composition." *Desalination*. 206:279-285.

Kato, F., M. Takaoka., K. Oshita., and N. Takeshita. 2007. "Present Stage of Phosphorus Recovery from Wastewater Treatment." *Journal of JSCE, Division G*. 63(4):413-424.

Murata, T. 1992. "*Advanced Process Technology of Sewage Water* " (in Japanese). Prepared for RIKOH TOSHO by K. Shibayama. 124-130.

Nakajima, H., Sasaki, Y. and Sakakibara, Y. 1998. "Fundamental study of advanced treatment aiming phosphate recovery." *Proceedings of the 53th annual conference of the Japan Society of Civil Engineers*, 7, 264–265.

Sakakibara, Y., and T. Nakayama. 2001. "A novel Multi-Electrode System for Electrolytic and Biological Water Treatments:Electric Charge Transfer and Application to Denitrification." *Water Research*. 35(3):768-778.

Sakakibara, Y. 2001. "Method for Removing Phosphorus from Water to be treated Using an Electric Field." US and EU patent #2001-175192.

Sakakibara, Y., and H. Nakajima. 2002. "Phosphate Removal and Recovery by a novel Electrolytic Process." *Water Science and Technology*. 46(11-12):147-152.

Tanaka, T., N. Koike., T. Sato., T. Arai., and N. Taira. 2009. "Recovery of Phosphate from Livestock Wastewater by Electrolysis." *Journal of Japan Society on Water Environment*. 32(2):79-85.

Tanaka, T., and K. Shimamura. 2005. "Biological Wastewater Treatment Process with Chemical-Phosphorus Recover Reactor." *Journal of Environmental Biotechnology*. 4(2):101-108.

NITROGEN REMOVAL PERFORMANCE IN A COMBINED BIOREACTOR

Junling Gao*, Yanling He and Cuiping Zhang
(Xi'an Jiaotong University, Xi'an, Shaanxi, China)

Experiments have been performed to investigate the nitrogen removal performance in a self-designed combined bioreactor using Industrial wastewater. In the reactor, one rectangle box was separated into three zones: aerobic zone, buffering zone and anoxic zone. Nitritation and denitrification were supposed to be mainly accomplished in the aerobic and anoxic zones, respectively. When the influent total nitrogen (TN) and organic carbon loadings were averaged at 0.12 and 0.56 kg/m^3.d, over 80% TN removal efficiency was achieved by adjusting the aeration rate. Continuous experimental results demonstrated that NH_3-N removal efficiency increased at a certain aeration rate. Energy produced by aeration was used for liquid recycle, so TN could be more efficiently removed at lower cost in this reactor.

ISBN 9780976885351

OPTIMIZATION OF AMMONIA-N OXIDATION BY *NITROSOMONAS EUROPAEA* USING EXPERIMENT DESIGN

Bao Yingling and Ye Zhengfang (*Peking University, Beijing, P. R. China*)

Medium and culture conditions for ammonia-N oxidation by *Nitrosomonas europaea* in discontinues culture were optimized using a statistical methodology. Plackett-Burman design (PBD) was used to study 19 factors that could potentially influence ammonia-N oxidation process. Inoculation size, dissolved oxygen (DO), pH control, and temperature were identified as key factors that significantly influenced biomass, ammonia monooxygenase activity and ammonium utilization ratio. The main and interaction effects of the four factors were further optimized via central composite design (CCD) using response-surface methodology (RSM). The maximum biomass (2.217×10^8 cells/ml), ammonia monooxygenase activity (2.778 ± 0.016 nitrite/protein) and ammonium utilization ratio (91.32±0.22 %) was obtained respectively through single-objective optimization. A total maximum strategy was subsequently obtained by multi-objectives optimization from the compromise of the three desirable objectives. With the inoculation size of 11.2%, cultivation at 28 ℃, pH of 7.6±0.2 and DO of 0.6±0.1mg l^{-1}, the biomass (1.829×10^8 cells/ml), ammonia monooxygenase activity (2.352 ± 0.016 nitrite/protein) and ammonium utilization ratio (89.19± 0.19%) were obtained simultaneous in a good agreement with models prediction.

ISBN 9780976885351

APPLICATION OF MAGNETITE MODIFIED WITH POLYACRYLAMIDE TO ADSORB PHOSPHATE IN AQUEOUS SOLUTION

Yi-Chen Chen, Ya-Fen Lin, and ***Chyow-San Chiou*** (National I-Lan University, I-Lan Taiwan)
Hua-Wei Chen (St. Mary's Medicine Nursing and Management College, I-Lan, Taiwan)

Phosphate is one of the main contaminants responsible for the eutrophication of surface waters, and adsorption is a potential treatment method of this pollutant. A magnetic adsorbent manufactured from magnetite (Fe_3O_4) can be easily recovered from treated water by magnetic force, without requiring further downstream treatment. In this research, the surface of magnetite modified with oleic acid and acrylamide (PAM/oleic acid/Fe_3O_4) was used to adsorb phosphate in an aqueous solution in a batch system. The optimum solution pH for phosphate adsorption by PAM/oleic acid/Fe_3O_4 was found to be 4.5. The phosphate adsorption behavior by PAM/oleic acid/$Fe_3O_4$was in good agreement both with the Langmuir and Freundlich adsorption isotherm, and the maximum adsorption capacity (q_m) and Gibbs free energy of phosphate was 28.143 mg g^{-1} and -13.094 kJ mol^{-1}, respectively. A pseudo-second-order model could best describe the adsorption kinetics, and the derived activation energy was 28.292 kJ mol^{-1}. The optimum condition to desorb phosphate from PAM/oleic acid/Fe_3O_4 is provided by a solution with 0.5 M NaOH.

ISBN 9780976885351

AGED REFUSE BIOREACTOR, A NOVEL PROCESS ON NITROGEN REMOVAL OF MATURE LANDFILL LEACHATE

Bing Xie
(Department of Environment Science, East China Normal University, Shanghai, PRChina, 200062)

Leachate irrigation to landfill is one of the best onsite technology to removal the pollutants. The aged refuse bioreactor is the well-decomposed waste through years in the landfill, the efficiency of pollutants removal is mainly from its physicochemical and microbiological properties, and bioreactor has already been found to be practical and operational in treating landfill leachate in previous reports, and received more and more attention.

However，The nitrogen remove in aged refuse reactor is not efficient enough especially for the mature leachate as well. In this study, the lab scale aged refuse bioreactor, of which landfill leachate nitrogen removal rate can reach to 90%. The nitrogen removal mechanism has been found with the anaerobic ammonia oxidation process (Anammox: Anaerobic ammonium oxidation). The 16S rRNA gene library and phylogenetic tree of planctomycetes was constructed to explore the community structure of anaerobic ammonium oxidation, and co-existence of denitrification mechanism in the aged refuse bioreactor. The results showed that Anammox bacteria distributed at various locations in the vertical direction in the bioreactor, which mainly concentrate in the lower part of the reactor. The anammox bacteria in the bioreactor are only *Candidatus Kuenenia stuttgartiensis*. The nitrogen removal efficiency could be controlled by influent nitrite and ammonia ratio and hydraulic retention time. This research would provide fundamental understanding on how to develop and efficiently operate high-rate bioreactor.

ISBN 9780976885351

TOXICITY FORMATION AND DISTRIBUTION IN ACTIVATED SLUDGE TREATING BISPHENOL A (BPA) WASTEWATER

Xiurong Chen, Na Yang, Wenlu Xu, Yuanyuan Hu (School of Resource and Environmental Engineering, East China University of Science and Technology, Shanghai 200237, China)

ABSTRACT: The synthetic wastewater with various Bisphenol A (BPA) concentrations as 2.5mg/L, 5.0mg/L, 7.5mg/L, 20mg/L was treated with sequential aerobic activated sludge reactor. The sludge acute toxicity indicated by the inhibitory ratio to Luminous bacteria T3 was taken as the investigated point. The original COD was 300±20 mg/L, operation period was 30d, and the hydraulic retention time (HRT) was 12h. As a result, there was a positive relationship between sludge acute toxicity indicated by inhibitory ratio to Luminous bacteria T3 and influent BPA concentration, and the toxicity centralized in intracellular and intersection of Extracellular polymeric substances (EPS) in sludge flocs. With the original BPA concentration from 2.5mg/L to 20mg/L, at the 12th hour of 28d, the difference between sludge fed with BPA and that without BPA was separately 2.23%、3.27%、5.41% and 9.96%. In the 12h treatment process, the peak content of BPA in sludge was at 2h due to the adsorption of BPA in sludge. However, the peak total toxicity of sludge was at 8h when the BPA was biodegraded to a great extent. Therefore, the organic toxicity in sludge flocs was contributed mostly by degradation of BPA and little by sludge adsorption.

INTRODUCTION

Land application is an important way for excess sludge disposal due to the high content of plants nutrient components[1,2]. It was indicated that crop yield was increased to a great extent with sludge addition to soil as fertilizer and physical properties reclamation[3,4,5]. Nevertheless, the key point which inhibit sludge being reused to soil is its toxicity. As to the organic and inorganic toxicity of sludge to soil, the latter one symbolized by heavy metals has been well known; while the organic toxicity has not caused people's wide concern. As a matter of fact, it is not a thorough ecological hazard assessment only with heavy metals toxicity for sludge land disposal[6]. Therefore, it is necessary to take the organic toxicity into account when recycle excess sludge to soil.

Typically, the relatively high content of various toxic organics in sludge leads to the organic toxicity. There are as much as 516 kinds organic matter[7] in sludge, and most of the persistent organic pollutants (POPs) must be introduced to food chain connecting human and ecology via sludge application to land[8]. A thorough survey for POPs distribution in sludge in wastewater treatment plants of Britain, Mediterranean, Australia and Spain indicated that Polychlorinated -p- two benzene dioxins / furans (PCDD/Fs), phthalate esters (PAEs), Poly Brominated Diphenyl Ethers (PBDEs), polybrominated biphenyls (PBBs) and Polycyclic Aromatic Hydrocarbons (PAHs) are detected[9-17]. Various kinds of excess sludge from more than hundreds of wastewater treatment plants in China (Beijing, Shanghai, Hongkong and Yangtze River delta) contain most of the above POPs and benzo[a]pyrene (B[a]P), polychiorinated (PCB) as well[18-23].

Besides the toxic products and residual organics after biodegradation, the process of toxic pollutants biodegradation contributes to the formation of sludge toxicity. Some research demonstrated that stress effects from toxic pollutants shock stimulated the microorganisms to produce toxic soluble microbial products (SMP) [24,25] and stress protein GroEL so as to change the characteristics of sludge[26]. When the Daphnia Magna Straus is taken as toxicity indicator, it is evaluated that wastewater containing toxic organics could lead to the toxicity formation of sludge indirectly [27].

In order to investigate the toxicity property and formation in sludge for the sake of exploring

---

ISBN 9780976885351

theory evidence for subsequent sludge disposal, the relationship between synthetic wastewater containing toxic Bisphenol A (BPA) treatment and toxicity of sludge was studied in Sequencing Batch Reactor (SBR). The reason to choose BPA as the target pollutant is based on its properties as follows:

1) BPA is a kind of widely used industrial materials [28,29], which exists in raw water of many industrial wastewater treatment plants. Therefore, the research conclusions from BPA biodegradation and sludge toxicity formation are representative for toxic wastewater treatment process;

2) BPA is a biodegradable [30] and toxic pollutant [31,32,33]. What is more important is that BPA is uneasily volatile [34] and low bioaccumulative [34]. Then, BPA decrease in treatment process is contributed by adsorption of biodegradation by active sludge. As a result, there are no other interference factors for analyzing the process of BPA degradation and sludge toxicity formation.

Up to now, literatures concerning BPA biological treatment are dominated by such aspects as BPA reduction from effluent, BPA biodegradation dominant bacteria cultivation and degradation pathway [34,35]. While the process of toxicity transferring from wastewater to sludge as BPA biodegradation and the toxicity distribution in sludge have not attracted wide attention, which are the key points in this research.

MATERIALS AND METHODS

Synthetic wastewater and SBR process. The study was carried out in two 10L bench-scale SBR process. The influent COD made by peptone for both SBR reactors was controlled at 300±23.5mg/L. In order to analyze the change of sludge toxicity caused by BPA degradation, the influent of one SBR was mixed by peptone and BPA original concentrations from 2.5mg/L, 5.0mg/L, 7.5mg/L and 20mg/L at different phase, the other SBR was fed only by peptone.

The operation parameters for both SBRs were kept to a "safety" range to ensure the good performance of BPA degradation: the operation phase for various BPA initial concentration was 30d; the hydraulic retention time (HRT) for both SBRs were 12h; the sludge retention time (SRT) for both SBRs were 20d.

In order to meet the aerobic BPA degradation bacteria activity, both SBR were regulated aeration intermittently to keep the dissolved oxygen (DO) in the range of 2.5-3.5mg/L, and the contents ratio of C (peptone or peptone+BPA), N (urea), P (potassium dihydrogen phosphate) was controlled as 100:5:1. The initial sludge used for both SBR acclimation was from Chang Qiao Wastewater Treatment Plant in Shanghai, China.

Analytical methods. The analytical items in this research included COD in liquid (APHA, 1995), BPA both in liquid and sludge, toxicity symbolized by inhibitory of Photobacterium phosphoreum T3 spp.. BPA in liquid and sludge was measured with High-performance Liquid Chromatography (HPLC, LC-10ATVP, Kyoto, Japan) after the sample was pretreated.

Inhibitory of Photobacterium phosphoreum T3 spp. was measured according to the Standard Methods of China (GB/T15441-1995, China). The Photobacterium phosphoreum T3 spp. can radiate a certain intensity visible light with wavelength of 50-490nm. When it is exposed to toxic matter, there is certain correlativity between the inhibitory extent to light intensity and toxic matter content. The change intensity of visible light is detected by Toxicity Determinator (DXY-2, Institute of Soil Science, Chinese Academy of Sciences). In this research, the toxicity was represented by the percent of inhibiting luminosity (%).

In order to investigate the toxicity (measured as inhibiting luminosity) spatial distribution in sludge, namely the total toxicity of sludge and the toxicity of outer section extracellular polymeric substances (EPS). The pretreatment procedures for two kinds of toxicity were respectively cell lysis and EPS extraction, which are listed as follows. The pretreatment for BPA detection in sludge with HPLC was cell lysis as well.

Cell lysis. The ultrasonic irradiation to sludge led to cell lysis so that Intracellular matter released to supernatant from sludge. The sludge was separated from mixed liquor through centrifugation at 4000r for 10 min twice, and then the sludge sediment was rinsed with buffer solution. The 50ml sludge mixed liquor was put into a plastic centrifuge tube and the ultrasound probe was switched on which emitting 20 KHz (0.5w/ml) ultrasonic frequency for 10 min. The ultrasonic probe was put 3 cm depth into mixed liquor and the centrifuge tube was kept on ice bath. With sludge disintegration and cells lysis under sonication, the organic matter in sludge would release to water. The sludge sample was centrifuged at 4000r for 20 min; the supernatant was centrifuged with 12000r at 4°Cfor 10 min. Finally, the supernatant after twice centrifugate was used to analyze BPA content with HPLC or sludge total toxicity with Photobacterium phosphoreum T3 spp..

EPS extraction. The EPS was extracted from sludge by being stirred with cation exchange resin (CER) under shearing effect. The CER was DOWEX 50×80, Na^+ form, 20-50 mesh in the sodium form (Fluka 44445). CER extraction was effective for EPS extraction because it was almost no cell lysis through the process. The 50ml sludge sample was centrifuged at 4000r for 10 min twice, and then the supernatant was removed and the sediment was rinsed in a buffer solution. The sludge mixed liquor was mixed with DOWEX (75g/g VSS), and then transferred into a conical flask where it was stirred with high rotating speed for 2 hours at 4°C. After stirring process, the extracted EPS was recycled by centrifugation at 12000r and 4°C for 10 min.

The variation of COD, BPA content and toxicity indexes through the treatment process was twice a week to investigate the relationship between BPA removal and sludge property especially toxicity formation and spatial distribution in sludge.

RESULTS AND DISCUSSION

Toxicity variation and property in sludge

COD removal with treatment time. The effluent COD at 12h in the whole treatment phase, e.g. 30d for two SBR processes is shown in Figure 1.

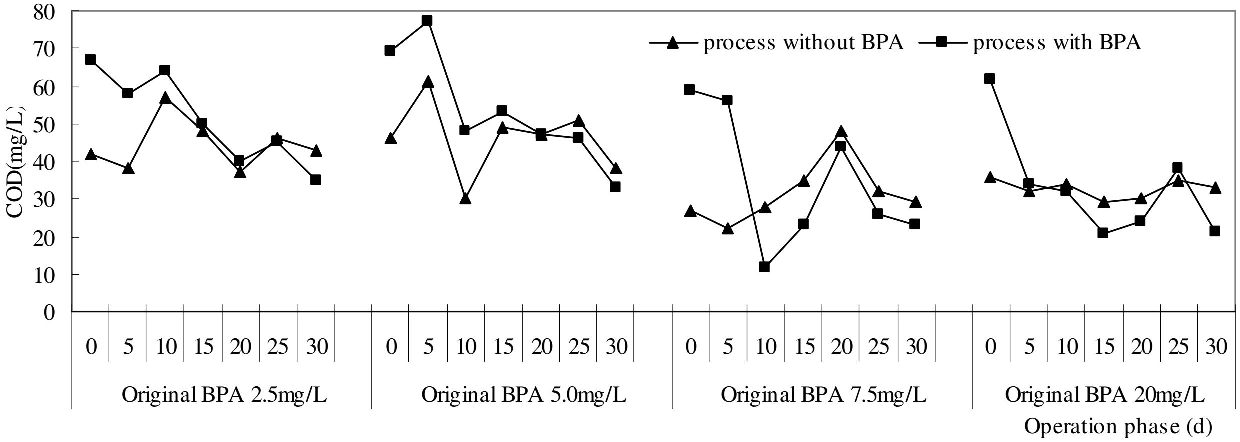

Figure 1. Effluent COD variation with operation phase

From Figure 1, it is shown that the effluent COD fluctuation was distinct for both processes during the operation phase as 30d. During the start stage before 10-15 days, the effluent COD of SBR fed with BPA from 2.5mg/L to 20mg/L was above that the SBR without BPA. While in the latter stage from 15 to 30d, the performance of COD removal of SBR with BPA was superior to that of SBR without BPA for the reason that sludge was acclimated to the influent BPA concentration as well as certain content of hormones pollutant as BPA stimulated sludge activity. In the end of the each operation phase as 30d, the effluent COD of both SBR process was below 45mg/L, which indicated that both SBR activated sludge showed perfect performance on COD removal. The SVI and SV of both SBR sludge were respectively around 100mL/g and 25-30%, which together with the good COD removal above embodied the activity of sludge was relatively high. Therefore, the contrast for toxicity of the sludge in two SBR processes was feasible with similar sludge activity.

Toxicity formation in sludge with treatment time. The variation of sludge total toxicity in two SBR processes with operation phase was illustrated in Figure 2. The toxicity is represented as percent of inhibiting luminosity to Photobacterium phosphoreum T3 spp..

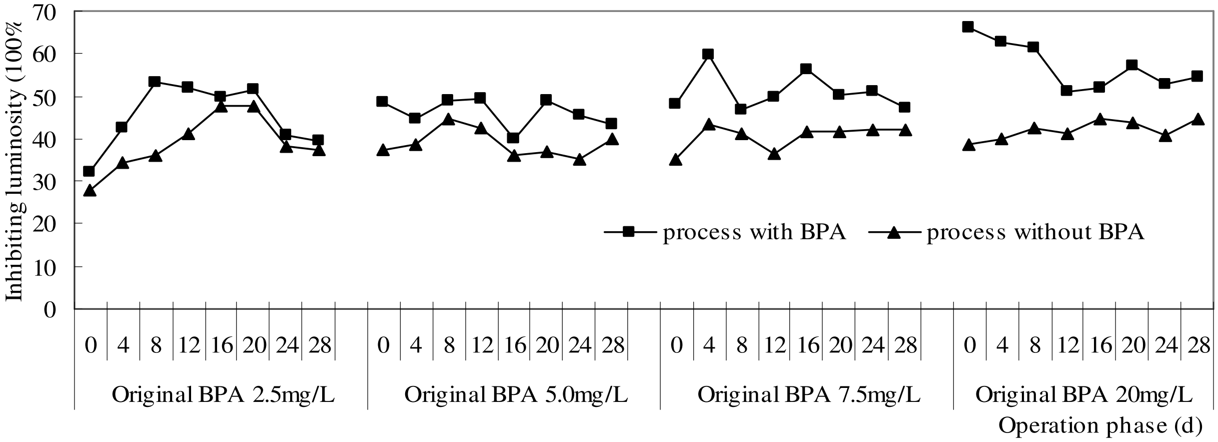

Figure 2. Variation of total toxicity of sludge with operation phase

For the 4 phases, the total toxicity of SBR with BPA is evidently higher relative to that of SBR without BPA. The difference of toxicity between these two kinds of sludge is gradually decreased to a stable level from the beginning stage to the end during each operation phase. Moreover, the average and the end gaps of the total sludge toxicity for two SBR processes become wider and wider with the influent BPA concentration increasing. When the influent BPA concentration was 2.5mg/L, 5.0mg/L, 7.5mg/L and 20mg/L, the total sludge toxicity of SBR with BPA was separately 2.23%, 3.27%, 5.41% and 9.96% higher than those of SBR without BPA.

Table 1. Variation of sludge total toxicity with various BPA original concentrations at different operation stage

Operation stage	Toxicity (%)	BPA 2.5mg/L	BPA 5.0mg/L	BPA 7.5mg/L	BPA 20mg/L
4th day	Process with BPA	42.55	44.67	59.85	62.61
	process without BPA	34.37	38.53	43.27	39.83
	Difference	8.18	6.14	16.58	22.78
28th day	Process with BPA	39.54	43.30	47.45	54.49
	process without BPA	37.31	40.03	42.04	44.53
	Difference	2.23	3.27	5.41	9.96

From the phenomena above, it is deduced that the toxicity extent had a positive relevance to the BPA content in influent synthetic wastewater, and the sludge toxicity is still evident even though the sludge had good performance on BPA removal.

For the whole process of each BPA concentration phase, the sludge total toxicity experienced unevenly variation at the start stage (before 10d), then went up to a high level in the middle stage (10-20d) and finally dropped to a stable range in the end stage (20-30d). The contrast between sludge total toxicity at the 4th day and 28th day is listed in Table 1.

The data in Table 1 indicate that the supplement of original BPA enhanced the sludge total toxicity, and the increasing extent for sludge toxicity is positively correlated to that of original BPA content variation. At the 4th day, namely the start stage, for each BPA concentration stage, the toxicity difference between sludge with BPA and that of sludge without BPA is 2 to 3 times that at the 28th day, namely the end stage. It suggests that the increased BPA was not completely biodegraded as the activated sludge did not adapt to it in the beginning. Consequently, there was considerable toxic intermediate biodegradation product or influent BPA stimulated sludge to produce toxic secretion when sludge was not acclimated to BPA addition, both of which led to the obvious sludge toxicity formation. In contrast, when the sludge was accustomed to the enhancement of influent BPA, the BPA was removed more thoroughly, so there was less accumulation of toxic intermediate byproducts or secretion in sludge. As a result, the sludge total toxicity at the 28th day reduced to a great extent.

Relevance between sludge toxicity and BPA removal. In order to investigate the correlation between sludge toxicity formation and BPA removal in SBR process, the sludge toxicity and BPA content in various sections during 12h treatment cycle as influent BPA was 20mg/L are concluded in Table 2.

Table 2. Sludge toxicity and content of BPA in liquid and sludge in 12h treatment process cycle

Time of a cycle (h)	0	0.5	1	1.5	2	2.5	4	6	8	10	12
BPA in liquid (mg/L)	20	7.72	2.67	1.13	0.85	0.41	0.34	0.03	0.01	0	0
BPA in sludge (mg/L)	0	0.9	1.81	3.32	1.28	0.37	0.038	0.021	0.015	0.01	0
Sludge total toxicity with BPA (%)	43.62	43.85	44.93	46.32	47.68	51.09	53.87	54.07	61.66	55.59	54.49
Sludge total toxicity without BPA (%)	41.48	42.12	43.05	45.32	46.23	45.71	44.75	47.66	46.52	48.54	44.53

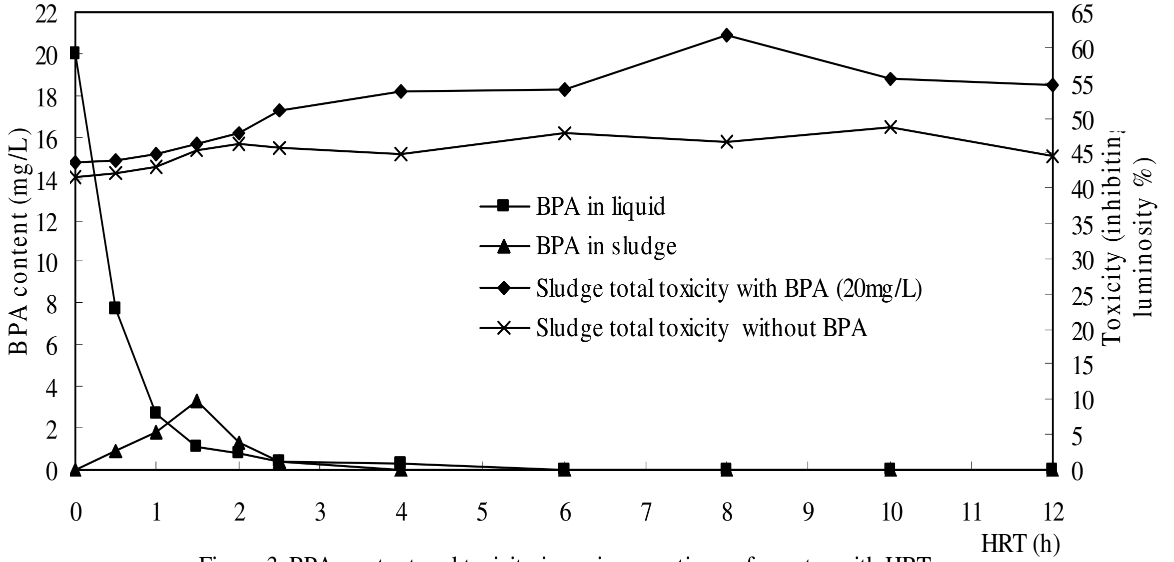

Figure 3. BPA content and toxicity in various sections of reactor with HRT

The BPA content in liquid decreased sharply in the first hour and below 1.0mg/L after 2h. At the same time, BPA adsorbed in sludge reached peak value as 3.32mg/L at 1.5h and reduced soon later. Except for the beginning of the 12h cycle, the sum of BPA in liquid and sludge was below the initial 20mg/L. Since BPA loss by volatilization is insignificant [34], the content of BPA loss in SBR was considered to be biodegraded by activated sludge. From the data from Table 2, the sum of BPA content in liquid and sludge was below 1mg/L after 2.5h. That is to say, the BPA removed by biodegradation in SBR was close to that in raw wastewater after 2.5h. Nevertheless, the time for the peak value of sludge toxicity was at 8h for SBR fed with BPA, which lagged behind the peak content of BPA in sludge by adsorption for 6.5 hours. Therefore, the toxicity peak value was not caused by BPA adsorption in sludge.

The variation of sludge toxicity and BPA contents in various sections in SBR along 12h cycle is shown in Figure 3. The curves trends for BPA adsorption in sludge and sludge toxicity in Figure 3 indicate that there was no significant correlation between the two processes. The peak content of BPA absorbed in sludge resulted to little rise of sludge toxicity, while peak toxicity of sludge appeared at the 8th hour when BPA in either sludge or liquid disappeared almost completely. So it could be concluded from above that the toxicity of sludge was caused not by BPA adsorption in sludge but by BPA degradation process. For the SBR without BPA in raw wastewater, the sludge toxicity was comparatively steady in a narrow range for the reason that peptone was more easily biodegraded and less toxic than BPA.

In the BPA degradation process, there were two possibilities for contribution to sludge toxicity formation: one was the toxic intermediate products of BPA biodegradation accumulated in sludge phase; the other was the toxic matter secreted by sludge as it was impacted by influent BPA. As to the two possibilities above, further investigation is still needed to proceed.

Toxicity spatial distribution in sludge. In order to evaluate the ratio of content of EPS extracted via CER and high speed centrifugation to that of total sludge, the BPA adsorption experiment was performed. In this experiment, BPA was the sludge unacclimated by BPA was inactivated under conditions as 0.1MPa and 120°C for 30 minutes. Since the construction of sludge flocs was destroyed in the inactivation process, the property of sludge dispersed evenly. When BPA adsorption got to equilibrium, EPS was extracted via CER and high speed centrifugation, and BPA contents in both total inactivated sludge and EPS were analyzed through HPLC. The adsorption result indicated that the ratio of BPA content in EPS to that in total sludge was 1:4.49. That is to say, EPS extracted by CER and high speed centrifugation accounted for only 22.27% of total sludge. Therefore, EPS extracted in this research was considered as the outer section part of sludge.

The toxicity spatial distribution in sludge was evaluated to build up the theoretic basis for sequential sludge disposal. Figure 4 presents the toxicity spatial distribution in sludge for various influent BPA concentrations during the 30d operation phase.

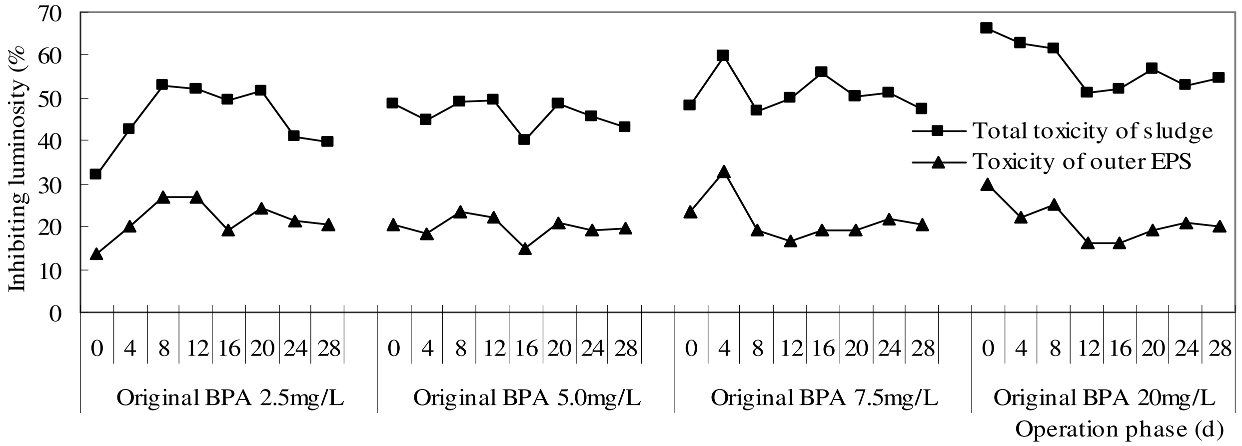

Figure 4. Toxicity in various sections of sludge operation time

For every BPA concentration phase, the total toxicity of sludge was more than twice of outer EPS toxicity, and furthermore, the discrepancy enhanced with the increase of influent BPA concentration. In conclusion, in the end of each 12h treatment cycle, toxicity resulted by BPA biodegradation process concentrated to inner section of sludge flocs, namely the intracellular section and inner EPS. The outer

EPS only contained a minor part of toxicity.

Figure 5 summarizes the toxicity distribution along 12h treatment cycle in sludge for two SBRs. The toxicity of outer EPS for sludge in two SBRs was similar to each other in the 12h treatment cycle. While there was remarkable difference between total toxicity of sludge fed with BPA and that without BPA. For sludge of both SBRs, the total toxicity of sludge was almost thrice of outer EPS toxicity. So the intracellular and inner EPS toxicity took up the main part of sludge toxicity. From Figure 5, it is shown that the toxicity difference between sludge in two SBRs existed in the inner section of sludge flocs. In other words, the influent BPA led to the toxicity accumulation in the inner section of sludge flocs, namely intracellular and inner EPS.

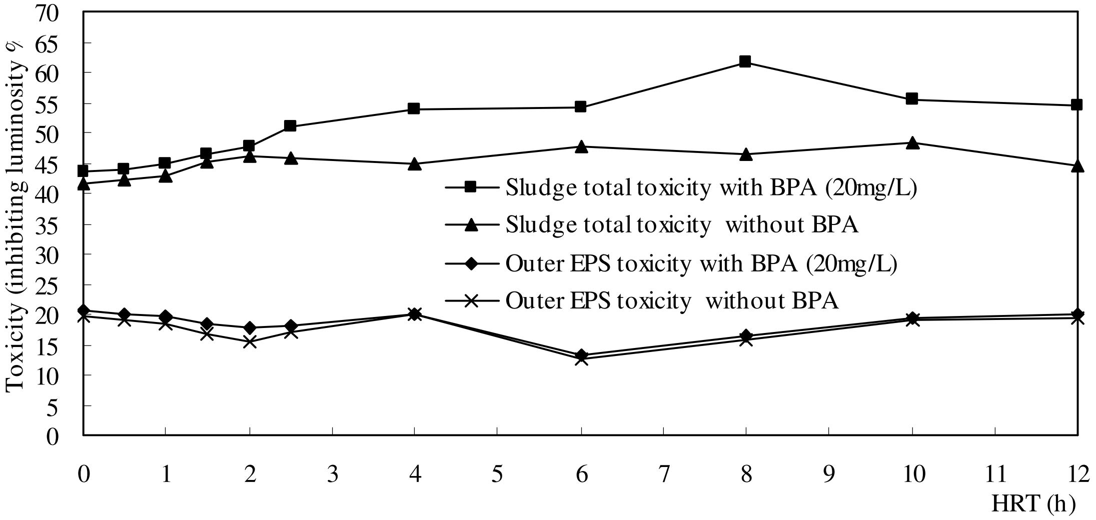

Figure 5. Toxicity in various sludge sections with BPA influent or not with HRT

CONCLUSION

By contrast of the sludge toxicity in two SBRs fed with BPA or not, the toxicity formation and spatial distribution in sludge flocs were investigated in this research. There are three items of conclusions as follows:

1) The toxicity was contributed most by BPA biodegradation, not by adsorption. And furthermore, the toxicity was positively correlated with the initial BPA concentration;

2) The toxicity of sludge which was not completely acclimated to BPA was most significant due to the accumulation of toxic intermediate biodegradation products of BPA or secretion of activated sludge stimulated by BPA. As the BPA was removed most by adsorption in the beginning and thoroughly degradation in the end phase, the sludge toxicity dropped relatively low;

3) The sludge toxicity caused by BPA biodegradation process concentrated in the inner section of sludge flocs.

The characteristics of toxicity formation and distribution in sludge flocs were the theoretic basis for subsequent sludge disposal for toxicity removal.

ACKNOWLEDGEMENTS

The authors would like to thank the National Natural Science Foundation of China (51008124) for financial support.

REFERENCES

1. R.P. Singh, M. Agrawal. Potential benefits and risks of land application of sewage sludge [J]. Waste Management, 2008,28:347-358.

2. Pilar Andrés, Eduardo Mateos, David Tarrasón, Cristina Cabrera, Blanca Figuerola. Effects of digested, composted, and thermally dried sewage sludge on soil microbiota and mesofauna [J]. Applied Soil Ecology, 2011,48:236-242.

3. M. Carmen Antolín, Inmaculada Pascual, Carlos García, Alfredo Polo, Manuel Sánchez-Díaz. Growth, yield and solute content of barley in soils treated with sewage sludge under semiarid Mediterranean conditions [J]. Field Crops Research, 2005,94:224-237.

4. Nicola Senesi,Cesar Plaza, Gennaro Brunetti, Alfredo Polo. A comparative survey of recent results on humic-like fractions in organic amendments and effects on native soil humic substances [J]. Soil Biology & Biochemistry, 2007,39:1244-1262.

5. F. Gallardo, M. Cea, G.R. Tortella, M.C. Diez. Effect of pulp mill sludge on soil characteristics, microbial community and vegetal production of Lolium Perenne [J]. Journal of Environmental Management, 2012,95:S193-S198.

6. P. Alvarenga, P. Palma, A.P. Gonçalves, R.M. Fernandes, A.C. Cunha-Queda, E. Duarte, G. Vallini. Evaluation of chemical and ecotoxicological characteristics of biodegradable organic residues for application to agricultural land [J]. Environmental International, 2007,33:505-513.

7. Ellen Z. Harrison, Summer Rayne Oakes, Matthew Hysell, Anthony Hay. Organic chemicals in sewage sludges [J]. Science of the Total Environment, 2006,367:481-497.

8. Bradley O. Clarke, Stephen R. Smith. Review of ‘emerging’ organic contaminants in biosolids and assessment of international research priorities for the agricultural use of biosolids [J]. Environment International, 2011,37:226-247.

9. D.A. Bright, N. Healey. Contaminant risks from biosolids land application: Contemporary organic contaminant levels in digested sewage sludge from five treatment plants in Greater Vancouver, British Columbia [J]. Environmental Pollution, 2003,126:39-49.

10. M. Francisca Gomez-Rico, Rafael Font, Jose Vera, David Fuentes , Karen Disante, Jordi Cortina. Degradation of organic pollutants in Mediterranean forest soils amended with sewage sludge [J]. Chemosphere, 2008,71:2129-2138.

11. Bradley Clarke, Nichola Porter, Robert Symons, Judy Blackbeard , Peter Ades, Philip Marriott. Dioxin-like compounds in Australian sewage sludge – Review and national survey [J]. Chemosphere, 2008,72:1215-1228.

12. Bradley Clarke, Nichola Porter, Robert Symons, Philip Marriott, Peter Ades, Gavin Stevenson, Judy Blackbeard. Polybrominated diphenyl ethers and polybrominated biphenyls in Australian sewage sludge [J]. Chemosphere, 2008,73:980-989.

13. Bradley O. Clarke, Nichola A. Porter, Philip J. Marriott, Judy R. Blackbeard. Investigating the levels and trends of organochlorine pesticides and polychlorinated biphenyl in sewage sludge [J]. Environment International, 2010,36:323-329.

14. M.M. González, J. Martín, J.L. Santos, I. Aparicio, E. Alonso. Occurrence and risk assessment of nonylphenol and nonylphenol ethoxylates in sewage sludge from different conventional treatment processes [J]. Science of the Total Environment, 2010,408:563-570.

15. E. Abad, K. Martínez, C. Planas, O. Palacios, J. Caixach, J. Rivera. Priority organic pollutant assessment of sludges for agricultural purposes [J]. Chemosphere, 2005,61:1358-1369.

16. Samuel Cantarero, Carlos A. Prieto, Ignacio López. Occurrence of high-tonnage anionic surfactants in Spanish sewage sludge [J]. Journal of Environmental Management, 2012,95:S149-S153.

17. I. Aparicio, J.L. Santos, E. Alonso. Limitation of the concentration of organic pollutants in sewage sludge for agricultural purposes: A case study in South Spain [J]. Waste Management, 2009,29:1747-1753.

18. Quan-Ying Cai, Ce-Hui Mo, Qi-Tang Wu , Qiao-Yun Zeng, Athanasios Katsoyiannis. Occurrence of organic contaminants in sewage sludges from eleven wastewater treatment plants, China [J]. Chemosphere, 2007,68:1751-1762.

19. Lixi Zeng, Thanh Wang, Ting Ruan, Qian Liu, Yawei Wang, Guibin Jiang. Levels and distribution patterns of short chain chlorinated paraffins in sewage sludge of wastewater treatment plants in China [J]. Environmental Pollution, 2012,160:88-94.

20. Li Hua,Wei-Xiangwu,Yu-Xue Liu, C.M. Tientchen, Ying-Xu Chen. Heavy metals and PAHs in sewage sludge from twelve wastewater treatment plants in Zhejiang province [J]. Biomedical and Environvironmental Sciences, 2008,21:345-352.

21. Shen Rong-Yan, Luo Yong-Ming, Feng Sheng, Zhang Gang-Ya, Wu Long-Hua, Li Zhen-Gao,Teng Ying and P. Christie. Benzo[a]pyrene and phenanthrene in municipal sludge from the Yangtze River Delta, China [J]. Pedosphere, 2009,19(4):523-531.

22. Jiayin Dai, Muqi Xu, Jiping Chen, Xiangping Yang, Zhenshan Ke. PCDD/F, PAH and heavy metals in the sewage sludge from six wastewater treatment plants in Beijing, China [J]. Chemosphere, 2007,66:353-361.

23. Chao Yang, Xiang-Zhou Meng, Ling Chen, Siqing Xia. Polybrominated diphenyl ethers in sewage sludge from Shanghai, China: Possible ecological risk applied to agricultural land [J]. Chemosphere, 2011,85:418-423.

24. Ping Yu, Xin Yu, Qihong Ji, Zhihua Qi, Gu Wei, Jianping Zhai. The formation mechanism and characteristics of soluble microbial products (SMP) in wastewater biological treatments [J]. Environmental Pollution and Control, 2006,28(5):352-355. (Chinese)

25. Juan Xu. Characteristics of Soluble microbial products(SMP) in wastewater biological treatment process [D]. University of Science and Technology of China, 2010, Environmental Engineering, 3-13. (Chinese)

26. Charles B. Bottm, Nancy G. Love. The immunochemical detection of stress proteins in activated sludge exposed to toxic chemicals [J]. Water. Research, 2001,35(1):91-100.

27. Yu Hongxia, Cheng Jing, Cui Yuxia, Shang Huihua, Ding Zhonghai, Jin Hongjun. Application of toxicity identification evaluation procedures on wastewaters and sludge from a municipal sewage treatment works with industrial input [J]. Ecotoxicology and Environmental Safety, 2004,57:426-430.

28. Nansheng Deng, Feng Wu. Endocrine Disrupting Chemicals in Environment [M]. Beijing: Chemical Industry Press, ISBN：7502552324, 2004:1-63, 209-214. (Chinese)

29. Craig D R, Brown E, Craft J A, et al. Effects of sewage efflrent and ethynyl oestradiol upon molecular markers of oestrogenic exposure, maturation and reproductive success in the sand goby [J]. Aquatic Toxicology, 2003, 62(2): 119-134.

30. IKE M. Biodegradation of bisphenol A in the aquatic environment [J]. Water Science and Technology, 1999,42(7-8): 31-38.

31. Dan Yang, Dandan Li, Shanshan Liu, et al. The effect of Bisphenol A on organism and its mechanism of action [J]. Modern Preventive Medicine, 2008, 35(17): 3280-3287. (Chinese)

32. Can A, Semiz O, Cinar O. Bisphenol A induces cell cycle delay and alters centrosome and spindle

microtubular organization in oocytes during meiosis [J]. Mol Hum Reprod, 2005, 11(6): 389-396.

33. Yong Lin, Xianggui Zeng, Desheng Wu, et al. Study on bisphenol A induced primary cultured mesencephalic neuronal cell injury by oxidative stress [J]. Journal of Hygiene Research, 2006, 35(4): 19-23. (Chinsese)

34. Xiaocun Wang, Xiaoxiang Zhao. Study on Discharge and Degeneration of Environmental Hormone Biophenol A [J]. Envionmental Science Survey, 2007, 26(1):17-20. (Chinese)

35. Jianhua Chen, Xia Huang, Shuyuan Li, Yunbo Xiao. Removal of bisphenol A in a membrane bioreactor [J]. Journal of Tsinghua University (Science and Technology), 2008， 48(6):999-1003. (Chinese).

UTILIZATION OF RAW SEWAGE SLUDGE (RSS) FOR THE PRODUCTION OF CONSTRUCTION MATERIALS.

Alaa Hamood and Jamal Khatib (School of Technology, University of Wolverhampton, Wolverhampton, West Midlands, UK)

ABSTRACT: The aim of this study was to introduce an effective alternative to the traditional treatment methods of Raw Sewage Sludge (RSS). This included the utilization of RSS as a water replacement in cement-based mixes for the production of sustainable construction materials. Four mixes, incorporating Portland cement, fine aggregate (1:4.5 respectively) and RSS (97.5% water content as a water replacing), were prepared and tested for their engineering properties. One more mix incorporating drinking water was also investigated for comparison purposes. Prepared specimens were cured for 28 days and tested for their compressive strength, specific gravity (SG), ultrasonic pulse velocity (UPV), total water absorption and length change. Results showed that RSS could potentially be used as a water replacement in cement based materials for the production of construction materials. Mixes incorporating RSS presented relatively good engineering properties in comparison with mix incorporating drinking water. Engineering properties were mainly affected by the amount of RSS added, as with the decreasing of RSS amount the better the engineering properties. This included compressive strength, specific gravity, UPV, total water absorption and drying shrinkage. The best properties was achieved in M1 (0.5 RSS:C). The amount of RSS added should be designed carefully to meet the required engineering properties.

INTRODUCTION

Raw Sewage Sludge (RSS) is the residual stream of suspended/dissolved organic and inorganic materials that result from the treatment processes of municipal wastewaters. Raw Sewage Sludge is usually in the form of liquid or semisolid liquid that typically contains, depending on operation and processes applied, from 2 to 8 present solids by weight. (Metcalf & Eddy Inc. 1991).

Raw Sewage Sludge is mainly collected from primary sedimentation tanks in wastewater plants, which are large round or rectangular tanks where heavier particles are allowed to settle to the bottom and to be later swept by scrapers to a submerged outlet. Settled stream is pumped in the form of slurry to the sludge storage tanks for further treatment at the sludge treatment unit. RSS may also be collected from secondary and tertiary sedimentation tanks. The composition of RSS is variant depending not only on collection seasons, but also on applied operations and processes.

There are approximately 35 million of tonnes of Raw Sewage Sludge produced in the UK each year. These quantities are reduced to 25 million tonnes per year by applying further on site physical and chemical processes.(Waste on line). In 2005, 1.4 million tons of dry solids were produced from sewage sludge in England and Wales, and it is estimated to increase to 1.6 million tons by 2010. (DEFRA 2007).

Biological, chemical and physical treatments are applied to Raw Sewage Sludge to reduce water content and to eliminate potential associated hazards. Such hazards including high heavy metal contents, presence of harmful pathogens and risks associated with the biodegradation of organic matters (production of flammable gases and unpleasant odours). Treatment includes preliminary operations, thickening, stabilisation, conditioning, dewatering, heat drying & other processing and thermal reduction. (Metcalf & Eddy Inc. 1991).

An effective Raw Sewage Sludge treatment is required to be in place in order to meet the requirements and guidelines stipulated by national and European environmental agencies. This generates great financial challenges to both local authorities and water companies as well as would involve high levels of energy consumption and large amount of greenhouse gases production. Such factors have,

---

ISBN 9780976885351

therefore, encouraged engineers and researchers to obtain sustainable alternatives to the traditional treatment methods of RSS.

BACKGROUND LITERATURE

Sewage sludge products were introduced as sustainable substances that could potentially be used as replacement for the traditional building materials. Different sewage sludge products (fully or partially treated) were internationally investigated for being used in the construction industry for the production of sustainable construction materials. Produced materials were examined for their engineering, chemical and environmental properties. Used Sewage sludge products included Dewatered Sewage Sludge, Dry Sewage Sludge and Incinerated Sewage Sludge Ash (ISSA). Previous relevant researches are shown below.

Monzó, Payá et al. (1998) used Incinerated Sewage Sludge Ashes (15% of total weight replacement) as a Portland cement replacement in mortars. Prepared mortar samples were tested for their engineering properties, including compressive and flexural strength. The results reviled that the addition of sewage sludge ash would enhance the strength properties due to pozzolanic properties of used Sewage Sludge Ashes.

Cyr, Coutand et al. (2007) examined the addition of high proportion of Incinerated Sewage Sludge Ashes (25 and 50% cement replacement). Results showed that the addition of ISSA induced short delays of cement hydration and lower compressive strength compared to that with cement only. It was also shown that presence of ISSA has a long term positive impacts which might be related the pozzlanic nature of the used ashes. The amount of elements leached from samples incorporated ISSA was slightly higher than from the reference mixes without residue but it remains of the same order of magnitude.

Garcés, Pérez Carrión et al. (2008) investigated the impact of using different proportions of Incinerated Sewage Sludge Ashes (10-30% of total weight replacement) as a cement replacement on some engineering properties, such as workability, compressive strength, porosity and shrinkage/expansion. Results showed that best compressive strength were obtained when 10% substitution was used, as well as, this ratio gave the best result for the other properties.

Wang, Chiou et al. (2005) investigated the possibility of producing lightweight cement based materials by adding Incinerated Sewage Sludge Ash (ISSA) to cement mixes and it was noted that the hydration process generated pores with diameter less than 0.1 micrometre. The study concluded that ISSA can be used for its lightweight properties and can be used as heat-insulation materials.

Mun, K (2007) produced lightweight aggregate by mixing natural clay, as main material, with different proportions of Dewatered Sewage Sludge (80-90% water content). Uniform pellets with similar diameter of 5-10mm was made and then sintered at a temperature of 1050-1150 Co for 10-20min. pellets then tested for their engineering and environmental properties. Results showed that total water absorption for mixes containing sewage sludge was better than that for those without it; also it was shown that no heavy metals were detected when leaching test was applied.

Valls, S (2001) prepared various mixes containing Dewatered Sewage Sludge (68% water content), Portland cement, sand and water with either flay ash or accelerating agent (CaCl2). Samples were tested for their engineering and environmental properties. The results generally showed that the greater the amount of sewage sludge the less the values of compressive strength with higher compressive strength values for samples without flay ash compared to those containing it. As well, results showed high degree of heavy metal retention in all mortar mixes, which ranged between 84-100%.

A study was undertaking by Cheilas, Katsioti et al. (2007) to investigate the effectiveness of applying solidification/stabilization technology to Dewatered Sewage Sludge (78% water content) by mixing it with Portland cement, sand and jarosite/alunite (JA) (waste produced from hydrometallurgical process). Two curing types were applied, traditional and Autoclave treatment (16 bar for 3hrs at 200˚C). Samples were then tested for their engineering and environment properties. Results showed that compressive strength for samples with jarosite/alunite (JA) was generally less than what for samples without it. The results showed as well high degree of heavy metal retention in both samples (with and without JA) for different metals, which ranged between 25.7-100%.

Physical and mechanical properties of concrete with added Dry Sewage Sludge (15% water content) was undertaken by Valls, S (2004). Four mixes incorporating Portland cement, sand, coarse aggregate and water with different ratios of Dry Sewage Sludge (0%, 2.5%, 5% & 10% of total weight) were prepared and then tested for their physical and mechanical/engineering properties. The results showed that samples with more sewage sludge proportion gave less density, less compressive strength and less flexural strength values. Durability properties for concrete samples containing materials above were examined by doing a set of durability tests. Tests included; combined wet–dry cycles using fresh water, seawater & water containing 5% sulphates; accelerated ageing in an autoclave and accelerated carbonation. Results for samples incorporated sewage sludge showed an acceptable and comparable to the results of reference concrete samples without sludge. (Yagüe, Valls et al. 2005)

MATERIALS AND MIXES COMPOSITION

The aim of this research was to utilize Raw Sewage Sludge (RSS) as a water replacement in cement based mixes to produce sustainable construction materials. Four mixes, incorporating Portland cement, fine aggregate (1:4.5 respectively) and RSS (97.5% water content as a water replacement), were prepared and tested for their engineering properties. Tests included compressive strength, specific gravity (SG), ultrasonic pulse velocity (UPV), total water absorption and drying shrinkage. One reference mix, incorporating drinking water (the same water content as in M3 after deducting the amount of solid content in RSS), was also prepared and tested for comparison purposes. Table 1 below shows the composition of used mixes.

Table 1: Mixes composition

Mix	Cement Ratio	Sand Ratio	RSS:C
M1	1	4.5	0.5
M2	1	4.5	0.65
M3	1	4.5	0.8
M4	1	4.5	1
Ref	1	4.5	0.77 (drinking water)

Raw sewage sludge was collected from Barnhart Sewage Treatment Works in Wolverhampton in the form of thick slurry (97.5% total water content). Collected Raw Sewage Sludge was later emptied into smaller containers (2.5 litre containers) and sent to a freezer. Raw Sewage Sludge samples were frozen for health and safety reasons and to prevent possible with time properties change as a result of natural decaying process. The cement used was Cem1 Portland Cement (PC) complies with the requirements of BS EN 197-1:2000 type CEM I Portland cement strength class 42.5/52.5N and used sand was size 0/4 that complies with the requirements of BS EN 12620:2002+A1:2008 category GF85.

CASTING, CURING AND TESTING

Cubes of 50 mm in size and specimens of dimensions 40mm x 40mm x 160mm were prepared. Specimens were casted in steel moulds, covered with plastic sheets and placed in a room at a temperature of 20°C for 24 hours until demoulding. Thereafter, cubes were cured for 28 days by wrapping them with sealed cling film (refer to Figure 1), while prisms were immediately placed in a room at 20°C to monitor length change. Cubes were used for the determination of compressive strength, specific gravity (SG), UPV and total water absorption, whereas the other specimens (prisms) were used to obtain drying shrinkage. For drying shrinkage specimens (prisms), 8mm in diameter steel locations disks were fixed on prisms' sides using superglue and length change was consecutively monitored using dial gauges (refer to Figure 2). For total water absorption, cured specimens were sent to oven at 75°C until a constant weight and thereafter were immersed in shallow water until full saturation was achieved.

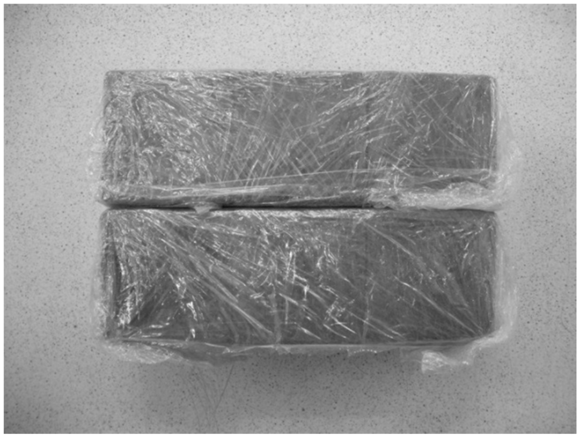

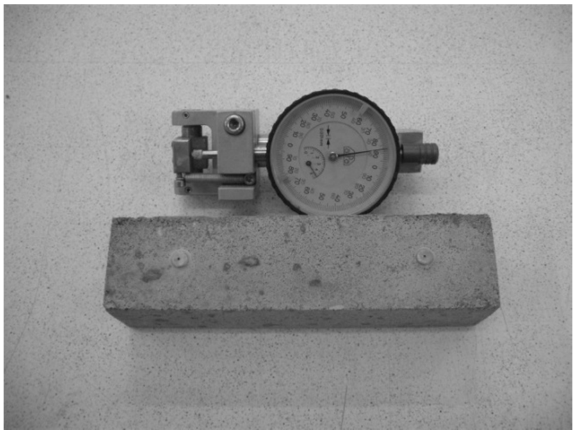

Figure 1: Specimens curing **Figure 2**: Length change monitoring

RESULTS AND DISCUSSION

The compressive strength of mortar mixes at 28 curing days is shown in Figure 3. There is a systematic trend in compressive strength for the various mixes and results showed that the less the amount of RSS/C ratio the greater the value of compressive strength and the best result of 36.0 Mpa was achieved for M1 with RSS/C ratio of 0.5. The compressive strength for M3 was about 59.6% of what was achieved for reference mix (Ref).

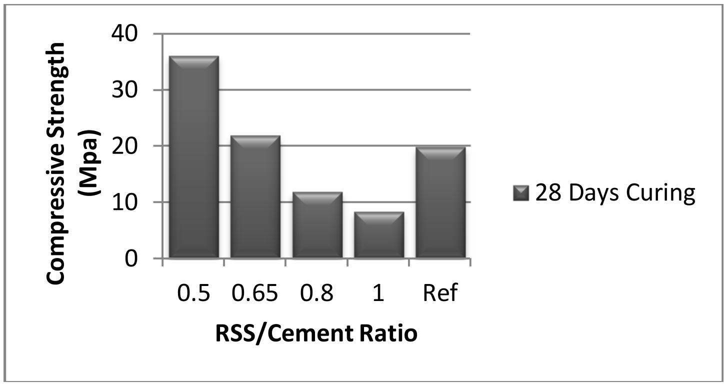

Figure 3: Compressive strength for mixes with RSS and with Water (Ref)

Specific gravity (SG) for mixes with RSS and water at 28 curing days is shown in Figure 4 below. The result showed that SG is systematically declining with the increasing of RSS amount and the best value of 2.28 was observed for M1. SG value for M3 was 96.7% of Ref mix. Ultrasonic pulse velocity (UPV) results (refer to Figure 5) showed an orderly trend, as the values of UPV rose with the reduction of RSS ratios and the best result of 4110 m/s was obtained for M1. The UPV value for M3 was about 95.3% of the reference mix (Ref).

Figure 6 below shows the results for total water absorption for mixes at 28 curing days. Total water absorption is an indirect method to determine air voids content in mortar mixes. Results showed a systematic increase in total water absorption with the increase of RSS amount. The best result of 6.4% was observed in M1, as well as, it was noted that there was not a considerable difference in total water absorption for M3 and Ref. Results for draying shrinkage after 28 days is shown in Figure 7 below, which shows a clear tendency of higher shrinkage values for mixes with higher RSS content.

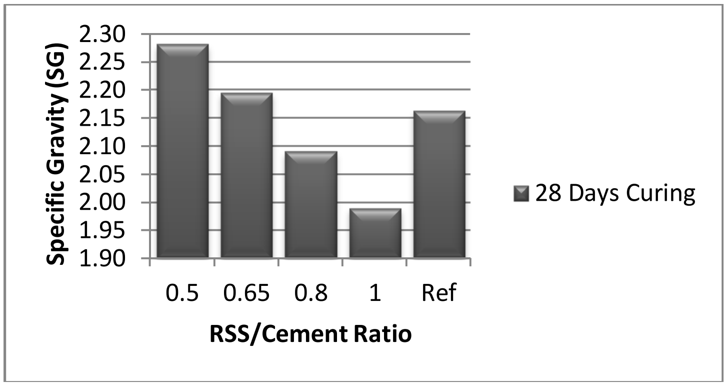

Figure 4: Specific gravity (SG) for mixes with RSS and with Water (Ref)

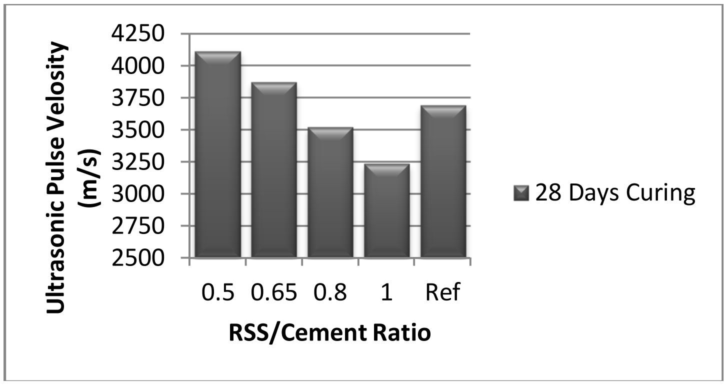

Figure 5: Ultrasonic pulse velocity (UPV) for mixes with RSS and with Water (Ref)

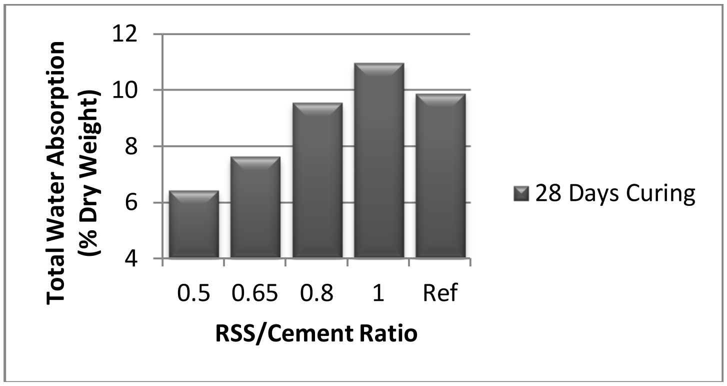

Figure 6: Total water absorption for mixes with RSS and with Water (Ref)

CONCLUSION

Results showed that RSS could potentially be used as a water replacement in cement based materials for the production of construction materials. Mixes incorporating RSS presented relatively good engineering properties in comparison with mix incorporating drinking water. Engineering properties were mainly affected by the amount of RSS added, as with the decreasing of RSS amount the better the engineering properties. This included compressive strength, specific gravity, UPV, total water absorption and drying shrinkage. The best properties was achieved in M1 (0.5 RSS:C). The amount of RSS added should be designed carefully to meet the required engineering properties.

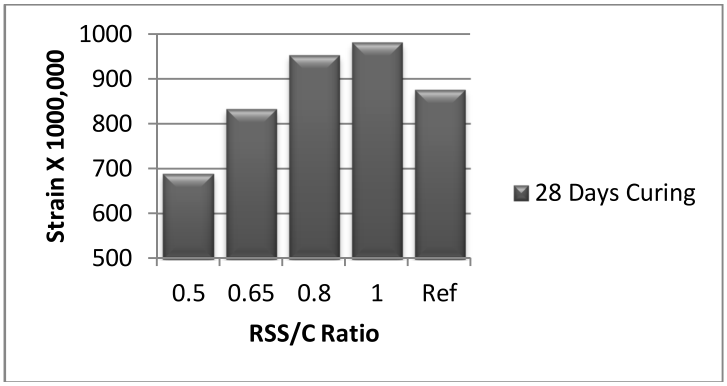

Figure 7: Drying shrinkage for mixes with RSS and with Water (Ref)

The outcome of this research could see huge financial savings to current economic constraints by the by-passing of current traditional RSS treatments. This would also lead to the reduction in huge amounts of energy consumption. Furthermore, there are huge environmental benefits from the prevention of RSS being transported to landfills and incinerators.

ACKNOWLEDGEMENT

The authors would like to acknowledge the support of technical staff in the laboratory, Mr G. Cooper and Mr R. Bradley- School of Technology-University of Wolverhampton.

REFERENCES

Cheilas, A., M. Katsioti, et al. (2007). "Impact of hardening conditions on to stabilized/solidified products of cement–sewage sludge–jarosite/alunite." Cement and Concrete Composites **29**(4): 263-269.

Cyr, M., M. Coutand, et al. (2007). "Technological and environmental behavior of sewage sludge ash (SSA) in cement-based materials." Cement and Concrete Research 37(8): 1278-1289.

DEFRA. (2007). "Waste strategy for England, Annex C6: Sewage Sludge." 17/10/2010.

Garcés, P., M. Pérez Carrión, et al. (2008). "Mechanical and physical properties of cement blended with sewage sludge ash." Waste Management 28(12): 2495-2502.

Metcalf & Eddy Inc. (1991). Wastewater engineering : treatment, disposal, reuse. Singapore, McGraw-Hill.

Monzó, J., J. Payá, et al. (1998). "Mechanical behavior of mortars containing sewage sludge ash (SSA) and Portland cements with different tricalcium aluminate content."

Mun, K. (2007). "Development and tests of lightweight aggregate using sewage sludge for nonstructural concrete." Construction and Building Materials 21(7): 1583-1588.

Valls, S. (2001). "Leaching properties of stabilised/solidified cement-admixtures-sewage sludges systems."

Valls, S. (2004). "Physical and mechanical properties of concrete with added dry sludge from a sewage treatment plant." Cement and Concrete Research 34(12): 2203-2208.

Wang, K., I. Chiou, et al. (2005). "Lightweight properties and pore structure of foamed material made from sewage sludge ash." Construction and Building Materials 19(8): 627-633.

Waste on line. "Sewage Sludge." Retrieved 4/9/2006, from http://www.wasteonline.org.uk/resources/Wasteguide/mn_wastetypes_sewagesludge.html/.

Yagüe, A., S. Valls, et al. (2005). "Durability of concrete with addition of dry sludge from waste water treatment plants." Cement and Concrete Research 35(6): 1064-1073.

REMOVAL OF ACID-GASES FROM DIGESTED SLUDGE USING MICROBUBBLE GENERATED BY FLUIDIC OSCILLATION

Mahamood K. H. Al-Mashhadani**,** Stephen J.Wilkinson, William B. Zimmerman
Department of Chemical and Biological Engineering, University of Sheffield, Mappin Street, Sheffield S1 3JD, United Kingdom

ABSTRACT: Anaerobic digestion is commonly used for nutrient and energy recovery from biomass. The largest share of biogases is generated through mesophilic anaerobic digestion yet. The remaining dissolved gases in the digested sludge still can cause pejorative effects on the environment, as well as disrupting operations such as corrosion of piping and process equipment. Moreover, continuous generation of biogas in digested sludge increases cavitation phenomena and exacerbates pump load. The present paper addresses the mechanism of post anaerobic digestion of digested sludge for removal of acid gases (CO_2 and H_2S) using microbubbles generated by fluidic oscillator. Design and simulation of gaslift bioreactor are presented. Throughout seven days of processing, the experimental data showed that the removal of carbon dioxide and hydrogen sulphide were more than that for the conventional digester.

INTRODUCTION

In wastewater treatment plant, an anaerobic digester is a processing unit, in which organic materials is broken down by anaerobic bacteria in the absence of oxygen through four steps (hydrolysis, acidogenesis, acetatogenesis and methanogenesis) to produce CH_4, CO_2 and trace of gases H_2S and N_2. The hydraulic retention time (HRT) applied in conventional mesophilic anaerobic digesters is normally in the range of 20 days, after which the sludge is discharged as effluent(Appels et al.,2008, Metcalf and Eddy, 2003). The digested sludge (effluent) contains organic matters biodegradable and some dissolved gases, for example CO_2 and H_2S that have a negative impact on the pipelines and eventually cause problems to the downstream units. Corrosion is one potential problem in metal pipelines. In addition, continuous generation of biogas in the digested sludge during its transfer and handling could lead to a creation of gas-liquid mixture; which, even if little, causes reduction of performance of pumps due to cavitation phenomena. In addition, and due to large density differences between the two phases, the gas and liquid tend to separate in pipelines and the pumps, consequently, handling this mixture will become a difficult task and inefficient (Lester and phil 1969, Garber and Ohara, 1972).

The present paper addresses utilization of a gaslift bioreactor (GLR) for removal of acid gases (CO_2 and H_2S) from digested sludge. Due to advantages over stirred tanks for instance, no moving parts inside the reactor, low cost of instillation and maintenance, and low energy consumption, gaslift reactors have been widely used in various biological processes. Nevertheless, it still needs further advanced technical developments to increase the efficiency of mass and heat transfer rates at the gas-liquid interface. This challenge can be solved by equipping the GLR with *microbubbles* generation.

In spite of the successive developments of microbubble generation systems, the energy requirements are still reasonably high. Zimmerman et al. (2009 and 2011) have developed a novel aeration system by fluidic oscillation, which is capable of producing gas bubbles with micron size to achieve a great heat and mass transfer rate, as well as an increased mixing efficiency by reducing the bubble diameter. The hydrodynamic stabilisation, longer residence times, and low energy demands could be achieved by using this technique. The essential idea of this novel system is to limit the required time for growth of the bubble by using fluidic oscillator, and hence, prevents the bubble size to grow bigger as shown in Figure (1). Al-Mashhadani et al.(2012) used this technology for stripping carbon dioxide. They reported that the efficiency of CO_2 stripping was about 29% more than that for fine bubble sparging.

ISBN 9780976885351

Therefore, the present article suggested, also, using this technique with gaslift digester for removal the acid cases.

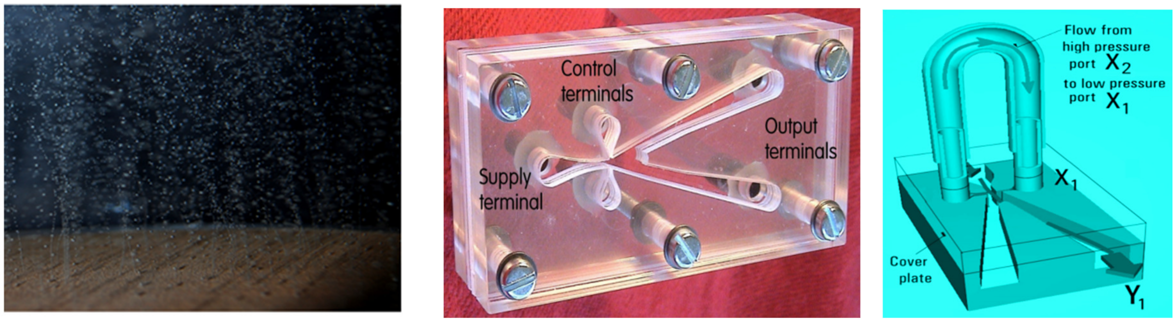

Microbubble generation fluidic oscillator

FIGURE1 Microbubbles generated by fluidic oscillator and fluidic jet-deflection amplifier

MATERIALS AND METHODS

In this study, experimental work is carried out with two bench-scale gaslift anaerobic digesters. Each digester has an overall volume of 15 litres with a working volume of 9 litres of digested sludge collected from a wastewater treatment plant in Sheffield city, UK. The gaslift digester was fitted with a circular ceramic diffuser at the bottom zone for nitrogen sparging which was generated by using a nitrogen gas generator (Peak Scientific Ltd). Before sparging, purity of generated nitrogen, which was about 99.9%, was checked by using gas analyzer (Gas data analyzer, Model 0518). The working duration of the experimental work was seven days under mesophilic conditions (i.e temperature was about 34±1^{o}C). The time of bubbling was set at one hour per day for 170 hours, and the average flow rate was 300±50 ml/min. Continuous measurement of biogas production was accomplished by downward displacement of acidified water (0.2 M HCL, pH<4). Concentration of CO_2 and H_2S was measured by the biogas analyzer.

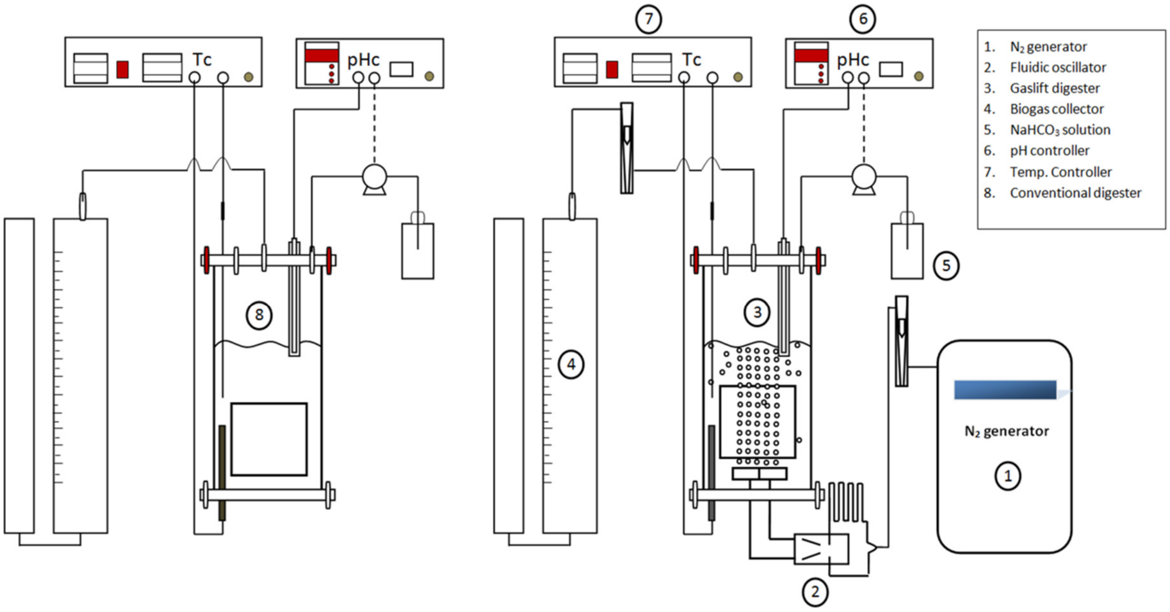

FIGURE2 A schematic diagram of the experimental apparatus

In duplicate conditions, the two digesters were sparged with pure nitrogen just in first day to provide an anaerobic environment. Then bubbling starts with the gaslift digester only. A schematic diagram of the experimental apparatus is shown in Figure (2).

MICROBUBBLE SIZE ANALYSIS

The micro-bubbles size generated by fluidic oscillator was analysed in the present study. The analysis was carried out using water as a liquid and air as a gas, while the measure of micro-bubbles size was achieved by high speed camera and image processing software. Estimate of the bubble diameter depended on the assumption that the shape of the micro-bubble is circular shape. Study of distributed size analysis for micro-bubbles was achieved using a ceramic diffuser and fluidic oscillator with same air flow rate (300 ml/min). The image containing more than 130 bubbles was analysed. The average diameter of these bubbles was 550 μm. Figure (3) shows the micro-bubbles with diameter 400-500 μm have relative frequency of 0.37 higher than other diameters, while the lowest relative frequency was in the range 0-400 of bubble diameter. It can be seen that the range 400-600 was more dominant than any other sizes with 64%.

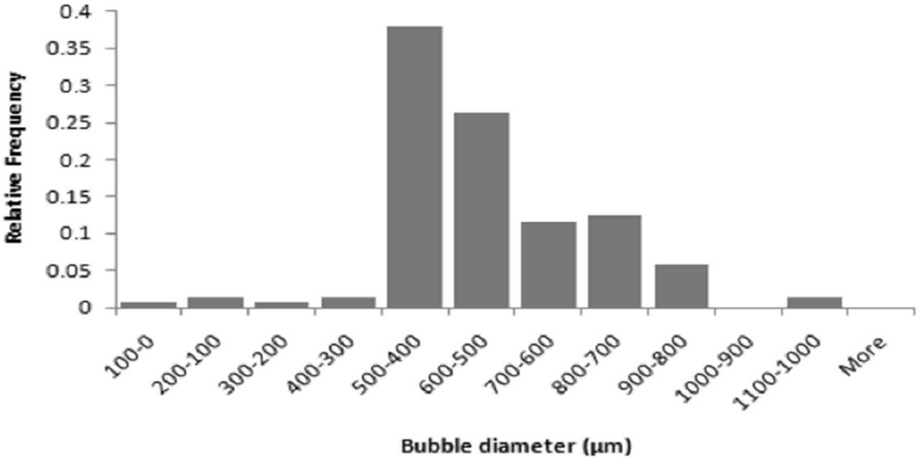

FIGURE3 Micro-bubble size distribution using ceramic diffuser

SIMULATION OF GASLIFT DIGESTER

Since the sludge is, usually, dark colour slurry containing organic materials, solids, bacteria, and various nutrients, it is difficult to visibly see the efficiency in the mixing process even when using high-speed cameras, due to their opaque characteristic. Therefore, use of simulation programs is necessary to study the efficiency of mixing in the anaerobic digester. The gaslift digester used in the present paper was designed as shown in the figure (4, a). In addition, and in order to investigate the proposed design, the gaslift digester with microbubbles generator, was simulated using COMSOL Multiphysics version 4.1. The gas concentration and arrows and streamlines of the liquid velocity during 120 seconds are presented in figure (4, b).

The microbubble size in the present simulation is the same that used in our experimental work (i.e. 550 microns). Many parameters were tested with this simulation, for example, position of diffuser, diameter of draft tube, liquid velocity, gas velocity, dead zones, and penetration of bubble at different bubble sizes. According to these parameters the proposal design was assembled.

RESULTS AND DISCUSSION

Removal of Produced Carbon Dioxide. The ability of the gases to stay in a liquid phase is mainly dependent on their relative solubility. Because water content in digested sludge is about 95%, whereas the remaining 5% consist of micro-organisms, organic matters, elements and suspended solids. The carbon dioxide, relatively, has a higher solubility compared with other gases. Thus, it would stay in digested sludge as (CO_2 (aq)) longer time than other gases. Produced carbon dioxide, which dissolved in sludge, converts to CO_2(aq), and then reacts with water to produce carbonic acid. According to kinetic conditions, 0.2% of carbon dioxide only, converts to carbonic acid ($H_2CO_{3(l)}$) and its ions; whilst, 99.8% of the carbon dioxide remains as dissolved gas CO_2 (aq).

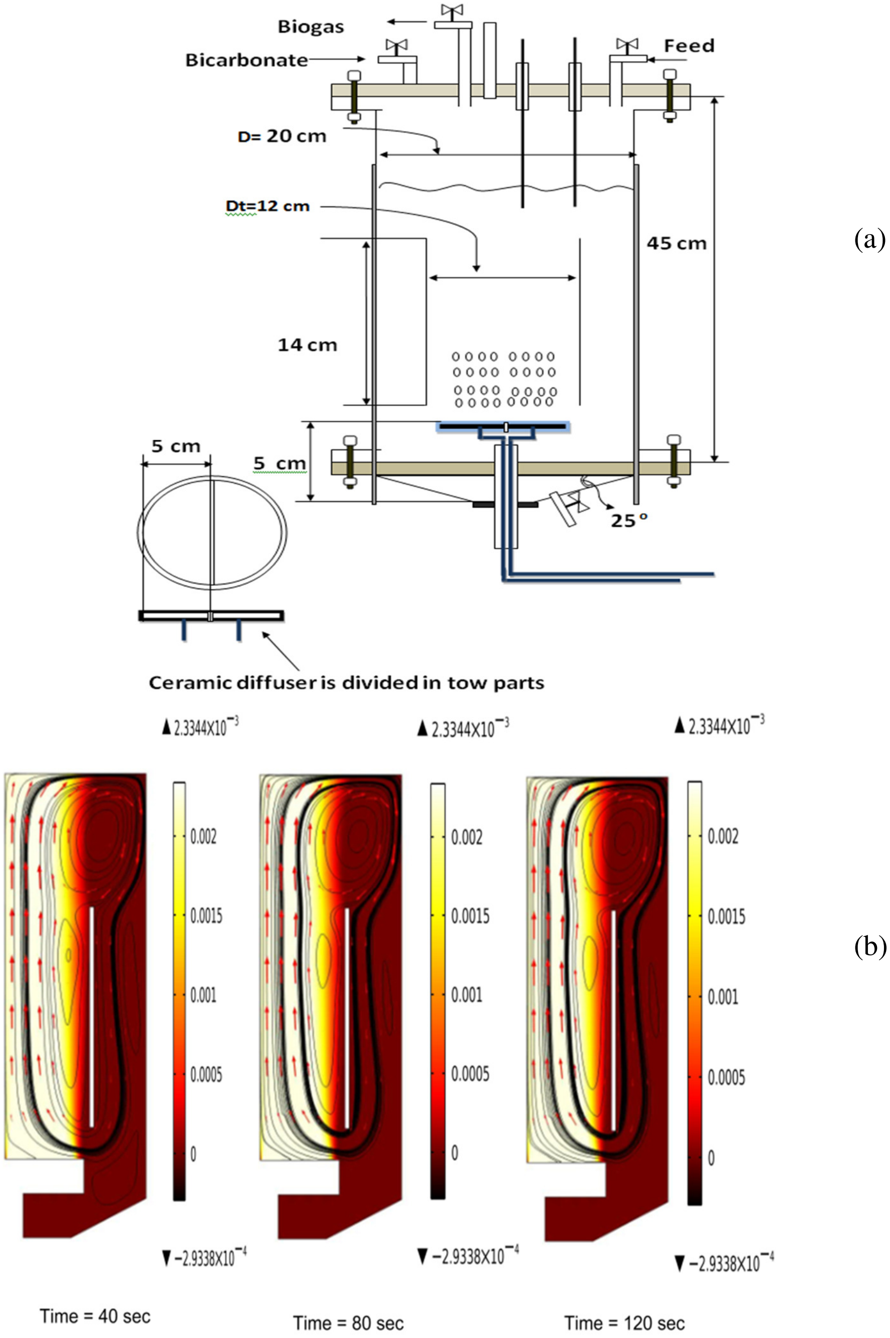

FIGURE4 (a) Design of gaslift digester used and (b) Snapshot of gas concentration and arrows streamlines of the liquid velocity after 120 sec with microbubble diameter 550 um.

$$CO_{2(g)} \leftrightarrow CO_{2(aq)} \qquad (1)$$

$$CO_{2(aq)} + H_2O_{(l)} \leftrightarrow H_2CO_{3(l)} \qquad (2)$$

Carbonic acid is a diprotic acid, thus it contains two hydrogen atoms ionisable in water and dissociates into bicarbonate and carbonate ions as shown in the following equations:

$$H_2CO_3 \leftrightarrow HCO_3^- + H^+ \qquad (3)$$

$$HCO_3^- \leftrightarrow CO_3^{2-} + H^+ \qquad (4)$$

Hence, the presence of dissolved carbon dioxide in digested sludge produces two hydrogen ions that would lead to decreasing the pH values. However, generally, the pH was observed to be stable in gaslift anaerobic digester as well as in the conventional anaerobic digester during the experimental work, except for a little change in gaslift digester was observed during sparging nitrogen as shown in the Figure (5). The reason was that the produced carbonic acid from dissolved carbon dioxide was immediately buffered by the ammonia produced from biodegrading of proteins in the solution. Most of carbon dioxide adsorbed in the sludge was in the form of "dissolved gas"; until a suitable chance to transfer from digested sludge is available. Therefore; a driving force for this transfer is being created when nitrogen was sparged.

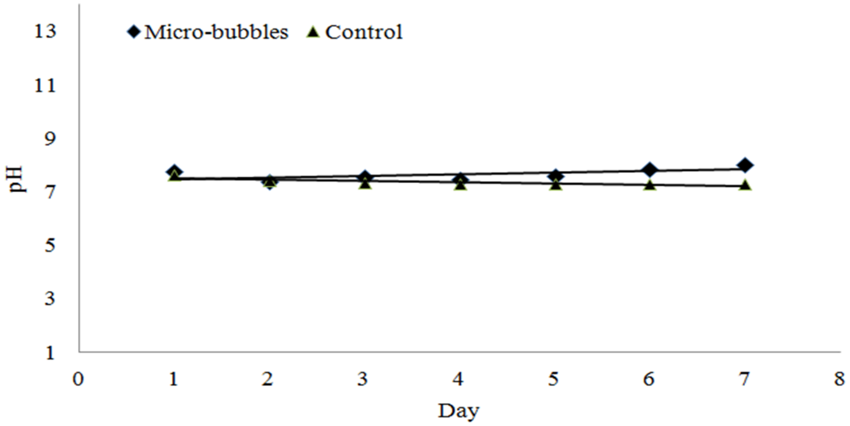

FIGURE5 pH values of both airlift digester and the conventional digester

Figure (6) shows trends of carbon dioxide production rate in the anaerobic digester with and without N_2 gas sparging. It is obvious that the bubbling system in the gaslift digester, highly contributed in stripping of produced carbon dioxide. With the use of micro-bubble technology of N_2 gas sparging, the CO_2 production has increased compared to that for the conventional digester. Experimentally, the characteristic complexity of the sludge has played an important role in enhancement of biogas stripping.

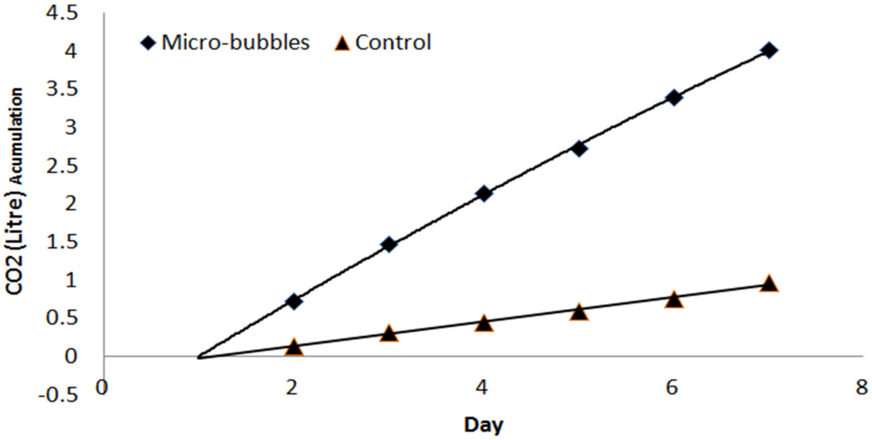

FIGURE6 Carbon dioxide produced from airlift digester with and without nitrogen bubbling

Removal of Produced Hydrogen Sulfide. By analogy H_2S, with its high solubility, should preferentially exist in an aqueous state in the sludge (e.g. $H_2S_{(aq)}$). When H_2S dissolves in sludge, the pH, also, would drop due to releasing hydrogen ions and forming week acid. Basically, the behaviour of the solubility of hydrogen sulphide is similar to carbon dioxide, as both gases form diprotic acid in water as is shown in following reactions:

$$H_2S_{(g)} \leftrightarrow H_2S_{(aq)} \qquad (5)$$

$$H_2S_{(aq)} \leftrightarrow HS^-_{(aq)} + H^+ \qquad (6)$$

$$HS^-_{(aq)} \leftrightarrow S^{2-}_{(aq)} + H^+ \qquad (7)$$

In an anaerobic digestion process, sulphate dissolved with a high concentration, can inhibit the generation of biogas produced from wastewater. The most important reason which leads to this inhibition is that the excessive accumulation of sulphate in wastewater encourages growth of the sulphate-reducing bacteria, which consume the acetic acid and hydrogen that are the main food for other bacteria to produce biogas (Hilton and Archer 1988). This competition between the sulphate-reducing bacteria and other bacteria on consumption the hydrogen are dependent on thermodynamic conditions (i.e. Gibbs free energy). The previous study suggested that the concentration of H_2S in the reactor can be taken as an indicator of inhibition of the biogas (Geradi, 2003).

In the current article, removal of dissolved H_2S, which produced in anaerobic conditions, from sludge is a necessary practice in order to prevent odours from digested sludge or corrosion in pipelines and control systems, thus, causing problems to downstream units. Normally, the removal of CO_2 and H_2S procedure takes place either by generated biogas or by contact with head space at the top of reactor (headspace). However, these methods are insufficient to remove all dissolved gases in the sludge. Mechanical mixing of the digested sludge capable to remove theses gases by the digester provides intimate contact between the sludge and bubbles of biogas or headspace. However; the characteristics of digested sludge requires high energy to achieve good mixing. Using a gaslift digester with microbubble generated by fluidic oscillation, with low energy requirements, can contribute to remove most of the generated hydrogen sulphate. Figure (7) shows the hydrogen sulphide removal from digested sludge during nitrogen bubbling. The figure indicates with one hour of nitrogen, sparging as microbubbles, increased removal of hydrogen sulphate as order of magnitude more than the unsparged conventional digester.

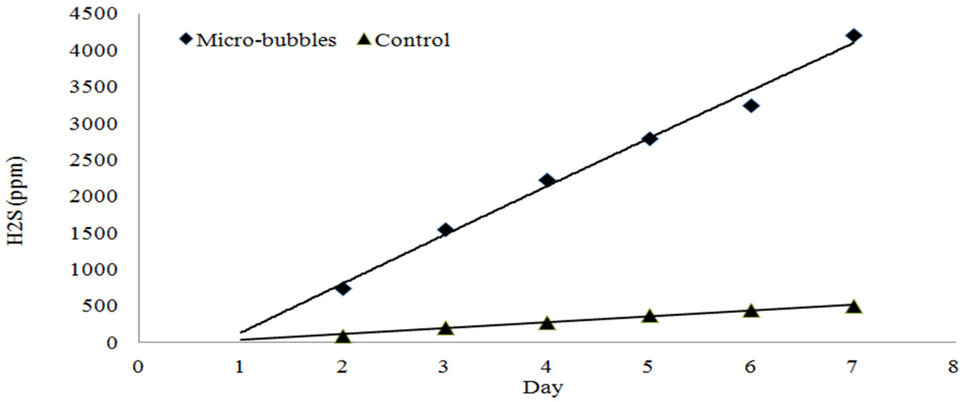

FIGURE7 Hydrogen sulphate produced from anaerobic digestion with and without nitrogen sparging.

From above, it can be summarised that the benefits of a gaslift bioreactor with microbubbles are illustrated through above results. Low energy, good mixing, and enhancement of gas stripping are the most important of characteristics of the gaslift bioreactor that were utilized in this study. More stripping of carbon dioxide and hydrogen sulphate were obtained from this utilization. Finally, the current paper has shown one of important applications, which utilized the proposal design and micro-bubble generated by fluidic oscillator with great mixing for stripping with lower energy requirements. In addition, there are various applications which take advantage of this technology. The results which obtained from this study, showed, also, that using the gaslift bioreactor with microbubble technology can leads to increase the efficiency of mass transfer between gas-liquid contact systems.

CONCLUSION

This paper addresses the mechanism of post anaerobic digestion of pre-digested sludge for removal of acid gases (CO_2 and H_2S). The benefits of the application of gaslift bioreactor with microbubble generated by fluidic oscillator for removal CO_2 and H_2S from digested sludge are demonstrated in this work. The proposed design of this application was simulated in the present article using COMSOL Multiphysics. Throughout 170 hours of processing, the experimental data showed that the removal of carbon dioxide and hydrogen sulphide, in gaslift anaerobic digester with microbubble generated by fluidic oscillator were more than that for the conventional digester.

ACKNOWLEDGMENT

W.Z. would like to acknowledge support from the EPSRC (Grant No. EP/I019790/1). W.Z. would like to acknowledge the Royal Society for a Brian Mercer Innovation award and the Royal Academy of Engineering for an industrial secondment with AECOM Design Build. MKHaM would like to thank the Iraqi Ministry of Education for a doctoral scholarship. S. W. acknowledges support from the ChELSI Institute and MWH UK Limited.

REFERENCE

AL-Mashhadani MKH, Bandalusena HCH, Zimmerman WB, 2012, "CO_2 mass transfer induced through an airlift loop by a microbubble cloud generated by fluidic oscillation", *Industrial and Engineering Chemistry Research*, 51 (4): pp 1864–1877.

Appels L., Baeyens, J., Degreve J. Dewil R. 2008, "Principles and potential of the anaerobic digestion of waste-activated sludge", *Progress in Energy and Combustion Science*, 34:755-781.

Garber, W. F. Ohara, G. T. 1972,"Operation and maintenance experience in screening digested sludge" *Journal Water Pollution Control Federation,* 44**:** 1518-1526.

Gerardi M. H. *Microbiology of anaerobic digestion.* John Wiley and sons, Inc., publication, 2003.

Hilton, M. G., Archer, D. B. 1988, "Anaerobic digestion of a sulfate-rich molasses wastewater: Inhibition of hydrogen sulfide production", *Biotechnology and Bioengineering*, 31, 885-888.

Lester W. G. S., Phil M. A. D. 1969, Temperature and fluid property effects on cavitation in Aircraft fuel pumps, Eng. Phys. Dept. Farnborough C. P. No. 1128

Metcalf and Eddy, .*Wastewater Engineering Treatment and Reuse*. Fourth edition, McGraw Hill, 2003

Zimmerman W.B., Hewakandamby B.N. , Tesar V. , Bandulasena H.C.H., Omotowa O. A. 2009 "On the design and simulation of an airlift loop bioreactor with microbubble generation by fluidic oscillation", *Food and Bioproducts Processing*, 87:215-227.

Zimmerman, W. B., Tesař, V., Bandulasena, H. C. H. 2011. "Towards energy efficient nanobubble generation with fluidic oscillation". *Current Opinion in Colloid and Interface Science*, 16, 350-356.

DEGRADATION AND MICROBIAL PROFILES IN SINGLE-STAGE AND 2-PHASE CSTR SLUDGE DIGESTION

Guo C H, Maspolim Y, Xiao K K, Zhou Y and Ng W J (Nanyang Environment & Water Research Institute, Nanyang Technological University, Singapore)
Zhai B, and Yeo K C (Keppel Environmental Technology Centre Pte Ltd, Singapore)

The degradation of mixed sewage sludge in single-stage and 2-phase systems was investigated in laboratory scale CSTR reactors. For example, the results showed hydrolysis and acidogenesis were achieved in the acid reactor operated at 5 days HRT and pH 5.5. The VFAs produced (with propionic acid predominant) were subsequently degraded in the methane reactor operated at 25 days HRT and pH 7. The 2-phase system achieved 42.97% TCOD and 34.29% VS reduction, compared to 38.67% TCOD and 30.84% VS reduction achieved in the single-stage system operated at 30 days HRT and pH 7. Methane was 45%, 68% and 66.9% in the gas from the acid, methane and single-stage reactors, respectively; the production rate of methane in the 2-phase system was about 8% more compared to the single-stage system. The microbial communities in the reactors were analysed by qPCR using primer/probes specific for orders of Archaea involved in methanogenesis. Hydrogen and acetate utilizing methanogens were present but hydrogen utilizing methanogens were predominant in all three reactors. The relevance of the predominance of the hydrogen utilizing methanogens in process design shall be discussed. Relative abundance of methanogens in the acid reactor was, as expected from the VFA production, lower compared to the methane and single-stage reactors. Acidogenic and methanogenic process dynamic studies showed that loadings on the acid and methane reactors in the 2-phase system have potential for further increase.

ISBN 9780976885351

APPLICATION OF CASCADE DIELECTRIC BARRIER DISCHARGE PLASMA ATOMIZERS FOR WASTE WATER TREATMENT

Wameath S. Abdul-Majeed, Esther Karunakaran, Catherine Biggs, and William B. Zimmerman
(Department of Chemical and Biological Engineering, The University of Sheffield, Sheffield, UK)

ABSTRACT: In this work, we apply a novel design for a cascade dielectric barrier discharge (DBD) atomizer for treating samples of water containing biological and organic contaminants. Several experimental investigations are conducted on artificial samples and a real waste water sample (Digested sludge collected from a WWTP). The artificial water samples are prepared by using different concentrations of *E.coli* for biological samples whereas acetic acid is used to prepare the organic samples. The biological samples are subjected to the plasma effect for different treatment periods and the growth curves of *E.coli* are generated for 24 hours after treatment. Moreover, the viable cells are counted after each treatment period and the change in *E.coli* morphology was monitored. The results show that a significant reduction in the viable cell number, by 3 orders of magnitude, occurs for an artificial biological sample after only five minutes treatment. The treatment of organic samples for 10 minutes shows a significant reduction in the concentration of acetic acid by 50 %. Furthermore, treatment of real waste water sample for 10 minutes results in more than 70% reduction in BOD_5 and 30% reduction in COD.

INTRODUCTION

An efficient scheme applied in the fields of waste water treatment is to subject target bulk material to a strong electrical field, which is utilized for treating different levels of organic and biological contaminants (Miichi et al., 2000; Sunka, 2001; Akiyama, 2000). Generally speaking, applying streamer discharges in the liquid phase results in several effects such as inducing highly energetic electrons and producing chemically active species as well as UV radiation and shock waves. These effects are able to decompose practically any kind of compound and result in water disinfection. Plasma discharge may cause direct effects from electron collisions or other effects caused by molecular, ionic or radical species such as the pyrolysis and photolysis reactions. On the other hand, the mechanism of biological cell degradation due to application of an electrical field is attributed to the phenomenon called electromechanical compression. Applying a sufficient electrical field could result in creation of pores in the membrane, which consequently causes a disruption of its biological structure. If the ratio of the total pores to the total membrane area becomes significant, the membrane will not be able to repair the disruption and such effects (e.g. electroporation or electrofusion) might be formed. Other studies reported that the electrical field could result in either local action due to the chemical reactions in plasma bulk or non local action due to the UV radiation and shock waves (Locke et al., 2006).

It is worth noting that UV radiation in the range of (200-400 nm) may induce organism mutation (i.e. mutagenic effects), whereas the shock waves in the range (5 – 20 kBar) could lead to deform the structure of the cell. The shock waves could be formed due to the effect of electrohydraulic discharge when a plasma channel is rapidly expanded leading to different radical reactions. In this regard, two kinds of radical reactions are distinguished in the literature and attributed to the electrohydraulic cavitations phenomenon; namely pyrolytic reactions and indirect free radicals reactions. The interaction between the aforementioned effects would consequently lead to deactivate the microorganisms and dissociate the organic compounds in the contaminated sample of water.

In most studies shown in the literature, the treatments of aqueous samples by applying a high potential field are conducted in batch mode; i.e. a bulk of water is subjected to a strong electrical field for known periods. The adoption of a high potential field for treatment of waste water disposal from industrial

---

ISBN 9780976885351

applications requires development of unique reactor able to impose online, continuous effects on the disposed stream with high efficiency.

It is hypothesized in this research that an annular plasma reactor based on dielectric barrier discharge (DBD) concept is appropriate to conduct the online continuous treatment for a water stream disposed from a contaminated source. An important microplasma category is the dielectric barrier discharge (DBD), which is also referred to as silent discharges. It was invented for ozone generation and utilized later for other applications such as surface treatment and waste gas treatment. DBD microplasma is non-thermodynamic equilibrium plasma formed at low or atmospheric pressure systems and classified to be cold plasma, in which the electron temperature is much higher than the temperature of heavy particles. The important feature of the DBD plasma atomizer is its low operating cost, which is attributed to limited gas and power consumption. The light weight and possibility of embedding the DBD atomizer in proximity with other compartments, are other advantages. Practically, DBD discharges are considered ideal for several applications due to availability of high electron energy (1- 10 eV) while keeping the gas at room temperature (Karanassios, 2004; Zhu et al., 2008).

In this research, we examined a novel design cascade annular DBD atomizer for treating artificial samples contain organic and biological contaminants as well as a real waste water sample collected from a waste water treatment plant. The work is described in three sections. An overview on the design parameters and the equipment used is described in the materials and methods section. The experimental investigations and the results are described in the results and discussion section, while the research outcomes are summarized in the conclusions section.

MATERIALS AND METHODS

Design of a cascade annular DBD atomizer and the equipment used. A cascade annular DBD atomizer has been designed as illustrated in figure (1A). The main concept is to utilize two atomization stages combined in series and separated by an interface in the centre, which is used to insert supporting gas. The gas inserted from the centre interface could be similar to that applied from the top section, or could be different gas. The insertion of different gas from the centre interface is aimed to imply changes in plasma characteristics, which might eventually affect the plasma chemistry and the radical's formation. The outer shell cylinder (10 mm ID, 12 mm OD) was made of quartz glass to enable the spectrometric data acquisition in the UV region, whereas the inner cylinder was a simple glass test tube (6 mm ID, 7 mm OD).

It is worth noting that the inner glass tube, which houses the live electrode, has been wrapped with a metal strip (very fine diameter) to form a corrugated screw shape on the outer surface. The aim is to generate a thin film of the falling liquid along the electrode which would result in several advantageous effects such as rapid release of any generated species and efficient contact between the falling film and the UV radiation. Two experimental sets were conducted, the first by applying one cascade atomizer whereas two cascade atomizers linked in series were adopted in the second experimental set to maintain longer irradiation time for the sample, as illustrated in figure (1B). A single channel peristaltic pump with a feed rate 2.8 ml/min (Williamson pumps Ltd. – UK) was used to inject the liquid sample into a T-junction (3 mm ID). A supporting gas (a dried air at 20 ml/min) was also injected through the T-junction in order to generate air/water plasma in the top section of the cascade atomizer, which gives rise for active species and radical formation in the system. In other experiments, argon (35 ml/min) is also injected to the system from the centre interface in addition to the main air stream. The resulted liquid/gas mixture was directed from the T-junction through a Tygon tubing (3 mm ID, 30 cm length) into the first cascade atomizer, in which approximately 5 seconds estimated for the sample irradiation. In the case of applying two cascade atomizers, the outlet stream from the first atomizer is directed into the top section of the second atomizer, and the total irradiation period in both atomizers is estimated to be approximately 15 seconds. Some treatment experiments are conducted by re-circulating the examined sample through a single and two DBD atomization stages for different periods; this is to deduce the enhancement in treatment efficiency. The air and argon gas flow rates are controlled manually by using gas flow meters purchased from (BOC special products – UK). A high voltage power source from (Entwicklung Leistungselectronic – Germany) and USB 2000 spectrometer integrated with Spectra Suite software from Ocean Optics are applied, the full details of these devices are described in (Abdul-Majeed et al., 2011).

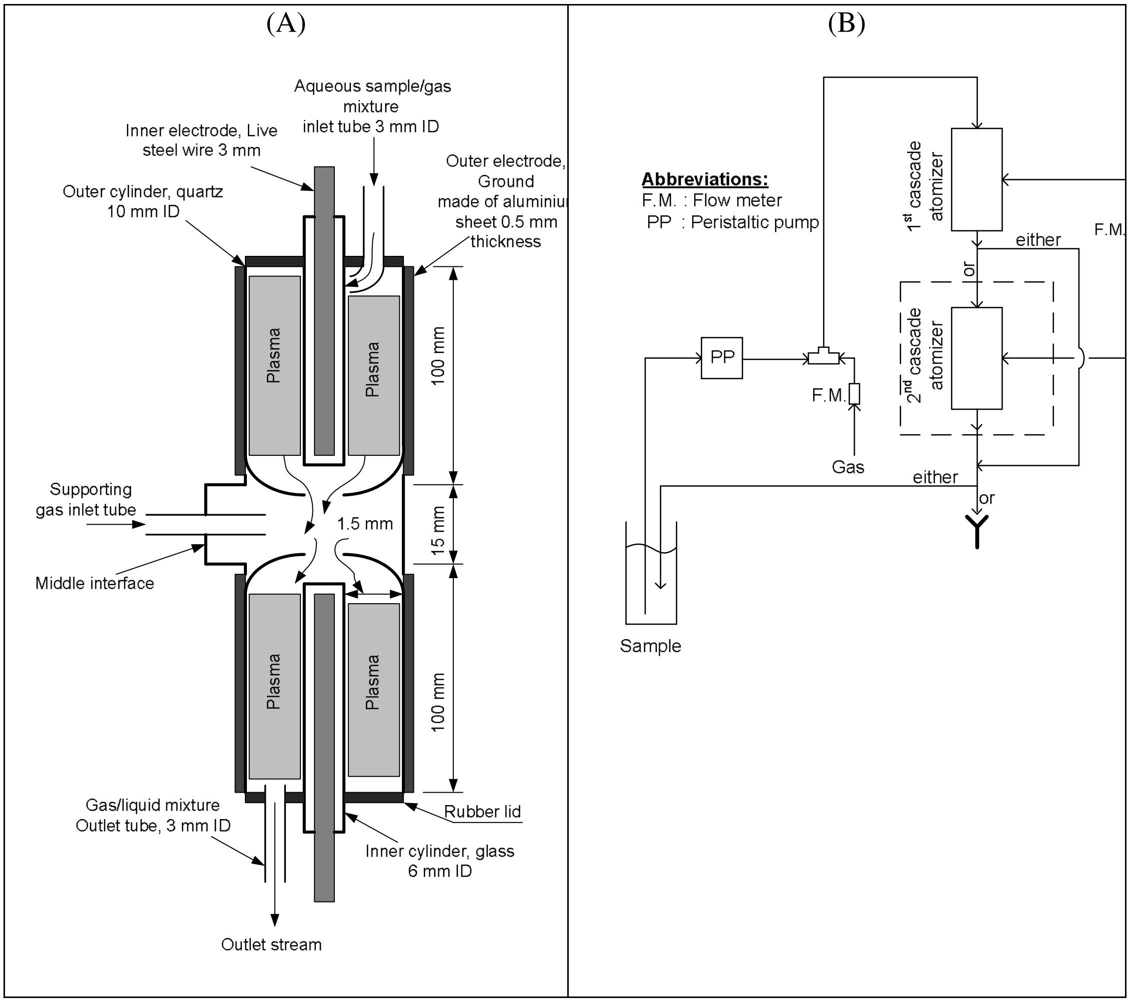

Figure 1. Treatment scheme; (A) annular DBD atomizer , (B) process flow diagram

Preparation of artificial organic and biological water samples. Two kinds of artificial samples, biological and organic were prepared and treated by using DBD plasma treatment scheme proposed in this study. The biological samples were prepared from (bacteria – *E. coli*) while acetic acid was used for organic samples preparation, as follows:

E. coli samples. All safety issues were taken into consideration when applying the full set of experiments in this part of work. The effect of the treatment on the viability of *E. coli* was assessed in this study by using two methods: 1) monitoring the lag in the batch growth curve during culturing treated cells in rich medium (Luria broth) , and 2) by using viable plate count technique.

Monitoring the growth of E.coli: Escherichia coli K-12 MG1655 was used in these experiments. *E. coli* was grown on LB agar medium (BPE1425, Fisher Scientific, UK; tryptone 10 g/L, yeast extract 5 g/L, sodium chloride 10 g/L, agar 15 g/L) from glycerol stocks (20% glycerol) stored in -80°C. The cells were transferred from LB agar to 5 ml LB broth (BPE1426, Fisher Scientific, UK; tryptone 10 g/L, yeast extract 5 g/L, sodium chloride 10 g/L) and grown for 16 hours at 37°C with aeration (orbital shaking at

200 rpm) for use as starter culture. The cells were diluted in fresh LB broth to the required concentrations measured as optical density at 595 nm (OD_{595}). The diluted cell suspensions were treated for different times in the annular DBD atomizer. The treated cells were incubated at 37°C and the increase in the optical density was measured at 595 nm every 30 minutes for 24 hours using a Tecan multi-well plate reader (Genios, UK). The growth curve was obtained as a plot of OD_{595} against time. Un-inoculated LB broth and untreated LB broth containing *E. coli* were set up as controls in the experiment. The results were reported as average and standard deviation of OD_{595} of cultures setup in 8 separate wells in a 96-well plate (TKT-180-070U, Fisher Scientific, UK) after a single round of treatment. The viability of cells after treatment was interpreted as being inversely proportional to the length of the lag phase in the growth curve of the treated cells when compared to that of the untreated controls.

Viable plate counts: Starter cultures of *E. coli* were grown in 5 ml of LB medium for 16 hours at 37°C. After incubation, the cells were harvested by centrifugation at 5000 xg for 10 minutes. The supernatant containing spent culture medium was discarded and the cells were washed and re-suspended in 5 ml sterile distilled water. The OD_{595} of the cell suspension was measured and the starter culture was diluted to 0.5 OD_{595}. The diluted cell suspensions were treated for different times in the annular DBD atomizer. An untreated control was setup in the experiment. The controls and the samples were serially diluted (dilution factor of untreated control 10^6; dilution factor of treated samples 10^4) and plated on LB agar plates. The dilution factors differed between the untreated control and the treated samples to account for the potential reduction in the number of viable cells in the sample. The agar plates were incubated overnight at 37°C. The resulting colonies were counted and adjusted with the appropriate dilution factors to obtain the number of viable cells in the samples and the untreated control.

Organic samples. Acetic acid (CH_3COOH, 99.8% - from BDH) was used to prepare artificial samples of different concentrations through dilution with distilled water.

RESULTS AND DISCUSSION

Treatment of biological samples – *E. coli* The effect of the treatment strategy on the biological components of the waste water was tested by subjecting pure cultures of *E. coli* grown in nutrient-rich medium, Luria broth, to viability tests after the treatment process. A semi-quantitative approach to viability testing based on batch growth curves, was undertaken in this study. As outlined in the Methods section, the relative number of viable cells in the treated samples was defined by the length of the lag phase in a typical batch growth curve of *E. coli* , which means the length of the lag phase increases proportionally with the decrease in the concentration of viable cells. As a proof of concept, different starting concentrations of *E. coli* were subjected to batch growth. The results (figure 2A) demonstrate the increase in the lag phase with a decrease in the initial concentration, represented by the number of viable cells of *E. coli*. The effect of treatment time on the reduction in the number of viable cells was then determined. *E.coli* diluted to a starting concentration of 0.5 OD_{595} was treated for different time intervals then subjected to batch growth. The increase in the length of the lag phase in the treated samples when compared to the untreated control (UTC) suggests a reduction in the viability of the cells after treatment, figure (2B).

The results shown in figure (2B) also suggest that the efficiency of the treatment, demonstrated by the reduction of viable cells number, increases in a time dependent manner with 20 minutes resulting in the most reduction of viable cells. Two separate replicates from different starting cultures (biological replicates) were setup for the UTC to determine the magnitude of biological variation in the batch growth of *E. coli*. Although the viability of *E. coli* was reduced significantly after plasma treatment, it was questionable whether the reduction has occurred due to the effects on the live cells or nutrient deterioration (e.g. Peptone in the culture medium). In this sense, two separate experiments were conducted, in which the effect of treatment conditions on the nutrients in the culture medium is investigated by monitoring the growth of *E. coli* in LB subject to different treatment times. The progressive reduction in the ability of *E. coli* to grow in LB medium treated for increasing periods of time suggest that the treatment indeed targeted the nutrients in the culture medium. Therefore, the effect of the treatment conditions on the viability of *E. coli* was investigated by using a viable plate count assay. As outlined in the Methods section, a $0.5OD_{595}$ suspension of *E. coli* in sterile distilled water was subjected to treatment for different periods. Viable plate counts were made of the treated samples and compared to that of the untreated control. The results show that the treatment is certainly proved effective against *E. coli* and significantly reduced the number of viable cells, from approximately 5×10^7 cells in the untreated control to approximately 5×10^4 cells (3 orders of magnitude) after only 5 minutes of treatment. The treated samples were visualised under a light microscope, where an extensive lysis of cells was seen (irregular shapes) with no change in the structure of the intact cells, figure (3A).

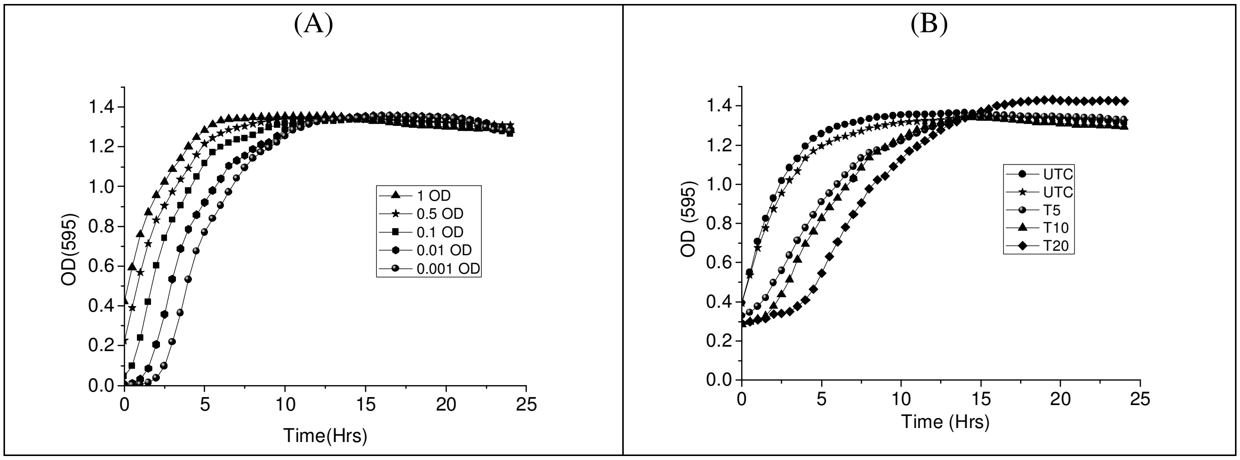

Figure 2. Growth curves generated for *E. coli* grown in LB media; (A) several concentrations of *E. coli* (1, 0.5, 0.1, 0.01, and 0.001 OD_{595}) grown at normal conditions (37 °C for 24 hours), (B) UTC (two samples) indicates untreated *E. coli* samples (at 0.5 OD_{595} concentration) grown at normal conditions, while T5, T10, and T20 refers to a 0.5 OD_{595} *E. coli* samples treated for 5, 10, and 20 minutes respectively and then grown at normal conditions.

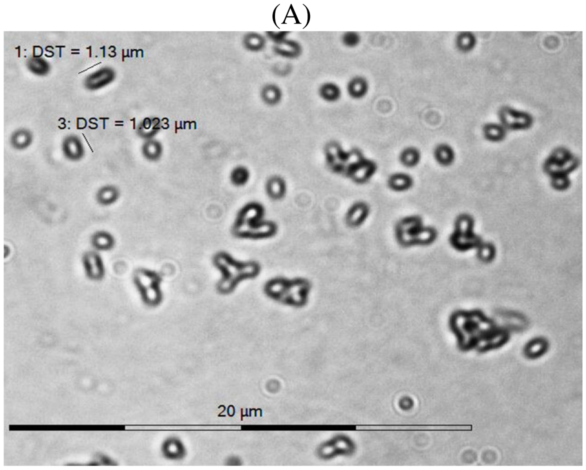

(B)

Figure 3. Treatment results; (A) a picture shows *E. coli* after 25 minutes treatment where the unaffected cells appears either circular or cylindrical while the lysed cells form irregular shapes, (B) the spectrum recorded when applying (water + air + argon) plasma in the annular DBD atomizer

Taken together, the results of the above experiments demonstrate the exceptional efficiency of the DBD plasma treatment not only in reducing the number of viable *E. coli* in the samples but also in the treatment of organic components in the nutrient medium. The reduction in the bacteria activity could be attributed to a well known treatment mechanisms such as live cell destruction which is occurred due to the electrical field (electroporation), the species produced in plasma bulk (e.g. O_3, H_2O_2, OH^* , H^*), the thermal effects as well as UV radiation. It should be mentioned that the temperature of the re-circulated solution through the DBD atomizer was measured outside the plasma bulk and found to be 40 ^{o}C after 20 minutes circulation, which indicates a limited thermal effect has occurred.

It is noteworthy that OH species were clearly observed in the spectrum recorded from the annular DBD atomizer, figure (3B), especially in the band (302 to 317 nm) which was characterized to be OH molecular emission lines (Zhu et al., 2008). The signal at 309 nm was attributed to OH in the relaxation state $(\mathrm{A}^{2}\,{}^{\Sigma^{+}}\,(\mathrm{v}=0) \rightarrow \mathrm{x}^{2}\Pi\,(\mathrm{v}=0)$ (Shih and Locke, 2010), whereas the signal at 317 nm could be related to OH in the excited state.

Treatment of artificial organic samples Other valuable impact of DBD plasma was observed during the treatment of organics in the examined sample. The mechanism speculated for organic contaminants degradation in waste water was attributed to the hydroxyl radicals attack on the organic molecules which results in fragmenting the double bond long chain molecules, forming single bond molecules or even dissociating the molecules into other forms (Locke et al., 2006). Several experimental investigations conducted in this study on artificial samples based on acetic acid, in which the treatment effect was deduced by applying titration with 0.1 mol/L ($NaOH$) as well as measuring the interfacial tension and the absorbance at 241 nm before and after treatment. The results show a proportional reduction in the quantity of $NaOH$ amount that required for titration occurred in accordance with treatment time. Ultimately, about 50% reduction in the acetic acid concentration (for a sample contains 0.57 acetic acid/1.0 water) has resulted after 10 minutes treatment. Other proof of acetic acid dissociation is the increase in the measured interfacial tension (up to 14%) which has occurred after treating sample contains 1.2 acetic acid / 1.0 water. Moreover, the absorbance of the sample containing 0.57 acetic acid / 1.0 water is increased by 14% after 10 minutes treatment and could be attributed to the formation of other species due to acetic acid fragmentation. Upon comparing several treatment schemes based on applying one and two annular DBD atomizers, linked in series, as well increasing the applied power, the results show that applying two cascade atomizers lead to better treatment efficiency even when applying higher power rate in a single atomizer. Although the treatment scheme has combined many factors, it could be interpreted that longer contact time with UV radiation is more effective than other parameters.

Treatment of real waste water sample Other experiments were conducted to analyse real waste water sample (digested sludge), collected from a waste water treatment plant. The treatment scheme has been applied by utilizing one cascade atomizer and circulating the sample for 10 minutes. Accordingly, the five days biological oxygen demand (BOD$_5$) and the chemical oxygen demand (COD) were measured for the samples before and after treatment by using reagents purchased from (Hanch Lange Ltd. - UK) and applying the protocol specified by the company. The results show a reduction of 30% and more than 70% in the values of COD and BOD$_5$ has occurred respectively after treatment. Moreover, the colour of the treated sample was changed from dark brown to whitish, which apparently emphasized the extensive treatment action achieved.

CONCLUSIONS

A treatment scheme based on a novel design annular DBD atomizer has been tested in this study for treating artificial samples of biological and organic contaminants as well as real waste water sample. The results show an exceptional treatment efficiency represented by the significant reduction in the viable cells number of *E-coli* by 3 orders of magnitude as well as considerable reduction in the measured values of COD and BOD$_5$ for real waste water sample. The treatment action has been attributed to several parameters led by the species generated in plasma bulk (e.g. OH radicals) as well as UV radiation and shock waves. The treatment results achieved promise the possibility of adopting the proposed scheme in the waste water treatment units upon producing optimized cascade DBD atomizers in a large scale. The developed design could be utilized to apply online treatment for a continuous waste water disposal. Further investigations are required in a pilot scale unit, which is planned for future work.

ACKNOWLEDGEMENTS

The authors thank Dr. Paul Dobson for helpful discussions. W. Abdul-Majeed acknowledges IMOHE for a doctoral scholarship. E. Karunakaran thanks EPSRC for a doctoral scholarship.

REFERENCES

Abdul-Majeed, W. S., J. Lozano Parada, and W. Zimmerman. 2011. "Optimization of a miniaturized DBD plasma chip for mercury detection in water samples." *Anal Bioanal Chem.* 401 (9): 2713-2722.

Akiyama, H. 2000. "Streamer discharges in liquids and their applications." *IEEE Trans. Dielectrics Electr. Insul.* 7: 646-653.

Karanassios, V. 2004. "Microplasmas for chemical analysis: analytical tools or research toys?. " *Spectrochimica Acta Part B*. 59: 909– 928.

Locke, B., M. Sato, P. Sunka, M. Hoffmann, and J. Chang. 2006. "Electrohydraulic discharge and nonthermal plasma for water treatment." *Industrial & engineering chemistry research.* 45**:** 882-905.

Miichi, T., N. Hayashi, S. Ihara, S. Satoh, and C. Yamabe. 2002. "Generation of radicals using discharge inside bubbles in water for water treatment." *Ozone Sci. Eng.* 24:471-477.

Shih, K., and B. Locke. 2010. "Optical and electrical diagnostics of the effects of conductivity on liquid phase electrical discharge." *Plasma Science, IEEE Transactions on***:** 1-10.

Sunka, P. 2001. "Pulse electrical discharges in water and their applications." *Phys. Plasmas*. 8: 2587-2594.

Zhu, Z., G. Chan, S. Ray, X. Zhang, and G. Hieftje. 2008. "Microplasma source based on a dielectric barrier discharge for the determination of mercury by atomic emission spectrometry."*Anal. Chem.* 80: 8622–8627.

EFFECT OF SEED SLUDGE TYPE ON AEROBIC GRANULATION AND TREATMENT EFFICIENCY OF GRANULES

Yusuf Çağatay Erşan[a,b], İrem Kocatürk[a] and ***Tuba Hande Erguder***[a] ([a]Middle East Technical University, Ankara, Turkey; [b]Abdullah Gul University, Kayseri, Turkey)

ABSTRACT: Two sequencing batch reactors seeded with different seed sludge type, namely, membrane bioreactor sludge (R1) and conventional activated sludge (R2), were operated to develop granular sludge and to investigate the effect of suspended seed sludge type on granulation. Granules were developed from both sludge types, but due to the free ammonia inhibition expected high removal efficiencies could not be achieved. During well operating conditions, COD removal efficiencies were 50-85% and 45-77% for R1 and R2, and total nitrogen removal efficiencies were generally between 35-46% and 20-44%, respectively. Although efficiencies were low relative to literature, there were enough implications to discriminate seed sludge types in terms of effectiveness. As a result, granules cultivated from membrane bioreactor sludge were found to be advantageous in terms of size, resistance to toxic effects, stability and recovery.

INTRODUCTION

Granular sludge as well as aerobic granules are more advantageous compared to suspended sludge for containing high amount of microorganisms in compact form, having high settling velocity, being resistant to toxic compounds and high loading rates. Therefore, aerobic granulation usually performed in sequencing batch reactors (SBRs) is offered as an efficient treatment technology for wastewater treatment (Liu and Tay, 2004). Yet, the studies on aerobic granulation are mainly limited to laboratory-scale researches. To our knowledge, there are only 2 municipal plants (1 pilot, 1 full-scale) and 3 industrial pilot plants started to operate since 2005 (Giesen et al., 2012). Main reason of this limitation is encountered with the stability of granular sludge due to the high growth rates of heterotrophic microorganisms (Adav et al., 2008).

Granular sludge is obtained by agglomeration of sludge flocs without adding any packing material. Driving forces for granulation are selective pressures like short settling time in SBRs, starvation and hydrodynamic shear forces. Exchange ratio, reactor design, substrate composition and seed sludge are also suggested to affect granulation (Liu and Tay, 2004; Adav et al., 2008). Most of these factors and their effects are still being studied. The researches on seed sludge mainly focus on the effect of the physical structure of the seed (initial floc size, crashed granules and pellet-form) on granulation (Xu et al., 2011; Verawaty et al., 2012). To our knowledge, all these researches were performed with activated sludge. There is a lack in literature on the effect of the seed sludge type of different sources on granulation and granular treatment. Therefore, in this study, two different sludge types, namely, membrane bioreactor (MBR) sludge and conventional activated sludge (CAS) were used in order to determine the effects of suspended seed sludge type on aerobic granulation process and the treatment efficiency of granules. This is a unique study about the effects of seed sludge type on aerobic granulation.

MATERIALS AND METHODS

Wastewater Composition and Seed Sludge. The synthetic wastewater content was arranged to compensate the dilution effect resultant of 50% exchange ratio. The composition of the two-times concentrated wastewater was as follows: COD 2000 mg/L (acetic acid as the carbon source, 1.78 mL/L); NH_4-N 400 mg/L; NO_3-N 80 mg/L; $NaHCO_3$ 3000 mg/L; $MgSO_4.7H_2O$ 180 mg/L; $CaCl_2.2H_2O$ 160

ISBN 9780976885351

mg/L; $Na_3PO_4.12H_2O$ 244 mg/L; yeast extract 2 mg/L; micro nutrients 0.6 ml/L (Smolders et al., 1994; Erguder and Demirer, 2005; Shi et al., 2010).

MBR sludge used in the experiments was obtained from METU-MBR Wastewater Treatment Plant. CAS was obtained from Ankara Municipal Wastewater Treatment Plant. Reactors were initially seeded with mixed liquor volatile suspended solids (MLVSS) concentration of 5000 mg/L.

Reactors and Operational Conditions. Two sequencing batch reactors (R1 and R2) with a height of 60 cm, diameter of 8 cm, effective volume of 2.45 L and exchange ratio of 50% were operated for 37 days with a cycle time of 6 h. Both reactors were operated under similar operational conditions. The only difference was the seed sludge type. R1 was seeded with MBR sludge while R2 was seeded with CAS. At the beginning of the operational period, MLVSS concentrations of R1 and R2 were 7670 ± 325 and 4570 ± 183 mg/L, respectively.

Before the operational period of 37 days, 2-days of acclimation period was applied. During acclimation period, one cycle consisted of 5 min of feeding, 120 min of anoxic period, 198 min of aerobic period, 35 min of settling period and 2 min of withdrawal period. After 2-days of acclimation, anoxic, aerobic and settling periods were changed in time as given in Table 1 to promote granulation and improve treatment efficiency. Reactors were operated at an upflow air velocity of 1.2 cm/s (during aerobic period) and a hydraulic retention time (HRT) of 12.3 h. Theoretical organic and nitrogen loading rates of the reactors were 2 g COD/L.d and 0.47 g N/L.d, respectively.

TABLE 1. Cycle details during operational period of 37 days

Periods	**Operation days**						
	1-5	**6-7**	**8-13**	**14-20**	**21-24**	**25-26**	**27-37**
Anoxic period	120	120	120	90	90	90	90
Aerobic period	208	213	218	248	253	255	258
Settling period	25	20	15	15	10	8	5

Analytical Methods. pH and DO values of reactor contents were measured at the middle of anoxic and aerobic periods via probes. Wastewater samples were collected at the beginning of the cycles (after feeding period; as the influent) and at the end of the anoxic and aerobic periods of the same cycles (as the effluents). Samples were analyzed for their sCOD, Total Ammonium Nitrogen (TAN), NO_2 and NO_3 contents after filtering through 0.45µm filter paper. sCOD, NO_3 and NO_2 were analyzed by EPA approved digestion method, ferric sulfate and cadmium reduction methods, respectively (Hach Water Analysis Handbook, 1989). NO_2 and NO_3 were also analyzed by Ion Chromatograph, when necessary. TAN, MLSS and MLVSS analyses were done according to Standard Methods (APHA, AWWA and WEF, 2005).

Granulation of sludge was observed through weekly sampling. Particle sizes were measured via ocular micrometer and light microscope (Leitz Wetzlar Microscope). Granule pictures were taken by 3.2 Megapixel camera. SVI_5 and SVI_{30} values were measured following the Standard Methods (APHA, AWWA and WEF, 2005) and used to determine percent of granulation in the sludge (Liu et al., 2010).

RESULTS

During anoxic period, average pH values of R1 and R2 contents were 8.2±0.4 and 8.3±0.2, respectively. During aerobic period, average pH values of R1 and R2 were recorded as 8.5±0.3 and 8.7±0.1, respectively. Dissolved oxygen (DO) concentrations of both reactor contents were in the range of 8.0-8.8 mg/L and 0.1-0.5 mg/L during aerobic and anoxic periods, respectively.

For better representation of operational conditions and results, operational period of 37 days was described in 3 periods. Period 1 corresponds to the Days 1-10, Period 2 (challenging conditions) to the Days 11-27 and Period 3 (recovery) to the Days 28-37. During Period 1, experimental influent concentrations were close to the theoretical influent values (i.e., 1000 mg/L COD, 200 mg/L TAN). During Period 2, treatment efficiencies of the reactors decreased. Due to cyclic nature of SBR operation, treatment efficiency of each cycle affects the influent concentration of the next cycle. In other words, the decrease in the removal efficiency of one cycle means the increased effluent concentrations, which results in the increase in the influent wastewater concentrations of the following cycle. During Period 2, due to the decrease in the treatment performances, the influent characteristics cumulatively increased. Therefore, before the start of Period 3, the contents of both reactors were washed with distilled water to achieve theoretical conditions. The average influent TAN concentrations of R1 during Periods 1, 2 and 3 were 263±73 mg/L, 343±25 mg/L and 250±44 mg/L, respectively, and of R2 were 240±73 mg/L, 327±21 mg/L, 248±45 mg/L (at the beginning of the cycles) for Periods 1, 2 and 3, respectively. Average influent COD values of R1 were 1252±92 mg/L, 1411±311 mg/L, 1154±73mg/L COD and of R2 were 1243±97 mg/L, 1226±145 mg/L, 1187±161 mg/L COD for Periods 1, 2 and 3, respectively.

Treatment Performances. Figure 1 shows the profiles of TAN concentrations and nitrification efficiencies (TAN removal efficiencies) observed during aerobic and anoxic periods of cycles. During experiments, TAN removal of both reactors was negligible during anoxic periods. During Period 1, nitrification efficiencies of R1 and R2 were fluctuating between 25-40% and 10-30%, respectively. In Period 2, the nitrification efficiency of R1 decreased and fluctuated around 10-20%. Average TAN removal in R1 was calculated as 12.5±5% (Table 2). R2, on the other hand, reached its maximum efficiency (45%) at the beginning of Period 2 only for one day. Following that day (Day 15), nitrification efficiency of R2 drastically decreased to 10-15%. After the reactors' content were washed with water and the theoretical influent concentrations were achieved (Period 3), the nitrification efficiency of R1 gradually recovered and increased to 40-45%. Yet, the nitrification efficiency of R2 remained same as in Period 2 and could not rise over 15% until the end of the operation.

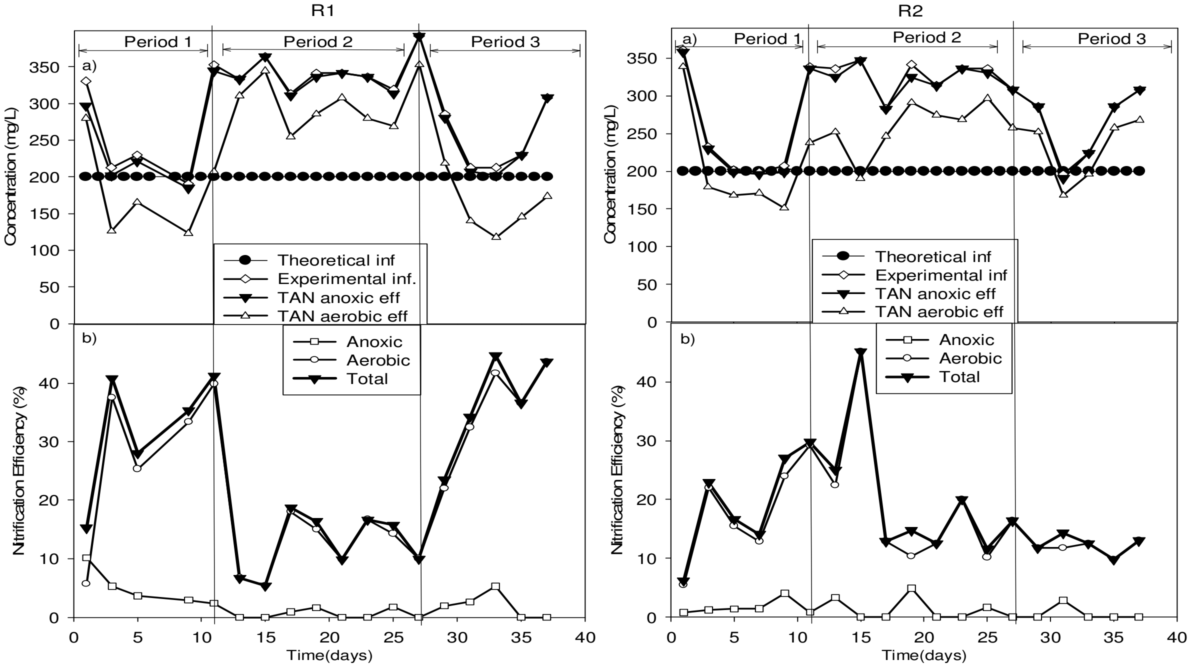

FIGURE 1. a) TAN concentrations of R1 (left figure) and R2 (right figure), b) TAN treatment efficiencies of R1 (left figure) and R2 (right figure)

Denitrification was achieved during both anoxic and aerobic periods of the cycles for both reactors (Table 2). Denitrification efficiencies fluctuated between 60% and 90%. Simultaneous denitrification (calculated from nitrogen loss) was also observed during aerobic periods of the cycles.

Average TAN and Total Nitrogen (TN) removal efficiencies were nearly similar. This was due to the high TAN content of TN and low nitrification efficiency.

Figure 2 shows the profiles of COD concentrations and removal efficiencies observed during the aerobic and anoxic periods of cycles. During Period 1, total COD removal efficiencies of R1 and R2 gradually increased from 47 to 85% and from 46 to 77%, respectively. During Period 2, the removal efficiencies of both reactors decreased to 30-35%. During Period 3, COD removal efficiency of R1 gradually increased, yet, the low COD removal performance of R2 remained still. The average COD removal efficiencies of R1 and R2 were calculated as 70±16 and 36±4%, respectively (Table 2).

TABLE 2. Average cyclic removal efficiencies (RE) of each operational period

Parameter	R1			R2		
	Period 1	Period 2	Period 3	Period 1	Period 2	Period 3
COD RE, %	70±13	39±12	70±16	67±11	54±15	36±4
TAN RE, %	32±11	13±5	37±8	20±8	16±11	12±2
Total Nitrogen (TN) RE, %	34±10	14±3	38±8	26±8	19±11	20±3
Denitrification in anoxic period-P, %	77±30	87±17	70±8	82±20	88±8	74±10
Denitrification in aerobic P., (mg/L)	9±1	-	18±11	10±3	-	8±1

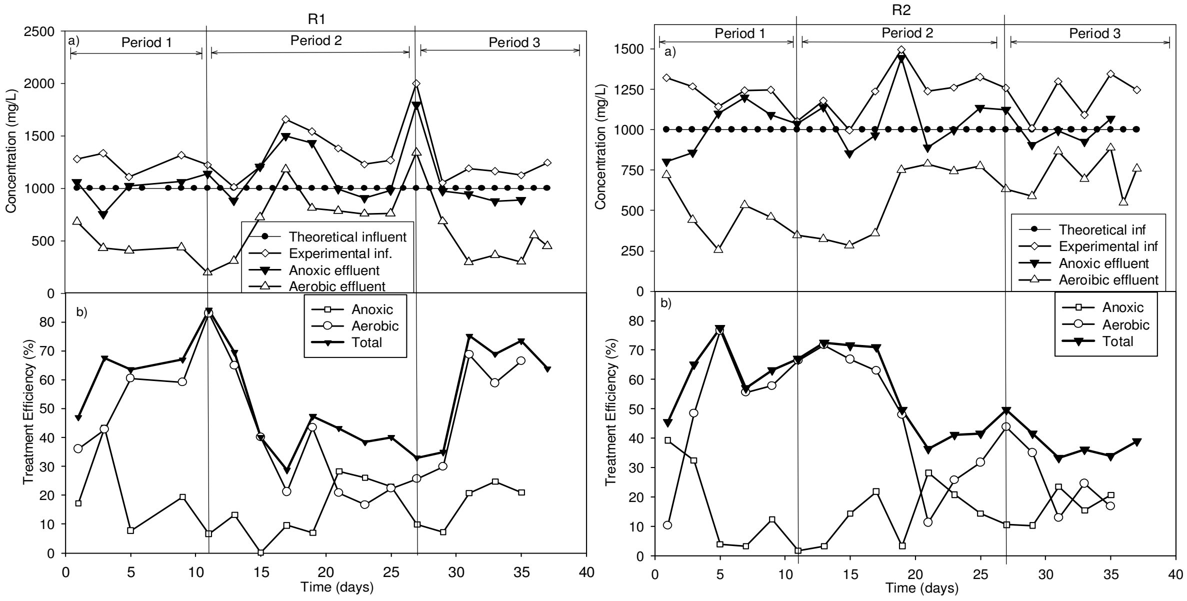

FIGURE 2. a) COD concentrations of R1 (left figure) and R2 (right figure), b) Treatment Efficiencies of R1 (left figure) and R2 (right figure)

Granulation. Both seed sludge types had a loose floc structure as shown in Figures 3a and 4a for R1 and R2, respectively. First granules were observed on Day 9 in both reactors. Granules randomly sampled from both reactors on Day 14 had compact structure and non-filamentous smooth outer surface (Figures 3b and 4b). The average particle sizes of the granules sampled from R1 and R2 on Day 14 were 1.58±0.83 and 2.19±0.82 mm, respectively. During Period 2, disintegration was observed for both reactors being severe in R2. Granules of R2 became loose and had filamentous structure, while R1 granules preserved their compact structure. The average particle sizes of the granules of R1 and R2 on Day 28 (Period 2) were 2.48±1.28 and 1.08±0.54 mm, respectively. During Period 3 (recovery period), R1 granules, despite the decrease in size, remained their intact structure, while R2 granules decreased in size and had a fluffy structure (Figures 3d and 4d). The average particle sizes of the granules sampled from R1 and R2 at the end of the experiment (Day 37) were 0.97± 0.47 and 0.56±0.23 mm, respectively.

Disintegration and degradation of the granules in R2 was also confirmed by the decreasing trends of VSS/TSS values and percent of granules through Periods 1 to 3, as well as lower settling velocities of R2 granules (Table 3). Granulation and disintegration patterns were also followed by extracellular polymeric substrates (EPS) of granules developed (data not shown). Protein- and carbohydrate-EPS contents of sludge in both reactors were similar (around 100 and 60-70 mg/g VSS, respectively). With the granulation, as expected, protein-EPS content increased to 180 and 150 mg/g VSS for R1 and R2 granules, respectively. However, with the decrease in removal efficiencies, protein-EPS contents of R1 and R2 granules significantly increased to almost 250-300 and 250-400 mg/g VSS, respectively. The increase continued up to 500 mg/g VSS in R2 during Period 3, indicating the stressful conditions and further disintegration/degradation.

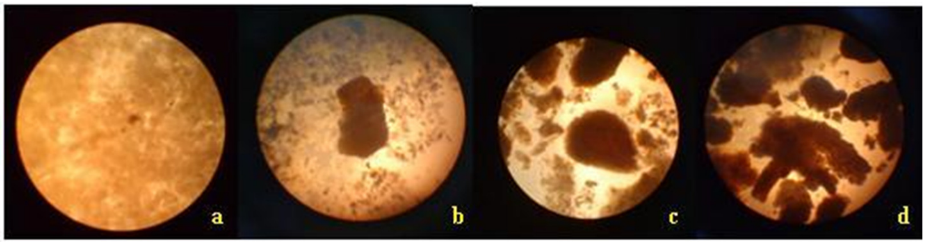

FIGURE 3. Granulation in R1 a) seed, b) day 14, c) day 28, d) day 37 (6.3 x 4 magnification)

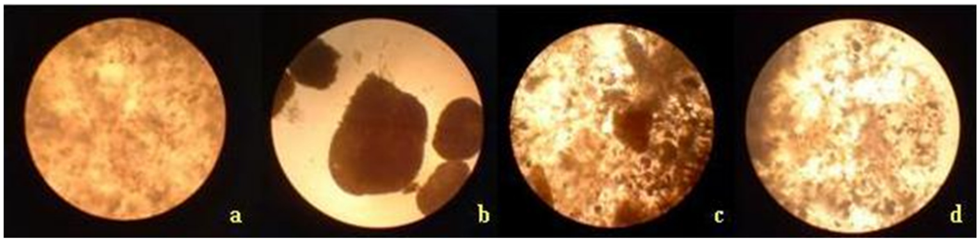

FIGURE 4. Granulation in R2 a) seed, b) day 14, c) day 28, d) day 37 (6.3 x 4 magnification)

TABLE 3. Characteristics of the flocs - granules of R1 and R2 in each operational period

Parameter	R1			R2		
	Period 1	Period 2	Period 3	Period 1	Period 2	Period 3
Granule percentage, %	34	37	32	33	37	22
Biomass in reactors, g/L	4.2	2	2.8	2.7	1.7	1.5
VSS/TSS	0.71	0.84	0.75	0.90	0.77	0.52
Granule settling velocity, m/h	-	36	39.6	-	19.1	20.2

DISCUSSION

Experiments indicated that both reactors seeded with different sludge types displayed similar COD treatment performances in Period 1. Yet, TN treatment performances were 10% and 20% higher in R1 compared to R2 during Periods 1 and 3, respectively. This was attributed to the source of sludge which is MBR system (for R1) designed for nitrogen removal. On the other hand, CAS system (source of R2) achieves only carbon removal. At the beginning of Period 2, free ammonia (FA) concentrations in R1 and R2 increased from 19 mg N/L to 32 mg N/L (at pH 8.4, T=20^{o}C) and from 26 mg N/L to 38.7 mg N/L (at pH 8.5, T=20^{o}C), respectively. COD and TAN removal efficiencies of both reactors further decreased and displayed similar low performances. This was attributed to the inhibitory FA concentrations of 32-39 mg N/L, which is comparable to the findings of Yang et al. (2004). Yang et al. (2004) reported that the increase in FA concentration to 39.6 mg N/L decreased the specific oxygen uptake rates of aerobic heterotrophs and nitrifiers by 5 and 2.5 times, respectively. After the concentrated reactor contents were washed away in Period 3, R1 recovered. Yet, low treatment performances and disintegration of granular sludge in R2 continued, which was related to the seed sludge type used.

Both seeds followed a similar granulation pattern during Period 1. However, during high FA concentrations and high COD and TAN loading rates as in Period 2 (32-39 mg/L NH_3-N, 2.4 g-2.8 g COD/L.d, 0.76-0.80 g N/L.d), and during Period 3, R1 granules remained their intact structure unlike those of R2. In addition, R1 granules recovered faster than R2 granules.

CONCLUSION

This study revealed the seed sludge type to be effective in achievement of stable granular structure and better recovery performance. Granules of 0.56±0.23 mm to 2.48±1.28 mm were developed from both suspended sludge cultures under the operational conditions studied. Yet, the granules cultivated from MBR seed had regular and smooth shape, better settleability, higher biomass retention, higher ability to withstand at high loading rates (0.8 g N/L and 2.8 g COD/L) and more tolerant to toxicity (32-39 mg/L NH_3-N) when compared to granules cultivated from CAS seed. MBR granules+sludge had capacity to recover much better and acclimate to the new conditions much faster than that of CAS.

The highest removal efficiencies for MBR and CAS seeded reactors were recorded as 85% COD – 46% TN, and 77% COD – 45% TN, respectively. Even these highest values were lower compared to the nutrient removal systems, which was attributed to the low granulation percent of the sludge. Optimum SBR operational conditions and nutrient contents should be further researched to improve treatment performances and to achieve full granulation.

ACKNOWLEDGEMENTS

The authors wish to thank The Scientific and Technological Research Council of Turkey for the support of this study with Project No 111Y176.

REFERENCES

Adav, S.S., D.J. Lee, K.Y. Show, and J.H. Tay. 2008. “Aerobic granular sludge: Recent advances.” *Biotechnol. Adv.* 26: 411-423.

APHA, AWWA, WEF, 2005. *Standard Methods for the Examination of Water and Wastewater.* 21st ed., American Public Health Association Press, Washington, DC.

Erguder, T.H., and G.N. Demirer. 2005. “Granulation of a mixture of suspended anaerobic and aerobic cultures under alternating anaerobic / microaerobic / aerobic conditions: A preliminary study.” *J. Chem. Technol. Biotechnol.* 80(7): 837-842.

Giesen A., R. Niermans, and M. van Loosdrecht. 2012. “Aerobic granular biomass: the new standard for domestic and industrial wastewater treatment?” *Water21* April: 28-30.

Hach Water Analysis Handbook, 1989. Hach Company, Colorado, U.S.A.

Liu, Y., and J.H. Tay. 2004. “State of art of biogranulation technology for wastewater treatment.” *Biotech. Adv*. 22: 533-563.

Liu, Y.Q., B. Moy, Y.H. Kong and J.H. Tay. 2010. “Formation, physical characteristics and microbial community structure of aerobic granules in a pilot-scale sequencing batch reactor for real wastewater treatment.” *Enzyme Microbial. Technol.* 46: 520-525.

Shi, X.Y., G.P. Sheng, X.Y. Li, and H.Q.Yu. 2010. “Operation of a sequencing batch reactor for cultivating autotrophic nitrifying granules.” *Biores. Technol.* 101: 2960-2964.

Smolders, G.J.F., J. van der Meij, and M. van Loosdrecht. 1994. “Model of the anaerobic metabolism of the biological phosphorus removal process: stocihiometry and pH influence.” *Biotechnol. Bioeng.* 43(6): 461-470.

Verawaty, M., M. Pijuan, Z. Yuan, and P.L. Bond. 2012. “Determining the mechanisms for aerobic granulation from mixed seed of floccular and crushed granules in activated sludge wastewater treatment.” *Wat. Res.* 46: 761-771.

Xu, H.C., P.J. He, G.Z. Wang, and L.M. Shao. 2011. “Effects of activated sludge flocs and pellets seeds on aerobic granule properties.” *J. Environ. Sci.* 23(4): 537-544.

Yang, S.F., J.W. Tay, and Y. Liu. 2004. “Inhibition of free ammonia to the formation of aerobic granules.*” Biochem. Eng. Journal* 17: 41-48.

ANALYSIS OF PHARMACEUTICAL AND ESTROGEN CONTAMINANTS FROM A RURAL WASTEWATER TREATMENT FACILITY

Xiaolin Li and ***Wei Zheng**** (Illinois Sustainable Technology Center, University of Illinois, Champaign, IL, USA)
Walton R. Kelly (Illinois State Water Survey, University of Illinois, Champaign, IL, USA)

Rural communities in the United States usually use a series of aerated lagoons to treat domestic wastewater. Effluent from these systems is typically discharged to a receiving creek or stream, which leads to a potential transfer of untreated hormone and pharmaceutical residues from sanitary sewage to the environment. The primary objective of this study is to identify and quantify pharmaceutical and estrogen contaminants in a lagoon wastewater treatment facility, to investigate the removal efficiency of these emerging contaminants in the treatment processes, and to monitor their occurrence in the surrounding watershed. In this study, a method has been developed for the trace analysis of thirteen pharmaceuticals and personal care products (PPCPs) and seven steroid estrogens in various waters. Among all of the PPCPs considered, ten chemicals were detected in sewage influents, lagoon waters of different treatment stages, or effluents at concentrations in the ng L-1 to low mg L-1 range. Three estrogens were observed in the influents at total concentrations as high as 164 ng L-1, but no estrogen residues were detected in the effluents. It indicates that the aerated lagoons may effectively remove estrogen contaminants. With the exception of carbamazepine, removal rates for the other nine PPCPs were relatively high with a range of 65.1~100%. But the removal efficiency of nine PPCPs in the wastewater treatment facility exhibited large temporal variability. The concentrations of PPCPs in the lagoon waters and effluents collected in November were 1-2 orders of magnitude higher than those sampled in September, suggesting that the temperature significantly impacts the aerobic biodegradation of PPCPs in the aerated lagoons. Occurrence of these compounds in the surrounding watershed was also monitored. The discharge of effluents significantly elevated the PPCP concentrations in the receiving creek. Most of PPCPs were still detected in the adjacent river, 10 km downstream of the rural wastewater treatment facility.

*Email: wzheng@istc.illinois.edu

BIODEGRADATION OF HIGHLY CONTAMINATED PENTACHLOROPHENOL PROCESSWATER

H. Borazjani, K. Wallace Walker, and S. Langroodi
(Mississippi Forest Products Department, Mississippi State University, MS, USA)

ABSTRACT: This study included two phases. In phase I, the efficacy of a pure culture, *Arthrobacter sp.*was evaluated in bioreactors containing pentachlorophenol(PCP)processwater during a period of 120 days. This bacterium was found to be highly effective in degrading PCP and its carrier oil. The biochemical oxygen demand (BOD), chemical oxygen demand (COD), and toxicity of the wastewater were also significantly reduced. In phase II, the usefulness of the *Arthrobacter sp.* was further explored in a cell immobilization silica and celite column study. A solution of mineral salt media containing PCP passed through the columns and effluents collected every 24 hours. . The effluent analytical results revealed that this method of treatment appeared to be more useful as physical than a biological method of PCP removal.

INTRODUCTION

PCP has been used extensively since its development by the Monsanto chemical company in 1935. In 1981, the use of this chemical in the US was estimated at 23 million Kg per year(Crosby *et al.* 1981).

PCP is most frequently used as wood preservatives for utility poles.There are over 160 million utility poles in service in North America. Currently, pentachlorophenol is used for treatment of 50% of utility poles in the US(KeshaniLangroodi *et al.* 2011, Morrell 2003). Although the products of the wood preserving industry do not represent a threat to the environment during use, accidental spilage and improper disposal methods have resulted in extensive contamination of some surface water and ground aquifers. Sites with this type of contamination are considered hazardous and require remedial action. In 1974, it was estimated that only 60% of the wood treatment plants in the wood treatment plants in the United States met water pollution standards, while 17% of the plants released their waste without any treatment (Walker *et al.* 1976). Since 1974, wastewater disposal regulations have become more stringent. These regulations have spurred research to develop more effective and economical methods of treating contaminated waste water.

One of the safest and most economical forms of remediation is degradation by microorganisms. This form of treatment is called bioremediation. The process uses microorganisms to reduce the quantity and toxicity of organic compounds in hazardous waste. The objective of this study was to determine the effectiveness of a selected microorganism(*Arthrobacter sp*) in the degrading PCP contaminated wastewater from wood treating facilities under batch tank reactor conditions. The ability of a pure culture, *Arthrobacter sp.,* to degrade PCP was also examined in a phase II by a cell immobilization study.

METHODS AND MATERIALS

ISBN 9780976885351

Phase I . The processwater used in phase I and II of this study was untreated process water obtained from wood treating facilities in Wiggins, Mississippi. This water contained high levels of oil and PCP. The wastewater was plated on nutrient agar to determine the presence of viable organisms. No growth was observed. The bacterium *Arthrobacter sp.* used for treatment in Phase I and Phase II of this study was first isolated previously from the process water of a wood treatment plant in Joplin, Missouri. This bacteria has been characterized as an *Arthrobacter sp.(Borazjani et al. 1990, Samuel 1991)* .

Treatment Condition. Three 16.5 liter batch bioreactors containing wastewater were seeded with bacteria in Phase I of this study. Environmental conditions were regulated to ensure optimum growth conditions for the bacteria. Air was supplied to the reactors at a rate of 2.5 liters per minute by a 30.5 mm sparge and room temperature ranged from 22-24 °C. The total nitrogen and phosphorous content and pH of the wastewater were analyzed periodically to ensure that nutrient levels were adequate. The microbial population was monitored throughout the treatment period.

Theprocesswater was sampled every 15 days in phase I and every 24 hours for phases II for PCP and oil and grease concentration. The microbial degradation of organic materials was also assessed by the five day biochemical oxygen demand (BOD) and chemical oxygen demand (COD) analyses. Microtox tests were performed to determine any change in the wastewater toxicity.Viable plate counts were performed in order to assess the rate of microbial reproduction and to determine the number of microorganisms present. In this procedure, serial dilutions are plated onto a suitable solid growth medium using the spread plate technique. Each plate inoculated with 0.5 ml of the diluted waste water sample. The agar plates were then incubated at 28 °C for 24- 48 hours.All water samples were extracted by EPA method 3520(continuous liquid-liquid extraction)and solid samples by EPA method3540 (USEPA 1986) . EPA method 555 (High performance liquid chromatography) was used to analyze PCP (USEPA 1992).The (BOD) was determined in accordance with standard methods(Clesceri *et al.* 1998).The COD test was performed according to standard methods (Clesceri *et al.* 1998)for water analysis (section 5220C). This analysis was performed according to standard method(Clesceri *et al.* 1998), for the examination of wastewater (section 5520 B).The toxicity of wastewater sample was determined with Microtox model 2055 toxicity autoanalyzer (Microbics Corporation, Carlsbad, California) according to the manufacturer's specifications.The results obtained from these experiments were analyzed using complete random design with three replications for each data point. Duncan's multiple range test was used to compare mean differences at (p= 0.05). Data were processed using the statistical analysis system (SAS)(Barr *et al.* 1976) .

Table 1. Composition of Mineral Salts Media

KNO3	1.0 g/L
K2HPO4	0.38 g/L
MgSO4.7H2O	0.20 g/L
FeCl3.6H2O	0.05 g/L
Deionized water	1L
pentachlorophenol	0.02 g/L

Phase II - Bacterial Immobilization. In this study, a bacterial culture (the same as phase I) was evaluated for its ability to degrade PCP in a cell immobilization study. The cells were immobilized in either celite or silica in sterilized glass columns. Mineral salts media containing 20 mg/L PCP (Table 1) was allowed to flow through the column. The effluent was collected and analyzed for PCP concentration and bacterial population.

RESULTS AND DISCUSSION

PHASE I

The data presented in Figure 1 show a significant decrease in the concentration of PCP over the 120 day treatment period. The initial and final concentrations were 83 mg/L and 20 mg/L, respectively. These results show a 76% reduction in the concentration of PCP. There was no significant decrease in PCP concentration prior to day 60. Due to the stability of PCP, it is not degraded as rapidly as other less stable compounds.

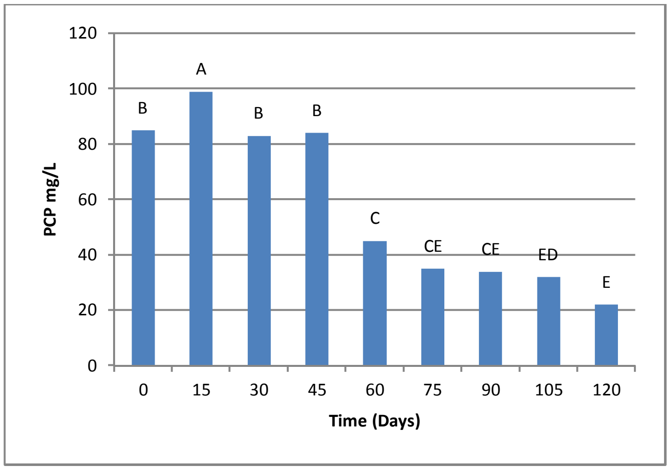

FIGURE 1. Rate of degradation for PCP in wastewater

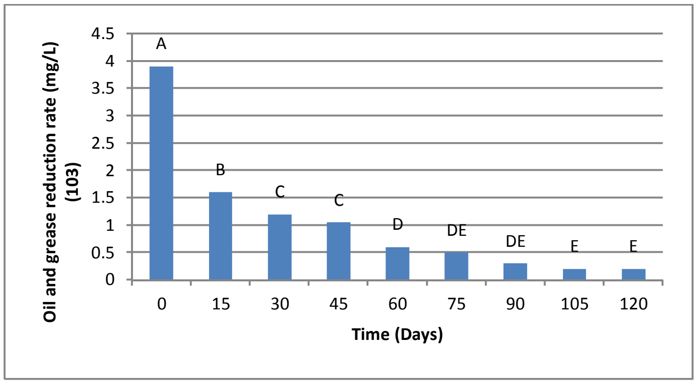

FIGURE 2. Rate of reduction in oil and grease concentration from wastewater

The data obtained from oil and grease analysis, COD, and BOD analysis reflect the degradation of straight chain alkanes, branched alkanes and many other compounds as well as cyclo-alkanes and other polycyclic aromatic hydrocarbons. The data obtained from oil and grease analysis is summarized in figure 2, these data show a significant decrease in the concentration of oils and greases found in the wastewater. Over the 120 day treatment period, the oil and grease concentration was reduced from 3,965 to a final concentration of 198 mg/L. this represents a 95% reduction in oil and grease concentration. The concentration was reduced 63%during the first 15 days of treatment.

The data obtained from the 5-day biochemical oxygen demand (BOD) shown in Figure 3 represent the decrease in oxidizable organic matter present in the wastewater. The 5-day BOD was significantly reduced from initial demand of 2,494.2 mg O_2/L at day 0 to a final demand of 173.1 mg O_2/L. this decrease can be attributed to the complete oxidation of organic compounds into CO_2 and H_2O, incorporation into cell biomass, and the conversion of these compounds into non-useable forms.

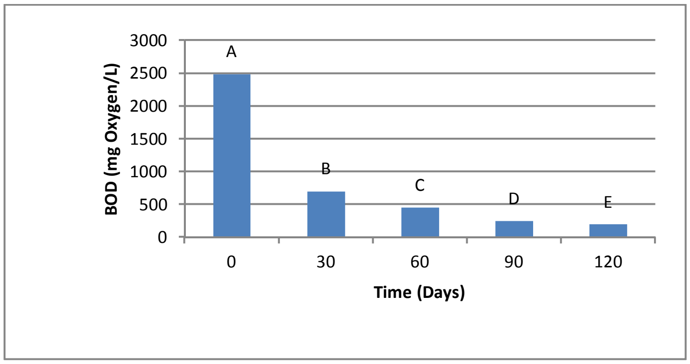

FIGURE 3. rate of reduction in BOD of wastewater

Figure 4 data represent the total amount of organic material present a determined by the chemical oxygen demand. The data obtained from COD analysis demonstrates a reduction in the COD from 11,368 mg O_2/L to 1,376 mg O_2/L in 120 days. This data represents an overall 87.8% reduction in the chemical oxygen demand. The COD decreased 18.4% during the first 15 days of treatment. This rapid reduction may be attributed to the rapid utilization of sample compounds present in the wastewater and possibly the volatilization of certain low molecular weight petroleum components.

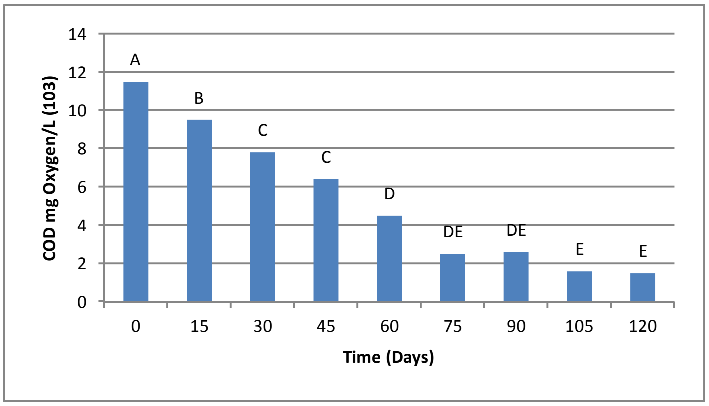

FIGURE 4. rate of reduction in COD of wastewater

Results of toxicity tests using the Microtox method of analysis are presented in Figure 5. The results of these analyses demonstrate a significant decrease in the toxicity of the wastewater between day 90 and 120. The toxicity of the processwater and the concentration required to reduce the light output by 50% (EC_{50}) are inversely related. Microbial counts peaked by day 60 and higher than starting population (Figure 6).

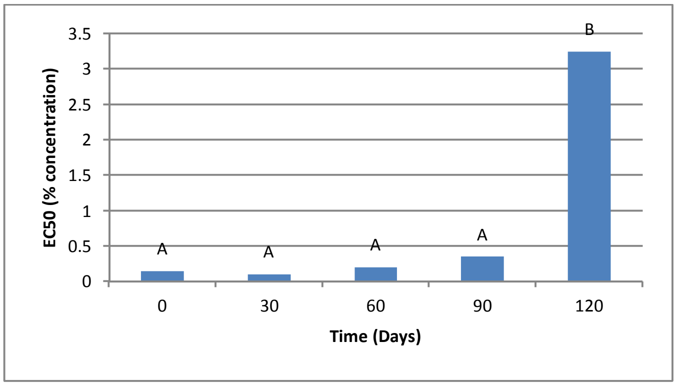

FIGURE 5. Reduction in wastewater toxicity as observed by Microtox Analysis

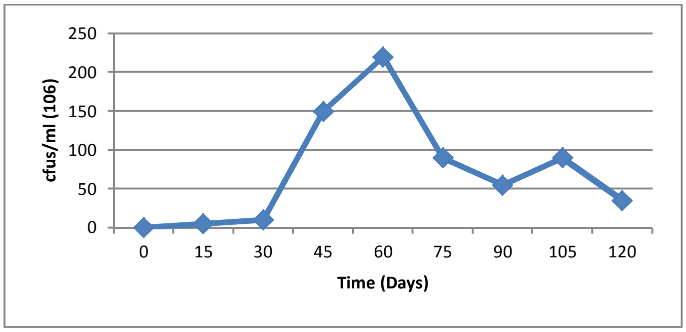

FIGURE 6. Rate of microbial reproduction as observed on nutrient agar amended with PCP

PHASE II

Analysis of the influent used in this study showed the PCP concentration was 18.6 mg/L. Results from HPLC analysis of the effluent from the silica treatment and control column are shown in Table 2. The PCP concentration in the effluent from the treatment and control columns varied over the 96 hour sampling period. The lowest concentration for both columns was observed after 24 hours. Results for the treatment and control columns show similar PCP concentration remaining in effluent.

TABLE 2. PCP concentration in effluent from Silica and Celite treatment and control columns

Time (Hours)	Silica (mg/l)		Celite (mg/l)	
	Treatment	Control	Treatment	Control
24	2.8	1.8	11.8	11.8
48	1.5	6.5	15.5	15
72	8.5	6.8	15	14.8
96	7.3	4.5	13.5	13.1

Extraction of silica contained in the treatment columns after 16 hours (not reported here) showed approximately 42 µg/g PCP. The treatment column may have had some degradation within the first hours of treatment causing the lower PCP concentration remaining in the packing material. Results from the analysis of effluent from the celeite control and treatment columns as shown in Table 2 show similar results for both treatment and control columns. The PCP concentration in the effluent from the celite treatment column was 11.5 mg/L at 24 hours, approximately 15 mg/L after 48 hours and 13.6 mg/L after 96 hours.

The celite packing material from the treatment column contained 14.8 µg/g PCP while the material from the control column contained 8.4 µg/g PCP.

Results from these analyses do not reflect a difference in the PCP concentration of the effluent from the treatment and control columns packed with silica or celite.

Plate counts of the effluent from the silica treatment column(not reported here due to page limitation) showed microbial population of 20,000 cfus/ml at 24 hours, which decreased to approximately 15,000 cfus/ml after 96 hours treatment. The silica control column contained approximately 4,000 cfus/ml after 24 hours.

CONCLUSION

Laboratory results from these experiments have demonstrated that batch tank reactor treatment can be effectively used for bioremediation of highly contaminated processwater when the appropriate conditions are met for microbial growth. Reduction in toxicity showed that metabolites from the degradation of PCP were significantly less toxic at the end of the experiment confirming that no hazardous by-products are produced during microbial activities. The use of immobilized cells in phase II for treatment of PCP contaminated water was not successful and is not recommended for remediation of this type wastewater.

ACKNOWLEDGMENT

This article was approved for publication as Journal article FP- 651of Forest and Wildlife Research Center, Mississippi State University, Mississippi State, MS.

REFERENCES

Barr, AJ, Goodnight, JH, Sall, JP and Helwig, JT (1976): A User's Guide to SAS 76. SAS Institute Raleigh, NC.

Borazjani, H, Strobel, D, Templeton, C, Wagner, J, Hannigan, M, Hendrix, F, Welch, M and Prewitt, L (1990): Applications of four bacteria and fungi species for bioremediation of selected polyclinic hydrocarbons (PAH's) and Pentachlorophenol (PCP), First Annual Hazamat Conference South, Atlanta, Ga, pp. 217-240.

Clesceri, LS, Greenberg, AE and Eaton, AD (1998): Standard methods for the examination of water and wastewater. Washington, DC.

Crosby, D, Beynon, K and Greve, P (1981): Environmental chemistry of pentachlorophenol. Pure Appl. Chem, **53**(5), 1051-1080.

KeshaniLangroodi, S, Borazjani, H, Nicholas, D, Lynn Prewitt, Diehl, SV and Kitchens, S (2011): Remediation of Pentachlorophenol (PCP) in Biodiesel versus Diesel Carriers In: *International Research Group on Wood Protection*. IRG/WP/11-50279, Queenstown, Newzeland, pp. 12.

Morrell, JJ (2003): Disposal of Treated Wood: Option and Perils. In: *American Wood Preservers' Association Seminar*, Boston, Massachusetts, pp. 7-14.

Samuel, BA (1991): Bioremediation of pentachlorophenol and creosote treated utility poles, Master Thesis, Mississippi State University, Mississippi State, MS.

USEPA, USEPA (1986): Test method for evaluating solid wastewates, SW-846. 3rdedition.

USEPA, USEPA (1992): Determination of chlorinated acids in water by HPLC with photodide array ultraviolet detector. , Revision 1. Environmental monitoring system laboratory office of research and development., Cincinati, OH.

Walker, J, Colwell, R and Petrakis, L (1976): Biodegradation of petroleum by Chesapeake Bay sediment bacteria. Canadian journal of microbiology, **22**(3), 423-428.

PHENANTHRENE BIODEGRADATION BY ISOLATED STRAINS-KINETIC STUDIES

M. Brinda Lakshmi and **M. Velan**
(Anna University, Chennai, Tamilnadu, India)

ABSTRACT: Two bacterial Strains were isolated from petroleum contaminated soil with phenanthrene as sole energy and carbon source. Biochemical and 16S rRNA gene sequence analysis confirmed the strains to be *Bacillus* sp. MVMB4 and *Rhodopseudomonas* sp. MVMB5. The effect of inoculum concentration (2.0 to 6.0 % (v/v)), pH (6.0 to 7.5) and substrate concentration (20- 100 mg/l) on the biodegradation of phenanthrene by the two strains were experimented considering bacterial growth and phenanthrene concentrations as measured parameters. The optimum inoculum concentration and pH for both the strains were same which was 4.0 % (v/v) and 7.0 respectively. But, the optimum initial phenanthrene concentrations was 60 mg/l for strain MVMB4 which was slightly greater when compared to strain MVMB5 (40 mg/l). Five kinetic models were applied to the experimental growth data to predict substrate inhibition on growth of the microorganism using MATLAB® 7.0. It is evident that the kinetic constants obtained coincided well with the literature. Thus the isolated bacterial strains *Bacillus sp. and Rhodopseudomonas sp.* seems to be promising strains for using in the processes of the bioaugmentation because of their ability to degrade phenanthrene and to grow on the substrate.

Keywords: phenanthrene / kinetic models / *Bacillus* sp. *and Rhodopseudomonas* sp.

INTRODUCTION

Phenanthrene is one among the perilous polycyclic aromatic hydrocarbons (PAHs) that are produced during the incomplete combustion of organic matter (HSDB 2001). It has been found in particle emissions from natural gas combustion and municipal incinerator waste, and in the particulates present in ambient air pollution near high vehicular traffic and industrial or urban areas (Rehwagen et al 2005; Fang et al 2006). To protect freshwater aquatic life from phototoxic and long-term effects, Ministry of Environment, Lands and Parks, British Columbia guidelines recommended that phenanthrene concentrations in water and sediments should not exceed 0.3μg L^{-1} and 0.04 μg g^{-1}. According to a study for Dutch Ministry of Environment, the Maximum Permissible Concentration of phenanthrene for water, soil and sediments are 0.30 μg L^{-1}, 0.51, mg Kg^{-1}, and 0.51, mg Kg^{-1}, respectively (Kalf et al 1997). In spite of its hazardous nature, phenanthrene compound is used in the manufacture of explosives, pesticides, drugs, the chemical phenanthrene-quinone, (intermediate for pesticides), the chemical diphenic acid (intermediate for resins), some dyes and in research (ATSDR 1995). Biodegradation of such compounds offers an advantage over other methods because it enables complete removal with the help of naturally occurring microorganism. Thus exploration of such organisms that occur in various polluted environment abets more information to bioremediation.

Bacterial growth factors such as substrate concentration, pH, and nutrient level can have an impact on the exploitation of substrates, influence on protein synthesis, alteration in cytoplasm synthesis and change of transferred intermediates (Skladany and Baker (1994). For a successful biodegradation, our attention should warrant on optimal process design. Selection of physiochemical parameter are as important as choice of suitable bacterial culture. All parameters either in excess or low will jeopardize the biodegradation process by deactivating the bacterial enzymes. Thus, operating conditions have to be determined priory to ensure the success of such biodegradation process. Also, kinetic models have been applied to the experimental growth data to estimate the biokinetic constants. Strains that can degrade

---

ISBN 9780976885351

PAHs completely and rapidly with good adjustment will be more favored although many bacteria capable of degrading PAHs have been isolated (Zhao et al., 2009). Microbial degradation of phenanthrene has been studied extensively and the pathway of microbial phenanthrene metabolism is well elucidated, aerobically as well as anaerobically (Morzik et al., 2003; Puntus et al., 2008).

In this study, the effects of certain factors and kinetics on the degradation of 3-ring PAH, phenanthrene by MVMB4 and MVMB5, isolated in India, were examined. This work was performed as a preliminary assessment of the potential usefulness of the isolated strains in the bioremediation of PAH pollutants.

MATERIALS AND METHODS

Microorganism isolation and acclimatization. Soil sample was collected from a petroleum contaminated site near Ennore, Chennai. Phenanthrene degrading bacteria were isolated from the soil sample by enrichment culture technique on minimal salt medium by using phenanthrene as sole carbon and energy source. The Minimal salt medium (MSM)composed of (pH 7) : KH_2PO_4- 1.0 g L^{-1}; $Na_2HPO_4.2H_2O$ -1.25 g L^{-1}; $MgSO_4.7H_2O$- 0.5 g L^{-1}; $CaCl_2.2H_2O$ – 0.05g L^{-1}; $FeSO_4.7H_2O$ – 0.005 g L^{-1} and $(NH_4)_2SO_4$ – 1.0 g L^{-1}. Concentrated solutions of all components were prepared and autoclaved at 121 °C for 20 min. Phenanthrene stock prepared with acetone was added to the flasks and evaporated before autoclaving with MSM (100 ml, pH 7.0). 1 gm soil sample was inoculated into MSM containing phenanthrene and isolates were obtained by enrichment technique. Pure cultures were tested for clearing zones on the phenanthrene sprayed coated plates (Kiyohara et al., 1982). The isolates were stored at −20 °C as liquid cultures containing 20% glycerol (v/v). The strains were identified through morphological, biochemical and 16S rRNA gene sequence analysis. Nucleotide sequence similarity searches were conducted by NCBI, BLAST (N). Phylogenetic tree was constructed using mega software version 5.

Experimental procedure for optimizations and kinetics. 1 ml culture grown in nutrient medium of 1.9 OD600 was used as inoculums for preparation of inoculum in MSM. The cells in late exponential growth phase was centrifuged, washed and used as a source of inoculum for the experiments. Batch experiments were carried out at 30 °C, 7 pH and 0.1g L^{-1} substrate concentration unless otherwise stated. After the optimization of each parameter, optimum conditions were adapted for further experiments. The range of inoculum concentration studied was from 2 to 6% (v/v). For pH studies, the desired pH in the range of 6.0 to 7.5 was maintained by adding HCl or NaOH at the beginning of the experiment and not controlled afterwards. Kinetic studies were conducted from the results obtained by optimization experiments at different initial substrate concentration ranging from 20- 100 mg L^{-1}. Suitable substrate models found in the literature (Monod, 1949; Edward, 1970; Shular and Kargi, 2002) and adopted is shown in Table 1.

TABLE1. Kinetic models used in this study

Models	Equations
Monod model	$\mu_g = \mu_{\max}[S]/K_S + [S]$
Haldane model	$\mu_g = \mu_{\max}[S]/K_S + [S] + ([S^2]/K_i)$
Yano model	$\mu_g = \mu_{\max}[S]/\{K_S + [S] + ([S^2]/K_i)\}\{1 + (1/K)\}$
Edward model	$\mu_g = \mu_{\max}[S]/\{K_S + [S] + ([S^2]/K_i)\}\{1 + ([S]/K)\}$
Competitive model	$\mu_g = \mu_{\max}[S]/\{K_S(1 + I/K_i)\} + [S]$

Analytical methods. Bacterial concentrations were determined as analysis of protein content by Lowry's method using UV–visible spectrophotometer (Hitachi U-2000, Japan) at 640 nm. Phenanthrene was quantified using high-performance liquid chromatography (Shimaduzu, 10 ATVP, Japan) equipped with a UV – Visible detector , M925 pump, Rheodyne injector, and C18 column (150× 4.6 mm; Phenomenex, Torrance, CA, USA) at a wavelength of 254 nm. The samples were extracted with hexane, evaporated and redissolved in acetonitrile. The elution gradient was 80: 20 acetonitrile: water with a flow rate of 1.0

ml/min. Degrading efficiency was calculated as follow: Degrading Percentage $=[C_i - C_f / C_i] \times 100\%$ where C stands for the concentration of phenanthrene.

Data analysis. Regression analysis was performed with the data analysis tool pack of Microsoft Excel®. The model equations were solved using nonlinear regression method using MATLAB® 7.0.

RESULTS AND DISCUSSION

Identification of microorganisms. Two isolates, MVMB4 and MVMB5, which out grew the other strains on phenanthrene, was analyzed morphologically and biochemically to identify the genus (Table 2). The 16S rRNA sequence analysis of the strains helped us to identify them as *Bacillus* sp. and *Rhodopseudomonas* sp. showing 97 & 78% homology respectively. The complete 16S rRNA sequence was used to establish the phylogram (Fig. 1) using MEGA 5 software.

TABLE2. Morphology and Biochemical analysis of microorganisms

	MVMB4	**MVMB5**
Cell Morphology	White, smooth colonies with irregular edges	Light orange, smooth colonies with regular edges
	aerobe	Facultative anaerobes
Gram Staining	Gram Positive Rods	Gram Negative Rods
	Motile	Motile
Indole Test	Positive	Positive
Methyl Red Test	Negative	Negative
Voges Proskauer Test	Positive	Positive
Citrate Utilization	Positive	Positive
Oxidase	Negative	Positive
Catalase	Positive	Positive
Lysine decarboxylase	Positive	Positive
Ornithine decarboxylase	Positive	Positive
Urease Production	Negative	Negative
PhenylalanineDeamination	Negative	Negative
Nitrate Reduction	Positive	Positive
H_2S Production	Negative	Negative
Glucuronidase utilization	Negative	Negative
ONPG utilization	Positive	Positive

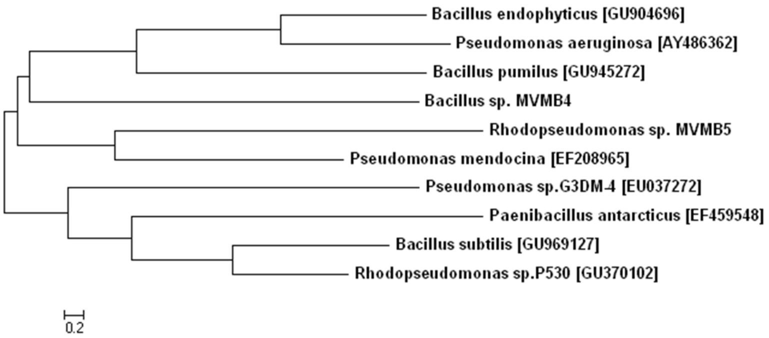

FIGURE1. Phylogenetic relationship by neighbour-joining analysis of 16S rDNA sequences; The scale represents the evolutionary branch length .

Biodegradation of Phenanthrene by *Bacillus* sp. and *Rhodopseudomonas* sp. Growth of the bacterial strains on phenanthrene showed biomass increase i.e the log phase ranging nearly 14 to 16 h with a short stationary phase up to 20 h. Thus for degradation experiments the culture was incubated upto 35 h and then held for phenanthrene estimation.

Effect of Inoculum Concentration. In order to find out the optimum inoculum needed for faster and higher % degradation, the degrading ability and biomass concentration was tested at different inoculum concentrations (Fig. 2a). Of the different initial biomass concentration, 4 % (v/v) proved to be optimum for both the strains with maximum biomass of 18.5 & 34.3 mg protein L^{-1} cell density and degradation of 45.13 & 33.53 % respectively. There was no lag phase because of good acclimatization. The increase of biomass concentration perhaps reduces the lag time and later becomes low at 4 % (v/v) biomass concentration, facilitating the organism to reach the exponential growth phase rapidly (Bandyopadhyay et al 1998). Except 4 % (v/v) all other inoculum concentrations showed low growth and degradation.

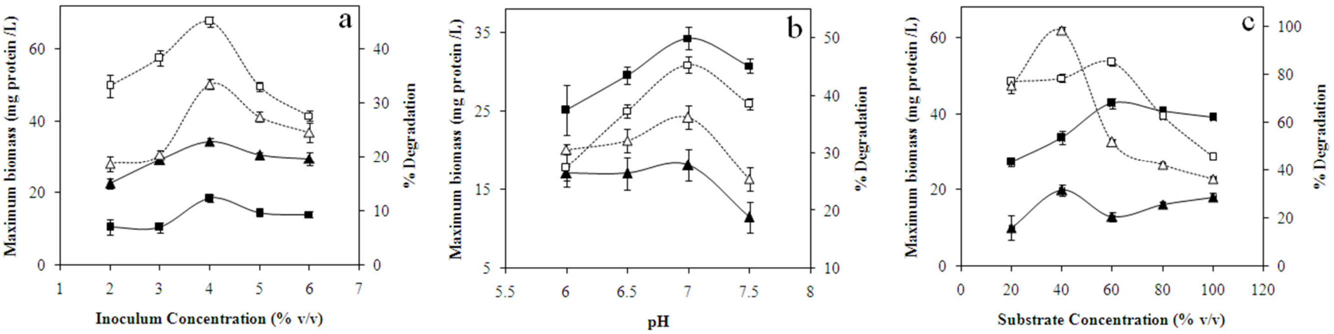

FIGURE2. Effect of (a) inoculum concentrations, (b) pH and (c) Substrate concentration on biomass and % phenanthrene degradation (□-*Bacillus* sp., Δ-*Rhodopseudomonas* sp., bold line- Biomass, dotted lines- Degradation).

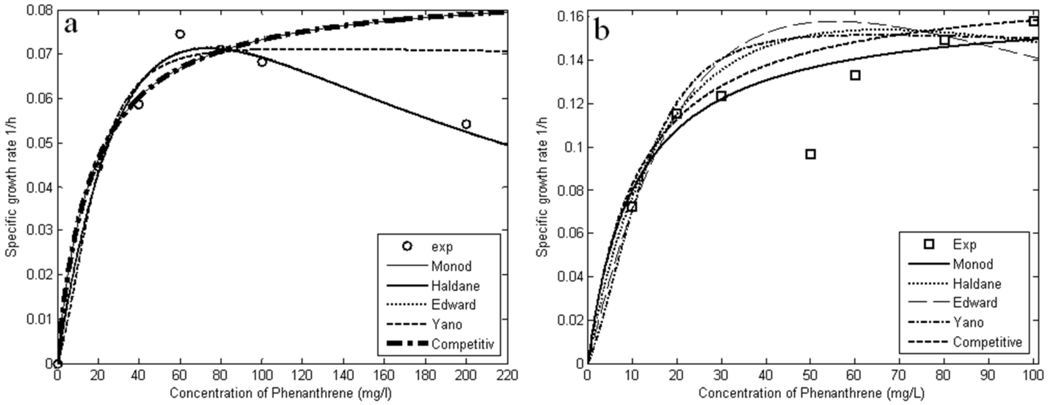

Figure3. Models fitted to the results of experimental data at optimized conditions for the degradation of phenanthrene by (a) *Bacillus* sp. and (b) *Rhodopseudomonas* sp.

Effect of Ph. The structure and permeability of the cell membrane depends mainly on the pH of the external medium. The improvement in the hydrocarbon degradation of the microbial environment in contaminated soils can be accomplished at different pH, acidic (Piddington et al 2000; Uyttebroek et al

2007) or alkaline (Margesin and Schinner 2001). The results on the influence of initial pH on phenanthrene degradation by the strains in the range of 6.0 to 7.5 are shown in Fig. 2b. There was simultaneous increase in growth for all the pH range studied with maximum biomass obtained at pH 7.0 for both the strains. No apparent increase in biomass occurred at other pH range studied. The optimal phenanthrene degradation also resulted at the neutral pH 7.0 with 45.34 & 36.2 % respectively for *Bacillus* sp. and *Rhodopseudomonas* sp. The optimum pH value reported in the literature and the results obtained in the present investigation were almost similar (Shafiee et al 2006; Abdelhay et al 2009; Zhou et al 2008).

Effect of Initial Concentration. The effect of substrate concentration for microbial growth and degradation on phenanthrene was varied from 20 to 100 mg L^{-1} and the results are plotted in Fig. 2c. The maximum or optimal growth resulted at the concentration of 60 & 40 mg L^{-1} for *Bacillus* sp. and *Rhodopseudomonas* sp. respectively above which the growth as well as the % degradation decreased. More than 80% degradation was observed at optimum concentrations for both the strains, whereas below above the optimum concentrations, the % degradation decreased. There was high rate of degradation during log phase and slow rate of degradation in stationary phase. This might be due to the higher concentration of substrate at the beginning and higher concentration of metabolites later (Jing et al 2008). Similar result has been reported (Tian et al 2002) for *Pseudomonas mendocina* after 60 h incubation on phenanthrene.

TABLE3. Fitted Equations for the Strains

Models	*Bacillus* sp.	*Rhodopseudomonas* sp.
Haldane	$\mu_g = 0.2175[S]/76.15+[S]+([S^2]/72.19)$	$\mu_g = 0.2652[S]/23.91+[S]+([S^2]/181.1)$
Edward	$\mu_g = 0.2223[S]/\{78.35+[S]+([S^2]/73.55)\}\{1+(1/20.14)\}$	$\mu_g = 0.4518[S]/\{51.78+[S]+([S^2]/62.8)\}\{1+(1/17.96)\}$
Yano	$\mu_g = 0.6946[S]/\{(531.6+[S]+([S^2])(1+([S]/10.14)\}$	$\mu_g = 1.643[S]/\{(317.7+[S]+([S^2])(1+([S]/11.77)\}$

Cell growth and kinetics. Transformations of the non-linear modeling equations to linear modeling equations, such as Line weaver– Burk linear equation, are always considered as low accuracy simulations (Smith et al, 1998). The calculations for percent deviation of predicted values of μ_g from experimental values for both the organisms show that Haldane, Yano and Edward models (Fig. 3) are more suitable models for the studied substrate concentration range. Observations on R^2 values also conclude that Haldane, Yano and Edward kinetic models give comparable predictions with high R^2 values (>0.95). The fitted equations for the models are as shown in Table 3. It is evident that the kinetic constants obtained coincides as well as exceeds the values in the literature (Rodrigues et al, 2005; Boldrin et al, 1993; Chen et al, 2001; Keuth and Rehm, 1991; Guha et al, 1999; Mallick and Dutta, 2008; Juang and Tsai, 2006; Kumaran and Paruchuri, 1997; Kumar et al, 2005) (the maximum specific growth rate (μ_{max}) for phenanthrene using popular microorganism system lies in the range of 0.03 –0.18 h^{-1} , Ks values fall in the range of 12.12-36.2 mg L^{-1} and K_i between 118 -324 mg L^{-1})

CONCLUSION

Biokinetic constants at optimized conditions for the phenanthrene degradation by *Bacillus* sp. and *Rhodopseudomonas* sp. were obtained by fitting the experimental rates at different concentration to suitable substrate inhibition models found in the literature. It is clear from the end results that the isolates MVMB4 and MVMB5 had the excellent capacity to oxidize phenanthrene. Since the rate of conversion was faster, it is concluded that *Bacillus* sp. and *Rhodopseudomonas* sp. can be used in any microbial consortium for the bioremediation of polycyclic aromatic compound.

REFERENCE

Abdelhay, A., J. P. Magnin, N. Gondrexon, S. Baup, and J. Willison. 2009. “Adaptation of a *Mycobacterium* strain to phenanthrene degradation in a biphasic culture system: influence on interfacial area and droplet size.” *Biotechnol. Lett.* 31:57-63.

Agency for Toxic Substances and Disease Registry (ATSDR) 1995. *Toxicological profile for polycyclic aromatic hydrocarbons*, Department Of Health And Human Services, Public Health Service, Atlanta, Georgia.

Bandyopadhyay, K., D. Das, and B. R. Maiti. 1998. “Kinetics of phenol degradation using *Pseudomonas putida* MTCC 1194.” *Bioprocess Engg.* 18:373-377.

Boldrin, B., A. Tiehm, and C. Fritzsche. 1993. “Degradation of phenanthrene, fluorene, fluoranthene, and pyrene by a *Mycobacterium* sp.” *Appl. Environ. Microbiol.* 59(6):1927–1930.

Chen, G., K. A. Strevett, and A. Vanegas. 2001. “Naphthalene, phenanthrene and surfactant biodegradation.” *Biodegradation.* 12(6):433–442.

Edward V. H. 1970. “The influence of high substrate concentrations on microbial kinetics.” *Biotechnol. Bioeng.* 12:679-712.

Fang, G. -C., Y. -S. Wu, J. -C. Chen, C. -N. Chang, and T. –T. Ho. 2006. “Characteristic of polycyclic aromatic hydrocarbon concentrations and source identification for fine and coarse particulates at Taichung Harbor near Taiwan Strait during 2004–2005.” *Sci. Tot. Environ.* 366:729-738.

Guha, S., C. A. Peters, and P. R. Jaffe. 1999. “Multisubstrate biodegradation kinetics of naphthalene, phenanthrene, and pyrene mixtures.” *Biotecnol. Bioengg.* 65(5):491- 499.

Hazardous Substances Databank (HSDB). 2001. *On-line Database*. National Library of Medicine. Washington, DC.

Jing, X., W. Hongke, A. Mingquan, and Y. Guiwen. 2008. “Kinetics and characteristics of phenanthrene degradation by a Microbial consortium.” *Pet. Sci.* 5:73-78.

Juang R. and S. Tsai. 2006. “Growth kinetics of *Pseudomonas putida* in the biodegradation of single and mixed mixed phenol and sodium salicylate.” *Biochem. Eng. J.* 31(2):133-140.

Kalf, D. F, T. Crommentuijn, and E. J. Van De Plassche. 1997. “Environmental quality objectives for 10 polycyclic aromatic hydrocarbons (PAHs).” *Ecotoxicol. Environ. Saf.* 36(1):89-97.

Keuth, S. and H. J. Rehm. 1991. “Biodegradation of phenanthrene by *Arthrobacter polychromogenes* isolated from a contaminated soil.” *Appl. Microbiol. Biotechnol.* 34(6):804-808.

Kiyohara, H., K. Nagao, K. Kouno, and K. Yano. 1982. “Phenanthrene degrading phenotype of *Alcaligenes faecalis* AFK2.” *Appl. Environ. Microbiol.* 43:458-461.

Kumar, A., S. Kumar, and S. Kumar. 2005. “Biodegradation of phenol and catechol using *Pseudomonas putida* MTCC 1194.” *Biochem. Eng. J.* 22(2):151-159.

Kumaran, P. and Y. L. Paruchuri. 1997. “Kinetics of phenol biotransformation.” *Water Res.*31(1):11-22.

Mallick, S. and T. K. Dutta. 2008. “Kinetic of phenanthrene degradation by *Staphylococcus sp.* strain PN/Y involving 2-hydroxy-1-naphthoic acid in a novel metabolic pathway.” *Process Biochem.* 43:1004-1008.

Margesin, R. and F. Schinner. 2001. “Biodegradation and bioremediation of hydrocarbons in extreme environments.” *Appl. Microbiol. Biotechnol.* 56:650-663.

Monod, J. 1949. “The growth of bacterial cultures.” *Ann. Review of Microbiol.* 3:371-394.

Mrozik, A., Z. Piotrowska-Seget, and S. Labuzek. 2003. "Bacterial degradation and bioremediation of polycyclic aromatic hydrocarbons." *Pol.J.Environ.Studies*, 12:15-25.

Piddington, D. L., A. Kashkouli, and N. A. Buchmeier. 2000. "Growth of *Mycobacterium tuberculosis* in a defined medium is very restricted by acid pH and Mg^{2+} levels." *Infect. Immun.* 68:4518-4522.

Puntus, F., A. E. Filonov, L. I. Akhmetov, A. V. Karpov, and A. M. Boronin. 2008. "Phenanthrene Degradation by Bacteria of the Genera *Pseudomonas* and *Burkholderia* in Model Soil Systems," *Microbiol.* 77(1):7–15.

Rehwagen, M., A. Muller, L. Massolo, O. Herbarth, and A. Ronco. 2005. "Polycyclic aromatic hydrocarbons associated with particles in ambient air from urban and industrial areas." *Sci Tot Environ.* 348:199-210.

Rodrigues, A. C., S. Wuertz, A. G. Brito, and L. F. Melo. 2005. "Fluorene and Phenanthrene uptake by *Pseudomonas putida* ATCC 17514: Kinetics and Physiological aspects." *Biotechnol. Bioengg.* 90(3):281-289.

Shafiee, P., S. A. Shojaosadati, and A. H. Charkhabi. 2006. "Biodegradation of polycyclic aromatic hydrocarbons by aerobic mixed bacterial culture isolated from hydrocarbon polluted soils." *Iran. J. Chem. Chem. Eng.* 25:73-78.

Shuler, M. L. and F. Kargi. 2002. *Bioprocess Engineering: Basic Concept.* 2nd ed. Prentice-Hall India, New Delhi.

Skladany, G. J. and K. H. Baker. 1994. *Laboratory biotreatability studies, Bioremediation*. McGraw-Hill Inc; New York.

Smith, L. H., P. L. McCarty, and P. K. Kitanidis. 1998. "Spreadsheet method for evaluation of biochemical reaction rate coefficients and their uncertainties by weighted nonlinear least squares analysis of the integrated Monod equation." *Appl. Environ. Microbiol.* 64(6):2044–2050.

Tian, L., P. Ma, and J. J. Zhong. 2002. "Kinetics and key enzyme activities of phenanthrene degradation by *Pseudomonas mendocina*." *Process Biochem.* 32:1431-1437.

Uyttebroek, M., S. Vermeir, P. Wattiau, A. Ryngaert, and D. Springael. 2007. "Characterization of cultures enriched from acidic polycyclic aromatic hydrocarbon-contaminated soil for growth on pyrene at low pH." *Appl. Environ. Microbiol.* 73(10):3159-3164.

Zhao H. P., Q. S. Wu, L. Wang, X. T. Zhao, and H. W. Gao. 2009. "Degradation of phenanthrene by bacterial strain isolated from soil in oil refinery fields in Shanghai China." *J. Hazard. Mater.* 164(2-3): 863–869.

Zhou, Y., J. Zhang, E. Su, G. Wei, Y. Ma, and D. Wei. 2008. "Phenanthrene biodegradation by an indigenous *Pseudomonas* sp". ZJF08 with TX100 as surfactant." *Annal. Microbiol.* 58:439-442

START-UP OF AN AEROBIC GRANULAR SLUDGE NON TUBULAR REACTOR

Ana M. T. Mata (Institute for Biotechnology and Bioengineering, Lisbon, Portugal,
Polytechnic Institute of Setúbal, Setúbal, Portugal)
Nídia Dana Lourenço (Institute for Biotechnology and Bioengineering, Lisbon, Portugal)
Helena Maria Pinheiro (Institute for Biotechnology and Bioengineering, Lisbon, Portugal)

ABSTRACT: Granular activated sludge is a new, promising wastewater treatment bioprocess. The aim of this study was to produce granular sludge in a laboratory sequential batch reactor (SBR) with a height/diameter ratio of 2.5, differing from the tubular reactors usually described. The SBR was seeded with flocs from a full-scale activated sludge reactor, and operated with a 50% exchange volume ratio in a 6-h cycle (5-h aeration). The settling time was gradually reduced from 40 to 2 minutes. The feed solution contained basic nutrients, and a starch-derived C-source delivered at 1.5-2.0 $kgCOD.m^{-3}.d^{-1}$. After 25 days of operation with 3 min of settling time, a drop in Sludge Volume Index (SVI_{30}) from 280 to 28mL/g was observed, granules reaching 1mm being obtained. Further settling time reduction deteriorated the settling properties. A low SVI_{30} value was restored back at 3 min, and biomass accumulation from 2 to 7 g/L resulted, with good granule integrity. COD removal averaged 88%. The successful generation of granular activated sludge from a flocculent inoculum was demonstrated in a laboratory non tubular reactor, settling time being a critical process parameter. The granules were stored for 7 months and their former performance ranges were restored within 10 days.

INTRODUCTION

Granular activated sludge is a new and promising biological process for wastewater treatment (Liu, 2008), with the advantages of fast biomass settling and the possibility of creating aerobic and anoxic/anaerobic zones within the same granule. The latter can improve the biodegradation of several types of compounds, namely xenobiotics. Generating the granules is the first step in the implementation of this technology. In almost all cases reported, aerobic granules were produced in column-type up flow reactors (Liu, 2004), but in this study the used sequential batch reactor (SBR) had a height/diameter ratio of 2.5, differing from the tubular reactors usually described (Muda et al., 2010; Tay, 2005, Beun et al.,1999) and closer to that of full-scale SBR units. The aim of this study was thus to produce granular sludge in this SBR type, from flocculent sludge harvested at a full-scale, conventional activated sludge reactor, to examine the parameters influencing this process and to characterize the obtained granules, including the possibility of long-term storage for the inoculation of other reactors.

MATERIALS AND METHODS

Carbon Source Stock Solution A starch derivative (Emsize E1) was used as carbon source. Emsize E1 was obtained from Emsland-Starke GmbH, Germany, and was pre-hydrolyzed in alkaline conditions, in order to produce a 100 $g.L^{-1}$ stock solution (Lourenço et al. 2001).

Feed Solution The feed solution had a Chemical Oxygen Demand (COD) concentration of 750-1000 $mg.L^{-1}$ (hydrolysed Emsize E1) and a nutrient base composed of KH_2PO_4 (760 $mg.L^{-1}$), $Na_2HPO_4.7H_2O$ (920 $mg.L^{-1}$), NH_4Cl (140 $mg.L^{-1}$), $MgSO_4.7H_2O$ (11 $mg.L^{-1}$), $CaCl_2$ (28 $mg.L^{-1}$), $FeCl_3.6H_2O$ (24 $ng.L^{-1}$), $MnSO_4.4H_2O$ (27 $ng.L^{-1}$), H_3BO_3 (57 $ng.L^{-1}$), $ZnSO_4.7H_2O$ (24 $ng.L^{-1}$), and $(NH_4)_6Mo_7O_{24}.4H_2O$ (35 $ng.L^{-1}$). It was prepared in aerated tap water. The salts were analytical grade.

ISBN 9780976885351

Activated Sludge Inoculum The reactor was seeded with flocs harvested at a full-scale, conventional activated sludge reactor from a municipal wastewater treatment plant, operated in continuous mode with advanced nitrogen removal (Chelas, Lisbon, Portugal). The sludge was washed and sieved (1mm net) before use. In a second experimental period, the emptied reactors were re-started using the stored granules described below, as sole inoculum.

Experimental System The granulation experiment was performed in a 1.5L SBR reactor with height/diameter ratio of 2.5, operated with a volume exchange ratio of 50% (effluent is discharged at the reactor half-height). The reactor was operated on a 6h-cycle with 5h of aeration, and 1 hour for the feeding, settling, discharge and idle stages. Feeding time was 15 min and settling time was reduced progressively from 40 min to 2 min, being always followed by rapid discharge (3 min). Aeration was achieved with an air compressor through a porous membrane (bubble wall air curtain) placed at the bottom of the reactor, together with stirring by an anchor type magnetic mixer at approximately 200rpm. The pumping, discharge, aeration and agitation functions were automatically controlled by a computer. Hydraulic retention time was set at 12h. Biomass wastage was limited to the sampling needs, resulting in sludge age values varying from 2 days in the beginning to 15 days after biomass accumulation. The fed organic load was set at 1.5 and 2.0 kgCOD.m^3.d^{-1} (operational days 1-63 and 64-96, respectively). In the reactor startup with stored granules, the fed organic load was 2.0 kgCOD.m^3.d^{-1}. The pH was not controlled, but the phosphate buffer present in the feeding solution was enough to maintain it the 6.4-6.8 range. The reactor was operated at room temperature that varied within the 21-26ºC range.

Long Time Granules Storage The granules obtained in the granulation experiment were harvested on day 96. They were divided into two equal portions and stored for 7 months, with no aeration, in the following conditions:

- Long-term storage SBR1: 25ºC, stored in the residual medium from the granulation experiment after going through 4, 6-h operational cycles without feeding or discharge.
- Long-term storage SBR2: 4ºC, washed with aerated tap water before storage in the latter.

Analyses Soluble COD and total suspended solids (TSS) were measured in the mixed liquor and the effluent; Sludge Volume Index at 5 and 30 minutes (SVI_5 and SVI_{30}, offline in an Imhoff cone), pH, and oxygen uptake rate (OUR) were measured on the mixed liquor. The settling velocity of sludge aggregates was measured by recording the average time taken for individual aggregates to drop from a given height in a 1 L measuring cylinder. Granule integrity (GI) evaluation was based on the method of Muda et al. (2010), i.e., 50mL of mixed liquor was agitated for 5 min at 200 rpm in an orbital shaker. The percentage of biomass detached was the ratio between the TSS value of the 1-min settled supernatant (50mL cylinder) and the TSS value of the initial mixed liquor sample; granule integrity (GI) was expressed (in percentage) as GI = 100 - percentage of biomass detached.

Microscopy and Gram Stain Biomass was observed under a light microscope to follow granule formation. Granules were also observed under Gram stain applied with a ViaGram™ Red+ Bacterial Gram Stain Viability Kit (V-7023) from Molecular Probes, following the supplier's protocol. The kit provides a simple fluorescent staining protocol that differentially stains many gram-positive and gram-negative bacterial species and, at the same time, discriminates live from dead cells on the basis of plasma membrane integrity (Product Information, Molecular Probes).

RESULTS AND DISCUSSION

Reactor Operation for Granule Production The SBR was started up with a flocculent inoculum and operated at 40 min sedimentation time. The latter was reduced to 10 min on day 6, to 5 min on day10 to 3 min on day 17, to 2 min on day 29, and back to 3 min on day 64. As it can be seen in Figure 1, the initial SVI_{30} value was high even for flocculent sludge (above 400 mL/g), but both the SVI_5 and the SVI_{30} values lowered sharply after the first operational days. After 10 days, at 10 min settling time, the SVI_{30} value was already 152 mL/g, corresponding to a settling velocity of 3.5 m/h. After 25 days, the SVI_{30} dropped to 28mg/L, with a settling velocity of 14.9 m/h. It can also be seen in Figure 1 that at this point the SVI_5 and SVI_{30} values were very similar, an important confirmation of the very good settling ability only reported for granular biomass. Microscopy observations indicated that granules with a size around 1mm were dominant, as it can be seen in Figure 2. The latter shows aggregates from the initial inoculum and from a biomass sample collected from the SBR on day 25. At this time the mixed liquor biomass concentration was slightly above 2 gTSS/L (Figure 3).

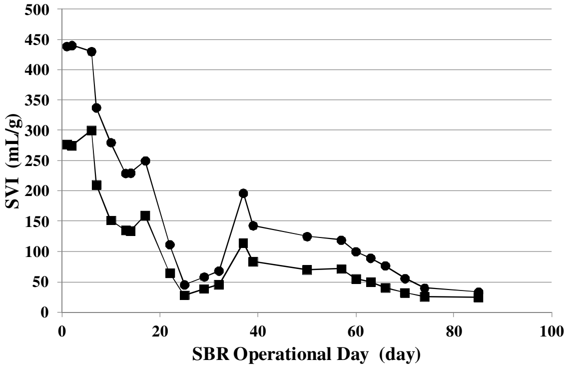

FIGURE 1 - Sludge volume index values *versus* SBR operational time, ■ SVI_{30}, ● SVI_5

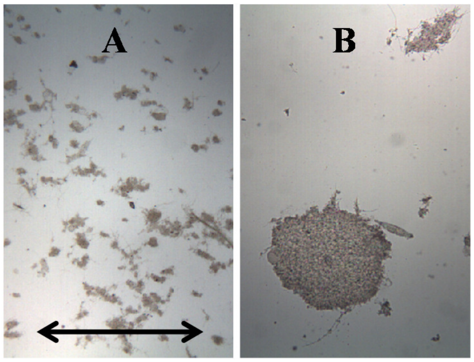

FIGURE 2 – Light microscopy observations, scale is 1 mm, A - flocculent inoculum, B - granular sludge sampled from the SBR on day 25

A further reduction in the settling time to 2 min deteriorated the settling properties of the aggregates, with the SVI_{30} reaching values above 100mL/g. Upon returning to the 3-min settling regime a low SVI_{30} was gradually restored, again approaching the SVI_5 value. From day 60 on, biomass accumulation was finally achieved in the SBR, raising the mixed liquor TSS values from 2 to 7 g/L, as can be seen in Figure 3. The evolution of COD removal along the SBR cycles can be seen on Figure 4. The removal rate increased with operational time and, on day 24, 65% removal was achieved 1h into the aerobic reaction stage. At the end of the experiment good effluent quality was being obtained, with average residuals 220 mgTSS/L and 65 mgCOD/L. The latter corresponds to an average COD removal of 88%.

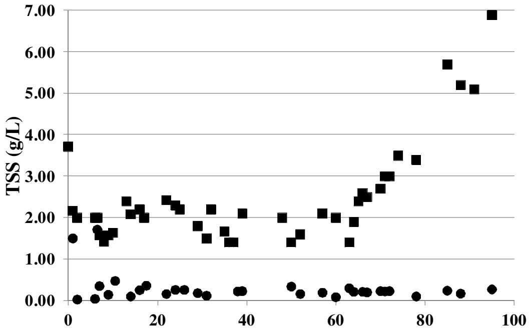

FIGURE 3 - TSS values in the SBR *versus* SBR operational time, ■ mixed liquor, ● effluent

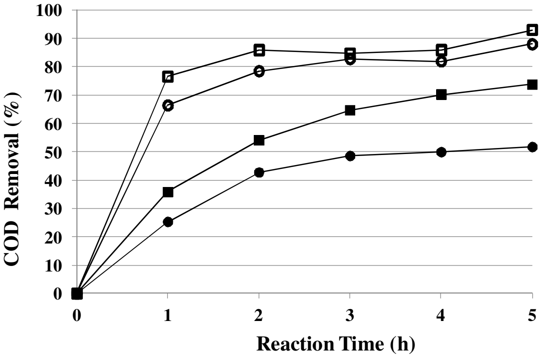

FIGURE 4 – COD removal along selected SBR cycles, ■ day 2, ● day 6, □ day 24, ○ day 87

Granule integrity tests were performed, showing good levels, reaching 85% on day 96. Specific oxygen uptake rate (SOUR) was measured in some of the cycles in the operational period between days 66 and 72. Average values of 55 and 9 mg $O_2.gSST^{-1}.h^{-1}$ were found at the start and end of the aerobic reaction stage, respectively. In this period, granules were observed under Gram/viability stain, and found to be almost only composed of Gram negative bacteria, as expected, with only one or to spots of Gram positive bacteria present in the observed slides. The majority of cells were stained as viable but clusters of dead cells were easily found, evenly spread on the granules.

Reactor Operation with Long-Term Stored Granules Two reactors, SBR1 and SBR2, were inoculated with granules stored for 7 months at 4ºC and at 25ºC, respectively, and operated in the same conditions as previously described. Both were operated at 3 min settling time, so there was some loss of biomass on day 1, as can be seen in Figure 4. A ready recovery in TSS levels followed, indicating good biomass growth in both reactors. The settling properties also improved rapidly, reaching on operational day 7, low values for SVI_{30} and SVI_5, comparable to those obtained in the previous SBR operational period. In both these aspects, granules stored at 4ºC performed better than granules stored at 25ºC, as expected. Regarding COD levels, on day 7, removal yields of 71% and 52% were achieved in SBR1 (4ºC storage) and SBR2 (25ºC storage), respectively. Nevertheless the fast recovery in performance of the biomass left for 7 months at 25ºC is notable. This result evidences the robustness and feasibility of granular activated sludge technology for industrial wastewater treatment, even in the face of production shutdown periods of days or weeks, with the corresponding absence of feed to the biological reactor.

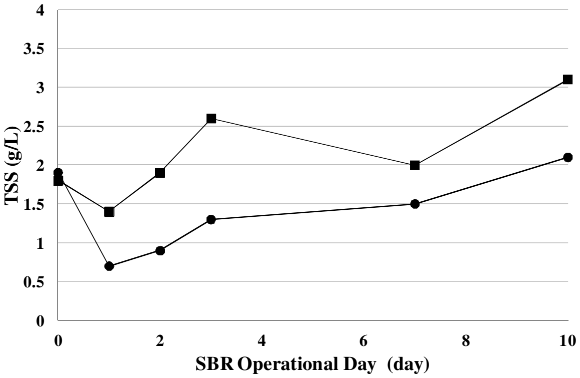

FIGURE 5 - TSS values in the SBR mixed liquor *versus* SBR operational time (second period), ■ SBR1 (4ºC storage) ● SBR2 (25ºC storage)

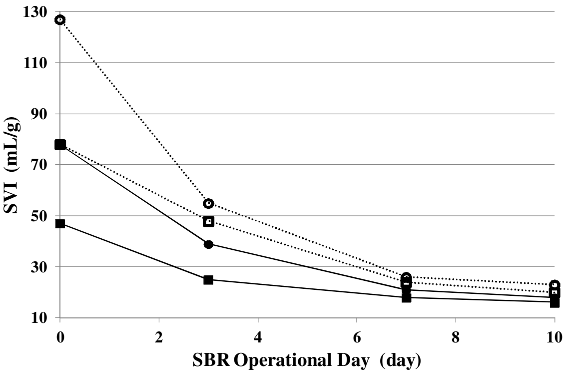

FIGURE 6 – Sludge volume index values *versus* SBR operational time (second period), ■ SVI_{30} (4ºC storage), ● SVI_{30} (25ºC storage) □ SVI_5 (4ºC storage), ○ SVI_5 (25ºC storage)

Microscopy images os sludge samples from this operational period are shown on Figure 7. Clearly, storage at 4ºC preserved the granule structure better, and storage at 25ºC lead to granule breakup. However, after SBR start up, already on operational day 10 granule structure was recovered and no significant differences could be observed between the two reactor sludges. This is in agreement with granule integrity measurements, with respective values of 26% and 15% (day 0) and 92% and 98% (day 10), for granules stored at 4ºC and at 25ºC.

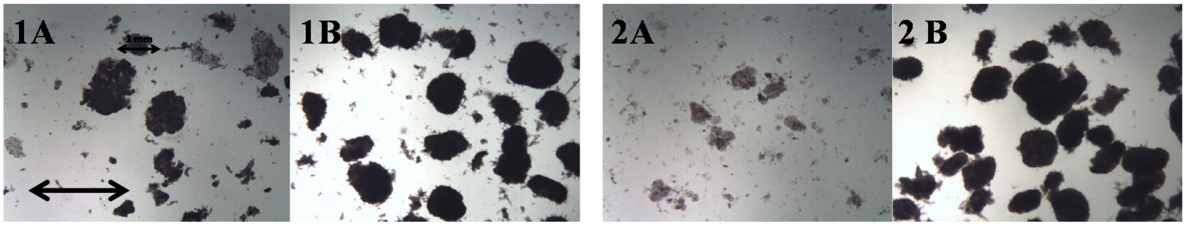

FIGURE 7 – Light microscopy observations (second period), scale is 1 mm, 1A- 4ºC storage, day 0; 1B- 4ºC storage, day 10; 2A- 25ºC storage, day 0; 2B- 25ºC storage, day 10

Granules were observed under Gram/viability stain (ViaGram™ Red+ Bacterial Gram Stain Viability Kit), and in both cases a semi-quantitative evaluation gave a 50% or higher proportion of viable cells in the sludge sampled on day 10.

CONCLUSIONS

This work demonstrated the successful generation of granular activated sludge from a flocculent inoculum in a laboratory, non tubular reactor, granules with very high settling velocity and good COD removal yields being obtained. The start up of the SBR with granules submitted to long-term storage gave remarkable results, showing fast recovery of the settling properties, growth rate and granule structure even for the biomass stored at 25ºC for 7 months. This indicates the robustness and feasibility of granular activated technology for wastewater treatment of varied origins, even under prolonged feed and aeration interruptions.

ACKNOWLEDGEMENTS

This work was partially financed by Fundação para a Ciência e a Tecnologia (FCT), Portugal, project BIOTEXTILE (PTDC/EBB-EBI/120624/2010). A. M. T. Mata and N. D. Lourenço acknowledge a doctoral grant (SFRH/BD/49432/2009) and a post-doctoral research grant (SFRH/BPD/31497/2006), respectively, from FCT (Portugal).

REFERENCES

Beun, J. J., A. Hendriks, M. C. M. Van Loodsdrecht, E. Morgenroth, P. A. Wilderer, J. J. Heijen. 1999. "Aerobic Granulation in a sequencing batch reactor" *Water Research* 33 (10), 2283-2290

Liu, Y., J. H. Tay. 2004. "State of the art of biogranulation technology for wastewater treatment" *Biotechnology Advances*. 22, 533–563

Liu, Y. 2008. *Wastewater Purification, Aerobic Granulation in Sequencing Batch Reactors*. CRC Press, Taylor & Francis Group.

Lourenço, N. D., J. M. Novais, H. M. Pinheiro. 2001. "Effect of some operational parameters on textile dye biodegradation in a sequential batch reactor" *J. Biotechnol.* 89(2-3), 163-172.

Muda, K., A. Aris, M. R. Salim, Z. I. A. Yahya, M. C. M. Van Loodsdrecht, A. Ahmad, M.Z. Nawahwi. 2010. "Development of granular sludge for textile wastewater treatment". *Water Research* 44 (15), 4341-4350

Tay, S. T., B. Y. Moy, H. Jiang, J. H. Tay. 2005. "Rapid cultivation of stable aerobic phenol-degrading granules using acetate-fed granules as microbial seed" *Journal of Biotechnology*. 115, 387–395

LINKING NUTRIENTS, METALS AND PRODUCTIVITY IN GULF OF MANNAR MANGROVE ISLANDS, INDIA

Nabeel M. Alikunhi (King Abdullah University of Science and Technology, Thuwal, KSA)
Kathiresan Kandasamy (Annamalai University, Tamil Nadu, India)

ABSTRACT: Influence of metals (Fe, Mn, Zn, Cu, Cd, Pb & Ni) and nutrients (N, P & K) on mangrove productivity (net canopy photosynthesis - NCP & complex index - CI) were investigated in Mandappam, Keelakarai and Tuticorin island groups in Gulf of Mannar (GoM), India. Tuticorin was less diverse, lower NCP (1.23±0.3 $gCm^{-2}d^{-1}$) and CI (420±56), but with higher salinity (55.0±5.2). Mandappam was more diverse, highest NCP and CI (2.89±0.8 $gC/m^2/d$ & 2737±145) but lower salinity (21.2±2.1). The nutrients (kg ha^{-1}) varied significantly; N (121±12 -22±3), P (15.6±2.9 - 6.2±0.8) and K (259±23.9 - 57±8.6) were maximum in Mandappam and minimum in Tuticorin. The concentration (μg g^{-1}) of Fe (1653 - 481), Mn (750 - 115), Zn (95 -11), Cu (156 - 19), Cd (2.12 - 0.53), Pb (137 - 0.5) and Ni (15.21 - 2.36) were higher in Tuticorin and lower in Mandappam. NCP and CI exhibited positive correlation with nutrients (N, P & K) but negative correlation with salinity and Cu, Pb & Zn. Principal component ordination, BIOENVI and Global BEST match tests revealed salinity, Cu and Pb are most influential parameters on NCP. Results indicate GoM mangroves are under degradation due to environmental and anthropogenic stress.

INTRODUCTION

Mangroves are among the most productive ecosystems of the world and are linked directly and indirectly with the adjacent ecosystems (Alikunhi and Kathiresan, 2012; Kathiresan and Bingham, 2001). They are extremely important coastal resources which provide food and habitat for numerous organisms and serve as breeding, feeding and nursery grounds for many marine organisms (Mumby et al., 2004). They protect coastal populations by stabilizing shorelines and functions as a 'bio-shield' against sea waves, coastal erosion and natural calamities (Kathiresan and Bingham, 2001). Mangroves play a major role in the global cycling of carbon, nitrogen and sulphur as well as act as reservoirs of waste materials (Kathiresan and Bingham, 2001). Despite of these facts, mangroves continue to disappear globally at a rate of 0.66% per year during the 2000-2005 period (FAO, 2007) in which 11 of the 70 mangrove species in the world (16%) are at threat of extinction (Polidoro et al., 2010) and consequently at least 40% of the animal species that are restricted to mangrove habitat are also at elevated risk of extinction (Luther and Greenburg, 2009). It is predicted that the ecosystem services offered by mangroves may be totally lost within 100 years (Duke et al., 2007). The global mangroves are under serious threat due to the collective effects of natural and anthropogenic pressures (Gilman et al., 2006). However, it is necessary to identify the natural and anthropogenic threats that affect the mangrove productivity at regional scales in order to void the aftermaths of mangrove degradations. The present investigation therefore was undertaken to study the influence of trace metals and nutrients on mangrove productivity in mangroves forest of the Gulf of Mannar (GoM) Biosphere Reserve of India.

MATERIALS AND METHODS

GoM Biosphere Reserve is the first Marine Biosphere Reserve in the south and south east Asia, that lie along the 140 km stretch between Tuticorin and Rameswaram, located between latitude 8°47′ N and 9°15′ N and longitude 78° 12′ E and 79° 14′ E with an area of about 623 hectares . The islands lie at an average distance of 8 km from the main land. The present study was conducted in 21 islands of the Gulf of Mannar area, divided under three groups *viz.* Mandappam, Keelakarai and Tuticorin group based

---

ISBN 9780976885351

on their spatial distribution. Each group was with 7 Islands. The field work was carried out during April-June, the dry season of the study area. A total of 130 plots of 10 × 10m dimension from all the islands were studied for their mangrove productivity (NCP & CI), and rhizosphere sediments were analyzed for pore water salinity, nutrients (N, P & K) and metal (Fe, Mn, Zn, Cu, Cd, Pb & Ni). Since two islands of Tuticorin were without mangroves, only metals and nutrients were analyzed.

Net canopy photosynthesis (NCP) and Complex index (CI) were calculated from the various measured values by using the method described by English et al., (1997). Pore water salinity was measured by using a hand refractometer (Atago hand refractometer, Japan). For other analysis, mangrove rhizosphere sediments were collected using a hand corer in clean polythene bags and transported to the laboratory. The plant roots and other debris were removed from the sediment samples, dried in an oven at 110°C and were ground before analysis of K by method described by Guzman and Jimenez (1992), N & P using Kjeldahl method (Subbiah and Asija, 1956) and trace metals using method by Chester and Hughes (1967). Differences in the values of various parameters between the island groups were tested using ANOVA (SPSS 17). To explore the relation between various groups, Pearson's correlation with two tailed test of significance was performed. The sediments were compared by principal component analysis (PCA), BIOENVI and Global BEST match tests using PRIMER 6 (Plymouth Routines in Multivariate Ecological Research).

RESULTS

A total of 9 mangrove species belonging to 5 botanical families, represented dominantly by Rhizophoraceae were recorded. In general, *Avicennia marina* is most abundant followed by *Pemphis acidula.* This is followed in descending order by: *Ceriops tagal, Rhizophora mucronata*, *Bruguiera cylindrica, Lumnitzera racemosa*, *Exoecoecaria agallocha R. apiculata* & *B. gymnorrhiza.* The Mandappam group has all the 9 mangrove species and hence was more diverse than other two groups. Keelakarai and Tuticorin group have 5 (*A. marina P. acidula, C. tagal, L. racemosa* & *E. agallocha*) and 2 (*A. marina* & *P. acidula*) mangrove species respectively. Two islands of Tuticorin group were without any mangroves. The biodiversity indices such as Shanon diversity, Margalef richness, Plieiou's evenness and Simpson dominance were higher in Mandappam and lower in Tuticorin group. Keelakarai group exhibited intermediate values. The mean NCP ($gCm^{-2}d^{-1}$) and CI of the mangroves varied significantly between the Island groups ($F_{(2,\ 97)} = 4.09$, & $F_{(2,\ 97)} = 7.14$; $P<0.05$ respectively) and was found maximum in Mandappam (2.89±0.8 & 2737 ±145) and minimum in Tuticorin group (1.23±0.3 & 420±56) as shown in the Figure 1.

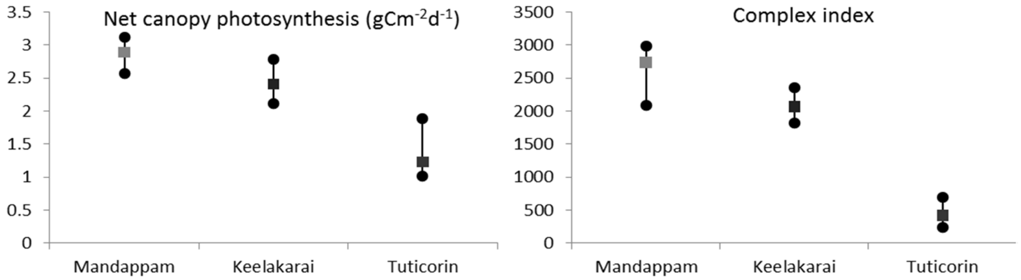

FIGURE 1. The complex index and net canopy photosynthesis in three Island groups

The values of salinity (psu), trace elements ($\mu g\ g^{-1}$) and nutrients ($kg\ ha^{-1}$) in the mangrove sediments varied significantly between different Island groups ($P<0.05$) as depicted in the Figure 2. The salinity ($F_{(2,\ 97)} = 4.09$) was maximum in Mandappam (55.0±5.2) and minimum in Tuticorin group (21.2±2.1). Among the metals Fe ($F_{(2,\ 118)} = 3.11$) ranged between 1653±145 & 481±39, Mn ($F_{(2,\ 118)} = 4.71$) between 750±81 & 115 ±14, Zn ($F_{(2,\ 118)} = 7.9$) between 95±8 & 11±1.4, Cu ($F_{(2,\ 118)} = 12.1$)

between 156±14 & 19±2.1, Cd ($F_{(2,\ 118)}$ = 4.25) between 2.12±0.23 & 0.53±0.04, Pb ($F_{(2,\ 118)}$ = 9.5) between 137±12 & 0.5±0.03 and Ni ($F_{(2,\ 118)}$ = 3.92) between 15.21±1.73 & 2.36±0.25 were higher in the mangrove sediments of Tuticorin and lower in Mandappam group of Islands. N ($F_{(2,\ 118)}$ = 9.34) ranged from 22±3 to 121±12, P ($F_{(2,\ 118)}$ = 8.74) from 6.2±0.8 to 15.6±2.9 and K ($F_{(2,\ 118)}$ = 6.91) from 57±8.6 to 259±23.9 were maximum in Mandappam group and minimum in Tuticorin group of Islands.

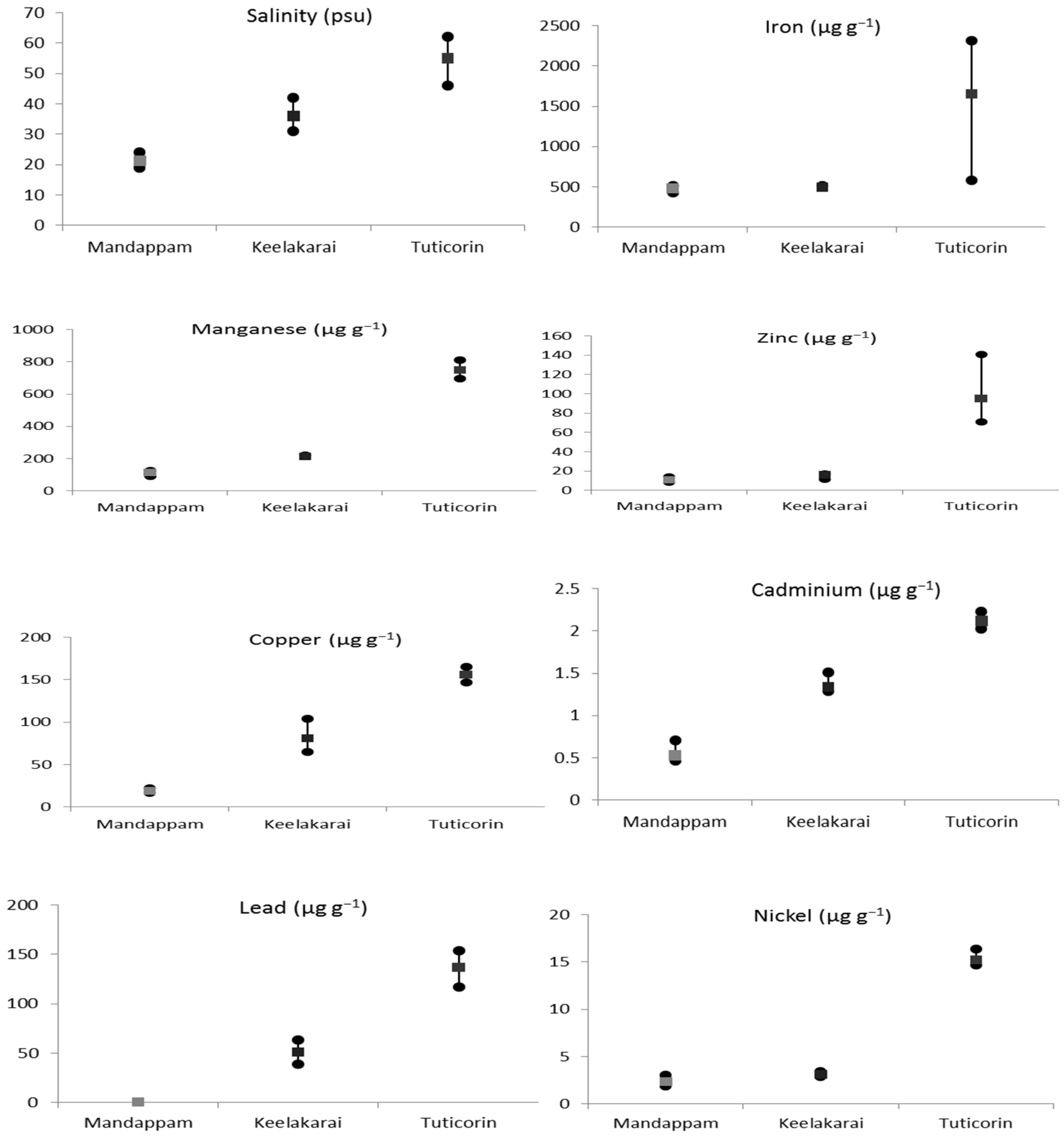

FIGURE 2(a). The values of salinity, metal and nutrients in rhizosphere sediment of three island groups.

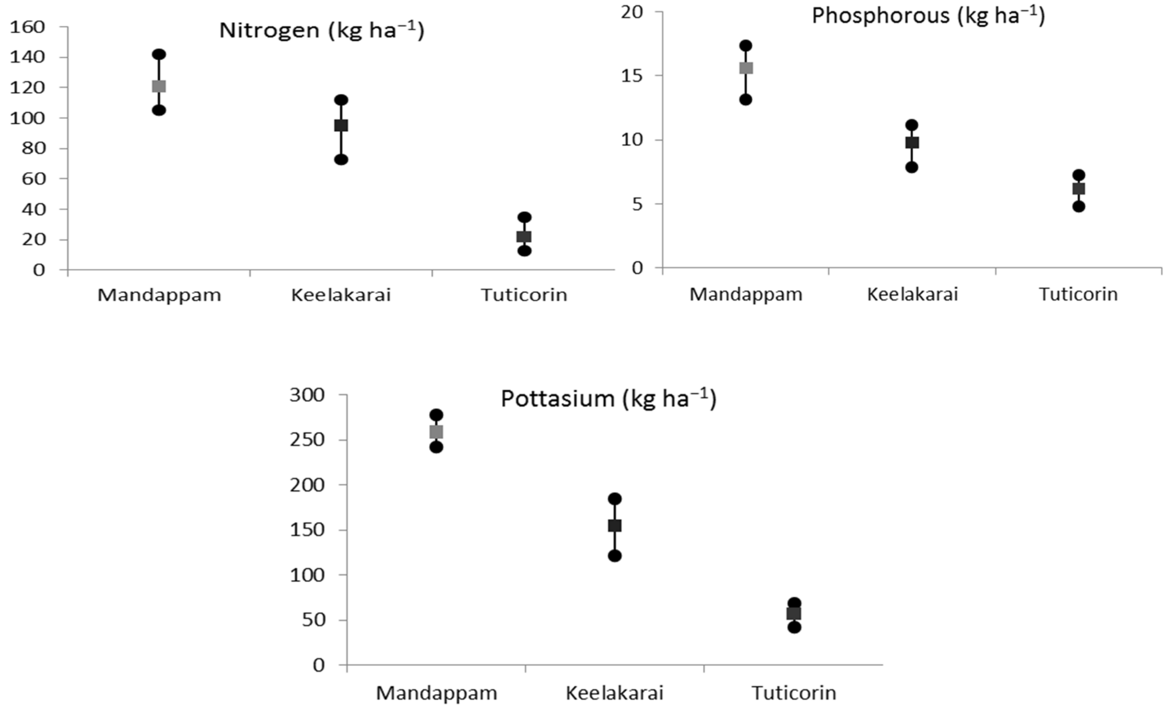

FIGURE 2(b). The values of salinity, metal and nutrients in rhizosphere sediment of three island groups.

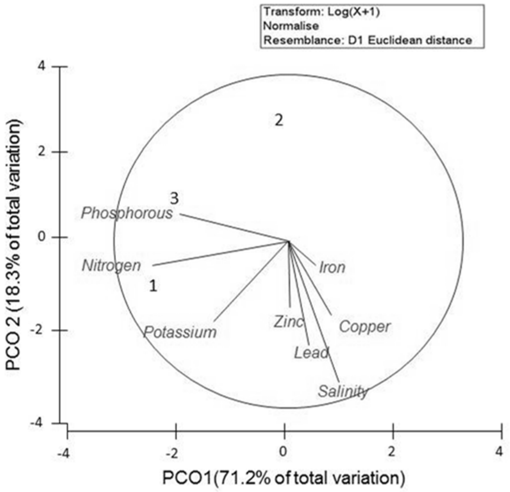

FIGURE 3. Principle coordination plot showing the coordination of various parameters tested

The NCP and CI exhibited positive correlation with nutrients (N, P & K) but negative correlation with salinity and metals (Cu, Pb & Zn).The PCA ordination exhibited a good coordination of stations based on various parameters tested in the present study (Figure 3). This first component accounted for 71.2% of variability and the second for 18.3% which makes a total of 89.5% of variability. The PCA eigenvector plot revealed that salinity influenced more for the variability of stations, as reflected in the length of the vector, followed by N and Cu. The BIOENVI was employed to find the best match of variables influencing net canopy photosynthesis. The results revealed that salinity, Cu and Pb were the best combination of variables influencing NCP with a correlation of 0.841 (Table 1). The histogram (Fig. not shown) obtained for Global BEST match test displayed Rho (ρ) value = 0.831, explaining the significant relationship between variables with NCP.

TABLE 1. BIOENVI results for best combination of variables influencing net canopy photosynthesis of mangroves at Gulf of Mannar islands

No.	Correlation	Selections
1	0.841	Salinity, Cu, Pb
2	0.792	Salinity, N, Pb,
3	0.719	Salinity, N, P,
4	0.704	N, Cu, Pb,
5	0.669	Cu, P, K

DISCUSSION

GoM biosphere reserve retains various critical ecosystems such as mangroves, seagrasses and corals with amazing biological diversity and hence has long been recognized as a national priority. The mangroves of GoM are under severe threat which is presumed due to anthropogenic pressures from the adjacent cities. But unfortunately no comprehensive efforts have been made to find out the scientific reason for the mangrove degradation. Thus, the present study investigated Island mangroves of GoM for its productivity and the influential factors on mangrove productivity. Among the island groups, Mandappam was more diverse with higher biodiversity indices such as Shanon diversity Margalef richness, Plieiou's evenness and Simpson dominance. Tuticorin was less diverse and two of its island were without any mangrove species. Similarly, the NCP and CI were also higher in Mandappam and lower in Tuticorin group.

Mangroves are tightly bound to tropical coastal environment thriving between land and water, characterized with variable gradients of physico-chemical parameters (Kathiresan and Bingham, 2001). The present study found that the CI and NCP of the mangroves was negatively correlated with pore water salinity of the rhizosphere soil. In general, mangrove vegetation is more luxuriant in lower salinities (Kathiresan et al. 1996) and hypersalinity stunts tree growth in a mangrove species (Selvam et al., 1991), reduces biomass (Naidoo, 1990), and causes denaturing of terminal buds in seedlings (Koch and Snedaker, 1997). Experimental evidences indicate that at high salinity, mangroves spend more energy to maintain water balance and ion concentration rather than for primary production and growth (Clough, 1984). Apart from salinity, N, P & K exhibited high correlation with the CI and NCP. This reveals that soil nutrients have direct control on mangrove ecosystems as stated by Boto and Wellington (1984). This has also been proved by fertilization experiment of dwarf trees and found that tree growth was strongly enhanced with P and N fertilization (Lovelock et al., 2004). In contrast the trace elements such as Cu, Pb and Zn exhibited higher negative correlation with NCP in this study. Recent industrialization of various tropical regions resulted in significant accumulation of pollutants into mangrove environment (Tam and Wang, 1998). The increased concentration of trace element pollution in many natural environments has resulted in toxicity to the biota and eventually leading to biodiversity reduction. Hence, excessive accumulation of trace metals would have negative effect on photosynthetic productivity of mangroves.

CONCLUSIONS

The assessment of environmental entities revealed that CI and NPR exhibited positive correlation with N, P & K, but negative correlation with salinity as well as trace elements (Cu, Pb & Zn). Thus the mangrove forest structure cannot be linked to one single factor but to complex interactions between various factors. The degradation and shrinkage of mangrove species of GoM ecosystem is well-known. The rapid industrialization all along the mainland coast caused increased metal pollutants particularly around Tuticorin, which is evident from the higher trace metal concentration in mangrove sediment. This could be attributed to the mangrove degradation in GoM. Increase in the extent of salt pans is yet another factor leading to the shrinkage of mangroves (Daniel and Uma Maheswari, 2001). This was supported by higher salinity values of the present study in the degrading mangrove regions. The information gained through the present study warns for immediate remedial measures for effective conservation of degrading mangrove ecosystems in the GOM islands.

ACKNOWLEDGEMENTS

The authors are thankful to the authorities of Annamalai University for providing facilities. We are also grateful to Gulf of Mannar Biosphere Reserve Trust, Ramanathapuram, TamilNadu- India for providing financial support from GEF-UNDP sponsored project.

REFERENCES

Alikunhi, N. M., and K. Kathiresan. 2012. “Phytoplankton productivity in interlinked mangroves, seagrass and coral reefs and its ecotones in Gulf of Mannar Biosphere Reserve South East India.” *Mar. Biol. Res.* 8(1): 61-73.

Boto, K. G., J. S. Bunt, and J. T. Wellington. 1984. “Variations in mangrove forest productivity in Northern Australia and Papua New Guinea.” *Estuar. Coast. Shelf Sci.* 19: 312-329.

Chester, R., and F. G. Huges. 1967. “A chemical technique for the separation of ferrow manganese minerals, carbonate minerals and absorbed trace elements from pelagic sediment.” *Chem. Geol.* 2: 249-262.

Clough, B. F. 1984. “Growth and salt balance in the mangroves *Avicennia marina* (Forsk.)Vierh. and *Rhizophora stylosa* Griff. in relation to salinity.” *Aus. J. Plant Physiol.* 11: 419-430.

Daniel, P., and P. Umamaheswari. 2001. *The Flora of the Gulf of Mannar. Botanical Survey of India*, Calcutta.

Duke, N. C, O. J. Meynecket, and S. Dittmann. 2007. A world without mangroves? *Sciencemag.org*. 41.

English, S., C. Wilkinson, and V. Baker. 1997. *Survey Manual for Tropical Marine Resources*. 2nd ed., Australian Institute of Marine Science, Australia.

FAO. 2007. *The World’s mangroves 1980-2005*. Food and Agriculture Organization of the United Nations, Rome.

Gilman, E., J. Ellison, V. Jungblat, H.VanLavieren, L. Wilson, F. Areki, G. Brighouse, J. Bungitak, E. Dus, M. Henry, I. Sauni Jr., M. Kilman, E. Matthews, N. Teariki-Ruatu, S. Tukia, and K. Yuknavage, 2006. “Adapting to Pacific Island mangrove responses to sea level rise and other climate change effects.” *Climate Res.,* 32:161–176.

Guzman, H. M., and C. E. Jimenez. 1992. “Contamination of coral reefs by heavy metals along the Carribeen coast of central America. (Coastal Rica and Panama).” *Mar Poll Bull.* 24(11): 554-561.

Kathiresan, K., B.L. Bingham. 2001. “Biology of mangroves and mangrove ecosystems.” *Adv. Mar. Biol.* 40: 81-251.

Kathiresan, K., N. Rajendran, and G. Thangadurai. 1996. “Growth of mangrove seedlings in intertidal area of Vellar estuary, southeast coast of India.” *Ind. J. Mar. Sci.* 25: 240-243.

Koch, M. S, and S. C Snedaker, 1997. “Factors influencing Rhizophora mangle L. seedling development in Everglades carbonate soils.” *Aqua. Bot.* 59(1-2): 87-98.

Lovelock, C. E., I. C. Feller, K. L. McKee, B. M. J Engelbrecht, and M. C. Ball. 2004. "Nutrient limitation growth in extensive scrub mangroves in Bocas del Toro, Panama." *Func. Ecol.* 18: 25-33.

Luther, D., and R. Greenburg. 2009. "Mangroves; a global perspective on the evolution and conservation of their terrestrial vertebrates." *Biosci.* 59: 602-612.

Mumby, P. J., A. J. Edwards, J. E. Arias-González, K. C. Lindeman, P. G. Blackwell, A. Gall, M. I.

Gorczynska, A. R. Harborne, C. L. Pescod, H. Renken, C. C. Wabnitz, and G. Llewellyn. 2004. "Mangroves enhance the biomass of coral reef fish communities in the Caribbean." *Nature* 427: 533-536.

Naidoo, G., 1990. "Effects of nitrate, ammonium and salinity on growth of the mangrove *Bruguiera gymnorrhiza* (L.) Lam." *Aqua. Bot.* 38(3): 210-219.

Polidoro, B. A., K. E. Carpenter, L. Collins, N. C. Duke, A. M. Ellison, J. C. Ellison, E. J. Farnsworth, E. S. Fernando, K. Kathiresan, N. E. Koedam, S. R. Livingstone, T. Miyagi, G. E. Moore, N. V. Nam, J. E. Ong, J. H. Primavera, S. G. Salmo III, J. C. Sanciangco, S. Sukardjo, Y. Wang, and J. W. H. Yong. 2010. "The loss of species: Mangrove extinction risk and geographic areas of global concern." *PLoS ONE.* 5(4): 1-10.

Selvam, V., R. Mohan, R. Ramasubramanian, and J. Azariah. 1991. "Plantcommunities and soil properties of three mangrove stands of Madras Coast." *Ind. J. Mar. Sci.* 20: 67-69.

Subbiah, B. V., and G. L. Asija. 1956. "A rapid procedure for the determination of available nitrogen in soils." *Cur. Sci.* 31: 196-200.

Tam, N.F.Y., and Y.S. Wang. 1998. "Variations of Soil Nutrient and Organic Matter Content in a Subtropical Mangrove Ecosystem." *Water Air Soil Poll.* 103(1-4): 245-261.

DECOLORIZATION AND DETOXIFICATION OF REACTIVE DYE BY *PSEUDOMONAS STUTZERI* ISOLATED FROM TEXTILE EFFLUENT

Naresh V. Butani* (Bhagwan Mahavir College of Biotechnology, Surat, India)
Nilesh D. Pandya (Arts, Science & Commerce College, Kamrej Char Rasta, Surat, India)
S. K. Tank (Veer Narmad South Gujarat University, Surat, India)
Piyush V. Desai (Veer Narmad South Gujarat University, Surat, India)

Azo reactive dyes, an important class of dyes, are commonly used to dye cellulosic fibers and appear in wastewater due to their lower fixation on fiber. Large volumes of effluent are generated at different stages of textile manufacturing as a result of the use of copious amounts of dyes. Colored textile water requires efficient & ecofriendly treatment before its discharge. An efficient dye decolorizing Gram negative bacterial strain *Pseudomonas stutzeri* was isolated from colored textile effluent and characterized by 16s rDNA sequencing. Biodecolorization study of Reactive Red 141 was carried out in Bushnell Hass medium where dyes were used as sole source of carbon and nitrogen. Decolorization was observed up to 91%, when dye was used as sole source of carbon and nitrogen. Various parameters like addition of carbon source, nitrogen source, pH and temperature, were optimized for maximum decolorization of dye. Complete dye decolorization was obtained in Bushnell Hass broth medium when the bacterial culture was incubated at 31 °C for 7 day at pH 8.0 on rotary shaker in presence of C & N source. Decolourization & degradation of dye was analyzed by HPLC & FTIR. The toxicity of dye & microbialy treated dye was assessed by bioassay test by using seed germination assay, *Lemna minor* bioassay, Daphnia & brine shrimp bio assays. Results of ecotoxicity test suggest environment friendly nature of degraded metabolites.

ISBN 9780976885351

ASSESSING ACUTE TOXICITY OF BLACK LIQUOR GENERATED FROM REFINED COTTON PRODUCTION

Xu Zhao, Quanlin Zhao, Zhengfang Ye (Peking University, Beijing, P.R. China)

The compositions of black liquor generated from refined cotton production were characterized by using UV-vis spectroscopy and Fourier Transform Infrared Spectroscopy (FTIR). The acute toxicity was evaluated by bacterium bioluminescence assays using a freshwater luminescent bacterium (*Vibrio qinghaiensis sp. Nov.*) and a marine luminescent bacterium (*Photobacterium phosphoreum*). The results showed that the wastewater was poorly biodegradable due to the high amount of chemical oxygen demand (COD). The main organic components of the black liquor are guaiacyl (G-) and hydroxyphenyl (H-) lignin. It was highly toxic to luminescent bacteria *P. phosphoreum* and *V. qinghaiensis sp. Nov.*. After reaction time of 15 min, the dilution ratio at 50% luminescence inhibition ratio was 370 for *P. phosphoreum,* while that was 133 for *V. qinghaiensis*. *P. phosphoreum* is more sensitive for evaluating black liquor's acute toxicity than *V. qinghaiensis*. After adsorption by activated carbon fiber, the acute toxicity can be greatly reduced, which is helpful for further treatment by biological methods.

ISBN 9780976885351

BIOSORPTION AND BIOACCUMULATION OF CHROMIUM (III) FROM AQUEOUS SOLUTION EMPLOYING *ASPERGILLUS LENTULUS*

Abhishek Mishra* and Anushree Malik (Indian Institute of Technology Delhi, INDIA)

Chromium(III) salts are the most widely used chemicals for tanning processes. Nevertheless, only 60% - 70% of total chromium salts react with the hides while about 30% - 40% of the chromium remains in solid and liquid wastes (especially spent tanning solutions). Although Cr(III) is less toxic than Cr(VI), long-term exposure to Cr(III) is known to cause allergic skin reactions and cancer. Moreover, there are always chances of the conversion of Cr(III) to Cr (VI) form. Therefore, the removal and recovery of chromium from these wastewaters is necessary for environmental protection and economic reasons. In view of the above, the aim of the present study was to investigate the Cr(III) removal potential of previously isolated strain of *Aspergillus lentulus* from aqueous solutions. Batch experiments were conducted with various initial concentrations of chromium ions to obtain the metal uptake capacity in growing (1000-5000 ppm) as well as in biosorption (50-500 ppm) mode. The tolerance data with a high range of Cr(III) concentrations revealed the *A. lentulus* could tolerate chromium toxicity up to 15,000 ppm. The kinetics of growth and Cr(III) removal by *A. lentulus* was studied using the optimized media. At higher concentrations (> 5000 ppm), presence of Cr(III) resulted in delayed growth and decreased growth rate of the fungal strain. In bioaccumulation mode, the Cr(III) uptake efficiency of *A. lentulus* were found to be 44.42, 192.29, 430.86, 658.37 and 917.77 mg/g in presence of 1000, 2000, 3000, 4000 and 5000 ppm initial metal concentrations, respectively. In the biosorption mode, in presence of 1000 ppm initial Cr(III) concentration, the biosorption rate increased from 41.95 mg/g to 80.8 mg/g when contact time was increased from 30 min to 60 min while at 120 min it further increased to 101.28 mg/g. Similar trend was followed by fungal biomass at higher initial concentration of Cr(III). Results indicate the applicability of this *A. lentulus* strain for the removal of chromium from industrial wastewater.

ISBN 9780976885351

ASSESSMENT OF PHYTOEXTRACTION EFFICIENCY OF NATURALLY GROWN PLANT SPECIES IN THE FORMER TIN MINING CATCHMENT

Muhammad Aqeel Ashraf [*], Mohd. Jamil Maah and Ismail Yusoff
(University of Malaya, Kuala Lumpur, Malaysia)

Removal of heavy metals from soil and water by plants (Phytoremediation) has appeared as a promising cost-effective technology. Nine plant species such as *Cyperus rotundus L., Imperata cylindrica, Lycopodium cernuum, Melastoma malabathricum, Mimosa pudica Linn, Nelumbo nucifera, Phragmites australis L., Pteris vittata L.* and *Salvinia molesta,* were selected according to previous studies on these plant species conducted by author. These plant species analysed to assess the phytoextraxtion potential for remediation of lead (Pb), copper (Cu), zinc (Zn), arsenic (As) and tin (Sn) from contaminated tin tailings. Results showed that *Cyperus rotundus L.*, accumulated 658 mg kg^{-1}, *Imperata cylindrica* accumulated 245 mg kg^{-1}, *Nelumbo nucifera* accumulated 288 mg kg^{-1}, *Phragmites australis L.,* accumulated 345 mg kg^{-1} and *Pteris vittata L.* accumulated 278 mg kg^{-1} (dry weight) with bioconcentration factors up to 0.40, 0.32, 0.57, 0.71 and .65, respectively. The phytoextraction rates of *Cyperus rotundus L.* (86%) for Sn, *Imperata cylindrica* (42%) for Zn, *Nelumbo nucifera* (56%) for As, *Phragmites australis L.*(49%) for Cu and *Pteris vittata L.* (31%) for Pb, were recorded. It can be concluded that these plant species could successfully be used for phytoremediation of mining tin tailings in Peninsular Malaysia.

ISBN 9780976885351

TWO-PHASE BIODEGRADATION OF PHENOL IN A HOLLOW FIBER MEMBRANE BIOREACTOR

Prashant Praveen and Kai-Chee Loh (National University of Singapore, Singapore)

Over the past few years, aqueous-organic two-phase biodegradation systems have emerged as a very efficient technique to avert substrate inhibition in the biodegradation of aromatic compounds. These biphasic bioreactors attain high cell growth and biodegradation rates and could make an ideal system; but the plethora of problems resulting from phase dispersion hamper bioreactor operation and render the technology relatively impractical.

The objective of this research was to mitigate the operational challenges encountered in a biphasic biodegradation system by designing a dispersion-free two phase membrane bioreactor. The strategy was to use hydrophobic hollow fiber membranes to physically separate the aqueous and organic phases using phenol as the model pollutant. The high surface area and porosity of the fibers facilitated the mass transfer of the substrate between the phases while the low pore size prevented any cell immobilization and helped in retaining the bacteria in suspension. Microorganisms in the membrane bioreactor were characterized by absence of lag phase and high specific growth rates of 0.52, 0.48 and 0.42 hr-1 for phenol concentrations of 600, 1000 and 2000 mgL-1 respectively. Biodegradation time was relatively shorter and 1000 mgL-1 phenol was biodegraded within 46 hours. It was found that biodegradation rates increased with interfacial mass transfer area. When fiber length was doubled, biodegradation time for 2000 mgL-1 phenol was shortened by 25 % and phenol could be mineralized within 43 hours. During the entire operation of the membrane bioreactor, no foaming, emulsification or solvent loss was observed. In the absence of high energy agitation for phase mixing, the bioreactor design demanded lower energy. The results of the study also indicate that by judiciously adjusting the mass transfer area, biodegradation kinetics of the membrane bioreactor can be made comparable and even better than that of dispersion-based two phase biodegradation systems.

ISBN 9780976885351

BIOSORPTION OF CU, ZN AND NI BY GROWING *ASPERGILLUS* SP. IN CHEESE WHEY

Reena Pundir and **M. G. Dastidar**
(Centre for Energy Studies, Indian Institute of Technology-Delhi, New Delhi, India)

Anthropogenic activities are the main sources of heavy metals contaminants causing serious environmental pollution problems and health hazards for living beings. The removal of heavy metals by physico-chemical techniques is not economically viable for small and medium scale industries. Biosorption of heavy metals has received serious attention in recent years as a low energy process. Microorganisms (algae/fungi/yeasts) have been reported as potent bio-remediators for heavy metals by various researchers mostly by using non-living biomass. The advantages of using growing cells over non-living cells are that simultaneous removal of metal could be obtained during the growth of the organism and additional unit processes of cell harvesting, drying etc. can be avoided. However, microorganisms require an energy source for their growth. In most of the laboratory studies on biosorption of heavy metals using growing cells of microorganisms, glucose has been used as an energy source, thus making the bioremediation process economically non-viable. In search for a cheaper energy source, the batch biosorption of Cu, Zn and Ni ions by *Aspergillus* sp. was investigated in the present study as a function of initial metal ion concentration (0-500mg/L), pH (2.0-6.0), inoculum concentration (v/v) and different concentrations of total sugar contained in cheese whey(2, 4, 6, 8 and 10g/L). Cheese whey which is generated as waste in food industry can act as a cheaper energy source due to the presence of high organic matter content such as lactos, protein, vitamins etc., disposal of which into the environment is again a cause of serious concern due to the high BOD and COD contents. The growth of *Aspergillus* sp. was examined at different pH using 50 mg/L initial metal ion concentration of each metal separately. A maximum biomass concentration (5.62 g/L) was observed at pH 5 in the absence of metal. The biomass concentration decreased from 5.62 g/L to 2.65 g/L , 2.8 g/L and 1.82 g/L in presence of 500 mg/L Cu, Zn and Ni respectively. The maximum specific uptake was found to be 9.4 ± 0.15 to 62.2 ± 0.20 mg/g, 9.5 ± 0.1 to 64.0 ± 0.25 mg/g and 7.2 ± 0.2 to 29.43 ± 0.08 mg/g by increasing initial concentration from 50 to 500 mg/L for copper, zinc and nickel respectively under similar conditions**.** The studies conducted with different concentrations of total sugar contained in cheese whey clearly indicate an increase in biomass concentrations with increase in total sugar concentration. The specific Cu uptake increased from 3.2 mg/g to 9.4 mg/g, specific Zn uptake from 3.5 mg/g to 9.6 mg/g and specific Ni uptake from 1.8 mg/g to 6.6 mg/g with increase in total sugar concentration from 2 to10 g/L. The possible cell metal ions interaction was evident from Scanning Electron Microscopy and X–Ray Energy Dispersion Analysis.

ISBN 9780976885351

DEGRADATION OF POLYCYCLIC AROMATIC HYDROCARBONS IN CRUDE OIL CONTAMINATED SALINE WATER BY A HALOTOLERANT BACTERIAL CONSORTIUM

Namasivayam Vasudevan* (Anna University, Chennai, India)
P. Aulazhagan, King Abdulaziz (University, Jeddah, Saudi Arabia)

Biodegradation of polycyclic aromatic hydrocarbons (PAHs) plays vital role due to its ubiquitous distribution and deleterious effects on human health. Hydrophobic nature of polycyclic aromatic hydrocarbons makes their clean up extremely difficult and persists for longer period. Polycyclic aromatic hydrocarbons (PAHs) are released into the environment through the incomplete combustion of solid and liquid fuels. Suspected to possess toxic, mutagenic and carcinogenic properties. PAH genotoxicity also increases with size, up to at least four or five fused benzene rings. Oil spillage leads to contamination of seawater by hydrocarbons. PAHs require effective remediation strategies due to growing production from anthropogenic sources. The present study is focused on degradation of PAHs by a halotolerant bacterial consortium crude oil contaminated saline water. Bacterial consortium degraded both low and high molecular weight PAH substrates. A BOD and COD removal efficiency above 90 % was observed with a MLSS concentration of 5000 mg/L. The degradation of phenanthrene, fluorene, anthracene, pyrene, and benzo(e) pyrene were monitored during the treatment of the crude oil contaminated saline water. A molecular characterization of the bacterial strains in the consortium was carried out to ascertain culturable bacterial strains in the mixture. The individual strains of the consortium has been shown to degrade the PAHs. The bacterial strains in the consortium can be used selectively or together for the bioremediation of contaminated wastewater and soil.

ISBN 9780976885351

ELECTROCHEMICAL TREATMENT OF INDUSTRIAL ELECTROPLATING RINSE WATERS

Meyyappan Revathi, Kaliyan Hemampujavalli, ***Manickam Velan*** (AC College of Technology, Anna University, Chennai, India)
Chiya Ahmed Basha (Central Electrochemical Research Institute, Karaikudi, India)

ABSTRACT: The present investigation reports removal of Cu (II), SO_4^{2-} ions and COD of the industrial electroplating rinse water (IEPRW) and the simultaneous recovery Cu (II) ions using an hybrid electrochemical ion exchange (EIX) and electro oxidation (EO) reactor (EIX–EO). The results obtained for voltage–current characteristics of EIX system with different inter electrode distance such as 0.5, 0.6 and 0.75dm showed that the electric current flow inside the stack cell increased with the decrease in inter electrode distance. The optimized conditions for current flow across the EIX stack were found to be 10g resin loading, Ti/RuO_2 anode and Nafion 117 membrane. Experiments were carried out in hybrid EIX-EO reactor in a batch recirculation mode at different applied current density (0.5-2.5Amp dm^{-2}). The Cu (II), SO_4^{2-} ions concentration and COD in the process compartment decreased with electrolysis time while in the receiver compartment Cu (II) ions concentration increased. Maximum recovery of Cu (II) ions into the receiver compartment was observed at an applied current density 2.0 Amp dm^{-2}.While varying the NaCl loading in the anolyte and applied current density, the amount of OCl^- produced was determined. Maximum of 106 mg L^{-1} hypochlorite was produced in 0.45h with 6 g L^{-1} of NaCl and 1.5 Amp dm^{-2} of applied current density. Breakpoint comparative analysis with ion exchange process alone showed that IX process has an efficiency to discharge 4.48L of treated IEPRW, the EIX discharged 19.5L of treated IEPRW.

Keywords: Ion exchange; electrochemical ion exchange (EIX); ion permeable membranes, Electro dialysis

INTRODUCTION

Wastewater from different industrial sectors, such as electroplating, metal finishing, photographic development, printed circuit board production or battery technology, requires special treatment to remove toxic metal ions or recycling of valuable material. Copper is very essential nutrient in animal metabolism. But the excessive intake of copper causes serious toxicological concerns, such as vomiting, cramps, convulsions, or even death [1]. Conventional waste-water treatment methods for Cu(II) removal is precipitation as hydroxides causing the formation of waste sludge. Conventional Ion Exchange technology has found wide application for the removal of low levels of dissolved contaminants from large volume of process and wastewater. But for industrial application when the resin gets saturated, it should be regenerated with suitable acid or alkali. The use of an electric potential in place of chemical reagents to elute ion exchange media by ion migration, as well as redox and pH changing reactions is of considerable importance in simplifying subsequent processing stages. The process has become known as electrochemical ion exchange (EIX) [2]. The principal objective of the present study is to develop effective treatment method for the removal, concentration of Cu(II) ions and removal of COD from the wastewater using EIX-EO process.

MATERIALS AND METHODS

ISBN 9780976885351

All the reagents and chemicals used were of analytical grade. All the solutions were made with double distilled water. The Ceralite IR120 cation exchange resin was purchased from CDH, New Delhi. The surface of the ion exchange resin was modified by Polyethyleneimine (PEI) (An Aldrich product (Mn – 60,000, Mw - 7,50,000, 50% aqueous solution) purchased from Sigma Alrich Chem. Co (USA). Stainless steel cathode, Titanium (Ti), Ti/RuO_2, Ti/PbO_2 anodes were purchased from Tianno, Ti anode fabricators Pvt. Ltd, Chennai. Anion exchange membranes (AEM), cation exchange membranes (CEM) used in the experiment were NEOSEPTA and NAFION 117 membranes were purchased from Tokuyama Corp., Japan.

Industrial electroplating rinse water (IEPRW) sample prior to any wastewater treatment was collected from an electroplating industry located at Balaji Nagar, Padi, Chennai. Samples of IEPRW were collected directly from the first rinse tank of the electro plating unit prior to any treatment. The IEPRW samples were diluted and analyzed for metal ions in Varian spectraa 220 Atomic absorption spectrophotometer (AAS). Concentration of chemical oxygen demand (COD) was analyzed by reflux condensation method in Lavibond ET 125 COD digester. The presence of sulphate was analyzed by Spectrophotometry in Elico Ltd, SL 160 spectrophotometer.

A schematic of batch recirculation system is shown in Figure. 1. The setup consists of a reservoir, a peristaltic pump, an Electrochemical ion exchange cell (EIX part) and an electro oxidation cell (EO part) connected to an electrical circuit consists of 5A, 30V DC power supply.

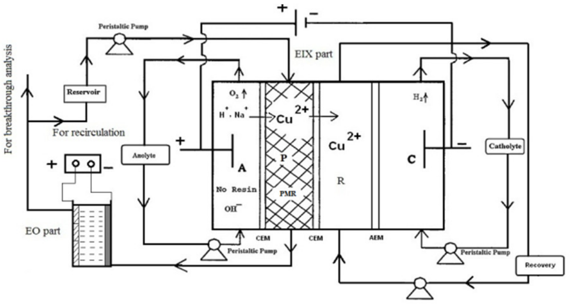

FIGURE 1. EIX-EO Reactor Design

Since membranes divide the EIX cell, it comprise of four parts of experimental solutions anolyte, process stream, concentrated and catholyte. The solutions taken in the reservoirs and their concentrations are given in Table.1. Solutions in the four reservoirs were allowed to flow in batch recirculation mode through the respective compartments of the reactor using peristaltic pump at particular flow rate (Figure 1).

Table: 1. Type of solution for the different compartments of EIX-EO reactor

Parameter	Process stream (P)	Anolyte (A)	Catholyte (C)	Receiver (R)
Solution	Electro plating rinse water	Sodium chloride	Sulphuric acid	Distilled water
Concentration	500 mg L^{-1}	1 to 5 g L^{-1}	0.05 M	-
Volume	1 L	1 L	0.5L	0.2L

Experiments were conducted at various applied current densities specifically at 0.5, 1.0, 1.5, 2.0, 2.5 Amp dm^{-2}. Initially, the Cu(II) ions present in the rinse water gets adsorbed by Polyethyleneimine modified resin (PMR) and then migrated to the receiver compartment. The organic matter present in the rinse water gets oxidized to oxygen and carbon dioxide at the anode surface of the EO part. At regular time interval samples were collected and analyzed.

RESULTS AND DISCUSSION

EIX part of the reactor component optimization. The components of the EIX part of the reactor varied to minimize the resistance between anode and cathode. For this all the four streams were recirculated through their respective compartments, desired voltage (2.5, 5.0, 7.5, 10.0 and 12.5V) was applied between the electrodes and the current flows in the EIX part was measured. The distance between the electrodes, resin loading, type of anode used, stripping agents in receiver compartment and type of membrane used were varied.

The Voltage – Current curve (E-I curve) gives the required information about the extent of Cu(II) ions migration from the ion exchange medium to the receiver compartment. The voltage–current characteristics of this EIX system with different inter electrode distance such as 0.7, 0.6 and 0.5dm have been studied and the results observed were illustrated in Figure. 2a.

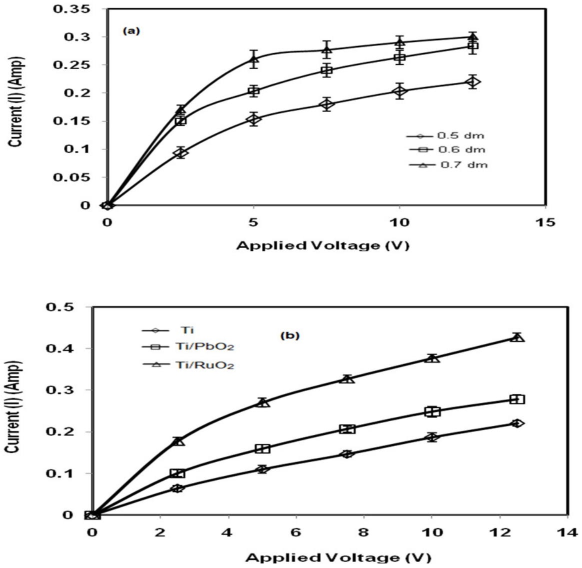

FIGURE: 2 Effect of reactor components (a) inter electrode distance, (b) electrode material on E-I behavior

As can be seen, in the three possible electrode distances varied, the electrical current flows of the stack cell increases with decrease of inter electrode distance. Three different anode materials were tried to give better current discharge to the system. For this Titanium (Ti), Lead oxide coated titanium substrate (Ti/PbO_2) and Ruthenium oxide coated Titanium substrate (Ti/RuO_2) was used as anode material. Their E–I behaviour was observed and represented in Figure.2b. The bed width of the process compartment was varied by loading different amount of resin (10, 20 and 40 g), the resulting current was noted. The current flow of the stack increases with decrease in amount of resin loading inside the process compartment (Figure not given). For 10 g resin loading in the process compartment, the maximum of 0.34 Amp current was flowed across the stack cell due to decreasing of resistance inside the stack [3].

The effect of usage of membrane types on the voltage – current characteristics of this EIX system have been studied (Figure not given). It was observed that the current flow increases sharply with increase of applied voltage in the case of Nafion 117 membrane than the Neosepta. Nafion 117 membrane gave 1.32 Amp current flows through the stack cell for an applied voltage of 7.5V. This proves that the Nafion 117 membrane allows more ionic transport through them by providing lower electrical resistance to the stack.

Process Parameter Optimization by Batch Recirculation Process. The experiments have been carried out in hybrid EIX–EO reactor in a batch recirculation mode. IEPRW samples were allowed to pass through the central compartment of the EIX part of the reactor and through the EO part at the flow rate of 0.005 L min^{-1} in batch recirculation mode. Desired current density was passed between two electrodes of the system. The Cu(II) ions gets dissociated due to electric force and gets adsorbed by the PMR from the flowing solution and then slowly migrated to receiver compartment. In EO part some of the escaped Cu(II) ions from EIX part gets deposited at the cathode surface and simultaneously the organic matter present in the rinse water gets oxidized. The sulphate anion undergoes redox reactions with H^+ ions and converted to sulphur and water. The Cu(II), COD concentration and sulphate concentration in the process compartment gets decreased with electrolysis time while in the receiver compartment Cu(II) concentration keeps on increasing.

Effect of applied current density. The percentage of Cu(II), COD and SO_4^{2-} ion removal from the IEPRW with respect to time at different applied current densities is illustrated in Figure 3 and 4. By comparison of the results of different current densities, it was noted that all applied current densities gave almost similar Cu(II) ions removal efficiency nearly 96.95%, only the reaction time needed was varied. The minimum concentration in the IEPRW reservoir attains in 3.5 h with 2.0 Amp dm^{-2} applied current density. Whereas, current density greater than 2 Amp dm^{-2} made excessive H^+ ion generation from the electrode surface in fraction of seconds so they combined and gets evolved as free hydrogen gas, and thus caused loss of efficiency [4]. Similarly, the increasing of current density from 0.5 to 2.5 Amp dm^{-2} results, increasing of the Cu(II) ions transport from process compartment to the receiver compartment (Figure 3b). The migration of Cu(II) ions from process to receiver compartment via membrane is purely depends on applied current [5]. Hence the increasing of process time and current density increases the Cu(II) ions recovery as almost linear (Figure. 3b). It could be noted from the figure that the receiver compartment Cu(II) ion concentration was more or less similar with 2.0, 2.5 Amp dm^{-2}. Hence, the minimum of 2 Amp dm^{-2} was fixed as optimum current density for this EIX part of the system.

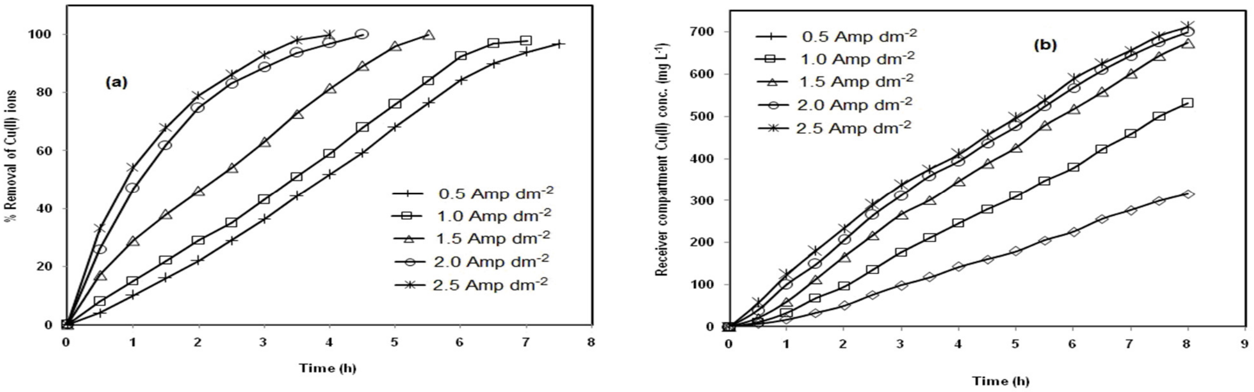

. **FIGURE 3. Applied current density Vs (a) % Removal of Cu(II) ion, (b) Recovery of Cu(II) ion**

COD and SO_4^{2-} ions removal. The IEPRW gets treated in the EIX part of the reactor where almost all Cu(II) ions removed was allowed to pass through the EO part. In EO part COD; SO_4^{2-} ions present in the IEPRW were removed by Electro oxidation process [6, 7]. The trend of COD, SO_4^{2-} removal is given in Figure 4 (a) & (b). For nearly 97.56% of COD, 98.51% SO_4^{2-} removal was achieved with 1.5, 1.0 Amp dm^{-2} respectively. Hence, for further experiments the EO part applied current density was fixed at 1.5 Amp dm^{-2} as optimum.

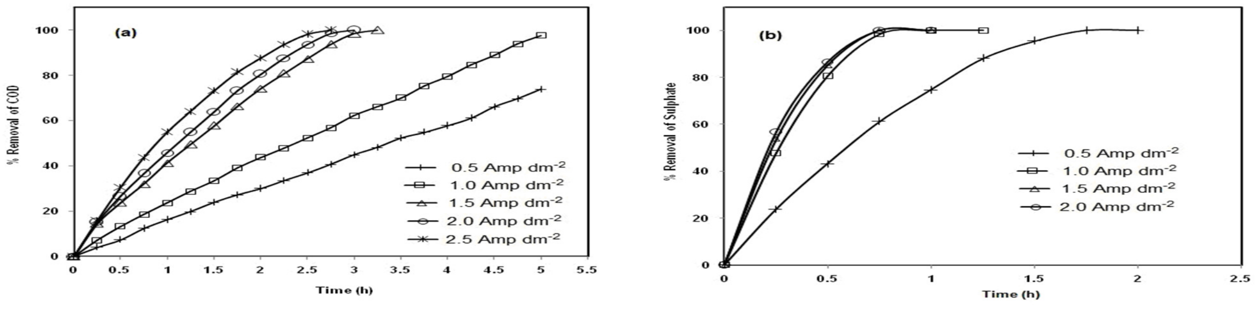

. **FIGURE 4. Effect of applied current density on (a) COD (b) SO_4^{2-} from the IEPRW**

Effect of concentration of NaCl and production of hypochlorite. The concentration of NaCl in the anolyte was varied (2.0 to 8.0 g L^{-1}) to study the extent of Cu(II) ions extraction to the receiver compartment was studied. Figure 5(a) shows that the increasing of NaCl concentration increases the extraction of Cu(II) ions. This may due to that while applying electric field, more Na^+ ions formed in the anolyte and move towards the process compartment for the online regeneration of ion exchange resin while increasing the concentration of NaCl. The maximum extraction was achieved at 6.0 g L^{-1} of NaCl used.

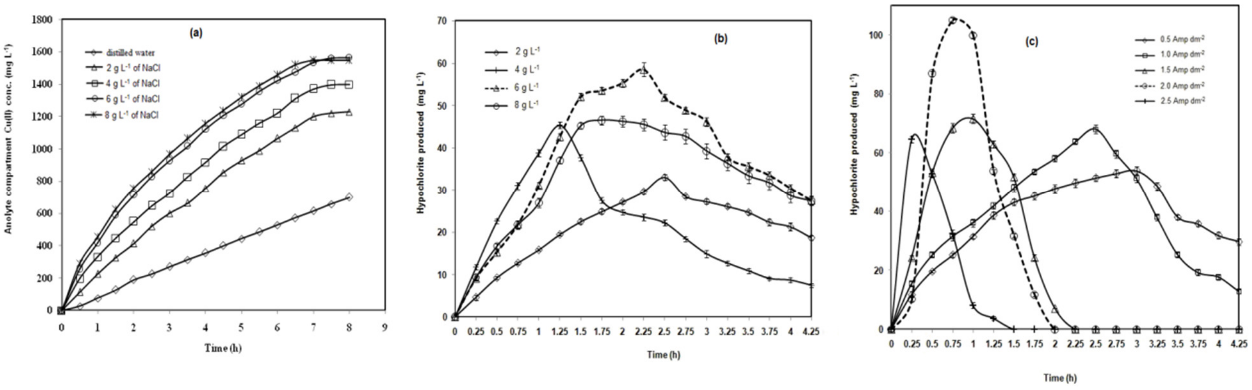

FIGURE 5. Production of hypochlorite (a) at different NaCl concentrations, (b) at different current densities

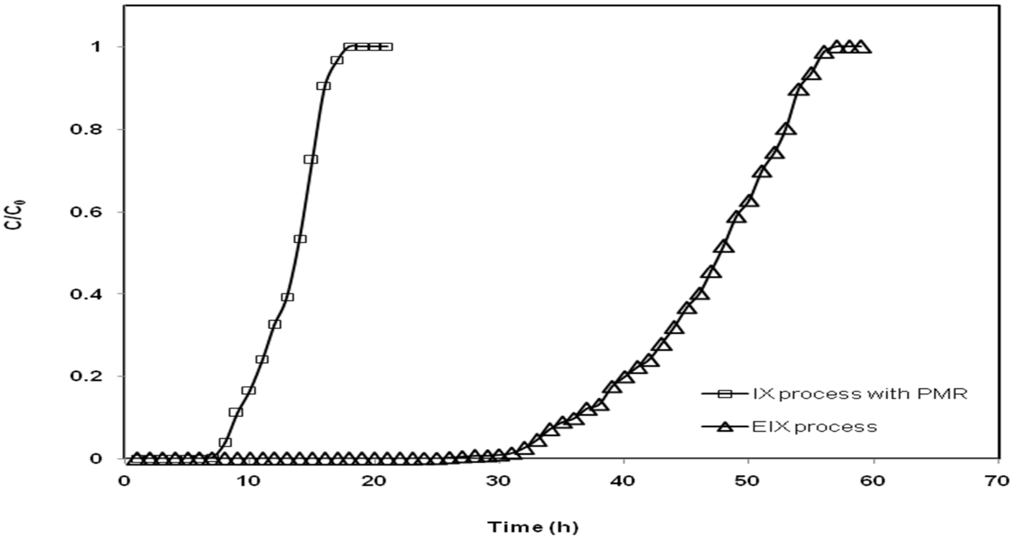

Figure 6 Breakthrough analysis

Hypochlorite was produced simultaneously with the removal/ Recovery of Cu(II) ions in the EIX part of the reactor as a useful side product. Hypochlorite was produced at different NaCl concentration in the anolyte (2.0, 4.0, 6.0 and 8.0 g L^{-1}) and at different applied current densities (0.5, 1.0, 1.5, 2.0 and 2.5Amp dm^{-2}) with respect to reaction time. The results obtained are given in Figure 5 (b), (c). It is observed from Figure that the production of hypochlorite increases with increase of time initially and then decreases due to the oxidation of hypochlorite to chlorine. Higher the initial concentration of NaCl in the anolyte higher the production of hypochlorite was obtained due to more NaCl was undergoing anodic reaction and produces hypochlorite. At 6.0 g L^{-1} of NaCl concentration, 58.5 mg L^{-1} of hypochlorite was produced in 2.25 h. Similarly increase of applied current density from 0.5 to 1.5Amp dm^{-2} hypochlorite production also increase and reaches to 106 mgL^{-1} in 0.45 hours on EIX process and then decreases. In order to get efficient Cu(II) elution and hypo production the NaCl concentration in the anolyte was fixed at 6 g L^{-1}; the hypo thus formed was periodically drawn at 0.45 h of treatment process and fresh NaCl solution was placed.

Continuous EIX Process. The rinse water contains 500 mg L^{-1} of Cu(II) ions was continuously passed through the EIX–EO reactor. The applied current density for the EIX part was fixed at 2.0 Amp dm^{-2}, for EO part 1.5 Amp dm^{-2}. The break point of the reactor was noted by the increase of Cu(II) ions concentration in the outlet from zero to some value. During this break point study the anolyte NaCl solution not changed periodically. Due to this at particular point of time the concentration of Cu(II) in the receiver compartment was higher and opposes the Cu(II) ionic flow from low to high

The outlet concentration of Cu(II) from the central compartment with respect to the discharged volume is presented in Figure 6. When the EIX–EO was operated at 2.0 Amp dm^{-2}, it is observed (Figure 6) that the concentration of Cu(II) ion was approximately zero up to the discharge of 19.5 L of IEPRW afterward the concentration of the Cu(II) ion in outlet increases and reaches the initial value. This breakpoint was compared with ion exchange process which shows that this system was able to discharge only 4.5L of Cu(II) ions free treated IEPRW.

CONCLUSION

In-situ removal and recovery of Cu(II) ions from an IEPRW have been studied by using hybrid technique of EIX–EO processes. Cu(II) ion, COD and SO_4^{2-} were removed from the IEPRW by batch recirculation mode of operation at various experimental conditions. In batch recirculation and continuous process of EIX the maximum Cu(II) removal achieved was 96.95%, for an applied current density of 2.0 Amp dm^{-2}. 97.56% of COD and 98.51% of SO_4^{2-} can be removed at 1.5 and 1.0 Amp dm^{-2} respectively from IEPRW in the EO part of the reactor. The optimum flow rate required for better treatment was found as 0.020 L min^{-1}. The comparative study with Ion exchange process showed that IX process has an efficiency to discharge 4.48 L of treated IEPRW whereas the EIX discharged 19.5 L of treated IEPRW.

REFERENCES

1) Fenglian, Fu and Qi Wang. 2011. “Removal of heavy metal ions from wastewaters: A review”, Journal of Environmental Management 92: 407.
2) Marshal, S., 1979. Hazardous and toxic effects of Industrial Chemicals, NDC Publication, USA, pp. 137.
3) Smara, A., Delimi, R., Chainet, E. and Sandeaux, J. 2007. “Removal of heavy metals from diluted mixtures by a hybrid ion-exchange/electrodialysis process”, Separation and Purification Technology,57: 103.
4) Ahmed Basha, C., Ramanathan, K., Rajkumar, R., Mahalakshmi, M. and Senthil Kumar, P. 2008. “Management of Chromium Plating Rinsewater Using Electrochemical Ion Exchange”, Ind. Eng. Chem. Res., 47: 2279.
5) Mansfield, R.L. 1979. “Lange’s Handbook of Chemistry”, 12th Edn., McGrawHill, Inc., New York.
6) Ahmed Basha, C., Bhadrinarayana, N.S., Anantharaman, N. and Meera Sheriffa Begum, K.M. 2008. “Heavy metal removal from copper smelting effluent using electrochemical cylindrical flow reactor”, J. Hazard. Mater., 152:71.
7) Szpyrkowicz, L., Grandi, F.Z., Kaul, S.N. and Polcaro, N.M. 2000. “Copper Electrodeposition and Oxidation of Complex Cyanide from Wastewater in an Electrochemical Reactor with a Ti/Pt Anode”, Ind. Eng. Chem. Res., 39:2132.

SILICA-ALUMINA ADSORBENTS FOR REMOVAL OF DISSOLVED OR DISPERSED OIL FROM WASTEWATER

A. De Folly D'Auris, R. Bagatin, M. Tagliabue (eni S.p.A., Research Center for Unconventional Energies, Novara, ITALY), A. Carati (eni S.p.A., Refining & Marketing Division, San Donato M.se, ITALY).

ABSTRACT: Production water represents the largest volume waste stream associated with hydrocarbon exploration and production. Generally, production water contains wide spectra of organic and inorganic contaminants, both dissolved and dispersed. eni S.p.A. proprietary mesoporous amorphous silica-alumina (MSA) was successfully employed to remove organics from such wastewater. Results from laboratory adsorption tests are reported.

INTRODUCTION

Freshwater resources on Earth are limited. Over 97% of water is seawater while less than 1% is available as freshwater for direct human consumption or for agricultural and industrial uses. About 69 % of that is located in glaciers and icecaps. The remaining freshwater is present as groundwater. Only about 0.3% is contained in rivers and lakes.

The demand for freshwater and population growth are directly correlated. World population is approximately 6 billion people and is projected to double in the next 50 to 90 y, while our renewable freshwater resources remain constant. Currently, over 400 million people live in regions with severe water shortages; this is estimated to climb to 2.8 billion people by 2025 and is roughly 35% of the projected total population. [Watson I.C. 2003]. While overall improvements in standards of living are positive for people, the demand for water resources increases. Additionally, increased standard of living results in demand for goods which increases industrialisation. As a result, consumption for industrial applications is expected to increase in the near future, thus contributing to global water shortage.

Water pollution by hydrocarbons and their derivatives represents a relevant problem. In particular, wastewater from oil and gas exploration and production (also called produced water) is a complex mixture of inorganic salts together with a wide variety of organic compounds (*e.g.* aromatics, aliphatic hydrocarbons and their derivatives). The latter ones can be traced in three different forms: 1) dispersed oil as little droplets on the water surface; 2) emulsified oil with smaller than 20 µm droplets dispersed in the water; 3) dissolved oil for the presence of organic soluble compounds.

Produced water *vs.* oil volumetric ratio ranges from 2 to 3 (with peaks of 50) depending from the age of reservoir and exploitation technology. Nowadays, energy industry is forced to develop effective technologies for produced water treatment in order to minimise environmental pollution and to exploit such large water resource. Several primary treatments, including oil separation, coagulation, flocculation, floatation and filtration have been successfully used to remove oil and suspended solids from produced water [Lu J. 2006. Deng S.B. 2002. Rubio J. 2002.]. Biological treatments, also known as secondary treatments, should be also considered when these effluents are discharged into natural receiving bodies [Tellez G.T. 1995, Campos J.C. 2002].

Water treatment by selective adsorption has drawn operator attention due to equipment compactness, limited use of auxiliary chemicals and low waste production. A wide spectra of adsorbents has been suggested (*e.g.* carbons, zeolites, polymers, biomaterials and even wastes) seeking for the optimal trade off between effectiveness and cost.

Zeolites are microporous crystalline alumino-silicates with frameworks based on a three-dimensional network of corner-sharing [TO_4] tetrahedra. Commonly, T corresponds to Si and Al but

---

ISBN 9780976885351

structures based on other cations (*e.g.* Be, Ge, Fe, P, Zn) have been described, as well [Weitkamp J. 2000]. They are characterised by the presence of regular channels with free diameter ranging from about 3 Å to over 10 Å, able to allow uptake and diffusion of ions and molecules. On this feature is based the use of zeolites as adsorbents.

A process for treatment of wastewater contaminated by organic compounds by adsorption on hydrophobic (siliceous) zeolites has been recently reported [Vignola R. 2011]. Quite good results have been described in case of dissolved hydrocarbons while reduced effectiveness has been noticed in presence oil droplets, due to pore clogging.

In order to overcome this limitation, mesoporous amorphous silica-alumina has been proposed as adsorbent of oil droplets from wastewater [Reynolds J.G. 2001]. Thanks to their wide pore size and large specific pore volume, mesoporous materials have been expected to be able to adsorb considerable amount of hydrocarbons, with particular reference to those characterised by large kinetic molecular diameter, thus unable to enter zeolite micropores.

In this context, use of eni S.p.A. proprietary mesoporous amorphous silica-alumina (MSA) [Bellussi G. 1994] for the treatment of wastewater containing organic compounds (both dissolved and as emulsified oil) is described in this paper.

MATERIALS AND METHODS

MSA adsorbents characterised by different porous texture and chemical composition were synthesised via sol-gel in alkali-free medium using $Si(OC_2H_5)_4$ (Dynasil-A, Nobel), $Al(sec\text{-}OC_4H_9)_3$ (Aldrich), tetrapropylammonium hydroxide (TPAOH, Sachem), alcohol (ROH) selected among C_2H_5OH or $n\text{-}C_3H_7OH$ (Aldrich). All preparations were performed at the same molar ratios: $TPAOH/SiO_2 = 0.09$, $H_2O/SiO_2 = 8$ and $alcohol/SiO_2 = 8$.

A typical synthesis preparation is following described. $Al(sec\text{-}OC_4H_9)_3$ was dissolved in $Si(OC_2H_5)_4$ at 60 °C. The obtained homogeneous solution was cooled at room temperature, then the required alcohol and TPA-OH in aqueous solution were added in sequence. Monophasic clear solutions were obtained, then transformed in homogeneous compact gel without separation of phases. The SiO_2/Al_2O_3 (SAR) molar ratio and the selected alcohol are reported in Table 1 for each preparation. After 15 hour ageing at room temperature, the gels were dried at 100 °C and calcined 8 h in air at 550 °C.

Synthetic mordenite zeolite (MOR) with SAR = 100 (Tosoh) was employed as benchmark. MSA samples textural characterisation was carried out by nitrogen adsorption at -196 °C on Micromeritics ASAP 2010 apparatus. Before determination of adsorption-desorption isotherms the samples (~ 0.2 g) were outgassed for 16 h at 350 °C under vacuum.

Apparent specific surface area (A-SSA, Brunauer Emmett and Teller method), specific pore volume (V_P, Gurvitsh rule) and mean pore size (d_p, non-local density functional theory algorithm) were evaluated from the acquired isotherms.

Before water treatment experiments, materials were sifted between 0.12 and 0.5 mm and calcined at 550 °C for 8 h. Table 1 reports the main characteristics of the used adsorbents.

TABLE 1. MSA synthesis parameters and chemical-physical characteristics.

Adsorbent	SAR	A - SSA (m^2/g)	Alcohol	V_P (ml/g)	d_P (Å)
MSA (1)	∞	668	C_2H_5OH	0.53	31
MSA (2)	100	990	C_3H_7OH	1	43
MSA (3)	∞	667	C_3H_7OH	1	72

Tests were run by using produced water coming from an eni S.p.A. oil processing site. Specifically, 30 mg of adsorbent were kept under stirring with 40 ml of contaminated water. Absorbance measurements were conducted using Hach DR/2500 spectrophotometer, setting the wavelength at 450 nm. Water composition was determined using GC-mass spectroscopy analyser:

- Analyser GC-mass spectroscopy Agilent equipped with OI Analytic 4460A purge and trap device;
- DB-5MS column, 60 m length, 0.25 mm internal diameter;
- Initial oven temperature 40 °C, final oven temperature 300 °C, 5 °C / min increasing, final temperature kept constant for 10 min.
- Helium as carrier gas.

On the same samples GC-head space analysis and total organic carbon (TOC) were also conducted. TOC analyses were performed without any sample pre-treatment, using Hach IL550 TOC-TN instrument. It was evaluated as the difference between total carbon and inorganic carbon. Instead, before GC analysis, samples were extracted in CH_2Cl_2.The organic solution was then passed through a Na_2SO_4 column for drying, concentrated to 2 ml and analysed.

RESULTS AND DISCUSSION

In MSA synthesis, the TPAOH role is to provide the pore formation through the TPA^+ clusters as well as to organise SiO_2 and AlO_2^- units into polymeric structure. The volume fraction of TPA^+ in the dried precursors addresses towards the formation of micro- or meso-porous materials [Perego G. 1997]. In agreement with previous results, mesoporous MSA samples were obtained, by using 40 % volume fraction of TPA^+ (calculated by assuming a mass density of 0.9 g/ml for TPA^+ and 2.0 g/ml for SiO_2). The kind of alcohol affects the solvation sphere of the TPA^+ clusters: higher pore volume and diameter were obtained using n-C_3H_7OH respect to C_2H_5OH. An increase of A-SSA, associated to a decrease in pore diameter, was observed by aluminium introduction.

Preliminary tests were performed to compare adsorbents (reported in Table 1) with different pore sizes. Results (Figure 1) emphasize that mesoporous adsorbents are able to reduce emulsified oil in water, with an absorbance reduction from 0.65 to 0.2 arbitrary units (a.u.). No effects from chemical composition and porous texture are evident. On the contrary, zeolite appears to be uneffective.

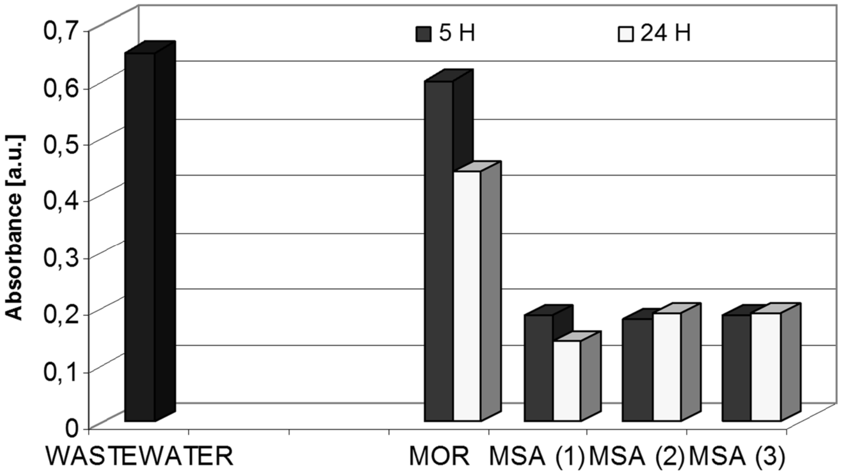

FIGURE 1. Absorbance (a.u. = arbitrary units) measurements (λ = 450 nm) of raw wastewater: comparison between MOR zeolite and MSA samples with 31, 43 and 72 Å mean pore size. Experimental conditions: 30 mg of sorbent material *vs.* 40 ml of water.

Once checked the efficiency of different mesoporous materials, only MSA with 72 Å mean pore size, was considered.

Results (Table 2) show the decreasing of TOC measured and the adsorption capacity after 24, 48 and 72 h of contact time with the adsorbent.

TABLE 2. Variation in TOC content and adsorption capacity for water sample treated for different contact time with MSA (3).

Contact time (h)	TOC (mg/l)	Adsorbed quantity (mg/g)
0	465	-
24	138	436
48	83	509
72	50	553

GC-MS (Figure 2A) and GC-head-space chromatograms (Figure 2B) were recorded on the wastewater before the treatment, to identify contaminants. A wide number of organics, ranging from light to heavy ones were detected. In particular, heavy hydrocarbons (until C_{33}), typical of oil were identified.

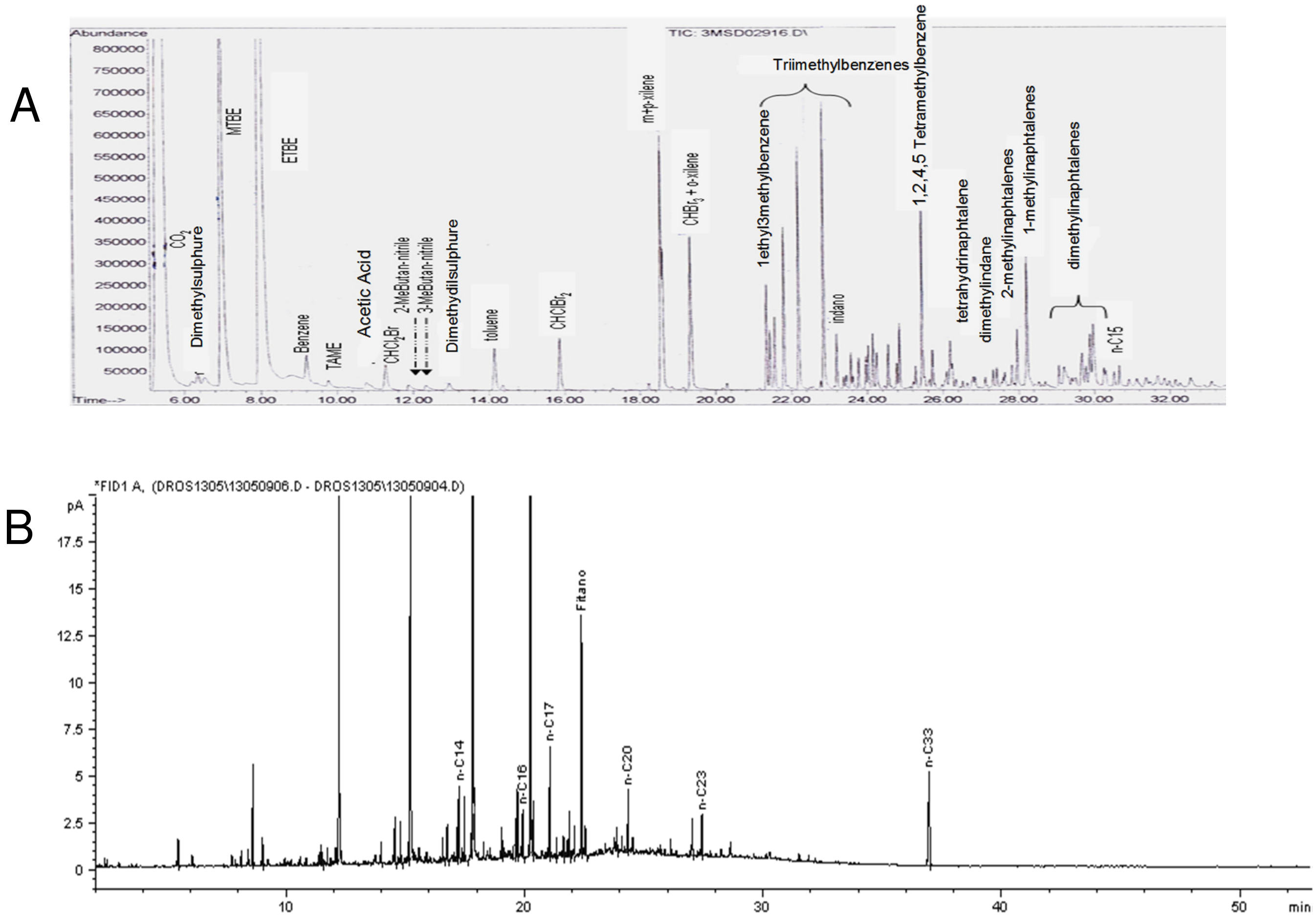

FIGURE 2. GC-mass spectrometry (A) and GC-head space (B) chromatograms of wastewater.

Wastewater was contacted with MSA (3) for 24 h. Then analyses were repeated. Disappearance of opaqueness due to oil dispersion was observed.

Chromatogram reported in Figure 3 show that several compounds were totally or partially removed, pointing to MSA effectiveness in oily water treatment by adsorption.

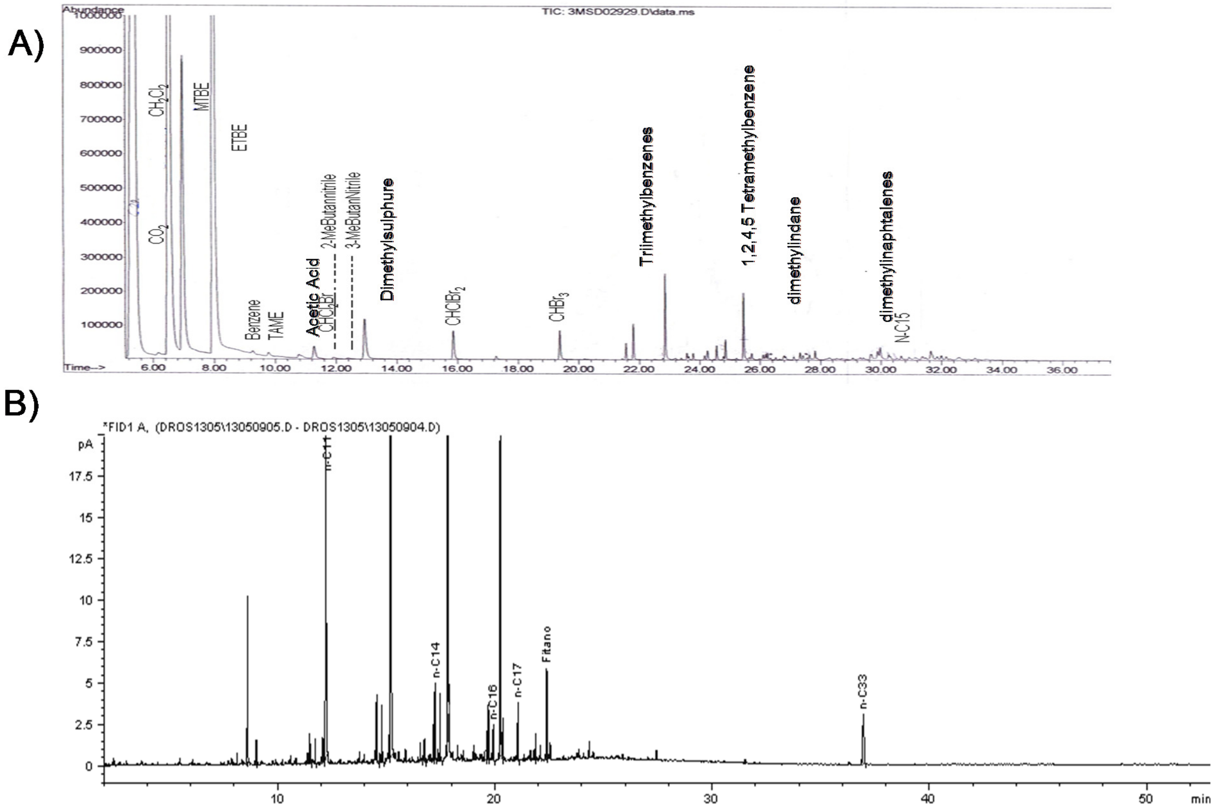

FIGURE 3. GC-mass spectroscopy (A) and GC-head - space (B) chromatograms of the wastewater treated with MSA (3).

CONCLUSIONS

Effectiveness of eni S.p.A. proprietary mesoporous amorphous silico-alumina in removing dispersed hydrocarbons from wastewater has been demonstrated through laboratory experiments [Vignola R. 2010]. Mesoporous materials have demonstrated an adsorption capacity about 50% by weight. No relation among performances, adsorbent chemical composition and/or porous texture has been registered in this specific studied range (SAR > 100, 31 Å < d_P < 72 Å). On the other hand, zeolite has been noticed to be inadequate for this task.

REFERENCES

Bellussi G., C. Perego, A. Carati, S. Peratello, E. Previde Massara, and G. Perego. 1994. “Amorphous Mesoporous Silica - alumina with Controlled Pore Size as Acid Catalysts”. *Stud. Surf. Sci. Catal.* 84: 85 – 92.

Campos, J.C., R.M.H. Borges, and A.M. Oliveira Filho. 2002. “Oilfield Wastewater Treatment by Combined Microfiltration and Biological Process. *Water Res.* 36: 95 – 104.

Deng S., R. Bai, J.P. Chen, Z. Jiang, G. Yu, F. Zhou, and Z. Chen. 2002. “Produced Water from Polymer Flooding Process in Crude Oil Extraction: Characterization and Treatment by a Novel Crossflow Oil–water Separator”. *Sep. Purif. Technol.* 29: 207–216.

Lu J., X. Wang, B. Shan, X. Li, and W. Wang. 2006. “Analysis of Chemical Compositions Contributable to Chemical Oxygen Demand (COD) of Oilfield Produced Water”. *Chemosphere* 62: 322 – 331.

Perego G., R. Millini, C. Perego, A. Carati, G. Pazzuconi and G. Bellussi. 1997. “ERS-8: a New Class of Microporous Alumino-silicates”. *Stud. Surf. Sci. Catal.* 105: 205 - 212.

Reynolds J.G., P.L. Coronado, L.W. Hrubesch. 2001. “Hydrophobic Aerogels for Oil Spill Cleanup - Intrinsic Absorbing Properties”. *Energy Source* 23: 831 – 843.

Rubio, J., M.L. Souza, and R.W. Smith. 2002. “Overview of Floatation as a Wastewater Treatment Technique”. *Miner. Eng.* 15: 139 – 155.

Tellez G.T., N. Nirmalakhandan, and J.L. Gardea Torresdey. 1995. “Evaluation of Bio-kinetic Coefficients in Degradation of Oilfield Produced Water Under Varying Salt Concentrations”. *Water Res.* 29: 1711 – 1718.

Vignola R., R. Bagatin, A. De Folly D’Auris, C. Flego, M. Nalli, D. Ghisletti, R. Millini, and R. Sisto. 2011. “Zeolites in a Permeable Reactive Barrier (PRB): One year of field experience in a Refinery Groundwater — Part 1: The Performances”. *Chem. Eng. J.* 178: 204 – 209.

Vignola R., A. Carati, A. De Folly D’Auris and R. Tuffi. 2010. Procedimento per il Trattamento di Acqua Contaminata Comprendente Composti Organici Disciolti ed Olio Disperso o in Emulsione, *Italian Patent Application N° MI10A002062* (submitted by eni S.p.A and La Sapienza Universiy of Rome).

Watson I.C., O.J. Morin, and L. Henthorne. 2003. *Desalting Handbook for Planners 3rd Edition,* Desalination and Water Purification Research and Development Program United States Department of the Interior Water Treatment Engineering and Research Group, Bureau of Reclamation, Denver, CO.

Weitkamp J. 2000. “Zeolite and Catalysis”. *Solid State Ionics*. 131: 175 – 188.

SYNTHESIS AND SURFACE MODIFICATION OF ORDERED MESOPOROUS CARBONS FOR RESORCINAL REMOVAL

Ruixuan Guo and Daniel Dianchen Gang
(Department of Civil Engineering, University of Louisiana at Lafayette, Lafayette, LA 70503 USA)

ABSTRACT: Ordered mesoporous carbons (OMCs) have gained global interests for applications in adsorption, separation and purification in recent decades. Due to their high specific surface areas, large pore volume and tunable pore size, ordered mesoporous carbons have shown unprecedented adsorption performance towards a wide range of inorganic and organic chemicals with fast adsorption kinetics, high adsorption capacity and good stability. Moreover, the easy modification of surface of ordered mesoporous carbon provides the possibility of creating specific binding sit for different chemicals. In this research, OMCs were synthesized using different templates made from four different temperatures (70°C, 90°C, 110°C and 150°C). Surface functionalization was carried out by nitric acid oxidation at 70°C. XRD patterns and TEM images showed that the ordered structure was well maintained during the synthesis and surface modification processes. Adsorption study showed that the modified OMC has the highest adsorption capacity of 39.2 mg/g for resorcinol removal, compared with the original OMC (36.3 mg/g) and the commercial Norit activated carbon (38 mg/g).

INTRODUCTION

Molecular sieves have been used broadly as catalysts, adsorbent, air purification, energy storage and ion-exchange media [Ryoo et al., 1999, Liang et al., 2008]. Most of these materials have the pore size less than 2 nm and the key drawbacks of microporous material are slow mass transport, low conductivity and collapse of microporous structures at high temperature [Liang et al., 2008]. To overcome these limitations, there have been growing interests in synthesis of new molecular sieves which can increase the pore diameter to the mesoporous region (2 nm < pore size < 50 nm). Ordered mesoporous carbons (OMCs), with controlled mesoporous pore size, and stable frameworks, have shown unprecedented adsorption performance towards a wide range of inorganic and organic chemicals with fast adsorption kinetics, high adsorption capacity and good stability.

Much work has been devoted to synthesize mesoporous carbons with uniform mesopores and large surface areas. The common way to prepare ordered mesoporous carbons (OMCs) with controllable pore size is using mesostructed silica materials as templates [Lu et al., 2006]. Ryoo et al. prepared an ordered mesoporous carbon named as CMK-1 by using MCM-48 silica as the template in 1999 [Ryoo et al., 1999]. In the synthesis developed by Ryoo's group, the mesostructed material MCM-48 was impregnated with solutions of sucrose and sulfuric acid. The acid acts as a catalyst during carbonization at temperatures of up to 1073°C. The silica framework was finally removed using a hot ethanolic solution of NaOH. This synthetic process resulted in a cubically structured mesoporous carbon, CMK-1. The Ryoo's group also developed a nanopipe-like ordered mesoporous carbon material, CMK-5, which has a hexagonally ordered array of amorphous carbon nanopipes. During this synthesis, aluminum was incorporated onto the surface of SBA-15 silica to introduce acidic sites that would catalyze the

---

ISBN 9780976885351

polymerization of furfuryl alcohol on the pore walls [Joo et al. 2001, Kruk et al., 2003]. Zhao et al. reported the synthesis of rod-like, hexagonally ordered CMK-3 mesoporous carbon material by using a rod-shaped SBA-15 as template [Zhao et al., 1998].

The effort led to discovery numerous new silica mesophases including SBA-1 and SBA-6, SBA-2, SBA-12, SBA-8, SBA-15, MSU-G and others. In addition, the supra molecular templating approach was extended to the synthesis of transition and other metal substituted silicas. Furthermore, silica mesophases were in turn uses as templates for the synthesis of a variety of other materials such as nanoporous carbon and polymers, as well as metallic and semiconductor nanowires. This extensive effort not only in conventional fields such as adsorption, separation and catalysis, but also in the area of advanced materials based on their unique electronic, magnetic and optical properties, or as host for quantum dots and sensing species.

The surface modification of ordered mesoporous carbon has been recognized as an attractive approach to improve aromatic removal from wastewater. One technique of functionalize the carbon surface involves oxidizing it with acids or ozone, through which oxygenated functionalities, such as carboxylic acids, quinines are generated [?????]. Ordered mesoporous carbon surface oxidation with HNO_3 is a typical modification method, which can increase the functional oxygen groups, such as carboxylic acids.

Overall, the objective of the study is to develop and examine the efficiency of surface modified ordered mesoporous carbons (OMCs) material for resorcinol removal. The long-term goal of this research is to develop a novel adsorbent with high adsorption capacity, less weight and less volume for removing organic matters from water and wastewater.

MATERIALS AND METHODS

In a typical aqueous solutions synthesis, 100 ml of concentrated hydrochloride acid (HCL, 37%) was added into 525 ml of distilled water while magnetically stirring. Twenty (20) grams of triblock copolymer Pluronic P123 was added. After Pluronic P123 was completely dissolved with stirring for 1 h, 46.5 ml of tetraethylorthosilicate (TEOS, 98%, Aldrich) was added to the homogenous solution with vigorous stirring for 10 min. The mixture was then placed in a constant temperature water bath (Precision Scientific) for 4 h at 40°C, followed by aging for 24 h under different temperatures (70°C, 90°C, 110°C and 150°C) . The solid product was filtered, washed with 500 ml 80 ~ 90°C hot distilled water, and dried in an oven at 105°C overnight. After drying, the product was calcined in a muffle furnace at 550°C for 8 h. The white silica template SBA-15 was stored for the next preparation of OMC.

Ninety ml of acrylic acid (>99%, Aldrich) was added into 180 ml of distilled water with stirring, then 9 g of SBA-15 was added and suspended in the acrylic acid solution. After the mixture was stirred for 30 min, 0.02 g of 2.2-azobisisobutyronitrile (AIBN) was added as a free radical initiator. The mixture was then heated to 60°C for in situ polymerization. The polyacrylic acid (PAA) and silica template composite was dried by oven at 200°C overnight. Afterwards, the sample mixture was heated under N_2 flow at a temperature ramp rate of 5°C min^{-1} to 700°C and held for 8 h for carbonization. Surface functionalization of ordered mesoporous carbons was carried out by nitric acid oxidation at 70°C. Ordered mesoporous carbon (0.1 g) was mixture with 5 ml 70% HNO_3. The mixture was heated at 90°C for formation of functional groups. The residual was washed with 500 ml deionized water until the pH is larger than 5, then the modified ordered mesoporous carbon was dried at 110°C for 4 hours and then in the protection of N_2 at 300°C for 1 hour. Batch adsorption experiments were conducted in 200 ml conical flasks placed in an E 24 Incubator Shaker (New Brunswick Scientific). The mixture of OMCs and resorcinol solutions was placed in a shaker (200 rpm, room temperature). After 24 hours, the conical flasks were removed and solution filtered using the 0.45 μm glass filter paper. The filtered solution was analyzed for the final concentration of TOC model compound – resorcinol.

RESULTS AND DISCUSSIONS

Figure 1 shows the small XRD patterns of four different silica templates. It can be seen that all silica templates present three XRD peaks and have excellent periodic structures. The three XRD peaks of templates can be assigned to (100), (110), and (200) reflections. The intensity of the (100) reflection is the strongest of all. The results are consistent with the results reported by Fuertes [2004]. Cell parameters calculated from the (1 0 0) reflection change with temperature. The pore size varies from 9.8 nm (150°C) to 10.9 nm (90°C). SBA-15 prepared at 90°C has the largest pore size (10.9 nm). The XRD patterns of ordered mesoporous carbons are presented in figure 2. The structure of ordered mesoporous carbons (OMCs) are negative replication of silica templates. All ordered mesoporous carbon samples show XRD patterns with an intense diffraction peak at (1 0 0) reflection and two weaker peaks at (1 1 0) and (2 0 0). These patterns are consistent with the 2-D hexagonal symmetry (*p6mm*) derived from the SBA-15. The structure of the carbon obtained by templating SBA-15 was faithful replica of the corresponding original silica. All of the ordered mesoporous carbons (OMCs) show the periodic structure, but the intensity of ordered mesoporous carbon is weaker than the intensity of silica templates. The intensity of ordered mesoporous carbons (OMCs) is about 30% weaker than corresponding silica templates.

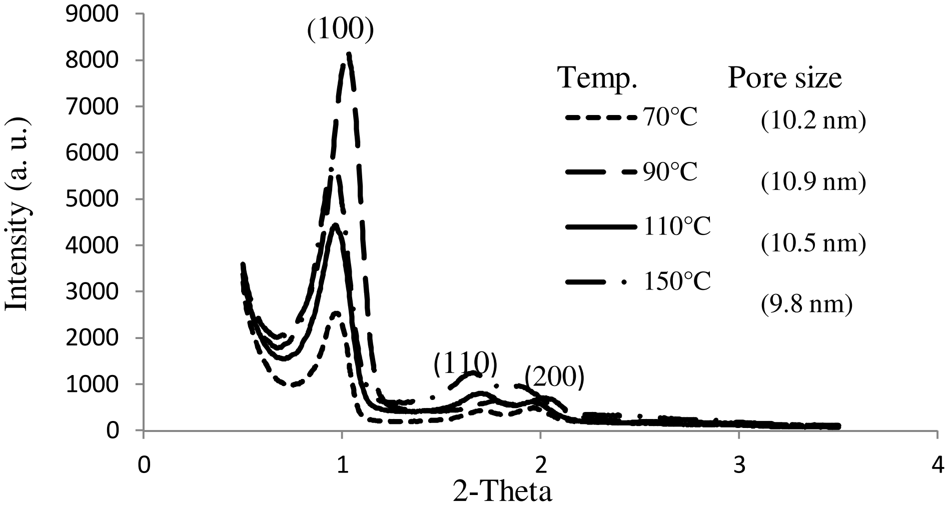

FIGURE 1. XRD patterns of SBA-15 prepared at different temperatures.

Transmission electron microscopy (TEM) analysis confirms the well-ordered hexagonal arrays of 2-D mesoporous channels of the SBA-15 silica template. Figure 3 is TEM image of the silica template taken from channel direction (100). Figure 3 illustrates the parallel array of SBA-15 template and the diameter of silica rods is about 10 nm. Figure 4 (100) illustrate the TEM images of OMC. The pore size of ordered mesoporous carbon is about 10 nm and the pore size is almost the same with that of SBA-15. The structure of ordered mesoporous carbon is faithfully duplicates the structure of the silica template.

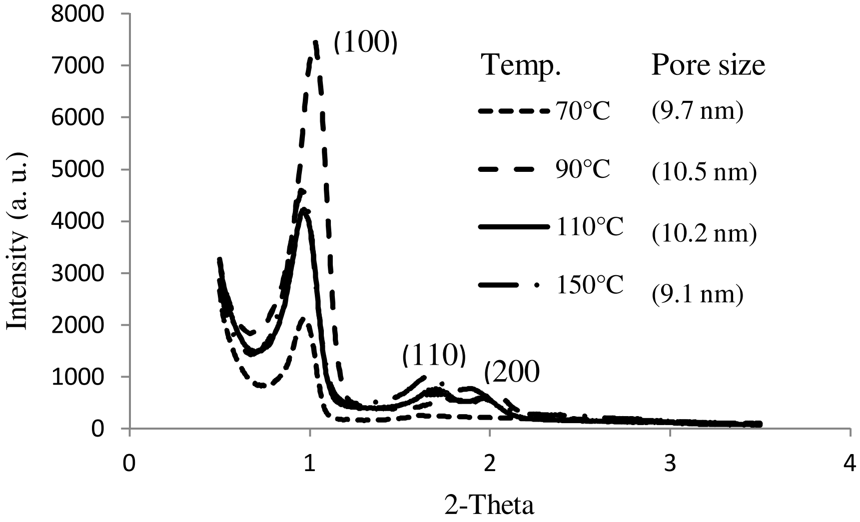

FIGURE 2. XRD patterns of OMC prepared from corresponding SBA-15 templates.

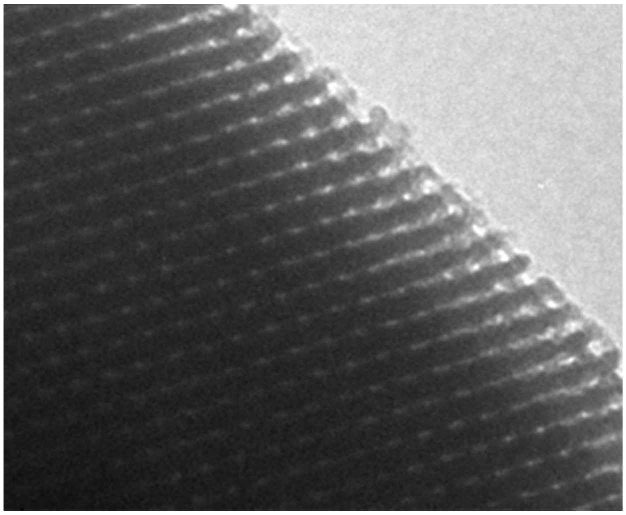

FIGURE 3. TEM image of SBA-15 (100).

The adsorption capacities of Norit activated carbon and four different ordered mesoporous carbon for resorcinol removal are shown in figure 5. From figure 5, it can be seen that the Norit activated carbon has the highest adsorption capacity of 38 mg/g. The mesoporous carbons made from 90°C SBA-15 has the best adsorption of 36.3 mg/g among all OMCs, but the adsorption capacity is still lower than that of the commercial Norit activated carbon. This is due to lacking functional group in the surface of OMCs. Figure 6 compared the adsorption capacity of original OMC and modified OMC. It can be seen that the modified ordered mesoporous carbon has higher adsorption capacity than Norit activated carbon and original OMC. The modified OMC has an adsorption capacity of 39.2 mg/g. This is because functional groups in the surface of the modified ordered mesoporous carbon attach to the resorcinol molecular through the hydrogen bonds.

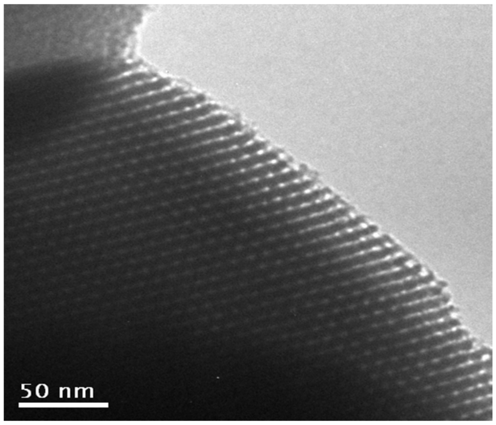

FIGURE 4. TEM image of ordered mesoporous carbon (100).

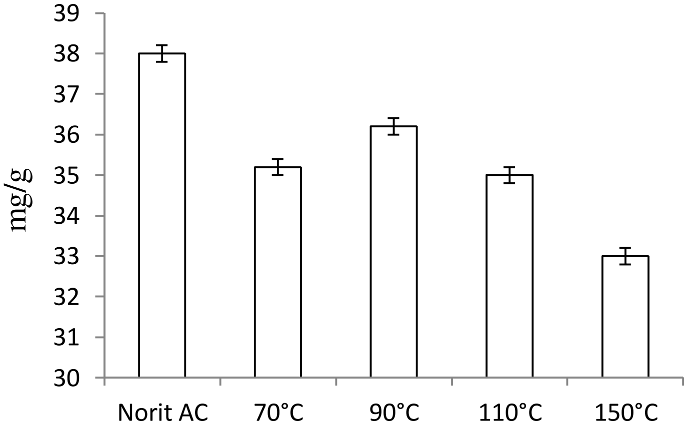

FIGURE 5. Adsorption capacity of Norit activated carbon and four different OMCs.

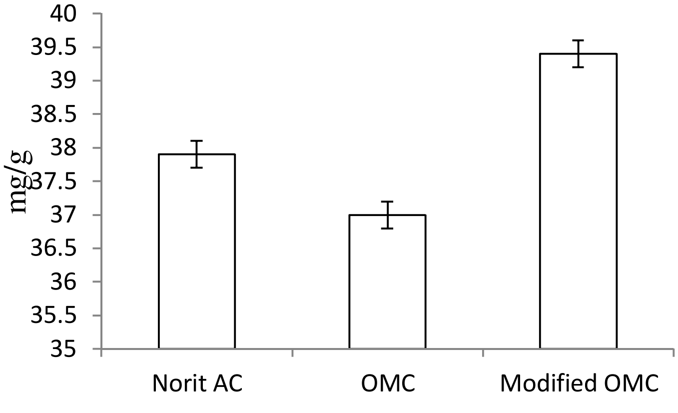

FIGURE 6. Adsorption capacity of Norit activated carbon, OMC and modified OMC.

CONCLUSIONS

Ordered mesoporous silica templates are made at four different temperatures. Ordered mesoporous carbons are synthesized using these silica templates as templates. Surface functionalization of ordered mesoporous carbons was carried out by nitric acid oxidation at 70°C. The adsorption capacity of ordered mesoporous carbons are measured by removal of resorcinol from aqueous system. The TEM images show that silica templates and OMCs have highly ordered structure. Batch adsorption studies show that all OMCs could remove resorcinol from water, but the OMCs made from 90 °C silica template have better performance than other OMCs with the adsorption capacity of 36.3 mg/g. The modified ordered mesoporous carbon has the highest adsorption capacity of 39.2 mg/g.

ACKNOWLEGMENTS

Support for this research by NASA (National Aeronautics and Space Administration) and LaSPACE is gratefully acknowledged.

REFERENCES

R. Ryoo, S. H. Joo, and S. Jun, 1999. “Synthesis of highly ordered carbon molecular sieves via template-mediated structural transformation”. *J. Phys. Chem. B*, 103: 7743-7746.

C. Liang, Z. Li, and S. Dai, 2008. “Mesoporous carbon materials: Synthesis and modification”. *Angew. Chem. Int. Ed.*, 47: 3696-3717.

A. H. Lu, and F. Schuth, 2006. “Nanocasting: A versatile strategy for creating nanostructured porous materials”. *Adv. Mater.*, 18: 1793-1805.

C. G. Wu, and T. Bein, 1994. “Conducting carbon wires in ordered, nanometered-sized channels”. *Science*, 266: 1013-1015.

D. Zhao, J. Feng, Q. Huo, N. Melosh, G. H. Fredirckson, B. F. Chemlka, and G.D. Stucky, 1998. “Triblock copolymer syntheses of mesoporous silica with periodic 50 to 300 angstrom pores”. *Science*, 279: 548-552.

M. Kaneda, T. Tsubakiyama, A. Carlsson, Y. Sakamoto, T. Ohsuna, O. Terasaki, S. H. Joo, and R. Ryoo, 2002. “Structural Study of Mesoporous MCM-48 and Carbon Networks Synthesized in the Spaces of MCM-48 by Electron Crystallography”. *J. Phys. Chem. B*, 106: 1256-1266.

S. H. Joo, S. J. Choi, I. Oh, J. Kwak, Z. Liu, O. Terasaki, and R. Ryoo, 2001. “Ordered nanoporous arrays of carbon supporting high dispersions of platinum nanoparticles”. *Nature*, 412: 169-172.

M. Kruk, M. Jaroniec, T. W. Kim, and R. Ryoo, 2003. “Synthesis and characterization of hexagonally ordered carbon nanopipes”. *Chem. Mater.*, 15: 2815-2823.

A. B. Fuertes, 2004. “Synthesis of ordered nanoporous carbons of tunable mesopore size by templating SBA-15 silica materials”. *Micropor. Mesopor. Mater.*, 67: 273-281.

BREAKTHROUGH CURVES FOR NICKEL REMOVAL FROM AQUEOUS SOLUTIONS USING A CATION EXCHANGE RESIN

M. Hamdzah, Z. Ujang, and M.M. Nasef (Institute of Environmental and Water Resource Management (IPASA), Water Research Alliance, Universiti Teknologi Malaysia, 81310 JB, Malaysia)

ABSTRACT: Breakthrough curves for the removal of Ni (II) from aqueous solutions using a cation exchange resin (Dowex 50W) were determined at ambient temperature under dynamic condition in a packed bed. The experimental data were obtained using a response surface methodology, so the observed behavior could be investigated as a function of the given operating parameter using response surface analysis. Three operating conditions were investigated: flow rate (15–25 mL/min), pH (4.5–8.5), and bed height (3–5 cm). The results indicated that the removal of Ni (II) as possible using cation-exchange resin. A Bohart-Adam model describing the dynamics of metal adsorption in the column was obtained from the mass balances in the fluid and resin phases. The model parameters, known as the kinetic constant k_{BA} (mg min cm^{-3}) and the maximum amount of metal exchange N_0 (mg cm^{-3}), were fitted to the experimental data.

INTRODUCTION

The increasing amounts of metals and chemicals used in various industrial processes such as metal plating, mining, fertilizer production, tanning, battery manufacture, and paper making has resulted in the generation of large quantities of effluents containing high levels of heavy metals. These contaminated effluents pose environmental problems in terms of their disposal, because their non-biodegradability and tendency to accumulate in living organisms (Petrus and Warchol, 2003). Furthermore, the leaking of heavy metals into the soil can lead to groundwater and surface water contamination, and consequently, can adversely affect human, animal, and aquatic life.

Industrial wastewater from the manufacture of batteries contains large amounts of Cd(II), Hg(II), Cu(II), Pb(II), Ni (II), and Zn (II), and must be treated prior to disposal. Nickel ions are non-biodegradable toxic heavy metal ions that may cause dermatitis and allergic sensitization (Kandah and Meunier, 2007). According to the Malaysian-Environmental Quality Act 1974 (Sewage and Industrial Effluents) 1979 the maximum discharge limits for Ni (II) under standard B is 1.0 mg/L, while according to World Health Organization (WHO) guidelines, the amount in drinking water should be less than 0.1 mg/L.

In the present work, this process is investigated by through determination of the breakthrough curves in a fixed bed column. An experimental design with response surface analysis is used to evaluate the significance of operating parameters such as the flow rate, pH, and bed height on the column performance. This statistical approach allows systematic and more appropriate variation of the experimental conditions. In addition, the experimental data for the breakthrough curves are analyzed using the Bohart-Adam model.

MATERIALS AND METHODS

Materials: Dowex 50W was obtained from Fluka Co. The properties of the resins are presented in Table 1. The resin was washed with deionized water and then dried in a vacuum oven at 50°C overnight, prior to use. All chemicals and reagents used were of analytical grade. ($Ni(NO_3)_2.6H_2O$) from QRec (Mw =

ISBN 9780976885351

290.81g/mol) was used to prepare Ni(II) solution. Solutions of 0.1 M NaOH and 0.1 M HNO_3 were used for pH adjustment.

Breakthrough Experiments: Breakthrough curves were planed using a 3^2 factorial design with varying feed flow rate (Q, mL/min), pH, and bed height (BH, cm). Each factor was changed to a different levels according to the experimental design given in Table 2, resulting in a total of 20 experiments.

TABLE 1. Properties of Dowex 50W

Type	Strong acid cation exchanger Dowex 50W-X8
Active group	Sulfonic acid
Matrix	Gel(microporous)-styrene divinylbenzene
Ionic forms as shipped	H^+
Physical form	Spherical beads
Standard mesh sizes (wet)	20-50
Mean particle size (μm)	560
Effective pH range	0-14
Total exchange capacity	H^+ form
mequiv./g dry resin	4.8

These experiments were carried out at room temperature in a clear perspex column with an internal diameter of 2 cm and length of 20 cm. The up-flow ion-exchange column was fed by a peristaltic pump. The samples in the outlet were taken at predetermined time intervals until resin saturation; this saturation was monitored by analyzing the concentration of each ion in the collected samples. A new batch of cationic resin was used in each experimental run. According to the literature, the effects of near-wall disturbances and preferential channels in the column can be neglected if the ratio of the internal column diameter to the resin particle diameter is higher than 10 (approximately 14.5) (Hamdaoui, 2009).

The total metal ions removal per mass unit of dry resin up to saturation calculated from each breakthrough curve using the following equation:

$$q = \frac{C_F Q}{m_R} \int_0^{t_{end}} \left(1 - \frac{C}{C_0}\right) dt \tag{1}$$

For the evaluation process efficiency, the breakthrough curves were divided into different areas associated with the resin uptake capacity, as indicated in Figure 1.

A is associated with the resin capacity used before the breakthrough point. B is related to the solute amount that leaves the column before the breakthrough point, without being adsorbed and C is related to the resin capacity that is not used efficiently, since part of the adsorption process occurs after the breakthrough point but before t_{end}, which is the first instant corresponding to $C/C_o \approx 1.0$.

On the basis of these areas, two different efficiencies can be calculated: $\mathcal{E}_r$ is the efficiency of solute removal, and, $\mathcal{E}_f$ is the efficiency of resin utilization, defined by Equations 2 and 3, respectively. Using these values, we could develop a statistical analysis of the results, which allowed the evaluation of the process performance.

$$\varepsilon_r = \frac{Q.C_0.(t_{br} - \int_0^{t_{br}} \left(\frac{C}{C_0}\right) dt}{Q.C_F.t_{br}} = \frac{A}{A+B} \tag{2}$$

$$\varepsilon_f = \frac{Q.C_0.(t_{br} - \int_0^{t_{br}} \left(\frac{C}{C_0}\right) dt}{Q.C_F.(t_{end} - \int_0^{t_{end}} \left(\frac{C}{C_0}\right) dt)} = \frac{A}{A+C} \tag{3}$$

The following response function, (Eq. (4)) is suggested in order to use the experimental breakthrough curves for process optimization. Since it is important to maximize the solute removal as well as the consumption of the resin capacity, this response function takes into account both efficiencies. The formulation also considers the breakthrough time: for process productivity, it is important that the time period for maximum solute removal is minimized. In fact, this response function seems to be the best form to represent the process performance because it combines both resin utilization and solute removal (i.e., the period before breakthrough time).

$$Response\ Function\ (RF) = \frac{\varepsilon_r \varepsilon_f}{t_{br}} \tag{4}$$

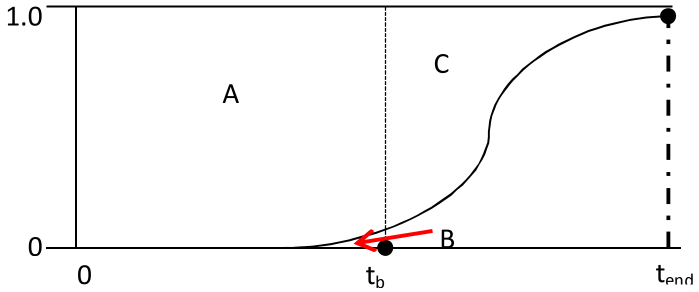

FIGURE 1. Areas A, B and C along the breakthrough curve

Mathematical model:-Bohart-Adams model: Prediction of the breakthrough curve and exchange capacity under specific operating conditions is required for the design of a column exchange process. The Bohart-Adams model assumes that the adsorption rate is proportional to both the residual capacity of the resins and the concentration of the sorbing species:-

$$ln\left(\frac{C_o}{C} - 1\right) = \frac{K_{BA} N_o Z}{U_o} - K_{BA} C_o t \tag{5}$$

where C is the effluent concentration (mg/L), C_o is the influent concentration (mg/L), K_{BA} is the rate coefficient (L mg^{-1} min^{-1}), N_o is the exchange capacity (mg/L), Z is the bed height (cm), U_o is the linear velocity (cm min^{-1}) and t is the time (min).

The model constants K_{BA} and N_o can be determined from a plot of ln[(C/C$_o$)-1] against t for a given flow rate and bed height.

RESULTS AND DISCUSSION

Effect of flow rate. The efficiencies calculated according to Eqs, (2) and (3) and the corresponding experimental conditions are given in Table 2. As expected the results indicate that for higher flow rates, the breakthrough time (t_b) and saturation time (t_{end}) occur sooner. The efficiency of resin utilization decreases as the flow rate increases. This behavior can be explained in terms of the residence time of the metal in the column. An increasing flow rate would reduce the volume treated efficiently until the breakthrough point (Cren *et.al*, 2009). This is because of the insufficient contact time between the metal ions and the cation exchange resin (Dowex 50W), which limits the number of available sites, thus reducing the volume of nickel solution to be treated. However, when the flow rate is decreases, the contact time in the column is longer, and the resin utilization becomes more effective (Hamdaoui, 2009; Dwivedi et. al, 2008).

Effect of bed height. From Table 2, it can be observed that the breakthrough volume varies with bed height. This is because of mass transfer during the process (Gandhimathi, et al., 2011). As the height of the bed decreases, the times required to reach breakthrough and saturation decrease. The mass of the cation exchange resin is proportional to the bed height, thus, a higher bed height lead to a larger exchange capacity and delay the occurrence of both breakthrough and saturation points. This means that the volume of aqueous solution that can be treated is effectively increased (Hamdaoui, 2009).

Response surface analysis. A very high efficiency of metal removal was obtained for all experiments (average 97.5%). The efficiency of resin utilization (ε_f) varied in the range 37-92%. This shows that the potential capacity of the resin bed was used efficiently. These results also indicate that a decrease in the solution flow rate increases the efficiency of resin utilization. The experiment with the best performance ($\varepsilon_f = 0.9229$) was the one conducted at a flow rate 20 mL/min, at pH 6, and with a resin bed height of 6.0 cm. The statistical analysis generates the CCRD model presented in Eq. (6), which describes the response function in terms of the three operating parameters (only two are significant). Figure 2 presents the response surface obtained for Eq. (6), and illustrates the behavior discussed above.

TABLE 2. Efficiency for the experimental breakthrough curves

Flowrate (mL/min) (±0.5)	**pH (±0.5)**	**Bed Height (cm)**	**T_{br} (min) (±2)**	**T_{end} (min) (±2)**	**ε_r**	**ε_f**	**RF**
15.2	4.2	2.8	90	240	0.97500	0.49717	0.00539
24.8	4.2	2.8	60	210	0.99250	0.46688	0.00772
15.2	7.8	2.8	90	300	0.99500	0.50224	0.00555
24.8	7.8	2.8	60	240	0.99500	0.46750	0.00775
15.2	4.2	5.2	120	270	0.99875	0.72264	0.00601
24.8	4.2	5.2	90	240	0.97500	0.74522	0.00807
15.2	7.8	5.2	120	300	0.99750	0.72678	0.00604
24.8	7.8	5.2	90	270	0.99333	0.73339	0.00809
12.0	6.0	4.0	150	240	0.99800	0.76888	0.00512
28.0	6.0	4.0	30	150	0.92500	0.36634	0.01130
20.0	3.0	4.0	60	240	0.96250	0.42308	0.00679
20.0	9.0	4.0	60	240	0.96250	0.42308	0.00679
20.0	6.0	2.0	60	150	0.86667	0.40000	0.00578
20.0	6.0	6.0	120	270	0.99750	0.92290	0.00767
20.0	6.0	4.0	60	240	0.99500	0.40420	0.00670
20.0	6.0	4.0	60	240	0.99500	0.40420	0.00670
20.0	6.0	4.0	90	270	0.99667	0.60731	0.00673
20.0	6.0	4.0	60	240	0.96167	0.42520	0.00682
20.0	6.0	4.0	60	240	0.96167	0.42520	0.00682
20.0	6.0	4.0	90	270	0.97444	0.61891	0.00670

On the basis of the results in Table 2, further analysis was carried out to develop a model to show the combined effect of the independent parameters investigated for the response function. From the *p*-values, the results indicate that the flow rate (*p*=0.000) and bed height (*p*=0.031) are the most significant parameters determining the response function of the breakthrough curve. The R-squared value of the model is acceptable (91.5%) and the *p*-value of the lack of fit test (0.000) indicates that it is significant, implying the inadequacy of the fitted model.

However, to improve the model, another attempt was carried out with only two parameters which are significant in the full quadratic terms analysis. On omission of the other terms that were insignificant in the first attempt, the R-squared term was reduced to 82.6%, while the *p*-value for lack of fit test remained equal to 0.000. The statistical model for this process, based on the experimental conditions of this study as obtained from the response surface analysis is:-

$$Response\ Function = \frac{\varepsilon_r \varepsilon_f}{t_b} = -0.0002 + 0.0003 + 0.0003BH \qquad (6)$$

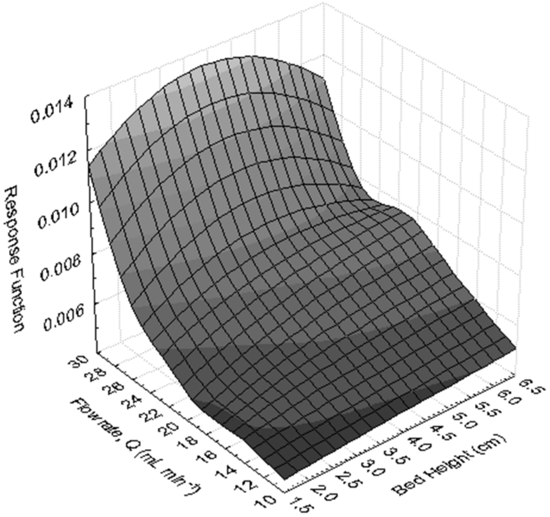

FIGURE 2. Response surface 3D plot representing the relationship between Response Function (RF), flow rate (mL min^{-1}) and bed height (cm).

Table 3. Value of the Bohart-Adams model parameters

Parameter	Q = 12mL min^{-1}	Q = 20mL min^{-1}
Z (cm)	4.00	6.00
u (cm min^{-1})	3.82	6.37
C_0 (mg cm^{-3})	0.001	0.001
k_{BA} (mg.min.cm^{-3})	0.187	0.203
N_0 (mg cm^{-3})	35.01	29.97
t_{br} (min)	150	120
R-squared	0.9031	0.8379

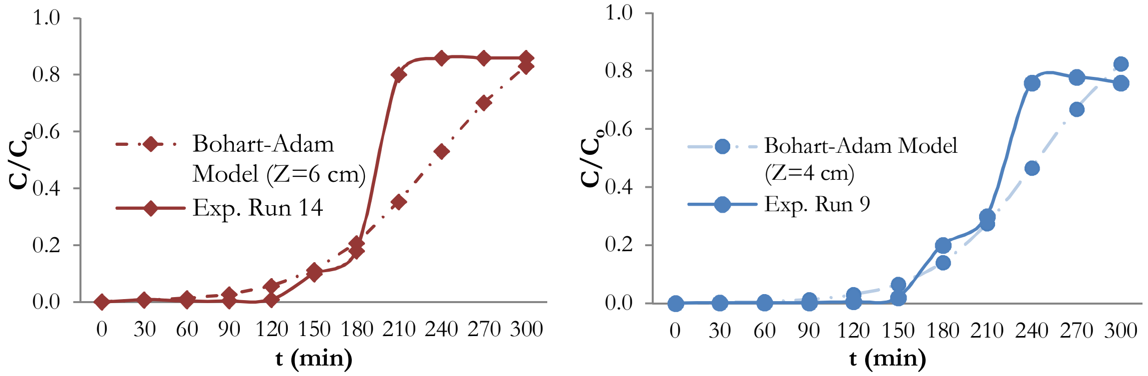

FIGURE 3. Comparison of the experimental and theoretical breakthrough curves obtained at different flow rates and bed heights for Bohart-Adam Model for Ni (II) removal by the cation exchange resin.

Bohart-Adams model. The calculation of the theoretical breakthrough curves for a single-component system requires the determination of the parameters K_{BA} and N_0 for the solute of interest. These values are also listed in Table 4.The approach involves a plot of ln[(C/C_0)-1] versus time according to Eq. (5)(Chu, 2010; Hamdaoui, 2009). The Bohart-Adams model is applied to investigate the breakthrough behavior of Ni (II) removal by the ion exchange resin. The values of the kinetic constant and the maximum amount of metal exchange are determined from the approached plot above at different bed height (4 and 6 cm) and different flow rates (12 and 20 mL min^{-1}). These values are then used to determine the breakthrough curve.

The theoretical curves are compared with the corresponding experimental data in Figure 3. It is shown that the experimental breakthrough curves are very close to those predicted by this model. Thus, this model provided a good correlation between the effects of bed height and flow rate when compared with the experimental results.

CONCLUSIONS

Experiments were carried out to study the breakthrough curves of nickel ions from aqueous solution using cation exchange resins. The effects of the flow rate, pH and bed height on the response function of the column were considered in order to investigate the ion-exchange efficiency. The efficiency of solute removal was in the range 96-99%, and the values obtained for the efficiency of resin utilization were, in most cases, above 40%. The obtained results indicated that both the breakthrough and saturation times increases at lower value of flow rates and higher resin bed heights. This is because at a lower flow rate and higher bed height, longer contact time is achieved, with a greater number of available binding sites, and the interaction between the metal and the resin is stronger. The response surface analysis and the application of the Bohart-Adams model gave good approximations of the observed experimental behavior. The theoretical models and their parameters fitted the experimental breakthrough curves well.

ACKNOWLEDGEMENT

The authors wish to acknowledge the financial support for this research from the Malaysian Ministry of Science, Technology, and Innovation (MOSTI)(Vot No. 79283), the Ministry of Higher Education (MOHE)(Vot No. 78400), and the Universiti Teknologi Malaysia (Vot No. 00L16 & 00L15).

REFERENCES

Alyuz B, Veli S. 2009. Kinetics and equilibrium studies for the removal of nickel and zinc from aqueous solutions by ion exchange resins. *J. Hazard. Mater.* 167(1-3):482-488.

Chu K.H. 2010. “Fixed bed sorption: Setting the record straight on the Bohart-Adams and Thomas models.” *J. Hazard. Mater.* 177:1006-1012.

Clifford, D.A. 1999. “Ion exchange and inorganic adsorption.” In *Water quality and treatment*, 5th ed., chap. 9. McGraw Hill, New York.

Cren E.C, Filho L.C., Silva E.A., Meirelles A.J.A. 2009. “Breakthrough curves for oleic acid removal from ethanolic solutions using a strong anion exchange resin.” *Separation and Purification Technology*, 69:1-6.

Department of Environment, Ministry of Science, Technology and Environment, *Environmental Quality Report 1997*, Kuala Lumpur.

Dwivedi C.P, Sahu J.N, Mohanty C.R., Raj Mohan B, Meikap B.C. 2008. “Column performance of granular activated carbon packed bed for Pb(II) removal.” *J. Hazard. Mater.* 156:596-603

Edebali S, Pehlivan E. 2010. Evaluation of Amberlite IRA96 and Dowex 1×8 ion-exchange resins for the removal of Cr(VI) from aqueous solution. *Chem. Eng. Journal* 161:161-166.

Gandhimathi R., Ramesh S.T., Nidheesh P.V., Nagendra B., Bharathi K.S. 2011. "Breakthrough data analysis of adsorption of Cd(II) on coir pith column." *EJEAFChe*. 10(7):2487-2505.

Hamdaoui O. 2009. "Removal of copper(II) from aqueous phase by Purolite C100-MB cation exchange resin in fixed bed columns: Modeling." *J. Hazard. Mater.* 161:737-746.

Kandah M.I. and Meunier, J.L., 2007. "Removal of nickel ions from water by multi-walled carbon nanotubes" *J. Hazard. Mater.*, 146(1-2): 283-288.

Kang, M.S., Choi, Y.J., Moon S.H. 2004. Effects of Charge Density on Water Splitting at Cation-Exchange Membrane Surface in the Over-Limiting Current Region. *Korean J. Chem. Eng.* 21 (1):221-229.

Pehlivan, E and Altun, T. 2006. The study of various parameters affecting the ion exchange of Cu^{2+}, Zn^{2+}, Ni^{2+}, Cd^{2+}, and Pb^{2+} from aqueous solution on Dowex 50W synthetic resin. *J. Hazard. Mater.* 134(1-3):149-156.

Pehlivan, E and Altun, T. 2007. Ion-exchange of Pb2+, Cu2+, Zn2+, Cd2+, and Ni2+ ions from aqueous solution by Lewatit CNP 80. *J. Hazard. Mater.* 140: 299-307.

Petrus R. and Warchol J. 2003. "Ion exchange equilibria between clinoptilolite and aqueous solutions of Na^+/Cu^{2+}, Na^+/Cd^{2+} and Na^+/Pb^{2+}" *Microporous and Mesoporous Materials*, 61(1-3): 137-146.

PERFORMANCE STUDY OF ADSORPTION PROPERTIES OF LATERITE SOIL IN REMOVING OIL AND GREASE FROM WASTEWATER

Ajith Hebbar H, Jayantha K. S.
(Vivekananda College of Engineering and Technology, Puttur, Karnataka, India)

ABSTRACT: Wastewater coming out of automobile garages mainly contains oil and grease of petroleum origin. It can make considerable nuisance by clogging the sewer pipes, resulting in frequent maintenance. In treatment plants, it can interfere with functioning of aeration tanks and biological treatment units. Conventionally, devices like Grease Traps and Oil and Grease interceptors are used to remove oil and grease. But these methods proved to be costly and inefficient. The present study focuses on the performance evaluation of adsorption property of Laterite bricks and granules in removing oil and grease and developing an efficient cost effective pre-treatment method. Studies were made by passing the synthetic wastewater into a channel between laterite baffle bricks both in the presence and absence of laterite granules at the bottom of channel. The results obtained in the various stages of experiments were found to be encouraging. In the absence of granules at the channel bottom, for slowest flow rate of 0.435 litres per second (lps) and closest brick spacing of 0.25m, the maximum Oil and Grease removal efficiency found to be 97.7%. Due to the addition of laterite granules at the channel bottom, the efficiency increased from 67.66% to 80.99 % for a flow rate of 1.667 lps with a brick spacing of 0.44m. Based on these results, it is quite evident that laterite is a powerful adsorbing medium may be used as adsorbent medium to pre-treat Oil and Grease laden water from vehicle service stations.

INTRODUCTION

Many studies have been made on the removal of Oil and Grease of organic and petroleum origin by using adsorption technique, using different adsorbent materials. Using thermally activated illite clay adsorption technique it was possible to remove oil and grease to an extent of 93.8% from oil-water mixture. Contact time, amount of adsorbent, pH, activation temperature and size of the adsorbent were varied for optimum results (Fatma Turak and Hüseyin Afşar, 2006). It was proved by practical results that, Sand Bio films can be used in the bio-remediation of vegetable oil and grease from polluted wastewater to an extent of 92%. It was adsorption that played an important role in the removal the oil and grease in this experiment (Mohamed H. El-Masry et al., 2004). A laterite column study revealed that Laterite adsorption can be used for defluoridation of drinking water (Jayantha et al., 2004). An experimental study on removing oil from synthetic oil-water mixture found that, Bentonite Organoclay was excellent adsorbent. The concentrations of oil in the oil- water mixture were varied from 26 to 381 milligram/litre in a batch reactor. An equilibrium time of one hour was observed in the experiment for the adsorption (Moazed and Viraraghavan, 2005).

MATERIALS AND METHODS

Study was made on wastewater containing petroleum based oil and grease. A synthetic wastewater was used for the study and it was prepared by using discarded automobile lubricants from the garages. Further to make the method more cost effective, cheaply available undressed laterite bricks from the local quarry were used as adsorbents. The batch flow study was carried out by passing the stored synthetic wastewater with a constant rate in a channel containing laterite brick baffles placed in a staggered manner. As the wastewater travelled through a zigzag path, floating oily particles adhered to laterite surface through adsorption phenomenon. The focus of the study was to monitor the oil and grease

---

ISBN 9780976885351

concentration levels in the wastewater along channel length and at the outlet. Studies were made in two stages by altering various parameters such as flow rate, length of the flow channel, contact area and baffle spacing. The samples were collected from regular intervals of the channel and tested for oil and grease concentration. In stage 1, trials were conducted for baffle spacing of 0.25m, 0.33m and 0.44m by varying the flow rates to 0.435 lps, 0.821 lps and 1.667 lps. In stage 2, laterite granules were added to the bottom of the channel and trials were conducted for a baffle spacing of 0.44m with varying flow rates. Figure 1 shows the bench scale unit used for the study.

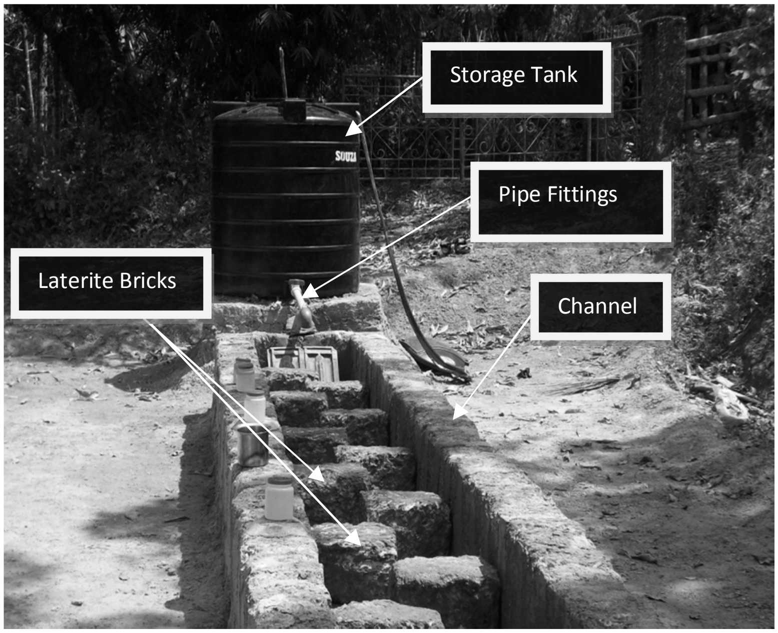

Figure1. A photographic view of the bench scale unit

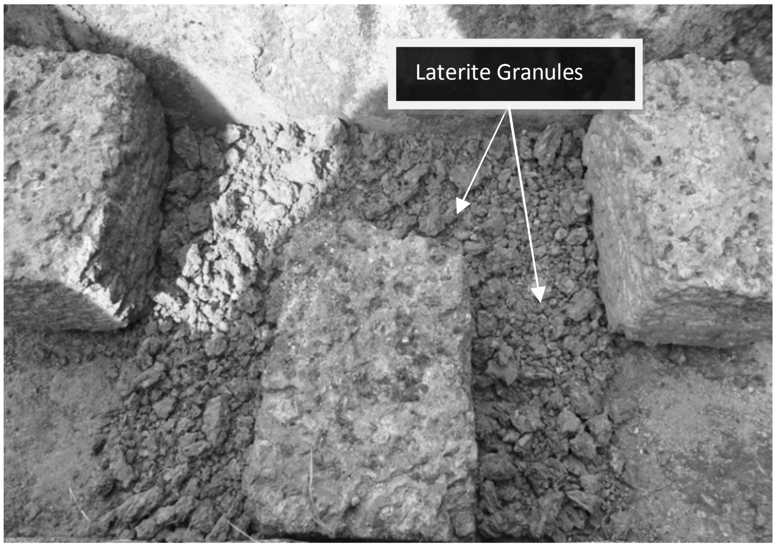

Figure2. A photographic view of the laterite granules placed at channel bottom

Figure 2 shows a photographic view of laterite granules placed at the channel bottom in stage 2.

RESULTS AND DICUSSION

The results of both stages are quite encouraging. In both stages it was observed that efficiency of oil and grease removal increased with the distance of travel in the channel as shown in Table 1 .

Table 1. Variation of oil and grease removal efficiency along the length of the channel

Distance of travel (in meters)		0 (start)	1.5	3	4.5	6	7.5	9	10.5 (end)
Oil and Grease removal efficiency (%)	**Stage 1**	0	12.4	38.7	55.5	67.4	79.9	91.2	97.7
	Stage 2	0	3.6	14.3	25.0	39.3	71.4	78.6	85.8

In stage 1, for given brick spacing, the efficiency decreased with respect to the increase in the flow rate (Figure 3). This depicts that for higher contact period of wastewater with adsorbent, the efficiency increased.

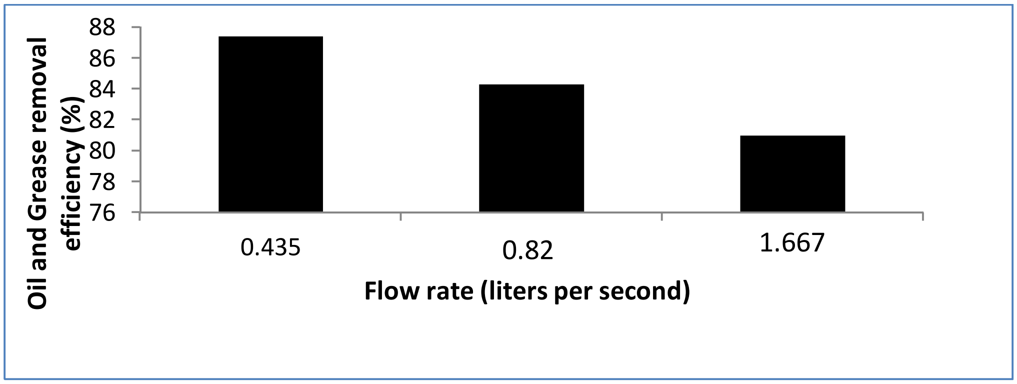

Figure 3. Variation of Oil and Grease removal efficiency with respect to flow rate

Table2. Variation of oil and grease removal efficiency with respect to brick spacing

Brick Spacing (meter)	**Oil and Grease removal efficiency (%)**
0.25	97.7
0.33	90.4
0.44	86.4

It was also observed in the stage 1, for a given flow rate the maximum efficiency of oil and grease removal decreased with respect increase in baffle brick spacing (Table2). This was due to the fact that, when spacing increased the number of bricks in contact with oil decreased.

In stage 2, for a spacing of 0.44m efficiencies found to be on higher side for all flow rates as compared to stage 1 (Table3). This is due the additional contact developed due the presence of laterite granules.

Table3. Variation of oil and grease removal efficiencies with respect to brick spacing

Flow rate(lps)	**Maximum Oil and grease removal efficiency (%)**	
	In the absence of granules	**In the presence of granules**
0.435	86.4	87.4
0.82	80.6	84.3
1.667	67.7	80.99

CONCLUSION

It is quite evident from the results that the laterite is a very powerful adsorbent medium, both in brick and granular form. Flow rate of wastewater, distance of travel of wastewater in the channel, spacing between two adjacent laterite bricks have played an important role in deciding the efficiency of the oil and grease removal. Slower rates of flow, closer baffle spacing and presence additional grains have increased the efficiencies. Moreover, the operations involved during the experiments were simple like flow regulation and repositioning of laterite bricks. Further, in areas where if laterite is very cheaply and locally available, the expenses incurred may be very low. Hence in establishments like vehicle garages and service stations in the urban areas this method can be conveniently used to pre-treat the oil laden wastewater and bring down the oil and grease concentration level to the permissible limits, in line with effluent standards.

REFERENCES

Fatma Turak and Hüseyin Afşar, 2006. “Treatment of Oil-Water Mixture Using Illite Clay Material”. Innovations in Chemical Biology - *A book of proceedings of 9th Eurasia conference on Chemical Sciences held in Turkey,* pp. 205-211

Mohamed H. El-Masry, Ebtesam El-Bestawy and Nawal I. El-Adl., 2004. “Bioremediation of Vegetable Oil and Grease from Polluted Wastewater using a Sand Biofilm System”. *World Journal of Microbiology and Biotechnology.* 20(6): 551-557

Jayantha K. S., Ranjana, G. R., Sheela, H. R., Modang Ritu and Shivananni,Y. S., 2004 “Defluoridation studies using Laterite material”. *J. Environmental Science and Engg.* 46(1): 282-288

Moazed R. H and Viraraghavan. T., 2005. “Removal of Oil from Water by Bentonite Organoclay”, *Pract. Periodical of Hazardous. Toxic, and Radioactive Waste Management.* 9(2): 130-134

MODELING COMPETITIVE BIOSORPTION OF CADMIUM(II) AND ZINC(II) IONS BY PROTONATED CITRUS PEELS

Abhijit Chatterjee and Silke Schiewer
(University of Alaska Fairbanks, Fairbanks, AK, USA)

ABSTRACT: Biosorption by low cost biological sorbent materials can be used as a technique to remove heavy metals from wastewater. Equilibrium batch experiments were performed to investigate the simultaneous biosorption of cadmium and zinc by protonated citrus peels in a mixed metal solution. Four binary metal biosorption models, all modifications of the Langmuir isotherm, were applied to explain the influence of each metal cation on the sorption of other. The competitive Langmuir model was identified as the best model, providing a good description of the data with a minimum number of model parameters. The influence of different objective functions minimized to optimize model parameters was also considered. Protonated citrus peels showed a preference for Cd over Zn sorption in both single and binary metal system.

INTRODUCTION

Decades of research established that different inexpensive biomass types can be employed to adsorb metal pollutants (Lodeiro et al. 2006; Vijayaraghavan and Yun 2008) from aqueous solution, making this process (biosorption) a potential low cost alternative to the traditional metal removal technologies. Even though a lot of research has been done on the subject of biosorption, little commercial success has been achieved to date. One reason is that biosorption research was more focused on searching novel biosorbents with higher uptake capacity for a single metal, rather than continuing study on any given biosorbent to investigate features essential for commercial success, such as its behavior in the presence of other heavy metals which are likely to be encountered in a mining effluent. This demands a long-term step by step study focusing on a single biosorbent. Past research of present authors established that citrus peels are more suitable for adsorption of cadmium (Schiewer and Patil 2008) than other citrus and non citrus fruit waste in a batch reactor and that it can also be used in the commercially preferred fixed bed reactor (Chatterjee and Schiewer 2011). Pectin is a major peel constituent and was found to be instrumental in binding heavy metals (Schiewer and Iqbal 2010). The purpose of this article was to study the simultaneous biosorption of cadmium and zinc using citrus peels. In a binary system, the uptake of each cation depends on the equilibrium concentrations of all metals. This article investigated the suitability of different multi-metal sorption isotherm models in explaining the mutual influence of each metal cation on sorption of other.

THEORY

Langmuir predictive model (LPM) The Langmuir isotherm is the most frequently used single metal isotherm (n=1, i=1 or 2 in Eq. (1)). Here b signifies the affinity of the metal to form M1-S and/or M2-S complexes where S denotes a binding site. The other parameter q_{mi} denotes the maximum uptake capacity of biosorbent for the i^{th} metal. This model can be extended (n=2, i=1, 2 in Eq. (1)) to incorporate the second metal. This is the most simplistic approach as it does not require any additional parameter other than those obtained from single metal isotherms and hence does not require any fitting specifically to binary experimental data.

ISBN 9780976885351

$$q_i = \frac{q_{mi} b_i C_i}{1 + \sum_{j=1}^{n} b_j C_j} (i = 1, 2) \tag{1}$$

Modified Langmuir type models The influence of a second metal on the biosorption of a target metal may be compared with enzyme inhibition. The Langmuir model for one component is mathematically similar to the Michalis-Menten model used to describe enzyme-substrate kinetics, and can also be extended by hypothesizing a series of reactions similar to those used for describing enzyme inhibition, which are classified as competitive, uncompetitive or partially competitive using modifications of the classical Michalis-Menten Model. The Competitive Langmuir model (CLM) Eq. (2) assumes that both metal ions compete for a single site to form M1-S and M2-S complexes. It is mathematically identical to the LPM, just that model parameters are fitted to the bimetal system. The uncompetitive Langmuir model (ULM) Eq. (3) considers also the formation of an M1-M2-S complex. The partially competitive Langmuir model (PCM) Eq. (4) is derived assuming that a metal cation can attach to a site which is free or already occupied by a co cation to form M1-(M2-S) and M2-(M1-S) type complexes. All b values used in Eq. (2)-(4) are equilibrium constants denoting the affinity for the formation of corresponding complexes. Details of the derivation of these equations can be found elsewhere. (Apiratikul and Pavasant 2006)

$$q_i = \frac{q_m b_i C_i}{1 + \sum_{j=1}^{2} b_j C_j} (i = 1,2) \tag{2}$$

$$q_i = \frac{q_m (b_i C_i + b C_i C_j)}{1 + b_i C_i + b_j C_j + 2 b C_i C_j} \text{ [for i, j = 1,2 with i} \neq \text{j]} \tag{3}$$

$$q_i = \frac{q_m (b_i C_i + b_j b_{ji} C_i C_j)}{1 + b_i C_i + b_j C_j + C_i C_j (b_i b_{ij} + b_j b_{ji})} \text{ [for i, j=1,2 with i} \neq \text{j]} \tag{4}$$

MATERIALS AND METHODS

Protonation of Citrus Peels 10 g of dry orange peels were suspended in 500 ml of 0.1 N nitric acid for 4 hours with constant stirring on an orbital shaker (120 rpm) at 25° C so that peels release naturally occurring light metals such as Na, K and Ca. These so called 'protonated peels' were then filtered, thoroughly washed with distilled water, dried overnight at 45° C and sieved into different size fractions. Enhanced biosorptive capacity was reported for protonated peels in comparison to raw peels (Schiewer and Balaria 2009). There was no significant weight loss in this process.

Batch Experiment All batch experiments were performed at 25 °C for 4 hours in a Metrohm auto-titrator using protonated peels of 1-2 mm size. A constant pH of 5 was maintained through the programmed addition of 0.01 N NaOH into the magnetically stirred titrating vessel containing a suspension of about 0.1 g protonated peels (M) in 100 ml of metal solution (V), prepared from 10,000 mg/L AAS standard stock solution purchased from VWR. The initial Cd and Zn concentration (C_0) ranged from 0 to 500 mg/L. The final equilibrium concentration (C) was measured using a flame AAS (Perkin Elmer). The metal uptake (q) was calculated from the mass balance Equation (5).

$$q \times M = V(C_0 - C) \tag{5}$$

RESULTS AND DISCUSSION

Single Metal Biosorption. Figure 1 showed that experimental data obtained from single metal sorption of Zn and Cd can be modeled by the Langmuir isotherm.

TABLE 1 Single metal isotherm parameters

Langmuir Model	b (L/mmol)	q_m (mmol/g)	s^2	R^2
Zn	1.66	0.51	1.49E-03	0.968
Cd	4.90	0.34	6.15E-04	0.972

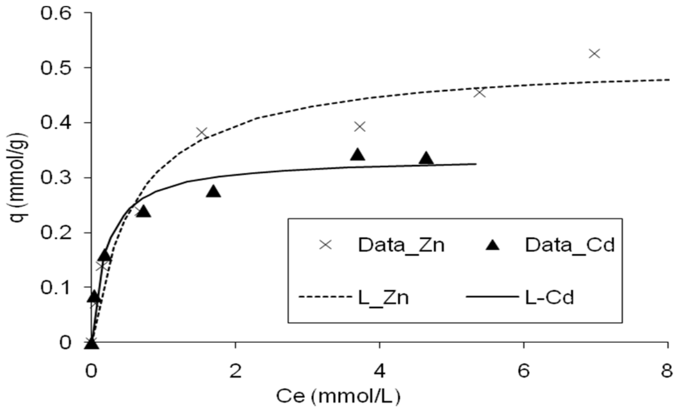

FIGURE 1. Single metal isotherm

Model parameters were optimized by iterative non linear least square fitting using the solver function in excel, minimizing the sum of squared absolute errors. Optimized parameters along with error variance (s^2) and regression coefficients (R^2) are reported in Table 1.

Binary Metal Model fitting All four Langmuir type models (Eq. (2)-(5)) were applied to the experimental data obtained from simultaneous sorption of Cd and Zn. For the LPM, model parameters were known from single metal isotherms (Table 1). For other models, parameters were obtained by applying the same numerical method as for single metal sorption but using two different objective functions, one based on the relative error (Eq. (6)) and another based on the absolute error (Eq. (7)) were employed for the purpose of optimization. The results are reported in Table 2 and 3.

$$F_{rel} = F1 + F2 = \sum_{i=1}^{N}\left(\frac{q1_{i,\exp} - q1_{i,\mathrm{mod}}}{q1_{i,\exp}}\right)^2 + \sum_{i=1}^{N}\left(\frac{q2_{i,\exp} - q2_{i,\mathrm{mod}}}{q2_{i,\exp}}\right)^2 \tag{6}$$

$$F_{abs} = F1 + F2 = \sum_{i=1}^{N}\left(q1_{i,\exp} - q1_{i,\mathrm{mod}}\right)^2 + \sum_{i=1}^{N}\left(q2_{i,\exp} - q2_{i,\mathrm{mod}}\right)^2 \tag{7}$$

For this particular set of data, the relative order among b values remains same, with Cd showing the higher affinity irrespective of the objective function used. However, the optimal set of parameters differed depending on the objective function used (Table 2). This is because an objective function based on the absolute error does not differentiate between data with low or high average experimental uptake. For a given absolute error, the relative error would be higher for the data point showing a lower experimental uptake. In general, the fraction of error contributed by individual metals (F1/F or F2/F) would be very different for F_{rel} and F_{abs} and the impact of each metal on the goodness of fit would be different: the optimization algorithm tends to give a undue weight to the points with larger q_{exp} values associated with a larger average scatter and ignores points with lower q_{exp} values when F_{abs} is used. An objective function based on the relative error F_{rel} removed this bias by scaling the error with the factor ($1/q_{exp}^2$), but the relative error becomes larger for very low q_{exp} values and a reverse bias may occur: points with lower q values will receive more weight due to having more scatter in their relative error due to typically higher relative measurement error. The final choice of the objective function would then depend on whether both metals are equally important and have similar uptake or not, or more generally, whether data with high or low metal uptake are more important.

To compare among models, scatter plots (figure not shown) of (q_{mod} vs q_{exp}) were prepared. Comparing relevant parameters (slope (m) and intercept (c) for these scatter plots, squared regression coefficient (R^2) and error variance (s^2)) in Table 3, the LPM was found to fit worse than the other four models. This is not surprising because model parameters were derived from a different experimental data set, namely the single-metal systems of each metal. Even then, the regression coefficient value is statistically significant, which means the influence of one metal on other metal in a binary system may be qualitatively predicted from this model based on mono-metal data. Based on the high regression coefficient, a near zero intercept and a slope close to unity, the other models seem to perform equally well.

For the ULM, a negative affinity value, obtained by using F_{rel} signifies that formation of a M1-M2-S complex is very unlikely. This was also observed in biosorption of other binary combination of metals (Pb/Cu, Pb/Cd, Cd/Cu) using a macro-alga (Apiratikul and Pavasant 2006). Similarly, b12 and b21 for the PCM were found orders of magnitude lower than b1 and b2, implying that cations were reluctant to bind to an already occupied site.

Since the CLM was found to fit the experimental data satisfactorily, having lower or equal error variance as other models with more parameters, this model was chosen for as the best one for this study.

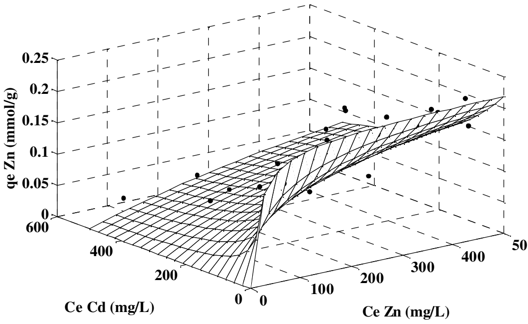

FIGURE 2. Uptake of Zn in bimetal system

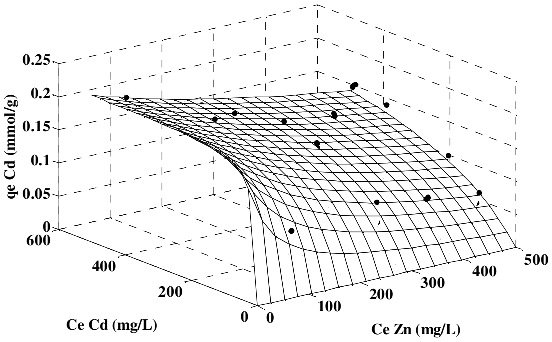

FIGURE 3. Uptake of Cd in bimetal system

Binary Metal 3D Biosorption surface In multi-metal systems, the final metal concentrations, unlike the respective initial concentrations, cannot be deliberately adjusted; it is impossible to obtain a desired equilibrium concentration in the batch experiment. Incidentally, most of the relevant published articles analyzed the biosorption of a primary metal as a function of the easily adjustable initial co-cation concentration. However, this is not a meaningful analysis; an isotherm at a particular initial co-ion concentration is not 'fixed', but will vary depending on biosorbent dose and other factors which alter the equilibrium concentration of co-ion for any given initial concentration. A 3D plot helps to depict the uptake as a function of the final concentration of two metals. Figures 2 and 3 illustrate the uptake of Zn and Cd respectively as a function of equilibrium concentration of both metals. The smooth surface represents CLM. An interpolated surface is avoided as it passes through all experimental points and creates ups and downs.

Influence of co- cation on biosorption of primary metal A more quantitative assessment of inhibition can be obtained by “cutting” the 3D surface plot at suitable x or y values, resulting in a series of 2D plots, which can be constructed from the CLM, as shown in figure 4. Figures 4 and 5 were produced from the CLM using model parameters obtained by minimizing F_{rel} (Table 2). Figure 4 compares the single-component Langmuir isotherm (using parameters from table 1) with a binary system (Zn and Cd) at high (2 mmol/L) and low (0.2 mmol/L) co-cation concentration. It can be observed that the presence of a co cation always lowers the uptake the primary metal, but the extent of inhibition differs from metal to metal. Biosorption of Zn in the presence of Cd was found to be affected more severely than vice versa. Presence of 0.2 mmol/L Cd lowers Zn uptake substantially while the effect was not so pronounced for Cd binding at the same Zn concentration. Increase in the co-cation concentration from 0.2 to 2 mmol/L depressed the metal uptake more heavily and that reduction was more pronounced for Zn binding in the presence of Cd.

TABLE 2 Binary Metal Model Parameters (i=1 for Zn, 2 for Cd)

Model	Model Parameters	F_{rel}	F_{abs}
CLM, Eq. 2 3 parameters	b_1(L/mmol)	7.69	6.06
	b_2(L/mmol)	21.06	16.15
	q_m(mmol/g)	0.230	0.288
ULM Eq. 3 4 parameters	b(L^2/$mmol^2$)	-0.24	1.01
	b_1(L/mmol)	7.54	5.99
	b_2(L/mmol)	20.65	16.38
	q_m(mmol/g)	0.232	0.293
PCM Eq. 4 5 parameters	b_{12}(L/mmol)	0.09	0.36
	b_{21}(L/mmol)	-0.02	0.08
	b_1(L/mmol)	8.52	6.71
	b_2(L/mmol)	17.66	11.84
	q_m(mmol/g)	0.232	0.292

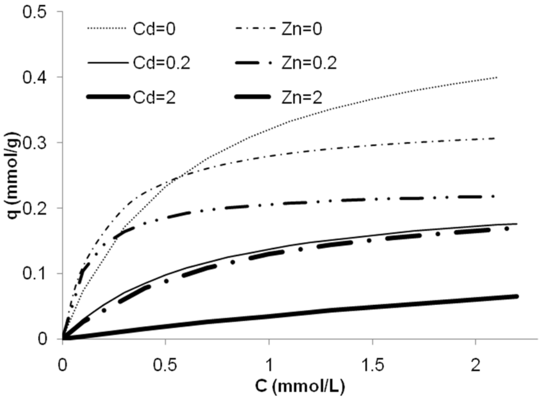

FIGURE 4. Cd and Zn isotherm at 0.2 and 2 mmol/L co-cation concentration

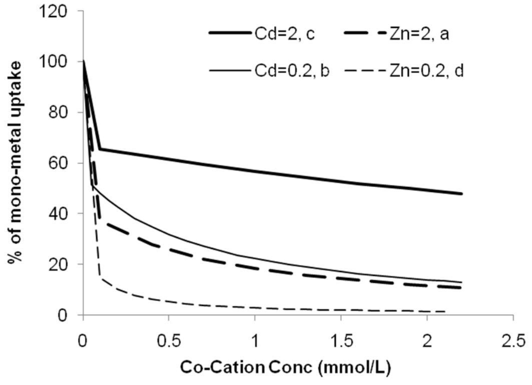

FIGURE 5. Reduction of Cd and Zn uptake with increasing co-cation concentration

This situation is further illustrated in figure 5 which demonstrates how the uptake of metal M1 (as percent of the uptake in the mono-metal system) is influenced by progressively increasing concentrations of metal M2 at a fixed residual concentration of metal M1. At higher Cd concentration (curve a), its uptake is gradually reduced to about 40 percent of its original mono-metal system value when the Zn equilibrium concentration is gradually increased to 2 mmol/L. In the same situation, (curve b, Zn concentration is 2 mmol/L), Zn was able to retain only about 15 percent of its original uptake when the Cd concentration is progressively increased to 2 mmol/L. Also, curve b lies below a, which means, at any co-cation concentration, Zn uptake is more strongly reduced than that of Cd, implying stronger inhibition power of Cd. A similar extent of Cd sorption inhibition only occurs when the Cd concentration is an order of magnitude lower, 0.2 mmol/L which is shown in curve c. At this low concentration of 0.2 mmol/L, Zn uptake is reduced to less than 5% of its original value. In a similar study (Perez-Marin et al. 2008) using orange waste, both Zn and Cd sorption were found to be only moderately affected by the co-cation. Here isotherms were compared by varying the initial concentration. Sorption of Cd was found to be competitively preferred to Zn by seaweed sp (Apiratikul and Pavasant 2006; Luna et al. 2010).

TABLE 3 Statistical parameters for binary metal biosorption

F_{rel}					**F_{abs}**			
	R^2	**m**	**c**	**s^2**	**R^2**	**m**	**c**	**s^2**
LPM					0.70	1.49	0.02	0.44
CLM	0.88	0.88	0.01	0.0008	0.88	0.93	0.01	0.0007
ULM	0.88	0.89	0	0.0390	0.88	0.91	0.01	0.0007
PCM	0.88	0.89	0	0.0395	0.88	0.90	0.01	0.0007

CONCLUSIONS

The protonated peels show a higher affinity for Cd compared to Zn sorption in both mono-component and binary metal systems. Metals-Peels interaction is likely to be ‘competitive’ in nature with no or negligible formation of M1-M2-S and M1-(M2-S) type complexes. Experimental data can be modeled using the CLM but model parameters depend on whether the absolute or relative error is minimized during parameter optimization.

ACKNOWLEDGMENTS

This research was supported in part by the National Research Initiative of the USDA Cooperative State Research, Education, and Extension Service, grant number 2005-35504-16092 and by a USGS NIWR grant. Orange peels were provided by Alarma Consulting Corporation in Florida.

REFERENCES

Apiratikul, R. and P. Pavasant (2006). "Sorption Isotherm Model for Binary Component Sorption of Copper, Cadmium, and Lead Ions Using Dried Green Macroalga, *Caulerpa lentillifera.*" *Chemical Engineering Journal* 119(2-3): 135-145.

Chatterjee, A. and S. Schiewer (2011). "Biosorption of Cadmium(II) Ions by Citrus Peels in a Packed Bed Column: Effect of Process Parameters and Comparison of Different Breakthrough Curve Models." *Clean-Soil Air Water* 39(9): 874-881.

Lodeiro, P., R. Herrero and M. E. S. de Vicente (2006). "Thermodynamic and Kinetic Aspects on the Biosorption of Cadmium by Low Cost Materials: A Review." *Environmental Chemistry* 3(6): 400-418.

Luna, A. S., A. L. H. Costa, A. C. A. da Costa and C. A. Henriques (2010). "Competitive Biosorption of

Cadmium(II) and Zinc(II) Ions from Binary Systems by *Sargassum filipendula*." *Bioresource Technology* 101(14): 5104-5111.

Perez-Marin, A. B., A. Ballester, F. Gonzalez, M. L. Blazquez, J. A. Munoz, J. Saez and V. M. Zapata (2008). "Study of Cadmium, Zinc and Lead Biosorption by Orange Wastes Using the Subsequent Addition Method." *Bioresource Technology* 99(17): 8101-8106.

Schiewer, S. and A. Balaria (2009). "Biosorption of Pb2+ by Original and Protonated Citrus Peels: Equilibrium, Kinetics, and Mechanism." *Chemical Engineering Journal* 146(2): 211-219.

Schiewer, S. and M. Iqbal (2010). "The Role of Pectin in Cd Binding by Orange Peel Biosorbents: A Comparison of Peels, Depectinated Peels and Pectic Acid." *Journal of Hazardous Materials* 177(1-3): 899-907.

Schiewer, S. and S. B. Patil (2008). "Pectin-Rich Fruit Wastes as Biosorbents for Heavy Metal Removal: Equilibrium and Kinetics." *Bioresource Technology* 99(6): 1896-1903.

Vijayaraghavan, K. and Y. S. Yun (2008). "Bacterial Biosorbents and Biosorption." *Biotechnology Advances* 26(3): 266-291.

NOVEL PRODUCTION OF ACTIVATED CARBON FOR HAMPERING OLIGOMERIZATION OF PHENOLIC COMPOUNDS

Liang Yan and George A. Sorial (University of Cincinnati, Cincinnati, OH, USA)

Phenol and its derivatives have been regarded as one major environmental concern around the world because they exist widely in industrial effluents. Among all treatment processes, activated carbon adsorption has been designated as the most widely effective technique in phenolic compounds removal. However, the major concern in activated carbon usage is due to poor regeneration efficiency of activated carbon. The main reason for the drawback is that the presence of molecular oxygen in the aqueous phase promotes oligomerization of the phenolic compounds absorbed onto the carbon surface. To solve this problem, this study proposes a novel approach to produce activated carbon for hampering oligomerization, and will eventually render the activated carbon more cost effective. In this study, a factorial experimental design has been conducted for obtaining the best activation process that will provide BET surface area similar to commercial activated carbon but with a percent of microporosity greater than 80%. The impact of the developed activated carbon on oligomerization of organic contaminants was examined by conducting isotherm experiments for single and multi-solute adsorption systems. Adsorption isotherms of single solute (2,4-dimethylphenol), binary solute (2-methylphenol/2,4-dimethylphenol) and ternary solute (phenol/2-methylphenol/2,4-dimethylphenol) were studied, using the developed activated carbon and commercial activated carbon (Calgon F400). All single solute, binary solute and ternary solute adsorption on developed activated carbon showed that no impact of the presence of molecular oxygen on the adsorptive capacity, indicating that the developed activated carbon is very effective in hampering the oligomerization of phenolic compounds. These results were compared to a commercially produced activated carbon (Calgon F400) where significant oligomerizations of these compounds were noticed.

ISBN 9780976885351

ADSORPTION OF DYE ON PYROLYSED RESIDUE (BIO-CHAR) OF NON-EDIBLE OIL SEEDCAKE

Vaibhav Bansal and ***M. G. Dastidar*** (Centre for Energy Studies, Indian Institute of Technology-Delhi, New Delhi, India)

Now-a-days, considerable attention has been given to bio-diesel production as an alternative to petro-diesel. In India, attempts are being made for using non-edible and under-exploited oils for production of bio-diesel. Most of these oil seeds yield about 25% oil and 70% seed cakes with approximately 5% loss in the mechanical oil extraction process. The seed cakes from non-edible oil being toxic in nature, their disposal in an environmental friendly manner is of great concern. On the other hand, dyes are widely used in various industries and discharge of coloured waste water into the environment is another major problem faced by the industries. In the present study, an attempt was made to convert non-edible *Pongamia pinnata* (Karanja) oil seed cake into useful products through pyrolysis. The potential of bio-char produced alongwith bio-oil during pyrolysis was examined as an adsorbent for the removal of methylene blue (MB) dye from aqueous solution. The pyrolysis experiments were conducted in a fluidized bed pyrolysis reactor and a maximum of about 25% (by weight) bio-char was obtained under controlled conditions at 480^{o}C temperature of pyrolysis. Batch adsorption studies were conducted using MB as adsorbate and bio-char as adsorbent. The performance of bio-char was compared with raw seed cake and standard adsorbent i.e., activated carbon. The effects of initial dye concentration, adsorbent dose, pH and contact time of the adsorbent on the adsorption of dye were examined. It was observed that maximum adsorption with bio-char took place within 15 minutes at 100 mg/l initial concentration of MB indicating about 85% removal. The concentration of MB adsorbed increased with increase in initial dye concentration and increase in pH from 2 to 10. The adsorption of MB increased from 75 to 85% by increasing adsorbent dose from 0.2 to 1 g/50 ml. The percentage of MB removed by bio-char was found to be more than 74% and 72% obtained with raw seed cake and activated carbon respectively. The experimental data obtained with bio-char fitted well with Freundlich adsorption isotherm model. An integrated approach of bio-char production alongwith bio-oil production for vehicular application utilizing waste oil seed cake is expected to give a sustainable development with tangible outcome of energy self sufficiency and environmental benefits.

ISBN 9780976885351

SUSTAINABLE TREATMENT TECHNOLOGY USING NANOSTRUCTURED IRON FOR COMBINED REMOVAL OF HEAVY METAL AND ORGANIC CHEMICALS

Indumathi M Nambi, Ambika M,
(IITMadras, India)

ABSTRACT: Leachate or industrial wastewater contains multiple organic compounds and heavy metals out of which Cr^{6+} were chosen as a representative heavy metal and phenol chosen as a representative organic compound. In this study, a sustainable and effective technology for rapid removal of organic chemical and inorganic heavy metal was developed. Out of many technologies coupling of chemical oxidation reduction and advanced oxidation process system (AOPs) was used in combination with nanostructured zero valent iron(nsZVI) to remove hexavalent Chromium and Phenol.

Batch experiments were conducted with mm sized ZVI and nsZVI to compare their performances. The optimum dosage of iron was found to be 2 g/l and 20mg/l for nsZVI and optimum pH as 4 for both the iron systems. Similar batch experiments were conducted to removal of 5 mg/l of phenol. Coupled experiments with both Cr and Phenol were conducted with the optimized conditions and the treatment process was successful and adequate iron remained in solution even upto three cycles of treatment. Low to neutral pH favoured more iron and Chromium (III) to remain in the dissolved phase which is advantageous for insitu systems. The results of the batch experiments proved that this technology can be used successfully for both for ex-situ system for collected leachate and for in-situ systems to remediate existing contaminated aquifers.

INTRODUCTION

Heavy metal and organic chemical contamination. Most of the developing countries like India, open dumping of solid waste in low lying areas without any engineered system is practiced. Leachate from this solid waste disposal site is generally found to contain organic, inorganic substances and heavy metals and causes ground water contamination. There are also many industries such as electroplating, e-waste processing facilities, paint industry and laboratories where heavy metals and organic compounds are discharged together in the effluent streams. In this study, hexavalent Chromium is chosen to represent the heavy metals in the ground water and phenol for organic chemicals.

Many treatment processes have been developed for removal of Cr(VI) and Phenol as individual compounds. Physio-chemical adsorption has long been researched, but the cost is high and the contaminant is just transferred to solid phase but not removed. Bioremediation by specific strains of bacteria can effectively degrade Cr(VI) and Phenol which is also economically favoured but it is slow and bactericidal toxicants, indigenous organisms and substrate limitations would limit their growth and effectiveness.

Chemical reduction and Chemical oxidation is known to remove Cr(VI) and Phenol respectively in a fairly rapid and effective manner. Many reductants such as H_2S, Fe^{2+}, Fe^0 etc. Fe^0, Zero valent iron (ZVI) has been proposed as a promising material for the reduction of hexavalent chromium into trivalent chromium. Christophoridis et al (2009) suggested that the mechanisms of Cr(VI) reduction by ZVI consists of multiple reactions electrochemical corrosion. Phenol can be removed by Fenton's oxidation process where H_2O_2 is activated by Fe^{2+} to generate strong reactive OH^o species to decompose organic chemicals.

The use of Nano zero valent iron (nZVI) in the place of usual mm sized ZVI (mmZVI) with enhanced surface area have been proven to accelerate the oxidation-reduction process several fold in

---

ISBN 9780976885351

various laboratory and pilot studies Rivero(2009). This can translate into smaller reactor volumes for ex-situ systems and longer life time for in-situ remediation systems which inturn can result in better economics. However, the cost of nZVI is quite prohibitive and its stability questionable due to high rates of oxidation. Moreover, the mobility of nanomaterials are definitely a cause of concern particularly when dispersed in natural systems such as ground water. There is a need to develop an accelerated red-ox based technology to treat a combined waste stream effectively without serious cost or environmental implications.

Coupling Chromium and Phenol removal with nano structured ZVI (ns-ZVI). In this work, new nano-structured zerovalent iron particles (ns-ZVI) with size range of 50-60 microns are synthesized and used in the oxidation and reduction processes. TIn order to reduce cost of replacing the ns-iron consumed in the reactions, the two reactions for Chromium and Phenol removal are coupled in such a way that the iron cycles between the two reactions and is never lost.

During this coupling process, it is hypothesised that the ferric iron generated from the chromium reduction process acts as the electron acceptor and catalyst for the Fenton's Phenol oxidation process. The Ferrous iron formed from the Fenton reactions during Phenol oxidation can be reused for the Chromium reduction and thus the iron can be made to recycle between the two reactions changing back and forth between Ferrous and Ferric forms.

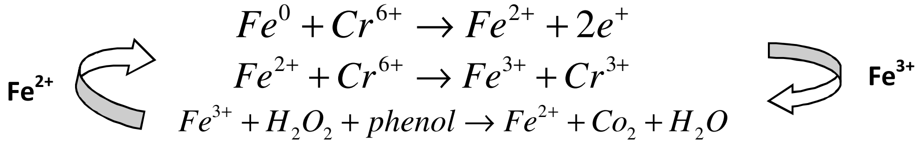

$$Fe^{0} + Cr^{6+} \rightarrow Fe^{2+} + 2e^{+}$$

$$Fe^{2+} + Cr^{6+} \rightarrow Fe^{3+} + Cr^{3+}$$

$$Fe^{3+} + H_2O_2 + phenol \rightarrow Fe^{2+} + Co_2 + H_2O$$

This cycling of iron between the two redox reactions is hypothesized to be a continuous process without having to refurbish the ZVI constantly by external addition. Hence the entire process will be a sustainable, maintenance free system with extended life time.

The objective of this work is to test the proposed sustainable treatment system hypothesis, compare the effectiveness of the nsZVI with that of mmZVI, identify the optimal conditions for removal and limitations if any.

MATERIALS AND METHODS

Chemicals and reagents. Potassium chromate ($K_2Cr_2O_7$, 99.8%), hydrochloric acid (HCl), sodium hydroxide (NaOH), Diphenyl carbazide, glacial acetic acid, 1,10-Phenanthroline, acetone (≥99.5%), sulfuric acid (95–98%), ferrous ammonium sulfate ($Fe(NH_4)_2(SO4)_2 .6H_2O$), ethanol (C_2H_6O, >99.7%) were all of analytical grade. All the reagents were prepared in deionized water.

Synthesis of nanostructure zerovalent iron particles. Iron filings about 2mm long were collected from a local workshop, washed several times with hexane and acetone to remove the oil and grease and oven dried. The dried iron fillings were again washed with acetone, and allowed to dry in an oxygen free environment by purging nitrogen gas. These iron filings were ground to 62nm using Fritsch P-5 High Energy Planetary Ball Mills and then sequentially washed with ethanol and acetone several times to remove the oxide layer and then stored in ethanol in an oxygen-free nitrogen environment until required.

Experimental Methodology

Single compound removal. In order to determine the removal of Cr(VI) using Fe^0, batch experiments were conducted. Separate batch reactors of 100ml volume were setup with initial concentration of 2mg/l of hexavalent Chromium and 5mg/l Phenol. Varying dosages of mmZVI and nsZVI (5, 10, 15, 20 mg/L) were experimented at different pH conditions (2, 4, 6, 8 and 10). The batch bottles were sealed with rubber and aluminium caps and mixed on a shaker table at 150 rpm. The pH was adjusted by using 0.01N HCL and 0.01N NaOH to maintain acidic and alkaline conditions respectively.

Coupled removal in series. In the second set of experiments**,** Phenol and Chromium were added in succession with Phenol reactions initiated first to oxidize the ZVI. The initial concentrations were maintained at 5ppm for Phenol and 2 ppm for Chromium at the beginning of each cycle respectively. The phenol oxidation experiment was initiated by the addition of 1.5ml Hydrogen peroxide solution for mmZVI and 1ml for mZVI determined based on optimization studies. The two reactors were operated parallelly with one time dosage of 20mg/l of nsZVI and 2000mg/l of mmZVI respectively based on the optimization studies done earlier. The experiments repeated for three pHs of 4, 7 and 10. For all the experiments, a blank was maintained without adding any ZVI.

Analytical methods. Samples were collected periodically and filtered using nupore cellulose syringe filter of size 0.45 µm for the measurements of solute Cr(VI) and Fe(II) concentration. Cr(VI) and Fe(II) concentration was measured using the diphenylcarbohydrazide method and phenonthroline method at the wave length of 540 nm, 510 nm respectively, accepted by USEPA and listed in the Standard Methods for the Examination of Water and Wastewater. This method is insensitive to Cr(III) and Fe(III). Total Cr and Fe were determined by atomic absorption (AA) spectroscopy. From this, Cr(III) and Fe(III) can be calculated. The solids retained on the filter were digested with HCl and analyzed for total Cr and Fe, Cr(VI) and Fe(II).

RESULTS AND DISCUSSION

Removal of Phenol and Chromium(VI) as single compounds - comparison of mmZVI and nsZVI and process optimization. Figure.1a and 1b indicate that in case of both mmZVI and the nsZVI removal efficiency increased with iron dosage resulting in an optimum of 2g/l and 20mg/l respectively. The dosages of nsZVI were significantly less by about 100 times as compared to mmZVI to achieve same or better removal of Cr(VI).The removal pathway involves initial reduction of Cr(VI) to Cr(III), followed by adsorption of Cr(III) onto the surfaces, or by precipitation of Cr(III)/Fe(III) hydroxides. All these depends on the available surface area, so that it can offer more electrons and offer more chance for the adsorption and precipitation.

Figures 2a and b and 3a and b illustrate the effect of pH on Chromium(VI) removal and Phenol removal respectively using mmZVI and mZVI. It is evident that the reduction rate of Cr(VI) was greatly enhanced under acidic conditions and reduced under alkaline conditions in both the iron systems. When pH is less than 4.5, iron corrosion is mostly driven by H_2O reduction; when pH is larger than 4.5 the extent of iron corrosion depends on the effect of oxide films on the solubility of Fe and the speciation of the Cr. The reductive remediation of chromate in aqueous media is strongly affected by the passivation of the metal surface with the consequent loss of reactivity (Junxi Liu et al 2009). After the start of the experiments, maintaining the low pH can avoid the formation of oxide film thus increase the reduction rate of Cr(VI).

The increase in pH value will promote the Cr(III) adsorption and co-precipitation which is also not desirable. (Rivero-Huguet et al 2009). It is also possible that the large removal rates of Cr (VI) at low pH could be due to sorption of Cr(VI). It has been reported that the anion form of Cr(VI) is preferentially adsorbed at low pH because the hydrous surface is more positively charged at lower pH (Xiao-qin Li et al, 2008). Similar to Cr(VI), phenol removal also dependent on the corrosion rate of ZVI used in the reaction and lower pH favored the phenol degradation more than the alkaline pH although the difference was not very much.

Coupled Removal of Phenol and Chromium. It can be observed from Figure 4a and 4b that complete removal of Phenol and Chromium(VI) is achievable in both the iron systems upto three cycles without any addition of extra ZVI or Hydrogen peroxide. Also, for both the iron systems, the time taken for removal of Phenol and Chromium decreased significantly with reductions in pH. At higher pH, passive

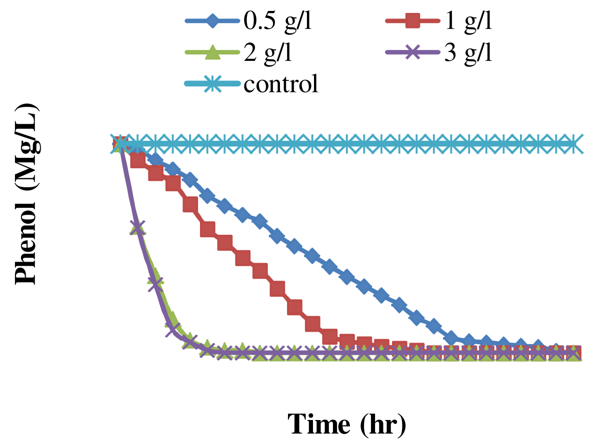

Figure 1a. Optimization of mmZVI dosage

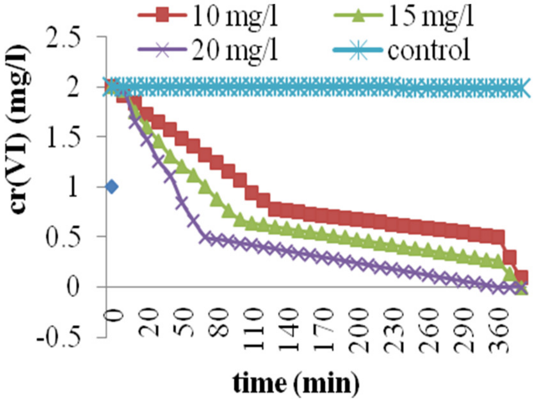

Figure 1b.Optimization of mZVI dosage

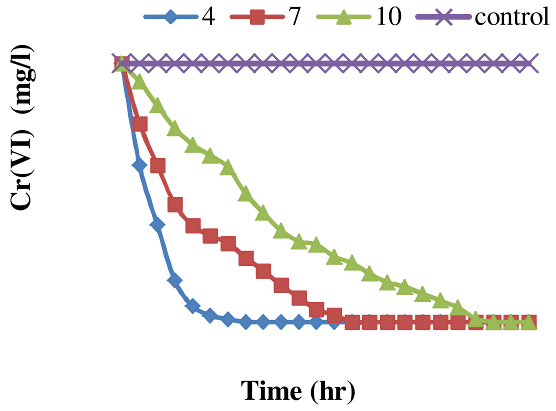

Figure.2a Cr(VI) removal using mmZVI for vavious pH

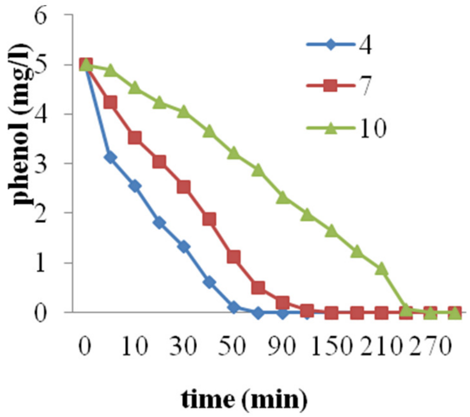

Figure.2b Cr(VI) removal using mZVI for various pH

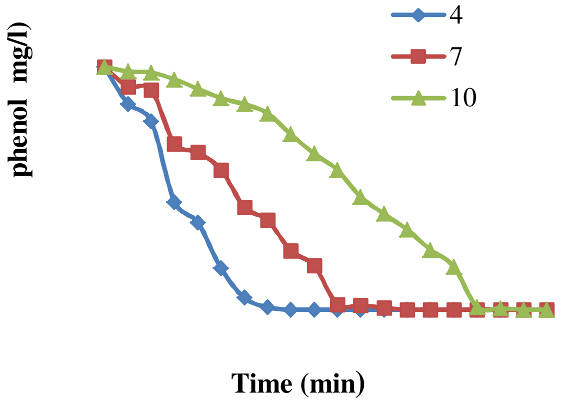

Fig.3a Phenol removal using mmZVI

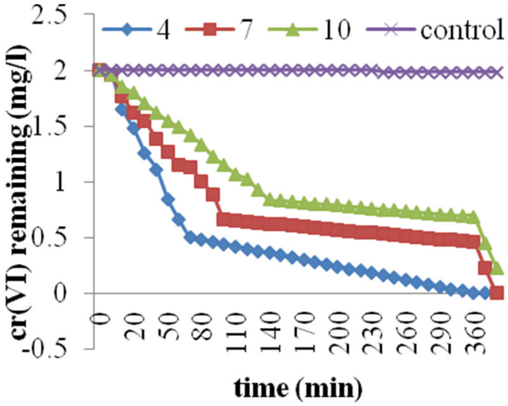

Fig.3b Phenol removal using mmZVI

layer formation on the iron surface and the reduction in the rate of corrosion of iron could inhibit Chromium reduction. A small lag in the Chromium VI reduction was observed for pH 7 and 10 in the beginning of the second cycle which stabilized in the third cycle for both the iron systems.

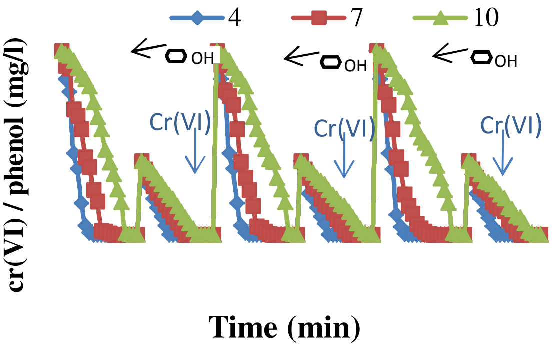

Figure.4a Phenol and Cr removal using mmZVI for various pH

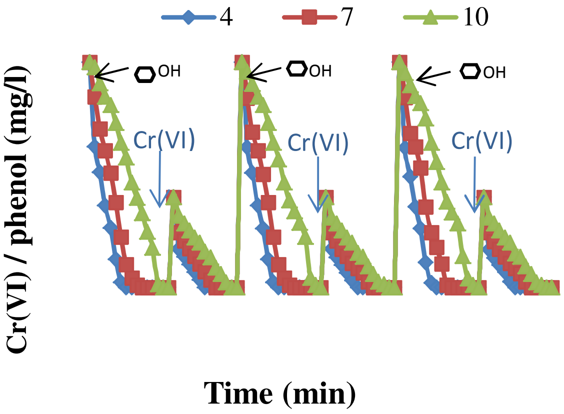

Figure.4b Phenol and Cr removal using nsZVI for various pH

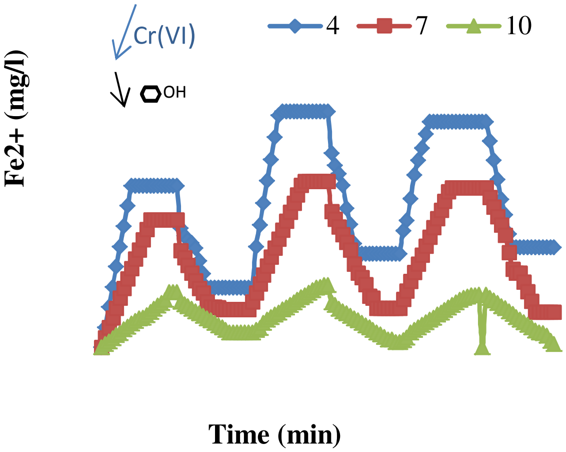

Figure.5a Fe(II) concentration in phenol-Cr(VI) removal system using mmZVI at various pH

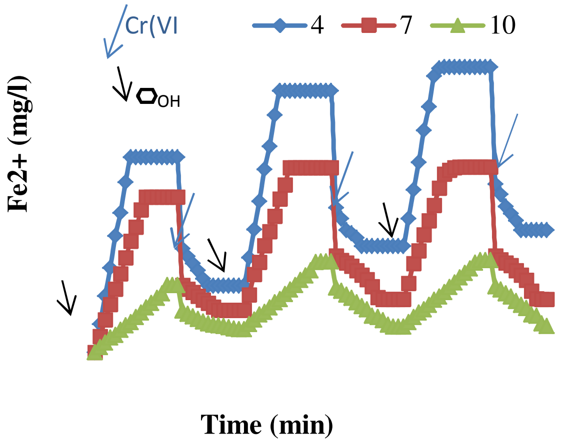

Figure.5b Fe(II) concentration in phenol-Cr(VI) removal system using nsZVI at various pH

However, in the nsZVI system for every cycle, the reaction was completed in less than fifty percent of the time taken in mmZVI system even though the quantity of iron was hundred times more in the latter. This demonstrates the effect of the large surface area available in this nanostructured material.

The concentration of Fe(II) was measured at every time step to track the iron transformation and confirm the cycling of iron during the Phenol and Chromium removals.

Figures 5a and 5b show the Fe(II) build up in both the iron systems with every successive cycle of Cr(VI)-phenol removal for experiments with varying pH. It can be observed that as the pH increased, the concentration of Fe(II) in solution decreased and this could be reason for the delayed removal of Cr(VI) and phenol removal in both the system as the pH increases.

It can also be observed that Cr(VI) removal in coupled removal of phenol and Cr(VI) system, was taking lesser time compared to the system which consisted only Cr(VI) as shown in Figure 1a and b. The reason for this phenomenon may be the readily available Fe(II) which was produced during the phenol removal phase in the first cycle of the coupled experiments.

CONCLUSIONS

The newly synthesized material nsZVI showed better Cr(VI) removal compared to mmZVI because of its enormous surface area even when ZVI concentrations were hundred times lower. Increase in iron concentration resulted in the improvement in the Cr(VI) removal efficiency, since increase in surface area facilitated effective electron transfer and precipitation sites. Low to neutral pH favours the remediation process by reducing the passive layer formation and Cr and Iron precipitation. As the pH increased, the removal rates of Cr(VI) decreased and the Cr(III) precipated which is also not desirable. The hypothesis of sustainable coupled removal of Cr(VI) and Phenol was proved to be successful since the removal rates for both Cr(VI) and Phenol were significantly enhanced with nsZVI which also sustained for several cycles. Hence this treatment process can be applied for treatment of combined Chromium and Phenol in effluents with proper pH control. Further soil column studies and speciation studies are required to identify the insitu application of this technology and the fate of the reduced Chromium and oxidized iron.

REFERENCES

Chirwa EN,Wang Y-T.2000 “Simultaneous chromium(VI) reduction and phenol degradation in an anaerobic consortium of bacteria”. Water Res.;33:2376–84.

Christophoridis C, Fytianos K, 2009 “Parameters affecting the removal of Cr(VI) using zero-valent iron” “Proceedings of the 11 th international conference on Environmental Science and Technology, Chania, Greece, 3-5 September.

Hamdaoui O, Naffrechoux E, Tifouti L, Pe´trier C. 2003 “Effects of ultrasound on adsorption–desorption of p-chlorophenol on granular activated carbon”. Ultrason Sonochem;10:109–14.

Junxi Liu, ChuanWang, Jianying Shi, Hong Liu, Yexiang Tong,2009 “Aqueous Cr(VI) reduction by electrodeposited zero-valent iron at neutral pH:Acceleration by organic matters” Journal of Hazardous Materials 163 pp. 370–375

Patterson RR, Fendorf S and Fendorf M, Reduction of hexavalent chromium by amorphous iron sulfide. Environ Sci Technol **31**:2039–2044 (1997).

Quintelas C, Tavares T. 2001 “Removal of chromium(VI) and cadmium(II) from aqueous solution by a bacterial biofilm supported on granular activated carbon”. Biotechnol Lett ;23:1349–53.

Rivero-Huguet M, W.D. Marshall, 2009 “Reduction of hexavalent chromium mediated by micro- and nano-sized mixed metallic particles”, J. Hazard. Mater. 169, pp1081–1087.

Xiao-qin Li, Jiasheng Cao, and Wei-xian Zhang, 2008 “Stoichiometry of Cr(VI) Immobilization Using Nanoscale Zerovalent Iron (nZVI):A Study with High-Resolution X-Ray Photoelectron Spectroscopy (HR-XPS)” Ind. Eng. Chem. Res., 47, 2131-2139.

ENGINEERING DEHALOGENATION OF TRICHLOROETHYLENE IN INDUSTRIAL WASTEWATER BY FE-NI ALLOY POWDER

Aibin Zeng
(Hangzhou Wanxiang Polytechnic, Hangzhou 310023, China)

ABSTRACT: Trichloroethylene (TCE) is regarded as a high potential toxic and hazardous halogenated organic for animal and human being. In a chemical plant that produced trichloroethylene as product, TCE was of the main pollutant in the wastewater. High concentration of TCE was found in the wastewater of ~ 240 m^3/d. A setup to treat the wastewater was constructed, where Fe-Ni alloy powder was employed as reductant to dehalogenate TCE in three reactors in series, following by neutralization and coagulation with carbide slag and polyacrylamide. After ~14 hr hydraulic retention time (HRT), the removal efficiencies up to 98.6% for TCE were achieved at initial pH 1.5 - 2.5. TCE reacted with metal media in a corrosion-like process to reduce TCE to those less halogenated products. The setup and processes proved to be efficient, stable and economic for the dehalogenation of TCE.

Keywords: Trichloroethylene; Dehalogenation; Wastewater; Fe -Ni Alloy Powder; Carbide Slag.

INTRODUCTION

Halogenated solvents are widely used in industries, resulting in a consequence of widespread contaminants in environment, including water and soil (Vogel, T.M. et al., 1987). The widespread presence of halogenated hydrocarbons poses a potentially serious environmental problem, since such ubiquitous halocarbons as trichloroethylene (TCE) are carcinogenic and toxic (Green T. 2000). As a persistent organic pollutant， TCE is clarified as one of the widest spread organic pollutants in soil and groundwater (Tian, X.M. et al., 2005).

To prevent the pollution, many technologies have been developed to remove TCE from water or wastewater or to reduce its toxicity to less halogenated, such as photo-assisted heterogeneous catalysis (Pruden A.L. et al., 1983), dissolved molecular oxygen oxidation catalyzed by Pt-Ru (Atwater J.E. et al., 1996), Fenton oxidation (Teel A.L., C.R. et al., 2001) and biological contactor process (Bar S.K., et al., 2000). Since Sweeny (Sweeny, K. H. et al., 1972) reported iron could reduce chlorinated hydrocarbon, dehalogenation by iron metal attracted wide attention (Senzaki, T., 1991), leading to the development of permeable reactive barrier technology (O'Hannesin, S. F. et al., 1998). The metal reduction method seems to be more efficient to dehalogenate organichalide (Muftikian R., Q. et al., 1995). Though nano metal particles appear more efficient (Gotpagar J, E. et al, 1997; Wang W. et al., 2009), the common zero-valent metals are still of more considerable interest in the dehalogenation for TCE (2004; Farrell, J. et al., 2000).

Unfortunately, most of the experiments were carried out in lab scale with composite waste water other than industrial one. In the present work, the metal reductive method is used to remove TCE from industrial wastewater to evaluate the performance of the processes, and a better appreciation of the metal reduction method for TCE removal from the wastewater.

MATERIALS AND METHODS

Materials. The chemical factory that produced TCE as product discharged wastewater containing high concentration of TCE 240 m^3/d with pH <1.0. The concentration of TCE was high up to ~387.5 mg/L. The scrap Fe-Ni alloy was grinded into powder in 30-80 mesh and employed as reductive agent for

---

ISBN 9780976885351

dehalogenation. Hydrochloric acid (25%) was used to adjust the pH of the wastewater. Carbide slag (the main composition was calcium hydroxide) was used as alkali for coagulation.

Analysis Method. TCE was measured by a gas chromatograph (Fuli GC 9790A, Fuli Analytical Instrument Co. Ltd., China) equipped with a headspace auto-sampler (DK-3001A, Beijing Zhongxing Huili Science and Technology Co., Ltd., China), a SE-54 capillary column (30 m × 0.25 mm × 0.25 μm) and an electron capture detector. The wastewater was fed into a 10 ml auto-sampler vial and equilibrated at 50 ^{o}C for 30 min. The headspace gas of 1.0 ml was injected with a split ratio of 30:1. Pure nitrogen gas was employed as carrier gas at a flow rate of 1.0 ml/min. The temperature was 120 ^{o}C for injector, 250 ^{o}C for detector and 70 ^{o}C for column. The test sensitivity was 0.001μm L^{-1}.

RESULTS AND DISCUSSION

Engineering Design and Operation. The wastewater treatment was designed into two groups with each in a capacity of 120 m^3/d in continuous flow. As shown in Fig. 1, the process is divided into three sections: (1) pretreatment, (2) dehalogenation, and (3) coagulation and separation. In section 1, the industrial wastewater was first kept in a concrete wastewater pool underplayed with anti-corrosion material to separate floating oil and other trash, HRT 24h. Then, the wastewater was pumped into section 2, which was composed by three tower reactors with each followed a homogenizer tank, where the wastewater was adjusted by adding hydrochloric acid or alkali to control pH in a range of 1.5-2.5 and the catalyst for dehalogenation was added. The tower reactor was divided into three zones, named as mixing and reaction zone, solid and liquid separation zone and the clarifying zone, from the bottom to the top. An out circle of wastewater was employed to support the complete mixing in the reaction zone. Metal powder was added to the reactors from top hopper. To save energy, the three tower reactors are installed in a decreasing level. The wastewater after dechlorination for 12 hours flowed into section 3, which assembled by neutralizing tank, coagulation tank and precipitation tank. Carbide slag was fed into neutralizing tank to adjust pH in a range of 7-9. Next, wastewater was pumped into coagulation tank and mixed with PAM to form floc for half an hour. Then, the slurry was pumped into precipitation tank, where the clear wastewater was separated and the sludge was removed by a scraper and pumped to a filter for dewatering.

The above operating parameters, such as the addition of metal powder, pH and HRT of dehalogenation, were chosen based on the preliminary laboratory scale investigations and practical considerations including the TCE removal efficiency, chemicals cost and power consumption.

TCE Removal. A continuous run of wastewater treatment for 20 days was recorded in Fig. 2. The concentrations of TCE in influent varied from 24.1 to 95.2mg/L, showing a great rise and decline. Three tower reactors displayed high dehalogenation efficiencies and decreased TCE to 2.2-20.6 mg/L in about 12 hours. It is notable that the effluent of tower reactors showed only one time sample above 20 mg/L and other three samples above 10 mg/L. Obviously, the sudden impulsion flow with high concentration of TCE tended to result in low dehalogenation efficiencies. The coagulation by Fe^{2+} and Fe^{3+} formed from metal reduction under assistance of carbide and PAM exhibited a pretty contribution to TCE removal with quite stable efficiencies. TCE in the effluent from precipitation tank varied between 0.1-2.6 mg/L, with only 2 samples were higher than 1.0 mg/L。

The impulsion of influent could lead to a dehalogenation fluctuation. Thus the pretreatment and homogenizer are important to ensure a stable concentration of TCE in effluent. Alternatively, the HRTs in tower reactors should be extended to control the fluctuation at a high concentration of TCE.

The dehalogenation products determined by GC-MS are listed in table 1. In reactor 1, both TCE and dichloroethylene (DCE) were detected, revealing that TCE was decomposed through reductive way. In reactor 2, vinyl chloride (VC) was found together with TCE, DCE and even less molecular weight products, such as acetylene and ethene. In reactor 3, alkane and chloroacetylene were produced. The results show that a long HRTs for TCE in the reactors benefited the decomposition of TCE. Finally TCE was reductive decomposed into less halogenated organics and even alkanes.

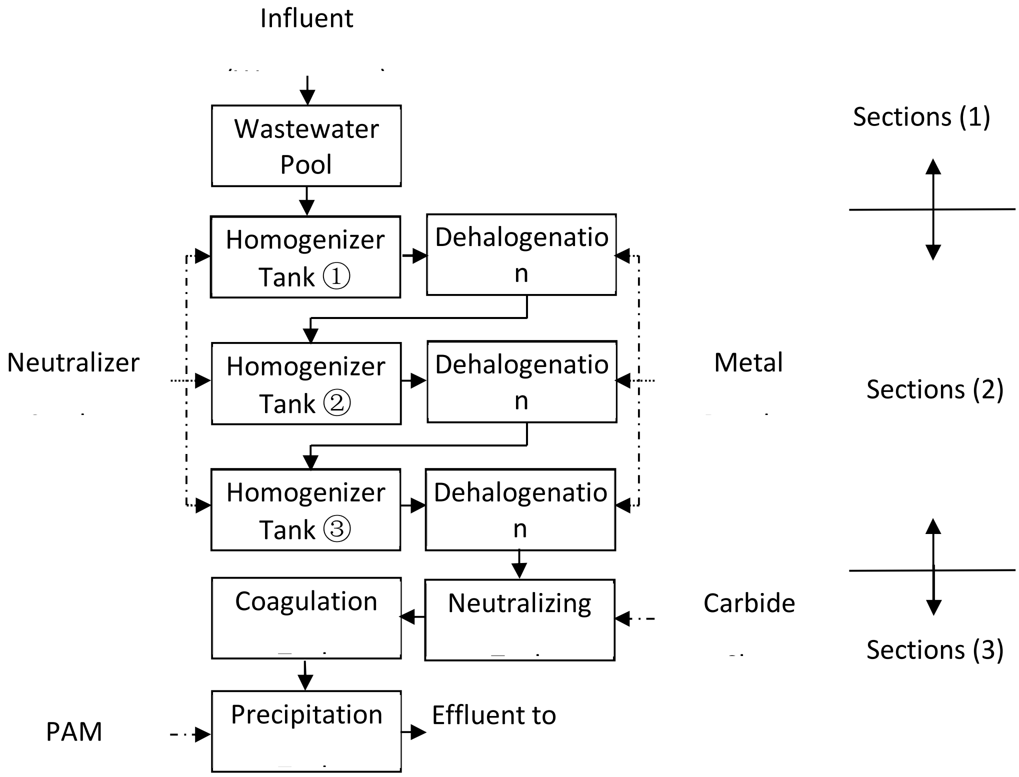

FIGURE 1. Flow chart of the dechlorination processes for TCE wastewater treatment

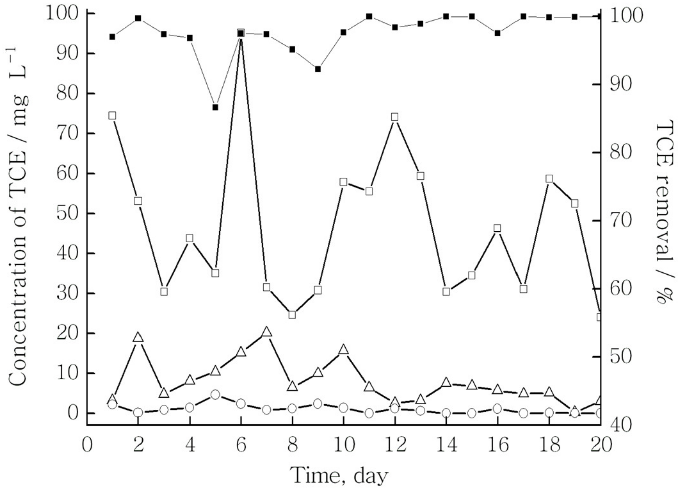

FIGURE 2. TCE removal from wastewater by dehalogenation and coagulation during continuous treatment for 20 days (□ influent; △ effluent from dechlorination reactor; ○ effluent from precipitation tank; ■ TCE removal efficiency)

TABLE 1 Products of TCE dehalogenation by metal reductive treatment

Influent	Dehalogenation treatment		
	Reactor 1	**Reactor 2**	**Reactor** 3
TCE	TCE Dichloroethylene (DCE)	TCE, DCE, Vinyl chloride (VC), Acetylene, Ethene	TCE, DCE, Chloroacetylene, C3 alkanes, Ethane

Economical Analysis. Economy is a crucial factor under consideration when dehalogenation technology is applied in industry. The total investment is $ 435,000, including architecture, equipments and technology service. However the customer pays more attention on the operation outgoing. Here an economic evaluation for the operation based on 1.0 m^3 wastewater is proceeded by calculating consumptions of energy and chemical on current average market price. The cost includes: (1) electricity 11 kWh, that is, $ 0.88; (2) metal powder 3.0 kg, which is converted into $2.36; (3) catalyst consumed 1.0-2.0 kg， equals to $0.1-0.2. The carbide slag and hydrochloric acid used as neutralizer are waste or byproduct in this chemical factory, are not included into the cost. Hence the cost of the operation amounts to $3.34-3.44 /$m^3$ wastewater, if the manual work and depreciation are excluded.

CONCLUSIONS

The process used scrap Fe-Ni alloy as reducer, carbide slag as alkali neutralizer, and Fe ions formed from dehalogenation as coagulant assisted by PAM, providing an economic technology for TCE removal. The setup mainly consisted with three dehalogenation reactors, a coagulation tank and a precipitation tank ensured a stable removal efficiency of TCE as high as 90-99 %. The less halogenated products determined in the metal reductive reactor proved that TCE was reductively decomposed gradually and an extension of HRT was needed for higher removal efficiency.

ACKNOWLEDGEMENTS

The research is supported by Project 2004C33068, Zhejiang Province, China.

REFERENCES

Atwater J.E., J.R. Akse, J.A. McKinnis, and J.O. Thompson. 1996. “Aqueous Phase Heterogeneous Catalytic Oxidation of Trichloroethylene”. *Appl Catal B: Environ*. 11: Ll l-L18L.

Bar S.K., and S. K. Gupta. 2000. “Biodegradation of Trichloroethylene in a Rotating Biological Contactor”. *Water Res*. 34(17): 4207-4214.

Farrell, J.; Kason, M.; Melitas, N., and Li, T. 2000. “Investigation of the long-term performance of zero-valent iron for reductive dechlorination of trichloroethylene”. *Environ. Sci. Technol*., 34, 514-521.

Gotpagar J, E. Grulke, T. Tsang, and D. Bhattacharyya. 1997. “Reductive Dehalogenation of Trichloroethylene Using Zero-valent Iron”. *Environ Progress*. 16(2): 137-143.

Green T. 2000. “Pulmonary toxicity and carcinogenicity of trichloroethylene: species differences and modes of action”. *Environ Health Perspect*. 108(Suppl 2): 261–264.

Muftikian R., Q. Fernando, and N. Korte. 1995. “A Method for the Rapid Dechlorination of Low Molecular Weight Chlorinated Hydrocarbons in Water”. *Water Res*. 29(10): 2434-2439.

O’Hannesin, S. F., and Gillham, R. W. 1998. “ Long-term performance of an in situ “iron wall” for remediation of VOCs”. *Ground Water*, *36*, 164-170.

Pruden A.L. and D.F. Ollis. 1983. “Photoassisted Heterogeneous Catalysis: the Degradation of Trichloroethylene in Water”. *J Catal*. 82: 404-417.

Teel A.L., C.R. Warberg, D.A. Atkinson, and R.J. Watts. 2001. "Comparison of Mineral And Siluble Iron Fenton's Catalysts for the Treatment of Trichloroethylene". *Water Res*. 35(4): 977-984.

Tian, X.M., Q.X. Zhou, and L.S. Wang. 2005. "Research Advances in Ecological Behavior and Toxicological Effects of Chlorohydrocarbon Pollutants"(in Chinese). *Chinese J. Ecology*. 24(10): 1204-1210.

Senzaki, T. 1991. "Removal of Chlorinated Organic Compounds from Wastewater by Reduction Process: III. Treatment of Trichloroethylene with Iron Powder II". *Kogyo Yosui*. 391: 29-35.

Sweeny, K. H., and Fischer, J. R. 1972. "Reductive Degradation of Halogenated Pesticides". U.S. Patent 3640821.

Vogel, T.M., C.S. Criddle, and P.L. McCarty. 1987. "Transformations of Halogenated Aliphatic Compounds." *Environ. Sci. Technol.* 21: 722-736.

Wang W., C.H. Jing, and T.L. Li. 2009. "Synthesis of Coated Nanoiron Particles for Trichloroethene removal"(in Chinese). *China Envoron Sci*. 29(8): 811-815.

STUDY ON THE DESALINATION AND CONCENTRATION OF DYE FROM WASTEWATER BY NANOFILTRATION

DONG Hang, DAI Xingguo, ZHOU Zhijun, ZHANG Lin*, CHEN Huanlin
(Department of Chemical and Biological Engineering, Zhejiang University, Hangzhou, 310027, China)
XIE Lin (China Kunlun Contracting & Engineering Corporation, Beijing, 100037, China)

ABSTRACT: Naphthalenesulfonic acids have been widely used in the chemical industry, especially in the textile industry as intermediate compounds of azoic dyes. A large amount of discharge effluent containing naphthalenesulfonic acids is regarded as a major industrial polluter, and recovery of naphthalenesulfonic acids from the effluence will decrease the discharge value of wastewater. In this work, polyamide nanofiltration membrane was prepared by interfacial polymerization and applied to desalinate and concentrate naphthalenesulfonic acids from the wastewater, which contains a large quantity of T acid and ammonium sulfate. The influences of feed composition and pH on nanofiltration process were investigated. The performance of batch operation and membrane fouling were also evaluated. The results showed that the concentration of salt and T acid, pH, temperature and operating pressure had a significant influence on the membrane separation performance. The permeate flux was more than 23 $L/m^2 \cdot h$, the rejection of T acid was over 92% and the rejection of salt was less than 40% under optimal operation conditions. The permeate flux retained steadily for about 18h, then decreased rapidly due to the membrane fouling.

INTRODUCTION

Naphthalenesulfonic acids are widely used in textile industry as intermediate compounds of azoic dyes. These compounds are highly water-soluble because of their sulfonic groups and stable against biological degradation due to their aromatic rings. So their widespread use results in the pollution of both surface and subterranean water (Zerbinati,O. et al.,1993). Therefore, wastewater treatment technologies are required urgently to eliminate these contaminants from environment.

Traditional processes such as adsorption, stripping and coagulation are not widely employed due to the complex composition of this kind of wastewater and the expensive regeneration of these adsorbents and coagulants. Biological treatment is also less efficient because these compounds are difficult to metabolize or may even inhibit microbial activity (Stolz,A.,1999). Consequently, technologically viable and economically feasible alternatives are required to eliminate and reclaim these aromatic sulfonic compounds from the wastewater.

Nanofiltration (NF) is a novel membrane separation technique, which generally has different retentions of monovalent anions and divalent anions. The separation of dye and salt using NF process has been intensively investigated recently (Capar,G. et al.,2006; Yu SC. et al.2010). The influence factors on the separation and recovery of dye in aqueous solution include three primary aspects: the membrane characteristics such as molecular weight cut off, porosity, surface charge and hydrophobicity, the dye characteristics such as molecular weight, charge and hydrophobicity and the system operating conditions such as feed composition, pH, ionic strength, applied pressure, temperature, and cross flow velocity. Thus, for the same nanofiltration membrane and dye wastewater, the separation performance is mainly determined by the system operating conditions of NF process.

In spite of many researches about separation of dyes by nanofiltration have been presented, there is few research basing on separating naphthalenesulfonic acids from real industrial wastewater. Otherwise, most of the researches are limited to separate different dyes and inorganic salts with

---

ISBN 9780976885351

monovalent anions by nanofiltration, and few of them separate dyes and inorganic salts with divalent anions. This is because the extremely complicated composition of this industrial wastewater and the lack of suitable membranes.

In this work, nanofiltration polyamide (PA) composite membrane was prepared to desalinate and concentrate naphthalenesulfonic acids from the real wastewater, which is produced in the preparation process of H acid with T acid. The composition of this wastewater contains a great deal of T acid and ammonium sulfate as well as a little sulfuric acid, sodium sulfate, sodium chloride and H acid. The COD of the wastewater could reach up to 50000~80000mg/L, and pH value is about 2~3. The T acid in this wastewater cannot be reused due to its high concentration of salts. Thus, nanofiltration technology was used to desalinate and concentrate the T acid, so as to solve the problem of discharge effluent in the production process and implement the recovery and utilization of T acid in the wastewater. The influences of feed composition, pH and temperature on the permeate flux and rejections of both naphthalenesulfonic acids and ammonium sulfate were investigated. In addition, the performance of batch operation and membrane fouling were also studied.

MATERIALS AND METHODS

Composition of Dye Wastewater: The naphthalenesulfonic acid used in this experiment is 1-naphthylamine-3,6,8-trisulfonic acid (T acid). T acid is one of the important raw materials for preparing both 1-amino-8-naphthol-4,6-disulfonic acid (K acid) and 1-Amino-8-naphthol-3,6- disulfonic acid (H acid), which are the primary intermediates in the synthesis of azoic dyes. The chemical structures of three acids mentioned above are given in Fig.1.

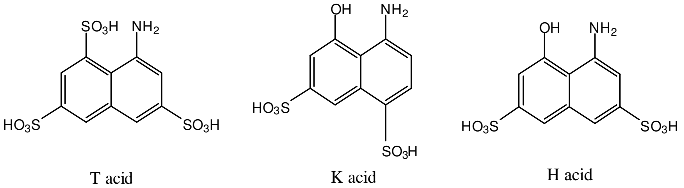

Fig.1. Chemical structure of three kinds of naphthalenesulfonic acids

Membrane Preparation: The nanofiltration polyamide (PA) composite membrane was prepared through the interfacial polymerization reaction between piperazine (PIP, Sinopharm Chemical Reagent Co. Ltd., China, purity >99.0%)) and trimesoyl chloride (TMC, Qingdao Sanli Chemical Engineering Technology Co. Ltd., China, purity >99.0%) on the polysulfone (PSf) support membrane (provided by Hangzhou Development Center of Water Treatment Technology) with 0.05%(w/v) sodium hydroxide as an addition in aqueous solution. After the membrane was held in an oven at 60°C for a certain period, it was washed by pure water and kept in 1% $NaHSO_3$ solution.

Nanofiltration Process: NF process of dye wastewater was carried out in a cross-flow membrane test unit. Circular membranes with a diameter of 70mm were placed in three parallel modules, respectively. The effective area of each membrane was 38.5cm^2. The temperature of the feed was controlled by a heat exchanger. The flow rate of the feed was regulated to 1.5L/min. During the experiment, the operating pressure was varied from 1.0 to 2.0MPa, and the operation temperature was set from 20 to 50°C. All experiments were carried out for 0.5h to reach the steady-state condition before the samples were collected and each experimental point reported was averaged over three polyamide membranes.

Analysis and Definitions: The concentration of T acid was determined with a UV-vis spectrophotometer (Spectrumlab54, Lengguang Tech, China). The concentration of ammonium sulfate was determined using a conductivity meter (DDS-11A, Leici Instruments, China). The pH was measured by a pH meter (Model 868, Thermo Orion, USA). The permeate flux can be calculated by the volumetric permeate flow (L/m^{2}h). The rejections of both T acid and ammonium sulfate were calculated by the solute concentration of permeate and feed solution.

RESULTS AND DISCUSSION

Preparation of Membranes: Tab.1 listed the effect of TMC and PIP concentrations on the performances of NF membranes. It showed that the rejections of T acid and $(NH_4)_2SO_4$ decreased with decreasing TMC and PIP concentrations, while the flux increased. Considered the rejections of T acid and $(NH_4)_2SO_4$, the optimized TMC and PIP concentrations ought to be 0.1% and 0.15% respectively.

Tab.1. Effect of TMC and PIP concentrations on NF membrane performance [a]

TMC% (w/v)	PIP% (w/v)	T acid rejection (%)	$(NH_4)_2SO_4$ rejection (%)	Flux (L/m^{2}h)
0.2	0.2	93.2	60.7	19.5
0.1	0.3	92.2	51.3	18.6
0.1	0.2	91.5	43.6	22.7
0.1	0.15	91.3	41.7	23.9
0.05	0.2	87.3	41.2	24.6
0.1	0.1	87	38.2	26.2

a: Performance of NF membrane was measured in wastewater (salt concentration: 20g/L; T acid concentration: 1.0g/L; temperature: 25.0°C; pressure: 1.5MP; pH: 5;).

Co-influence of salt and T acid concentrations: The co-effect of salt and T acid concentrations on the performance of NF process at P=1.5 MPa, pH=5 and T=25.0°C was shown in Fig.2. The results showed that for a constant T acid concentration in the mixed solution, flux, salt rejection and T acid rejection all decreased with increasing salt concentration. And for a constant salt concentration, both flux and salt rejection decreased with increasing T acid concentration, but the T acid rejection appeared to be insensitive to the adjustment of T acid concentration.

Compared to the T acid concentration, the change of salt concentration had a greater impact on the performance of NF process. A straightforward explanation of this phenomenon was that T acid concentration in the feed was quite low relatively to salt, so the change of T acid concentration had little contribution to the total concentration of the feed. On the other hand, the increase of salt concentration was more likely to make the counter ions concentrate on the surface of the membrane and diminish the dielectric effect of membrane. For these reasons, salt concentration had stronger influence on the separation efficiency of nanofiltration membrane.

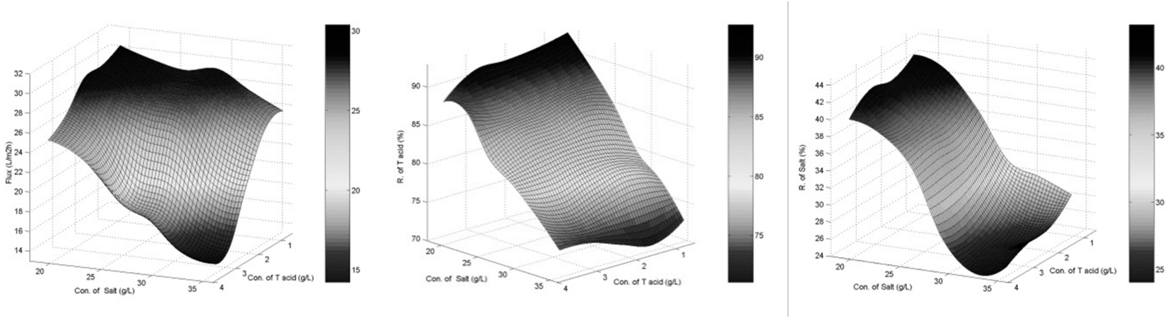

Fig.2. Co-effect of the two solutes on permeate flux, rejection of T acid and rejection of salt in mixed-solute solutions. (temperature: 25.0°C; pressure: 1.5MPa; pH: 5).

Influence of feed pH and temperature. The skin layer of the membrane used in this experiment was made of polyamide material, which possessed dissociable carboxylic and amine groups, and could exhibit negative or positive surface charge depending on feed pH (Manttari,M. et al.,2006). Therefore, the performance of NF process would be highly dependent on the solution pH, which could significantly affect the electrostatic interaction between charged solutes and membrane surface. The pH of feed in this experiment was adjusted from 2.8 to 6.5 by 0.1M H_2SO_4 and 0.1M NaOH respectively.

Fig.3 showed the flux and rejections of solutes at different pH value. The flux decreased moderately from 25.6L/m^{2}h to 21.5L/m^{2}h with the increasing pH value. This phenomenon was probably due to the different pH value in the feed changed charge distribution on the membrane, and resulted in skin shrinkage (Freger,V. et al.,2000), which decreased the permeate flux of NF process. The rejection of T acid increased with the increasing pH value. This was caused by the increasing electrostatic repulsion between membrane surface and T acid. The T acid molecule held negative charge and the sulphonic acid groups were completely dissociated over the studied pH range. So the electrostatic repulsion between membrane surface and negatively charged dye solute increased. In addition, membrane skin shrinkage should happen when the pH of feed changed, which could reduce the diameter of micropores on the membrane surface so as to improve the retention of T acid. The salt rejection showed a different trend with the variation of pH. It appeared to be moderately dependent on pH with a shallow minimum at pH=4.5. This trend was similar to the results of other researchers (Childress,A.E. and M.Elimelech, 2000). The ions ionized from ammonium sulfate were much smaller than the micropores on the membrane surface, so the retention of ammonium sulfate was mainly decided by the electrostatic interaction between ions and charged membrane. In this experiment, the salt retention minimum of membrane was in accordance with zeta potential measurements, with which the iso-electric point was determined to be pH=4.3 with 1mM KCl at 25^{o}C.

The effects of temperature on permeate flux and solutes rejections were shown in Fig.3. The permeate flux increased with increasing temperature linearly. As the viscosity of dye solution decreased when temperature was raised, the diffusion coefficient increased accordingly. As a result, the permeate flux increased with an increase of temperature. The rejections of solutes showed different patterns, the rejection of T acid seemed not to be sensitive to the change in operating temperature, but along with an increase in temperature, the rejection of salt increased apparently. These results may cause by the effects of temperature on the sorption and charge distribution of the membrane.

Fig.11. Influence of solution pH and temperature on permeate flux and rejections of both T acid and salt (salt concentration: 25g/L; T acid concentration: 3.0g/L; temperature: 25.0^{o}C; pressure: 1.5MPa;).

Performance of batch operation and membrane fouling: NF process was operated for ten hours a day and persisted for six days in this experiment. Fig.15 presented the variation of permeate flux and rejections of both T acid and salt with the operating time. It could be observed that the permeate flux reduced drastically in the first six hours, which was caused by the unsteady-state of membrane. Then it retained steadily at about 24L/m^{2}h for the next 18h. After that, the permeate flux decreased again, which was attributed to the fouling of the membrane. This gel layer formed by the rejected dye on membrane surface operated as an additional resistance to permeate.

The trends of T acid and salt rejections with operation time were apparently different to each other. For the retention of T acid, the main interaction between the membrane and solute was steric effect, which was increasing with the gel layer formed on membrane surface. As a result, the T acid rejection increased directly with the operation time. However, for the retention of salt, the main interaction between them was electrostatic effect. As the gel layer formed on membrane surface, the charge on the membrane surface was shielded continuously, this resulted in the decline of electrostatic effect. And after an idle period, the charge on the membrane surface was more likely to be shielded. Therefore, the trend of salt rejection was presented as in Fig.15.

Fig.16 showed the dye layer accumulated on the surface of the membrane after 60h. There was a very thick and hard dye cake layer on the membrane surface, and the cake layer had a great deal of fissuring after drying. This gel layer caused the permeate flux declined by about 25%. In order to avoid such membrane-fouling problem, pretreatment of the dye solution with chemical coagulant and cleaning of membrane polluted were often needed (Mo, J.H. et al.,2008; Zator,M. et al.,2009).

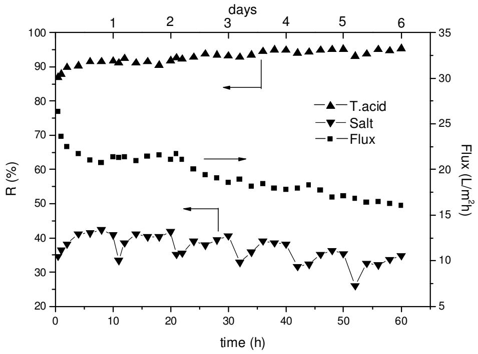

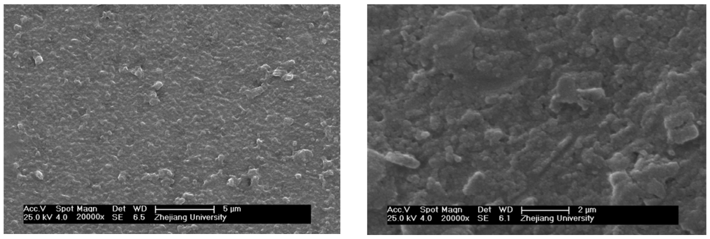

Fig.15. Performance of batch operation of NF process. (salt concentration: 25g/L; T acid concentration: 3.0g/L; pH: 5; temperature: 25^{o}C; pressure: 1.5MPa)

CONCLUSIONS

Nanofiltration membrane was prepared for naphthalenesulfonic acids desalination and concentration. When this process was operated under optimal conditions, the permeate flux exceeded 23 L/m^{2}h, and the rejection of T acid was over 92.0% and the rejection of ammonium sulfate was less than 40.0%. After investigating the influence of different operating conditions on the performance of NF process, the results indicated that: Flux increased with increasing temperature and decreased with increasing pH and concentration of both T acid and salt. Rejection of T acid increased while pH increased, whereas the rejection of T acid decreased along with increasing salt concentration. Rejection of salt increased with increasing temperature and operating pressure, and declined as the concentration of both T acid and salt increased. The salt retention gained its minimum when the charge of membrane was close to zero at pH=4.3. The permeate flux retained steadily for about 18h, then it decreased by about 25% due to a gel layer formed on the membrane surface.

ACKNOWLEDGEMENTS

The authors acknowledge financial support from The National Basic Research Program of China (2009CB623402), National Key Technologies R&D Program (2008ZX07424-001) and the Fundamental Research Funds for the Central Universities.

REFERENCES

Zerbinati,O., G.Ostacoli, D.Gastaldi, and V.Zelano. 1993. “Determination and identification by high-performance liquid chromatography and spectrofluorimetry of twenty-three aromatic sulphonates in natural waters.” *J. Chromatogr. A.* 640(1-2): 231-240

Stolz,A. 1999. “Degradation of substituted naphthalenesulfonic acids by Sphingomonas xenophaga BN6” *J. Ind. Microbiol. Biotechnol.* 23:391-399

Capar,G., L.Yilmaz and U.Yetis. 2006. “Reclamation of acid dye bath wastewater: Effect of pH on nanofiltration performance” *J. Membr. Sci.* 281(1-2):560-569

Yu S.C., M.H. Liu, M. Ma, M. Qi, Z.H. Lu and C.J. Gao. 2010. “Impacts of membrane properties on reactive dye removal from dye/salt mixtures by asymmetric cellulose acetate and composite polyamide nanofiltration membranes” *J. Membr. Sci.* 350(1-2):83-91

Manttari,M., A.Pihlajamaki and M.Nystrom. 2006. “Effect of pH on hydrophilicity and charge and their effect on the filtration efficiency of NF membranes at different pH” *J. Membr. Sci.* 280(1-2):311-320

Freger,V., T.C.Arnot, J.A.Howell. 2000. “Separation of concentrated organic/inorganic salt mixtures by nanofiltration” *J. Membr. Sci.* 178(1-2):185-193

Childress,A.E. and M.Elimelech. 2000. “Relating Nanofiltration Membrane Performance to Membrane Charge (Electrokinetic) Characteristics” *Environ. Sci. Technol.* 34:3710-3716

Mo, J.H., Y.H. Lee, J. Kim, J.Y. Jeong and J.G. Jegal. 2008. “Treatment of dye aqueous solutions using nanofiltration polyamide composite membranes for the dye wastewater reuse” *Dyes Pigment.* 76:429-434

Zator,M., J.Warczok, M.Ferrando, F.López and C.Güell. 2009. “Chemical cleaning of polycarbonate membranes fouled by BSA/dextran mixtures” *J. Membr. Sci.* 327(1-2):59-68

COMPARATIVE EVALUATION OF PRE- AND POST-OZONATION ON THE BIOLOGICAL TREATMENT OF DISTILLERY SPENT WASH

Namasivayam Vasudevan and Ramalingam Kanimozhi (Centre for Environmental Studies, Anna University Chennai, Chennai 600 025, India)

ABSTRACT: The present study investigates the treatment of anaerobically digested distillery spent wash (ANDSW) with biological treatment followed by ozonation process. The aerobic biological system (SBR) used in this study was able to treat the distillery wastewater (ANDSW) containing high COD to the extent of 70% and BOD to the extent of 96%, respectively at an optimized OLR of 3.6 kgCOD/m^3/d and HRT of 24 h. The SBR treated effluent was subjected to ozonation. Two different ozone application rates of 0.2 g/h and 1 g/h were used in the ozonation experiments with ozonation times of 5, 10, 15, 25, 30 and 35 minutes, respectively. For the lowest ozone application rate of 0.2 g/h, a COD and colour removal of 33% and 87% respectively was observed in 30 minutes of ozonation. While for the highest ozone application rate of 1 g/h, COD and colour removal of 42% and 89% respectively was achieved in 30 minutes. Hence, in the present SBR treated effluent, a low ozone dosage of 0.2 g/h for 30 min was effective for partial oxidation of persistent compounds and colour removal.

Keywords: Distillery; Wastewater; Sequencing batch reactor; Ozonation; COD removal; Colour removal

INTRODUCTION

Distillery industry is one of the most highly polluting and growth oriented industries in India based on the quantity of wastewater generated. Molasses from sugarcane industry is the common raw material used in ethanol production due to its easy availability and low cost (CPCB 2003; Kalavathi et al 2001). At present, there are 319 distilleries in India with an annual alcohol production of 2.3 billion litres (Tewari et al 2007) and approximately 40 billion litres of spentwash are generated annually (Ghosh et al 2002).

Distillery wastewater is well known for its tremendous pollution potential due to high organic and inorganic load, low pH and dark colour (Dikshit and Chakraborty 2006). The biochemical oxygen demand (BOD) and chemical oxygen demand (COD) are an index of its polluting character, typically range between 35,000 – 50,000 and 80,000 – 1,00,00 mg/L respectively (CPCB 2003).

Among the various biological treatment methods available, anaerobic treatment process is widely employed for the treatment of distillery effluents for methane recovery (Akunna and Clark 2000; Xiangwen et al 2008). Spentwash even after anaerobic digestion has high residual COD and BOD (COD: 36,000 – 40,000 mg/L and BOD: 8,000 – 10,000 mg/L). The existing treatment technology is inadequate and therefore a feasible technology is required for the treatment of anaerobically digested distillery wastewater before its disposal into the environment.

Aerobic biological system is considered as an effective method for the removal of residual organic load (Dosta et al 2008; Torrijos and Moletta 1997); however biological treatment still presents problems due to the presence of recalcitrant compounds like melanoidin (Sirianuntapiboon and Prasertsong 2008), which are mostly coloured and in a highly complex state and that makes the biological treatment quite inadequate for colour removal from this stream (Satyawali and Balakrishnan 2007). Currently, treatment processes such as chemical methods, adsorption using activated charcoal (Chandra and Pandey 2001), flocculation (Migo et al 1993) are used for the removal of melanoidins from the biologically treated wastewater. However, these processes still have disadvantages due to high operation cost, high consumption of chemical agents, and variations in the colour removal efficiency and high

---

ISBN 9780976885351

volume of solid waste produced (Kumar and Chandra 2006). Since polyphenols are aromatic compounds and are prone to the attack of electrophilic agents like ozone, ozonation seems to be an alternative technology to degrade the recalcitrants (Beltran et al 1993). Hence the present study investigates the treatment of anaerobically digested distillery wastewater by aerobic sequencing batch reactor followed by ozonation process.

MATERIALS AND METHODS

Spent wash. The anaerobically digested distillery wastewater (ANDSW) was collected from the anaerobic unit of a distillery near Chennai, Tamilnadu, India. The wastewater was degasified for 2 hours and the degasified wastewater was used in the study. Table 1 shows the characteristics of ANDSW after degasification.

Table 1 CHARACTERISTICS OF ANAEROBICALLY DIGESTED DISTILLERY SPENT WASH

S.No.	Parameters	Sample 1	Sample 2	Sample 3	Sample 4	Sample 5	Mean
1	pH	8	7.9	8.1	8.1	8.3	8.08
2	BOD	8,000	8,450	8,000	9,200	8,150	8,360
3	COD	36,600	37,400	37,000	38,600	38,200	37,560
4	BOD/COD	0.21	0.22	0.21	0.23	0.21	0.21
4	TSS	12,675	17,000	17,260	20,000	15,600	16,507
5	TDS	20,800	27,300	29,500	27,340	26,360	26,260
6	TKN	1332	1047	1277	1338	1297	1258.2
7	Phosphorus (PO4)	56	63	70	69	67	65
8	Alkalinity	2960	2760	3200	2900	2820	2928

Bioreactor. Biological treatment was carried out in a laboratory scale Sequencing batch reactor (SBR) of 6 L capacity made of acrylic (6mm thick) with a dimension of 230 mm x 190 mm. The working volume of the reactor was 4 L equipped with air sparger. Mixing was carried out by overhead stirrers (IKA Labortecnik) with paddles for homogenization of reactor content. Filling of the influent wastewater and decanting of treated effluent were carried out by peristaltic pump (Miclins make).

Ozonation. The Ozonator used for the study was an air cooled ozonator, (CDS 2G INDIZONE model) supplied by Ozone Technologies and Systems India Ltd., Chennai. It can produce 2% ozone (Percentage weight of ozone in outlet gas) if fed with air. A single phase 220 V AC power supply was used as the source of power. The Ozonator used in this study generates ozone by Corona discharge method. The ozone generated by the ozonator was passed through three bubble column reactors connected in series and trapped in KI solution.

Biological oxidation of ANDSW. The mixed bacterial culture used in the study was isolated from the soils of distillery premises, which had been saturated with spilled distillery effluent for a prolonged period was used as inoculum for SBR along with the activated sludge from municipal wastewater treatment plant for highest treatment efficiency. Each SBR cycle lasted for 24 h. The cycle consists of 30 min fill phase, 22 h Aerate phase, 1 h sludge Settling phase and 30 min Decant phase. The fill phase took place under anoxic conditions, providing only mixing of the reactor content. Throughout the react phase, air was supplied to the system ensuring a dissolved oxygen (DO) concentration above 2 mg/L. Aeration and mixing was stopped during the settle phase and the sludge was allowed to settle under quiescent conditions. During the decant phase, the clarified supernatant was withdrawn by using peristaltic pump.

Anaerobically digested spentwash was combined with domestic wastewater in a ratio of 1: 4 v/v and used as an influent in the laboratory scale SBR. The COD, BOD and TKN of the influent wastewater were 9,500-10,000 mg/L, 1100 – 1135 and 300-330 mg/L, respectively. The influent was delivered to the bioreactor at a rate of 1.5 litres per day. Consequently the Organic loading rate was 3.6 kgCOD/m^3/d and the Hydraulic Retention Time was 24 hours. A sludge retention time (SRT) of 10 days was fixed to limit sludge production.

The influent and effluent samples of the SBR were analysed for Chemical Oxygen Demand (COD), Biological Oxygen Demand (BOD), Total Kjeldahl Nitrogen (TKN) and Total Phosphorus (TP). In addition, reactor pH, DO, SVI and MLVSS were measured on a regular basis. Analysis of COD, BOD, TKN, Phosphate, TSS and MLVSS were carried out in accordance with the Standard methods for the examination of water and wastewater (2005).

Ozonation of Wastewater. All the decolourisation studies were conducted at the laboratory ambient temperature of about 30±3ºC. The optimum contact time, pH and ozone consumption at the optimum conditions were determined for the treatment of distillery wastewater.

For every experiment, the reactor was filled with the required volume of the wastewater (approx. 350 mL) in the first bubble column reactor. The second and third column contained about 250 mL of 2% solution of aqueous potassium iodide. Ozone thus generated, was bubbled through the aeration port of the first column reactor with the help of air diffuser. The ozone gas was allowed to react with the sample for a specific time interval (5, 10, 15, 20, 25, 30 & 35 minutes).

All the ozonation experiments were conducted inside the fume hood to avoid the ozone toxicity in the laboratory. All the experiments were carried out at the original pH of the effluent sample of 8 – 8.5. Ozonation experiments were carried out at different ozone dosages of 0.2 g/h and 1 g/h. Ozonated effluent sample (10 mL) was from the reactor at regular time intervals was analyzed for pH, COD, colour and UV_{254}.

RESULTS AND DISCUSSION

Biological treatment of ANDSW. The performance of Sequencing batch reactor for the treatment of anaerobically digested distillery wastewater combined with domestic wastewater (1:4 v/v) are presented and discussed in this section. Figure 1 illustrates the removal of BOD and COD in the SBR effluent during this study. The average concentration of COD and BOD in the influent wastewater were approximately 10,000 and 1350 mg/L, respectively.

A significant amount of COD reduction (73%) was observed with 1 day HRT. The effluent COD was approximately 2740 mg/L. This increase in removal efficiency might be due to the presence of sufficient nutrients in the domestic wastewater that aids for the growth of biomass and COD reduction. The high percentage of organic removal could also be attributed to the fact that the ANDSW along with domestic wastewater gives a relatively high biomass yield. Zhang et al (2003) reported that high biomass concentration will provide higher organic removal. The system provides good settleability of sludge which implies that wash out of microorganism does not take place.

The BOD reduction was relatively higher (98%) compared to the COD reduction. The effluent BOD was around 30 – 45 mg/L. The data showed that the initial BOD/COD ratio of the influent wastewater was around 0.135, which decreased to 0.0009 after aerobic treatment with SBR. Therefore SBR treatment system seems to utilize full potential of the microorganisms in the reduction of BOD and COD. The residual organics (2740 mg/L of COD) in the treated effluent might be due to the recalcitrant/non biodegradable organics.

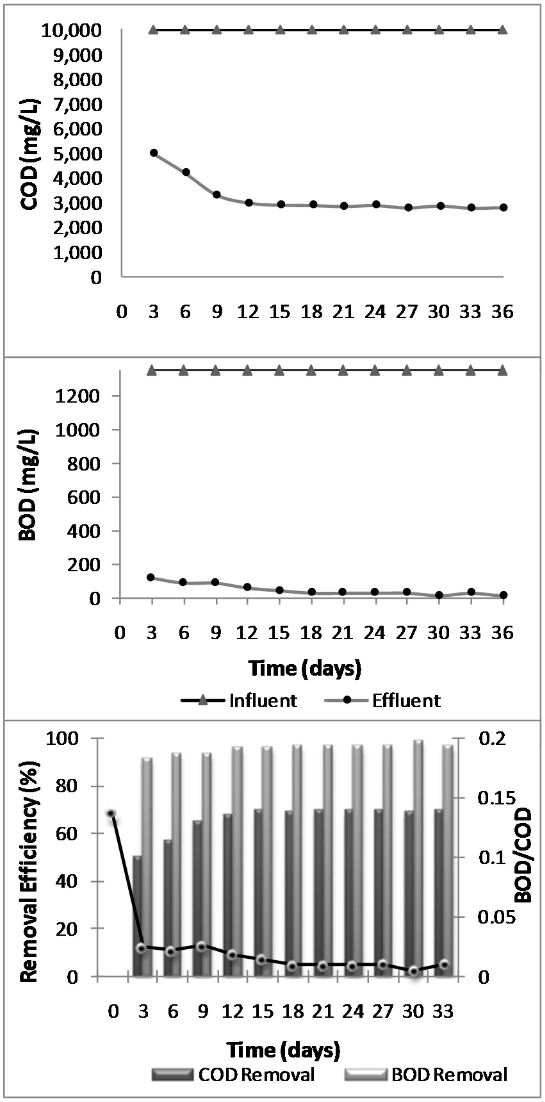

FIGURE 1. Removal of cod and bod of combined wastewater

Pathade et al (2001) were able to achieve 88% COD reduction for an influent COD of 3000 mg/L only at 6 d HRT during the treatment of anaerobically digested distillery wastewater under aerobic conditions using developed mixed microbial seed culture. Wherein the present study attains 73% COD removal with 24 h HRT itself for the higher organic loading rate.

Kanetkar et al (1990) reported 89% reduction of BOD at 6.6 d HRT in the activated sludge treatment of anaerobic lagoon distillery effluent using acclimatized biomass. Whereas the SBR with acclimatized biomass achieved 98% BOD removal in the present study.

Ozonation of SBR treated distillery effluent

Removal of COD. The SBR treated effluent having a COD of 2700 mg/L was subjected to ozonation in the present study. Figure 2 gives the reduction in the COD of the effluent as a result of ozonation of SBR effluent.

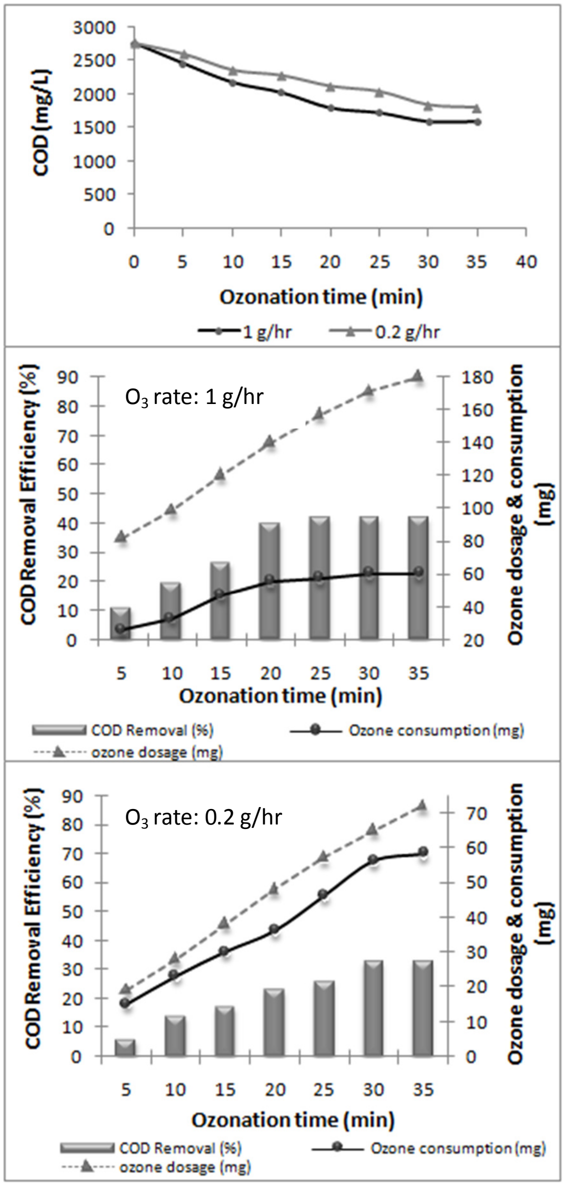

FIGURE 2 Removal of cod of the effluent during ozonation of sbr treated effluent (post ozonation)

A comparison of COD removal between two different ozone application rates of 1g/h and 0.2 g/h, are also shown in figure. The influent COD of 2760 mg/L reduced to a maximum of 1600 mg/L and 1800 mg/L for the ozone application rates of 1 g/h and 0.2 g/h, respectively at the end of 30 minutes of ozonation and no further decrease in the COD was observed after 30 min. The COD values remained constant after 30 min of ozonation. Lesser amount of COD reduction indicates that only molecular level transformations (breaking of complex molecules into simpler lower carbon chain molecules) have taken place during ozonation.

For the highest ozone application rate of 1 g/h, 42% COD removal was achieved in 30 min of ozonation. While for the lowest ozone application rate of 0.2 g/h, a COD removal of 33% was observed with 30 min of ozonation. No significant difference was observed between the two ozone application rates. Therefore, it is not practical to increase the flow rate in the ozonation system. This shows that lower ozone application rate produces significant COD reduction.

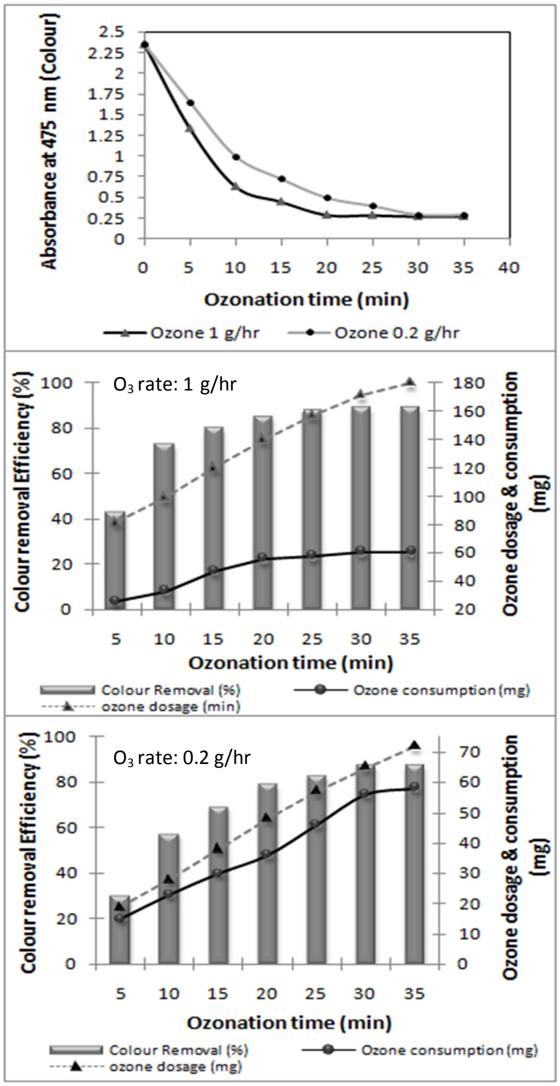

FIGURE 3 Removal of colour of the effluent during ozonation of sbr treated effluent (post ozonation)

Kim et al (1985) also reported that carboxylic acids have been indicated as products of melanoidin ozonation and carboxylic acids hardly react with ozone (Hoigne and Bader, 1983) but they contribute to COD. Jammes et al (1994) also supported this view. Ozonation of SBR effluent led to the reduction in the COD value, in other words, it brought about the mineralization of some of its contents during the aerobic SBR treatment step itself. From the figure it is clear that for a given time, an increase in the ozone dosage applied to the wastewater led to an increase in COD removal. For the highest ozone application rate of 1 g/h, the ozone dosage was around 180 mg for 30 min of ozonation, wherein the ozone reacted with the organics in the wastewater was only 60 mg, i.e. only one-third of the applied ozone was consumed by the wastewater and the remaining unreacted ozone was let out from the reactor without being consumed. Whereas at an ozone application rate of 0.2 g/h, the applied ozone of 60 mg was consumed completely for the reaction and only 4 mg of ozone remained unreacted.

Removal of Colour. Ozonation of SBR effluent results in significant colour removal. The colour removal in wastewater measured as absorbance at 475 nm during ozonation is shown in Figure 3. The colour was effectively reduced from an initial absorbance value of 2.35 to 0.272 and 0.295 for the ozone application rates of 1 g/h and 0.2 g/h for 30 min which amounted to 89% and 87% of colour reduction respectively. There was a significant decrease in colour during the first 20 min due to direct reactions between ozone molecules and colorants and slight decrease during the remaining period of ozonation. After 30 min, the absorbance value remained almost constant.

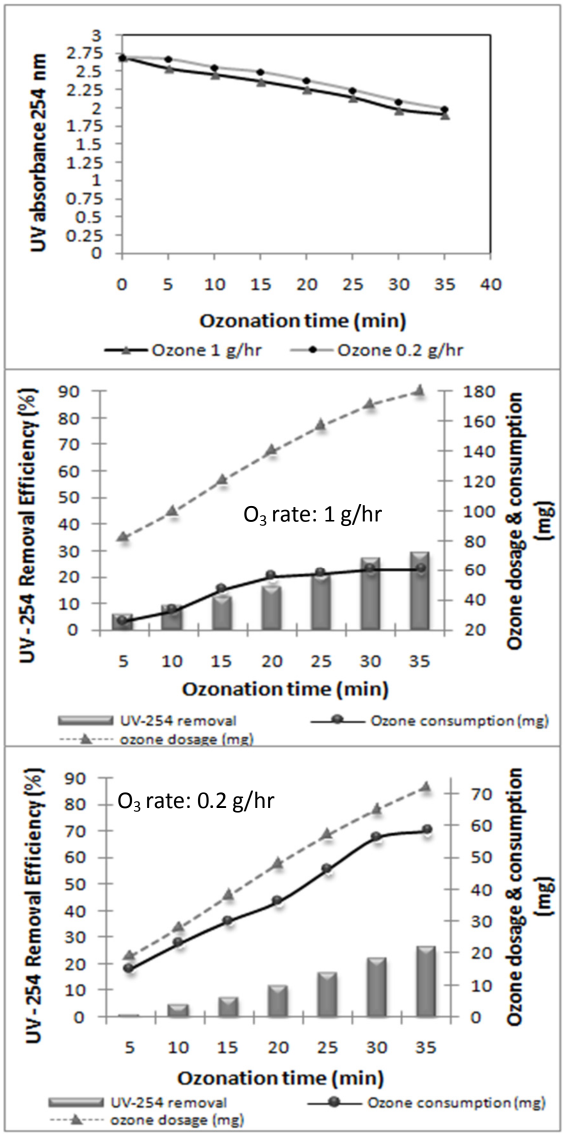

FIGURE 4 Reduction of absorbance (uv$_{254}$) of the Effluent during ozonation of sbr treated effluent (post ozonation)

Though ozonation step led to a significant reduction in colour, higher ozonation time did not enhance the colour removal efficiency and ozone left the reactor without being consumed. Melanoidins have conjugated carbon-carbon double bonds in their structure. The colour removal was probably due to the fact that ozone is able to cleavage these conjugated carbon-carbon double bonds (Kim et al 1985). However in this study, the efficiencies achieved for colour removal were much higher than those for COD removal. It is likely that ozone transforms the visible chromophores groups instead of breaking high molecular weight compounds into lower molecular weight components (Pena et al 2003) and mineralization of compounds does not take place. Therefore, COD reduction was lower compared to the colour removal efficiency.

Coca et al (2007), in their study on molasses wastewater ozonation have reported colour reduction of about 70 -75% in 20 minutes, increasing up to 85 – 87% after 40 min ozonation for an ozone flow rate of 1.7 g/h for ozonation of anerobic/aerobic effluent. Wherein, this study achieved colour reduction of 89% and 87% in 30 minutes for ozone application rate of 0.2 g/h and 1 g/h, respectively. Pena et al (2003) reported that ozone does not oxidizes functional groups responsible for colour but it only transforms chromophore groups, and ozone do not break brown polymers into smaller compounds.

Reduction of UV_{254} Absorbance. The variation in aromatic content during the ozonation of SBR effluent observed at 254 nm is presented in Figure 4. A measure of absorbance at 254 nm indicated that the ozonation of SBR effluent led to decrease in the absorbance value from 2.7 to 1.9 at ozone application rate of 1 g/h and 2.7 to 1.98 for ozone rate of 0.2 g/h showing a removal efficiency of 29 and 26 %, respectively. Ozonation at low pH favours highest removal of unsaturated and aromatic compounds (i.e. polyphenol and other UV_{254} absorbing compounds). Therefore, the UV_{254} absorbance removal was very lower for distillery wastewater ozonated at basic pH. Killops (1986) and Gilbert (1998) reported that ozonation led to quick decolorization and a decreased in UV absorbance of humic substances due to loss of aromaticity. The experimental results clearly reveal that an increase in the ozone application rate from 0.2 g/hr to 1 g/hr showed an insignificant effect on the removal efficiencies.

CONCLUSIONS

According to the results obtained, it may be concluded that the mixed bacterial consortium could reduce the BOD of the combined wastewater in the SBR reactor followed by ozonation as an effective treatment to remove the organics and colour but less effective against recalcitrant organic matter causing colour in wastewater. It is recommended that low ozone dosage (0.2 g/h) and 30 min of reaction time were effective for colour removal and partial oxidation of persistent compounds present in the biologically treated distillery wastewater.

REFERENCES

Akunna, J.C..; Clark, M. Bioresource Technology 2000, 74, 257-261.

American Public Health Association (APHA) (2005) Standard Method for Examination of Water and Wastewater, 21st ed. APHA, AWWA and WEF, Washington, DC 2005.

Beltran, F.J.; Encinar, J.M.; Garcia-Araya, J.F. Wat Res. 1993, 27, 1023.

Beltran, F.J.; Garcia-Araya, J.F.; Alvarez, P.M. Water Research 2001, 35, 929-936.

Central Pollution Control Board (CPCB), Environmental management in selected industrial sectors Status and Needs, In PROBES/97/2002-03, CPCB, Ministry of Environment and Forest, New Delhi, 2003.

Chandra, R.; Pandey, P.K. Indian Journal of Environmental Protection 2000, 21, 134–137.

Coca, M.; Pena, M.; Gonzalez, G. J. of Haz. Mat 2007, 149, 364 – 370.

Dikshit, A.K.; Chakraborty, D. Clean Techn Environ Policy 2006, 8, 273-285.

Dosta, J.; Rovira, J.; Gali, S.; Mace, S.; Mata-Alvarez, J. Bioresource Technology, 99, 5722-5730.

Ghosh, M.; Ganguli, A.; Tripathi, A.K. Process Biochemistry 2002, 7, 857-862.

Gilbert, E. Water Research 1998, 22, 123 – 126.

Hoigne, J.; Bader, Water Research 1983, 17, 173 – 194

Jammes, C.; Hochereau, C.; Bruchet, A. Occurrence and behaviour of some disinfection by-products during ozonation step; In: Proceedings of the first international research symposium on water treatement by-products, Poitiers, France, 29 30, September 1994, Vol.1, 10.0 – 10.17.

Kalavathi, D.F.; Uma, L.; Subramanian, G. Enzyme and Microbial Technology 2001, 29, 246-251.

Kanekar, S.N. Studies on Secondary Aerobic Treatment of Distillery Waste, PhD Thesis 1990, Shivaji University, Kolhapur, India.

Killops, S.D. Wat. Res. 1986, 20, 153 – 165.

Kumar, P.; Chandra, R. Biores. Technol. 2006, 97, 2096–2102.

Migo, V.P.; Matsumura, M.; Rosario, E.J.D.; Kataoka, H. Journal of Fermentation Bioengineering 1993, Vol. 75, pp.438–442.

Pathade, G.R. Indian J. Environ. Prot. 2001, 21, 114–121.

Satyawali, Y.; Balakrishnan, M.; Bioresource Technology 2007, 98, 2629-2635.

Sirianuntapiboon, S.; Prasertsong, K.; Bioresource Technology 2008, 99, 1806-1815.

Tewari, P.K.; Batra, V.S.; Balakrishnan, M. Resources Conservation Recycling 2007, 52, 351-367.

Torrijos, M.; Moletta, R. Water Science and Technology 1997, 35, 249 -257.

Xiangwen, S.; Dangcong, P.; Zhaohua, T.; Xinghua, J. Bioresource Technology 2008, 99, 3182-3186.

Zhang, S.Y.; Van Houten, R.; Eikelboom, D.H.; Doddema, H.; Jiang, Z.C.; Fan, Y.; Wang, J.S. Biores. Technol 2003, 90, 185-192.

ELECTRO-REGENERATION OF Ce(IV) IN REAL SPENT Cr-ETCHING SOLUTIONS: COMPARISON OF SEPARATORS

Kuo-Lin Huang, Te-San Chen, Shui-Jen Chen, and Yi-Min Ding
(National Pingtung University of Science and Technology, Pingtung, Taiwan)

ABSTRACT: Different separators (membranes) were investigated for the electro-regeneration of Ce(IV) from Ce(III) in real spent Cr-etching solutions. The experiments were performed at 2 A and 40°C in a divided cell using real spent Cr-etching solutions as the anolyte and 4 M HNO_3 as the catholyte. The anode and cathode materials were platinum (2.25 cm^2) and titanium (1 cm^2), respectively. Among the tested separators (Neosepta CMX, Neosepta AMX, Nafion 117, and Nafion 212), the CMX membrane had the best performance in terms of Ce(IV) yield and current efficiency for the electro-regeneration of Ce(IV); the greatest apparent rate constant for Ce(IV) electro-regeneration was 9.4×10^{-5} s^{-1} when using the CMX membrane. The Ce(IV) yield and current efficiency were more influenced by separator thickness than by separator selectivity to anions/cations.

INTRODUCTION

Recently, liquid crystal displays (LCDs) have been widely used in notebook computers, desktop computer monitors, and televisions. The thin film transistor (TFT)-LCD industry has developed rapidly, but the manufacture of such panels requires many complex procedures and suffers from enormous waste production. For example, in TFT-LCD upstream material manufacturing, the black matrix (mainly made of complex Cr/CrO materials) is usually etched using cerium ammonium nitrate $[Ce(NH_4)_2(NO_3)_6]$ (CAN) dissolved in HNO_3. After use, the spent Cr-etching solutions are regarded as hazardous wastes. Spent Cr-etching solutions are commonly treated with chemical coagulation followed by precipitation, which produces considerable amounts of hazardous sludge with over-limit leaching of total-Cr (Cr(III) + Cr(VI)) in the Toxicity Characteristic Leaching Procedure (TCLP). To alleviate this situation, it is attractive to recover spent Cr-etching solutions. One option is to regenerate Ce(IV) from Ce(III) by electro-oxidation in spent Cr-etching solutions, and the regenerated solutions can be used for recycling purposes.

The electro-oxidation of Ce(III) may be conducted in a divided cell equiped a separator to divide anolyte and catholyte (Been and Oloman, 1993). For the electro-regeneration of spent Cr-etching solutions, the divided cell needs a separator which is resistant to strong acidic conditions (pH < 1). In our earlier study, an anion-exchange separator (AMI-7001) was found to be better than a cation-exchange one (CMI-7000) for use in the Ce(IV) electro-regeneration in simulated spent Cr-etching solutions (Huang and Chen, 2009). In this study, four different separators (Neosepta CMX, Neosepta AMX, Nafion 117, and Nafion 212) were tested and compared for the Ce(IV) regeneration in terms of Ce(IV) yield and current efficiency.

MATERIALS AND METHODS

Real Cr-etching solutions used in experiments were obtained from a waste treatment plant in southern Taiwan. Three cation-exchange (Neosepta CMX, Nafion-117, and Nafion-212) and one anion-exchange (Neosepta AMX) membranes were used as the separator in a divided cell for test. Prior to use, the membranes were heated at 65°C in 1 M (~3%) H_2O_2 for 1 h to remove organic impurities, rinsed at 65°C in deionized water for 1 h, and then heated at 65°C in 1 M $NaNO_3$ or HNO_3 solution for 1.5 h, to convert into NO_3^- or H^+ type, respectively. Finally, the membranes were washed three times with deionized water (Millipore Milli-Q), and then stored in deionized water. All the electrolytic experiments

ISBN 9780976885351

were performed under constant current electrolysis using a DC power supply (Good Will Instrument CO., LTD GPS-2303). A redox potential titrator (Metrohm 702 SM Titrino) equipped with the solution of ferrous ammonium sulfate (in 1 M nitric acid) was used to quantitatively determine the Ce(IV) concentrations of samples.

The theoretical amount of Ce(IV) production (m_t) at electrolysis time t can be calculated as follows.

$$m_t = MIt/zF \tag{1}$$

where M: molecular weight of Ce, I: current, z: electrons transferred per Ce(III) ion ($z = 1$ in Ce(III) → Ce(IV) + e^-), and F: the Faraday's constant. The current efficiency is calculated based on the following equation

$$\text{current efficiency (CE)} = (m_e/m_t)\times 100\% \tag{2}$$

where m_e is the Ce (IV) amount obtained experimentally. The Ce(IV) percent yield is calculated using

$$\text{yield (\%)} = (C_e(IV)_A/C_e(IV)_T)\times 100\% \tag{3}$$

where $Ce(IV)_A$ is the actual amount of Ce(IV) generated in electrolysis for a period of time and $Ce(IV)_T$ is the theoretical amount of Ce(IV) that can be generated. In this study, $Ce(IV)_T$ = electrolyte volume × ($[Ce(III)]_{initial} + [Ce(IV)]_{initial}$) = electrolyte volume × ($[Ce(III)]_{initial}$) because the $[Ce(IV)]_{initial} = 0$.

RESULTS AND DISCUSSION

When the Neosepta AMX was used as the separator in the divided cell, operated at 2 A/2.25 cm^2, the Ce(IV) yield increased but the current efficiency (CE) of Ce(III) oxidation decreased with increasing electrolysis time (Fig. 1).

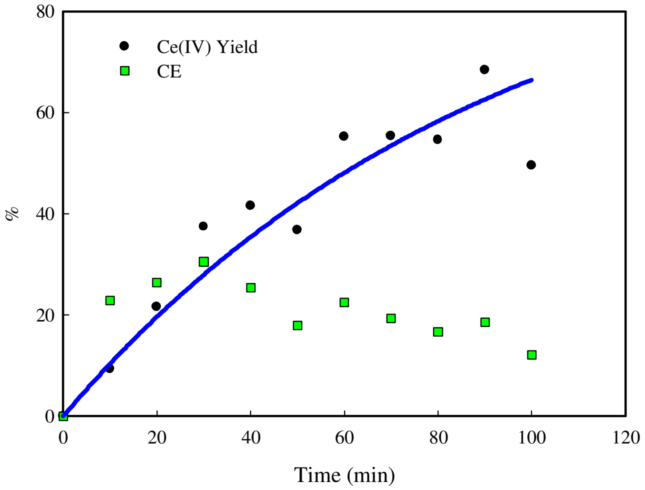

FIGURE 1. Variation of Ce(IV) yield and current efficiency (CE) when using a AMX membrane as the cell separator (line: fitted curve).

Regardless of the difference in membrane, a similar trend was also observed when the cell separator was replaced with Neosepta CMX, Nafion 117, or Nafion 212 (Figs. 2–4). For simplification, the modeling of Ce(IV) yield (Y) in the divided cell with membranes is equivalent to that of fractional conversion ($X_A = 1 - \exp(-kt)$) (k: apparent rate constant) in a simple batch reactor. By this approximation, the k values can be obtained using Y (%) = aX_A in data fitting. The fitted apparent rate constants (k) for Neosepta AMX, Neosepta CMX, Nafion-117, and Nafion-212 were 8.1×10^{-5}, 9.4×10^{-5}, 9.0×10^{-5}, and 6.5×10^{-5} s^{-1}, respectively. Accordingly, the Ce(IV) yields in the cell using different separators were in order CMX > Nafion-117 > AMX > Nafion-212. Of all the tested separators, only the AMX is anion-exchange membrane, while the others are cation-exchange membranes. Interestingly, the effect of positive or negative charge of Ce(III)/Ce(IV) species on Ce(IV) yield was noticeably lower that of separator thickness (CMX ≈ AMX > Nafion-117 > Nafion-212). The Ce(III)/Ce(IV) species in real Cr-etching solutions have not been explored yet, and further study is necessary.

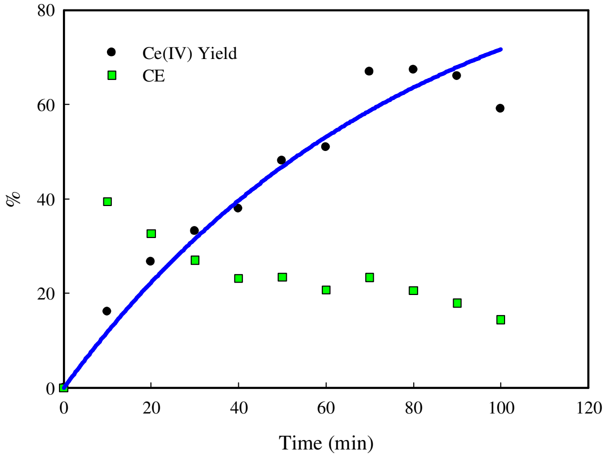

FIGURE 2. Variation of Ce(IV) yield and current efficiency (CE) when using a CMX membrane as the cell separator (line: fitted curve).

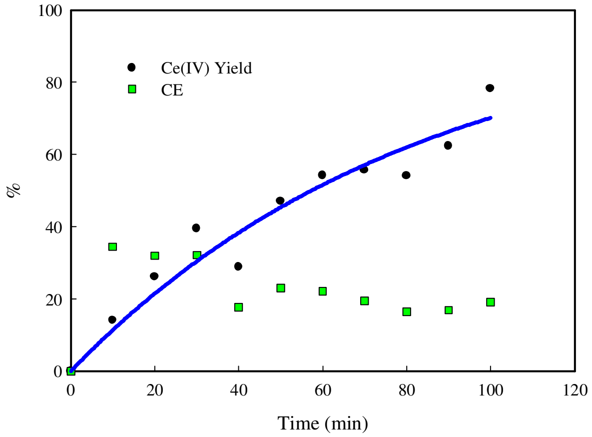

FIGURE 3. Variation of Ce(IV) yield and current efficiency (CE) when using a Nafion-117 membrane as the cell separator (line: fitted curve).

The apparent mass transfer coefficients (k_L) can be calculated by $k_L = k(V/Ae)$ where V and Ae are volume of electrolyte and projected geometric area of electrode, respectively. Accordingly, the corresponding k_L for Neosepta AMX, Neosepta CMX, Nafion-117, and Nafion-212 were 3.6×10^{-3}, 4.2×10^{-3}, 4.0×10^{-3}, and 2.9×10^{-3} cm s^{-1}, respectively. Among the tested separators, the CMX membrane had the best performance in terms of Ce(IV) yield, CE, k and k_L for the electro-regeneration of Ce(IV), so the CMX was better than the other tested membranes to be used as the separator in the divided cell for electro-regeneration of Ce(IV) in real spent Cr-etching solutions.

CONCLUSIONS

Among the tested separators, the CMX membrane had the best performance in terms of Ce(IV) yield, CE, k and k_L for the electro-regeneration of Ce(IV), so the CMX was better than the other tested membranes to be used as the separator in the divided cell for electro-regeneration of Ce(IV) in real spent Cr-etching solutions. The Ce(IV) yield was influenced more by separator thickness than by positively/negatively charged Ce(III)/Ce(IV) species.

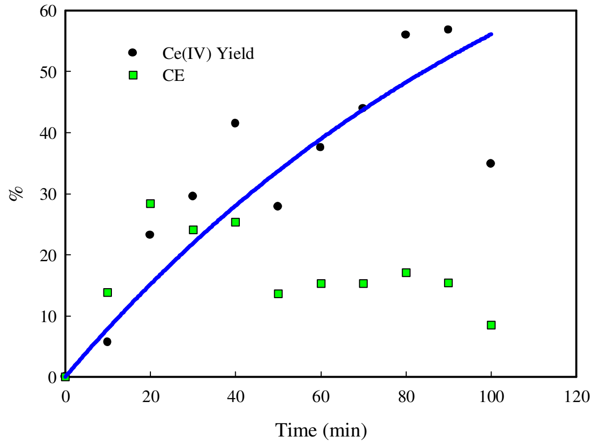

FIGURE 4. Variation of Ce(IV) yield and current efficiency (CE) when using a Nafion-212 membrane as the cell separator (line: fitted curve).

ACKNOWLEDGEMENTS

This research is financially supported by Taiwan National Science Council (NSC), under Contract No. NSC–100–2221–E–020–007–MY2.)

REFERENCES

Been, J. and C. W. Oloman, 1993. “Electrochemical regeneration of ceric sulphate in an undivided cell”. *Journal of Applied Electrochem*istry, 23: 1301–1309.

Huang, K.-L. and T.-S. Chen, 2009. “Electro-regeneration of Ce(IV) in simulated spent Cr-etching solutions containing abundant Ce(III)”. *Journal of The Electrochemical Society*, 156(12): E192–E198.

$Fe\text{-}Mn_2O_3$ COMPOSITE: PREPARATION, IDENTIFICATION AND CHARACTERISTICS IN FENTON-LIKE REACTION

Si-Hyun Do*, Su-Jin Bang and Yong-Jae Kwon
(Hanyang University, Seoul, Republic of Korea)

Iron oxide has been known as a catalyst in Fenton-like reaction and the reaction preferably produces hydroxyl radical in acidic condition. Recently, it was revealed that the reaction of hydrogen peroxide and manganese oxide produced superoxide anion and it could degrade the reduction-favored organic contaminants above neutral condition. Therefore, the reaction of H_2O_2 and Fe-Mn composites possibly provides the specific reactive species (i.e. hydroxyl radical or superoxide anion), depending on the pH of solution. This study consists of two milestones, which are a synthesis of Fe-Mn composite and an application of Fe-Mn composite as catalyst to treat organic contaminants.

First of all, manganese oxides (i.e. MnO_2, Mn_2O_3 and MnO) were mixed with $FeSO_4$. After that, Fe-Mn composites were synthesized by the addition of either NaOH or $Ca(OH)_2$. The surface area was generally increased by the modification. Based on the results of SEM, TEM, XPS and XRD analysis, iron oxides were identified and the types of synthesized iron oxides depended on the types of manganese oxide and hydroxide sources (NaOH or $Ca(OH)_2$). In addition, the decomposition of H_2O_2 on Fe-Mn composites including pure manganese oxides revealed that the decomposition rates on composites were less than that on pure oxides. This possibly indicated that the decomposition pathway with Fe-Mn composites was different from that with pure manganese oxides. In general, decomposition rates for Mn_2O_3 and MnO_2 were higher than that for MnO. Fe-Mn composite synthesized using Mn_2O_3 and NaOH had the highest H_2O_2 decomposition rates. Degradation of carbon tetrachloride and benzene as the representative compounds (i.e. easily reduced or oxidized) will be investigated and discussed.

ISBN 9780976885351

SIMULTANEOUS REMOVAL OF A_S (III) AND A_S (V) BY ADVANCED OXIDATION

Sil-hee Hong*, Young-hoon Jo and Sung-ho Kong
(Hanyang University, Seoul, Republic of Korea)

Recently, many researches have worked on removing non-biodegradable materials using Fenton reaction with UV radiation system. By using this system, it generates more ·OH radicals and it is more effective than using a single Fenton reaction or UV system. In this study it was investigated the removal of total arsenic, As(III) and As(V), simultaneously by Fenton reaction under UV radiation. Conventionally, two step processes, oxidation of As(III) in one reactor and adsorption of As(V) in another reactor, were applied; however, in this study Fenton reaction with UV system was applied in one-step single reactor to process oxidation of As(III) and adsorption of As(V).

The concentrations of As(III) and As(V) were measured by atomic absorption spectrophotometer (AAS) and Molybdenum method, respectively. Experiments were performed for oxidation of As(III) when the ratio of As(III) and H_2O_2 was 1:3 at pH 7; reaction systems for experiments are as followed: 1) only with H_2O_2, 2) only with UV system, 3) with combination of H_2O_2 and UV system. Oxidation efficiencies for each system were 23, 15 and 90%, respectively. Removal efficiency of As(V) in H_2O_2/UV system with the addition of irons was also investigated. The types of iron tested were Fe(II), Fe(III) and Fe(II)/Fe(III) (ration of Fe(II):Fe(III): 1:2). When the ratio of H_2O_2 and iron was 1:4, removal efficiencies of total arsenic were 39, 98 and 100%, respectively. Among them, Fe(III) showed the highest removal efficiency and removal efficiency of As(V) was increased as the doses of iron increased. Overall, when the ratio of H_2O_2 and Fe(III) was 1:4, total arsenic, As(III) and As(V), was completely removed within 30 min of reaction time.

ISBN 9780976885351

COLOR AND COD REDUCTION OF SYNTHETIC REACTIVE DYE WASTEWATER USING THERMOLYSIS

Ruchika Agnihotri and ***Pradeep Kumar***
(Institute of Technology, Banaras Hindu University, Varanasi, India)

Treatment of synthetic wastewater containing Reactive Pink MB dye (Reactive Red 74) using catalytic thermal treatment (Thermolysis) has been reported in this work. Local carpet dying industries, situated near Varanasi, India are the major source of pollution of Reactive Red 74 dye. Catalytic thermal treatment has been mostly used to wreck the bonding in the dye molecules. Homogenous $CuSO_4$ has been reported to possess good catalytic activity for this reaction. Reaction was carried out using a 100 mg/L dye concentration with colour concentration 494 PCU. The concentration of dye coming out of dye bath is 1300 PCU, which is much higher than maximum permissible limit set by Pollution Control Board of India.

Catalytic thermal reaction experiments were conducted at various reaction parameters, such as, pH, temperature, time and catalyst dose. A removal of about 95% chemical oxygen demand (COD) and 67.6% colour of synthetic wastewater were achieved using a catalyst concentration of 4 g/L at 60˚C, 90 min duration and at pH 11. The initial pH value of the wastewater showed pronounced effect on the precipitation process and so on the COD and colour reductions. During the thermolysis, copper gets leached into the aqueous phase. The solution was filtered and the precipitates were characterized.

ISBN 9780976885351

ELECTROCHEMISTRY AND AQUEOUS CHEMISTRY OF ZERO-VALENT TITANIUM FOR REMOVAL OF PERCHLORATE IN WATER

Dong Suk Han* and Ahmed Abdel-Wahab (Texas A&M University at Qatar, Doha, Qatar)
Chunwoo Lee (Doosan Hydro Technology, Tampa, FL, USA)
Sung Hyuk Park (GS Engineering & Construction Research Institute, Youngin-si, Korea)
Bill Batchelor (Texas A&M University, College Station, TX, USA)

Perchlorate has entered human and environmental food chains and has received a great deal of attention because of its toxicity to humans. In this study, two approaches have been investigated for chemical degradation of perchlorate using zero-valent titanium (ZVT). The first one was to use electrochemically developed pitting corrosion of ZVT anode and the other one was to use partially oxidized aqueous titanium ions (Ti(II) and Ti(III)) under acidic condition. Results of laboratory experiments showed that perchlorate reduction was believed to be caused by an active reductant (dissolved Ti(II)) during the pitting corrosion of ZVT. The rate of perchlorate reduction was independent of the imposed potential as long as the potential was maintained above the pitting potential of ZVT, but it was proportional to the applied current. For application of aqueous titanium ions that were produced by strong acidic conditions (mixture of HF and HCl or H_2SO_4), titanium ions were able to degrade perchlorate ions very rapidly with half-life less than one hour. A new reactor system using ion exchange membrane was adapted which promotes the reactions of perchlorate destruction and suitable for applications in water treatment systems. Consequently, this study can be a starting point for development of a new treatment process that applies titanium or titanium metal ions to abate contaminants present in natural and engineered systems by chemical reduction.

ISBN 9780976885351

ADVANCED REDUCTION PROCESS FOR DEGRADATION OF CHLORINATED ALIPHATIC COMPOUNDS USING SULFUR COMPOUNDS AND UV LIGHT

Sun Hee Yoon, Dong Suk Han, and Ahmed Abdel-Wahab (Texas A&M University at Qatar, Doha, Qatar)
Bill Batchelor (Texas A&M University, College Station, TX, USA)

Chlorinated aliphatic compounds such as 1,2-dichloroethane (1,2-DCA) and vinyl chloride (VC) have been of great environmental concern because of their adverse effects on human health and the environment. These compounds are persistent oxidized compounds and therefore, available treatment processes are neither efficient nor cost-effective in destroying them. This study proposed a new treatment approach called advanced reduction processes (ARPs) in which a reducing agent (RA) is combined with activating methods. This combination can generate reactive electron-rich anion radicals to break C-Cl bond under UV irradiation. To investigate the feasibility of ARPs for 1,2-DCA and VC, a variety of reducing agents such as dithionite, sulfite and sulfide combined with UV light were examined and the effects of irradiation time, pH, and doses of reducing agent were evaluated. Experimental results showed that the use of reducing agent alone or activating method alone was limited by showing a rate-limiting step. However, combination of reducing agent and UV light achieved more than 99 % of degradation efficiency and showed fast kinetic behavior of both contaminants. The extent of degradation of 1,2-DCA and VC was found to be dependent on solution pH. This study provides fundamental information for the development of ARP as potential treatment process for destroying electron-deficient contaminants (chlorinated chemicals, perchlorate, bromate, arsenate or chromate) in natural or engineered system.

ISBN 9780976885351

EFFECT OF HEAVY METALS Cd^{2+} AND Cu^{2+} ON K^+ TRANSPORT THROUGH NSCCs*

Feng Ke, ***Shan Yuhua***, Wang Xiaoli and Wang Yuqian (College of Environmental Science and Engineering, Yangzhou University, Yangzhou, China)

Higher K^+/Na^+ ratio in cells is of key importance in growth maintenance of plants under salt stress. Recent studies have demonstrated that non-selective cation channels (NSCCs), in addition to some specific carriers and pathways on the membrane, play an important role in the uptake of many cations including K^+ and Na^+. NSCCs are dually conductive and can regulate K^+ and Na^+ concentration in plant cells by controlling their influx and efflux across the membrane. However, reports pertaining to the response of NSCCs to heavy metal stress and its impacts on K^+ and Na^+ transmembrane transport and on plant tolerance to salt stress have been so far in scarce. With a salt-tolerant wheat cultivar 'Shijiazhuang 8' as material, the effect of heavy metal (Cu^{2+} and Cd^{2+}) stress on transmembrane transport of K^+ and Na^+ through NSCCs was investigated in this study. Results showed that K^+ uptake through both specific pathways and NSCCs was affected by Cd^{2+} stress. The contribution rate of K^+ transport through NSCCs to total K^+ uptake increased with the elevation of Cd^{2+} concentration in the media, which indicated that K^+ uptake through NSCCs was less sensitive to Cd stress, compared with that through specific pathways. The influx of K^+ through NSCCs was not apparently affect by low Cu^{2+} concentration, but this process could be inhibited by high Cu^{2+} level. In contrast to Cd^{2+}, higher Cu^{2+} concentration reduced the contribution rate of K^+ transport through NSCCs to total K^+ uptake. To the process of K^+ transport, NSCCs was more sensitive to Cu^{2+} stress than the specific pathways.

*The study was sponsored by Natural Science Foundation of China (NSFC, No. 30171845)

ISBN 9780976885351

SULFATE RADICALS-BASED ADVANCED OXIDATION TECHNOLOGIES FOR THE DECOMPOSITION OF TRICLOSAN

Prince Nfodzo and Hyeok Choi (The University of Texas at Arlington, Arlington, TX, USA)

ABSTRACT: The presence of triclosan (TCS, 5-chloro-2-(2, 4-dichlorophenoxy)phenol) in water resources, as an important and widely used antimicrobial agent, has drawn significant concerns from water authorities and industries because of its endocrine disruption potential. Sulfate radicals (SRs) generated via the transition metal-mediated activation of peroxymonosulfate (PMS) and persulfate have been proposed to be effective to decompose TCS and many other recalcitrant contaminants. In spite of its significance as a key to understanding the efficiency of SR generation and catalytic/non-catalytic nature of the oxidation reaction, metal speciation has not been properly highlighted in previous studies probably due to associated analytical challenges. We have conducted experiments using SRs generated by the activation of PMS with Co to elucidate the effects of pH-dependent speciation of Co on TCS decomposition. Results showed that a rapid oxidation of Co^{2+} to Co^{3+} generally corresponds with pseudo-steady state decomposition of TCS after its initial fast decomposition. The presence of a potential threshold concentration of Co^{2+} to effectively activate PMS was found. A strong catalytic activity was observed at pH 3, where most of Co was present in form of dissolved Co^{2+}.

INTRODUCTION

Recent advances in environmental health and analytical chemistry make it possible to detect and identify many toxic organic compounds in the environment at trace levels (Daughton and Ternes, 1999). Among these compounds, pharmaceuticals and personal care products (PPCPs) are the most significant (Ankley, et al., 2007). Many PPCPs have been classified as emerging chemicals of concern (ECCs) and endocrine disrupting compounds. Meanwhile, some industries continue to emphasize the benefits of such PPCPs in their products. In particular, triclosan (TCS, 5-chloro-2-(2,4-dichlorophenoxy)phenol), an antimicrobial agent widely used in PPCPs, has attracted significant concern because of the toxicity and prevalence of its derivatives (Rule, et al., 2005). The US Environmental Protection Agency (EPA) is particularly worried about the potential for antibiotic resistance and endocrine disruption resulting from human exposure to TCS because of recent findings about the estrogenic effects of TCS in rats (Zorrilla et al., 2009). The EPA is thus re-examining the health risks of TCS (Erickson, 2010). Like several other recalcitrant organic contaminants, TCS is not effectively degraded during conventional water and wastewater treatment processes. TCS is reported to be capable of destroying some microorganisms that are beneficial to biological wastewater treatment processes (Krishnakumar et al., 2011). In response to the growing concerns about the presence of potentially toxic PPCPs and other ECCs in water resources, advanced oxidation processes (AOPs) have been widely studied and proposed to be effective for the complete degradation of such contaminants. AOPs involve the generation of transitional reactive free radicals, particularly hydroxyl radicals (HRs, $^{\bullet}OH$) and sulfate radicals (SRs, $SO_4^{\bullet -}$), which are stronger oxidizing species than conventional oxidants (Anipsitakis and Dionysiou, 2004; Son et al., 2007). However, most of the researches have focused on HRs-based processes. More recently, there has also been a growing interest in the application of SRs-based processes for the degradation of organic contaminants in water. SRs are typically generated by the metal-mediated activation of common oxidants such as peroxymonosulfate (HSO_5^-, PMS) and persulfate ($S_2O_8^{2-}$, PS), as shown in Equations (1) and (2) (Anipsitakis and Dionysiou, 2003).

$$HSO_5^- + Me^{2+} \rightarrow Me^{3+} + SO_4^{\bullet -} + OH^- \tag{1}$$

ISBN 9780976885351

$$S_2O_8^{2-} + Me^{2+} \rightarrow Me^{3+} + SO_4^{\bullet -} + SO_4^{2-} \quad (2)$$

The presence of low oxidation state ions, such as Fe^{2+} and Co^{2+}, is important for the activation of oxidants. Consequently, the ability of the system to maintain adequate amount of useful metal species (i.e., dissolved Fe^{2+} and Co^{2+}) determines the efficiency of SRs generation and the catalytic/non-catalytic nature of the overall reaction. In spite of the importance of metal speciation, there have been few studies on determining the speciation of metals over time in order to correlate the metal speciation with organic decomposition. Measuring metal species in real time, however, poses an analytical challenge since changes in metal species occur rapidly over time, especially under oxygenated environments (Safarzadeh-Amiri et al., 1996). The speciation changes are also influenced by pH conditions. (Anipsitakis and Dionysiou, 2004; Safarzadeh-Amiri et al., 1996).

Our research has explored the degradation of TCS using SRs in our effort to propose SRs-based AOPs as an alternative to the most common and established HRs-based AOPs for the degradation of ECCs (Nfodzo and Choi, 2011a; 2011b). As part of the research activities, the objective of this present study is to elucidate the effects of pH-dependent metal speciation on the decomposition of TCS. This study will provide the basis for a more detailed analysis to identify the unique reaction mechanisms and pathways for TCS degradation by SRs-based AOPs.

MATERIALS AND METHODS

Chemicals. Triclosan (TCS) was in a salt form as irgasan. Potassium peroxymonosulfate ($KHSO_5$) for PMS derived from the triple salt oxone was used as oxidant. $CoSO_4$ salt was used as the source of Co^{2+} ions. These analytical chemicals, and HPLC grade acetonitrile and methanol were obtained from Sigma-Aldrich and used as received. The chemicals for ion chromatography analysis, including Metpac PDCA eluent, MetPac PAR post column eluent, and 4-(2-pyridylazo) resorchol monosodium salt, were obtained from Dionex. Phosphate buffers for pH adjustment were prepared from the salts of sodium phosphate monobasic monohydrate ($H_2NaPO_4 \cdot H_2O$) and sodium phosphate dibasic heptahydrate ($HNa_2PO_4 \cdot 7H_2O$) obtained from Sigma-Aldrich. All solutions were prepared in high-purity water except for the standard solution of Co, which was prepared in 2 % ultra-pure nitric acid.

Generation of Sulfate Radicals. SRs were generated by the activation of PMS with Co. The experiments were conducted in batch reactors at ambient temperature. Specific aliquot of TCS was transferred into a glass reactor and appropriate volumes of PMS and Co stock solutions were added to achieve a 100 mL reaction solution at a TCS:PMS:Co molar ratio of 1:2:2. The solution was continuously agitated using a magnetic stirring bar. Our preliminary experiments confirmed the immediate and natural transformation of molecular TCS to its ionic form at pH higher than 8.1 (pK_a of TCS), and thus this study to investigate the effect of pH was conducted exclusively at pH 3, 5 and 7. The pH was maintained with the phosphate buffers.

Analysis of Samples. Samples were drawn at 15 minutes intervals for 2 hrs, immediately mixed with methanol (a well-known quenching agent for SRs), and filtered through 0.45 µm membranes. TCS concentration was monitored with a reversed-phase high performance liquid chromatography (1200 series, Agilent) equipped with a quaternary pump, C18 column, and ultraviolet (UV) detector. A mixture of water and acetonitrile was used as the mobile phase at water:acetonitrile ratio of 25:75% v/v with a flow rate of 1 ml/min. The UV detector was operated at a wavelength of 280 nm for TCS detection, which was pre-determined using a UV-visible spectrophotometer (UV 2550, Shimadzu). The concentrations of the various metal species were monitored over time in order to make distinctions between solid metals and dissolved metals and to identify the oxidation states of dissolved metals. Total metal concentration added to the initial reaction solution and dissolved metal concentrations in filtered samples were measured eventually to determine solid metal concentration. In filtered samples, specific ionic species (Co^{2+}) was instantaneously measured and compared to total dissolved metal concentration to determine the concentration of other ionic species (Co^{3+}). Measurements of the ionic species were performed with ion chromatograph (IC, Dionex LC 20), comprised of UV-visible multiple wavelength detector (AD 25), gradient pump (GP 50), IonPac analytical column (CS5A, Dionex), IonPac guard column (CG5A, Dionex), automated sampler (AS 40), and a postcolumn pneumatic controller. MetPac PDCA eluent was used as the mobile phase at a flow rate of 1.0 mL/min, and MetPac PAR was used as post-column reagent at a flow rate of 0.5 mL/min. The total metal and total dissolved metal concentrations were determined with a quadrupole inductively coupled plasma–mass spectrometry (ICP–MS) system (PerkinElmer/SCIEX, Sheldon, CT) after the samples were acid-digested.

RESULTS AND DISCUSSION

The efficiency of SRs generated from the Co-assisted activation of PMS to degrade TCS was correlated with changes in the speciation of Co under different pH regimes. Among many transition metal activators, Co was selected because it is known to be the best activator of PMS (Anipsitakis and Dionysiou, 2004; Nfodzo and Choi, 2011b). It has been reported that at pH values above 8.1 (pKa of TCS), TCS exists primarily in its ionic form (Lindstrom et al., 2002), which was confirmed in our preliminary studies. The effects of pH on the speciation of Co conjugated with PMS, and consequent effect on TCS degradation were therefore examined exclusively at pH 3, 5 and 7. The decomposition of TCS in the aqueous solution was significantly affected by pH, as shown in Figure 1. The results show that pH 5 was most effective, which is in agreement with other studies that suggested that pH 5 was optimal for organic decomposition by Co/PMS system (Anipsitakis and Dionysiou, 2003; Huang et al., 2009).

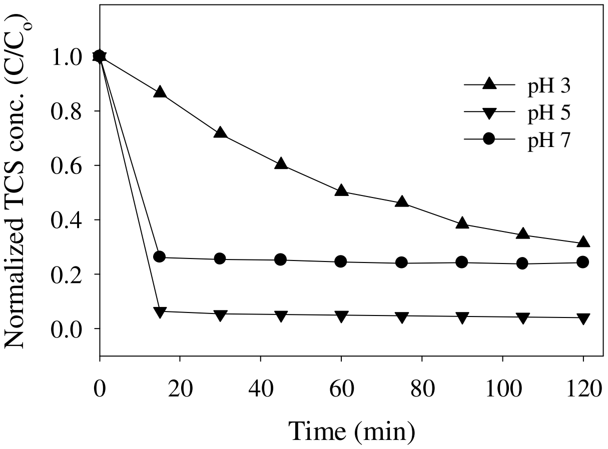

FIGURE 1. Effect of pH on TCS decomposition over time using PMS/Co. $[TCS]_o$=9 mg/L, $[Co^{2+}]_o$=3.66 mg/L, and [PMS]=19.14 mg/L.

In order to elucidate the catalytic/non-catalytic behavior of the oxidation reaction, Co species were monitored over time, as shown in Figures 2 and 3. Considering that the heterogeneous activation of oxidants by solid state metals is not as effective as the homogeneous activation by dissolved metal ions, determining fractional changes of the solid state and ionic state metals was of particular interest. Though small amounts of Co precipitate were observed at pH of 7 and 5, a high level of dissolved Co species was constantly maintained at all pH values, as shown in Figure 2.

Some of the dissolved Co species, however, may not be effective to activate PMS. Figure 3 shows the fractionalization of the dissolved Co species. At pH 3, most of dissolved Co was present as Co^{2+} which is important for inducing the catalytic behavior of the overall reaction in order to continuously generate SRs and thus decompose TCS. The constant high concentration of Co^{2+} can explain the continuous decomposition of TCS observed in Figure 1. On the other hand, a rapid oxidation of Co^{2+} to

Co^{3+} was observed at pH 5 and 7. Though a certain level of Co^{2+} was continuously available in solution, TCS decomposition seemed to have stopped, resulting in the initial fast then pseudo-steady state decomposition of TCS (Figure 1). Similar results showing an initial sharp drop followed by no further reaction were reported in literature (Anipsitakis and Dionysiou, 2003; 2004). One notable explanation for this behavior is the presence of a potential threshold concentration of Co^{2+} minimally required to activate PMS.

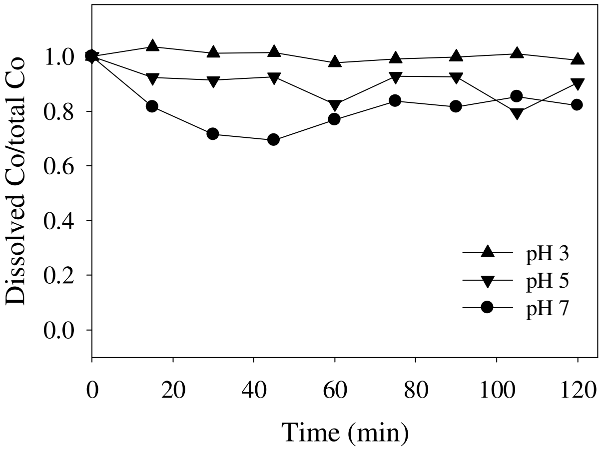

FIGURE 2. Effect of pH on speciation of Co (fraction of dissolved Co/total Co) in Co/PMS system for TCS decomposition. $[TCS]_o$=9 mg/L, $[Co^{2+}]_o$=3.66 mg/L, and [PMS]=19.14 mg/L.

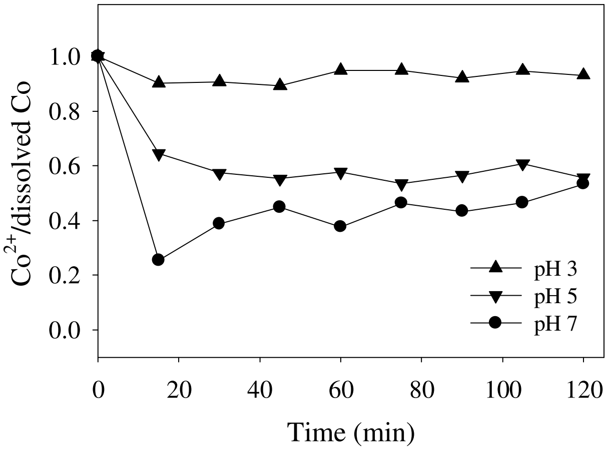

FIGURE 3. Effect of pH on speciation of Co (fraction of Co^{2+}/dissolved Co) in Co/PMS system for TCS decomposition. $[TCS]_o$=9 mg/L, $[Co^{2+}]_o$=3.66 mg/L, and [PMS]=19.14 mg/L.

For all the experiments, we added reactants in the order of TCS, PMS and Co^{2+}, since oxidation of TCS by PMS was found to be negligible and thus the addition of Co^{2+} last was expected to initiate the overall advanced oxidation. In a separate test, we first added PMS and Co^{2+} before immediately adding TCS in order to further prove the importance of maintaining high Co^{2+} concentration for the ecomposition of TCS. As shown in Figure 4, there was a substantial decrease in TCS decomposition when TCS was added later. Significant amount of Co^{2+} added was rapidly converted to Co^{3+} during its instantaneous reaction with PMS before TCS addition.

We are also conducting studies on the speciation of other metals by the activation of PMS with Fe, Cu and Ag, as well as investigating the effectiveness of SRs generated by the activation of PS with transition metals to decompose TCS. Finally we will conduct studies to identify the reaction intermediates of TCS degradation in order to propose a degradation pathway for the sulfate radicals-based degradation of TCS.

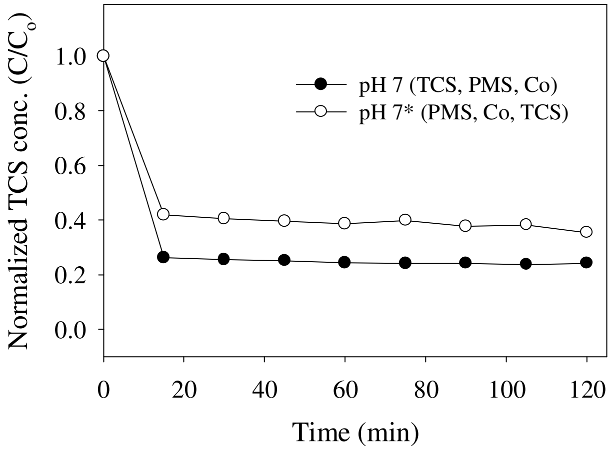

FIGURE 4. Effect of the order of addition of reagents on TCS decomposition using PMS/Co.

CONCLUSION

This study has demonstrated the detailed changes in Co speciation in Co/PMS system over time and correlated it with TCS decomposition under different pH regimes. A strong catalytic activity was observed at pH 3, where Co^{3+} seemed successfully regenerated back to Co^{2+}. Although this study does not completely address many fundamental questions, it contributes towards taking an important first step in understanding the catalytic/non-catalytic nature of the metal-mediated activation of PMS to decompose organic contaminants in water. A detailed study on Fe/PMS system is also being conducted since Fe occurs abundantly in water resources.

ACKNOWLEDGEMENTS

Dr. Choi appreciates the financial support of the University of Texas at Arlington in form of startup fund to initiate this study.

REFERNCES

Anipsitakis, G. P., and D. D. Dionysiou. 2003. “Degradation of organic contaminants in water with sulfate radicals generated by the conjunction of peroxymonosulfate with cobalt.” *Environ. Sci. Technol.* 37(20):4790-4797.

Anipsitakis, G. P., and D. D. Dionysiou. 2004. “Radical Generation by the Interaction of Transition Metals with Common Oxidants.” *Environ. Sci. Technol.* 38(13):3705-3712.

Ankley, G.T., B. W. Brooks, D. B. Huggett, and J. P. Sumpter. 2007. “Repeating history: pharmaceuticals in the environment.” *Environ. Sci. Technol.* 41(24):8211-8217.

Daughton, C.G., and T. A. Ternes. 1999. “Pharmaceuticals and personal care products in the environment: Agents of subtle change?” *Environmental Health Perspectives Supplements.*107(6):907-938.

Erickson, B. 2010. “Targeting Triclosan.” *Chem. Eng. News* 88:8.

House, D. A. 1962. “Kinetics and Mechanism of Oxidations by Peroxydisulfate.” *Chem. Rev*. 62(3):185-203.

Huang, Y., Y. Huang, C. Huang, and C. Chen. 2009. “Efficient decolorization of azo dye Reactive Black B involving aromatic fragment degradation in buffered Co^{2+}/PMS oxidative processes with a ppb level dosage of Co^{2+}-catalyst.” *J. Hazard. Mater*. 170(2-3):1110-1118.

Krishnakumar, B., V. N. Anupama, S. Anju, and M. Rugminisukumar. 2011. “Effect of triclosan on protozoa in wastewater treating bioreactors.” *Water Sci. Technol.* 63(4):754-760.

Lindström, A., I. J. Buerge, T. Poiger, P. A. Bergqvist, M. D. Müller, and H. R. Buser. 2002. “Occurrence and environmental behavior of the bactericide triclosan and its methyl derivative in surface waters and in wastewater.” *Environ. Sci. Technol*. 36(11):2322-2329.

Nfodzo, P., and H. Choi. 2011a. “Sulfate Radicals Destroy Pharmaceuticals and Personal Care Products.” *Environ. Eng. Sci.* 28(8):605-609.

Nfodzo, P., and H. Choi. 2011b. “Triclosan decomposition by sulfate radicals: Effects of oxidant and metal doses.” *Chem. Eng. J*. 174 (2-3):629-634.

Rule, K. L., V. R. Ebbett, and P. J. Vikesland. 2005. “Formation of Chloroform and Chlorinated Organics by Free-Chlorine-Mediated Oxidation of Triclosan.” *Environ. Sci. Technol*. 39(9):3176-3185.

Safarzadeh-Amiri, A., J. R. Bolton, and S. R. Cater. 1996. “The use of iron in advanced oxidation processes.” *J. Adv. Oxid. Technol.* 1(1):18-26.

Son, H. S., S. B. Chol, K. D. Zoh, and E. Khan. 2007. “Effects of ultraviolet intensity and wavelength on the photolysis of triclosan.” *Water Sci. Technol.* 55(1-2):209-216.

Spiro, M. 1979. “The standard potential of the peroxosulphate/sulphate couple.” *Electrochim. Acta.* 24(3):313-314.

Zorrilla, L. M., E. K. Gibson, S. C. Jeffay, K. M. Crofton, W. R. Setzer, R.L. Cooper, and T. E. Stoker. 2009. “The effects of triclosan on puberty and thyroid hormones in male Wistar rats.” *Toxicol. Sci.* 107(1):56-64.

SOLID RETENTION TIME (SRT) EFFECTS ON LANDFILL LEACHATE TREATABILITY BY MEMBRANE BIOREACTOR

Rouhallah Mahmoudkhani (Tehran medical Branch, Islamic Azad University, Tehran, Iran)
Ali Torabian (University of Tehran, Tehran, Iran)
Amir Hessam Hassani and Seyed Mehdi Borghei (Science and Research Branch, Islamic Azad University, Tehran, Iran)

ABSTRACT: One of the most important concerns in Tehran municipal landfill is the production of leachate and its potential risks to the surrounding water resources. Average COD of the leachate in aerobic submerged membrane bioreactor was 60000 mg/L. The dissolved oxygen (DO) concentration were maintained at 3.2 and 2.3 mg/L and For each aeration ratio, MLSS concentration were considered in base of sludge retention time (SRT). With increasing Sludge age of 55 days to infinity, the concentration of chloride and sulfate ions and electrical conductivity of the membrane is increased about 3, 2 and 2 times, respectively, in a way that the kinetic coefficients obtained showed a serious reduction in specific growth (μ) and the reaction coefficient (K), yield coefficient (Y), decay coefficient (K_d) and saturation constant (K_s) were in the about of 0.0093 day^{-1}, 0.18 day^{-1}, 0.085 mg VSS/mg COD, 0.036 day^{-1} and 2295 mg COD/L, respectively, than the MBR kinetic coefficients with SRT of 55 days were, 0.013 day^{-1}, 0.236 day^{-1}, 0.08 mg VSS/mg COD, 0.035 day^{-1} and 1065 mg COD/L, respectively, in order to increasing leachate treatability and reducing leachate treatment inhibitors, it is required that appropriate SRT with high MLSS and kinetic coefficient to be used.

INTRODUCTION

Landfilling of municipal solid waste (MSW) has been economically quite accepted method for municipal solid waste (MSW) disposal throughout the world (Safari et al., 2011). Landfill leachate, which is often characterized as a high strength wastewater with high Chemical Oxygen Demand (COD), Biochemical Oxygen Demand (BOD), chloride and ammonia nitrogen should be considered as an integrated part of landfill operation (Safari et al., 2011).

Determination of the biokinetic coefficients is usually achieved by collecting data from lab-scale or pilot-scale experimental setups operated at various hydraulic retention times (HRTs) and/or at various sludge retention times (SRTs) (Tchobanoglous et al., 2003).Various kinetic models have been presented to describe biological degradation of organic compounds. Despite its drawbacks, Monod model is still an important and a fundamental model in the calculations of all active sludge processes. The capabilities of this model outweigh its shortcomings and defects. The pollutants concentration effect on reactors exiting concentration, the variation of the half-velocity constant (K_s) and the effect of inhibitor pollutants in the environment are some of the shortcomings which are attributed to this model. This relation has been reported as the reduction of growth rate constant when the concentration of the inhibitor increases. In the absence of the inhibitor of growth, the variations of X_{max}/ M with respect of F/M has a ascending function; otherwise the presence of the inhibitor in the environment is predictable which affects the rate of live micro organism and their activities. The above-mentioned points make Monod model to be less than 100% precise in matching the experimental data and the outcomes of the model. In the present study, there has been an attempt to simulate the Membrane Bioreactor process based on the Monod model. According to this model, specific growth can be related to substrate by the following relations 1 and 2.

$$\mu = \mu_{\max} \frac{s}{k_s + s} \qquad (1)$$

ISBN 9780976885351

Where μ = Specific growth rate of microorganism (day^{-1}), μ_m = Maximum specific growth rate (day^{-1}), S = Substrate concentration (mg/L), K_S = Half-velocity constant or Monod constant (mg/L).and Webb's model presents ion-strength inhibition for microorganism growth (Nguyen Phuoc, 2001):

$$\mu = \mu_{max}\frac{s}{s + k_s\left(1 + {}^{\sigma}/_{k_I}\right)}exp(1.17\sigma) \tag{2}$$

Where σ = Ion strength, The method of kinetic parameter determination is based on linearization of mass balance equations with the assumption, that Monod kinetics is applicable for this type of wastewater and treatment technology. It is also assumed, that the plant is operated at a steady state conditions under all loadings models. The linearized form of mass balance equations for substrate (COD) are presented in equations 3 and 4, respectively (Marais, 1994; Eid Abbassi, 2008).

$$\frac{1}{SRT} = YU - k_d = Y\frac{S_0 - S}{\theta X} - k_d$$

$$\frac{X\,\theta}{S_0 - S} = \frac{K_s}{k}\frac{1}{S} + \frac{1}{k} = \frac{1}{U}$$

Where SRT= Solids retention time (d), Y= Biomass yield (mg VSS/mg sCOD), U= Substrate utilization rate (mg sCOD/mg VSS.d), k_d= Endogenous decay coefficient (1/d), S_0= Influent substrate concentration (mg sCOD/L), S= Effluent substrate concentration (mg sCOD/L), X= Biomass concentration (mg VSS/L), Θ= Hydraulic retention time (d), K_s= Half-velocity constant (mg sCOD/L), k= Maximum rate of substrate utilization (mg sCOD/mg VSS.d), the main purpose of presenting the above equation is to determine biosynthetic parameters Y, K_d, μ_{Max} and K_s in the membrane bioreactor process in order to optimize the design of the leachate treatment system.

The main objective of this study was to make an initial assessment on the possibility of aerobic treatment of the extremely high strength leachate streams generated at Kahrizak landfill by MBR. This paper presents the results of leachate characterization and laboratory scale MBR degradation characteristics. Conventional biological treatment were explored for extended application in salin wastewater but were not successful, this study focused on MBR system function and kinetic reaction under chloride, sulfat and EC affected conditions.

MATERIALS AND METHODS

Leachate *Feed:* The leachate used in this study was collected from a municipal landfill located in a suburban area of Tehran, Kahrizak. The landfill site has been in operation since 1985. The age of the landfill for sampling is 0.5-1 year. The leachate used for this study was young because it contained readily biodegradable organic matter (Hasar et al., 2009).

Process Configuration and System Design: The investigations were carried out at a laboratory scale in a MBR. The MBR with a working volume of 175 L was made of Plexiglas. Dissolved oxygen was supplied using 2 fine bubble disc diffusers (Ecoflex 250 Cv), made by USA Diffuser Tech Co., placed at the bottom of the reactor, producing bubbles of pour size. The amount of oxygen supplied to the reactor was regulated for aeration at two rates of 4 (1.03 kg O_2/kg COD) and 2 (0.58 kg O_2/kg COD) m^3/h and The dissolved oxygen (DO) concentration were maintained at 3.2 and 2.3 mg/L and For each aeration ratio, MLSS concentration were considered in base of sludge retention time (SRT). Ultimately, sludge retention times (SRTs) were controlled at 55 days and unlimited with zero sludge waste. After each time of aeration rate change, 55 days (SRT) was given to the system to adapt with the new condition. Sludge abstraction directly from the MBR, leads to a method of control of the SRT (called the Hydraulic Control of SRT) that was used in this study (Marais, 1994), In this pilot-plant test, a hollow-fiber pp microfiltration (MF) membrane was used with pore size of 0.1 µm and the effective surface area of the MF membrane module at 4 m^2. Membrane flux was between 0.5 and 0.8 m^3/d.

A lab scale MBR was set up for COD and biological nutrient removal with a flow rate of 12 L/day which operated under a total SRT of 55 and unlimited days, and an HRT of 15 days. Influent characteristics were measured once a week. The effluent BOD_5, COD, NO_3-N, PO_4-P, NH_4-N, NO_2-N, EC, Cl^-, SO_4 and turbidity were monitored for ten months. All experiments were conducted under the conditions of constant temperature (21 C^o) and controlled pH (9-9.5). Determination of COD, BOD5, nitrite, nitrate, ammonium, phosphate, sulfate, Cl^-, Conductivity, MLSS and turbidity were performed according to standards methods, 20th ed. (APHA, 1998). Chemical oxidation demand was analyzed colorimetrically using tests and photometer of the HACH firm (DR 2010).

RESULTS AND DISCUSSION

Aeration Rate Effects in MBR: In this work the attention was specifically focused on the mechanisms of COD and NH_4 removal on MBR with high and low aeration rates with 55 and high aeration with unlimited days SRT. The concentration of the mixed liquor suspended solids (MLSS) at high aeration ratio (4 m^3/h) in both 55 and unlimited days were 6300 and at low aeration ratio (2 m^3/h) was 3800 mg/L. Figure 1, demonstrates the changes to the MLSS and shows the sludge age in days.

The results of the MBR treatment are summarized in Table 1; Effluent quality at high aeration with 55 days SRT was very high with regard to all parameters studied. Effluent COD and NH_4 were below 1733 and 8.1 mg/L respectively. The other investigated fact was related to the capability of COD and NH_4 removals from the leachate through MBR with tow aeration rate and tow SRTs. in this regard, the concentration of the Cl^-, SO_4, and EC, were slightly different from other parameters. The average concentration of the Cl^-, SO_4, and EC in MBR with high aeration were 8620, 2060 and 40680 mg/L, respectively, in MBR with low aeration were 10795, 2504 and 44180 mg/L, respectively and in MBR with unlimited SRT were 26447, 4257 and 85200 mg/L, respectively. The results show that, with decrease in the aeration rate, the concentration of the Cl, SO_4 and electrical conductivity increase 20%, 21% and 8.6% respectively, and with the relative increase, the removal efficiency of COD is reduced by 45%. This reduction, to some extent, may be due to the concentration of Cl, SO_4 and electrical conductivity.

SRT Effects in MBR: Considering the outcomes (figure 1), the MLSS variations in the 55 days and unlimited SRT, almost remained the same which indicates that the increase in the SRT and the concentration increase of the Cl, SO4, and electrical conductivity have no effect on the growth, and mortality rate of micro organisms. As it is illustrated in table 2, the increase of the SRT from 55 days to unlimited days and in turn the increase of the concentration of Cl, SO4, and electrical conductivity inside the reactor are 3, 2 and 2 times higher respectively, have no considerable effect on the efficiency coefficient (Y) and mortality rate of bacteria (K_d). The effect was so that the efficiency coefficient under same conditions (aeration rate and Temperature) with 55 days and unlimited days SRT were 0.082 and 0.085 mg VSS/mg COD respectively. With the low-aeration rate it was about 0.034 mg VSS/ mg COD which indicates a considerable effect of aeration rate on the efficiency coefficient (Y) of micro organisms. Mortality rate of micro organisms (K_d) under the same condition with 55 days sludge and unlimited sludge were 0.035 and 0.036 respectively on day-1. With low aeration rate the mortality rate of micro organisms was about 0.017. The conclusion drawn from all this is that the increase in the sludge age from 55 days to unlimited and the increase of the Cl, SO4, and electrical conductivity from 8620 to 26447 mg/L; from 2060 to 4257 mg/L and from 40680 to 85200 mg/L respectively, has no noticeable effect on efficiency coefficient (Y) and the mortality rate (K_d) of micro organisms. But, as it is illustrated in table 2, what affects the quality reduction of exiting COD from 1733 to 3436 mg/L and the increase in the concentration of exiting NH4 from 8.1 to 60.6 mg/L and the increase of nitrite concentration inside the reactor, from about 0.7 to 40 mg/L, under 55 days and unlimited SRT respectively, is extremely important and it is the effect of Cl, SO4, and electrical conductivity on the performance of micro organisms in removing COD and NH4. This, in turn, causes the reduction of reaction constant (K), half- velocity constant (Ks) and the maximum specific growth rate from 0.23 to 0.18 day^{-1}, from 1065 to 2265 mg COD/L and from 0.212 to 0.0156 day^{-1} respectively.

TABLE1. Physical and Chemical Parameter Concentrations in the MBR Inlet and Outlet

parameters		COD (mg/L)	NO3 (mg/L)	NO2 (mg/L)	NH4 (mg/L)	PO4 (mg/L)	CL (mg/L)	SO4 (mg/L)	EC (µmhos/cm)	TUR (NTU)	BOD (mg/L)	pH
Influent	average	49383	303	0.003	1575	219.2	10712	2804	44150	190	25801	6.9
	standard deviation	15061	330	0.01	713	293.9	3649	1882	3635.4	6.56	14144	0.2
Effluent with high aeration	average	1733	209	0.76	8.1	12.94	8620	2060	40680	58	270.8	9.1
	standard deviation	116.4	192	0.24	3.11	9.80	192.3	307	1428.9	1.03	184.6	0.1
Effluent with low aeration	average	2514	126	20.78	49.2	9.422	10795	2504	44180	58.6	1247	9.2
	standard deviation	132.3	63.8	13.60	17.7	2.65	2497	180.7	3472.3	1.82	184.1	0.1
Effluent with unlimited SRT	average	3436	213.3	40.02	60.64	-	26447	4257	85200	62	-	9.35
	standard deviation	92.11	142	26.40	3.28	-	208.6	13.04	381.75	0.45	-	0.1

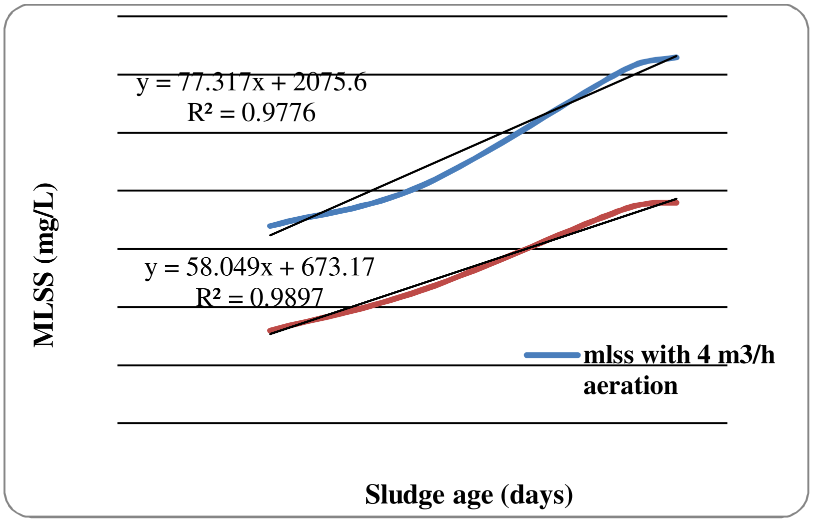

FIGURE1. MLSS Changes with Sludge Age and Aeration

As it is shown in figure 2 the inhibition amount of Cl, SO_4, and electrical conductivity have been compared the inhibition amount of low aeration rate regarding their effect on micro organisms. The difference is that in the low aeration conditions, the concentration of Y, MLSS and K_d inside the reactor decreases considerably, while in inhibition conditions Cl, SO_4, and electrical conductivity, the concentration of MLSS, Y and K_d which relate to the mortality of micro organisms inside the reactor, is always constant. The inhibition rate of ions, related to the poor performance of micro organisms in removing COD and NH_4 can be determined before the concentration of MLSS reaches its maximum constant amount with the minimum ions of Cl, SO_4, and electrical conductivity. Figure 3 also shows the amount of inhibitors gained from ions and electrical conductivity based on the results obtained from Webb's model, compared to the results obtained from reactor. According to the results, the specific growth rate inside the MBR is much less than the Webb's model. This means that there are other inhibitors inside the reactor including the high concentration of the entering organic materials and the lack of nutrients such as phosphate, which affect the specific growth rate.

TABLE2. Biokinetic Coefficient Characteristics of Membrane Bioreactor

Reactor condition	HRT (Days)	SRT (Days)	reaction coficient - K (d^{-1})	Kinetic model	MLSS (mg/l)	Y (mg/mg)	K_d (Day^{-1})	K_s (mg COD/l)	μ (Day^{-1})	μ_{max} (Day^{-1})	COD $_{in}$ (mg/l)
High aeration	15	55	0.236	$C=C_0e^{-0.236T}$	6300	0.073- 0.09	0.035	1065	0.013	0.0212	60250± 8000
Low aeration	15	55	0.205	$C=C_0e^{-0.205T}$	3800	0.03- 0.038	0.017	2062	0.0043	0.0078	60250± 8000
Unlimited SRT	15	∞	0.18	$C=C_0e^{-0.18T}$	6330	0.085	0.036	2295	0.0093	0.0156	60250± 8000

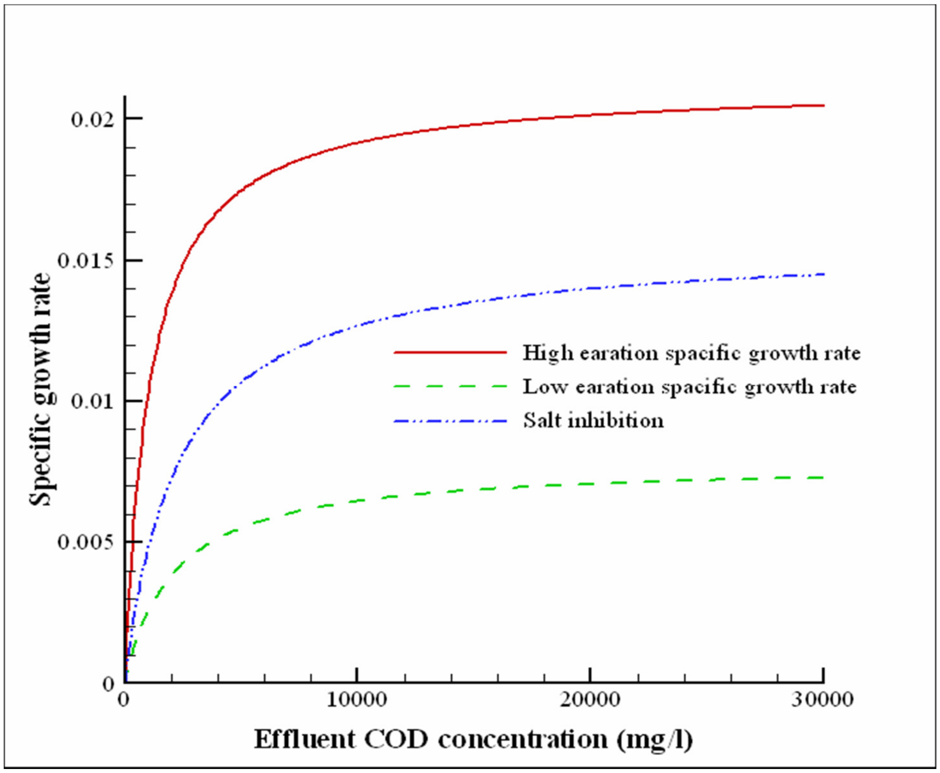

FIGURE2. The Effects of Electrical Conductivity and Aeration Inhibition on Specific Growth Rate

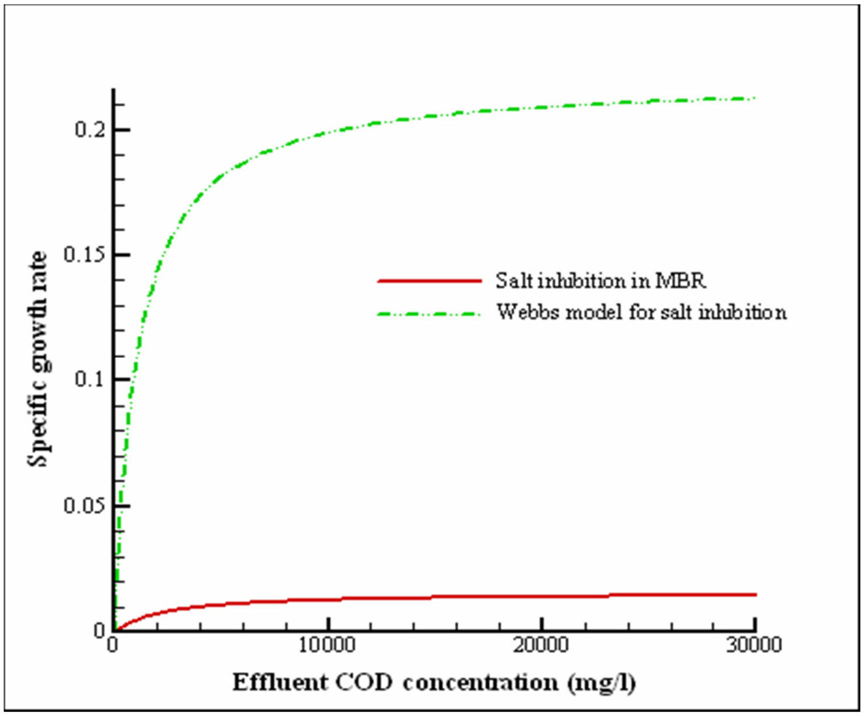

FIGURE3. The Effects of Ion Inhibitors on the Specific Growth Rate Based on Webb's Model and the Results of MBR

CONCLUSIONS

The present study contains results of landfill leachate treat ability by Membrane Bioreactor that is important for modeling, design, and operation of landfill leachate treatment MBRs and determination of discharge limits. Suitable treatment strategy depends on two major criteria, the initial leachate quality and the final requirements given by local discharge water standards, the presented data indicate that the landfill leachate composition has a significant effect on treatability and According to the finding of this study, in order to increasing leachate treatability and reducing leachate treatment inhibitors, it is required that appropriate SRT with high MLSS and kinetic coefficient to be used. Apart from the factors affecting the function of Monod equation such as the primary concentration of the entering leachate and other inhibitors, the age of the sludge is another important factor which makes the application of Monod equation difficult under various circumstances.

REFERENCES

American Public Health Association (APHA). 1998. Standard methods for the examination of water and wastewater, 20th ed., American Public Health Association, Washington, DC, USA.

Eid Abbassi B. 2008." Effect of Hydraulic Loading Variations on the Performance of Decentralized Small Scale Activated Sludge Treatment Plant" American-Eurasian J. Agric. & Environ. Sci., 4(5): 617-624.

Hasar H., S. A. Unsal, U. Ipek, S. Karatas, O. Cınar, C. Yaman, C. Kınac. 2009."Stripping/ Flocculation/ Membrane Bioreactor/Reverse Osmosis Treatment of Municipal Landfill Leachate", Journal of Hazardous Materials. 171: 309–317.

Marais G.V.R. 1994. Wastewater Treatment by Activated Sludge Process. Lecture notes. University of Cape Town. South Africa. International Institute for Infrastructural, Hydraulic and Environmental Engineering, the Netherlands.

Nguyen Phuoc D. 2001." Biological Treatment of High Salinity Wastewater Using Yeast and Bacterial Systems ".Bangkok, Thailand. Asian Institute of Technology, school of Environment, Resources and Development.

Safari E., M. Jalili Ghazizade, A. Shokouh, Gh. R. Nabi Bidhendi. 2011." „Anaerobic Removal of COD from High Stregth Fresh and Partially Stabilized Leachates and Application of Multi Stage Kinetic Model ".Int. J. Environ. Res. VOL(5)2,: 255-270.

Tchobanoglous G., F. L. Burton, H.David Stensel. 2003. Wastewater Engineering Treatment and Reuse. Fourth Edition, Metcalf & Eddy, Inc.

ELECTROCHEMICAL TREATMENT OF TRACE ENDOCRINE DISRUPTING CHEMICALS BY A NOVEL GRANULAR-ELECTRODES REACTOR

Huu Cong Vo and Yutaka Sakakibara
(Waseda University, Shinjuku, Tokyo, JAPAN)

ABSTRACT: Electrochemical treatments of trace endocrine disrupting chemicals containing Estrone (E1), 17β-Estradiol (E2) and 17α-Ethinyl Estradiol (EE2) were conducted at laboratory scale using granular glassy carbon electrodes. Synthetic wastewater was prepared and treated under different operating conditions. Electrochemical responses of electrode were analyzed by cyclic voltammetric (CV) technique for each estrogen. The results show that oxidation current peaks of E1, E2, and EE2 occurred in the range of 660-760mV. However, the peaks were subsequently decreased or disappeared from the second scans. No reduction peak was observed. The results from batch treatments have shown that removals of three estrogens similarly occurred within three hours regardless different currents were applied. Moreover, the electrochemical removal of the estrogens could be reasonably well simulated by a mathematical model developed assuming the external liquid-film mass transfer as a rate-limiting step. The X-ray Photoelectron Spectroscopy analysis of electrode surface composition has demonstrated the electrodes were hindered by a polymeric film containing carbon and oxygen bounds. The overall treatment performance achieved about 80% of removal efficiency within 4 hours. It was suggested that the electrochemical response of electrode in multi-anode systems were taking place at low potential and the composition of electrode surface has changed after several treatments.

INTRODUCTION

In recent years, environmental hormones such as natural and synthetic estrogens, Estrone (E1), Estradiol (E2) and Ethinylestradiol (EE2), have been drawn high attention due to their adverse impact on the aquatic life forms even at trace concentrations. Extremely strong estrogenic effects of E1, E2 and EE2 have been identified for aquatic life form at very low concentration ranging from 0.2-10 ng/L on Medaka and Zebrafish (Tilton et al., 2005, Oern et al., 2006). These threshold values are extremely lower in comparison with other synthetic EDCs such as bisphenol-A (BPA), nonylephenol (NP), 4-t-octyl phenol (4-t-OP) and pentachlorophenol (PCP) and their presence in the wastewater treatment plans. Due to extremely low threshold values of E1, E2, and EE2 for aquatic life forms, conventional treatment processes are not always able to remove or detoxify them below acceptable levels (Koh et al., 2008).

Advanced Oxidation Process (AOPs) can achieve more than 96% of estrogen removals (E2 and EE2) at different ozone dosages and O_3/H_2O_2 in aqueous solution (Maniero et al., 2008) but it was reported that this process required large amounts of energy up to several thousand kWh/m^3 (Sakakibara et al. 2005). In our recent studies, we showed that EDCs such as BPA, NP, 4-t-OP, and PCP could be removed with extremely low energy consumptions by direct electrolysis where they exchange electrons directly with the anode surface without involvement of other substances through the formation of polymeric film. In addition, mass transfers of EDCs were a rate-limiting step, so that the use of electrode

---

ISBN 9780976885351

having high specific surface areas is important for enhanced and high rate treatment (Sakakibara et al, 2010).

In direct oxidation process, electro-polymerization reaction involving two-electron process consumed less than two electrons per phenol molecule transformed into polymer (Tahar and Savall, 2011). It is noted that E1, E2 and EE2 have similar structures to phenolic EDCs with three phenolic rings, therefore, it is supposed that E1, E2 and EE2 may be removed by electrolytic reactor. However, to our knowledge no literatures on the removals of E1 and EE2 via electro-polymerization have been reported. This study was conducted to know the possibility and characteristics of removing the natural and synthetic estrogens, E1, E2 and EE2 by electro-polymerization process.

MATERIALS AND METHODS

Materials: Estrone (CAS 58-05023), 17β-Estradiol (CAS 58-04043), Ethynylestradiol (CAS 57-63-6), and 17β-Estradiol 16, 16, 17-d_3 standard (CAS 054-06941) were purchased from Wako Chemical Company, Japan. All chemicals are over 97% purity for GC analysis. Granular glassy carbon electrodes (ϕ: 2000-3150μm) were purchased from HTW, Germany.

Cyclic voltammetr: The CV analysis was conducted using a conventional three-electrode system consisted of a glassy carbon (0.07 cm^2), Pt wire counter and Ag/AgCl reference electrode. The PK-3 electrode polishing kit consisted of a coarse diamond 1μm (Cat.No. 012621) and a polishing alumina 0.05 μm (Cat.No. 012620) was used to clean the electrodes. A solution containing E1, E2 and EE2 5mg/L with 10mM Na_2SO_4 in de-ionized water was separately prepared. CV analysises were conducted at 100mV/s, in the potential ranges of 0-1300 mV using Hokuto HZ-5000 (Hokuto Electronics Inc.).

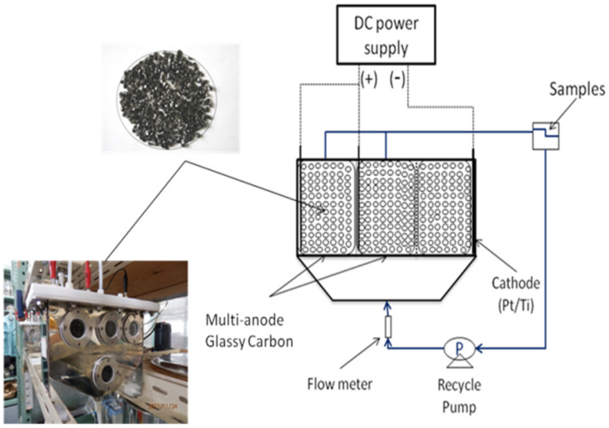

FIGURE 1. Scheme of batch experiment apparatus

Batch treatment by granular electrochemical reactor: The batch experimental apparatus of this study includes two compartments consisting of 3-dimensional granular glassy carbon electrodes (anodes) and a Pt/Ti mesh as cathode (FIGURE 1). Total liquid volume and surface area of the working electrode (anode) were 500 cm^3 and 2,000 cm^2, respectively. The batch experiments were carried out at electric currents in the range of 0-1000μA. The initial concentration of E1, E2 and EE2 was prepared at 100μg/L with 10mM Na_2SO_4 in de-ionized water. Recirculation flow rate was set at 500ml/min. Samples were taken at the initial time, 20, 30, 40, 60, 120, 180, and 240 minutes of the operation. Estrogens extractions were carried out based on the tentative investigation manual for Endocrine Disrupting Chemicals (JEA, 1998). The concentrations of estrogens were analyzed by GCMS (Shimadzu QP5050).

Mathematical models: In our former kinetic study (Sakakibara et al, 2010), it was demonstrated that removal rates of EDCs such as BPA, NP, 4-t-OP, and PCP were controlled by mass transfer rates in liquid film between electrode surface and bulk liquid. In this research, the same kinetic approach was applied to the electrochemical removals of estrogens. From an assumption that overall removal rates of estrogens are governed by mass transfer rates, the estrogens removals in batch treatment would be represented by the following equation.

$$V\left(\frac{dCi}{dt}\right) = -kAC_i \qquad (1)$$

Where, V is the total liquid volume of reactor, C_i is the effluent concentrations, k is the mass transfer coefficient of estrogen, t is time, and A is the total surface area of working electrode, respectively.

In the batch treatment, removals of estrogens from aqueous solution could be simplified by the following equation (2):

$$C = C_0 \mathrm{Exp}^{(-\frac{A}{V}kt)} \qquad (2)$$

Where, C is concentration of estrogens and C_0 is initial concentration.

In this research, the packed bed reactor composed of granular electrodes was used. Therefore, the mass transfer coefficient calculated from the Wilson-Geankoplis (1966) was adopted. The equation can be written as:

$$k = \frac{1.09\,(u)^{1/3}}{\varepsilon}\left(\frac{Dm}{d}\right)^{2/3} \qquad (3)$$

Where, u is the superficial velocity (cm/s), ε is the void fraction, and d is diameter of glassy carbon granular electrodes, respectively.

Diffusivity in Eq. (3) is estimated by the following Wilke and Chang (1955) with accuracy within 10% for small to medium size molecules [10]. The calculated diffusivities of E1, E2, and EE2 are 2.06 x 10^{-6}, 2.06 x 10^{-6}, and 1.91 x 10^{-6}, respectively.

RESULTS AND DISCUSSION

Electrochemical behaviour of estrogens: FIGURES 2, 3 and 4 demonstrate the progressive cyclic voltamograms of E1, E2, and EE2 at 5 mg/L in the range of 0-1.3V with 10mM Na_2SO_4. The result shows that only oxidation process was occurred in the experiments. The oxidation peaks of E1, E2, and EE2 (dotted lines) occurred at 660-760 (mV vs Ag/AgCl reference electrode) at 3.2 µA, 1.3 µA, and 2.6µA, respectively, but there is no reduction peak on the reverse scans. However, the oxidation peaks were reduced in subsequent cycles (dotted and dashed lines). This result implies that electro-polymerization of organic compounds have taken place on the surface of electrode. The same phenomena were reported elsewhere (Kuramitz et al., 2004, Sakakibara et al., 2010, Tahar et al., 2011).

Electrochemical mineralization of organic pollutants normally occurred at high potential in the region of water discharge where strong oxidant like •OH radicals are produced, but huge amount of energy is consumed (Murugananthan et al., 2007). Within the region below the electrolysis of water, the energy is consumed for chemical reaction rather than oxygen and •OH radical production. In the case of estrogens, at the first step one electron and one proton will be released to create a phenoxy radical. Then, one more electron is released to form phenoxonium ion which is playing role as an active species in the solution (Ngundi et al., 2003). If no electrochemical polymerization occurred, one proton will be released to form a stable form. The passivation may be assumed due to the electro-polymerization through two electrons process in which two electrons are transfer from the estrogens to create the active and free radical on phenoxy radical which may further lead to a reaction with other estrogens in the bulk solution.

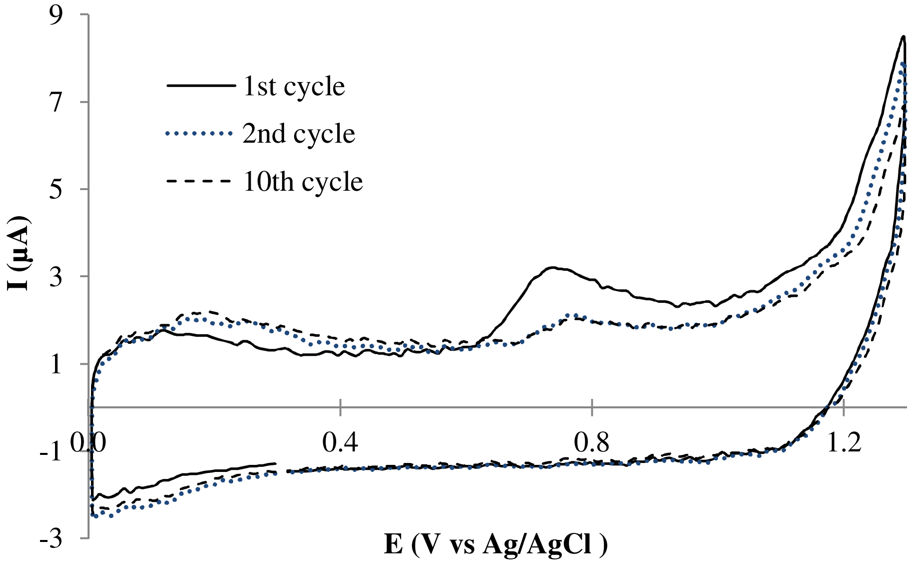

FIGURE 2. Progressive cyclic votammograms of E1

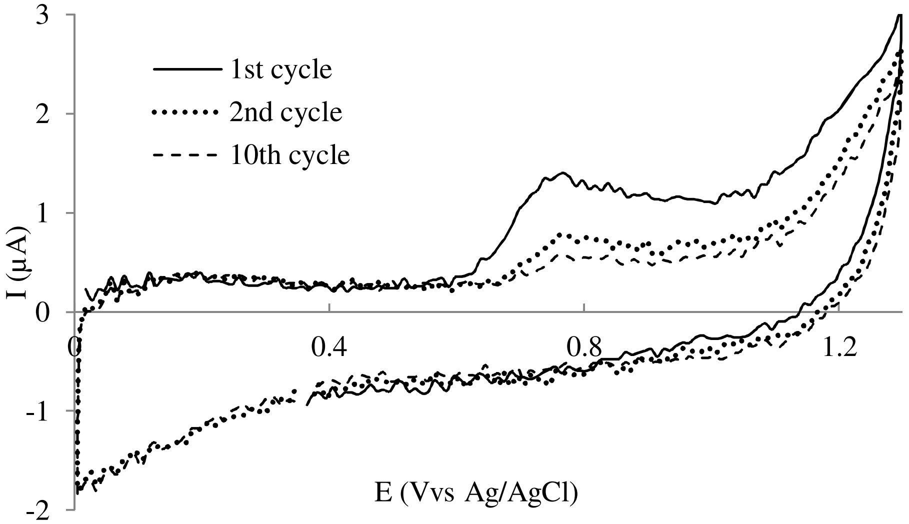

FIGURE 3. Progressive cyclic votammograms of E2

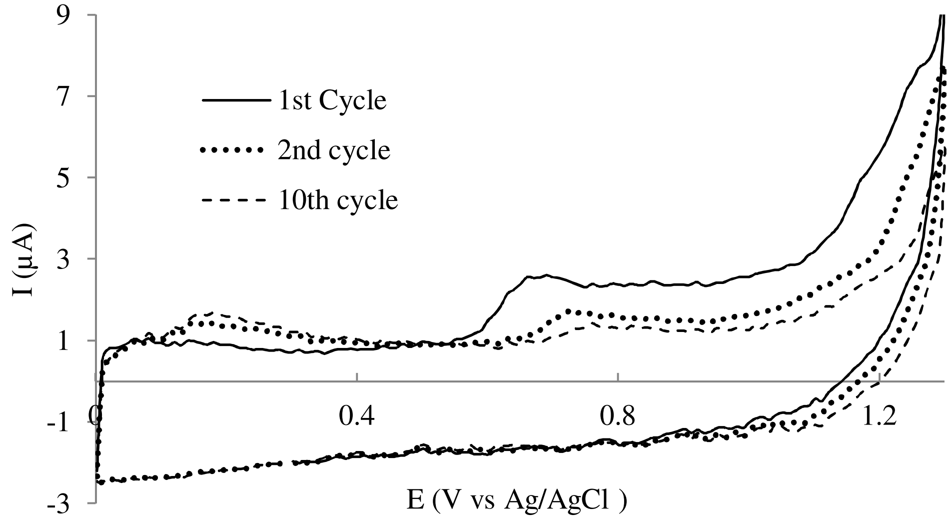

FIGURE 4. Progressive cyclic votammograms of EE2

Electrolytic removals of estrogens: Electrochemical removals of estrogens (E1, E2, and EE2) were studied at different currents. FIGURE 5 shows the removals of E1, E2, and EE2 at 0.1 and 1mA. The result shows that concentration of E1, E2, and EE2 dropped significantly by an application of electric current. When the current increased about 10 times (0.1 to 1mA), the removals of estrogens revealed almost the same. This suggests that the removals of estrogens were governed by the mass transfer rate (Eq. (2)). To our knowledge, this result is the first experimental verification that the estrogens can be removed by an electrochemical oxidation process. A solid line in FIGURE 5 shows calculated results for E1, E2, and EE2 by Eq. (2). As molecular diffusivities of the estrogens are almost the same, the results were represented by the solid line. As shown, the calculated result fitted reasonably well to observed data regardless of the estrogens. After 4 hours of treatment, about 80% of E1, E2 and EE2 were removed by the application of electric current.

It was reported that an electrolytic reactor consisted of granular electrodes have enlarged the working surface of anode which increases the net mass transfer rates from bulk solution to the active electrode for chemical reactions (Sakakibara et al., 2010). This study shows a possible treatment of trace estrogens at low current 5×10^{-3}A/m^2 which is 4-5 orders lower compared to 2×10^{2}A/m^2 applied in the treatment of E2 by BDD electrode (Murugananthan et al., 2007). This may indicate that granular electrodes contribute the reduction of energy consumption besides the enhancement of treatment performance. Energy consumption was in the range of 0.16-3.6 Wh/m^3 which was 2-3 orders of magnitude smaller than that of conventional activated sludge used in sewage treatment plan.

Polymeric formation: In FIGURE 6 (A) and (B), observed results of X-ray Photoelecctron Spectroscopy (XPS) analysis of carbon and oxygen elements on anode surface were compared before and 4 hours after the treatment. As shown, the Carbon peak decreased, while the Oxygen peak increased during the treatment. It is thought that during the trreatment of estrogen on glassy carbon, the oxidized products of estrogens may cover the electrode surfaces. Taking into consideration of results shown in FIGURES 2 to 5, and referring to former studies (Pannizza et al., 2003, Kuramitz et al., 2004, Muruganathan et al., 2007, Sakakibara et al., 2010, and Tahar and Savall 2011), it is thought that polymer formations occurs during the treatment of estrogens. In our former studies (Sakakibara et al., 2010), the polymer can be easily decomposed to generate anodes through the generation of ·OH radicals by Fenton reaction or by advanced electrochemical oxidation process (Shimura et al., 2011). A further study will be needed to quantify and control the electro-polymerization of estrogens.

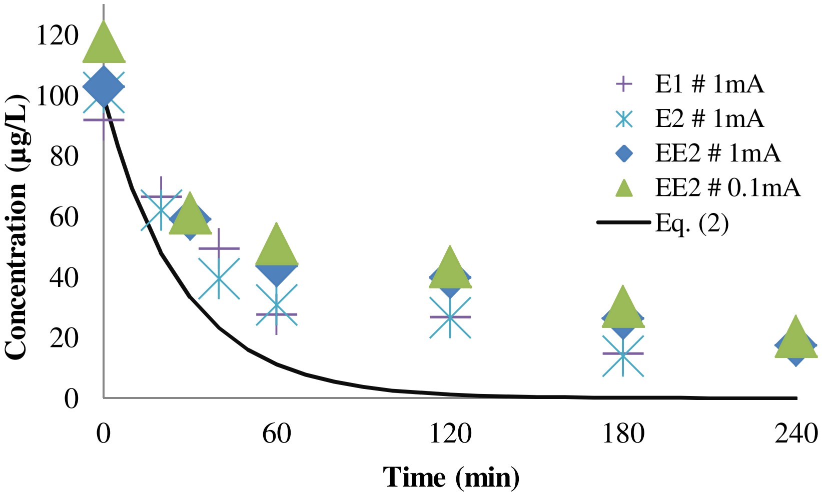

FIGURE 5. Electrochemical removals of estrogens

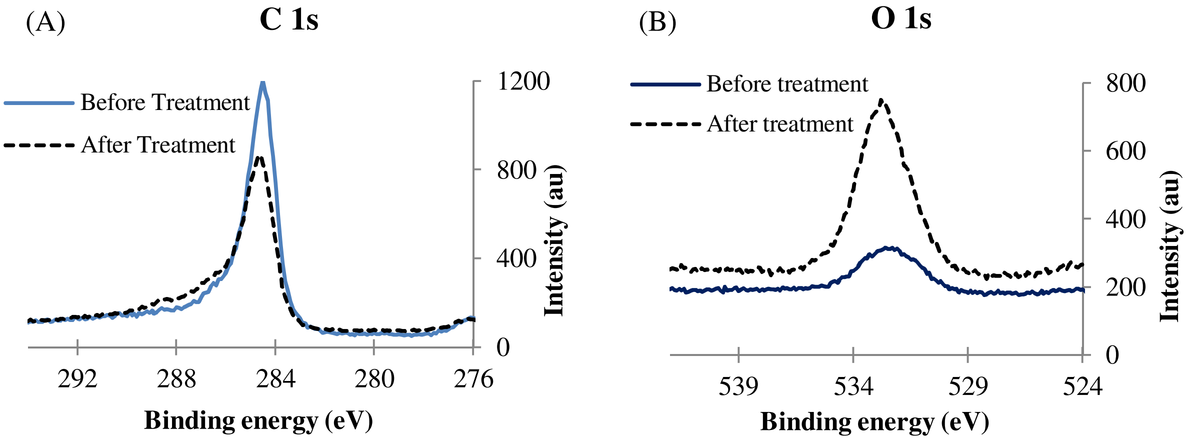

FIGURE 6. Carbon and oxygen elements on glassy carbon electrode before and after treatment

CONCLUSIONS

Electrochemical oxidations and removals of estrogens, E1, E2, and EE2 were possible by an application of electric current about 5×10^{-3}A/m^2. The overall treatment performance achieved about 80% of removal efficiency within 4 hours of operation and consumed an energy amount 0.16-3.6 Wh/m^3. Moreover, from the comparisons of observed results with calculated results by a mathematical model (Eq. (2)), it was shown that estrogens removal rates were mainly controlled by mass transfer rates in liquid film between electrode and bulk liquid. In addition, the oxidation of estrogens occurred at low potential around 660-760mV but the oxidation reaction decreased from the subsequent second scans. It was supposed that estrogen removals were made through polymerizations of estrogens. In long-term treatment, a further study will be needed to quantify and control the electro-polymerization of estrogens. In addition, electrode regeneration should be taking into considerations of reactor design to enhance the removal performance of estrogens.

ACKNOWLEDGMENTS

The authors would like to thank the Grant-in-Aid for Scientific Research (B) (#24360219), the Ministry of Education, Culture, Sports, Science and Technology (MEXT) for financial support for this research. We would also like to thank Mr. Takahiro Gotoh at Material Characterization Central Laboratory, Waseda Unvesity for technical assistance and supports, and to whom the authors are very grateful.

REFERENCES

Japan Environmental Agency (JEA). 1998. “Tentative Investigation Manual for Endocrine Disrupter Chemicals” (in Japanese).

Koh, Y. K. K., T. Y. Chiu, A. Boobis, E. Cartmell, M. D. Scrimshaw and J. N. Lester. 2008. “Treatment and removal strategies for estrogens from wastewater”. *Environmental Technology* 29: 245-267.

Kuramitz, H., Y. Nakata, M. Kawasaki and S. Tanaka. 2004. “Electrochemical oxidation of bisphenol A. An application to the removal of Bisphenol A using carbon fiber electrode”. *Chemosphere* 45: 36-43.

Maniero, M.G., D.M. Bila, M. Dezotti. 2008. “Degradation and estrogenic activity removal of 17β-estradiol and 17α-ethinylestradiol by ozonation and O_3/H_2O_2”. *Science of the total environment* 407: 105-115.

Murugananthan, M, S. Yoshihara, T. Rakuma, N. Uehara and T. Shirakashi. 2007. “Electrochemical degradation of 17β-estradiol (E2) at boron-doped diamond (Si/BDD) thin film electrode”. *Electrochemical Acta* 52: 3242-3249.

Ngundi, M.M, O.A Sadik, T. Yamaguchi and S. Suye. 2003. “First comparative reaction mechanisms of b-estradiol and selected environmental hormones in a redox environment”. *Electrochemistry Communications* 5: 61-67.

Oern, S., S. Yamani and L. Norrgren. 2006. “Comparison of Vitellogenin Induction, Sex Ratio, and Gonad Morphology Between Zebrafish and Japanese Medaka After Exposure to 17a-Ethinylestradiol and 17b-Trenbolone”. *Archives of Environmental Contamination and Toxicology*, 51, (2): 237-243.

Panizza, M. and G. Cerisola. 2003. “Influence of anode material on the electrochemical oxidation of 2-naphthol Part 1. Cyclic voltammetry and potential step experiments”. *Electrochimica Acta* 48: 3491-3497.

Sakakibara, Y., Sekine, M., Tsuneda, S., Sumino, T., Emori, H., -Morita, A. & Takakura, A. 2005 “Development of advanced wastewater treatment process to reduce levels of endocrine disrupting chemicals (EDCs) in water environment”. Final report to the Ministry of Land, Infrastructure and Transport, Government of Japan (in Japanese).

Sakakibara, Y., T. Kounoike and H. Kashimura. 2010. “Enhanced Treatment of Endocrine Disrupting Chemicals (EDCs) by A Granular Bed Electrochemical Reactor”. *Water Science & Technology* 62: 2218-2224.

Shimura, M., M. H. Uddin, Y. Sakakibara, and T. Tanaka: Generation of O_3 and OH radicals by a 3-dimensional electrolytic reactor, *JSCE, Ser. G (Environmental Research)*, **67**(7), 697-703 (2011).

Tahar N.B. and A. Savall. 2011. "Electropolymerization of phenol on a vitreous carbon electrode in alkaline aqueous solution at different temperature". *Electrochimica Acta* 55: 465-469.

Tilton, S. C., C. M. Foran and W. H. Benson. 2005. "Relationship between ethinylestradiol mediated changes in endocrine function and reproductive impairment in Japanese medaka (Oryzias latipes)". *Environmental Toxicology and Chemistry*, 24, (2): 352-359.

Wilke C.R. and P. Chang. 1955. "Correlation of Diffusion coefficients in dilute solutions", *A.I.Ch.E. Journal*: 264-270.

Wilson E.J. and C.J. Geankoplis.1966. "Liquid mass transfer at very low Reynolds numbers in packed beds". *I&EC fundamentals* 5: 9-14.

ELECTRON SPIN RESONANCE ANALYSIS OF BIO-FENTON PROCESS

Shoichi NAGAHASHI and Yutaka SAKAKIBARA
(Waseda University, Tokyo, Japan)

ABSTRACT: A biological Fenton process (Bio-Fenton process) using aquatic plants, where refractory compounds are decomposed through reduction of endogenous hydrogen peroxide in the presence of ferrous ion, has been proposed in our former studies. In this study, OH radical production in Bio-Fenton process and abiotic Fenton process were studied by Electron Spin Resonance (ESR) Spectroscopy using DEPMPO as a spin trapping probe. In abiotic system, Fenton's reagents containing 0.1mM H_2O_2 and 0.05mM ferrous ions were prepared, referring to endogenous H_2O_2 levels in aquatic plants. ESR results in abiotic system showed a clear peak indicating the formation of OH radicals. On the other hand, in biotic system, reagents were prepared by mixing cell extracts from aquatic plant with and without 0.05mM ferrous ion, and the same ESR analyses were conducted. Results using 200 mM DEPMPO showed a small peak and no peak for OH radical formation in the presence and absence of ferrous ion, respectively. It was considered that there existed OH radical scavengers in plant extracts which reduced OH radical peaks. From these results, it was concluded that Bio-Fenton process would be an innovative advanced treatment process for refractory pollutants.

INTRODUCTION

In recent years, water demand has been increasing due to the population increase and economic growth. With such an increase in water demand, advanced oxidation processes (AOPs) have received great attention in the field of water and wastewater treatment and reuse (Roberto et al., 1999), which are characterized by hydroxyl radical (OH radical) production. OH radical can decompose almost all persistent substances due to its high reactivity.

Fenton process is one of AOPs and is represented by Reaction (1), where OH radical is produced through the reaction between hydrogen peroxide and ferrous ion (E. and Baeyens, 2003).

$$Fe^{2+} + H_2O_2 \rightarrow Fe^{3+} + OH^- + OH^\bullet \qquad (1)$$

Although AOPs have superior performances in decomposing persistent and toxic substances, it is still a costly technology for wastewater treatment. We proposed a Biological Fenton process (Bio-Fenton process) using aquatic plants, where refractory compounds such as chlorinated phenols and PCP are decomposed through the reduction of endogenous hydrogen peroxide in the presence of ferrous ion. Enhanced decomposition rates and the production of chloride ions were observed during the process (Reis and Sakakibara, 2011, 2012). If AOP such as Bio-Fenton process is adopted into practical use, it will contribute significantly to the field of wastewater treatment thanks to its advantage in treating wastewater containing persistent substances with low cost and low energy consumption.

Detection of OH radicals is facing problems due to its extremely short life-time existence. Thus, a number of methods of OH radical detection and measurement have been proposed. Recently, spin

---

ISBN 9780976885351

trapping method with Electron spin resonance (ESR) spectroscopy is one of the most effective methods to detect OH radical. It could help to keep OH radical for a longer-lived adduct by scavenging OH radicals. It have been suggested that one of the most effective spin trapping reagents is 5-diethoxyl-phosphoryl-5-methyl-1pyrroline-*N*-oxide (DEPMPO) or a phosphorylated derivative of the widely used 5,5-dimethyl-1-pyrroline-*N*-oxide (DMPO) (Ke et al., 1998). The DEPMPO has been used in researches on the biological field (Biljana et al., 2009). However, no literature on the application of DEPMPO for quantifying OH radicals in the Bio-Fenton reaction has been reported.

The objective of this study was to investigate the OH radical production in Bio-Fenton process with ESR spectroscopy and spin trapping techniques by comparison between biotic and abiotic Fenton systems.

MATERIALS AND METHODS

Materials and Reagents. Duckweed (*Spirodela Polyrhiza*) aquatic plants taken in Chiba prefecture Japan were used as an experimental host plant (PHOTOGRAPH 1). DEPMPO was obtained from Radical Research Inc. (Tokyo). H_2O_2 and other chemicals were purchased from Wako Pure Chemical Industries, Ltd. (Osaka).

PHOTOGRAPH 1. Duckweed (*Spirodela Polyrhiza*)

Sampling for ESR Experiments. OH radical generation in Bio-Fenton reaction was studied using Electron Spin Resonance (ESR) Spectroscopy. ESR analysis was conducted using spin trapping probe DEPMPO to detect OH radical. In the first run of experiments, OH radical formations in abiotic and biotic systems were studied with 10mM DEPMPO. In abiotic system, the final concentrations of 0.1mM H_2O_2, 0.05mM $FeSO_4$ and 10mM DEPMPO solution was prepared. H_2O_2 concentration was referred to H_2O_2 levels in aquatic plants (Reis and Sakakibara, 2011 and 2012). ESR analysis of the sample was carried out immediately. In the case of biotic system, Fenton's reagents were prepared by mixing cell extracts from aquatic plant with ferrous ion solution. Plant extracts were obtained by the following method. Duckweed was crushed in a mortar with the 50mM phosphate buffer 2 mL per 1 g F.W. duckweed. The mixture was centrifuged for 10 min (13000 rpm, 4℃), after that, the supernatant was collected. Then same ESR analysis was conducted.

Another ESR experiments were conducted in which a much higher concentration of the spin trapping probe DEPMPO (around 200 mM) was used to detect OH radicals. An amount of 0.3g F.W. of duckweed was ground in a mortar with 1mL solution containing 200 mM DEPMPO and 0.05 mM ferrous ion. Then, the mixture was centrifuged for 3 min (13000 rpm, 4℃). The supernatant was collected and ESR analysis was carried out immediately. For comparison, another sample was obtained by the same method except ferrous ion (i.e. no ferrous ion) and ESR analysis was conducted.

ESR Spectroscopy. ESR measurements were carried out using pulsed electron spin resonance apparatus (JEOL JES-TE200) and the flat-type water sample cell (JEOL JES-JC11). Conditions for analysis were as follows: frequency, 9.456GHz; microwave power, 4mW; center of magnetic field, 336.5mT; scan range, 15mT; scan time, 2min; modulation width, 0.1mT; amplitude, 200; time constant, 0.1sec; at ordinary temperatures and pressures.

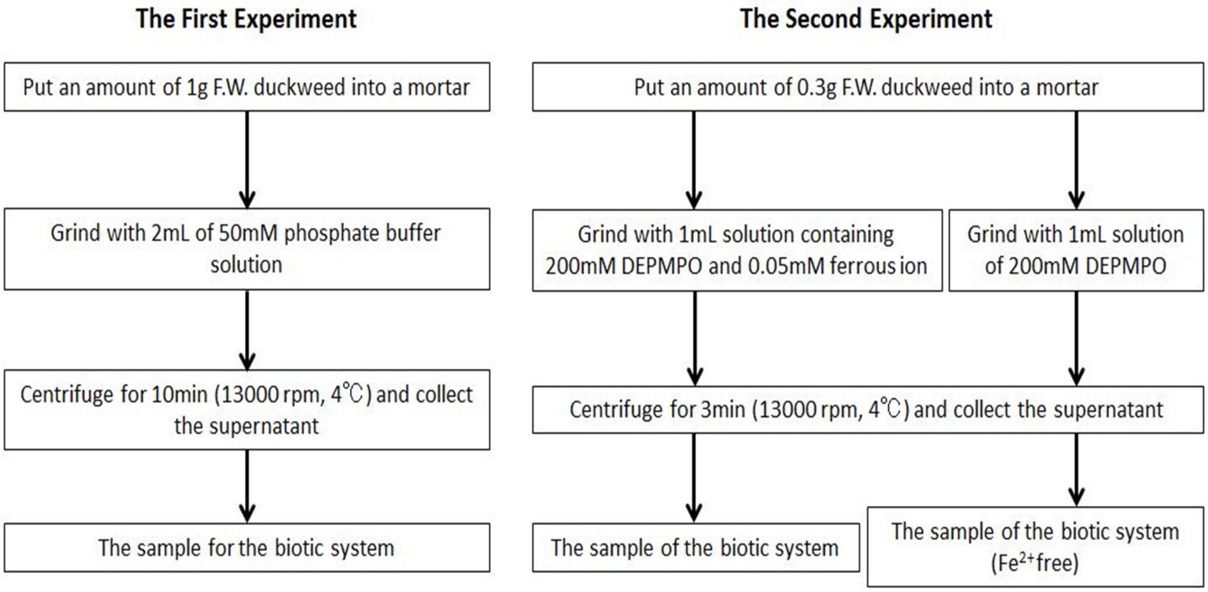

FIGURE 1. Flow chart for the preparation of samples

RESULTS AND DISCUSSION

Comparison of Abiotic and Biotic System. In the first set of experiments, the comparison of results between biotic system (FIGURE 2-A) and abiotic system (FIGURE 2-B) is shown in FIGURE 2, where DEPMPO and ferrous ion concentrations were 10 mM and 0.05 mM, respectively. In the abiotic system, ESR results indicated the formation of OH radicals which is confirmed by the characterization peak of OH radical (denoted by the arrow) (Kazunori et al., 2003). On the other hand, in the biotic system, results showed several low peaks. In comparison with the characterization peaks, it was found that results of biotic system indicated no clear peaks for OH radical formation. It was considered that there existed substances in plant extracts which reduced OH radical peaks.

In former studies on Fenton process, concentration levels of H_2O_2 were set in the range of several to 1,000 mM. Comparing these levels, the concentration in this study was 1 to 5 orders of magnitude smaller (Joseph et al., 2006). Therefore, it is interesting to note that the production of OH radicals is still possible under trace H_2O_2 levels.

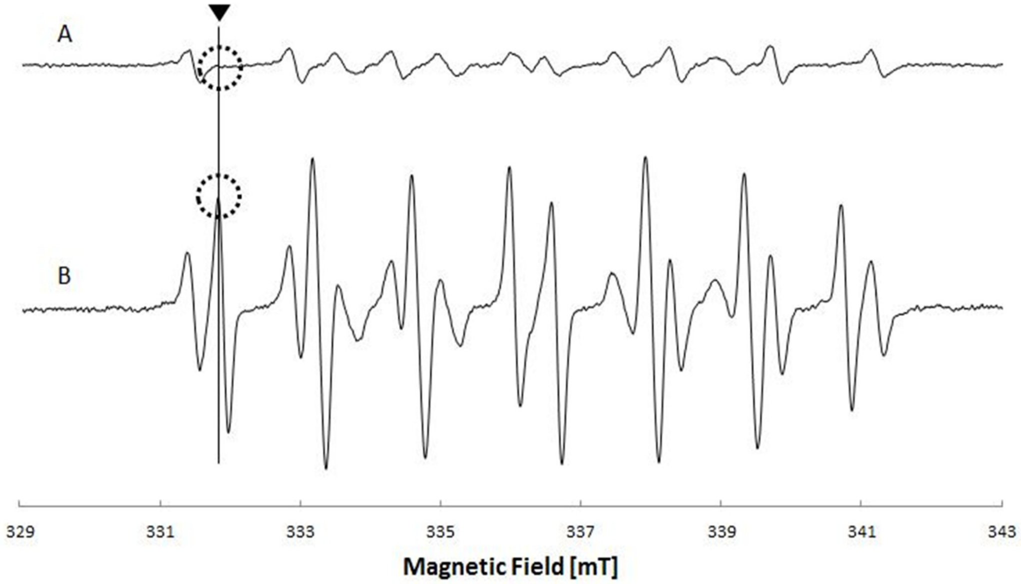

FIGURE 2. Comparison of ESR results of (A)biotic system and (B)abiotic system

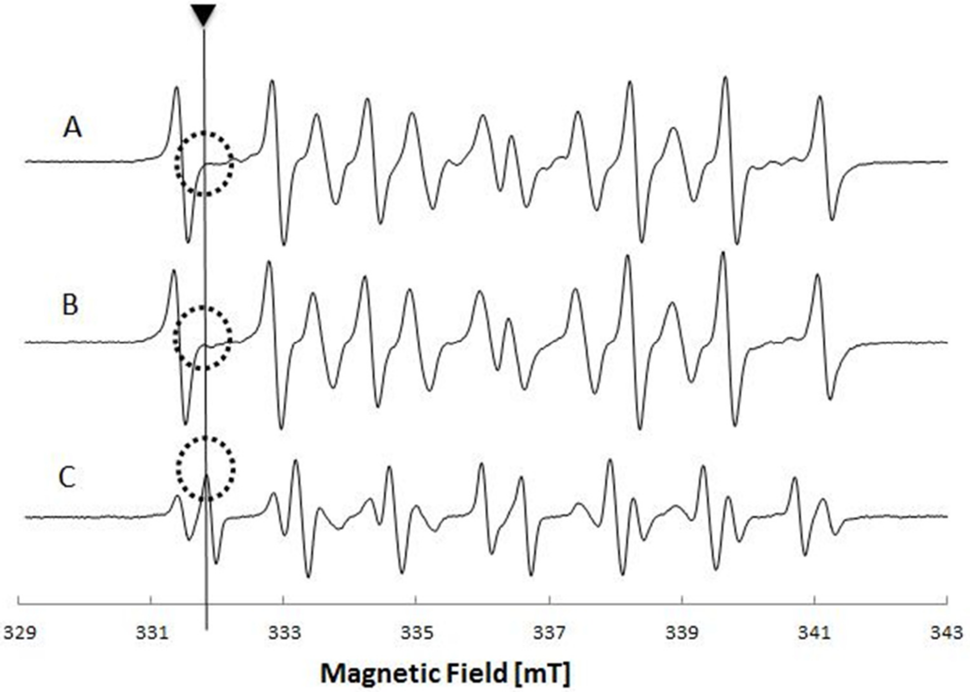

FIGURE 3. Comparison of ESR results of (A)biotic system (Fe^{2+} free), (B)biotic system and (C) abiotic system

ESR Analysis with the High Concentration DEPMPO. In the second set of experiments, ESR analyses were conducted at a much higher concentration of the spin trapping probe (around 200mM). The comparison of results between biotic system without ferrous ion (FIGURE 3-A), biotic system (FIGURE 3-B) and abiotic system (FIGURE 3-C) was shown in FIGURE 3. In the both results of the biotic system without ferrous ion and biotic system, with focusing on the point of OH radical's characteristic peak, there is no peak which is the same levels as abiotic system. However, in the result biotic system, there is a small peak at the point whereas no peak was detected in the result of biotic system without ferrous ion. From these results, it is considered that OH radical production was promoted by the addition of ferrous ion.

CONCLUSIONS

In the case of Fenton reagents in abiotic system, which contains H_2O_2 at the level of endogenous H_2O_2 in aquatic plants, clear OH radical production was detected. On the other hand, the results of the same ESR analysis conducted to the biotic system using plant extracts did not indicate clear OH radical formation. However, in experiments using a high concentration of spin trapping probe DEPMPO, results indicated the appearance of small peaks showing OH radical formation in the biotic system. From these results, it was concluded that there is possibility of OH radical production in Bio-Fenton process and Bio-Fenton process would be used as an innovative advanced treatment process for refractory pollutants. A further study will be needed to optimize the process performance.

ACKNOWKEDGEMENTS

This research was partially supported by Grant-in-Aid for challenging Exploratory Research (#23656334), The Ministry of Education, Culture, Sports, Science and Technology (MEXT), Japan; and Research fund of JST Project on "Development for water reuse technology in tropical region".

REFERENCES

Biljana K., M. Mojović, Ž. Vučinić, V. Maksimović, U. Takahama and S. V. Jovanović. 2009. "Generation of Hydroxyl Radical in Isolated Pea Root Cell Wall, and the Role of Cell Wall-Bound Peroxidase, Mn-SOD and Phenolic in Their Production" *Plant Cell Physiol.* **50**(2): 304-317.

E. N. and J. Baeyens. 2003. "A review of classic Fenton's peroxidation as an advanced oxidation technique" *Journal of Hazardous Materials.* B98: 33-50.

Joseph J. P., E. Oliveros and A. MacKay. 2006. "Advanced oxidation process for organic contaminant destruction based on the fenton reaction and related chemistry" *Critical reviews in Environmental Science and Technology,* **36**: 1-84

Julio A. Z. and K. F. Reardon. 2009. "Fenton's oxidation of pentachlorophenol" *Water research.* **43**: 1831-1840.

Katharina F. P., K. Stolze, T. G. Reichenauer and B. A. Goodman. 2009. "Free radical generation in uncooked carrot (*Daucus carota*) root tissue after cell disruption – A model for chemical reactions during mastication" *Food Chemistry*. **112**: 400-405.

Kazunori A., T. Aikawa, Y. Furukawa, Y. Matsushima, S. Urano and T. Ozawa. 2003. "ESR measurement of rapid penetration of DMPO and DEPMPO spin traps through lipid bilayer membranes" *Archives of Biochemistry and Biophysics.* **415**: 251-256.

Ke J. L., M. Miyake, T. Panz and H. Swartz. 1998. “Evaluation of DEPMPO as a spin trapping agent in biological systems” *Free Radical Biology and Medicine.* **26**(5): 714-721.

Reis, A.R., and Y. Sakakibara. 2011. “Continuous treatment of endocrine disrupting chemicals by aquatic plants and biological Fenton reaction”. *Jap. Soc. Civil Eng., Series G (Environmental Research).* **67**(7):725-734.

Reis, A. R. and Y. Sakakibara. 2012. “Enzymatic Degradation of Endocrine Disrupting Chemicals in Aquatic Plants and Relations to Biological Fenton Reaction”, *Wat. Sci. and Technol.* (in press).

Roberto A, V. Caprio, A. Insola and R. Marotta. 1999. “Advances oxidation processes (AOP) for water purification and recovery” *Catalysis Today.* **53**: 51-59.

CATALYTIC WET DECOMPOSITION OF DIMETHYL PHTHALATE

Chia-Chi Chang[1], Shih-Yun Chen[1], Ching-Yuan Chang[1]*, Sheng-Wei Chiang[1], Chiung-Fen Chang[2], Yi-Hung Chen[3]

1. Graduate Institute of Environmental Engineering, National Taiwan University, Taipei 106, Taiwan; 2. Department of Environmental Science and Engineering, Tunghai University, Taichung 407, Taiwan; 3. Department of Chemical Engineering and Biotechnology, National Taipei University of Technology, Taipei 106, Taiwan

This study investigated the treatment of dimethyl phthalate (DMP) via wet oxidation (WO) and catalytic wet decomposition (CWD) processes. Pt/γ-Al_2O_3 and γ-Al_2O_3 were used as catalysts to enhance the decomposition efficiency of DMP (η_{DMP}) and mineralization efficiency of total organic carbons (TOC_S) (η_{TOC}).

The results showed that η_{DMP} and η_{TOC} of WO process are affected by the rotating speed (N_r), reaction temperature (T) and pressure (P_T), with T being the key factor. An increase of T can promote the decomposition of DMP. The decomposition of DMP via WO process was performed in two steps. (1) During the temperature rising stage (298 to 483 K), the DMP was pyrolyzed without O_2. (2) It followed by introducing the oxidizing gas into the batch system and then proceeded the oxidation at 483 K for 3 h in which DMP and intermediates were decomposed into acid intermediates (such as formic acid), CO_2 and H_2O. At $N_r = 500$ rpm and $P_T = 2.41$ MPa, η_{DMP} and η_{TOC} are about 93 and 36%, respectively.

The addition of catalyst results in a different pathway for the decomposition of DMP. The working gas plays an important role in CWD process. In aerobic CWD (with working gases such as O_2, air and their mixing gas), the oxygen molecule is adsorbed on the active site of the catalyst surface and excited as O* with high activity. The DMP and intermediates react with O* and are decomposed into CO_2 and H_2O. At $N_r = 500$ rpm, $P_T = 1.03$ MPa and $T = 298$-483 K using working gas O_2 and catalyst Pt/γ-Al_2O_3 (mass of catalyst/sample liquid volume (m_S/V_L) = 0.079 g mL^{-1}), η_{DMP} reaches about 100% at 473 K while η_{TOC} is about 24%.

The mechanism of anaerobic CWD (with working gas such as N_2) is quite different from that of aerobic CWD. The intermediates produced during pyrolysis using N_2 can be absorbed by both Pt/γ-Al_2O_3 and γ-Al_2O_3 yielding η_{TOC} of 80 and 29%, respectively at $T = 298$-483 K, $P_T = 1.03$ MPa and m_S/V_L = 0.079 g mL^{-1}. It indicated that Pt on the γ-Al_2O_3 surface not only can absorb the pyrolysis intermediates but also further catalyze the decomposition of intermediates.

ISBN 9780976885351

DEGRADATION KINETICS AND MECHANISM OF CONJUGATED STEROID ESTROGENS IN DAIRY LAGOON WASTEWATER

Wei Zheng, Xiaolin Li, and Yonghong Zhou (Illinois Sustainable Technology Center, University of Illinois, Champaign, IL, USA)
Michael L. Machesky (Illinois State Water Survey, University of Illinois, Champaign, IL, USA)

Land application of concentrated animal feeding operation (CAFO) wastewater is a feasible and economical water reuse strategy, which can provide nutrients and organic matter for plant growth and offer an alternative water source to reduce the demand for high quality water. An emerging threshold issue to this reuse, however, is the potential transfer of organic contaminants such as natural steroid estrogens from the animal wastewater to soil, which may subsequently enter into the surrounding aquatic environments by leaching and runoff. In this study, we investigated the degradation kinetics and mechanisms of three natural estrogen conjugates (17α-estradiol-3-sulfate, 17β-estradiol-3-sulfate, and estrone-3-sulfate) in aqueous solutions blended with dairy lagoon water under aerobic and anaerobic conditions. The degradation of the three conjugated estrogens in the dairy lagoon water was predominated by biodegradation. The biodegradation rates were temperature-dependent and the most suitable temperature for the degradation of all of estrogens was 35 oC. The anaerobic biodegradation of three estrogen conjugates was much slower than aerobic biodegradation, suggesting that these compounds may persist in anaerobic or anoxic environments such as anaerobic CAFO lagoons. Estrone-3-sulfate was identified as a major metabolite for the biodegradation of both estradiol conjugates in aqueous solutions in the presence of dairy lagoon water. The estrone conjugate could be further deconjugated to non-conjugated product. The information in this study is useful for assessing the potential environmental risk of natural steroid hormones derived from the CAFO wastewater reuse.

ISBN 9780976885351

TiO_2-BASED PHOTOCATALYTIC OXIDATION OF VOCs: COATING TO REACTOR PERFORMANCE AND DESIGN

Indramani Dhada, ***Mukesh Sharma***, Tarun Gupta, Suraj Agarwal and Rajesh Mohan
(Department of Civil Engineering, Indian Institute of Technology Kanpur,
Kanpur- 208016, India)

ABSTRACT: Majority of harmful volatile organic compounds (VOCs) in ambient air include benzene, toluene, ethyl benzene and xylene (BTEX). The control of VOCs requires innovations as the quantities are small and not easily degradable to harmless compounds. The specific objectives of the research were: (i) synthesis of TiO_2 nanoparticles and evaluation of their coating on the substrate, (ii) photocatalytic oxidation (PCO) of BTEX and estimate their degradation rates and (iii) fabrication and demonstration of a continuous annular reactor for photodegradation of BTEX. Two sol-gel methods; one prepared using titanium tetra iso-butoxide, ethanol, acetyl acetone and deionized water (M1) and other prepared using titanium tetra iso-propoxide, diethanolamine, ethanol, acetyl acetone and deionized water (M2). M2 was the optimal method for VOCs removal and used in a laboratory scale continuous annular photo catalytic reactor. It was possible to achieve 90 percent removal of BTEX in about 28 to 33 minutes. This study can be used for designing a prototype reactor for field applications.

INTRODUCTION

Volatile organic compounds (VOCs), having vapor pressure ≥ 0.1 mm Hg, are important group of chemicals as many of the VOCs are carcinogenic and have other health impacts (Burstyn et al., 2007; You et al., 2007). Among the VOCs present in ambient air, benzene toluene and xylene (BTEX) are listed as hazardous air pollutants and also in the list of priority pollutants by USEPA. Sources of emissions of VOCs include combustion, cooking, building materials, furnishings, office equipment and consumer products (Dutta et al., 2009). Use of air purifiers based on the principle of heterogeneous photocatalysis (PCO) is a novel and effective method to remove harmful organic compounds from indoor air and emitting sources. PCO involves irradiation of semiconductor materials with UV light of intensity sufficient enough to excite the valance band electrons of the catalyst molecule. The process is heterogeneous, as it involves a phase transfer of the pollutants from gaseous to solid catalyst surface. PCO technique commonly uses nano-semiconductor catalysts and ultraviolet (UV) radiation to convert organic compounds into odorless and simple constituents such as water vapor (H_2O) and carbon dioxide (CO_2). TiO_2 is widely used as catalyst for PCO as it is relatively inexpensive, chemically stable, and the photogenerated holes are highly oxidizing (Fujishima et al., 2006). The other advantage of TiO_2 based PCO is that destruction of VOCs is possible at room temperature.

Photocatalyst, TiO_2, a semi-conductor contains equally spaced energy levels with electron surplus "valency band" and at a higher state, electron deficient “conduction band". When a photocatalyst undergoes illumination by a light source emitting radiation at a specific wavelength with energy equal or greater than that of the band gap, it absorbs the energy promoting an electron excitation from the valence band, to the conduction band. This leaves a fraction of the surface with electron deficiency, forming a hole denoted as h^+ ($TiO_2 + h\upsilon \rightarrow h^+ + e^-$). This electron in conduction band lowers the activation energy of the oxidation reaction of pollutants with oxygen. Sol-gel based coating is the preferred method for coating of nano sized TiO_2 that adheres to the substrate surface as thin films. For PCO applications, these thin films should consist of anatase phase particles of diameter not more than 50 nm (Jang et al., 2000).

Although the principle of PCO is well established, the technology development poses several challenges including synthesis of TiO_2 nanoparticles of controlled size, their characterization,

---

ISBN 9780976885351

understanding the factors affecting the adhesion of the particles to the filter material of different geometries for enhanced lifetime of system. To improve the technology development to control the VOCs, the specific objectives of this research were: (i) synthesis of TiO_2 nanoparticles and evaluation of their coating on the substrate, (ii) photocatalytic oxidation of BTEX and estimate their degradation rates, and (iii) fabrication and demonstration of a continuous annular reactor for photo-degradation of BTEX.

MATERIALS AND METHODS

All chemicals used were of analytical reagent grade. BTEX standard mix (2000 µg/ml; Supleco make) was used for calibration purposes. Other chemicals include: gases (Sigma), de-ionized water (Milli-Q system), titanium tetra iso-propoxide (Spectrochem), titanium tetra isobutoxide (Merck) and tetra n-butyl ortho titanate (Merck), ethanol, n-propanol, iso-propanol, acetone (Qualigen), toluene anhydrous (99.8%), ethyl benzene (99.8%), benzene anhydrous (99.8%) and o, p, m - xylene anhydrous (99.5%) (Loba Chemicals).

TiO_2 nanoparticles were produced using different sol-gel methods and were coated as thin films on borosilicate glass substrate and aluminum substrate. Two sol-gel methods; one prepared using titanium tetra iso-butoxide, ethanol, acetyl acetone and deionized water (referred to as M1; Shen et al., 2005) and other prepared using titanium tetra iso-propoxide, diethanolamine, ethanol, acetyl acetone and deionized water (referred to as M2; Nguyen *et al.,* 2004), were identified as potential methods for coating for PCO of BTEX.

Preliminary analysis showed that the films formed on glass substrate were more uniform and stable than the films coated on aluminum. Films prepared on glass supports were selected for further characterization studies to obtain information about the average particle size, absorption spectra, transmission spectra, band gap, elemental composition, surface morphology, thickness of catalytic film, surface roughness, surface area and photoactivity of the coating. The characterization of the above coated TiO_2 thin films was done by X-ray diffraction analysis model: ISO Debye Flex1001, Field emission-scanning electron microscopy (FE-SEM) Model: SUPRA 40VP (Make: Carl Zeiss NTS GmbH, Germany), Energy dispersive X-ray spectroscopy (EDAX or EDX method) model: FEI Quanta 200 HV, Atomic force microscopy (AFM) model: PicoSPM II, Molecular Imaging, AZ, USA, UV spectrophotometry using Lambda 750 spectrophotometer, Profilometry through Tencor Alpha X-100 Profilometer and Surface area measurement using SMART SORBS 92/93 based on the BET (Brunauer, Emmett and Teller) principle at various laboratory facilities in IIT Kanpur campus.

A cylindrical batch reactor system was used to check the effectiveness of coating techniques for potential PCO application. The effective techniques identified after characterization study were used for coating the reactor. The reactor consisting of a glass socket dimension as 50 mm inside diameter, 370 mm height (volume 1800 cm^3) and cone made of glass was used in this study. A UV lamp (8 W, 10 mm outside diameter, 300 mm length) was placed coaxially inside the reactor. Sensors for monitoring the temperature and the relative humidity inside the reactor were also installed. The reactor was made airtight with port facility to draw gas samples and inject known concentrations of BTEX (benzene, toluene, o,p,m- xylenes) as well. The actual effective volume of the reactor was (1776 cm^3). TiO_2 coated glass strips (30 cm × 3 cm) were placed inside the reactor to study the effectiveness of two coatings, between M1 and M2 for one set-up. Later on, for another similar set up, a thin film of nano sized TiO_2 particles was coated on the inner wall surface of the glass reactor by the methods M1 and M2. A TiO_2 loading density of 3.2×10^{-3} g cm^{-2} was obtained by weighing the tube before and after the coating.

RESULTS AND DISCUSSION

Characterization of TiO_2 Coating: Thin films prepared on glass support were characterized for elemental composition, grain size, surface morphology, thickness, surface roughness, surface area and photoactivity. Using X-ray diffraction techniques the average particle sizes were found to be 19 nm and 21 nm for M1 and M2 coating methods. The photocatalytic activity of TiO_2 increases with decreasing particle size, especially when the particle size is below 30 nm (Jang et al., 2000). With a smaller particle size, the number of active surface sites increases and so does the surface charge carrier transfer rate in the photo catalysis. The phase of TiO_2 nanoparticles was confirmed to be mainly anatase on comparing their XRD pattern with the standard XRD patterns. FE-SEM and UV-spectrophotometry analyses showed the band gap of 3.24 eV for M1 and 3.27 eV for M2 and were found to be almost equal to the reported band gap of 3.23 eV for TiO_2 anatase phase (Mo et al., 2009). This confirms that both coating techniques are optimal and should efficient to use in a laboratory scale reactor. The thickness of TiO_2 coated thin film for M1 and M2, were done through thickness profilometry and found to be 19.2 µm and 23.9 µm respectively, which were in the range of desirable thickness (10-50 µm; Keshmiri et. al., 2006). BET surface areas of the M1 and M2 coatings of nanoparticles were 24.8 $m^2 g^{-1}$ and 30.9 $m^2 g^{-1}$ respectively. Atomic force microscopy analysis of both the samples was performed. The surface roughness was 733.91 nm for M1 and 813.19 nm for M2 which indicates that the thin film consists of rough surface, contributing a higher surface area exposure for the pollutants as compared to the smoother film.

Various sets of batch experiments were performed based on different combinations of target pollutants (benzene, toluene, ethylbenzene, o,p,m-xylene and BTEX mix) in the blank reactor and in TiO_2 coated borosilicate glass strips (30 cm × 3 cm). M1 and M2 were selected for coating TiO_2 to eventually assess that which method was suitable for coating that will give the maximum reduction in VOCs. Figure 1 shows the reduction in benzene in a blank reactor, reactor with UV light (no TiO_2) and with methods M1 and M2 used for coating on the strips. A similar trend was obtained for other VOCs (not shown here).

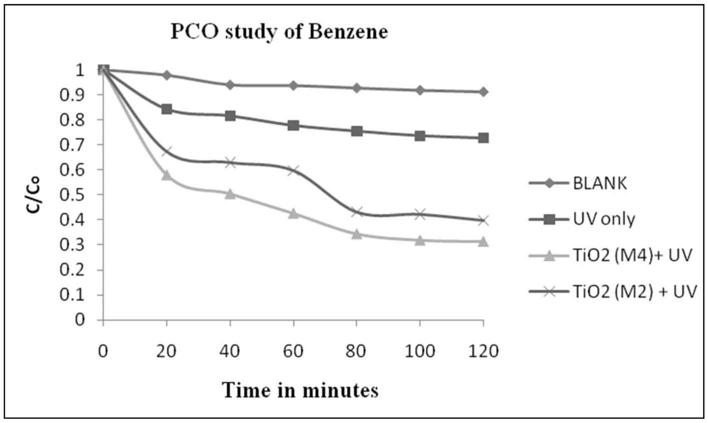

FIGURE1. Degradation of benzene under different combinations

For the blank reactor, there was no significant change in the pollutant concentration. On illuminating the reactor with UV light, the conversion of the pollutant was observed up to 27% (approx.) in two hours. On introduction of TiO_2 catalyst with UV illumination, the conversion increased to 60% for method M1 and 68% for method M2. Thus, the PCO method (i.e., use of UV-TiO_2 combination) was found to be more effective for degradation of benzene. It can be concluded that TiO_2 thin film coated, using method M2 is more effective for PCO of benzene, as compared to the thin films coated with method M1. This conclusion was true for all other pollutants that M2 was a better coating technique than M1. The rest of the studies were carried out using M2 technique and fully coated reactor which had a catalyst surface area to volume (CSV) ratio of 0.33 (strip coated reactor had CSV ratio of 0.2).

The following conclusions can be drawn from the results of experiment through the TiO_2 coated batch reactor (Figure 2). This is to be noted that due to limitation of the manuscript size, we have not shown other figures in this paper.

Degradation of BTEX (individual as well as mixture) in presence of UV-illuminated TiO_2 with large CSV ratio is considerably higher as compared with small CSV ratio (e.g., compare

Figure 2(a) with Figure 1). BTEX when degraded individually shows first order decay but the mixture slightly deviates from the first order degradation (not shown here).

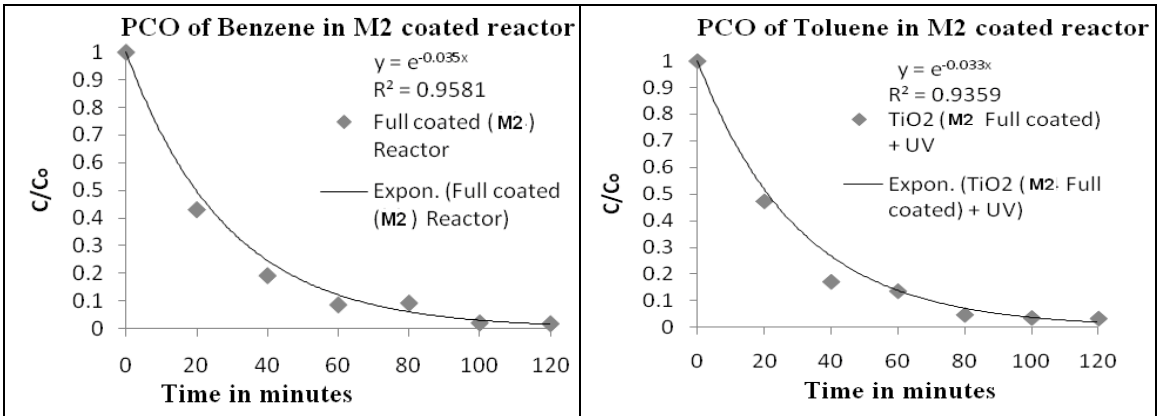

2(a). Degradation of Benzene **2(b).** Degradation of Toluene

FIGURE2. Degradation of benzene and toluene using UV and TiO_2 (M2) coated reactor

Continuous Annular Plug Flow Reactor (CAPF): The results of batch reactor were encouraging in VOCs removal and this led to development of a CAPF reactor for possible application of VOCs control in the field; reactor dimension: 65 mm inner diameter, 270 mm length. The schematic of the experiment for assessing the performance of annular reactor is shown in Figure 3.

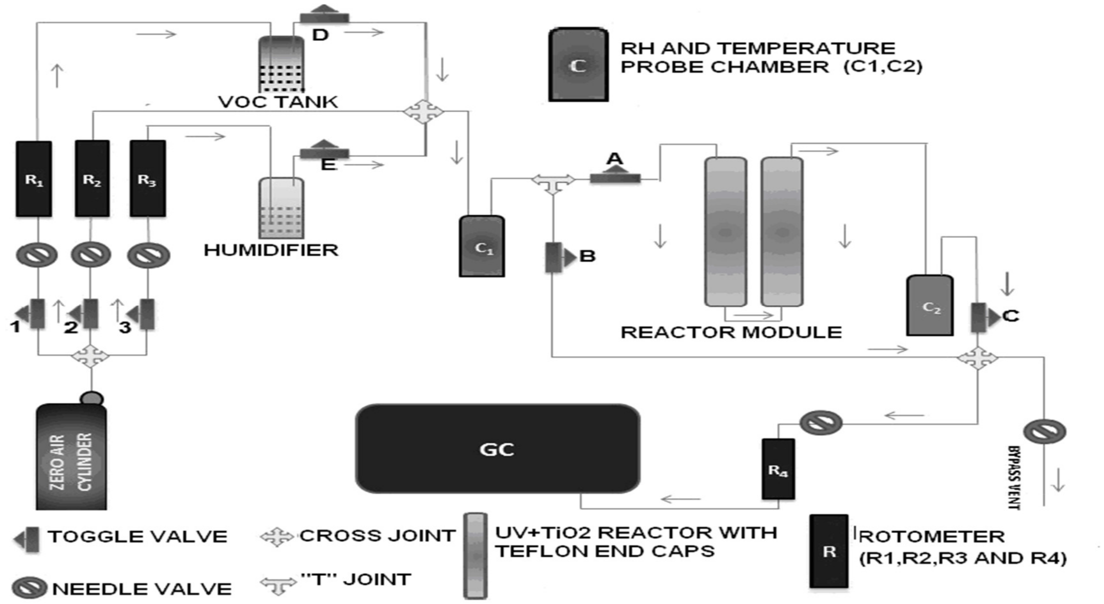

FIGURE3. Schematic diagram for the CAPF photo-reactor setup

Like benzene (Figure 4(a)) and o-xylene (Figure 4(b)), PCO of all BTEX compounds were studied (figures not shown in this paper).The degradation rate of each compound has been estimated and required size of the reactor in terms of retention time for achieving 50% and 90% reduction in the VOC concentration for individual VOC were calculated given in Table 1.

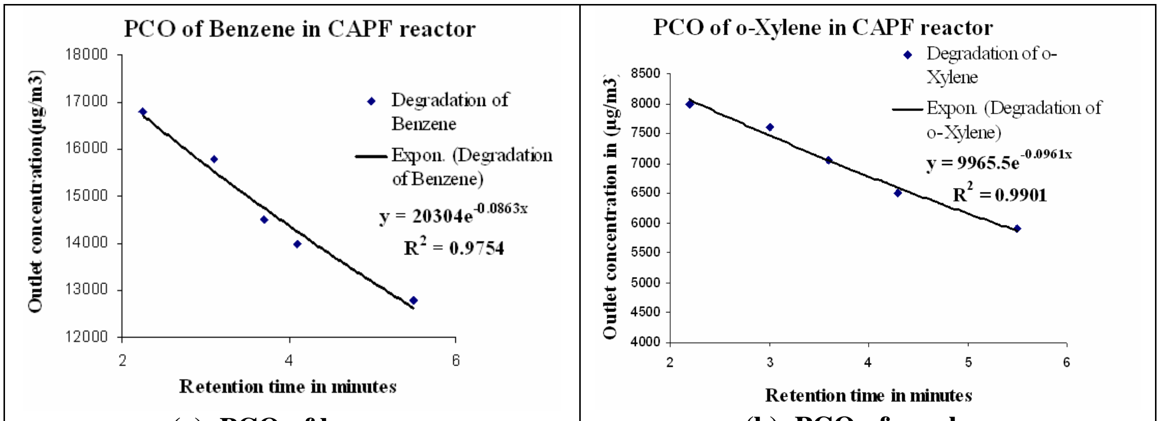

(a). PCO of benzene **(b). PCO of o-xylene**

FIGURE4. (a) PCO of benzene in CAPF reactor with TiO_2 coated (M2) reactor in presence of UV light.(b) PCO of o-xylene in CAPF reactor with TiO_2 coated(M2) reactor in presence of UV light.

TABLE1. **Size of the reactor in terms of retention time for achieving 50% and 90% reduction in the VOC concentration**

Name of Compound	Inlet Concentration (mg/m^3)	Retention Time (minutes)	
		for 50%	for 90%
Benzene	17.9	10.67	33.5
Toluene	8.66	9.96	32.7
Ethyl Benzene	4.34	9.48	31.8
P, m -Xylene	4.2	9.4	31.0
o- Xylene	3.97	8.72	28.4

CONCLUSIONS

The developed reactor was found effective in degrading BTEX with the conversion efficiency for different VOCs in the order o-xylene (36.5%) > p,m- xylene (33%) > ethyl benzene (30%) > toluene (28%) > benzene (26%), with the limited residence time available in the reactor (5.48 min). It was found that 90 percent removal of BTEX could be achieved in about 28 to 33 minutes of run. Such a reactor can be used in situations where continuous streams of the gases are to be cleaned for VOCs. However, there is still room for more research to optimize the operational and design parameters for increasing the efficiency of the reactor.

REFERENCES

Burstyna, I., S. You, N. Cherry and A. Senthilselvan, 2007. “Determinants of airborne benzene concentrations in rural areas of western Canada”. *Atmospheric Environment*, 41: 7778–7787.

You, X., A. Senthilselvan, N.M. Cherry, H.G. Kim and I. Burstyn, 2008. “Determinants of airborne concentrations of volatile organic compounds in rural areas of Western Canada”. *Journal of Exposure Science and Environmental Epidemiology,* 18: 117-128.

Dutta, C., D. Som, A. Chatterjee, A.K. Mukherjee, T. K. Jana and S. Sen, 2009. “Mixing ratios of carbonyls and BTEX in ambient air of Kolkata, India and their associated health risk”. *Environmental Monitoring and Assessment*, 148: 97–107.

Fujishima, A. and X. Zhang, 2006. “Titanium dioxide photocatalysis: present situation and future approaches”. *Comptes Rendus Chimie*, 9: 750-760.

Jang, H.D., S. K. Kim and S.J. Kim, 2000. “Effect of particle size and phase composition of titanium dioxide nanoparticles on the photocatalytic properties”. *Journal of Nanoparticle Research,* 3: 141–147.

Shen, G.X., Y.C. Chen and C.J. Lin, 2005. “Corrosion protection of 316 L stainless steel by a TiO_2 nanoparticle coating prepared by sol–gel method”. *Thin Solid Films,* 489**:** 130 – 136.

Nguyen, H. T., I. Miao and S. Tanemura, 2004. “Structural and morphological characterization of anatase TiO_2 coating on χ-Alumina scale fiber fabricated by sol–gel dip-coating method”. *Journal of Crystal Growth,* 271: 245-271.

Mo, J., Y. Zhang, Q. Xu, J.J. Lamson and R. Zhao, 2009. “Photocatalytic purification of volatile organic compounds in indoor air: A literature review”. *Atmospheric Environment,* 43**:** 2229–2246.

Keshmiri, M.,T. Troczynski and M. Mohseni, 2006. “Oxidation of gas phase trichloroethylene and toluene using composite sol–gel TiO_2 photocatalytic coatings”. *Journal of Hazardous Materials,* B128: 130–137.

REDUCTIVE/OXIDATIVE DECOMPOSITION OF PERFLUOROOCTANE SULFONATE USING NZVI CONJUGATED WITH OXIDANTS

Wasiu A. Lawal and Hyeok Choi
(The University of Texas at Arlington, Arlington, TX, USA)

ABSTRACT: Perfluoroalkyl compounds (PFACs) are fluorinated surfactants which are widely used as fire retardants in the semiconductor, textiles and paper industries in addition to a number of other applications. These chemicals are non-biodegradable and have been found in various environmental matrices. There is a great need of innovative technologies to remediate PFACs-contaminated sites in situ. This present study investigates the decomposition of perfluorooctane sulfonate (PFOS), one of the most important PFACs, via advanced oxidation technologies (AOTs). We are testing the destruction of PFOS through Fenton processes which involves hydroxyl radicals and sulfate. Both radicals are generated in the presence of ferrous ions (Fe^{2+}) provided by nanoscale zerovalent iron (nZVI). nZVI was used as the source of Fe^{2+} as earlier studies have shown that it is more effective than regular ZVI in releasing the Fe^{2+} required for oxidation. This study shows that ferrous ions are indeed produced in solution by nZVI and that the amount produced increases over time starting from 15 minutes to at least 3 hours with detected concentrations ranging from 1.508mg/L to 4.859mg/L. Fluoride ions were also detected in the solution indicating the defluorination of PFOS. The detected fluoride concentrations ranged from 29.6µg/L to 113.0µg/L.

INTRODUCTION

Perfluoroalkyl compounds (PFACs) are substituted alkyl compounds with all the alky hydrogen atoms replaced by fluorine (Benford et al., 2008), as demonstrated in Figure 1 showing some representative PFACs; perfluorooctane sulfonate (PFOS) and perfluorooctanoic acid. PFACs are currently among one of the most studied chemicals in the field of environmental research as they have been recognized as emerging environmental pollutants (Takagi et al., 2008) Generally, PFACs are thermally and chemically stable (Benford et al., 2008; Skutlarek et al., 2006) and are able to resist processes such as hydrolysis and photolysis all due to the strength of the carbon-fluorine bond (Benford et al., 2008; Skutlarek et al., 2006; Takagi et al., 2008). These properties help make PFACs useful as liquid repellent coatings for textiles, carpeting, paper and leather (Benford et al., 2008; Martin et al., 2004; Skutlarek et al., 2006,)and also in firefighting foams (Benford et al., 2008; Martin et al., 2004; Taniyasu et al., 2003; Thompson et al.; 2011). The importance of these compounds that in 2000, their production in the United States alone reached about 6.5 million pounds (Takagi et al., 2008) and then there was an article published in 2010, which suggested that PFACs might be too useful for consumers and manufacturers to easily jettison (Ritter., 2010). The aforementioned properties, however, also mean that PFACs are also non-biodegradable and as such are recalcitrant which means that they have the ability to persist in the environment (soil, sediment and water).

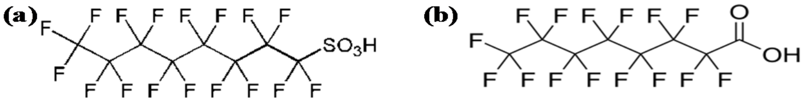

FIGURE 1. Molecular structure of (a) perfluorooctane sulfonate and (b) perfluorooctanoic acid.

ISBN 9780976885351

Numerous studies have detected PFACs in seawater, surface waters and even drinking water which obviously indicates a direct path of exposure to humans (Takagi et al., 2008; Skutlarek et al., 2006; Taniyasu et al., 2003; Thompson et al., 2011; Powley et al., 2005; Moody et al., 2003; Saito et al,. 2004; Hansen et al., 2002) and because of their physical/chemical properties (also mentioned earlier), these compounds cannot be removed by conventional water/wastewater treatment processes (Benford et al., 2008; Takagi et al., 2008; Thompson et al., 2011). It is therefore important that a method that decomposes PFACs to harmless or less toxic species at ambient conditions is developed.

Over time, many different technologies have reported for the decomposition of PFACs. Some techniques that have been employed involve photocatalysis, sonolysis and UV irradiation as well as subcritical conditions (Vecitis et al., 2009). While these aforementioned technologies had varying degrees of success, there are also implementation issues associated with them such as high energy requirements. Perfluorooctane sulfonate (PFOS) happens to be one of the most commonly encountered PFACs and as such, will be the focus of this paper from here on.

One process that can be potentially effective for the decomposition of PFOS is reductive dehalogenation. In many halogenated organic compounds, this process is mediated by free electrons and involves the replacement of the halogen atom with hydrogen (Agarwal et al., 2008; Zhang et al., 2006). ZVI particles have been widely used as an electron donor for the reaction (Lowry and Johnson 2004, Choi et al., 2008; Ghauch 2008) as shown below and nanoscale ZVI (nZVI) has been shown to have better kinetics than regular ZVI due to the increased surface area (Lowry and Johnson., 2004).

$$Fe^0 + R\text{-}X + H^+ \rightarrow Fe^{2+} + R\text{-}H + X^- \qquad (1)$$

Since PFOS is an emerging contaminant, extensive studies have not yet been reported on the electrochemical dehalogenation of it and other similar fluorinated compounds.

One major issue with simple reductive dehalogenation is that there is no further decomposition of the molecule after the halogens have been removed (Choi et al. 2008) which still leaves other unwanted byproducts. One possible solution to this is the addition of oxidants such as hydrogen peroxide, persulfate (PS) and peroxymonosulfate (PMS). In equation (1), Fe^{2+} ions are produced and the addition of these oxidants induces the Fenton or modified Fenton reaction as shown below:

$$Fe^{2+} + H_2O_2 \rightarrow Fe^{3+} + OH^{\cdot} + OH^- \qquad (2)$$

$$Fe^{2+} + HSO_5^- \rightarrow Fe^{3+} + SO_4^{\cdot -} + OH^- \qquad (3)$$

$$Fe^{2+} + S_2O_8^{2-} \rightarrow Fe^{3+} + SO_4^{\cdot -} + SO_4^{2-} \qquad (4)$$

The hydroxyl radicals (HRs, $OH^{\cdot}$) generated in equation (2) and the and sulfate radicals (SRs,$SO_4^{\cdot 2-}$) produced in equations (3) and (4) are highly reactive intermediates which then attack organic contaminants in water resulting in less toxic products (Brillas et al. 1998; Nfodzo and Choi., 2011a; Nfodzo and Choi., 2011b.).

The combination of the aforementioned reductive dehalogenation and oxidative pathways for the complete mineralization of PFOS is something that has not yet been extensively studied and therefore is the aim of this particular investigation.

MATERIALS AND METHODS

Materials: Perfluorooctane sulfonic acid, potassium peroxymonosulfate, potassium persulfate and hydrogen peroxide were purchased from Aldrich (St. Louis, MO). Nanoscale ZVI was purchased as reactive nanoscale iron particles (RNIP) from Toda America (Schaumburg, IL), regular ZVI from Aldrich (St. Louis, MO). HPLC grade methanol was obtained from Acros (New Jersey) and ultra-pure water was produced by a Milli-Q filtration system (Millipore; Billerica, MA). 1, 10-phenanthroline was obtained from LabChem Inc (Pittsburgh, PA). All materials were used as received.

Reaction procedure: The reactions were carried out in a 100mL batch reactor starting with 100µM of PFOS for all reactions. Control reactions were initially run using 50mM of each oxidant (Hydrogen peroxide, potassium peroxymonosulfate and potassium persulfate) just to confirm that no degradation occurs at this condition. The next set of tests involved nZVI and regular ZVI added to the reactor in the absence of oxidants and concentrations ranged from 1.5 to 15mM. This set of reactions was set up to compare the effectiveness of regular ZVI and nZVI and demonstrate the heterogeneous defluorination by reduction of PFOS using ZVI. The next step was to add oxidants to the reactor and this was done in 3 phases. First was to add each oxidant to solution containing PFOS just before adding ZVI and the second was to add oxidants 2 hours after adding ZVI. Third, was to repeat the first phase but this time using free ferrous ions instead of ZVI. Since there would not be any free electrons in this case, we would be able to roughly determine how much PFOS is decomposed by oxidation alone. The concentrations of ZVI and oxidants added were the same as those mentioned earlier. For each reactor that was set up, samples were collected initially and also at various time intervals (0.25, 0.5, 1, 2, 4, 6 and 8 hours) and excess methanol was added at each step to quench any radicals that might be in solution. Each sample was briefly vortexed and filtered using a 0.45µm syringe filter. Samples collected at each interval were split into three and sent for analysis. All reactions were conducted at ambient temperature.

Analyses: PFOS was analyzed using a high-performance liquid chromatography (HPLC, Agilent 1200 series) which included a quaternary pump and C18 column. The signal from a Shimadzu CDD-10AVP conductivity detector with ion suppressor (Shimadzu Scientific, Columbia MD) was transmitted to the Chemstation software for processing by an Agilent 35900E A/D interface (Agilent Technologies, USA). Sample elution was done via a gradient flow of acetonitrile with a solution of boric acid and sodium hydroxide. Concentrations of fluoride ions (to estimate the rate of defluorination) and sulfate ions were measured based on a procedure described in a separate study (Lee et al., 2010) with an ion-chromatograph system (DIONEX, ICS-3000) consisting of an automatic sample injector, a degasser, a pump, a guard column (Ion Pac AS4A Guard Column, DIONEX), a separation column (Ion Pac AS4A Analytical Column, water research), and a conductivity detector with a suppressor device. The mobile phase was an aqueous solution containing $NaHCO_3$ (1.7 mM), Na_2CO_3 (1.8 mM), and the flow rate was 2 mL/min. The LODs (S/N ¼ 3, injected at 50 mL) were 0.024 and 0.089 mg/L for F^- and SO_4^{2-} respectively. Ferrous ion was measured with a Shimadzu UV-2550 spectrophotometer using 1, 10-phenanthroline at a wavelength of 510nm. This method was adapted from the Standard Methods for the Examination of Water and Wastewater. For all of the above analyses, each sample was run in triplicate.

FIGURE 2. Nanosize zerovalent iron particles .

RESULTS AND DISCUSSION

Preliminary results show that there is some decomposition of PFOS in the presence of nZVI. As nZVI particles (shown in FIGURE 2 below) start to release Fe^{2+} into solution, free electrons are also available. These free electrons can then be accepted by the fluorine atoms on thus releasing free fluoride ions into the aqueous solution and these fluoride ions were tested for using ion chromatography.

Fluoride ion formation. Initial analysis run using 100µM PFOS alone showed no fluoride ions in solution but upon the addition of nZVI, some fluoride ions were detected at as little as 0 minutes (sample was taken as soon as nZVI was added). Samples taken after 15, 30, 60 and 120 minutes showed a general increase in the amount of fluoride in water with time which points to the fact that PFOS is being reductively defluorinated as time goes on. This is shown in FIGURE 3 below.

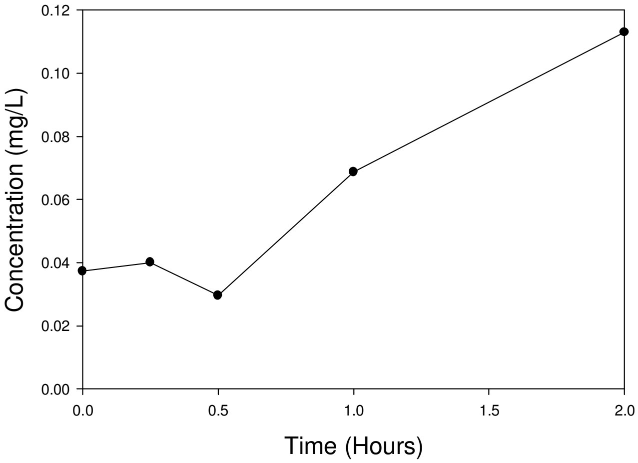

FIGURE 3 The appearance of Fluoride ions in solution over time.

The figure above shows that 0.0373 mg/L of fluoride is detected in solution as soon as nZVI is added and the fluoride concentration rises up to 0.1130 mg/L after 4 hours although there is a dip at 30 minutes which at this point cannot be explained until further studies are conducted.

Ferrous ion production: FIGURE 4 Below shows that while there were no detectable ferrous ions in solution at the very beginning, samples taken from minute 15 onwards showed a presence of Fe^{2+} (0.027 mM at 15 mins to 0.087 at 3 hours). This is significant for two reasons. First, the presence of ferrous ions indicates that there might be electrons available for onto the fluorine atoms on PFOS thus resulting in defluorination. Second is that the ferrous ions in solution can be used for the generation of hydroxyl or sulfate radicals thus leading to further degradation of PFOS.

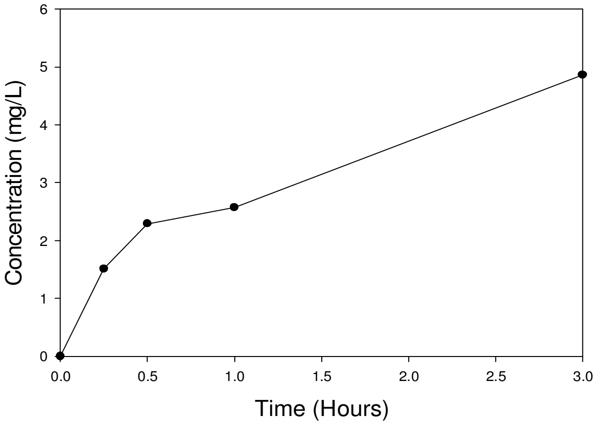

FIGURE 4 The appearance of ferrous ions in solution over time.

CONCLUSION

The preliminary results shown in this paper indicate that nanoscale zerovalent iron does have some effect on the decomposition PFOS at ambient conditions. The amount of fluoride found in solution is seen to increase with reaction time which strongly suggests a corresponding decomposition. Additional tests are required to confirm this using the HPLC and then the effects of oxidants which is an integral part of this study will also be very important.

ACKNOWLEDGEMENTS

Dr. Choi appreciates the financial support of the University of Texas at Arlington in the form of startup funds to initiate this study.

REFERENCES

Agarwal, S., S. R. Al-Abed, D. D. Dionysiou, and E. Graybill. 2008, "Reactivity of substituted chlorines and ensuing dechlorination pathways of select PCB congeners with Pd/Mg bimetallics", *Environmental science & technology,* vol. 43, no. 3, pp. 915-921.

Benford, D., J. d. Boer, A. Carere, d. A. Domenico, N. Johansson, D. Schrenk, G. Schoeters, d. P. Voogt, and E. Dellatte. 2008, "Opinion of the Scientific Panel on Contaminants in the Food chain on perfluorooctane sulfonate (PFOS), perfluorooctanoic acid (PFOA) and their salts", *EFSA Journal,* , no. 653, pp. 1-131.

Brillas, E., E. Mur, R. Sauleda, L. Sanchez, J. Peral, X. Domenech, and J. Casado. 1998, "Aniline mineralization by AOP's: anodic oxidation, photocatalysis, electro-Fenton and photoelectro-Fenton processes.", *Applied Catalysis B: Environmental,* vol. 16, no. 1, pp. 31-42.

Choi, H., S. R. Al-Abed, S. Agarwal, and D. D. Dionysiou. 2008, "Synthesis of reactive nano-Fe/Pd bimetallic system-impregnated activated carbon for the simultaneous adsorption and dechlorination of PCBs", *Chemistry of Materials,* vol. 20, no. 11, pp. 3649-3655.

Ghauch, A. 2008. "Rapid removal of flutriafol in water by zero-valent iron powder", *Chemosphere,* vol. 71, no. 5, pp. 816-826.

Hansen, K., H. Johnson, J. Eldridge, J. Butenhoff, and L. Dick. 2002, "Quantitative characterization of trace levels of PFOS and PFOA in the Tennessee River", *Environmental science & technology,* vol. 36, no. 8, pp. 1681-1685.

Lee, Y., S. Lo, P. Chiueh, Y. Liou, and M. Chen,. 2010, "Microwave-hydrothermal decomposition of perfluorooctanoic acid in water by iron-activated persulfate oxidation", *Water research,* vol. 44, no. 3, pp. 886-892.

Lowry, G.V. and K. M. Johnson. 2004, "Congener-Specific Dechlorination of Dissolved PCBs by Microscale and Nanoscale Zerovalent Iron in a Water/Methanol Solution", *Environmental science & technology,* vol. 38, no. 19, pp. 5208-5216.

Martin, J.W., K. Kannan, U. Berger, P. D Voogt, J. Field, J. Franklin, J. P. Giesy, T. Harner, D. C. G Muir, B. Scott, M. Kaiser, U. Jãrnberg, K. C. Jones, S. A. Mabury, H. Schroeder, M. Simcik, C. Sottani, B. V. Bavel, A. Kãrrman, G. Lindstrom, and S. V. Leeuwen, 2004, "Peer Reviewed: Analytical Challenges Hamper Perfluoroalkyl Research", *Environmental science & technology,* vol. 38, no. 13, pp. 248A-255A.

Moody, C.A., G. N. Hebert, S. H. Strauss, and J. A. Field. 2003, "Occurrence and persistence of perfluorooctanesulfonate and other perfluorinated surfactants in groundwater at a fire-training area at Wurtsmith Air Force Base, Michigan, USA", *Journal of Environmental Monitoring,* vol. 5, no. 2, pp. 341-345.

Nfodzo, P. and H. Choi. 2011a, "Sulfate Radicals Destroy Pharmaceuticals and Personal Care Products", *Environmental Engineering Science,* vol. 28, no. 8, pp. 605-609.

Nfodzo, P. and H. Choi. 2011b, "Triclosan decomposition by sulfate radicals: Effects of oxidant and metal doses", *Chemical Engineering Journal,* vol. 174, no. 2-3, pp. 629-634.

Powley, C. R., S. W. George, T. W. Ryan, and R. C. Buck. 2005, "Matrix effect-free analytical methods for determination of perfluorinated carboxylic acids in environmental matrixes", *Analytical Chemistry,* vol. 77, no. 19, pp. 6353-6358.

Ritter, S.K. 2010, "Fluorochemicals go short", *Chemical & engineering news,* vol. 88, no. 5, pp. 12-17.

Saito, N., K. Harada, K. Inoue, K. Sasaki, T. Yoshinaga, and A. Koizumi. 2004, "Perfluorooctanoate and perfluorooctane sulfonate concentrations in surface water in Japan", *Journal of occupational health,* vol. 46, no. 1, pp. 49-59.

Skutlarek, D., M. Exner, and H. Farber. 2006, "Perfluorinated surfactants in surface and drinking waters", *Environ Sci Pollut Res Int,* vol. 13, no. 5, pp. 299-307.

Takagi, S., F. Adachi, K. Miyano, Y. Koizumi, H. Tanaka, M. Mimura, I. Watanabe, S. Tanabe, and K. Kannan. 2008, "Perfluorooctanesulfonate and perfluorooctanoate in raw and treated tap water from Osaka, Japan", *Chemosphere,* vol. 72, no. 10, pp. 1409-1412.

Taniyasu, S., K. Kannan, Y. Horii, N. Hanari, and N. Yamashita. 2003, "A Survey of Perfluorooctane Sulfonate and Related Perfluorinated Organic Compounds in Water, Fish, Birds, and Humans from Japan", *Environmental science & technology,* vol. 37, no. 12, pp. 2634-2639.

Thompson, J., G. Eaglesham, J. Reungoat, Y. Poussade, M. Bartkow, M. Lawrence, and J. F. Mueller. 2011, "Removal of PFOS, PFOA and other perfluoroalkyl acids at water reclamation plants in South East Queensland Australia", *Chemosphere,* vol. 82, no. 1, pp. 9-17.

Vecitis, C. D., H. Park, J. Cheng, B. T. Mader, and M. R. Hoffmann. 2009, "Treatment technologies for aqueous perfluorooctanesulfonate (PFOS) and perfluorooctanoate (PFOA)", *Frontiers of Environmental Science & Engineering in China,* vol. 3, no. 2, pp. 129-151.

Zhang, C. H., H. J Wan, Y. Yang, H. W. Xiang, and Y. W. Li. 2006, "Study on the iron-silica interaction of a co-precipitated Fe/SiO2 Fischer-Tropsch synthesis catalyst", *Catalysis Communications,* vol. 7, no. 9, pp. 733-738.

ENHANCING SELECTIVE OXIDATION OF TARGET POLLUTANTS USING TiO_2 PHOTOCATALYST

Abolfazl Zakersalehi and Hyeok Choi
(The University of Texas at Arlington, Arlington, TX, USA)

ABSTRACT: Recently, the photocatalytic decomposition of water contaminants using TiO_2 photocatalyst has been of great interest due to its effectiveness and green properties. In spite of numerous advantages of TiO_2 photocatalyst, TiO_2-based reactions suffer from non-selective decomposition of organic compounds which contribute to significant reduction in their effectiveness, particularly in the presence of other competing compounds. Controlling porous structure of TiO_2 nanoparticles is one of the proposed approaches for enhancing selective oxidation, which has not been properly highlighted in previous studies. In this study, the effect of porous structure of TiO_2 nanoparticle, or more specifically size exclusion mechanism, on selective decomposition of ibuprofen (2-[4-(2-methylpropyl) phenyl]propanoic acid), as a model target compound, in the presence of humic acids as competing compounds was investigated. Porous structure of TiO_2 nanoparticles was tailor-designed via sol-gel method employing different molar ratios of polyoxyethylen sorbitant monooleate (Tween 80) as a pore-directing agent. The results from photodegradation experiments show that the size exclusion strategy was effective for enhanced selectivity.

INTRODUCTION

In recent years, the treatment of water contaminants employing advanced oxidation technologies (AOTs) has attracted a great attention. The ability of AOTs to completely degrade highly persistent pollutants including emerging chemicals of concern (ECCs) have made AOTs promising for water and wastewater treatment. AOTs are particularly useful in removing emerging compounds such as endocrine disrupting compounds, and pharmaceutical and personal care products that are not completely degraded in conventional water and wastewater treatment processes (Choi *et al*., 2006.b). AOTs involve processes that generate strong transient oxidizing species such as hydroxyl radicals (HRs). Among AOTs, TiO_2 photocatalysis is of particular interest due to its green properties and effectiveness. The activation of TiO_2 with UV radiation produces HRs which can attack and mineralize most organic contaminants (Munter, 2001). However, due to the non-selective nature of HRs, the presence of competing organic compounds such as natural organic matter (NOMs) and humic acids (HAs) can significantly decrease the effectiveness of TiO_2-UV system (Liu et al., 2008; Lin et al. 2007). Though several studies have been conducted on TiO_2-based AOTs, relatively few reports are available on enhancing selective decomposition by TiO_2 nanoparticles. Considering the heterogeneous nature of photocatalytic reactions, controlling the preferential adsorption of target compound onto TiO_2 surface is key to efficiently adsorb and decompose target compounds. As illustrated in Figure 1, a practical approach for enhancing selective adsorption of target compounds is based on the size exclusion mechanism. In this approach, porous structures of TiO_2 nanoparticles are strategically designed so that only favorable chemicals are allowed to enter the porous network of particles.

It has been demonstrated that modification of sol-gel method by introducing self-assembly agents can enhance controllability of TiO_2 porous structure (Guo et al., 2009; Yoshitake et al. 2002). In this method, a self-assembly agent (such as surfactant) acts as a template for titania precursor. The templates are later removed during the thermal treatment, leaving behind a porous network of titania. Previous studies showed that, changing surfactant type and concentration effectively changes the pore size and porosity of titania network (Choi et al. 2006.a), which can be an effective way for tailor-designing

ISBN 9780976885351

particles with controlled porosity and consequently selective adsorption. Our research focuses on enhancing the selectivity of engineered TiO_2nanoparticles using ibuprofen (2-[4-(2-methylpropyl) phenyl]propanoic acid) (IBP) and HAs as model target and competing compounds respectively. IBP has a molecular size (206 g/mole) which is close to the molecular size of many of ECCs. The Aldrich HA which has a high molecular size was selected as competing compound to demonstrate the effect of molecular size on selective adsorption/degradation. Both target and competing compounds were of similar hydrophilicity to minimize the effect of other adsorption parameters. In order to obtain further insight into adsorption mechanism, different fractions of HAs with different molecular sizes were used in each set of experiment.

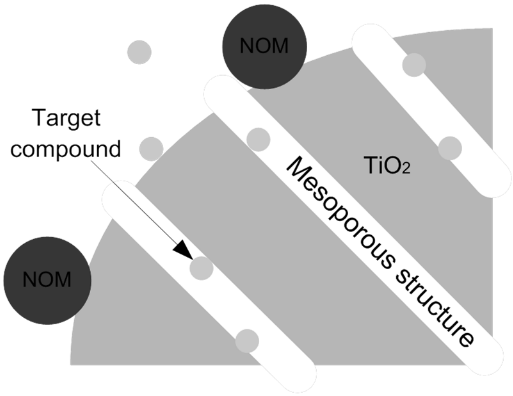

FIGURE1. Size exclusion mechanism on TiO_2. Due to small size of porous structure which provides most of active adsorption sites, large molecules such as NOM are excluded from the adsorption while small target chemicals freely enter the porous structure followed by chemical reaction

MATERIALS AND METHODS

Materials: Ibuprofen, humic acid, Polyoxyethylenesorbitan monooleate (Tween 80) surfactant, isopropyl alcohol (iPrOH,) titanium tetraisopropoxide (TTIP) and HPLC grade acetonitrile (ACN) were purchased from Sigma-Aldrich Company and were used as received.

Synthesis of TiO_2 Nanoparticles: Procedure for the synthesis of TiO_2 nanoparticles previously reported by Choi et al. 2006.a was adopted with slight modifications to synthesize three different types of TiO_2 nanoparticles. For each set of particles, considering surfactant content (R), appropriate amount of Tween 80 was dissolved in isopropanol. Acetic acid was then added for esterification reaction with alcohol, after which TTIP was added and stirred. For obtaining particles, sol was sprayed on a petri dish and dried at room temperature for 12 hours, t heat-treated and calcinated at a ramp rate of 3 °C/min up to 500 °C, maintained at this temperature for 120 minutes, and cooled at room temperature. The high temperature removes all organics including templating agents. The film was scraped and sieved to achieve three sets (P_1 R=0, P_2 R=1, P_3 R=3) of TiO_2 nanoparticles.

Photocatalytic Degradation Experiment: The photocatalytic experiments were conducted in batch reactors at ambient temperature. The 50 ml Petri dishes were placed inside UV chamber (Blak-Ray, HG-UV lamps) and continuously agitated using a magnetic stirring bar throughout the irradiation time. TiO_2 loading was adjusted to 0.5 g/L for all of the batches and IBP with initial concentration of 12 mg/L was used in experiment. In the batches with HAs, the initial concentration of HAs was same as IBP concentration (12 mg/L).

Analytical Methods: Samples were taken at 30 minutes intervals and filtered through 0.45 µm syringe filters to remove TiO_2 nanoparticles. Concentration of IBP was monitored using a reversed-phase high performance liquid chromatography (1200 series, Agilent) equipped with ultraviolet (UV) detector. A mixture of phosphoric acid buffer and acetonitrile was used as the mobile phase at buffer:ACN ratio of 50:50% v/v The UV detector was set at a wavelength of 214 nm for detection of IBP.

RESULTS AND DISCUSSION

The adsorption of species was correlated with their molecular size and interaction with the porous structure of TiO_2 nanoparticles. Figure 2 shows molecular structure of IBP and typical structure of HAs.

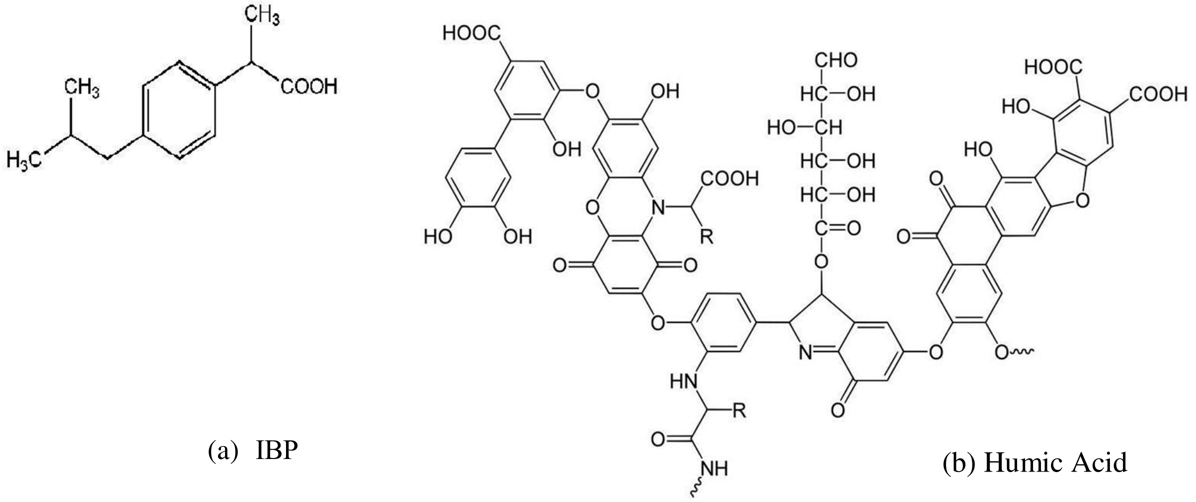

(a) IBP

(b) Humic Acid

FIGURE2. a) Molecular structure of Ibuprofen with molecular weight of 206 g/mole. b) Typical molecular structure of humic acid with molecular weight of many thousands g/mole

As shown in Figure 2(a), IBP has a relatively smaller molecular size which facilitates its penetration into mesoporous structure of TiO_2 followed by its photocatalytic degradation. Thus the porous structure of synthesized particles should be precisely designed so that competing compounds could be effectively retained on the outer surface of particles.

The selectivity of synthesized particles was evaluated through comparison of their photoactivity in the batches with and without HAs. Particles with the highest selectivity, exhibit the lowest decline in photocatalytic degradation of IBP. As shown in Figure 3(a), photocatalytic activity of particles with non-porous structure (P_1) significantly decreased when HAs are present. In this case, the degradation of IPB reduced from 62% to 15 % after 1 hr reaction time (more than 4 times reduction in photo-activity). This phenomenon can be attributed to the degradation of competing HAs.

Figure 3(b) shows photocatalytic degradation of IBP using mesoporous TiO_2 nanoparticles with targeted pore size of 2-6 nm (P_2). In spite of significant decline observed in non-porous particles, photocatalytic activity shows milder decline using mesoporous particles. In this case overall photocatalytic degradation of IBP decreases from 88% to 41% when HAs are present. Increasing pore size to 5-11 nm (P_3) results in a reduction in overall degradation but contributes to higher selectivity (39% degradation in the presence of HAs compared to 71% using pure IBP solution) as shown in Figure 3(c). The results confirm the dependency of specific adsorption of compounds on their molecular size. It is also notable that, regardless of selectivity, overall photoactivity was enhanced in the case of porous TiO_2 particles, which can be correlated to increase in active sites for photocatalytic activity.

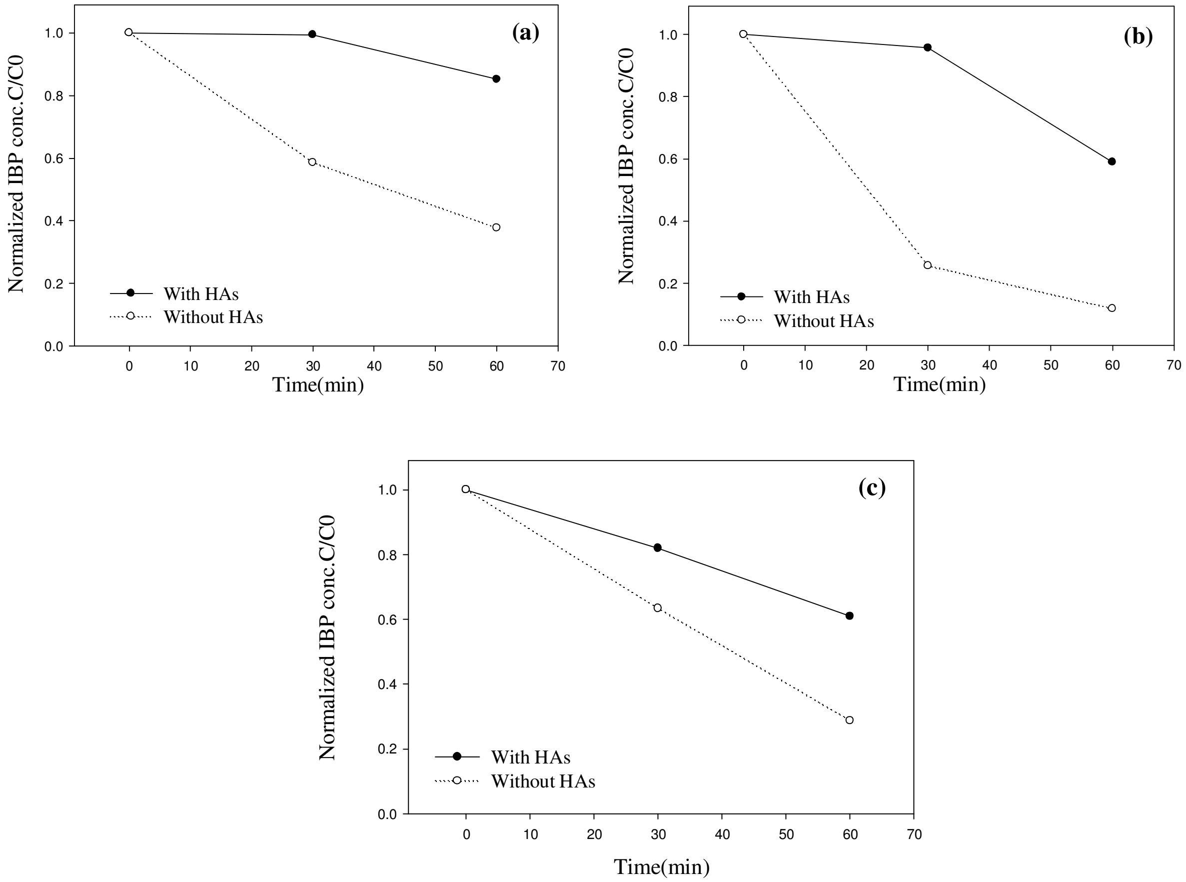

FIGURE3. a) IBP decomposition using P_1 non-porous, control particles. b) IBP decomposition using P_2 meso-porous particles. c) IBP decomposition using P_3 meso-porous particles.

CONCLUSION

This study has demonstrated the important role of size exclusion mechanism in adsorption process and the practical usefulness for enhancing selectivity of TiO_2 nanoparticles. It is also notable that, although these results are for specific target and competing compounds, it is expected to be applicable for a broad range of compounds with similar molecular size, considering the significant role of size-exclusion mechanism in preferential adsorption. A detailed study is being conducted to optimize the porous structure of synthesized particles for this special case and also parallel experiments are being conducted to evaluate the effectiveness of synthesized particles for other target compounds. Studies also will be conducted to maximize the selectivity by coupling the size exclusion approach with other proposed approaches.

ACKNOWLEDGEMENTS

Dr. Choi appreciates the financial support of the University of Texas at Arlington in form of startup fund to initiate this study.

REFERNCES

Choi, H., A. C. Sofranko and D. D. Dionysiou. 2006.a. “Nanocrystalline TiO_2 Photocatalytic Membranes with a Hierarchical Mesoporous Multilayer Structure: Synthesis, Characterization, and Multifunction” . *Adv. Funct. Mater.*, 16(8):1067–1074.

Choi, K. J., S. G. Kim, C. W. Kim, and J. K. Park. 2006.b. “Removal efficiencies of endocrine disrupting chemicals by coagulation/flocculation, ozonation, powdered/granular activated carbon adsorption, and chlorination.” . *Korean J. Chem. Eng.*, 23(3):399-408.

Choi, H., E. Stathatos, D. D. Dionysiou. 2006. “Synthesis of nanocrystalline photocatalytic TiO_2 thin films and particles using sol – gel method modified with nonionic surfactants”. *Thin Solid Films.,* 510(1-2):107 – 114.

Guo, B., H. Shen, K. Shu, Y. Zeng and W. Ning. 2009. “The study of the relationship between pore structure and photocatalysis of mesoporous TiO_2”. *J. Chem. Sci.,* 121(3):317–321.

Idrissi-Kandri, N., A. Ayral, M. Klotz, P.A. Albouy, A. Mansouri, A. V. D. Lee and C. Guizard. 2001. “Porous alumina thin layers using mesophase templating”. *J. Mater. Sci.,* 50(2-3):57-60.

Kitazawa, N. , K. Sakaguchi, M. Aono and Y. Watanabe. 2003. “Synthesis of mesostructured titanium dioxide films by surfactant-templated sol-gel method”. *J. Mater. Sci.,* 38(14):3069-3072.

Liu, G. J., X. R. Zhang, L. Mcwilliams, J.W. Talley and C.R. Neal. 2008. “Influence of ionic strength, electrolyte type, and NOM on As(V) adsorption onto TiO_2”. *J. Environ. Sci. Health,* 43(4):430–436.

Lin, C., K. S. Lin. 2007. “Photocatalytic oxidation of toxic organohalides with TiO_2/UV:The effects of humic substances and organic mixtures”. *Chemosphere,* 66(10):1872–1877.

Munter, R.. 2001. “Advanced Oxidation Processes-Current Status and Prospects”. *Proc. Estonian Acad. Sci. Chem.,* 50(2):59–80.

Yoshitake, H., T. Sugihara and T. Tatsumi. 2002. “Preparation of wormhole-like mesoporous TiO_2 with an extremely large surface area and stabilization of its surface by chemical vapor deposition”. *Chem. Mater.,* 14(3):1023–1029.

PHOTOCATALYTIC DEGRADATION OF 17β-ESTRADIOL UNDER SOLAR IRRADIATION

Cheng-Ling Hu, Wei-Fu Wang and Yung-Hsu Hsieh
(National Chung Hsing University, Taichung, Taiwan)

ABSTRACT: Natural steroid 17β-estradiol (E2) is one of endocrine disrupting chemicals (EDCs). Estrogenic steroids are detected in both the influent and effluent of sewage treatment plants in different countries at various concentrations. Among the various environmental degradation processes (abiotic/ biotic), photodegradation under solar irradiation is one of the most important factors for determining the ultimate fate of the persistent pollutants in aquatic environments. In this research, TiO_2 prepared by sol-gel method achieve nano particle size about 30 nm can improve photodegradation rate constant of E2. Photocatalytic degradation of E2 by TiO_2 under solar irradiation can increase rate constant (k = 2.20-2.42 hr^{-1}) and mineralization (65-95% after 5 hr irradiation). The E2 photodegradation followed pseudo-first-order kinetics, with the rate constant increasing slightly with increased pH. In the presence of NO_3^-, the photodegradation rate increased significantly, attributed to photosensitization by the reactive species.

INTRODUCTION

The present of low concentration of EDCs in the environment has been reported over the last 30 years (Tabak, Bloomhuff, and Bunch 1981; Baronti et al. 2000). However, EDCs have been detected over the past decade in effluents of domestic sewage treatment plant in many countries (Nasu et al. 2001). It effects reproduction and development in wildlife, especially in ecosystem stability and balance (Hayes et al. 2002).

17β-estradiol (E2) is one of the natural steroid, has activity in low concentration (about 10^{-9} M) (Arnold et al. 1996). The E2 released about 60μg per day from women to aquatic environment, and up to 200 to 400 μg in pregnancy period (Adlercreutz et al. 1986). Therefore, reducing the concentration of EDCs in environment is currently as a decisive stage.

Semiconductor photocatalysis, one of advanced oxidation processes, combined with UV light has been developed rapidly in recent decades (Ohko et al. 2002; Brugnera et al. 2010). Titanium dioxide was widely used on liquid and gas advanced oxidation processes because of its advantages about non-toxic, light stability, inexpensive and low water solubility, etc. Hydroxyl radical, a strong oxidant, produced by the photocatalytic processes and applied to oxidize organic matter in air or water, can achieve the degradation and mineralization (Ohko et al. 1998; Fujishima, Rao, and Tryk 2000).

In this study, we explore the factors of natural water parameters and reaction kinetics on solar photocatalytic degradation of E2, and then infer the fate of E2 in this degradation system.

MATERIALS AND METHODS

Standard and Sample Preparation. Stock solutions (1 mM) of E2 ($C_{18}H_{24}O_2$, Sigma-Aldrich, ≥ 98 %) were prepare by dissolving an appropriate amount of E2 and 0.25 M NaOH (Sigma-Aldrich, ≥ 97.0 %) in super purified water in 500 mL volumetric flask by stirring overnight to ensure complete dissolution. The

---

ISBN 9780976885351

stock solutions were filtered by 0.22 μm pore size filter and stored at 4 °C. All experiments were used NaOH or HCl to adjust the pH.

Preparation of TiO_2 . TiO_2 powders were synthesized with the sol-gel method by mixing 40 mL Titanium (IV) isopropoxide (TTIP, $Ti[OCH(CH_3)_2]_4$, Acros, $\geq$ 98 %), 20.5 mL 2-Propanol (IPA, C_3H_7OH, Mallinckrodt chemicals, 99.5 %) and 61.2 mL acetic acid (CH_3COOH, J. T. Baker, 98 %) in 125 ml flask, and parafilm was used to prevent water vapor losing and stirred 24 hr. The gel was treated hydrothermally at 120 °C for 12 hr without stirring and calcined at 500 °C for 24 hr. The resulting powder was grinded by agate mortar.

Photocaltalytic Degradation Experiments. All experiments were used solar irradiation at Taiwan, located at 24 degrees north latitude. The batch system during photocatalytic degradation in 1 L Pyrex reaction bottle with thin glass cover to prevent contamination, irradiated solar without shelter. The initial E2 concentration was 10 μM for all experiments, and sampled 12 mL at time series.

Analytical Methods. The concentration of E2 in aqueous solutions was determined with fluorescence spectrophotometer FP-6200 (Jasco, Japen) in a 1-cm quartz cuvette. The peak intensities on condition λ_{ex}=280 nm and λ_{em}=308 nm have a good liner relation with concentration of E2 (R^2=0.9995, 0.02 μM to 12 μM). Total organic carbon (TOC) was measured by Shimadzu TOC-V_{CSN} analyzer with an ASI-V auto sampler, and the pH was measured using a Melter pH meter (SevenEasy pH S20).

TiO_2 surface characters were analyzed by field emission scanning electron microscope (FE-SEM, JEOL JSM-7041F, Japan) and high resolution X-ray diffractometer (HRXRD, BRUKER D8 Discover SSS, Germany), respectively.

RESULTS AND DISCUSSION

Analysis of Tio_2 Surface. The surface of TiO_2 particles is uniform and average particle size is 30 nm shown in Fig. 1a. The crystal of TiO_2 prepared by sol-gel method content 88.6% anatase and 11.4% rutile (show in Fig. 1b.). Higher ratio of anatase presents higher photoactivity and smaller crystal size achieves higher contact area. It is reasonable to indicate that TiO_2 was successfully prepared.

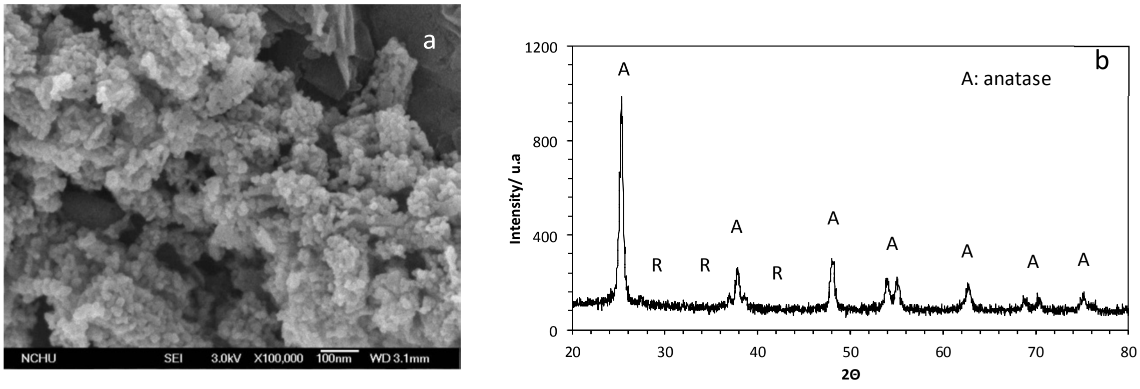

FIGURE 1. SEM image (a) and XRD pattern (b) of TiO_2 prepared by sol-gel method.

Kinetics of Solar Photocatalysis of E2 In Aqueous Solution. In the experimental period, control experiment without TiO_2 was irradiated under solar for 5 hr and sampled at the same time serial. The kinetic experiments were carried out with an initial E2 concentration of 10 μM at pH 7.0 ± 0.1, and with 0.5 g/L TiO_2 or absence conditions. All results show in Fig. 2, indicating the photocatalysis degradation of E2 in aqueous solution under solar irradiation followed pseudo-first-order kinetics. There was no evidence of E2 degradation at ambient condition in the absence of TiO_2.

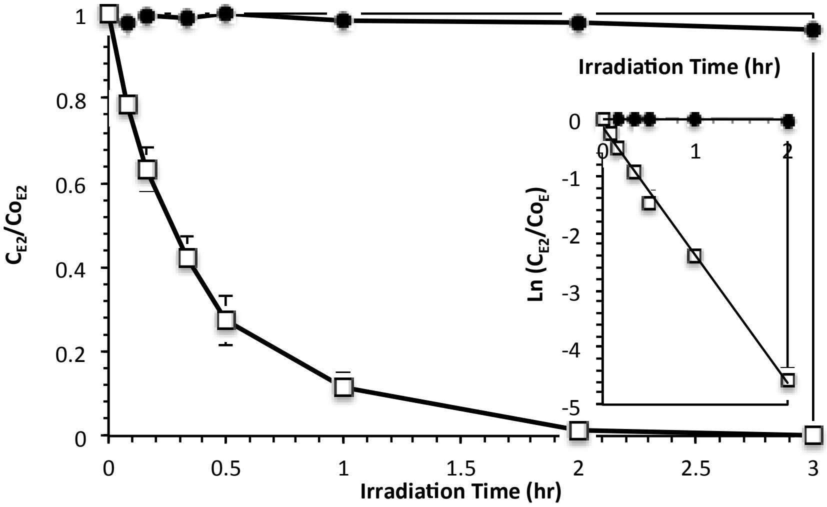

FIGURE 2. Photodegradation of E2 in aqueous solution under solar irradiation. All solution were adjusted initial pH at 7. Direct photolysis degradation of E2 without TiO_2 (circles) and photocatalysis degradation of E2 with 0.5 g/L TiO_2 (square).

E2 has absorption over 265-385 nm (Chowdhury, Charpentier, and Ray 2011) and present in nature solar irradiation only 7.8% in UV-A and UV-B region (Gibson), therefore the direct photodegradation of E2 has lower rate constant ($k = 0.004\ hr^{-1}$) and longer half-life time (t = 6.7 days). The addition of TiO_2 can improve the kinetic rate due to OH radicals produced by the H_2O and holes of TiO_2 separated when absorb UV wavelength energy. It exists a higher rate constant ($k = 2.1 \pm 0.2\ hr^{-1}$) and shorter half-life time (t = 20 min). After 2 hr irradiation, the concentration of E2 was not detected in aqueous solution.

Influence of pH. The pH of aqueous solution is one of the important parameter affecting the solar photocatalytic degradation in natural environment. To understand the effect of pH on photodegradation, experiments were conducted by adjusting pH at 6, 7, 8, and 9 respectively, using solar irradiation at the same time with 0.5 g/L TiO_2. Fig. 3 shows the rate constants of E2 photodegradation in different pH under solar irradiation with 0.5 g/L TiO_2. Photocatalytic degradation rate constant of E2 is slightly higher in basic condition. Due to the photocatalytic system, the holes of TiO_2 produce OH radical and H^+ ions neutralizing by hydroxyl ions (OH^-) (see equation [1] and [2]). Higher H^+ concentration, decreases the rate of OH radical production. Therefore, higher pH condition would increase the photocatalytic oxidation. In addition, the rate constant of E2 under direct photolysis is higher in high pH aqueous solution (Chowdhury, Charpentier, and Ray 2011). The pH above the pk_a of E2, the phenol group of E2 structure would form phenoxide ions, increasing the degradation rate.

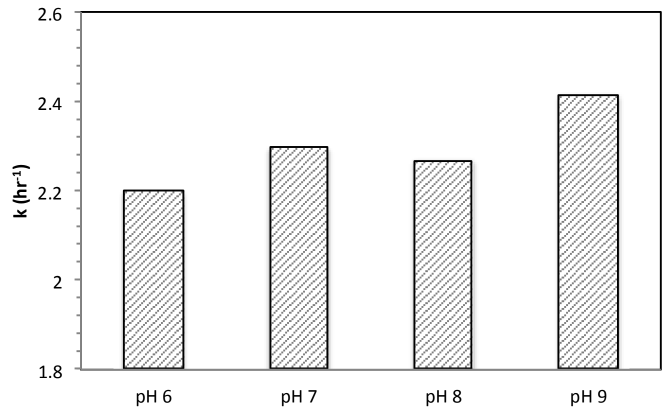

FIGURE 3. Rate constant of E2 photocatalytic degradation with 0.5 g/L TiO_2 in different pH.

$$TiO_2 \overset{hv}{\rightarrow} TiO_2(e_{cb}^{-} + h_{vb}^{+}) \quad [1]$$

$$TiO_2(h_{vb}^{+}) + H_2O \rightarrow TiO_2 + H^{+} + OH^{\cdot} \quad [2]$$

Influence of NO_3^-. Nitrate is generally present in natural aqueous system at different concentration depending on geographic location (Shankar et al. 2007). The experiments were conducted based on several nitrate concentrations between 4 and 40 μM. The source of nitrate was from nitrate acid and pH was adjusted to 7 using HCl and NaOH. As results show in Fig. 4, the experiments content nitrate of 30 μM and 40 μM have higher rate constant (k = 2.67 hr^{-1}) and shorter half time (t = 16 min). The present of nitrate can improve the photocatalytic degradation rate. It is well known that nitrate produces OH radical when irradiated at wavelengths between 290 and 330 nm (Nélieu et al. 2004).

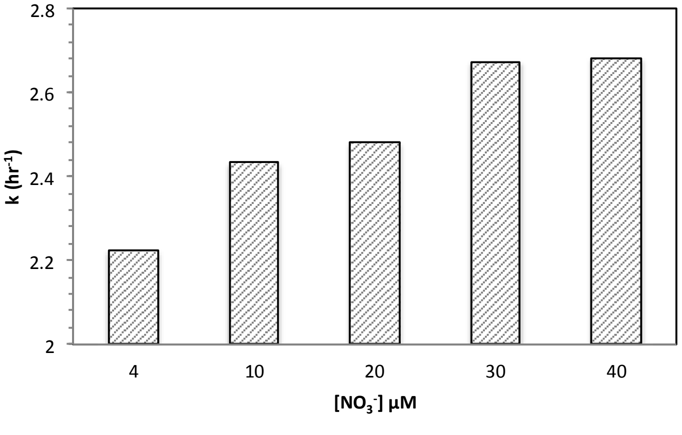

FIGURE 4. Rate constants of E2 photocatalysis degradation in different nitrate concentration. All experiments were conducted by adjusting initial pH at 7.

Mineralization. By-product is an important issue in the fate of environmental pollutants, which may cause more toxicity than parent pollutants. In order to quantify the mineralization of E2 in photocatalytic system, we use TOC value to estimate the amount of organic by-product produced during photocatalytic degradation of E2. The results are presented in Table 1. The TOC removal is slightly higher at high pH condition based on the more OH radical produced. In the presence of nitrate, TOC removal increases 34% even up to 100% removal, attributed to photosensitization by the reactive species.

CONCLUSIONS

The surface of TiO_2 powder prepared by sol-gel method can achieve nano particle size and anatase crystal. TiO_2 photocatalysis has higher kinetic rate of E2 degradation than direct photolysis. When the concentration of E2 is 10 μM under solar irradiation, the presence of TiO_2 has decreased the half-life time from 6.7 days to 18 min and mineralization achieved to 71% after 5 hr irradiation. In the presence of nitrate, slightly high kinetic rate constant and mineralization were observed.

TABLE 1. Mineralization of E2 at different parameters by photocatalytic degradation with 0.5 g/L TiO_2 after 5 hr solar irradiation.

pH	**Nitrate (μM)**	**TOC Removal %**
6	0	65
7	0	71
8	0	95
9	0	87
7	4	94
7	10	88
7	20	100
7	30	95
7	40	100

ACKNOWLEDGEMENTS

We thanks for Instrument Center of National Chung Hsing University for FE-SEM, XRD, and BET analysis.

REFERENCES

Adlercreutz, H., T. Fotsis, C. Bannwart, Hämäläinen E., S. Bloigu, and A. Ollus. 1986. Urinary estrogen profile determination in young finnish vegetarian and omnivorous women. *Journal of Steroid Biochemistry* 24 (1):289-296.

Arnold, Steven F., Diane M. Klotz, Bridgette M. Collins, Peter M. Vonier, Louis J. Guillette Jr, and John A. McLachlan. 1996. Synergistic Activation of Estrogen Receptor with Combinations of Environmental Chemicals. *Science* 272 (5267):1489-1492.

Baronti, Chiara, Roberta Curini, Giuseppe D'Ascenzo, Antonio Di Corcia, Alessandra Gentili, and Roberto Samperi. 2000. Monitoring Natural and Synthetic Estrogens at Activated Sludge Sewage Treatment Plants and in a Receiving River Water. *Environmental Science & Technology* 34 (24):5059-5066.

Brugnera, Michelle Fernanda, Krishnan Rajeshwar, Juliano C. Cardoso, and Maria Valnice Boldrin Zanoni. 2010. Bisphenol A removal from wastewater using self-organized TIO2 nanotubular array electrodes. *Chemosphere* 78 (5):569-575.

Chowdhury, Rajib Roy, Paul A. Charpentier, and Madhumita B. Ray. 2011. Photodegradation of 17β-estradiol in aquatic solution under solar irradiation: Kinetics and influencing water parameters. *Journal of Photochemistry and Photobiology A: Chemistry* 219 (1):67-75.

Fujishima, A., Tata N. Rao, and D. A. Tryk. 2000. TiO2 photocatalysts and diamond electrodes. *Electrochimica Acta* 45 (28):4683-4690.

Gibson, J. H. UVB radiation: definition and characteristics.

Hayes, Tyrone B., Atif Collins, Melissa Lee, Magdelena Mendoza, Nigel Noriega, A. Ali Stuart, and Aaron Vonk. 2002. Hermaphroditic, demasculinized frogs after exposure to the herbicide atrazine at low ecologically relevant doses. *Proceedings of the National Academy of Sciences of the United States of America* 99 (8):5476-5480.

Nasu, M., M. Goto, H. Kato, Y. Oshima, and H. Tanaka. 2001. Study on endocrine disrupting chemicals in wastewater treatment plants. *Water Science & Technology* 43 (2):101-108.

Nélieu, S., L. Kerhoas, M. Sarakha, and J. Einhorn. 2004. Nitrite and nitrate induced photodegradation of monolinuron in aqueous solution. *Environmental Chemistry Letters* 2 (2):83-87.

Ohko, Yoshihisa, Ken-ichiro Iuchi, Chisa Niwa, Tetsu Tatsuma, Tetsuto Nakashima, Taisen Iguchi, Yoshinobu Kubota, and Akira Fujishima. 2002. 17β-estradiol degradation by TiO2 photocatalysis as a means of reducing estrogenic activity. *Environmental Science & Technology* 36 (19):4175-4181.

Ohko, Yoshihisa, Donald A. Tryk, Kazuhito Hashimoto, and Akira Fujishima. 1998. Autoxidation of Acetaldehyde Initiated by TiO2 Photocatalysis under Weak UV Illumination. *The Journal of Physical Chemistry B* 102 (15):2699-2704.

Shankar, M. V., S. Nélieu, L. Kerhoas, and J. Einhorn. 2007. Photo-induced degradation of diuron in aqueous solution by nitrites and nitrates: Kinetics and pathways. *Chemosphere* 66 (4):767-774.

Tabak, H. H., R. N. Bloomhuff, and R. L. Bunch. 1981. Steroid hormones as water pollutants. II. Studies on the persistence and stability of natural and synthetic ovulation-inhibiting hormones in untreated and treated wastewaters. *Develoment in Industrial Microbiology* 11:497-519.

DEGRADATION OF REFRACTORY POLLUTANTS USING CARBON-IRON MODIFIED TITANIA UNDER NATURAL SUN-LIGHT

K. Palanivelu and R. Jeevitha Raji
(Centre for Environmental studies, Anna University, Chennai-600025, India)

ABSTRACT: NanoTiO_2 was synthesized by ultrasonication assisted sol-gel process doped with carbon in 1:0.1 w/w ratio using natural coconut oil as carbon precursor and subjected to C-Fe codoping with ferrous sulphate as iron precursor. The characterization of the pure, carbon doped and C-Fe codoped TiO_2 catalysts were accomplished by XRD, BET, HR-SEM and EDS analysis. The characterization reveals the presence of anatase form of titania in both the pure and modified catalysts and the average size of the pure TiO_2 catalyst was found to be in the range of 90 nm with a large specific surface area of 180 m^2/g. In the solar photoactivity studies, the degradation of dye pollutants was evaluated by the degradation of a cationic dye, methylene blue, and an anionic dye, methyl orange. In the case of solar photocatalyic oxidation with the pure and C-TiO_2, the cationic non-azo dye, methylene blue was found to be decolorized at a faster rate than the anionic azo dye, methyl orange. Whereas interestingly, in the case of the solar photo-Fenton's oxidation with C-Fe TiO_2, a complete and rapid decolorization of the anionic azo dye was acheived in 15 min when the experiments were conducted at acidic pH.

INTRODUCTION

Textile dyeing industries are now the major source of pollution which release various organic dyes in the effluent and many of the dyes are considered to be carcinogenic by U. S. regulatory agencies and thus textile wastewater put forward a serious threat not only to the human population but to the entire biosphere. The increased public concern with these dyes and the stringent international environmental standards (ISO 14001) necessitate the development of novel, advanced and reliable technologies for converting these organic dyes to harmless compounds (Tsumura et al., 2002; Inagaki et al., 2003). In this sense, photocatalysis is a rapidly emerging and promising technology coming up with clean, green and sustainable innovation in environmental applications (Wong et al., 2004) and titanium(IV) dioxide (TiO_2) is the most widely used photocatalytic semiconductor, because of its superior physical and chemical properties (Seery et al., 2007). Enormous research works have been carried out on TiO_2 photocatalysis under artificial UV light sources and found successful. But those light sources depend on fossil fuels which pose several drawbacks since they are non-renewable and are likely not to continue to remain abundant for the next generations. One of the possible solutions to the energy challenge is to make efficient use of solar energy, which is abundant, long lasting and clean. In the case of TiO_2, though it acts as an efficient photocatalyst, its wide band gap restricts solar applications. To enhance the photoactivity of TiO_2 and broaden the absorption to solar spectrum, a number of attempts have been made to change its physical and chemical porperties by metal/non-metal doping as it extends the optical absorption of the catalyst to the visible spectral region (Xiao et al., 2006).

India is endowed with rich solar energy resource since it is located in the equatorial sun belt of the earth with about 300 clear sunny days in a year. The daily average solar luminance over India varies from 32,000 LUX to 1,20,000 LUX with about 2,300–3,200 sunshine hours per year, depending upon location. This is far more than current total energy consumption. Thus the present study aimed to utilize the natural, abundant and renewable solar source for the photocatalytic degradation of refractory pollutants. The study involved the synthesis of nano-sized titanium dioxide in a more economical way and making it solar active by tailoring the properties by doping with carbon and codoping with carbon and iron (Fe^{2+}). The solar photoactivity of the carbon doped and carbon-iron codoped catalysts was then

---

ISBN 9780976885351

monitored by the decolorization of a cationic dye, methylene blue and an anionic dye, methyl orange in the presence of natural sunlight.

MATERIALS AND METHODS

Preparation of Pure, Carbon doped and carbon-iron codoped TiO_2. Undoped TiO_2 was prepared by ultra sonication assisted sol-gel process with titanium isopropoxide as the titania precursor. The calcination of TiO_2 was carried out at low temperature in the range of 80 ^{0}C – 150 ^{0}C for 12 h in a hot air oven to provide an economical way of calcination and also to prevent the agglomeration of TiO_2 particles through sintering thus avoiding the formation of rutile phase (Jeevitha Raji and Palanivelu 2011). The as-synthesized undoped titania was then designated as "Pure TiO_2".

A portion of it was then taken for carbon modification using coconut oil as carbon precursor. In the preparation procedure, the carbon source was added to titania in the w/w ratio of 1 : 0.1 and subjected to thermal treatment at 250 ^{0}C till there were no fumes in closed environment. It was subsequently subjected to microwave irradiation for 1 h in medium-high mode using a domestic microwave oven to augment the crystallinity of the catalyst particles[16] and the resulting catalyst was designated as "C-TiO_2".

C-Fe codoping process was carried out by wet impregnation method in which the percentage of Fe^{2+} was 0.5 wt% with respect to C-TiO_2. In the preparation procedure, a portion of C-TiO_2 was soaked in ferrous sulphate aqueous solution overnight and the supernatant was decanted. The residue was then washed with distilled water to remove unfixed iron and impurities and then dried in an oven at 150 ^{0}C for 3 hours. It was then thermally heated for 30 min and finally subjected to microwave irradiation for 30 min in medium-high mode. The resulting C-Fe codoped titania was designated as "C-Fe TiO_2".

Sunlight induced photocatalytic experiments. The photochemical experiments were carried out in glass beakers with 200 mL of aqueous solution containing 0.1 g of catalyst and 10 mg/L of the dye (methylene blue/methyl orange). The dye suspensions were stirred in the dark for 15 min to attain the adsorption equilibrium and then subjected to daylight solar irradiation at noon for 3 h when the intensity of sunlight was ~ 90,000 LUX, measured using a LUX meter (Model: TES 1332). The residual concentration of the dye in the suspension after adsorption was taken as the initial concentration before solar irradiation. For every 15 min, an aliquot of 5 mL was taken and centrifuged to eliminate the catalyst and the absorbance of the supernatant was then measured at the corresponding wavelength of the dye using a spectrophotometer (Model: Systronics Visiscan 167).

In case of the solar Photo-Fenton's degradation experiments with C-Fe TiO_2, 1 mL of 50% H_2O_2 was added to each of the dye suspensions the moment before solar irradiation. Since the decolorization was rapid, an aliquot of 5 mL was taken for every 5 min.

RESULTS AND DISCUSSION

Crystal characterization. In order to determine the crystal phase and crystalline nature of the undoped and carbon modified titania catalysts, powder X-ray diffraction patterns of the catalysts were taken. Figure 1a, 1b and 1c represent the X-ray diffraction patterns of Pure TiO_2, C-TiO_2 and C-Fe TiO_2 catalysts respectively. For all the catalysts, the peaks related to anatase phase were predominantly obtained at the corresponding 2θ values[16] of 25^0, 37^0, 48^0, 55^0 and 62^0 (Bunjerd et al., 2005). Thus, the X-ray diffraction patterns reveal the predominant presence of anatase phase in both undoped and modified samples which may be attributed to the low temperature calcination of TiO_2 (80 ^{0}C to 150 ^{0}C) during the synthesis rather than calcination at higher temperatures.

Morphological characterization. The surface morphology of the pure and carbon modified titania catalysts was characterized by scanning electron microscopy. High magnification SEM images of the undoped and modified titania samples shown that most of the undoped titania particles were agglomerated whereas the particles shown in the SEM micrographs of microwave treated C-TiO_2 samples were present as tiny individual particles which facilitate the effective degradation of organic contaminants on each catalyst particle. This beneficial nature of the microwave treated C-TiO_2 particles was due to the rapid, homogeneous and selective heating produced by the microwaves which induces better crystallinity (Liu et al., 2007). The particle size of the pure and modifiedTiO_2 catalysts was studied with the aid of HR-SEM and wasv found to be in the range of 90 nm.

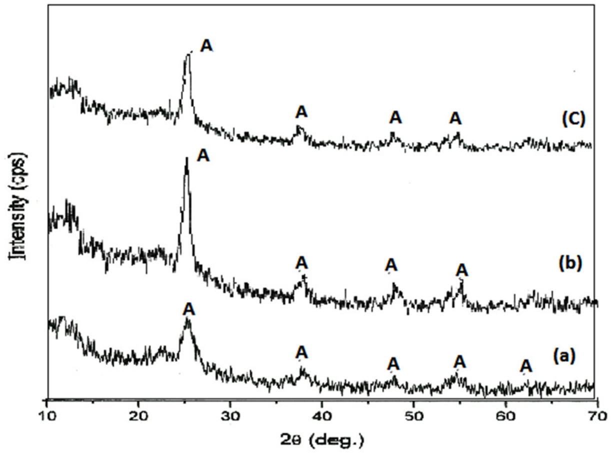

Fig. 1. XRD patterns of a) Pure TiO_2 b) C-TiO_2 and c) C-Fe TiO_2

Compositional Analysis. In order to determine the wt% of carbon and iron in the modified titania samples, EDS analysis was performed. Figure 2 shows the EDS spectrum of C-TiO_2. The percentage of coconut oil added in the synthesis procedure was 10 wt % and the amount of carbon shown in the corresponding EDS spectrum was 8.27 wt%. Remaining composition was contributed chiefly by titanium then by oxygen. Figure 3 shows the EDS spectrum of C-Fe-TiO_2. The percentage of iron added to the catalyst was 0.5wt% and the amount of iron impregnated on to the sample was found to be 0.06 wt%.

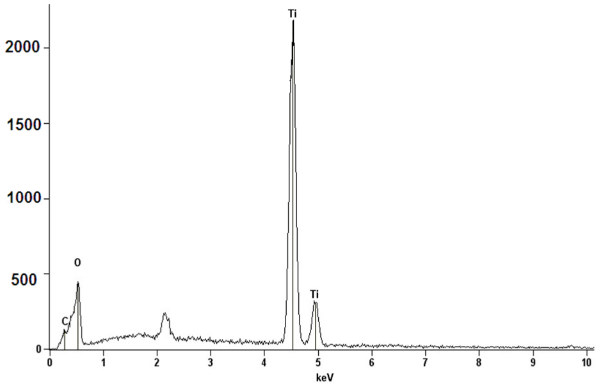

Fig. 2. EDS spectra of C – TiO_2

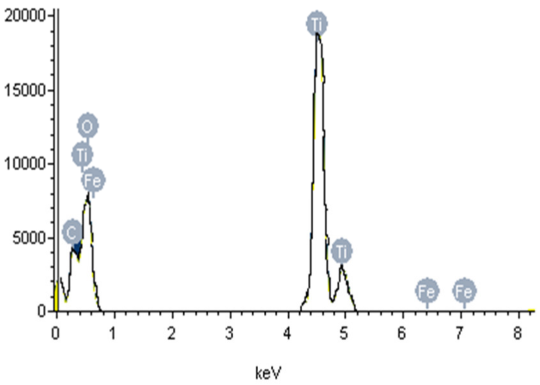

Fig. 3. EDS spectra of C-Fe TiO_2

Solar photoactivity of pure and carbon doped titania. In order to evaluate the solar light induced photoactivity of pure and carbon doped titania catalysts in the degradation of refractory organic compounds, a study was conducted to monitor the decolorization of methylene blue and methyl orange as model organic pollutants. The decolorization profile of methylene blue with pure TiO_2 and C-TiO_2 catalysts at different pH is given in Figure 4a.

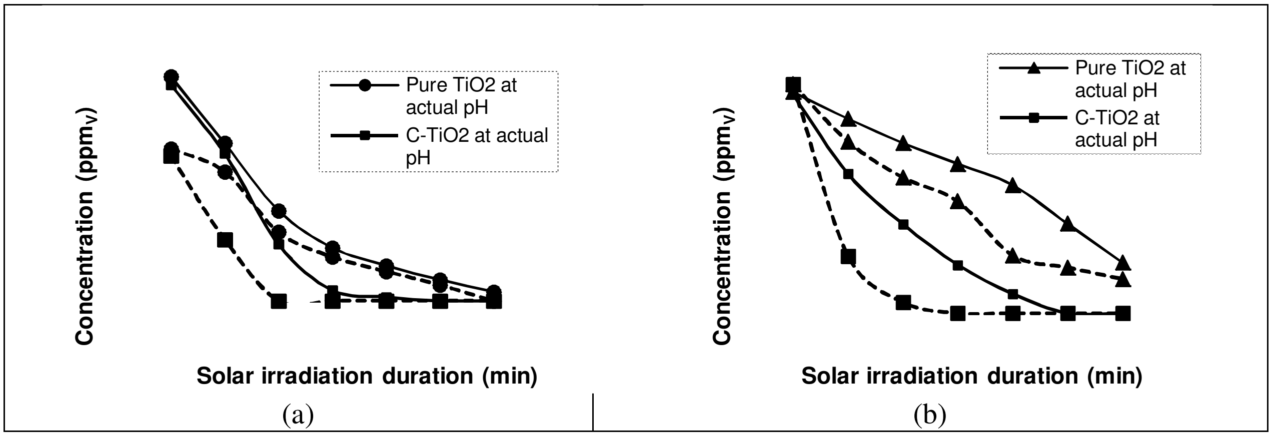

(a) (b)

Fig. 4. Decolorization profile of (a)methylene blue and (b)methyl orange with pure TiO_2 and C-TiO_2

Figure 4a shows that at actual pH, 93.9% of methylene blue dye decolorization was observed in the case of the pure titania at the end of 3 h of sunlight irradiation. But, complete decolorization of the dye was observed after 2.5 h of irradiation in the presence of the carbon doped titania catalyst. This enhanced efficiency in the decolorization of the dye of the carbon doped catalysts was due to the enhanced visible light absorption from the sunlight due to the red shift after doping with carbon. The results also reveal that a complete decolorization of methylene blue dye was observed at the end of 60 min in the case of C -TiO_2 at pH 9. Thus the rate of decolorization of methylene blue was higher in the presence of the catalyst at pH 9 when compared to the decolorization rate at the actual pH of the dye where the complete decolorization was observed only after 150 min. This increase in the rate of decolorization of the dye at pH 9 could be explained as follows. The measured value of the pH of zero point of charge pHzpc for TiO_2 is around 5.7, evincing that the particle surface is predominantly positively charged below pH 5 and negatively charged in neutral and alkaline solutions. Since, methylene blue is a cationic dye, it is expected to be predominantly in its cationic form in alkaline pH, and hence, it prefers to electrostatically interact with the negatively charged catalyst surface and undergoes better degradation. Thus, due to the dissociation nature of the dye, the decolorization of was maximum and faster in the alkaline pH when compared to that in the actual pH (Yun et al., 2008).

In the case of methyl orange, the decolorization profile observed was similar to that in the case of methylene blue decolorization. As observed in the case of methylene blue, the decolorization of methyl orange was maximum in the pH at which the dissociation of the dye is maximum. Thus, decolorization was favored at pH 3.5 than at the actual pH, since the pKa of methyl orange is close to 3.7.

When comparing the rate of decolorization of the two dyes, methylene blue was found to be decolorized faster and better than methyl orange. This is due to the obvious reason that methyl orange is an azo dye and hence its degradation is complicated when compared to the degradation of non-azo dyes like methylene blue (Marugan et al., 2007).

Thus at optimum pH, the solar photoactivity of carbon doped TiO_2 catalyst was found to be threefold higher than pure titania in degrading methylene blue and the photoactivity is nearly double than pure titania in the degradation of the azo dye, methyl orange.

Solar Photo-Fenton's activity of C-Fe-TiO_2. Preliminary Fenton's experiments were conducted at the laboratory with the pure and carbon-iron codoped titania in the absence of light source. Since the Fenton's degradation of the model pollutants were observed to be very slow compared to the solar light induced photoFenton's reactions, further emphasis was given to evaluate the solar photo-Fenton's activity of the catalysts. The decolorization profile of methylene blue and methyl orange with the C-Fe-TiO_2 at acidic, actual and alkaline pH is depicted in Figure 5a and Figure 5b respectively.

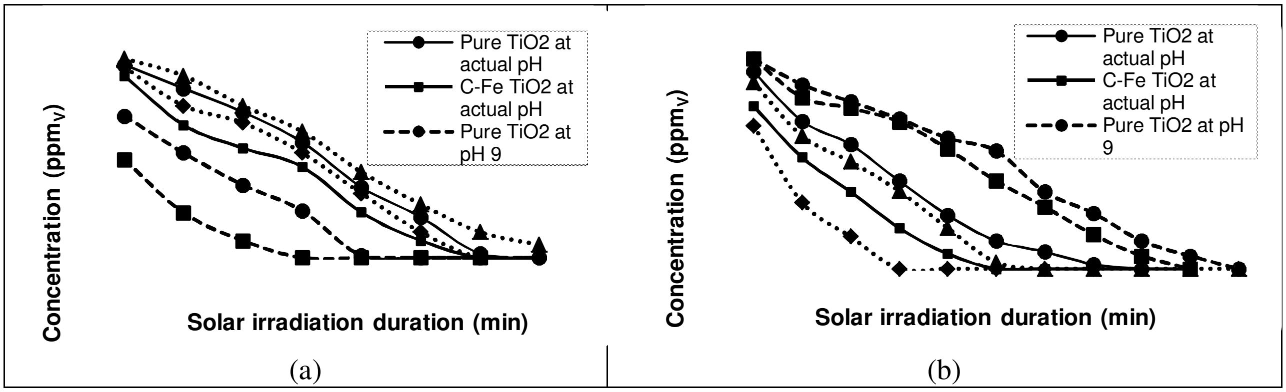

(a) (b)

Fig. 5. Decolorization profile of (a)methylene blue and (b)methyl orange with pure TiO_2 and C-Fe-TiO_2 [Conditions: Dye concentration = 10 ppm$_v$; H_2O_2 concentration = 0.07 M]

From Figure 5a, it is clear that at pH 9, the initial residual concentration of methylene blue in dye suspension before solar irradiation was very low (around 6.6 ppm$_v$ in the case of pure TiO_2 and 4.8 ppm$_v$ in the case of C-Fe-TiO_2). This clearly reveals that majority of dissociation of the dye and adsorption onto the catalyst surface takes place at the pH which corresponds to the pKa of the dye. The dissociation and adsorption of the cationic dye was found to very minimum at acidic pH. When compared to the pure titania, C-Fe-TiO_2 was found to well adsorb the dye pollutant which could be due to the enhanced adsorption nature of both carbon and iron. While observing the decolorization profile, the results very well support the expected trend. The rate of decolorization is very high at the pH which corresponds to the pKa of the dye pollutant. Thus, methylene blue was found to be completely decolorized in a very short duration of 15 min at pH 9 with C-Fe-TiO_2 when compared to all other catalysts at actual and acidic pH. Least degradation of the dye was observed at pH 3, at which the dissociation of the dye is minimum.

The enhanced photoactivity of C-Fe-TiO_2 when compared with pure titania could be attributed to the three possible electronic transitions such as i) From the anionic (carbon) impurity level to the cationic (Fe^{2+}) impurity level, ii) From the anionic impurity level to the conductor band of TiO_2, iii) From the valence band to the cationic impurity level. All of them enhance the quantity of the photo-induced electrons and holes and the red shift of band edge adsorption threshold. Therefore, co-doped sample is in favor of visible absorption than that of single doped titania or undoped titania, due to the narrower band gap and multiform exciting approach (Arabatzis et al., 2003).

While observing the decolorization profile of methyl orange from Figure 5b, initial residual dye concentration before solar irradiation was very low at acidic pH (pH 3.5). This indicates that the maximum adsorption of the anionic dye was favored at the pH which corresponds to the pKa 3.7 of the dye. The rate of degradation was also found to be very high at this pH, which is not only since the pH 3.5 is favorable for the dissociation of the anionic dye and also because the acidic pH enhances the Fenton's reaction and the subsequent organic pollutant oxidation.

When comparing the results in Figure 5a and Figure 5b, the decolorization of the non-azo dye and the azo dye could be achieved at an equally faster rate with the C-Fe-TiO_2, which denotes that the anionic nature of the azo dye facilitates its degradation in Fenton's process.

Thus, the solar photo-Fenton's activity of C-Fe-TiO_2 is almost twelvefold higher than the solar photoactivity of pure titania in the degradation of the cationic dye, methylene blue, and the anionic dye, methyl orange.

CONCLUSIONS

In summary, titanium dioxide nanoparticles were prepared using ultrasonication assisted Sol-gel process with low temperature calcination, modified by doping with carbon and codoping with carbon-iron, characterized and evaluated for the degradation of methylene blue and methyl orange. The XRD characterization reveals the predominant presence of highly active anatase phase in both the pure and doped catalysts, thus shows that low temperature calcination prevented the formation of less photoactive rutile phase. The results of the dye degradation studies lead us to a conclusion that,

- Efficient degradation of the dye pollutants could be rapidly achieved at the pH in which the dissociation of the dye is maximum
- Dyes could be degraded at a very faster rate by solar photo-Fenton's process using C-Fe codoped titania than by the solar photooxidation using pure and carbon doped titania.
- Degradation of the anionic azo dye could be achieved at a faster rate than that of the cationic non-azo dye when the solar photo-Fenton's experiments are conducted at acidic pH.

Thus, the study revealed that the natural and energy efficient sunlight-induced photo-Fenton's process using C-Fe codoped titania could be a viable alternative for the energy consuming treatment technologies for the degradation of organic pollutants.

ACKNOWLEDGEMENTS

We gratefully acknowledge the Centre for International Affairs, Anna University Chennai for the financial help rendered to participate in the 6th International Conference on Environmental Science and Technology 2012. We are also thankful to the University Grants Commission (UGC), New Delhi (India), for UGC Research Fellowship to Ms. R. Jeevitha Raji.

REFERENCES

1. Arabatzis, I.L., T. Stergiopoulos, M. C. Bernard, D. Labou, S. G. Neophytides. 2003. " Silver-modified titanium dioxide thin films for efficient photodegradation of methyl orange". *Appl. Catal. B. Env*. 42:187-201.
2. Bunjerd, Jongsomjit, Tipnapa Wongsalee, Piyasan Praserthdam. (2005). "Study of cobalt dispersion on titania consisting various rutile:anatase ratios". *Materials Chemistry and Physics*. 92: 572.
3. Inagaki, M.; Y. Hirose, T. Matsunaga, T. Tsumura, M. Toyoda. 2003. "Carbon coating of anatase-type TiO2 through their precipitation in PVA aqueous solution". *Carbon*. 41: 2619–2624.
4. Jeevitha Raji, R., and K. Palanivelu. (2008). "Sunlight-Induced Photocatalytic Degradation of Organic Pollutants by Carbon-Modified Nanotitania with Vegetable Oil as Precursor". *Ind. Eng. Chem. Res.* 50**:** 3130.
5. Liu, Y.; S. Yang, J. Hong, C. Sun. 2007. "Low temperature preparation and microwave photocatalytic activity of TiO2 mounted activated carbon". *J. Haz. Mater.* 142: 208.
6. Marugan, J.; M. Munoz, R. Grieken, J. Aguado. 2007. "Photocatalytic Decolorization and Mineralization of Dyes with Nanocrystalline TiO_2/SiO_2 Materials". *Ind. Eng. Chem. Res.* 46 (23): 7605.
7. Seery, M. K.; R. George, P. Floris, S. C. Pillai. 2007. "Silver doped titanium dioxide nanomaterials for enhanced visible light photocatalysis". *J. Photochem. Photobio. A: Chem.* 189: 258.
8. Tsumura, T.;N. Kojitani, I. Izumi, N. Iwashita, M. Toyoda, M. Inagaki. 2002. " Carbon coating of anatase-type TiO2 and photoactivity". *J. Mater. Chem.* 12: 1391.
9. Wong, S.K.; Jiyun Feng; Xijun Hu and Po Lock Yue. 2004. "Discoloration and Mineralisation of Non-bioidegradable azo dye orangeII by copper doped TiO nanocatalysts". *J. Env. Sci & Health.* 39, 2583.
10. Xiao, J.; T. Peng, T. R. Li, Z. Peng, C. Yan. 2006. "Preparation, phase transformation and photocatalytic activities of cerium doped mesoporous titania nanoparticles". *J. Sol. State Chem.* 179: 1161.

11. Yun, S.; K. Palanivelu, Y. Kim, P. Kang, Y. Lee. 2008. ”Preparation and characterization of carbon covered TiO_2 using sucrose for solar photodegradation”. *J. Ind. Eng. Chem.* 14: 667.

SYNTHESIS OF V-TiO_2 NANOPARTICLES AND APPLICATION FOR REDUCTION OF Cd^{2+} FROM AQUEOUS SOLUTION

Reyad Shawabkeh, Musab Mirgani (Department of Chemical engineering, King Fahd University of Petroleum & Minerals, Dhahtan 31261, Saudi Arabia)

Vanadium-doped titania nanoparticles were synthesized by sol-gel technique from alkoxide precursor. Different reaction conditions such as vanadium concentration, acids and alcohol type, water content, sonication time and calcination temperature were investigated and optimized. ANOVA analysis proved that anatase phase of TiO_2 nanoparticles with average size of 7.6 nm and 1.7 wt% doped vanadium were obtained using 5 ml titanium isoporopoxide, 0.65 mmol HCl, 50 ml methanol, 5 g/L NH_4VO_3, 60 min sonication time and 450 ^oC calcination temperature. The produced catalyst was characterized for its surface area and morphology, particle size distribution and crystalline phase. XRD analysis proved the presence of polycrystalline anatase structure with minor peak for rutile phase. SEM and BET showed a spheroidal shape of the particles with surface area of 66 m^2/g and total pore volume and width of 0.0248 cm^3/g and 57.3 Å, respectively. PSA analyses provided a normally distributed particle sizes with mean of 7.6 nm and standard deviation of 8.02 over a range of 3.8-15.19 nm. The photocatalytic activity for reduction of Cd^{2+} showed an average of 70% reduction obtained within 20 min. This percentage is increased with increasing the mass of the catalyst and mixing speed, and decreasing the initial pollutant concentration and solution pH. Two-resistant kinetic model coupled with reaction rate was developed and showed that the external mass transfer coefficient, internal diffusivity and reaction constant are of order of magnitude of $1:10^5:10^4$, respectively, which suggests that the overall rate at times is controlled by external mass transfer resistance.

ISBN 9780976885351

PROTECTION OF STAINLESS STEEL SURFACES AGAINST BIOFILM FORMATION AND CORROSION BY NANOCOMPOSITE COATINGS

Farid Ahmed, Catherine M. Santos, Rigoberto Advincula and Debora F. Rodrigues (University of Houston, Houston, TX, USA)

This study aims in developing novel nanocomposite coatings for stateless steel (SS) surfaces to prevent chemical corrosion and biofilm formation. The electroactive polymer polyvinyl-*N*-carbazole (PVK) was used to synthesize two nanocomposites. One of the nanocomposites contained single-walled carbon nanotubes (SWNT) and the other contained multi-walled carbon nanotubes (MWNT) as fillers. It was observed that carbon nanotubes were highly stable and well dispersed in the presence of PVK in the following ratios: PVK-SWNT (97:3, wt %) and PVK-MWNT (96:6, wt %). Stainless steel (SS) surfaces were coated with a thin and homogeneous film of PVK-SWNT and PVK-MWNT nanocomposite via electrochemical deposition. Excellent chemical corrosion resistance of coated SS with these nanocomposites were demonstrated with prolonged exposure to 0.5M NaCl solution when compared to uncoated surfaces. Furthermore, SS coated surfaces with these nanocomposites inhibited both *Escherichia coli* (Gram- negative bacteria) and *Bacillus subtilis* (Gram-positive bacteria) biofilm formation. These results showed that PVK-SWNT and PVK-MWNT nanocomposites can be used as coating on SS surfaces to prevent chemical corrosion and biofilm formation.

ISBN 9780976885351

LOOPED CARBON CAPTURING AND ENVIRONMENTAL REMEDIATION: CASE STUDY OF MAGNETIC POLYPROPYLENE NANOCOMPOSITES

Suying Wei (Department of Chemistry and Biochemistry, Lamar University, Beaumont, TX 77710, USA)
Zhanhu Guo, Jiahua Zhu, Hongbo Gu, Sowjanya B. Rapole (Integrated Composites Laboratory (ICL), Dan F. Smith Department of Chemical Engineering, Lamar University, Beaumont, TX 77710 USA)

A waste-free process to recycle Fe@Fe_2O_3/polypropylene (PP) polymer nanocomposites (PNCs) is introduced to synthesize magnetic carbon nanocomposites (MCNs) and simultaneously produce useful chemical species which can be utilized as feedstock in petrochemical industry. The Fe@Fe_2O_3 NPs are found to have an effective catalytic activity on the pyrolysis of PP. The PNCs undergo a complete degradation with 2-hour pyrolysis at 500 ^oC in the H_2/Ar atmosphere and the degradation components exhibit an even distribution of different carbon number species, while only 40% of pure PP is decomposed after applying the same pyrolytic conditions. The coked solid waste in the conventional process has been utilized as carbon source to form a protective carbon shell surrounding the magnetic NPs. The carbon-coated magnetic nanocomposites pyrolyzed from PNCs containing 20.0 wt% NPs demonstrate an extremely fast Cr(VI) removal from the wastewater with an almost complete removal of Cr(VI) within 10 min. The pH effect on the Cr(VI) removal efficiency is investigated. These MCNC adsorbents exhibit much higher adsorption capacity in acidic solutions than that in alkali solutions. The large saturation magnetization (32.5 emu g^{-1}) of these novel magnetic carbon nanocomposites allows fast recycling of both the adsorbents and the adsorbed Cr(VI) from liquid suspension in a more energetically and economically sustainable way by simply applying a permanent magnet. The significantly reduced treatment time required to remove the Cr(VI) makes these magnetic carbon nanocomposites (MCNCs) promising for efficient removal of the heavy metals from the wastewater. Kinetic investigation reveals a pseudo-second-order adsorption of Cr(VI) on these novel magnetic carbon nanocomposite adsorbents.

ISBN 9780976885351

ENVIRONMENTAL TRANSFORMATION OF MULTI-WALLED CARBON NANOTUBES AND CARBON NANO-FIBER COMPOSITES USING THERMAL ANALYSIS AND RELATED HYPHENATED TECHNIQUES

E. Sahle-Demessie[1], Amy Zhao[1],
Andrew W. Salamon[2], Bruce Cassel[2],
[1]U.S. EPA, Office of Research and Development, NRMRL, 26 W. Martin Luther King Drive
[2]PerkinElmer Inc. 710 Bridgeport Ave., Shelton, CT 06484

Thermogravimetric analysis (TGA) coupled with gas chromatography and mass spectroscopy (TGA/GCMS), for the evolved gas analysis, has provided deeper knowledge to the stability and kinetics of structural changes and determining adsorbed organics to nanomaterials and nanocomposites. TGA is also an effective technique to confirm dimensions and homogeneity of MWCNT including the presence of trace metal catalyst or other contaminants, and structural defects. The use of TGA/GC-MS brings insight to the affects of UV exposure on MWCNT and CNT-composites. Fast scanning differential scanning calorimetry (Hyper®DSC) was used to accurately determine the heat capacity and investigate the relationship of the rigid-amorphous fraction (RAF) in semicrystalline polymers of nanocomposite systems. These results were compared with other characterization techniques, electron microscopy (SEM and TEM) and X-ray diffraction. With the increase in the commercialization of engineered nanomaterials and the future of nanotechnology rests upon innovative approaches to characterize and manufacture useful complex nanomaterial systems, and assess their use phase and endo-of-life environmental transformation. Nanomaterials could undergo oxidation processes or undesired aging or degradation due to exposure to certain environmental factors. These exposures may result in changes of surface chemistry and other structural changes which affects the fate, transport and toxicity of these materials. Unlike the mature analytical market for bulk and molecular matter, the current advance from discovery to application in nanotechnology is constrained due to the lack of quick, rapid, reliable and low cost analytical techniques.

ISBN 9780976885351

MICROCYSTIS AERUGINOSA REMOVAL USING NATURAL CLAY NANOMATERIALS

Chen-Hao Li, Yu-Han Yu ***Shu-Chi Chang***, (National Chung Hsing University, Taichung, Taiwan)

Drinking water quality is under crisis at Taiwan's isolated islands because more than 90% of 34 water reservoirs are usually eutrophic. Cyanobacteria proliferation and toxin generation in these reservoirs elevated the concerns of health effects. *Microcystis aeruginosa* is the top priority because it releases microcystin which cannot be effectively removed by current water treatment processes. In this study, we tested the growth inhibition effects of two natural clay nanomaterials (NNM-1 and NNM-2) on *Microcystis aeruginosa.* After exposure to NNM-1 and NNM-2 for 30 minutes, the LC_{50}'s are 90.11 ($R2=0.9537$) and 142.87 ($R2=0.7732$) ppm, respectively. After exposure to NNM-1 and NNM-2 for 12 hours, the LC_{50}'s are 18.74 ($R2=0.9973$) and 0.02 ($R2=0.9908$) ppm, respectively. These results suggest that treatment by natural clay nanomaterials is a cost-effective option for *Microcystis aeruginosa* removal and their prolonged inhibiting power can significantly reduce the impact of cell death related toxin release.

ISBN 9780976885351

PHOTOCATALYTIC DEGRADATION OF CHLORINATED ORGANIC COMPOUNDS USING NEWLY-DEVELOPED NANOPOROUS ZINC OXIDE-LAPONITE COMPOSITES

J. C. Joo, C. H. Ahn, and J. H. Kwon (Korea Institute of Construction Technology, Korea)
J. Kim and L. Campos (University College London, U.K.)
M. Song (Kangwon National University, Korea)

The removal efficiency of trichloroethylene (TCE) in aqueous phase was evaluated through photocatalytic decomposition using newly-developed nanoporous zinc oxide-laponite composites (NZL) as a function of initial concentration of TCE, pH of aqueous solution, wavelength and time of UV irradiation. The experiments were performed using only TCE solution (control test), TCE solution with NZL, TCE solution with UV irradiation, and TCE solution with both NZL and UV irradiation in batch photo reactor. Sorption of TCE to nanoporous composites was found to be dominant at relatively low aqueous concentration of TCE (i.e., ≤ 10 mg/L), whereas photocatalysis was found to be dominant at relatively high aqueous concentration of TCE. As pH increased, the removal efficiency of TCE increased due to the greater hydroxyl radicals enhancing the reactivity and rate of photocatalysis. Removal efficiency of TCE by UV-C irradiation was greater than that by UV-A irradiation, however, the TCE removal efficiency increased with UV irradiation time, irrespective of UV wavelength. Based on these results, the application of NZL as a possible alternative to TiO_2 through photocatalytic decomposition of recalcitrant chlorinated organic compounds may be feasible with low costs and effort.

ISBN 9780976885351

OPTIMIZATION OF ZIRCONIA NANOPARTICLE SUFACE AREA IN HYDROTHERMAL SYNTHESIS UNDER SUPERCRITICAL WATER CONDITION

A. Golzary and ***S. Gitipour**** (University of Tehran, Tehran, Iran)

In recent years, Zirconium dioxide (zirconia) has attracted much attention as a catalyst, photocatalyst and catalyst support due to its unique amphoteric character and redox properties. Photocatalysis is a rapidly expanding technology for wastewater treatment. Photocatalytic process have potential for widespread applications in indoor air and environmental health, biological, medical applications, laboratory and hospital applications, pharmaceutical and food industry, plant protection applications, drinking water disinfection and organic and inorganic contaminant removals. In case of necessity, photocatalyst performance can be improved by reducing the particle size (increasing the specific surface area). In this research, synthesis of zirconia nanoparticles using supercritical water for optimization of specific surface area (SSA) as a reaction medium in batch type reactor was studied. Characterization of product were performed by x-ray diffraction (XRD), transmission electron microscopy (TEM), induced couple plasma (ICP) and Brunauer-Emmett-Teller (BET) measurements. The effect of four parameters including temperature, reaction time, primary concentration of aqueous solution of zirconium nitrate and pH of solution on the specific surface area and yield of reaction were investigated. Response surface method (RSM) was used to optimize the process parameters. The reaction temperature; 405 ^{o}C, the reaction time; 1.38 hr, the primary concentration of zirconyl nitrate, 0.19 M and starting solution PH, 1.21 were found to be the optimum condition to achieve the maximum SSA of zirconia nanoparticle. Under the optimum conditions, the experimental value was well in close agreement with value predicted by the model, thus indicating suitability of the model employed and the success of response surface methodology in optimizing the ScWHS conditions.

ISBN 9780976885351

DEVELOPMENT OF CNT-TIO_2 PHOTOCATALYSTS USING SEPARATION OF CARBON NANOTUBE

Hyukmin Kweon, Thuy-Duong Nguyen-Phan and Eun Woo Shin (University of Ulsan,Ulsan, Ulsan, South Korea)

Recently anatase TiO_2 particles showed photocatalytic enhancements in many cases. This concept can be extended to defined carbon structures. Furthermore, single wall carbon nanotube(SWCNT) has excellent mechanical properties and a large specific surface area (>150 m^2/g). The mixture of titania and SWCNT also have a large area where pollutants can adsorb. Thus, SWCNT-TiO_2 mixtures and composites are able to achieve photocatalytic activities well beyond the anatase/rutile composites.

This study highlights the literature on the synthesis of SWCNT-titania composite structure, and addresses the enhancement of the SWCNT-TiO_2. The SWCNT is separated two parts metallic and semiconducting. The separated SWCNT was supplied from a research team in Kyungwon Univ. which has a SWCNT separation technique. The SWCNT-TiO_2 composites were prepared using a simple colloidal blending method. Photocatalysis performance under UV radiation was achieved. Separated semiconducting SWCNT-TiO_2 composites promoted the removal efficiency and correspondingly, facilitated the photodegradation rate of methylene blue. The good photocatalytic performance on the SWCNT-TiO_2 composite systems could be attributed to a synergy effects including the increase in specific surface area with SWCNT amount as well as the property of separated SWCNT. Furthermore, the SWCNT-TiO_2 composites in photocatalytic degradation studies are examined with focus toward understanding enhancement.

ISBN 9780976885351

SYNTHESIS OF TUNGSTEN-DOPED TITANIA NANOPARTICLES AND APPLICATIONS FOR PHOTO-DEGRADATION OF METHYLENE BLUE, Zn^{2+} AND Pb^{2+} FROM AQUEOUS SOLUTIONS

Naim M. Faqir (Department of Chemical engineering, King Fahd University of Petroleum & Minerals, Dhahran 31261, Saudi Arabia)

Nanocrystalline tungsten-doped titania was synthesized by sol-gel method with continuous ultrasonication using titanium isopropoxide as a precursor. Different concentrations of tungsten solutions were used in order to obtain the maximum loading of tungsten oxide on Titania surface. Energy dispersive spectroscopy (EDS) technique was used to measure the amount of tungsten on the surface of titania and BET was used to investigate the total surface area which is found to be 152.26 m^2/g for the sample with maximum tungsten loading (2.7 wt%). SEM images showed spherical shape of the catalyst that has anatase form of Titania as found by XRD patterns. The photocatalytic activity of tungsten doped Titania was investigated by the degradation of Methylene Blue (MB) at different solution pH values of 4, 6 and 10. Pure and tungsten doped titania were further applied for removal of Zn and Lead form aqueous solutions and it was noticed that addition of tungsten to titania enhanced the photocatalytic activity, which results in the increment of the catalyst maximum uptake from 7 to 15 mg/g for Zn and from 15 to 26 mg/g for Pb.

ISBN 9780976885351

DIATOMACEOUS EARTH MODIFIED BY MAGNETITE NANOPARTICLES FOR CONTAMINANTS REMOVAL

Xinchao Wei and F. Andrew Wolfe
(The State University of New York Institute of Technology, Utica, NY, USA)

As a lightweight sedimentary mineral with a porous structure, diatomaceous earth (DE) is an important material for use as a filter media for water treatment. However, the surfaces of DE are inert silica lacking chemically active sites to adsorb dissolved contaminants from water or wastewater. The objective of this study was to modify the surfaces of DE with a layer of magnetite nanoparticles and to investigate the removal of selenium anions and lead cations using the modified DE as an adsorbent. Batch adsorption experiments were conducted to evaluate the effects of pH, temperature, adsorbent concentration, selenium speciation, and presence of competing anions in conjunction with studies on adsorption kinetics, isotherms, and adsorptive thermodynamics. The new adsorbent showed great potential in reducing Se to a very low level and its applicability in adsorption columns indicated it could be a very promising adsorbent for full-scale processes. The maximum removal of selenite and selenate was achieved under acidic conditions (pH 2 – 3.5), indicating the adsorption process was suitable for treating Se-impaired acid mine drainage. The adsorption of Pb was found to be highly dependent on pH, with the highest removal obtained at pH 6.0. The thermodynamic parameters obtained indicated that Pb(II) adsorption onto nano-magnetite modified DE was feasible, spontaneous and endothermic.

ISBN 9780976885351

EFFECT OF ANNEALING ON PHYSICAL CHARACTERISTICS AND PHOTOELECTROCHEMICAL RESPONSE OF NANOSTRUCTURED ZnO

Pushpendra Kumar*, Vidhika Sharma, Nirupama Singh, Babita Kumari, Shailja Sharma, Sumant Upadhyay, Surbhi Choudhary (Dept. of Chemistry, Dayalbagh Educational Institute, Agra, India – 282 110), Vibha Rani Satsangi (Dept. of Physics & Comp. Science, Dayalbagh Educational Institute, Agra, India – 282 110) , Sahab Dass and Rohit Shrivastav (Dept. of Chemistry, Dayalbagh Educational Institute, Agra, India – 282 110)

Nanostructured zinc oxide (NZO) is a promising material for photoelectrochemical (PEC) splitting of water to produce hydrogen. This report deals with the effect of annealing on the physical properties and the PEC behaviour of sol-gel derived ZnO thin films coated on conducting glass substrates. Zinc acetate (ZnAc.) dihydrate was used as precursor, which was dissolved in monoethonalamine (MEA) and isopropanol. Resulting sol was spin coated on conducting glass substrate. Obtained films were sintered in two stages; firstly at 250°C for 30 minutes followed by second stage sintering at 400, 500 and 600°C for 1 h. Samples, characterization included: XRD for phase analysis, UV absorption for band gap, AFM for surface topography and SEM for morphological study. As synthesized films were used as working electrode in conjunction with platinum counter electrode and saturated calomal reference electrode in PEC cell filled with NaOH solution (pH 13) under 150 W xenon arc lamp illumination. XRD analysis indicated dominant evolution of hexagonal wurtzite ZnO. The surface of the film appeared uniform, homogeneous and exhibited granular nanostructured morphology, especially for two stage sintered films, as evident from AFM and SEM analysis. Nature of I-V curves confirmed n-type nature of NZO films. It was observed that as the sintering temperature was increased PEC current density increased significantly and short circuit current of 1 mA/cm^2 was recorded with the film sintered at 600°C. Sintering played a crucial role to modify the texture, optical and electrical properties of films and thus influencing their PEC cell performance.

ISBN 9780976885351

AIR POLLUTION
AND
AIR QUALITY CONTROL

VEHICULAR POLLUTION IN KURNOOL - ACASE STUDY

C. V. Rajeswari
(Govt. Degree College, PATTIKONDA, Kurnool Dist., A.P. India)

ABSTRACT: Vehicular pollution is one of the burning environmental issues of all cities in India as well as the world where the maximum extent of population is exposed to poor air quality. The increase in population, urbanization and also rise in per capita income has resulted in tremendous increase in the number of motor vehicles. In recent times number of vehicles are either doubled or tripled in most of the cities and towns of India. As the number of vehicles is increasing, congestion of roads is resulting and vehicles are now becoming the main source of air pollution due to their unwanted emissions. This paper presents a detailed account of vehicular pollution in Kurnool and nearby villages.

Key Words: Vehicular Pollution, Urbanization, Air Quality

INTRODUCTION

Kurnool Town is one of the important towns of Andhra Pradesh State in India which is rapidly growing with population and vehicles. It is a town with population of nearing 500000 and registered number of vehicles with more than 300000. According to Regional Transport Authority, more than one hundred two wheelers and at least ten four wheelers or being registered every day. This is a clear proof for the abnormal increase in the number of personalized vehicles and insufficient mass transport system. The enormous increase in the number of vehicles leads to increase in vehicular emissions which have maximum impact on the surroundings. Hence vehicles contribute to air pollution (1,2). The other reasons which are contributing for the deterioration of the air quality in the town are:

1. Very congested and poorly maintained roads;
2. Use of old vehicles without proper maintenance;
3. Insufficient pollution checks and inspection by authorities concerned;
4. Use of 2-stroke vehicles (two wheelers and three wheelers);
5. Use of adulterated fuel especially in three wheelers (Autorikshaws);
6. Improper traffic –management; and
7. Absence of effective, rapid mass transport system and lastly encroachments and unauthorized constructions on road sides.

The various pollutants emitted by vehicles are Carbon monoxide (CO), un burnt hydrocarbons (HC), Sulfur dioxide (SO_2), Nitrogen dioxide (NO_2), Carbon particles, Suspended particulate matter (SPM) and Respirable Suspended particulate matter (RSPM) (3,4) Most of the vehicles, especially autorikshaws use diesel and 2T oil for lubrication of engine and this oil is partially burnt and comes out as smoke and suspended particulate matter. About 15-20% un burnt fuel comes out from 2-stroke engine exhaust (5). Usage of diesel also leads to high concentration of nitrogen dioxide. Many studies reveal the effect of vehicular pollution on public (6,7,8) in general and traffic policemen and auto men (9,10) in particular.

ISBN 9780976885351

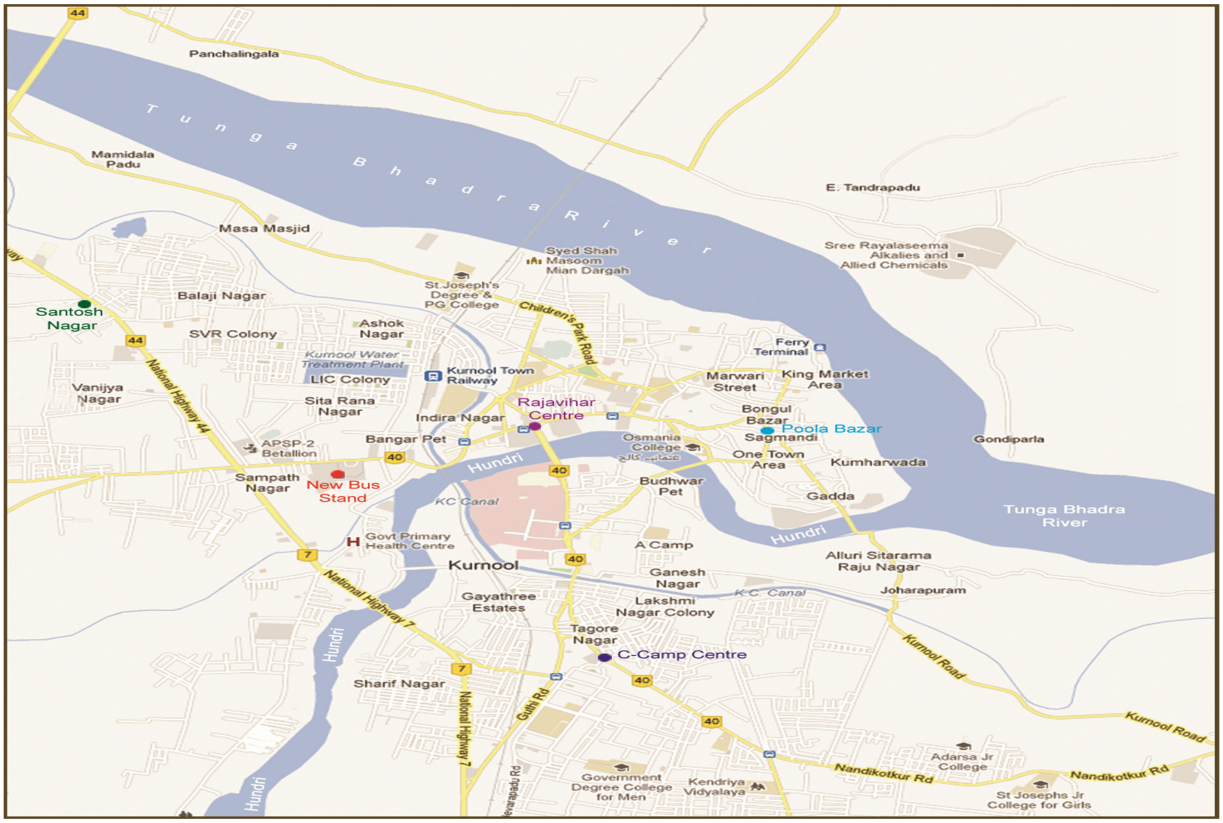

Figure 1. The Selected Areas in Kurnool Town

Table 1. Description of Sampling Locations

S.No.	Locations	Nature
1	Rajvihar Center	Traffic Junction
2	New Bus Stand	Traffic Junction
3	C Camp Center	Traffic Junction
4	Poola Bazaar	Semi Residential (market area)
5	Santhosh Nagar	Residential area

The present study deals with comparative increase in the number of vehicles for the past ten years as shown in the Table 1 and also comparative increase in vehicular emissions at five places of Kurnool Town.

MATERIALS AND METHODS

Five different places in Kunool Town shown in Table 2 and Figure 1 were selected to detect ambient air quality by monitoring sulfur dioxide, nitrogen dioxide, suspended particulate matter and Respirable suspended particulate matter. The air monitoring was done from 6AM to 2PM and 2PM to 9PM. The concentration of gaseous pollutants was recorded with the help of SO_2 and NO_2 analyzers. SPM and RSPM were monitored with the help of Respirable Dust Sampler RDS provided by Andhra

Pradesh Pollution Control Board, Zonal Office, Kurnool. Among the five places three places are traffic junctions in the town and other two are residential areas.

Table 2. Motor Vehicles on Road as on May 2012 when compared to 2002

S.No.	Type of Vehicles	Number in 2002	Number in 2012
1	Two wheelers	35064	1,79426
2	Three wheelers	1486	23048
3	Motor Cars	565	13267
4	Heavy Vehicles(Goods carrier)	796	8059
5	Education Institutional Buses	15	442
6	Ambulances	04	120
7	R.T.C Buses	150	500
8	3-Wheeled Goods Vehicles	18	1491
9	Tractors	564	11414
10	13 Seat private vehicles	14	1506

Table 3. Ambient Air Quality Standards in microgms/m^3

Area	SO_2	NO_x	SPM	RSPM
Sensitive Area Rural	30	30	100	75
Residential Area	80	80	200	100
Industrial Area	120	120	500	120

RESULTS AND DISCUSSION

The ambient air quality parameters for all selected sites are presented in the Table 4 along with previous years values (11). There is enormous increase in the amount of SPM and RSPM levels and even though the values of Sulfur dioxide and Nitrogen dioxide are in permissible limits there is gradual increase of these pollutants.

Table 4. Ambient Air Quality Parameters for All Selected Sites along with Previous Years Values

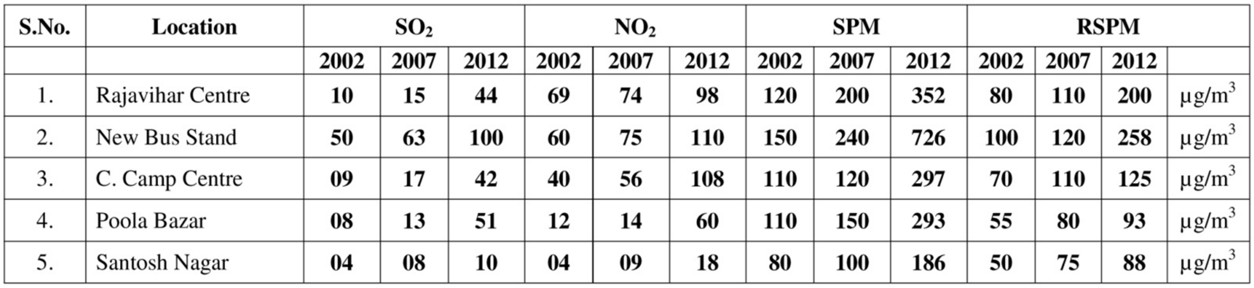

S.No.	Location	SO_2			NO_2			SPM			RSPM			
		2002	2007	2012	2002	2007	2012	2002	2007	2012	2002	2007	2012	
1.	Rajavihar Centre	10	15	44	69	74	98	120	200	352	80	110	200	µg/m^3
2.	New Bus Stand	50	63	100	60	75	110	150	240	726	100	120	258	µg/m^3
3.	C. Camp Centre	09	17	42	40	56	108	110	120	297	70	110	125	µg/m^3
4.	Poola Bazar	08	13	51	12	14	60	110	150	293	55	80	93	µg/m^3
5.	Santosh Nagar	04	08	10	04	09	18	80	100	186	50	75	88	µg/m^3

Sulfur dioxide: The concentration values of SO_2 in all places except New Bus stand is more than permissible limits and below in other places.

Nitrogen dioxide: The values of NO_2 are in permissible limits in two residential areas and more in other three places. This can be attributed to the huge increase in the number of vehicles passing through these junctions.

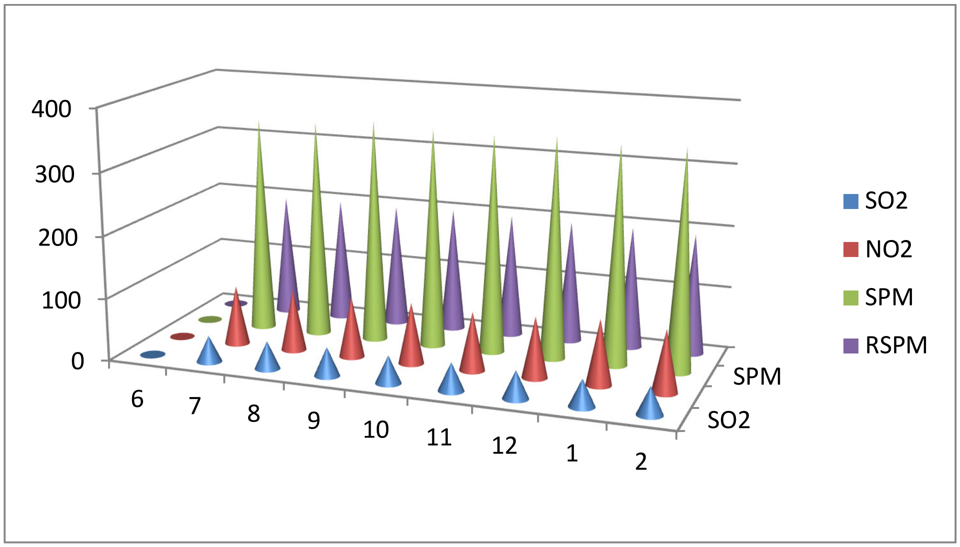

Figure 2. Concentrations of Different Air Pollutants at Rajavihar Centre

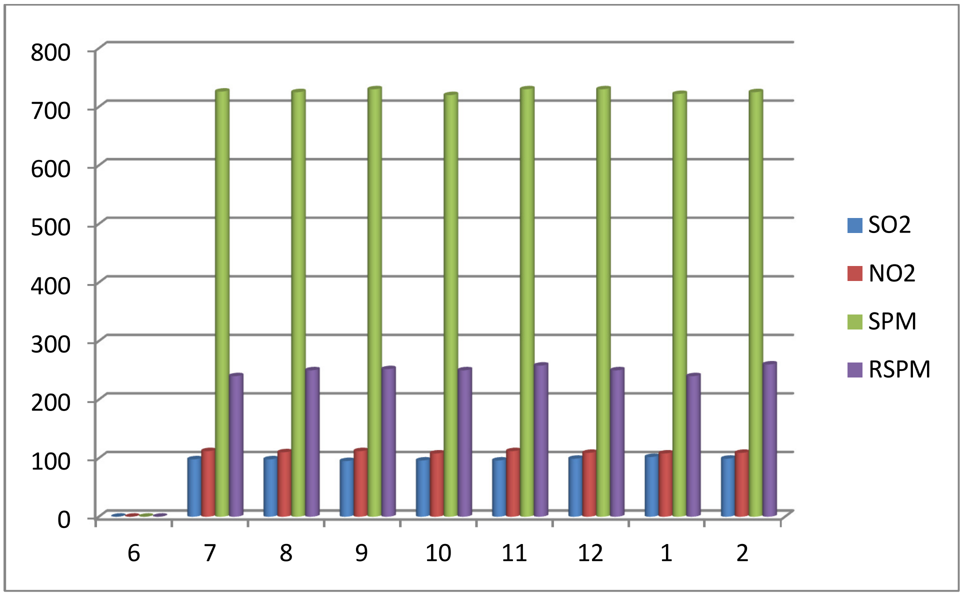

Figure 3. Concentrations of Different Air Pollutants at New Bus Stand

Suspended Particulate Matter: The SPM concentration is very high in all four places except in Santhosh nagar (residential area). It is highest in New bus stand which is mainly due increased number of vehicles.

From the above study it can be concluded that mainly due to large number of vehicles plying through the roads, the ambient air quality is being deteriorated. There are evidences from the people staying at Raj Vihar Centre and New Bus Stand that there is incidence of eye irritation, sneezing, cough and skin allergy due to exposure to vehicular emissions longer period of time (Figures 2-6).

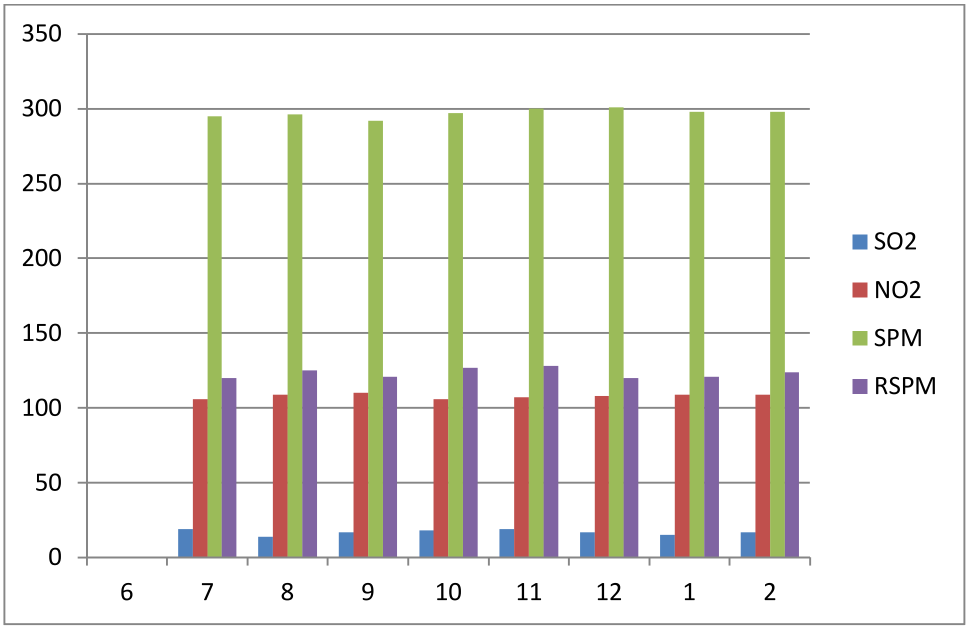

Figure 4. Concentrations of Different Air Pollutants at C-Camp Centre

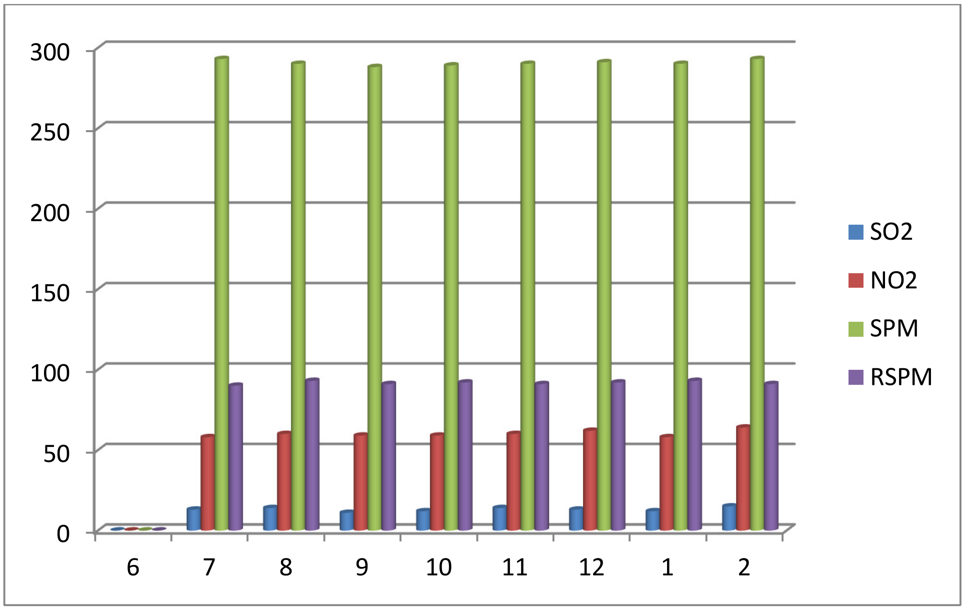

Figure 5. Concentrations of Different Air Pollutants at Poola Bazar

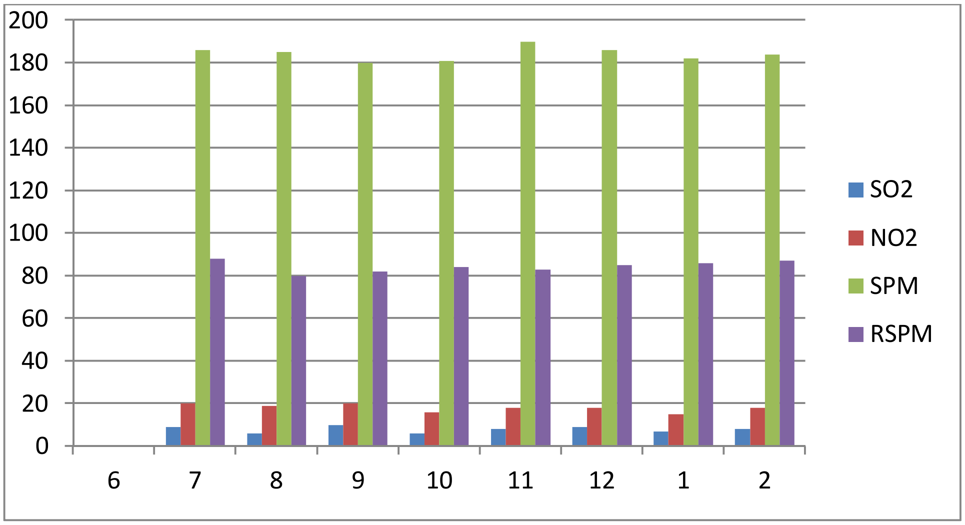

Figure 6. Concentrations of Different Air Pollutants at Santosh Nagar

CONCLUSION

After monitoring ambient air quality at Kurnool it can be concluded that mainly the increase in the number of vehicles is the root cause for air quality deterioration. Hence an integrated and holistic approach should be adopted to control vehicular pollution.

- It should be made mandatory for the heavy vehicles like goods carriers to pass through by pass roads.
- The public transport system should be improved and increased.
- Stringent emission norms should be followed for vehicles.
- Frequent inspections and checks should be there by the authorities concerned.
- Noise pollution is another byproduct of vehicular pollution should be reduced by having silent zones.
- There should be proper traffic planning and management.
- Two stroke engine vehicles should be replaced by CNG (Compressed Natural Gas) vehicles.
- There should be strict check on usage of adulterated fuel.

Last but not least that there should be strict implementation of law and punishment for the violation of rules and regulations laid down by the authorities concerned.

ACKNOWLEDGEMENTS

The author thankful to A.P. Pollution Control Board, Zonal Office, Kurnool, A.P. India for the help and cooperation rendered.

REFERENCES

1. Cortse, A.D., Cleaning the Air J. of Environmental Science and Technology 24(4) 442 448. 1990.

2. CPCB, Air Pollution and its Control Parivesh Newsletter 2 (1) Central Pollution Control Board 20pp 1995.
3. Pandey, V., and Kumar,A., Status of Air Quality in Lucknow City Indian J of Environmental Protection 19(3) 193-199, 1999.
4. Glose, M.K., Paul,R., and Banerjee,S.K., Assessment of the Impacts of Vehicular Emissions on Urban Air Quality and its Management in Indian Context: The Case Study of Kolkata. Environment Science and Policy 7(2) 345-351, 2004.
5. Pundir, B.P., Vehicular Air Pollution: Recent Control Measures and Related Issues in India Infrastructure Report, Oxford University Press. New Delhi.2001.
6. Mohanty,S.K., Ambient Air Quality in Koraput. Indian J. of Environmental Protection 19(3) 181-184 , 1999.
7. Lone . P .M., Khan, A.A. ,and Shah, A.A., Study Of Dust Pollution caused by Traffic in Aligarh City. Indian .J. of Environmental Health 47(4), 33-36 2005
8. Mazher.S., Sakuntala.K., and Jayaraj S.S., Study of Dust Pollution caused by Traffic in Tiruvanmiyur area in Chennai City, Nature Environment and Pollution Technology. 7(4) 643-646, 2008.
9. Prasanthi Sam,R., and Rajeswari, C.V., Effect Of Vehicular Pollution On health of traffic Police men in Kurnool Town, Pollution Research 22(3) 373-375 2003.
10. Prasanthi Sam,R., and Rajeswari, C.V., Effect Of Vehicular Pollution On health of Auto men in Kurnool Town, Pollution Research 26(3) 427-428 2007.
11. Investigation of Air and Water Pollutants in Kurnool and Nearby Villages, UGC Major Research Project by Dr. C.V. Rajeswari Principal Investigator.

AIR POLLUTANT EMISSIONS FROM A NON-ROD DIESEL GENERATOR ON B20

Lora Monti[1], Zifei Liu[2] and ***Mingming Lu***[2]

[1]Northwest high school, 10761 Pippin Road, Cincinnati, OH 45231
[2]University of Cincinnati, 2600 Clifton Avenue, Cincinnati, Ohio, 45221

ABSTRACT: Diesel particulate emissions have been recognized as carcinogenic by various agencies, including the US EPA, NIOSH (National Institute of Occupational Safety and Health), WHO, etc., and diesel emission is a significant source of fine particulate matter (PM) in many urban centers. In this study, the diesel emissions from the use of a B20 biodiesel blend were measured and compared against that of petro-diesel. Diesel particulate matter (DPM), the carbon speciation of DPM, CO, and NOx were measured. The measurements were performed on a non-road source and under various loads from idle to full load. The DPM from B20 is 10-15% lower than that of petro-diesel by weight. The emissions of CO and NOx were close for the two fuels. The organic and elemental carbon speciation were found to be close also for the two fuels.

INTRODUCTION

Diesel particulate emissions have been recognized as carcinogenic to health by various agencies, including the EPA and NIOSH (National Institute of Occupational Safety and Health), etc. [1-2] and it is an important source in the Cincinnati area, like many other urban locations. Diesel particulate matter (DPM) emitted from trucks, buses and construction equipment constitutes of a large fraction of $PM_{2.5}$ in may urban centers around the world. Cincinnati is ranked as the top 25 metropolitan areas most polluted by short term (24 hours) and long term (annaul) particulate matter ($PM_{2.5}$) pollution, number 18 and 10 [3] in the United States respectively. There are approximately 12,000 to 16,000 trucks that travel on the highways every day emitting particulate matter and gases in the Cincinnati vicinity. In fact, I-75 is the most traveled truck route in the United States. [4]

Biodiesel, meanwhile, can offer a solution to both the DPM issue as well as the declining petroleum diesel supply. This environmentally friendly diesel fuel alternative can be made from vegetable oil, recycled cooking oil from restaurants or animal fat. According to an EPA study, both 100% biodiesel (B100) and even 20% biodiesel (blended with petroleum also called B20) result in emissions reductions of unburned hydrocarbons, CO, and PM. One limitation may be that the concentration of NO_x slightly increases.

In this project, the emission of CO, NOx and DPM were quantified from the use of B20 and are compared with that of petroleum diesel (referred to as normal diesel in this paper). The goal is to verify the pollution reduction benefits of biodiesel from a non-road source. As part of the RET (Research Experience for Teachers) effort, one of the high school teacher participated in this research, who will develop more effective classroom examples in teaching Science and Chemistry subjects back in the high school.

EXPERIMENTAL DESIGN

The research was conducted on a non-road diesel generator at the University of Cincinnati's Center Hill Research Facility. Two types of fuel were analyzed, normal diesel (low sulfur diesel with about 500 ppm sulfur) and B20 (20% biodiesel with 80% normal diesel). Each fuel was tested at four

---

ISBN 9780976885351

load conditions with multiple measurements, *i.e.,* 0 (idle), 25, 50 and 75 kW. The biodiesel was obtained from Griffin Industries and was made from used cooking oil.

The EPA Method 5 (the Determination of Particulate Matter Emissions from Stationary Sources) sampling train was used to determine the amount of DPM generated from each fuel and the organic carbon and elemental carbon concentrations.[5] The setup is a sampling train with a nozzle, a filter box, a control system, a pump, and an impinger box, where the exhaust gas is collected isokinetically to ensure a representative collection of particles from the exhaust stream. The samples were collected on quartz filter instead of glass fiber filters in order to perform carbon speciation. Four impingers (three filled with water and one empty) were placed in an icebox, in order to capture any condensable, such as moisture, traveling through the system. The amount of moisture in the impingers was used to calculate the dry volume of sample gas. The diesel particulate matter concentration was determined from the differential weight of the filter before and after running Method 5. After the filters were desiccated and weighed, they were taken to a NIOSH lab for the organic carbon and elemental carbon (OC/EC) concentration determination using the Thermal Optical NIOSH Method 5040.[6] A Testo Gas Analyzer was used to obtain the concentration of O_2, CO, CO_2, NO_x, and EA (extra air). Most of the data points have two of more repeated tests.

RESULTS AND DISCUSSION

Figure 1 shows the DPM emissions from B20 and normal diesel. DPM of B20 was slightly lower at loads of 25, 50, and 75kW, which is approximately a 10.5 to 15.4% reduction. However, the DPM of B20 was somewhat higher than low sulfur diesel at 0 kW. Further research is needed to determine why this occurred.

Figure 2 shows the CO concentrations for the two fuels. The concentrations went down as the load was increased on the generator. Perhaps this is due to more CO being oxidized to CO_2. The CO concentration for B20 at 0 kW is noticeably lower than that of petro-diesel. At the 25 to 75 kW load conditions the concentration of CO were approximately the same for both types of fuels. The NOx measurement for B20 and petro-diesel were also very close (not shown here).

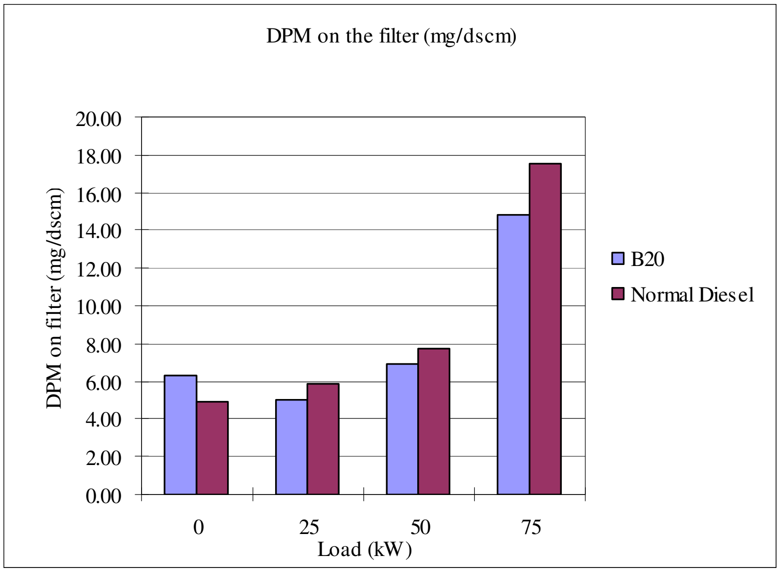

FIGURE 1. The DPM emission with different load.

Figure 3 shows the ratio of elemental carbon to total carbon (EC to TC) obtained by the thermo-optical method using NIOSH 5040. Average values have been used at each of the data points. The B20 emission followed similar trends as the DPM with load: the higher the load, the more EC in the carbon fraction.[7] During the conference presentation, we will further compare this results with other studies on B20. Also the comparison of sampling methods, Method 5 vs. the dilution method, will be provided in the future.

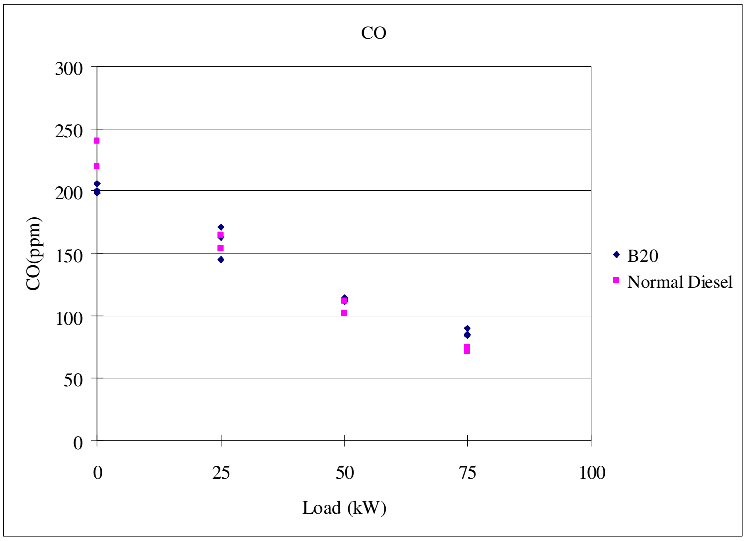

FIGURE 2. The CO emissions for B20 and petro-diesel.

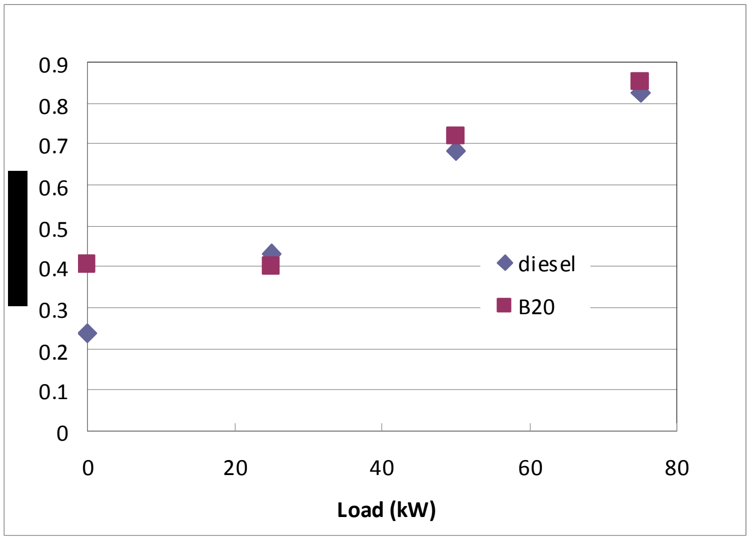

FIGURE 3. The carbon analysis of the PM from the two fuels

CONCLUSIONS

The DPM for B20 was 10-15% lower than the DPM for normal diesel. B20 and normal diesel had slight reductions of CO, and the carbon analysis of the two types of PM did not show statistical differences. This may be due to the low percentage of biodiesel used, and also the setup of the method 5, it is a heated and non-dilution method, whereas the majority of the other studies used dilution and cooling when the PM samples were taken. Further comparison with the literature and comparisons with the dilution method will be conducted in the future.

ACKNOWLEDGEMENTS

The author acknowledges the RET Planning Grant by the National Science Foundation for support and Drs. Fuyan Liang and M. Eileen Birch from The National Institute of Occupational Safety and Health for the OC/EC analysis.

REFERENCES

1. U.S. Department of Health and Human Services, Public Health Service, Centers for Disease Control, National Institute for Occupational Safety and Health, DHHS (NIOSH). (1988). *Current Intelligence Bulletin No 50 - Carcinogenic Effects of Exposure to Diesel Exhaust.* Publication No. 88-116. Cincinnati, OH.
2. U.S. Environmental Protection Agency, National Center for Environmental Assessment. (2000). *Health Assessment Document for Diesel Emission.* Review Draft EPA/600/8-90/057E. Washington, DC.
3. American Lung Association. (2005). *State of the Air 2005*. Retrieved on July 20, 2005, from http://lungaction.org/reports/sota05_cities.html.
4. Private communication with ARTIMIS.
5. Federal Register, Part II, Environmental Protection Agency, 40 CFR Part 60, 61, and 63, Amendments for Testing and Monitoring Provisions; Final Rule. Tuesday, October 17, 2000. Also available at http://www.epa.gov/ttn/emc/promgate.html (accessed April 2005).
6. U.S. Department of Health and Human Services (DHHS), Public Health Service, Centers for Disease Control, National Institute for Occupational Safety and Health (NIOSH). NIOSH Manual of Analytical Methods (*NMAM*), Cassinelli, M.E., O'Connor, P.F., Eds. Second Supplement to *NMAM*, 4th Edition. Publication No. 94-113. Cincinnati, OH. 1998.
7. Z. Liu, M. Lu, T. Keener, E. Birch, S. Khang, F. Liang, "Variations of the particulate carbon distribution for a nonroad diesel generator", *Environmental Science and Technology*, 39: 7840-7844 (2005).

CHARACTERISTICS AND SHIP TRAFFIC SOURCE IDENTIFICATION OF AIR POLLUTANTS IN SHANGHAI PORT, CHINA

Yan Zhang[1], Minjiang Zhao[1], Weichun Ma[1], Qingyan Fu[2], Xin Yang[1], Chunlei Li[1], Bin Zhou[1], Qi Yu[1], Limin Chen[1]
1. Department of Environmental Science and Engineering, Fudan University, Shanghai, 200433, China
2. Shanghai Environmental Monitoring Center, Shanghai, 200030, China

ABSTRACT: To know the characteristics of air pollutants in Shanghai Port and contribution of the ship traffic emission to them, field measurements have been conducted in 2011. The trace gases SO2, NO2 and O3 were monitored and aerosol samples of TSP, PM2.5 and size-segregated particles were collected in one working area of Shanghai Port. Also elements including V, Ni, Al, Fe, Si, Ca, Na, Mg, Mn, Zn, Co, Cr in aerosol samples and heavy fuel oils samples were analyzed. The results revealed that average hourly SO2 and NO2 concentrations in Shanghai Port were respectively 0.029 and 0.064 mg m-3, concentrations of TSP and PM2.5 were 114.39 and 62.60μg m-3, comparable with the ones in Shanghai land area. Ni and V were found enriched and mainly accumulate in fine particles with averaged concentrations of 80.0 and 14.8ng m-3 in PM2.5 respectively. Also ratio of V/Ni in aerosol under summertime airflow was 3.4, very close to the ratio of averaged V and Ni content in international Heavy Fule Oil used in Shanghai Port. The backward trajectory analysis further revealed that SO2, NO2, and V under coastal airflows were mainly from ship traffic emission. The mean concentration of vanadium was 15.84ng m-3 under hybrid coastal airflows, much higher than that of 9.84ng m-3 under continental airflows. Furthermore, V was found to be obviously positively correlated with ship fluxes, and was selected as an indicator of ship traffic emission in Shanghai. The estimated primary PM2.5 contribution from ship traffic ranged from 0.63 to 3.58μg m-3, with an average of 1.96μg m-3. This PM2.5 fraction accounted for 4.23% of the total PM2.5 in an average level, and reached to a maximum of 12.80%. Further, there would be 62% of primary PM2.5 contributed by ships in Shanghai Port transported to a land site estimated by the parallel sampling measurement. Our results suggest that ship traffic has an important impact on ambient levels of fine particles as well as SO2 and NO2 and major part of ship traffic emission could be transported to the surrounding land area.

Keywords: PM2.5, Chemical composition, Shipping emission, V, Ni, Shanghai

INTRODUCTION

Ships are making a non-negligible contribution to global and regional emission inventories of SOx, NOx and PM in recent studies (Corbett and Fischbeck, 1997; 2000; Eyring et al., 2005; Endresen et al., 2007; Wang et al., 2008; Jalkanen et al, 2009). Also the impacts of ship emissions on global climate, air quality and human health in coastal areas have been reported worldwide (Capaldo et al., 1999; Isakson et al., 2001; Lu et al., 2006; Corbett et al., 2007; Vutukuru and Dabdub, 2008; Agrawal et al., 2009; Ault et al., 2009; Matthias et al, 2010; Hellebust et al., 2010; Lonati et al., 2010). The various impacts caused by ship emission not only depend on their emission fluxes, concentrations, but also on their chemical compositions. Oceangoing ships running large diesel engines generally burn low-quality residual fuels that tend to contain high amounts of sulfur and heavy metals (Lack et al., 2009; Lack et al., 2011). Recently, Ni, associated with cardiovascular hazards emission has attracted public attention because of their adverse effects on human health, and Ni were being contributed a lot by ship emissions from Port of New York in summertime (Lippmann et al., 2006; Peltier et al, 2009; Peltier and Lippmann, 2010). Several recent studies have clearly revealed ship exhaust particles as containing V and Ni by Aerosol

---

ISBN 9780976885351

Time-of-Flight Mass Spectrometer monitoring (Healy et al., 2009; Ault et al., 2009) or in-stack emission measurements (Agrawal et al., 2008). Furthermore, it has tackled the problem that estimate the fine particles contributed by ship traffic via using certain chemical components as markers (Agrawal et al., 2009; Pandolfi et al., 2011).

Now a majority of 10 largest marine ports in the world comes under the Asian continent and mostly emerge from China, of which the biggest one is Shanghai Port. Shanghai Port became the world's largest container shipping port since 2008. Yang et al (2007) has developed an emission inventory from marine ships, from which NOx, SO2 from ships accounting for 13.4%, 9.5% of all sources in Shanghai in 2003, respectively. The amounts of throughput goods and 20-foot-equivalent units (TEU) in 2010 were 653 million tons and 29.1 million TEU, respectively, more than 2 and 2.6 times the amounts in 2003. However, few studies have reported the air quality situation in Shanghai Port, even in ports of China. This study aims to understand the characteristics of air pollutants in one typical Port and try to identify the contribution of ship traffic source on local and regional air pollutants by in situ atmospheric field measurements and Heavy Fuel Oil (HFO) survey.

LOCATION AND MEASUREMENTS

Samples Collecting. As one of five working areas of Shanghai Port, the Yangshan Port, located 20 miles off the coast of Shanghai in the East China Sea is a deep water port opened in late 2005. With annual throughput of 10.1 million TEUs in 2010 (Shao and Wu, 2011), Yangshan Port is well representative of Shanghai Port. Field measurements were chosen to be conducted in Yangshan Port (30.63N, 122.06E) on Xiaoyangshan Island in the East China Sea, connected to the mainland via the world's longest sea bridge (Fig. 1). The site was on the roof of a building, with a height of 10m above the ground and a distance of 600m to the shipping berths. There were no other industry activities on the island except the mechanical work in the port and few inhabitants lived there. Thus, the measurement site can be considered as a coastal port background station.

Fig. 1. Map of the sampling site in this study (from Google Map)

Three field measurement campaigns were carried out in the year of 2011. Aerosol samples of TSP and PM2.5 in winter (January13-19), spring (May11-21) and summer (August1-11) were collected by Anderson medium-flow samplers. In spring and summer, an Andersen eight-stage impactor was used to collect fine particles of different sizes. The aerodynamic size cuts for each stage of the impactor were 0.4, 0.7, 1.1, 2.1, 3.3, 4.7, 5.8 and 9μm. All the aerosol samples were collected onto Whatman-42 cellulose filters. The sampling time of TSP and PM2.5 in winter and summer were 24h, with the daily filter changing time of 08:00 (Beijing time, the same hereafter), while the time of spring sampling was generally 12h, with the filters changed twice at 08:00 and 20:00. The size-segregated air particles were collected with 48−72 hours at a flow rate of 28.3L min-1. After finishing the sampling, every sample was immediately put in a polyethylene plastic bag and reserved in a refrigerator subsequently. All those filters were weighed before and after sampling for mass by an analytical balance (Sartorius BP211D). Before weighing, the substrates were equilibrated in the weighing room at relative humidity of 40±2% and temperature of 25±2℃. Totally 35 TSP, 35 PM2.5 and 9 sets of size-segregated particle samples were collected throughout the sampling periods. It should be noted that the experimental study was interrupted on 6-7 August due to the passage of typhoon “Meihua”.

Trace gaseous pollutants (SO2, NO2 and O3) were simultaneously monitored by DOAS (differential optical absorption spectroscopy) technique. The detailed information about DOAS was given elsewhere (Hao et al., 2006). The integration time of per spectrum was about 5 minutes. All the gas concentration data used were recalculated in the time resolution of one hour. Only data obtained in May and August were available since no gas monitoring campaign was performed in January. Additionally, ship traffic intensity (numbers of ships enrolled per day) was provided by marine administration in the port and hourly averaged SO2, NO2 and O3 concentration data of Shanghai urban area were provided by Shanghai Environmental Monitoring Center.

It should be mentioned that PM2.5 samples with sampling periods of 24h were also collected at a site in Binhai Site in Pudong District (Fig. 1) during the spring period. Moreover, 25 Heavy Fuel Oil (HFO) samples have been collected from China Marine Bunker, the biggest HFO supplier company, accounting for 60% of oil market for ships passing by Shanghai Port. The HFO samples composed of 19 domestic samples and 6 international samples derived from CMB’s oil samples in 2011.

Chemical Analysis. All the PM2.5 and size-segregated particle samples were selected for element analysis. In order to avoid any possible contamination of the samples, all the following procedures were strictly quality-controlled.

Half of each sample filter and blank filter was cut into pieces (about 1cm2) and put in a high-pressure Teflon digestion vessel with 7mL HNO3 and 0.6mL HF. It takes about 45min for the microwave digestion system (CEM MARS5) to digest the filters. After cooling, the solutions were dried to about 0.5mL, and then added 0.2mL HNO3, and diluted to 10mL with deionized water (18MΩ cm-1). All the acids used were in the quality of guaranteed reagent. Elements including S, Al, Fe, Ca, Mg, Mn, Ba, Cu, Cr, Na, Zn, Ti, Ni, V, K, Pb, As, Sr, I and P were determined by Inductively Coupled Plasma Spectrometer (ICP, model: SPECTRO ARCOS, made in Germany). Each element got concentration values by subtracting blank values from determinations and had the recovery range of 95-105%. Some other studies also used very similar methods (Li et al., 2008a; Deng et al., 2011).

The oil samples were sent to Shanghai INTERTEK lab to analyze the trace metal contents using ICP method after ashing. The 8 of 25 samples were selected for 12 elements analysis (V, Ni, Ca, Al, Fe, Si, Na, Mg, Mn, Zn, Co, Cr), including 6 domestic and 2 international samples. The left 17 samples were analyzed just for V and Ni contents.

METEOROLOGICAL BACKGROUND

Surface Meteorological Conditions. The meteorological data, including wind speed, wind direction, temperature, visibility, and relative humidity with six-hour resolution were provided by the local meteorological station in the port. The visibility was not observed at 02:00. The variations of the meteorological factors in the sampling period were described in Fig. 2. The prevailing wind directions were from north and northwest in January and were from south in May and August. In summer, there were evident southern airflows reaching the port from the sea side. The average temperatures in January, May and August were 1.6, 20.5 and 27.9℃, respectively. Relative humidity ranged from 35 to 95% with an average of 76%, while visibility ranged from 1.2 to 50km with an average of 19km and a frequency of 23% lower than 10km. In addition, low visibilities were more frequently occurred in May than in January and August.

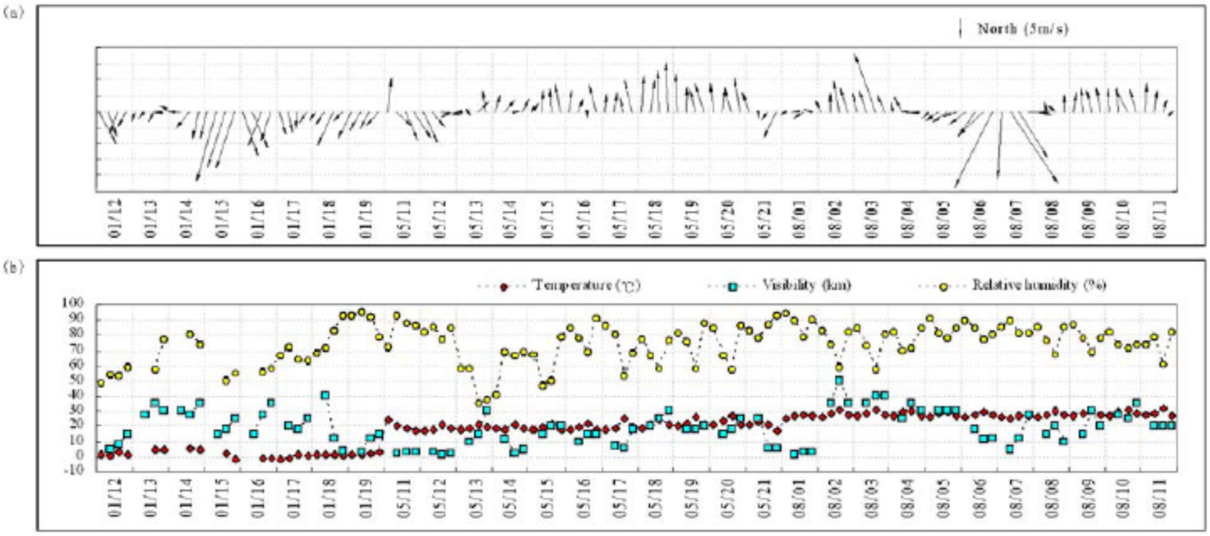

Fig. 2. Meteorological variables during the sampling period: (a) wind vector, (b) temperature, visibility and relative humidity.

Air Mass Trajectories Above 500m. To better understand the potential influences of different source regions on aerosol composition at the sampling site, the daily air mass trajectories at an altitude of 500m above ground level were calculated using the HYSPLIT 4 model (Draxler and Rolph, 2003). The backward trajectory began at 00:00 UTC (local time: 08:00), and every 6h per calculation. FNL meteorological data were used as input. Based on the transport pathways of air masses, there were existing three typical types of air mass trajectories, representing continental dominant, marine dominant, and mixing (continental plus marine) airflows, during the sampling period and plotted in Fig. 3.

RESULTS AND DISCUSSION

Chemical Characteristics of Air Pollutants in Yangshan Port

Concentrations of trace gases and particle matters. The measured average hourly SO2 and NO2 concentrations in Yangshan Port were 0.029 and 0.064mg m-3, respectively. Compared with Shanghai land area, SO2 level was about the same (mean hourly SO2 concentration in land area: 0.029mg m-3) while NO2 level was generally higher in Yangshan Port (Fig. 4). The high levels of the two gases in the port were mainly linked with the emissions from ship exhaust since our sampling site was very close to the shipping berths. During the monitoring period, SO2 in Yangshan Port had reached a maximum hourly concentration of 0.119mg m-3, which was 2.4 times higher than the daily Chinese national ambient air quality standard Ⅱ (0.05mg m-3). NO2 seemed more polluted in the port since its highest hourly concentration (0.200 mg m-3) even exceeded daily Chinese national ambient air quality standard Ⅳ

(0.18mg m-3). However, a much lower level of O3 was observed in Yangshan Port when compared with Shanghai land area.

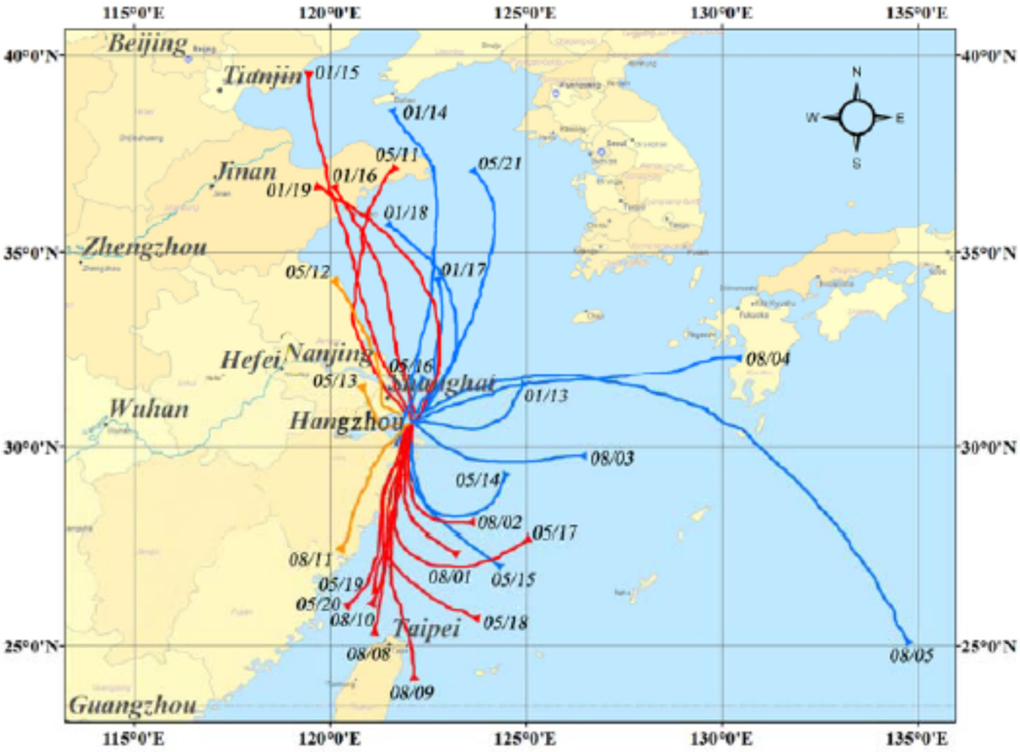

Fig. 3. Daily trajectories of air masses arriving at Yangshan Port during the sampling period. The date labels near the start-points of the trajectories are the starting dates. The yellow, blue, and red lines represent the trajectories of continental dominant, marine dominant and mixing air flow, respectively.

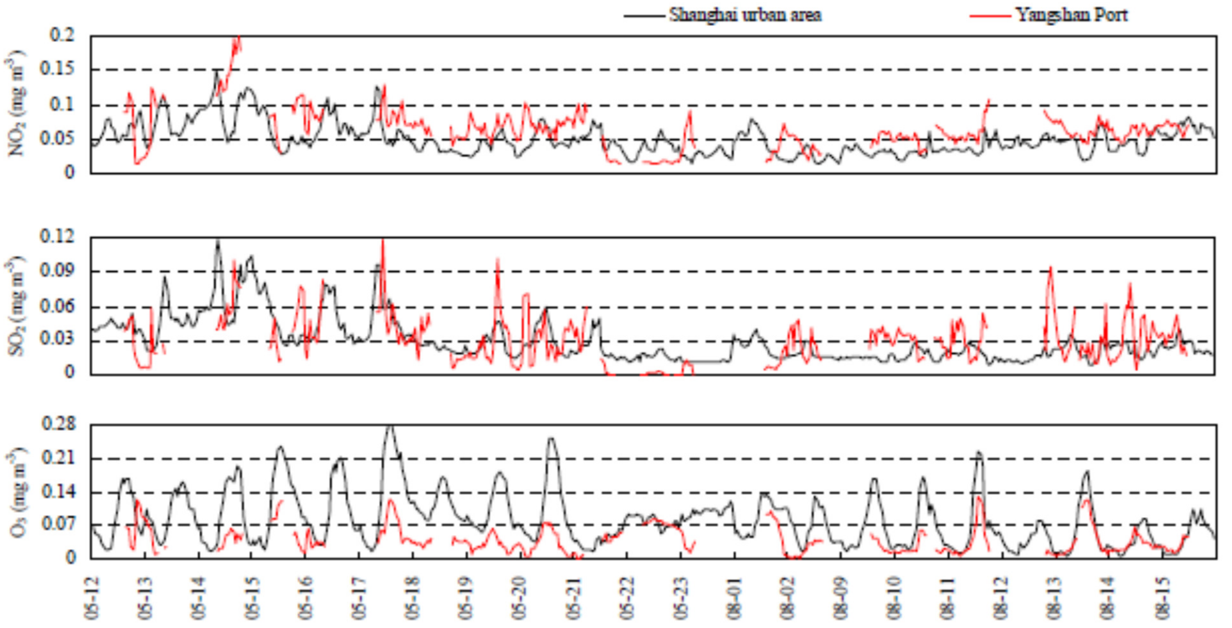

Fig. 4. Hourly SO_2, NO_2 and O_3 concentrations.

The daily TSP and PM2.5 mass concentrations obtained from the samples, as well as the corresponding ratios of PM2.5/TSP during the sampling periods were shown in Fig.5. The concentration values of TSP ranged from 48.06 to 404.63μg m-3, while those of PM2.5 ranged from 20.35 to 158.12μg m-3. The maximum value was about 8 times higher than the minimum one for both TSP and PM2.5, which showed wide variation ranges of particle concentrations in Yangshan port. Average concentrations of TSP and PM2.5 were 96.03 and 60.95μg m-3 in winter, 174.99 and 80.25μg m-3 in spring, and 72.14 and 46.61μg m-3 in summer, respectively. Although TSP and PM2.5 concentrations were in the highest average levels in spring, the lowest mean PM2.5/TSP ratio (0.49) was observed in this season compared with those of winter (0.59) and summer (0.64). PM2.5 concentrations in Yangshan Port were lower than those previously reported in urban Shanghai in 2003-2005 (Wang et al., 2006), comparable with those in coastal sites of Qingdao in 1997-2000 (Hu et al., 2002), but much higher than those in some coastal harbour sites (Hellebust et al., 2010; Contini et al., 2011; Pandolfi et al., 2011).

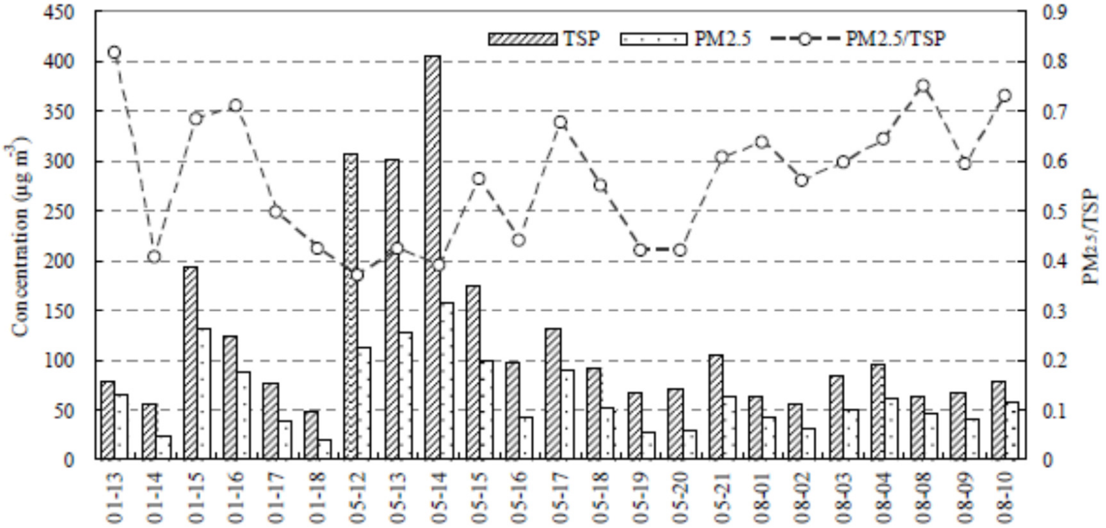

Fig. 5. Daily concentrations of TSP and PM$_{2.5}$ together with PM$_{2.5}$/TSP ratios measured in Yangshan Port.

Elemental contents and enrichment factors in PM2.5. Comparing the average concentrations of selected elements in PM2.5 samples, it was found that S, Na, Ca, Fe, Mg and Al had relatively high proportions of the 20 target elements. They accounted up to 92.3% of the elements. The mean values obtained in the sampling period for the group of elements analyzed lay in the range of 4.50ng m-3-5.94μg m-3, with only S, Na, Ca and Fe exceeding 1μg m-3.

In terms of some trace heavy metals, the concentration ranges of Ni, Pb and V were 0.2-376.3, 0.9-86.8 and 3.4-38.5ng m-3, respectively. In brief, the average concentration observed during the sampling period in our study was 80.0ng m-3 for Ni, 24.4ng m-3 for Pb, and 14.8ng m-3 for V. The temporal trend of daily concentrations of V and Ni in PM2.5 samples was shown in Fig. 6. It can be seen that the fluctuation of V level in Yangshan Port was always stable in each season. The concentration of Ni varied largely in the sampling periods, with very high value on Jan15-16 under the airflow via Jiaodong peninsula with a lot of heavy industries and power plants. However, the concentration of Ni tended to be stable in summer and lower than that of V. The averaged ratios of Ni/V were seasonally different, reached 15, 4 and 0.3, respectively in winter, spring and summer. The similar situation for Ni/V in winter and summer is found in NYC region, but the Ni concentration in Shanghai Port in winter is much higher than that in the Port of New York (Peltier and Lippmann, 2010).

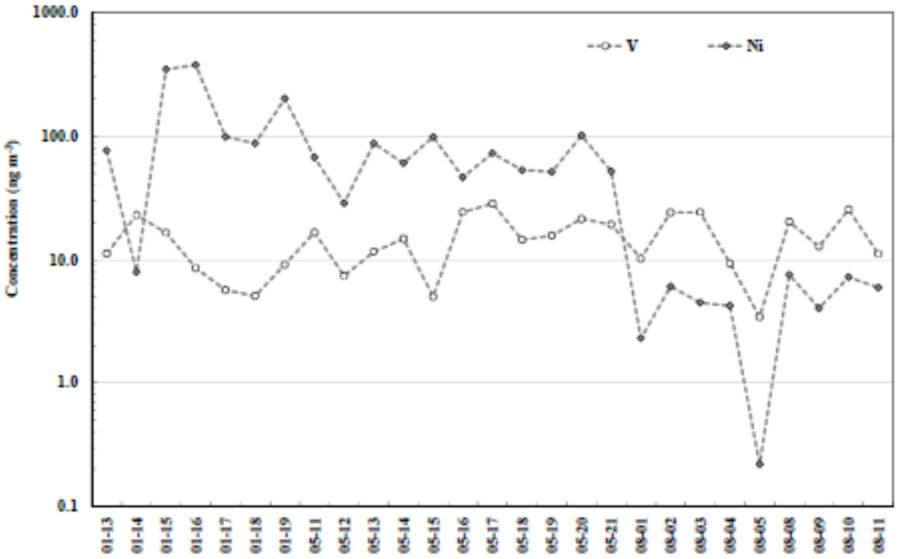

Fig. 6. Temporal trend of daily concentrations of V and Ni in $PM_{2.5}$

Enrichment factor (EF) is used in this study to evaluate influences of non-crustal sources on observed concentrations of elements. Mathematically, EF is expressed as EF = (X/R)aerosol/(X/R)crust, where (X/R)aerosol is the concentration ratio of the interest element X to the reference element R in aerosol, and (X/R)crust is the concentration ratio of X to R in crust. Species with EFs less than 10 usually have a major mineral source, while species with high EFs probably have a significant anthropogenic source. The composition of the continental crust was given by Wedepohl (1995) and Al was selected as the reference element when EFs were being calculated.

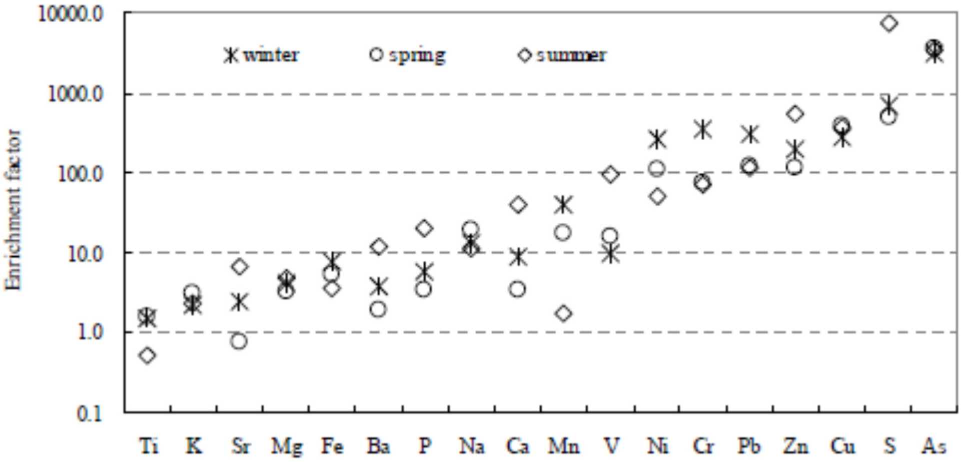

Fig. 7. Enrichment factor of elements in $PM_{2.5}$ in Yangshan Port

Totally eighteen elements obtained EF values through calculation and the results are depicted in Fig. 7. The EF values of Ti, K, Sr, Mg, Fe, Ba, P, Na and Ca were mostly less than 10, indicating that these nine elements were largely contributed by the mineral dust. However, among these crustal elements, Ba, P, Na and Ca with EF values a bit higher than 10 sometimes can be explained by the contribution of sea salt. Elements Mn and V are moderately (EF<100) and Ni, Cr, Pb, Zn, Cu, S and As are highly

(EF>100) enriched due to the contribution of non-crustal sources to aerosol composition. EFs reaching more than 1000 for the most enriched elements S and As, and EFs of heavy metals V, Ni, Cr, Pb, Zn and Cu were mostly within the range of several hundred revealed the severe aerosol pollution in Yangshan Port.

Among the pollution related elements, the EFs of some of them (for instance, Mn and Ni, Cr and Pb, Zn and S, Cu and As) shared the similar seasonal variation pattern, which might be a result of the same source. It should be noted that V probably derived from certain anthropogenic sources different from other elements, which was suggested by its unique EF seasonal variation pattern. The EF of V reached a remarkable value of 98 in summer and with the lowest value in wintertime.

Size distribution of chemical components. Based on the concentration data of chemical components in size-segregated aerosol samples collected in May and August, there were three different size distribution types in Shanghai Port: evenly distributed, coarse mode gathered and fine mode gathered. The calculated mass fractions of size-segregated elements in PM9 were presented in Fig. 8.

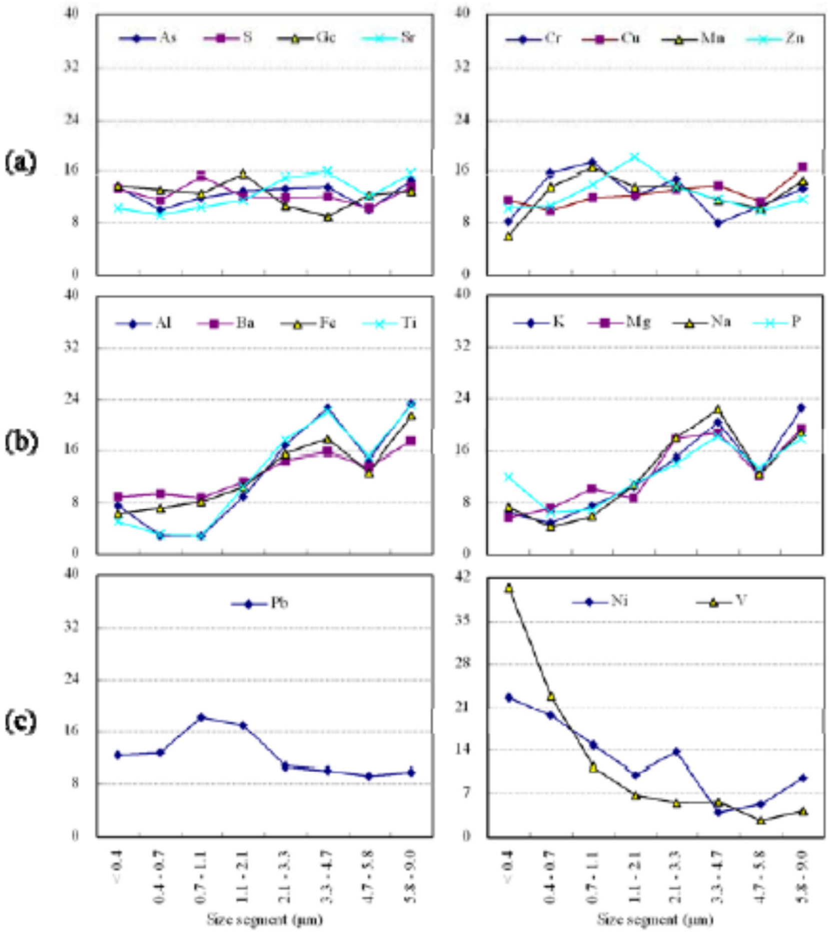

Fig. 8. Mass size distribution of chemical components in size-segregated aerosol samples collected in Yangshan Port: (a) evenly distributed, (b) coarse mode gathered, (c) fine mode gathered.

Elements like As, S, Ge, Sr, Cr, Cu, Mn, Zn were evenly distributed in most of the size ranges. Crustal elements Al, Ti, Fe, K, Ba, Mg, P and Na, based on EF study, were found mostly in the larger size ranges. Nevertheless, heavy metals Pb, Ni, and V, all of which were predominantly of anthropogenic origin, tended to accumulate in fine particles rather than coarse particles. Among them, V exhibited strongest enrichment trend in fine mode with above 40.5% mass fraction below 0.4μm. Similar to V, Ni also showed more enriched in fine particles than coarse particles, suggested by mass fraction values in smaller size ranges were much higher than those in larger size ranges. It should be noted here the size distribution was just for spring and summer, high concentration of Ni coming from long distance transport in Janurary was not included here. Jang et al. (2007) also reported that V and Ni were more enriched in fine particles, particularly in ultra-fine particles by studying the characteristics of fine particles. Since high levels of V and Ni were observed at sites close to heavy ship traffic in early studies (Querol et al., 2007), the notable fine mode gathering characteristics of the two elements shed some light on the fact that emissions released by ships are prevalently composed of fine particles.

Ship Traffic Source Identification of Air Pollutants in Yangshan Port

Characteristics of elements in Heavy Fuel Oil used in Shanghai Port. The HFO used by ships in Shanghai Port comes from multiple kinds of sources, mainly divided two categories, domestic and international ones, which are supplied for the domestic and international ships, respectively. Among 25 HFO samples, 6 domestic and 2 international samples were selected for multiple element analysis. In terms of averaged contents in the 8 HFO samples, vanadium and nickel ranked the top two of all the 12 elements, with the average concentrations of 103 and 37 mg kg-1, respectively. The concentrations of Ca, Al, Fe, Si, and Na ranged from 14.3 to 20.3 mg kg-1. The concentrations of Zn, Mg, Cr, Mn, and Co were below 10 mg kg-1. The vanadium and nickel contents in 25 HFO samples were listed in Table 1. The averaged V and Ni contents were 56±35.6 and 30±13.1 mg kg-1 for domestic HFO, and 93±77.9 and 24±8.3 mg kg-1 for international HFO, respectively. The ratio of V/Ni varied from 0.5 to 3.5 for domestic HFO, and from 1.9 to 6.5 for international HFO. Overall, the averaged ratio of V/Ni in international HFO was 3.6, much higher than 1.9 in domestic HFO. The average ratio of V/Ni in summertime aerosol samples was 3.4, very close to the value in international HFO. That implied the V and Ni predominantly coming from ship traffic emission during the summer by the marine wind.

Table 1 Vanadium and nickel contents in the selected Heavy Fuel Oil (HFO) samples (unit: mg kg^{-1})

	Domestic HFO (n=19)				International HFO (n=6)			
	Average	Minimum	Maximum	Standard deviation	Average	Minimum	Maximum	Standard deviation
Vanadium	56	10	164	35.6	93	43	266	77.9
Nickel	30	14	65	13.1	24	14	41	8.3
Ratio of V/Ni	**1.9**	0.5	3.5	0.9	**3.6**	1.9	6.5	1.5

Source identification by backward trajectory analysis. As presented in Fig.3, three major types of airflow including dominant terrestrial, dominant marine and mixing airflow were influencing Yangshan Port. Following that, the correlation analysis between hourly SO2 and NO2 concentrations under different airflows was carried out, and the result was depicted in Fig. 9. Also the concentrations of elements in PM2.5 under different airflows were compared and the corresponding data were listed in Table 2.

Weak correlation between SO2 and NO2 were found with correlation coefficient of 0.42 under continental airflows. However, larger correlation coefficient (r = 0.63) occurred between the two gases under mixing airflows. Meanwhile, the strongest correlation (r = 0.91) between SO2 and NO2 were found under marine airflows, suggesting a significant common source. Allowing for the fact that SO2 and NOx are key compounds emitted by seagoing ships (Lloyd's, 1995), the main source responsible for SO2 and NO2 under marine airflows in Yangshan Port would be the heavy ship traffic.

For most elements, concentrations under the three different airflow types did not exhibit significant differences. However, under continental airflows, as expected, average concentrations of typical crustal metal Al and Ti were highest, exceeding the levels under the other two by notable higher concentration values. The concentration ratio under hybrid coastal airflows to continental airflows was 0.5 for Al and 0.6 for Ti, respectively. On the contrary, concentrations of V and Ni, 15.84 and 71.37ng/m3 under hybrid coastal airflows, were much higher than 9.84 and 47.62ng/m3 under continental airflows. The concentration ratios of V and Ni under hybrid coastal versus continental airflows were separately 1.6 and 1.5, indicating the significant effect of ship traffic associated with heavy fuel oil combustion.

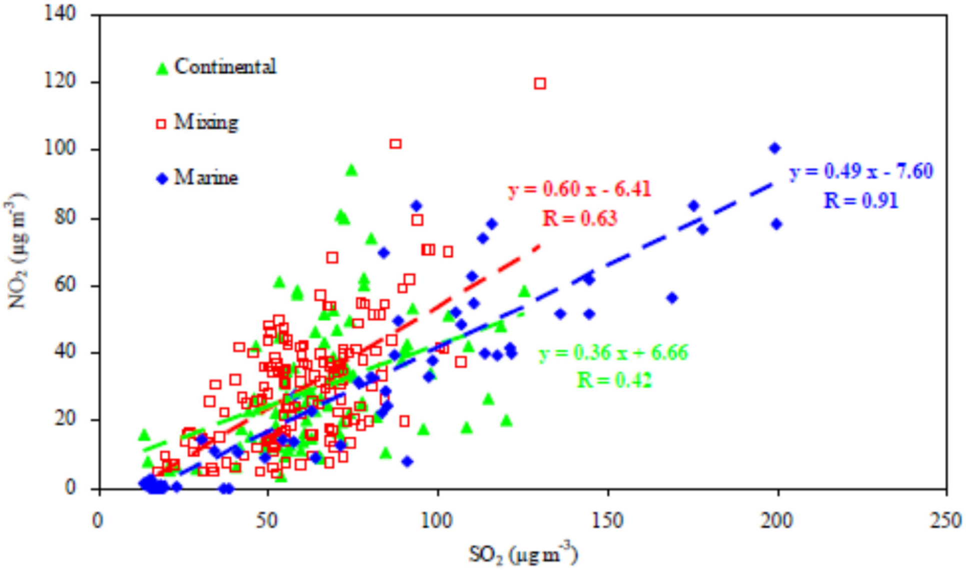

Fig. 9. Correlation analysis between hourly SO_2 and NO_2 concentrations under different airflows

Table 2 Comparison of concentrations of chemical components in $PM_{2.5}$ under different airflows

Component	Unit	Continental	Marine	Mixing	Hybrid coastal^a	Hybrid coastal/Continental
Al	μg m^{-3}	1.27	0.61	0.53	0.57	**0.5**
Ti	ng m^{-3}	82.00	51.93	40.22	46.08	**0.6**
Pb	ng m^{-3}	26.38	24.02	17.32	20.67	0.8
Na	μg m^{-3}	3.72	2.53	4.08	3.30	0.9
As	ng m^{-3}	47.52	48.32	49.74	49.03	1.0
P	ng m^{-3}	32.29	30.28	31.18	30.73	1.0
Zn	ng m^{-3}	86.54	79.11	94.44	86.78	1.0
Fe	μg m^{-3}	1.97	1.87	2.33	2.10	1.1
S	μg m^{-3}	4.79	5.17	5.54	5.36	1.1
Mg	ng m^{-3}	536.76	702.74	653.44	678.09	1.3
Mn	ng m^{-3}	110.42	117.19	168.07	142.63	1.3
Ca	μg m^{-3}	1.52	2.21	2.33	2.27	1.5
Ni	ng m^{-3}	47.62	49.98	92.77	71.37	**1.5**
V	ng m^{-3}	9.84	13.79	17.89	15.84	**1.6**

^{a} *Average concentration under marine and mixing airflows.*

When the correlation of daily ship fluxes with the concentrations of elements in PM2.5 was analyzed, V was found to be the one that most positively correlated with ship fluxes. Furthermore, as illustrated in Fig. 10 that V had its stronger correlation with international ships than domestic ones, pointing to the fact that international ship emissions were playing more important roles on the concentrations of V in Yangshan port.

However, in our study weak correlation was found between mass concentrations of V and Ni in the PM2.5 samples. Taking into account that Ni had relative weak positive correlations with ship fluxes and relative high EF values when compared with V, it was concluded that some unidentified Ni sources might also affect the PM2.5 composition at our sampling site. Based on all the statistical analysis above, ships running on heavy fuel oil were identified as the only significant source of V in ambient PM2.5 in Yangshan Port and therefore V could serve as a tracer for PM2.5 emission from ship traffic.

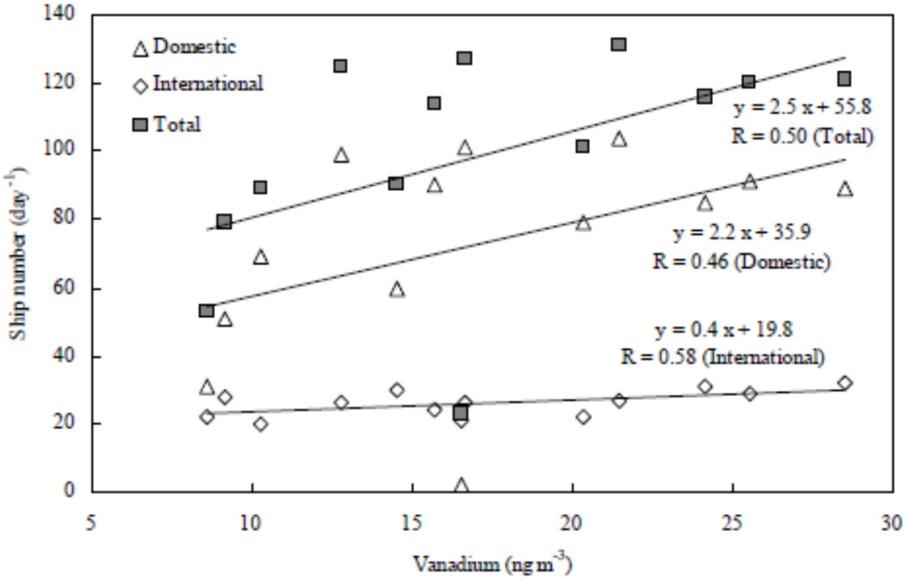

Fig. 10. Relationship between daily vanadium concentrations and ship fluxes under mixing airflows

Contribution Estimate to PM2.5 from Ship Traffic Emissions with V as the Indicator. Based on the background of our sampling site combined with the results mentioned above in this paper, it was reasonable to use V as a tracer for the combustion of heavy fuel oil typically burned by ships. It should be mentioned that the result of the estimation using the equation would be more reliable if no other major sources of V are present. Following the method reported by Agrawal et al. (2009), the PM2.5 contribution in Shanghai Port from ship traffic was calculated using the equation: $PMa = r \times Va/FV, HFO$ (2009). where *PMa* is primary PM2.5 concentration estimate (μg m-3), *r* is average ratio of PM2.5 to normalized V emitted (ppm) according to the HFO burning experiment, *Va* is ambient V concentration (μg m-3) and *FV, HFO* is average V content of the heavy fuel oil from all vessels (ppm). In this study, the value of FV, HFO used 65.3 ppm of the average vanadium content in the domestic and international HFO samples collected from China Marine Bunker. Fig. 11 showed the resulting contribution estimate of primary PM2.5 due to ship traffic in Yangshan Port.

The result revealed that primary PM2.5 concentrations contributed by ship traffic ranged from 0.63 to 3.58μg m-3, with an average of 1.96μg m-3. This PM2.5 fraction accounted for 4.23% of the total PM2.5 in an average level, and reached to a maximum of 12.8% on the day of 14 January. The averaged primary PM2.5 concentration and fraction from ship traffic would be respectively 1.38 μg m-3 and 2.97% if taking 93 ppm of average V in international HFO as the value of FV, HFO. This also means that ship traffic has a non-negligible impact on ambient PM2.5 levels since this only included the primary contribution. In addition, our estimated primary PM2.5 from ship traffic was at similar level of 1.2-2.3μg m-3 ,0.39-0.47μg m-3, and 0.18-0.42μg m-3 primary PM2.5 contribution reported by Pandolfi et al. (2011) , Kim and Hopke (2008) using PMF model, and Minguillón et al. (2008) using CMB model, respectively.

It was found that the prevailing wind direction was from south in spring and summer time of our sampling period, which indicated that the meteorological conditions favored the transport of pollutants from Yangshan Port to Shanghai land areas. The four PM2.5 samples collected at Binhai site in Pudong District revealed that about 1.22μg m-3 primary PM2.5 were from ship traffic, accounting 2.7% of the total PM2.5 concentration. However, this contributed primary PM2.5 reaching this site could account for

62% of that estimated one in Yangshan Port from ship traffic contribution. The results confirmed that ship traffic had important influences on local and regional scale air quality.

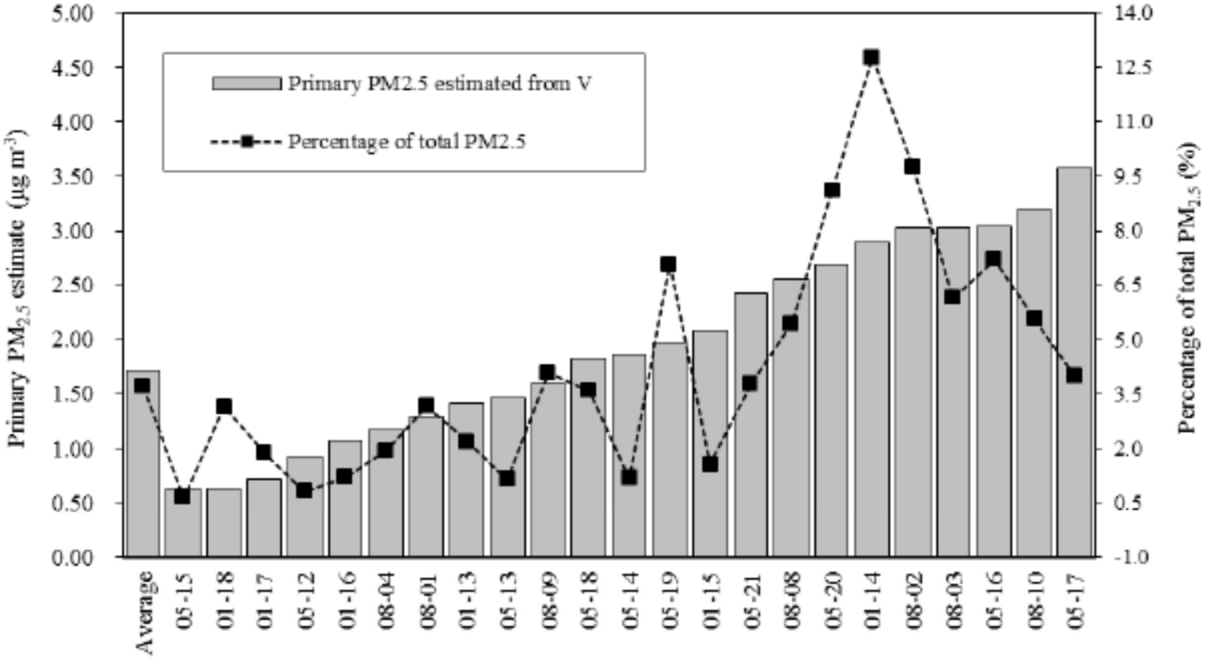

Fig. 11. Contribution estimate to primary $PM_{2.5}$ from ship traffic emissions in Yangshan Port

CONCLUSIONS

The concentrations of trace gases and PM as well as elements in the collected fine particle and HFO samples have been used to understand the chemical characteristic of air quality in Shanghai Port and to estimate the possible contribution of ship traffic. Average hourly SO2 and NO2 concentrations measured in Shanghai Port were 0.029 and 0.064mg m-3, respectively. Average daily concentrations of TSP and PM2.5 were found separately 114.39 and 62.60μg m-3 with seasonal PM2.5/TSP ratios ranged from 0.49 to 0.64. There were evident seasonal variations in Ni concentration in PM2.5, however, relatively stable concentrations for V in PM2.5. Size-segregated elements showed Ni and V were enriched due to anthropogenic activities and tended to accumulate in fine particles in spring and summer. The backward trajectory analysis revealed that ship traffic was mainly responsible for SO2, NO2 and V under marine airflows. Further, V was found to be the most positively correlated with ship fluxes and in conjunction with all statistical analysis, and was selected as an indicator for PM2.5 emission from ship traffic source. The estimated primary PM2.5 from ships ranged from 0.63 to 3.58μg m-3. This fraction by ships could account for 4.23% of the total PM2.5 in an average level, and reached to a maximum of 12.80% in Shanghai Port. Also The PM2.5 emitted by ship traffic could be transported to Shanghai land area.

Our results suggest that ship traffic has a non-negligible impact on primary particles as well as SO2 and NO2 in port and surrounding land area. However, ship traffic also could release precursors of secondary particles. The potential contribution of secondary fine particles caused by ship traffic would not be neglected for a robust project deals with the contribution estimation. So, further research to assess both primary and secondary particles contributed by ship traffic is necessary.

ACKNOWLEDGMENTS

This work was supported by the Foundation for National Natural Science Foundation of China (Grant Nos.41005076). Thanks for helps of Professor Jianmin Cheng in the observational site and the data support by Yangshan Meteorological Station and Marinetime Safety Administration of Shanghai. Also great thanks to China Marine Bunker for supplying HFO samples.

REFERENCE

Agrawal H, Q Malloy, W. Welchb, J. Millera, D Cocker III, 2008. In-use gaseous and particulate matter emissions from a modern ocean going container vessel, Atmospheric Environment 42, 5504-5510.

Agrawal, H., Eden, R., Zhang, X., Fine, P.M., Katzenstein, A., Miller, J.W., Ospital, J., Teffera, S., Cocker Ⅲ, D.R., 2009. Primary particulate matter from ocean-going engines in the Southern California Air Basin. Environmental Science & Technology 43, 5398-5402.

Ault, A.P., Moore, M.J., Furutani, H., Prather, K.A., 2009. Impact of emissions from the Los Angeles Port region on San Diego air quality during regional transport events. Environmental Science & Technology 43, 3500-3506.

Bućko, M.S., Magiera, T., Johanson, B., Petrovský, E., Pesonen, L.J., 2011. Identification of magnetic particulates in road dust accumulated on roadside snow using magnetic, geochemical and micro-morphological analyses. Environmental Pollution 159, 1266-1276.

Capaldo, K. P.,Corbett, J. J., Kasibhatla, P., Fischbeck, P., Pandis, S. N. Effects of Ship Emissions on Sulphur Cycling and Radiative Climate Forcing Over the Ocean. *Nature* **1999**, *400*, 743–746.

Chen, X., Teng, H., Wang, F., He, J., Zhou, S., Jian, Y., Xiao, X., 2003. Blood lead level and related risk factors among children aged 0-6 years in Beijing. Chinese Journal of Epidemiology 24(10), 868-871 (in Chinese).

Contini, D., Gambaro, A., Belosi, F., De Pieri, S., Cairns, W.R.L., Donateo, A., Zanotto, E., Citron, M., 2011. The direct influence of ship traffic on atmospheric PM2.5, PM10 and PAH in Venice. Journal of Environmental Management 92, 2119-2129.

Corbett, J. J., Fischbeck, P. S. Emissions from Ships. *Science* **1997**, *278* (5339), 823–824.

Corbett, J. J.,Fischbeck, P. S. Emissions from WaterborneCommerce Vessels in United States Continental and Inland Waterways. *Environ. Sci. Technol.* **2000**, *34* (15), 3254–3260.

Corbett J., Winebrake J., Green E., Kasibhatla P., Eyring V., Lauer A. Mortality from ship emissions: A global Assessment. Environ. Sci. Technol. 2007,418512-8518.

Deng, C., Zhuang, G., Huang, K., Li, J., Zhang, R., Wang, Q., Liu, T., Sun, Y., Guo, Z., Fu, J.S., Wang, Z., 2011. Chemical characterization of aerosols at summit of Mountain Tai in central east China. Atmospheric Chemistry and Physics 11, 7319-7332.

Draxler, R.R., Rolph, G.D., 2003. HYSPLIT (HYbrid Single-Particle Lagrangian Integrated Trajectory). NOAA Air Resources Laboratory, Silver Spring, MD Model access via NOAA ARL READY Website http://www.arl.noaa.gov/ready/hysplit4.html.

Endresen, O; Sørgard, E.; Sundet, J. K.; Dalsøren, S. B.; Isaksen, I. S. A.; Berglen, T. F.; Gravir, G. Emission from International Sea Transportation and Environmental Impact. *J. Geophys. Res.* **2003**, *108*, 4560.

Eyring, V., H. W. Köhler, J. van Aardenne, and A. Lauer (2005), Emissions from international shipping: 1. The last 50 years, *J. Geophys. Res.*, 110, D17305, doi:10.1029/2004JD005619.

Han, L., Zhuang, G., Cheng, S., Li, J., 2007. The mineral aerosol and its impact on urban pollution aerosols over Beijing, China. Atmospheric Environment 41, 7533-7546.

Hao, N., Zhou, B., Chen, D., Sun, Y., Gao, S., Chen, L., 2006. Measurements of NO2, SO2, O3, benzene and toluene using differential optical absorption spectroscopy (DOAS) in Shanghai, China. Annali di Chimica 96, 365-375.

Healy, R.M., O'Connor, I.P., Hellebust, S., Allanic, A., Sodeau, J.R., Wenger, J.C., 2009. Characterisation of single particles from in-port ship emissions. Atmospheric Environment 43, 6408-6414.

Hellebust, S., Allanic, A., O'Connor, I.P., Jourdan, C., Healy, D., Sodeau, J.R., 2010. Sources of ambient concentrations and chemical composition of PM2.5–0.1 in Cork Harbour, Ireland. Atmospheric Research 95, 136-149.

Hu, M., He, L., Zhang, Y., Wang, M., Kim, Y.P., Moon, K.C., 2002. Seasonal variation of ionic species in fine particles at Qingdao, China. Atmospheric Environment 36, 5853-5859.

Huang, W., Tan, J., Kan, H., Zhao, N., Song, W., Song, G., Chen, G., Jiang, L., Jiang, C., Chen, R., Chen, B., 2009. Visibility, air quality and daily mortality in Shanghai, China. Science of the Total Environment 407, 3295–3300.

Huo, M., Sun, Q., Xie, P., Bai, Y., Liu, Z., Li, J., Lu, S., 2009. Relationship between atmospheric particles and rain water chemistry character. Environmental Science 30(11), 3159-3166 (in Chinese).

Isakson, J., Persson, T.A., Lindgren, E.S., 2001. Identification and assessment of ship emissions and their effects in the harbour of Göteborg, Sweden. Atmospheric Environment 35, 3659-3666.

Jalkanen J.-P., A. Brink, J. Kalli, H. Pettersson, J. Kukkonen, and T. Stipa, 2009A modelling system for the exhaust emissions of marine traffic and its application in the Baltic Sea area, Atmos. Chem. Phys., 9, 9209–9223

Jang, H., Seo, Y., Lee, J., Hwang, K., Yoo, J., Sok, C., Kim, S., 2007. Formation of fine particles enriched by V and Ni from heavy oil combustion: Anthropogenic sources and drop-tube furnace experiments. Atmospheric Environment 41(5), 1053-1063.

Kim, E., Hopke, P.K., 2008. Source characterization of ambient fine particles at multiple sites in the Seattle area. Atmospheric Environment 42, 6047-6056.

Lack, D.A., Corbett, J.J., Onasch, T., Lerner, B., Massoli, P., Quinn, P.K., Bates, T.S., Covert, D.S., Coffman, D., Sierau, B., Herndon, S., Allan, J., Baynard, T., Lovejoy, E., Ravishankara, A.R., Williams, E., 2009. Particulate emissions from commercial shipping: Chemical, physical, and optical properties. Journal of Geophysical Research 114, D00F04.

Lack, D.A., Cappa, C.D., Langridge, J., Bahreini, R., Buffaloe, G., Brock, C., Cerully, K., Coffman, D., Hayden, K., Holloway, J., Lerner, B., Massoli, P., Li, S., McLaren, R., Middlebrook, A.M., Moore, R., Nenes, A., Nuaaman, I., Onasch, T.B., Peischl, J., Perring, A., Quinn, P.K., Ryerson, T., Schwartz,

J.P., Spackman, R., Wofsy, S.C., Worsnop, D., Xiang, B., Williams, E., 2011. Impact of fuel quality regulation and speed reductions on shipping emissions: Implications for climate and air quality. Environmental Science & Technology 45, 9052-9060.

Li, J., Zhuang, G., Huang, K., Lin, Y., Xu, C., Yu, S., 2008a. Characteristics and sources of air-borne particulate in Urumqi, China, the upstream area of Asia dust. Atmospheric Environment 42, 776-787.

Li, J., Zhuang, G., Huang, K., Lin, Y., Wang, Q., Guo, Y., Guo, J., Yu, S., Cui, C., Fu, J.S., 2008b. The chemistry of heavy haze over Urumqi, Central Asia. Journal of Atmospheric Chemistry 61, 57-72.

Lippmann, M., Ito, K., Hwang, J., Maciejczyk, P., Chen, L., 2006. Cardiovascular Effects of Nickel in Ambient Air. Environmental Health Perspectives 114, 1662-1669.

Lippmann M, Peltier R E., 2010. Residual oil combustion: 2. Distributions of airborne nickel and vanadium within New York City. Journal of Exposure Science and Environmental Epidemiology 20, 342–350

Lloyd’s Register of Shipping (LR), 1995. Marine Exhaust Emissions Research Programme. Lloyd’s Register Engineering Services, UK, London.

Lonati, G., Cernuschi, S., Sidi, S., 2010. Air quality impact assessment of at-berth ship emissions: Case-study for the project of a new freight port. Science of the Total Environment 409, 192-200.

Lu, G., Brook, J.R., Alfarra, M.R., Anlauf, K., Leaitch, W.R., Sharma, S., Wang, D., Worsnop, D.R., Phinney, L., 2006. Identification and characterization of inland ship plumes over Vancouver, BC. Atmospheric Environment 40, 2767-2782.

Mariani, R.L., Mello, W. Z., 2007. PM2.5–10, PM2.5 and associated water-soluble inorganic species at a coastal urban site in the metropolitan region of Rio de Janeiro. Atmospheric Environment 41, 2887-2892.

Matthias V, I Bewersdorff, A Aulinger, M Quante, 2010. The contribution of ship emissions to air pollution in the North Sea regions. Environmental Pollution 158, 2241-2250

Millero, F.J., Sohn, M.L., 1992. Chemical Oceanography. CRC Press, Boca Raton, FL, 531pp.

Minguillón, M.C., Arhami, M., Schauer, J.J., Sioutas, C., 2008. Seasonal and spatial variations of sources of fine and quasi-ultrafine particulate matter in neighborhoods near the Los Angeles-Long Beach harbour. Atmospheric Environment 42, 7317-7328.

Pandolfi, M., Gonzalez-Castanedo, Y., Alastuey, A., de la Rosa, J.D., Mantilla, E., de la Campa, A.S., Querol, X., Pey, J., Amato, F., Moreno, T., 2011. Source apportionment of PM10 and PM2.5 at multiple sites in the strait of Gibraltar by PMF: impact of shipping emissions. Environmental Science and Pollution Research 18, 260-269.

Peltier R E., S Hsu, R Lall, M Lippmann, 2009. Residual oil combustion: a major source of airborne nickel in New York City. Journal of Exposure Science and Environmental Epidemiology 19, 603–612.

Pope Ⅲ, C.A., Burnett, R.T., Thun, M.J., Calle, E.E., Krewski, D., Ito, K., Thurston, G.D., 2002. Lung cancer, cardiopulmonary mortality, and long-term exposure to fine particulate air pollution. Journal of the American Medical Association 287, 1132-1141.

Querol, X., Viana, M., Alastuey, A., Amato, F., Moreno, T., Castillo, S., Pey, J., de la Rosa, J., Sánchez de la Campa, A., Artíñano, B., Salvador, P., García Dos Santos, S., Fernández-Patier, R.,

Moreno-Grau, S., Negral, L., Minguillón, M.C., Monfort, E., Gil, J.I., Inza, A., Ortega, L.A., Santamaría, J.M., Zabalza, J., 2007. Source origin of trace elements in PM from regional background, urban and industrial sites of Spain. Atmospheric Environment 41, 7219-7231.

Salvador, P., Artíñano, B., Querol, X., Alastuey, A., Costoya, M., 2007. Characterisation of local and external contributions of atmospheric particulate matter at a background coastal site. Atmospheric Environment 41, 1-17.

Shao, R., Wu, M., 2011. Site selection and planning of Yangshan deepwater port. Waterway Engineering 7, 51-57 (in Chinese).

Tagaris, E., Liao, K., Delucia, A.J., Deck. L., Amar, P., Russell, A.G., 2009. Potential impact of climate change on air pollution-related human health effects. Environmental Science & Technology 43(13), 4979-4988.

Vutukuru S, D Dabdub, 2008. Modeling the effects of ship emissions on coastal air quality: A case study of southern California. Atmospheric Environment 42, 3751–3764

Wang C., James J. Corbett, and J. Firestone. Improving Spatial Representation of Global Ship Emissions Inventories. *Environ. Sci. Technol.*, **2008**, 42 (1), 193-199

Wang, Y., Zhuang, G., Zhang, Tang, A., Yuan, H., Sun, Y., Chen, S., Zheng, A., 2005. The ion chemistry and the source of PM2.5 aerosol in Beijing. Atmospheric Environment 39, 3771-3784.

Wang, Y., Zhuang, G., Zhang, X., Huang, K., Xu, C., Tang, A., Chen, J., An, Z., 2006. The ion chemistry, seasonal cycle, and sources of PM2.5 and TSP aerosol in Shanghai. Atmospheric Environment 40, 2935-2952.

Wedepohl, K.H., 1995. The composition of the continental crust. Geochimica et Cosmochimica Acta 59(7), 1217-1232.

Yang D., Kwan H., Lu T., **Fu Q.**, et al. 2007. An emission inventory marine vessels in shanghai in 2003. *Environmental Science and Technology*, 41(15),5183-5190.

Yuan, C., Lee, C., Liu, S., Chang, J., Yuan, C., Yang, H., 2006. Correlation of atmospheric visibility with chemical composition of Kaohsiung aerosols. Atmospheric Research 82, 663-679.

Zhang, X., Zhuang, G., Guo, J., Yin, K., Zhang, P., 2007. Characterization of aerosol over the Northern South China Sea during two cruises in 2003. Atmospheric Environment 41, 7821-7836.

Zhang, Y., Yu, Q., Ma, W., Chen. L., 2010. Influence of continental outflows on marine aerosols over Xiaoyangshan Island in the East China Sea: An episode of heavy air pollution. Terrestrial Atmospheric and Oceanic Sciences 21(6), 939-953.

2-02,873

ROLE OF CARBONACEOUS AEROSOL IN VISIBILITY IMPAIRMENT IN A TROPICAL MEGACITY

P. S. Khillare, Sayantan Sarkar and Darpa Saurav Jyethi
(Jawaharlal Nehru University, New Delhi, India)

ABSTRACT: Size-fractionated aerosol samples collected at two sites in Delhi in 2003 were analyzed for carbonaceous species (elemental and organic carbon, EC and OC) and water-soluble ions. Light extinction coefficients (b_{ext}) and standard visual range (SVR) were calculated from chemical speciation data. The visual air quality of Delhi was found to be poor with SVRs of 7.4-10.8 km and EC (16-23%) and OC (33-39%) being the major visibility impairing species. This led to the second study where aerosol samples collected at two sites in Delhi in 2008-09 were analyzed for EC, OC and total carbon (TC). A significant portion of aerosol mass (34-37%) was found to be carbonaceous and a moderately high positive correlation ($r = 0.63$, $p < 0.01$) between EC and OC indicated that OC might have secondary sources. OC/EC and EC/TC ratios indicated coal combustion and biomass burning sources along with some non-combustion primary OC. Secondary organic carbon (SOC) was quantified using the minimum OC/EC method and was found to contribute heavily (44-68%) to OC levels. It was therefore concluded that along with EC, a significant part of the visibility reduction in Delhi could be due to the high concentrations of SOC.

INTRODUCTION

Visual air quality is an important aspect of ambient air quality and visibility impairment is probably the most easily recognizable effect of atmospheric pollution. Visibility impairing aerosols are associated with economic and aesthetic losses and deleterious effects on human health and property. High loadings of atmospheric particulate matter (PM) and associated chemical species such as elemental and organic carbon (EC and OC) and inorganic ions such as SO_4^{2-}, NO_3^-, NH_4^+ etc. are determining factors for atmospheric visibility reduction. High atmospheric pressure and stability and increased relative humidity are also known to exacerbate visibility impairment. Therefore, investigation of the size distribution and chemical speciation of these aerosols is of vital importance to understand the phenomenon of visibility impairment, especially in urban areas that are affected by a multitude of sources. Towards this objective, two studies with a separation of 6 years were undertaken in the tropical megacity of Delhi, India. The results obtained in the first study (2003) consequently led to the second study during 2008-09. Results obtained in the second study forms the basic framework of this paper.

MATERIALS AND METHODS

Study area and sampling sites: Delhi (28°37'N, 77°12'E, population 17 million), the capital of India, is spread over an area of 1483 km^2 with an average elevation of 216 m above mean sea level. The region is characterized by intensely hot summers (monthly mean temperatures of 32°-34°C in May-June) and cold winters (monthly mean temperatures of 12°-14°C in December-January). The mean annual rainfall is 714 mm, of which ~80% is received during the monsoon months (July-October). Ground based temperature inversions are common during winters. The predominant wind direction is from the north and northwest (Fig. 1) except during the monsoon season that is characterized by easterly and southeasterly winds. Delhi houses three coal-fired power plants (combined capacity ~1100 MW) and around 130,000 industrial units. It is also home to a vehicular population of around 6.6 million.

ISBN 9780976885351

The whole study involved a total of three sampling sites, i) SN - a residential area with very heavy traffic in north-west Delhi, ii) MV - an urban residential area with moderate traffic in east Delhi and iii) JNU - a relatively clean residential/institutional area with good vegetation cover in south Delhi. The first study (2003) involved SN and JNU while the second study (2008-09) involved MV and JNU sites. Locations of the sampling sites are shown in Figure 1.

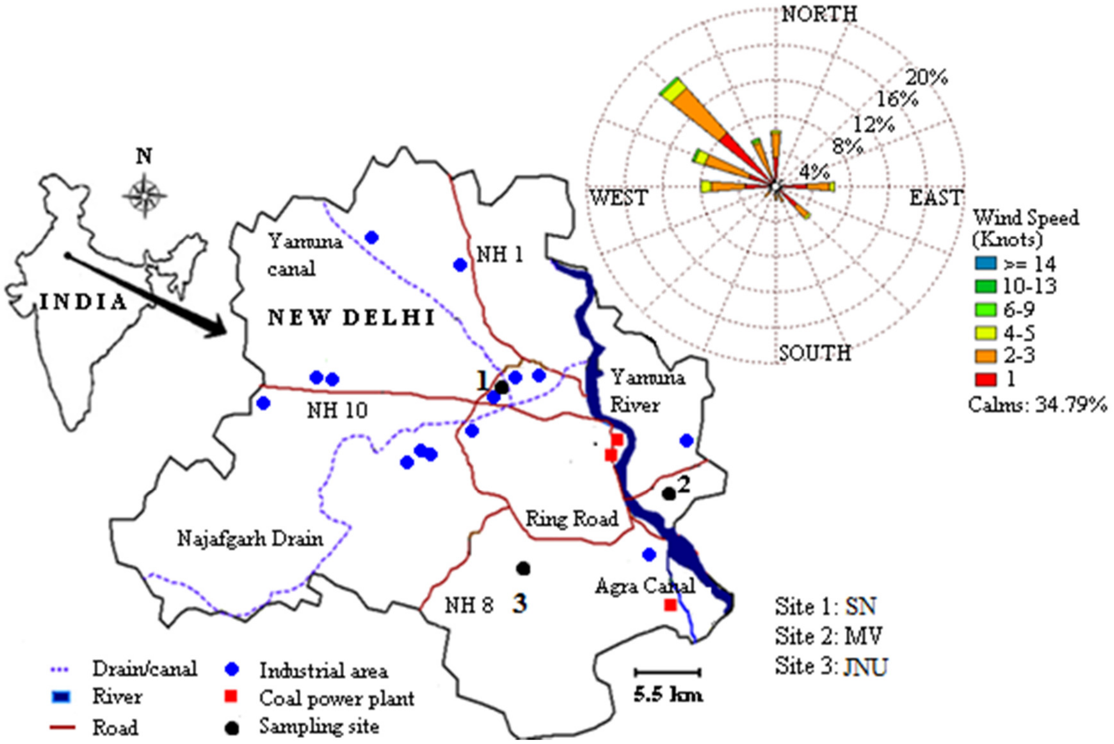

FIGURE 1. Map of Delhi showing the sampling sites and location of point sources in the study area. Also shown is a representative wind rose (December 2008-November 2009) for the study area.

Sampling and analysis protocols: In the first study (2003), aerosol sampling was carried out from June 2003 to November 2003 using the Andersen cascade aerosol sampler. Five samples were collected at each site during this period. Sampling was done for 72-80 hours at a time with a flow rate of 28.3 L min^{-1} using a preseparator for PM > 10 µm. The sampling substrate was glass fibre filters (Gelman Type A/E). Filters were pre-baked at 60°C overnight and were desiccated before and after use. The eight stages of exposed filter papers were separated as stages 1-5 for coarse fraction (>2.1 µm) and stages 6-F for fine fraction (<2.1 µm). In the second study (2008-09), 24-hour PM_{10} samples were collected simultaneously at the two sites from December 2008 to February 2009. The sampling frequency was once a week. A total of 12 samples were obtained per site during this period. PM_{10} was trapped on Whatman GF/A (8” × 10”) glass fibre filters (precombusted at 450°C for 12 hours) using high-volume samplers (Respirable Dust Sampler, Model MBLRDS-002, Mars Bioanalytical Pvt. Ltd.) having a constant flow rate of 1.2 m^{3} min^{-1}. Filters were desiccated for 48 hours before and after sampling.

In the first study, ions were extracted by sonication (20 kHz) in 20 ml of Milli-Q water for 20 min followed by filtration. Sulfate was determined by turbidity method (APHA, 1992), nitrate by Brucine method (Katz, 1977) and ammonium by Indophenol Blue method (Allen, 1989) using a VARIAN (Carry 300 Bio) spectrophotometer. OC and total carbon (TC) were determined by burning the filters in oxygen atmosphere at 620°C and 700°C, respectively, and measuring the released CO_2 by IR spectroscopy

(ELTRA 500 Carbon Analyzer). EC was determined by subtracting OC from TC (Roosli et al., 2001). In the second study, sample filters were pre-treated by heating them at 340°C in a muffle furnace for ~100 minutes in order to remove OC, and were subsequently analyzed by an elemental analyzer (EuroEA3000, EuroVector Instruments and Software) to obtain the EC content (Lin and Tai, 2001). Another portion of the filter was fed directly to the elemental analyzer without any pre-treatment to obtain the TC content. The evolved CO_2 was separated in a gas chromatography column and identified by a thermal conductivity detector (TCD). OC was calculated as the difference between TC and EC.

RESULTS AND DISCUSSION

First study: Overall mean values of PM_{10}, ions and carbonaceous species observed in the first study is provided in Table 1. Mean PM_{10} at SN and JNU were observed to be 347.5 ± 142.4 and 211.4 ± 116.8 $\mu g\ m^{-3}$, respectively. These values were 3-6 times the national ambient air quality standard of 60 $\mu g\ m^{-3}$(annual average). Mean percentages of coarse and fine fractions in PM_{10} were 63.4% and 36.6% at SN and 69% and 31% at JNU. Highest aerosol loadings, especially in the fine fraction, were observed for the months of October and November, which was possibly due to very little dispersion because of stable atmospheric conditions during this period. On the other hand, lowest particulate loadings, especially in the coarse fraction, were observed in the month of August, possibly due to wash-out effects of monsoon precipitation.

Concentrations of ions and carbonaceous species were higher at SN possibly because of its nearness to traffic and industrial point sources. At JNU, which has a good vegetation cover, OC was higher than EC both in the coarse and fine fractions. High OC in coarse fraction was possibly due to resuspension of decomposed vegetal debris, spores, pollen etc while higher values of OC in the fine fraction indicated condensation of biogenic VOCs in the fine mode. Higher OC in the coarse fraction at SN was possibly contributed by carbonaceous waste aerosol from cardboard industries and tire rubber dust.

Using the aforementioned aerosol chemical speciation data, the light extinction was estimated as the sum of the products of concentration of individual species and their respective light extinction efficiency (Sisler and Malm, 1999)

$$b_{ext} = b_{Ray} + (3)f(RH)[SO_4^{2-}] + (3)f(RH)[NO_3^-] + (4)[OMC] + [soil] + (0.6)[coarse\ mass] + (10)[EC]$$

where b_i is the light extinction efficiency ($m^2\ g^{-1}$) of species i, OMC is organic mass carbon given as (1.4)[OC] and f(RH) signifies the ratio of change in scattering efficiencies of species. The contribution from gaseous Rayleigh scattering (b_{Ray}) is considered to be a constant as 200 Mm^{-1}. A simple model allows the observer visual range to be estimated from the extinction coefficient by dividing a constant by the extinction coefficient. To compare the visibility data from different sites, visual range estimates can be normalized to a Rayleigh scattering coefficient of 10 Mm^{-1} (particle-free atmospheric conditions at an altitude of 1.524 km or 5000 ft). This normalized estimate is called the standard visual range (SVR) and can be expressed as

$$SVR = 3912 / (b_{ext} - Ray + 10)$$

where the units for SVR are km, Ray is the Rayleigh value, 10 is the Rayleigh coefficient used to normalize visual range and 3912 is a constant derived assuming a 2% contrast detection threshold.

At SN, the average b_{ext} and SVR were 784 Mm^{-1} and 7.4 km, respectively, while those at JNU were 562.3 Mm^{-1} and 10.8 km, respectively. Leavy and Sweeney (1990) reported that in a non-polluted atmosphere, visibility would be of the order of 250 km while for an urban atmosphere, Gomez and Smith (1987) defined very good visibility as >19 km. In view of this, the visual air quality of Delhi was found to be poor. Percentage contributions of species such as SO_4^{2-}, NO_3^-, EC, OC, soil and coarse particles to visibility impairment, i.e. b_{ext}, were 7%, 3%, 23%, 33%, 10% and 24%, respectively, at SN and 10%, 4%, 16%, 39%, 5% and 26%, respectively, at JNU. It was apparent that visibility impairment in Delhi was mainly due to carbonaceous aerosol. Increased release of carbonaceous aerosol from biomass burning in agricultural fields and from consumption of organic matter for energy requirement in household activities in tropical and sub-tropical regions is responsible for its dominant role in visibility reduction (Singh et al., 2008 and references therein). On the other hand, sulphate is the major component of visibility reducing aerosol in temperate regions due to heavy emission of SO_2 from electricity generation in power plants, oil refineries, steel mills and favourable conditions for sulphate formation. The enhanced role of carbonaceous compounds (EC and OC) in visibility impairment in Delhi as observed in this study prompted us to investigate its role in greater detail and thus led to the second study.

TABLE 1. Mean values (± one standard deviation) of analyzed species concentrations in the first and second study.

First study **Species (µg m^{-3})**		**SN**	**JNU**
PM	Fine	127.1	65.5
	Coarse	220.4	145.8
	PM_{10}	347.5 ± 142.4	211.4 ± 116.8
SO_4^{-2}	Fine	6.1	6
	Coarse	6.4	5.7
	PM_{10}	12.5 ± 3.2	11.7 ± 2.4
NO_3^-	Fine	2.9	2.9
	Coarse	3.4	2.9
	PM_{10}	6.3 ± 1.9	5.7 ± 2.2
NH_4^+	Fine	7.5	7.4
	Coarse	4.7	3.4
	PM_{10}	12.1 ± 5	10.8 ± 2.5
OC	Fine	32.2	25.6
	Coarse	36.3	31.1
	PM_{10}	68.6 ± 13.3	56.7 ± 10
EC	Fine	14.8	6.2
	Coarse	23.7	7.6
	PM_{10}	38.5 ± 21	13.9 ± 2.6
Second Study **Species (µg m^{-3})**		**MV**	**JNU**
PM_{10}		183.1 ± 39.2	133.9 ± 43.1
EC		17 ± 5.9	7.2 ± 2.2
OC		51.1 ± 13.4	38.2 ± 16.9
TC		68.1 ± 18.5	45.4 ± 17.5

Second study: Overall mean PM_{10} concentrations along with concentrations of carbonaceous species (EC, OC and TC) observed at MV and JNU sites in 2008-09 are presented in Table 1. Mean 24-h PM_{10} concentrations at RG and JNU were 183.1 ± 39.2 and 133.9 ± 43.1 µg m^{-3}, respectively. These values are 2-3 times the annual average PM_{10} standard. The 24-h PM_{10} standard (100 µg m^{-3}) was violated on 100% of the sampling days at MV and on 83% of the days at JNU.

A significant portion of PM_{10} mass (37% at MV and 34% at JNU) was found to be carbonaceous at the sites. Lower EC and OC concentrations observed at JNU can be attributed to the absence of heavy traffic and stationary combustion sources in the vicinity. OC contributed 75% and 82% to TC concentrations at MV and JNU, respectively. OC in ambient air has both primary and secondary origins; vehicular emissions, coal combustion and biomass burning are the major contributors of primary OC, while secondary OC is formed through gas-to-particle partitioning of volatile organic compounds (VOCs) in the atmosphere under favourable conditions. A moderately high positive correlation ($r = 0.63$, $p < 0.01$) observed between EC and OC concentrations indicated that along with co-emission with EC from combustion sources, OC might have secondary sources in Delhi's atmosphere. Favourable meteorological conditions during the study period (low ambient temperature, stable atmospheric conditions etc.) may have aided in the gas-to-particle partitioning of VOCs, thus resulting in increased secondary OC formation. Another potential source of OC could be in the form of non-combustion primary OC such as tyre dust, brake dust and vegetative sources (spores, pollen, detritus etc.).

OC/EC ratios can be used to trace the origin of carbonaceous particles where an OC/EC ratio of 1.1 is related with traffic-related emissions, and that of 2.7 with coal combustion (Watson et al., 2001). Higher OC/EC ratios of 4 – 9 are generally associated with biomass burning (Salam et al., 2003). In the present study, the mean OC/EC ratio at MV was 3.1, which is somewhat near the coal combustion boundary. At JNU, the OC/EC ratio was 5.5, indicating biomass burning as the chief source. Dry-leaf burning is common at this site during winter, which could be a possible source of OC along with gas-to-particle partitioning of VOCs emitted by plants. The EC/TC ratio at MV was 0.25, which is excellent agreement with the averaged EC/TC ratio (0.25) of total biomass combustion emissions of India (Salam et al., 2003). A lower EC/TC ratio (0.18) at JNU is probably due to the presence of some non-combustion OC (presumably in the form of vegetative detritus, spores, pollens etc., given the nature of the site).

An attempt was made to quantify secondary organic carbon (SOC) by utilizing the minimum OC/EC ratio method (Castro et al., 1999). The following equation was used for estimating SOC

$$\text{SOC} = \text{OC}_{\text{tot}} - \text{EC} \times (\text{OC/EC})_{\text{min}}$$

where OC_{tot} is the total OC and $(\text{OC/EC})_{\text{min}}$ is the minimum OC/EC ratio observed. The assumptions regarding the use of this method have been discussed in detail by Castro et al., (1999). Here, 24 samples were collected from two sites during the study period. It seems reasonable to consider that the amount of SOC was negligible in the samples exhibiting the minimum OC/EC ratio. Secondly, contributions of semi-volatile organics was considered to be low in comparison to non-volatile organics. Source contributions to primary carbonaceous aerosols were assumed to be spatially constant since the study was limited to Delhi only. Furthermore, the study was performed only during the winter period of 2008-09, which rules out any possibility of seasonal effects on source composition and contributions. Lastly, the contribution of non-pyrogenic primary OC was also assumed to be small.

Mean SOC concentrations at MV and JNU sites were 22.7 and 28.5 $\mu g\ m^{-3}$, respectively, and contributed heavily (44% at MV and 68% at JNU) to OC levels in Delhi's air. SOC was also found to represent a sizeable fraction (13% at MV and 20% at JNU) of PM_{10} concentration. Atmospheric SOC is known to play a vital role in visibility reduction and formation of regional haze. The present study therefore indicates that along with EC, a significant part of the visibility reduction in Delhi could be due to the high concentrations of SOC. This finding has enormous implications for policy-makers in order to channel mitigation efforts to preserve the visual air quality of Delhi.

CONCLUSIONS

The findings of this study indicate that the visual air quality of Delhi is poor and visibility impairment could mainly be attributed to the dominance of carbonaceous aerosol in its atmospheric environment. Specifically, EC and SOC were found to be the major visibility impairing species in this pilot study. This has tremendous implications for the local atmospheric chemistry of this area and needs to be investigated further. Future directions of research would therefore include seasonal variation in sampling (especially summertime, when atmospheric SOC concentrations are expected to be even higher) and expansion of the spatial distribution.

REFERENCES

APHA, 1992. *Standard method for the examination of water and wastewater*. Washington, DC. American Public Health Association.

Katz, M. 1977. *Methods of air sampling and analysis.* 2nd ed., APHA, Washington, DC.

Roosli, M., Theis, G., Kunzli, N., Staehlin, J., Mathys, P., and Oglesby, L. 2001. "Temporal and spatial variation of the chemical composition of PM10 at urban and rural sites in the Basel area, Switzerland." *Atmos. Environ*. 35:3701-3713.

Allen, S.E. 1989. *Chemical analysis of ecological materials*. pp. 124-125. Blackwell, Oxford, UK.

Sisler, J., and Malm, W. 1999. "Interpretation of trends of PM2.5 and reconstructed visibility from the IMPROVE network." *J. Air Waste Manage. Assoc.* 50:775-785.

Leavey, M., and Sweeney, J. 1990. "The influence of long-range transport of air pollutants on summer visibility at Dublin." *Int. J. Climatol.* 10:191-201.

Gomez, B., and Smith, C.G. 1987. "Visibility at Oxford 1926-1985." *Weather* 42:98-106.

Salam, A., Bauer, H., Kassin, K., Ullah, S.M., and Puxbaum, H. 2003. "Aerosol chemical characteristics of a mega-city in Southeast Asia (Dhaka - Bangladesh)." *Atmos. Environ*. 37:2517-2528.

Watson, J.G., Chow, J.C., and Houck, J.E. 2001. "$PM_{2.5}$ chemical source profiles for vehicle exhaust, vegetative burning, geological material and coal burning in northwestern Colorado during 1995." *Chemosphere* 43:1141-1151.

Lin, J.J., and Tai, H-S. 2001. "Concentrations and distributions of carbonaceous species in ambient particles in Kaohsiung City, Taiwan." *Atmos. Environ*. 35:2627-2636.

Castro, L.M., Pio, C.A., Harrison, R.M., and Smith, D.J.T. 1999. "Carbonaceous aerosol in urban and rural European atmospheres: estimation of secondary organic carbon concentrations." *Atmos. Environ*. 33:2771-2781.

TOXICITY AND CHEMICAL COMPOSITION OF AMBIENT PARTICULATE MATTER FROM THE REGION OF AACHEN, GERMANY

Sabrina Michael and Wolfgang Dott (RWTH Aachen University, Aachen, Germany)

ABSTRACT: In recent years, numerous studies have investigated the association between the air pollution level and various health effects. In this context ambient airborne particulate matter (PM) concentrations are considered one of the important environmental cofactors for cardiovascular and respiratory diseases. However, to what extent such effects are various for PM obtained from different sites and sources is still unknown. Therefore this study compares the toxicological effects of different source-related particles in regard to their chemical composition. In this context we investigated airborne PM from different sites in the Region of Aachen. For the toxicological characterization human alveolar epithelial cells (A549) were exposed to increasing PM concentrations (0-100 µg/ml) followed by analyses of cell viability, pro-inflammatory and oxidative stress response. The chemical analysis of these particles indicated the presence of 21 elements, water-soluble ions and a multitude of different PAH. For the toxicological investigations the water-soluble particulate matter extracts induced a concentration - and time-dependent decrease in cell viability and an increase in pro-inflammatory and oxidative stress markers. The cell responses to ambient PM were markedly different comparing samples from different sites and emission sources and support other investigations regarding the importance of the chemical compositions and their PM-induced toxicity.

INTRODUCTION

Clean air is a basic requirement for the human health and well-being. An average daily inhalation of 20 m^3 of air is characterized by an exposure to many different pollutants. Apart from the classic gaseous pollutants (e.g. SO_2, NO_x, O_3) airborne particulates continue to pose a significant threat to human health worldwide (WHO 2006). Many studies show that particulate matter (PM) air pollution is related to adverse health effects with increased mortality and morbidity. In this context oxidative stress-induced inflammation is one of the most discussed pathways of PM-induced respiratory diseases (Valavanidis et al., 2008, Yang et al., 2009). PM mediated oxidative stress mainly caused by reactive oxygen species (ROS), such as hydrogen peroxide, superoxide, and hydroxyl radical. ROS may be generated by free radicals present on particle surface, by the chemical reaction of specific PM constituents. The inflammatory response is involved through upregulation of various signaling molecules, such as cytokines, chemokines and adhesion molecules, in the lung (Akhtar et al., 2010). Thus, the incidence and degree of oxidative stress as well as inflammatory response induced by particulate air pollution can depend on the chemical reactivity of PM (Steenhof et al., 2011).

Generally, airborne PM is a complex mixture of inorganic and organic components, such as metals, salt, carbonaceous material, volatile organic compounds (VOC), polycyclic aromatic hydrocarbons (PAH) and allergens (pollen and mold spores). Some of the components, e.g. transition metals and PAH, have been identified for several mechanisms with adverse cellular effects including cytotoxicity, oxidative stress, mutagenicity and stimulation of pro-inflammatory factors (Merbitz et al., 2012, Riley et al., 2003).

The objective of this study was to compare the toxicological effects of different source-related particles in regard to their chemical composition. In this context we investigate airborne PM from different sites in the Region of Aachen. The special topography of Aachen within a basin with up to 200 m of altitude difference and its location in the centre of the densely populated region Maas-Rhine makes Aachen (population 250.000) an excellent case study for air quality analyses. Human alveolar

---

ISBN 9780976885351

epithelial cells (A549) were exposed to increasing PM concentrations followed by analyses of cell viability, pro-inflammatory and oxidative stress response.

MATERIALS AND METHODS

Sampling and chemical characterization of ambient particulate matter. Ambient airborne particulate matter samples were collected at two selected permanent air quality stations representing urban and rural areas in the City of Aachen, Germany. Sampling was carried out by the NRW Ministry for Environment and Nature Protection, Agriculture and Consumer Protection with a high volume sampler coupled with a LVS sampling head (PM10). PM samples at each of the two sampling sites were being collected for 24 hours (~700 m^3) on quartz fiber filter from September to October 2010. The PM samples were extracted and examined for the content of inorganic elements with inductively coupled plasma mass spectrometry (ICP-MS), CHN elemental analyzer and ion chromatography (IC). The detection of PAH level was measured by high-performance liquid chromatography with fluorescence detection (HPLC-FLD). All procedures were performed according to DIN EN (12341, 14902, 14907) or U. S. EPA (1984, 1999) methods. Additionally to the chemical investigations a scanning electron microscope analysis with energy dispersive X-ray spectroscopy (SEM-EDX) of the loaded quartz fiber filters was carried out.

Analyses of the toxicological endpoints. Human alveolar epithelial cells (A549) were exposed to a water-soluble PM suspension at concentrations of 1-100 µg/ml for 0-96 h. For cell viability, cytokine (IL-6, IL-8, TNF-α) and oxidative stress (SOD, KAT, GSH) detection, cells were exposed to PM in triplicate at each PM concentration and incubation period. Cell viability was determined using a viability staining test. Cytokine levels were immunochemically detected using commercial enzyme-linked immunosorbent assay (ELISA) kits performed according to the manufacturer´s instructions. The determination of oxidative stress was carried out after cell disruption by commercial colorimetric assays.

RESULTS

PM mass concentration and chemical composition. The selected ambient PM10 samples were collected at two different sites in the region of Aachen, Germany during the sampling period September - October 2010 (Fig. 1). PM samples demonstrated a clear location-dependent variability of the PM concentration. The lowest mass concentrations were measured at the rural site, whereas the highest concentrations were detected at the urban traffic site. The median particle mass concentration ranged from 9.9 (rural site) to 25.1 particles/m^3 (urban site).

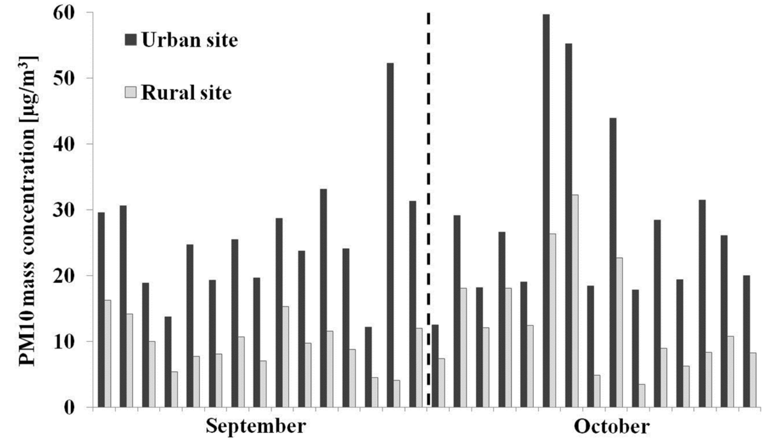

FIGURE 5 PM mass concentration [µg/m^3] during the sampling period September - October 2010 at the urban and rural site in the region of Aachen, Germany. (Source: NRW Ministry for Environment and Nature Protection, Agriculture and Consumer Protection)

The chemical analysis of these particles indicated the presence of 21 elements, water-soluble ions and a multitude of different PAH (Fig. 2). The major inorganic components are the crustal elements (Ca, K, Mg, Na) and the (transition) metals Al, Fe, Zn. But an exceeding of the regularized limits for As, Cd, Ni and Pb could not be detected. In contrast to metals, carbon and PAH, the concentration of ionic species is approx. 25 % higher at the rural site compared to the urban site.

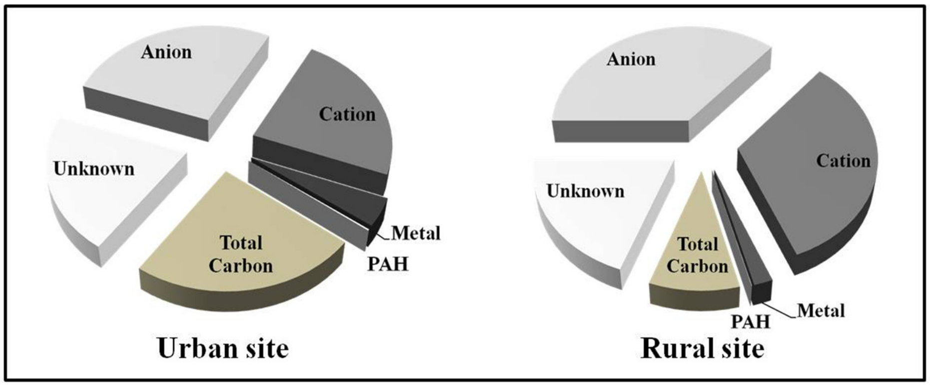

FIGURE 6 Mean values of the chemical composition of PM10 collected during the sampling campaign Sept/Oct 2010 at urban and rural sites in the region of Aachen, Germany.

Additionally to the chemical investigations an exemplary scanning electron microscope analysis with energy dispersive X-ray spectroscopy (SEM-EDX) of the loaded quartz fiber filter was realized (Fig. 3). The results confirm the chemical analysis and show strong distinctions between both sampling sites. Particularly the content of carbon black and metals differentiate the particles from urban and rural locations. In contrast to the urban site, the rural PM contains a huge amount of organic components such as fungal spores. The peaks for Si and Au in the EDX- spectrums result from the filter background and the gold coating of the EDX-analysis.

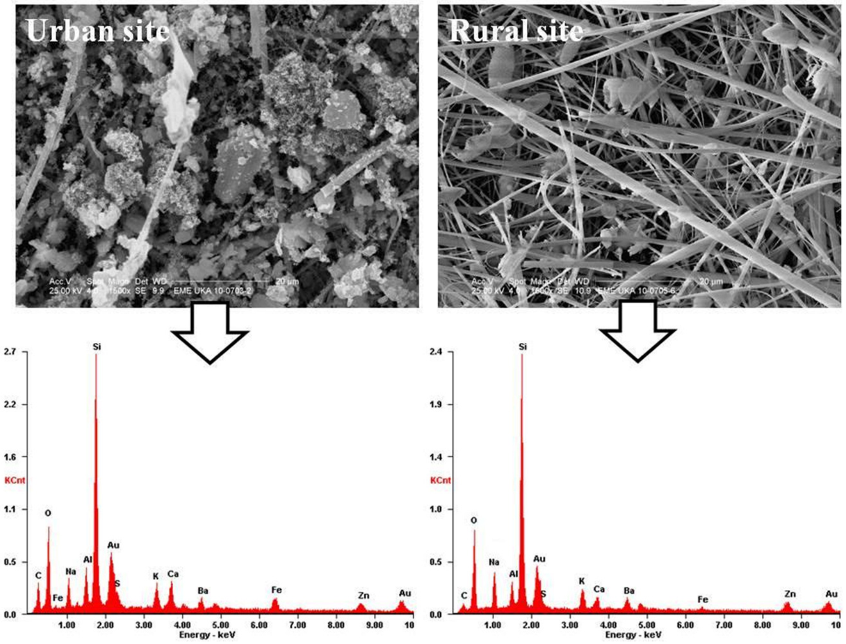

FIGURE 7 SEM – EDX analysis of PM loaded quartz fiber filter from urban and rural sites.

Toxicological investigations. For the toxicological characterization the human alveolar epithelial cells (A549) were exposed to increasing concentrations of PM–extracts from urban and rural sites (1-100 µg/ml). After the incubation period of 0-96 h, viability and the release of oxidative stress and pro-inflammatory markers were determined.

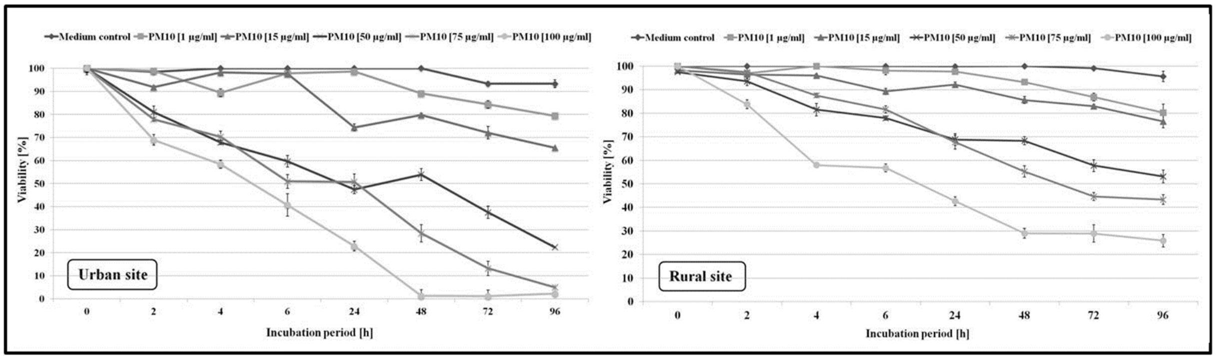

FIGURE 8 Viability [%] of A549 cells during a 0-96 h incubation with PM samples from urban and rural sites. Each measuring point shows mean ± standard deviation of one exposure in triplicate.

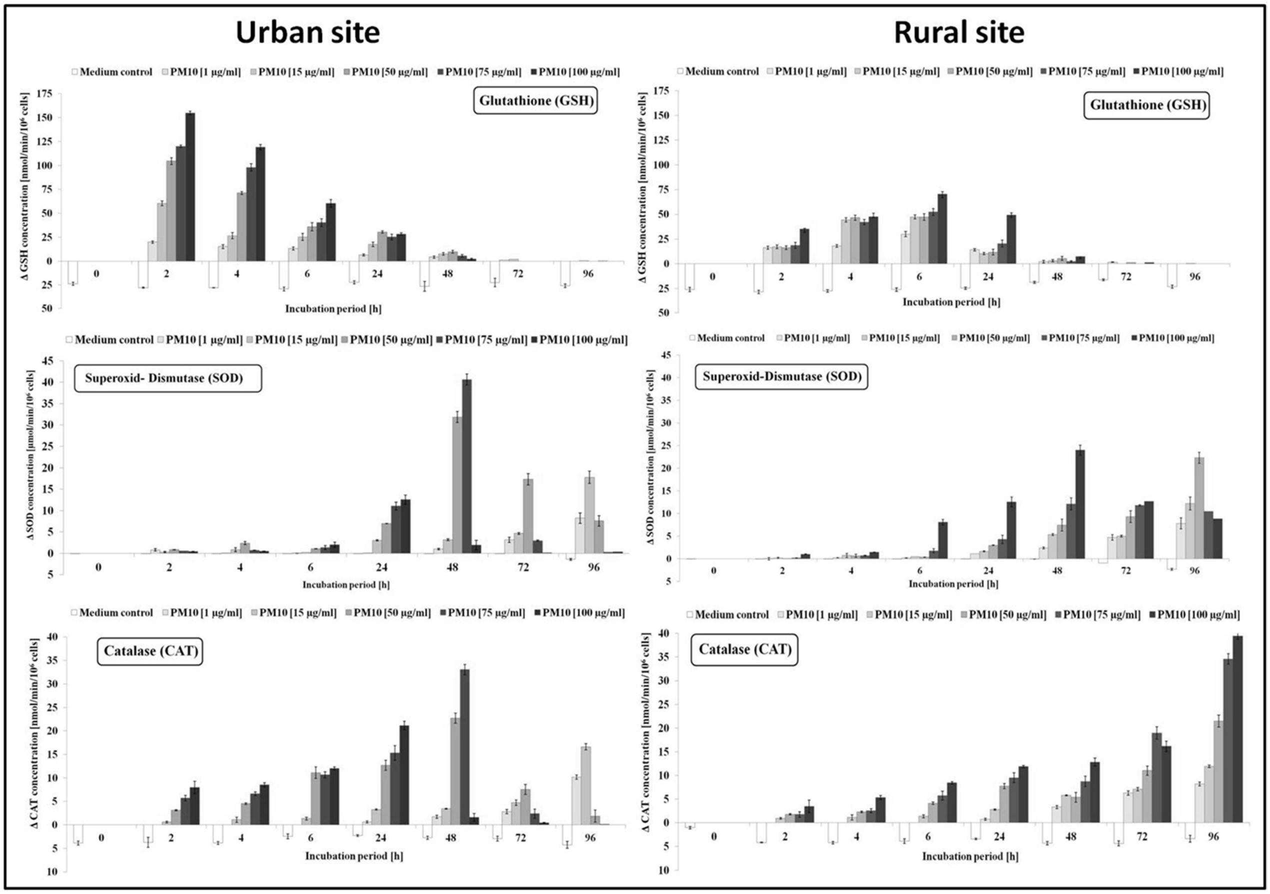

FIGURE 9 Release of different oxidative stress markers (GSH, SOD, CAT) by A549 cells after 0-96 h incubation with PM samples from urban and rural sites. Each bar shows mean ± deviation of one exposure in triplicate.

Viability staining test. Figure 4 represents the viability [%] of alveolar epithelial cells during 96 hours exposure to the concentrated PM samples. PM-extracts from both sites caused a concentration- and time-dependent decrease in cell viability. The most potent cytotoxic effect shows the PM from the urban site. After 48 h only a viability of < 5 % (100 µg/ml) could be detected.

Oxidative stress markers. The activity of oxidative stress markers superoxid-dismustase (SOD), catalase (CAT) and total glutathione (GSH) were determined in the cell´s extract after cell disruption for every measurement point (Fig. 5).

PM10 collected at urban and rural sites induced a clear concentration- and time-dependent increase in oxidative stress markers release. According to the known cellular defense system all three involved markers show a coordinated response. Furthermore the results show a clear correlation between cytotoxicity and oxidative stress. Similar to the viability reduction (Figure 4) the high urban PM concentrations (> 50 µg/ml) induced a decrease of oxidative stress markers after 48 hours.

Pro-inflammatory markers. Parallel to the determination of oxidative stress response the study includes the detection of pro-inflammatory cytokines such as TNF-α, IL-6 and IL-8. The production of these cytokines was determined in the cell´s supernatant for every measurement point (Figure 6).

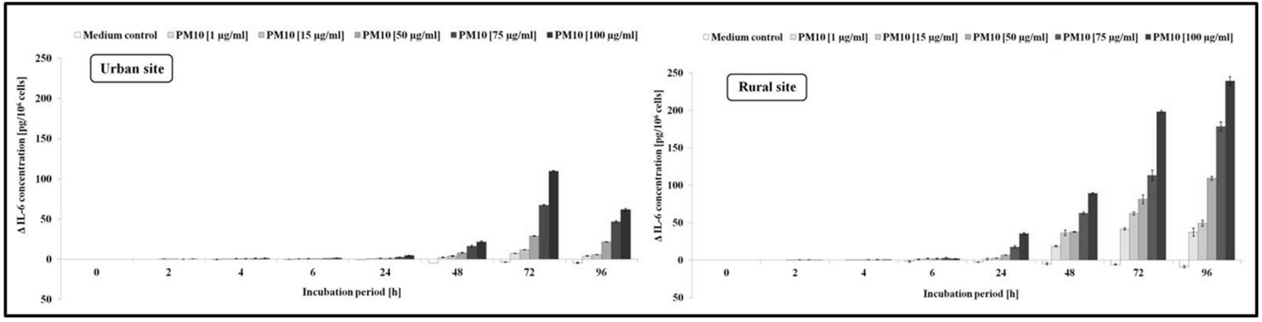

FIGURE 10 IL-6 produced by A549 cells after 0-96 h incubation with PM samples from urban and rural sites. Each bar shows mean ± deviation of one exposure in triplicate.

Airborne particles from both sampling sites induced a clear concentration- and time- dependent increase in IL-6 and IL-8 (not shown) production. Generally, a TNF-α release could not be detected for the alveolar epithelial cells. In direct comparison, the PM from the rural site induced the highest pro-inflammatory (IL-6 and IL8) release. The high level of IL-6 secretion after 48 hours induced by PM from the urban site, based on residually suspended and degraded cells in the incubation medium (Figure 6).

DISCUSSION

The main focus of this study was the analysis of the in vitro PM induced oxidative stress, pro-inflammatory and cytotoxic effects of different sites in the region of Aachen, Germany. PM10 samples caused a concentration-, time- and site dependent decrease in cell viability and an increase in oxidative stress markers (GSH, SOD, CAT) as well as pro-inflammatory response (IL-8 and IL-8).

This effect on cell viability from the urban site might be linked to the high metal and total carbon content which were substantially higher compared to the rural site (Fig. 2). At the urban location, the most abundant metal species were iron and zinc. For PM10, the amount of iron per µg PM was 12 times higher and the amount of zinc was 5 times higher compared to the rural site. Similar differences were observed in the total carbon content.

Several other studies described that PM with high metal and/or carbon content caused oxidative stress-induced inflammatory response as well as cytotoxic effects (Steenhof et al., 2011, Riley et al., 2003). In most of these studies, the oxidative stress and pro-inflammatory activity was triggered by linked compounds at the PM or carbon surface, such as transition metals or PAHs, rather than by carbons themselves. However a final conclusion about the PM-induced toxicity is still unclear. But our results support these investigations regarding the importance of the chemical, particularly the metal, compositions and their PM-induced toxicity.

CONCLUSION

In summary, the response of A549 cells to ambient PM was clearly different comparing specific samples from various sampling sites and emission sources in the region of Aachen. Our results support other investigations regarding the importance of the chemical compositions and their PM-induced toxicity. Parallel to this toxicological analysis, further investigations with murine macrophages (RAW 264.7 cells), human skin kreatinocytes (HaCaT) and hepatocellular carcinoma cells (Hep-G2) have been already carried out with the same PM extracts as in this project.

ACKNOWLEDGMENT

The study is embedded in the project City2020+ which is part of the interdisciplinary Project House HumTec (Human Technology Center) at RWTH Aachen University funded by the Excellence Initiative of the German federal and state governments through the German Research Foundation (Deutsche Forschungsgemeinschaft, DFG). Furthermore, we would like to thank the NRW Ministry for Environment and Nature Protection, Agriculture and Consumer Protection for the technical support.

REFERENCES

WHO Air quality guidelines for particulate matter, ozone, nitrogen dioxide and sulphur dioxide. 2006.Available at the following website adress:
http://www.euro.who.int/__data/assets/pdf_file/0006/78657/E88189.pdf

Steenhof, M., I. Gosens, M. Strak, K. J. Godri, G. Hoek, R. C. Flemming, I. S. Mudway, F. J. Kelly, R. M. Harrison, E. Lebert, B. Brunekreef, N. AH. Janssen and R. HH. Pieters. 2011. *Particle and fibre toxicology*, 8:26

Valavanidis A., K. Fiotakis, T. Vlachogianni. 2008. Airborne particulate matter and human health: Toxicological assessment and importance of size and composition of particles for oxidative damage and carcinogenic mechanisms, *Journal of Environmental Science and Health* Part C, 26: 339-362

Yang W., Omaye S. T. 2009. Air pollutants, oxidative stress and human health. *Mutation Research/Genetic Toxicology and Environmental Mutagenesis*. 674: 45-54

Merbitz, H., M. Buttstädt, S. Michael, W. Dott, C. Schneider. 2012. GIS-based identification of spatial variables enhancing heat and poor air quality in urban areas. *Applied Geography*. 33: 94-106

Akhtar, U. S., R. D. McWhinney, N. Rastogi, J. P. D. Abbatt, G. J. Evans, and J. A. Scott. 2010. Cytotoxic and proinflammatory effects of ambient and source-related particulate matter (PM) in relation to the production of reactive oxygen species (ROS) and cytokine adsorption by particles. *Inhalation Toxicology*, 22: 37-47

DIN EN 12341. Air quality – Determination of the PM10 fraction of suspended particulate matter – reference method and field test procedure to demonstrate references equivalence of measurement methods. 1998.German version EN 12341.

DIN EN 14902. Ambient air quality – Standard method for the measurement of Pb, Cd, As and Ni in the PM10 fraction of suspended particulate matter. 2005. German version EN 14902.

DIN EN 14907. Ambient air quality – Standard gravimetric measurement method for the determination of the PM2.5 mass fraction of suspended particulate matter. 2005. German version EN 14907.

U. S. Environmental Protection Agency (EPA) Report. 1984. Methods for determination of toxic organic compounds in ambient air. No. 600/4-84-041.

U. S. Environmental Protection Agency (EPA) Report .1999. Methods for determination of toxic organic compounds in ambient air, Compendium method TO-13A. NO. 625/R-96/010b.

Riley, M.R., D. E. Boesewetter, A. M. Kim, F. P. Sirvent. 2003. Effects of metals Cu, Fe, Ni, V, and Zn on rat lung epithelial cells. *Toxicology*. 190:171-184

NEAR-ROAD BLACK CARBON EMISSION AT AN URBAN CAMPUS INTERSECTION

Jiangchuan Hu and ***Mingming Lu*** (School of Energy, Environmental, Biological and Medical Engineering, University of Cincinnati, 2600 Clifton Avenue, Cincinnati, Ohio, 45221, USA)

ABSTRACT: Traffic-related air pollutants are receiving increasing attention with the increasing traffic volume in recent years. In this study, traffic-related air pollutants were investigated at a busy urban intersection near the University of Cincinnati. Near-road ambient concentrations of black carbon were monitored and related to traffic volumes and meteorology conditions in different seasons and different times of the day throughout years 2010 to 2011. Black carbon concentrations were observed following the similar seasonal trends of the ambient particulate matters and always higher during the morning peak hours of the day. The samplings on Fridays were found to be not statistically different from other weekdays. Relationship between black carbon concentrations and traffic volumes were investigated and diesel heavy duty vehicles were associated with the near-road black carbon concentrations.

INTRODUCTION

Traffic-related air pollution is increasingly emphasized in human health exposure management as well as in environmental protection. Black carbon is one of the particulate carbonaceous emissions generated by diesel engines and biomass burnings, leading to negative human health effects (Samet and Krewski, 2007). Thus better characterization and quantification of the vehicular emissions in inner cities of concentrated populations offer better understandings to the human exposure. Little emphasis has been placed to date on urban settings, such as intersections, rather than highway. However, the urban intersections are important areas to investigate due to high pedestrian volumes. In this study, a busy traffic intersection was selected for a quantitative investigation on the black carbon emissions.

The goal of this study is to quantify the black carbon emissions from transportation sources at an urban intersection, and to determine contributing factors influencing the emissions. Seasonal and diurnal trends of the black carbon emissions were characterized as the first step to fulfill the goal. Linear regressions and correlation analyses were performed to identify the relationship between black carbon emissions and influencing factors, including traffic volume, traffic delay, temperature, relative humidity and wind conditions.

EXPERIMENTAL METHODS

Sampling Site and Data Collection. The intersection of Martin Luther King Dr. W. and Clifton Ave in Cincinnati area, OH was selected as the sampling site. The average traffic flow is approximately 50,000 vehicles per day, including an approximately 1-3% heavy duty trucks. There are four lanes both on Martin Luther King Dr. W. and Clifton Ave including a left-turn only lane, two go-through lanes and a right-turn only lane. A full-actuated signal plan is applied at this intersection with loop detectors installed on the left-turn lane and go-through lanes. The sampling site was shown in Figure 1.

A total of four sampling campaigns in different seasons of the year were conducted to ensure sufficient sample size. October 2010, February to March 2011, and July 2011 were selected to represent

---

ISBN 9780976885351

fall, winter, and summer season. The meteorology conditions at the intersection during the spring season in Cincinnati are typically similar to the fall season. Thus no spring season was selected for data collection. During each season, 10-16 samplings were taken in three different 2-hour periods of the day, morning peak hours (AM), noon hours (Noon), and evening peak hours (PM). The instruments were placed on the grassy land at the southeast of the intersection, with an inlet tube being placed at approximately 1.5 meters above ground to represent human exposure height.

FIGURE 1. Sampling Site at Urban Intersection

Instrumentation. Aethalometers, model AE22 (*Anderson,* Fultonville, NY) was used during the samplings. Both aethalometers operated by a filter basis. Air samples were absorbed onto a Teflon coated glass filter installed inside the instrument, and analyzed by under specific light wavelengths (880 nm). Real-time readings were obtained from the aethalometer at an interval of 1 minute. A Camcorder was placed at site to record the traffic conditions for all four approaches. A weather station, model Vantage Pro2 (*Davis Instruments*, Canon Beach, OR) or a meteorology tower developed by graduate students at the University of Cincinnati was used to collect meteorology information, including temperature, relative humidity, wind speed and direction, at an interval of 1 minute.

RESULTS AND DISCUSSIONS

Seasonal and Diurnal Trend: Near-road black carbon concentrations were measured for a total of 40 sampling periods in three different seasons. There were 2 AM periods in fall season (Oct 20, 2010 and Oct 22, 2010), 1 AM periods in winter season (Mar 25, 2011), and 1 AM periods in summer season (Jul 6, 2011) when the measured black carbon concentrations were significantly larger than any other monitoring periods in the same season. Meteorology Skew-T plots of these sampling date were obtained from NOAA/ESRL radiosonde database (NOAA and ESRL, 2011). The Skew-T plots for all 4 periods indicate the occurance of temperature inversion.

During the sampling campaigns, there were 6 periods of sampling were conducted during Friday. Friday was typically considered different than the other weekdays, due to possible reduction of traffic volume. However, in this study, no significant differences were observed between samplings on Friday and on the other weekdays. Table 1 listed the traffic volume and black carbon concentrations for the samplings on Friday, with comparison to the averages of other weekdays.

TABLE 1. Traffic Volume and Black Carbon Concentration Comparison between Friday Samplings and the Other Weekdays Samplings

	Total Traffic Volume (Heavy Duty Vehicle Volume)			**BC Concentration ($\mu g/m^3$)**		
	Friday	**Average on Other Weekday**	**Difference**	**Friday**	**Average on Other Weekday**	**Difference**
Oct 22, 2010, AM Period	7618 (182)	7058 (211)	7.9%	6.1	2.2	179.7%[1]
Oct 28, 2011, AM Period	6503 (76)	7058 (211)	7.8%	2.2	2.2	2.2%
Oct 28, 2011 Noon Period	6706 (45)	6567 (184)	2.1%	1.2	1.0	22.2%
Mar 25, 2011, AM Period	4945 (219)	6556 (210)	24.6%[2]	2.0	1.6	20.8%
Jul 22, 2011, AM Period	5720 (156)	5853 (169)	2.3%	2.4	1.9	30.2%
Jul 22, 2011, Noon Period	5511 (172)	5462 (158)	0.9%	1.7	1.8	6.3%

[1] The significantly higher black carbon concentration on Friday during fall 2010 season was mainly due to the temperature inversion, not to the traffic condition.

[2] On Mar-25 the university was on spring break, which led to a significant reduction of the traffic volume.

Figure 2 shows the average black carbon concentrations in each period in each season, without the periods during temperature inversion. Error bars indicate standard deviation. During the noon and PM periods, the black carbon concentrations were slightly higher during the summer season. During the AM periods, there were no significant differences between the different seasons, due to large variations. The results agrees with the trend of ambient particulate matters less than 2.5 microns in diameter ($PM_{2.5}$) concentrations monitored by Hamilton County Department of Environmental Services (HCDOES), showing in Figure 3 (Pacas, 2011). In all seasons, the black carbon concentrations were measured significantly higher during the AM period than the other periods, along with more diesel heavy duty vehicles observed during the AM periods than the other periods. This diurnal variability is consistent with the yearly trend of BC concentrations in a Chinese city as reported by Cao et al (2009). The ambient black carbon concentrations were monitored by HCDOES in the winter 2011. The average of the black carbon concentrations measured at the intersection were 78%, 17%, and 37% higher than those measured at HCDOES, which is an indication that the on-road vehicles could be a major source of the near-road black carbon emissions.

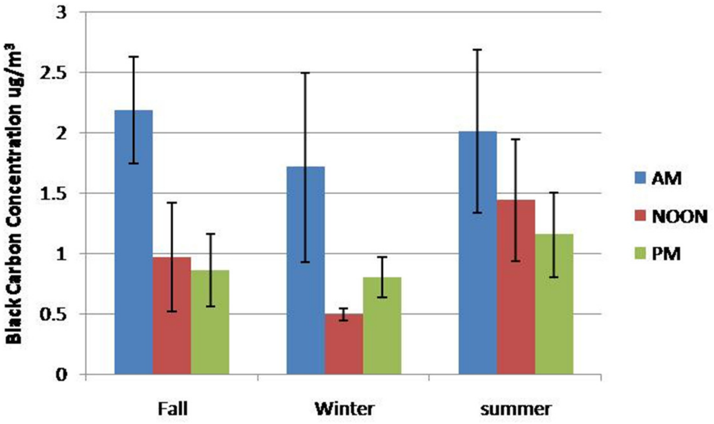

FIGURE 2. Average Black Carbon Concentrations in Each Period in Each Season

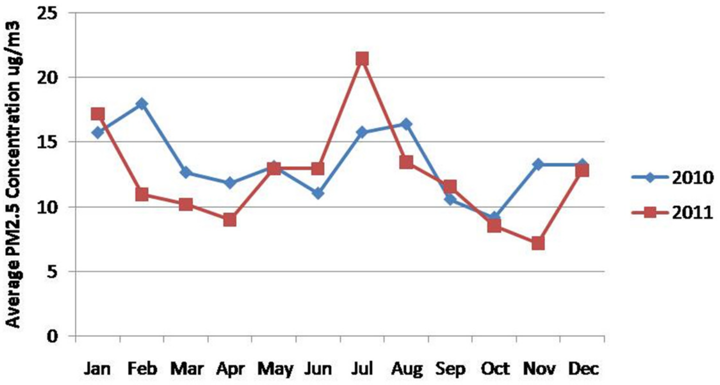

FIGURE 3. Average Monthly Particulate Matter ($PM_{2.5}$) Concentrations in Cincinnati from 2010 to 2011.

Influencing Factors on Black Carbon Concentrations: The near-road black carbon concentrations were influenced by a number of factors, and traffic conditions would be one. The diesel engines were believed to be one of the major sources of ambient black carbon emissions. During each sampling period, the black carbon concentrations as well as the traffic volumes were measured at an interval of 1 minute.

The traffic volumes were in additionally separated into two categories: passenger cars (PC) and diesel heavy duty vehicles (HDV). A linear regression were done for each sampling period to investigate the relationship between black carbon concentrations and the traffic volumes. Table 2 lists the correlation coefficient (R) for the linear regression of black carbon concentration against PC volumes and HDV volumes in all sampling periods. Compared with coefficients for black carbon concentrations versus PC volume, the coefficients for black carbon concentrations versus HDV volume were generally more positive and larger, indicating a monotonically increasing trend between black carbon concentrations and HDV volumes. This coincides with the hypothesis of that the near-road black carbon emissions partly come from on-road diesel engine vehicles.

TABLE 2. Correlation Coefficients of Black Carbon Concentrations versus Passenger Car (PC) Volumes and Heavy Duty Vehicle (HDV) Volumes in All Sampling Periods

Fall	PC	HDV	Winter	PC	HDV	Summer	PC	HDV
10-18PM	0.08	0.58	2-17PM	(0.25)	0.58	7-5PM	(0.03)	0.30
10-19AM	(0.10)	0.34	2-22AM	(0.19)	0.35	7-6AM	0.15	0.18
10-19NOON	(0.05)	0.24	2-23PM	0.15	0.15	7-6NOON	(0.06)	0.30
10-19PM	0.28	0.27	3-1AM	0.44	0.12	7-6PM	(0.12)	0.32
10-20AM	0.15	0.12	3-1NOON	(0.47)	(0.04)	7-12AM	(0.51)	0.36
10-20PM	(0.23)	0.25	3-2PM	(0.02)	0.05	7-12NOON	0.21	0.56
10-21AM	0.08	(0.07)	3-3AM	0.15	(0.17)	7-14AM	0.21	0.08
10-21NOON	(0.26)	(0.29)	3-3NOON	0.05	(0.12)	7-14NOON	0.12	0.02
10-21PM	(0.24)	0.48	3-16PM	0.19	0.49	7-14PM	(0.12)	0.38
10-22AM	0.60	0.48	3-25AM	(0.27)	0.22	7-18AM	0.16	0.09
10-27AM	(0.13)	0.64				7-18NOON	(0.33)	0.14
10-27NOON	(0.60)	0.02				7-18PM	0.21	0.55
10-27PM	0.20	0.01				7-22AM	0.12	0.40
10-28AM	0.35	(0.40)				7-22NOON	0.18	0.12
10-28NOON	(0.18)	0.13						
10-28PM	(0.17)	0.01						

Note: numbers in red in parentheses are negative values.

CONCLUSION

A busy intersection near the UC campus was investigated for black carbon emissions. The black carbon concentrations were monitored and their association with automobile traffic was examined. A total of 40 measurements of black carbon concentrations, traffic volumes, and meteorology conditions were conducted in different seasons, and during different periods of the day. During 4 AM periods, the black carbon concentrations were significantly higher, due to the temperature inversion. No significant difference was found between Friday samples and samplings on other weekdays during the same season.

The black carbon concentrations followed the same seasonal trend as the ambient $PM_{2.5}$ concentrations measured by local environmental agency. Higher AM period black carbon concentrations were observed than the other periods, due to the increased HDV volumes. The HDV volumes were also found to have consistently high impact on black carbon emissions.

REFERENCES

Cao, J.J., C.S. Zhu, J.C. Chow, J.G. Watson, Y.M. Han, G.H. Wang, Z.X. Shen, and Z.S. An. 2009. "Black Carbon Relationships with Emissions and Meteorology in Xi'an, China." *Atmospheric Research*. 94(2): 194-202.

Samet, J. and, D. Krewski. 2007. "Health Effects Associated with Exposure to Ambient Air Pollution." *Journal of Toxicology and Environmental Health-Part A-Current Issues*, 70: 227-242.

NOAA and ESRL, 2011. NOAA/ESRL Radiosonde Database. http://www.esrl.noaa.gov/raobs/. Accessed 2012-4-15.

Pacas, C.R. 2011. *The Evaluation of $PM_{2.5}$ Measurements by Federal Reference Method and Continuous Instruments in Cincinnati, Ohio.* M.S. Thesis, University of Cincinnati, Cincinnati, OH.

IMPACT OF FUJAIRAH POWER PLANT-UAE ON AIR QUALITY

Muthanna Al Omar, Fadi Al Jallad and Santosh K.L
(National Energy and Water Research Center (NEWRC), Abu Dhabi Emirate, United Arab Emirates)

ABSTRACT: The growth in water and electricity demand in United Arab Emirates (UAE) has remarkably increased during recent years due to population growth and rapid industrial and economic development. In the north eastern part of the UAE namely Fujairah Emirate, two cogeneration plants were lately commissioned, thus according to the operation permit, impact on air quality of the surrounding should be assessed. Air quality station was installed at approximately 2.5 km downwind of the plants in Fujairah city, whose population was estimated as 145,261 in 2008. Continuous monitoring analysers (Environment S.A, France, 2M Series) were used in this project. The present work represents the outcome data for the period January to December, 2011, during which, the hourly and daily average values were estimated along with investigations regarding the temporal variation patterns.

Based on hourly data, the dominant wind direction was found to be south east with a maximum value of 14.8 m/second was reported. Temperature was ranging between 22.1ºC as a minimum value reported in January and 35.4 ºC reported in June. Relative humidity was ranging between 53.4% reported in December and 83.6 reported in August. Maximum hourly values of criteria pollutants were as follow: nitrogen oxides (NO_x) 280.6 µg/m^3, sulphur dioxide 179.7 µg/m^3, carbon monoxide 2.9 mg/m^3, ozone 227.5 µg/m^3 and particulate matter 1175.9 µg/m^3. Whereas annual average values were as follow: nitrogen oxides (NO_x) 22.8 µg/m^3, sulphur dioxide 11.4 µg/m^3, carbon monoxide 0.3 mg/m^3, ozone 61.6 µg/m^3 and particulate matter 103.5 µg/m^3. Ozone and sulphur dioxides showed their peak values in the afternoon, while other pollutants showed different diurnal variations with the peak values were mostly reported in the midnight. Exceedance was reported for ozone and particulate matters only in 10 incidences out of 8346 hourly readings for the former and 60 incidences out of 341 daily readings for particulate matter. It is worth to mention that the maximum limits for ozone 200 µg/m^3 (hourly average) and 150 µg/m^3 for particulate matter (daily average). It can be concluded that Fujairah cogeneration plant as a source of air pollution has insignificant effect on air quality of the city of Fujairah. Nevertheless the next step is to assess the impact of the plant using air pollution dispersion model.

INTRODUCTION

Water and electricity demand in United Arab Emirates has remarkably increased during the recent years due to population growth and rapid industrial and economic developments (SCAD, 2009). Operation of cogeneration plants may results in undesirable emissions to the surrounding atmosphere (Heinsohn and Kabel, 1999) which may include –but not limited to- nitrogen oxides (NOx), sulphur dioxide (SO_2), ozone (O_3), particulate matter (PM) and carbon monoxide (CO) (Smith, 1993), which are commonly called "criteria pollutants", according to World Health Organization (WHO) U.S. Environmental Protection Agency (US-EPA), and can harm health and the environment (Nazaroff, and Lisa, 2001; Baldauf et al., 2009). International and national entities use these pollutants as indicators of air quality. Standards for ambient air quality were established in United Arab Emirate for the criteria pollutants as per the Council of Ministers Decree No. (12) of 2006 (CoM, 2006).

Fujairah is one of the seven Emirates in UAE, whose population was estimated as 145261 in 2008. In this Emirate two Integrated Water and Power Plants (IWPP) exist and are operated with fossil oil to produce both water and electricity, hereinafter will be known as the source. However, scarce information is available regarding emissions and air quality in the area. As part of its commitment in conservation and protection of the environment, Abu Dhabi Water and Electricity Authority (ADWEA)

ISBN 9780976885351

installed Ambient Air Quality Monitoring (AAQM) station in the sensitive area in Fujairah city downwind of the power plants to monitor and assess their impact on ambient air quality.

This work presents the results of the monitoring process during the period from January to December, 2011.

EXPERIMENTAL

The source is located in the Emirate of Fujairah-UAE on the coast of the Gulf of Oman, approximately 20km north of Fujairah city. AAQM station is installed downwind of the source where sensitive receptors exist. The longitude and latitude coordinates of monitoring site are N25° 17.407 and E56° 22.041, respectively. The entire area is a desert with considerably poor vegetation cover.

The monitoring station is equipped with air quality monitors, data loggers, meteorological sensors, sampling system and advanced calibration system to ensure high quality data and has direct communication to a central data acquisition system which was utilized to retrieve and process the monitoring data.

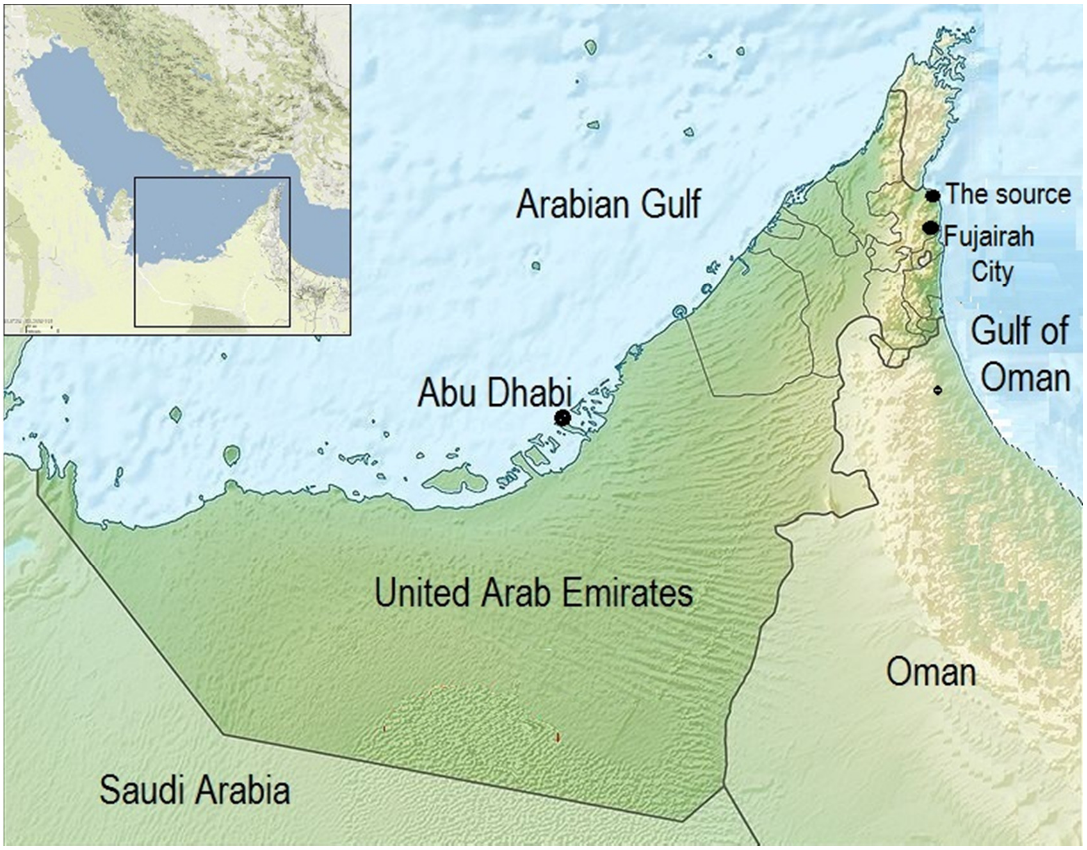

FIGURE 11 Location of the source and the sensitive receptors (Fujairah) with respect to UAE and the Arabian Gulf region.

Analysers (Environment S.A, France, 2M Series) used in this work are as follow along with their models and principle of operation: Sulphur dioxide analyser (AF22M, UV Fluorescence); Carbon monoxide analyser (CO12M, Non Dispersive Infrared); Nitrogen oxides analyser (AC32M,Chemiluminescence); Ozone analyser (O342M, UV photometry); Inhalable particulate matter monitor (MP101, Beta attenuation); Combined ultrasonic wind speed and direction anemometer (Gill WindDSonic, Ultrasonic transit time); and temperature and humidity sensors (Lastem DNA021, Thermohygrometric). Data flow from the monitoring stations is continuous at 5 minutes intervals. Analysers are calibrated by a calibration system of zero air and a multi gas calibrator and accordance to international standards and guidelines (US-EPA, 2008). All instruments are placed in an air-conditioned shelter.

Monitoring started by the end of 2010 and on-going; however, this work is limited to the period 1st Jan. 2011 to 31st Dec. 2011, in order to estimate the average values on annual basis as well as daily basis. Estimation was based on hourly average and daily average values for most pollutants, however, 8-hours average values was estimated for CO and O_3 in order to match the maximum allowable concentrations as mentioned in the national standards.

RESULTS AND DISCUSSION

The availability of the data was found to be more than 92% of all parameters during the study period. Minimum, maximum and average values of meteorological parameters are presented in Table 1. The months of June to August are usually the hottest in this region, with temperatures climbing to over 45.6 °C with an average value of 29.2°C based on hourly average and almost similar value based on daily basis. Relative humidity may reach sometimes 100% and 90.3% based on hourly and daily average, respectively.

TABLE 1 Meteorological parameters in Fujairah city for the period Jan.-Dec. 2011.

Parameter	Units	Hourly basis			Daily basis		
		Min.	Max.	Avg.	Min.	Max.	Avg.
Temperature	°C	9.5	45.6	29.2	20.1	39.7	29.3
Relative Humidity	%	0.1	100.0	68.0	0.2	90.3	68.0
Wind speed	m/s	0.0	14.8	1.6	0.7	14.8	1.6

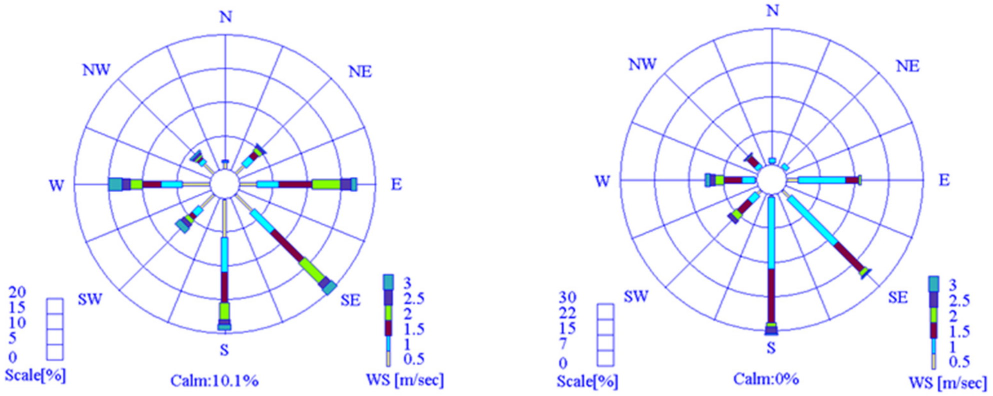

Wind rose based on hourly values

Wind rose based on daily values

FIGURE 2 Wind rose in Fujairah in 2011, based on hourly values and daily values

Figure 2 demonstrates wind rose in Fujairah city where the prevailing wind direction was found to be southeast based on hourly values. Southern and eastern winds were the second and third dominant directions. Nevertheless other directions were not uncommon, whereas plotting the wind rose based on daily average values revealed that southern wind was the dominant wind direction.

Table 2 demonstrates hourly and daily average concentrations of criteria pollutants. The maximum daily and hourly average concentrations of SO_2 were 45.8µg/m³ and 179.7µg/m³, respectively. Pollution rose indicated that highest concentrations were associated with east and southeast wind directions. No exceedance events were recorded neither for daily limit of 150µg/m³ nor for hourly limit of 350µg/m³ specified in the national standard.

TABLE 2 Hourly and daily average values of criteria pollutants in Fujairah during the study period 2011.

Pollutant	Units	Type of Datum	Values	
			Hourly basis	Daily basis
SO_2	µg/m^3	Min.	0.1	0.9
		Max.	179.7	45.8
		Avg.	11.3	11.4
CO	mg/m^3	Min.	0.0	0.0
		Max.	2.9	1.5
		Avg.	0.3	0.3
NO_2	µg/m^3	Min.	0.0	1.6
		Max.	157.7	60.4
		Avg.	16.4	16.3
O_3	µg/m^3	Min.	0.0	0.3
		Max.	227.5	185.2
		Avg.	61.5	61.8
PM10	µg/m^3	Min.	2	22
		Max.	1176	622
		Avg.	104	104

Hourly and daily average concentrations of carbon monoxide (CO) were ranging between 0.01 mg/m³ and 2.95 mg/m³, respectively. Hourly and eight-hour average concentrations of CO were well below the relevant allowable limits of 30 mg/m³ and 10 mg/m³, respectively.

Maximum daily NO, NO_2 and NOx average concentrations were 36.02µg/m³, 60.41µg/m³ and 90.85µg/m³, respectively, whereas the maximum hourly NO, NO_2 and NOx average concentrations were 182.72µg/m³, 157.71µg/m³ and 280.61µg/m³, respectively. No exceedance events for NO_2 hourly and daily limits were recorded during the study period.

Those three criteria pollutants (i.e. SO_2 , CO and NOx) are associated with vehicles as well as any combustion source (Baldauf et al., 2009), however, levels reported in this work were considerably low, since Fujairah city overlooks the open sea, vehicles are relatively new and low in numbers whose vast majority works on gasoline; on the other hand industrial combustion sources are rather limited among them is the two power plants.

The maximum hourly average concentration of O_3 was found to be 227.5µg/m³. Ten exceedance instants for the hourly limit of 200µg/m³ were recorded and there were 55 days (percentage of 15%) of high ozone concentrations (i.e. the maximum daily values for ozone 8hours rolling averages were higher than limit value). The highest daily maximum 8-hour average concentrations were 185.24µg/m^3 reported on 3rd May, 179.40µg/m^3 on 17th June, 174.29µg/m^3 on 22nd March and 167.66µg/m^3 on 23rd March 2011.

However, according to US-EPA guidelines on reporting and handling ozone data (US-EPA, 1998), and to verify the compliance with the standards, a valid 8-hr daily maximum concentration values should be based on three year intervals' among which each year should have 75% availability of data.

Taking into consideration that Gulf of Oman region is characterized by elevated ground level of ozone due to intensive sunlight, high temperatures, and stagnant wind, these climate conditions improve the dynamic photochemical reaction and trap the air within a region for several days (Camalier et al., 2007).

Daily average concentration values of PM_{10} ranged between 22µg/m^3 and 622µg/m^3, Sixty exceedance instants (16%) were recorded to the daily allowable limit of 150µg/m^3. However, elevated levels of PM_{10} in the entire region are thought to be caused by natural sources such as windblown desert sand and sea spray.

As a conclusion, it can be said that generally speaking, the study area has good air quality hourly and daily average concentrations of sulfur dioxide (SO_2), carbon monoxide (CO) and nitrogen dioxide (NO_2) were well below allowable limits stated in the National Air Quality Standard. High levels of ozone were recorded to exceed the limits in a few incidences. However, it is a secondary pollutant and cannot be attributed to the industrial activates. On the other hand, daily concentrations of PM10 were found to exceed the standard limit which can be attributed to both natural source and some non-combustion source known to be found in the area.

REFERENCES

Baldauf W.R., N. Watkins, D. Heist, C. Bailey, P. Rowley and R. Shores, 2009. Near-road air quality monitoring: Factors affecting network design and interpretation of data. *Air Quality, Atmosphere & Health*, 2:1–9

Camalier, L., W. Cox and P. Dolwick, 2007. The effects of meteorology on ozone in urban areas and their use in assessing ozone trends. *Atmospheric Environment*, 41(33): 7127-713.

CoM (Council of Ministers). Regulation Concerning Protection of Air from Pollution, 2006. Decree No. (12) of 2006, Annex #8, Ambient Air Quality Standards (Air Pollutants Limits in the Ambient Air).

Heinsohn, R. J. and R. L. Kabel, 1999. Source and Control of Air Pollution. Prentice Hall, Upper Saddle River, New Jersey.

Nazaroff, W. W. and A.C. Lisa. 2001. Environmental Engineering Science, John Wiley & Sons.

SCAD (Statistics Center-Abu Dhabi), 2009. *Abu Dhabi in Figures*.

Smith, K. R., 1993. "Fuel Combustion, Air Pollution Exposure, and Health: Situation in Developing Countries", *Annual Review of Energy and the Environment,* 18: 529-566.

US- Environmental Protection Agency, 1998. Guidelines on data handling conventions for the eight hour ozone National Ambient Air Quality Standard (NAAQS). U.S. EPA-454/R-98-017, December, 1998.

US- Environmental Protection Agency, 2008. Quality Assurance handbook for Air Pollution Measurement System, Volume II, Ambient Air Quality Monitoring Program. U.S. EPA- 454/B-08-003, December, 2008.

CHARACTERIZATION OF SIZE RESOLVED AIR PARTICULATES IN THE VICINITY OF ELECTRIC ARC FURNACE STEELMAKING FACILITY

K. Mohiuddin[a], V. Strezov[a], E. Stelcer[b] A. Morrison[a] and P. Nelson[a]
[a]Graduate School of the Environment, Macquarie University, North Ryde, NSW, Australia
[b]Australian Nuclear Science and Technology Organisation, Lucas Heights, NSW, Australia

Electric arc furnace (EAF) steelmaking process can produces particulates containing metals such as iron, zinc, manganese and lead, mainly originated from recycled galvanized scrap materials. The release of these particulates in the air can have significant impact on air quality, human health and environment. To understand the physicochemical characteristics of these air particulates, an eight staged Micro Orifice Uniform Deposit Impactor (MOUDI) sampler with 47 mm Teflon substrates was deployed from June to August 2011 in the vicinity of an EAF steelmaking facility at Rooty Hill located in the western Sydney of Australia to collect the different size fractions (18 µm to 0.18 µm) of air particulates. Elemental analysis of collected air particulates was performed using Proton Induced X-ray Emission (PIXE) and Proton Induced Gamma-ray Emission (PIGE) techniques. Scanning electron microscopy (SEM) examination was performed to observe the morphology and microstructure of particulates. The results were compared to those obtained from samples collected on the Macquarie University campus at North Ryde in the north-western Sydney suburbs, which is located away from any major industrial activity.

ISBN 9780976885351

A STUDY OF LIVE BACTERIAL PATHOGENS IN AIRBORNE PARTICLES

R. Kaushik and ***R. Balasubramanian*** (National University of Singapore, Singapore)

Airborne particles (PM) that contain biological components such as infectious agents, allergens, bacterial and fungal agents are usually measured by collecting them in solid, liquid, or agar media followed by qualitative and/or quantitative sample analysis using microscopic, biochemical, immunochemical, or molecular techniques. Culture-based techniques are time consuming, requiring microorganisms to grow on specific media at time scales ranging from days to weeks. Microscopic methods are tedious, and lack identification specificity. In addition, the classical microbiological methods lack the ability to represent the non-cultivable population of microorganisms. As a consequence, disease-causing pathogens could remain uncharacterized. In view of these drawbacks, there is a critical need to develop bioanalytical techniques that can provide accurate and reliable quantitative data on live pathogens in environmental samples for health risk assessments.

In this study, we investigated the use of PMA to distinguish viable from non-viable potential bacterial pathogens in fine particles in the atmosphere ($PM_{2.5}$; airborne particulate matter with aerodynamic diameter $\leq$ 2.5 µm). We identified a suitable DNA extraction procedure for $PM_{2.5,}$, optimized and validated a PMA-qPCR method for quantification of four live potential bacterial pathogens with pure cultures, and demonstrated the practical application of the modified qPCR method for quantification of the selected live pathogens in collected in $PM_{2.5}$, impacted by biomass burning emissions. To our knowledge, this is the first report of the application of the PMA technique in conjunction with qPCR to potential bacterial pathogens in PM. Previous reports in the literature detected total dead and live potential bacterial pathogens in PM, which limits conclusions regarding the significance for public health.

ISBN 9780976885351

EFFECT OF VARIOUS BIOWASTES ON EMISSIONS İN COMBUSTION OF LIGNITE COAL İN A CIRCULATING FLUIDIZED BED COMBUSTOR

Aysel Atimtay and Murat Varol (Middle East Technical University, Ankara, Turkey)
Hayati Olgun, Ufuk Kayahan, Alper Unlu (TUBITAK-MRC, Gebze, Kocaeli, Turkey)
Hüsnü Atakül (Istanbul Technical University, Istanbul, Turkey)

In this study, combustion of biomass and coal was carried out in a circulating fluidized bed combustor. A lignite coal which has high sulfur content and three biomasses were used in the experiments. The biomasses were hazelnut shells; woodchips and olive cake which is a waste of olive oil industry. Olive cake is a quite common biomass in Mediterranean countries. The experimental setup consists of a circulating fluidized bed combustor column, a fuel feeding system, electrical heaters, and two cyclones. Its thermal capacity is 30 kW. The combustor column has an inside diameter of 108 mm and a height of 6 m. The temperatures along the column are observed with thermocouples located at specific heights. The temperature of the column is kept at 850 oC during the combustion experiments. The pressure drops along the combustor column, cyclone, downcomer, and loopseal are continuously measured and observed in order to determine the solid mass flux within the combustor. A series of combustion tests for each fuel was performed in order to investigate the effect of excess air ratio and secondary air ratio on the flue gas emissions and combustion efficiency. Optimum Ca/S ratio was determined for each combustion tests in order to minimize SO2 emissions. During the combustion experiments, CO2, CO, O2, NO, and SO2, emissions in the flue gas was continuously measured and recorded by Gasmet DX-4000 flue gas analyzer.

The results of the experiments showed that as the biomass ratio in the fuel mixture increases for co-combustion, the combustion takes place more in the freeboard of the main column. Therefore, the maximum temperatures are seen in the freeboard rather than in the bed. Also the CO and CmHn emissions increase as the biomass percentage increases in the fuel. Biomass fuels have high CO emission which indicates that a secondary air addition is required for the system. As the biomass content in the fuel mixture increases, a decrease in the overall combustion efficiency is observed. Secondary air injection into the freeboard has been a useful solution to decrease the CO and hydrocarbon emissions and to increase the combustion efficiency. Addition of secondary air during the combustion of biomass-coal mixtures is found to increase the NOx emissions slightly. These results suggest that during the design of the CFBC, one has to be careful about the VM content of the biomass. Agglomeration properties were also investigated. High sulfur content of lignite coal seemed to help to solve the agglomeration problem. The results are promising.

ISBN 9780976885351

RADON & CHEMICAL CONTAMINANTS IN INDOOR AIR & “SOIL GAS SAFE” COMMUNITIES

Schuver, H., Jalbert, P. (USEPA, Wash. DC, USA), Steck, D. (St. Johns Univ., MN, USA), Siegel, L. (CPEO, Mt. View, CA, USA), Nicol, A., McKenzie, A., and Blewett, C. (Univ. BC, Vancouver, Canada)

The intrusion of hazardous soil gas contaminants into the indoor air of homes, schools, and other buildings is a significant public concern because human exposure may be continuous and, in the absence of mitigation, unavoidable. The recent focus of environmental regulation has been on the intrusion of chlorinated solvents such as TCE and PCE, released by industrial polluters, yet the threat of naturally occurring radon is more widespread and poses a greater overall threat to public health. This presentation will propose an integrated approach to investigating and mitigating radon and chemical vapor intrusion that is designed to maximize the protection of public health and better inform the public about the hazards of vapor intrusion, using radon as a general indicator of all intrusion and risk driver.

The intrusion of soil gas into the indoor air of buildings in contact with the soil can degrade the quality of indoor air and can significantly impact human health. For example, radon is the leading carcinogen for the general public that is addressed by the USEPA and it is typically the most potent environmental toxin in a home (EPA 1990). Radon commonly presents risks 100-1000 times chemical risk action levels. The scientific evidence for radon risk and the impact on public health in the US (e.g., ~21,000 deaths/yr (EPA 2003)) is now clear (WHO 2009). Despite significant efforts to educate the public on radon risks, studies indicate that the public generally comprehends the material but discounts these largely natural risks despite the scientific evidence for their seriousness (CAREX, 2011). It is hypothesized that the individual building owners/occupants may sample for radon but many e.g., without high education and income levels, often fail to take action on these risks (i.e., mitigate), not solely due to the cost of mitigation (shown to be cost-effective in high-radon areas based primarily on medical costs alone), but also because they perceive that society has a generally negative understanding or stigma for soil gas controls. Many believe soil gas controls degrade the value their property (e.g., for resale to members of the public) and consider that to be more of concern than the health risks presented. To address this long-established society-wide misunderstanding of the benefits of keeping soil gases out of indoor air, health authorities such as the USEPA are considering a voluntary public health approach highlighting the positive values and benefits of soil gas controls. To acknowledge the value added to buildings with controls preventing soil gas intrusion they are considering issuing certificates of LEED credits (Leadership in Environmental and Energy Designs (LEED 2010)) for new and existing residential buildings with designs/control systems preventing/reducing soil gas intrusion. Furthermore, they are considering designating “Soil Gas Safe” Communities where the majority of the buildings have designs/systems keeping soil gas out of indoor air. These areas could be mapped to highlight the positive value of community-wide reduced risks. The continuous monitoring of radon, prior to and following mitigation, would allow the health benefits, e.g., estimates of the number of lives saved/extended, due to radon alone, per state and nationally, to be tracked and compared to areas without soil gas controls. These efforts are intended to make it clear to the broad public the value added by preventing soil gases from intruding into indoor air and that such added protection should be desired and expected in their current and/or future homes. It has been estimated that over the last 50 years as many as one million persons have died from indoor-air radon-related lung cancer (Field 2011). The objective of this effort is to significantly reduce that number over the next 50 years, and also to reduce all soil gas intrusion hazards, including those with less easily documented health risks (e.g., chemicals, etc.).

ISBN 9780976885351

ESTIMATION OF HISTORIC BLACK CARBON REDUCTION CO-BENEFIT FROM PM CONTROL IN MAINLAND CHINA

Wei Wei Song (Harbin Institute of Technology, Harbin, China)
Ke Bin He and Jeremy Schreifels (Tsinghua University, Beijng, China)
Yu Lei (Chinese Academy for Environmental Planning, Beijing, China)

Black carbon (BC) is a short-lived climate forcer that contributes to global climate change and is the second biggest contributor to positive radiative forcing after carbon dioxide. Several studies have shown that abatement of BC emissions may provide a cost- and environmentally-effective approach to mitigate global climate change. Since 1990, mainland China has undertaken significant efforts to reduce PM emissions, providing significant co-benefit reductions of BC. In this study, we estimate historical BC emissions and reductions from key sectors. The analysis accounts for changes in combustion and control technologies, and established polices and strategies of industry, power plants, transportation, and bio-fuel burning sectors. The analysis is based on earlier studies, but includes new information from surveys of stationary sources and their activity levels. The paper aims to provide a quantitative understanding of BC emission trends and co-benefit emission reductions from existing PM control approaches. It also provides data that can support future research and projections, technology selection, and control technology optimization.

ISBN 9780976885351

ENVIRONMENTAL EFFECT OF ROAD DEVELOPMENT ON SOME AIR QUALITY PARAMETERS IN NIGER DELTA, NIGERIA

John U. Akpabio (Department of Environmental Management Enugu State University, Enugu State, Nigeria)
MANDU A. ESSIEN- IBOK (Department of Fisheries, University of Uyo, Akwa Ibom State, Nigeria)
ANTHONY W. AKPAN (Department of Zoology, University of Uyo, Akwa Ibom State, Nigeria)

The effect of road development on some air quality parameters in an urban oil producing community east of the Niger Delta (Nigeria) was studied for 24 months using standard air quality gas monitors. Pre and post construction measurements were made for NH_3, CL_2, SPM, heat, radiation and HCN. Emission levels for NH_3 varied between 2.0-3.0ppm and exhibited both spatial and temporal variation and post-construction emission levels lower than pre-construction phase and 0.30-0.90ppm during the post construction period with significant difference between the two phases. SPM levels were significantly higher during pre-construction period than the post-construction indicating remarkable reduction in air-borne load of suspended matter. Heat and radiation levels were significantly higher during post-construction period indicating that the road development projects spewed off higher pollutant emissions. Emission levels of HCN varied during pre and post construction phases but not significantly different. The development of infrastructure facilities such as roads particularly in the developing societies is very needful but the environmental burdens of such development need also to be considered particularly in the oil rich areas with gas flares.

ISBN 9780976885351

EMISSION OF VOLATILE ORGANIC COMPOUNDS FROM GREEN WASTE COMPOSTING: AN OVERVIEW

Anuj Kumar
(Carlsbad Environmental Monitoring and Research Center, New Mexico State University, Carlsbad-88220, NM, USA)

Composting of green waste separated from the disposed solid waste stream reduces biodegradable inputs into landfills, and contributes valuable soil amendments to agriculture. The study was conducted to determine the emission estimation with a detailed speciation profile of VOCs for more accurate input on the contribution of compost operations to tropospheric ozone production. Multiple sampling and analytical approaches were applied to ensure the detection of most gaseous organic components emitted from green waste compost piles of different ages (fresh tipped piles, 3-6 day old windrows, and 2-3 week old windrows). More than 100 VOCs were detected and measured in this study, including aliphatic alkanes, alkenes, aromatic hydrocarbons, biogenic organics, aldehydes, ketones, alcohols, furans, acids, esters, ether, halogenated hydrocarbons and dimethyl disulfide (DMDS). Alcohols were found to be the dominating VOC in the emissions from a compost pile regardless of age, with fluxes ranging from 2.6 to 13.0 mg m^{-2} min^{-1} with the highest emissions coming from the younger composting windrows (3-6 days). Average VOC emissions other than alcohols were determined to be 2.3 mg m^{-2} min^{-1} from younger windrows, which was roughly two times higher than either the fresh tipping pile (1.2 mg m^{-2} min^{-1}) or the older windrows (1.4 mg m^{-2} min^{-1}). It was also observed that the older windrows emit a slightly larger proportion of more reactive compounds. Approximately 90% of the total VOCs were found to have maximum incremental reactivity of less than 2. Net ozone formation potential of the emissions was also assessed.

ISBN 9780976885351

INDOOR AIR QUALITY SURVEY OF BOSTON NAIL SALONS

Meda Kisivuli, Liza Ansher, Ariana Berlin, Jenny Cheng, Deena Kanopkin, Anna Khazan, Molly Lortie,
Emily Peterson, Laura Pohl, Sam Porter, Vivian Zeng, Joseph Allen, Matt Fragala, Theodore Myatt,
James Stewart, Laura Goldin (Brandeis University, Waltham, MA, USA)
Tiffany Skogstrom (Boston Public Health Commission, Boston, MA, USA)

Employees in nail salons are exposed to a range of volatile organic chemicals from the products used in nail care, including solvents, glues and polishes (Spencer, Estill et al. 1997). Some of these chemicals have the potential to cause short and long-term adverse health effects (LoSasso, Rapport et al. 2001; LoSasso, Rapport et al. 2002; Roelofs, Azaroff et al. 2008). Only limited research has been performed on assessing occupational exposures in nail salons and very little has focused on evaluating ventilation characteristics. Additionally, the nail salon workforce is largely composed of immigrant Vietnamese workers which can add to the complexity of this issue in regard to public health awareness campaigns and outreach (Quach, Nguyen et al. 2008). This project aimed to characterize total volatile organic compound (TVOC) concentrations in nail salons as a function of ventilation characteristics, building size, customer and employee occupancy, and type of services being performed. Students conducted sampling in 21 salons in Boston, MA (USA) from September to December, 2011. Study visits consisted of three parts: indoor environmental quality measurements (total volatile organic compounds, carbon dioxide (CO2) and particulate matter less than 2.5 microns in diameter [PM2.5]), site observations, and a short interview with each salon owner. Six to eight sampling locations were selected in each salon. CO2 levels in 15 of 21 salons exceeded 800 ppm indicating that these salons may have insufficient ventilation. Higher TVOC and PM2.5 levels were found in salons with poorer ventilation (as determined by elevated CO2 concentrations). Contrary to our *a priori* hypothesis, average levels of TVOCs , CO2 and PM2.5 were consistent throughout salons, indicating that elevated exposures may not be restricted to areas in the salon where work is being performed (e.g., at the manicure table). Higher TVOC concentrations were observed when tasks were being performed, and were not dependent upon the number of tasks being performed. Salons with open doors and/or windows had significantly reduced TVOC concentrations. Improving ventilation conditions in salons to meet minimum outdoor air delivery requirements can reduce exposures to TVOCs. Weather permitting, increasing outdoor-indoor air exchange by opening doors and windows may be a simple approach to reducing exposures.

ISBN 9780976885351

LICHEN BIOMONITORING ALONG A POTENTIAL POLLUTION GRADIENT IN SOUTH WEST WESTERN AUSTRALIA

M.C. Vitarana, W.D. Stock, A. Hinwood (Centre for Ecosystem Management, Edith Cowan University, Western Australia)

During the last few decades, various techniques for using lichens as biomonitors have been developed for monitoring air pollution and forest ecosystem health. Literature confirms that lichen diversity and density can be effectively used to determine the dispersion of pollutants, however the approach has not been used in Australia. This study investigated the distribution of lichen populations along a potential pollution gradient from coal-fired power plants, in native Jarrah forests of Collie, South West Western Australia. Questions addressed were: (1) Which site characteristics play a key role in the distribution of lichen communities and abundance in the Jarrah forests surrounding Collie? (2) Do forest management practices play an important role in the distribution of lichen communities and their abundance? (3) Are industrial pollutants controlling the distribution of lichen species richness and abundance along the potential pollution gradient?

Our study found a total of twenty lichen taxa in thirty six sites, with the highest number of species and lichen cover observed in control sites. A positive correlation was observed between distance to coal-fired power plants and lichen abundance data, indicating a higher lichen density away from these pollution point sources. A principal component analysis was performed and the ordination plot showed distinct differences in lichen communities along the pollution gradient. No correlations were observed between forest characteristics such as fragment size, stand density, canopy cover, fire history, harvesting history and lichen diversity or abundance data. A significant correlation was observed between log/stump density and lichen abundance data. These results confirm the use of lichens community structure as a cost-effective tool for monitoring the impacts of pollutants in native forests of South West Western Australia.

ISBN 9780976885351

TOLUENE AND N-HEXANE ADSORPTION ON ALMOND SHELL BASED ACTIVATED CARBONS

Alicia Martínez de Yuso* (Universidad San Jorge, Zaragoza, Spain), Mª Teresa Izquierdo, Begoña Rubio (Instituto de Carboquímica, Zaragoza, Spain) and Rosa Pino (Universidad San Jorge, Zaragoza, Spain)

Among atmospheric pollutants, volatile organic compounds emissions have reached a great relevance in recent years due to the risks for human health and for the environment that they present. These compounds may cause headache, nauseas or even damage to central nervous system with long exposure, some of them are carcinogenic. VOCs are considering like ozone precursors due to they participate in reactions with other contaminants in the atmosphere to form photochemical smog. VOCs are widely used like organic solvents in industrial applications like coating or painting and they are emitted by the storage, distribution and use of fossil fuels.

There are different methods to VOCs control but activated carbon present several advantages over other alternatives. Adsorption on activated carbon permits not only the removal of VOCs but also the recovery of the VOC for later uses and provides high removal efficiency at low inlet concentrations. Another advantage of these materials is that can be prepared from low cost precursor like lignocellulosic wastes.

The goal of this study is the adsorption of volatile organic compounds that act like solvents in gas streams, such as toluene and n-hexane, using almond shell based activated carbons prepared by chemical activation with phosphoric acid. The effect of porous structure, chemical surface and the presence of water vapour have been analyzed in a series of activated carbons prepared under different conditions in order to identify the most adequate parameters to prepare activated carbons for VOC adsorption. With the view of reduce the environmental cost of the activated carbon a very common lignocellulosic waste was choice as precursor and the preparations of the activated carbons was carried out under moderate conditions of impregnation ratio, time of activation and temperature of activation.

The characterization of the samples was carried out to determine their pore structure and their surface chemistry showing different characteristics of the activated carbons prepared. This demonstrates that the conditions of preparation have a great influence in the final physicochemical characteristics of the activated carbons permitting to adjust the characteristics of the carbons in function of the final application changing the conditions of preparation.

High adsorption capacities have been obtained for VOCs with high values of 60 wt% for toluene and 40 wt% for n-hexane. Dynamic adsorption was carried out in a bench-scale custom build set up to simulate the adsorption in a real application. Breakthrough curves obtained show high breakthrough times for both VOCs. Dynamic adsorption in presence of 3% of water vapour confirms a reduction in the amount of VOC adsorbed of at least a 75% for n-hexane but much lower for toluene, from 50% of reduction to a slight change in the amount adsorbed. Breakthrough curves show a higher reduction in breakthrough times for n-hexane, between 75 % and 95 %, than for toluene, between a slight decrease and 70 %. It can be concluded that the presence of water vapour has a great influence in the adsorption of VOCs, however high breakthrough times were still observed.

Activated carbons prepared present only a slight decrease of the adsorption capacity along several cycles adsorption-desorption. This is an important characteristic for solvents recovery in industrial applications.

ISBN 9780976885351

NOVEL REGENERABLE SORBENTS FOR MERCURY RETENTION IN ENERGY POWER PLANTS

D. Ballestero (Universidad San Jorge, Zaragoza, Spain), M.T. Izquierdo, R. Juan, E. García-Díez, C. Gómez-Giménez, C. Ruiz, B. Rubio (Instituto de Carboquímica, Zaragoza, Spain)

Mercury is a highly toxic trace metal of environmental concern because of its properties like volatility, persistence, bioaccumulation in the environment and its neurological health impacts. This metal is readily methylated by microorganisms, bioaccumulates in biota and consistently biomagnifies through the food chain. Mercury can be emitted in a natural way like volcanoes and anthropogenic way. Due to anthropogenic mercury emissions, the concentrations of mercury are three times higher than in pre-industrial days. Between all mercury anthropogenic sources, electrical power plants are estimated to account for about 25% of the global anthropogenic mercury emissions. Technologies like activated carbon injection are used for mercury abatement, but large amount of toxic wastes are obtained during these abatement processes. The objectives of this job is to develop a waste free process for mercury capture based on novel gold nanoparticles/carbon regenerable sorbent. A regenerable sorbent based on gold /carbon monolith for the capture of elemental mercury has been developed with a new methodology for gold nanoparticles deposition onto carbon monolith support.

A honeycomb structure monolith is selected in order to avoid pressure drop and particle entrainment. Carbon-based supports were chosen because the possibility to modify the surface chemistry to favour the gold nanoparticles dispersion. Once the sorbents are obtained, are characterized by SEM, SEM-FE, BET, elemental analysis, TPD, N_2 physisorption and IR. Sorbents are tested in a bench scale experimental installation working at high space velocities 25000-50000 h^{-1}, 120ºC for retention temperature and at Hg inlet concentration of 22 ppb. Mechanism of mercury retention is the amalgamating and deamalgamating property of mercury for gold. The appropriate regeneration temperature was obtained and it was in the range of 220ºC. The regenerelability has been tested performing cycles of adsorption-desorption at low temperatures. High mercury capture efficiencies are obtained for the sorbents tested, with low gold content, indicating that this novel regenerable sorbent is a promising material for mercury capture in a waste free process.

ISBN 9780976885351

STRUCTURED PACKING CORROSION EVALUATION IN SOUR GASES TREATMENT AT BRICK KILN PRODUCTION

Rosa-Hilda Chavez* and Araceli Salazar (Instituto Nacional de Investigaciones Nucleares, La Marquesa, Ocoyoacac, Mexico, Mexico)
Javier de J. Guadarrama (Instituto Tecnologico de Toluca, Metepec, Mexico, Mexico).

The burning of pieces manufactured with clays to be used in the construction industry, contributes to environmental imbalance due to it is used combustible material that produce emissions released to the atmosphere, up to now kilns have been used with combustion processes precarious and fuels highly polluting, which favors climate change emissions for CO2, NOx and acid rain by SOx, endangering the health of those living near these facilities. The treatment of combustion gases by means of a packed absorption column with a high efficiency liquid-gas contactor reduces pollutant emissions to the atmosphere, when combustion gases are in contact with aqueous amine solution of Mono Ethanol Amine (MEA), using different structured packing material which can be metallic, polymeric or ceramic. The objective of this work is to study which one of three materials presents the lowest deterioration in presence of combustion gases with MEA. The materials were tested according the ASTM G31-2004 corrosion testing, and the procedure NRF-194 PEMEX-2007. The properties studied were tensile strength, hardness and elastic modulus, before and after structured packing materials were in contact with combustion gases in MEA aqueous solution. The results showed that in acid and basic medium, the metallic material was the most resistant to abrasion; it has the major tensile strength, and presented more resistance in the stress test.

ISBN 9780976885351

PARTICULATE MATTER FLUX DEPOSITION IN THE VICINITY OF A COAL-FIRED POWER PLANT

Maria de Lurdes Dinis, Joaquim Góis, António Fiúza, José Soeiro de Carvalho, Ana Meira Castro
(Geo-Environment and Resources Research Center (CIGAR), Porto University, Porto, Portugal)

ABSTRACT: This paper describes the methodology adopted to assess local air quality impact in the vicinity of a coal power plant located in the south of Portugal. Two sampling areas were selected to assess the deposition flux of dust fallout and its potential spatial heterogeneity. The sampling area was divided into two subareas: the inner, with higher sampling density and urban and suburban characteristics, inside a 6-km circle centered on the stacks, and an outer subarea, mainly rural, with lower sampling density within a radius of 20 km. Particulate matter deposition was studied in the vicinity of the coal fired power plant during three seasonal sampling campaigns. For the first one, the average annual flux of dust fallout was 22.51 g/(m^2 yr), ranging from 4.20 to 65.94 g/(m^2 yr); for the second one was 9.47 g/(m^2 yr), ranging from 0.78 to 32.72 g/(m^2 yr) and for the last one was 38.42 g/(m^2 yr), ranging from 1.41 to 117.48 g/(m^2 yr). The fallout during the second campaign turned out to be much lower than for others. This was in part due to meteorological local patterns but mostly due to the fact that the power plant was not working at full power during the second sampling campaign.

INTRODUCTION

One of the main adverse impacts from coal-fired power plants emissions is related to local air quality. Many hazardous air pollutants are associated with coal-fired power plant releases, including sulfur dioxide, oxides of nitrogen and particulate matter. Hazardous air pollutant emissions from coal power plants can originate several health effects in the nearby population. Also, airborne fine particulate matter may be a source of heavy metals transport, dispersion and deposition in the environment. These heavy metals include As, Be, Cd, Cr, Pb, Mn, Ni, Ra, Se and other metals, which are attached to fine particulate matter released from coal-fired power plants (Azimi et al., 2003; Mehra et al., 1998).

Particulate matter (PM) is defined as the solid and condensable matter emitted from an industrial process, like coal combustion, and is identified according to their aerodynamic diameter as either PM_{10} (particles with an aerodynamic diameter smaller than 10 µm) or $PM_{2.5}$ also called fine particulate matter (aerodynamic diameter smaller than 2.5 µm) (EEA, 2009).

Coal power plants are a major source of particulate matter pollution resulting both from unburned fuel particles and from chemicals that react to form new particles. Further, PM pollution from coal plants includes a high proportion of $PM_{2.5}$, the smallest and most damaging size.

Primary PM is formed in the process itself, such as in the combustion of coal. Secondary PM is formed outside the process when pollutants react with each other in the atmosphere. Examples are nitrates, sulfates, and other organics formed by a reaction with sulfur oxides and nitrogen oxides emitted to the atmosphere (XiaoWei et al., 2009).

Fine particles can remain suspended in the air for long periods of time (as smaller particles are lighter) and travel long distances before settling down. When inhaled they are able to penetrate deep into the lungs. In contrast, larger particles such as dust travel shorter distances and are more effectively trapped in the body's upper respiratory track. Also chemicals released from coal-fired boilers may remain in the gas form for distances up to several kilometers from the stack, forming PM at significant distances downstream from the pollution source (WHO, 2006).

This paper describes the methodology adopted to assess local air quality impact in the vicinity of a plant located in southern of Portugal. This research work was particularly focused on flux deposition of

---

ISBN 9780976885351

particulate matter and is part of a national research project supported by the Portuguese Foundation for Science and Technology for three years.

Two sampling areas were selected to assess the deposition flux of dust fallout and its potential spatial heterogeneity; atmospheric dust was collected by a passive system following the French norm NF X43-007 (1973). Both areas were defined taking for referential the stacks, and considering the wind direction, as well as its velocity and frequency, in order to take into account the possible exposure of a population living up to 20 km from the source. Local meteorological conditions were studied using a portable self standing station placed near the coal-power plant as well as additional data from other sources (Dinis et al., 2011).

Two annual sampling campaigns were carried out to collect variable data according to potential seasonal meteorological patterns considering rainy or dry atmospheric conditions. The first campaign was performed between mid September and mid October 2010 (nº 1) and the other one during the month April of 2011 (nº 2). The sampling campaigns were repeated one year after for the same seasonal periods: mid September to mid October 2011 (nº 3) and mid March to April of 2012 (nº 4). The research described here refers to three sampling campaigns (nº 1, nº 2 and nº 3).

MATERIALS AND METHODS

Study Area. The studied area is located in the southwest coastline of Portugal, at 6 km south-east from the city of Sines and about 150 km south of the country's capital, Lisbon. The coal-fired power plant is a conventional one working with four coal fired units, each one with an electrical energy output of 314 MW (Cianci et al., 2007). The first unit started working in 1985 and the last one in 1989. The power plant operates with efficiency in the range of 32 to 35%.

The facility has two operational stacks both with 225 m height and supplies about 20 to 25% of all electrical energy produced in Portugal. The power station burns bituminous coal as a primary fuel, imported from many different countries (Dinis et al., 2011). The coal-fired power plant is one of the several industrial plants (at least 14) located in this area which includes a petrochemical complex, a refinery and a resins plant among others.

The PM_{10} releases from this coal-fired power plant are reported in the European database E-PRTR (2010) for 2001, 2004, 2007, 2008, 2009 and 2010 with the values of 1740, 812, 587, 394, 130 and 100 tons, respectively. There is no information about $PM_{2.5}$ releases in this database.

Sampling and analysis. The area of stack's emissions influence and, consequently, the sampling areas were defined considering the possible effect on the people living in the neighborhood of the coal-fired power plant, up to distances of 20 km.

Two sampling areas were selected to assess the spatial heterogeneity and deposition flux of dust fallout. The sampling area was divided into two subareas: the inner, with higher sampling density and urban and suburban characteristics, inside a 6-km circle centered on the stacks, and an outer subarea, mainly rural, with lower sampling density within a radius of 20 km (FIGURE 1).

The atmospheric fallout was quantified by a passive collection system following the norm NF X43-007 (1973). This collection system consists of a 50 cm^2 stainless steel slice horizontally fixed at a defined height above the ground with a silicone cover (Polydimethylsiloxane) to trap dust fallout. Same sampling procedures were carried out at sampling points selected as a control, away from possible influence of the power plant.

About 40 samplings points were defined in the influence area (FIGURE 1): 13 dust sedimentation plates were placed inside the inner circle around the plant and 27 other were placed in the outer subarea, at about 3 meters above the ground. This height above the ground was adopted in order to assure that the collectors were recovered after the collecting period without being damaged.

Seasonal sampling campaigns for dust fallout are being carried out in the study area twice a year, since September 2010. A month period was chosen for the determination of the deposition flux according to the previous procedure and the norm NF X43-007. The aerosols attached to the resin were removed after this period. The slices were then rinsed with an organic solution (dichloromethane) at the laboratory. The solvent was filtered in a glass filtration system (Buchner funnel) over a 0.22 μm Polyvinylidene Difluoride (PVDF) membrane filters with 47 mm diameter. Filters were dried and weighted to obtain dust quantity expressed in weight per area per time (μg m^{-2} d^{-1} or g m^{-2} yr^{-1}) which represents the dust fallout deposition flux.

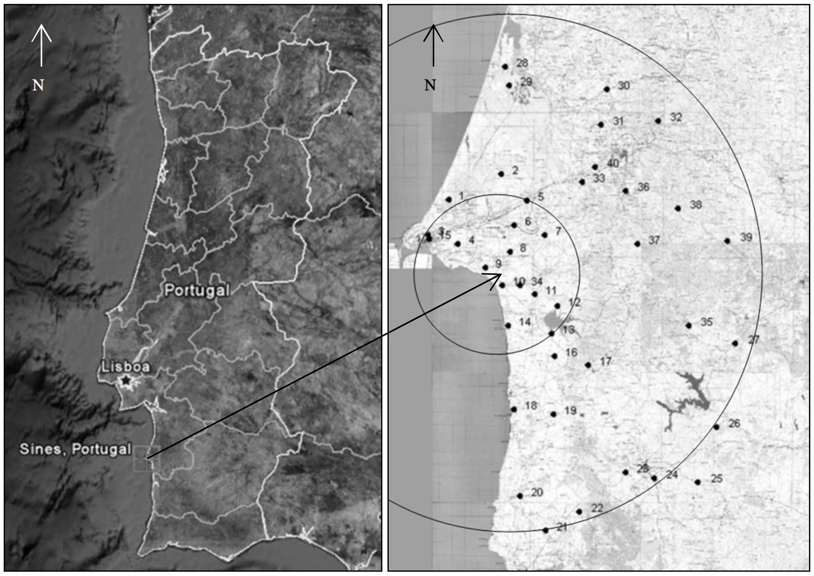

FIGURE 1: Sines location and sampling area around Sines coal power-fired power plant.

Meteorological Conditions. Meteorological data was continuously collected from a meteorological station placed at south of the coal power plant at about 10 meters height from the ground. Wind data of each 10 minutes observations were extracted referring to the sampling periods of each campaign. Daily average, maximum and minimum values were automatic extracted for temperature, rainfall, relative humidity, insulation as well as wind velocity, direction and frequency.

The historical data referent to the study area indicates that the prevailing wind direction is from the sector N-NW (frequency of 26 and 25%, respectively) with the exception for the month of October, when the prevailing winds direction is from SW and S. In autumn there is a significant decrease in wind directions blowing from NW indicating the prevailing winds to be from N with a frequency of 34.5%. Less frequency is associated to sectors E and SE (with frequency of 4 and 6.4%, respectively).

Wind velocity is relatively constant during all year with long calm periods; stronger winds blow from N-NW and SW with maximum velocities during the winter season. Annual average wind velocity range between 11 and 22 km/h. Higher velocities are associated to NW and N sectors (22 and 17 km/h respectively) while lower wind velocity is associated with E and SW sectors (≅ 11 km/h).

As the sampling periods were carried out during mid September to mid October (sampling campaigns nº 1 and nº 3) and during the month of April (sampling campaign nº 2), the prevailing wind direction for these periods were from N-NW and from N-NE, respectively. For these same periods, wind velocity was in average 2.57 m/s, ranging from 0.18 to 13.31 m/s for sampling campaign nº 1; 2.6 m/s, ranging from 0.21 to 8.16 m/s for sampling campaign nº 2 and 2.43 m/s, ranging from 0.18 to 11.51 m/s for campaign nº 3.

RESULTS AND DISCUSSION

Particulate matter deposition was studied in the vicinity of the coal-fired power plant during three campaigns. Data on deposition flux was calculated according to the norm NF X43-007 and are presented in TABLE 1 and TABLE 2 for each one of the considered sampling campaigns as well as for both sampling areas.

TABLE 1: Dust fallout in selected sampling points within the 6 km sampling area

Sampling point Nº	Sampling Campaign Nº 1	Sampling Campaign Nº 2	Sampling Campaign Nº 3
4	3.134	1.185	3.758
8	2.364	0.212	7.799
11	5.702	1.198	1.078
34	2.867	0.504	2.132
Average	**3.517**	**0.775**	**3.692**

For the sampling area within 6 km around the stacks the average dust flux depositions are in a good agreement for the first and third sampling campaigns (equivalent seasonal periods). For the second sampling campaign the flux deposition was much lower.

TABLE 2: Dust fallout in selected sampling points within the 20 km sampling area

Sampling point Nº	Sampling Campaign Nº 1	Sampling Campaign Nº 2	Sampling Campaign Nº 3
1	4.915	1.272	3.198
18	2.237	0.568	0.703
23	3.280	0.356	6.716
24	2.799	0.315	3.353
25	2.381	0.419	0.868
26	2.499	0.545	9.442
32	2.403	0.326	5.866
33	2.313	0.413	2.398
39	5.407	0.931	2.180
40	4.007	0.065	1.837
Average	**3.224**	**0.521**	**3.656**

The same variation pattern was observed for the sampling area between 6 and 20 km around the stacks. This may be related with the fact that the power plant was not operating at full power during the second sampling campaign; 17 days out of 28 fully sampling days. The results also showed a high variability among the sampling points for both areas. The average annual dust flux deposition as well as the deposition flux per month for the 40 sampling points is presented in TABLE 3.

TABLE 3: Dust flux deposition for the sampling campaigns nº 1, nº 2 and nº 3

Dust flux deposition Sampling campaign	Min.	Mean ± σ ($g\ m^{-2}$ per month)	Max.	Min.	Mean ± σ ($g\ m^{-2}$ per year)	Max.
Nº 1	0.36	1.90 ± 1.32	5.70	4.32	22.79 ±15.83	68.43
Nº 2	0.02	0.79 ± 0.73	3.10	0.25	9.48 ± 8.76	32.23
Nº 3	0.12	3.20 ± 2.58	9.83	1.41	38.42 ± 30.96	117.98

The parameters that influence the dispersion of solid particles and the velocity of their descendents through the atmosphere (according to their weight and velocity) are mainly the wind force and direction, rainfall intensity and frequency, other larges sources of emissions, resuspension of dust from earth's surface, intensified agricultural activities and road traffic (Mejstrik and Svacha, 1988).

In cases where none of these factors are present the intensity of particles deposition should decrease with the distance to the main source of pollution as found in some sectors of the studied area within the 6 km; the exceptions are the sampling points nº 4, 8, 11 and 34. In what concerns to the outer area (20 km), the exceptions are points nº 1, 18, 21, 23, 24, 25, 26, 27, 31, 32, 33, 38, 39 and 40.

The distance from most of these sampling points to the stacks as well as their orientation is presented in TABLE 4.

TABLE 4: Sampling points distance and orientation to the power plant stacks

Sampling Point Nº	Distance to the stacks (m)	Orientation to the stacks
1	6695	NW
4	5924	NW
8	2013	NE
11	3399	E
18	10537	S
23	18208	SE
24	19898	SE
25	22328	SE
26	20648	SE
32	17124	NE
33	9686	NE
34	2126	E
39	17963	E
40	11180	NE

In these cases we may have the presence of point sources of particle emissions or emissions from more than one source overlapping which may reverse the normal pattern of dust deposition. In the studied area, beside the existence of others industrial plants, a huge open air coal pile deposit is located near the stacks.

The exceptions observed for sampling points nº 4 and nº 8 may be explained by the dispersion of unburned coal particles from this pile. The other exceptions may be explained by the emissions from further industrial plants located at NW and N, road traffic and agricultural practices for the sampling points more distant from the stacks where rural and agricultural areas prevail. On the other hand, the height of the stacks (225 m) may influence fallout dispersion up to a distance of 20 km.

The dispersion of particle emissions with wind parameters as well as the dispersion in the dominant wind direction is a little more complex as the observed pattern does not completely follows the wind patterns.

The total fallout particle values at NW, SE and E are in the same order of magnitude for sampling campaigns nº 1 and nº 3 although emissions were expected to be transported to SE; this occur only at some extent being more expressive for sampling campaign nº 3.

In sampling campaign nº 2 the deposition occurs mostly at NW, N and NE. In the E-SE sector at distances relatively close to the stacks the flux deposition pattern is similar. A peak deposition flux occurs for sampling points nº 11 (campaign nº 1), nº 13 (campaign nº 2) and nº 12 (campaign nº 3). These sampling points are located at distances comprised between 4150 and 6300 meters S-SE from the stacks. This may be explained by the dispersion, and subsequently the deposition, of the unburned coal particles from the deposit around the stacks, in the prevailing wind direction observed for the respective sampling periods.

The fallout particles observed in the NW sector may be attributed to other pollution sources located either to N and NW of the coal power plant that influence particle fallout in the northern sector and at some extent in the eastern sector where such pollution sources do not exist (in particular, samplings points nº 1, 2, 4, 5, 9, 30, 32, 33 and 38).

For sampling point's nº 26 and nº39 located at distances of 18 and 21 km from the stacks, respectively, it was observed an increased average dust fallout flux deposition in the southeastern and eastern sectors. This must be due to a contribution from other sources; in particular, these two sampling points are located in rural areas near to the road. The contribution may come from either agricultural practices or from road traffic.

Another point of discussion concerns the wind velocity; higher values due to the strong winds occurring at NE direction may be responsible for the increasing deposition flux as it observed at sampling point nº 40. Also terrestrial breeze, which occurs in particular at night, may reverse the expected flux deposition pattern as it is observable at sampling point nº 18 located at south of the coal power plant.

Finally, the flux deposition during sampling campaign nº 2 follows a different pattern as wind parameters are also different. The influence of intense rainfall periods during this sampling campaign increased the precipitation in approximately 36.6% comparing with the sampling period of campaign nº 1. This may suggest particles washout by precipitation as the dispersion occurred downwind from the source causing lower deposition fluxes.

CONCLUSIONS

This study provides an analysis of the particulate matter deposition affecting urban, suburban and rural areas in the vicinity of a coal-fired power plant and evaluates de flux deposition patterns associated with local factors such as meteorological conditions and the presence of other sources. Several factors were identified as having possible influence in the dispersion and deposition of the collected particulate matter: wind parameters such as direction, velocity, frequency and strength, rainfall, others emitting sources such as other industrial plants, the contribution from road traffic and agricultural practices and the presence of an open air coal deposit.

The average total quantity of particle fallout in the study area for the considered sampling periods was 22.79 g m^{-2} per year for campaign nº 1; 9.48 g m^{-2} per year for campaign nº 2 and 38.42 g m^{-2} per year for campaign nº 3. The fallout during the first campaign was much higher than for the second one. This was in part due to meteorological local patterns but mostly due to the fact that the power plant was not working between March and April of 2011.

In general, wind direction promotes the particulate matter dispersion in to the Atlantic Ocean. However, for higher wind speeds an inversion of wind direction occurs and the particles are transported in the opposite direction from SW to NE.

An evaluation of particles deposition flux with respect to meteorological conditions showed a directed influence by NE directed emissions.

For all sampling campaigns it is possible to observe two preferential flux deposition areas at SE from the coal power plant which follows first the prevailing wind direction for sampling campaigns nº 1 and nº 3 and one of the directions with higher frequency for sampling campaign nº 2. It is also noticeable the important contribution from the coal deposit located at SE.

The deposition flux at NW may be explained by either the direction inversion due to higher wind speeds already mentioned.

In order to identify the contribution from each one of the existent industrial plants morphological and chemical analysis area needed. Particles submitted to high combustion temperatures are completely rounded and Sines coal-fired power plant is the only local plant which uses coal as fuel. Chemical analysis will allow calculating the enrichment factor which is based on the fact that some elements originating from well-defined sources can be distinguished from other elements derived from different sources (Papaefthymiou, 2008).

ACKNOWLEDGMENTS

This work is being supported by FEDER grants through the COMPETE (Programa Operacional Factores de Competitividade) and by national grants through the FCT (Fundação para a Ciência e Tecnologia) namely via the project FCOMP01-0124-FEDER-009745 (FCT reference: PTDC/ECM/100735/2008).

REFERENCES

Azimi S., A. Ludwig, D. R. Thévenot and J. L. Colin 2003. "Trace metal in total atmospheric deposition in rural and urban areas". *The Science of Total Environment*, 308: 247-256.

Cianci V., D. Coppola and W. Sunk 2007. “Dry Ash Collection at Coal Fired Power Plants and Potential for WTE Facilities”, *Proceedings of the 15th Annual North American Waste to Energy Conference NAWTEC15*: 41(12).

Dinis M. L., A. Fiúza, J. Góis, J. S. de Carvalho and A. C. M. Castro 2011. “Assessment of direct radiological risk and indirect associated toxic risks originated by Coal-Fired Power Plants”. *Radioprotection Journal*, 46, n◦ 6: S137–S143.

EEA 2009. “Spatial assessment of PM_{10} and ozone concentrations in Europe (2005)”. *European Environment Agency, Technical Report 1/2009.*

E-PRTR 2010. European Pollutant Release and Transfer Register. http://prtr.ec.europa.eu/Home.aspx.

Mehra A., M. E. Farago and D. K. Banerjee 1998. “Impact of Fly Ash from Coal-Fired Power Stations in Delhi, with Particular Reference to Metal Contamination”. *Environmental Monitoring and Assessment*, 50: 15-35.

Mejstrik V. and J. Svacha 1988. “The fallout of particles in the vicinity of coal-fired power plants in Checoslovakia”. *The Science of Total Environment*, 72: 43-55.

Papaefthymiou H. 2008. “Elemental deposition in the vicinity of a lignite power plant in Southern Greece”. *Journal of Radiochemical and Nuclear chemistry*, 275, nº 2: 433-439.

WHO 2006. “Health risks of particulate matter from long-range transboundary air pollution”. *World Health Organization, European Centre for Environment and Health.* Copenhagen, Denmark.

XiaoWei L., X. MingHou, Y. Hong, Y. DunXi, Z. ZhongHua and L. DangZhen 2009. “Characteristics and composition of particulate matter from coal-fired power plants”. Sci China Ser E-Tech Sci, Vol. 52, no. 6: 1521-1526.

SPATIAL VARIABILITY OF PARTICULATE MATTER ON A CALIFORNIA UNIVERSITY CAMPUS

Harmonie Hawley* and Diep Vu
(California State University, Fullerton, Fullerton, CA USA)

ABSTRACT: This study measured fine and coarse particulate matter (PM) in a relatively small space on a Southern California college campus over a 3 month period. The fine PM ranged from 2.77 to 27.71 $\mu g/m^3$ and the coarse PM ranged from 9.23 to 102.35 $\mu g/m^3$. Linear correlations and coefficients of divergence (COD) were calculated to assess the spatial variation of fine and coarse PM. The fine PM linear correlations ranged from 0.95 to 0.40 and the COD ranged from 0.05 to 0.26. The coarse PM linear correlations ranged from 0.74 to 0.86 and the COD ranged from 0.10 to 0.17. The statistical analyses showed that the fine PM had a larger spatial variation than the coarse PM on the campus. Additionally it was found that the higher levels of PM and the highest divergence in PM homogeneity were near an on-campus fast food restaurant.

INTRODUCTION

California State University, Fullerton (CSUF) is located in Orange County in Southern California and is part of the South Coast Air Basin. The South Coast Air Basin is currently one of the most polluted areas in the United States in regards to particulate matter (PM) and is in non-attainment status as specified by the National Ambient Air Quality Standards (through the Environmental Protection Agency, EPA) and the more stringent California Air Resources Board (CARB) standards.

Particulate Matter originates from natural and anthropogenic sources and can be characterized as primary or secondary. Primary PM is directly emitted into the atmosphere, whereas secondary PM is formed by reactions in the atmosphere. There are many sources of PM in the atmosphere; automotive emissions and residential heating are examples of anthropogenic sources and sea salt, dust and wildfires are examples of natural emissions. Adverse health effects have been associated with atmospheric PM. PM_{10} can penetrate into the lower respiratory system and $PM_{2.5}$ can enter the lungs (Wilson et al., 2005; Pakbin, 2010).

MATERIALS AND METHODS

Handheld airborne particle counters are easier to use than traditional fine and coarse particulate matter sampling methods. A Lighthouse® Airborne Particle Counter 3016 6-channel with fine and coarse PM mass adaptation was used to monitor ambient concentrations of PM at four locations on the campus to assess the air quality.

Samples were collected from February 2, 2011 to May 4, 2011. The samples were collected for five to ten minutes in 1-minute intervals; the reported values are the average of the 1-minute readings. Four locations on the college campus were chosen for sampling: a high traffic parking lot, the students' common area (high person traffic), outside of a fast food restaurant, and in the athletic fields (low traffic, "background" site).

ISBN 9780976885351

Linear correlations were determined by plotting two sites against each other in Microsoft Excel® and determining the linear regression line and the subsequent coefficient of determination (R^2). A value of 0 for the R^2 indicates no correlation between the paired data and a value of 1 indicates perfect correlation between the paired data. However, caution needs to be taken with R^2 interpretation in environmental settings. High correlation can be seen in data that simply varies at a consistent factor or if the positive and negative deviations from the regression line are similar. Therefore the R^2 may be a better evaluation of temporal variation than spatial variation in ambient samples (Moore et al., 2009).

An additional statistical test was performed on the data to assess spatial variation given the limitations of the coefficient of determination. The coefficient of divergence was calculated by:

$$COD_{jk}=\sqrt{\frac{1}{n}\sum_{i=1}^{n}\frac{\left(x_{ij}-x_{ik}\right)^2}{\left(x_{ij}+x_{ik}\right)^2}}$$

Where x_{ij} is the *i*th concentration measured at site j for a specified sampling period, the two different sites are represented as *j* and *k*, and n is the number of observations. A COD ranges from 0 where the concentrations are identical to 1 where the concentrations are different; a value of 0.20 or greater indicates heterogeneity between two sites (Wilson et al., 2005). All data was compared by date, so if one location was missing a sample it was deleted from the linear correlation and COD analysis, but was included in the plots and in the average concentrations of the locations.

RESULTS

The highest concentrations were found near the fast food restaurant, which is an anthropogenic, primary emission of PM. The lowest concentrations were found at the background site and the students' common area (see Table 1). The four sites followed the same general trend and the PM_{10} and $PM_{2.5}$ followed the same generalized trend. The lower concentrations observed at the four sites were during or after a precipitation event. This is consistent with a study conducted by McCully et al. (1956) that found the greater the rainfall intensity the greater removal of particles from the atmosphere. Additionally, the campus has a lower traffic flow of vehicles and people on Fridays and the weekends, this Friday samples showed lower levels of PM. The restaurant closes early on Fridays and is closed all weekend; thus samples collected on Friday were collected when the restaurant was closed and not in operation which would lower the PM emissions in the area.

The average concentration for the sampling period was compared to the EPA and CARB annual average standards and the maximum concentration was compared to the 24-hour standards in order to assess the air quality. For the restaurant site, the fine PM exceeded both the CARB and EPA annual standards of 12 $\mu g/m^3$and 15 $\mu g/m^3$, respectively. None of the CSUF monitoring sites exceeded the EPA $PM_{2.5}$ 24-hr standard of 35 $\mu g/m^3$. For all CSUF monitoring sites, the PM_{10} currently exceeded the CARB annual standard of 20 $\mu g/m^3$. None of the CSUF monitoring sites exceeded the PM_{10} EPA 24-hr standard of 150 $\mu g/m^3$, but did exceed the PM_{10} CARB 24-hr standard of 50 $\mu g/m^3$.

Figures 1 through 4 illustrate the PM concentrations for each location. The horizontal lines represent the different 24-hour average regulations. The error bars are the standard deviation of the individual one-minute readings taken during each sample collection day. The error bars are usually not visible. There are some readings, however, where the error bars are visible. This indicates a deviation within the sample. The main reason for such deviations is a rapid change in air quality for a short period of time (one minute). A reason for the change could be the wind increasing particulates in the air from the ground. All of these samples were collected near ground-level.

TABLE 1: $PM_{2.5}$ and PM_{10} concentrations (bold values exceed standards)

		Background Site	Parking Lot	Student Commons	Restaurant
$PM_{2.5}$ (µg/m^3)	Average	10.90	11.41	11.27	**15.26**
	Max	21.70	27.71	20.75	25.62
	Min	3.06	2.77	3.31	3.16
PM_{10} (µg/m^3)	Average	**41.20**	**41.11**	**42.76**	**50.01**
	Max	**80.82**	**93.01**	**69.88**	**102.35**
	Min	10.84	9.23	11.55	12.12

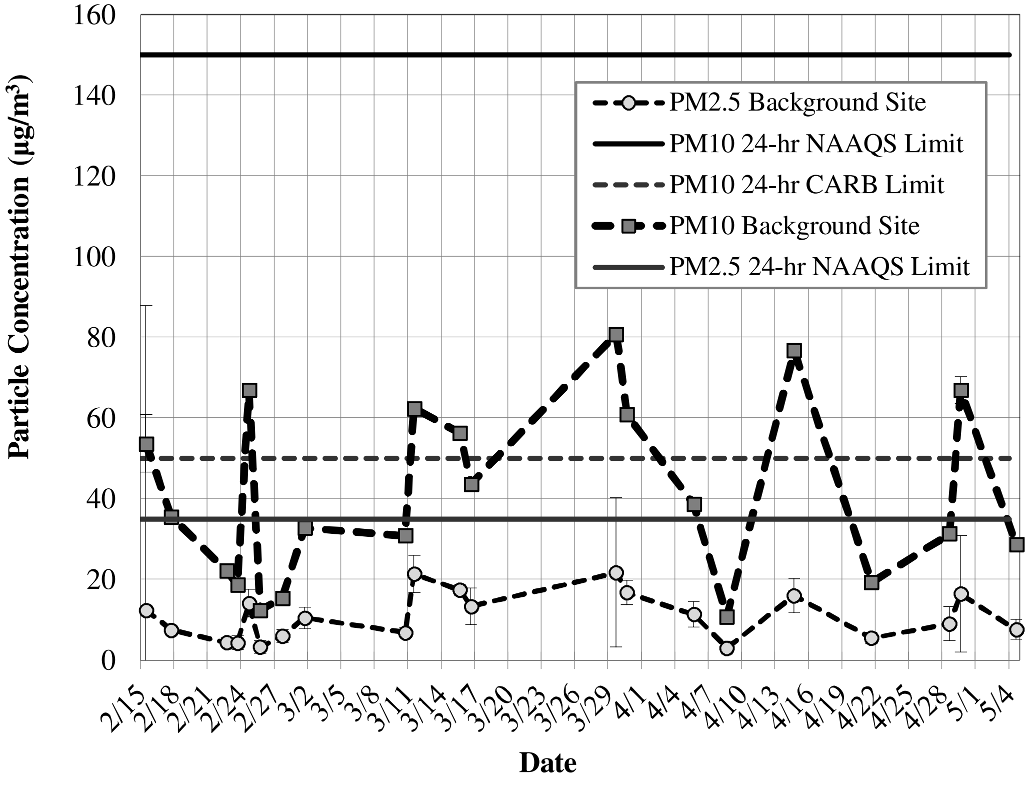

FIGURE 1: PM concentrations at the "Background" site

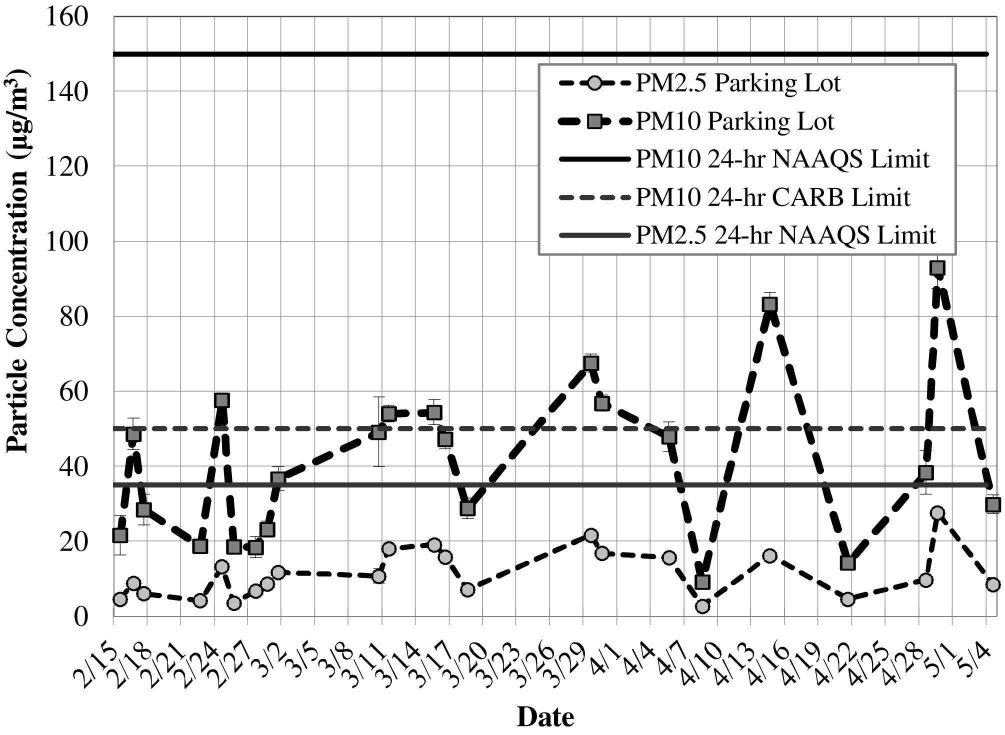

FIGURE 2: PM concentrations at the Parking Lot

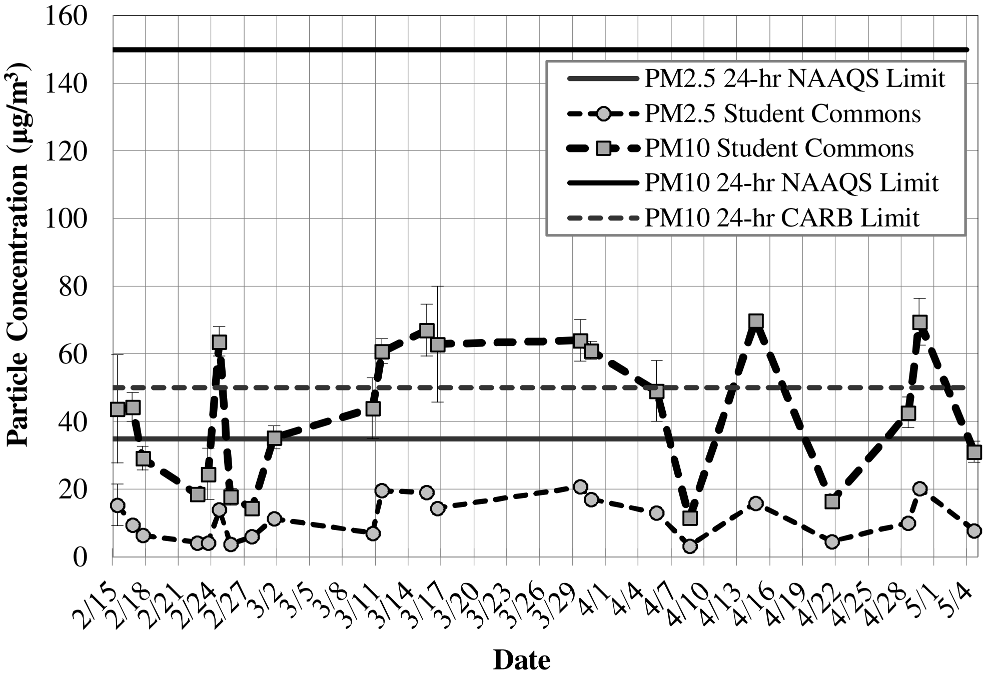

FIGURE 3: PM concentrations at the Student Commons

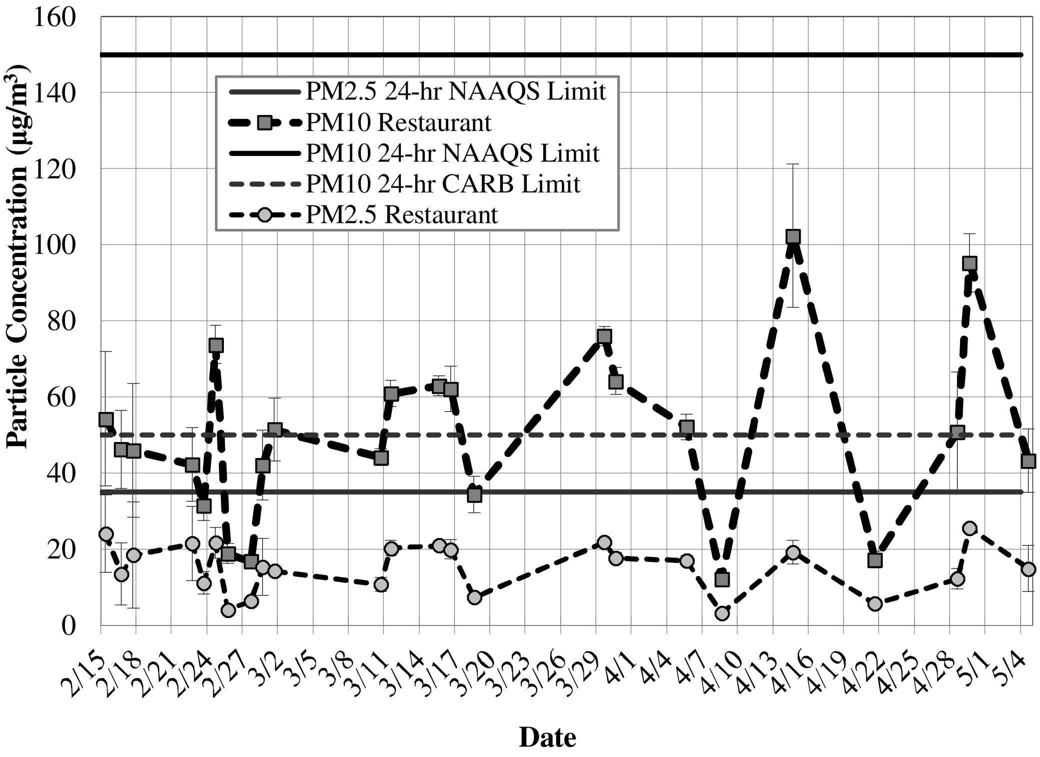

FIGURE 4: PM concentrations at the Restaurant

DISCUSSION

Linear correlations (R^2) between sites for $PM_{2.5}$ ranged from 0.95 to 0.40 and the linear correlation of PM_{10} between the sites ranged from 0.74 to 0.86. These results indicate that the fine PM is more localized than the PM_{10} on the campus, even in such a small space range as the lower correlations were found between sites for fine PM. These results could also indicate a larger temporal variation in the fine PM on campus as the R^2 does not distinguish between temporal and spatial variation. The three lowest correlations of $PM_{2.5}$ were the comparisons of the three other sites to the restaurant location, which also had the highest average concentration of $PM_{2.5}$, indicating that the restaurant is a localized emission source of fine PM.

Coefficient of Divergence (COD) values ranged from 0.05 to 0.26 for $PM_{2.5}$ and followed the same trend as the linear correlations for $PM_{2.5}$. The COD for the restaurant site compared to the background site, parking lot and students' common area were 0.24, 0.26, and 0.23, respectively. The next highest COD for fine PM was 0.14 which was a comparison between the background site and the parking lot, which would be expected to be different as motor vehicles are a known source of fine PM. The COD ranged from 0.10 to 0.17 for the PM_{10}. This indicates that there is more similarity of the PM_{10} concentrations than the $PM_{2.5}$ concentrations between the locations. The CODs and the linear correlations indicate the same results in this data set.

If a COD of 0.2 or less is considered homogeneous, the PM_{10} is homogenous on campus. The $PM_{2.5}$ was homogeneous on the campus except for the location near the on-campus fast-food restaurant. This would indicate that the restaurant is a distinct source of fine PM and that the fine PM is getting "trapped" in the area around the restaurant.

Pinto et al. (2004) studied fine PM concentrations in Los Angeles, Riverside and Orange Counties in Southern California. The COD ranged from 0.14 to 0.26 between the sites in 1999-2000. Krudysz et al. (2008) studied PM samples that ranged in size from 0.25 to 2.5 (slightly different than this study) in the Long Beach, CA area. The approximate average COD for the study sites was 0.15. Pakbin et al. (2010) conducted a study in the Los Angeles, CA area from 2008 to 2009. Particulate matter samples were collected for particles with diameters between 10 and 2.5 μm (different than this study). The average CODs for comparison of urban sites ranged from 0.10 to 0.18. The aforementioned studies are in a similar location (Southern California) to this study conducted on a college campus, although it is important to note that the college campus evaluated was a smaller sized area than the studies to which it was compared. The CODs found in this study are in the same range as the CODs found in the aforementioned PM studies in the Southern California area.

CONCLUSION

In conclusion, a straight evaluation of the data indicated that the area near the fast food restaurant had the highest levels of particulate matter for both coarse and fine PM. The CODs verified the original evaluation that the fast food restaurant area was the least homogeneous in terms of air quality on the campus. However, further analysis showed that the difference in PM_{10} was lower than the difference in $PM_{2.5}$ throughout the campus. The data reveals that cooking operations are a source of fine PM on campus. As restaurants are a point source discharge, the pollutants could be reduced by restaurant modifications.

REFERENCES

Krudysz, Margaret A.; Froines, John R.; Fine, Philip M.; Sioutas, Constantinos. Intra-Community Spatial Variation of Size-Fractionated PM Mass, OC, EC, and Trace Elements in the Long Beach, CA Area. Atmospheric Environment. 2008, 42: 5374-5389.

McCully, C.; Fisher, M.; Langer, G.; Rosinski, J.; Glaess, H.; Werle, D.; Scavenging Action of Rain on Air-Borne Particulate Matter. Industrial & Engineering Chemistry. 1956, 48 (9): 1512-1516.

Moore, Katharine; Krudysz, Margaret; Pakbin, Payam; Hudda, Neelakshi; Sioutas, Constantinos. Intra-Community Variability in Total Particle Number Concentrations in the San Pedro Harbor Area (Los Angeles, California). Aerosol Science and Technology. 2009, 43: 587-603.

Pakbin, Payam; Hudda, Neelakshi; Cheung, Ka Lam; Moore, Katharine F.; Sioutas, Constantinos. Spatial and Temporal Variability of Coarse ($PM_{10-2.5}$) Particulate Matter Concentrations in the Los Angeles Area. Aerosol Science & Technology. 2010, 44:514-525.

Pinto, Joseph P.; Lefohn, Allen S.; Shadwick, Douglas S. Spatial Variability of $PM_{2.5}$ in Urban Areas in the United States. Journal of Air & Waste Management Association. 2004, 54: 440-449.

Wilson, J. Gaines; Kingham, Simon; Pearce, Jamie; Sturman, Andrew P. A Review of Intraurban Variations in Particulate Air Pollution: Implications for Epidemiological Research. Atmospheric Environment. 2005, 39: 6444-6462.

FIRST RESULTS OF AIR MONITORING IN SOUTH EAST EUROPEAN PORT OF BOURGAS

Ekaterina Bachvarova, Hristomir Branzov, Anna Jordanova, Svilen Borisov and ***Jordan Marinski***
(National Institute of Meteorology and Hydrology, Sofia 1784, Bulgaria)

ABSTRACT: First results of field measurements and analysis of the air pollution, in particular PM10 concentrations in Bourgas port, located in South East Europe, along the Black Sea are presented. The Bourgas port is chosen as a pilot site during implementation of Ecoport8 project. The monitoring of air aims: controlling of air quality according the required standards, identifying and determining the sources and scale of emissions, determining the effects of air pollution on the environment, analyzing the processes which occur in the atmosphere. The sampling station for atmospheric air is located in the area of an existing workshop for repair and storage of stock of Bulgarian Ports Infrastructure Company and records the impact of the old and new bulk cargo terminals in northwest direction, in the direction of the central part of the city. The monitoring includes a number of physical-chemical parameters: Particulate matter PM10, sulphur dioxide, Nitrogen oxides, Persistent Organic Pollutants (POPs), Volatile organic compounds (VOC), Asbestos, Heavy metals (Lead, Mercury, Tin, etc.) and Odors. The monitoring system is equipped with specific software for information servicing, collection and accumulation of database in real time.

INTRODUCTION

The impact of ports and ship traffic to the air quality in coastal areas is drawing specific attention during the last decade. A number of studies investigate the ship emissions on the main routes and the complex emissions at big ports in order to quantify their impact (IMO, 2000). Air quality as one of the main environmental priorities of the European port sector becomes with higher significance over time. This trend is caused principally by the traffic intensification, cargoes operations increase and high prices for modernization and introduction of new technologies. Air quality, which largely affects on environmental quality, is among main relevant aspects in the SEE port areas.

The most common sources of air pollution in port are ships, cars, trucks, equipment, of cargo handling. Dust concentration may be caused by open storage and handling of bulk cargoes. Fine particles require little wind to create dust. Dust is also included within this key aspect since it is a set of particles emitted to air and can constitute visual, physical, chemical, or health hazards for employees and the public.

Accordingly, the port authorities need to focus on creating and maintaining air quality monitoring systems. The aims of such systems should be multipurpose – to assess emissions of various no organized sources, to assess air quality on the entire territory of the port, to assess the impact of the port activities on the air quality in the adjacent territories.

THE CITY OF BURGAS – CLIMATE AND INDUSTRY

Burgas is a regional and municipal centre, as well as the fourth largest town in Bulgaria, with a population of 230 000 inhabitants, Figure 1. The largest refinery at the Balkan Peninsula, Lukoil, is situated close to the city. The city is built on a complex coastline in a large and deep bay. Several lakes bring additional complexity to the terrain and meteorological conditions.

ISBN 9780976885351

Figure 1. Bourgas on the map of Bulgaria

The air quality of the city is defined by the emissions due to the operation of the refinery, several power stations and industrial sites, the Port and the traffic, from one site, and by the meteorological conditions from another site, AQR, 2002; Assessment, 2004 and Veleva et al, 2012. Situated at the Black Sea coast, the city is characterized by breeze circulation from March to October. During July, typically, more than 95% of the days are characterized by breeze circulation (or winds from NE, E and SE) as seen in Figure 2.

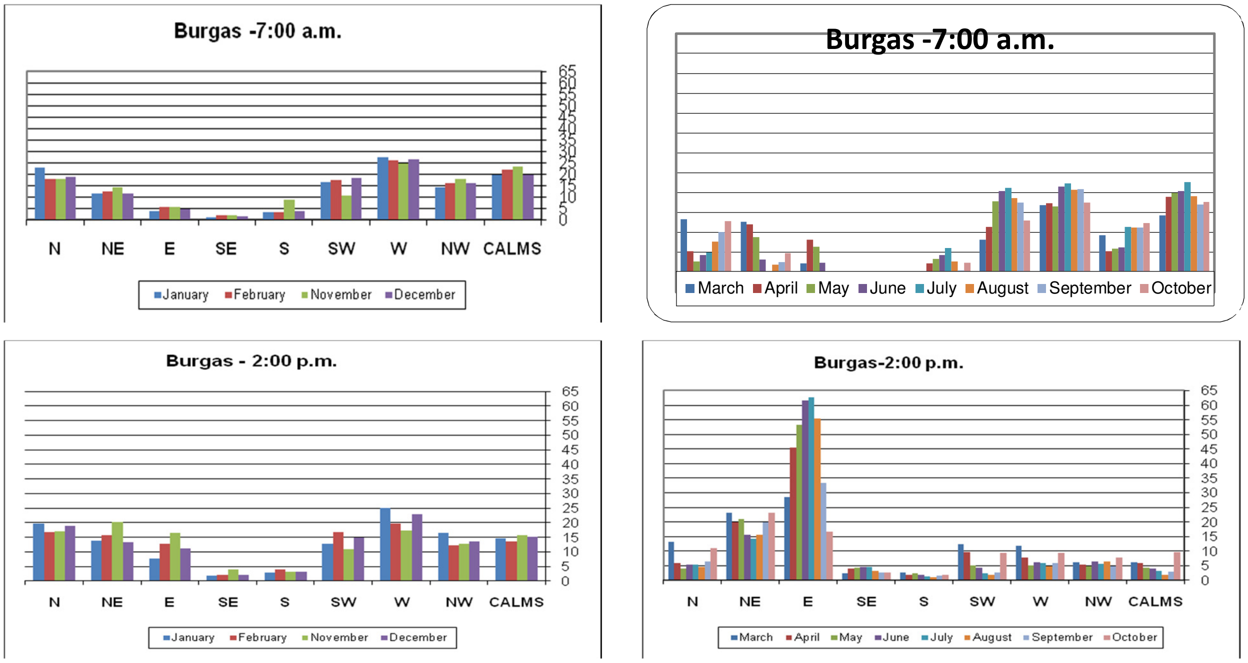

Figure 2. Wind direction frequency (in %) for the period 1931 – 1970 based on monthly averaged values at 7 am and 2 pm for Meteorological Observatory Bourgas. In the left panels the groups of bars for given wind direction correspond in sequence to January,February, November and December. In the right panels the sequence of bars in the groups by wind direction is for March, April; May; June, July, August, September and October.

THE MONITORING NETWORK OF THE PORT

The monitoring programme at the Port, presently includes 3 sampling sites of water quality measurements and one for air quality measurements, Figure 3 (left panel): **Sampling site 1**, with coordinates 42°29'01.1" N; 27°28'44.7"E, is representative for the seawaters from the current activities related to the loading-unloading operations at berths 0-20, including the old bulk cargo terminal. In the area of aquatory 1 there are several inflows from emergency sewerages of Burgas city where rain waters during storm flow into. **Sampling station 2** is for atmospheric air quality. It is located in the area of an existing workshop for repair and storage of stock of Bulgarian Ports Infrastructure Company and shows the impact of the old and new bulk cargo terminals in northwest direction. It can indicate to some extend the impact of the Port on the air quality in the central part of the city. **Sampling station 3** covers the waters of the activities related to loading-unloading operations at berth 20a where liquid cargos (mostly oil products) are mainly handled. This is the berth with one of the most dangerous cargos. In this part of Port of Bourgas aquatory there is a storm water inflow from bulk cargo Terminal 2A. According to the existing project these storm waters should flow through sedimentation tanks and then flow into the aquatory. **Sampling station 4** is assumed to monitor the busiest part of Port of Bourgas at the moment and in the near future. Therefore, the maximum range of controlled parameters will be here.

At **sampling station 2**, a MULTI-COMPONENT OUTDOOR AIR QUALITY MONITOR ETL 3000 of UniTec – Italy is mounted to measure concentrations of NO_2, CO, H_2S, SO_2 and PM10. The data are averaged for 1-hour periods and constantly archived. An indicator for the validity of the data is applied every hour. The error of the NO_2 and CO measurements is below 2% for full scale and within the range 0.1 to 100 mg/m^3 for CO and the range 0.1 to 500 µg/m^3 for NO_2. The error of the H_2S, SO_2 and PM10 measurements is not defined by the manufacturer. The range of measurements is declared to be 0 to 30 µg/m^3 for SO_2, 0 to 15 µg/m^3 for H_2S and 0 to 10 000 µg/m^3 for PM10. It has to be noted that the health norms are fixed in the Bulgarian law and directives of the Ministry of Environment and Waters and Ministry of Health (Directive 12/2010 for SO_2, NO_2 and PM10).

The synoptic station of the National Institute of Meteorology and Hydrology is located on the coast in the park "Morska gradina" and is shown with an arrow in Figure 3 (left panel). The wind rose for the period 2005 – 2010 for the year and for winter and summer is shown in the right panel.

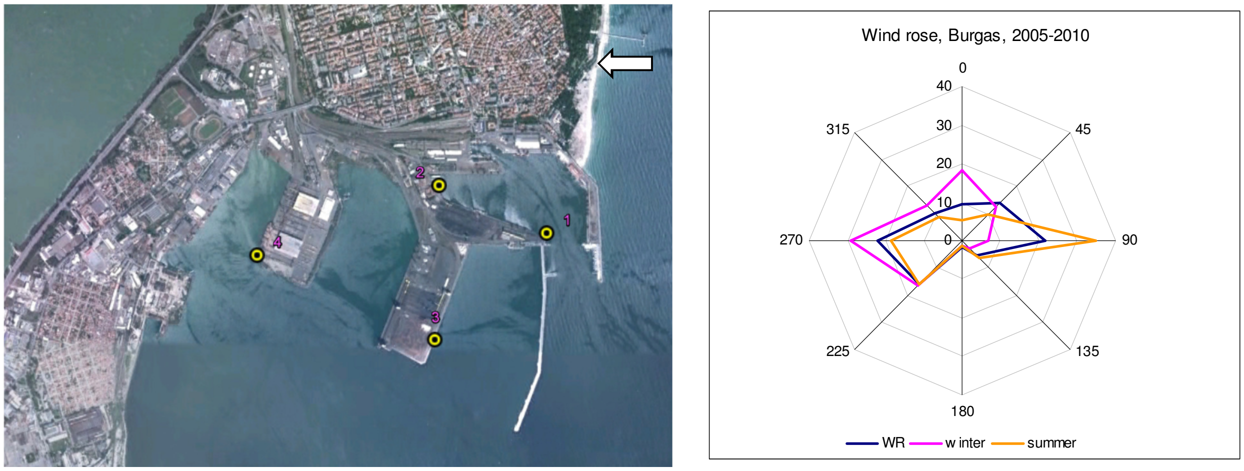

Figure 3. View of Port of Burgas and the monitoring sites (left panel). The arrow shoes the location of the wind measurements of the Meteorological observatory Burgas of NIMH and the wind rose for this site for recent 5 years (right panel).

AIR QUALITY DATA ANALYSIS

The air quality monitoring system in Bourgas is maintained currently by the regional center of the ministry of Environment and waters. Two automatic stations operate in the districts Dolno Ezerovo and

Meden Rudnik, situated close to the refinery. Another station is situated in the center north of the Meteorological observatory where air quality measurements were also performed until July 2011, Batchvarova et al, 2008 and Valkov at al, 2007. The prevailing winds (easterly and westerly) suggest that the Port might have restricted impact on the air quality of the city center, but further monitoring and analysis is needed to identify the flow characteristics of the area. The combination of complex coast line, lakes and breeze circulation creates specific conditions of pollutants dispersion.

The records of the stations in operation of the regional center and from sampling station 2 of the port for the period 10 – 31 March 2011 are presented in Figure 5.

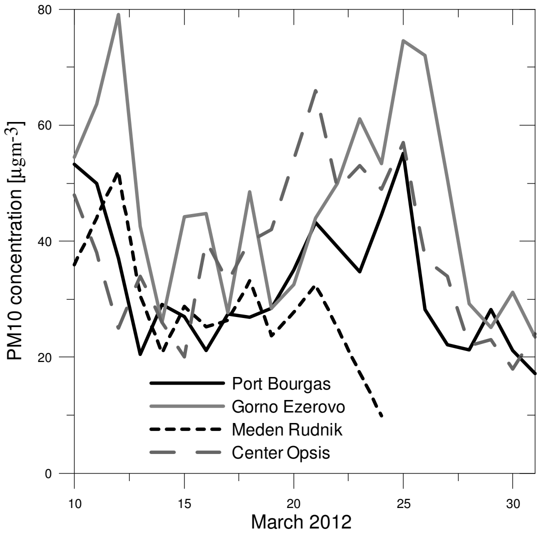

Figure 5. Records of PM10 concentrations in the air at Port Burgas 8sampling station 2) and three monitoring sites of the regional center of the Ministry of Environment and waters.

During this specific period, no bulk cargo activities were maintained and the Port was not large PM10 source. The measured concentrations are close to those published by the regional center of the Ministry of Environment and waters.

CONCLUSIONS

The monitoring station 2 at port Bourgas is operating since March 2012. Therefore only short period of data is analyzed here. The main result concerning PM10 concentrations is that in situations of no bulk cargo emissions, the PM10 concentrations at the port are comparable or even smaller than those in the center of the city or close to industrial areas.

ACKNOLEDGEMENTS

This research was made possible thanks to a research grant provided by South East Europe Transnational Cooperation Program within Environmental Management of Transborder Corridor Ports, ECOPORT 8 project Code SEE/A/218/2.2/X.

REFERENCES

Veleva, B., H. Kirova, E. Batchvarova, and M. Kolarova. 2012, “TSP and NO2 Variation in the Urban Air under Different Meteorological Conditions”. Balwois2012, Ohrid, FYROM, 28 May – 2 June 2012.

Valkov, N., E. Batchvarova, and B. Veleva. 2007. “Bulgarian contribution to the WMO WDCGG”. 14th WMO/IAEA Meeting of Experts on Carbon Dioxide, Other Greenhouse Gases, and Related Tracer Measurement Techniques, September 10-13, Helsinki, Finland, 59.

Batchvarova, E., N. Valkov, B. Veleva. 2008. “Study of long term air pollution and meteorological data in five Bulgarian towns”. Proc. of 17th International Symp. Ecology&Safety 2008, 9-13 June 2008, Sunny Beach Resort, Bulgaria, International Scientific Publications, publ. by INFO INVEST, Bulgaria, (www.science-journals.eu) ISSN:1313-2563, Vol.2, Part 1, 571-577.

AQR. 2004. “Air Quality Report for the Municipality of Burgas for the period 1998 – 2002”. http://file.burgas.bg/ecology/Binder2.pdf

Assessment. 2002. “Assessment of the influence of the auto transport on the air quality in the Municipality of Burgas”. http://air.burgas.bg/uploads/files/Binder1.pdf

IMO. 2000. “INTERNATIONAL MARITIME ORGANIZATION Study of Greenhouse Gas Emissions from Ships”, Issue no. 2, 169 p. http://unfccc.int/files/methods_and_science/emissions_from_intl_transport/ application/pdf/imoghgmain.pdf

MONITORING THE KINETICS OF THE PHOTO-DEGRADATION OF BENZENE WITH HYDROXYL RADICALS

Aubrey A. Heath, Franz S. Ehrenhauser, Kalliat T. Valsaraj
(Louisiana State University, Baton Rouge, LA, USA)

Each day aromatic compounds are released into the environment, both in aquatic environments and in the air. Although aromatic compounds are stable, they will react with hydroxyl radicals, which are abundant oxidative species in the atmosphere. In order to assess the environmental degradation of aromatic compounds in the atmosphere, benzene serves as a model aromatic compound because of its basic representative structure and its oxidative products, phenol and biphenyl, are straightforward to follow. The oxidation pathway of benzene to phenol has been studied extensively, but less consideration has been given to the alternative pathway of benzene to biphenyl.

In this work, the photo-oxidation (UV-B light) of benzene in the presence of hydrogen peroxide as a hydroxyl radical source is first monitored in a bulk phase reactor. Salinity, pH, and temperature are then varied in order to represent typical environmental conditions and to pinpoint their effect on biphenyl formation. This concept is then extended from the bulk aqueous phase to monitor aerosols present in the atmosphere by the use of a thin film reactor. Unlike the bulk phase experiments, the thin film reactor can model these smaller aerosol droplets by varying the film thickness of the aqueous surface. The reactivity of these two regimes is compared.

ISBN 9780976885351

RELATIONSHIP BETWEEN AIR AND WATER TEMPERATURE IN THE EBRO RIVER (SPAIN)

Mª Rosa Pino Otín (1) , Hugo Saiz Bustamante (2) , Jonatan Val Pulido(1), Cecilia Español Latorre(1)
((1)San Jorge University, Zaragoza, Spain; (2) Pyrenean Institute of Ecology (IPE-CSIC), Zaragoza, Spain)

Global warming due to climatic change is one of the most important threats to ecosystems conservation, due to its major influence in biotic and environmental forces that drive ecosystems organization. Several future climate scenarios have been developed in recent years in order to predict the most reliable future conditions. However, predictions focus in air temperature while this may not be the most important parameter shaping biotic communities. For example, stream communities are more influenced by water temperature.

In the present study we analyze the present relationship between air and water temperature in the Gállego River, Ebro River basin (NE Spain), in order to predict the water temperature changes in future climatic scenarios. We employed historic daily data for air and water temperature for the 2006-2011 period in two stations (Villanueva and Jabarrella), and 30 minutes data from field sensors for 2011 year in the same places. The relationship between water and air temperature in both cases was modelled employing two models: a logistic function, and a Markov type model that links air temperature to water temperature residuals (water temperature is represented as a sum of two components: a long-term annual component and the short-term residuals) for daily and weekly data. The goodness of fit for the model was calculated employing the Root Mean Square Errors between the calculated and the real values.

In order to model the water temperature, the best model depends on the time lag that we are interested in. For daily processes the Markov model performs better (RMSE I = 2,16, RMSE II = 1,51 for Villanueva Station, and RMSE I = 2,81, RMSE II = 1,51 for Jabarrella station), while for weekly ones the first model is preferred (RMSE = 1,49 for Villanueva and 1,49 for Jabarrella). Future directions will aim in predicting the variation of water temperature employing simulated climatic data in order to evaluate the most vulnerable sites in the river basin.

ISBN 9780976885351

NERIUM OLEANDER AS BIOMONITOR TOOL FOR MAPPING HEAVY METAL IMMISSION IN CITIES

Ana Martín, Mª Rosa Pino (Universidad San Jorge. Villanueva de Gállego, Zaragoza, Spain)
Mercedes García, Enrique Navarro (Instituto Pirenaico de Ecología-CSIC. Zaragoza, Spain)

Cities suffer severe air pollution due to the release of different pollutants. The knowledge of emission and immission patterns of these is a requirement to assess the associated environmental and human risks. Urban immission assessment relies on the use of automatic quality-air sampling stations. But the limited number of stations prevents us from creating detailed immission maps. It is well known that plants accumulate trace elements from the atmosphere and have been used in several bio-monitoring studies offering a low-cost method for gathering environmental quality data. This study assesses the feasibility of *Nerium oleander* as bio-monitor tool for airborne heavy metal (Pb, Zn, Ni, Cr) immission in Zaragoza (NE Spain). This plant is widely distributed across the city.

Routine acid digestion of leaf tissues and soils and ICP-OES analysis of heavy metals were performed in 118 plants. Metal concentration in soils and plants were mapped, upon geostatistical methods (krigging). Heavy metal related with traffic emissions (Pb) appears in soils and plants from areas with high traffic density. Even if the higher Cr concentrations were detected in soils located in city-periphery districts, plants with higher content of Cr were located in districts exposed to the predominant winds. Ni presents a similar distribution in soils and plants than Cr, although in concentrations 10 times smaller; Zn presented similar patterns. These results indicate two main sources of heavy metals in Zaragoza: a) local emissions (such as those related with traffic) and b) dust transport from upwind regions. The resulting maps are a detailed and reliable tool for environmental and human risk managers.

ISBN 9780976885351

PM2.5 / PM10 CHARACTERS DURING *MEJI* BURNING IN THE BRAHMAPUTRA VALLEY (INDIA)

Pratibha Deka, Raza R. Hoque† and Ratan Boruah (Tezpur University, Tezpur, 784028, Assam, India)

Meji is an annual festive biomass burning event, of large dimension, in the Brahmaputra valley of the Northeast India. We grabbed atmospheric PM10, 12 hourly in a time series for 16 days in January 2009, and monitored PM2.5 and CO at a receptor site in Tezpur. The average mass concentration of PM10 was found to be 148.79±45 µgm-3 with maximum and minimum concentrations of 292.59 µgm-3 and 93.04 µgm-3 respectively during the experiment. PM2.5 and CO did show a high correlation indicating their source being *meji* burning. Elemental analysis of the PM10 samples exhibit high levels of carbon and bromine, besides several heavy metals with convincing levels. A rotated PCA of the data showed that the sources of PM10 during that period could be vehicular, crustal and industrial coal burning beside biomass burning.

ISBN 9780976885351

TOXIC METALS FROM ILLEGAL OPEN BURNING AND SOURCE APPORTIONMENT OF PM2.5

Jin-Hong Lee and Jin-Hee Jeong (Chungnam National University, Daejeon, Korea)
Jong-Myoung Lim (Korea Atomic Energy Research Institute, Daejeon, Korea)
Ki-Hyun Kim (Sejong University, Seoul, Korea)

To establish proper strategies to cost-effectively reduce the inhalation exposure level of PM2.5 in agricultural areas, it is desirable to accurately apportion their sources using long-term measurement data based on receptor model. In this study, we investigated emission inventories of PM2.5 and the associated toxic metals from illegal open burning of waste (e.g., municipal solid waste, agricultural waste vinyl, etc). The elemental concentrations of PM2.5 were determined by instrumental neutron activation analysis (INAA) and inductively coupled plasma-mass spectrometry (ICP-MS). According to the open burning experiments using bench-scale combustion chamber, the emission rate of toxic metals (e.g., As, Cd, Cr, Ni, Pb, and Zn) were 348 ± 205, 2.40 ± 1.21, 302 ± 178, 23.1 ± 10.4, 165 ± 97.2, and 11493 ± 5769 mg kg^{-1}, respectively. Annual average PM2.5 concentrations at an agricultural area in Korea were 22.0 ± 11.0 µg m^{-3} in the range of 4.8 - 53.9 µg m^{-3}. Finally, based on the data matrix including the concentrations of metals, ions, and black carbon, the sources of PM2.5 in the agricultural area were identified to estimate its contributions by positive matrix factorization.

ISBN 9780976885351

DEVELOPMENT AND APPLICATION OF THERMAL DESORPTION METHOD FOR AIRBORNE POLYFLUORINATED ALKYL SUBSTANCES

Yaoxing Wu and Victor W.-C. Chang (Nanyang Technological University, Singapore)

A new, simple, and highly reliable method was developed to analyze the airborne volatile polyfluorinated alkyl substances (PFASs) using thermal desorption (TD) coupled with gas chromatography–mass spectrometry (GC–MS). The targeted PFASs included four fluorinated alcohols (FTOHs), two fluorooctane sulfonamides (FOSAs), and two fluorooctane sulfonamidoethanols (FOSEs). All targeted compounds are considered as the major contributors to the ubiquitous occurrence of the ionic PFASs, which were reported to be persistent in environment and pose potential adverse health effects. Low-volume sampling approach at flow rate of 0.009 m^3/h has been proven successful in this method. The adsorptive enrichment and thermal desorption of PFASs on different sorbent materials including one porous polymer (Tenax TA) as well as two graphitized carbon blacks (Carbograph 2 TD and Carbograph 1 TD) were also investigated to quantify the sample breakthrough and method recovery. Results indicated the combination of Tenax TA (150 mg) and Carbograph 2TD (200 mg) provided the minimal breakthrough and optimal method recoveries. This method exhibited significant improvement compared with the other existing methods, which typically hindered by poor method recoveries for the most volatile FTOHs. The approach has been successfully applied to routine monitoring of airborne PFASs in both indoor and outdoor environments in Singapore. The data also indicated that indoor concentrations of targeted PFASs (2411–16838 pg/m^3) are typically several orders of magnitude higher than that collected outdoor (22–147 pg/m^3), indicated the existence of indoor sources. It also indicated that FTOHs were the most abundant class of compounds of total volatile PFASs observed. Furthermore, the significantly shorter sampling time required in this method makes it possible to observe the concentration variations of indoor airborne PFASs at different period time during a day, which provides further insights toward the source identification and the impacts from building ventilation system.

ISBN 9780976885351

PCDD/F AND PBDE EMISSIONS FROM CO-COMBUSTION OF WOODCHIP AND WASTEWATER SLUDGE

Shun-Shiang Chang and Wen-Jhy Lee (National Cheng Kung University, Tainan, Taiwan)
Lin-Chi Wang and Guo-Pin Chang-Chian (Cheng Shiu University, Kaohsiung, Taiwan)

The co-combustion of both woodchip and industrial wastewater sludge has been recognized as a green alternative fuel in the industrial boilers. However, mass distributions of polychlorinated dibenzo-p-dioxin and dibenzo furans (PCDD/Fs) and polybrominated dibenzo ether (PBDEs) in the burning processes are seldom studied. In this study, the co-combustion of 90% woodchip (w/w) mixed with 10% industrial wastewater sludge (w/w) in an industrial boiler was investigated for the mass distributions of PCDD/Fs (17 congeners) and PBDEs (30 congeners) in the feeding mass (woodchip and sludge, respectively) and in the discharged media (the stack flue gases, the bottom residue, the cyclone ash, and the bag filter ash, respectively). Of the mixed feeding fuel, the total PCDD/F and total PBDE contents were 12.5 and 20,601 ng/kg, respectively. As to the discharged media, the mean emission factors of total PCDD/Fs and total PBDEs were 0.645 and 2.58 ng/kg-fuel in the bottom residue, 0.820 and 8.31 ng/kg-fuel in the cyclone ash, 3.50 and 6.24 ng/kg-fuel in the bag filter ash, and 28.7 and 88.5 ng/kg-fuel in the stack flue gas, respectively. The above results showed that the emission factors in the discharge media of the total PBDEs were all higher than that of the total PCDD/Fs which are related to the PCDD/F and PBDE contents in the feeding fuel (total PCDD/F and PBDE contents were 12.5 and 20,601 ng/kg). For the total PCDD/F and total PBDE mass distributions, they were 1.91% and 2.45% in the bottom residue, 2.44% and 7.86% in the cyclone ash, 10.4% and 5.91% in the bag filter ash, and 85.2% and 83.8% in the stack flue gas, respectively. The mass distribution results showed that the major PCDD/F and PBDE emission routes of the boiler system were from the stack flue gas but the fraction of the total PCDD/Fs was higher than that of the total PBDEs in the bag filter ash. In Taiwan, PCDD/F emissions from stack flue gases and residues/ashes are strictly regulated but those of PBDE emissions did not established yet. The PBDE emissions from thermal processes, such as industrial boilers and incinerators, needs we pay more attention to.

ISBN 9780976885351

PCDD/FS IN THE AMBIENT AIR OF TAIPEI CITY, TAIWAN

Shun-I Shih (Kun Shan University, Tainan, Taiwan)
Shun-Shiang Chang and Wen-Jhy Lee (National Cheng Kung University, Tainan, Taiwan)
Yi-Chieh Lai (Chung Yuan Christian University, Taoyuan, Taiwan)
Lin-Chi Wang and Guo-Ping Chang-Chien (Cheng Shiu University, Kaohsiung, Taiwan)

Seventeen 2,3,7,8-substituted polychlorinated dibenzo-*p*-dioxins and dibenzofurans (PCDD/Fs) in northern Taiwan were investigated during four sampling periods: September-October in 2009 (A), February-March in 2010 (B), September-October in 2010 (C), and February-March in 2011 (D). During period A, the PCDD/F I-TEQ concentrations in atmosphere ranged from 0.00780 to 0.0307 pg I-TEQ/Nm^3 and averaged 0.0161 pg I-TEQ/Nm^3 (RSD = 42%); while during period B, they were between 0.0220 and 0.0575 pg I-TEQ/Nm^3 with an average of 0.0364 pg I-TEQ/Nm^3 (RSD = 28%). As to the period C, they were between 0.00396 and 0.0778 pg I-TEQ/Nm^3 and averaged 0.0138 pg I-TEQ/Nm^3 (RSD = 108%). However, during period D, they were in the range between 0.00322 and 0.0737 pg I-TEQ/Nm^3 and in an average of 0.0215 pg I-TEQ/Nm^3 (RSD = 61%). Regarding the impact of season variation, The above results showed that, the mean PCDD/F I-TEQ concentration of B (D) was higher than that of A (C), which were due that the atmospheric mixing height during February-March (winter-spring) was much lower than that of September-October (summer-autumn). A lower atmospheric mixing height did cause poor pollutants dispersion. The PCDDs/PCDFs mass ratios were 0.91, 0.73, 1.67, and 0.53 during periods A, B, C, and D, respectively. During the periods A, B, and D, the atmospheric PCDD/F masses were contributed by PCDFs which were resulted from the de novo synthesis from combustion sources. While the dominant PCDDs during period C was probably associated with precursor formation. Of the three most dominant PCDD/F congeners, OCDD (29~36%) was predominant congener followed by 1,2,3,4,6,7,8-HpCDF and OCDF during periods A and B; whereas they were predominated by OCDD (23~48%) followed by OCDF and 1,2,3,4,6,7,8-HpCDF during periods C and D. By the principal component analysis (PCA), the atmospheric PCDD/F congener profiles in this study are similar with those of fossil fuelled vehicles. The ambient air PCDD/F I-TEQ concentrations (0.0160~0.0364 pg I-TEQ/Nm^3) from 2009 to 2011 (periods A to D) are close to that in the northern Taiwan (0.024 pg I-TEQ/Nm^3) reported by Taiwan EPA. However, they were smaller than the ambient air regulation of PCDD/Fs and dioxin-like compounds (0.6 pg I-TEQ/Nm^3) in Japan. The atmospheric PCDD/Fs of 2009-2010 (periods A and B) were lower than those of 2010-2011 (periods C and D). This result may attribute to less on-road fossil fuelled vehicles and/or less incinerated wastes in the MSWIs. With the human health reason, a continuous monitoring work is needed in the future.

ISBN 9780976885351

GREENHOUSE GAS EMISSION INVENTORIES IN COMPANY ENVIRONMENTAL REPORTING

Nina Braschel and Alfred Posch (University of Graz, Graz, Austria)

Describing the environmental impact of a company, a product or a production process needs to be just as essential for business success as the drafting of conventional financial reports. Environmental impact may be identified, analyzed and assessed by means of ecological balance sheets (environmental performance evaluations). One particular and well-known type of environmental performance evaluation is the greenhouse gas (GHG) emission inventory. Such inventories are based on assessing the carbon intensities of a company, a product or a production process, i.e. the ´carbon footprint´. Carbon intensities can be assessed in terms of a specific product, a whole company or manufacturing site, or even in terms of a whole economic sector. Unfortunately, several different methods are currently available for developing a GHG emission inventory. This raises numerous difficulties, the main one being that lack of consistency among the assessment methods makes inventory comparability extremely difficult.

There are two main objectives in the current paper. First, to describe the existing calculation methods and tools used in establishing a GHG emission inventory, to compare them with regard to the most common areas of difficulties and to provide an ideal type of procedure for developing a GHG emission inventory. Second, to reveal the difficulties arising when defining system or sectoral boundaries and to demonstrate how sensitive the calculation of GHG emission inventories is to such definitions. An analysis of the waste sector and its three interfaces with collection / transport, incineration / co-combustion and biogas plants is used as an example to clarify the whole issue.

The aim is to provide a description of how best to proceed when calculating a GHG emission inventory and to enumerate in seven steps those specific items which need to be considered exactly. Justifications for the proposed procedure, as well as the related difficulties, are also presented.

ISBN 9780976885351

ANAEROBIC REMOVAL OF CHLOROFORM USING TRICKLING BED GAS BIOFILTERS

Bineyam Mezgebe and George Sorial (University of Cincinnati, Cincinnati, OH, USA)
Ashraf Aly Hassan, PhD and Endalkachew A Sahle-Demessie (NRMRL, U.S. Environmental Protection Agency, Cincinnati, OH, USA)

Disinfection by-products (DBPs) are formed in water due to the interaction of Cl_2 gas, a common disinfectant, with natural organic matter present in the water. DBPs are present in most drinking water supplies that have been subject to chlorination, chloramination or ozonation. Studies have shown that disinfection byproducts (DBP), such as trihalomethanes, are carcinogenic and can cause adverse reproductive or developmental effects in laboratory animals. They are not destroyed by the body and can accumulate in body tissues and may cause cardiac irregularities, loss of a fetus, and low birth. Municipal water systems are required to meet maximum contaminant levels (80 ppb for trihalomethane, 60 ppb for haloacetic acids) as an average at each compliance monitoring location (instead of as a system-wide average as in previous rules).

Removing DBP by physical and chemical methods can be expensive and may generate a secondary pollutant. Although carbon adsorption has been commonly used to remove DBP innovative technologies are being developed. The high volatility of many of the DBP (for example chloroform Henry's law constant 25˚C, is 0.0025 atm.m^3/mol), allows alternative approaches such as use of gas stripping in tandem with biological treatment of the gas. A novel technology is applied to achieve stable removal efficiencies of chloroform as a model disinfection by-product, by utilizing trickling bed biofilters. The trickle bed biofiltration is operated under anaerobic conditions. The dechlorination process is designed to achieve desirable elimination rate and sustained removal of chloroform, with little or no by-product formation.

ISBN 9780976885351

BENEFIT OF ALTERNATE USE OF HYDROPHILIC VOC IN BIOFILTRATION OF HYDROPHBIC VOCs

Abderrahman Zehraoui and George A. Sorial (University of Cincinnati, Cincinnati, OH, USA)

The main research objective of this work is the removal of recalcitrant compounds that are not readily bio-available due to the mass transfer rate limiting between the liquid and gas phases. The emphasis is being place on an initial start-up by alternating the addition and removal of hydrophilic VOC to hydrophobic VOC. For this purpose n-hexane is used in this study as a model hydrophobic compound to represent recalcitrant compounds while methanol was chosen to denote hydrophilic VOC.

In order to increase the bioavailability of n-hexane, a mixture of n-hexane and methanol with the following ratios by volume: 70% methanol & 30% n-hexane, and 80% methanol & 20% n-hexane were investigated at start-up. Four biofilters were run and fed with different nutrient pH buffers. Two biofilters were operated at neutral pH with each receiving a different methanol:n-hexane ratio. The remaining two were operated at acidic pH in order to enhance the growth of fungi with each biofilter receiving a different methanol:n-hexane mixing ratio

The experimental setup was such that at n-hexane loading rate of 13.2 g $m^{-3}h^{-1}$ each TBAB was subjected to removal and addition of methanol for a specific time. When the loading rate of n-hexane was increased beyond 13.2 g $m^{-3}h^{-1}$, it was the sole feed to the TBABs. The methods used to control biomass growth were a combination of stagnation & flow-switching and periodical backwashing depending on the VOCs loading rates.

Experimental results have shown that n-hexane degradation is greatly enhanced by optimizing the alternate use of methanol at n-hexane loading rate of 13.2 g $m^{-3}h^{-1}$. For both mixture ratios of methanol to n-hexane studied, TBABs receiving nutrients buffered at pH 7, n-hexane removal efficiency increased by 53% (from 41% to 88%) and 20% (from 65% to 85%) when methanol was stopped for mixture ratio of 80% : 20% and 70%:30%, respectively. On the other hand, for nutrient buffered at pH4 more significant improvement were noticed which was more pronounced at 80%:20% ratio than at the 70%:30% ratio.

After the alternate use of methanol, the study was continued by feeding n-hexane alone and increasing its loading rate. The results have shown that for nutrient feed at pH 4, n-hexane removal efficiency was over 90% at loading rate up to 31.0 g $m^{-3}h^{-1}$. While for biofilter with nutrient feed at pH 7, the removal efficiency did not exceed 68% for the same loading rates. At a loading rate of 41.5g $m^{-3}h^{-1}$, the removal efficiency of n-hexane was above 83% for biofilters operating at pH 4.

In general, n-hexane removal efficiencies obtained in this study are considerably higher as compared to other published values in treating n-hexane alone, with surfactant or in mixture with benzene either at pH 4 or 7. This implies that optimizing the alternate use of hydrophilic VOCs in TBAB could be a promising means in helping the long term elimination of hydrophobic odors and hence fulfilling the regulatory requirements.

ISBN 9780976885351

SCENARIOS FOR IMPROVING HYDROPHOBIC VOCS ELIMINATION IN TRICKLE-BED-AIR-BIOFILTERS

Abderrahman Zehraoui and George A. Sorial (University of Cincinnati, Cincinnati, OH, USA)
Ashraf Aly Hassan (USEPA, Cincinnati, OH, USA)

Biological treatment represents low-cost and environmental friendly option for air pollution as compared to incineration, catalytic oxidation and adsorption. It has several advantages such as low power consumption, few byproducts and cost effectiveness. However, several challenges face biological treatment processes such as variability of flow rate and composition of contaminants in waste streams. And most importantly, hydrophobic compounds are not readily available for the microorganisms, creating a deficiency for the use of biological treatment in the industry. The main research objective of this study is to introduce biological treatment as an effective technique for non-methane hydrocarbon removal from air under stressed operating conditions. Emphasis is being placed on increasing bioavailability of hydrophobic compounds which are known to be recalcitrant to biological treatment due to the mass transfer rate limiting between the gas and liquid phases.

For this purpose, and in order to increase the bioavailability of n-hexane, different scenarios were considered to overcome the mass transfer rate limiting by either increasing n-hexane solubility or augmenting surface area of the media. The following techniques were tested for enhancing n-hexane biodegradation: introduction of surfactant in the nutrient feed, use in mixture with benzene, change of medium from bacteria to fungi, and finally in mixture with methanol.

The results showed that using the surfactant Tomadol® 25-7 successfully enhanced the biodegradation process of n-hexane in the TBAB by 20% and provided more stable performance by having smaller standard deviation in the removal efficiency as compared to a control TBAB. On the other hand, at the best mixture ratio of benzene to n-hexane, the removal efficiency of n-hexane was negatively affected by the presence of benzene, but the presence of n-hexane did not had any significant impact on the performance of benzene at the concentration levels studied. Feeding the system with an acidic nutrient (pH4) greatly enhanced the biodegradation of n-hexane by around 50% in a fungi medium.

Finally, the presence of methanol greatly enhanced the removal efficiency of n-hexane biodegradation in bacterial consortium (pH7) as compared to degradation of n-hexane alone using bacterial community, in mixture with benzene, or using surfactant. This result was obtained for 70%:30% mixing ratio of methanol to n-hexane. A 3% increase was observed for n-hexane biodegradation using fungi microorganisms as compared to the degradation of n-hexane alone using acidic nutrient buffers. For both cases, methanol elimination capacity was not affected by the presence of n-hexane.

ISBN 9780976885351

SIMULTANEOUS MINERALIZATION OF COAL COMBUSTION FLUE GAS CO_2, SO_2, AND HG WITH FLY ASH

Brandon Reynolds and KJ Reddy (University of Wyoming, Laramie, WY, USA)

Flue gas emissions from coal-fired power plants are a major source for the release of anthropogenic CO_2 into the atmosphere. Concurrently, coal-fired power plants also generate significant quantities of solid residues e.g., fly ash and bottom ash, as by-products. Simultaneous capture and mineralization of flue gas CO_2 at these point sources is invaluable in addressing greenhouse gas problems. A pilot scale accelerated mineral carbonation (AMC) process was developed and installed at JBPP.

The AMC process has been successfully tested at the pilot scale at JBPP. Among the various temperature and pressure conditions, 60°C and ≈16% moisture, respectively, showed the highest mineralization of flue gas CO_2, SO_2, and Hg. The novel AMC process utilizes coal combustion by-products, i.e., flue gas and fly ash particles, to produce environmentally safe and stable carbonate minerals in the fly ash. Overall, the novel AMC process demonstrates, in one step, simultaneous capture and mineralization of significant amounts of coal combustion flue gas CO_2, SO_2, and Hg, without separation, under field conditions. In addition the AMC process is environmentally safe, cost-effective, and energy efficient with minimum carbon footprint.

ISBN 9780976885351

MERCURY ADSORPTION BY A MODIFIED ACTIVATED CARBON

Jinjing Luo and Qiang Niu, Zhongye Wang (Xiamen University, Xiamen, FJ, China)

This study evaluated the mercury capture ability of a novel modified activated carbon (BPL-CX). Mercury adsorption tests were performed under pure nitrogen atmosphere and the presence of flue gas component(s) (CO_2, O_2, SO_2, NO, NO_2, HCl and water vapor). Results show that BPL-CX has a relatively large mercury adsorption capacity under pure N_2 atmosphere. O_2 can strongly increase the mercury adsorption capacity of BPL-CX. On the contrary, SO_2 can significantly inhibit mercury adsorption by BPL-CX. In addition, HCl does not play important roles in determining the mercury adsorption capacity in this study. Adsorption tests under the flue gas mixture revealed that the mercury adsorption capacity for BPL-CX is more than 10 times to that obtained under pure N_2, 1.7 times to that for DARCO FGD and 6.3 times to that for FLUEPAC. Based on this study, BPL-CX is a promising sorbent for capturing elemental mercury in flue gas and an efficient catalyst for mercury oxidation.

ISBN 9780976885351

STRUCTURED PACKING CORROSION EVALUATION IN SOUR GASES TREATMENT AT BRICK KILN PRODUCTION

Rosa-Hilda Chavez and Araceli Salazar (Instituto Nacional de Investigaciones Nucleares, La Marquesa, Ocoyoacac, Mexico, Mexico)
Javier de J. Guadarrama (Instituto Tecnologico de Toluca, Metepec, Mexico, Mexico).

ABSTRACT: The burning of pieces manufactured with clays to be used in the construction industry, contributes to environmental imbalance due to it is used combustible material that produce emissions released to the atmosphere, up to now kilns have been used with combustion processes precarious and fuels highly polluting, which favors climate change emissions for CO_2, NOx and acid rain by SOx, endangering the health of those living near these facilities. The treatment of combustion gases by means of a packed absorption column with a high efficiency liquid-gas contactor reduces pollutant emissions to the atmosphere, when combustion gases are in contact with aqueous amine solution of Mono Ethanol Amine (MEA), using different structured packing material which can be metallic, polymeric or ceramic. The objective of this work is to study which one of three materials presents the lowest deterioration in presence of combustion gases with MEA. The materials were tested according American Society for Testing Materials ASTM G31-2004 corrosion testing, and the procedure NRF-194 PEMEX-2007. The properties studied were tensile strength, hardness and elastic modulus, before and after structured packing materials were in contact with combustion gases in MEA aqueous solution. The results showed that in acid and basic medium, the metallic material was the most resistant to abrasion; it has the major tensile strength, and presented more resistance in the stress test.

INTRODUCTION

The study of gas-liquid contactors (structured packing), which are the elements directly contact with the acid gases with solution of Mono Ethanol Amine (MEA), lead the actions of delivering on environmental legislation regarding emissions into the atmosphere and increase the separation efficiency in the absorption columns (Back, 1972, Chavez *et al.* 2005).

The burning of pieces manufactured with clays to be used in the construction industry, contributes to environmental imbalance due to it is used combustible material that produce emissions released to the atmosphere, up to now kilns have been used with combustion processes precarious and fuels highly polluting, which favors climate change emissions for CO_2, NOx and acid rain by SOx, endangering the health of those living near these facilities (Chavez, 2008). The treatment of combustion gases by means of a packed absorption column with a high efficiency liquid-gas contactor reduces pollutant emissions to the atmosphere, when combustion gases are in contact with aqueous amine solution, using different structured packing material which can be metallic, polymeric or ceramic.

Some factors that decrease the lifespan of the materials and devices are radiation, thermal shock, pressure, velocity and turbulence of fluids, the presence of solid particles and action of air moisture. Substantial corrosion problems are presented in gas-liquid contactors such as wear, clogging and detachment of material, causing deterioration in the acid gases separation processes, due to loss of absorption efficiency (Kladkaew et al. 2009; Veawab et al., 1997; Wagner and Traud, 1938).

ISBN 9780976885351

Corrosion problems are generated in the materials, largely due to the presence of sour gases such as CO_2, SO_2, and other substances such as MEA, which in contact with water, become aggressive media that promote destructive oxidation of metallic alloys and the deterioration of non-metallic materials, into they are in contact (Mendoza et al., 2002). Table 1 presents the parameters of acceptance for materials tested in corrosive media PEMEX NRF-194-2007.

METHODOLOGY

In order to assess the interaction of the gas-liquid contactors in separating acid gases, there were considered two aspects: i) shelf life for corrosion problems and ii) physical-chemical properties of the materials contactors, to determine their abrasion resistance and mechanical strength.

Shelf life for corrosion by ASTM G5-1999 and ASTM G31-2004. For the study of materials contactors the *Tafel* extrapolation electrochemical technique was used, using two electrochemical corrosion cells, which were composed of a working electrode (sample), an electrode of graphite, a saturated electrode of *Calomel*, and one electrolyte aqueous solutions of an aqueous solution of MEA (monoethanolamine) at 30% in weight, and electronic measurement was made. The sample was prepared so as to expose an area of 1 cm^2, as a reference electrode was used as saturated *Calomel* electrode and a counter electrode or auxiliary graphite electrode holder used a reference electrode, partly immersed in electrolyte solution, to minimize ohmic resistance (Wagner and Traud, 1938; Mendoza et al., 2002).

If the concentration of the reactants and products is uniform in the middle, the Butler-Volmer equation for the current density j is:

$$j = j_0 exp\left(\frac{\eta_a}{\beta_a}\right) - j_0 exp\left(\frac{\eta_a}{\beta_c}\right)$$

Where β_a y β_c, are the coefficients of anodic and cathodic *Tafel*, respectively. The equations are applied to the electrode reactions in which the speed is controlled by the charge transfer process at the electrode/electrolyte. This situation is often known as activation on corresponding potential as activation overpotential, η_A. The value of the coefficients *Tafel*, β_a y β_c, depend on the mechanism of the reactions taking place at the electrodes, which often include several stages. By means of Butler-Volmer equation, it is described the whole kinetics of charge transfer process, regardless of the mechanism, based on three easily measured variables: j_0, β_a y β_c (Mendoza et al., 2002).

Table 1. Accepted parameters for the materials tested in corrosive media NRF-194 PEMEX-2007

Materials tested in corrosive media	mpy	mmpy
Exceptional	Less than 1	Less then 0.02
Excellent	1-5	0.02-1
Good	5-20	0.1-0.5
Acceptable	20-50	0.5-1.0
Poor	50-200	1.0-5.0
Unacceptable	Greater than 200	Greater than 5

Physical-chemical properties of the materials contactors by ASTM E8-1998 and ASTM E384-1990. Mechanical properties: Hardness, tension and elastic modulus of three materials were evaluated as follows:

Hardness. The property of hardness of the materials was determined before and after contact with the MEA solution at 30% by weight, in the presence of CO_2. Samples of the materials metallic, polymeric and ceramic were assembled on the resin of polymethylmethacrylate (PMMA) in a press *Buehler* to 150°C and pressure of 28 MPa, in order to manipulate the samples during the polishing process with sandpaper 240 grit, 320, 400, 600, on up fine finish. Later they were given a polished mirror finish with *Buehler* microcloth cloth and aqueous alumina (Al_2O_3) of 0.1 microns. *Knoop* hardness (HK) was measured on a *Shimadzu* microhardness of the mark, using a diamond indenter diamond pyramid shape with angles of 172° and 130°, in accordance with ASTM E 384-90, at ambient temperature of 23°C.

Tensile strength and modulus of elasticity measurements. Measuring the tensile strength and modulus of elasticity were performed with a Universal Testing machine *Monsanto* trademark and according to ASTM E 8-98. This assay was performed on specimens of 2 inches (0.05 m) long for each of the three materials, before being in contact with the aqueous solution of MEA at 30 wt% and after contact with the same solution with speed test of 5 mm/min, capacity from 0 to 10 000 MPa and ambient temperature of 25°C.

Morphology. The morphology of the materials was analyzed before and after being in contact with the aqueous solution of MEA with a Scanning Electron Microscopy (SEM) *JEOLJSM5900LV* brand, using secondary electrons to the metal material and backscattered electrons in the polymer and ceramic voltage 20kV (see Figures 1, 2, 3, 4, 5, 6, 7, 8, 9, 10, 11, 12).

RESULTS

Table 2 shows the metallic material presented a rate of corrosion of 0.0642 mpy, 2.3 times more resistant than the polymeric material the polymer of 0.148 mpy, the second in resistant and the ceramic 0.56, 3.78 times less resistant than the polymeric material.

Table 2. Corrosion rate of materials contactors at MEA solution at 30% in weight, mmpy (mm per year) and mpy (miles per year)

Contactor material	Corrosion rate in aqueous solution of MEA at 30% weight	
	mm/y	**mpy**
Metallic	1.63068×10^{-3}	6.42×10^{-2}
Polymeric	3.7592×10^{-3}	1.48×10^{-1}
Ceramic	1.4224×10^{-2}	$5.6 \times ^{10-1}$

In Table 3, ceramic material decreased by 2.86% as compared with the value before contact with the MEA. The hardness of the polymeric material decreased by 5%, while in the metallic material rose 2.6%. These results indicate that the metallic material resists most efforts to friction and pressure that are exhibited in the absorption column. Table 3 shows the analysis results of tensile strength. This parameter provides information on the tensile strength, rigidity and ductility of the materials. The metallic material showed the highest zone of plastic deformation, which means the more able to withstand higher pressures within the absorption column. The polymeric material was the most ductile causing not breaking easily. The ceramic one is the most fragile and prone to break easily due to the efforts within the absorption column.

Table 3. Results of change in the mechanical properties of structured packing before and after contact with the aqueous solution of MEA at 30% weight

Mechanical properties	Metallic	Polymeric	Ceramic
Knoop hardness (HK) before contact with MEA	190 HK	20 HK	700 HK
Knoop hardness (HK) after contact with MEA	195 HK	19 HK	680 HK
Change of hardness (%) after contact with MEA	+ 2.63 %	-5.0%	-2.86%
Tensile strength (MPa) before contact with MEA	841 MPa	35 MPa	90 MPa
Tensile strength (MPa) after contact with MEA	797 MPa	33 MPa	65 MPa
Change of tensile strength (%) after contact with MEA	- 0.36 %	- 5.71%	- 27.8 %

Elemental composition of the structured packing before and after contact with the aqueous solution of MEA at 30% by weight is shown at Table 4. It is observed that after contact with the MEA solution at 30%, the metallic material introduced the presence of oxygen, corresponding to an oxidation process that results in a surface layer of chromium oxide and nickel, which serves to protect the material to reduce the corrosion process.

Table 4. Elemental composition of the structured packing before and after contact with the aqueous solution of MEA at 30% by weight

Elemental composición	Metallic (%)		Polymeric (%)		Ceramic (%)	
	Before	After	Before	After	Before	After
Aluminum					16.62	11.83
Manganese	0.72	1.00				
Sulfur	0.015	0.31				
Carbon	0.07	0.19	87.34	96.15		4.5
Phosphorus	0.01	0				
Silicon	0.01	0.05			22.92	24.53
Chromium	18	14.3				
Nickel	13	8.0				
Potassium					1.69	2.26
Iron	66.775	71.01				0.65
Molybdenum	1.4	0.68				
Oxygen		4.46			58.76	55.1
Sodium						0.59
Magnesium						0.45

The morphology of the three materials before and after contact with the MEA solution at 30% by weight and in the presence of acid gases are shown in Figures 1, 2, 3, 4, 5, 6, 7, 8, 9, 10, 11, 12. The ceramic material after contact with the MEA solution and acid gas has a morphology less rough surface, while the polymeric material does not change substantially and the metallic material introduced a greater surface roughness favoring the formation of liquid film to carry after the absorption process between the liquid and gas, helping to improve the mass transfer in the capture of carbon dioxide, is also dark areas of Cr_2O_3 and NiO, which provide protection against an acid medium.

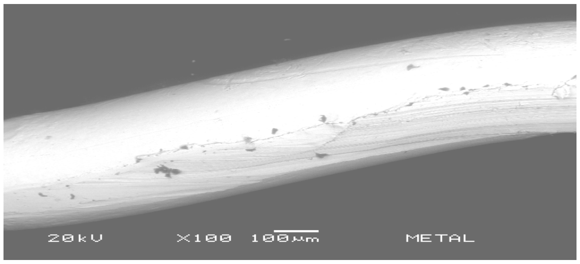

Figure 1. SEM of the surface of the metallic material at 100X, before contact with MEA.

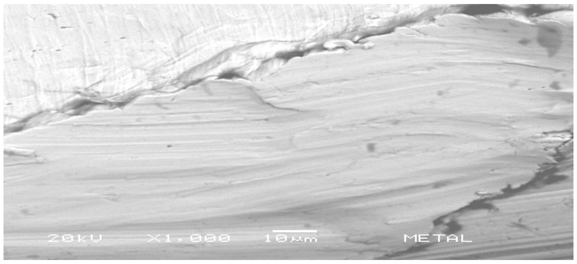

Figure 2. SEM of the surface of the metallic material at 1000X, before contact with MEA, with rough spots.

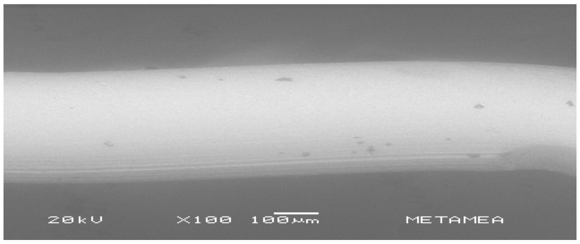

Figure 3. SEM of the surface of the metallic material at 100X, after contact with MEA.

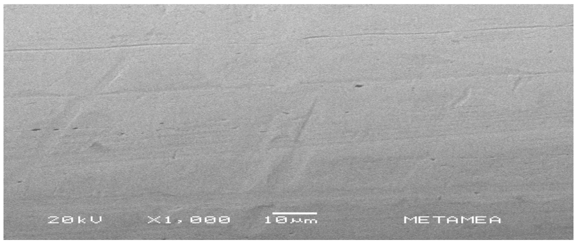

Figure 4. SEM of the surface of the metallic material at 1000X, after contact with MEA.

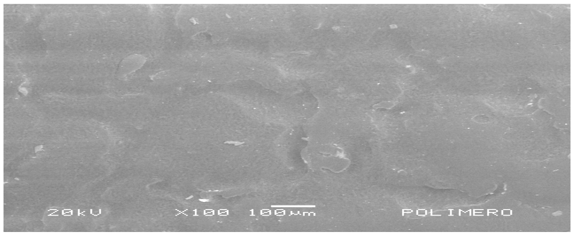

Figure 5. SEM of the surface of the polymeric material at 100X, before contact with MEA.

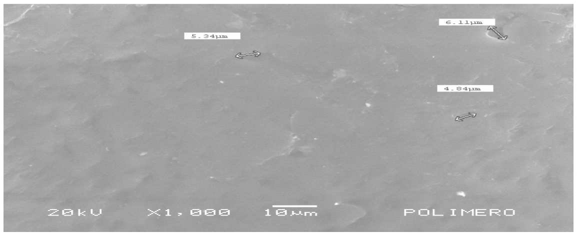

Figure 6. SEM of the surface of the polymeric material at 1000X, before contact with MEA.

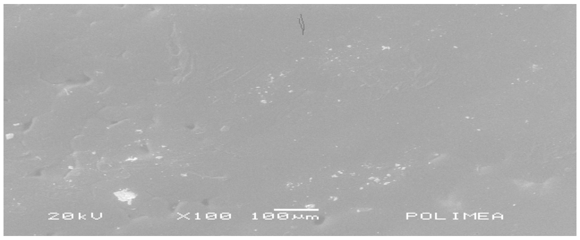

Figure 7. SEM of the surface of the polymeric material at 100X, after contact with MEA.

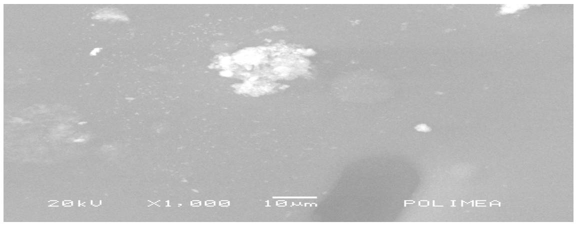

Figure 8. SEM of the surface of the polymeric material at 1000X, after contact with MEA.

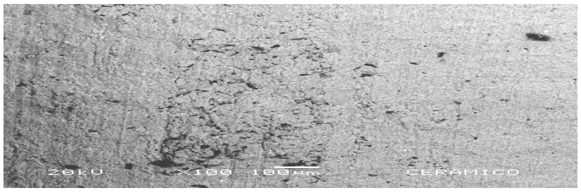

Figure 9. SEM of the surface of the ceramic material at 100X, before contact with MEA.

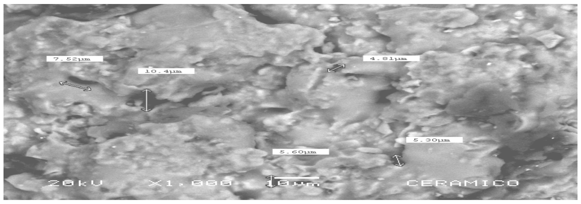

Figure10. SEM of the surface of the ceramic material at 1000X, before contact with MEA.

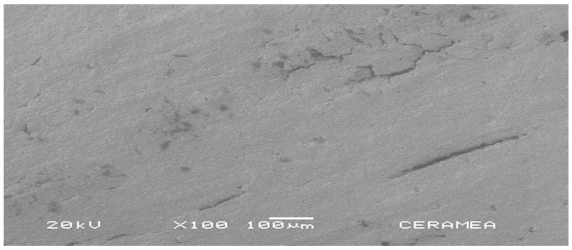

Figure 11. SEM of the surface of the ceramic material at 100X, after contact with MEA.

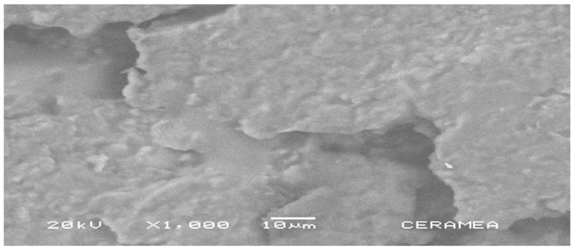

Figura 12. SEM of the surface of the ceramic material at 1000X, after contact with MEA.

CONCLUSIONS

The ceramic was the most susceptible to be attacked when the concentration of MEA rose above the reference value and because of its fragility and porosity was found to be less suitable for use in the treatment of acid gas with MEA, in absorption processes.

The polymeric material showed higher resistance to attack in presence of MEA aqueous solution, which makes it suitable for treatment of acid gases.

The metallic material was identified as the best suited for the treatment of CO_2, due to their mechanical properties which can withstand higher loads before failing and able to withstand higher pressures within the absorption column. After contact with the aqueous solution of MEA, layers of Cr_2O_3 and NiO were formed on its surface due to react with a passive anode, and became resistant to corrosion.

ACKNOWLEDGMENTS

For partial funding to carry out this work to the National Council for Science and Technology (CONACyT), Projects: EDOMEX-2009-C02-135728 and SEP-CONACyT-CB-2007-01-82987.

REFERENCES

ASTM E8-1998. American Society for Testing Materials, Standard Test Methods of Tension Testing of Metallic Materials.

ASTM E384-1990. American Society for Testing Materials, Standard Test Method for Microhardness of Materials.

ASTM G5-1999. American Society for Testing Materials, Test Method for Measurement of Anodic polarization and potentialdynamic and Potentialstatic.

ASTM G31-2004 American Society for Testing Materials, Corrosion testing.

Mendoza J., Duran R. and Garcia E., Corrosion 2002, Paper Num. 02491, Houston, 2002.

Bach, W., 1972, Atmospheric pollution, Mc Graw-Hill Book Company, New York, USA, 3rd. edition.

Chavez Rosa Hilda, Guadarrama Javier de J., and Segovia Nuria, 2005, “A Removal of sulfur dioxide from exhaust gases using hazardous and structured packing”, International Journal of Environmental and Pollution 23:1, 81-91.

Chavez, (2008). Pollution reduction and energy savings of a coupled two kilns system for bricks system for bricks system for bricks making, Journal of Environmental Progress, Online ISSN: 1547-5921, Print ISSN: 0278-4491.

Kladkaew, N., Idem, R., Tontiwachwuthkul, P., Saiwan, C. (2009). Corrosion Behavior of Carbon Steel in the Monoethanolamine-H_2O-CO_2-O_2-SO_2 System *Ind. Eng.Chem. Res*, 48. 19, 8913.

Veawab A., Tontiwachwuthikul P. and Sanjiwan D.B. (1997). Studies of Corrosion and Corrosion Control in a CO_2-2-Amino-2-methyl 1-1-propanol (AMP), *Environment, Ind. Eng. Chem. Res.* 36, 254-269. Wagner C. and Traud W., Z. Elektrochem, (1938), 44(391).

THREE INTERACTIVE TEXAS STATE REGULATORY PROGRAMS TO DECREASE AMBIENT AIR TOXIC LEVELS

Susana Hildebrand, Tara Capobianco, Michael Honeycutt, Jong-Song Lee, Darrell McCant, and Roberta L. Grant (Texas Commission on Environmental Quality, Austin, TX, USA)

The United States Environmental Protection Agency (USEPA) under the authority of the Clean Air Act (CAA) regulates air pollution and air quality by numerous methods: National Ambient Air Quality Standards for Criteria Pollutants, Maximum Available Control Technology (MACT) standards for specific industries that emit Hazardous Air Pollutants (HAP), etc. The framework for the CAA envisions a federal-state partnership whereby the development of regulations to satisfy the CAA requirements may be strictly at the federal level or at the state level with federal oversight. The CAA framework leaves the states responsible for ensuring that actual measured concentrations of pollutants are not occurring at levels that may be harmful to health. Texas Commission on Environmental Quality (TCEQ), the Texas state environmental agency, employs three interactive programs to ensure concentrations of air toxics do not exceed levels of potential health concern: comprehensive air permit reviews, use of extensive air monitoring systems, and establishment of Air Pollutant Watch List (APWL) areas for locations in the state where air toxics are monitored at a level of a potential health concern. Air permit reviews occur when a change at an existing site (or a newly proposed site) may increase emissions. Two key features of the state's air permitting program are the requirement for Best Available Control Technology (BACT) to be applied and that the permit ensures the protection of public health and welfare. The protection of public health and welfare provision may be demonstrated by a number of means including demonstration that the predicted ambient concentrations for the permitted emissions, evaluated on a case-by-case and chemical-by-chemical basis, do not cause or contribute to a level of concern. Ambient air monitoring provides data to help assess the potential for adverse health effects from all operational emission equipment near a monitor. If air toxics are persistently monitored at a level of potential health concern, an APWL area is established. The purpose of the APWL is to reduce ambient air toxic concentrations below levels of concern by focusing TCEQ resources and heightening awareness for interested parties in areas of concern. This paper will discuss examples of decreases in air toxic levels in Houston, Texas, as a result of the interactive nature of these programs.

ISBN 9780976885351

MODELING EVAPORATIVE VOC EMISSIONS FROM PASSENGER CARS

Heidi Davidson and ***Michael Tschantz*** (MeadWestvaco Corporation, North Charleston, SC, USA)

Evaporative VOC emissions are generated anytime a passenger car is refueled or heated by diurnal temperature changes and are precursors in the production of ground-level ozone and secondary organic aerosol formation. The US EPA and California Air Resources Board have progressively implemented stringent passenger car regulations to effectively manage these emissions to near-zero levels. European regulators, as well as those regulators in nations following European norms, have not applied the same level of focus on controlling these emissions. It is hypothesized that European source models significantly under-represent the magnitude of diurnal emissions and that the effectiveness of Stage II refueling vapor recovery controls at petrol stations is over-estimated. Improved models that better estimate baseline evaporative VOC generation from passenger cars and accurately predict the effectiveness of existing and available refueling controls will quickly lead regulators to focus on reducing these remaining VOC emissions using cost-effective measures demonstrated in the United States.

The objective of this empirical modeling work is to accurately estimate monthly evaporative VOC emissions for a nation's existing and future vehicle fleet. The model allows input of a range of potential vehicle-based refueling and diurnal evaporative controls, vehicle fleet makeup, anticipated new-vehicle sales, monthly gasoline volatility expectations, monthly diurnal temperature statistics, existing and future petrol station Stage II vapor recovery controls, and representative parking and driving activity. The model estimates diurnal parking emissions based on representative vehicle activity and an empirical emissions relationship that was developed from a matrix of canister capacities, fuel tank volumes, and fuel volatilities.

The model was applied to describe evaporative emissions from the South Korean existing and future vehicle fleet. South Korea has been following the European evaporative requirements but recently announced it will implement a 48-hour portion of the U.S. Tier I evaporative requirements beginning in 2013. Korea has already implemented Stage II refueling vapor recovery controls. The results of the modeling analysis suggest that while the new standards will reduce VOC emissions by 15,000 mt/year, evaporative VOC emissions will continue to be two to three times higher than exhaust VOC emissions through 2025. Adding Onboard Refueling Vapor Recovery regulations by 2015 could reduce annual evaporative VOC emissions by 30,000 mt/year in 2025, and adding California's LEV III diurnal regulations could reduce VOC emissions by an additional 8,000 mt/year.

Current evaporative emissions models used by regulators and policy-makers outside the United States calculate diurnal emissions for parking events lasting no longer than twelve hours, which under-estimates evaporative emissions. The model constructed in this research suggests that including parking events with durations between 24 and 120 hours triples prior evaporative emissions estimates. The model also offers an improvement by including refueling emissions both with and without Stage II. The model can serve as a tool to evaluate the effectiveness and cost-benefit of regulatory options. The paper will discuss global VOC emissions control, shortcomings of existing predictive models, and present the general empirical emissions model and results of the South Korean case study.

ISBN 9780976885351

ECOSYSTEM ASSESSMENT
AND
RESTORATION

A GAP ANALYSIS OF THE EFFECTIVENESS OF THE ENVIRONMENTAL SMALL BUSINESS OMBUDSMAN AND SMALL BUSINESS ENVIRONMENTAL ASSISTANCE PROGRAM OFFICES (SBEAP)

Terry L. Polen
(West Virginia Department of Environmental Protection, Charleston, WV 25304, USA)

ABSTRACT: Small Businesses are a vital part of the economy of the United States. Governmental Small Business Environmental Assistance Programs have been tasked with helping these clients through the complexity of environmental regulations. The federally unfunded mandate that created these programs has placed them in a situation where the increased needs of the small businesses intersect with the governmental limitations of available funding and resources. In a time of limited budgets and economic uncertainty, the state assistance programs need to realize that they cannot be all things to all people (or businesses). The focus should be on the needs of the small businesses with an emphasis on the necessity to examine the processes within their operations. According to the research (based in a Delphi Analysis), the prioritization of service needs that should be supplied to the clients (the small businesses) are: Permit & Technical Assistance, Hotlines, Comprehensive Site Visits, Programmatic specific workshops and training, Websites, and Involvement with trade and sector associations. In regards to the content prioritization, the governmental entities need to focus on: Hazardous Air Pollutants, Air, Pollution Prevention, Solid Waste, Stormwater, Industrial Wastewater, and Hazardous Waste to best assist those small businesses. In this way, the Small Business Environmental Assistance Programs can fulfill their mandate in the most effective manner to meet the needs of their small business clientele throughout the nation.

INTRODUCTION

The 1990 federal Clean Air Act required that individual states establish programs to assist small businesses with the myriad of regulatory requirements to which they must comply. To comply with this Act, the states created the governmental offices of the Small Businesses Environmental Assistance Programs (SBEAP) (Public Health and Welfare & Air Pollution Prevention and Control, 2004; U.S. Government Printing Office, 2004). The SBEAPs, along with the non-mandated Small Business Compliance Advisory Panels (SB CAP) were created to fulfill the Clean Air Act requirement. The programs worked with new and existing small businesses providing environmental assistance to small businesses and have been critical to their profitability as well as their operations (SBA Office of Advocacy, 2008). Small businesses pay roughly 5 times more, per employee, to comply with environmental regulations than do their larger brethren. Since the burden on these businesses is so (comparatively) high, an important opportunity was available to not only assess the gap between what the programs can and do offer (including the needs); but also to bring forth a procedure which will assist governmental Small Business Environmental Assistance Programs in re-prioritizing their focus towards the needs of this critical segment of the business sector.

Purpose. The purposes of this study were to: 1) identify the gap between environmental content and services offered by the Small Business Environmental Assistance Programs and those that were needed by the Small Business community; 2) to suggest strategies that the governmental programs that could use to prioritize their services and environmental content.

Problem Statement. The SBEAPs did not appear to meet the compliance needs of the small business community; therefore, there seemed to be a gap between the offering by the government and the needs of the SBs. Many of the governmental Small Business Environmental Assistance Programs were

ISBN 9780976885351

air-only and were statutorily unable to provide assistance to small businesses with other environmental contents such as hazardous waste or stormwater requirements (which are defined within this study as 'content'). It also appeared that the way that the SBEAPs presented this information was different than the way the SBs needed the information supplied to them (which are defined within this study as 'services').

Many Small Business Environmental Assistance Programs were:

-Small;
-Had additional duties assigned (including enforcement);
-Were housed outside of environmental programs;
-Were required to assist with the substantial new environmental requirements for small businesses.

Thus, one would presume there was a gap between current services from the SBEAPs and the needs of the SBs.

METHODS

Study Variables. For the purposes of this study, the Small Business Environmental Assistance Programs were broken into individual topical components of environmental contents and services. Program responsibilities such as air quality, used oil, hazardous waste, storm water, pollution prevention, sustainability, and others were defined as environmental content items within this study. Services within this study included subjects such as: hotlines, permit & technical assistance, publications, and comprehensive site visits. The state governmental Small Business Environmental Assistance Programs (SBEAP) helped small businesses (SB) with the various environmental contents (air quality, hazardous waste, storm water, etc.) by the services (permit and technical assistance, etc.) that were offered to those businesses. Therefore, any individual service (e.g. site visits), could have provided assistance to the SB with any, or all, of the environmental contents. For example, from a single visit by the state Small Business Environmental Assistance Program (SBEAP) to a small business, the SBEAP program might need to help the business with any (or all) of the environmental contents such as air quality, water, and hazardous waste.

Description of the Experts. The Delphi process used experts in the field for this study. The population of experts that were sampled consisted of state government program managers within the Small Business Environmental Assistance Programs, as well as small business owners across the nation. Specifically, the expert group included current and former members of both the National Steering Committee* (the steering committee consisted of elected representatives from the state SBEAP programs) and the small business owners that comprise the Small Business Compliance Advisory Panels (SB CAP)** . Each state (50) and territory (three) were required by section 507 of the 1990 Clean Air Act to have the governmental Small Business Environmental Assistance Programs, as well as the SB CAP according to (Public Health and Welfare & Air Pollution Prevention and Control, 2004; U.S. Government Printing Office, 2004). The Small Business Environmental Assistance governmental representatives on the National Steering Committee and the small business owners on the SB CAP were selected from states or territories within the 10 individual USEPA regions to represent the states within their region to the nation. Because of their selection, it was important for these individuals to be aware of the various environmental needs of small businesses, as well as the full operation of the governmental Small Business

---

*The National Steering Committee was not required by law, but was an association of the existing state and territorial Small Business Environmental Assistance programs.

**The members of the Compliance Advisory Panels were small business owners that were legislatively and gubernatorially appointed. The Compliance Advisory Panels are required by the 1990 Clean Air Act, and are to work in conjunction with the SBEAP programs.

Environmental Assistance Programs. Due to the responsibilities of these individuals regarding state and national issues, they were considered as experts for the Delphi portion of this study.

Structure of the Study. This study consisted of three phases: scoping, reflection, and validation. The first phase of the study consisted of the initial scoping analysis that incorporated responses from twenty-nine (29) individuals (nine (9) SBs and twenty (20) SBEAPs). The second (reflection) phase of the study incorporated responses from thirty-four (34) individuals (seven (7) SBs and twenty-seven (27) SBEAPs). The third (validation) phase of the study incorporated responses from ten (10) individuals (five (5) SBs and five (5) SBEAPs).

In the first two phases (scoping and reflection), the mean rank and the Kendall coefficient of conformance was used to analyze the data. The mean rank, commonly described as the average, was used for the overall ranking of the responses and the Kendall coefficient of conformance was used to allow for a quantitative measure of the agreement of the views within each group that was researched. A Kendall coefficient of conformance of 0.5 or higher represents acceptable agreement (Schmidt, 1997).

The analysis of the data for the Kendall coefficient of conformance performed in the first phase began by using the weighted responses from the data collection in the first phase. These weightings were converted into rankings by using a simple correlation (e.g. a weighting of ten (10) would convert to a ranking of one (1)). These groupings were separated, since the intention was to analyze the rankings between small businesses and the state Small Business Environmental Assistance Programs, and to consider the level of agreement. The second phase rankings were performed in the same way as the first phase, except that instead of weighting (as was done in the first phase, in the second phase specific rankings for the items of service and environmental content were recorded. The results from the ranking and correlation data from the second phase were again used to interview individuals in the expert groups for Phase III. Five (5) randomly selected individuals from the SB and five (5) individuals from the state SBEAP group were chosen. The interviews were performed to validate the study findings.

Description of the Instruments. Consistent with the Delphi method approach (Linstone and Turoff, 2002), a Likert scale series of iterative questionnaires were developed where the instruments build and refine upon the previous set of inputs.

Some of the open ended questions in the Phase I analysis were specifically asked to identify relevant concepts that may have been missed in the Phase I data collection instrument. The Phase II (reflection) instrument was then created by using the responses from Phase I (scoping). The Phase III (validity) instrument used the Phase II rankings and questioned the validity of these rankings.

Data Collection Process. In the first (scoping) phase, the respondents were asked a series of open ended interview questions, and they were asked to provide weighted responses to closed ended questions in a questionnaire. The process of weighting was done by asking the respondent to note the importance or value (i.e. weight) of an item. For the first questionnaire, the construct began from information collected by the US Environmental Protection Agency for their annual reports to Congress regarding the state Small Business Assistance Programs (USEPA, 2008), data collected by the SBEAP group amongst themselves (Small Business Environmental Assistance Programs, 2008), as well as breadth issues regarding small businesses that are related to environmental protection (SBA Office of Advocacy, 2008).

Certain of the open ended questions in the Phase I analysis were specifically asked to identify relevant concepts that may have been missed in the Phase I data collection instrument where individuals were asked to weight, in levels of importance, certain environmental issues. The Phase II instrument then was created by using the responses from Phase I. The Phase III instrument used the Phase II rankings and questions regarding the validity of these rankings. The data captured during the first phase was analyzed using coding methods. Coding techniques were used to incorporate the broader responses to the data of the interview questions. These data from the questionnaires were analyzed for statistical consistency by using the Kendall coefficient of conformance. This allowed respondents, within the interviews, to note the importance of certain environmental content and services that were offered by the programs. This was done by their priority weighting, or by referencing items that were not already listed. The open ended questions also allowed the respondents to provide comments as to what the greatest needs were for the small businesses within their states.

The categories of service and environmental content that were developed through this process of open coding (Northcutt & McCoy, 2004) from the first (scoping) phase interviews were used to create the list for the second (reflection) phase. This second list was created by removing responses from the first phase questionnaire that were not considered a priority to the SBs and SBEAPs. Items of service and environmental content that did not hold strong agreement (i.e., items whose average weight were less than two) during the first phase were dropped in an attempt to gain a greater consensus for the next round. Through the expert input process, a second priority listing of twenty (20) services and twenty (20) environmental content offerings were created.

The respondents in the second (reflection) phase were then asked to again rank both the services and environmental content lists that were created from the first phase information. The items were ranked from one to twenty, with one being the most important to the respondent. The second phase incorporated responses from thirty-four (34) individuals (seven (7) SBs and twenty-seven (27) SBEAPs).

The ranking and correlation data was then used to interview individuals in the expert groups for the third phase validation process. Five (5) randomly selected individuals from both the SB group and five (5) individuals from the state SBEAP group were chosen. This process did not require ranking or weighting from the respondents, but asked the individual respondents to comment on the rankings created from the responses in the second phase.

RESEARCH FINDINGS AND DISCUSSION

This research investigated the following questions:

1. Was there a gap between the needs of the small businesses (SB) and the environmental content and services that were funded and offered by the state Small Business Environmental Assistance Programs (SBEAP)?
2. How should the Small Business Environmental Assistance Programs prioritize the environmental content and services to assist small businesses?

Research Question One. Was there a gap between the needs of the small businesses (SB) the environmental content and services that were funded and offered by the state Small Business Environmental Assistance Programs (SBEAP)?

The data revealed that there was no gap. The environmental content priorities by the state Small Business Environmental Assistance Programs closely matched those of the small businesses. However, a reprioritization of the services offered by the SBEAPs will allow them to more closely meet the needs of the small business community.

Regarding the environmental content and services offered, an analysis of the Small Business Environmental Assistance Programs showed that they funded and offered varied environmental contents (e.g. air quality, hazardous waste, storm water) as well as services (permit and technical assistance, hotlines, etc.) which were needed by the small businesses. The services that were offered by the SBEAPs helped the SBs with their environmental content needs. The services offered by the SBEAP included: permit and technical assistance, site visits, hotlines, and websites (see Table one). For example, a small business may have a need for environmental assistance related to air quality permits. The opportunity for that business to obtain help may be from a visit to the site by the state Small Business Environmental Assistance Program, information obtained through a hotline or website, or from direct permit and technical assistance. The permit and technical assistance could also have included items such as the calculation of air pollutant emissions from a new source that the business was planning to build. Within this same scenario, the SBEAPs may also have found themselves helping a small business with additional requirements for proper hazardous waste storage and disposal, or dealing with the requirements for stormwater management from their site. Permit and technical assistance* (for example) by the SBEAPs to a business can be time consuming due to the complexity of environmental permitting (Buchholz, R. A., 1993). This leads to a resource limitation due to the amount of time that each SBEAP program office has available to them to meet the growing requests for services from the SBs.

The services provided by the SBEAPs to the SBs allow the SBs to comply with environmental content requirements. The total service assists by the SBEAPs have increased from slightly less than 2 million in 2004 to more than 3.1 million in 2006 (Small Business Environmental Assistance Programs, 2008). This total includes an increase of site visits by the SBEAPs from 6,120 in 2004 to 9,376 in 2006, and an increase in workshops that have been offered from 958 to 2807 (with the corresponding attendance increase from 39,401 to 108, 296). The permits that were assisted by the SBEAPs increased from 16,328 to 23,615 during the same time period. In regards to the services offered, the total assists to the SBs have increased by more than one million, and permit assists have increased by almost 7,300 (approximately 44.6%), while the full time employees (FTEs) in the SBEAPs had only increased by roughly three (1.3%)from 2004 to 2006 (Small Business Environmental Assistance Programs, 2008).

The research findings also included several comments noting that SBs needed ‘more’ services including: funding, training, and people for the SBEAPs, enhanced communication (including sector specific brochures), sector specific workshops, engineering assistance, funding (i.e. loan programs), site visits for the SBs, and involvement by the SBEAPs across silos within the agencies.

As noted, the hypothesis was that there was a gap between the needs of small businesses and the offerings of the government Small Business Environmental Assistance Programs. Instead, the data revealed that there was no gap. The SBs and SBEAPs generally agreed on the services and environmental content. Both groups of experts (the SB and the SBEAPs), generally viewed the same overall issues as important (Tables one and two). The data showed that the SBEAPs and the SBs differed in their opinion of importance of individual items. This was shown in their priority rankings for both environmental content and services. Both groups of experts also agreed on the priority of the environmental content (air quality, hazardous waste, etc.) that were to be provided, but differed in the way that that environmental content was to be delivered via the services offered. For example, hazardous air pollutants and air quality environmental contents were ranked one or two by both the SBEAPs and the SBs (see Table two). However, the way that the SBEAPs were to provide that information (i.e. services) to the SBs was different (see Table one).

With respect to the rankings of the services offered, both the government Small Business Environmental Assistance Programs and the small businesses ranked comprehensive site visits** (ranked second (SBEAPs) and fourth (SBs)) near the top in their priority rankings. In contrast, the ‘air quality only’ site visits were ranked significantly lower by the SBs. The services that were designated as ‘air quality only’ site visits received little interest from the SBs (ranked eighteenth), in contrast the Small Business Environmental Assistance Programs considered this item important enough to rank in their top ten, it seemed that the small business owners were more concerned with the comprehensive*** site visits. As noted by the SBs interviewed, since the small businesses are required to comply with all applicable environmental regulations (as noted by the SBs interviewed) air quality only site visits offer limited assistance.

---

*Permit and Technical Assistance is a term assigned to a service rendered by the SBEAP programs to the SBs. This service could include items such as: preparation of an air permit (a complex process), the calculation of pollution control device emission efficiencies, the preparation of a stormwater permit application with rainwater runoff calculations, or hazardous air pollutant sector requirements for a small business.

**Site visits are when the SBEAP programs go to the SB site and help that business with environmental issues. Comprehensive site visits are services that the SBEAP performs that are not ‘air quality’ only.

***The term comprehensive, whether used in relation to site visits to a SB, or in relation to the offerings of an entire SBEAP program, describes the work by the SBEAPs that offer content that is more that air quality only. For example, the SBEAP may offer assistance with hazardous waste and stormwater issues in addition to assistance with air quality issues.

The interest in the services that were funded and offered by the state Small Business Environmental Assistance Programs (SBEAP), as well as the need for that assistance has grown in the last few years as evidenced by states moving toward comprehensive environmental assistance for environmental content. Businesses are not required to avail themselves of the services offered by the SBEAPs. However, services such as permit assists that are requested by the SBs (and are voluntary) have increased by 44.6% from 2004 to 2006. Nationally, from 2004 to 2006, the overall increase in state total budgets was ~15%, average budget ~15.5%, and median budget ~9%, while full time employees (FTEs) during that time have increased by ~1.3%. During that time (2004 to 2006), four (4) additional states have become comprehensive assistance providers (those which provide multiple environmental content), to a total of thirty-nine (39). Additionally, two (2) states added air quality only programs, which were up from ten (10) states in 2005 and 2004.

The data showed that the funding and the economy were not a strongly noted issue by the respondents. Only six (6) of the respondents noted funding at all, and only two (2) of these individuals referred to the needs of these funds for the small businesses themselves (e.g. loans, grants, rebates, etc.). Only one (1) person noted the overall national economy as a concern for small businesses and this was a government employee manager and not a small business owner. Since this research was performed prior to the current economic difficulties (nationally and internationally), it is assumed that the economy would be mentioned more readily if the interviews were redone today.

Table 1. Ranking comparison of the Services from the perspective of the SBs and the SBEAPs

	SB	SBEAP
Permit and Technical Assistance	1	1
Hotlines	2	8
Funding Assistance (pollution equipment, etc.)	3	19
Comprehensive Site Visits	4	2
Programmatic specific (permitting, etc.) workshops & training	5	7
Involvement with trade and sector associations	6	4
Websites	7	3
Involvement with Chamber's of commerce, SBA, SBDC, etc.	8	9
Involvement with environmental enforcement programs	9	12
Sector specific workshops & training	10	5

Note: Sector specific workshops & training means the type of business, i.e., drycleaners, autobody shops, etc.

Table 2. Ranking comparison of the Environmental Content from the perspective of the SBs and the SBEAPs

	SB	SBEAP
Hazardous Air Pollutants	1	2
Air Quality	2	1
Pollution Prevention (P2)	2	8
Solid Waste	4	6
Stormwater	5	3
Industrial Wastewater	6	5
Energy (inc. waste to energy)	7	9
Hazardous Waste	7	4
Underground and Aboveground Storage Tanks	9	10
Used Oil	10	7

Research Question Two. How should the Small Business Environmental Assistance Programs prioritize the environmental contents and services to assist small businesses?

The hypothesis was that there was a gap between the needs of the SBs (environmental contents and services) and those offered by the SBEAPs. The data revealed that there was no gap, instead, it was found that the environmental content needs of the SBs were quite similar to the priorities of the Small Business Environmental Assistance Programs. The services that were offered were prioritized differently by each group. The SBEAPs need to reprioritize their services (site visits, hotlines, etc.), to meet the SBs' needs since the SBs cannot reprioritize. The small business needs were set by the environmental regulatory and enforcement agencies. Similarly, the needs of the SBs regarding the environmental content (e.g. hazardous air pollutants, etc.) were also set by the environmental agencies.

Both the SBEAP and SB groups agree internally with regards to services, but disagree with each other. The conformity of rankings in services rose from 0.32 to 0.95 for the SBs and 0.41 to 0.69 for the SBEAPs. The conformity of rankings in environmental content rose from 0.36 to 0.53 for the SBs, and actually dropped somewhat for the SBEAPs from 0.91 to 0.79. However, 0.79 still is considered a strong agreement. Agreement is defined as a Kendall Coefficient of Conformance of 0.5 or higher (Schmidt, 1997). The views showed moderate to unusually high agreement within both groups.

The following sections (environmental content and services) describe how the Small Business Environmental Assistance Programs should prioritize their work to assist small businesses as asked in research question two.

Environmental Content. The data showed that the environmental content priorities that were expressed by both the SBEAPs and the SB were consistent across both groups. This section describes those rankings and priorities.

During the third phase of this study, which is the validation phase, the respondents were consistent in their comments that the environmental content of hazardous air pollutants and air quality environmental contents should be ranked highly (Table two). The SBs ranked the hazardous air pollutants higher than the SBEAPs. New hazardous air pollutant regulations that were specifically focused on SBs have created a level of concern for that group due to the amount of new regulations based on these pollutants (USEPA, 2008).

The rankings that followed the top two environmental content needs were: pollution prevention, solid waste, energy, stormwater, hazardous waste, and industrial wastewater, tracked with the Phase I interviews. Both the SBs and the SBEAPs considered stormwater (#5, SB and #3, SBEAP), and industrial wastewater (#6, SB and #5, SBEAP), as important, and rank both highly. These high rankings may be due to the perceived need for the service rather than the actual need. For example, industrial wastewater permits were regulated under the Clean Water Act (CWA) (USEPA Office of Wastewater Management, 2008). These permits can be issued individually to sources of wastewater. More typically, sources (especially SBs) would become part of an overall umbrella permit that would be obtained from a Publically Owned Treatment Works and therefore, the SB would not generally be concerned with obtaining a wastewater permit.

Certain of the environmental contents ranked toward the bottom of the ranking analysis. These consisted of: emergency planning, remediation & brownfields, OSHA (safety and health), and special wastes. The brownfields program assisted counties, municipalities, and non-profit organizations in bringing former industrial sites back to productive use (Polen & Carico, 2006). The interview responses from the first phase of the study indicated that brownfields and remediation were of interest to both SBs and SBEAPs. Interest (as shown in the first phase), in this case, does not translate to a high priority.

The results suggest that little effort at additional improvement needs to be made in the areas of specific funding for small businesses, energy (energy audit within specific companies, as well as commodities), greenhouse gas and global warming issues, and the economy. These areas have very little interest from the experts regarding the prioritization that the governmental Small Business Assistance Programs should tackle. While these topics were of specific concern due to current environmental and economic issues nationally and internationally, they held very little value to the SBEAP programs in their prioritization hierarchy.

Services. The data showed that the service priorities that were expressed by both the SBEAPs and the SB were not consistent across both groups. This section describes those rankings and priorities. The data showed that the overall responses (from both the SBEAP and SB responses) regarding the services offered can be separated into two broad categories of: information distribution and technical issue assistance.

Within the service category of information distribution, Permit and Technical Assistance is the top ranking item on the service lists (Table one). The permit and technical assistance is at the core of the Small Business Environmental Assistance Programs that allow them to get and keep small businesses in compliance with environmental regulations. The data also showed that within the top ten (10) services' category, the small businesses ranked the following items which included: second (hotlines), the fifth (programmatic specific workshops and training), the sixth (involvement with trade and sector associations), the seventh (website), and the tenth (sector specific workshops and training) suggest that a consensus of SB regarding knowledge of new and existing environmental regulations are strong.

Additionally, six (6) of the top ten (10) services (the third, fourth, fifth, sixth, seventh, eighth) of the SBEAPs also show that they too believe that information sharing is critical. Numerous regulations of all types are issued annually by states and the federal government and it is difficult for any small business to keep up with all new and modified requirements. This was noted by the respondents during the first phase of the study.

Funding assistance for pollution control equipment, etc., ranked highly in the research finding from the SBs, but ranked poorly at nineteenth from the SBEAP responses. The idea of the SBEAPs expanding their customer base to large businesses was ranked poorly by both SBs and SBEAPs. The small businesses rated this as nineteenth and the SBEAPs rated this as twentieth. Since the Small Business Environmental Assistance Programs already have a drain on resources (as seen in research question two), it would be difficult for the programs to open up to larger business clients. The concept of the large business' mentoring ranked seventeenth out of twenty on both the SB and SBEAP service lists. The service idea of using trinkets that could increase environmental awareness by SBs ranked poorly with both groups as the Small Business Environmental Assistance Programs ranked this service eighteenth, and the SBs ranked this as twentieth.

In the third phase of the analysis, a respondent noted that due to the complexity of the topic and the arcane language that is used within environmental issues, there was a language barrier which added to the difficulty of SBs understanding the environmental regulatory programs and their requirements. The research reflected this comment within the rankings. In the service rankings from the SBs, half of the top ten (10) rankings were related to the clarification of regulatory requirements. These services that were offered by the SBEAPs include: permit and technical assistance, hotlines, and programmatic specific workshops, and training.

CONCLUSIONS

The findings show that there was not a gap between environmental contents (e.g. air quality, hazardous waste) provided by the SBEAPs and those that were needed by the SBs, however, the research also revealed that the Small Business Environmental Assistance Programs needed to reprioritize the services provided to the small businesses to match the needs of the SBs. The service needs of the SBs have increased dramatically (as shown by requests for assistance) while the budget and staffing levels for the SBEAPs have remained relatively constant. Because the requests by the SBs continued to increase while the staffing and budget levels of the SBEAPs remained fairly constant, continuing to fulfill those needs may be difficult for the SBEAPs. The re-prioritization of these services by the Small Business Environmental Assistance Programs will assist the government programs in providing for the needs of the SBs. This re-prioritization did not seem to pose a problem for the government according to the interviewees.

The re-prioritization of services offered to the small businesses should be reprioritized as: Permit & Technical Assistance, Hotlines, Comprehensive Site Visits, Programmatic specific workshops and training, Websites, and Involvement with trade and sector associations. In regards to the environmental content prioritization, the SBEAPs need to continue to focus as they have previously on: Hazardous air pollutants, Air Quality, Pollution Prevention, Solid Waste, Stormwater, Industrial Wastewater, and Hazardous Waste.

The implementation of this analysis has the potential to allow states to prioritize limited resources to best assist the small businesses within their state on environmental issues. It also could allow states to manage their Small Business Environmental Assistance Programs by providing a solution to this management problem.

REFERENCES

Buchholz, R. A. (1993). *Principles of Environmental Management---The Greening of Business.* Englewood Cliffs, New Jersey: Prentice-Hall.

Linstone, H. A., & Turoff, M. (2002). *Delphi Method.* Retrieved May 2, 2008, from New Jersey Institute of Technology Web site: http://is.njit.edu/pubs/delphibook/

Northcutt, N., & McCoy, D. (2004). *Interactive qualitative analysis*. Thousand Oaks, CA: Sage Publications.

Polen, T., & Carico, G. (2006, October). Brownfields. *EM-Environmental Managers.*

Public health and welfare, air pollution prevention and control. (2004, January 8). *42 U.S. Code 7401.* Retrieved March 12, 2008, from U.S. Government Printing Office Web Site: http://www.access.gpo.gov/uscode/title42/chapter85_subchapteri_.html

SBA Office of Advocacy. (2008). Retrieved January 22, 2008, from United States Small Business Administration Web site: http://www.sba.gov/advo

SBEAP National Steering Committee. (2007, June). *Summary of the 2007 SBEAP multimedia surveys.* Retrieved June 1, 2008, from National Steering Committee of the Small Business Assistance Programs Web site: http://www.smallbiz-enviroweb.org/sba/multimediafiles/2007MultimediaSurveyResults.pdf

Schmidt, R. C. (1997). Managing Delphi surveys using nonparametric statistical techniques. *Decision Sciences,* 28 (3), 763-774.

USEPA, Office of Wastewater Management. (2008). *NPDES Permit Writers' Manual.* Retrieved October 30, 2008 from USEPA National Pollutant Discharge Elimination System (NPDES) website: http://cfpub.epa.gov/npdes/index.cfm

USEPA. (2008, June 5). *Report to Congress-Section 213 Informal Guidance Program, the Small Business Regulatory Enforcement Fairness Act.* Retrieved September 24, 2008, from United States Environmental Protection Agency Web site: http://www.epa.gov/sbo/rep1.htm#2.2.1

PROXIMITY OF CANCER CASES TO AIRPORTS WITHIN THE STATE OF TEXAS

Author Block S. N. Senkayi,[1,2] M. Sattler,[1] V. Chen[1];
([1]University of Texas at Arlington, Arlington, TX, USA; [2]EPA Region 6, USA)

Determining whether the incidence of cancer may be associated with pollutants emitted from airports is important in order to better plan cities to reduce such incidences. This research aims to answer the following questions: 1) Is there a trend between the incidence of various kinds of cancer and proximity to air emission sources, including airports, in Texas? and 2) Specifically, is there a relationship between childhood leukemia and airport benzene emissions? Texas has two airports ranked among the top 10 U.S. airports in terms of enplanements for Jan.-March 2010: Houston ranked 7th, while Dallas was 3rd.[1] State-wide cancer incidence data was obtained in July of 2009[2]; additionally, state-wide data on age, race and gender-specific cancer rates[3,4,5,6] were obtained from the Texas Department of State Health Services (DSHS)[7]. These rates were applied to the demographic make-up of each geographical unit to compute the number of cancer cases which would be expected in each area. The observed number of cases in each area was compared to the expected number for leukemia, lymphoma (both for children 9 years and under), colon and respiratory (both for all ages) cancers at the state-wide block group level. Colon cancer was used as a negative control because benzene exposures are not expected to be associated with the incidence of colon cancer. The ratio of the number of observed cases was divided by the number of expected cases for each block group and was then plotted against the distance to major emission sources (railroads, airports, industrial facilities and roads), using Geographical Information Systems (GIS). In order to address the second question of a relationship between childhood leukemia and airport benzene emissions, a Poisson regression model was developed using county emissions as the predictor variables and childhood leukemia as the response variable. Additionally, distance to the emission sources for children under age 9 with and without leukemia was compared. The 3 analyses all suggest that airport benzene emissions contribute to incidences of childhood leukemia in Texas.

REFERENCES

1. Administration Bureau of Transportation. March 2010 Airline Traffic Data: System Traffic Up 2.4 Percent from March 2009 (See table 5 titled Top 10 U.S. Airports (ranked by January-March 2010 System Scheduled Enplanements on U.S. Airlines)). http://www.bts.gov/press_releases/2010/bts029_10/html/bts029_10.html. Accessed June 12, 2010

2. Cancer data have been provided by the Texas Cancer Registry statewide incidence file, 1995-2007, Department of State Health Services, created December, 2008.

3. Texas statewide Age-Specific Rates, Average Annual Rates, 1995-2000, Selected Age Groups, and by race and ethnicity and sex for All Childhood Leukemias combined (ICCC-3 Group I) Rates are per 1,000,000. Data Request 11/5/2010 Incidence Source: prepared by Texas Department of State Health Services, Cancer Epidemiology and Surveillance Branch, Texas Cancer Registry, Incidence - Texas, 1995-2007, Cut-off 11-19-09, SEER*Prep 2.4.3, .

4. Texas Statewide Age-Specific Rates, Average Annual Rates, 1995-2000 Selected Age Groups, and by race and ethnicity and sex (Data Release #10385) All Childhood Lymphomas (ICCC-3: II Lymphomas and reticuloendothelial neoplasms) Rates are per 1,000,000. Data Request # 10385 11/16/2010 Incidence Source: prepared by Texas Department of State Health Services, Cancer Epidemiology and Surveillance Branch, Texas Cancer Registry, Incidence - Texas, 1995-2007, Cut-off 11-19-09, SEER*Prep 2.4.3, .

ISBN 9780976885351

5. Texas Statewide Age-Specific Rates, Average Annual Rates, 1995-2000, Five-Year Age Groups, and by race and ethnicity and sex (Data request # 10385) All Respiratory System Cancers (ICD-O-3), Rates per 100,000. Data Request # 10385 (table 2) 11/19/2010 Incidence Source: prepared by Texas Department of State Health Services, Cancer Epidemiology and Surveillance Branch, Texas Cancer Registry, Incidence - Texas, 1995-2007, Cut-off 11-19-09, SEER*Prep 2.4.3, .

6. Texas statewide Age-Specific Rates, Average Annual Rates, 1995-2000, Five-Year Age Groups, and by race and ethnicity and sex Colon Cancer (ICD-O-3), Rates are per 100,000. Data Request 11/5/2010 Incidence Source: prepared by Texas Department of State Health Services, Cancer Epidemiology and Surveillance Branch, Texas Cancer Registry, Incidence - Texas, 1995-2007, Cut-off 11-19-09, SEER*Prep 2.4.3, .

7. Cancer data have been provided by the Texas Cancer Registry, Cancer Epidemiology and Surveillance Branch, Texas Department of State Health Services, 1100 W. 49th Street, Austin, Texas, 78756, http://www.dshs.state.tx.us/tcr/default.shtm, or (512) 458-7523. Viewed 2009.

HEALTH RISKS EVALUATION OF HEAVY METALS IN SEA FOOD FROM PERSIAN GULF

Majid Afkhami (Yung Researches Club, Islamic Azad University, Bandar Abbas Branch, P.O.Box:79159-1311, Bandar Abbas, Iran.)
Maryam Ehsanpour (Islamic Azad University, Bandar Abbas Branch, P.O.Box:79159-1311, Bandar Abbas, Iran)
Reza khoshnood (Islamic Azad University, Tehran Central Branch, Iran)

ABSTRACT: Heavy metals are increasingly being released into natural waters from geological and anthropogenic sources. The distribution of several heavy metals (Cd, Pb) was investigated in muscle, Liver in six different fish species seasonally collected in Persian Gulf (autumn 2009-summer 2010). The concentrations of all metals were lower in flesh than those recorded in liver due to their physiological roles. The THQ index for fish was calculated. Estimation of Target Hazard quotients calculations for the contaminated fish consumption was calculated to evaluate the effect of pollution on health. Total metal THQs values (Pb and Cd) for adults were 0.05 and 0.04 in Bushehr and Bandar-Genaveh, respectively, and for children was 0.08 and 0.05 in Bandar-Bushehr and Bandar-Genaveh, respectively.

INTRODUCTION

Over the last few decades, there has been growing interest in determining heavy metal levels in the marine environment and attention was drawn to the measurement of contamination levels in public food supplies, particularly fish (Mora et al., 2004). Toxicological and environmental studies have prompted interest in the determination of toxic elements in food. The ingestion of food is an obvious means of exposure to metals, not only because many metals are natural components of food stuffs but also because of environmental contamination and contamination during processing Daviglus et al. 2002) .With the exception of occupational exposure, fish are acknowledged to be the single largest source of heavy metals for man. In some instances, fish catches were banned for human consumption because their total mercury or other metals content (like as cadmium) exceeded the maximum limits recommended by the FAO and WHO (WHO/FAO 1972).The probability risk assessment technique has been adopted by a number of researchers to fully utilize available exposure and toxicity data(Wang et al. 2005). However, these methods are only applied to quantify the magnitude of health risks of carcinogenic pollutants, but not for quantifying non-carcinogenic risks. Current non-carcinogenic risk assessment methods do not provide quantitative estimates on the probability of experiencing non-carcinogenic effects from contaminant exposures. These are typically based on the target hazard quotient (THQ), which is a ratio of determined dose of a pollutant to the dose level (a Reference Dose or RfD). If the ratio is less than 1, there will not be any obvious risk. Conversely, an exposed population of concern will experience health risks if the dose is equal to or greater than the RfD. The US Environmental Protection Agency (US EPA) has described the methodology for estimating target hazard quotients (THQ) for non-carcinogenic risk (EPA 1989), which is applicable to assess the health risk of some metals.

The suburban and urban areas of Bushehr and Bandar-Genaveh cities, Iran, are polluted by some sources of heavy metals, but information on the health risks of these elements is quite limited. The main objective of this study is to estimate the health risks of heavy metals, such as Pb, Cd, via consumption of fish to the general public in above districts by using the target hazard quotient (THQ) concept.

MATERIAL AND METHODS

The selected fish species belong to different families and have different trophic /ecological characteristics i.e. they include demersal top carnivores (e.g. Grooper) and Benthos feeders (e.g. Flat fishes). In September 2010 to April 2011, the fish species were randomly collected from commercial

---

ISBN 9780976885351

catches landed at local fishing ports, and the biometrics of collected fishes samples were determined and noted. Immediately after the collection, fish samples were stored on ice in an isolated box (Chien et al. 2002) , and transferred to reference laboratory. After that a part of dorsal muscle (edible tissue) from each of the samples dissected as target sample, and prepared for processing. All of the samples were dried at 60°C for 48 h in laboratory oven (Rajotte et al. 2005).

Table 1: Overview of Sampled Species

Scientific name	Common Name	Station	Length (cm)	Weight (g)
Euryglossa orientalis	Oriental sole	Bushehr	32.3±4.31 24.5-36.5	585.0±140.09 240-710
		Bandar Genave	32.1±6.49 24.0-41.0	604.0±252.51 209-1010
Psettodes erumei	Deep flounder	Bushehr	48.1±5.36 39.0-58.0	1672.0±289.52 754-2650
		Bandar Genave	43.0±6.37 31.5-51.0	1309.0±320.25 497-2286
Epinephelus coioides	Orange spotted grouper	Bushehr	48.0±9.50 34.0-63.0	2278.9±360.95 277-4310
		Bandar Genave	54.3±6.58 40.0-67.0	2437.9±350.26 420-4950
Lethrinus nebulosus	Spangled emperor	Bushehr	21.7±4.3 16.0-26.0	310.5±70.25 150-470
		Bandar Genave	26.8±4.89 20.0-33.0	582.9±39.25 325-790

All glassware's was cleaned prior using by soaking in 10% v/v HNO_3 for 12h and then rinsed with ultra-pure water. Between 0.2 to 0.4 g of dried sample material were weighted and then digested in acid-cleaned teflon beaker with 5ml of ultra-pure nitric acid (65%v/v). Typical microwave digester operated for 30-40 min at a target digestion temperature at 200°c and after then allowed for 1h to cooling. Digested samples transferred to a graduated plastic test tube and brought up to volume (50ml) with Mili-Q-water(MOOPAM 1999).All samples were analyzed three times for Cd, Pb by inductively coupled plasma-atomic emission spectrometry (ICP-AES) (Varian Model- liberty series II) and for Hg by LECO AMA254 Advanced Mercury Analyzer.In order to assess the analytical capability of the proposed methodology, accuracy of heavy metals analyzing was tested with reference matrices of dogfish liver tissue (DORM 2), and muscle tissues (DOLT 2). Results confirms that observed and reference values have not statistically differences ($P<0.05$) (Table1).

The methodology for estimation of target hazard quotients (THQ) used was provided in USEPA region III risk based concentration table(EPA 2000). For carcinogenic effects, risk is expressed as excess probability of contracting cancer over a lifetime. For non-carcinogenic effects, risk is expressed as a target hazard quotient, the ratio between the exposure and the reference dose.

A THQ below 1, means the exposed population is unlikely to experience obvious adverse effects. The dose calculations were carried out by using the standard assumption from an integrated U.S. EPA risk analysis considering an average adult body weight of 55.9 kg, and 32.7 kg for children. The health risks were separately considered the contact pathway with each exposure medium (e.g. food) changes with age. Furthermore, children are more sensitive to pollutants. There will be a certain amount of discrepancy in health risks between age groups and the locality of the inhabitants. In this respect, the THQ was determined based on the methods by USEPA described by the equation 1:

$$THQ = \frac{E_F \times E_D \times F_{IR} \times C}{R_{FD} \times W_{AB} \times T_A} \times 10^{-3}$$

Equation 1: THQ equation

In this equation E_F is the exposure frequency (365 days/year); E_D is the exposure duration (72 years), equivalent to the average lifetime in Iran; F_{IR} is the food ingestion rate (g/person/day); C is the metal concentration in food (Ag/g); R_{FD} is the oral reference dose (mg/kg/day); W_{AB} is the average body weight (55.9 kg for adults and 32.7 kg for children), and T_A is the averaging exposure time for noncarcinogens (365 days/year number of exposure years, assuming 70 years in this study).For adult inhabitants of the two study area, the daily fish consumption was 19.17 g/person/day and 14.06 g/person/day for children.

RESULTS

Concentration of Pb, Cd for fishes in two studied areas has shown in table 2. Because the residents of two study areas consume 4 kind of fish samples, we used average of heavy metal concentrations for calculate of THQ. Mean concentration of Pb ranging from 0.09 to 0.55 µg/g in Bushehr and 0.01 to 0.30 µg/g in Bandar-Genave, and for Cd, ranging from 0.02 to 0.40 µg/g in Bushehr and 0.01 to 0.32 µg/g in Bandar-Genave, (table 3).The average concentrations of the three metals are higher in Bushehr than other stations.

Table 2: Concentrations of Pb , Cd In 4 Kinds of Fish Samples (µg.G^{-1} Dry Weight).

Station\metals	species	Pb		Cd		Hg	
		Range	Mean	Range	Mean	Range	Mean
Bandar Bushehr	*E.orientalis*	0.10-0.20	0.15	0.06-0.40	0.20	0.14-0.27	0.21
	P. erumei	0.17-0.44	0.27	0.10-0.25	0.15	0.10- 0.55	0.28
	E.coioides	0.10-0.55	0.22	0.02-0.18	0.15	0.12-0.23	0.19
	L.nebulosus	0.09-0.35	0.17	0.01-0.10	0.07	0.07-0.26	0.17
Bandar Genaveh	*E.orientalis*	0.07-0.28	0.14	0.01-0.32	0.13	0.15-0.24	0.21
	P. erumei	0.01-0.25	0.15	0.05-0.18	0.10	0.14-0.31	0.26
	E.coioides	0.01-0.30	0.21	0.01-0.25	0.13	0.09-0.17	0.11
	L.nebulosus	0.09-0.18	0.14	0.01-0.17	0.09	0.11-0.21	0.14

This result is mainly due to unmanaged shipping activities, river runoff, and untreated sewage discharge by coastal settlements, and dumping of toxic and industrial wastes into the sea which accrue adjacent of Bushehr. Averaged heavy metal concentrations in fish used for calculation of the THQ.

DISCUSSION

Concentration of,Cd and Pb in fish from Bushehr which receives municipal and industrial wastewater From Bushehr city ,were higher than those observed at the other location(Bandar-Genave).Mean values of Cd, in our investigation except for *Letherinus nebulosus* were less than those reported for *Lethrinus lentjan* in Al-Yousuf et al (2000) reported from United Arab Emirates. Totally , about Cadmium Concentration, our results were Lowere than concentration reported from Gulf of California(Soto-Jimenze, Amezcua et al. 2009), and higher than reported from Jingsu River (Liu, Ge et al. 2009).Concentration of Cd observed in our study were similar to concentration in *Hexagrammos otakii* and *Sebastiscus marmoratus* fishes from Masan Bay(Kwon and Lee 2001).The concentration of Pb in Current study were lowere than reported from Gulf of California in *Istiphorus platypterus* and *Terrapturus audax* (Soto-Jimenze, Amezcua et al. 2009).The health risks posed by exposure to Pb, Cd to the local inhabitants in two coastal regions of Persian Gulf, Iran through the consumption of contaminated fishes were investigated based on estimated target hazard quotients (THQs). The results showed that THQ values are less than 1 for both adults and children by either consuming fish alone .The consumption of fish provides health benefits, but some of them have high heavy metals levels, contributing to possible adverse effects, particularly in fetuses and young children. Health benefits and risks from consumption of fish has mainly focused on recreational and subsistence fish, and only more recently on commercial fish (Burger and Gochfeld 2007), although Yess (Yess 1993) reported on levels of canned tuna much earlier.Oral reference doses were based on 1×10^{-3} µg/g/day for Cd and 4×10^{-3} µg/g/day for Pb (EPA 2000).It is shown that there are no THQ values over 1 through the consumption of fish, suggesting that health risks associated with heavy metals exposure is insignificant. An important aspect in assessing risk to human health from potentially harmful chemicals in food is the knowledge of the dietary intake of such substances that must remain within determined safety margins. For Cd and Pb the World Health Organization has established as “safe” intake level a Provisional Tolerable Weekly Intake (PTWI) of 5 µg/kg body weight, 7 µg/kg body weight, 25 µg/kg body weight, respectively (WHO/FAO 2003).

Table 3: Estimated Target Quotients (THQ) and Estimated Weekly Intake (EWI) For Individual Metals Caused By Fish Consumption.

		Pb		**Cd**	
		THQ	EWI	THQ	EWI
Adult	**Bushehr**	0.01	0.55	0.04	0.17
	Bandar-Genave	0.01	0.55	0.03	0.13
Children	**Bushehr**	0.02	0.18	0.06	0.25
	Bandar-Genave	0.01	0.55	0.04	0.17

In our case Cd, Pb weekly intakes through the consumption of fish (Pb: 0.18 – 0.55 µg/kg body weight, Cd: 0.13 – 0.25 µg/kg body weight,) were lesser than tolerable weekly intake limit. The availability of information on both of the risks and benefits of specific species of fishes from particular areas is key to making informed decisions about fish consumption. To be effective, development of risk communication tools should involve not only scientists, health professionals, and regulators, but the public as well (Burger, Gochfeld et al. 2007).

CONCLUSION

From the human health point of view, Cd and Pb THQ values (<1) show a situation of no risk for the consumer. Consequently, intake might be significantly underestimated and might be of concern, above all in the cases where the exposure is closer to the tolerable weekly intake. As a final conclusion, we suggest that more specific recommendations regarding human consumption (kind of species and frequency and size of meals) are done according to the data concerning levels of environmental pollutants in the most consumed fish and seafood species.

REFERENCES

Burger J. Gochfeld M. Jeitner C. Burke S. Stamm T. (2007). Metal levels in flathead sole (Hippoglossoideselassodon) and great sculpin (Myoxocephaluspolyacanthocephalus) from Adak Island, Alaska:potential risk to predators and fishermen. Environ. Res. 103, 62–69.

Chien LC, Hung TC, Choang KY, Yeh CY, Meng PJ, Shieh MJ, et al. Daily intake of TBT, Cu, Zn, Cd and As for fishermen in Taiwan. Sci Total Environ 2002; 285; 177– 85.

Daviglus, M., Sheeshka, J., Murkin, E., 2002. Health benefits from eating fish. Comments Toxicol. 8, 345–374.

EPA (1989). Risk assessment guidance for superfund,Human health evaluation manual. Washington DC, USEPA,United States Environmental Protection Agency. vol 1.

Hamrick, K., Smith, J., 2003. Subsistence Food Use in Unalaska and Nikolski. Aleutian Pribilof Island Association,Anchorage, AL.

MOOPAM (1999). manual of oceanographic observations and pollutant analyses. 3th. Kuwait, regional organization for the protection of the marine environment.

Mora S.D. Fowler S.W. Wyse E. Azemard S. (2004).Distribution of heavy metals in marine bivalves, fish and coastal sediments in Gulf and Gulf of Oman. Marine pollution bulletin. 49, 410-424.

Pyle, G. G., J. W. Rajotte, et al. (2005). "Effects of industrial metals on wild fish populations along a metal contamination gradient." Ecotoxicology and Environmental Safety 61(3): 287-312.

Patrick, R., 2002. How local Alaska native communities view the Amchitka issue. In: Proceedings of the Amchitka Long-term Stewardship Workshop. CRESP/University of Alaska, Fairbanks, AK.

Sofuoglu, S.C., Kavcar, P., 2008. An exposure and risk assessment for fluoride and trace metals in black tea. J. Hazard. Mater. 158, 392–400.

Wang, X., T. Sato, et al. (2005). "Health risks of heavy metals to the general public in Tianjin, China via consumption of vegetables and fish." Science of The Total Environment 350(1-3): 28-37.

WHO/FAO (1972). Evalution of Certain Food Additives and the Contaminants Mercury, Cadmium and Lead. Geneva, WHO/FAO.

Yess, N. J. (1993). "Food and Drug Administration Survay of Methylmercury in Canned tunna." Journal of Association of Official Analytical Chemists International 76: 36-38.

ECOTOXICOLOGICAL RISK ASSESSMENT OF THREE INSECTICIDES USING AN EPIGEIC EARTHWORM

Anilava Kaviraj (University of Kalyani, Kalyani, W.B, India), Rupa Dasgupta and Partha Pratim Chakravorty (Raja N.L. Khan Women's College, Paschim Medinipore, WB, India)

ABSTRACT: Bioassays were made in the laboratory with age synchronized specimens of the epigeic earthworm *Eisenia fetida* using OECD guidelines to assess ecological implications of application of three insecticides carbaryl, chlorpyrifos and endosulfan in the crop fields. The specimens were exposed to control (T1) and three sub-lethal doses representing 12.5 % (T2), 25 % (T3) and 50 % (T4) of the LC_{50} value of the respective insecticide to *E. fetida*. Biomass of earthworms increased from the initial value under all treatments of chlorpyrifos and T2 of carbaryl, though significantly lower than the control, but reduced from the initial value under T3 and T4 treatments of carbaryl and all treatments of endosulfan. Cocoon production, hatching success and juvenile production of the earthworms significantly reduced under T2 dose of endosulfan and T2-T4 doses of carbaryl and chlorpyrifos as compared to control. The earthworms failed to produce cocoon even at 0.5 $\mu g.kg^{-1}$ soil of endosulfan (T3), which was only 2.0 % of the recommended agricultural dose (RAD) of this insecticide. Activitiy of the enzyme alkaline phosphatase was elevated and that of acetylcholinesterase inhibited by the sub-lethal doses of all insecticides, except endosulfan, which produced no effect on acetylcholinesterase activity. It was concluded that application of carbaryl and endosulfan in the agricultural fields at the recommended agricultural dose (RAD) was ecologically dangerous for soil agro-ecosystems and unsafe for soil organisms like earthworms.

INTRODUCTION

Concern for contamination of the environment by insecticides has assumed tremendous importance in recent years because of sharp rise in the magnitude of insecticide application in the agricultural fields (Zhu et al., 2004). The ecological implications of such rise in insecticide application, particularly their effects on subsoil systems remained largely unexplored. Therefore, the fate of insecticides in the soil and their effects on non-target soil organisms are priority research in recent years (Holmstrup, 2000, Amorim et al., 2002, Mosleh et al., 2003 a). Earthworms are most conspicuous non-target organisms in soil and are worst victims of insecticide application in the agro-ecosystems. They have been adopted as standard organisms for eco-toxicological testing by several researchers (Conder and Lanno, 2000) and organizations (OECD, 1984, 2004).

The main objectives of the present study were to determine effects of sub-lethal doses of carbaryl (carbamate), chlorpyrifos (organophosphate) and endosulfan (chlorinated hydrocarbon), three most common insecticides used in the agricultural fields in India, on growth, reproduction and activities of key enzymes of an epigeic earthworm species *Eisenia fetida* and to evaluate ecological implications of indiscriminate use of these insecticides at their recommended agricultural dose (RAD).

MATERIALS AND METHODS

ISBN 9780976885351

Collection and culture of the test specimens. Specimens of *Eisenia fetida* were collected from a vermicompost unit located at Midnapore town (W. Bengal, India) and were cultured in earthen pots (diameter 45.72 cm, mean depth 30.48 cm) in the laboratory to produce fresh stock of specimens for bioassays. Finely ground uncultivated grassland soil (pH: 6.72 ± 0.02, Organic carbon: 1.28 ± 0.37 %) sieved through 0.25 mm mesh and mixed with dry and ground cow dung (1:1) was used as the culture medium (Ismail, 1997). The earthen pots, each containing 150-200 earthworms, were covered with fine meshed iron nets and were kept inside environmental chambers at 28 ± 0.5°C and 60-70 % moisture. Dried and finely ground cow dung were added to the culture pots every week to maintain supply of foods for the earthworms. Cocoons were obtained from the culture pots from 10-15 days onwards. The healthy cocoons were hand sorted and were further cultured in separate culture pots to obtain test specimens for bioassays following the guidelines for testing of chemicals for earthworm (OECD, 1984, 2004).

Bioassay methods. Bioassays were made in small inert polythene boxes each measuring 192 cm^2 and containing 500 g of the same soil that has been used for culture of the specimens. Required amount of insecticides were administered into the experimental box by a micropipette and the boxes were left undisturbed for uniform spreading of the insecticide in the medium. Altogether twenty boxes were used for each insecticide so that there were five replicates for each of the four treatments used (Table 1). Ten age synchronized adult specimens were introduced in each experimental box. Before introduction, the worms were rinsed with water, blotted dry on a filter paper and biomass per ten worms was determined. Finally the experimental boxes were kept in an environmental chamber at a constant temperature of 28 ± 0.5° C and 60-70 % moisture level. Finely ground cow dung (5 g dry weight) moistened to 50% (w/w) was added to each pot every week to provide food for the growing worms. Additional food was given when all the food added was consumed. Moisture loss from the test soil was checked by weighing the test containers at weekly intervals and replenished if needed (OECD, 2004).

TABLE1. Sub-lethal doses of the insecticides used in the bioassay

Dose	Carbaryl (mg/kg soil)	Chlorpyrifos (mg/kg soil)	Endosulfan (µg/kg soil)
$T_{1\ (control)}$	0	0	0
T_2	1.85	3.6	0.25
T_3	3.7	7.2	0.5
T_4	7.4	14.4	1.0

The worms were removed from the test box and weighed on the 28th day to determine the change in biomass following the protocols recommended by OECD (2004). The cocoons were left undisturbed in the test boxes after removal of the adults till 56th day. Numbers of cocoons that hatched were also counted each week to determine the hatching success. Hatchlings per box were counted on the 56th day to determine the number of juveniles produced (OECD, 2004).

Adult earthworm specimens removed from the test boxes on 28th day of the experiment were also used to determine the activities of the enzymes alkaline phosphatase and acetylcholinesterase and total protein of the earthworms following the methods of Walter and Schutt (1974), Ellman et al. (1961) and Lowry et al. (1951) respectively.

The data were subjected to MANOVA using factorial design with types of pesticide and treatments as fixed factors. If the interaction between the insecticides and the treatments were found significant, the data for each insecticide was analyzed for single factor ANOVA followed by Least Significance Difference (LSD) test to determine significant variation between treatments at 5 % level of probability (Gomez and Gomez, 1984).

RESULTS

Earthworms exposed to control and sub-lethal doses of chlorpyrifos did not exhibit any mortality while those exposed to sub-lethal doses of carbaryl and endosulfan exhibited 9.5-20 % and 29-54% mortality respectively. The control earthworms showed an increase of 76.1 ± 5.1 % of biomass from the initial value during the 28 days of culture. Biomass also increased from the initial value in T2 of carbaryl and all the treatments of chlorpyrifos (Figure 1), but the increase was significantly lower than the control. Biomass, on the other hand, reduced from the initial value in all the treatments of endosulfan and T3 and T4 of carbaryl. Maximum reduction in biomass was found in T4 of endosulfan (40.3 % from initial value) followed by T4 of carbaryl (32.9 %).

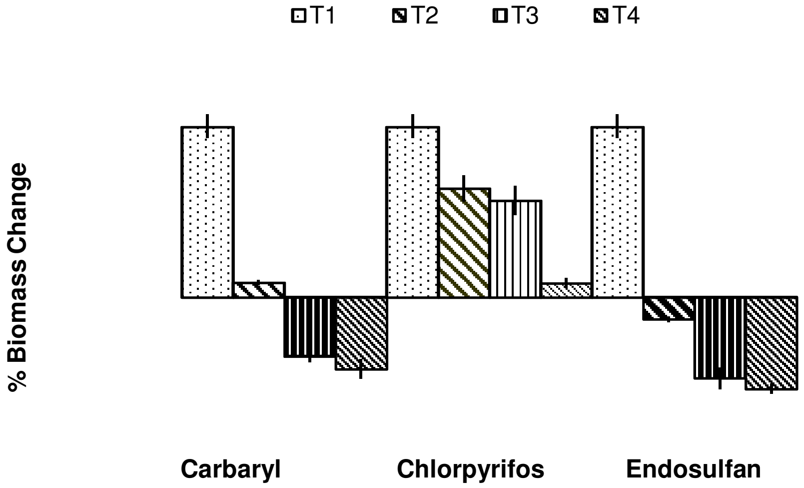

FIGURE1. Change in biomass of *E. fetida* after 28 d exposure to control (T1) and sub-lethal doses (T2,T3 & T4) of carbaryl, chlorpyrifos and endosulfan.

Mean number of cocoons produced, hatching success and number of juveniles produced in control and treatments have been recorded in Table 2. The sub-lethal doses of the insecticides significantly affected the reproductive performance of the earthworms even at the lowest dose (T2), endosulfan producing the most severe effects followed by carbaryl and chlorpyrifos.

Activities of the enzymes alkaline phosphatase and acetylcholinesterase of the earthworms have been shown in Figure 2. Activity of alkaline phosphatase was elevated by the sub-lethal doses of all three insecticides, except T2 and T3 doses of carbaryl, which did not produce any significant change in the activity of this enzyme from the control. Acetylcholinesterase activity was severely inhibited by all the sub-lethal doses (T2-T4) of carbaryl and chlorpyrifos. But there was no change in the activity of acetylcholinesterase enzyme under endosulfan treatment.

TABLE2. Cocoon production, hatching success and juvenile production of *E. fetida* exposed to control (T1) and sub-lethal doses (T2, T3 & T4)^{1} of carbaryl, chlorpyrifos and endosulfan. Different superscripts between two treatments in a column denote significant difference at $p<0.05$.

Parameters^{2}	Treatments	Carbaryl	Chlorpyrifos	Endosulfan
Cocoons/worm/week	T1	1.04 ± 0.05^{a}	1.04 ± 0.05^{a}	1.04 ± 00.05^{a}
	T2	0.16 ± 0.06^{b}	0.28 ± 0.02^{b}	0.12 ± 0.01^{b}
	T3	0.19 ± 0.04^{b}	0.26 ± 0.02^{b}	0^{b}
	T4	0.14 ± 0.08^{b}	0.27 ± 0.02^{b}	0^{b}
Hatching success (%)	T1	74.92 ± 3.40^{a}	74.92 ± 3.40^{a}	74.92 ± 3.40^{a}
	T2	36.00 ± 2.11^{b}	28.31 ± 5.22^{b}	0^{b}
	T3	30.00 ± 7.94^{b}	48.31 ± 7.19^{b}	0^{b}
	T4	20.00 ± 2.29^{b}	43.75 ± 7.13^{b}	0^{b}
Juveniles	T1	31.0 ± 1.58^{a}	31.00 ± 1.58^{a}	31 ± 1.58^{a}
(No. per ten worms)	T2	0.85 ± 0.30^{b}	15.00 ± 1.70^{b}	0^{b}
	T3	0.80 ± 0.4 0^{b}	05.00 ± 0.70^{b}	0^{b}
	T4	0.40 ± 0.01^{b}	04.60 ± 0.54^{b}	0^{b}

1, Sub-lethal doses are mentioned in Table 1
2, Values are expressed as mean ± S.D

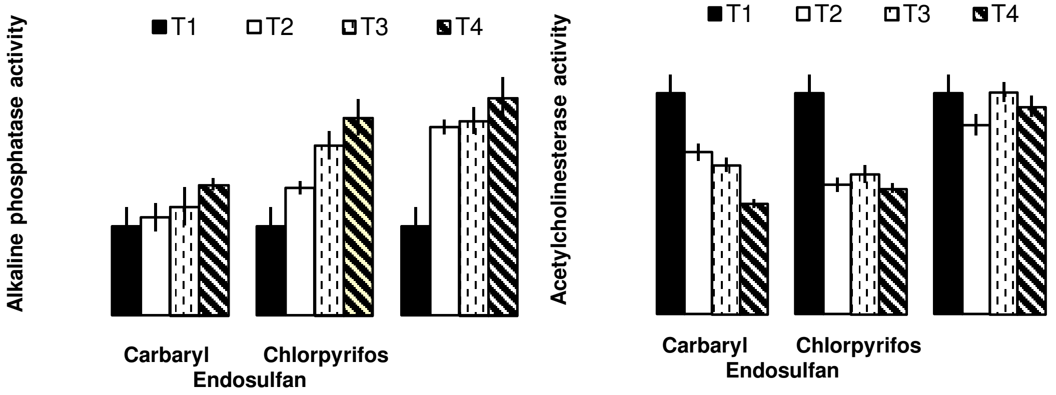

FIGURE2. Activities of the enzymes alkaline phosphatase (µg pnp released/ 30 mins/ mg protein) and acetylcholinesterase (n mole thiocholine/min/mg protein) of *E. fetida* exposed to sub-lethal doses of carbaryl, chlorpyrifos and endosulfan.

DISCUSSION

Results of the present study indicated that carbaryl, chlorpyrifos and endosulfan could significantly affect growth and reproduction of earthworms at doses lower or close to doses recommended for their application in agricultural fields (RAD). Change in biomass, cocoon production and juvenile production are most sensitive parameters of earthworms exposed to insecticides (Helling et al., 2000; Mosleh et al., 2002, 2003 a, b; Bustos-Obregon and Goicochea, 2002). Earthworms, when exposed to insecticides, often reduce feeding to regulate intake of insecticides (Mosleh et al., 2002, 2003 a), resulting in reduction of biomass. However, the reduction in biomass from the initial value under high doses of carbaryl and all doses of endosulfan in the present study were probably due to high mortality of the earthworms. The lowest dose that could reduce the biomass of earthworms from initial value was less than 20% of RAD of carbaryl (T3) and 1 % of the RAD of endosulfan (T2). The earthworms failed to produce cocoon at T3 dose of endosulfan, which was about 2 % of RAD of this insecticide. The effects of chlorpyrifos were rather moderate. The two higher doses (T3 and T4) of this insecticide that produced significant changes in biomass and reproduction as compared to control were higher than RAD. The lowest dose (T2), that produced a mild effects on growth and reproduction was about 72 % of RAD of chlorpyrifos. However, activity of the enzyme alkaline phosphates was higher under all treatments of chlorpyrifos than control and carbaryl. There is strong evidence that increase in the activity of alkaline phosphatase is related to reduction in growth and soluble protein in earthworms contaminated by pesticides (Mosleh et al., 2003 c). Therefore, sensitivity of *E. fetida* to chlorpyrifos, as evident from the activity of alkaline phosphatase, can not be ignored. The present results also indicated that ability of chlorpyrifos to inhibit acetylcholinesterase activity was no less than carbaryl. Endosulfan, on the other hand, did not affect acetylcholinesterase activity because, it was known to inhibit gamma amino butyric acid instead of acetylcholinesterase (Klassen and Watkins, 1999).

CONCLUSION

It is concluded from the present study that application of carbaryl and endosulfan in the agricultural fields at the current recommended agricultural dose (RAD) is ecologically most dangerous for soil agro-ecosystems. Growth and reproduction of earthworms, the most conspicuous soil organism, are severely affected by these two insecticides at doses much lower than their RAD. Careful monitoring of chlorpyrifos is also required to check that its wide spread uses do not cross RAD of this insecticide.

ACKNOWLEDGEMENTS

We thank the Head, Department of Zoology, University of Kalyani and Principal, Raja N.L. Khan Women's College for providing necessary laboratory facilities. Financial assistance from CPE-UGC and DST-FIST to Raja N. L. Khan Women's College and DST-PURSE to University of Kalyani are thankfully acknowledged.

REFERENCES

Amorim, M. J., J. P. Sousa, A. J. A. Nogueira, and A. M. V. M. Scares. 2002. "Bioavailability and toxicokinetics of C-14-Lindane (Gamma-HCH) in the enchytraeid *Enchvtraeus albiduf*, in two soil types: The aging effect". *Arch. Environ. Contam. Toxicol.* 43: 221-228

Bustos-Obregon, E., and R. I. Goicochea. 2002. "Pesticide soil contamination mainly effects earthworm male reproductive parameters". *Asian. J. Androl.* 4(3):195-199

Conder, J. N., and R. P. Lanno. 2000. "Evaluation of surrogate measures of cadmium, lead and zinc bioavalability to *Eisenia fetida*". *Chemosphere.* 41:1659-1668

Ellman, G. L., K. D. Courtney, V. J. R. Andres, and R. M. Feathertone. 1961. "A new and rapid colorimrtric determination of acetylcholinesterase activity". *Biochem. Pharmacol.* 7: 88-95

Gomez, K. A., and A. A. Gomez. 1984. *Statistical procedures for agricultural research.* 2nd ed., Wiley-Interscience , NY.

Holmstrup, M. 2000. "Field assessment of toxic effects on reproduction in the earthworms *Apporrectodea longa* and *Aporrectodea rosea*". *Environ. Toxicol. Chem.* 19:1781-1787

Helling, B., S. A. Reinecke, and A. J. Reinecke. 2000. "Effects of the fungicide copper oxychloride on the growth and reproduction of *Eisenia fetida* (Oligochaeta)". *Ecotoxicol. Environ. Saf.* 46(1): 108–116

Ismail, S. A. 1997. *Vermicology- the biology of earthworms.* Orient Longman, Chennai, India.

Klassen, C. D., and J. B. Watkins. 1999. *Casarett and Doull's toxicology: the basic science of poisons.* 5th ed., McGraw Hill, NY.

Lowry, O. H., N. R. Roberts, W. U. Mei-Ring, W. S. Hixon, and E. J. Crawford. 1951. "The quantitative histochemistry of brain enzyme measurements". *J. Biol. Chem.* 207: 19

Mosleh, Y. Y., S. Paris-Palacios, M. Couderchet, and G. Vernet. 2002. "Biological effects of two insecticides on earthworms (*Lumbricus terrestris* L.) under laboratory conditions". *Mededelingen Rijksuniversiteit te Gent. Fakulteit van de Landbouwkundige en Toegepaste Biologische Wetenschappen.* 67(2): 59–68

Mosleh, Y. Y., S. Paris-Palacios, M. Couderchet, and G. Vernet. 2003 a. "Effects of the herbicide isoproturon on survival, growth rate, and protein content of mature earthworm (*Lumbricus terrestris L.*) and its fate in the soil". *Appl. Soil Ecol.* 23:69–77

Mosleh, Y. Y., S. Paris-Palacios, M. Couderchet, and G. Vernet. 2003 b. "Acute and sub-lethal effects of two insecticides on earthworms (*Lumbricus terrestris*) under laboratory conditions". *Environ. Toxicol.* 18: 1–8

Mosleh, Y. Y., S. M. M. Ismail, M. T. Ahmed, and Y. M. Ahmed. 2003 c. "Comparative toxicity and biochemical responses of certain pesticides to the mature earthworm *Aporrectodea caliginosa* under laboratory conditions". *Environ. Toxicol.* 18: 338-346

OECD. 1984. *Guidelines for testing of chemicals No 207, Earthworm Acute Toxicity Test.* Organization for Economic Co-Operation and Development, Paris, France.

OECD. 2004. *Guidelines for testing of chemicals No 222, Earthworm Reproduction Test. (Eisenia fetida/andrei).* Organization for Economic Co-Operation and Development, Paris, France.

Walter, K., and C. Schutt. 1974. "Acid and alkaline phosphatase in serum". In H. U. Bergmeyer (Ed.), *Methods of Enzymatic analysis*, pp.856-864. Academic Press, NY.

Zhu, G., H. Wu, J. Guo, and F. M. E. Kimaro. 2004. "Microbial degradation of fipronil in clay loam soil". *Water. Air. Soil. Poll.* 153(1): 35-44

COST EFFECTIVE ENVIRONMENTAL MAGNETIC FIELD MITIGATION BY ACTIVE LOOPS NEAR POWER LINES

Ayman Aboud (Electrical Engineering Department, Fayoum University, Fayoum, Egypt)
Hussein Anis (Electric Power Department, Cairo University, Cairo, Egypt)

ABSTRACT: In this paper, the two most relevant components of the shielding action are considered, namely, reduction in magnetic field intensity near the power line and the cost involved in the shielding process. It is required to simultaneously maximize mitigation while minimizing the cost involved in the mitigation technique. The paper formulates an optimization problem in which a fitness function combines the above two factors. Optimization is based on genetic algorithm optimization. The paper uses a number of different power lines as case study. The results are compared to the cases when the cost element is ignored and the focus is then only on reducing the magnetic field in a specific area in the vicinity of a power line.

INTRODUCTION

The potential hazard due to exposure to magnetic fields produced by electric power systems and installations still represents a public and environmental concern and raises valid questions concerning safe limits of such exposure (Aboud and Anis, 2009; Svendsen et al., 2007; McBride et al., 1999). Shielding by active loops is one of the most effective means of mitigating magnetic field in the neighborhood of high voltage power lines (Memari et al. 1996; Reta-Herna´ndez, et al. 1998; Celozzi, 2002; Celozzi et al. 2004;).

At the time when more current injected in the shielding conductors ensures more efficient mitigation the conductor material plays an opposite role, where larger conductor cross sections, which allows more current to flow, cost more. In this paper, the two components of the shielding action are considered: (1) reduction in magnetic field intensity near the power line and (2) the cost involved in the shielding process. It is required to simultaneously maximize mitigation while minimizing the cost involved in the mitigation technique. The primary element of cost is the shielding conductor material. Other cost elements involved in the process of shielding, e.g. cost of joints on line towers, labor, etc., can be neglected. The cost of conductor material, in turn, is proportional to the conductor cross-sectional area. The cross section of the shielding conductor relates to both the above factors. Increasing shielding conductor cross sectional reduces the conductor resistance and allows the magnetic field-induced voltage to pass more current into the shielding conductor thus improving mitigation, which is contrary to the then increased cost. The paper formulates an optimization problem in which a fitness function combines the above two factors.

Evolutionary computation lends itself to solving this optimization problem, where it enjoys the advantage that it uses probabilistic rather than deterministic transition rules. It uses payoff information (fitness function), not derivatives, and it works with a coding of solution set, not the solutions itself (Sivanandam and Deepa, 2008). In this paper, Optimization is based on genetic algorithm optimization. The problem seeks the best combination of shield conductors' locations, the active shielding current's magnitude and phase and the cost of those conductors. To be able to combine the above two components in the same fitness function it was necessary to determine the relative relevance (weight) of each component to the combined function. The paper first examines the impact of shield conductor size on magnetic field mitigation to determine its weight. The relation between conductor size and cost is then investigated to determine the weight of its role. It is noted that –within the range of conductor sizes used for sub-transmission and transmission lines- the conductor price per ton is nearly constant, a fact which

---

ISBN 9780976885351

makes the cost linearly related to the conductor's cross section for a given line length. The paper uses a number of different power lines as case study. The results are compared to the cases when the cost element is ignored and the focus is then only on reducing the magnetic field is a specific area in the vicinity of a power line. The trade-off between field mitigation and cost is quantitatively assessed**.**

MATERIALS AND METHODS

Impact of Shield Conductor Size: To demonstrate the effect of shield conductor size on the efficiency of mitigation the results shown in Figure 1 are produced. It is evident that decreasing the resistance of the active shield circuit by using larger conductors, without changing the position of those conductors, improves magnetic field mitigation –as expressed by the rise in the field reduction factor.

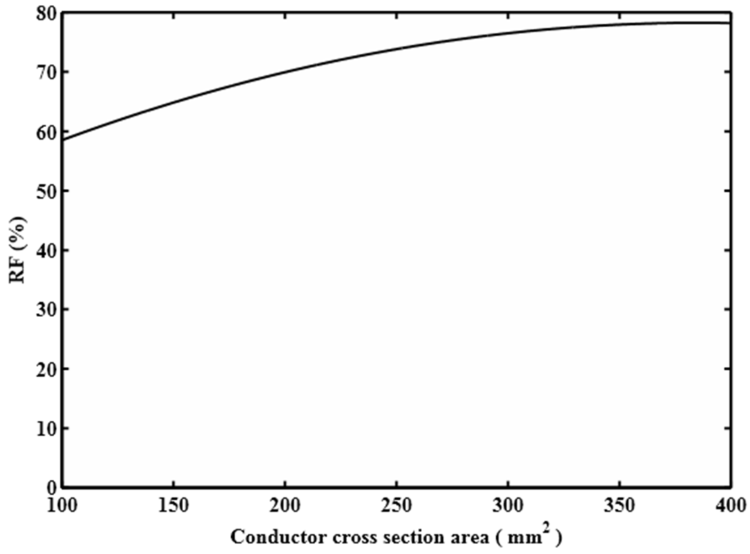

FIGURE 1 REDUCTION FACTOR VS. CONDUCTOR CROSS SECTIONAL AREA FOR 500 KV LINE.

Cost of Shield Conductor Material. By soliciting current market prices of conductors, it is found out that –within the range of conductor sizes used for sub-transmission and transmission lines- the conductor price per ton is constant. This fact makes the cost linearly related to the conductor's cross-sectional area (CSA) for a given length. By setting the price of the phase conductors (500 mm^2 for 500 kV lines and 250 mm^2 for 66 kV lines) as base, the per-unit conductor cost C_{pu} is related to its CSA by

$$C_{pu} = 0.2\,a \quad \text{for 500 kV lines} \tag{1}$$

$$C_{pu} = 0.4\,a \quad \text{for 66 kV lines} \tag{2}$$

Where, a, being the shield conductors CSA in mm^2.

Fitness Function. Optimization is based on genetic algorithm optimization. The fitness function in that algorithm is made up of two components, one relating to targeted reduction in magnetic field intensity and the other relates to cost. It may thus take the form:

$$F = \frac{w_1\,RF + w_2\,S}{w_1 + w_2} \tag{3}$$

Where,

RF is magnetic field reduction factor
S= (1- C_{pu}) is the cost saving

The two components (RF and S) of the fitness function are weighted by factors w_1 and w_2, which determine the relative relevance of the two components.

RF Weight Factor (w_1). The weight w_1 could be determined by showing the effect of active current on the magnetic field reduction factor RF, which is demonstrated in Figures 2 and 3 for 500 kV and 66 kV lines, respectively. The weight w_1 is arbitrarily taken as the relative increase in RF over the range of active current values relative to the RF's maximum value, which in this case equals to 0.32 and 0.63 for 500 kV and 66 kV lines, respectively. It is worth mentioning that the point at which the active current is zero corresponds to the case of passive shielding.

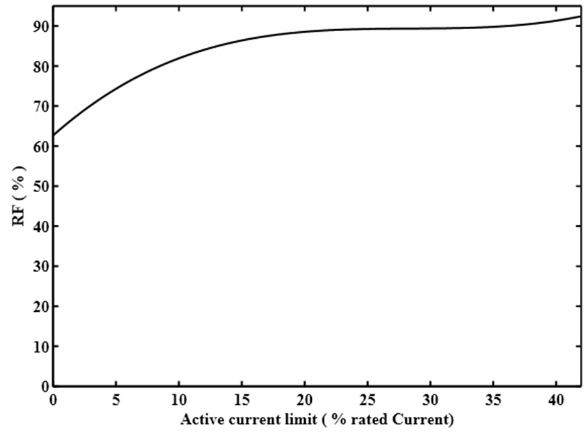

FIGURE 2 ACTIVE CURRENT LIMITS FOR 500 kV LINE

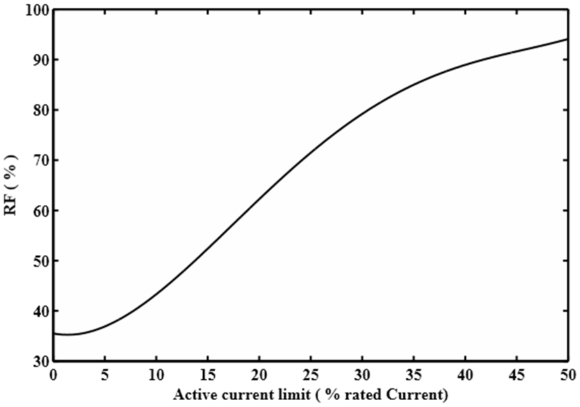

FIGURE 3 ACTIVE CURRENT LIMITS FOR 66 kV LINE

Cost Saving Weight Factor (w_2). The weight w_2 could be determined in light of the influence of shield conductor's cross sectional area on the induced current in the shielding loop. This is demonstrated in Figures 4 and 5 for 500 kV and 66 kV lines, respectively. The weight w_2 is arbitrarily taken as the rise in induced current -as the CSA reaches a maximum value equal to the phase conductors' CSA- relative to the induced maximum current, which in the present cases equals to 0.45 and 0.17 for the 500 kV and 66 kV lines of the rated line current, respectively.

Evolutionary Computational Application. Possible algorithms that can serve the paper's prime goal have been investigated, namely, optimizing the cost-effective fitness function, where mitigation would be ensured to be effective. The evolutionary computational approach, customarily known as the genetic algorithm, appears to lend itself well to the problem as it inherently–during the optimization process-avoids falling into local optima and thus producing less than accurate results (Rao, 2009).

Genetic Algorithms (GAs) simulate the natural evolutionary process in searching for the best solution based on the mechanism of natural selection and natural genetic operation. The evolution starts from a population of completely random solutions and searches for the best generation by generation. In each iteration, multiple solutions are stochastically selected from the current population, modified (mutated or recombined) to form a new population, which is used in the next iteration.

The identification of the coefficients present in the reduction factor is made using a genetic algorithm, with the following characteristics:

i. Population size: 100

ii. Fitness function: F (equation 3)
iii. Selection operator: Roulette
iv. Mutation operator: Adaptive feasible
v. Crossover operator: Two point
vi. Probability of crossover: 0.8
vii. Stopping criteria: Stall (20 generations)

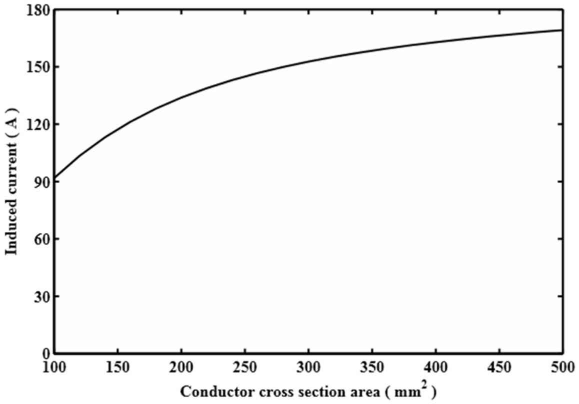

Figure 4 Conductor cross sectional area vs. induced current for 500 kV line

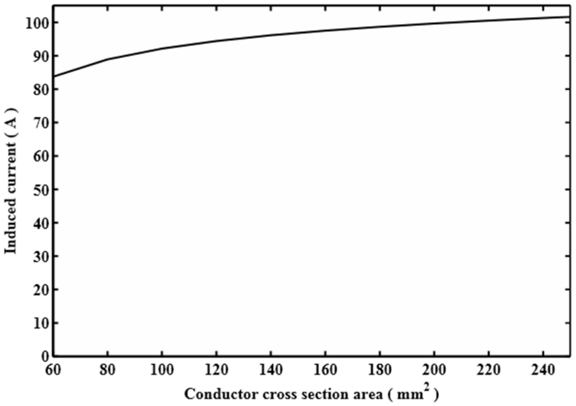

Figure 5 Conductor cross sectional area vs. induced current for 66 kV line

RESULTS AND DISCUSSION

Tables 1 and 2 summarize the results obtained by using the proposed algorithm, while Figures 6 and 7 display the field mitigation for the different cases.

The obtained results show that accounting for the factor of cost in the optimization process is appropriate, since in case of 500 kV line the cross section area of shield conductor decreased by 60% (from CSA =500 mm^2 without considering cost to 200 mm^2 when cost was accounted for). The corresponding sacrifice in the field reduction was relatively small (the field reduction factor went down from RF = 87% without cost consideration to 75.7% when cost was accounted for). In case of 66 kV line the cross section area of conductor decreased by 58.4% (from CSA =250 mm^2 without considering cost to 146 mm^2 when cost was accounted for) with a corresponding small sacrifice in the reduction factor (the field reduction factor went down from RF = 78.6% without cost consideration to 74.7% when cost was accounted for).

Table 1 Active Loop Conductor Coordinates And Currents

Line	w_1	w_2	Loop coordinates		I_{act} (% I_{rated})	phase angle
			(x_1, y_1)	(x_2, y_2)		
500 kV	1	0	(20.8, 7.4)	(-20.9, 6.6)	20	-9.9°
	0.5	0.5	(21.5, 6.5)	(-9.8 , 10)	20	272 °
	0.32	0.45	(22, 5.3)	(-7.9, 9.7)	20	291°
66 kV	1	0	(10,14.6)	(6.7, 5.3)	30	-94.7°
	0.5	0.5	(5.6, 5.2)	(4.3, 14.9)	30	82°
	0.63	0.17	(5.4, 5)	(4.7, 14.8)	30	81°

Table 2. Field Reduction Factor, Cost Saving and Cross Sectional Area

Line	w_1	w_2	RF	Cost saving (%)	Cross sectional area (mm^2)
500 kV	1	0	87.6	0	500
	0.5	0.5	80.2	23.8	381
	0.32	0.45	75.7	60.0	200
66 kV	1	0	78.6	0	250
	0.5	0.5	71.6	51.6	121
	0.63	0.17	74.7	41.6	146

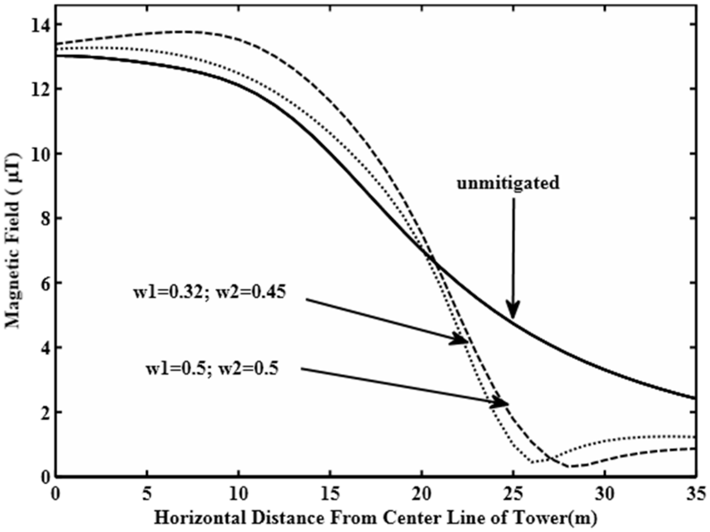

Figure 6 Magnetic Field Distributions for Single-Circuit 500 kV Line

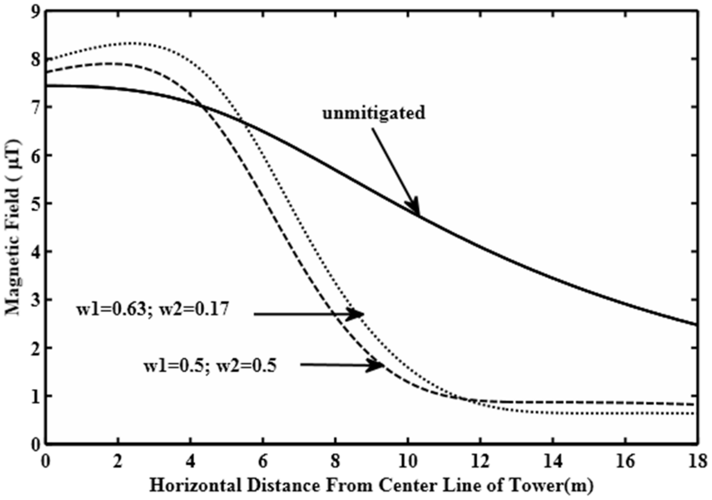

Figure 7 Magnetic Field Distributions for Double-Circuit 66 kV Line

CONCLUSIONS

Magnetic fields can be effectively reduced near power lines using active shield conductors. Targeting cost effective magnetic field mitigation represents an improvement over designing a mitigating arrangement without due consideration to cost.

Accounting for the cost of material of shielding conductors results in significant differences in shielding conductor location by as much as 50%.

Saving on conductor material cost causes inevitable slight sacrifices in field reduction, which are less than 8%.

Using optimization techniques an overall magnetic field reduction in the power line vicinity while simultaneously minimizing the cost involved in the mitigation technique.

The use of genetic algorithms, in particular, allows proper application of the newly cost-effective mitigation technique, where it seeks an efficiently quasi-optimal solution that would otherwise be difficult to find due to the number of parameters involved in the optimization problem.

REFERENCES

Aboud A., and H. Anis. 2009. "Probabilistically-Based Risk of Exposure to Power Lines Magnetic Fields" *J. Electric Power Components and Systems*, 37(11): 1241-1259.

Svendsen A. L., T. Weihkopf, P. Kaatsch, and J. Schuz. 2007. "Exposure to magnetic fields and survival after diagnosis of childhood leukemia: a German cohort study". *Cancer Epidemiol Biomarkers*. 16(6): 1167-1171.

McBride M.L., R.P. Gallagher. 1999. "Power-frequency electric and magnetic fields and risk of childhood leukemia in Canada". *American Journal of Epidemiology*, 149 (9): 831–842,.

Memari A.R., W. Janischewskyj. 1996. "Mitigation of magnetic field near power lines". IEEE Trans. Power Delivery 11(3): 1577–1586.

Reta-Herna´ndez M. and G. Karady. 1998. "Attenuation of low frequency magnetic fields using active shielding". *Electric Power Systems Research*. 45(1):57-63

Celozzi, S. 2002. "Active compensation and partial shields for the power frequency magnetic field reduction". *Proc. IEEE Int. Symp. On Electromagnetic Compatibility*, 222–226

Celozzi S., and F. Garzia. 2004. "Active shielding for power-frequency magnetic field reduction using genetic algorithms optimization". *IEE Proc.-Sci. Meas. Technol.*, 151(1): 2-7.

Sivanandam S. N., S. N. Deepa. 2008. *Introduction to Genetic Algorithms*. Springer-Verlag, Berlin.

Rao S.S. 2009. *Engineering optimization: theory and practice*. 4th ed.,Wiley.

THE CONCEPT OF ECOSYSTEM MANIPULATION: WHAT IS IT, AND HOW DOES IT WORK IN BIOREMEDIATION?

Guangzhi Sun, and Kirsten Heimann (James Cook University, Townsville, Australia)

ABSTRACT: This paper discusses how the general efficiency of a natural wastewater treatment system can be classified as being inherently, passively or actively efficient. A new concept, ecosystem manipulation, is described. Rather than providing a specific set of tools and methods, this concept reflects the philosophy of inherent efficiency that should be embedded in the design of natural wastewater treatment or other pollution control systems. Three case studies are presented to illustrate how this concept was instinctively adopted in the past.

INTRODUCTION

According to their main source of energy, wastewater treatment (or bioremediation) systems can be classified into two broad groups: conventional (steel-and-concrete) treatment systems, and natural systems (also known as ecological or green systems). Steel-and-concrete systems, such as an activated sludge plant, are typical energy-intensive but highly efficient in terms of pollutant mass removal. Natural systems, such as constructed wetlands and facultative ponds, are land-intensive but energy-efficient, i.e. they occupy larger land surfaces but consume smaller amounts of energy in the treatment of each m^3 of wastewater (Brix, 1999). Since the mid-1990s, natural treatment systems (in particular, the constructed wetlands) have been increasingly used in water pollution control, partly spurred by the rising cost of fossil fuel energies and concern about climate change.

Considerable progress has been made to understand pollutant degradation mechanisms, effects of environmental factors, and identities of microbial communities in natural treatment systems. However, significant knowledge gaps, and many design and operating problems, still remain. Constructed wetlands, for example, often have poor performances in terms of total nitrogen removal that are caused by conflicting requirements for environmental conditions (such as redox potential), and shortage of substances for microbial activities (such as organic carbon for denitrification). To further improve the competitiveness and robustness of the natural systems, it is desirable to: (1) increase pollutant mass removal rate per m^3 of system volume (or m^2 of land surface) by providing optimal environmental conditions for microbial activities and various physico-chemical processes, and (2) direct the mass flow of substances to avoid the addition of extra chemical substance into the system (such as to avoid adding methanol to aid denitrification), or alter the routes of substance mass flow to reduce pollution effect (such as assimilating carbon dioxide into algae cells, instead of releasing into the atmosphere as greenhouse gas).

Achievement of the above objectives requires continual research and discovery in process mechanisms and environmental conditions in the natural treatment systems. At the same time, it also requires a new way of thinking to be embedded into research and design. Similar to the principle used in process safety, an effective bioremediation or wastewater treatment system may be considered as being *inherently*, *passively*, or *actively* effective. For example, when a well designed vertical flow wetland is used to remove ammonia by nitrification, the inherent character (natural upwards air circulation, growth of nitrifying bacteria, etc) of the wetland will facilitate the nitrification process. If a temporary adverse condition occurs, such as a large dose of biodegradable organics enters into the wastewater that restricts the activities of nitrifying bacteria, the character of the vertical flow system will tend to re-establish nitrification process once the adverse condition passes - in this case, the organics will eventually be degraded albeit it may takes some time. An example of passive efficiency is the use of a subsurface

---

ISBN 9780976885351

horizontal flow wetland for denitrification - its efficiency will depend on external conditions such as the availability of organic carbon and sufficiently low dissolved oxygen level for denitrification bacteria to function. The characters of the horizontal flow wetland neither facilitate nor restrict the denitrification process. A hypothetical example of active efficiency is the use a horizontal flow wetland for nitrification process. In this case, compressed air must be supplied so that the activities of nitrifying bacteria can be sustained; once the active support (i.e. compressed air) is removed, the character of the system will tend to inhibit nitrification. As such, the preference for effective functioning of a pollution control system is:

Inherent → Passive → Active

When a system is designed for bioremediation of contaminated water, how inherent efficiency can be embedded into the system will depend on up-to-date research development, e.g. understanding about various factors affecting pollutant removal processes. Although many knowledge gaps still remain, rapid advance in various green technologies in recent years has opened up the possibility of such approach. For example, it is now possible to meticulously arrange (manipulate) different media (which have major effects on microbial population and environmental conditions such as redox potential, alkalinity, dissolved oxygen, etc), or sequence of events (such as various steps of nitrogen transformations), in a treatment wetland system to improve its efficiency. The approach of building inherent efficiency into an ecological treatment system may be named *ecosystem manipulation* (or *ecosystem coordination*), to reflect the distinct philosophy behind such approach.

Without stressing the principle behind it, ecosystem manipulation has been practiced in the past, in wastewater treatment and control of greenhouse gas emission. Here, three case studies are briefly described: (1) a combined tidal-vertical flow wetland system that generates temporal variations in DO level to improve organics removal; (2) a lab-scale wetland system with unconventional media arrangement to enhance total nitrogen removal as a result of inherent efficiency; and (3) a microalgae growth study that demonstrates the potential of assimilating CO_2 into algal biomass.

CASE STUDY I

System Description. A constructed wetland system was installed near a pig farm at Rugeley, UK, to treat agricultural (piggery) wastewater at a fixed flow rate of 2 m^3 per day (Sun, 1999). As shown in Figure 1, the system was arranged to form four treatment stages: stage 1 - tidal flow wetlands; stage 2 - vertical flow wetlands without effluent recirculation; stages 3 and 4 - vertical flow wetlands with recirculation. All wetland cells were packed with river gravel as main media where common reeds, *Phragmites australis*, were planted.

The intention of such system arrangement was to generate regular water level fluctuations in the tidal flow stage to improve aeration, as the rising and falling tides acted as air 'pumps', whereas the subsequent stages supported further removal of organics (stage two) and nitrification (stages three and four). The system was operated continuously for three months. As intended, rhythmical water and air movement in the tidal flow part of the system was generated by controlling the operation of the pumps. Water samples were collected on a weekly basis from the feed tank and outlets of each stage, and analysed for BOD_5, COD, SS, NH_4-N, NO_3-N, NO_2-N, PO_4-P and pH.

Results and Discussion. Table 1 presents the average performances of the system during the experimental period. A unique character of the system is its high efficiency in the removal of organic matter; on average, BOD was reduced by 98%, and COD by 71%. Compared with the efficiency of BOD_5 removal (74%) achieved in a previous study on the same system without tidal flow operation (Sun et al, 1998), the performance had clearly improved. No experimental data are available to compare how the robustness (such as its performance after a spike of influent BOD value or flow rate) of the system may differ if it is operated with and without the artificial tides. Nevertheless, it is logical to consider that if a disturbance in the operating condition had occurred (such as temporary anoxic condition due to pollutant overload), the regular aerations of the tidal flow wetland matrices would have facilitated the activities of heterotrophic bacteria, leading towards the re-establishment of high BOD removal efficiency. Thus, the tidal flow part of the wetland system has inherent character to provide aerobic condition for its intended function (i.e. bulk removal of organic matter).

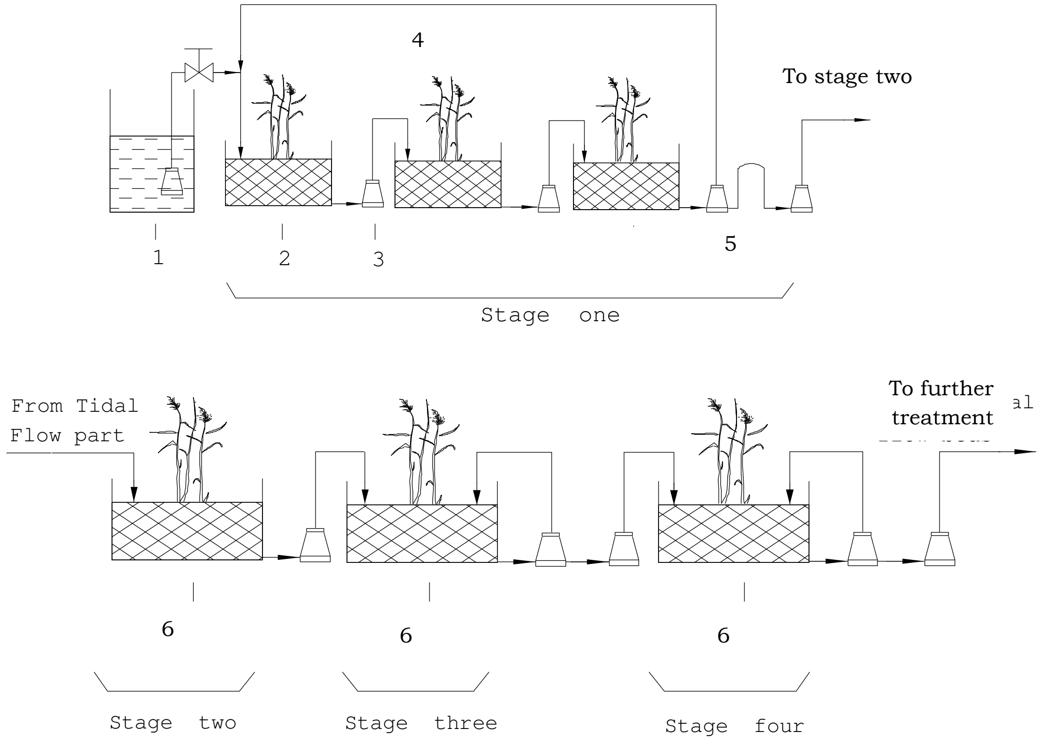

FIGURE 1. Combined tidal-vertical flow wetland system at Rugeley (1-feed tank; 2-tidal flow wetland cell; 3-pump; 4-*Phragmites*; 5-water level control; 6-vertical flow wetland cell)

TABLE 1. Performances of the combined tidal-vertical flow wetland system

	Influent	Stage one outlet	Stage two outlet	Stage three outlet	Stage four outlet	Total removal, %
BOD_5, mg/L	1100	452	295	50	26	98
COD, mg/L	1465	965	827	463	421	71
SS, mg/L	677	397	300	137	118	83
PO_4-P, mg/L	70.4	54.5	48.1	33.7	31.6	55
NH_4-N, mg/L	330	190	136	28.0	22.9	93
NO_2-N, mg/L	3.9	32.9	28.1	4.1	2.0	---
NO_3-N, mg/L	1.4	24.6	55.8	176	182	---
pH	7.8	7.3	7.3	5.7	5.6	---

Note: The above results represent the average of 18 sets of data.

CASE STUDY II

System Description. A pilot-scale hybrid wetland system was studied for the treatment of a tannery wastewater (Saeed et al, 2012). The hybrid system consisted of three treatment stages, a vertical flow (VF) wetland as the first stage, followed by a horizontal flow (HF) wetland as the second stage, and another VF wetland as the third stage, as illustrated in Figure 2. The length, width, and height of the HF unit were 1.32, 1.01, and 0.78 m, respectively. The height and diameter of each VF wetland were 0.73 and 0.91 m, respectively. The main media of the VF systems was 0.6 m deep, overlying on large stones (that added additional depth of 0.1 m) to facilitate effluent drainage.

Three different substrates (i.e. organic coco-peat, cupola slag, and pea gravel) were employed as the main media. The first stage VF wetland (A) was packed with organic coco-peat, extracted from coconut husks (size 1.2-2.3 mm). The HF wetland (B) was packed with cupola slag, a by-product of cast iron melting process; the size of the employed cupola slag ranged 19-20 mm. The final stage VF wetland (C) was packed with pea gravel of size 1.2-2.3mm range.

The intention of system design was to seek inherent efficiency in all three treatment stages. Stage 1 was designed to utilise the character of greater void space to enhance aerobic degradation of organic matter, while utilising packed coco-peat media to provide anaerobic micro-zones to allow simultaneous nitrification and denitrification. The intended function of the second stage was to remove phosphorus by adsorption on the slag media, while stage 3 was designed to provide final polishing of the effluent.

The hybrid system was manually dosed with the tannery wastewater, on a daily basis, for 18 weeks; giving theoretical hydraulic retention time of 4.80, 12.5 and 2.43 d in wetlands A, B and C, respectively. During the experiment, 10 sets of samples were collected from the influent and effluent of each stage. The samples were analysed for values of pH, Eh, DO, NH_4, NO_2, NO_3, PO_4, total solids (TS), BOD_5, and COD.

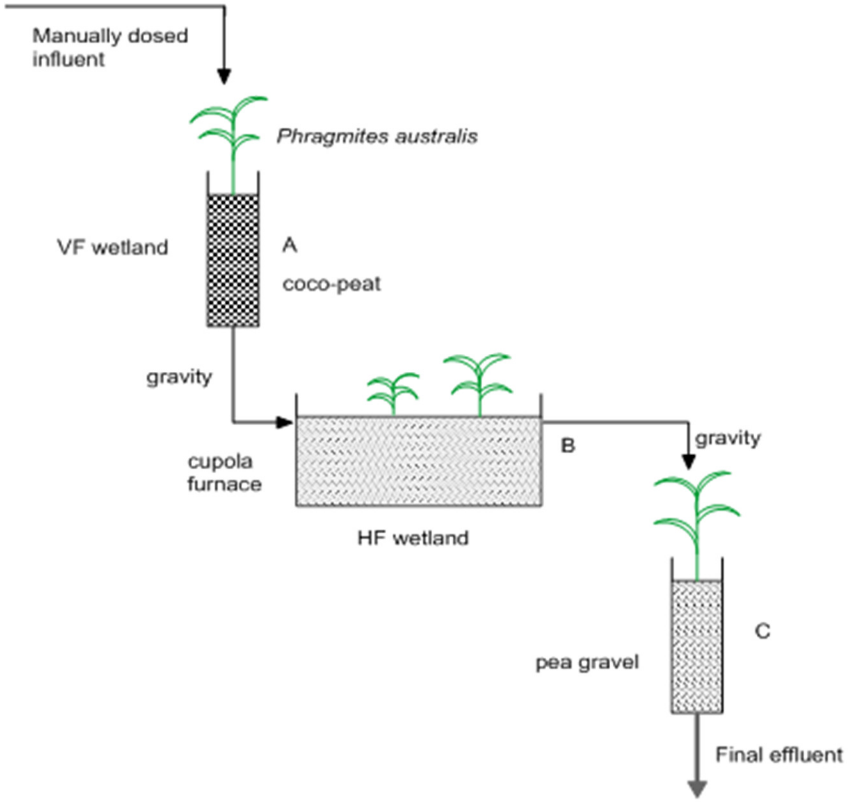

FIGURE 2. Schematic diagram of the pilot-scale wetland system treating tannery wastewater

TABLE 2. Average performances of the hybrid wetland system (SD in brackets)

Para-meter	Unit	Influent	VF wetland (A) *(Coco-peat media)*		HF Wetland (B) *(Cupola slag media)*		VF wetland (C) *(Pea gravel media)*		Overall removal %
			Effluent	Removal %	Effluent	Removal %	Effluent	Removal %	
BOD	g L^{-1}	4.2 (2.8)	0.9 (0.6)	78	0.3 (0.2)	66	0.08 (0.04)	73	98
COD	g L^{-1}	11.5 (6)	4.9 (3.6)	57	1.2 (0.4)	75	0.2 (0.06)	83	98
PO$_4$	mg L^{-1}	30 (10)	15 (7)	48	6 (2)	61	3 (1)	34	87
NH$_4$	mg L^{-1}	111 (39)	53 (20)	52	41 (13)	22	15 (12)	62	86
NO$_2$	mg L^{-1}	4.3 (1.8)	5.4 (5.7)	---	21.3 (26.0)	---	16.8 (16.5)	21	---
NO$_3$	mg L^{-1}	66 (35)	30 (14)	54	22 (6)	25	33 (12)	---	50
DO	mg L^{-1}	0.02 (0.01)	0.04 (0.02)	---	0.06 (0.03)	---	0.12 (0.03)	---	---
E$_h$	mV	-317 (122)	-187 (117)	---	-81 (92)	---	47 (78)	---	---
pH*	---	7.5-9.2	6.5-7.5	---	7.5-7.9	---	5.7-7.3	---	---

*Note: value range (minimum to maximum) is provided for pH

Results and Discussion. Table 2 indicates mean pollutant removal performances across each wetland unit. As intended, the first stage VF wetland provided simultaneous NH$_4$, NO$_3$ and organics removal, under high pollutant loadings. Second stage HF wetland removed 61% PO$_4$ and 75% COD, due to absorption ability of the cupola slag media, while the last stage VF wetland (C) provided further ammonia and organics removal. On average, NH$_4$ and NO$_3$ mass removal rates across the whole system reached up to 6 and 2 g m^{-2} d^{-1}, respectively. The system also produced average removal of 249 g m^{-2} d^{-1} for BOD, and 678 g m^{-2} d^{-1} for COD. In terms of pollutant mass removal rates, the hybrid system was one of the most efficient constructed wetland systems reported in literatures. The combination of different media, and arrangement of the three treatment stages, allowed different microbial and physico-chemical processes to take place in appropriate sequence (simultaneous organics and nitrogen removal, followed by phosphorus removal, followed by organics removal); helping to sustain the high efficiency of the system.

CASE STUDY III

The concept of ecosystem manipulation (or coordination) was instinctively adopted in this study (Huerlimann et al, 2010), as four species of microalgae (*Nannochloropsis* sp., *Isochrysis* sp., *Tetraselmis* sp., and *Rhodomonas* sp.) were investigated for their growth efficiency in three different media. Measured by biomass and lipid productivity (in mg L^{-1} d^{-1}), the study discovered that *Tetraselmis* sp. is the species of choice among the tested species, for large-scale cultivation of microalgae for biomass or lipid production. The cultivation of microalgae has the potential to immobilise carbon dioxide generated at an industrial source (such as a power generation plant) into algal biomass, instead of releasing it into the atmosphere as a greenhouse gas. The main products of the cultivation, algal lipids, have a diverse range of applications; they can be used as raw materials for biodiesel production, as ingredients of animal feedstock, or as food additives. The assimilation of CO$_2$ into algal biomass effectively interferes (manipulates) carbon mass flow, with two-fold benefits: (1) high level of CO$_2$ sequestration into biomass to control air pollution, and (2) the transformation of CO$_2$ from a pollutant into a valuable product.

CONCLUSIONS

Ecosystem manipulation refers to the approach of managing the environmental conditions (such as redox potential) in a pollution control system, and altering material mass flow (such as the flow of carbon dioxide), to optimise pollutant removal efficiency via microbial and physico-chemical processes. Three case studies, which reflect such approach, have been briefly introduced. In each case, discussion is made on how improved system performance, or potential benefit, becomes obtainable by instinctively embedding inherent efficiency in experiment design.

REFERENCES

Brix, H. 1999. "How 'Green' are Aquaculture, Constructed Wetlands and Conventional Wastewater Treatment Systems". *Water Sci. Technol.*, 40(3): 45-50.

Huerlimann, R, R. de Nys, and K. Heimann. 2010. "Growth, Lipid Content, Productivity, and Fatty Acid Composition of Tropical Microalgae for Scale-Up Production". *Biotechnol. Bioeng.*, 107: 245-257.

Saeed, T., F. Azam, Z. Quiyum, A. E-Rabbi, and G. Sun. 2012. "Tannery Wastewater Treatment in a Pilot-Scale Wetland System with Coco-Peat, Slag and Gravel Media". Submitted to: *13th International Conference on Wetland Systems for Water Pollution Control*. To be held in 25-29 November, Perth, Australia.

Sun, G. 1999. *Treatment of High Strength Wastewaters in Constructed Reed Bed Systems*. PhD thesis. The University of Birmingham, UK.

Sun, G., K.R. Gray, and A.J. Biddlestone. 1998. "Treatment of Agricultural Wastewater in Downflow Reed Beds: Experimental Trials and Mathematical Model". *J. Agr. Eng. Res.*, 69: 63-71.

MAPPING AND ANALYZING TRADEOFFS BETWEEN ECOSYSTEM SERVICES UNDER LANDSCAPE CHANGE

Tao Huang , Chun-Wei Huang , Yu-Pin Lin

(National Taiwan University, Taipei, Taiwan)

ABSTRACT: Human-driven changes in land use typically resulted in large threats on biodiversity and ecosystem service supply. Expanding urban and croplands to meet the needs of a growing population comes at the cost of reduced biodiversity and ecosystem services. Efficient management of ecosystems can sustain the provision of vital ecosystem services. Challenges of ecosystem management are the need for spatial analyst and how to manage multiple ecosystem services across landscapes. The article presents a case study in Keelung River Watershed. In the study, the CLUE model is used to predict the changes of land use/land cover, then applying InVEST, a spatial explicitly model, to estimate the value and spatial patterns of ecosystem services. The results are analyzed spatially and temporally. The study use landscape metrics to quantify the impact of land use composition and configuration on ecosystem services. Furthermore, most of the ecosystem services are lack of model validation. Due to the water flow validation, the study is more reliable than past studies. The aim of the study is to provide a new perspective for future landscape management and decision-making.

INTRODUCTION

Ecosystem service is defined as “The benefits that people obtain from ecosystems (Millennium Ecosystem Assessment 2005), including provisioning services, such as food, freshwater, and fibre; cultural services that provide non-material benefits, such as places for recreation and inspiration; and regulating services that provide benefits due to the regulation of ecosystem processes, such as flood control and climate regulation (Millennium Ecosystem Assessment 2005)”.

Land use has great impact on hydrology, habitat, and ecosystem services. Studies relevant to ecosystem service can be traced back to the 1980s; however, it is still a relatively new research field. R. Costanza (1997) estimated the value of ecosystem services based on biome type. E. Nelson (2009) developed a modeling tool InVEST to determine the cost of ecosystem service.

The purpose of the study is to assess the impact of land use on ecosystem services with the application of InVEST model in watershed scale. With the help of CLUE model, the ecosystem services under future scenarios could be predicted. The flow chart of the study is as follow:

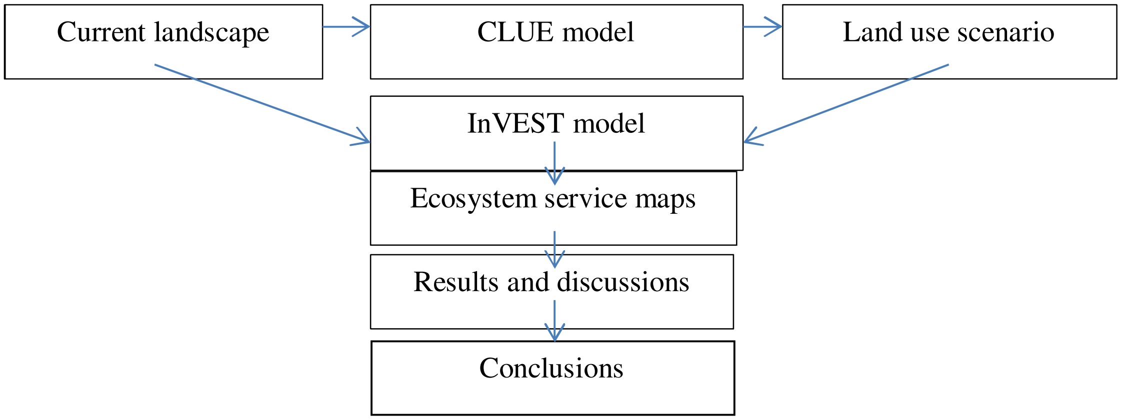

ISBN 9780976885351

STUDY AREA

Wutu watershed is located in Keelung River basin, the size of the watershed is 204 km^2 . The government started prohibiting the harvest of natural forest since 1992, the main land use type is forest in the watershed. Population cluster is the major environmental problem in Keelung River Basin, resulting in the degradation of water quality and habitat quality. The water quality of Hsin-Shan Reservoir is in eutrophication level. For comparing the landscape impact on ecosystem services, the study used baseline (Year 1994) climate condition for water-related ecosystem service simulation for all scenarios.

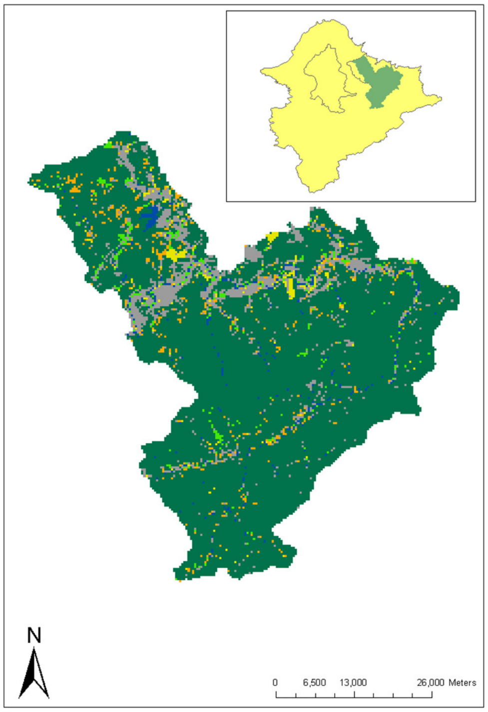

Figure 1. Location of Wutu watershed

METHODS

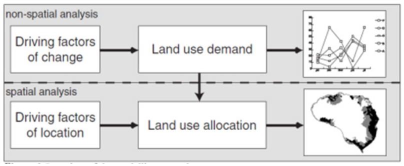

Figure 12 2. Model procedure (Verburg et al., 2004)

Land use modeling. In the study, CLUE model is applied. The CLUE model was developed to simulate land-use change by quantifying empirical relationships between land use and its driving factors by Peter H. Verburg in Wageningen University (Verburg et al. 2004).

Markov chain was used as a stochastic model to make quantitative comparisons of the land-use changes between discrete time periods extending from 1994 to 2008. The relationship between current land-cover and land-use configuration of the study area is established through logistic regression for each land-cover type and a set of defined driving forces. Probability maps for all land uses can be established using logistic regression models.

Ecosystem service modeling. InVEST models the production of a single service in a small area with an "ecological production function" – how provision of that service depends on local ecological variables (eg

Ricketts et al. 2004). InVEST consists of a suite of models that use LU/LC patterns to estimate levels and economic values of ecosystem services, biodiversity conservation, and the market value of commodities provided by the landscape.

Carbon storage. Carbon sequestration as used in this study refers to the ability of vegetation to take up carbon dioxide through photosynthesis and store it for long periods of time in their woody tissues and the soil. To determine how much carbon is stored in an area, the InVEST model estimates above- and below-ground biomass and soil carbon pools as a function of the distribution of present and historic LU/LC and biomass age of a particular area (Nelson et al., 2009).

Water yield. A number of previous ecosystem service studies have used water production, i.e. the volume of water produced by area, as an ecosystem service or as a surrogate for an ecosystem service (Chan et al., 2006). The nature and quantity of hydrologic ecosystem services is intimately linked with the management of the territory, and the capacity of the different land uses to partition rainfall into green (evapotranspiration) and blue (runoff) freshwater flows (Barbara A. Willaarts, 2012). Annual water yield is equal to the precipitation that falls during the course of a year less the water that evaporates or transpires .

Nutrient retention. Export coefficients, developed by Reckhow et al. 1980, are annual averages of pollutant fluxes derived from various field studies. The purification service may be determined by taking the value of the ecosystem as a nutrient sink. The Water Purification Nutrient Retention model calculates the amount of nutrients exported based on export coefficient and retained on every pixel of a watershed.

Soil retention. Although the USLE has been criticized, it is an excellent planning tool for estimating the relative values of varying land uses and conservation measures (Stanley W. Trimble and Pierre Crosson, 2000). In first step, USLE is used to calculate soil loss. In second step, the model estimates how much of the sediment eroded on all pixels will be trapped by downstream vegetation based on the ability of vegetation in each pixel to capture and retain sediment.

RESULTS

Land use simulation. Built-up is the only land use type increased constantly, forest increased in 2008 then decreasing, other land use type decreased.

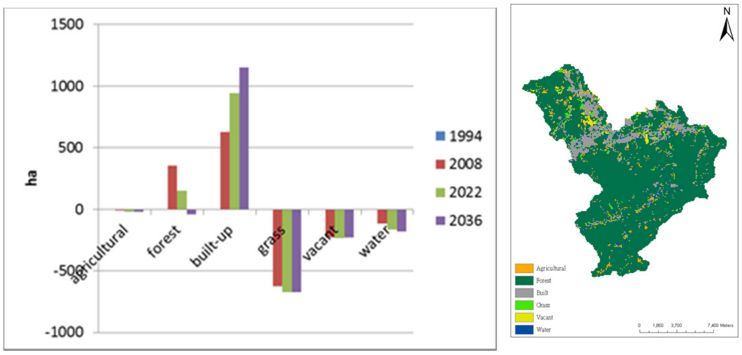

Figure13 3. Land use area change and the distribution map of Year 2036

Ecosystem service simulation. The results are shown in Figure 4.

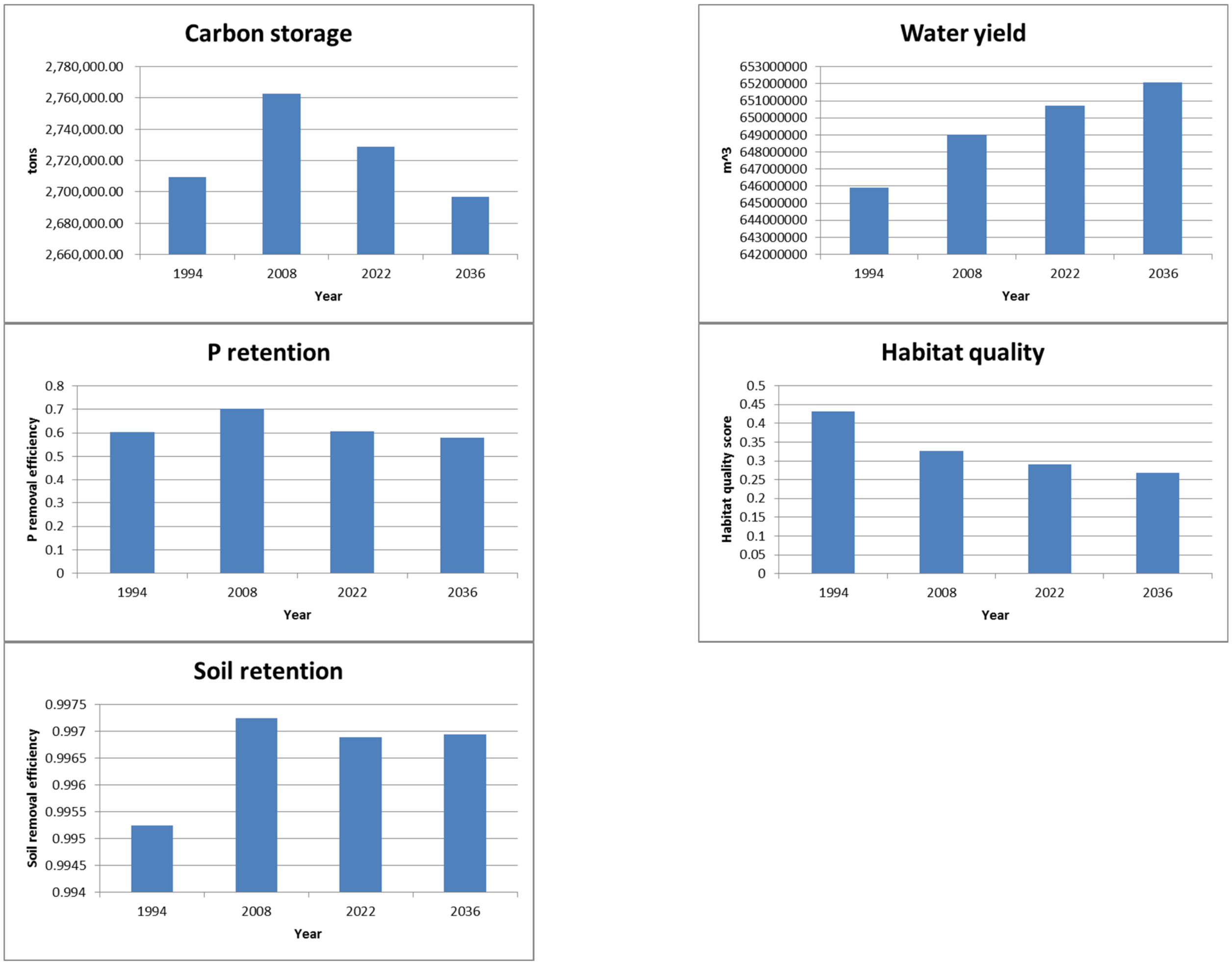

Figure 14 4. Ecosystem service under difference scenarios

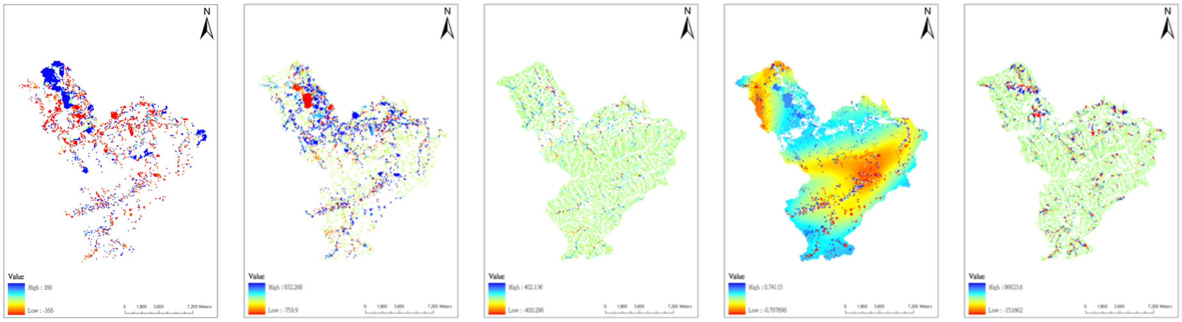

Figure 15 5. Ecosystem service change maps between 2036 and baseline for carbon storage, water yield, P retention, habitat quality, and soil retention

Carbon storage. Carbon storage increased in 2008 due to the increase of forest, then decreasing with the decreasing forest.

Water yield. All the maps show that water yield is high near the stream. The areas with more water yield cluster in 1994, while the areas scatters after 1994. Annual water yield increases because urban areas increase, while urban areas do not take as much water as natural land cover. The study also compared simulation stream flow with observed flow. As table 1 shows, the simulated flow is -0.05978% and -0.04063% lower than observed flow, indicating the model performance is acceptable in the watershed.

Table 1. Model validation (Unit: m^3)

	Observation	InVEST
1994	695053440	653500000
2008	792184320	760000000

Phosphorus retention. Urban growth generated more phosphorus than before, the role of forest to filter the pollution is more important. The trend of P retention is similar as forest area, increasing in 2008 then decreasing.

Habitat quality. As human activities changed over time, one would expect to see corresponding changes in the threats to biodiversity. The habitat quality score decreases with time due to urban expansion. The habitat quality of the North part of the watershed is lower, resulting from the threat post by urban.

Soil retention. Soil retention increased in 2008, decreasing in predicted scenarios. In predicted scenarios, land use conversion mainly occurred in low slope area near the urban, where the service value is low. As a consequence, the service affected less in predicted scenarios.

DISCUSSIONS

The ecosystem services have distinctly different spatial distributions, although some areas are of high value to multiple services and other areas are of low value to many. For example, the mountain areas are characterized by forest cover (accounting for carbon storage) and high quality habitat. In the study, the increase of urban area and decline of forest enhanced water yield, however; resulting in the loss of other services. The main limitation of the study is that the model runs on annual basis and not including many biological interactions.

CONCLUSIONS

With urban expansion, most ecosystem functions were obviously damaged in the watershed. Ecosystem services trade-offs arise from land use management choices made by humans. Increasing urban land will lead to enhancing water yield at the cost of other regulating and supporting ecosystem services. There are some area providing multiple ecosystem services, which are suitable for conservation area to protect both biodiversity and ecosystem services.

REFERENCE

Chan, K. M. A., M. R. Shaw, et al. 2006. "Conservation Planning for Ecosystem Services." PLoS BIOLOGY.

Costanza, R., R. d'Arge, et al. 1997. "The value of the world's ecosystem services and natural capital." NATURE.

Millennium ecosystem assessment .2005. Ecosystems and human well-being.

Nelson, E., G. Mendoza, et al. 2009. "Modeling multiple ecosystem services, biodiversity conservation, commodity production, and tradeoffs at landscape scales." Frontiers in Ecology and the Environment.

Ricketts, T. H., G. C. Daily, et al. 2004. "Economic value of tropical forest to coffee production." PNAS.

Trimble, S. W. and P. Crosson. 2000. U.S. Soil Erosion Rates--Myth and Reality. Science.

Verburg, P. H. and A. Veldkamp. 2004. "Projecting land use transitions at forest fringes in the Philippines at two spatial scales." Landscape Ecology.

Willaarts, B. A., M. Volkb, et al. 2012. "Assessing the ecosystem services supplied by freshwater flows in Mediterranean agroecosystems." Agricultural Water Management.

STRATEGIC ENVIRONMENTAL ASSESSMENT WITH QUANTITATIVE EVALUATION TECHNIQUE IN ZERO WASTE TO LANDFILL

Chotiwan Seangprasertkij and Yutaka Sakakibara (Waseda University, Tokyo, Japan) Takehiko Murayama (Tokyo Institute of Technology, Yokohama, Japan)

ABSTRACT: In pulp and paper mill located in Thailand, large amount of ash is generated from coal-based power generation and sent to landfill for disposal. Driving by sustainability aspiration, zero waste to landfill policy was initiated. In this study, six alternative projects with seventeen options were proposed to cope with ash generated, which are landfilling, disposing in cement kiln, selling for ready mix concrete production, selling for concrete masonry producer, implementing internal concrete masonry plant, and executing fly ash recirculation. Strategic Environmental Assessment with quantitative evaluation technique was conducted to identify the most sustainable option taking into account environmental, economic and social aspects. The assessment results indicated that the most sustainable option would be to utilize bottom ash by implementing an internal concrete masonry plant and to sale fly ash for ready mix concrete production and recirculation, because it demonstrated the highest degree of criteria satisfaction. This infers better economic impacts to paper company and local businesses, lower generation of carbon oxide, lower environmental risk, and more opportunities in land use and social structure.

INTRODUCTION

To overcome some deficiencies remaining in Environmental Impact Assessment (EIA), Strategic Environmental Assessment (SEA) has been introduced to Thailand as the more promising tool in the current National Environmental Quality Management Plan 2007-2011(ONEP, 2006) and used so far for supporting decision-making process on governmental projects pertaining to area development planning (ONEP, 2005) and river management (HSRI, 2007).

In recent years the attention towards sustainable development and cooperate social responsibility has increased in both governmental and private sectors of Thailand. Now that the so-called “triple bottom line” is being referred to in many companies’ development directions, their performances are appraised not only economic but environmental and social as well. Adopting SEA as a systematic process for evaluating environmental consequences of proposed strategic actions is one promising approach to ensure they are appropriately addressed and considered at the early stage of decision making. It enables not only objective discussion among options but also upstream adjustment as well as reduction of possible adverse impacts and conflicts.

Zero waste to landfill policy of a pulp and paper mill indicates environmentally benign aim. Still, apart from financial concerns, many measures are obscure on their consequent impacts on both stakeholders and environment. In this research, SEA was applied to industrial waste management plan to serve company’s decision-making process towards sustainable development. Based on quantitative technique integrated to SEA’s evaluation step, degree of criteria satisfaction by option was quantified so as to be simply comparable across projects and options as well as easily comprehensible for the decision makers. Furthermore, in response to SEA’s problem nationwide, this study was intended to restructure the

---

ISBN 9780976885351

top-down planning tradition, to create the opportunity of public participation and to originate new institutional culture.

APPROACH IN SEA

FIGURE 1 shows SEA procedures proposed by Therivel (2004).

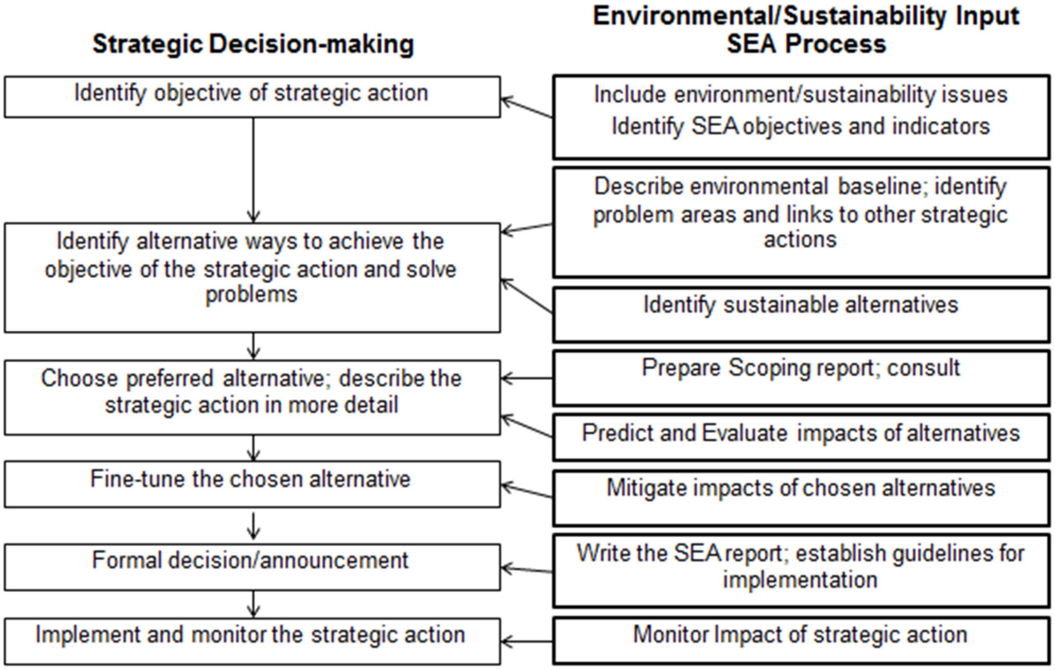

FIGURE 1. Illustration of SEA procedures proposed by Therivel (2004)

In this study, similar approach was followed for the case of zero waste to landfill plan. Important procedures in this study are shown as follows:

1) Screening and links for decision-making: Implementing SEA to this strategic action was not legally required but for examining new approach towards organizational sustainability.
2) Describing the environmental baseline and identifying problems: Data of related projects were gathered and documented as baseline data. Identification of impact areas was defined by literature review and field survey at projects' sites.
3) Identifying alternatives or options: Since some individual projects alone were not possible to cope with all generated ash, options were designed for eliminating 100% of both Bottom Ash (BA) and Fly Ash (FA). In this paper, "project" was defined as an activity for eliminating ash (see Table 1), while "option" was defined as a combination of projects (see Table 2). Totally six different waste management projects were proposed and seventeen options were considered with varyingly realistic percentage of manageable ash.
4) Predicting, evaluating, public consulting and mitigating impacts: Preceded by preliminary impacts prediction based on literature review and onsite data, direct interviews were conducted with seven stakeholders in order to help predicting, evaluating and mitigating impacts. In this stage, elicitation techniques (Ribeiro, 1996) were used as well as the specifically constituted algorithms to achieve quantitative evaluation.

RESULTS AND DISCUSSION

Proposed Waste Management Projects and Options-The differences in physical and chemical characteristics between BA and FA govern their potential utilization. Based on the differences, the following ash management projects were proposed and assessed:

1. Landfill Continuation: The consideration is made for illustrating the situation in the absence of zero waste to landfill policy.
2. Kiln Disposal: This is a legal waste disposal by a cement company within the same group of the paper company. Both FA and BA can be eliminated in cement kiln. Nevertheless, due to remote location of cement kiln, long distance transportation is mandatory.
3. Sale for Ready Mix Concrete (RMC): FA is broadly used in Thai RMC industry. It can partially replace cement in the mix. This project can be beneficial depending on FA quality.
4. Sale for Concrete Masonry Producer: BA has suitable properties to be used in concrete masonry as crushed stone alternate. BA was sold to concrete masonry producer. Then, the ash concrete masonry was bought back for paper company's internal use or charitable activities for local temples, schools, and public places. However, the production capacity of this local masonry plant was very limited.
5. Internal Concrete Masonry Plant: It was proposed for the idea of high BA consumption and commercializing concrete masonry production.
6. Fly Ash Recirculation: FA was to be recirculated in Circulating Fluidized Bed boiler for substituting sand and the outflow FA can be sold to RMC.

Based on these 6 projects, 17 options were considered, which were summarized in Table 2.

TABLE 1. Degree of criteria satisfaction by project-level of satisfaction for all relevant attributes derived from its importance and impacts in stakeholders' viewpoint

Projects	Social Weight	Social Score	Economic Weight	Economic Score	Environmental Weight	Environmental Score	Degree of Criteria Satisfaction
Landfill Continuation	0.250	0.624	0.279	0.705	0.471	0.440	0.560
Landfill Closure	0.250	0.576	0.279	0.705	0.471	0.760	0.699
Kiln Disposal	0.250	0.682	0.279	0.318	0.471	0.572	0.529
Sale for RMC (FA)	0.250	0.662	0.279	1.121	0.471	0.540	0.732
Sale to Contract Manufacture (BA)	0.250	0.702	0.279	0.526	0.471	0.558	0.585
Internal Concrete Masonry Plant	0.250	0.772	0.279	0.637	0.471	0.560	0.635
FA Recirculation	0.250	0.600	0.279	0.530	0.471	0.547	0.555

Best Option Based on Degree of Criteria Satisfactory-To select the best option, the degree of criteria satisfaction was calculated by Equation (1):

$$\mathrm{D}(A_i) = \sum \in_j * D(P_j) \qquad (1)$$

where D represents degree of criteria satisfaction: A_i represents option i: and P_j represents project j: $\in_j$ represents percentage of ash taken by project j.

$$\mathrm{D}(P_j) = \sum_{j=1}^{n} W_k * S_{jk} \qquad (2)$$

where W_k represents the weight of aspect k: and S_{jk} represents score of aspect k for project j. The weight of each aspect was calculated according to the result of stakeholder interview. To represent the aspect's importance, stakeholders have been asked to allocate ten points among the three aspects (environmental, social, and economic) based upon their opinions. These points from each stakeholder were aggregated to get a singular weighting value for each aspect as shown in Equation (3). The algorithm used was termed as weighted average rating (Ribeiro, 1996).

$$W_k = \frac{\sum \omega_k}{\sum w_k} \qquad (3)$$

where ω_k represents the weight of aspect k assigned by each stakeholder; and w_k represents total points from each stakeholder which, in this case, was equally worth ten points for all stakeholders.

TABLE 2. Options and degree of criteria satisfaction

Options	Waste Management Projects									
	Landfill		Kiln Disposal		Sale for RMC (FA)	FA Recirculation	Sale to Contract Manufacture (BA)	Internal Concrete Block Plant		Degree of criteria satisfaction
	BA	FA	BA	FA	FA	FA	BA	Sale	Charity	
1	100%	100%	0%	0%	0%	0%	0%	0%	0%	1.119
2	100%	70%	0%	0%	30%	0%	0%	0%	0%	1.171
3	100%	0%	0%	0%	70%	30%	0%	0%	0%	1.239
4	0%	0%	100%	100%	0%	0%	0%	0%	0%	1.057
5	0%	0%	100%	70%	30%	0%	0%	0%	0%	1.119
6	0%	0%	100%	0%	70%	30%	0%	0%	0%	1.208
7	90%	100%	0%	0%	0%	0%	10%	0%	0%	1.122
8	0%	0%	90%	100%	0%	0%	10%	0%	0%	1.063
9	0%	0%	0%	100%	0%	0%	0%	0%	100%	1.163
10	0%	0%	0%	100%	0%	0%	0%	50%	50%	1.163
11	0%	0%	0%	100%	0%	0%	0%	100%	0%	1.163
12	0%	0%	50%	100%	0%	0%	0%	0%	50%	1.110
13	0%	0%	50%	100%	0%	0%	0%	25%	25%	1.110
14	0%	0%	50%	100%	0%	0%	0%	50%	0%	1.110
15	0%	0%	0%	0%	70%	30%	0%	0%	100%	1.314
16	0%	0%	0%	0%	70%	30%	0%	50%	50%	1.314
17	0%	0%	0%	0%	70%	30%	0%	100%	0%	1.314

The score of aspect k for project j, S_{jk} was calculated by,

$$S_{jk} = \sum_{l=1}^{n} w_l * s_l \qquad (4)$$

where w_l represents the weight of attribute *l*. The attributes were also ranked from most important as the first to least important as the last. The environmental attributes consisted of air quality, public health and safety, noise, ecology, soil and sediment, water quality, and aesthetic, whereas the social attributes included induced development, cultural heritage, local social structure, land use, local employment, and social benefit. The calculation followed rank (decreasing) method (Ribeiro, 1996). Then, the weight of each attribute was calculated by weighted average rating in accordance with Equation (3). Lastly, weighting of second-level attributes where exist was assigned equally.

Calculated degrees of criteria satisfaction, D(P_i) and D(A_i) were shown in Tables 1 and 2, respectively. Referring to Table 1, the landfill closure indicates more satisfactory over landfill continuation. Additionally, sale FA for RMC is the most supported project. In Table 2, option 15, 16, and 17 indicate the highest degree of criteria satisfaction. Varying proportion between sale and charity of masonry has insignificant result among the best three options. By way of explanation, FA should be utilized for producing RMC combining with substituting sand in furnace recirculation project, while, internal concrete masonry plant should be constructed to cope with BA.

Discussion-In order to convert numerous and linguistic data into a compatible form, some assumptions were used which any change might impact on the study's conclusion concerning order of most to least preferred options. Hence, simple sensitivities (Pannell, 1997) were carried out for observing the effect from changing the interval of ranked aspects and changing scoring scale. The parameters were trialed for both smaller and greater interval as well as the scale of scoring. The results were observed through the changed degree of criteria satisfaction by option. According to sensitivity analysis, most of preferred option trends stay the same after varying interval of ranked aspects and changing scoring.

Life Cycle Analysis (LCA) is an evaluation technique that can be utilized with SEA since it analyzes through strategic action from cradle to grave both direct and indirect impacts. However, during the environmental baseline gathering, LCA was not completed since some emissions from certain operations were not monitored. For example, carbon dioxide emission from cement kiln was not able to be compared between using and not using ash. The ash burnt in cement kiln was viewed as disposal drawing no attention for monitoring the change of emitting carbon dioxide. Therefore, further study will be needed for adjusting attributes such as focusing on the amount of carbon dioxide emitted from each project's life cycle towards global warming oriented assessment.

CONCLUSIONS

This study demonstrates that it is possible to use SEA as a tool for organizational decision-making towards sustainable waste management plan. The degree of criteria satisfaction enhances quantitative comparison across various projects and options. The new paradigm of integrating public participation in to organizational planning process was introduced. While this approach is directed for assessing zero waste to landfill options, similar assessment method can be conducted for other strategic actions as well.

ACKNOWLEDGEMENTS

Support for this research by SCG is gratefully acknowledged.

REFERENCES

HSRI. Final report, *management of Yom River Basin by using SEA*. Thailand: Health Systems Research Institute; 2007.

ONEP. Final report, *SEA in the border area in Chiang Rai Province*. Thailand: Office of natural resources and environmental policy and planning; 2005.

ONEP. Project report: *study and technical analysis of environmental quality management plan 2007–2011development*. Thailand: Office of natural resources and environmental policy and planning; 2006.

Pannell, D.J. 1997. "*Sensitivity analysis of normative economic models: Theoretical framework and practical strategies.*" Agricultural Economics 16: 139-152.

Ribeiro R. A., 1996. *"Fuzzy multiple attribute decision making: A review and new preference elicitation techniques"* Fuzzy Sets and Systems 78(1996) 155-181

Therivel R., 2004. *"Strategic Environmental Assessment in Action."* Cromwell Press, Trowbridge, UK

SURVEY OF THE ENGINEERING IMPACTS OF ACID MINE DRAINAGE ON INFRASTRUCTURE

Stephen O. Ekolu (University of the Witwatersrand, Johannesburg, South Africa)
Firehiwot Azene (Council for Geoscience, Pretoria, South Africa)

ABSTRACT: This paper highlights the engineering and economic impacts of acidic mine water on physical infrastructure, typically comprising buildings, highway structures, roads, equipment. Existing literature shows that an overwhelming focus of research on the subject has been placed on environmental considerations, ecological impacts of acid mine drainage (AMD) and the AMD hydrogeology. Relatively little scientific attention has been given to the impacts of acid mine drainage on infrastructure. It is understood that the physical infrastructure are essential intermediate operational agents contributing to major societal needs of the economy and community services. Efficient functioning of these engineering structures can be severely hampered upon exposure to acidic water, resulting in their degradation, disruption of services, high maintenance and replacement costs.

Herein discussed are selected case studies from the literature and from field survey in South Africa, showing the adverse impacts of acidic mine water on engineering infrastructure. These real life cases of damage caused by AMD include the corrosion of equipment in a hydro-power station, corrosive degradation of a bridge structure, clogging of pumps, incrustation of pipes. It is evident from the survey that the corrosive actions of AMD can cause failure of the engineering performance of infrastructure, which in turn translates to significant economic consequences. Acid corrosion and incrustation effects are the most common damage types in metal-based infrastructure while acid corrosion and sulphate attack appear to be the main processes of concern in concrete structures affected by AMD. Against this background, it should be considered essential to develop thorough understanding of the AMD attack processes on common infrastructure materials in order to define the boundary of public fears pertaining to the risks and threats that often arise from exposure of engineering infrastructure to polluted mine water.

INTRODUCTION

The impacts of acid mine drainage to engineering infrastructure has generally not received much attention while most research efforts have largely been devoted to the adverse environmental and ecological effects of AMD, along with hydrogeological studies. While the importance of the critical impacts of AMD to the environment are undisputable, due to their life-threatening effects, it should also be appreciated that AMD can bear significant adverse effects on engineering materials and structures, which in themselves are the intermediate operational agents for economic activities and community services. Engineering structures are relied upon in addressing challenges associated with economic development and alleviation of poverty. They contribute to various societal needs by:- (i) providing the physical infrastructure needed by businesses and financial institutions to conduct economic activities such as agriculture, trade and industry, (ii) improving productivity of industries, thus enabling efficiency and high value product chain capable of promoting industrial competitiveness for economic transformation, (iii) being a vehicle for essential municipal and communal services needed in the functioning of urban and rural communities. However, the efficient functioning of engineering structures can be severely hampered upon their exposure to acidic mine water, resulting in their degradation. CISA (2004) reports of research conducted at University of the Witwatersrand, which gave an estimate of the direct costs of corrosion in South Africa to be about 5.2% of the Gross Domestic Product (GDP), translating to 154 billion Rand annually.

ISBN 9780976885351

OVERVIEW OF ACID MINE DRAINAGE

The occurrence of acid mine drainage is synonymous with mining activity. The term *acid mine drainage* refers to polluted mine water, characterisized by acidity and/or high concentration of heavy metals, well in excess of the loads acceptable for normal water quality. AMD typically occurs in long abandoned mines. Most mineral ore deposits including copper, coal, gold, platinum, nickel etc. contain pyrites. After several years from mine closure, the pyrites or iron disulphide (FeS_2) exposed to moisture and oxygen in the atmosphere (during the past mining operations), will undergo oxidation, resulting in production of sulphuric acid. The chemical process is simplified as (Petrik et al., 2006):

$$2\,FeS_2 + 7.5O_2 + 7H_2O \longrightarrow 2Fe(OH)_3 + 4H_2SO_4$$

The mines may be surface /open pit mines or underground mines. In any case, the acidic mine water formed infiltrates underground water and water pathways including rivers and streams which interlink with the surrounding environment from which the adverse impacts of the acidic mine water will emanate.

ENGINEERING IMPACTS OF ACID MNE DRAINAGE

Vulnerable Infrastructure: There is little literature available on the engineering and economic impacts of acid mine drainage worldwide. Yet several real life cases exist where AMD attack on infrastructure has been experienced with major consequences. An examination of scientific literature worldwide reveals that corrosivity of acid mine drainage can be extremely destructive to infrastructure. The most commonly affected forms of infrastructure are those constructed of metals and concrete. The list (which is by no means exhaustive) of vulnerable infrastructure includes:

- Water handling equipment such as pumps, irrigation systems, navigation equipment, municipal water supplies, turbines of hydro-power dams
- Industrial equipment such as boilers, textile dying, metal plating
- Civil engineering structures such as bridges, culverts, buried pipes and other highway structures, electricity transmission lines, underground storage tanks
- Ore processing plants and structures i.e. plant buildings and machinery
- Ground subsidence and sinkholes
- Buildings, highway and urban infrastructure affected by ground subsidence, sinkholes, corrosion damage, soil acidification (geotechnical impacts)

In the United States, a 1937 report (Earlie and Callaghan, 1998) gave an account of the adverse effects that AMD inflicted on water supplies, various equipment and infrastructure. It cites the extent to which AMD caused intensive corrosion of federal navigation locks and dams, ships and barges, bridges and culverts, pipelines and plumbing. The report goes further to mention how the ‘reddish’ water destroyed fish and aquatic life, inhibited self-purification of streams, made water unfit for drinking or household use by causing scum in wash bowls, sinks and tubs. Other reported effects include causing of spots on clothing fabric in laundries and textile factories. Further mention is made of AMD’s scale formation on equipment, rendering its use unsuitable in locomotives, power plant boilers, manufacturing industries and municipal works.

In South Africa, Johannesburg City overlies a deeply mined gold basin. In November 2010, acid mine water level was determined to be 510 m below the ground surface and rising at a rate of 0.59 m per day. Among the public fears concerning AMD rise are its potential to cause acid and durability attacks, ground de-stabilization and increased seismic activity. It is feared that major urban infrastructure in the central business district could be affected including high-storey structures of deep foundations, bridges, culverts, pavements, other transportation and municipal infrastructure.

Corrosion Attack Processes of AMD on Metals. Acid mine drainage can cause corrosion of metals through several different kinds of attack. While there are different forms of metal corrosion including chemical, electrochemical and bacterial corrosion, the most predominant attack processes of acid mine drainage on metallic infrastructure are the *acid attack* and *incrustation*. The pH or acidity of the electrolyte has a marked effect, causing rusting by dissolution of metals. The high acidity of AMD can attack pipes, pumps/metal casings, valves, tanks, screens, conveyances (chutes) and other metal fixtures, among others. Considering the corrosion of pumping equipment alone, the cumulative cost due to replacement of parts, short life of parts, labour, maintenance and other related costs are conceivably enormous. *Incrustation* can affect industrial equipment and water handling infrastructure. Precipitated minerals from underground water, form depositions on metal surfaces that can affect performance and efficiency. The common elements responsible for incrustation are carbonates or sulphates of calcium and magnesium, hydroxides of iron and manganese, slime-forming bacteria. These problems are common in well pumping stations, where slime bacteria can also plug well screens while scales formed by carbonates fill voids by binding together the sand grains (used as screens) and consequently blocking water flow into the well.

Corrosion Attack Processes of AMD on Concrete: Major urban settings, city suburbs and mining towns, typically consist of high-value stocks of concrete infrastructure which provide economic and social services including housing; transport systems such as roads, bridges, airports; dams and water supply systems; municipal sewerage and waste disposal networks; buildings for offices, conferences and shopping centres; community amenities such as schools, theatres and restaurants, hospitals, sports centres and stadiums; agricultural and farm infrastructure, among many others. All these involve cement and concrete consumption. These and other structures close to mine fields can be at the risk of exposure to acid mine drainage. The corrosive nature of AMD typically causes attack on concrete, affecting its durability and service life, which can result in prohibitively expensive maintenance and repair costs. In some cases, deterioration, settlement and ground subsidence can induce catastrophic failures and collapse of structures.

AMD may cause degradation of concrete through the *acid or sulphate attack* mechanisms. Acids severely attack and destroy the basic components of concrete. The attack is considered to occur at a pH below 6.5 but becomes significant at pH 3 to 4. The attacking compounds must be in solution. In concrete or cementitious systems, acids dissolve calcium hydroxide (CH), calcium silicate hydrate, and aggregates. Eventually, total disintegration of concrete is inevitable. For groundwater, conditions suggestive of potential acid attack are: water of pH ≤ 5.0, total acidity ≥ 25 mg per 100g of soil, and sufficient groundwater rate of replenishment (Earlie and Callaghan, 1998; Bearly, 1980). The acid will typically attack and destroy the surface concrete which in turn neutralizes the acid by its high alkalinity. A fresh supply of acid will launch further attacks progressively into the interior of concrete. An acid solution concentration of 1% H_2SO_4 will attack and significantly cause corrosion damage within 1 to 12 months (Ash et al., 1951). Most concrete structures also contain steel reinforcement which is protected by a thin layer of typically no greater than 50 mm thickness of concrete cover. Erosion of the cover concrete by even light acid will expose the steel reinforcement not only to acid attack but also to corrosion deterioration. Different types of sulphate salts typically, Na_2SO_4 (Glaubers salt), $MgSO_4$ (Epsom salts) and $CaSO_4$ (Gypsum), can result in sulphate attack. AMD typically contains a rich source of these various types of salts making it a potential prime source for sulphate attack. A concentration of $SO_4^{2-} > 1500$ ppm in water may cause severe sulphate attack. Other external sources of sulphates in underground conditions are soils, groundwater or other mine effluents. The sulphate salts react with tricalcium aluminate (C_3A) and cement hydrates, forming ettringite in already hardened concrete. The formation of ettringite is expansive resulting in cracking. In the case of external sulphate attack, sulphates from an external source penetrate concrete and dissolve into solution. The sulphate ions then react with CH to form gypsum in the pore solution, which in turn converts monosulphate to ettringite.

CASE STUDIES

Case Study 1 - Corrosion of Hydro-Power Dam Equipment (India). In India (Pankaj et al., 2011), two major hydro-power stations from the Kopili H.E project were severely damaged by acid mine water emanating from the nearby coal mines, resulting in frequent power breakdowns. The 50 MW Khadong power generating station commissioned in 1984 and 200 MW Kopili power station commissioned in 1988, were reported to have performed excellently and rarely experienced breakdowns for over 22 years. But from 2006 to 2010, the stations experienced up to fifty (50) equipment breakdowns due to failures in various equipment parts. The critical parts that were severely corroded include the cooler tubes, fixtures, and turbine components as shown in Figure 1. It was found that the materials of the severely corroded components were made of copper-nickel alloy, mild steel and high carbon alloy. It was also reported that even stainless steel components had corroded, indicating the high severity of the attack seen on the metals. Failure frequency was mainly found in those components exposed to high water turbulence in the upstream side, consisting of cooling header water pipe, bends, valves, and pressure equalizer pipes of the turbine.

FIGURE 1 Corrosion of hydro-power dam equipment by acid mine water (Pankaj et al., 2011)

In the downstream side, similar corrosion of components was observed but to a lesser severity compared to the upstream side, implying that the combination of acid corrosion and abrasive action of water inflicted a more damaging impact. The cause of corrosion was attributed to exposure of hydro-power equipment to low pH reservoir water ranging from as low as 2.76 to 5.0, monitored from 2007 to 2009. Coal mining had been practiced within the catchment areas of the river tributaries. Later the abandoned open cast and "rat hole" mines resulted in oxidation of the pyrites in the sandstone rocks, forming sulphuric acid that in turn flowed into the reservoirs, aided by rainwater run-off.

FIGURE 2 Corrosion of manhole and pipe fittings (Du Toit 2010 (right insets)) due to exposure to acid mine drainage

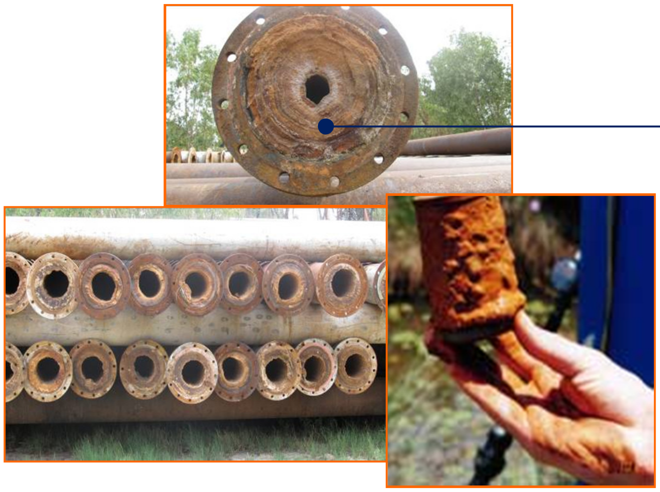

FIGURE 3 Incrusted pipes and pump filter (DERM, 2011 (right inset)) with heavy metals in acid mine discharge water

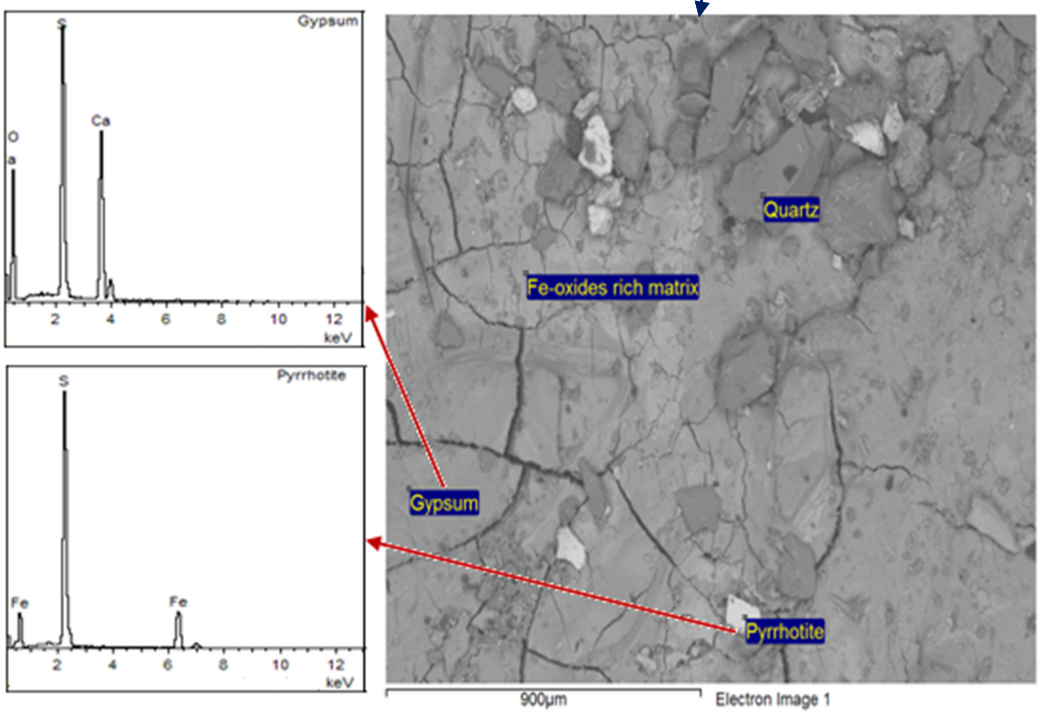

Case Study 2 - Corrosion and Incrustation of Pipes (South Africa). Corrosion problems related to AMD attack on infrastructure have been observed in South Africa including corrosion of pipes and pipe fittings as shown in Figure 2. It can be seen that the metal T-junction and other parts of the pipe have severely corroded while the rest of the plastic pipe is not corroded as expected. The cover of the manhole is also exhibiting aggressive corrosion. The process of incrustation is known to be a result of precipitation of heavy metals, causing clogging of equipment and de-generation of its performance and efficiency. Some of the most vulnerable infrastructure include pumps, well screens, pipes etc. In Figure 3 shows a pump filter and water pipes that have been severely clogged with precipitates of iron and calcium, rendering them dysfunctional. An analysis by scanning electron microscopy determined the pipe precipitates to be a mixture of gypsum and possibly iron-hydroxides. Also seen are the residual pyrrhotites, being the primary reactant in AMD formation (see Figure 3). Frequent and costly pump /pipe maintenance would typically be necessary as a result of such incrustation by polluted mine water.

Case Study 3 - Deterioration of Concrete Bridges (Australia). The deterioration of concrete structures due to exposure to acid mine drainage has been reported albeit in circumstances related to the proximity of structures to the mining environment. The attack is related to acid corrosion and/or sulphate corrosion of the structural concrete, the vulnerable elements being foundations and piers. The attack may emanate from soils, underground water or acid polluted rivers. In New South Wales Australia, a bridge crossing over an AMD polluted river experienced severe deterioration in the substructure, as shown in Figure 4. It can be seen that the concrete matrix has been dissolved by the acidic water, leaving behind exposed aggregates. It follows that foundations of the structure are likely to have been similarly affected. Without any remedial actions, the observed condition will in turn propagate other attack mechanisms such as carbonation and acid corrosion of reinforcement, ultimately compromising the structural capacity of the bridge. The condition will typically demand costly repairs and maintenance of the structure.

FIGURE 4 Severely deteriorated bridge piers attacked by sulphuric acid water (DERM, 2011)

SUMMARY

The purpose of this article was to identify the engineering impacts of acid mine drainage on infrastructure. Concrete, steel and metal alloys are the most important materials involved in the interaction of acid mine water with infrastructure. Selected real-life case studies consisting of a hydro-power dam, a bridge structure, pipes and water conveyance infrastructure have been discussed in consideration of the type of infrastructure, the material of construction, the form of attack process, and economic implications of the damage. It is evident that a wide range of engineering infrastructure can be severely damaged upon exposure to acidic mine water, with some major structures having enormous economic impacts.

The attack process depends on the type of infrastructure material. Acid corrosion and incrustation effects are dominant in metal-based infrastructure. In concrete structures, acid corrosion and sulphate attack appear to be the main processes of concern. Also, there is little or no literature available on the damage processes of acidic mine water attack on infrastructure materials. Such understanding is essential in defining the boundary of fears and concerns pertaining to threats and risks that can be posed by acid mine drainage on infrastructure.

REFERENCES

Ash S.H, Felegy E.W, Kennedy D.O, Miller P.S. (1951) "Acid Mine Drainage Problems—Anthracite Region of Pennsylvania", *US Bureau of Mines Bulletin* 508, 72p

Bearly, M. (1980), *Concrete Pipe Handbook*, American Concrete Pipe Association, Chapter 6, p.1-21

CISA (2004), Corrosion Control in Southern Africa, *Corrosion Institute of Southern Africa* (CISA),

John.J McEwan (ed.), ISBN 0-620-32198-9, 136p

DERM (2011), *Potential Impacts of Acid Sulphate Soils*, Dept of Envir and Resource Mgt, Queensland Govt, AUS. http://www.derm.qld.gov.au/land/ass/impacts.html, Accessed 28 Oct 2011

Du Toit, S. (2010), "Hidden Footprint of Gold Mining Activities in the West Rand: Some Present and Future Concerns to be Addressed", Mogale City Local Municipality, PPT 29 Nov 2010, 52 slides

Earlie J., Callaghan T., "Impacts of Mine Drainage on Aquatic Life, Water Uses, and Man-Made Structures", *Department of Environmental Protection*, Harrisburg, PA 17105, 12p

Petrik L., Burgers C., Gitari W., Surrender D., Reynolds K., Ellendt A., Etcvhebers O., Vadaphalli

V.R.K., Key D., Iwuoha E., 2006, "Stability and Neutralisation Capacity of Potential Mine Backfilling Material formed by Neutralisation of Fly Ash and Acid Mine Drainage", *Water Research Commission*, WRC Report No. 1458/1/06, December 2006, 254p

ACID MINE WATER QUALITY - CAUSE OF DETERIORATION OBSERVED IN FIELD CONCRETE

Firehiwot Azene (Council For Geoscience, Pretoria, South Africa)
Stephen O. Ekolu (University of the Witwatersrand, Johannesburg, South Africa)

ABSTRACT: In an abandoned mine of the coalfields of South Africa, it was observed that concrete exposed to discharging acid mine drainage (AMD) exhibited severe deterioration associated with severe cracking, salt crystallization and efflorescence. Specimens of AMD water and the deteriorated concrete were taken from the field for purposes of laboratory investigation and analytical studies. Emphasis was placed on the aggressiveness of the acidic mine water on concrete. The chemical signature of the AMD water was determined and its corrosiveness assessed using the Langelier Saturation Index (LSI*)*, Ryznar Stability Index (RSI), Larson Ratio (LnR), Corrosion Ration (R) and the Aggressiveness Index (AI). All indexes indicate extreme aggressiveness by the AMD, with its AI being 20 times greater than the typical value for normal (non-aggressive) water. The indexes predictions are consistent with the observed severe degradation leading to exfoliation of the field concrete. Analytical studies conducted using differential thermal analysis were not confirmatory of the processes involved but sulphate and/or acid attack mechanisms are suspect.

INTRODUCTION

This paper describes the deterioration observed in field concrete exposed to acid mine drainage water in the coalfields of South Africa. While it is recognized that acid mine drainage is acidic and corrosive to life and materials, most of the literature on the subject has been devoted to environmental and ecological studies with little work done in consideration of the impacts of acid mine drainage on engineering infrastructure. Concrete is the most dominant material of construction whose use as a commodity is only second to water. The sheer volume of use of this material in construction of structures is indicative of the importance of these intermediate agents to modern economic development and societal needs. Concrete is used for a wide variety of infrastructure from mining shafts and plants to domestic and urban infrastructure. However, there are no reports or scientific investigations in South Africa, involving the effects of acid mine drainage on concrete.

The deterioration of concrete under acid mine drainage attack is highlighted by the evidence from recent field observation herein reported. Understanding of a wide range of issues associated with the nature of attack is necessary in order to explain the effects observed. For this reason, careful consideration was given in the approach undertaken to examine this real-life case of degradation due to AMD attack on concrete. The aims of this work are thus, to:

- Provide a report of the real case scenario of AMD attack on concrete, for practical purposes and information
- Apply index approaches for qualitative assessment of water for its degree of aggressiveness
- Conduct analytical study into the mechanism of attack
- Develop insights for research into AMD attack process on concrete

THE NATURE OF ACID MINE DRAINAGE

ISBN 9780976885351

AMD has been known to be a worldwide environmental problem of enormous proportions and consequences, identified and documented since the 1920's (EPA, 1973) to be a result of oxidation of pyrites abundantly present in abandoned mines or mine tailings. Years after abandonment of mining activity, oxidation of the pyrites in the presence of water through exposure to air, results in sulphuric acid formation. During seepage of the acid through the various rock strata, it dissolves heavy metals found in the substrate, carrying them into soils and water courses. The process of AMD formation is represented chemically as (Wildeman, 199):

$$4FeS_{2(s)} + 14O_{2(g)} + 4H_2O_{(l)} \rightarrow 4Fe^{2+}{}_{(aq)} + 8SO_{4(aq)}{}^{2-} + 8H^{+}{}_{(aq)} \qquad (1)$$

$$4Fe^{2+}{}_{(aq)} + O_{2(g)} + 4H^{+}{}_{(aq)} \rightarrow 4Fe^{3+}{}_{(aq)} + 2H_2O_{(l)} \qquad (2)$$

$$4Fe^{3+}{}_{(aq)} + 12H_2O_{(l)} \rightarrow 4Fe(OH)_{3(s)} + 12H^{+}{}_{(aq)} \qquad (3)$$

$$4FeS_{2(s)} + 15O_{2(g)} + 14H_2O_{(l)} \rightarrow 4Fe(OH)_{3(s)} + 8SO_4{}^{2-}{}_{(aq)} + 16H^{+}{}_{(aq)} \qquad \text{Summation of 1, 2 \&3}$$

Further reaction leads to formation of ferric hydroxide and more acid release, basically ensuring an increasing supply of the acid. Consequently, AMD is typically characterised by high acidity resulting in low pH, high sulphate concentrations, high heavy metal concentrations, and high total dissolved solids content. The actual composition of the AMD will vary depending on the geological setting of sulphide minerals. In fact, some polluted mine water may not at all be acidic but rather an alkaline polluted mine drainage (Younger, 2000). The AMD problem becomes complex when it manifests upon exposure at the surface, through infiltration of underground water and/or surface water run-off. Due to its corrosive nature, AMD is typically aggressive towards life and most engineering materials, causing damage attacks of different forms.

BACKGROUND

The site of investigation is located in one of the oldest collieries in Mpumalanga, South Africa. The coal mine was operated for at least 50 years before its closure in the 1950's. Human activity in and around the site is indicated by several footpaths that criss-cross the 750 ha coal mine. The mine is also close to a township and an industrial area. Well documented legacies of the colliery and other similar coal mines in the province have involved occurrences of ground subsidence, spontaneous coal fires and decant of acid mine drainage. Several coal fires have occurred underground some of which could be so intense with flames seen burning above ground surface level. Acid mine drainage decants from various parts of the large coal mine and drains into the nearby small Brugspruit stream which eventually joins the olifants river and flows through the Loskop dam.

Typically, the decant of acid mine drainage from the large coal mine is spread out but there were known specific major decant sources. Accordingly, some of the locations where large decant volumes occur within the mine were rehabilitated by government through channeling of the AMD decant into constructed evaporation ponds. Another important consideration in the rehabilitation effort was to provide protection to nearby communities. As mentioned earlier, adults invariably traverse the mine while children often find attractions such as the polluted water to be a playfield. Indeed, fatal incidents have been reported over the years due to these risks to the surrounding communities. To mitigate these issues, government fenced off the main decants locations to limit human access and highlight it as a high risk area. Fencing was constructed as a substructure consisting of a concrete wall lining which supports the concrete posts, as shown in Figure 1.

FIELD DETERIORATION

Closer inspection of the concrete wall lining used in the fence construction (Figure 1) revealed the presence of extremely severe deterioration in the concrete. Accordingly, understanding of concrete science and technology was deemed necessary to examine the condition of the deteriorated concrete. From the outset of the project, it was evident that severe exfoliation and dilapidation of the concrete had occurred. Severe deterioration particularly occurred in the concrete above the water line, and was characterized by the following features:

- A line of disintegration separating concrete above the water line from the foundation (see Figure 1)
- Map cracking pattern, seemingly oriented longitudinally along the length of the wall lining. Notice that the deterioration occurs across the full thickness of the 250 mm concrete wall (see Figure 2)
- Swelling and spalling of the concrete leading to falling out of disintegrated chunks of concrete
- Depositions of powdery salt crystals on the concrete surface.
- Erosion of cement past matrix leaving protruding aggregates

FIGURE1. Disintegration above water line

FIGURE2. Severe degradation on outer side of the concrete wall lining

With these alarming signs of degradation, it was necessary to delve into further investigation in order to develop insights into the nature of the attack observed in the concrete. Accordingly, the following assessments were conducted in the field and samples collected for use in the laboratory investigation:

- Inspection of the physical condition of the disintegrated concrete walls. Information gathered includes: the cracking patterns, sizes and orientations; spalling and planes of failure; salt depositions on the surface; wear and eroding of material
- A photographic record of the distress condition and features observed in the insitu concrete
- Samples consisting of solid chunks of concrete were broken off from damaged concrete wall and the samples were taken for use in laboratory analytical studies
- Acid mine drainage was collected for water analysis

ASSESSMENT OF WATER AGGRESSIVENESS

Index Evaluation Methods: Index approaches were used in this investigation for qualitative assessment of the corrosivity of the water from the coal mine. A total of six index methods were used and only two of them consisting of the Langelier Saturation Index (LSI) and the Aggressiveness Index (AI) evaluation were discussed in this paper. All the techniques are applied based on the water chemistry. The LSI is commonly used to assess the tendency of water to cause incrustation or corrosion attack. The index is calculated from pH, TDS, alkalinity, Ca hardness, and is defined by (Driscoll, (1986), Sasidhar and Vijay, (2008) as:

$$LSI = pH - pHs$$

Where pH is the measured pH of water, pHs is the saturation pH based on calcium carbonate and obtained from pHs = (9.3 + a + b) – (c + d) such that a = (log (TDS) - 1)/10; b = -13.12 x log (T) + 34.55; c = log(C) - 0.4; d = log (A). In the equations, TDS represents the total dissolved solids in mg/l, T is the temperature in Kelvin, C is the calcium hardness in mg/l (Ca as $CaCO_3$), and A is the alkalinity as mg $CaCO_3$/l. An LSI of zero indicates neutral water with no dissolution or precipitation effects. Water with a negative LSI is aggressive and likely to be corrosive as it tends to dissolve calcium carbonate but has no potential to produce encrusts and scaling. The larger the value of LSI, the greater the attacking effect of the AMD water. LSI>0 water is supersaturated with respect to calcium carbonate (CaCO3) and scale forming may occur with slighter corrosive action.

The AI of water is specifically relevant to its interaction with concrete. The method proposed by Basson (1989) is based on seven (7) corrodent properties of water identified as pH, $CaCO_3$ saturated pH, calcium hardness as $CaCO_3$, total ammonium ion, magnesium ion, total sulphate as SO_4 and chloride ion. AI is calculated as a cumulative contribution from each of the properties. A constant, C (from C1 to C7) and the measured value V (from V1 to V7) for concentration of the ions or parameter in water, are applied to calculate and scale the individual indices (see Figure 6 of Basson, 1989), giving:

$$AI = \sum_{1}^{7} N$$, Where N is the index value calculated for each property

Non-aggressive water has a Final Index (FI) < 350, FI 350 to 750 fairly aggressive, 750 to 1000 & over 1000 indicate high and very high aggressiveness, respectively. After performing the calculations for aggressiveness index (N), then make any necessary corrections for turbulent/stagnant conditions, temperature effects, for wet-dry cycling time ratios and frequencies to derive the final index (FI).

TABLE1. Average chemical composition of the acidic mine water from the coalfields

pH	**EC** *mS/m*	**$CaCO_3$** *mg/l*	**Cl** *mg/l*	**P** *mg/l*	**SO_4** *mg/l*	**TDS** *mg/l*	**Fe** *Mg/l*	**Ca** *mg/l*	**Mg** *mg/l*	**Mn** *mg/l*	**K** *mg/l*	**Na** *mg/l*
3.0	907	66	32	<0.1	5200	8555	23	990	247	14	32	1168

The observed degradation arises from corrosive attack by the aggressive ions present in water. Each form of attack is governed by the presence of specific ionic species, available in sufficient quantities as to induce chemical attack. Table 1 shows the chemical analyses of AMD water samples taken from the field site where the deterioration of concrete occurred. It can be seen that the predominant ion species present in the acidic water are calcium (Ca), sodium (Na), magnesium (Mg) and sulphate (SO_4). The Ca and Na+K ionic concentrations are 990 ppm and 1189 respectively, while the SO_4 anion which is the most dominant of all the ion species present exceeds 5000 mg/l. Potassium (K), iron (Fe), chloride (Cl), and manganese (Mn) are only present in negligible concentrations. Figure 3 is a pie chart plot showing the relative proportions of the main elements in the water. The Ca, Na, K ions are all alkaline species, leaving the presence of high concentrations of SO_4 to be the likely candidate species for aggressive actions of the water. The chloride ion, an agent known to be severely aggressive to materials, is negligible and likely to have no influence on corrosion actions of the water.

Index Results and Discussion. The six indexes determined for the acidic mine water are given in Table 2. By examining the main aggressive elements, properties or ions in water that are influential in corrosion, the indexes are used to classify the water quality for corrosiveness. Basing on water chemistry, it is clear that the AMD water from the coal mine source is highly acidic given its average pH of 3.0 (see Table 1).

The high negative LSI index value of -6.48 indicates the highly corrosive nature of the water on materials. An FI > 1000 is considered to be very highly aggressive. But the index value of 7382 obtained for the AMD water is much higher, being 7 times greater than the highest level of aggressiveness classified and 20 times greater than the FI value of normal and non-aggressive water. The extreme high FI index is suggestive of severe attacking nature of the AMD water, and is consistent with the observed exfoliation in the field concrete. Also included in the table are the RSI, LnR, R and AI for asbestos cement, determined by simple arithmetic rule basing on the chemical agents and parameters that characterise leaching, spalling, & scaling behaviours. The result of the indexes indicates leaching to be the dominant mode of water attack and confirm field observations showing intense efflorescence and salt depositions at the disintegrated concrete surface.

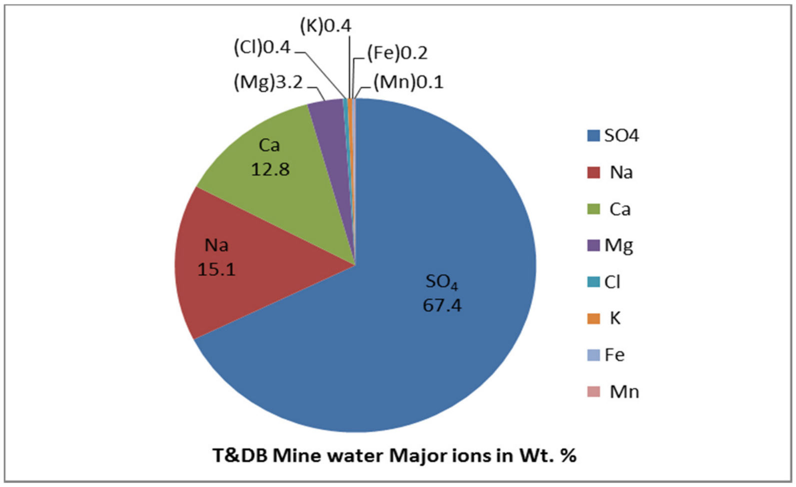

FIGURE3. Pie chart showing element concentrations in the acid mine drainage water

TABLE2. Classification the acidic mine water based on corrosion indexes

No	*Indexes*	*value*	*Aggressiveness classification*
1	*LSI-Langelier saturation index*	*-6.48*	*Water is undersaturated with respect to CaCO3*
2	*RSI-Ryznar stability index*	*15.96*	*Water is very aggressive*
3	*AI-Agreesiveness index (Basson, 1989)*	*7381.8*	*Very highly aggressive water*
4	*AI-Agreesiveness index for asbestos cement pipe*	*5.63*	*Highly aggressive water*
5	*LnR-Larson ratio*	***	*Strong corrosion potential (* Formula doesn't apply)*
6	*R- Corrosion ratio*	*5345*	*Aggressive water*

ATTACK PROCESS

Based on water chemistry (see Table 1) and the index analyses, it is thought that the possible attack processes that led to the observed concrete disintegration could be acid corrosion and/or sulphate attack mechanisms. In order to obtain insights into the attack process(es) involved in the concrete deterioration, thermogravimetric (TGA)/differential thermal analysis (DTA) was conducted on powder samples prepared from the deteriorated concrete. Figure 4 gives the TGA/DTA profile of the reaction products found in the distressed concrete.

The absence of the Ca(OH$_2$) is indicative of total loss of alkalinity associated with the acidic conditions. It is likely that the calcium hydroxide was destroyed by acid attack and/or converted by formation of CaCO$_3$ as a result of carbonation. Acid or sulphate attacks typically form gypsum and ettringite as the final reaction products. But the absence of a major peak for these products suggests lack of massive quantities, although a minor peak can be seen which indicates a trace (of the past) presence of the phases. It is possible that the gypsum and ettringite phases may have been converted by carbonation or they were simply unstable under the existing conditions, leading to their dissolution. There is also some brucite present, which is consistent with the relatively high concentration of magnesium in the water. Further analytical study of the concrete deterioration is being undertaken by using scanning electron microscopy and x-ray diffraction techniques.

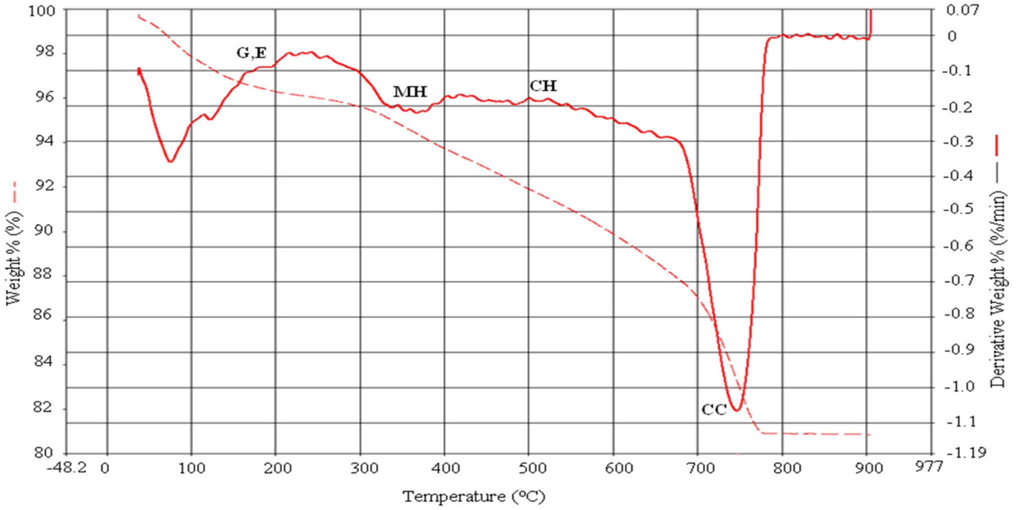

FIGUR4. TGA/DTA of the deteriorated concrete: G - gypsum, E - ettringite, MH – magnesium hydroxide (brucite), CH – calcium hydroxide, CC – calcium carbonate

CONCLUSIONS

Deterioration of a concrete wall lining was examined against the analytical understanding of the aggressiveness of the acidic mine water responsible for the physical degradation. The concrete deterioration observed included severe cracking notably above the water line, map cracking across the full wall thickness; swelling, spalling and exfoliation; surface deposition of yellow discolouration, and erosion of the cementitious matrix of the concrete leaving behind protruded aggregates. The chemical signature of the mine water revealed high toxicity, and can be classified as highly acidic, with a pH of 3.0. The water had elevated concentrations of calcium and sodium alkalis relative to others, and higher concentration of sulphates.

The *Langelier Saturation Index* of the acidic mine water was determined to be -6.5 while the *Aggressiveness Index* was found to be 20 times greater than the corresponding values expected of non-corrosive normal water quality. According to both indexes, the acidic mine water is classified as being extremely corrosive and could be expected to cause severe deterioration of the concrete. These findings are in agreement with the physical damage features observed in the distressed field concrete. Although acid and/or sulphate attack mechanisms are suspect, the mineralogical forms of the attack process could not be fully established through the thermal analytical technique employed. Further investigation on the deterioration mechanism is being conducted using other complementary analytical techniques.

ACKNOWLEDGEMENT

Support for this research by DMR (Department of Minerals Resources), CGS (Council For Geoscience) and University of Witwatersrand is gratefully acknowledged.

REFERENCES

Basson, J.J. 1989. *Deterioration of Concrete in Aggressive Waters- Measuring Aggressiveness and taking Countermeasures*, Portland Cement Institute, Midrand, South Africa, ISBN 0-620-13710-X, 22p.

Driscoll, F. 1986. *Groundwater and Wells*, Johnson Division, 2nd Ed., 1089p.

EPA 1973. Processes, Procedures, and Methods to Control Pollution from Mining Activities. *Environmental Protection Agency*, Publication EPA-430/9-73-011, Washington D.C.

Sasidhar, P. and K. S. B. Vijay 2008. "Assessment of Groundwater Corrosiveness for Unconfined Aquifer at Kalpakkam." *Environ Mon Assess*, 145:445-452.

Younger, P. L. 2000. "The Mine Water Pollution threat to Water Resources and its Remediation in Practice." *School of Civil Engrg and Geosciences*, University of Newcastle, Newcastle Upon Tyne, NE1 7RU, UK, 48p

MEASUREMENT AND ESTIMATION OF FOREST WATER RETENTION CAPACITY ALONG THE FOREST TRANSECT

Xuyong Li**,** Fei Mo, Xiaoxue Wang
(Research Center for Eco-environmental Sciences, Chinese Academy of Sciences, Beijing, China)

We investigated forest water retention characteristics and estimated forest water retention capacity at different spatial scales in Dongling Mountain area in Beijing, China during May-October of 2006-2009. The rainfall interception capacity of forest canopy, water hold capacity of forest litter and soil were investigated and compared among four long-term forest ecosystem study sites with the precipitation from low to high (Dongling, Changbai, Huitong and Dinghushan sites) along the forest transect in eastern China during May-October of 2006-2009. In Dongling Mountain, rainfall interception capacity of forest canopy, water hold capacity of forest soil and litter accounted for 44.5%, 53.2% and 2.3% of the total potential forest water retention capacity, respectively. Hillslope runoff was 54.9 mm under the mixed coniferous and broad-leaved forest, and 24.7 mm under the pinus tabulae-formis forest in Dongling Mountain. In raining season (May to October) during 2006-2009, hillslope runoff sharply dropped from 32.3 mm to 2.5 mm while the rainfall decreased from 500 mm to 300 mm. At the landscape scale in Dongling Mountain, the actual forest water retention capacity in raining season varied from 80.4 mm to 106.8 mm among four major forest types. Actual forest water retention capacity in raining season accounted for 60.5% of the total potential forest water retention capacity. Compared the forest water retention characteristics in two sites with similar climate and vegetation conditions, we found the average hillslope runoff was 63.1 mm and 37.2 mm in Dongling Mountian and Liupan Mountain, respectively; but the watershed runoff was 10.6 mm and 20.1 mm in Dongling Mountian and Liupan Mountain, respectively. Along the forest transect in eastern China with the rainfall from low to high (Dongling: 498 mm, Changbai: 599 mm, Huitong: 627 mm and Dinghushan: 1216 mm) from May to October, the rainfall interception capacity of forest canopy varied from 71.2 mm to 245.1 mm and positively correlated with rainfall, but water hold capacity of forest litter and soil did not correlate to rainfall. We concluded that the rainfall interception capacity of forest canopy and water hold capacity of forest soil contributed to most of the forest water retention. The forest water retention capacity is impacted not only by rainfall and forest type, but also by topology and soil hydraulic properties.

ISBN 9780976885351

ROLE OF ORGANIC MATERIALS IN DESERT GREENIFICATION TO IMPROVE THE ARID ENVIRONMENT

Ali A. AlJaloud and Ghulam Hussain (King Abdulaziz City for Science and Technology (KACST), P.O.
Box 6086 Riyadh 11442, Kingdom of Saudi Arabia)

A field experiment with one soil (sandy), four organic materials (compost, sewage sludge, dairy manure, poultry manure), three plants (*Prosopis juliflora, Acacia Arabica and Atriplex halimus*), four application rates (0.25, 50, 75 Mg ha^{-1}) and one irrigation level (irrigation at 20% depletion of maximum available water at field capacity) was carried out to determine the potential of these organic materials for desert reunification in Saudi Arabia.

Mean biomass yield of Acacia Arabica (Mg ha^{-1}) ranged between 31-39 (compost) 25-53 (sewage sludge)m 18-67 (dairy manure) and 19-82 (poultry manure). Mean protein contents of Acacia Arabica (%) ranged between 6.32-7.27 (compost), 6.11-8.10 (sewage sludge), 6.8-7.56 (dairy manure) and 7.59-8.43 (poultry manure) Mean biomass yield of prosopis juliflora (Mg ha^{-1}) ranged between 21-52 (compost), 51-107 (sewage sludge), 43-87 (dairy manure) and 52-156 (poultry manure). Mean protein contents of Prosopis Juliflora (%) ranged between 9.26-10.45 (compost), 10.41-11.37 (sewage sludge), 9.6-11.07 (dairy manure) and 9.3-10.93 (Poultry manure). Mean biomass yield of Artipex halimus (Mg ha^{-1}) ranged between 1.2-10.1 (compost), 11-37 (sewage), 5-45 (dairy manure) and 5-57 (poultry manure). Mean protein contents of Atriplex halimus (%) ranged between 7.35-8.38 (compost), 4.11-5.47 (sewage sludge), 4.40-4.93 (dairy manure) and 3.68-4.58 (poultry manure). Soil salinity increased considerably due to application of different organic waste materials than the control treatment.

Overall the mean biomass yield of all the plants increased significantly with increasing application rates of different organic materials. The order of increase in biomass yield was significantly higher in poultry manure> dairy manure> sewage sludge and the compost. The plant protein contents were not significantly affected by the application of different organic materials, these organic materials showed an excellent potential for improving the productivity of sandy soils.

ISBN 9780976885351

SCREENING OF SALT TOLERANT PLANTS FOR PROMOTING GREENERY IN SAUDI ARABIA

Ali A.ALjaloud, Ghulam Hassain (King Abdulaziz City for Science and Technology(KACST), P.O. Box:6086 Riyadh 11442 Saudi Arabia, E-mail: aljaloud@kacst.edu.sa)

A field experiment was carried out at Al-Muzahmiyia Research station, KACST, Riyadh, Saudi Arabia to determine salt tolerance of landscape trees. The experimental treatments were nine plants, one soil (sandy) and four levels of water salinity (2, 4, 8, and 12 thousand mg L^{-1}). The experiment was laid out by following "The Randomized Complete Block Design" with four replications. Mean plant yield(Kg/Plant) ranged between 8.2 - 11.24 kg (*Prosopis juliflora*), 0.7 - 1.3 kg (*Prosopis specigera*), 0.3 - 0.6 kg (*Prosopis tamarugo*), 2.7 - 5.8 kg (*Acacia nilotica*), 1.3 - 4.3 kg (*Leuceana leucocephola*), 0.2 - 1.7 kg (*Pithecellobium dulce*), 11.49 -15.88 kg (*Atriplex halimus*), 7.7 - 18.6 kg (*Atriplex nummularia*) and 1.5 - 1.9 kg (*Conocarpus erectus*), in different water salinity treatment. Mean plant height ranged between 230 - 261 cm (*P. juliflora*), 134 - 168 cm (*P. specigera*), 103 - 118 cm (*P. tamarugo*), 181 - 206 cm (*Atriplex halimus*), 172 - 216 cm (*Acacia nilotica*), 137 - 145 cm (*Atriplex nummularia*), 109 - 173 cm (*Pithecellobium dulce*), 91 - 118 cm (*Conocarpus erectus*) and 199 - 246 cm (*Leuceana leucocephola*) in different water salinity treatment. The results indicated that landscape plants such as *Atriplex halimus, Atriplex nummularia* and *P. juliflora* produced more than 50% biomass as compared to the control treatment. Overall, the experiment showed excellent potential for cultivation these plants for desert greenification under an arid environment.

ISBN 9780976885351

ASSESSMENT OF AGRICULTURAL ECOSYSTEM SERVICES VIA ECONOMIC AND SPATIAL SIMULATIONS

YenLan Liu**,** ***Jun-Wen Hsiao*** (National Taiwan University, Tapei, Tawan)

This study assesses the potential to improve agro-biocapacity on agricultural land in Taiwan by modeling a series of alternative scenarios and comparing the spatial distribution in land use. Agro-biocapacity is defined as the capacity of an agricultural area to provide ecological resources and services. In the paper different management scenarios aiming at the supply of agricultural ecosystem services by including fallow land with green manure in the cropping system are evaluated. Using an agricultural allocation model, this study examines four scenarios and finds that farming practices considering agricultural ecosystem services result in improved agro-biocapacity and increased yields. Inadequate governmental subsidy can cause low levels of the provision of ecosystem services due to soil degradation from accelerated soil acidification.

ISBN 9780976885351

INTER-SECTORAL POLICY COORDINATION IN THE FORESTRY AND AGRICULTURAL SECTORS OF GHANA: *WHAT ROLE FOR IDEAS, INTERESTS AND INSTITUTIONS (3Is)?*

***Yaw Amo Sarpong*, Daniel K. B. Inkoom
(Kwame Nkrumah University of Science and Technology, Kumasi, Ghana

Natural resources (NR) in most countries are key to sustaining the national economy and local livelihoods. The NR is made up of many sectors – land, forestry, agricultural, mining, fisheries, water, and oil and gas. There exist competitive claims among most of the sectors. This becomes problematic when there is a lack of inter-sectoral policy coordination (IPC) among sectors resulting in competition for resources and often, as a result, resource depletion. Almost all forestry and agricultural activities in Ghana happen in the forest zone. These two sectors have a tradition of sectoral approaches but have recently been pushed for coordination to help achieve sustainable development. This resulted in launching of some NR policy intervention programmes of which five are implemented by these two main sectors of the economy. Because success and failure of these initiatives in terms of (lack of) coordination are not clear so far, the objective of this research is to investigate and create an understanding of inter-sectoral policy coordination in Ghana. The question is: To what extent do the forestry and agricultural sectors in Ghana coordinate their policy initiatives and how can we understand this in terms of, the ideas, interests and institutions (3Is) within the two sectors? The 3Is framework will be used as the overarching theory to understand the role of interest, institutions and ideas in policy coordination at three governance levels (national, district and local). Methodology involving case and multi-sited ethnographic studies will be employed to study the five selected programs.

ISBN 9780976885351

HEALTH HAZARDS OF URBAN METAL CONTAMINATION TO WILDLIFE IN AN ARID ENVIRONMENT

Khadiga G. Adham[1 2], Nadia A. Al- Eisa[1], Manal H. Farhood[1]
[1]King Saud University, Malaz, P.O. Box 22452, Riyadh 11495, Saudi Arabia
[2]Alexandria University, Moharram Bey, Alexandria 21511, Egypt

Several aspects of the physiology of the wild libyan jird, *Meriones libycus* were investigated in the context of heavy metal (Cd, Cu, Hg, Ni and Pb) accumulation. Animals were collected from one of Riyadh's polluted districts and samples were assayed versus reference subjects. Study features included testing the biomonitoring potential of this species, setting up a baseline profile of its physiology and hematology versus other small mammalian species, evaluating the impact of inhabiting a metal-polluted area on the stress profile of hematology and serum biochemistry and assessing the relevance of *M. libycus* for evaluating environmental health hazards to humans. A unique species-specific stress leukogram for *M. libycus* was displayed by leukocytosis, monocytosis, lymphocytosis with eosinopenia and neutropenia. Data of platelets and mean platelet volume MPV acknowledged bone marrow suppression in affected jirds. Stress-related altered metabolism and utilization in energy synthesis were suggested to rationalize the deviation of the normal patterns of serum lactate dehydrogenase LDH, glucose, low-density and high-density lipoprotein, cholesterol, triglycerides and the stress hormone cortisol. Multiple organ dysfunction was suggested in view of the modified activities of serum pseudocholinesterase PChE, alanine aminotransferase ALT, aspartate aminotransferase AST and creatine kinase CK. Based upon adverse effects on several metabolic and physiologic pathways, *M. libycus* proved a relevant bioindicator species for contaminant biomonitoring and a potential sentinel species for evaluating the risk imposed upon human populations in urban polluted areas.

ISBN 9780976885351

LOSSES OF ECOSYSTEM SERVICES VALUE IN TAIHU WATERSHED FROM 1979 TO 2010

Hui Zhang*(Nanjing Institute of Environmental Science. Ministry of Environmental Protection of China, NanJing, JiangSu Province ,China,210042);Yan-Song Wang(Academy of Environmental Sciences of Liaoning Province, ShengYang,China,110031);Qiao Wang (Environmental Satellite Application Center, Ministry of Environmental Protection of China, BeiJing, China,100029)

The Taihu Watershed is one of the fastest growing metropolitan and the rapidest proceeding industrialization areas in China. Due to urban sprawl, some cultivated land and ponds become urban construction land. Meanwhile there are losses of ecosystem services in response to land use changes during urbanization. Based on researches of ecosystem service values per unit area by each land cover category of China. the Taihu watershed's ecosystem service values per unit area was given. Based on dynamic data of land use in 1979, 1987,2000 and 2010 , changes of ecosystem services was valuated delivered by each land cover category. Results showed the total value of ecosystem services in the Taihu Watershed had been diminished rapidly in recent 30 years. The whole watershed decreases from 40.489 billion yuan in 1979 to 32.512 billion yuan in 2010 and reduces by 19.7%. And the ecological service values of the cultivated land and the waters decrease faster than others. The ecosystem service values of the cultivated land and the waters decrease faster than others. The ecological service value of the cultivated land decreased from 18.018 billion yuan in 1979 to 13.997 billion yuan in 2010 and reduces by 22.31%. And ecosystem service values of water area decreased from 8.611 billion yuan in 1979 to 3.609 billion yuan in 2010 and reduced by 58.09%. However, the ecosystem service value of the forest land increased from 13.528 billion yuan in 1979 to 14.226 billion yuan in 2010.

ISBN 9780976885351

AN INVESTIGATION INTO CRUDE OIL EVAPORATION FROM ARID SOILS FOR OIL SPILLS REMEDIATION

Farid Benyahia* (Chemical Engineering, Qatar University, Qatar)

Crude oil spills are becoming one of the greatest environmental disasters humanity can witness. Whether these occur in the sea or inland, the environmental damages have been largely underestimated because of the inability to estimate to any degree of accuracy the amount and nature of fractions of crude oil evaporated following major spills. For inland spills, this can be traced to several related or independent factors that include complex composition of crude oil, temperature and wind speed variations, mechanisms regulating oil evaporation and mode of adhesion of oil onto soil particles.

In this investigation, oil evaporation studies have been conducted on free oil and on oil saturated desert soil over a period of time during which temperature and wind speeds were recorded. The amount of oil lost by evaporation was shown to follow the trend of daily temperature variation in a damped oscillatory manner. The damping element was explained in terms of shift towards heavier oil fractions as evaporation proceeds.

The evaporation rate of a medium to heavy weighted UAE crude oil was studied from a contaminated soil. The evaporation rate was very much dependents on the temperature primarily and solar radiation during the day. In a 48 hours experiments 37% of the initial crude in the soil has evaporated. This represents 86% of the light components in the soil. The evaporation process from soil has increased by 60% when ploughing of the soil was considered. Modeling of the evaporation process proved to be a challenging task and empirical modeling could give good answers but is constrained by the specific site and material. The issue that needs addressing is whether there could be better and yet simple to use modeling approaches such as neural networks that can relate prevailing conditions to oil evaporation. Such tools are urgently needed for oil spill and environmental impact assessment studies.

Our study has shown that oil evaporation poses serious concerns in terms of human health risk and water resources contamination. In this study 86% of the light components were evaporated to the atmosphere. These include many carcinogenic components like BTEX. In an attempt to mitigate such problem, a bioremediation study showed that a significant decrease in original PAH, and TPH in the soil can be achieved without shifting evaporated fractions to the atmosphere. The technology adopted made use of self contained biopile systems and addressed the concern on strongly adsorbed recalcitrant components. If not treated, these can be a serious risk associated to human and ground water.

ISBN 9780976885351

SYSTEMATIC CONSERVATION PATTERN FOR THE ECOSYSTEM IN QINBA REGION, CHINA

Ya-nan Tian, *Hongqi Wang*, Jingwen Sun, Zeqing Hou
(College of Water Sciences, Beijing Normal University. Beijing 100875, P. R. China)

With vast area of river basin and rich biodiversity, QinBa Region (QBR) has its uniqueness and irreplaceability at local, regional and global scales. QBR not only provides huge suitable habitats for various wildlives, but also plays very important role in providing great ecosystem service for the whole country. However, due to intensive human activities in QBR during the half past century, this region has long been suffering from large-scale destruction and increasing degradation. Though some National Nature Reserves have been established to protect the biodiversity and their habitats, it is still not enough to control the destruction and degradation. Therefore, it's essential to develop an efficient conservation network based on existing reserve system evaluation to ensure ecological security. In order to optimize ecosysem reserve system effectively, we firstly evaluated the status of existing reserves system. We then, taking ecological security as goal, identified conservation gaps based on the existing reserves system evaluation in considering the important of water conservation, biodiversity, soil conservation, wind prevention and sand-fixation, as well as desertification sensitivity, stony desertification sensitivity, salinization desertification sensitivity and soil erosion sensitivity. Before that the importance and sensitivity of ecosystem need to be considered and socio-economical factors also to be considered such as GDP, population, etc. Thirdly conservation scenarios and irreplaceable patterns had been established based on different conservation levels in QBR by using the theory and methodology of Systematic Conservation Planning (SCP) and worldwide Marxan space-optimized software. Finally, we, taking the consideration of integrity and connectivity, compared those scenarios to confirm the optimized planning and integrated with the existing reserve system to develop the optimized conservation network. In this process, we kept making sure that the results of planning can be overlapped onto the countys' maps. The results showed that: the existing reserve system covered only about 4.39% of region; lots of potential habitats and important reigon which had significant ecological function were still under the risk of human destroying. To improve and optimize the spatial pattern of existing conservation system in QBR, it was necessary to adjust the function zonings across provinces: Gansu (2 counties) , Sichuan (1 counties) , and Shaanxi (6 counties). As 7 counties have not been covered by current reserve system so far except 2 counties has intersect with existing reserves, we proposed to establish new reserves across these provinces which covered about 12.04% of region. These protected / adjusted areas proposed in this study should be well integrated with existing reserve system to form a larger and optimized conservation network system for QBR. The implications of this study are: on the one hand, SCP had been used not only in the biodiversity conservation but in the ecosystem protection; on the other hand, SCP had a good potential of application and extension in China with ecological zoning.

ISBN 9780976885351

URBAN ECOSYSTEMS ARE AMALGAMATIONS OF ECO-FRIENDLY & ADVERSE FACADES: CASE STUDY, INDIA

Prem Kumari Gupta (Indira Gandhi National College, Ladwa (Kurukshetra), India)

"Kurukshetra city" is the cultural capital of "Haryana" state in India and is located at a distance of 157Kms North of New Delhi on national Highway number one (Latitude $29^0$52' to $30^0$12' and Longitude $76^0$26' to $77^0$04').Albeit , it is a historical city having a rich historic past (Indus-valley civilization-remnants) and a universal recognition linked with LORD KRISHNA'S GOSPEL TRUTH: GEETA SCRIPT, yet from the viewpoints of URBAN ECOSYSTEMS its past 45 years events have transformed its façade drastically having few virtuous eco-friendly facets mingled with negative aspects like concrete jungles of over-excessive conflagration of urbanization processes dominated by modern human dwellings. The main objectives of the present study are to set aside good and bad aspects to the fore in reference to urban ecosystem in Kurukshetra district, India.

The results indicate that the distinctly visible positive parameters in the shape of vast spacious PUBLIC PARKS with ultramodern landscape patterns, attractive avenues of metallic roads lined with exotic shady trees, orchards of Guavas *Psidium guajava* and Jamun *Syzigium cumunii,* Deputy Commissioner's, state of the art, office, extremely beautiful JUDICIARY COMPLEX, POLICE HEAD QUARTERS are few positive virtues of a modern human dwellings in an upcoming world economy like India. Also, intensive tree cover in the area is distinctly an eco-friendly feature. Another eco-friendly feature of this urban ecosystem is the presence of multiple public parks. The results further reveal that negative aspects of this urban ecosystem, in its very inception, initiation and execution in 1975 on a vast patch of excellent fertile fields known for world class per acreage output of Rice and wheat can not be justified as development of new colonies should preferably be done in wastelands. Also, the huge mounds of Wheat/Rice packed gunny bags in the open yards display; in the first place, irresponsible behavior of Govt. of India by way of storing food grains in a most unscientific way thus spoiling the façade of urban ecosystem. The most significant finding is the practice related to zero sensitivity of public and Govt towards environment. Moreover, these polythene bags are accumulating in the very face of existing strict laws. These polythene bags are a very common site depicting the deterioration of this urban ecosystem.

In conclusion, one may say that in an upcoming world economy like India, urban ecosystems are an amalgamation of good and bad ecological parameters. A sensitive society and responsible Govt. can certainly catapult the situation towards the prevalence of eco-friendly ecosystems in India.

ISBN 9780976885351

EVALUATION OF GREENHOUSE GAS EMISSION POTENTIAL OF A EUTROPHIC LAKE

Ezgi Ogun and ***Selim L. Sanin*** (Hacettepe University, Ankara, Turkey)
Aysegul Aksoy (Middle East Technical University, Ankara, Turkey)

Eutrophication of lakes is well defined and accepted problem in the world. In recent years, effect of increasing nutrients in natural inland waters on GHG production is also verified. The objective of the study was to determine the production rate of GHGs in eutrophic lakes and to investigate the relationship between the nutrients, physical conditions of the lake and gas releases. Lake Eymir is a small eutrophic lake, used for recreational purposes. The lake is covered horizontally (E-W) and vertically (N-S) for water and sediments samples. Lake water samples are collected into 65 ml pre-cleaned brown glass bottles with Teflon septa and stored in ice packed cooler until delivering to the laboratory, within 5 hours. Sediments were collected from the field and 30 grams of sediment samples filled into 65 ml brown glass bottles. The samples immediately analysed upon arrival to the laboratory using a GC system equip with ECD and FID detectors (Agilent 6890N). All necessary calibration and method validation protocols are applied. Calibrated and verified detection kits are used for the measured parameters (COD, NO3, NH3, PO4, TN). Monitoring Eymir lake water and rate determination studies conducted in the microcosms showed that sediments are the GHG production locations, during spring and summer seasons. Hydrodynamic characteristics of the lake, which is affected form the climatic conditions) has an effect on GHG production. The lake can be treated as open system plug flow reactor with varying flow conditions. Although methane production is observed in all samples, nitrous oxide production is limited to sediment regions with high organic content. In microcosms N2O production rate is high for the first 24 hours. A stationary phase and decreasing period is followed. Light intensity is important for photosynthetic activities in the lake sediment but in the absence of light, anoxic microbial populations are also responsible for GHG production.

ISBN 9780976885351

DIVERSITY OF AQUATIC INSECTS OF URBAN LAKE DURING RESTORATION, GULBARGA DISTRICT, KARNATAKA

K.Vijaykumar (Gulbarga University, Gulbarga-585106, Karnataka, INDIA)

In this present investigation focused on diversity of aquatic insect present in Sharnabasaveshwara Lake. The study was conducted in two periods i.e. before restoration of lake (2005-06) and after restoration of lake (2009-10). The aquatic fauna of lake belonging to 6 orders viz., Hemiptera, Coleoptera, Diaptera, Ephemeroptera, Tricoptera and Odonata. Whereas after the restoration the aquatic insects composition of Sharanabasaveshwara lake was belonging to 7 orders viz, Hemiptera, Coleoptera, Diaptera, Odonata and Ephemeroptera ,Tricoptera and Plecoptera respectively. Seasonal occurrence of aquatic insects results indicate that the Dipetera family showed high in their abundance in all the seasons of 2005-06, while after restoration Diaptera group declined in all the seasons. Hemiptera and Ephemeroptera families were recorded low density in 2005-06 and increased their density and diversity in 2009-10. While less tolerance insects were showed high density after restoration (Odonata). Family biotic index, Dominance, Shannon index and Simpson index values reveals that after restoration the aquatic insect's diversity of lake is increased with comparison with results of before restoration.

ISBN 9780976885351

INTEGRATED ASSESSMENT FOR THE HEALTH OF THE MISSISSIPPI CANYON, N. GULF OF MEXICO

Y. S. Soliman (Qatar University, Qatar), T. L. Wade (Texas A&M University, USA) and G. T. Rowe (Texas A&M at Galveston, TX, USA)

Mississippi Canyon has diverse potential sources for Polynuclear Aromatic hydrocarbons (PAHs) including natural seepage, releases in areas where active oil and gas exploration and development are under way, and from the lateral transport from the Mississippi river and the surrounding shelves. PAHs are hydrophopic organics that can accumulate in sediment where they become available to the benthos, t thus imposing potential adverse impact to the ecosystems of the Gulf. Little work has been done on the fate and the quantitative effect of the PAHs in the deep-water environment.

We utilized the "Triad" approach in the head of the Mississippi Canyon to assess the quality of the sediment. This integrated information from chemical, biological and toxicological measurements in sediments and associated biota. Sediment PAHs were slightly above the back ground levels. However, benthic faunal abundance was unexpectedly high at the head of the Mississippi canyon (480m). Faunal parameters including high dominance, low diversity and species indicators for the stressed environment implied that the canyon is highly stressed.

The biomass and production were unexpectedly high for a deep ocean habitat, comparable to organically enriched shallow water habitats. This coincided with high levels of total PAHs in the dominant species amphipods (*Ampelisca mississippiana* Soliman and Wicksten, 2007), reaching 5000 ng/g. The distributions of individual PAH in sediments were different from that in the organisms, suggesting preferential uptake/depuration or uptake from pore or bottom waters. Benthic amphipods concentrated alkylated PAHs and dibenzothiophenes with bioaccumulation factors up to 132. The diagnostic ratios indicated that in the canyon the PAHs were petrogenic in origin, e.g., from oil and gas activities or natural seeps. The integrated study for the Mississippi canyon indicated that the head of the canyon has a degraded benthic habitat quality.

ISBN 9780976885351

EFFECT OF O_3 ENRICHMENT ON MICROELEMENTS IN WHEAT AND SOIL

Xiaozhi Wang, Xianchen Zhang, Yuhua Shan, Haitao Zhao and Ke Feng (Yangzhou University, Yangzhou, China)
Jianguo Zhu (Chinese Academy of Sciences, Nanjing, China)

Ozone Free-air Concentration Enrichment (O_3-FACE) system was used in this study to investigate the effects of atmospheric elevated O_3 on concentrations of DTPA-extractable microelements in soil and accumulation of microelement in wheat plant in the wheat season in 2009-2010. Concentrations of DTPA-extractable Fe, Mn, Cu ,Zn at different soil depths (0-5 cm, 5-10 cm and 10-15 cm) and microelement in wheat plant at mature stage were determined under ambient and elevated (target at 50% above ambient) ozone concentration treatment. The results showed that elevated O_3 increased the concentrations of DTPA- extractable Fe and Mn in soil at 0-15 cm depth with 11.7% and 6.2%, and reduced the concentrations of DTPA- extractable Cu and Zn in soil at 0-15 cm depth with 3.0% and 27.3%, respectively. Elevated O_3 significantly increased the concentrations of DTPA- extractable Fe, Mn, Cu and Zn in soil at 5-10cm. Concentrations of DTPA-extractable Fe, Mn and Zn in soil decreased with soil depth. Elevated O_3 significantly reduced the concentration of DTPA-extractable Zn in 5-10cm and 10-15cm soil ($P<0.05$), and decreased wheat biomass and microelement accumulation at mature stage. To understand the effect mechanism of elevated O_3 on biogeochemical cycling of microelements in agricultural ecosystem, soil properties and plant growth, together with the microelement status at different soil depths should be considered.

ISBN 9780976885351

PROPOSALS OF INDUSTRIAL ECOLOGY FOR LOCAL PRODUCTIVE ARRANGEMENTS

Adriana V. Saraceni* and Pedro Paulo de Andrade Júnior (Universidade Tecnológica Federal do Paraná,
Ponta Grossa, PR, 84016-210, Brasil)

Proposals of Industrial Ecology for Local Productive Arrangements were investigated. From the literature review, it was described the main features of Industrial Ecology and its implementation in the form of Ecological Industrial Park. The methodology used was by means of a theory survey and of qualitative and exploratory character. The common characteristics of Ecological Industrial Parks and Local Productive Arrangements were investigated. Also it was showed a application proposal for the Local Productive Arrangements. It was used as method, the theoretical conception of Industrial Ecology, Eco-Industrial Parks and the main approaches of Local Productive Arrangements. Results of this study showed that there is the prospect that a Local Productive Arrangement, by applying tools of Industrial Ecology, may move towards an Ecological Industrial Park.

ISBN 9780976885351

International Conference
on
Environmental Science and Technology

All information about the International Conference on Environmental Science and Technology can be found at http//:www.aasci.org/conference/env/index.html